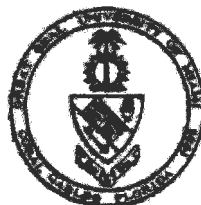
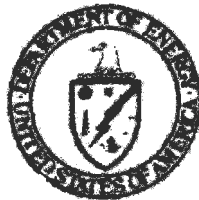


Research and Development



# Proceedings: Second Conference on Waste Heat Management and Utilization (December 1978, Miami Beach, FL) Volume 2



## **RESEARCH REPORTING SERIES**

Research reports of the Office of Research and Development, U.S. Environmental Protection Agency, have been grouped into nine series. These nine broad categories were established to facilitate further development and application of environmental technology. Elimination of traditional grouping was consciously planned to foster technology transfer and a maximum interface in related fields. The nine series are:

1. Environmental Health Effects Research
2. Environmental Protection Technology
3. Ecological Research
4. Environmental Monitoring
5. Socioeconomic Environmental Studies
6. Scientific and Technical Assessment Reports (STAR)
7. Interagency Energy-Environment Research and Development
8. "Special" Reports
9. Miscellaneous Reports

This report has been assigned to the MISCELLANEOUS REPORTS series. This series is reserved for reports whose content does not fit into one of the other specific series. Conference proceedings, annual reports, and bibliographies are examples of miscellaneous reports.

## **EPA REVIEW NOTICE**

This report has been reviewed by the U.S. Environmental Protection Agency, and approved for publication. Approval does not signify that the contents necessarily reflect the views and policy of the Agency, nor does mention of trade names or commercial products constitute endorsement or recommendation for use.

This document is available to the public through the National Technical Information Service, Springfield, Virginia 22161.

**EPA-600/9-79-031b**

**August 1979**

**Proceedings: Second Conference  
on Waste Heat Management and Utilization  
(December 1978, Miami Beach, FL)  
Volume 2**

S.S. Lee and Subrata Sengupta, Compilers

Mechanical Engineering Department  
University of Miami  
Coral Gables, Florida 33124

EPA Purchase Order DA 86256J  
Program Element No. EHE624A

EPA Project Officer: Theodore G. Brna

Industrial Environmental Research Laboratory  
Office of Energy, Minerals, and Industry  
Research Triangle Park, NC 27711

Cosponsors: Department of Energy, Electric Power Research Institute, Environmental Protection Agency, Florida Power and Light Company, Nuclear Regulatory Commission, and University of Miami's School of Continuing Studies (In cooperation with American Society of Mechanical Engineers' Miami Section)

Prepared for

U.S. ENVIRONMENTAL PROTECTION AGENCY  
Office of Research and Development  
Washington, DC 20460

## ORGANIZING COMMITTEE

Dr. John Neal  
Department of Energy

Dr. Theodore G. Brna  
Environmental Protection Agency

Mr. Frank Swanberg  
Nuclear Regulatory Commission

Dr. John Maulbetsch  
Electric Power Research Institute

Mr. Charles D. Henderson  
Florida Power & Light Company

Dr. Samuel S. Lee  
Conference Chairman,  
University of Miami

Dr. Subrata Sengupta  
Conference Co-Chairman,  
University of Miami

## ADVISORY COMMITTEE

Dr. C. C. Lee  
U.S. Environmental Protection Agency

Mr. Charles H. Kaplan  
U.S. Environmental Protection Agency

Dr. Mostafa A. Shirazi  
U.S. Environmental Protection Agency

Dr. Richard Dirks  
National Science Foundation

Dr. Donald R. T. Harleman  
Massachusetts Institute of Technology

Dr. Charles C. Coutant  
Oak Ridge National Laboratory

Dr. G. S. Rodenhuis  
Danish Hydraulic Institute, Denmark

Mr. H. Fuchs  
Consulting Engineers Inc., Switzerland

Dr. P. F. Chester  
Central Electricity Research Laboratory, England

## CONFERENCE SUPPORT

### Arrangements:

James Poissant  
Ruben Fuentes  
The School of Continuing Studies

### Special Assistant:

Sook Rhee

## ACKNOWLEDGEMENTS

The Conference Committee expresses its gratitude to the Keynote Speaker, Dr. Eric H. Willis. It also greatly appreciates the help of the Banquet Speaker, Dr. William C. Peters.

This Second Conference on Waste Heat Management has been shaped with help from the Advisory Committee members and the Session Chairmen. Their help is gratefully acknowledged.

The numerous students and faculty who have helped as Co-Chairmen of sessions and other organizational matters were invaluable to the Conference Committee.

The sustained interest of sponsoring organizations made this conference possible. The scientists and administrators who have provided a leadership role in nurturing this growing field of waste heat research deserve our sincerest gratitude.

The participating scientists, engineers and administrators have made this conference achieve the planned objectives of technical interaction and definition of future goals.

Conference Committee  
Miami, December, 1978

## FOREWORD

The first conference on Waste Heat Management and Utilization held in Miami during May 9-12, 1977 was a success in terms of participation, comprehensive technical representation and quality. A questionnaire submitted to the sponsors and participants at the meeting indicated a strong interest in an annual or biannual meeting. In response to this the second comprehensive conference in the subject area is being held during December 4-6, 1978. This will establish a biannual frequency and allow significant progress during meetings.

A perusal of the table of contents will indicate that causes, effects, prediction, monitoring, utilization and abatement of thermal discharges are represented. Utilization has become of prime importance owing to increased awareness, that waste heat is a valuable resource. Sessions on Co-generation and Recovery Systems have been added to reflect this emphasis.

This second conference has working sessions covering important topics in the subject area. This provides an interactive forum resulting in relevant recommendations regarding research directions.

A well balanced Organizing Committee with an Advisory Board with international composition has brought this conference to fruition. The sponsoring organizations include governmental and private organizations who are active in waste heat research and development.

Samuel S. Lee  
Subrata Sengupta

## CONTENTS

### WASTE HEAT MANAGEMENT AND UTILIZATION CONFERENCE

|   | <u>Page</u> |
|---|-------------|
| <b>OPENING SESSION</b>  |             |
| OPENING REMARKS   | ---         |
| Samuel S. Lee, Conference Chairman, University of Miami   |             |
| WELCOMING ADDRESS   | ---         |
| Norman Einspruch, Dean of Engineering and Architecture,<br>University of Miami                              |             |
| KEYNOTE ADDRESS   | 1           |
| Eric H. Willis, Deputy Assistant Secretary for Energy<br>Technology, Department of Energy, Washington, D.C. |             |
| PROGRAM REVIEW  | ---         |
| Subrata Sengupta, Conference Co-Chairman, University of Miami   |             |
| <b>GENERAL SESSION</b>  |             |
| A WASTE HEAT UTILIZATION PROGRAM  | 13          |
| J. Neal, Department of Energy, Washington, D.C.<br>W.F. Adolfson, Booz-Allen & Hamilton Inc., Bethesda, MD  |             |
| EPA PROGRAMS IN WASTE HEAT UTILIZATION  | 25          |
| T. Brna, EPA, Research Triangle Park, NC  |             |
| REVIEW OF EPRI PROGRAM  | 38          |
| Q. Looney, J. Maulbetsch, Electric Power Research Institute,<br>Palo Alto, CA                               |             |
| THE ENERGY SHORTAGE AND INDUSTRIAL ENERGY CONSERVATION  | 39          |
| E.H. Mergens, Shell Oil Company, Houston, TX  |             |
| <b>UTILIZATION I</b>  |             |
| USE OF SOIL WARMING AND WASTE WATER IRRIGATION FOR FOREST<br>BIOMASS PRODUCTION                             | 66          |
| D.R. DeWalle, W.E. Sopper, The Pennsylvania State University  |             |
| POWER PLANT LAND AVAILABILITY CONSTRAINTS ON WASTE HEAT<br>UTILIZATION                                      | 76          |
| M. Olszewski, H.R. Bigelow, Oak Ridge National Laboratory,<br>Oak Ridge, TN                                 |             |

|  | <u>Page</u> |
|--|-------------|
| COOLING PONDS AS RECREATIONAL FISHERIES - A READY MADE RESOURCE<br>J.H. Hughes, Commonwealth Edison Company, Chicago, IL   | 86          |
| HEAT RECOVERY AND UTILIZATION FOR GREEN BAY WASTE WATER TREATMENT FACILITY<br>R.W. Lanz, University of Wisconsin, Green Bay, WI  | 96          |
| <br>MATHEMATICAL MODELING I  |             |
| WHY FROUDE NUMBER REPLICATION DOES NOT NECESSARILY ENSURE MODELING SIMILARITY<br>W.E. Frick, L.D. Winiarski, U.S. Environmental Protection Agency, Corvallis, OR   | 106         |
| A CALIBRATED AND VERIFIED THERMAL PLUME MODEL FOR SHALLOW COASTAL SEAS AND EMBAYMENTS<br>S.L. Palmer, Florida Department of Environmental Regulation, Tallahassee, FL  | 114         |
| FARFIELD MODEL FOR WASTE HEAT DISCHARGE IN THE COASTAL ZONE<br>D.N. Brocard, J.T. Kirby, Jr., Alden Research Laboratory, Worcester Polytechnic Institute, Holden, MA   | 129         |
| THERMAL CHARACTERISTICS OF DEEP RESERVOIRS IN PUMPED STORAGE PLANTS<br>J.J. Shin, N.S. Shashidhara, Envirosphere Company, New York, NY   | 139         |
| ALGORITHMS FOR A MATHEMATICAL MODEL TO PREDICT ENVIRONMENTAL EFFECTS FROM THERMAL DISCHARGES IN RIVERS AND IN COASTAL AND OFFSHORE REGIONS<br>J. Häuser, Institut für Physik, Germany<br>F. Tanzer, Universität Giessen, Germany | 150         |
| EFFECT OF SALT UPON HOT-WATER DISPERSION IN WELL-MIXED ESTUARIES - PART 2 - LATERAL DISPERSION<br>R. Smith, University of Cambridge, United Kingdom  | 161         |
| <br>MATHEMATICAL MODELING II   |             |
| COST-EFFECTIVE MATHEMATICAL MODELING FOR THE ASSESSMENT OF HYDRODYNAMIC AND THERMAL IMPACT OF POWER PLANT OPERATIONS ON CONTROLLED-FLOW RESERVOIRS<br>A.H. Eraslan, K.H. Kim, University of Tennessee, Knoxville, TN             | 179         |
| HEAT LOAD IMPACTS ON DISSOLVED OXYGEN: A CASE STUDY IN STREAM MODELING<br>A.K. Deb, D.F. Lakatos, Roy F. Weston, Inc., West Chester, PA  | 187         |

|  | <u>Page</u> |
|--|-------------|
| A STOCHASTIC METHOD FOR PREDICTING THE DISPERSION OF THERMAL EFFLUENTS IN THE ENVIRONMENT<br>A.J. Witten, Oak Ridge National Laboratory, Oak Ridge, TN<br>J.E. Molyneux, University of Rochester, Rochester, NY  | 199         |
| A TWO-DIMENSIONAL NUMERICAL MODEL FOR SHALLOW COOLING PONDS<br>S. Chieh, A. Verma, Envirosphere Company, New York, NY  | 214         |
| UTILIZATION II   |             |
| WASTE HEAT FOR ROOT-ZONE HEATING - A PHYSICAL STUDY OF HEAT AND MOISTURE TRANSFER<br>D. Elwell, W. Roller, A. Ahmed, Ohio Agricultural Research and Development Center, Wooster, OH  | 225         |
| BENEFICIAL USE OF REJECTED HEAT IN MUNICIPAL WATER SUPPLIES<br>R.W. Porter, R.A. Wynn, Jr., Illinois Institute of Technology Chicago, IL   | 236         |
| SUPER GREENHOUSE PROJECT UTILIZING WASTE HEAT FROM ASTORIA 6 THERMAL POWER PLANT<br>R.G. Reines, Cornell University, Ithaca, NY  | 246         |
| EXPERIENCE WITH THE NEW MERCER PROOF-OF-CONCEPT WASTE HEAT AQUACULTURE FACILITY<br>B.L. Godfriaux, Public Service Electric and Gas Company, Newark, NJ. R.R. Shafer, Buchart-Horn: Consulting Engineers, York, PA. A.F. Eble, M.C. Evans, T. Passanza, C. Wainwright, H.L. Swindell, Trenton State College, Trenton, NJ. | 247         |
| UTILIZATION III  |             |
| WASTE HEAT RECOVERY IN THE FOOD PROCESSING INDUSTRY<br>W.L. Lundberg, J.A. Christenson, Westinghouse Electric Corporation, Pittsburgh, PA. F. Wojnar, H.J. Heinz Company, Pittsburgh, PA.  | 266         |
| GENERATION OF CHILLED WATER FROM CHEMICAL PROCESS WASTE HEAT<br>J. Entwistle, Fiber Industries, Inc., Charlotte, NC  | 277         |
| THE SHERCO GREENHOUSE PROJECT: FROM DEMONSTRATION TO COMMERCIAL USE OF CONDENSER WASTE HEAT<br>G.C. Ashley, J.S. Hietala, R.V. Stansfield, Northern States Power Company, Minneapolis, MN  | 286         |
| ANALYSIS OF ECONOMIC AND BIOLOGICAL FACTORS OF WASTE HEAT AQUACULTURE<br>J.S. Suffern, M. Olszewski, Oak Ridge National Laboratory, Oak Ridge, TN  | 296         |

|   | <u>Page</u> |
|---|-------------|
| ECOLOGICAL EFFECTS I  |             |
| A QUALITATIVE/QUANTITATIVE PROCEDURE FOR ASSESSING THE<br>BIOLOGICAL EFFECTS OF WASTE HEAT ON ECONOMICALLY IMPORTANT<br>POPULATIONS<br>J.M. Thomas, Battelle Pacific Northwest Laboratories,<br>Richland, WA  | 319         |
| A REVIEW OF STATISTICAL ANALYSIS METHODS FOR BENTHIC DATA<br>FROM MONITORING PROGRAMS AT NUCLEAR POWER PLANTS<br>D.H. McKenzie, Battelle Pacific Northwest Laboratories<br>Richland, WA   | 329         |
| FURTHER STUDIES IN SYSTEMS ANALYSIS OF COOLING LAKES:<br>HYDRODYNAMICS AND ENTRAINMENT<br>K.D. Robinson, R.J. Schafish, R.W. Beck and Associates,<br>Denver, CO. G. Comogis, New England Research, Inc.,<br>Worcester, MA.                                      | 344         |
| SYNTHESIS AND ANALYSES OF EXISTING COOLING IMPOUNDMENT<br>INFORMATION ON FISH POPULATIONS<br>K.L. Gore, D.H. McKenzie, Battelle Pacific Northwest<br>Laboratories, Richland, WA   | 353         |
| COOLING TOWER PLUMES  |             |
| A SIMPLE METHOD FOR PREDICTING PLUME BEHAVIOR FROM MULTIPLE<br>SOURCES<br>L.D. Winiarski, W.E. Frick, U.S. Environmental Protection<br>Agency, Corvallis, OR  | 367         |
| MODELING NEAR-FIELD BEHAVIOR OF PLUMES FROM MECHANICAL DRAFT<br>COOLING TOWERS<br>T.L. Crawford, Tennessee Valley Authority, Muscle Shoals, AL<br>P.R. Slawson, University of Waterloo, Ontario, Canada   | 377         |
| MECHANICAL-DRAFT COOLING TOWER PLUME BEHAVIOR AT THE GASTON<br>STEAM PLANT<br>P.R. Slawson, University of Waterloo, Ontario, Canada   | 388         |
| CRITICAL REVIEW OF THIRTEEN MODELS FOR PLUME DISPERSION<br>FROM NATURAL DRAFT COOLING TOWERS<br>R.A. Carhart, University of Illinois, Chicago, IL<br>A.J. Policastro, Argonne National Laboratory, Argonne, IL<br>W.E. Dunn, University of Illinois, Urbana, IL | 402         |
| EVALUATION OF METHODS FOR PREDICTING PLUME RISE FROM<br>MECHANICAL-DRAFT COOLING TOWERS<br>W.E. Dunn, P. Gavin, University of Illinois, Urbana, IL<br>G.K. Cooper, Mississippi State University, Mississippi  | 449         |

|   | <u>Page</u> |
|---|-------------|
| ECOLOGICAL EFFECTS II   |             |
| ENVIRONMENTAL COST OF POWER PLANT WASTE HEAT AND<br>CHEMICAL DISCHARGE IN TROPICAL MARINE WATERS<br>J.M. Lopez, Center for Energy and Environment Research<br>Mayaguez, Puerto Rico   | 461         |
| THEORY AND APPLICATION IN A BIOLOGICAL ASPECT<br>T. Kuroki, Tokyo University of Fisheries, Tokyo, Japan   | 468         |
| OCCURRENCE OF HIGHLY PATHOGENIC AMOEBAE IN THERMAL<br>DISCHARGES<br>J.F. De Jonckheere, Laboratorium voor Hygiene,<br>Katholieke Universiteit Leuven, Belgium   | 479         |
| RELATION BETWEEN ZOOPLANKTON MIGRATION AND ENTRAINMENT<br>IN A SOUTH CAROLINA COOLING RESERVOIR<br>P.L. Hudson, S.J. Nichols, U.S. Fish and Wildlife Service<br>Southeast Reservoir Investigations, Clemson, SC   | 490         |
| EFFECTS OF A HOT WATER EFFLUENT ON POPULATIONS OF<br>MARINE BORING CLAMS IN BARNEGAT BAY, NJ<br>K.E. Hoagland, Lehigh University, Bethlehem, PA<br>R.D. Turner, Harvard University, Cambridge, MA   | 505         |
| COOLING TOWERS I  |             |
| COLD INFLOW AND ITS IMPLICATIONS FOR DRY TOWER DESIGN<br>F.K. Moore, Cornell University, Ithaca, NY   | 516         |
| AN IMPROVED METHOD FOR EVAPORATIVE, CROSS-FLOW COOLING<br>TOWER PERFORMANCE ANALYSIS<br>K.L. Baker, T.E. Eaton, University of Kentucky, Lexington, KY   | 532         |
| THE IMPACT OF RECIRCULATION ON THE SITING, DESIGN,<br>SPECIFICATION, AND TESTING OF MECHANICAL DRAFT COOLING<br>TOWERS<br>K.R. Wilber, Environmental Systems Corporation<br>A. Johnson, Pacific Gas & Electric Co.<br>E. Champion, Consultant   | 535         |
| AN INVESTIGATION INTO THE MINERAL CONCENTRATION OF<br>INDIVIDUAL DRIFT DROPLETS FROM A SALTWATER COOLING TOWER<br>R.O. Webb, Environmental Systems Corporation, Knoxville, TN.<br>R.S. Nietubicz, State of Maryland, Department of Natural<br>Resources. J.W. Nelson, Florida State University, Tallahassee, FL | 547         |
| COGENERATION  |             |
| COGENERATION TECHNOLOGY AND OUR TRANSITION FROM<br>CONVENTIONAL FUELS<br>J.W. Neal, Department of Energy, Washington, DC  | 548         |

|   | <u>Page</u> |
|---|-------------|
| COGENERATION: THE POTENTIAL AND THE REALITY IN A<br>MIDWESTERN UTILITY SERVICE AREA<br>D.M. Stipanuk, Cornell University, Ithaca, NY<br>W.J. Hellen, Wisconsin Electric Power, Milwaukee, WI                                  | 558         |
| ALTERNATIVE APPROACHES IN INDUSTRIAL COGENERATION SYSTEMS<br>J.C. Solt, Solar Turbines International, San Diego, CA   | 572         |
| THE ENVIRONMENT FOR COGENERATION IN THE UNITED STATES<br>F.E. Dul, Envirosphere Company, New York, NY   | 582         |
| FUEL COST ALLOCATION FOR THE STEAM IN A COGENERATION<br>PLANT<br>K.W. Li, and P.P. Yang, North Dakota State University,<br>Fargo, ND  | 595         |
| <br>COOLING SYSTEMS   |             |
| APPLICATIONS OF MATHEMATICAL SPRAY COOLING MODEL<br>H.A. Frediani, Jr., Envirosphere Company, New York, NY  | 619         |
| THE DEVELOPMENT OF ORIENTED SPRAY COOLING SYSTEMS<br>D.A. Fender, Ecolaire Condenser, Inc. Bethlehem, PA<br>T.N. Chen, Ingersoll-Rand Research, Inc., Princeton, NJ   | 638         |
| ONCE-THROUGH COOLING POTENTIAL OF THE MISSOURI RIVER IN<br>THE STATE OF MISSOURI<br>A.R. Giaquinta, The University of Iowa, Iowa City, IA<br>T.C. Keng, Jenkins-Fleming, Inc., St. Louis, MO                                  | 651         |
| A MODEL FOR PREDICTION OF EVAPORATIVE HEAT FLUX IN LARGE<br>BODIES OF WATER<br>A.M. Mitry, Duke Power Company, Charlotte, NC<br>B.L. Sill, Clemson University, Clemson, NC  | 663         |
| <br>WORKING SESSIONS - WORKSHOPS  |             |
| (1) MANAGEMENT AND UTILIZATION  | 677         |
| (2) ENVIRONMENTAL EFFECTS   | 681         |
| (3) MATHEMATICAL MODELING   | 682         |
| (4) HEAT TRANSFER PROBLEMS IN WASTE HEAT MANAGEMENT AND<br>UTILIZATION  | 684         |
| <br>COOLING TOWERS II   |             |
| THE CHALK POINT DYE TRACER STUDY: VALIDATION OF MODELS AND<br>ANALYSIS OF FIELD DATA<br>A.J. Poliscastro, M. Breig, J. Ziebarth, Argonne National<br>Laboratory, Argonne, IL<br>W.E. Dunn, University of Illinois, Urbana, IL | 686         |

|  | <u>Page</u> |
|--|-------------|
| COOLING TOWERS AND THE LICENSING OF NUCLEAR POWER PLANTS<br>J.E. Carson, Argonne National Laboratory, Argonne, IL  | 720         |
| A DESIGN METHOD FOR DRY COOLING TOWERS<br>G.K.M. Vangala, T.E. Eaton, University of Kentucky,<br>Lexington, KY   | 732         |
| EVAPORATIVE HEAT REMOVAL IN WET COOLING TOWERS<br>T.E. Eaton, K.L. Baker, University of Kentucky,<br>Lexington, KY   | 742         |
| COMPARATIVE COST STUDY OF VARIOUS WET/DRY COOLING CONCEPTS<br>THAT USE AMMONIA AS THE INTERMEDIATE HEAT EXCHANGE FLUID<br>B.M. Johnson, R.D. Tokarz, D.J. Braun, R.T. Allemann,<br>Battelle Pacific Northwest Laboratory, Richland, WA | 772         |
| <br>UTILIZATION IV   |             |
| ENVIRONMENTAL ASPECTS OF EFFECTIVE ENERGY UTILIZATION<br>IN INDUSTRY<br>R.E. Mournighan, U.S. EPA, Cincinnati, OH<br>W.G. Heim, EEA, Inc., Arlington, VA   | 805         |
| WASTE HEAT RECOVERY POTENTIAL FOR ENVIRONMENTAL BENEFIT<br>IN SELECTED INDUSTRIES<br>S.R. Latour, DDS Engineers, Inc., Fort Lauderdale, FL<br>C.C. Lee, EPA, Cincinnati, OH  | 817         |
| WASTE HEAT UTILIZATION AND THE ENVIRONMENT<br>M.E. Gunn, Jr., Department of Energy, Washington, DC   | 830         |
| THERMAL STORAGE FOR INDUSTRIAL PROCESS AND REJECT HEAT<br>R.A. Duscha, W.J. Masica, NASA Lewis Research Center,<br>Cleveland, OH   | 855         |
| PERFORMANCE AND ECONOMICS OF STEAM POWER SYSTEMS<br>UTILIZING WASTE HEAT<br>J. Davis, Thermo Electron Corporation, Waltham, MA   | 866         |
| <br>COOLING LAKES  |             |
| A ONE-DIMENSIONAL VARIABLE CROSS-SECTION MODEL FOR THE<br>SEASONAL THERMOCLINE<br>S. Sengupta, S.S.Lee, E. Nwadike, University of Miami,<br>Coral Gables, FL   | 878         |
| HYDROTHERMAL STRUCTURE OF COOLING IMPOUNDMENTS<br>G.H. Jirka, Cornell University, Ithaca, NY   | 908         |
| HYDROTHERMAL PERFORMANCE OF SHALLOW COOLING PONDS<br>E.E. Adams, G.H. Jirka, A. Koussis, D.R.F. Harleman,<br>M. Watanabe, M.I.T., Cambridge, MA  | 909         |

|   | <u>Page</u> |
|---|-------------|
| TRANSIENT SIMULATION OF COOLING LAKE PERFORMANCE UNDER<br>HEAT LOADING FROM THE NORTH ANNA POWER STATION<br>D.R.F. Harleman, G.H. Jirka, D.N. Brocard, K.H. Octavio,<br>M. Watanabe, M.I.T., Cambridge, MA  | 919         |
| <br>RECOVERY SYSTEMS  |             |
| COMPARISON OF THE SURFACE AREA REQUIREMENTS OF A SURFACE<br>TYPE CONDENSER FOR A PURE STEAM CYCLE SYSTEM, A COMBINED<br>CYCLE SYSTEM AND A DUAL FLUID CYCLE SYSTEM<br>M.H. Waters, International Power Technology<br>E.R.G. Eckert, University of Minnesota | 931         |
| UTILIZATION OF TRANSFORMER WASTE HEAT<br>D.P. Hartmann, Department of Energy, Portland, OR<br>H. Hopkinson, Carrier Corporation, Syracuse, NY   | 960         |
| THE APPLICATION OF PRESSURE STAGED HEAT EXCHANGERS TO<br>THE GENERATION OF STEAM IN WASTE HEAT RECOVERY SYSTEMS<br>M.H. Waters, D.Y. Cheng, International Power Technology  | 980         |
| HEAT RECOVERY FROM WASTE FUEL<br>Y.H. Kiang, Trane Thermal Company, Conshohocke, PA   | 1000        |
| <br>AQUATIC THERMAL DISCHARGES I  |             |
| SURFACE SKIN-TEMPERATURE GRADIENTS IN COOLING LAKES<br>S.S. Lee, S. Sengupta, C.R. Lee, University of Miami,<br>Coral Gables, FL  | 1011        |
| FOUR THERMAL PLUME MONITORING TECHNIQUES: A COMPARATIVE<br>ASSESSMENT<br>R.S. Grove, Southern California Edison Company, Rosemead, CA<br>R.W. Pitman, J.E. Robertson, Brown and Caldwell, Pasadena, CA  | 1027        |
| EXPERIMENTAL RESULTS OF DESTRATIFICATION BY BUOYANT PLUMES<br>D.S. Graham, University of Florida, Gainesville, FL   | 1028        |
| THREE-DIMENSIONAL FIELD SURVEYS OF THERMAL PLUMES FROM<br>BACKWASHING OPERATIONS AT A COASTAL POWER PLANT SITE IN<br>MASSACHUSETTS<br>A.D. Hartwell, Normandeau Associates, Inc., Bedford, NH<br>F.J. Mogolesko, Boston Edison Company                      | 1047        |
| SHORT-TERM DYE DIFFUSION STUDIES IN NEARSHORE WATERS<br>D.E. Frye, EG&G, Environmental Consultants, Waltham, MA<br>S.M. Zivi, Argonne National Laboratory, Argonne, IL  | 1057        |
| EFFECTS OF BOTTOM SLOPE, FROUDE NUMBER, AND REYNOLDS<br>NUMBER VARIATION ON VIRTUAL ORIGINS OF SURFACE JETS:<br>A NUMERICAL INVESTIGATION<br>J. Venkata, S. Sengupta, S.S.Lee, University of Miami<br>Coral Gables, FL                                      | 1069        |

|   | <u>Page</u> |
|---|-------------|
| ATMOSPHERIC EFFECTS   |             |
| METEOROLOGICAL EFFECTS FROM LARGE COOLING LAKES<br>F.A. Huff, J.L. Vogel, Illinois State Water Survey, IL   | 1095        |
| COMPUTER SIMULATION OF MESO-SCALE METEOROLOGICAL EFFECTS<br>OF ALTERNATIVE WASTE-HEAT DISPOSAL METHODS<br>J.P. Pandolfo, C.A. Jacobs, The Center for the Environment<br>and Man, Inc., Hartford, CT   | 1104        |
| A NUMERICAL SIMULATION OF WASTE HEAT EFFECTS ON<br>SEVERE STORMS<br>H.D. Orville, P.A. Eckhoff, South Dakota School of Mines<br>and Technology, Rapid City, SD  | 1114        |
| ON THE PREDICTION OF LOCAL EFFECTS OF PROPOSED COOLING<br>PONDS<br>B.B. Hicks, Argonne National Laboratory, Argonne, IL   | 1124        |
| AQUATIC THERMAL DISCHARGES II   |             |
| MEASUREMENT AND EVALUATION OF THERMAL EFFECTS IN THE INTER-<br>MIXING ZONE AT LOW POWER NUCLEAR STATION OUTFALL<br>P.R. Kamath, R.P. Gurg, I.S. Bhat, P.V. Vyas, Environmental<br>Studies Section, Bhabha Atomic Research Centre, Bombay, India | 1131        |
| RIVER THERMAL STANDARDS EFFECTS ON COOLING-RELATED POWER<br>PRODUCTION COSTS<br>T.E. Croley II, A.R. Giaquinta, M.P. Cherian, R.A. Woodhouse,<br>The University of Iowa, Iowa City, IA  | 1146        |
| THERMAL PLUME MAPPING<br>J.R. Jackson, A.P. Verma, Envirosphere Company, New York, NY   | 1160        |
| THERMAL SURVEYS NEW HAVEN HARBOR - SUMMER AND FALL, 1976<br>W. Owen, J.D. Monk, Normandeau Associates, Nashua, NH   | 1167        |
| BEHAVIOR OF THE THERMAL SKIN OF COOLING POND WATERS<br>SUBJECTED TO MODERATE WIND SPEEDS<br>M.L. Wesely, Argonne National Laboratory, Argonne, IL   | 1191        |
| OPEN SESSION  |             |
| ALTERNATE ENERGY CONSERVATION APPLICATIONS FOR INDUSTRY<br>L.J. Schmerzler  | 1201        |
| MINERAL CYCLING MODEL OF THE <u>THALASSIA</u> COMMUNITY AS<br>AFFECTED BY THERMAL EFFLUENTS<br>P.B. Schroeder, A. Thorhaug, Florida International University<br>Miami, FL   | 1202        |

|  | <u>Page</u> |
|--|-------------|
| SYNERGISTIC EFFECTS OF SUBSTANCES EMITTED FROM POWER PLANTS ON SUBTROPICAL AND TROPICAL POPULATIONS OF THE SEAGRASS <u>THALASSIA TESTUDINUM</u> : TEMPERATURE, SALINITY AND HEAVY METALS | 1221        |
| A. Thorhaug, P.B. Schroeder, Florida International University, Miami, FL   |             |
| WASTE HEAT MANAGEMENT AND UTILIZATION: SOME REGULATORY CONSTRAINTS   | 1240        |
| W.A. Anderson II, P.O. Box 1535, Richmond, VA  |             |

## APPLICATIONS OF MATHEMATICAL SPRAY COOLING MODEL

H A Frediani Jr, Senior Engineer  
Envirosphere Company  
A Division of Ebasco Services Incorporated  
New York, New York USA

### ABSTRACT

A mathematical model to analyze the performance of large-scale spray cooling systems [1], has been applied to several different types of spray systems. This model is unique in that the basic heat and mass transfer mechanisms are modelled accurately over a wide range of parameter values that cooling systems encounter.

The model was first used to verify which vendors' systems would be expected to meet the design conditions and then to predict which vendors' performance curves were accurate. The model showed some sensitivity to wind direction, and to dry bulb temperature, which the manufacturers had assumed negligible.

Another application of this model has been to develop an optimum (economical) configuration of a spray system that met the design operating condition. To complete the economic optimization, average operating cold water temperatures and required spray motor horsepower were calculated and used to predict capability penalties.

A third application of this model was to design a fixed spray pond and predict its performance under the most severe operating conditions. Parameters optimized included nozzle separation, nozzle flow rate, and spray height. Performance was predicted, including evaporation rate and the effects of increasing solids concentrations during extended periods of operation without makeup.

Qualitative conclusions have also been drawn from the results of these applications concerning fogging and drift associated with closed loop spray systems. Further development of this model could lead to quantitative predictions in this regard.

### INTRODUCTION

Spray cooling systems have been utilized to dissipate heat rejected by electric generating stations. The cooling water includes both condensing water for the main turbine steam and cooling water for auxiliary and/or emergency heat exchangers. The spray systems include arrays of either fixed or floating nozzles. The traditional method of designing a spray

system has been to interpolate or extrapolate predicted performance from previously recorded data. Recently, a mathematical model was developed to predict performance from the physical characteristics of the given spray system and the basic principles of heat and mass transfer. The model has since been utilized in various applications and some of the results are described herein.

## MODEL DESCRIPTION

The model has been described in detail in the literature. Briefly, the continuity and energy equations were developed for a cellular model representing a single spray in a system of sprays. The equations were solved using a finite difference solution along a drop trajectory, for both water and air parameters. The results of the cellular analysis are incorporated into a system model in which the interaction between sprays for both the water and air is considered.

The model incorporates the following features:

1. A finite mass flow rate of air, as well as of water is calculated.
2. The amount of heat transferred from the water is added to the air.
3. The amount of mass transferred from the water is added to the air.
4. The air temperature, enthalpy, moisture content and density are calculated to reflect the heat and mass transferred to the air.
5. Physical parameters such as cooling water salinity, spray height, pattern, and droplet sizes, air dry bulb, and wind direction are specifically entered as data and incorporated in the basic equations.

## APPLICATIONS

### Proposal Evaluation

The first application of the model was to independently check the credibility of various proposed spray systems being considered for a proposed coal-fired plant. The design was a closed cycle, salt water cooling system. At that time, no successful closed cycle systems had been documented. Each manufacturer predicted system performance using empirical spray performance correlations, a method that is basically an extension of the "number-of-transfer-units" (NTU) concept, as applied to cooling towers [2]. An independent check was deemed necessary because of the following reasons:

1. Closed cycle systems typically operate at higher water temperatures than open cycle systems. Thus, the operating water temperatures of the proposed system would be outside the range of data available to any manufacturer.
2. The basic premise of the NTU concept that the amount of cooling is solely dependent on the wet bulb and wind speed is an approximation.

In actuality, the percentage of heat transfer in spray cooling which is sensible (i.e. non-evaporative) will approximate twenty percent when the air dry bulb temperature is significantly below the cooled water temperature.

3. The increase in enthalpy, through increased temperature and moisture content, of the air as it flows past a spray was not predicted rationally. Thus, for a large system of sprays, most of which are downwind from other sprays, the major ambient input to the performance correlation was estimated without benefit of either data or theoretical considerations.

Each manufacturer proposed a U-shaped spray canal containing an array of floating sprays (Figure 1). In this configuration, the hottest water is sprayed immediately upwind of the coolest water. Thus the air which has undergone the largest enthalpy increase will then pass the sprays with the lowest incoming water temperature. This is where the greatest potential exists for the incoming air dry bulb temperature to exceed the incoming water temperature for a particular spray. Under this condition, the sensible heat transfer is actually reversed and total cooling reduced. Under extreme conditions of very large systems, the incoming air wet bulb temperature can approach the cold water temperature closely enough that all heat transfer is stopped.

Each manufacturer had submitted performance curves plotting system cold water temperatures versus ambient wet bulb temperatures for several different wind speeds. The design condition was at an 81 degree wet bulb and a 5 mph wind speed, perpendicular to the canal axis. Runs were made at the design conditions for each proposed system. The results indicated that one manufacturer's system was slightly conservative (i.e. the desired cold water temperature would be achieved before the last pass of sprays). A second proposed system was estimated to be approximately 30 percent deficient. At this point, the first manufacturer's system was selected and examined further.

The next step was to synthesize the entire performance curve for the selected system. At each given point, the ambient wet bulb and the desired cooling range were known, but the equilibrium hot and cold water temperatures were unknown. Using the model to determine the latter, for a U-shaped canal, would have been a trial and error process. A hot water temperature would be assumed, the model run, and the cooling range obtained. Such a technique would have required a great deal of computer time and an alternative method was derived.

It was hypothesized that, as a heat dissipation system, the straight canal shown in Figure 2 would perform identically with the U-shaped canal shown in Figure 1. There are the same number of sprays, in the same locations. There are the same water flow rate in and air flow rate across. This hypothesis was tested, using the model, at various wet bulbs, hot water temperatures, and spray configurations. Close agreement was predicted, as can be seen in the typical case presented as Figure 3. The difference

in predicted cold water temperature, over a cooling range of 12.1 degrees F, was only .26 degrees, approximately two percent.

Utilizing a straight canal, only one computer run is required for each data point. The model is run for a longer canal than the one desired, for an initial hot water temperature known to exceed the desired result. An example run is illustrated in Table 1, in which the design number of spray passes is 19 and the total number of passes run is 30. From the Table, a plot of cooling range vs cold water temperature can be constructed, from which the cold water temperature corresponding to the desired cooling range can be estimated. Such a plot for this example is shown in Figure 4. In this example, the desired range of 16.6 degrees F, with a corresponding cold water temperature of 64.3 degrees F, represented a power plant operating at 80 percent of load capacity. The same plot can be used in synthesizing performance curves at other desired plant load capacities by simply varying the cooling range.

The performance curves were synthesized from the model runs for two different wind directions, parallel and perpendicular to the spray canal axis. The manufacturer had not specified any relative humidity for its performance curve. Comparative runs were made, at a given wet bulb, for relative humidities of 20%, 60%, and 100%. It was found that, as relative humidity was increased (i.e. air dry bulb temperature was decreased), the equilibrium cold water temperature decreased. This improvement in heat transfer is attributable to improved sensible heat transfer. For comparison, 60 percent relative humidity was used.

The curves for the parallel wind case were virtually identical over the full range of wet bulb examined. In the perpendicular wind case, the model predicted better performance. The improvement ranged from about 4 degrees F cooler equilibrium temperature at a 40 degree wet bulb, to about 2 degrees F at an 80 degree wet bulb, for 100 percent load. Since the manufacturer had guaranteed its performance curves for any wind direction, it was concluded that the model had verified those performance curves.

#### Alternative Cooling System Studies

The model has been utilized several times to provide input to alternative cooling system studies. This input is normally generated in two stages. The first stage involves sizing a system to meet a given design point, in order to estimate the system installation cost. The second stage is to predict the system operation in order to estimate annual operating costs. The total cost can then be estimated and compared to other types of alternatives.

For a typical new power plant, the floating type of spray device has a decided economic advantage over the fixed type, because of the large size of such a system. There are two opposing economic factors in optimizing a floating spray cooling system. Minimizing the number of spray devices requires minimizing the number of sprays arrayed across the canal.

However, this would maximize the length of the canal, and thus the costs for canal excavation, diking, and auxiliaries such as wiring for the spray motors. An example of these effects is given in Table 2, in which two systems with identical performance at a design point are described. Case 1 has approximately 74 percent of the number of sprays required in Case 2. However, the Case 1 canal is about twice as long. The economic optimum depends both on the spray device cost and the canal construction cost. Results from numerous model runs indicate that a width of 10 floating sprays (or 5 on each side of a U-shaped canal) is about the practical limit. The expense of additional sprays across the canal cannot be justified by the small increase in performance.

Once the particular system is sized, operating cold water temperatures are predicted. The gross output power from a generating station, at a given load factor, is a direct function of the condenser inlet temperature. A representative curve of this function is shown as gross power output in Figure 5. As the cold water temperature is increased, gross power out is decreased. For a particular spray system, at a given set of ambient meteorological conditions, the cold water temperature is a function of the number of sprays operating. By operating less than the full number of sprays, the power consumed by the spray pump motors can be reduced. Table 3 summarizes this effect for a spray system designed for the turbine generator of Figure 5. The net power output (gross power putput minus spray motor power consumption) is plotted on Figure 5. The optimum operating point for this system, at this particular meteorological condition, is with 79 percent of the sprays operating. This optimization increases plant output approximately 700 kilowatts over running 100 percent of the spray system.

In the preceding manner, monthly or seasonal average net power generation is predicted for the given spray system. The capitalized cost of the differential power outputs from each alternative are added to the estimated installation costs to obtain the total costs for comparisons.

### Fixed Spray Applications

The same model has also been utilized to evaluate fixed spray ponds. These traditionally employ smaller nozzles and are used for smaller flow rates. One example is the design of a reactor coolant spray cooling system for a nuclear power plant. This system was to function under both normal and emergency shutdown conditions. Thus two independent sets of design criteria had to be met by the same design.

Fixed spray design requires pumping the heated water through a distribution system of pipes to the spray nozzles. The total system flow is sprayed and collected. Should the cooling be insufficient, a second stage of sprays can respray the collected water. Manufacturers typically recommend one nozzle pressure and flow rate for a given nozzle. To size a system, the total flow rate is divided by the nozzle flow rate giving the number of nozzles required. These nozzles are then arranged in a rectangular array. For the example mentioned above, this process indicated

that two stages of sprays would be required to meet the desired design conditions.

Utilizing the model, an alternative design was considered. By increasing the pressure to the nozzles, the flow rate and spray height per nozzle can be increased. This requires fewer nozzles spaced further apart. However, the spray performance is improved for two reasons. Firstly, the water drops experience a higher velocity and travel time through the air. Secondly, the ratio of water to air mass flow is decreased. An example for a commonly used nozzle (approximate orifice diameter of 1.5 inches) is given in Table 4. In this example, a wind speed of 10 feet per second and a total cooling water flow rate of 30,000 gpm were used. By increasing the nozzle pressure from 7 to 15 psi, the spray height was increased by 40 percent, and the spray pattern diameter was increased by 23 percent. This resulted in sufficient improvement in cooling range so that one stage of sprays were adequate when two stages were required for the conventional layout.

Under shutdown conditions, this spray pond must operate without makeup for an extended period of time. This results in an increasing dissolved solids content and a decreasing total volume of cooling water in the system, both because of system evaporation without replacement water. The increased solids content decreases the water's ability to carry heat. This causes the cooling range and hot water temperatures to increase, without significant change to the cold water temperatures. The reduced water volume in the system causes lowering of the water level in the spray pond collection area, from which the circulating pumps draw suction. This increases the static head on the pumps, resulting in a reduced pumping rate and nozzle pressure. This in turn increases both the hot and cold water temperatures of the operating spray pond. Finally, the heat load of the system varies with time during this mode of operation.

The model is run, at the design meteorological conditions and the initial heat load to predict the evaporation rate. The change in solids content and water volume is calculated from this evaporation rate. A new pumping rate and cooling range are selected to provide the model input for the second heat load. This process is repeated for all the heat rates until plots of hot and cold water temperature, and solids content, versus time, are produced. The operating temperatures are then checked to insure satisfactory equipment operation. The solids content is used to estimate scaling tendencies. If necessary, spray system design is altered and the process repeated.

One item of interest in Table 4 is the predicted ratio of water to air mass flow in each system. All other spray models assume this quantity to be zero, i.e. that the air supply is infinite. Thus they are unable to quantitatively estimate performance for any spray system without a vast array of operating data. They are also unable to predict differential performance resulting from modification of a spray system. It should be noted that the ratios in Table 4 are for a fixed spray nozzle and that, for the floating nozzles available, higher ratios are typical.

## FUTURE APPLICATIONS

Two of the environmental impacts associated with evaporative cooling systems are fogging and drift. Examination of the psychrometric conditions the model predicts for the air leaving a spray canal leads to certain qualitative conclusions. With respect to fogging, it has previously been assumed that because a spray system discharges air over a relatively large area, in comparison with a comparable cooling tower, that the potential for fogging is much less for the spray system. Model predictions indicate that the air leaving spray canals is not as close to saturation as that from cooling towers. Thus, the previous assumption would appear to be correct. Since the air flow rate, temperature, and moisture content are all predicted, it should not be too difficult to construct a quantitative fogging prediction model in the future.

Intuitive assumptions with drift have not been so accurate. As recently as 1974, the lack of experience with closed-loop, salt water spray systems precluded the availability of any useful drift data. Impact analyses typically were based on limited data from a few sprays operating under insignificant heat load. It was predicted that all drift, from one proposed installation, would deposit within 600 feet of the spray canal [2].

In a large spray system the heat transfer causes an increase in moisture content and temperature in the air passing through the sprays. Thus the air leaving the system has an upward velocity component due to its relative buoyancy with respect to the ambient air. The resultant path of water droplets entrained in the air as drift is thus a parabolic arch (Figure 6). The path of a drift particle from a spray without heat load is a straight line (Figure 6). Thus the mechanism is different and predictions of one based on the other are invalid. The distance of 3400 feet for the heat load case in Figure 6 was reported for an actual system of the same type sprays which, without heat load, drifted within 600 feet [3].

As in the case of fogging, it should not be too difficult to predict, from the model output, the magnitude and direction of the air velocity leaving a spray canal. From this, a model could be constructed to predict drift deposition. It should be kept in mind that the system which attained drift deposition at 3400 feet is a relatively small system, and that greater ranges could be attained in the future.

## CONCLUSIONS

A mathematical spray cooling model has been used for a variety of applications, some of which are described herein. It was found that the model gives reasonable quantitative performance estimates over a wide range of configurations and operating regimes for both fixed and floating spray canals.

## REFERENCES

1. "Mathematical Model for Spray Cooling Systems", H A Frediani, Jr, and N Smith, Trans. ASME Journal of Engineering for Power, April 1977, pp 279-283.
2. Draft Environmental Statement for Surry Power Station, Units 3 & 4, USAEC, February, 1974, pp 3-11 through 3-15.
3. "Measured and Predicted Salt Deposition Rates, Closed Cycle Water Cooling Duty", PSM-SD-6A, Ceramic Cooling Tower Company, 1977.

TABLE 1  
PERFORMANCE CURVE GENERATION

Input Data

Desired Canal Length - 19 Passes  
Wind - Perpendicular to Canal Axis at 19 FPS  
C W Flow - 711348 GPM  
Flow Per Spray - 10000 GPM  
Inlet Water Temperature - 89.61 Deg F  
Ambient Dry Bulb - 47 Deg F  
Ambient Wet Bulb - 40 Deg F  
Initial Drop Diameter - .0165 ft  
Initial Salinity - 0.5 ppt  
Spray Height - 17 ft  
Spray Width - 160 ft  
Straight Canal of 30 Passes with 10 Sprays per Pass  
Desired Cooling Range - 16.6 Deg F

TABLE 1 (Cont'd)

## Output Data

| <u>Pass<br/>Number</u> | <u>Flow<br/>(gpm)</u> | <u>Temperature<br/>(deg F)</u> | <u>Pass<br/>Number</u> | <u>Flow<br/>(gpm)</u> | <u>Temperature<br/>(deg F)</u> |
|------------------------|-----------------------|--------------------------------|------------------------|-----------------------|--------------------------------|
| 1                      | 710528                | 88.0                           | 16                     | 702000                | 70.7                           |
| 2                      | 709751                | 86.5                           | 17                     | 701607                | 69.9                           |
| 3                      | 709011                | 85.0                           | 18                     | 701227                | 69.1                           |
| 4                      | 708307                | 83.6                           | 19                     | 700861                | 68.3                           |
| 5                      | 707634                | 82.2                           | 20                     | 700507                | 67.6                           |
| 6                      | 706993                | 80.9                           | 21                     | 700165                | 66.9                           |
| 7                      | 706393                | 79.7                           | 22                     | 699843                | 66.2                           |
| 8                      | 705818                | 78.5                           | 23                     | 699530                | 65.6                           |
| 9                      | 705267                | 77.4                           | 24                     | 699226                | 64.9                           |
| 10                     | 704739                | 76.3                           | 25                     | 698933                | 64.3                           |
| 11                     | 704232                | 75.3                           | 26                     | 698648                | 63.7                           |
| 12                     | 703746                | 74.3                           | 27                     | 698378                | 63.2                           |
| 13                     | 703278                | 73.3                           | 28                     | 698116                | 62.6                           |
| 14                     | 702829                | 72.4                           | 29                     | 697861                | 62.1                           |
| 15                     | 702407                | 71.5                           | 30                     | 697613                | 61.6                           |

TABLE 2

| <u>Case</u> | <u>Number of Sprays<br/>Across Canal</u> | <u>Number of Sprays<br/>Required</u> | <u>Canal Length<br/>(Number of Spray Lengths)</u> |
|-------------|--|--------------------------------------|---|
| 1           | 3  | 273                                  | 91  |
| 2           | 8  | 368                                  | 46  |

TABLE 3

## POWER OUTPUT VS CONDENSER INLET WATER TEMPERATURE

| <u>Percent Spray<br/>Canal Operating</u> | <u>Cold Water<br/>Temperature - Deg F</u> | <u>Gross Power<br/>Out - MW</u> | <u>Spray Motor<br/>Power - MW</u> | <u>Net Power*<br/>MW</u> |
|--|---|---------------------------------|-----------------------------------|--------------------------|
| 58                                       | 109.3                                     | 819.1                           | 6.2                               | 812.9                    |
| 63                                       | 106.6                                     | 820.3                           | 6.7                               | 813.6                    |
| 74                                       | 102.8                                     | 822.1                           | 7.8                               | 814.3                    |
| 79                                       | 100.6                                     | 823.0                           | 8.4                               | 814.6                    |
| 84                                       | 98.7                                      | 823.4                           | 9.0                               | 814.4                    |
| 89                                       | 97.0                                      | 823.8                           | 9.5                               | 814.3                    |
| 95                                       | 94.6                                      | 824.3                           | 10.1                              | 814.2                    |
| 100                                      | 92.7                                      | 824.5                           | 10.6                              | 813.9                    |
| 105                                      | 91.3                                      | 824.6                           | 11.2                              | 813.4                    |

\*Net Power = Gross Power - Spray Motor Power

**TABLE 4**  
**SPRAY NOZZLE PARAMETERS**

|  |      |      |
|--|------|------|
| Pressure (psi)                                 | 7    | 15   |
| Spray Height (ft)                              | 10   | 14   |
| Spray Diameter (ft)                            | 26   | 32   |
| Drop Airborne Time (seconds)                   | 1.6  | 1.9  |
| Maximum Vertical Velocity<br>(feet per second) | 20.2 | 22.0 |
| Ratio of Water to Air Mass Flow                | .058 | .048 |
| Required Number of Nozzles<br>Per Stage        | 380  | 272  |
| Required Area Per Stage (acres)                | 5.9  | 6.4  |
| Required Number of Stages                      | 2    | 1    |

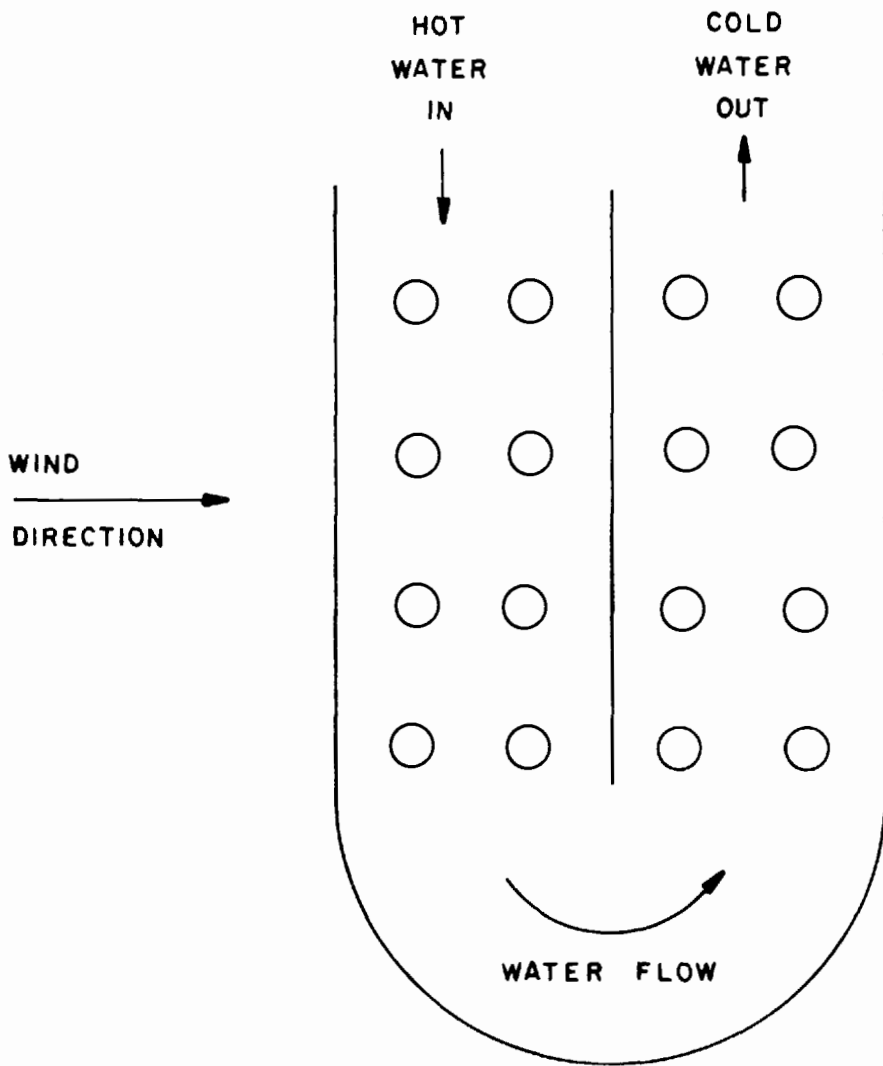


FIGURE 1 U-SHAPED SPRAY CANAL PLAN VIEW

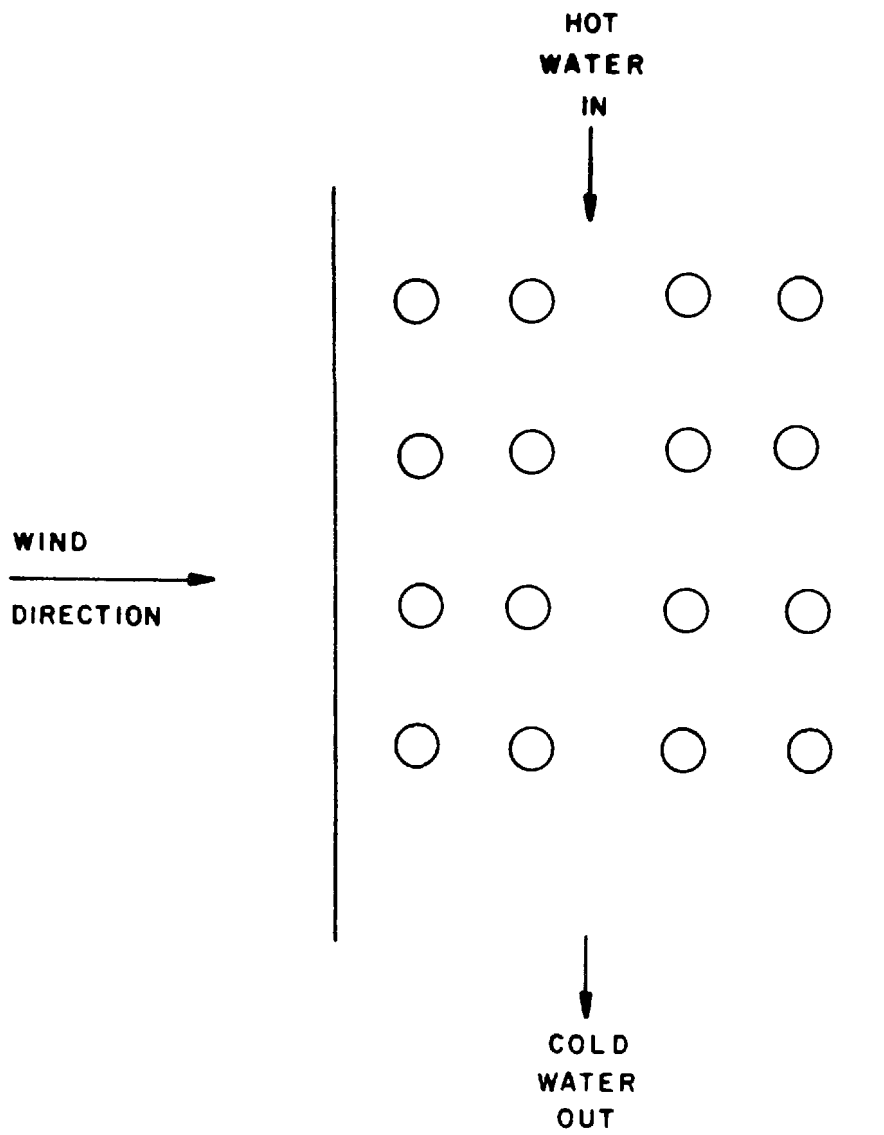


FIGURE 2 STRAIGHT SPRAY CANAL PLAN VIEW

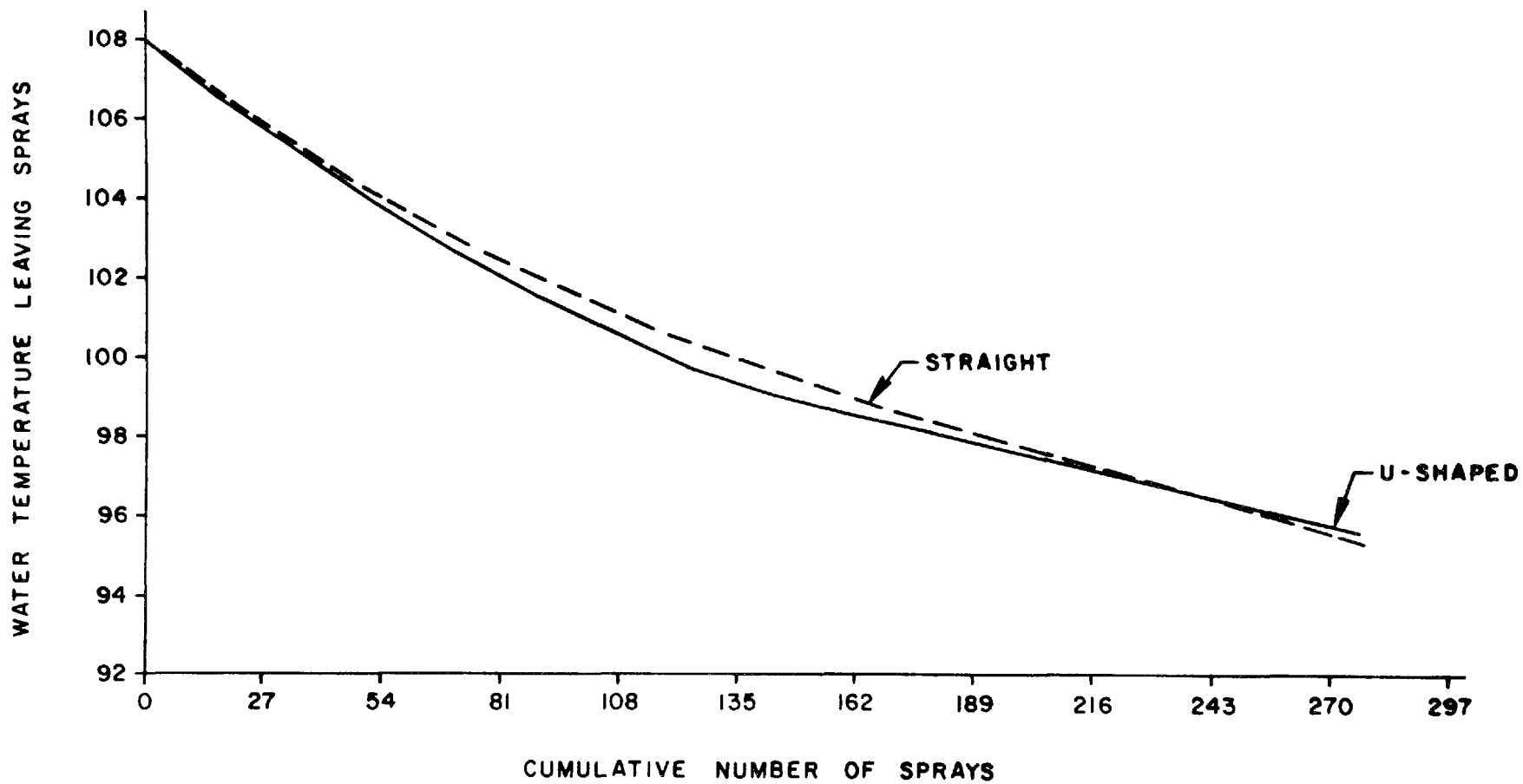


FIGURE 3 COLD WATER TEMPERATURE COMPARISON ALONG CANAL

635

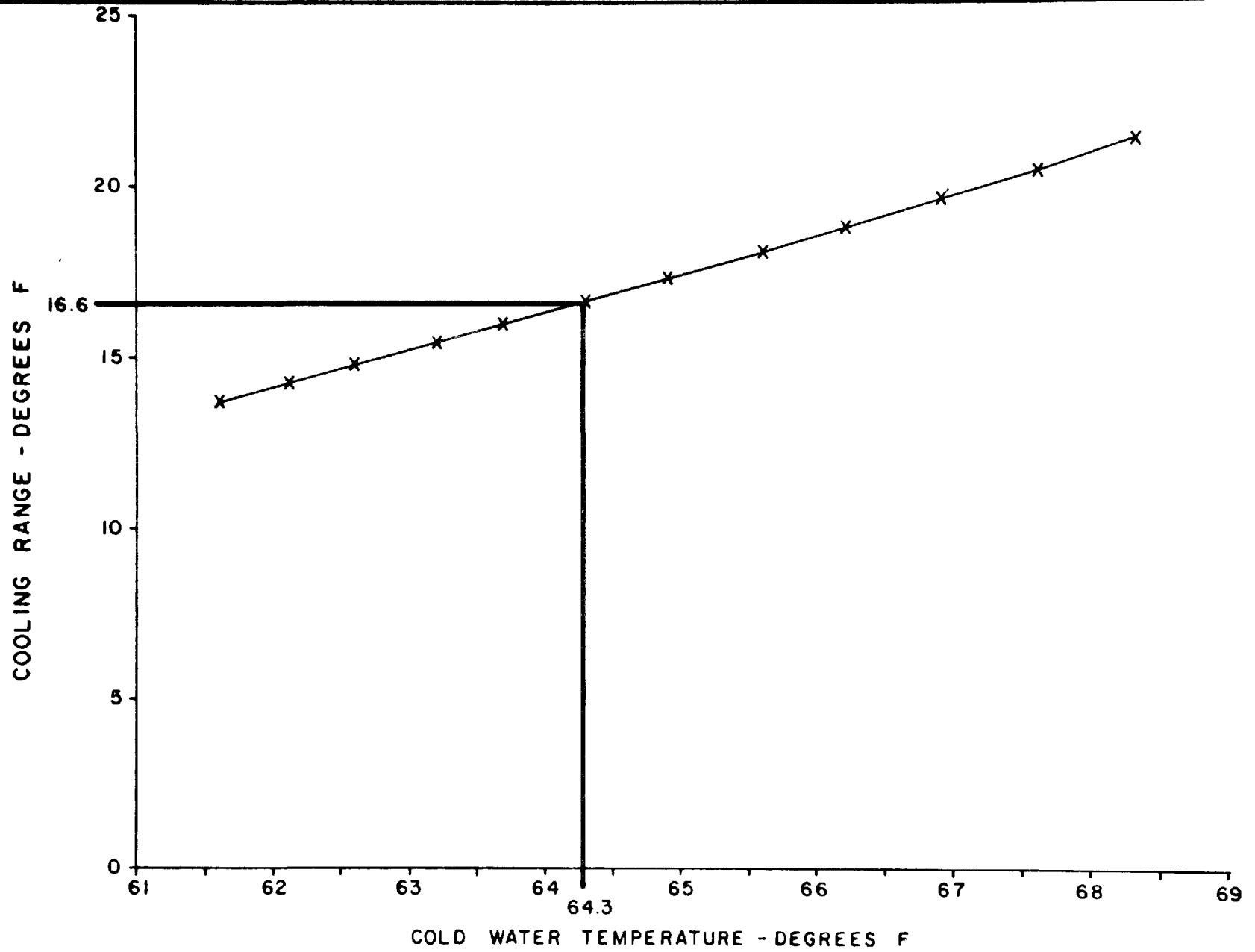


FIGURE 4 COOLING RANGE VS COLD WATER TEMPERATURE

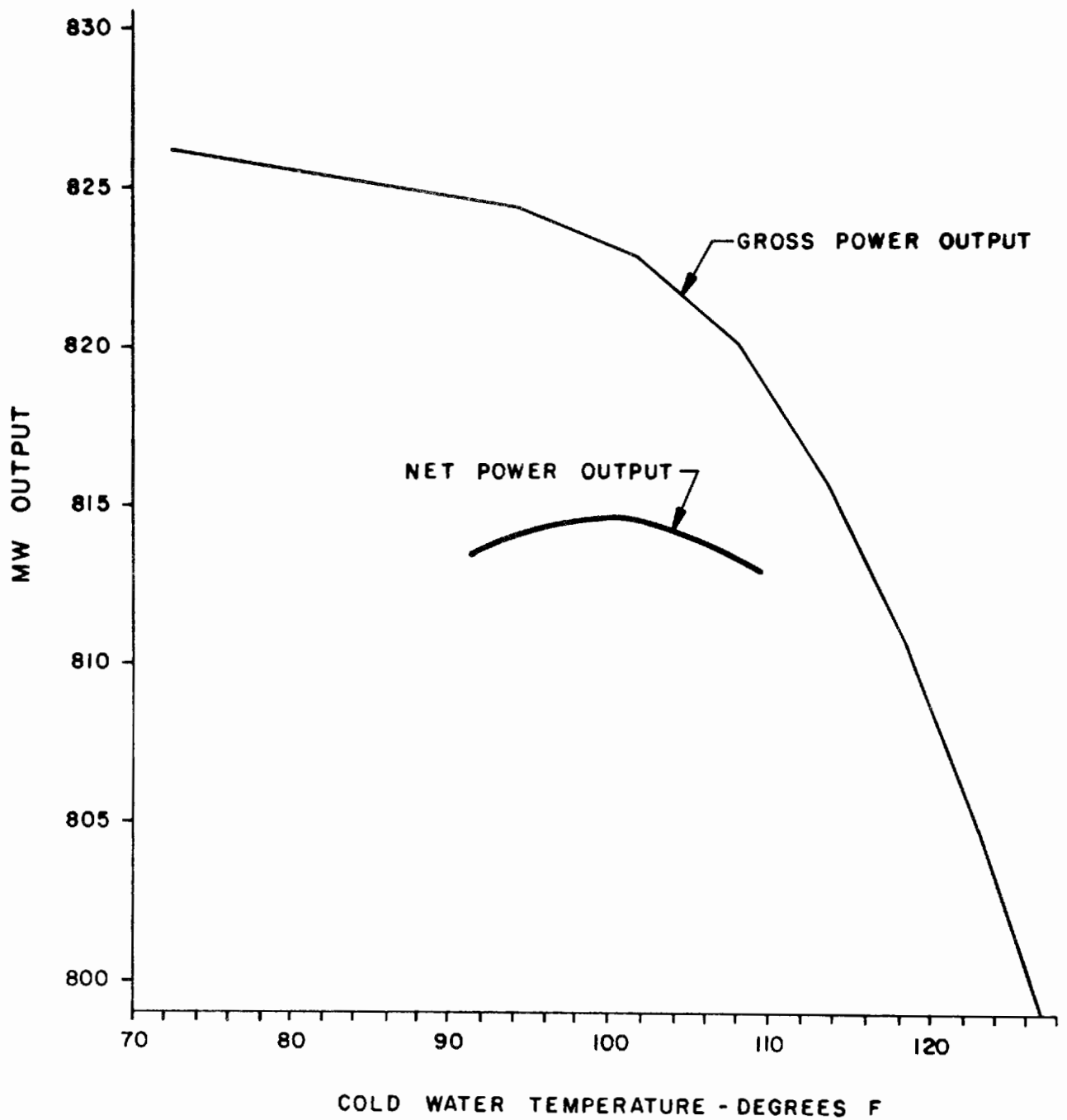


FIGURE 5 POWER OUTPUT VS. COLD WATER TEMPERATURE INTO CONDENSER - 100% LOAD

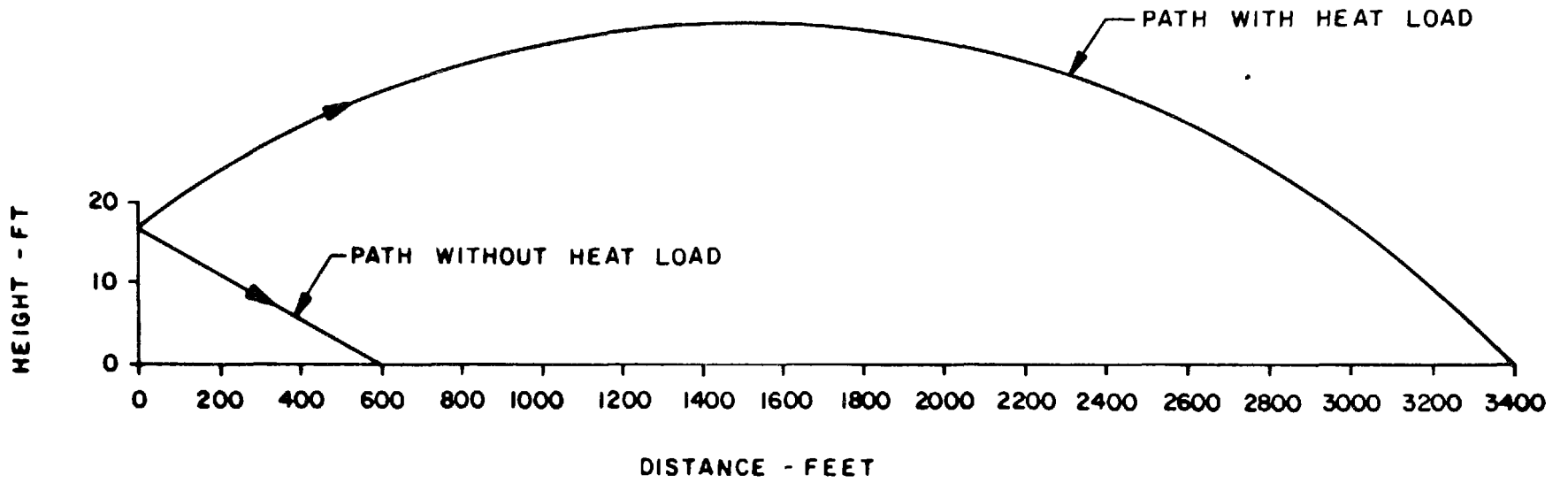


FIGURE 6 DRIFT DROPLET PATHS

## THE DEVELOPMENT OF ORIENTED SPRAY COOLING SYSTEMS

D. A. Fender  
Ecolaire Condenser, Inc.  
Bethlehem, PA U.S.A.

T. N. Chen  
Ingersoll-Rand Research, Inc.  
Princeton, New Jersey U.S.A.

### ABSTRACT

The historical and theoretical development of Oriented Spray Cooling Systems (OSCS) from conception to its current state is described. Originated by the Thermosciences Research Group of Ingersoll-Rand Research, Inc. in 1968, and being further developed after its purchase by Ecolaire Condenser, Inc. in 1977, OSCS was conceived as a method to induce air flow through a low stack cooling tower. Following numerical modeling and the laboratory testing of several scale systems, a full scale, two dimensional model cooling tower was constructed at South Carolina Electric and Gas Company's Canadys Power Station. Extensive performance testing of this demonstration model proved that system performance was unaffected by the tower enclosure. As a result, the design of spray pond systems having comparable performance to natural draft cooling towers without the typical spray pond dependence on ambient wind conditions was established. OSCS development culminated with the installation of an oriented spray cooling system for an industrial turbine condenser application located at Phillipsburg, New Jersey. Heat and mass transfer relationships are described, and performance curves are presented for these viable new industrial and utility heat rejection systems.

### INTRODUCTION

OSCS is a method of evaporative heat rejection proprietarily owned and patented by Ecolaire Condenser, Incorporated. These systems combine the low cost and environmental acceptability of conventional spray systems with the consistent and efficient performance of natural draft cooling towers. OSCS is intended for use in utility plant condenser cooling, industrial process cooling, or nuclear plant safety system cooling. It can be adapted to a wide variety of configurations, depending upon plant site topography, meteorology, and load requirements. This adaptability makes OSCS particularly appropriate for retrofit and supplemental application.

The standard OSCS arrangement consists of an annular array of vertical spray tree modules (refer to Figure 1). These spray trees each consist of a vertical riser pipe to which horizontal branch pipes are attached at equal height intervals and at right angles to each other such that the spray nozzles attached to the branch ends comprise a counter-clockwise helix with increasing height. The number of nozzles per tree

is selected according to the thermal performance characteristics required for the specific application. OSCS provides consistent performance for all ambient wind conditions, including no-wind periods, through its ability to induce air flow through the fill area by momentum exchange with the sprayed water droplets. Hence, the major task of the research effort expended on OSCS was to develop the ability to predict this performance for various meteorological and configurational conditions.

## EXISTING COOLING SYSTEMS

In 1968, the Condenser Division of Ingersoll-Rand conducted a market examination of the cooling requirements for commercial power generating plants. This survey indicated that closed system type condenser cooling would be showing a dramatic increase in usage. As environmental concern and activism began to restrict the use of once-through cooling systems fed from natural lakes and rivers, high efficiency cooling towers were being specified to provide the lowest condenser circulating water temperature possible. The survey led to the determination to investigate the feasibility of developing a viable evaporative cooling tower product line.

Natural draft cooling towers can be arranged for either counterflow, parallel flow, crossflow, or combinations of these. Typically, maximized air to water contact, necessary for efficient evaporation, is achieved by droplet formation from cascading trays, plates, or slats. Air movement through the "fill" section can be provided by the natural draft effect caused by the heated air buoyancy within a tall stack section. In some tower designs, spray nozzles are used to augment droplet formation and subsequently increase the evaporative heat transfer.

Preliminary fluid dynamics analysis of the various possible fill designs conducted by Ingersoll-Rand Research, Inc. (IRRI) indicated that in a crossflow tower independent hollow cone nozzle spraying offered the greatest potential for reducing tower fill pressure drop. Suggesting that a smaller tower stack could be used, this finding led to the decision to pursue the project as a natural draft crossflow spray cooling tower.

## SPRAY TOWER PERFORMANCE AND FEASIBILITY

Until that time, no known significant theoretical analysis had been conducted on spray towers. One spray cooling tower was found, and it was operated by the Electricity Supply Commission in Johannesburg, South Africa. In late 1969, IRRI undertook the development of an analytical model and computer simulation program of the proposed spray cooling tower. This model was to provide operating characteristics which would be subsequently used in determining the technical and economical feasibility of spray towers. A complete analytical model of the system was not possible due to the vastly complex trajectory and thermal history of the spray droplets. Therefore, the first step of the analytical study was to develop a simplified model of the actual process while retaining its essential physical description.

## Vertical Rain Model

By considering each hollow cone spray within the tower to be comprised of numerous pairs of spray droplets, the average spray cooling performance was shown to reasonably approximate that of those droplet pairs moving transverse to the air flow. This approximation is called the "vertical rain model" and was determined valid by a finite element computer analysis of both transverse and parallel spray models within a spray tower. In this analysis, the heat and mass transfer was calculated based on the average air and water properties entering each element, and air drag was assumed negligible. The air temperature and humidity variation was determined using a trial and error approach to satisfy the overall energy balance. Since each droplet trajectory was limited within a vertical plane perpendicular to the air flow, the analysis was greatly simplified.

## Tower Performance Simulation

The vertical rain model was subsequently used in the development of a spray tower computer simulation program. Again, a finite element grid was devised to allow numerical solution of the governing equation for heat and mass transfer, draft, pressure loss, and water surface area and distribution. The program also allowed the optional simulation of a draft-inducing fan to augment air movement through the fill.

The results which this program generated suggested that a crossflow spray tower could be designed to produce comparable cooling performance to a conventional state-of-the-art tower. This suggested that spray cooling towers were, indeed, technically feasible. The analysis also indicated that performance was strongly dependent upon the effective droplet size. Therefore, not only is the droplet size distribution important, but droplet collisions or "interference" have a strong effect.

## Spray Nozzle Orientation

Finally, the pressure drop through the spray fill was confirmed as the largest single pressure loss in the tower. To reduce this pressure loss, and thus reduce the tower stack cost, Dr. T. N. Chen of the IRRRI proposed that the fill spray nozzles be oriented towards the air flow direction. By reducing the horizontal relative velocity between the water drops and the air, fluid dynamic theory indicates that the viscous drag, and consequently the pressure drop, would be reduced. Hence, the stack height required for draft would be reduced as the water droplet horizontal velocity in the air flow direction is increased. Taken further, the principle indicated that the tower stack could be completely eliminated if the spray velocity were sufficient to drag the air through the spray section. This proposal has become the essential principle of the Oriented Spray Cooling System concept.

The spray tower computer model was consequently revised to allow the study of a spray nozzle orientation other than vertically upward. Parametric studies of the resultant oriented spray system confirmed both its technical feasibility and drop size dependence.

Since the droplet interference is a function of nozzle arrangement and operating pressure, and it has a strong effect on cooling performance, it was concluded that a full scale test program was necessary to establish the performance of OSCS.

## LABORATORY MODEL TESTING

Prior to engaging in a full scale prototype testing program, two laboratory scale model tests were devised. Using appropriate scaling analysis, much valuable data concerning various design parameters could be gathered at greatly reduced expense. The tests were primarily intended to examine air flow and recirculation phenomena, and to provide criteria for the design of the full scale prototype.

### Laboratory Flow Testing

Beginning in early 1970, this laboratory test program was intended to experimentally confirm the oriented spray principle of inducing air to create the draft necessary for cooling performance, and to determine the effects of various design parameters on this air flow. The test apparatus consisted of a long, narrow box with an array of horizontal spray manifolds at the inlet end and a roof opening at the outlet end to direct the sprayed induced air upward. The manifolds were drilled in a special multiple orifice arrangement to simulate hollow cone spray nozzle effect. This type of module was used because it could be scaled to the dimensions of a finite "slice" through an annular OSCS unit.

Thermal data were taken of air and water conditions, and smoke traces were recorded for air flow pattern determination. The test results clearly demonstrated the effectiveness of the oriented spray principle in inducing air movement. The test also confirmed the strong effects of droplet interference and spray distribution. The smoke traces of air motion through the spray apparatus did indicate that air flow deviated from the horizontal flow assumption used throughout the theoretical study. This is understandable because of the parabolic trajectory of the spray droplets inducing the air. In addition, by removing the apparatus roof, it was confirmed that a tower enclosure was unnecessary for performance. The results suggested that further testing of a full scale system would be needed for accurate performance prediction.

### Recirculating Testing

The recirculation of the exhaust plume effluent is a common problem of all evaporative cooling systems, causing a negative effect on cooling performance. Beginning in mid-1972, a laboratory model was constructed and tested to determine the general magnitude of the recirculation which an OSCS would exhibit (refer to Figures 2, 3, and 4).

The models consisted of pairs of small open boxes arranged in two different configurations in a horizontal air stream. The first arrangement consisted of two linear rows of these box pairs separated by a variable space.

The second consisted of an annular arrangement. A wind velocity profile was simulated by controlling the air velocity profile with a variable opening screen. The outer box of each set removed a quantity of air calculated to be equivalent to the air induced by the spray. This air was ducted to a heating device which raised its temperature as desired, returned it to the inner box, and discharged it to atmosphere (refer to Figure 2). Recirculation could then be determined for each of the downwind boxes by the increase in the air inlet temperature over the ambient. This procedure yielded a reliable quantitative recirculation allowance factor for the OSCS design.

#### FIELD DEMONSTRATION SYSTEM TESTING

Full scale testing of an actual prototype OSCS for performance determination would be substantially cost prohibitive. Hence, it was decided that these necessary tests would be performed on a full scale replica of the laboratory model. Again, this module represented a finite slice of a complete OSCS unit. The comparison between performance factors of this linear model and an annular section was determined to be equivalent by the use of appropriate flow area.

Construction of this 10,000 gpm capacity test module was begun in 1973 at South Carolina Electric and Gas Company's Canadys Power Station. Field tests were initiated that year, and were continued over an 18 month period. The tests were intended to provide full scale verification of the oriented spray principle. They also allowed determination of the effects of various design parameters such as nozzle size, orientation distribution, pressure, and exhaust area, as well as the effects of the operating heat load and ambient meteorological conditions on the overall cooling performance. Finally, the tests provided extensive data upon which a thermal performance model for the entire operating range could be accurately based.

During the testing period, 486 separate test runs provided specific point data over an extensive range of operating pressures, water loadings, nozzle arrangements, and meteorological conditions. The data were then correlated into empirical relationships.

Parallel to the test program, a design analysis was conducted to optimize the method for piping and distributing the water. This analysis led to the design of the helical pattern of the vertical riser spray tree, a major contributor to the OSCS patent.

#### DEVELOPMENT OF PERFORMANCE MODELS

The introduction of OSCS into the commercial marketplace also required the development of several mathematical models for various performance criteria. These models are essential to the proper application of OSCS to specific design conditions. They have enabled OSCS to be engineered to specific applications with a precision and efficiency not found in other spray ponds or spray towers.

## Thermal Performance Model

The thermal performance model was formulated from the conservation laws of mass and energy within a control volume within the spray zone. The energy balance is:

$$L C_p (T_{wh} - T_{wc}) = KAV(MhD) \quad (1)$$

where:

- L = total water loading rate
- C<sub>p</sub> = specific heat of water at constant pressure
- $\bar{T}_w$  = average temperature of all water drop at a point in their falling period
- T<sub>wh</sub> = temperature of hot water entering spray
- T<sub>wc</sub> = temperature of cold water after spray
- K = mass transfer coefficient
- A = average water surface area per unit volume
- V = total volume of spray zone
- $\bar{h}_{ws}$  = total enthalpy of air-water vapor mixture in equilibrium with the water drop at a surface temperature  $\bar{T}_{ws}$  and a bulk temperature  $\bar{T}_w$
- $\bar{h}_a$  = average total enthalpy of air in contact with the drops

MhD, the mean enthalpy difference between the vapor film at the water surface and the bulk air, is defined from:

$$MhD = \frac{T_{wh} - T_{wc}}{\int_{T_{wc}}^{T_{wh}} \frac{d\bar{T}_w}{(\bar{h}_{ws} - \bar{h}_a)}} \quad (2)$$

so that Equation (1) can be written in the familiar form:

$$\frac{KAV}{L} = \int_{T_{wc}}^{T_{wh}} \frac{C_p d\bar{T}_w}{(\bar{h}_{ws} - \bar{h}_{wa})} \quad (3)$$

The dimensionless KAV/L parameter, as it is for conventional cooling towers, is the performance factor for a given spray system. Examination of the left hand side terms of Equation (3) indicates that the KAV/L variation with temperature is small ( $\pm 5\%$ ). Hence, KAV/L is primarily a function of nozzle configuration and operating pressure, and not a significant function of temperature. Given a specific OSCS design, then Equation (3) becomes a simple relationship between  $T_{wc}$ ,  $T_{wh}$ , and the ambient air enthalpy,  $h_{ai}$ .

Since KAV/L cannot be analytically calculated, it must be determined empirically. Thus, the Canadys test data provided the KAV/L value for each different nozzle arrangement and pressure. By substituting the various temperature and enthalpy relationships for a variety of load and ambient conditions into Equation (3), the statistical KAV/L value could be determined. A typical OSCS performance curve for a specific arrangement or KAV/L is shown in Figure 5. It should be noted that an OSCS KAV/L value should not be compared with a conventional cooling tower KAV/L, because the KAV/L's in the two cases are not defined exactly the same. Furthermore, because the experimentally determined KAV/L is effectively a no-wind factor, and since inclusion of wind effects should improve cooling performance, we can deduce that these KAV/L values reflect the worst-case (no-wind) performance.

#### Theoretical Drift Models

All evaporative cooling systems require special attention to the problem of water droplets which become entrained in the air stream. This phenomenon is called "drift", and is, in many areas, a substantial environmental and/or economic problem.

Two separate numerical drift models were developed for computer simulation. First, the "low-wind" drift model considers the wind to be sufficiently low to allow the formation of a buoyant plume. By treating the notion of the water droplets carried upward in the buoyant plume in a cross wind, a finite difference computer model was generated. This program produces droplet fallout distances for various wind orientations, drop diameters, and operational/ambient conditions. Total drift is determined by using the drop size distribution curves for the nozzle used and the fraction entered and lifted by the plume to calculate the total mass of droplets which will fallout beyond the spray basin boundaries. Hence, the basin boundaries can be established to catch all but the allowable percentage of drift.

The second model developed was the "high-wind" drift model, which assumes that the wind forces are strong enough to prevent plume formation. Similarly to the low-wind model, the high-wind model uses numerical techniques to resolve the drag forces into particle trajectories. Again, the allowable percent drift can be met by appropriate design of the basin boundaries.

The worst case model for the specific application is used to determine the most conservative basin dimensions for a particular drift requirement.

## Theoretical System Model

Because the actual cooling accomplished by OSCS is complicated by the transient system response due to the thermal capacitance of the pond water mass, a computerized finite difference system cooling model was developed for predicting the temperature of the pond water being supplied to the service system. This model requires consideration of the supplied hot water load, ambient conditions, pond volume, surface radiation and convection, drift and evaporation loss, and mixing effects. While this system is helpful for condenser and industrial process applications, it is essential to nuclear power plant ultimate heat sink (UHS) design.

## PROTOTYPE INSTALLATION

The development of OSCS culminated in 1976 with the installation of an actual working system at Ingersoll-Rand Company's Phillipsburg, New Jersey, Turbo Division, plant. The plant cooling pond provides cold circulating water to various turbine test stand condensers according to a variable testing schedule. An approximately sixty-year-old flatbed spray cooling system was converted to OSCS to provide the most adequate and economical cooling for an increased thermal loading following test facility expansion.

After removal of the old flatbed headers, a new annular header system with 32 spray trees was installed. A helicopter was used for member placement, facilitating assembly without requiring the pond to be drained. The total cost of the 20,000 gpm installation, including pumps, was \$330,000. This Phillipsburg OSCS has been in service since its initial startup (refer to Figure 6), and has provided more than adequate cooling performance.

## FOLLOW-UP TESTING AND DEVELOPMENT

Ecolaire's OSCS development program is primarily aimed at further verification of the thermal performance model generated from the Canadys data by thermal testing of the Phillipsburg installation. Such results are expected in the near future.

Other development work includes computer optimized design methods to provide the user with the maximum efficiency cooling system at the minimum cost for the specific application. And, as with any other newly introduced technology, OSCS will require an ongoing development program to further reduce manufacturing and installation costs.

## CONCLUSIONS

The above historical review has shown how a unique large scale water cooling system utilizing water sprays to induce cooling air flows was successfully developed and expanded into a viable product line. OSCS offers users the advantages of low cost and environmental acceptability of the conventional spray pond and the consistent and efficient performance of natural draft

cooling towers. The development was conducted through a concerted and illustrative combination of analytical, numerical, and experimental procedures which should be insightful to all research and development engineers concerned with similar tasks. The resultant addition of OSCS to evaporative cooling technology represents a major contribution to the industry.

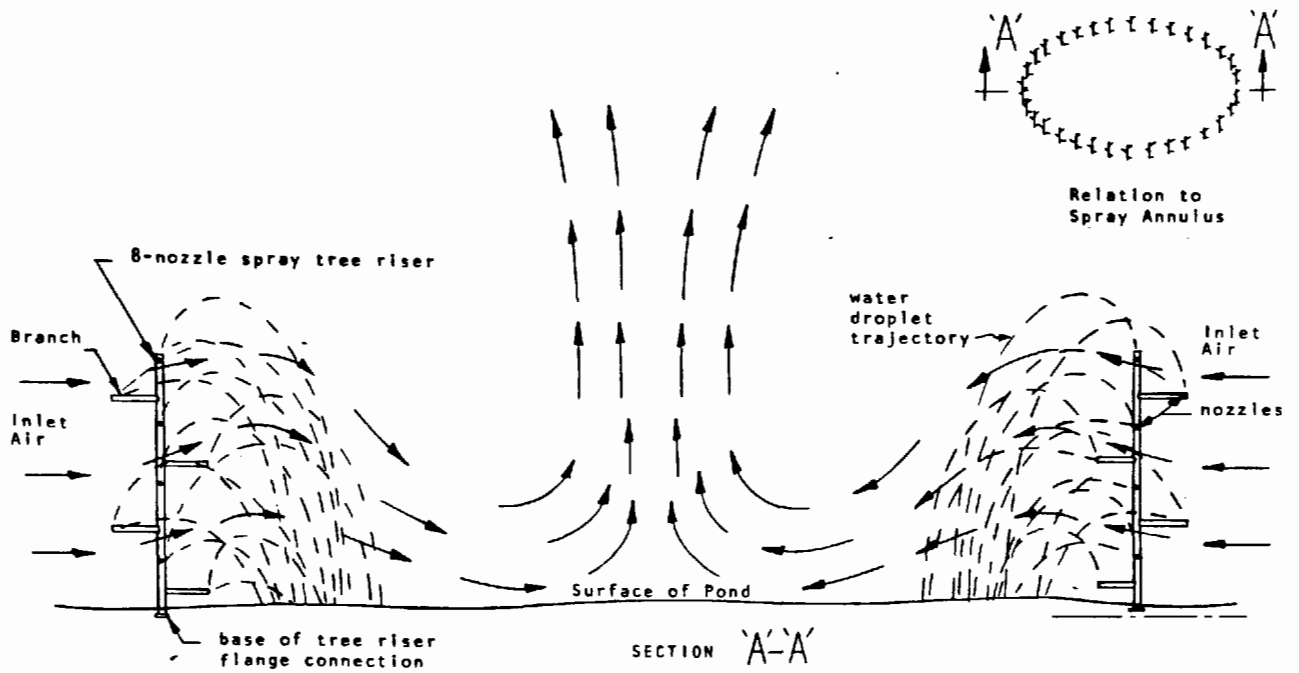


Figure 1: Oriented Spray Cooling System Cross Sectional View

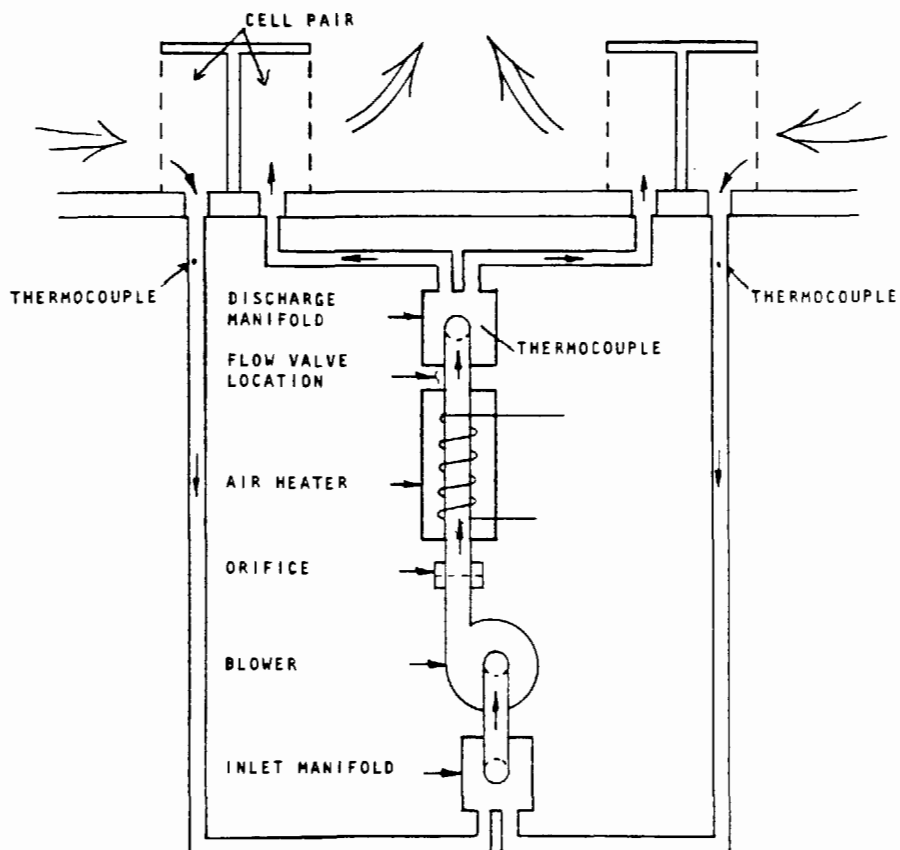
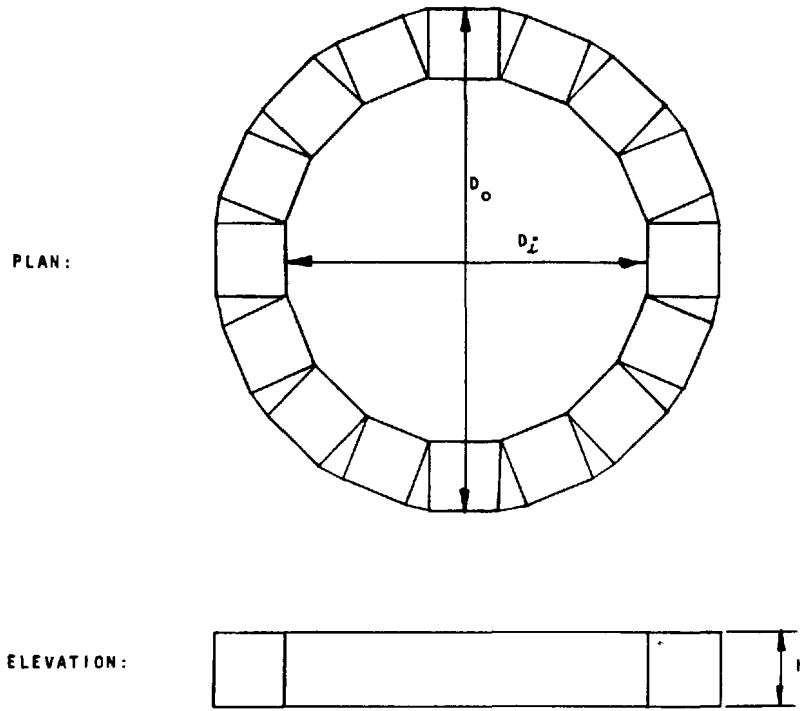


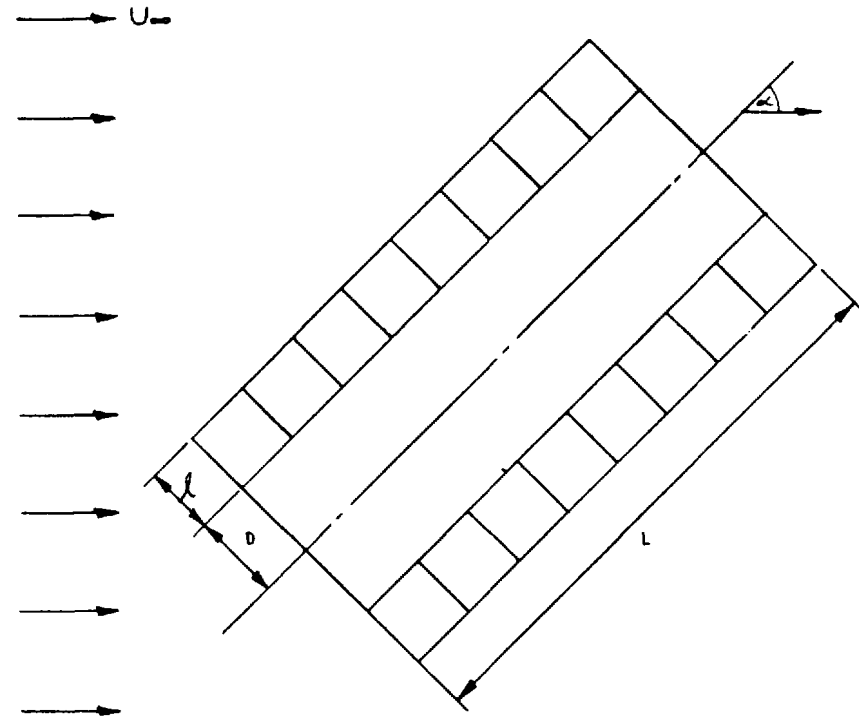
Figure 2: Schematic of Recirculation Testing Apparatus



Area Constraint:  $\frac{A_i}{A_e} = \frac{3}{4} \rightarrow \frac{D_o h}{D_i^2/4} \approx \frac{3}{4}$

$h$  = height of cells  
 $A_i$  = total area of the inlet to the test apparatus  
 $A_e$  = total exhaust area of the test apparatus

Figure 3: Recirculation Testing Apparatus Annular Arrangement



$L$  = overall length of OSCS installation  
 $l$  = width = depth = height of spray system =  $h$   
 $\therefore$  aspect ratio =  $L/h$

$$\frac{\text{inlet area}}{\text{exhaust area}} = \frac{3}{4} = \frac{h \times L \times 2}{D \times L \times \frac{2}{D}}$$

$\alpha$  = angle between wind,  $U_\infty$ , and centerline of model

Figure 4: Recirculation Testing Apparatus Linear Arrangement

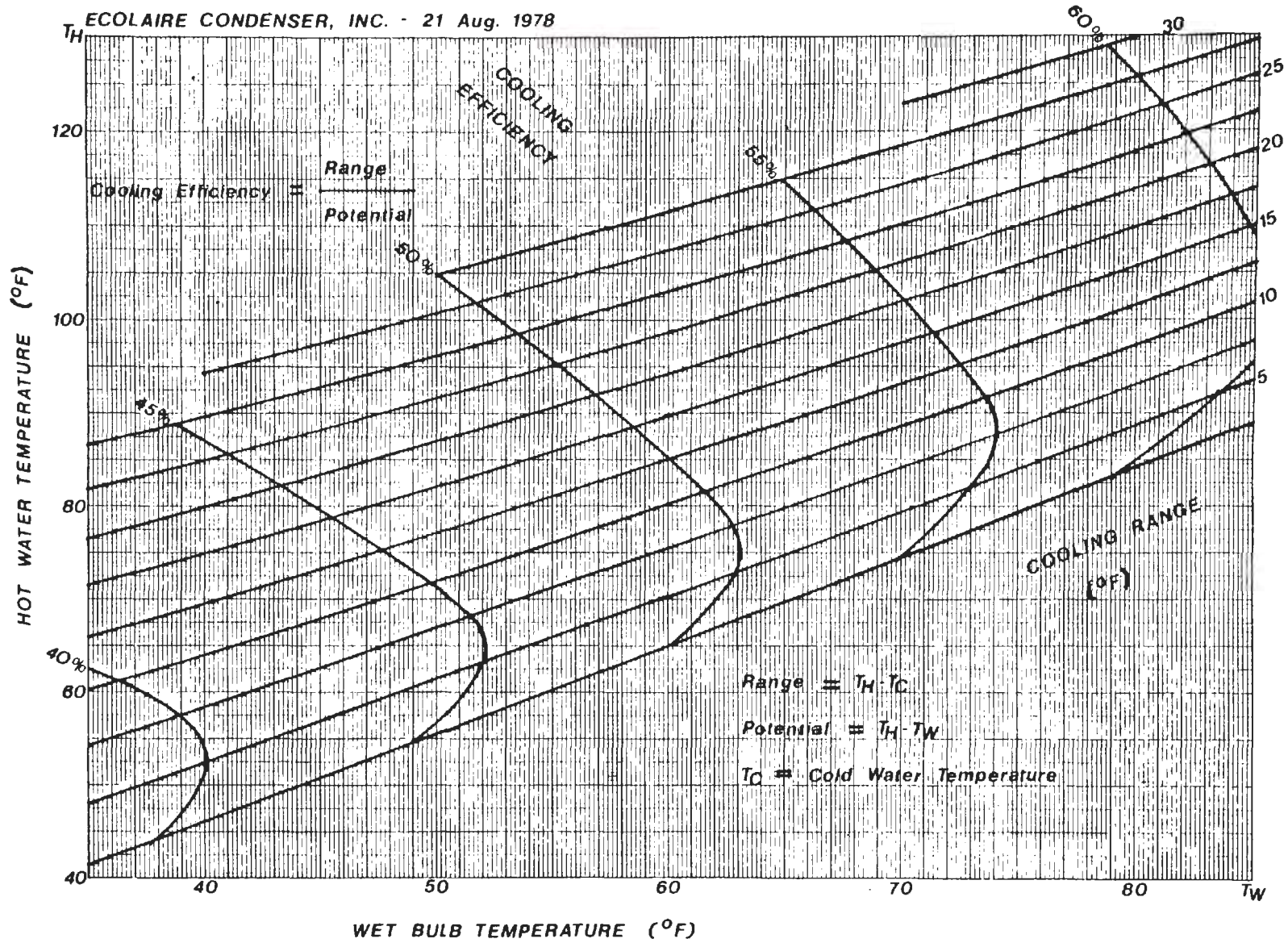


Figure 5: A Typical Oriented Spray Cooling System Performance Curve



Figure 6: OSCS Installation At Phillipsburg, New Jersey

ONCE-THROUGH COOLING POTENTIAL OF THE  
MISSOURI RIVER IN THE STATE OF MISSOURI

A.R. Giaquinta  
Institute of Hydraulic Research  
The University of Iowa  
Iowa City, Iowa U.S.A.

T.C. Keng  
Jenkins-Fleming, Inc.  
St. Louis, Missouri U.S.A.

ABSTRACT

The reach of the Missouri River bordering or crossing the state of Missouri is studied with regard to its potential for use in once-through cooling of steam-electric power plants. Based on the existing thermal standards of the state regulatory agencies, the remaining heat assimilation capacity of the river is computed, and sites and capacities of future permissible once-through-cooled power plants are determined.

The existing and future thermal regimes of the river are computed from a heat balance equation relating the rates of convective heat transfer, surface heat exchange between the river and the atmosphere, and heat inputs from power plants or other artificial sources. Streamwise temperature distributions with existing, future proposed, and future permissible heat loads are shown for average river flow conditions and for the 7-day, 10-year low flow condition.

It is demonstrated that this reach of the Missouri River can accommodate additional once-through-cooled power plants with a total capacity of several thousand megawatts at average flow conditions. These new plants must be properly sited to avoid the cumulative effects of upstream thermal loads. If thermal standards were based on the low flow condition, the total permissible capacity would be significantly reduced.

INTRODUCTION

The continuing increase in demand for electrical energy and the resultant growth of the electrical power industry in the United States have given rise to certain environmental problems related to the siting and design of new power plants. Once-through (open-cycle) cooling is known to be one of the most efficient methods for condenser cooling. This method is efficient economically, thermodynamically, and, if the cooling water outfall structure is designed properly, it is efficient ecologically.

However, the U.S. Environmental Protection Agency has mandated that in the near future new power plants will not be allowed to utilize open-cycle cooling and some older plants will have to backfit closed-cycle cooling systems. These regulations will incur tremendous expense and a great increase of energy consumption. As more studies are completed, it is being found that thermal pollution is not as ecologically harmful as

originally thought [1]. Therefore, in light of an expanding power industry, it is important to consider the future open-cycle cooling potential of our nation's major rivers.

In this study attention is focused on the reach of the Missouri River bordering or crossing the state of Missouri. Along this reach which passes through or near the two major population centers of Kansas City and St. Louis, the river is used for open-cycle cooling by several power plants, and more once-through-cooled units are proposed for construction within the next decade. To determine the once-through cooling potential of the river it is important to consider the cumulative effects of the existing and future power-plant discharges. It also is necessary to consider the availability of water for use in open-cycle cooling and the amount of evaporative water loss. It was shown in [2] that consumptive use is no problem.

The steady-state version of the Iowa Thermal Regime Model (ITRM), a numerical model for the calculation of streamwise temperature distributions in rivers, is used to determine the existing and future thermal regimes of the Missouri River downstream from the southern Iowa border. The basic equation governing the conservation of thermal energy in a free-surface flow is reviewed, and the numerical model is presented.

The steady-state ITRM is used to determine the thermal regimes of the Missouri River along the study reach corresponding to average meteorological and hydrological conditions for the months of February, May, August, and November (representing the four seasons of the year). The natural thermal regimes and the modified thermal regimes resulting from the imposition of external heat loads from power plants and other sources are calculated. Results are shown in the form of temperature distributions along the river for the cases of existing power plants and future power plants proposed for installation within the next decade. Based on the existing thermal standards of the state regulatory agencies, the remaining heat assimilation capacity of the river is computed, and sites and capacities of future permissible once-through-cooled power plants of reasonably large size are determined. The resultant temperature distributions corresponding to these future permissible plants are presented.

It is shown that there is no remaining heat assimilation capacity of the river in the vicinity of Kansas City. No additional future power plants using open-cycle cooling are permissible upstream from Kansas City because they would cause violations at downstream locations. The total capacity of future permissible plants at average flow conditions is about 6000 MW for fossil-fueled plants or about 4100 MW for nuclear-fueled plants, based on allowable increases above the natural temperature base. Thermal regimes at the 7-day, 10-year low flow hydrological condition also were studied by Giaquinta and Keng [2], and some results are presented herein. At the low flow condition, some existing and proposed future power plants are seen to violate the excess temperature limitation if they operate at full load. These plants would require derating or auxiliary cooling at this extreme condition. Based on the low flow the total future permissible plant capacity is about 1300 MW for fossil plants or about 900 MW for nuclear plants.

## THE MISSOURI RIVER SYSTEM

The source of the Missouri River is in the state of Montana, and it flows generally southeasterly 2315 miles to its junction with the Mississippi River about 15 miles above St. Louis, Missouri. River miles along its channel are measured upstream from the intersection of the thalwegs of the Missouri and Mississippi Rivers.

The river reach of concern in this study, starts at the Iowa-Missouri border (Mile 553) and continues to the confluence with the Mississippi River (Mile 0). This reach borders the states of Nebraska and Kansas and crosses the state of Missouri. The major tributary streams entering the river in the downstream order are the Kansas River (Mile 367), Grand River (Mile 250), Chariton River (Mile 239), Osage River (Mile 130), and Gasconade River (Mile 104). The general layout of the river system is shown in Fig. 1.

The climatic conditions are represented by data from five Class-A weather stations located along or close to the Missouri River in the study area. Monthly mean values of daily weather data for the 20-year period from 1954 through 1973 were used in the analysis. The locations of the weather stations and detailed tables of data are given in reference [2].

The Missouri River flow rate is regulated by six reservoirs upstream from Sioux City, Iowa. Because the present study reach is far downstream from the reservoirs, the thermal effects of the reservoir control are negligible, and only the obvious consequences of the reservoir regulation on flow rate are considered.

TABLE I gives a summary of the monthly mean values of daily flow rates for a 19-year period (1956-1974) at seven gaging stations along the study reach. Detailed flow-rate tables and a map showing the locations of the gaging stations are included in reference [2].

The thermal standards for the Missouri River are governed by the water pollution control agencies of the states bordering the river. The maximum allowable temperature rise is 5°F (2.78°C) and the maximum water temperature is 90°F (32.2°C) for the entire study reach. The allowable temperature increase is the governing standard for all the cases considered herein.

Eleven power plants utilizing open-cycle cooling with a total of 40 units are located along the study reach; their locations are shown in Fig. 1. Only steam-electric power plants with capacities greater than 50 MW are considered. TABLE II summarizes the loading and cooling system characteristics of these power plants. The major data source used in preparing the table was the FPC Form 67. For most of the power plants along the Missouri River, the forms were provided by the utilities for the year ended December 31, 1974. For those not supplied by the utilities reference [3] which covered the year ended December 31, 1973, was used. The list of utilities and their abbreviations are given in the appendix.

The total installed plant capacity is about 5690 MW, which consists of about 4880 MW fossil-fueled and 810 MW nuclear-fueled plants. All of these plants use once-through cooling systems. There are four future power plants proposed for construction through 1990, as listed in TABLE III. The total plant capacity proposed for installation is about 6620 MW, of which 4240 MW is planned for once-through cooling, and 2380 MW for natural draft cooling towers [2]. Heat loads from industrial and municipal sources were considered and found to be negligible compared to the heat loads due to power plants.

#### COMPUTATIONAL MODEL

The general differential equation that describes the conservation of heat in an elemental volume of water in a river is three-dimensional and unsteady. However, in most streams large temperature gradients in the transverse and vertical directions occur only in the near-field regions of sites where thermal loads are imposed. In considering the overall thermal regime of a river, the zones of the three-dimensional effects usually are small compared to the lengths of the river reaches, and, therefore, a one-dimensional formulation may be employed.

Also, in examining the thermal regime of a river, it frequently suffices to determine the steady-state temperature distributions corresponding to average meteorological, hydrological, and thermal loading conditions. Based on these simplifications, the one-dimensional, steady convection-diffusion equation expressing the conservation of thermal energy in a free surface flow may be expressed as

$$\frac{dT}{dx} = \frac{B}{Q} \frac{\phi^*(T)}{\rho c_p} + \frac{TI}{Q\rho c_p} \quad (1)$$

in which  $T$  = cross-sectional average river temperature,  $x$  = streamwise distance along the channel,  $B$  = top width of the river flow section,  $Q$  = river discharge,  $\phi^*$  = rate of surface heat exchange between the water and the atmosphere,  $TI$  = rate of heat input from power plants and tributary inflows per unit length along the stream,  $\rho$  = density of water, and  $c_p$  = specific heat of water. The terms of the equation represent the heat advected by the current, the heat transferred by the air-water interfacial transport processes, and the rates of artificial and tributary heat inputs to the river. This equation can be solved to obtain the steady-state longitudinal distribution of temperature in a river.

The computational technique to solve Eq. (1) is a finite-difference method based on the steady-state Iowa Thermal Regime Model (ITRM) developed by Paily and Kennedy [4]. This method was employed to study the thermal regimes of the Upper Mississippi and Missouri Rivers [5] and was validated in that study by comparing numerical results with measured field temperature data along both rivers.

To compute the temperature distribution along a river the total river length is divided into a convenient number of reaches. Each reach is subdivided

into a finite-difference grid defined by a number of meshpoints. The solutions for adjacent reaches are linked by the common conditions at the junction node points connecting them. If the temperature at any meshpoint,  $X_i$ , is  $T_i$ , the temperature at the next meshpoint,  $X_{i+1}$ , which is at a distance  $\Delta x$  downstream is given by

$$T_{i+1} = T_i + (\Delta x) \left[ \frac{(B_{i+1} + B_i)/2}{(Q_{i+1} + Q_i)/2} \right] \frac{\phi^*_{i+\frac{1}{2}}}{\rho c_p} + \frac{1}{(Q_{i+1} + Q_i)/2} \left[ \frac{(TI)_{i+1}}{\rho c_p} \right] \quad (2)$$

in which  $\phi^*_{i+\frac{1}{2}}$  is the surface heat exchange rate corresponding to  $T_{i+\frac{1}{2}}$ , the temperature at the middle of the mesh space,  $\Delta x$ . The temperature,  $T_{i+\frac{1}{2}}$  is determined by

$$T_{i+\frac{1}{2}} = T_i + \left( \frac{\Delta x}{2} \right) \left( \frac{B_{i+1} + B_i}{Q_{i+1} + Q_i} \right) \frac{(\phi^*)_i}{\rho c_p} + \frac{1}{2} \left( \frac{1}{(Q_{i+1} + Q_i)/2} \right) \left[ \frac{(TI)_{i+1}}{\rho c_p} \right] \quad (3)$$

in which  $\phi^*_i$  corresponds to the known temperature,  $T_i$ . If the temperature at the upstream boundary ( $i=1$ ) is known, Eqs. (2) and (3) can be used to calculate the temperature at downstream meshpoints  $i=2, 3, \dots, N$ , where  $N$  is the total number of meshpoints for the entire length of the reach under consideration.

In the above equations, the rate of surface heat exchange,  $\phi^*(T)$ , is one of the principal factors influencing the thermal regimes of the river. It depends upon several climatic factors, including solar radiation, air temperature, wind speed, relative humidity, atmospheric pressure, and cloud cover. The most important processes included in the mechanism of heat transfer between the water surface and the atmosphere are the net short-wave radiation entering the waterbody,  $\phi_R$ ; the net long-wave radiation leaving the waterbody,  $\phi_B$ ; evaporation,  $\phi_E$ ; conduction,  $\phi_H$ ; and the melting of snow,  $\phi_S$ . The heat transfer process is expressed as

$$\phi^* = \phi_R - \phi_B - \phi_E - \phi_H - \phi_S \quad (4)$$

Equations for computing the components of surface heat exchange are given elsewhere [2,5,6].

The input data required for the model include (1) river mile at the upstream boundary; (2) river temperature at the upstream boundary; (3) number and spacing of meshpoints in each reach; (4) top widths of the river at selected stations along the river; (5) main stem river flow rates at selected locations and tributary inflows; (6) weather conditions at suitable locations along or close to the stream including air temperature, wind speed, relative humidity, cloud cover, cloud height, visibility, atmospheric pressure, and solar radiation; and (7) thermal discharges into the river from power plants and other sources. It was assumed that flow rates, climatological data, and top widths varied linearly between measuring stations, and linear interpolation was used to distribute these variables from the measuring stations to each meshpoint.

## THERMAL REGIMES

The thermal regimes of the study reach for the months of February, May, August, and November were computed by the ITRM. In addition to the assumptions mentioned previously, additional assumptions were made for the interpretation and use of the Missouri River data as follows:

1. The upstream boundary condition temperatures at the Iowa-Missouri border (Mile 553) were obtained from reference [5].
2. Thermal impacts of tributary streams were neglected.
3. For the determination of future permissible power plants, temperature increases are considered relative to the natural-temperature base.
4. All existing, future proposed, and future permissible power plants operate at full load, and load capacity factors are not considered.
5. As noted in reference [5], Cooper No. 2 and 3, future units at Brownville, Nebraska, will be required to use closed-cycle cooling.

Four temperature profiles corresponding to average meteorological and hydrological conditions for each study month were predicted. (1) natural thermal regime of the river; (2) temperature distributions with existing heat loads (as of January 1975); (3) temperature distributions with existing and future proposed power plants; (4) temperature distributions with permissible new power plants which could be installed without violating present thermal standards.

The locations and sizes of future permissible plants were determined from the natural-temperature base. The sites were chosen arbitrarily, avoiding reaches already heavily loaded thermally, and spaced approximately 100 miles apart.

## PRESENTATION AND DISCUSSION OF RESULTS

The temperature distributions corresponding to average flow and weather conditions for the months of February, May, August, and November with the permissible future plants determined from the natural-temperature base were computed. The temperature distributions for the month of November are shown in Fig. 2. These curves are typical of the thermal regimes for all the study months which are given in reference [2]. It is seen that there is no more heat assimilation capacity of the river in the vicinity of Kansas City. Upstream from Kansas City no additional future power plants using open-cycle cooling are possible because they will cause temperature violations at downstream locations. Three sites are chosen well downstream from Kansas City for permissible new plants. At each site the maximum allowable plant capacity is found for each of the study months, and the future permissible capacity is taken as the lowest value for the four months. The permissible capacities of fossil-fueled power plants at the three sites are

(1) Mile 230.5 - 1980 MW, (2) Mile 113.1 - 2860 MW, and (3) Mile 19.1 - 1150 MW. If the plants were nuclear fueled, the permissible capacities would be reduced, because of efficiency differences, by about 31 percent to (1) 1370 MW, (2) 1970 MW, and (3) 790 MW.

The temperature distributions corresponding to the 7-day, 10-year low flow, combined with average weather conditions for the months of August and November and with the permissible future plants based on natural temperature is shown in Fig. 3. The figure shows that existing power plants in the vicinity of Brownville, Kansas City, and Sibley will violate the 5°F excess temperature limitation; the future proposed plants at Brownville, Iatan, and Nearman will violate the criterion also if it is assumed that they operate at full load. Closed-cycle cooling systems will be required during low flow conditions at these plants unless they operate at less than full capacity.

Owing to the rapid decay of temperature during low flow conditions some new plants may be permitted downstream from Kansas City. The allowable capacity at Mile 230.5 is 290 MW for a fossil-fueled unit or 200 MW for a nuclear-fueled unit; at Mile 19.9 the permissible capacity is 1000 MW - fossil or 690 MW - nuclear.

#### CONCLUSIONS

Steam-electric power plants will continue to play an important role in the power industry because of the increasing need of energy in the future. However, more stringent environmental regulations concerning waste heat released from power plants demand a better understanding of the thermal regimes and the heat assimilation capacity of rivers, particularly for the planning of future plants employing open-cycle cooling. The Iowa Thermal Regime Model can predict temperature distributions in a river downstream from imposed thermal loads provided that specific hydrological, meteorological, and geometrical parameters describing the river are known. This model was employed to show that the reach of the Missouri River bordering or crossing the state of Missouri can be used for once-through cooling of future power plants based on present thermal standards.

The total permissible future plant capacity for this reach of the river is about 6000 MW for fossil plants at average flow conditions and about 1300 MW for fossil plants at the 7-day, 10-year low flow condition. Permissible capacities of nuclear plants are reduced by about 31 percent to about 4100 MW for average flow conditions and to about 900 MW for low flow conditions.

The vicinity of Kansas City already is heavily loaded thermally. If the natural-temperature base is used, no additional future once-through-cooled power plants are permissible upstream of Kansas City because they would cause temperature violations at downstream locations.

If thermal standards were based on the 7-day, 10-year low flow, the total permissible plant capacity would be reduced by about 78 percent.

## ACKNOWLEDGEMENT

This project was financed in part by a grant from the U.S. Department of the Interior, Office of Water Research and Technology under Public Law 88-379 as amended, and made available through the Iowa State Water Resources Research Institute. Funds for computer time were provided by the Graduate College of The University of Iowa.

## APPENDIX

### List of Utilities and Abbreviations

|       |  |
|-------|--|
| CEPC  | Central Electric Power Co-op.                |
| KCBPU | Kansas City (Kan.) Board of Public Utilities |
| KCPL  | Kansas City (Mo.) Power & Light Co.          |
| MPS   | Missouri Public Service Co.                  |
| NPPD  | Nebraska Public Power District               |
| SJLP  | St. Joseph Light & Power Co.                 |
| UEC   | Union Electric Co.                           |

### LIST OF REFERENCES

1. Utility Water Act Group , "Biological Effects of Once-Through Cooling," Vol. 1, Introduction: Principles of Quantitative Impact Assessments, Vol. 4, Rivers and Reservoirs, submitted to U.S. Environmental Protection Agency, June 1978.
2. Giaquinta, A.R. and Keng, T.T.C., "Thermal Regimes of the Mississippi and Missouri Rivers Downstream from the Southern Iowa Border," IIHR Report No. 211, Iowa Institute of Hydraulic Research, The University of Iowa, Iowa City, Iowa, January 1978.
3. Federal Power Commission, "Steam-Electric Plant Air And Water Quality Control Data" (for the year ended December 31, 1973 based on FPC Form No. 67) Summary Report, FPC-S-253, Federal Power Commission, Washington, D.C., January 1976.
4. Paily, P.P. and Kennedy, J.F., "A Computational Model for Predicting the Thermal Regimes of Rivers," IIHR Report No. 169, Iowa Institute of Hydraulic Research, The University of Iowa, Iowa City, Iowa, November 1974.
5. Paily, P.P., Su, T.Y., Giaquinta, A.R., and Kennedy, J.F., "The Thermal Regime of the Upper Mississippi and Missouri Rivers," IIHR Report No. 182, Iowa Institute of Hydraulic Research, The University of Iowa, Iowa City, Iowa, October 1976.
6. Giaquinta, A.R. and Keng, T.T.C., "Thermal Regimes of the Middle and Lower Mississippi River During Low Flow Conditions," to be presented at the ASME Winter Annual Conference, San Francisco, California, December 10-15, 1978.

TABLE I

## SUMMARY OF MONTHLY MEAN VALUES OF DAILY FLOW RATES

| Gaging Station | River Mile | Mean Daily Flow Rates in cfs |        |        |        |        |
|----------------|------------|------------------------------|--------|--------|--------|--------|
|                |            | Averaging Period             | Feb.   | May    | Aug.   | Nov.   |
| Nebraska City  | 562.6      | 1956-74                      | 22,272 | 42,101 | 39,494 | 34,033 |
| Rulo           | 498.0      | 1956-74                      | 23,910 | 45,184 | 40,843 | 35,733 |
| St. Joseph     | 448.2      | 1956-74                      | 25,209 | 47,544 | 42,459 | 36,486 |
| Kansas City    | 366.1      | 1956-74                      | 31,696 | 59,134 | 49,047 | 42,935 |
| Waverly        | 294.4      | 1956-74                      | 32,040 | 59,884 | 49,108 | 43,506 |
| Boonville      | 196.6      | 1956-74                      | 39,613 | 71,237 | 53,546 | 50,576 |
| Hermann        | 97.9       | 1956-74                      | 53,621 | 99,149 | 61,151 | 63,073 |

TABLE II

## EXISTING POWER PLANTS ALONG THE LOWER MISSOURI RIVER

| POWER PLANT |                   | LOCATION        |            | INSTAL.            | CONDENSER FLOW      |                 |
|-------------|-------------------|-----------------|------------|--------------------|---------------------|-----------------|
| Utility     | Name              | City, State     | River Mile | Rated Capacity MWe | Quantity cfs        | Temp. Rise °F   |
| NPPD        | Cooper            | Brownville, NE  | 532.5      | 810 (N) a          | 1455                | 18              |
| SJLP        | Edmond St. #4,5,7 | St. Joseph, MO  | 449        | 51                 | 129.2               | 13              |
| SJLP        | Lake Road #1      | St. Joseph, MO  | 446        | 15                 | 47.8                | 18.3            |
|             | #2                |                 |            | 20                 | 62.3                | 12.2            |
|             | #3                |                 |            | 12.5               | 44.6                | 14.5            |
|             | #4                |                 |            | 90                 | 114.6               | 17.2            |
| KCBPU       | Quindaro #2       | Kansas City, KN | 374        | 94.5               | 262                 | 14              |
|             | #3                |                 |            | 239.1              | 340                 | 14.3            |
| KCBPU       | Kaw <sup>b</sup>  | Kansas City, KN | 367.5      | 161.3              | 273                 | 15.9            |
| KCPL        | Grand Ave.        | Kansas City, MO | 365.7      | 126.7              | 145.6 <sup>c</sup>  | 18 <sup>c</sup> |
| KCPL        | Northeast         | Kansas City, MO | 364.4      | 88                 | 101.8 <sup>c</sup>  | 18 <sup>c</sup> |
| KCPL        | Hawthorn          | Kansas City, MO | 358.3      | 910.1              | 1045.7 <sup>c</sup> | 18 <sup>c</sup> |
| MPS         | Sibley #1,2       | Sibley, MO      | 336.4      | 100                | 133                 | 19.2            |
|             | #3                |                 |            | 418.5              | 393                 | 17.5            |
| CEPC        | Chamois           | Chamois, MO     | 117        | 67.7               | 106.9               | 15              |
| UEC         | Labadie           | Labadie, MO     | 57.6       | 2482               | 1676                | 29.7            |

a N=Nuclear, all other units are fossil

b Plant located on the Kansas River close to Missouri River

c Assumed condenser temperature rise and calculated condenser flow rate

TABLE III

FUTURE PROPOSED POWER PLANTS ALONG THE LOWER MISSOURI RIVER

| POWER PLANT |             | LOCATION       |            | INSTALLATION                   |                        |                             | CONDENSER FLOW   |                 | SCHEDULED IN-SERVICE DATE |
|-------------|-------------|----------------|------------|--------------------------------|------------------------|-----------------------------|------------------|-----------------|---------------------------|
| Utility     | Name        | City, State    | River Mile | Rated Capacity MW <sub>e</sub> | Fuel Type <sup>a</sup> | Cooling System <sup>d</sup> | Quan. cfs        | Temp. Rise °F   |                           |
| NPPD/OPPD   | Cooper #2   | Brownville, NE | 532.5      | 1150                           | N                      | OTF                         | 2066             | 18 <sup>b</sup> | /85                       |
|             | Cooper #3   |                |            | 1300                           | N                      | OTF                         | 2335             | 18 <sup>b</sup> | 5/89                      |
| KCPL/SJLP   | Iatan #1    | Iatan, MO      | 411        | 630                            | F                      | OTF                         | 746              | 18.7            | 4/80                      |
|             | Iatan #2    |                |            | 630                            | F                      | OTF                         | 746              | 18.7            | 4/81                      |
| KCBPU       | Nearman #1  | Nearman, KN    | 380        | 235                            | F                      | OTF                         | 270 <sup>c</sup> | 18 <sup>c</sup> | 4/79                      |
|             | Nearman #2  |                |            | 300                            | F                      | OTF                         | 345 <sup>c</sup> | 18 <sup>c</sup> | 4/83                      |
| UEC         | Callaway #1 | Fulton, MO     | 128        | 1188                           | N                      | NDCT                        | 1220             | 30              | 10/81                     |
|             | Callaway #2 |                |            | 1188                           | N                      | NDCT                        | 1220             | 30              | 4/83                      |

a F = Fossil; N = Nuclear

b Assumed same condenser temperature rise and efficiencies as Cooper #1

c Assumed condenser temperature rise and calculated condenser flow rate

d OTF = Once-through fresh; NDCT = Natural draft cooling tower

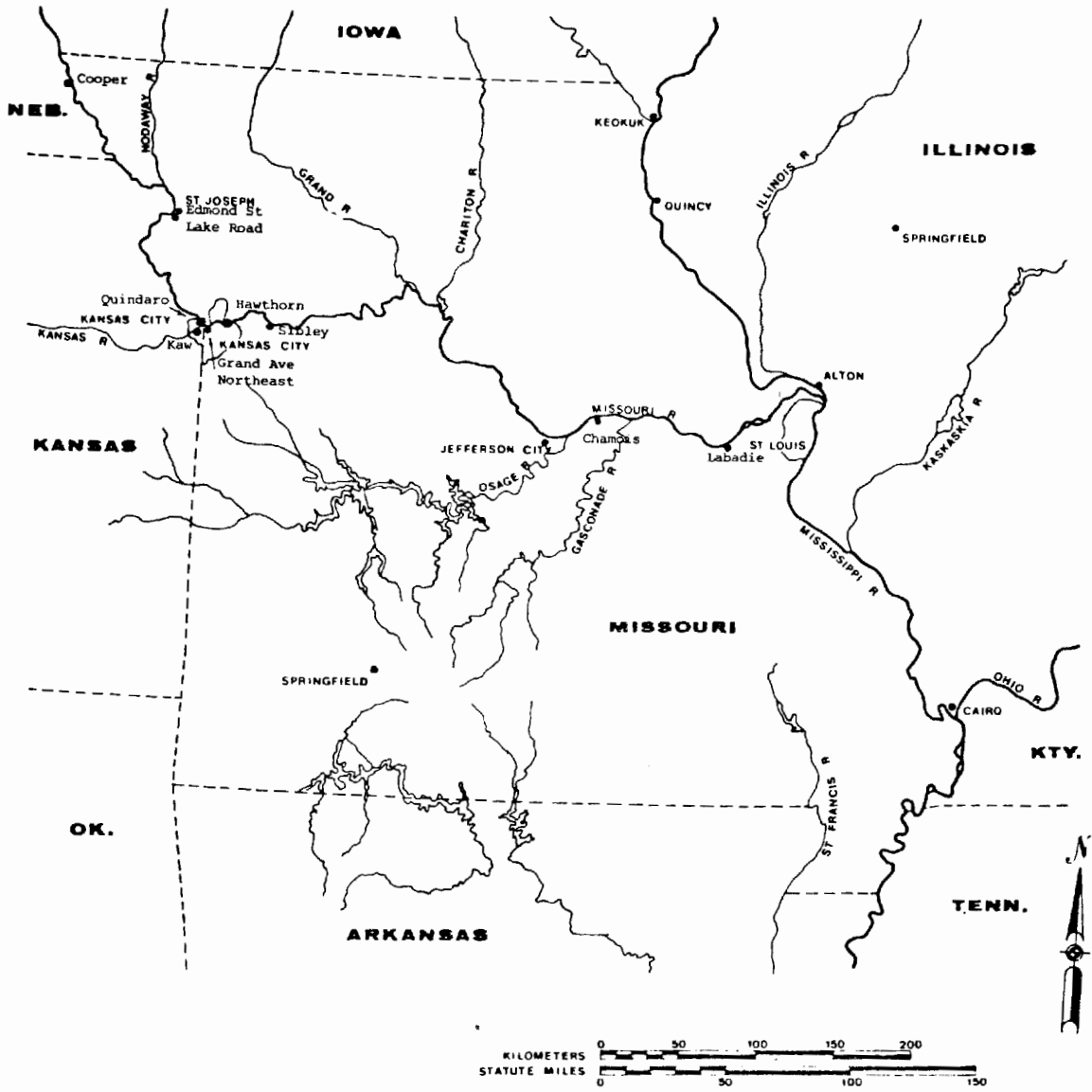


Figure 1. Location of Existing Thermal Power Plants Along the Lower Missouri River

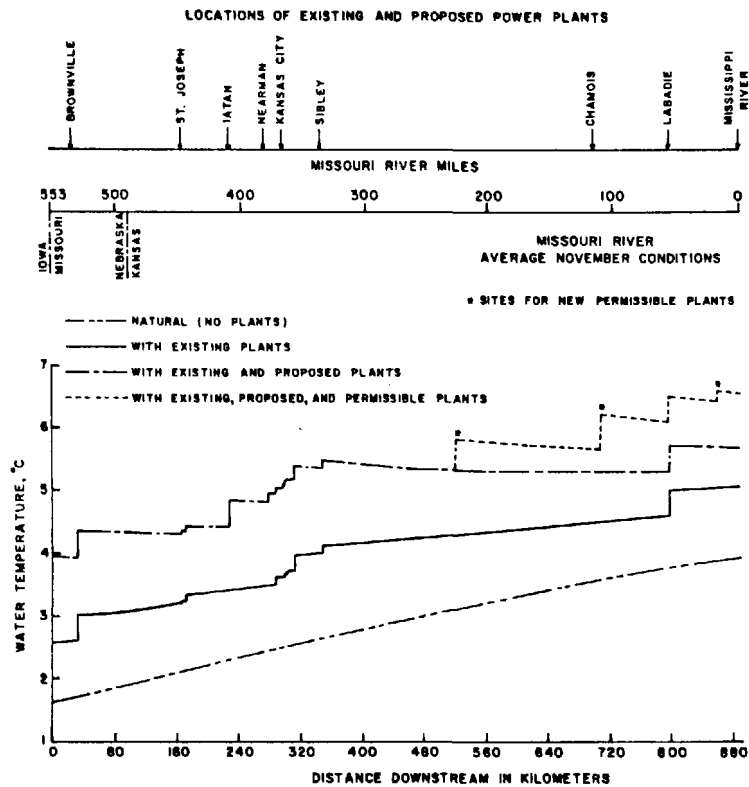


Figure 2. Temperature Distributions for Average November Conditions with Permissible New Plants Determined from the Natural-Temperature Base

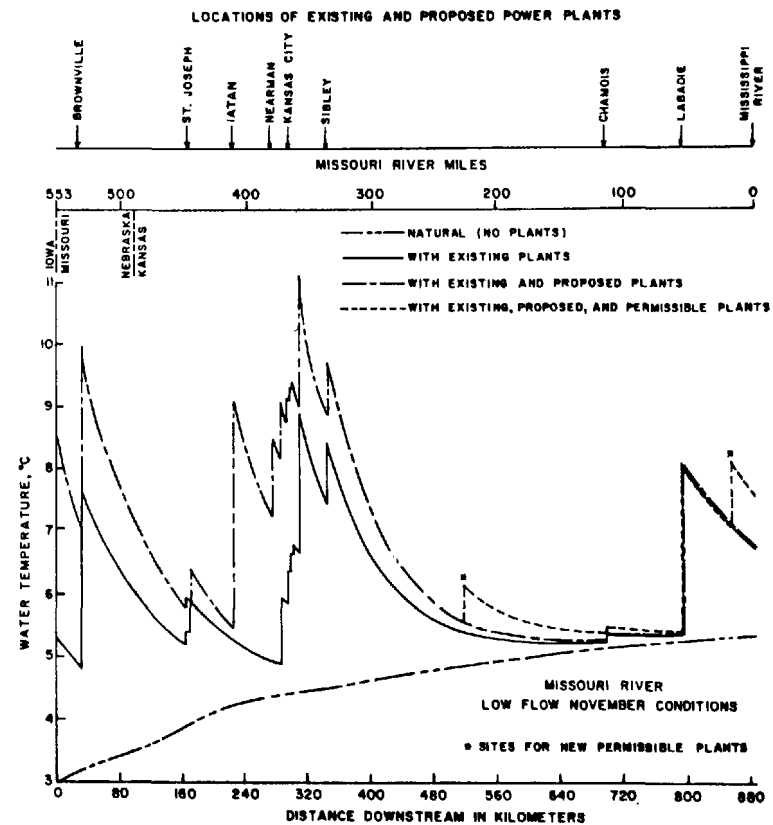


Figure 3. Temperature Distributions for Low Flow November Conditions with Permissible New Plants Determined from the Natural-Temperature Base

A MODEL FOR PREDICTION OF  
EVAPORATIVE HEAT FLUX IN LARGE BODIES OF WATER

A.M. Mitry  
Duke Power Company  
Charlotte, NC 28242, U.S.A.

B.L. Sill  
Department of Civil Engineering  
Clemson, SC 29631, U.S.A.

ABSTRACT

In earlier papers [1,2], one and two dimensional analytical models have been developed for the prediction of seasonal variation of the temperature distribution in large bodies of water. The one dimensional model, along with field data are used to evaluate various wind speed functions (used in calculating  $T_e$  and  $K'$  and evaporative heat flux) to determine their overall effect on temperature profiles in stratified lakes. Results indicate that temperature prediction is very insensitive to the particular wind speed function employed. Based on this conclusion, a direct and straightforward method which utilizes the model, but completely independent of wind speed function, is proposed to calculate evaporation from large, natural bodies of water. The method is applied to predict a daily evaporative heat flux from Lake Belews, N.C. The results agree well with the field data available.

INTRODUCTION

Evaporation from large bodies of water such as lakes is a topic of much current interest. Despite a large amount of work regarding the prediction of evaporation, the current state of practical predictions unfortunately is not completely satisfactory. Many predictive techniques assume that the evaporative flux is proportional to the vapor pressure difference between the water surface and the air, that is  $q_e = f(e_s - e_a)$ . The proportionality coefficient is usually a function of the wind speed only. Many different wind speed functions,  $f$ , have been proposed; these vary surprisingly in functional form and more importantly, in value. In the present work we first study the effect of wind speed function on the temperature profile of the body of water. Different wind speed functions are used to compute surface heat exchange coefficients and surface equilibrium temperatures. Such results are used in a previously reported analytical model [1] to predict the seasonal variation of temperature distribution in a natural stratified lake (no artificial heat load). It is found that lake temperature prediction is quite insensitive to the ultimate choice of wind speed function. This conclusion leads to the second portion of the study in

which a direct energy balance method is proposed to calculate evaporation from bodies of water.

## ANALYSIS

### Water Temperature

The analytical model used here has been presented in earlier papers [1,2] and verified with the field data from Cayuga Lake, New York. The model has been developed for the prediction of the seasonal variation of the temperature distribution in large stratified bodies of water. The analysis used in developing the model will be briefly outlined. The two-layer model consists of:

- (i) A well-mixed upper layer in the region  $0 \leq z \leq h$  where the vertical temperature distribution is considered uniform and taken as  $T_s$ .
- (ii) A lower layer in the region  $h \leq z \leq H$  where the temperature varies from  $T_s$  at  $z = h$  to a constant value  $T_H$  at the bottom of the lake where  $z = H$ .

The governing equations are taken as

$$\rho C_p \frac{\partial T}{\partial t} = - \frac{\partial}{\partial z} (q + q_r) \quad \text{in} \quad 0 \leq z \leq H \quad (1)$$

where

$$T \equiv T_s(t) \quad \text{in} \quad 0 \leq z \leq h(t) \quad (1a)$$

$$T \equiv T(z,t) \quad \text{in} \quad h(t) \leq z \leq H \quad (1b)$$

with the boundary conditions

$$T = T_H \quad \text{at} \quad z = H \quad (1c)$$

$$q = q_r = 0 \quad \text{at} \quad z = H \quad (1d)$$

In addition the net heat transfer flux at the surface,  $q_s$  is represented in the form [3]

$$q_s = K'(T_e - T_s) \quad (1e)$$

Here  $T$  is the temperature,  $t$  is the time,  $q$  and  $q_r$  are the turbulent and radiative heat fluxes respectively,  $z$  is the vertical coordinate measured from the surface,  $\rho$  is the density,  $C_p$  is the specific heat,  $K'$  is the surface heat exchange coefficient and  $T_s$  is water surface temperature. The annual variation of the equilibrium temperature  $T_e$ , is represented [4] as

$$T_e = \bar{T}_e + \Delta T_e \sin(\Omega t + \phi) \quad (2)$$

where  $\bar{T}_e$  is an average value,  $\Delta T_e$  is half of the annual variation,

$\Omega = 2\pi/365 \text{ day}^{-1}$  and  $\phi$  depends upon the conditions from which the computations begin.

A dimensionless temperature  $\theta(\eta)$  is defined for the lower layer as

$$\theta(\eta) = \frac{T_s(t) - T(t)}{T_s(t) - T_H} \quad , \quad \text{in} \quad h(t) \leq z \leq H \quad (3)$$

where

$$\eta = \frac{z - h(t)}{H - h(t)} \quad , \quad \text{in} \quad h(t) \leq z \leq H \quad (4)$$

The temperature profile  $\theta$  is represented by

$$\theta(\eta) = 3\eta - 3\eta^2 - \eta^3 \quad , \quad \text{in} \quad 0 \leq \eta \leq 1 \quad (5)$$

which satisfies the boundary conditions

$$\theta = 0 \quad , \quad \frac{d^2\theta}{d\eta^2} = 0 \quad \text{at} \quad \eta = 0 \quad (5a)$$

$$\theta(\eta) = 1 \quad , \quad \frac{d\theta}{d\eta} = 0 \quad \text{and} \quad \frac{d^2\theta}{d\eta^2} = 0 \quad \text{at} \quad \eta = 1 \quad (5b)$$

clearly if  $T_s(t)$  and  $h(t)$  are known the corresponding  $\eta$  and  $\theta(\eta)$  are determined from Eqs. (4) and (5) respectively, and the temperature distribution  $T(t,z)$  in the lower layer from Eq. (3).

Two equations that are needed for the determination of  $T_s(t)$  and  $h(t)$  are then derived from the energy Eq. (1). The turbulent heat transfer  $q$  can be related [4,5,6] to the wind stress acting on the water surface by making use of the fact that thermal stratification in a lake acts as a barrier to mixing while the wind stress creates turbulence that acts against the buoyancy gradient. Therefore, a mechanical energy balance in the water relates the kinetic energy input from the wind directly to the transformation of the potential energy into kinetic energy by convection within the layer if the turbulent energy dissipation due to viscosity is neglected; the kinetic energy input into the water is then related to the wind stress at the water surface [5,6]. With an analysis based on these considerations it can be shown that the turbulent heat flux  $q$  is related to the wind stress  $\tau_s$  at the surface by [4,5-8]

$$\int_0^H \frac{q}{\rho C_p} dz \approx \frac{W^*}{\delta g \psi} \quad (6)$$

where  $W^* = \sqrt{\tau_s/\rho}$  is the friction velocity,  $\delta$  is the coefficient of volumetric expansion of water,  $g$  is the gravitational acceleration and  $\psi$  is von Karman constant ( $\psi \approx 0.4$ ). The determination of the radiative heat flux,  $q_r$ , however, requires the solution of the equation of radiative transfer over the entire depth of the lake. The radiation part of the problem

to account for the bulk heating of the water due to the penetration of the solar radiation is treated by considering a plane parallel, absorbing, emitting, isotropically scattering gray medium with azimuthal symmetry. The  $P_1$ -approximation for the spherical harmonics method is used to solve the radiation problem. In this method the equation of radiative transfer takes the form [9]

$$\frac{d^2 G}{d\tau^2} - K^2 G(\tau) = -4K^2 \sigma T(\tau, t) \quad \text{in } 0 \leq \tau \leq \tau_0 \quad (7)$$

where

$$K^2 = 3(1 - \omega)$$

$\omega$  is the single scattering albedo,  $\tau = \beta z$  is the optical variable,  $\sigma$  is the Stefan Boltzmann constant and  $T(\tau, t)$  is the temperature distribution in the lake. Once the function  $G(\tau)$  is known from the solution of Eq. (7) subject to appropriate boundary conditions, the net radiative heat flux  $q_r(\tau)$  is determined from

$$q_r(\tau) = -\frac{1}{3} \frac{dG(\tau)}{d\tau} \quad (8)$$

For most lakes the source term on the right hand side of Eq. (8) is very small compared to the solar radiation energy incident on the lake surface. Then Eq. (7) is simplified as

$$\frac{dG(\tau)}{d\tau^2} - K^2 G(\tau) = 0 \quad \text{in } 0 \leq \tau \leq \tau_0 \quad (9)$$

The boundary conditions for this equation are established assuming that the solar radiation incident on the lake surface is specified and that no radiation is coming from the bottom of the lake. With this consideration the boundary conditions for Eq. (9) are taken in the Marshak boundary condition approximation as [9]

$$G(\tau) - \frac{2}{3} \frac{dG(\tau)}{d\tau} = 4\pi[\bar{I} + \Delta I \sin(\Omega t + \phi')], \quad \tau = 0 \quad (10a)$$

$$G(\tau) + \frac{2}{3} \frac{dG(\tau)}{d\tau} = 0, \quad \tau = \tau_0 \quad (10b)$$

The boundary condition (10a) assumes that the annual variation of the intensity  $I$  of the solar radiation incident on the water surface is specified [10,17] as

$$\bar{I} + \Delta I \sin(\Omega t + \phi')$$

where  $\bar{I}$  is an average value and  $\Delta I$  is half of the annual variation of the solar radiation intensity,  $\Omega = 2\pi/365 \text{ day}^{-1}$  and the value of  $\phi'$  depends on the conditions at the start of computations.

The solution of Eq. (9) subject to the boundary conditions (10) is straightforward. Knowing  $G(\tau)$ , the net radiative heat flux  $q_r(\tau)$  is obtained from Eq. (8) as

$$q_r(\tau) = \frac{\frac{4}{3} \pi K [\bar{I} + \Delta I \sin(\frac{2\pi}{365} t + \phi')]}{\frac{4}{3} K \cosh(K\tau_0) + (1 + \frac{4}{9} K^2) \sinh(K\tau_0)}$$

$$\{ [\cosh(K\tau_0) + \frac{2}{3} K \sinh(K\tau_0)] \cosh(K\tau) -$$

$$- [\sinh(K\tau_0) + \frac{2}{3} K \cosh(K\tau_0)] \sinh(K\tau) \} \quad (11)$$

Noting that  $\tau = \beta z$  and  $\tau_0 = \beta H$  we can write

$$\int_0^H q_r dz = \frac{\pi [I + \Delta I \sin(\frac{2\pi}{365} t + \phi')] \cdot \{ \tanh(K\beta H) + \frac{2}{3} K [1 - \frac{1}{\cosh(K\beta H)}] \}}{\beta K + (\frac{3}{4} + \frac{1}{3} K^2) \beta \tanh(K\beta H)} \quad (12)$$

Taking zeroth\* and first\*\* moments of Eq. (1) over the entire depth of the lake and making use of Eqs. (1e), (3), (4), (5), (11) and (12) and after some manipulation the desired two equations respectively become,

$$(H - \alpha H + \alpha h) \frac{dT_s}{dt} + \alpha (T_s - T_H) \frac{dh}{dt} = \frac{K'}{\rho C_p} (T_e - T_s) \quad (13)$$

$$[(\alpha - \gamma)h^2 + H(2\gamma - \alpha)h + H^2(\frac{1}{2} - \gamma)] \frac{dT_s}{dt} +$$

$$+ [2(\alpha - \gamma)h + 2(\gamma - \alpha)H] \cdot (T_s - T_H) \frac{dh}{dt} = \frac{W^*3}{\delta g \psi} +$$

$$+ \frac{\pi [\bar{I} + \Delta I \sin(\frac{2\pi}{365} t + \phi')] \cdot \{ \tanh(K\beta H) + \frac{2}{3} K [1 - \frac{1}{\cosh(K\beta H)}] \}}{\rho C_p [\beta K + (\frac{3}{4} + \frac{1}{3} K^2) \beta \tanh(K\beta H)]} \quad (14)$$

where  $\alpha = \int_0^1 \theta(\eta) d\eta = 0.75$

and  $\gamma = \int_0^1 \eta \theta d\eta = 0.45$

\* Integrate Eq. (1) from  $z = 0$  to  $z = H$ .

\*\* Multiply Eq. (1) by  $z$  and then integrate from  $z = 0$  to  $z = H$ .

Equations (13 and (14) provide two coupled, first order nonlinear ordinary differential equations for the determination of the temperature  $T_s(t)$  in the upper layer and the depth  $h(t)$  of the thermocline. A computer program based on a Runge Kutta method was developed to solve those two equations numerically. Then the temperature distribution is determined by Eqs. (3), (4) and (5) and the net heat flux,  $q_s$  at the surface by Eq. (1e).

### Equilibrium Temperature and Heat Exchange Coefficient

It is obvious from the above analysis that expressions for the equilibrium temperature  $T_e$  and the heat exchange coefficient  $K'$  are essential to the prediction of water temperature and the net heat flux at the surface. Various techniques for calculating  $T_e$  and  $K'$  have been presented in the literature and most of the approaches are similar. The procedure given by Ryan and Harleman [11] is used to yield the following expressions.

$$T_e = \frac{(q_{sw} + q_{lw}) + f(bT_d + 0.142 T_a) - 73.3}{1.30 + f(b + 0.142)}, \quad ^\circ\text{C} \quad (15)$$

$$K' = 1.30 + f(b_s + 0.142), \quad \text{cal/m}^2/\text{s}/^\circ\text{C} \quad (16)$$

where  $q_{sw}$  is the short wave solar radiative heat flux specified from meteorological data or calculated [11]. The long wave solar radiative heat flux  $q_{lw}$  and the constant  $b$  are respectively expressed as [11],

$$q_{lw} = (1.24 \times 10^{-13})(T_a + 273)^6 (1 + 0.172 C^2), \quad \text{cal/m}^2/\text{sec} \quad (17)$$

$$b = \frac{134,000}{(T^*)^2} \exp(17.62 - \frac{5300}{T^*}), \quad \frac{\text{mmHg}}{^\circ\text{C}} \quad (18a)$$

$$b_s = \frac{134,000}{(T_s^*)^2} \exp(17.62 - \frac{5300}{T_s^*}), \quad \frac{\text{mmHg}}{^\circ\text{C}} \quad (18b)$$

$$T^* = \frac{T_s + T_d}{2} + 273, \quad ^\circ\text{K} \quad (19a)$$

$$T_s^* = \frac{T_s + T_e}{2} + 273, \quad ^\circ\text{K} \quad (19b)$$

$T_a$  and  $T_d$  are dry bulb and dew point temperatures,  $C$  is the cloud cover in tenths and  $f$  is a specified wind speed function discussed in the following section.

## Effect of Wind Speed Function on Predicted Water Temperatures:

The wind speed function  $f$ , is usually experimentally derived and taken as dependent on the wind speed  $W$ , over the water surface. A number of wind speed functions have been proposed by several investigators [11, 12, 31] and all yield somewhat different values of  $T_e$  and  $K'$ . The following, chosen for their widely differing forms, are the particular functions used here

$$f = 0.91 W \quad (\text{ref. 11})$$

$$f = 2.20 + 0.11 W^2 \quad (\text{ref. 12})$$

$$f = 0.78 (e_s - e_a)^{1/3} + \frac{48.9W}{(\text{Re}_L)^{.2}} \quad (\text{ref. 13})$$

In these expressions,  $f$  has the units of  $\text{cal/s/m}^2\text{mmHg}$ ,  $W$  is the wind speed in  $\text{m/s}$  measured at 8 meters, and  $(\text{Re}_L)$  is the air Reynolds number based on fetch  $L$  and the free stream velocity  $W$ .

As a first investigation, the analytical model described above for the prediction of water temperature [1,2] was used to perform a sensitivity analysis of the effect of the choice of wind speed function on the ultimate prediction of lake temperature (coupled through  $K'$  and  $T_e$ ). Monthly average, meteorological data at Greensboro, N.C. for the period 1941 - 1970, along with Ryan, Brady and Goodling wind speed functions [11, 12, 13] were used in the procedure above to calculate the equilibrium, dry bulb, dew point temperatures, the incident solar radiation, and the surface heat exchange coefficient. These were then accurately expressed in the following simple forms [4, 10],

$$T_e = \bar{T}_e + \Delta T_e \sin (\Omega t + \phi_1) \quad (20)$$

$$K' = \bar{K}' + \Delta K' \sin (\Omega t + \phi_2) \quad (21)$$

$$T_a = \bar{T}_a + \Delta T_a \sin (\Omega t + \phi_3) \quad (22)$$

$$T_d = \bar{T}_d + \Delta T_d \sin (\Omega t + \phi_4) \quad (23)$$

$$I = \bar{I} + \Delta I \sin (\Omega t + \phi_5) \quad (24)$$

where  $\bar{T}_e$ ,  $\bar{K}'$ ,  $\bar{T}_d$ , and  $\bar{I}$  are average values,  $\Delta T_e$ ,  $\Delta K'$ ,  $\Delta T_a$ , and  $\Delta I$  are half of the annual variation,  $\Omega = 2\pi/365$ ,  $t$  is the time in days and  $\phi_1$ ,  $\phi_2$ ,  $\phi_3$ ,  $\phi_4$ ,  $\phi_5$  are phase angles dependent upon the conditions from which the computations begin.

Three computations, each corresponding to a different wind speed function, were presented for input conditions that correspond to Lake Belews, N.C. with input data taken as

First run:

$$T_e = 16.21 + 13.45 \sin \left( \frac{2\pi}{365} t - 0.994 \right), \text{ } ^\circ\text{C}$$

$$K' = 293.10 + 86.67 \sin \left( \frac{2\pi}{365} t - 0.762 \right), \text{ kcal/m}^2\text{/day/}^\circ\text{C}$$

Second run:

$$T_e = 16.06 + 13.22 \sin \left( \frac{2\pi}{365} t - 0.999 \right) , \text{ } ^\circ\text{C}$$

$$K' = 299.77 + 94.13 \sin \left( \frac{2\pi}{365} t - 0.793 \right) , \text{ kcal/m}^2\text{/day/}^\circ\text{C}$$

Third run:

$$T_e = 15.97 + 12.83 \sin \left( \frac{2\pi}{365} t - 0.985 \right) , \text{ } ^\circ\text{C}$$

$$K' = 321.92 + 144.58 \sin \left( \frac{2\pi}{365} t - 0.815 \right) , \text{ kcal/m}^2\text{/day/}^\circ\text{C}$$

The dry bulb temperature, the dew point temperature and the incident solar radiation are

$$T_a = 14.50 + 10.69 \sin \left( \frac{2\pi}{365} t - 1.141 \right) , \text{ } ^\circ\text{C}$$

$$T_d = 8.19 + 10.56 \sin \left( \frac{2\pi}{365} t - 0.683 \right) , \text{ } ^\circ\text{C}$$

$$I = 3645.73 + 2058.86 \sin \left( \frac{2\pi}{365} t - 0.683 \right) , \text{ kcal/m}^2\text{/day}$$

The semi-empirical relation between the wind stress  $\tau_s$  at the surface and the wind speed given by Munk and Anderson [14] was used to evaluate the friction velocity  $W^*$ . The minimum temperature during spring homothermy was assumed to be  $5.83^\circ\text{C}$  and calculations were started for this temperature on Julian day 45 ( $t = 0$ ). The absorption and scattering coefficients for water and the particles in suspension were assumed to be  $1.017 \text{ m}^{-1}$  and  $2.06 \text{ m}^{-1}$  respectively, and the depth of the lake was taken as 30.48 m. Figure (1) shows a comparison of the predicted water temperatures corresponding to the various wind speed functions. Examination of the values indicated that temperature predictions are very insensitive to choice of wind speed function. Thus it is felt that in most situations, model predictions for temperature in a non-heat loaded body of water will depend only very slightly on the choice of  $f$ , a conclusion of importance to those researchers who employ mathematical models for temperature analysis of large bodies of water.

#### Calculation of Evaporation

Now after having demonstrated that lake temperature predictions are insensitive to the wind speed function, we are in a position to propose a straightforward method for calculating evaporative heat flux from an unheated lake without the necessity of selecting a particular form of  $f$ .

An energy balance for the water body yields

$$q_s = q_{sw} + q_{lw} - q_{br} - q_e - q_c \quad (25)$$

The conductive heat flux  $q_c$  is related to the evaporative heat flux,  $q_e$  by [11],

$$q_c = Bq_e \quad (26)$$

where the Bowen ratio  $B$  is defined as

$$B = \left(\frac{0.142}{b}\right) \cdot \left(\frac{T_s - T_a}{T_s - T_d}\right) \quad (27)$$

Combining Eqs. (25) and (26) yields the required equation to calculate evaporative heat flux.

$$q_e = \left(\frac{1}{1+B}\right) \cdot (q_{sw} + q_{lw} - q_{br} - q_s) \quad (28)$$

A first order expression of the Stefan-Boltzmann relation for back radiation from the water surface is [11]

$$q_{br} = 73 + 1.3 T_s(^{\circ}\text{C}) \quad , \quad \text{cal/m}^2/\text{s} \quad (29)$$

The surface temperature  $T_s$  is determined by using the analytical model as indicated in section 1.,  $q_s$  and  $q_{lw}$  are computed by Eqs. (1e) and (17) and  $q_{sw}$  is specified from meteorological data or calculated as given in Ref. 11.

Using this method, daily evaporation rates were calculated for the previous test case. The evaporations are plotted in Figure (2) and give an annual evaporation of 1.18 m compared with values of 1.02 m and 0.96 m in Ref. 15 and 16 respectively. Such favorable agreement gives confidence in the use of this technique for predicting evaporation rates from unheated large bodies of water.

## CONCLUSIONS

A previously developed [1] analytical model for lake temperature prediction was used to evaluate the sensitivity of wind speed function choice on predicted temperatures. Results indicate that the predictions were very insensitive to the particular wind speed function used. Next, this result was utilized to allow evaporation calculations via the energy budget approach. This technique is satisfactory only because the insensitivity of calculated lake temperatures to wind speed function allows proper calculation of energy budget terms (such as long wave back radiation) which depend on the water temperature. An application of this approach was presented and the agreement of predictions with field data is encouraging.

## NOMENCLATURE

$b$ , defined by Equation (18);

$B$ , Bowen ratio defined by Equation (27);

$C$ , cloud cover;

|            |  |
|------------|--|
| $q_{br}$ , | back radiative heat flux;                                  |
| $q_c$ ,    | conductive heat flux;                                      |
| $q_e$ ,    | evaporative heat flux;                                     |
| $q_{lw}$ , | long wave solar radiative heat flux;                       |
| $q_r$ ,    | radiative heat flux incident on the water surface;         |
| $q_s$ ,    | net heat flux at water surface;                            |
| $q_{sw}$ , | short wave solar radiative heat flux;                      |
| $w^*$ ,    | friction velocity = $\sqrt{\tau_s/\rho}$ ;                 |
| $z$ ,      | vertical distance measured downward from the lake surface. |

Greek Symbols:

|                  |  |
|------------------|--|
| $\alpha$ ,       | $\int_0^1 \theta(\eta) d\eta = 0.75$ ;             |
| $\delta$ ,       | coefficient of volumetric expansion of water;      |
| $\psi$ ,         | von Karman constant $\approx 0.4$ ;                |
| $\beta$ ,        | extinction coefficient;                            |
| $\phi$ ,         | phase angle;                                       |
| $\gamma$ ,       | $\int_0^1 \eta \theta d\eta = 0.45$ ;              |
| $\eta$ ,         | dimensionless variable defined by Equation (4)     |
| $\omega$ ,       | single scattering albedo;                          |
| $\rho$ ,         | density of water;                                  |
| $\sigma$ ,       | Stefan-Boltzmann constant;                         |
| $\tau$ ,         | optical variable = $\beta z$ ;                     |
| $\tau_0$ ,       | optical depth of the lake = $\beta H$ ;            |
| $\tau_s$ ,       | surface shear stress induced by the wind;          |
| $\theta(\eta)$ , | dimensionless temperature defined by Equation (3). |

|                |  |
|----------------|--|
| $C_p$ ,        | specific heat;   |
| $e_a$ ,        | saturated vapor pressure at the dry bulb temperature;        |
| $e_s$ ,        | saturated vapor pressure at the water surface temperature;   |
| $f$ ,          | windspeed function;  |
| $g$ ,          | acceleration due to gravity;                                 |
| $H$ ,          | depth of lake  |
| $h(t)$ ,       | depth of upper layer;  |
| $I$ ,          | intensity of solar radiation incident on the water surface;  |
| $\bar{I}$ ,    | average value of the solar radiation intensity;              |
| $\Delta I$ ,   | half of the annual variation of solar radiation intensity;   |
| $K'$ ,         | heat exchange coefficient at water surface;                  |
| $\bar{K}'$ ,   | average value of the heat exchange coefficient;              |
| $\Delta K'$ ,  | half of the annual variation of heat exchange coefficient;   |
| $t$ ,          | time;  |
| $T_a$          | dry bulb temperature;  |
| $T(z,t)$ ,     | temperature of the lower layer;                              |
| $\bar{T}_a$ ,  | average value of the dry bulb temperature;                   |
| $\Delta T_a$ , | half of the annual variation of dry bulb temperature;        |
| $T_d$ ,        | dew point temperature;                                       |
| $\Delta T_d$ , | half of the annual variation of dew point temperature;       |
| $T_e$ ,        | equilibrium temperature defined by Equation (2);             |
| $\bar{T}_e$ ,  | an average value of the equilibrium temperature;             |
| $\Delta T_e$ , | half of the annual variation of the equilibrium temperature; |
| $T_H$ ,        | temperature at the bottom of the lake;                       |
| $T_s(t)$ ,     | temperature of the upper layer (epilimnion);                 |
| $q$ ,          | turbulent heat flux;   |

## REFERENCES

1. A. M. Mitry and M. N. Özisik, "One-Dimensional Model for Seasonal Variation of Temperature Distribution in Stratified Lakes," International Journal of Heat and Mass Transfer, 19, 201-205 1976.
2. A. M. Mitry and M. N. Özisik, "A Two-Dimensional Time Dependent Model for Seasonal Variation of Temperature Distribution in Stratified Lakes," Letter in Heat and Mass Transfer, 3, 475-484 1976.
3. J. E. Edinger and J. C. Geyer, "Heat Exchange in the Environment," Sanitary Engineering and Water Resources Report, Johns Hopkins University, Baltimore, Maryland 1967.
4. T. R. Sundaram and R. G. Rehm, "Formation and Maintenance of Thermoclines in Stratified Lakes Including the Effect of Plant Thermal Discharges," AIAA Paper, No. 70-238, 1970.
5. T. Y. Li, "Formation of Thermocline in Great Lakes," Paper presented at the 13th Conference on Great Lakes Research, Buffalo, New York, 1970.
6. E. B. Kraus and J. S. Turner, "A One-Dimensional Model for the Seasonal Thermocline, II. The General Theory and its Consequences," Tellus, 19 (1), 98-105 1967.
7. O. M. Phillips, The Dynamics of Upper Ocean, pp. 198-243 Cambridge University Press, Cambridge, 1966.
8. A. S. Monin and M. M. Obukhov, "Basic Regularity in Turbulent Mixing in The Surface Layer of the Atmosphere," U.S.S.R. Acad. Sci. Works Geophys. Met. No. 24, 163, 1954.
9. M. N. Özisik, Radiative Transfer. John Wiley, New York, 1973.
10. Unpublished field data, Lake Belews, N.C., Environmental Section, Duke Power Company, Charlotte, N.C., 1973.
11. P. J. Ryan and D. R. F. Harleman, "Analytical and Experimental Study of Transient Cooling Pond Behavior," Ralph M. Parsons Laboratory, Dept. of Civil Engineering, Report No. 161, Massachusetts Institute of Technology, Cambridge, Mass., Jan. 1973.
12. Edinger, J. E., D. K. Brady, and J. C. Geyer, "Heat Exchange and Transport in the Environment," Report No. 14, Electric Power Research Institute, Research Project RP-49, Johns Hopkins University, Baltimore, Maryland, November, 1974.
13. J. S. Goodling, B. L. Sill, and W. J. McCabe, "An Evaporation Equation for an Open Body of Water Exposed to the Atmosphere," Water Resources Bulletin, Vol. 12, No. 4, August, 1976.

14. W. H. Munk and E. R. Anderson, "Notes on the Theory of Thermocline," Journal of Marine Research, 7, 276-295, 1948.
15. J. J. Geraghty, D. W. Miller, F. Van der Leeden, and F. L. Troise, Water Atlas of the United States, Water Information Center Publication, Port Washington, N.Y., 1973.
16. W. L. Yonts, G. L. Giese, and E. F. Hubbard, "Evaporation From Lake Michie, North Carolina, 1961-1971," U.S. Geological Survey Water-Resource Investigation, 38-73, 1974.
17. T. R. Sundaram, C. C. Eastbrook, K. Piech and G. Rudinger, "An Investigation of the Physical Effects of Thermal Discharges into Cayuga Lake," Report VT-2616-0-2, Cornell Aeronautical Laboratory, Buffalo, New York, 1969.

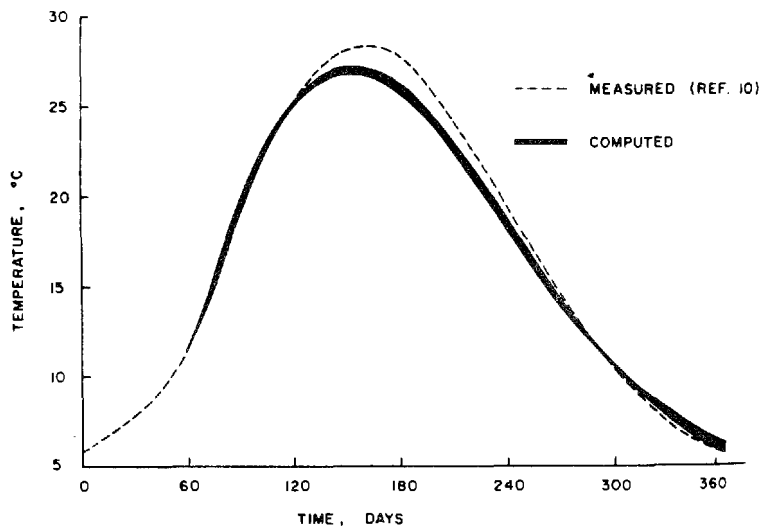


Fig. 1 Predicted surface water temperatures using three different wind speed functions (refs. 4, 5, 6) as compared with measurements.

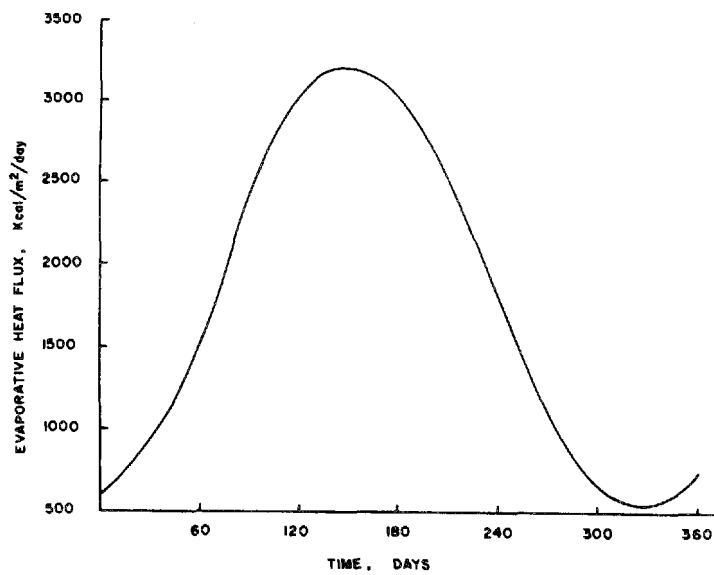


Fig. 2 Calculated evaporative heat flux for Lake Belews, North Carolina.

Second Conference  
on  
Waste Heat Management and Utilization  
WORKING SESSION W1 - MANAGEMENT AND UTILIZATION  
December 5, 1978

Co-chairmen: Theodore G. Brna, U.S. Environmental Protection Agency  
John Neal, U.S. Department of Energy

This session was divided into two parts: low grade (Part I) and high grade waste heat (Part II). Low grade waste heat was defined to apply to 93°C (200°F) and lower temperatures, while the high grade concerned waste heat available at temperatures above 93°C (200°F). Consequently, separate work session summaries, prepared by the co-chairmen in the order listed above, are presented below for these classifications.

PART I - Low Grade Waste Heat

The beneficial uses of this quality of waste heat include hot water district heating (with and without augmentation by heat pumps), agriculture, and aquaculture. Waste heat suppliers may be industries and power plants, while users could encompass the industrial, commercial and residential sectors.

The major constraint to low grade waste heat utilization was felt to be the lack of favorable economics. Thus, demonstrations of waste heat applications which are profitable and independent of government subsidies are needed. One mechanism for progressing toward successful demonstrations would be government-guaranteed loans, such as for waste heat aquaculture.

A suggestion that consideration of waste heat utilization alternatives be required as part of the permitting/licensing process for power plants received little comment. One utility representative opposed such a requirement on economic and scheduling grounds.

Relative to waste heat from steam-electric generating plants, the use of this resource as it is normally available seemed to be favored. Such use was seen as highly site dependent. Modification of plant operation to accommodate greater utilization of waste heat was viewed by some as enhancing a secondary benefit while lowering electrical output, the primary product. Use of this cogeneration concept could also adversely affect plant reliability because of two different outputs with variable demands.

Governmental regulation of fuel prices was pointed out to be an inhibitor to the use of heat pumps. Deregulation of fuel prices was suggested as necessary for making heat pumps economically feasible in low grade waste heat applications, particularly district heating.

Further consideration of governmental regulation concerned several areas. The consensus of those present was that environmental regulations should provide offsets for the beneficial uses of waste heat. One approach would be to permit exceptions to environmental standards to encourage the overall reduction of pollutants in a region via a less than proportionate increase in pollutants in the locale of the waste heat source. State rate regulatory agencies in not recognizing waste heat utilization as an energy conservation measure impede beneficial uses of waste heat. Some of the utility participants indicated that the support of waste heat research and development projects by utilities may adversely impact requests by utilities to these agencies as these projects are non-income generating and non-electrical generation activities.

## **PART II - High Grade Waste Heat**

High Grade Waste Heat Recovery was in general defined to include process heat cogeneration as opposed to the low grade heat definition which emphasized both beneficial uses of waste heat and district heating. Concern was expressed by various workshop participants that district heating should be categorized in high grade heat and separated for the purpose of management and planning, from the broader area of beneficial uses of waste heat. It was acknowledged by the chairman that for future meetings or policy decisions on this subject, it would be better to consider both process heat industrial cogeneration and residential/commercial district heating cogeneration together.

Three problem areas, or issues, were brought up for discussion by the group. These were: 1) should cogenerators be exempted from coal conversion, 2) should industrial cogenerators be regulated as utilities, and 3) what is the best way of permitting excess power to be sold back to the utilities from industrial cogenerators?

With regard to the first of these, concern was expressed that if exemption were granted unilaterally for cogeneration, many units "called cogeneration" would be installed just to promote the exemption. As a result the nation would not necessarily benefit from the potential national savings afforded by well planned cogeneration systems. After some discussion it was concluded by the chairman that great care should be taken in formulating the language for any such exemption since it is one of our primary goals in energy planning to move toward the use of more readily available domestic resources, such as coal and uranium.

Secondly, the group discussed the issue of regulation as to whether cogenerators should be regulated as utilities. Utility members of the

audience were very specific in their views that PUC Control should not extend to process steam. Examples were also given where cogenerators were considered municipal utilities and therefore not subject to PUC regulation.

The third topic concerned the best way of permitting excess power to be sold back by a cogenerator to the utility grid. In general the utility members of the group thought this would be a minimal problem. They were of the opinion that the net transfer of electricity would remain predominately from the utility to the industrial. It was more or less unanimously felt that the utility must remain in control of dispatching power. Bonneville Power in the Pacific Northwest cited their experience with cogeneration. They indicated that utility systems made up of a significant percentage of cogeneration, such as theirs, could be dispatched, power sold back and forth, etc., in a very acceptable manner. It was noted that Bonneville had large hydro capacity which eased the problem by in effect providing storage.

A more important problem than ownership or sellback was judged by the group to be the issue of standby power and its attendant charges. Several examples were given ranging from increased costs for standby due to cogenerators, to reduced cost of standby because of multiple cogenerators creating greater redundancy.

The conclusive remarks which seemed to receive overall endorsement by the group were to the effect that arrangements can be made without additional government or local regulations.

Additional discussions were then held on how the government could help. It was suggested by a group member who is involved now in cogeneration that the EPA could help the most by allowing an overall fuel efficiency credit in cogeneration emissions regulations. The entire group endorsed this concluding remark.

Second Conference  
on  
Waste Heat Management and Utilization  
WORKING SESSION W2  
ENVIRONMENTAL EFFECTS  
December 5, 1979

Co-Chairmen: C. Coutant, Oak Ridge National Laboratory,  
Oak Ridge, Tennessee  
R. Wilcox, Florida Power and Light Company,  
Miami, Florida

The working session on environmental effects were co-chaired by J. Ross Wilcox and Dan McKenzie on Tuesday, December 5, 1978. Approximately 41 persons were in attendance during all or part of the discussion period.

There were lively discussions centering around environmental effects of cooling water intake and thermal discharge systems. Most people felt that entrainment of zooplankton and phytoplankton was a non-problem; however, more review is required to determine the effects of entrainment on icythoplankton. Concerns were raised about the suitability of any baseline data set so that a natural perturbation or seasonal variations could be distinguished from a man-made perturbation. The question of mitigation was discussed as a means to soften an environmental impact. Many people were concerned about the continued standardization of techniques because one data set may be difficult or impossible to compare with another data set due to sampling gear differences. Suppression of data and its exchange was of concern to some individuals, but others countered that exchange of data among professionals is good and will improve when data banks are computerized and collected under the auspices of two or three national data centers.

Second Conference  
on  
Waste Heat Management and Utilization  
WORKING SESSION W3  
MATHEMATICAL MODELLING  
December 5, 1979

Co-Chairmen: D.R.F. Harleman, M.I.T., Cambridge, Massachusetts  
S. Sengupta, University of Miami, Coral Gables,  
Florida

Mathematical modelling is an attractive tool for predictive and diagnostic analyses of environmental effects of waste heat. The session was attended by approximately 30 people. The discussions were primarily related to physical effects and numerical techniques. However, some concerns regarding the state-of-the-art in biological modelling were expressed. A summary of the discussions is presented.

1. The merits of rigid-lid and free surface numerical-differential models for aquatic discharges were discussed. The rigid-lid models are appropriate for cooling lakes whereas free-surface models are more suited to coastal and estuarine domains. The discussion was in relation to three-dimensional models. More effort in calibration of 3-D models should be directed as computational costs become less prohibitive with more efficient numerical techniques and better computers.
2. Numerical matching between "near-field" and "far-field" regions of thermal discharges was perceived as a problem that needs more extensive investigation. Complete field models with horizontal stretching and variable diffusion coefficients is a direction of research that might avoid the problem of matching.
3. Open boundary conditions is a problem for almost all classes of mathematical models. The present techniques rely quite extensively on measured knowledge regarding flow fields and temperature and/or salinity distributions. Sensitivity analysis of existing models as a function of open boundary conditions is an useful direction for further research.
4. The state of the art in cooling tower plume models is somewhat more primitive than aquatic discharges. Integral models are being developed to include more complex physical effects. Basic research in determination of entrainment coefficients, mixing mechanisms and condensation processes is essential.
5. Lack of reliable data bases for verification of cooling tower plume models is also a problem. Extensive data bases under

diverse meteorological conditions are needed for evaluation of existing models and to provide bases for future model development.

6. The gap between the groups working in mathematical modelling of physical effects and biologists (the user community for physical data) is wide. Multidisciplinary demonstration projects may be a route to enhance greater exchange of information. It will also develop greater appreciation for cross-disciplinary needs.

Second Conference  
on  
Waste Heat Management and Utilization  
WORKING SESSION W4  
HEAT TRANSFER PROBLEMS IN WASTE HEAT  
MANAGEMENT AND UTILIZATION  
December 5, 1978

Co-Chairmen: W. Aung, National Science Foundation  
F. K. Moore, Cornell University

Research in heat transfer and related areas is necessary for the economic realization of various schemes for waste heat management and utilization. In recent years a number of symposia have been held in which heat transfer problems in waste heat technologies have received attention. These discussions were continued in one of the four workshop sessions held during the present conference. We list below a summary of the perceived research needs in heat transfer and related topics which if carried out would contribute towards effective waste heat management or utilization. Our sources are the recommendations provided at the latest workshop session. In addition we have also included some of the recommendations made at previous meetings of a similar nature.

- (1) There is a need to develop and understand the behavior of new heat exchanger surfaces for cooling tower applications. Cost and size reductions are important considerations in cooling tower designs and efforts in these directions are now limited by the existing heat exchanger technology. This field is in need of innovative new design concepts. New surfaces that are developed should be characterized not only in terms of thermal performance but also in terms of fluid flow fields and pressure drops.
- (2) More accurate information is needed on near-field plume behavior including the interaction of multiple plumes, the effect of atmospheric stratification, the factors leading to re-entrainment, etc. Better understanding in this field could lead to substantial savings in real estate and in transmission costs by making it possible to position towers closer together.
- (3) Methods of achieving flow uniformity over heat exchangers are needed especially for dry cooling towers. These methods should account for the movement of the ambient air since the dynamic pressure there is often of the same order of magnitude as the pressure drop across the heat exchanger.
- (4) There is a need to control and eliminate regions of separated

flow in cooling towers, sometimes evidenced as "cold inflow".

- (5) In relation to soil warming in waste heat utilization, improved methods for characterizing the transport of heat and moisture are needed. Laboratory experiments and theoretical simulation studies are both needed. Theoretical studies should not only focus on modelling through the use of the full transport equations but also on developing simplified mathematical models that are capable of elucidating important mechanisms.
- (6) The fouling properties of heat exchanger surfaces in cooling towers are in need of further understanding.
- (7) Novel experimental techniques should be exploited to provide detailed heat transfer information on new and existing surfaces of complicated design. Promising experimental methods include those based on the analogy of heat and mass transfer, such as the naphthalene sublimation technique used in the past for heat transfer in complex geometries.
- (8) Simulation studies are needed to facilitate power plant siting and design that include waste heat utilization and management options.
- (9) Research should be conducted to identify new fluids for refrigeration or heat engine application involving low temperature thermal energy.
- (10) Studies are needed to convert low temperature thermal energy into a form more suitable for practical utilization.
- (11) Research is needed to clarify the limitations of extended Reynolds analogies among heat, momentum and mass transfer, especially in turbulent flow. Current basic turbulence studies of "scalar transport" should be encouraged and applied to heat-exchange problems.
- (12) In general, increased understanding is needed in the areas of thermal discharges, spray cooling and in transport phenomena in cooling ponds.

THE CHALK POINT DYE TRACER STUDY: VALIDATION OF MODELS  
AND ANALYSIS OF FIELD DATA

A. J. Policastro\*  
W. E. Dunn<sup>□</sup>  
M. L. Breig<sup>●</sup>  
J. P. Ziebarth<sup>○</sup>

ABSTRACT

Predictions of ten models are compared with field data taken during the Chalk Point dye tracer study of June 1977. The ESC/Schrecker, Hosler-Pena-Pena, and Wigley-Slawson models compared most favorably with the deposition data from the cooling-tower alone and are generally within the error bounds of the data. Most models predict larger drop diameters at deposition than were measured. No model predicted each of the deposition parameters consistently within a factor of three. Predictions of stack deposition compared rather poorly with the stack deposition data probably due to the lack of good information on exit conditions.

A comparison of Johns Hopkins University (JHU) and Environmental Systems Corporation (ESC) ground-level drift data showed that the JHU data had larger drop counts in both the smallest and largest drop size ranges yet both sets of data agreed quite well in the intermediate drop size range. The JHU methodology appears superior since their data were more internally consistent and their technique of using large sensitive paper samplers and counting all drops on the paper yields a greater statistical accuracy.

INTRODUCTION

Drift refers to the small droplets of liquid water released from a cooling tower along with the warm, moist plume. These droplets, ranging in size from a few to more than 1000 microns in diameter, are transported through the atmosphere eventually evaporating totally or being deposited on the ground. If the droplets contain large concentrations of dissolved solids, as is particularly the case when brackish cooling water is used, then the drift deposition may damage vegetation and/or accelerate the corrosion and deterioration of structures.

---

\*Engineer, Div. of Environmental Impact Studies, Argonne National Lab.  
<sup>□</sup>Asst. Professor, Dept. of Mech. & Ind. Engr., Univ. of Ill., Urbana.  
<sup>●</sup>Visiting Scientist, Div. of Environmental Impact Studies, Argonne Nat. Lab.; Perm. Add.: Dept. of Physics, Eastern Ill. Univ., Charleston.  
<sup>○</sup>Engineer, Div. of Environmental Impact Studies, Argonne National Lab.

Therefore, predictions of anticipated drift-deposition rates are essential to an informed estimate of the environmental impact of a plant for which cooling towers are planned.

Once emitted from the tower, a drift drop moves under the combined influences of gravity and the aerodynamic drag force produced by the vector difference between the drop and local air velocities. Simultaneously, the drop experiences both heat and mass transfer. As a result, the drop temperature will approach the drop wet-bulb temperature and evaporation will occur as long as the vapor pressure at the drop surface exceeds that of the local ambient. For a drop containing salt, evaporation will increase the concentration within the drop and thus lower the vapor pressure at the drop's surface. The salt concentration will continue to increase until either (a) the droplet vapor pressure exactly equals that of the local ambient after which evaporation will cease or (b) the salt becomes saturated within the drop after which salt particles will begin to precipitate out as evaporation proceeds. In the latter case, the drop will eventually become a dry particle, although it may strike the ground before reaching its final state. The purpose of a drift model, then, is to predict the number, size, and character of drops and/or particles striking the ground at any given location with respect to the emitting tower.

Numerous mathematical models have been formulated to predict drift plumes and drift-deposition patterns. Although each of these models has a number of theoretical limitations, good quality field data have been lacking to determine the limits of reliability of these models. Field data taken at the Chalk Point Power Plant in 1975 and 1976 by the Environmental Systems Corporation suffered from several inherent deficiencies: ground samplers were too small in size and few in number, no separation of cooling tower and stack drift was made, etc. Those data provided a rough test of the models, yet the limitations of those data did not allow definitive conclusions to be made about the field performance of the models tested.

The field data taken at Chalk Point in June, 1977 by the Environmental Systems Corporation (ESC) [1] and independently by the Johns Hopkins University (JHU) [2,3] represent a significant improvement in the data collection methods and the culmination of more than three years of experience in drift data collection. The data, taken as a whole, are of good quality and sufficient to provide a true test of the models' capability. In fact, these data are presently the only good-quality field data on drift deposition available in the literature. The purpose of this paper then is to evaluate the performance of 10 drift models [4-11] with respect to these data and to provide an analysis of the data themselves to uncover special trends. Moreover, the ground-level data taken simultaneously by the two groups (ESC and JHU) will be intercompared as a test of their measurement and data reduction methods. It is important that such data be studied in detail due to the uniqueness of these good-quality data as well as the difficulty and expense of acquiring new data.

It must be noted that while these data are the best available and were obtained only through a very carefully executed measurement program, the data were obtained at only two radial distances from the tower. Thus the data encompass only one of several possible regimes of droplet behavior.

## THE FIELD EXPERIMENT

The Chalk Point Unit No. 3 cooling tower and stack effluent scrubber produce salt water drift because of the saline Patuxent River water used for the cooling tower circulating water and the stack particulate scrubbing agent. Previous drift measurements at Chalk Point have used sodium as a tracer and consequently separation of cooling tower and stack drift was not possible. To provide a positive identification of the drift deposition from the individual sources, JHU used a water soluble fluorescent dye (Rhodamine WT) as a tracer in the cooling tower circulating water. The photolytically unstable dye required that the experiment be performed at night. The drift dye tracer experiment was conducted during a four-hour period on June 16 and 17, 1977.

The instrumentation used by JHU consisted of 10.5 inch diameter modified deposition funnels for sodium and dye concentration measurements and 10.5 inch diameter Millipore HA type filter papers for measurement of total chloride and dyed drift droplet deposition. Three filter papers per sampling station were used for the deposition measurement of all water droplets (water sensitive filter paper), chloride containing droplets (plain filter paper) and dyed drift droplets (plain filter paper). A sketch of the sampler is shown in Fig. 1. The sampler consisted of a post with rectangular and triangular brackets for holding the funnel and sample bottle, and a filter paper holder plate with a can type candle heater. Filter paper heaters were required because of night time condensation which could affect the drop size measurements. The filter papers were photographed for fluorescent droplets using ultraviolet light. In this way, droplets deposited from the cooling tower could be identified. The water sensitive filter papers were used to define total drops deposited from all sources (stack and cooling tower). A calibration curve for droplet sizes was used to relate drop deposit size to falling drop size. The funnel samples were corrected to a standard volume (after being washed with distilled water) and split into two parts. One part was analyzed for sodium using an atomic absorption spectrophotometer while the other part was concentrated by boiling and analyzed for dye by fluorometry. The funnels could then give sodium deposition rate from all sources (tower and stack) by analyzing total sodium content of the sample. The funnels could also determine the part contributed by the tower alone by pro rating the dye deposited in the funnel to the ratio of the sodium to dye concentration in the basin water.

Fig. 1 also shows the Chalk Point power plant area and the JHU array of 8 stations on the 0.5 km arc (40 m apart) and 14 stations on the 1.0 km

are (40 m apart). Each sampling station consisted of three samplers (see Fig. 1) to ensure at least one good sample in case of accidents or contamination during sample collection and for good statistics. A total of 25 sampling stations were used by JHU on the night of the dye test. Each sampling station used during the experiment by JHU is identified with a number.

A number of drift parameters were measured at ground level downwind of the cooling tower by ESC. Typically, ESC uses four or five stations to measure the following ground-level drift quantities.

1. Sodium concentration in the air ( $\mu\text{g-Na}/\text{m}^3$ ) using a rotating tungsten mesh.
2. Liquid droplet concentration as a function of droplet size ( $\text{g-water}/\text{m}^3$ ) using a rotating sensitive paper disk.
3. Liquid droplet deposition flux as a function of droplet size ( $\text{kg-water}/\text{km}^2\text{-month}$ ) using a stationary sensitive paper disk.
4. Sodium mass deposition flux ( $\text{kg-Na}/\text{km}^2\text{-month}$ ) using a stationary funnel and bottle assembly.

The ESC sampling stations for the dye study are also located in Fig. 4 (denoted E1-E4). Some of the ESC ground-level stations were fixed in location and thus received drift only when the wind was blowing in the proper direction. Other stations were located beneath the cooling tower plume, being moved as the wind direction changed. For the purpose of model-data comparisons with the ESC data, we used the droplet number deposition flux measurements obtained using sensitive paper disks fixed to a petri dish and the sodium mass deposition flux obtained using the stationary funnel and bottle assembly. In addition to the ground-level measurements, source and ambient conditions were also measured by ESC.

Drift rates from the cooling tower were determined by ESC using an instrument package suspended in a plane approximately 13.6 m below the tower exit. The following measurements were made:

1. The drift droplet size spectrum was measured using sensitive paper and with a device based on scattering of infrared laser light (PILLS II-A, Particle Instrumentation by Laser Light Scattering).
2. The drift mineral mass flux was measured with a heated glass bead isokinetic (IK) sampling system.
3. The updraft air velocity (from which droplet velocity was determined) was measured using a Gill propeller-type anemometer.
4. The dry-bulb and wet-bulb exit temperatures of the plume were also measured.

The IK system sampled continuously during the traverse and yielded the sodium and magnesium mineral flux at the measurement plane. Updraft air velocities were acquired and averaged for each point. Grab samples of circulating water were also taken for chemical analysis of sodium and magnesium content. These two cations, which are present in the highest amounts in the water, were chosen as tracer elements for the IK measurements. No source measurements were made for the stack however.

Ambient meteorological measurements were made using the Chalk Point 100 meter instrument tower which has wind and temperature instruments at three levels (7 m, 50 m, and 92 m) and dew point sensors at two levels (7 m and 92 m). Ten minute averages of dry bulb and dew point temperature and wind speed were taken. Due to the location of the meteorological tower on a hill, the 92 meter level on the meteorological tower was at the same vertical elevation as the cooling tower exit plane. To supplement the meteorological tower measurements, rawinsonde flights were conducted at intervals of 1 hour by JHU in order to establish the short-term history of diurnal stability characteristics. Measurements of pressure (elevation), dry-bulb temperature, relative humidity, and wind speed (and direction) were made every 10 to 20 meters vertically.

#### ANALYSIS OF FIELD DATA AND COMPARISON OF JHU AND ESC DATA

The published presentation [2,3] of the JHU data revealed several interesting facts. A histogram plot of the total water and fluorescent droplet size distributions for the approximate cooling tower plume centerline sampling stations, 0.5 km/355 deg. and 1.0 km/350 deg., indicates a bimodal distribution (see Fig. 2). One peak occurs at about the 40-60 micron droplet size and the other between 200 to 400 microns. The second peak is expected from model calculations while the first one is not. Meyer and Stanbro [2,3] suggest that the source of these droplets is most probably blowoff from the cooling tower fill. The droplet distribution data for the other 22 sampling stations in the JHU net has yet to be reduced. Figure 3 presents the above droplet distribution data as percent mass fraction. The smaller droplets with their greater number contribute less than 1% to the total mass fraction. Note also that the fluorescent droplet distribution peak is separated from the total water peak by approximately 30 microns. The shift in the peaks between fluorescent and total drops is probably due to larger droplets originating in the stack. Also shown in Fig. 3 is a comparison of salt deposition contributions from the cooling tower and stack at near centerline locations 0.5 km and 1.0 km downwind of the tower. Note that each distribution is nearly bell-shaped and due, we believe, to the variation in wind direction with time during the measurement campaign. Also, the distinction between the contributions of the two sources is clearly seen at the 0.5 km distance and gets less distinct further from the tower as may be seen by the comparison at the 1.0 km location.

Figure 4 shows the placement on the ground of the four ESC and the two JHU samplers which have data reduced in the form of droplet size ranges. J1 and J2 indicate the two samplers of JHU, and E1 through E4 represent the locations of the appropriate ESC samplers.

The first parameter we studied for each of the six samplers was the drop size spectrum measured at particular sampler locations. Figure 4 gives the drop size distributions reported for the JHU and ESC data. The JHU spectra are clearly bimodal with a large peak of small drops (up to 100 microns) and a second peak of larger drops (approximately 250-280 microns). The ESC spectra also show bimodal tendencies, but the small drop count is smaller for samplers E2, E3, and E4.

Figure 5 shows the same data replotted in terms of mass distribution. Here, we see that very little mass is contributed by drops less than 100 microns in diameter. The largest drops also contribute very little except for ESC sampler E1 in which one drop contributed 8% of the total liquid mass. Problems with a few large drops contributing a significant fraction of the mass were evident in the 1976 ESC data as well.

It is instructive to examine next the average drop size measured at each of the ESC and JHU samplers. Defining an average drop size poses some interesting questions as several alternatives are possible.

1. Mass Mean Diameter -  $d_{MM}$

$$d_{MM} = (\sum C_i d_i^3 / \sum C_i)^{1/3}$$

where  $C_i$  is the number of drops in an interval and  $d_i$  is the corresponding drop diameter.

2. Mass Median Diameter -  $\bar{d}$

$\bar{d}$  is selected such that 50% of the total mass is contributed by drops larger than  $\bar{d}$  and 50% by drops less than  $\bar{d}$ .

3. Count Mean Diameter -  $d_{CM}$

$$d_{CM} = \sum C_i d_i / \sum C_i$$

4. Mass Peak Diameter -  $d_{MP}$

$d_{MP}$  is the diameter at which the greatest mass contribution occurs.

5. Count Peak Diameter -  $d_{CP}$

$d_{CP}$  is the drop diameter with the highest recorded count.

Listed in Table 1 are the values of these characteristic diameters computed from the JHU and ESC drop size distributions shown in Fig. 5.

The mass mean and mass median diameters are fairly representative of the corresponding distribution with the mass mean being roughly 40 to 50 microns smaller than the mass median. The mass peak diameter is intermediate between these two. The count mean is much smaller reflecting the large counts of small drops. The count peak diameter is not unique.

Among these, either the mass mean diameter or mass median diameter is preferable; however, neither of these is totally satisfactory. The mass mean diameter can be greatly affected by errors in the small drop data (large count, small mass). In contrast, the mass median diameter is sensitive to errors in the large drop data (small count, large mass). Since the greater uncertainty appears to be in the small drop counts for the 1977 data, we have chosen to use the mass median diameter to characterize these data.

Figure 6 shows how mass median diameter varies with distance from the tower. A trend of decreasing drop size with increasing distance from the tower is evident, but Sampler E4 does not follow the trend. This may be due to a greater influence of the stack. Recall that the JHU investigators found that the stack distribution has a greater number of larger drops. As shown in Fig. 4, Sampler E4 experiences a stronger stack influence than do the other samplers.

A fourth test of the data concerns the consistency between the four independent measurements: sodium deposition flux, liquid deposition flux, sodium concentration and liquid concentration. We can calculate from the data apparent droplet salt concentration and deposition velocity.

1. Apparent Droplet Concentration

$$C_{DD} = \left[ \begin{array}{l} \text{Apparent concentration} \\ \text{from deposition data} \end{array} \right] = \frac{\text{Sodium deposition flux}}{\text{Liquid deposition flux}}$$
$$C_{CD} = \left[ \begin{array}{l} \text{Apparent concentration} \\ \text{from concentration data} \end{array} \right] = \frac{\text{Sodium concentration}}{\text{Liquid concentration}}$$

## 2. Apparent Deposition Velocity

$$V_{SD} = \frac{\left[ \begin{array}{l} \text{Apparent velocity} \\ \text{from sodium data} \end{array} \right]}{\text{Sodium concentration}} = \frac{\text{Sodium deposition flux}}{\text{Sodium concentration}}$$
$$V_{LD} = \frac{\left[ \begin{array}{l} \text{Apparent velocity} \\ \text{from liquid data} \end{array} \right]}{\text{Liquid concentration}} = \frac{\text{Liquid deposition flux}}{\text{Liquid concentration}}$$

Table 1 summarizes the comparison of these calculated quantities. (Note that the basin-water salt concentration (for the tower) was 0.014 g/g.) The agreement here is within a factor of 2 with one exception, suggesting some consistency among the ESC data. Also, the magnitudes given are not unreasonable. Notably,  $C_{CD}$  is consistently larger than  $C_{DD}$ , and  $V_{LD}$  is consistently larger than  $V_{SD}$ . This may be fortuitous as a suitable explanation is presently lacking.

As it happens, Samplers J1 and E3 are within 26 meters of one another. Thus, we may compare almost directly the measurements obtained independently by these two different groups. Figure 6 compares the count and mass distributions as functions of drop diameter. The following observations can be made. First, the JHU sampler shows a greater droplet count both below about 100 microns and above about 300 microns, (although agreement above 600 microns is good). Second, the JHU mass distribution is clearly shifted toward greater diameters, although agreement above 550 microns is good. Despite this discrepancy, the mass median diameter computed from the JHU distribution is 400 microns whereas that computed from the ESC distribution is 336 microns, which is less than a 25% difference. It is possible, although unlikely, that the JHU sampler received a larger contribution of drops from the stack than did the ESC sampler.

### MODEL VALIDATION WITH JHU DATA

Critical reviews of the 10 models tested appear in References 12 and 13. Described below are the major features of the methodology used to make the model/data comparisons in this study.

1. Model predictions were made using the 10-minute averages of meteorological conditions acquired at the time of the dye study in order to better account for the variability of these conditions on deposition predictions. Predictions were made for each 10-minute period and the results summed over the four-hour duration of the study.
2. A 15 degree sector was chosen over the more common 22 1/2 degree sector due to the short duration of the averaging period.

3. For nine models, the 92-m level on the meteorological tower was used to provide the needed input. For one model (Wigley-Slawson), radiosonde profiles were used as well since that model has an option to accept full profiles.
4. At first, only the cooling tower was simulated and only the deposition acquired from the dye was used in the model/data comparisons. Sodium deposition rate, liquid mass deposition rate, number droplet deposition rate, and average diameter were computed by the models and also extracted from the data. The sodium deposition rate included contributions from all sizes; the other three ground-deposition variables were computed only from droplets of diameter greater than 100 microns. Average diameter was computed using the liquid mass deposition rate (droplets greater than 100 microns only) and number drop deposition rate (greater than 100 microns only). It should be noted that, although sodium deposition data were available from 8 locations along the 0.5 km arc and 12 locations along the 1.0 km arc, the data on droplet counts were reduced and made available only for the 0.5 km/355 deg. and 1.0 km/350 deg. locations. Thus data for number droplet deposition flux, liquid mass deposition rate and average diameter are available at only those two ground locations. We also made calculations for the stack separately and also combined cooling tower plus stack contributions at each sampler. No measurements at the stack were made during the dye study so we estimated the droplet size spectrum, liquid mass emission rate, exit temperature and velocity from measurements made in the stack during the previous study June, 1976. We will discuss those results later. The total of stack and cooling tower contributions were then compared with the plain filter paper results of JHU.

The results of the model/data comparisons for the cooling tower alone are given in Figs. 7 and 8 and Table 2. In Figs. 7 and 8, the model predictions of sodium deposition are plotted with respect to angle along the 0.5 km (Fig. 7) and 1.0 km arcs (Fig. 8) downwind of the tower. Tabular results of sodium deposition with angular position and distance from tower are listed in Table 2. Error estimates for the data are also shown. Notably, the plot of the observed sodium deposition rate is a bell-shaped curve on the angular range for which salt-drift data were acquired. Note also that the model predictions represent generally bell-shaped curves themselves. This is due to the variation in wind direction for the 10-minute averages of meteorological data. The usual procedure of averaging meteorological conditions over a four-hour period would provide only a single average value of deposition rate for the full four-hour period. Clearly then, wind direction variation with time is a likely explanation of the bell-shaped distribution of drift.

Some other general characteristics of the comparisons are noteworthy. First, wide variations among the predictions is striking. The Slinn I

predictions of sodium deposition rate are too large to fit on the scales of Figures 7 and 8. Second, the models tend to underpredict sodium deposition at the left and right end of the 0.5 km and 1.0 km arcs. This underprediction may be due, in part, to our choice of a 15 degree sector. A larger angle for sector-averaging may partially mitigate the discrepancy. Third, two predictions were made for both the ESC/Schrecker and Wigley-Slawson models in order to study the effects of changes in the input data on predictions. The second prediction of the ESC/Schrecker model, labeled "ESC/ Schrecker (limited)", was made by reducing the measured drop size spectrum from 25 to 3 intervals. Clearly, this modification of the spectrum led to a significant overprediction of sodium deposition in this case. The first prediction of the Wigley-Slawson model, labeled "Wigley-Slawson (profiles)", was made using the full ambient profiles as recorded by radiosonde flights with wind direction obtained from the meteorological tower. The second prediction was made using the met-tower data alone as was done for each of the other models. Here again, performance is degraded as the detail of the input data is degraded.

A few models, notably ESC/Schrecker, Wolf II, and Wigley-Slawson appear to be most accurate over the range of comparisons in Figs. 7 and 8. Observations on the performance of individual models will now be presented.

The ESC/Schrecker model (full spectrum) is rather good in its prediction of sodium deposition except at angles between 340 and 345 degrees on the 1 km arc, where the prediction is rather low. The predictions at 0.5 km are excellent. However, the prediction of number drop deposition (Table 2) at 1 km from the tower is too small by a factor of 3. This underprediction is carried through to the liquid mass deposition rate which is also too small by a factor of about 3. The prediction of final droplet diameter is quite good at both the 0.5 and 1.0 km distances from the tower.

The Wolf I and II model predictions are very similar at 0.5 km from the tower since evaporation is rather insignificant due to the high ambient relative humidity and the short time to deposition. Wolf II provides excellent predictions of sodium deposition except between angles of 330 and 335 degrees where low predictions occur. A larger difference between the predictions of the two Wolf models occurs at 1 km, where Wolf II now predicts noticeable evaporation; the effect of evaporation is to distribute the drift at the ground further downwind from the tower. The Wolf II predictions of final droplet diameter and liquid deposition rate give results that are low compared with the data probably due to excess evaporation predicted owing to the omission of solute effects in the model. Although the Wolf II predictions of sodium deposition are quite good at 0.5 and 1 km from the tower, the Wolf I model (which assumes no evaporation) overpredicts deposition.

The MRI model predicts sodium deposition reasonably well at both the 0.5 km and 1.0 km distance from the tower. However, the model underpredicts

number droplet deposition flux by a factor of 4 at 0.5 km from the tower and a factor of 5 at 1.0 km. No final drop size or liquid mass deposition is computed since the model is based on the equilibrium height concept which does not allow the computation of the final state of the drop. The model permits only two categories of relative humidity, greater than 50% and less than or equal to 50%. The case here of high relative humidity, approximately 93%, is perhaps not well represented by the formulas. The prediction of the Wigley-Slawson model with full ambient profiles is, overall, superior to the prediction of the model without profiles.

The Slinn I and II models were developed to provide upper and lower bounds on deposition. Clearly they do so. The Slinn II model predicts deposition just beginning to occur at 1 km. The prediction at 0.5 km is nearly zero. The Slinn I prediction for sodium deposition varies between a factor of 3 to 7 too large (see Table 2). Interestingly, the Slinn I prediction of average diameter at deposition is too small perhaps because the larger droplets have already deposited closer to the tower.

The Hanna model underpredicts sodium deposition probably due to the overprediction of evaporation in the model [14]. Predictions of number drop deposition rate and liquid mass deposition rate are also too low.

The Hosler-Pena-Pena model has in our previous model/data comparisons [12,13] underpredicted salt deposition rates (near the tower) but usually provided larger values than predicted by the Hanna model. Here, it does predict larger deposition rates than Hanna's model and performs quite well with the sodium ground flux data. The model, however, continues to underpredict the number drop deposition flux, here by factors of 2.5 and 3.6 at 0.5 and 1.0 km, respectively.

The Overcamp-Israel model underpredicts sodium deposition flux at 0.5 km from the tower. In addition, the deposition peak is shifted to the right. There is underprediction also at 1 km but only slightly. There is an underprediction in droplet number deposition rate and an overprediction in droplet size. In total, there is a consequent underprediction of liquid mass deposition flux by factors of 2.1 at 0.5 km and 2.7 at 1 km.

A few general comments should also be made. First, from Table 4, the models generally overpredict droplet diameter at deposition. Second, the peak deposition for sodium predicted by the models is generally coincident or nearly coincident with the observed peak along the two arcs. Third, it should be recalled that the sodium flux predicted and measured included droplets of all sizes, whereas, our droplet number deposition flux, average diameter, and liquid mass deposition rate include droplets only above 100 microns in size. We would expect the observed sodium deposition rate to be slightly larger than the predicted deposition rate since it includes some sodium coming from blow-off from the tower fill. The 100 micron cutoff for other deposition quantities

was set because it is difficult to accurately count drops less than this value and also it eliminates most of the blow-off droplets which are not considered by the models.

The models have also been run for the stack input data with results given in Figures 9 and 10 and Table 3. Combined results of model predictions from cooling tower and stack appear in Figs. 11 and 12 and Table 4. Field data taken from the water sensitive paper were used for comparison with model predictions. Some observations follow.

1. In the angular range (at 0.5 and 1.0 km distances) where the tower has a predominant effect, the models perform in a reasonable manner. However, in the angular range 350 to 365 degrees, the stack contribution becomes important and the tower contribution becomes insignificant (at 0.5 km). At 1.0 km, the stack contribution is about 3-4 times the tower contribution. From Figs. 11 and 12 and Table 4, the models overpredict by a factor of 5-15 in the angular range of 350-365 degrees. The poor comparison of models with stack plus tower data may be due to the use of average stack parameters from the year before. Among the unknowns for the stack exit were: (a) drop size spectrum, (b) liquid mass emission rate, (c) drop concentration at exit (we assumed saturated drops following ESC '15', 0.26 g/g), and (d) stack exit velocity and temperature.
2. The model predictions for the stack are quite consistent among themselves. One of the reasons may be our assumption that the drops are saturated with salt and evaporate only little out to the deposition samplers.
3. The cooling tower contribution to total deposition can be easily distinguished from the stack contribution at the 0.5 km distance but not as easily for the 1.0 km distance. Perhaps our assumed drop spectrum had too large a mass fraction in the large drop sizes.
4. In terms of total deposition there is less discrepancy between model predictions and data for the 1.0 km distance than for the 0.5 km distance. Here, the stack contributes 2-3 times more drift than does the cooling tower; in total, the predictions are about four times larger than observed. As expected from the earlier tower comparisons, the ESC/Schrecker (Limited) and Slinn I and II models perform very poorly.
5. It is interesting that the Wolf I and II predictions for the stack are very similar at both 0.5 and 1.0 km in contrast to the increasing effect of evaporation from 0.5 to 1.0 km seen for drift drops from the cooling tower. The similarity in predictions for Wolf I and II for the stack is due to the slower rate of evaporation which occurs for the larger size stack-emitted drops which fall from the stack plume to the nearby samplers at 0.5 and 1.0 km downwind of the tower.

## VALIDATION OF MODELS WITH ESC DATA

The locations of the ESC sensors are given in Fig. 4. Unfortunately, the data for only 4 of the 9 samplers ESC placed at the site were reduced. Tables 5 and 6 provide a comparison of the model predictions with the data in terms of sodium deposition rate, number deposition rate, liquid mass deposition rate, and average diameter (mass averaged). Clearly, significant discrepancies exist between the model predictions and the data. Notably the predicted averaged deposited diameter is 50-100% larger than that measured. Clearly then, the mass of salt in the predicted drop should then be about 2.3-4 times that in the observed drops. Also, the droplet deposition flux is predicted to be about twice as large as observed (considering only drops of size greater than 100 microns). In total, the deposited sodium mass should be predicted as 5-8 times observed. Actually an average value of overprediction of salt deposition flux is more like 10-13. The overprediction of deposition at these near-tower sensors may be due in part to the questionable assumptions we had to make concerning the conditions at the stack exit. However, in view of the fact that the models overpredict deposition due to the tower contribution alone (compared to the total observed deposition from tower and stack), the problem is much more disturbing. ESC uses a smaller sensitive paper (122 cm<sup>2</sup>) than the JHU sampler (700 cm<sup>2</sup>) leading to a less statistically significant sample. Moreover, ESC does not count all drops on the paper. In their method of data reduction, two squares are drawn on the 122 cm<sup>2</sup> area, the larger one to size the larger drops and the smaller one to size the smaller drops. JHU, on the other hand, sizes all drops on the full area of their sampler. This difference in data reduction methods may be at the root of the difference between ESC and JHU measurements. It would be advisable for each group to count the droplets on the other's samplers to judge the potential differences in data reduction methods.

## CONCLUSIONS

The field data acquired in the Chalk Point Dye Study represent the best thus far available for validation of salt-drift deposition models. Sodium deposition measurements taken on the ground along arcs 0.5 km and 1.0 km from the tower showed a bell-shaped profile. This shape was also evident in the model predictions when 10-minute average meteorological data were used and total deposition predictions were obtained by summing predictions made for each 10-minute period. Variation in wind direction thus appears to be a satisfactory explanation of the lateral distribution seen along arcs on the ground.

Comparison of JHU and ESC data yielded interesting results. The JHU measurements of drop size spectrum at ground locations yielded a clear bimodal distribution while the ESC measurements were at best weakly bimodal. The JHU measurements yielded a large peak of small drops (up to 100 microns and a second peak of larger drops (approximately 250-280 microns). The peak of small drops is thought to be due to blow-off from

the fill section of the tower and represents only a small fraction of the total mass deposited at any sampler. For a JHU and ESC sampler located close together (26 m apart), the following observations were made. The JHU sampler showed a greater droplet count both below 100 microns and above about 300 microns with reasonable agreement in between. In addition, the JHU mass distribution is clearly shifted toward greater diameters although agreement above 600 microns is good. The median diameters were only 25% different (JHU: 400 microns; ESC: 336 microns). Consistency checks on the ESC data revealed a factor of 2 difference between different methods of calculating droplet salt concentrations and droplet settling velocity at the ground sampler locations. In general, the JHU measurements were of better quality in terms of methodology of measurement, data reduction, and internal consistency. The general trends in ESC and JHU measurements agree although they differ in details. These details may be important in specific cases.

Ten drift-deposition models are compared with the JHU and ESC field data. For the cooling tower taken alone, a wide range in predictions occurs for sodium deposition flux, number drop deposition flux, liquid mass deposition flux, and average diameter. A number of models predicted very poorly; most, however, were not far off from the data, at least in terms of the sodium deposition predictions. The ESC/Schrecker, Hosler-Pena-Pena, and Wigley-Slawson Models compare best with the sodium deposition flux measurements and are generally within the error of the data. Those models which degrade the level of input data (e.g., use readings from one location on a meteorological tower rather than full profiles, or degrade the spectrum from 25 to 8 bins) lose accuracy in their predictions. Most models predict larger drop diameters at deposition than were measured. This may be due to an incorrect treatment of breakaway in which, in reality, smaller drops are breaking away from the plume sooner. The wind moving past the tower causes a wake or cavity effect with a resultant downdraft on the plume; this effect combined with complex internal circulations within the plume may be causing earlier breakaway. It should be noted that the comparative levels of performance of the models apply only to this special case: high relative humidity, moderate to large wind speed, very stable atmosphere. One cannot a priori extend the specific accuracy of any model to more general environmental conditions without further testing.

For the stack, calculations were made with average June conditions of the previous year since no stack parameters were measured on the date of the dye test. Average values from measurements on the previous June had to be used instead for model input; they were: droplet size spectrum, liquid mass emission rate, exit temperature and velocity. Also, the drops were assumed to be saturated at exit. Model/data comparisons yielded large overprediction of deposition by the models at 0.5 km but more realistic predictions at 1.0 km. In any case, the stack parameters need to be measured on any particular date calculations are required; this is due to the fact that a significantly larger discrepancy existed between stack plus tower predictions and data than with just tower

predictions and data. An important unknown is the salt concentration of droplets leaving the stack. Such exit conditions for the stack need to be measured because the impact of the stack can be as great as the tower, at least in terms of salt emitted.

#### ACKNOWLEDGMENTS

This work was funded by the Electric Power Research Institute. The authors also wish to express their appreciation to the modelers whose work was utilized for their cooperation.

#### REFERENCES

1. Environmental Systems Corporation. Cooling Tower Drift Dye Tracer Experiment. Chalk Point Cooling Tower Project, PPSP-CPCTP, August, 1977, pp.92-95.
2. J. H. Meyer and W. D. Stanbro. Cooling Tower Drift Dye Tracer Experiment. Johns Hopkins University Applied Physics Laboratory. Chalk Point Cooling Tower Project, PPSP-CPCTP-16, Volume 2, August, 1977, pp 5-18 through 5-26.
3. Meyer, J. H. and Stanbro, W. D., "Separation of Chalk Point Drift Sources Using a Fluorescent Dye." IN: Cooling-Tower Environment - 1978, A Symposium on Environmental Effects of Cooling Tower Emissions, May 2-4, 1978. Chalk Point Cooling Tower Project Report PPSP-CPCTP-22. WRRRC Special Report No. 9. Baltimore, Maryland. May, 1978.
4. Hosler, C., Pena, J., and Pena, R., "Determination of Salt Deposition Rates from Drift from Evaporative Cooling Tower," J. Eng. Power, Vol. 96, No. 3, 1974, p. 283.
5. Wolf, M., Personal Communication, Battelle Pacific Northwest Laboratory, Richland, Washington, July, 1976.
6. Slinn, W. G. N., Personal Communication, Battelle Pacific Northwest Laboratory, Richland, Washington, February, 1977.
7. Hanna, S. R., "Fog and Drift Deposition from Evaporative Cooling Towers." Nuclear Safety. Vol. 15, No. 2. March-April, 1974. pp. 190-196.
8. Slawson, P. R. and Kumar, A., "Cooling Tower Drift Deposition Program ENDRIFT II," Envirodyne Ltd., Tennessee Valley Authority Air Quality Branch, April, 1976.
9. Maas, S. J., "Salt Deposition from Cooling Towers for the San Joaquin Nuclear Project," MRI 75-FR-1361, September 15, 1975.

10. Schrecker, G. and Rutherford, D., Personal Communication, Environmental Systems Corp., Knoxville, Tennessee, 1976.
11. Overcamp, T., "Sensitivity Analysis and Comparison of Salt Deposition Models for Cooling Towers." Paper presented and published in Proceedings of the Conference on Waste Heat Management and Utilization. Miami Beach, Florida. May 9-11, 1977.
12. Policastro, A. J., Dunn, W. E., Breig, M., Ziebarth, J., and Ratcliff, M. Evaluation of Mathematical Models for the Prediction of Salt-Drift Deposition from Natural-Draft Cooling Towers (in preparation). Division of Environmental Impact Studies, Argonne National Laboratory, Argonne, Illinois. 1978.
13. Policastro, A. J., Dunn, W. E., Breig, M., and Ratcliff, M. "Evaluation of Theory and Performance of Salt-Drift Deposition Models for Natural-Draft Cooling Towers." IN: Environmental Effects of Atmospheric Heat/Moisture Releases, presented at the Second AIAA/ASME Thermophysics and Heat Transfer Conference. Palo Alto, California. May 24-26, 1978. (available from ASME, New York City).
14. Dunn, W. E., Boughton, B., and Policastro, A. J. "Evaluation of Droplet Evaporation Formulations Employed in Drift Deposition Models." IN: Cooling-Tower Environment - 1978, A Symposium on Environmental Effects of Cooling Tower Emissions, May 2-4, 1978. Chalk Point Cooling Tower Project Report PPSP-CPCTP-22. WRRC Special Report No. 9. Baltimore, Maryland. May, 1978.
15. Environmental Systems Corporation. Chalk Point Cooling Tower Project. Comprehensive Project Final Report for the Period October 1, 1975-June 30, 1976. Volume 2. PPSP-CPCTP-12. October 1975.

Table 1a. Comparison of Average Diameter (by Several Definitions) for the ESC and JHU Samplers

| Sampler | $d_{MM}$ | $\bar{d}$ | $d_{CM}$ | $d_{MP}$ | $d_{CP}$ (micron) |
|---------|----------|-----------|----------|----------|-------------------|
| JHU-J1  | 320      | 360       | 207      | 360      | 60,280            |
| JHU-J2  | 240      | 280       | 152      | 280      | 40,180,240        |
| E1      | 353      | 500       | 199      | 375      | 80,375            |
| E2      | 268      | 326       | 195      | 285      | 80,285            |
| E3      | 291      | 336       | 237      | 285      | 65,285            |
| E4      | 289      | 344       | 238      | 285      | 35,225            |

Table 1b. Comparison of Apparent Droplet Concentration and Droplet Settling Velocity at the ESC and JHU Samplers.

| Sampler | $C_{DD}$ (gm/gm) | $C_{CD}$ | $V_{SD}$ (m/s) | $V_{LD}$ |
|---------|------------------|----------|----------------|----------|
| JHU J1  | 0.029            | -        | -              | -        |
| JHU J2  | 0.019            | -        | -              | -        |
| ESC E1  | 0.006            | 0.009    | 1.29           | 1.76     |
| ESC E2  | 0.011            | 0.022    | 0.69           | 1.47     |
| ESC E3  | 0.018            | 0.020    | 1.41           | 1.53     |
| ESC E4  | 0.031            | 0.052    | 1.57           | 2.63     |

| Sampler      |      | JHU Dye Data<br>June 16-17, 1977<br>Sodium Deposition Flux<br>Tower<br>mg/m <sup>2</sup> -4 hours |      |      |      |       |      |   |      |      |      |      |      |      |
|--------------|------|---|------|------|------|-------|------|---|------|------|------|------|------|------|
| Distance (m) | Dir. | OBS.  | 1    | 2    | 3    | 4     | 5    | 6 | 7    | 8    | 9    | 10   | 11   | 12   |
| 500          | 350  | 1.9 ± .5  | 0.00 | 0.00 | 0.00 | 0.00  | 0.00 | 0 | 0.00 | 0.00 | 0.00 | 0.00 | 0.00 | 0.00 |
| 500          | 335  | 2.7 ± .7  | 1.11 | 3.22 | 0.08 | 0.00  | 10.3 | 0 | 1.66 | 1.48 | 3.50 | 1.57 | 2.19 | 5.59 |
| 500          | 340  | 4.7 ± 2.1   | 1.98 | 5.65 | 0.39 | 3.50  | 18.9 | 0 | 9.24 | 8.66 | 6.22 | 5.95 | 4.22 | 10.2 |
| 500          | 345  | 8.9 ± 2.6   | 3.97 | 10.0 | 0.76 | 5.65  | 32.8 | 0 | 13.7 | 12.3 | 10.8 | 6.74 | 7.46 | 18.3 |
| 500          | 350  | 10.9 ± 2.7  | 5.41 | 11.2 | 2.49 | 11.04 | 35.8 | 0 | 15.3 | 11.7 | 12.1 | 9.27 | 9.06 | 21.5 |
| 500          | 355  | 7.7 ± 2.5   | 5.25 | 9.38 | 5.18 | 10.53 | 29.5 | 0 | 12.9 | 11.0 | 10.4 | 7.33 | 7.78 | 18.9 |
| 500          | 0.0  | 6.1 ± 2.4   | 5.07 | 4.52 | 3.13 | 6.34  | 10.7 | 0 | 5.38 | 4.95 | 4.77 | 4.50 | 5.31 | 8.82 |
| 500          | 5.0  | 1.9 ± .3  | 0.93 | 1.57 | 1.28 | 3.55  | 2.64 | 0 | 0.89 | 0.74 | 1.35 | 1.12 | 0.95 | 2.52 |

| Sampler      |       | JHU Dye Data<br>June 16-17, 1977<br>Sodium Deposition Flux<br>Tower<br>mg/m <sup>2</sup> -4 hours |     |      |      |      |      |      |      |      |      |      |      |      |
|--------------|-------|---|-----|------|------|------|------|------|------|------|------|------|------|------|
| Distance (m) | Dir.  | OBS.  | 1   | 2    | 3    | 4    | 5    | 6    | 7    | 8    | 9    | 10   | 11   | 12   |
| 1000         | 340   | 1.4 ± .4  | 0.6 | 1.71 | 1.29 | 0.61 | 4.54 | 0.10 | 4.28 | 2.52 | 0.40 | 1.45 | 1.29 | 1.89 |
| 1000         | 342.5 | 3.6 ± .9  | 0.7 | 1.72 | 1.46 | 1.08 | 5.24 | 0.13 | 4.96 | 2.72 | 0.53 | 1.67 | 1.49 | 2.36 |
| 1000         | 345.0 | 2.4 ± .4  | 0.9 | 2.35 | 1.99 | 1.12 | 8.26 | 0.19 | 6.55 | 3.53 | 1.04 | 2.28 | 2.19 | 5.75 |
| 1000         | 347.5 | 3.5 ± .8  | 1.0 | 2.34 | 2.02 | 2.50 | 9.50 | 0.22 | 6.30 | 5.12 | 1.40 | 2.44 | 2.20 | 5.09 |
| 1000         | 350.0 | 2.4 ± 1.2   | 1.0 | 2.19 | 1.65 | 2.32 | 11.3 | 0.20 | 6.25 | 2.95 | 1.99 | 2.26 | 2.18 | 6.25 |
| 1000         | 352.5 | 2.4 ± 1.2   | 0.8 | 1.75 | 1.42 | 1.74 | 10.6 | 0.19 | 6.59 | 2.90 | 3.00 | 2.09 | 1.94 | 7.67 |
| 1000         | 355.0 | 1.2 ± .3  | 0.8 | 1.29 | 1.16 | 2.11 | 9.86 | 0.17 | 5.79 | 2.75 | 2.28 | 1.32 | 1.70 | 7.51 |
| 1000         | 357.5 | 1.2 ± .5  | 0.6 | 1.21 | 0.90 | 1.51 | 8.54 | 0.11 | 5.92 | 1.66 | 2.09 | 1.50 | 1.41 | 7.11 |
| 1000         | 0.0   | 1.4 ± .4  | 0.4 | 0.64 | 0.40 | 1.46 | 5.84 | 0.05 | 2.63 | 1.08 | 1.75 | 0.92 | 0.86 | 5.98 |
| 1000         | 5.0   | .51 ± .1  | 0.1 | 0.31 | 0.10 | 1.65 | 1.32 | 0.01 | 0.36 | 0.16 | 0.45 | 0.26 | 0.22 | 1.65 |
| 1000         | 7.5   | 0.0   | 0.0 | 0.00 | 0.00 | 0.00 | 0.00 | 0.00 | 0.00 | 0.00 | 0.00 | 0.00 | 0.68 | 0.00 |
| 1000         | 10.0  | .55 ± .2  | 0.0 | 0.00 | 0.00 | 0.00 | 0.00 | 0.00 | 0.00 | 0.00 | 0.00 | 0.00 | 0.00 | 0.00 |

| Sampler   |      | JHU Dye Data<br>June 16-17, 1977<br>Tower |     |      |     |      |        |   |       |      |      |      |      |      |
|---|------|---|-----|------|-----|------|--------|---|-------|------|------|------|------|------|
| Distance (m)  | Dir. | OBS.                                      | 1   | 2    | 3   | 4    | 5      | 6 | 7     | 8    | 9    | 10   | 11   | 12   |
| * Drops/m <sup>2</sup> -hour:                             |      |   |     |      |     |      |        |   |       |      |      |      |      |      |
| 500   | 355  | 6500                                      | 590 | 2475 | 408 | 1793 | 5537   | - | 6393  | 4706 | 4066 | 1495 | 2388 | 145  |
| 1000  | 350  | 7208                                      | 231 | 2019 | 537 | 2788 | 100240 | - | 15100 | 4432 | 2113 | 1505 | 1330 | 8066 |
| Average Diameter (µm)                                     |      |   |     |      |     |      |        |   |       |      |      |      |      |      |
| 500   | 355  | 510                                       | 519 | -    | 607 | 424  | 262    | - | 376   | 334  | 359  | -    | 484  | 398  |
| 1000  | 350  | 241                                       | 354 | -    | 411 | 307  | 157    | - | 225   | 119  | 241  | -    | 367  | 231  |
| Liquid Mass Deposition Flux<br>mg/m <sup>2</sup> -4 hours |      |   |     |      |     |      |        |   |       |      |      |      |      |      |
| 500   | 355  | 393                                       | 173 | -    | 191 | 768  | 2104   | - | 706   | 367  | 526  | -    | 567  | 945  |
| 1000  | 350  | 204                                       | 21  | -    | 78  | 169  | 806    | - | 360   | 15   | 62   | -    | 159  | 209  |

LEGEND

- |                              |                             |
|------------------------------|-----------------------------|
| 1. Hanna                     | 7. Wolf I                   |
| 2. Hosler-Pena-Pena          | 8. Wolf II                  |
| 3. Overcamp-Israel           | 9. ESC/Schrecker            |
| 4. Wigley-Slawson (profiles) | 10. MRI                     |
| 5. Slinn I                   | 11. Wigley-Slawson          |
| 6. Slinn II                  | 12. ESC/Schrecker (limited) |

Table 2. Comparison of Predictions of 10 Drift Deposition Models to Ground-Level Measurements of Sodium Deposition Flux, Number Drop Deposition Flux, Average Deposited Diameter, and Liquid Mass Deposition Flux . . . Cooling Tower Contribution at JHU Samplers.

| Sampler      |           | JHU Dye Data<br>June 16-17, 1977<br>Sodium Deposition Flux<br>Stack<br>mg/m <sup>2</sup> -4 hours |      |      |      |      |      |     |      |      |      |      |      |      |
|--------------|-----------|---|------|------|------|------|------|-----|------|------|------|------|------|------|
| Distance (m) | Direction | OBS.  | 1    | 2    | 3    | 4    | 5    | 6   | 7    | 8    | 9    | 10   | 11   | 12   |
| 589.5        | 319       |   | 0.0  | 0.0  | 0.0  | 0.0  | 0.0  | 0.0 | 0.0  | 0.0  | 0.0  | 0.0  | 0.0  | 0.0  |
| 580.7        | 323       |   | 0.0  | 0.0  | 0.0  | 0.0  | 0.0  | 0.0 | 0.0  | 0.0  | 0.0  | 0.0  | 0.0  | 0.0  |
| 571.4        | 327       |   | 0.0  | 0.0  | 0.0  | 0.0  | 0.0  | 0.0 | 0.0  | 0.0  | 0.0  | 0.0  | 0.0  | 0.0  |
| 561.5        | 332       |   | 0.0  | 0.0  | 0.0  | 0.0  | 0.0  | 0.0 | 2.41 | 2.14 | 0.0  | 0.0  | 0.0  | 0.0  |
| 551.1        | 336       |   | 18.5 | 18.0 | 24.0 | 0.0  | 21.2 | 0.0 | 15.0 | 15.6 | 26.3 | 18.9 | 3.26 | 24.2 |
| 540.5        | 340       |   | 24.5 | 22.5 | 29.0 | 0.0  | 26.6 | 0.0 | 45.5 | 44.9 | 51.6 | 25.0 | 11.0 | 50.7 |
| 529.1        | 345       |   | 51.2 | 46.7 | 65.1 | 0.0  | 55.4 | 0.0 | 80.4 | 87.1 | 61.7 | 48.1 | 21.3 | 61.9 |
| 517.6        | 350       |   | 54.4 | 56.3 | 54.1 | 31.6 | 75.5 | 0.0 | 70.6 | 75.6 | 71.8 | 52.6 | 29.0 | 61.7 |

| Sampler      |           | JHU Dye Data<br>June 16-17, 1977<br>Sodium Deposition Flux<br>Stack<br>mg/m <sup>2</sup> -4 hours |      |      |      |      |      |   |      |      |      |      |      |      |
|--------------|-----------|---|------|------|------|------|------|---|------|------|------|------|------|------|
| Distance (m) | Direction | OBS.  | 1    | 2    | 3    | 4    | 5    | 6 | 7    | 8    | 9    | 10   | 11   | 12   |
| 1064.8       | 335       |   | 0.74 | 2.15 | 0.67 | 0.0  | 5.49 | 0 | 0.39 | 0.18 | 1.05 | 0.77 | 0.56 | 4.62 |
| 1059.0       | 335.6     |   | 2.59 | 7.19 | 2.27 | 0.0  | 12.5 | 0 | 2.11 | 1.94 | 2.85 | 2.79 | 1.56 | 16.5 |
| 1054.3       | 338       |   | 3.32 | 9.05 | 2.95 | 0.0  | 15.0 | 0 | 3.15 | 3.34 | 3.65 | 3.72 | 1.84 | 21.9 |
| 1048.8       | 340.3     |   | 3.65 | 9.99 | 3.12 | 0.0  | 17.1 | 0 | 5.99 | 5.96 | 4.17 | 4.40 | 2.52 | 25.1 |
| 1043.3       | 343       |   | 4.96 | 15.1 | 4.74 | 0.0  | 24.1 | 0 | 7.59 | 7.09 | 6.45 | 6.19 | 2.95 | 27.0 |
| 1037.6       | 345       |   | 6.47 | 19.0 | 6.29 | 0.0  | 31.4 | 0 | 10.1 | 9.57 | 8.39 | 8.75 | 3.98 | 38.3 |
| 1031.9       | 347       |   | 7.94 | 21.2 | 7.52 | 0.0  | 35.4 | 0 | 12.0 | 10.7 | 9.10 | 10.1 | 4.79 | 42.5 |
| 1026.1       | 350       |   | 8.12 | 21.5 | 8.44 | 4.25 | 31.1 | 0 | 11.0 | 9.34 | 8.84 | 10.7 | 5.05 | 39.1 |
| 1020.2       | 352.2     |   | 7.65 | 19.5 | 8.18 | 5.99 | 26.8 | 0 | 11.2 | 9.60 | 9.19 | 9.95 | 5.25 | 55.6 |
| 1008.5       | 357.1     |   | 5.55 | 11.4 | 6.15 | 5.28 | 16.9 | 0 | 7.96 | 6.00 | 6.06 | 7.87 | 4.65 | 22.7 |
| 1002.3       | 359.6     |   | 4.55 | 8.02 | 5.06 | 5.44 | 10.1 | 0 | 5.58 | 4.11 | 4.57 | 5.98 | 4.15 | 16.0 |
| 992.5        | 361       |   | 2.52 | 3.28 | 2.95 | 5.99 | 4.99 | 0 | 4.28 | 2.86 | 4.96 | 5.29 | 2.96 | 4.52 |

| Sampler   |           | JHU Dye Data<br>June 16-17, 1977<br>Stack |     |      |     |   |      |   |     |     |      |     |     |      |
|---|-----------|---|-----|------|-----|---|------|---|-----|-----|------|-----|-----|------|
| Distance (m)  | Direction | OBS.                                      | 1   | 2    | 3   | 4 | 5    | 6 | 7   | 8   | 9    | 10  | 11  | 12   |
| # Drops/m <sup>2</sup> -hour                              |           |   |     |      |     |   |      |   |     |     |      |     |     |      |
| 540.2   | 340       |   | 578 | 1166 | 824 | 0 | 1390 | - | 862 | 800 | 762  | 555 | 404 | 889  |
| 1043.3  | 343       |   | 572 | 1994 | 553 | 0 | 9952 | - | 327 | 585 | 1327 | 620 | 525 | 4599 |
| Average Diameter (um)                                     |           |   |     |      |     |   |      |   |     |     |      |     |     |      |
| 300   | 355       |   | 699 | -    | 630 | 0 | 463  | - | 605 | 556 | 651  | -   | 551 | 594  |
| 1000  | 350       |   | 451 | -    | 419 | 0 | 255  | - | 559 | 222 | 508  | -   | 580 | 329  |
| Liquid Mass Deposition Flux<br>mg/m <sup>2</sup> -4 hours |           |   |     |      |     |   |      |   |     |     |      |     |     |      |
| 540.5   | 340       |   | 310 | -    | 525 | 0 | 217  | - | 500 | 316 | 500  | -   | 106 | 292  |
| 1043.3  | 343       |   | 72  | -    | 64  | 0 | 197  | - | 60  | 10  | 61   | -   | 28  | 157  |

LEGEND

- |                              |                             |
|------------------------------|-----------------------------|
| 1. Hanna                     | 7. Wolf I                   |
| 2. Hosler-Pena-Pena          | 8. Wolf II                  |
| 3. Overcamp-Israel           | 9. ESC/Schrecker            |
| 4. Wigley-Slawson (profiles) | 10. MRI                     |
| 5. Slinn I                   | 11. Wigley-Slawson          |
| 6. Slinn II                  | 12. ESC/Schrecker (limited) |

Table 3. Predictions of 10 Drift Deposition Models of Ground-Level Sodium Deposition Flux, Number Drop Deposition Flux, Average Deposited Diameter, and Liquid Mass Deposition Flux . . . Stack Contribution at JHU Samplers.

| Sampler      |           | JHU Dye Data<br>June 16-17, 1977<br>Tower and Stack<br>Sodium Deposition Flux<br>mg/m <sup>2</sup> -4 hours |      |      |      |      |      |     |      |      |      |      |      |      |
|--------------|-----------|---|------|------|------|------|------|-----|------|------|------|------|------|------|
| Distance (m) | Direction | OBS.  | 1    | 2    | 3    | 4    | 5    | 6   | 7    | 8    | 9    | 10   | 11   | 12   |
| 500(589.5)   | 350(319)  | 1.96 ± .26  | 0.0  | 0.0  | 0.0  | 0.0  | 0.0  | 0.0 | 0.0  | 0.0  | 0.0  | 0.0  | 0.0  | 0.0  |
| 500(580.7)   | 335(323)  | 5.16 ± .43  | 1.1  | 3.22 | 0.08 | 0.0  | 10.8 | 0.0 | 1.66 | 1.48 | 3.50 | 1.57 | 2.19 | 5.59 |
| 500(571.4)   | 340(327)  | 2.88 ± .96  | 1.98 | 5.65 | 0.39 | 3.50 | 18.9 | 0.0 | 9.24 | 8.66 | 5.43 | 3.95 | 4.22 | 10.2 |
| 500(561.5)   | 345(332)  | 5.44 ± .75  | 3.97 | 10.0 | 0.76 | 5.65 | 32.6 | 0.0 | 16.1 | 14.4 | 10.8 | 6.74 | 7.48 | 18.3 |
| 500(551.1)   | 350(356)  | 8.91 ± .44  | 23.7 | 29.2 | 26.4 | 11.0 | 56.4 | 0.0 | 26.8 | 27.5 | 38.9 | 28.2 | 17.3 | 45.7 |
| 500(540.3)   | 355(340)  | 7.99 ± .45  | 29.6 | 32.4 | 31.8 | 10.5 | 56.1 | 0.0 | 58.4 | 55.9 | 42.0 | 32.9 | 18.8 | 49.5 |
| 500(529.1)   | 0.0(345)  | 8.65 ± .78  | 54.3 | 51.0 | 66.1 | 6.34 | 64.1 | 0.0 | 85.8 | 92.1 | 66.5 | 52.4 | 25.6 | 70.7 |
| 500(517.6)   | 5.0(350)  | 12.6 ± .98  | 55.3 | 58.2 | 55.4 | 55.2 | 77.9 | 0.0 | 71.5 | 76.3 | 73.2 | 53.7 | 30.0 | 64.2 |

| Sampler      |              | JHU Dye Data<br>June 16-17, 1977<br>Tower and Stack<br>Sodium Deposition Flux<br>mg/m <sup>2</sup> -4 hours |      |      |      |      |      |      |      |      |      |      |      |      |
|--------------|--------------|---|------|------|------|------|------|------|------|------|------|------|------|------|
| Distance (m) | Direction    | OBS.  | 1    | 2    | 3    | 4    | 5    | 6    | 7    | 8    | 9    | 10   | 11   | 12   |
| 1000(1064.8) | 340(333)     | 2.00 ± .52  | 1.34 | 3.84 | 1.96 | 0.61 | 8.03 | 0.10 | 4.67 | 2.70 | 1.43 | 2.22 | 1.65 | 6.51 |
| 1000(1059.6) | 342.5(335.6) | 2.98 ± .26  | 5.29 | 8.91 | 3.73 | 1.08 | 17.5 | 0.13 | 7.07 | 4.66 | 3.56 | 4.46 | 2.85 | 18.9 |
| 1000(1054.3) | 345(338)     | 2.98 ± .34  | 4.22 | 11.4 | 4.94 | 1.12 | 23.3 | 0.19 | 9.70 | 6.67 | 4.67 | 6.00 | 3.98 | 24.8 |
| 1000(1048.8) | 347.5(340.3) | 5.67 ± .075   | 4.63 | 12.3 | 5.14 | 2.30 | 26.6 | 0.22 | 12.3 | 9.08 | 5.57 | 6.84 | 4.52 | 28.2 |
| 1000(1045.3) | 350(343)     | 5.71 ± .15  | 5.96 | 17.3 | 6.39 | 2.32 | 35.4 | 0.20 | 13.8 | 10.0 | 8.44 | 9.45 | 5.11 | 33.3 |
| 1000(1037.6) | 352.5(345)   | 5.18 ± .50  | 7.27 | 21.3 | 7.71 | 1.74 | 42.0 | 0.19 | 16.7 | 12.5 | 11.4 | 10.8 | 5.92 | 46.0 |
| 1000(1031.9) | 355(347)     | 4.31 ± .12  | 8.64 | 22.5 | 8.68 | 2.11 | 43.3 | 0.17 | 17.8 | 13.5 | 11.4 | 11.9 | 6.49 | 50.0 |
| 1000(1026.1) | 357.5(350)   | 4.81 ± .14  | 8.72 | 22.5 | 9.34 | 5.76 | 39.6 | 0.11 | 14.9 | 11.0 | 11.9 | 12.2 | 6.46 | 46.2 |
| 1000(1020.2) | 0.0(352.2)   | 4.98 ± .095   | 8.05 | 20.1 | 8.38 | 7.45 | 32.6 | 0.05 | 13.8 | 10.7 | 10.9 | 10.9 | 6.09 | 39.6 |
| 1000(1008.3) | 5.0(357.1)   | 4.72 ± .22  | 5.65 | 11.4 | 6.25 | 6.93 | 18.2 | 0.01 | 8.32 | 6.16 | 6.51 | 8.04 | 4.87 | 24.4 |
| 1000(1002.3) | 7.5(359.6)   | 2.87 ± .51  | 4.55 | 8.02 | 5.06 | 5.44 | 10.1 | 0.0  | 5.58 | 4.11 | 4.57 | 5.98 | 4.31 | 16.6 |
| 1000(996.5)  | 10.0(2.1)    | 5.49 ± .68  | 2.52 | 3.28 | 2.95 | 5.99 | 4.99 | 0.0  | 4.28 | 2.86 | 4.96 | 3.28 | 2.96 | 4.52 |

| Sampler   |           | JHU Dye Data<br>June 16-17, 1977<br>Tower and Stack |      |      |      |      |        |   |       |      |      |      |      |       |
|---|-----------|---|------|------|------|------|--------|---|-------|------|------|------|------|-------|
| Distance (m)  | Direction | OBS.  | 1    | 2    | 3    | 4    | 5      | 6 | 7     | 8    | 9    | 10   | 11   | 12    |
| # Drops/m <sup>2</sup> -hour                              |           |   |      |      |      |      |        |   |       |      |      |      |      |       |
| 500(540.3)  | 355(340)  | 7595  | 1168 | 3641 | 1232 | 4793 | 57127  | - | 7255  | 5506 | 4828 | 2050 | 2792 | 8032  |
| 1000(1043.3)  | 350(343)  | 7311  | 803  | 7013 | 1090 | 2788 | 110192 | - | 15927 | 5017 | 3440 | 2125 | 1855 | 12665 |
| Average Diameter (um)                                     |           |   |      |      |      |      |        |   |       |      |      |      |      |       |
| 500   | 355       | 358   | 582  | -    | 584  | 425  | 269    | - | 405   | 370  | 434  | -    | 486  | 419   |
| 1000  | 350       | 280   | 381  | -    | 396  | 307  | 163    | - | 253   | 134  | 258  | -    | 364  | 260   |
| Liquid Mass Deposition Flux<br>mg/m <sup>2</sup> -4 hours |           |   |      |      |      |      |        |   |       |      |      |      |      |       |
| 500(540.3)  | 355(340)  | 728   | 483  | -    | 514  | 768  | 2521   | - | 1006  | 583  | 827  | -    | 673  | 1237  |
| 1000(1043.3)  | 350(343)  | 338   | 93   | -    | 142  | 169  | 1003   | - | 420   | 25   | 123  | -    | 187  | 466   |

LEGEND

- |                              |                             |
|------------------------------|-----------------------------|
| 1. Hanna                     | 7. Wolf I                   |
| 2. Hosler-Pena-Pena          | 8. Wolf II                  |
| 3. Overcamp-Israel           | 9. ESC/Schrecker            |
| 4. Wigley-Slawson (profiles) | 10. MRI                     |
| 5. Slinn I                   | 11. Wigley-Slawson          |
| 6. Slinn II                  | 12. ESC/Schrecker (limited) |

Table 4. Comparison of Predictions of 10 Drift Deposition Models to Ground-Level Measurements of Sodium Deposition Flux, Number Drop Deposition Flux, Average Deposited Diameter, and Liquid Mass Deposition Flux . . . Contribution of Cooling Tower and Stack at JHU Samplers.

| Sampler    | ESC Dye Data (Evening)<br>June 16-17, 1977<br>Sodium Deposition Rate<br>Tower and Stack<br>mg/m <sup>2</sup> -4 hours |           |      |      |      |      |      |      |      |      |      |      |      |      |      |
|------------|---|-----------|------|------|------|------|------|------|------|------|------|------|------|------|------|
|            | Distance (m)  | Direction | OBS. | 1    | 2    | 3    | 4    | 5    | 6    | 7    | 8    | 9    | 10   | 11   | 12   |
| 230(261)   | 181(212.9)  |           | 0.02 | 0.0  | 0.0  | 0.0  | 0.0  | 0.0  | 0.0  | 0.0  | 0.0  | 0.0  | 0.0  | 0.0  | 0.0  |
| 300(346)   | 357(334)  |           | 6.58 | 62.0 | 75.5 | 42.6 | 24.2 | 105  | 0.0  | 65.6 | 62.0 | 33.5 | 56.4 | 80.2 | 58.5 |
| 400(461)   | 347(330)  |           | 1.54 | 12.2 | 15.9 | 4.56 | 17.3 | 36.4 | 0.0  | 21.5 | 20.2 | 35.4 | 14.4 | 7.24 | 40.3 |
| 500(547)   | 352(338)  |           | 1.24 | 29.1 | 32.4 | 31.4 | 7.56 | 52.8 | 0.0  | 37.7 | 37.3 | 42.9 | 29.1 | 19.3 | 49.6 |
| 750(778)   | 358(348)  |           | NR   | 17.3 | 21.4 | 16.9 | 1.01 | 37.6 | .002 | 16.4 | 12.3 | 29.1 | 17.5 | 18.1 | 30.8 |
| 750(800)   | 348(339)  |           | NR   | 8.93 | 12.4 | 7.73 | 3.56 | 26.1 | .003 | 16.1 | 12.2 | 11.6 | 10.5 | 9.93 | 5.68 |
| 1050(1110) | 342(335)  |           | NR   | 2.61 | 7.75 | 3.54 | 0.44 | 13.9 | 0.17 | 5.79 | 3.98 | 4.81 | 3.65 | 1.92 | 24.3 |
| 980(1023)  | 350(343)  |           | NR   | 5.19 | 4.28 | 5.31 | 2.32 | 31.1 | 0.15 | 14.3 | 9.85 | 7.15 | 7.90 | 4.79 | 33.5 |
| 1740(1756) | 0(356)  |           | NR   | 3.05 | 8.91 | 3.54 | 2.44 | 11.0 | 0.89 | 6.41 | 4.57 | 3.70 | 4.98 | 0.04 | 0.52 |

| Sampler    | ESC Dye Data (Evening)<br>June 16-17, 1977<br>Tower and Stack<br># Drops/m <sup>2</sup> -hr. |           |       |      |      |      |      |        |   |       |      |      |      |      |       |
|------------|--|-----------|-------|------|------|------|------|--------|---|-------|------|------|------|------|-------|
|            | Distance (m)   | Direction | OBS.  | 1    | 2    | 3    | 4    | 5      | 6 | 7     | 8    | 9    | 10   | 11   | 12    |
| 230(261)   | 181(212.9)   |           | 0     | 0    | 0    | 0    | 0    | 0      | 0 | 0     | 0    | 0    | 0    | 0    | 0     |
| 300(346)   | 357(334)   |           | 10766 | 2454 | 3020 | 5039 | 3064 | 14178  | 0 | 5055  | 4682 | 4460 | 2833 | 4672 | 4600  |
| 400(461)   | 347(330)   |           | 2101  | 1237 | 2480 | 584  | 5373 | 33308  | 0 | 7294  | 6485 | 4058 | 2222 | 1650 | 4468  |
| 500(547)   | 352(338)   |           | 3630  | 1164 | 3648 | 1213 | 3312 | 33317  | 0 | 7319  | 5373 | 4862 | 1953 | 2748 | 7958  |
| 750(778)   | 358(348)   |           | NR    | 1208 | 4278 | 1392 | 983  | 67187  | 0 | 6011  | 3189 | 5610 | 1857 | 2654 | 1735  |
| 750(800)   | 348(339)   |           | NR    | 812  | 4150 | 826  | 3214 | 90883  | 0 | 8398  | 4425 | 5630 | 1859 | 2364 | 1067  |
| 1050(1110) | 342(335)   |           | NR    | 424  | 4023 | 744  | 519  | 51377  | 0 | 11368 | 5239 | 3610 | 1371 | 892  | 15921 |
| 980(1023)  | 350(343)   |           | NR    | 699  | 5557 | 788  | 2844 | 101393 | 0 | 14006 | 4925 | 3223 | 1873 | 1777 | 13146 |
| 1740(1756) | 0(356)   |           | NR    | 605  | 8255 | 1127 | 1203 | 37684  | 0 | 8531  | 1572 | 3300 | 1523 | 44   | 390   |

LEGEND

- |                              |             |                             |
|------------------------------|-------------|-----------------------------|
| 1. Hanna                     | 5. Slinn I  | 9. ESC/Schrecker            |
| 2. Hosler-Pena-Pena          | 6. Slinn II | 10. MRI                     |
| 3. Overcamp-Israel           | 7. Wolf I   | 11. Wigley-Slawson          |
| 4. Wigley-Slawson (profiles) | 8. Wolf II  | 12. ESC/Schrecker (limited) |

NR - Not Reduced by ESC.

Table 5. Comparison of Predictions of 10 Drift Deposition Models to Ground Level Measurements of Sodium Deposition Flux and Number Drop Deposition Flux . . . Contribution of Cooling Tower and Stack at ESC Samplers.

| Sampler      |           | ESC Dye Data (Evening)<br>June 16-17, 1977<br>Average Diameter (µm)<br>Tower and Stack |     |   |     |     |     |   |     |     |     |    |     |     |
|--------------|-----------|--|-----|---|-----|-----|-----|---|-----|-----|-----|----|-----|-----|
| Distance (m) | Direction | OBS.   | 1   | 2 | 3   | 4   | 5   | 6 | 7   | 8   | 9   | 10 | 11  | 12  |
| 300(346)     | 357(334)  | 360  | 652 | - | 732 | 650 | 509 | - | 658 | 638 | 679 | -  | 663 | 662 |
| 400(461)     | 347(330)  | 306  | 678 | - | 622 | 482 | 334 | - | 475 | 461 | 652 | -  | 535 | 659 |
| 500(547)     | 352(338)  | 310  | 610 | - | 563 | 431 | 274 | - | 410 | 377 | 437 | -  | 482 | 422 |

| Sampler      |            | ESC Dye Data (Evening)<br>June 16-17, 1977<br>Liquid Mass Deposition Flux<br>Tower and Stack<br>mg/m <sup>2</sup> -4 hours |      |   |      |      |      |   |      |      |      |    |      |      |
|--------------|------------|--|------|---|------|------|------|---|------|------|------|----|------|------|
| Distance (m) | Direction  | OBS.   | 1    | 2 | 3    | 4    | 5    | 6 | 7    | 8    | 9    | 10 | 11   | 12   |
| 230(261)     | 181(212.9) | 0  | 0.0  | - | 0.0  | 0.0  | 0.0  | 0 | 0.0  | 0.0  | 0.0  | -  | 0.0  | 0.0  |
| 300(346)     | 357(334)   | 1047   | 1422 | - | 2485 | 1762 | 3914 | 0 | 3022 | 2542 | 2966 | -  | 2848 | 2794 |
| 400(461)     | 347(330)   | 126  | 806  | - | 294  | 1261 | 2604 | 0 | 1639 | 1327 | 2352 | -  | 528  | 2675 |
| 500(547)     | 352(338)   | 226  | 552  | - | 504  | 551  | 2301 | 0 | 1056 | 608  | 851  | -  | 660  | 1253 |
| 750(778)     | 358(348)   | NR   | 298  | - | 308  | 74   | 1196 | 0 | 491  | 147  | 498  | -  | 361  | 299  |
| 750(800)     | 348(339)   | NR   | 213  | - | 187  | 259  | 1146 | 0 | 471  | 173  | 391  | -  | 370  | 57   |
| 1050(1110)   | 342(335)   | NR   | 52   | - | 102  | 32   | 353  | 0 | 276  | 101  | 145  | -  | 79   | 696  |
| 980(1023)    | 350(343)   | NR   | 79   | - | 111  | 169  | 967  | 0 | 516  | 106  | 114  | -  | 183  | 476  |
| 1740(1756)   | 0(356)     | NR   | 25   | - | 44   | 36   | 183  | 0 | 144  | 4    | 92.3 | -  | 3    | 6    |

LEGEND

- |                              |             |                             |
|------------------------------|-------------|-----------------------------|
| 1. Hanna                     | 5. Slinn I  | 9. ESC/Schrecker            |
| 2. Hosler-Pena-Pena          | 6. Slinn II | 10. MRI                     |
| 3. Overcamp-Israel           | 7. Wolf I   | 11. Wigley-Slawson          |
| 4. Wigley-Slawson (profiles) | 8. Wolf II  | 12. ESC/Schrecker (limited) |

NR - Not Reduced by ESC.

Table 6. Comparison of Predictions of 10 Drift Deposition Models to Ground Level Measurements of Average Deposited Diameter and Liquid Mass Deposition Flux . . . Contribution of Cooling Tower and Stack at ESC Samplers.

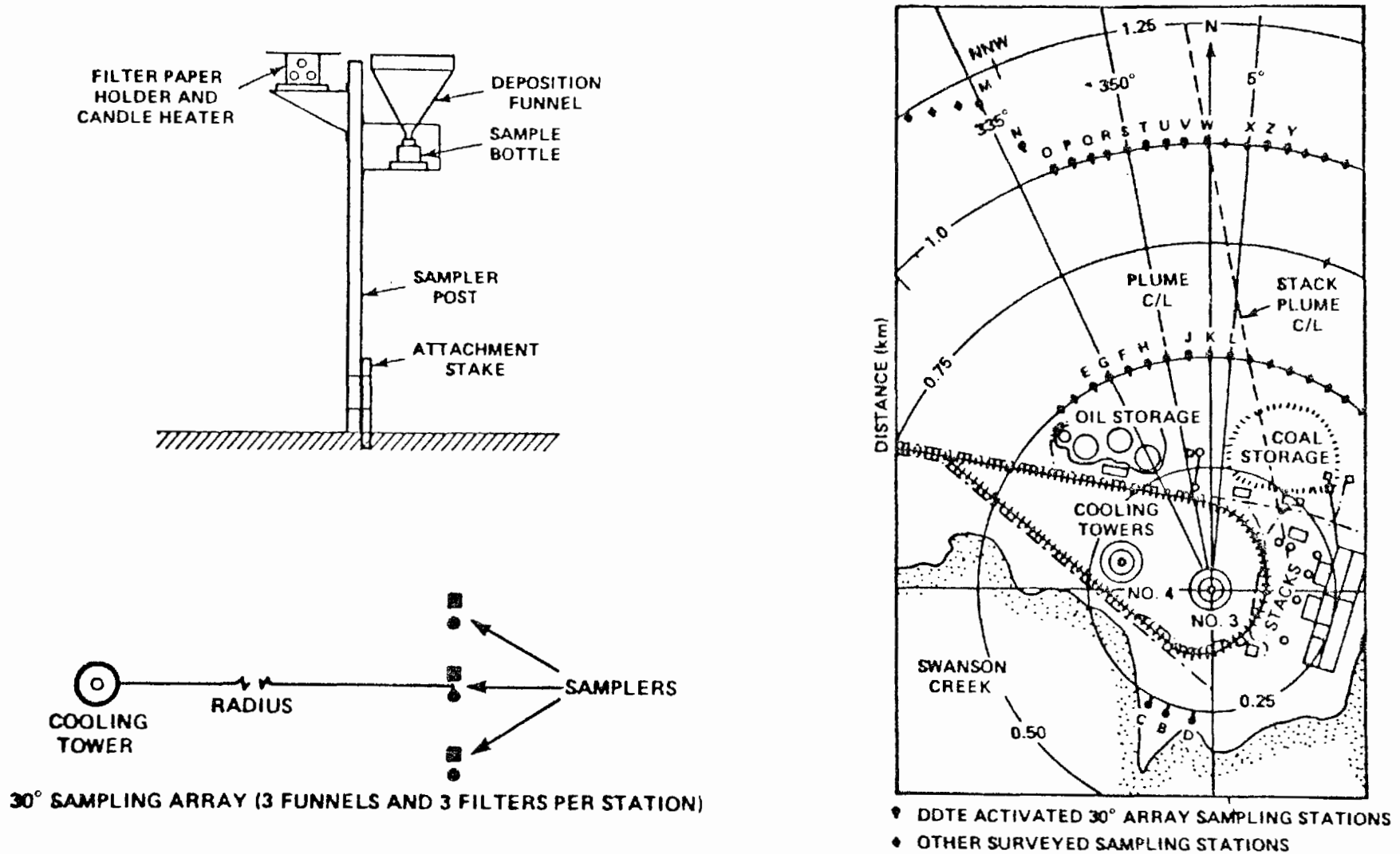


Fig. 1. (upper left) Sketch of Position of JIU Samplers at Typical Sampling Station. (lower left) Relative Position of Duplicate Samplers at a Sampling Location. (right) JIU and FSC Sampling Arrays at Chalk Point. (Adapted from Ref. 2).

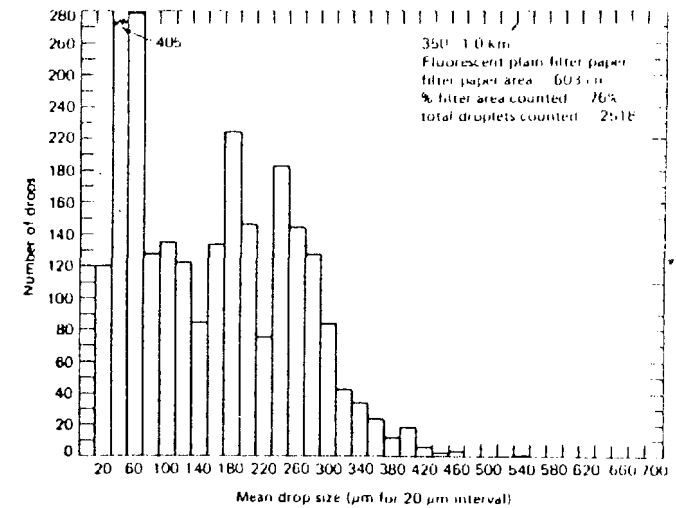
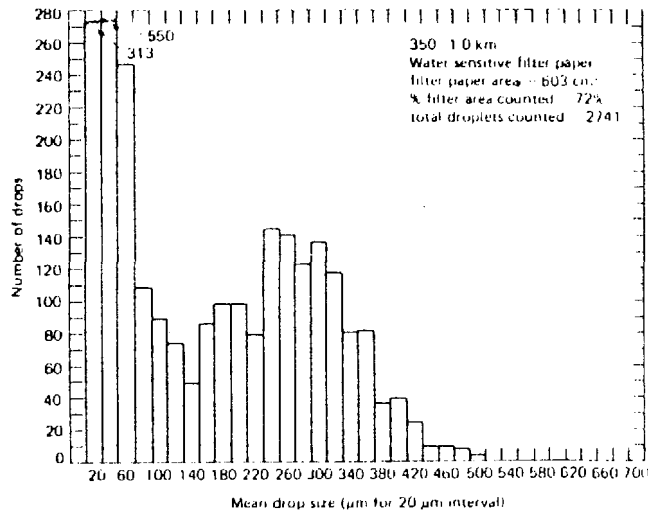
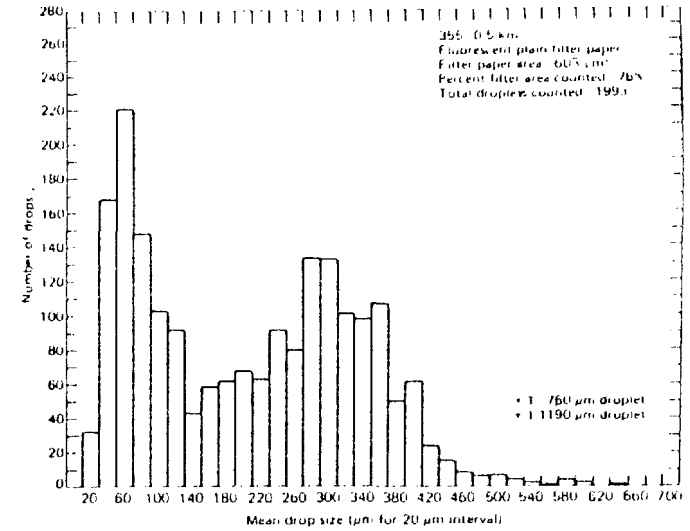
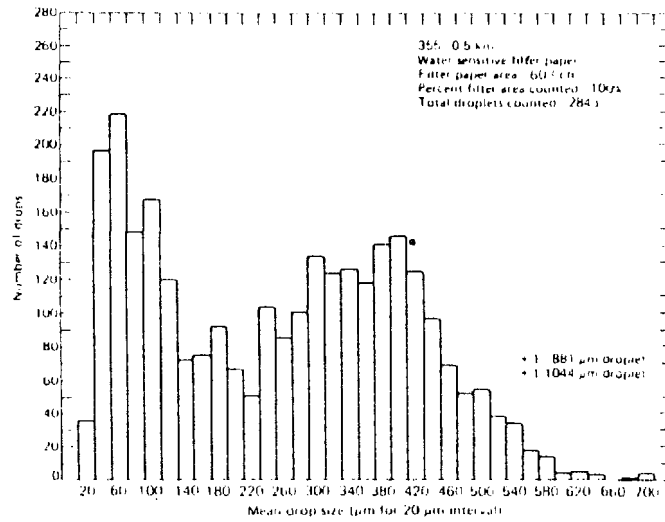


Fig. 2. Histogram Plots of Total Water and Fluorescent Droplet-Size Distribution for Sampling Stations Near Cooling Tower Plume Centerline. (Adapted from Ref. 2).

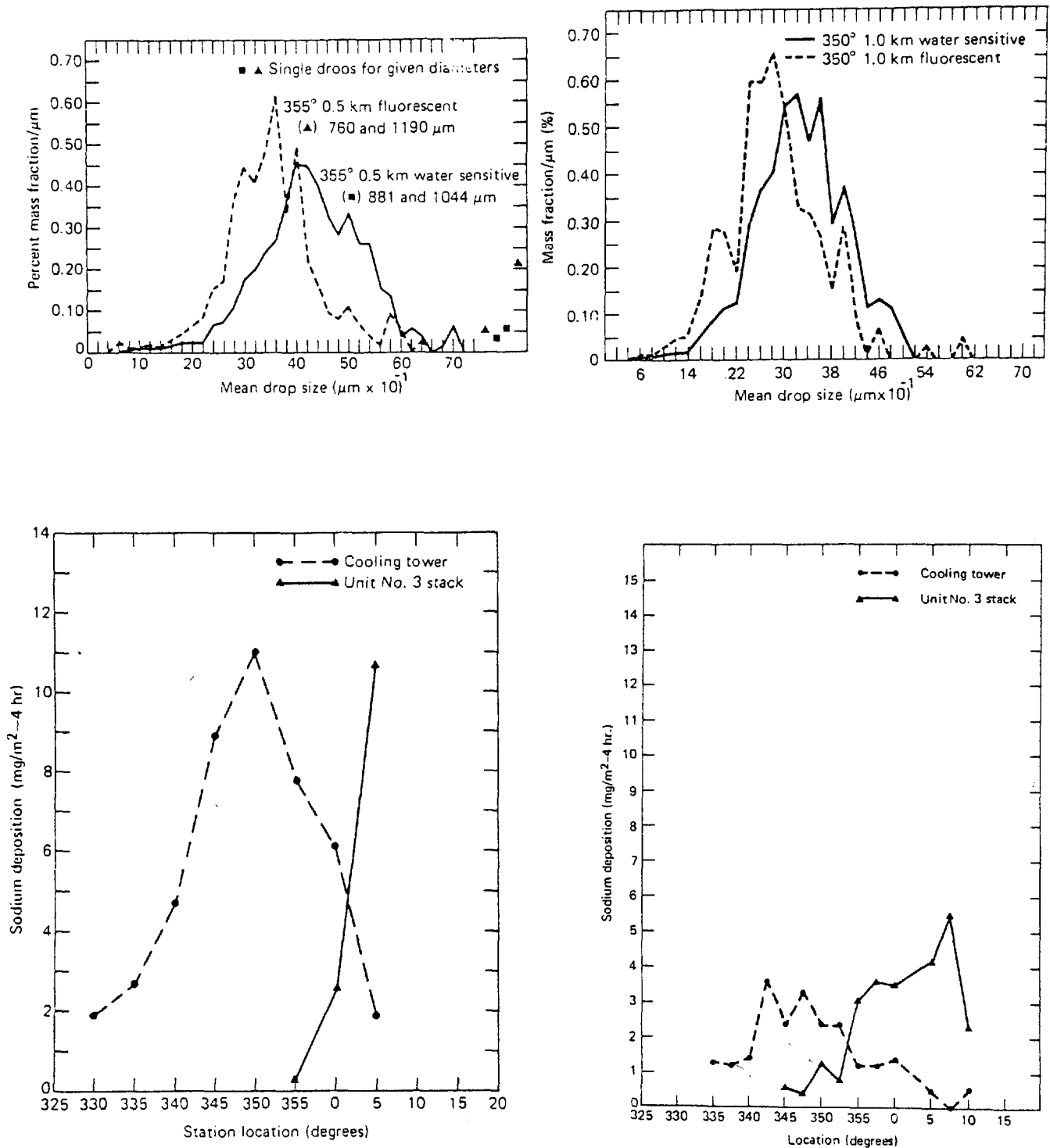


Fig. 3. (top) Percent Mass Fraction as a Function of Mean Drop Size at Two JHU Samplers. (bottom) Separation of Tower and Stack Sources of Sodium Deposition at the 0.5 km and 1.0 km Arcs. (Adapted from Ref. 2).

GROUND-LEVEL SAMPLER  
LOCATIONS FOR 6/6/77 DYE TEST

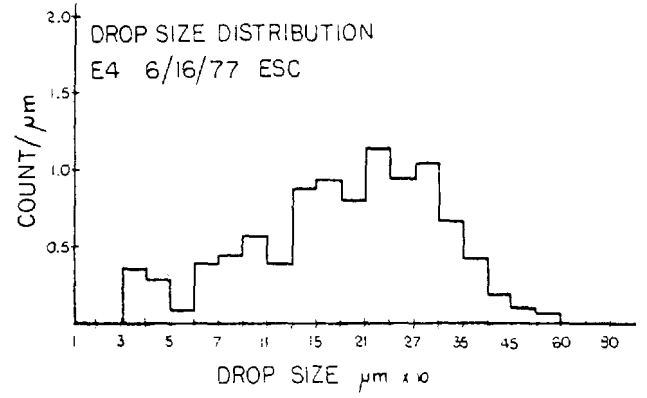
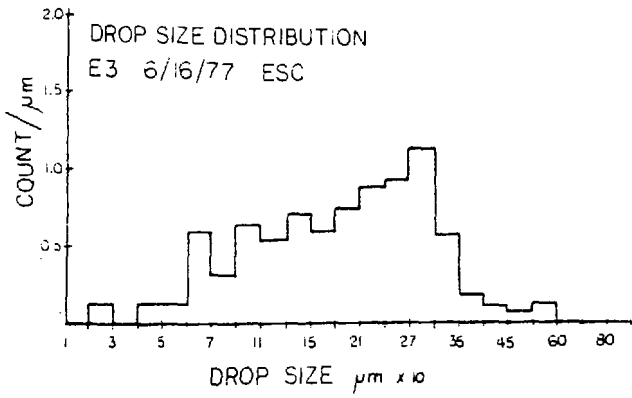
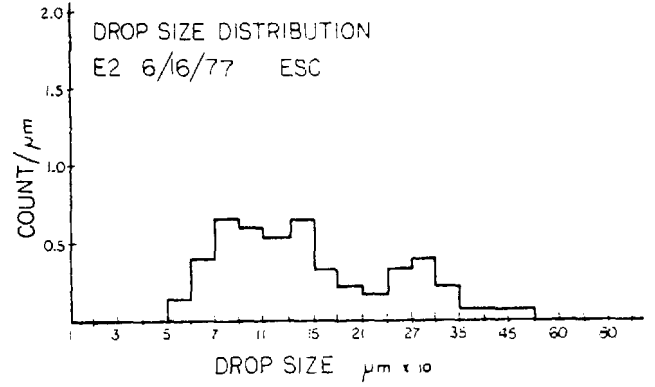
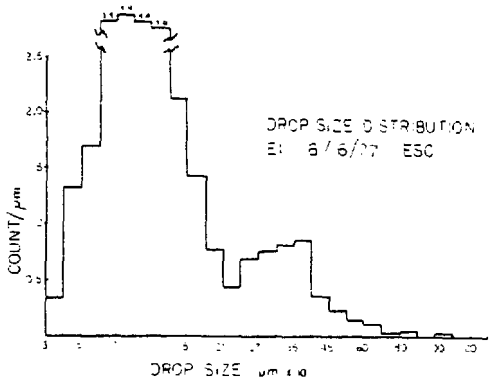
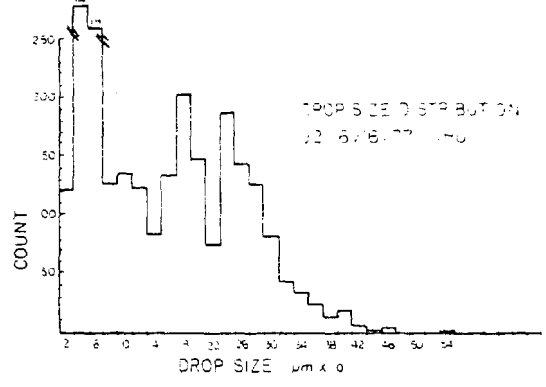
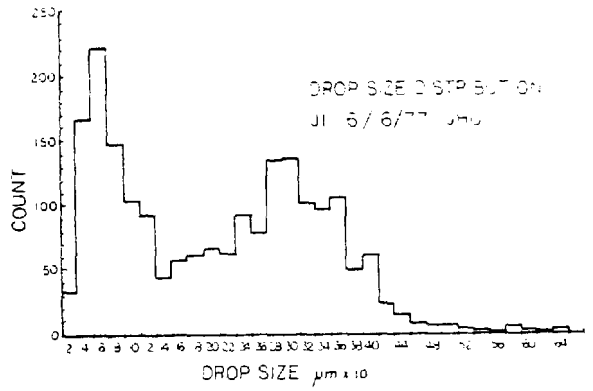
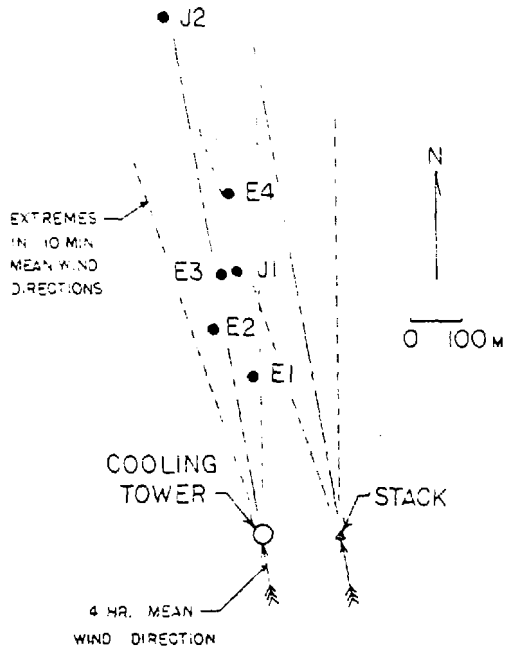


Fig. 4. (upper left) Location of 4 ESC and 2 JHU Samplers at which Drop Size Distributions were Measured. (lower left and right) Droplet Count as a Function of Droplet Size for All 6 Samplers.

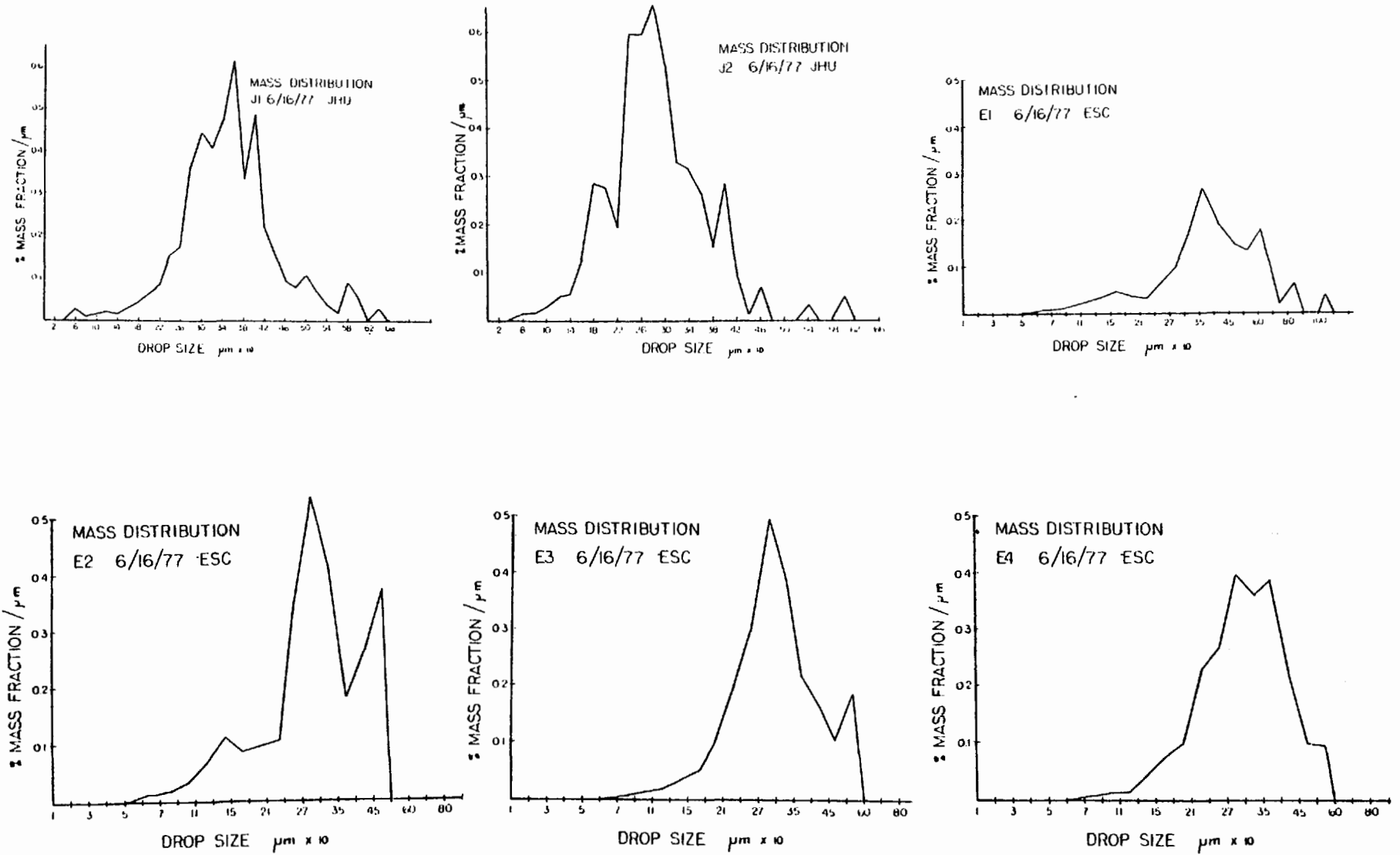


Fig. 5. Percent Mass Fraction as a Function of Droplet Size for the 4 ESC and 2 JHU Samplers.

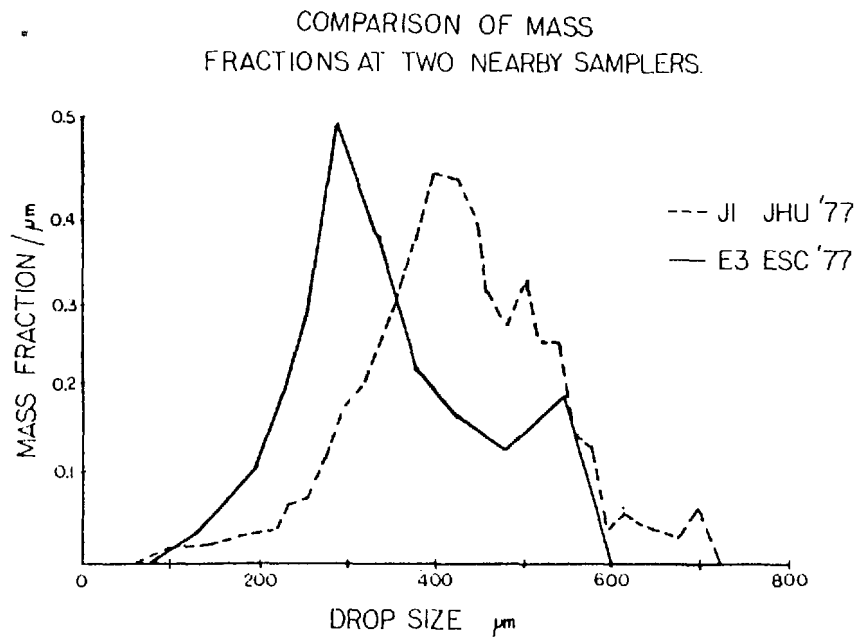
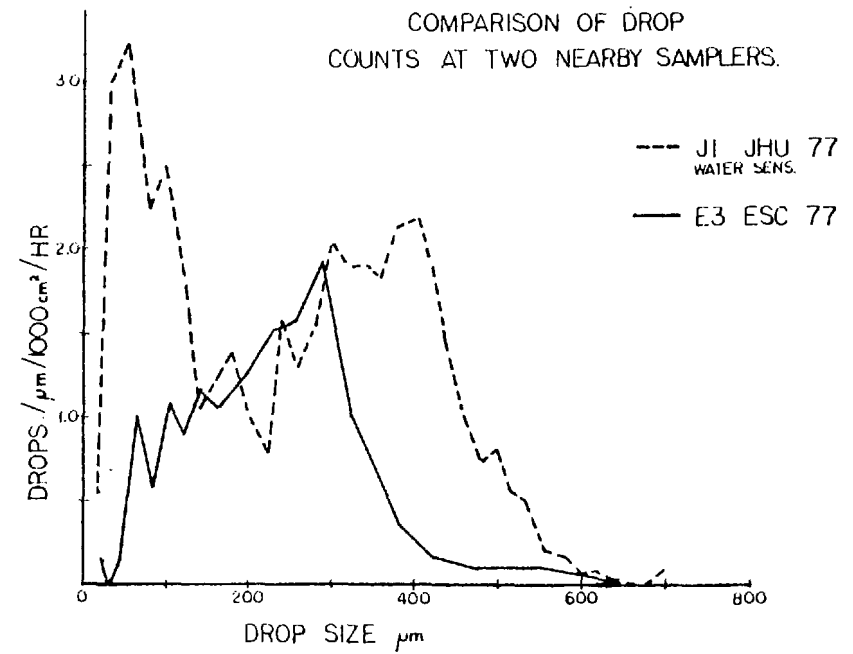
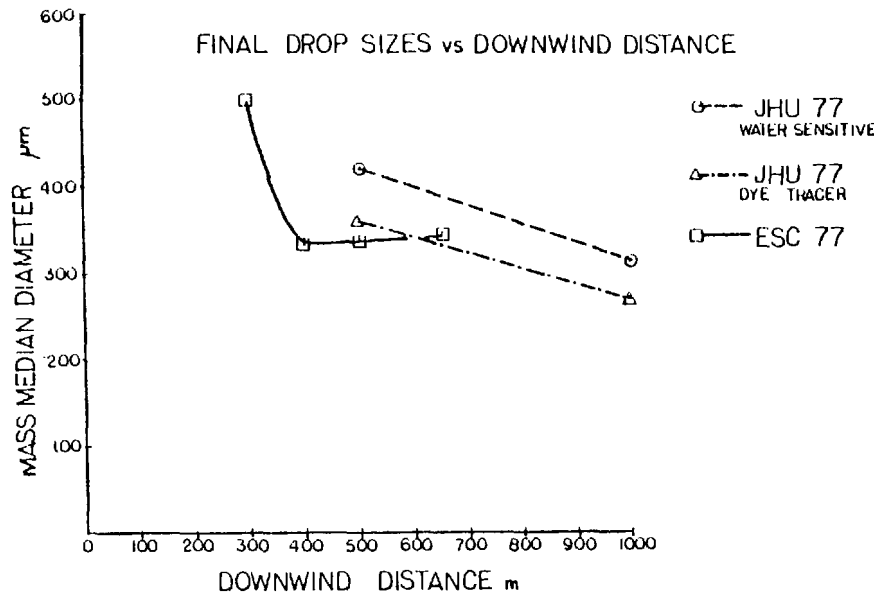


Fig. 6. (upper left) Variation of Mass Median Diameter with Distance from the Tower. (lower left) Comparison of Mass Fractions at Two Nearby Samplers. (above) Comparison of Drop Counts at the Same Two Nearby Samplers.

SODIUM DEPOSITION RATE  
 JHU DYE DATA -- 0.5 KM  
 JUNE 16-17, 1977  
 TOWER

SODIUM DEPOSITION RATE  
 JHU DYE DATA -- 0.5 KM  
 JUNE 16-17, 1977  
 TOWER

714

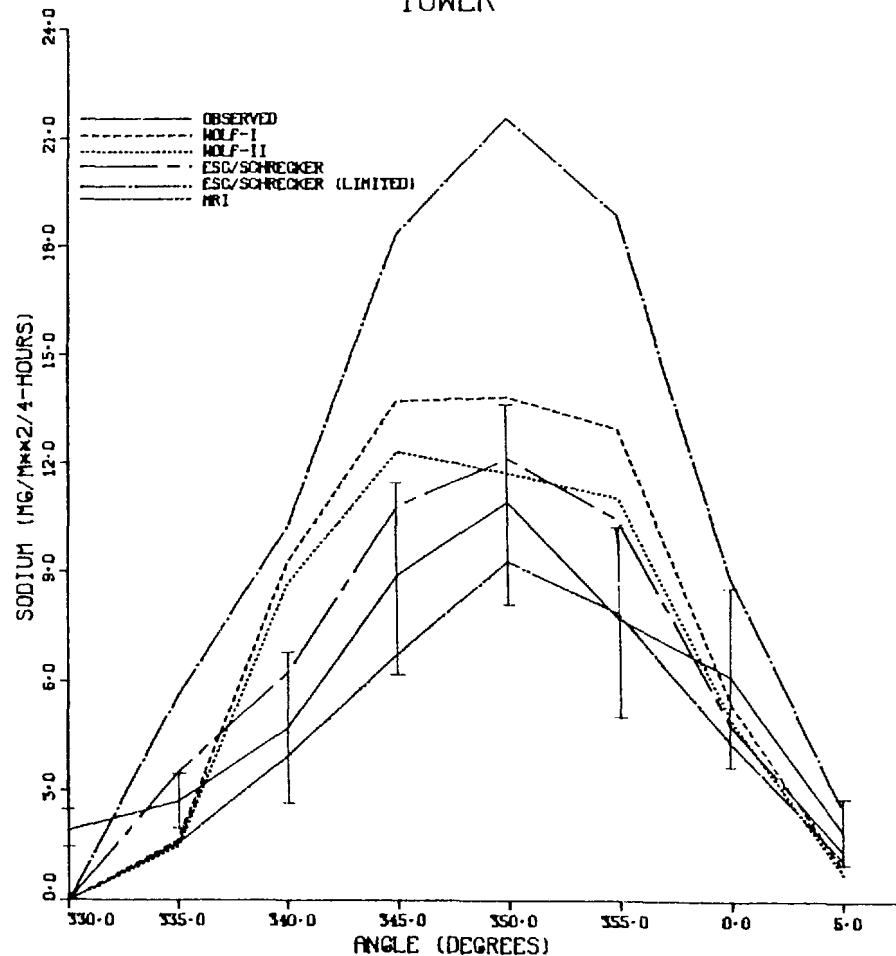
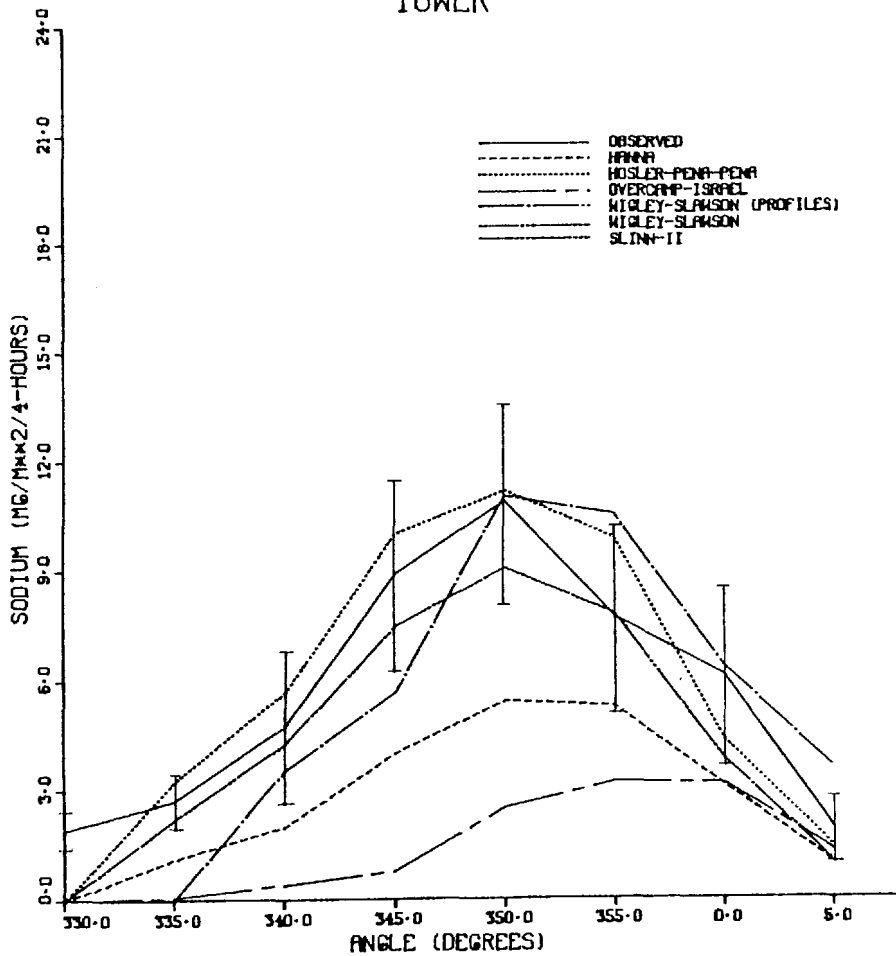


Fig. 7. Comparison of Predictions of 10 Drift Deposition Models to Sodium Deposition Flux Measurements at 8 Locations Along the 0.5 km Arc . . . Cooling Tower Contribution Alone.

SODIUM DEPOSITION RATE  
 JHU DYE DATA -- 1.0 KM  
 JUNE 16-17, 1977  
 TOWER

SODIUM DEPOSITION RATE  
 JHU DYE DATA -- 1.0 KM  
 JUNE 16-17, 1977  
 TOWER

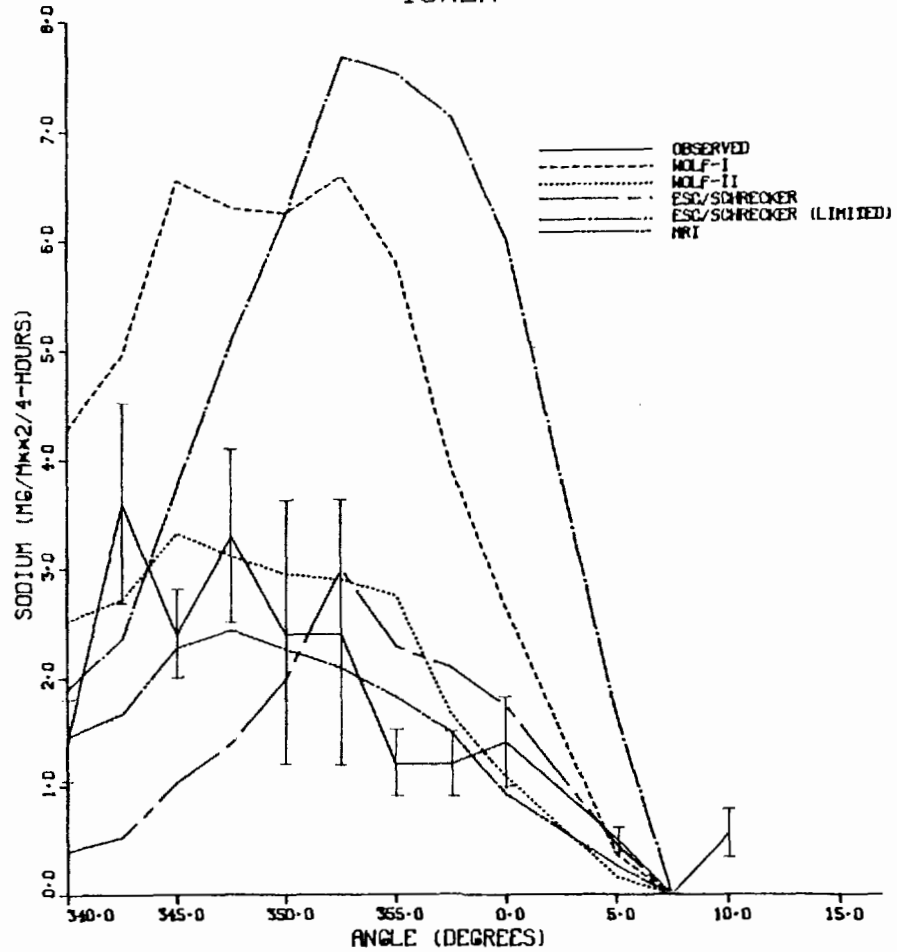
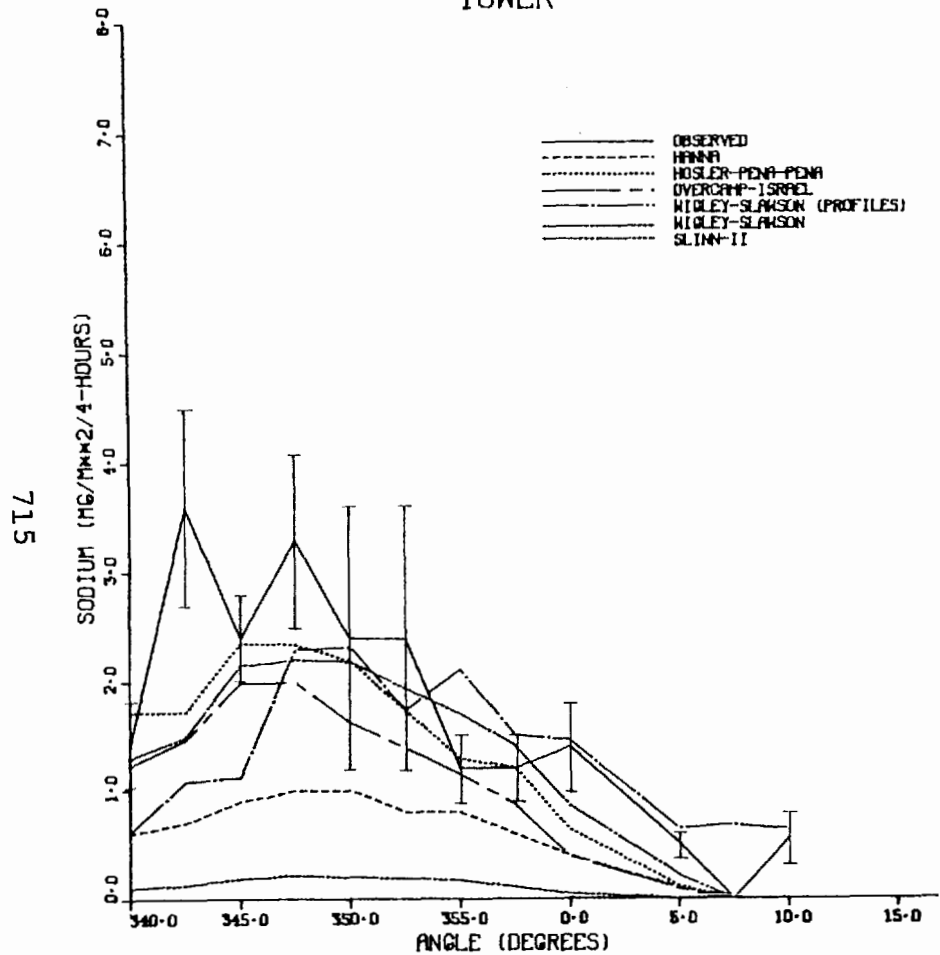


Fig. 8. Comparison of Predictions of 10 Drift Deposition Models to Sodium Deposition Flux Measurements at 8 Locations Along the 1.0 km Arc . . . Cooling Tower Contribution Alone.

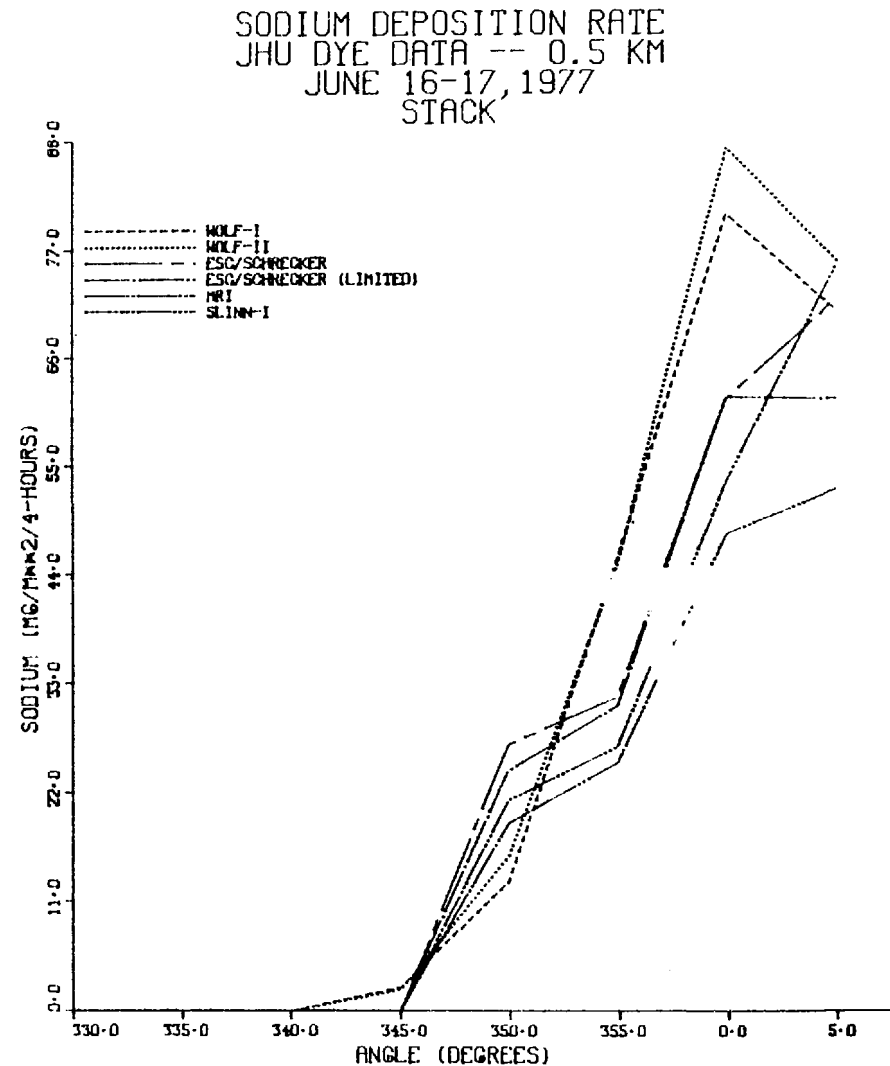
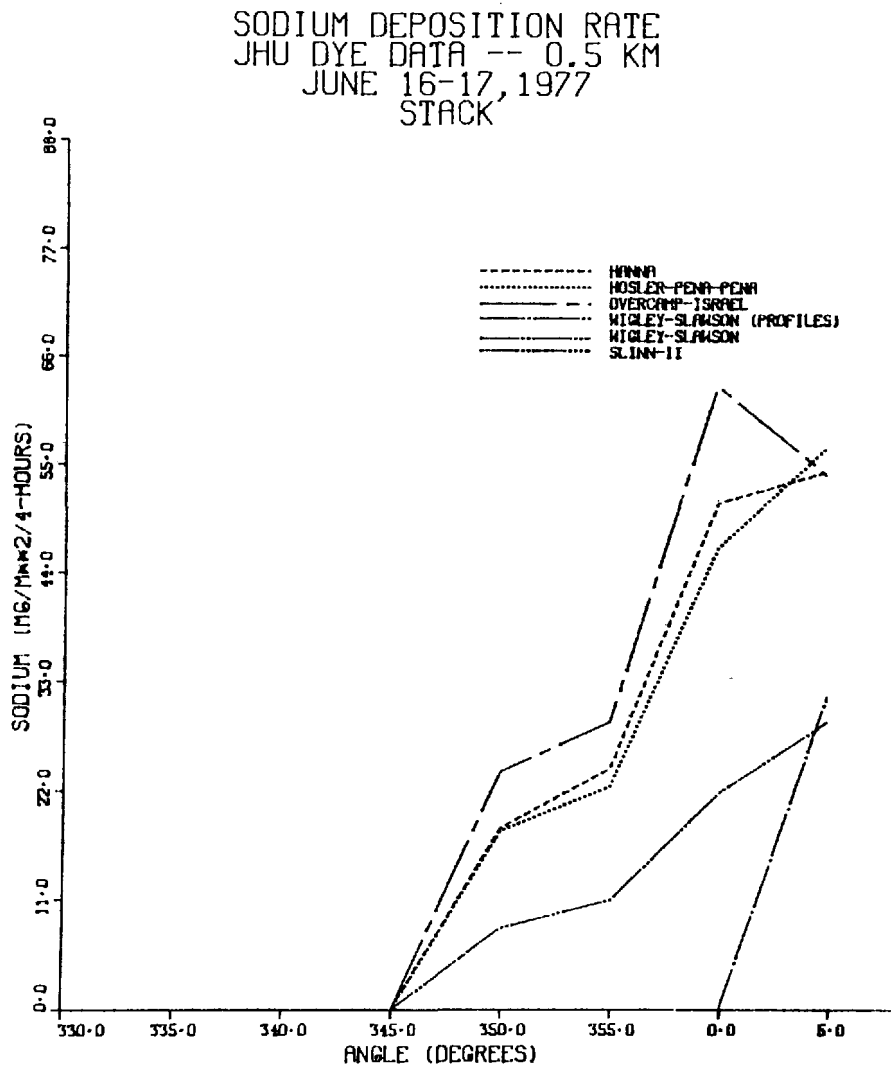
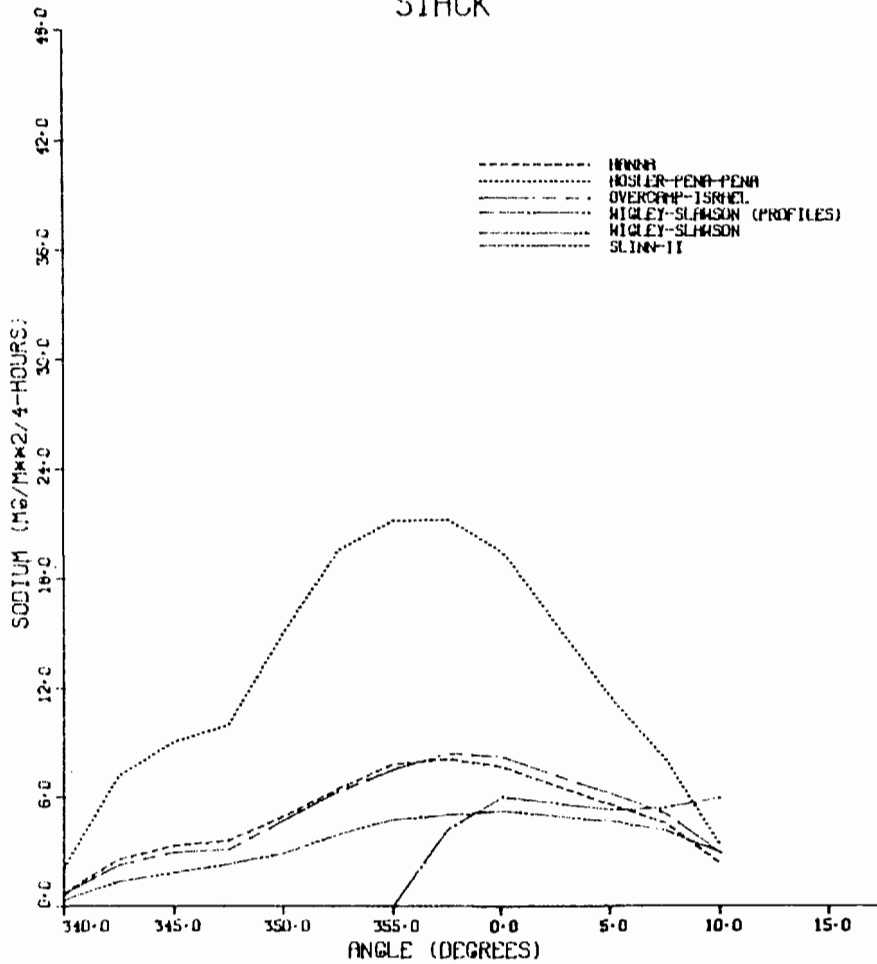
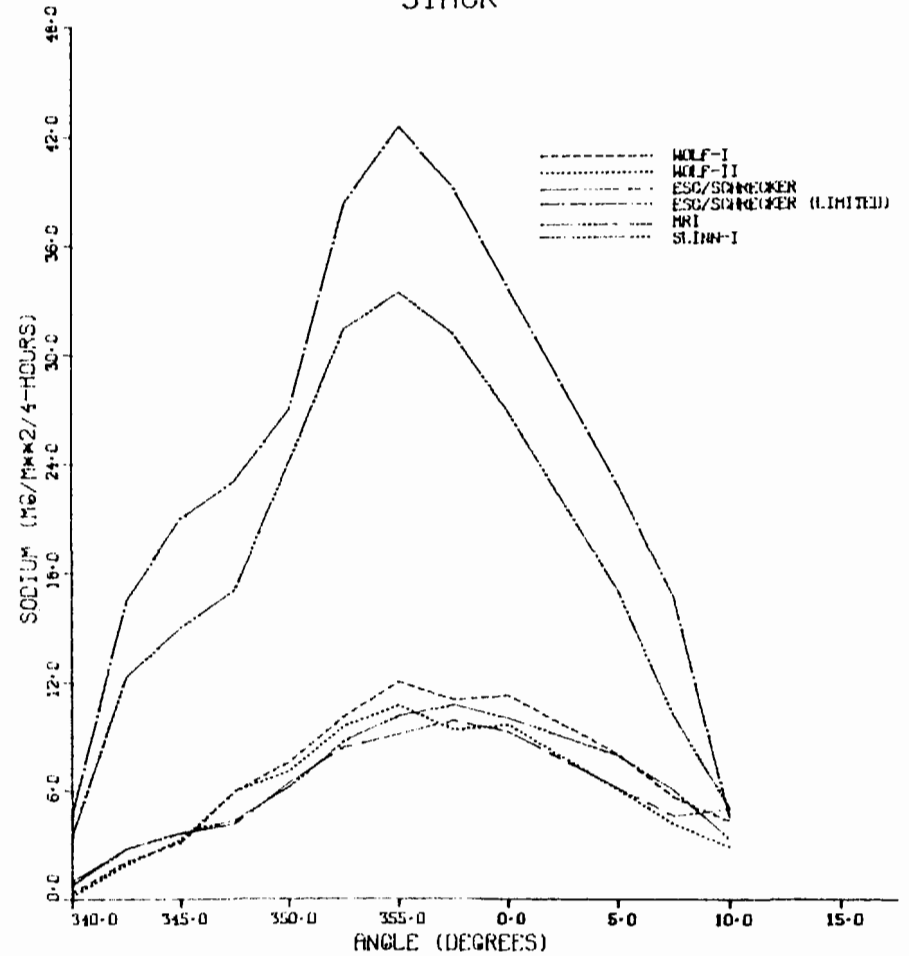


Fig. 9. Comparison of Predictions of 10 Drift Deposition Models of Sodium Deposition Flux at 8 Locations Along the 0.5 km Arc . . . Stack Contribution Only.

SODIUM DEPOSITION RATE  
 JHU DYE DATA -- 1.0 KM  
 JUNE 16-17, 1977  
 STACK



SODIUM DEPOSITION RATE  
 JHU DYE DATA -- 1.0 KM  
 JUNE 16-17, 1977  
 STACK



717

Fig. 10. Comparison of Predictions of 10 Drift Deposition Models of Sodium Deposition Flux at 8 Locations Along the 1.0 km Arc . . . Stack Contribution Only.

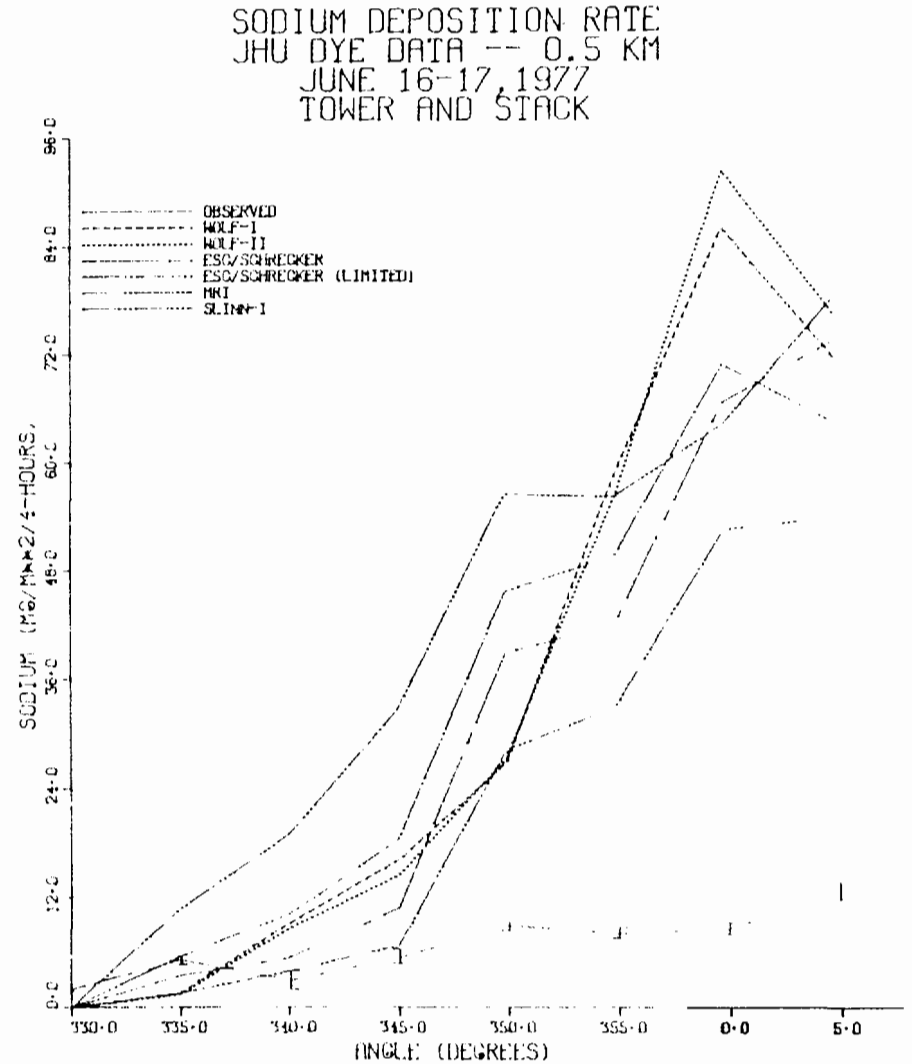
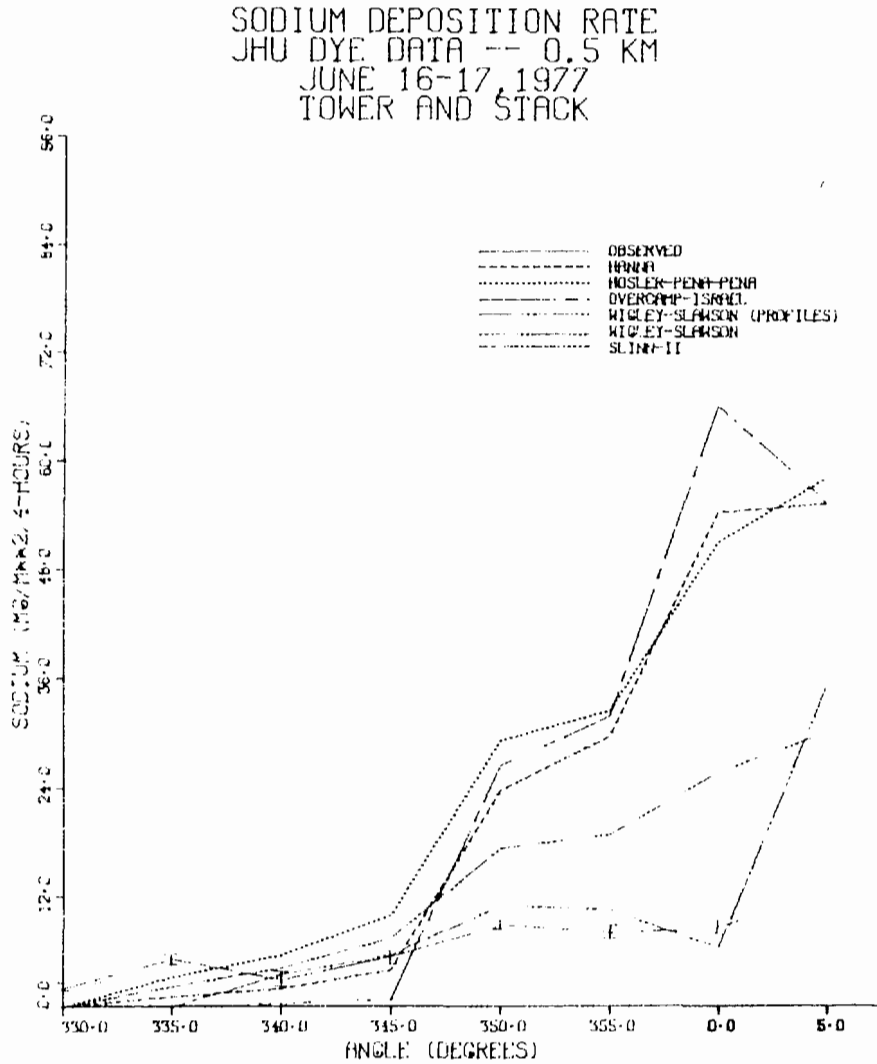


Fig. 11. Comparison of Predictions of 10 Drift Deposition Models to Sodium Deposition Flux Measurements at 8 Locations Along the 0.5 km Arc . . . Cooling Tower and Stack Contributions.

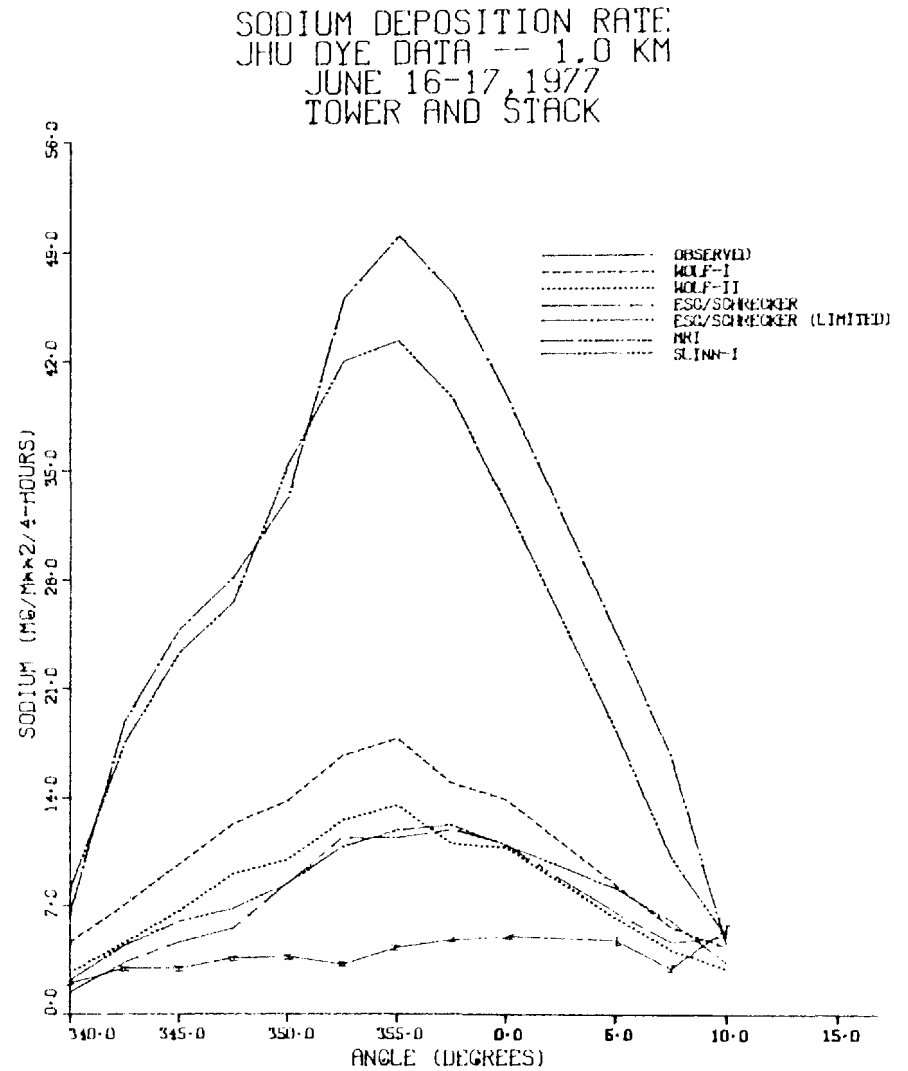
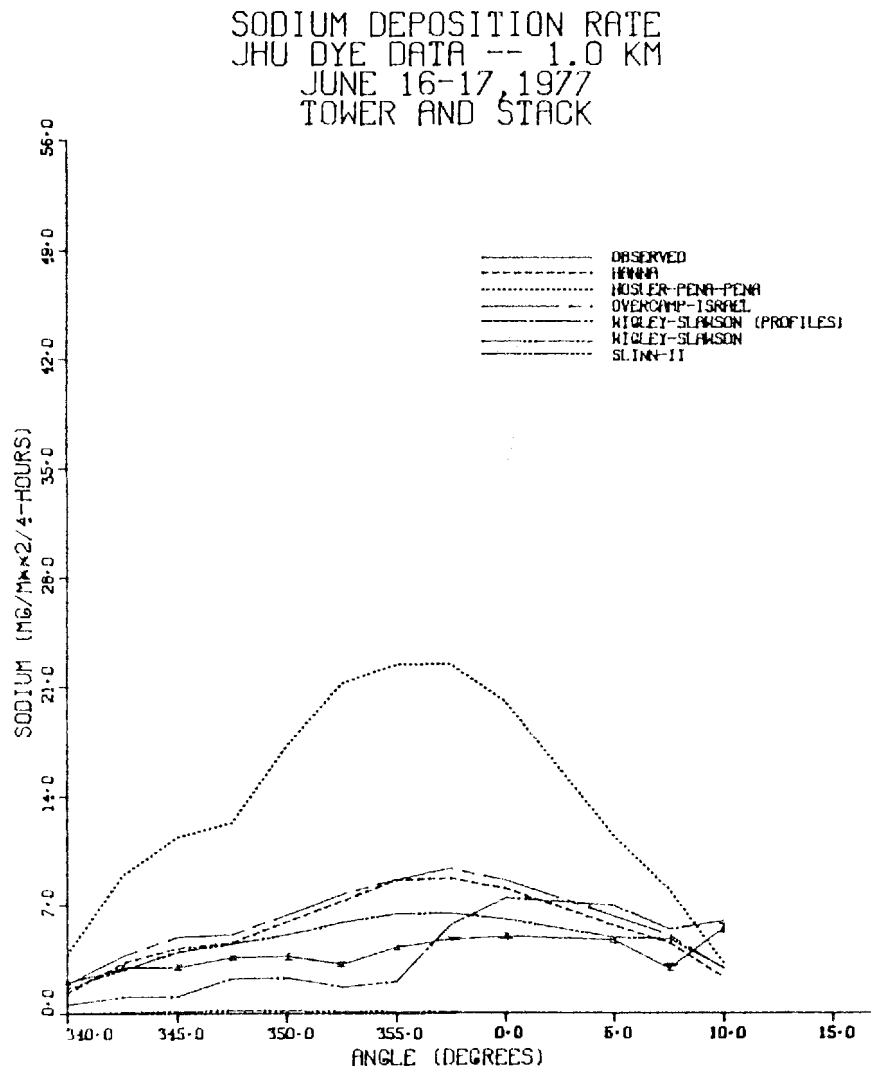


Fig. 12. Comparison of Predictions of 10 Drift Deposition Models to Sodium Deposition Flux Measurements at 8 Locations Along the 1.0 km Arc . . . Cooling Tower and Stack Contributions.

## COOLING TOWERS AND THE LICENSING OF NUCLEAR POWER PLANTS

J. E. Carson  
Division of Environmental Impact Studies  
Argonne National Laboratory  
Argonne, Illinois 60439, U.S.A.

### ABSTRACT

One provision of the National Environmental Policy Act of 1969 requires quantitative estimates of the effects of effluents from cooling towers used by nuclear power plants on the local air environment. Meteorologists were required to make these predictions even though adequate quantitative observational data at operating power plants were not available and for which accurate, proven models did not exist. Many of the environmental questions raised concerning the use of wet cooling towers in the early 1970's have been shown to be, in fact, non-problems: acid rain, plant damage due to salt drift from fresh water cooling towers, fogging and icing from natural-draft units, offsite fogging and icing from mechanical-draft towers, etc.

The procedures used in the environmental review process are discussed. Examples of the types of questions raised at environmental hearings, for some of which good answers are not available, will be discussed. Observations at hundreds of operating cooling towers in the United States and in Europe show that, except for the visual impact of the towers and their visible plumes, wet cooling towers are effective, economical heat sinks that are environmentally acceptable if properly constructed, maintained and sited.

### INTRODUCTION

The National Environmental Policy Act of 1969 (NEPA) completely altered the method of licensing of many facilities, including the issuance of construction and operating permits for nuclear power plants. The NEPA review process, as outlined in the Act and expanded by court decisions, requires a much more thorough, expensive and systematic review of the environmental impacts of the proposed facility than was previously required. Among other items, NEPA requires an analysis of all alternatives to the proposed action. For nuclear power plants, these include not building any new generating capacity, using other than nuclear fuels, locating the plant on other sites, and using other types of cooling systems. The benefit/cost ratio is one of the methods to be used to determine whether or not the license should be granted.

The bottom line of the NEPA process is the decision by the licensing agency (in this analysis, the Nuclear Regulatory Commission, NRC), whether or not to issue a permit for the construction or operation of the facility. A

"no" verdict is made if one or more of the environmental impacts is not acceptable for that site; for example, using mechanical-draft cooling towers next to a major highway. Another example would be a threat to an endangered species. Or the licensing agency, using a number of criteria including the benefit/cost analysis, may require that one of the alternative sites, cooling systems or fuels be used.

It should be remembered, and many opponents of nuclear power seem to ignore this fact, that it is not possible to generate energy from any source with creating some negative impacts on the environment. The NEPA review process is the method used to insure that the total environmental impact of the proposed power plant is low and acceptable.

As a result of the National Environmental Policy Act of 1969 and the Calvert Cliffs court decision, the Directorate of Licensing of the United States Atomic Energy Commission (AEC, now the U.S. Nuclear Regulatory Commission) entered into a crash program to write environmental impact statements (EIS's) as a step in the licensing of nuclear power plants and other facilities. Argonne National Laboratory (ANL) is one of the three national laboratories that have served as consultants to the AEC/NRC in the preparation of EIS's. I was assigned to write the meteorological sections of the EIS's prepared by ANL. In this paper, only those items related to the environmental impacts of waste heat on the atmosphere are discussed.

As part of the program to prepare EIS's, several meteorologists, including consultants for the utilities and the author, were forced to become "instant experts" on the effect of cooling-system effluents on the atmosphere. We were (and are) required to make quantitative predictions of the effects of the cooling system on the local air environment--effects such as fogging, icing, and drift. Recent trends indicate that EIS's may be required for fossil-fueled plants and many other types of facilities. Unfortunately, the state-of-the-art in atmospheric understanding and modeling is such that meteorologists are not able to make accurate, quantitative predictions on how the atmosphere will react to the large amounts of heat and water vapor generated from limited areas per unit of time from closed-cycle cooling systems.

A survey of the literature in the early 1970's indicated lots of generalities but very little factual information on cooling-tower effects. Statements with as little usefulness and authority as "cooling towers have the potential to cause fogging and icing" were found all too frequently. In addition, some of the facts presented were wrong (for example, the drift rates from cooling towers were quoted as about 0.2%). Also, the time available to become an "expert" was quite short. Nevertheless, meteorologists both for the NRC and the utilities are required to make these estimates and publish them in Environmental Reports (ER's prepared by the Utility) and Environmental Statements (ES's prepared by the NRC). We later have the dubious privilege of defending our analyses and conclusions in public hearings. These calculations and analyses must be made even though the complex processes involved are not understood and for which adequate, proven models are not available. Even in 1978, the amount of high quality

observational data on cooling tower drift and plumes is small. A large number of mathematical models have since been developed; however, none of the models has so far been shown to accurately simulate nature over a wide range of tower and atmospheric conditions with the degree of precision needed for the NEPA process.

#### STEPS IN THE PREPARATION OF ENVIRONMENTAL IMPACT STATEMENTS\*

It should be remembered that an EIS is a legal document whose primary function is to provide factual, quantitative information on the environmental impact of the proposed installation (and alternative plant designs and sites) to both the public and to licensing and regulatory agencies, who in turn use this information in their decision-making roles. The key word to be considered in writing a section of an EIS is impact rather than effect; the agencies and the public are more concerned with how the plant will affect people, fauna, flora, and the environment than with processes or effects. For example, if it can be shown that plumes from natural drift cooling towers never causes fog or that drift from a freshwater cooling tower with state-of-the-art drift eliminators never causes problems to the biota due to salts or wetting, no model or study should be required to prove it for each plant. Thus, it is not sufficient to only predict the frequency, extent, and severity of a specific event (such as fogging and icing from a mechanical-draft cooling tower or cooling pond); some effort must be made to estimate how these changes will affect people, traffic, flora, etc., which is usually a much more difficult problem. Frequent fog in winter from a MDCT or cooling pond over a vacant field owned by the utility is quite acceptable whereas fog only a few hours per year over a busy highway is not acceptable. The atmospheric effects of a cooling system depend primarily on the type of cooling system selected and on the local climate; the impact of the cooling system will be controlled to a considerable degree by the location of the cooling device with respect to roads, homes, trees, etc., and on the height of release.

A brief summary of the NEPA review process for the atmospheric effects of waste heat from a nuclear power plant is presented below (similar procedures are taken for the other environmental impacts as well). First, the utility (or its consultant meteorologist) prepares its assessment of the impacts of the cooling system selected for the plant (plus all of viable alternative cooling systems for that site) on the air environment. This massive document (up to 8 thick volumes), the ER, is sent to state and local agencies, the NRC, EPA and other federal agencies, and is made available to the public and to potential opponents. NRC meteorologists use this report, plus information from other sources (such as literature reports, field studies, models, personal observations of cooling towers in action, and the known environmental impacts from cooling systems) to prepare its own independent analysis. Independent is a key word in the description of the NRC analysis.

\*In this paper, the term Environmental Impact Statement includes both ER's, prepared by the applicants, and ES's, prepared by the regulatory agencies.

The NRC's environmental review for the plant is published in the Draft Environmental Statement (DES), which is circulated to local, state and federal, regulatory agencies, potential intervenors and the public for comments and criticisms. After a 45-day comment period, the responses to the DES are collected, studied, and responded to by the NRC staff. The NRC then issues a Final Environmental statement (FES), which includes the staff's responses to the comments and questions generated by the DES: a reproduction of all written messages received is included in the FES.

The FES is then recirculated to all interested parties and, after a suitable waiting period, a public hearing before the Atomic Safety and Licensing Board (ASLB) is held. These hearings are conducted in an adversary environment. Statements in the FES and ER are used by the ASLB in its deliberations as to whether or not the facility should be licensed. All parties to the legal process are free to challenge the accuracy or adequacy of the statements made in the FES and ER, present new information, or raise new issues; the NRC and the utility may use Supplemental Testimony (a written, signed, sworn document) or present expert testimony at the environmental hearing.

The rules-of-evidence at an ASLB hearing are quasi-legal; that is, they are not as strict as those in a civil or criminal case. Hearsay evidence, which includes observations and opinions not put in writing by plant personnel or others as to, for example, the actual extent and frequency of fogging and drift at an operating power plant, may be admitted into the record; such testimony is usually given "low probative value"--legal talk for "we hear you but we really don't believe it." An oral statement at a hearing that, for example, no one has reported damage from acid misting as a result of the merging of an SO<sub>2</sub> plume with that of a NDCT cannot be used as proof that it does not occur. The regulatory agencies are like other legal bodies; they want documentary evidence that can be placed into the record. Many of those participating in the review process and those in the hearing room have never seen a big cooling tower in operation.

It is my experience that the most useful type of evidence is a written report published in a quality, refereed journal. This report is then referenced in the ER, DES, FES or supplemental testimony, docketed and made available to the public by being placed in public reading rooms. Thus, all parties to the hearing can determine the accuracy and validity of your sources of information and the basis for your conclusions. The accuracy or validity of such references is rarely questioned. Big reports describing field studies are also very useful, as are theoretical (model) studies and generic reports.

It should be pointed out that the burden-of-proof that what is said in the ER and ES is true and complete rests with those who prepared them, and that intervenors, the utility or ASLB members can challenge any statement made or make their own independent assessment. It is of course hard to prove that postulated long-term or subtle effects will rarely or never happen, or are truly insignificant. A frequently heard phrase at these hearings is "if you cannot say with 100% confidence what will happen and then prove it, don't build the plant."

The objective of most intervenors is to either prevent the construction of the power plant, force a change in location, or force the utility to make a major change in plant design (for example, change from once-through cooling to cooling towers). (Some intervenors want to stop the construction and/or operation of all nuclear power plants; others are trying to prevent the construction of all new electric generating stations.) The best way for an intervenor to attain his objective is to present a positive case at the ASLB hearing; that is, present written evidence and/or expert testimony that some aspect of proposed nuclear power plant is in fact environmentally not acceptable. He can also attempt to show that the NRC staff's analyses are wrong or inadequate; the best way to do this is to present a positive case. The mere assertion that the NRC has not provided a satisfactory analysis is usually not sufficient.

The ASLB, which consists of three members, then makes its decision, based on the ER, FES and all of the other documents introduced into the "record" during the lengthy review process, plus transcripts of the hearing.

The ASLB's decision can be appealed within the NRC structure to the Atomic Safety and Licensing Appeal Board, or the Commission itself, which may reverse all or part of the decision, or call for further testimony and evidence on specific points.

Appeals to the civil courts have also been used to delay or suspend the issuance of a construction or operating licenses.

A large number of atmospheric effects of cooling systems can probably be answered by "too small to be measured" or "too small to be significant." However, merely saying it doesn't prove that the effect is too small--the conclusion must be proved by actual measurements or a validated model to become acceptable evidence. Mesoscale weather changes, such as the generation of clouds, additional precipitation and severe storms, should be items of major concern. An unfortunate consequence of the NEPA review processes is that it encourages the formation of energy parks--it takes very little additional effort, money and time to license multiple-unit power stations than a single unit. Power centers containing a nuclear capacity of 6500 MWe, are now being reviewed; even larger ones are being discussed. There must exist a critical heat load for a given site which, if exceeded, can create its own mesocirculation or heat island and thus create inadvertent weather changes. However, no one knows where this limit is.

#### MATHEMATICAL MODELS AND EIS's

One of the unfortunate features of the EIS work is the emphasis placed on quantitative estimates; the numbers generated by models which do not accurately simulate nature tend to be more acceptable and given higher probative value than are observations made at operating power plants. In one case, a utility spent money to hire a meteorological consultant to develop a computer simulation program for a NDCT at a proposed nuclear plant,

but has never taken a single plume measurement from his own operating NDCT's located 20 miles from the proposed site, or tried to compare actual plume behavior with his model.

Since the primary use of cooling tower models in EIS work is to determine the environmental acceptability of that tower for a specific heat load at a known location, only a model that has been shown to accurately predict plume and drift parameters for that tower size and for that climate (that is, a fully validated model) should be used. Unfortunately, none of the models now available has been proven to be sufficiently accurate. For example, a model was used to predict the frequency and extent of fogging from various types of cooling towers for a nuclear power plant which may be forced to convert from once-through to closed-cycle cooling. The model for mechanical draft cooling towers predicted a few hours per year of fog over a nearby (300-350 m) major highway. If we had complete faith in the model, the MDCT could have been listed as an acceptable cooling system. However, the lack of proven accuracy of the model for predicting the extent of surface fog, the irregular terrain at this site, and the consequences of a wrong decision forced NRC to reject this type of cooling tower as an acceptable alternative for this plant. The recommended cooling system for this power plant, natural-draft towers, would be more expensive and would have a much greater aesthetic impact.

In the past decade, a large number (more than 50) mathematical models have been developed and used to make quantitative predictions of plume rise, plume length, drift deposition, local changes of temperature and humidity, and other effects that are created by the heat and moisture discharges from cooling towers.

Although meteorologists have found that mathematical models are very useful in studying and understanding a wide range of atmospheric processes, the primary use for mathematical models of cooling tower plumes and drift has been to provide quantitative predictions of cooling tower effects at proposed power plants for use in environmental reports and environmental impact statements. Therefore, mathematical models for this use should be simple and easy to apply with available data, be inexpensive to run on the computer, and have been shown by tests with independent data to accurately simulate nature for the range of atmospheric conditions expected at the new location. Research-type models can and should be more complex and may require specialized data--such as vertical profile of wind speed and direction, air temperature, humidity, etc.--not readily available at other sites.

#### QUESTIONS RAISED AT ENVIRONMENTAL HEARINGS

Most of the issues raised at the public hearings concerning cooling tower impacts are valid ones that must be addressed. Typical of the type of question that does have an answer is one posed at a recent public hearing for a nuclear power plant in Indiana: "Will the heat, humidity, icing, water droplets (due to both fog and drift) and salts (due to drift) added to the atmosphere by a large group of mechanical-draft cooling towers less than

one kilometer away decrease the yield of fruit or increase the incidence of fungus diseases in a peach/apple orchard located within one kilometer of the towers? If yes, by how much? What can be done to mitigate or lessen the damage? If no, prove it in an adversary environment in a court of law." Models plus observations of cooling tower plumes in a similar climate and mathematical models were used to provide answers to this question. Unfortunately, because of the lack of demonstrated proof of the accuracy of the model used and the shortage of quantified observations at operating cooling towers of (comparable size in a similar climate), 100% confidence in the predicted changes of temperature and humidity in the orchard is not possible. Compounding the uncertainty of the conclusion is the fact that biologists cannot state how large the temperature and humidity changes would have to be in order to affect the fruit trees, lower crop yields, increase the incidence of fungus and other plant diseases, increase insect populations, etc.

There are a number of meteorological questions that are raised during the environmental review process that do not have provable (in either the scientific or legal sense) answers. These questions, which are valid ones, relate mostly to mesocale effects, such as local climatic changes, generation of clouds, snow showers, thunderstorms, and tornadoes. Unfortunately, the state-of-art in cloud physics and other phases of meteorological knowledge do not permit us to predict with any degree of certainty what will be observed downwind of a group of wet cooling towers. Snowfall from cooling towers has been reported many times under very cold winter conditions; in one case, 140 mm (5.5 in) of snow was measured downwind off a complex of natural draft cooling towers in West Virginia [1].

Given below are samples of questions, raised by the intervenors and the ASLB related to mesocale weather effects raised at the ASLB hearings for a proposed two-unit nuclear power plant in an area of high frequency of tornadoes:

"The waste heat released to the atmosphere could also increase the incidence of turbulent weather, fog, icing, inversions and possibly climate changes and tornado incidence."

"The PSAR\* recognizes the climatic effects of the thermal plume. Obviously tremendous amounts of energy are present as a result of the thermal plume, plus the effect of the up-drafts. Intervenors believe that, given the proper climatic conditions (conditions which are not unusual in this area) the energy and up-draft will contribute to the existence of additional precipitation and spawn tornadoes. The PSAR appears to admit that there are uncertainties in this area but dismiss the implications without conducting the necessary experimental basis for rejecting the consequences. As part of their answer, Intervenors request and require that Staff and Applicant test the effects of the thermal plume under appropriate climatic conditions and furnish the results thereof. If these tests were conducted, and it is the responsibility of Staff and Applicant to do so, the issue could be resolved."

\*Preliminary Safety Analysis Report, prepared by the utility.

"Intervenors contend that the applicant and regulatory staff have inadequately considered the effect of the plume of the (proposed facility) cooling towers in the following areas: increased precipitation: spawning tornadoes.

"Although we have the many days of sunshine and wind we also have many tornadoes and earthquakes. If you think you know someone who can predict those things are what will happen in them then you have fools for advisors." How would you like to try to answer this type of question, under oath, in a adversary environment?

Sometimes, intervenors use "overkill" in their questions and comments in an attempt to stop the licensing of the facility. These contentions usually are relatively easy to answer. Given below is the sworn testimony of a highly respected professional meteorologist given under oath at the environmental hearing for a proposed two-unit nuclear power in the northern part of the country using a cooling pond. "The second feature of this winter situation is that the fogging will almost certainly occur as liquid drops at sub-freezing temperatures. All exposed surfaces will be subject to riming and glazing. Roads within a mile or so downwind of the pond are likely to be impassable throughout the winter. How far out occasional episodes of hazardous driving conditions are likely to extend is speculation." Under cross examination, the witness was forced to admit he had never seen a cooling pond in operation, and that his estimates of distance of fogging and the duration of icing were too high.

If all or part of the written or oral testimony of a witness at the hearing is shown to be incorrect or otherwise unsatisfactory, the remainder of his testimony is (and should be) given low probative value. The above statement is especially true for witnesses for the utility or the NRC. In other words, one incorrect bit of information can destroy the creditability of the witness for all other issues as well.

Some contentions are false, and can easily be refuted. One example was made at a recent hearing (I have altered the wording of the question slightly):

"local observation indicated that when the plant was shut down on (date) for three months, it was because so much snow and ice had deposited on (a local major highway), about 0.8 km from the plant that the utility feared suit in case of accidents."

This nuclear power plant was shutdown for refueling before heavy natural snowstorms created this traffic hazard.

A question that has been asked of several locations that is hard to answer is that of acid rains caused by the merger of SO<sub>2</sub> and other gases from fossil smoke stacks and cooling tower plumes:

"the interactions of the plume and the vapors from said plant with emissions of oxides of sulfur and particulates from other existing fossil fuel plants in the area, including a fossil fuel plant located within one mile of the city of \_\_\_\_\_ and with temperature inversions, common to the area,

will produce unacceptable adverse effects on the historic building and property in the city of \_\_\_\_\_ and to the health of the citizens of the city of \_\_\_\_\_."

This particular contention was easy to answer, as wind conditions favorable for plume merger carried the merged plumes away from the city in question. But proving that significant impacts due to a merger of fossil chimney effluents and cooling tower moisture will not occur remains.

Fortuantely, one comment heard frequently a few years ago is rarely used now: "Build a cooling tower and all the thermal problems will disapear." This is simply a false statement. While certain thermal effects are reduced or eliminated, others are created which, for a specific location, could be worse. This is especially true if a plant is forced to retrofit to another cooling system either during construction or after the start of operation.

A problem of communications with the boards and the public is the lack of precise meaning of certain words. "Salt" means "NaCl" to most people; there is little of this material in the blowdown and drift from cooling towers at inland sites. The effects of NaCl on plants, metal, etc., are quite different from that of the CaSO<sub>4</sub> and other materials in drift. "Fog" and "ice" are other poorly understood terms. Most people at these hearings feel that fog is only present when "one cannot see his hand in front of this face" and ice is hard and dense like ice cubes. Cooling-tower fog that restricts visibility to 300 m (1000 ft) is not a traffic hazard but is "fog" to meteorologists. Ice produced by cooling tower plumes is light, friable rime ice of little strength and very low density; such ice does not cause damage to structures or vegetation. Cooling tower fogs rarely cause ice on clear road surfaces. At one hearing concerning a cooling pond, I showed photographs of steam fog over the pond; the reaction was "Is that what we are talking about? Forget it. Go on to the next topic." I have used movies and color slides at public hearings; they did a much better job of explaining what happens than several pages or days of testimony. I strongly urge all of you to document your observations with photographs and movies (be sure to include date, time, weather conditions, etc.), as they are very effective pieces of evidence. The old saying that a picture is worth a thousand words is very applicable in EIS work.

#### WAYS TO IMPROVE THE EIS PROCESS

In my opinion, which is shared by most people in the field, the primary reasons meteorologists are not able to make accurate, quantitative estimates of the atmospheric effects of cooling-system operation required by the NEPA review process is the lack of systematic detailed observations made at operating power plants. Therefore, there is a need for a series of major field experiments at power plants with mechanical-draft and natural-draft cooling towers, spray canals, once-through cooling, and cooling ponds. One result of these field observations would be to clearly identify and quantify the environmental problems caused by cooling systems, and to indicate which of

the postulated issues are in fact nonproblems and need not be considered further. Another result of equal importance would be the construction of a suitable data base that would allow mathematical and physical models to be developed and adequately tested. These models could then be used to predict, with accuracy and confidence, conditions at proposed power plants in other area areas. As a result, multimillion-dollar design decisions, which are now being based on very poor information, would be supported on a more accurate and complete assessment of cooling-system effects.

The observations would also be used to formulate "rules-of-thumb" that could be used in determining the environmental acceptability of a specific cooling system on a given site. For example, if more thorough observations show that fog from MDCTs and cooling ponds does, in fact, always or almost always evaporate or rise above the surface within a short distance, then no model would be needed for acceptance of such a cooling system on another site. But "how far is far enough" remains a valid question requiring a quantitative answer that can only come through observations over a wide range of meteorological conditions at operating cooling systems. Such "rules" could be used by the decision-making agencies without the need to model each and every proposed plant. These agencies could also dismiss with confidence those environmental concerns that have raised at public hearings but which are known to be insignificant (such as temperature and humidity changes downwind of NDCTs) or do not in fact occur (fog downwind of NDCTs).

Finally, the studies would lead to a series of generic reports that would be very useful to the regulatory and licensing agencies and for educating the general public. If such reports were now available, much of the wheel-spinning that is going on in the EIS procedure would be eliminated, with a considerable savings of time, effort and money for all parties involved. These generic reports should summarize and evaluate our present knowledge of cooling tower effluents, and include a critical comparison of the models now available. If such generic reports or "rules" were now available, each utility would not be required to "reinvent the wheel" each time it generated an ER.

There is a large amount of good factual data and information locked up in the files of cooling tower manufacturers, power companies and their consultants. This data, if properly summarized and published, would demonstrate the actual impact of cooling towers on the air environment, would shorten the time and effort to complete a NEPA review, and could lead to a better selection of cooling system for a specific power plant. The dollar and time savings would be very large. The legal and other values of such studies buried in classified files are zero.

## SUMMARY

Due both to shortages of cooling water and to regulatory actions, future power plants--both fossil and nuclear--will use evaporative closed-cycle cooling systems to dissipate their waste heat directly to the atmosphere.

Unfortunately, the state-of-the-art of atmospheric knowledge and modeling is such that meteorologists are not now able to predict quantitatively how the atmosphere will react to the large amounts of heat energy and water vapor that it will be forced to absorb from limited areas of cooling towers, cooling ponds, and spray canals. Conceivably, critical heat release rates may exist which, if exceeded, may lead to considerable effects, such as the formation of extra precipitation, severe storms and/or tornadoes.

Closed-cycle cooling methods reduce but do not eliminate chemical and thermal discharges into the aquatic medium; they transfer the primary area of impact from hydrosphere to the atmosphere. These cooling systems do create adverse atmospheric effects (such as fogging and icing, noise, drift, greater evaporative loss of water, esthetics, etc.) which may be environmentally unacceptable at some sites.

Because evaporative or wet cooling towers provide a convenient, dependable, economical, and well-understood method of rejecting heat directly to the atmosphere, they are usually chosen as the means of heat rejection for power plants and large industrial plants. Where sufficient level land is available near the plant at moderate (i.e., farmland) prices, cooling lakes or spray canals may be utilized. Occasionally, to meet some stringent condition such as the lack of cooling water at a mine-mouth plant, a dry cooling system will be installed, even for a large heat-load plant.

The primary impact of the operation of natural-draft cooling towers is their visual bulk and the formation of visible plumes that remain aloft. Plumes as long as 80 km may be generated; under certain weather conditions, snow does fall from these plumes. Most of the postulated adverse impacts--such as fogging, acid mist formation, noise, and the wetting, icing, and salt deposition due to drift with towers using fresh water for makeup and state-of-the-art drift eliminators--do not, in fact, occur.

Aerodynamic downwash frequently brings the plume from mechanical-draft cooling towers to the ground next to the tower. The plumes will evaporate or lift due to their buoyance to become a cloud deck within a short distance (of the order of 0.4 km). Thick deposits of light, friable rime ice may be generated in this zone. Most of the drift that does fall to the ground will do so within the same distance. Thus, areas of adverse impacts are limited to those quite close to the cooling towers--the exclusion area required for nuclear power plants. Observations at operating facilities indicate that the rate of deposition of salts from drift is very low and below the threshold of injuring to vegetation. Recent improvements in drift eliminator design reduce the already low drift rates by an addition order of magnitude or more. Salt-water towers equipped with these devices could become environmentally acceptable even in areas of salt-sensitive crops.

The question of the degree of mesoscale weather modification by cooling tower plumes, either wet or dry, cannot be satisfactorily answered at this time due to our lack of understanding of the atmospheric processes involved and the inadequacy of available modeling techniques. Very little information is currently available on the possible effects of large plumes on severe weather

events such as thunderstorms, hail, severe rainstorms, and tornadoes. Some observers think that severe thunderstorms, and even tornadoes, can be caused by cooling tower effluents during very unstable weather situations. This question remains unanswered.

Cooling ponds and spray canals will cause frequent fogging over the water surface; this fog may move inland several hundred meters before lifting, becoming very thin, or evaporating. Because of the larger area of heat release from ponds and canals, fogging and icing conditions are less severe near these cooling options than near mechanical-draft cooling towers. There is no drift from a cooling pond; drift and icing near spray canals can be heavy but restricted to a hundred meters or so from the canal.

When I was a graduate student at the University of Chicago many years ago, I was fortunate in having as one of my professors Dr. Carl-Gustaf Rossby, the great Swedish/American meteorologist. One day in class in the late 1940's (this is in the B.C. era: before computers), he had a long, complex set of partial differential equations on the blackboard. His comment, which still has relevance in the A.C. (after computers) era and should not be ignored, went something like this: "I cannot solve these equations. Nature can and does solve them, with no approximations or assumptions. All I need to do to get nature's accurate solution is to carefully read the weather map."

Nature can and does solve the complex set of equations related to cooling tower emissions; all we need do to find the exact solutions to these complex, not fully understood physical processes--with no approximations, no assumptions, no errors due to finite grid sizes and time steps--is to make careful, detailed observations at operating cooling towers. The answer is that modern cooling towers in good repair and properly sited, have a low and acceptable impact on the air environment.

#### REFERENCE

1. R. E. Otts, "Locally heavy snowfall from cooling towers," NOAA Tech. Memo. NWS ER-62, December 1976.

## A DESIGN METHOD FOR DRY COOLING TOWERS

G.K. Vangala and T.E. Eaton  
Mechanical Engineering Department  
University of Kentucky  
Lexington, Kentucky, USA 40506

### ABSTRACT

The cumulative cost of a large dry cooling tower is minimized by simultaneously optimizing the heat exchanger area and air friction losses; the optimization parameters are sensitive functions of the initial temperature difference (ITD).

For a given value of ITD, the air temperature rise varies from its optimum value because, even though the air friction losses are minimal at the optimum air temperature rise, the heat exchanger area decreases monotonically as the normalized air temperature rise decreases.

### INTRODUCTION

The continuing growth in demand for electric power requires planning, siting, and construction of large central generating stations. These stations use a regenerative Rankine energy conversion cycle which typically rejects two-thirds of the energy input as waste heat and which requires low heat sink temperatures for high efficiencies. Most power stations reject heat using cooling towers which transfer heat from water to air.

There are two basic cooling tower types, i.e., wet and dry; see Parker and Krenkel [1] for a detailed introductory discussion. However, few dry towers have been used for cooling central electric generating stations. The wet or evaporative cooling tower has the advantages of a lower cost and a lower sink temperature (the wet bulb temperature) than a dry tower. A major disadvantage of wet towers is the high water consumption and the associated environmental effects due to fog and drift. While the dry cooling tower approaches the dry bulb temperature, it neither consumes water nor releases moisture into the atmosphere.

Typical schematics of dry cooling towers are shown in Figure 1. The nomenclature used in this work is listed at the end of the text and illustrated in Figure 2.

### OBJECTIVES

Because of problems associated with power plant siting, the dry cooling tower is receiving serious consideration as a heat rejection technique

for large central generating stations. However, large dry cooling towers are inherently expensive, and a careful cost optimization results in large capital savings.

Although the optimization of various dry cooling tower design parameters has received considerable attention, little has been reported on the overall design of a cost optimized dry cooling tower. This paper presents a method for dry cooling tower design which uses the existing literature and standard sourcebooks on heat exchanger design and performance to arrive at a cost optimized dry cooling tower for a specific application. The general method presented incorporates a detailed analysis of heat exchanger performance and sizing based on the results of intensive work reported by others which pertains to dry cooling tower design.

#### DRY COOLING TOWER DESIGN METHOD

The design of a dry cooling tower is determined by the ambient dry bulb temperature, the hot fluid temperature, the heat rejection rate, the hot fluid properties, and the optimum cooling system cost.

The design method presented proceeds by determining the air friction losses and heat exchanger area based on the optimum air temperature rise across the heat exchanger. Next, a specific heat exchanger type is selected, and the number of tube columns and fluid passes, as well as the tube length are determined. The best heat exchanger type is selected from the alternatives considered based on an evaluation of cost and performance as is illustrated in Figure 3A.

With the type of heat exchanger selected, the optimum tower design is established based on cumulative cost while the air friction losses and air temperature rise are varied as is illustrated in Figure 3B.

#### Air Friction Losses

The basis of the air friction loss analysis for the design method presented is essentially adapted from work by Moore [2,4]. The tower is treated as a duct, and expressions for air friction losses, i.e., either tower height or fan power, are obtained.

Moore [3] has defined an air friction loss function as:

$$\Psi = \frac{\ln [(1 - \alpha_I) / Q_I]}{\alpha_I^2 (1 - Q_I - \alpha_I)} \quad (\text{Eq. 1})$$

$\Psi$  is minimized for various values of normalized approach, and corresponding values of normalized air temperature rise were found. From Table 1, it may be seen that the normalized air temperature rise is not a strong function of the normalized approach; therefore, in this work, iterations to establish the optimum tower cost were initiated with a normalized air

temperature rise of 0.83, irrespective of the value of the normalized approach.

### Heat Exchanger

With this, the heat exchanger is designed such that it operates at the predetermined optimum conditions. Knowing the heat rejection requirement and the optimum operating conditions, the total heat transfer area may be established [3,4].

Next, using heat exchanger design sourcebooks, cf., references [5], [6], and [7]) and work on the Rugley dry tower [8], a specific heat exchanger type and its design parameters, i.e., K, E, and F, are selected simultaneously. K is the ratio of friction coefficient to Stanton number ( $K = f/St$ ) [6]; E is a coefficient combining water side resistance and air side effectiveness, see reference [7]; F is a coefficient expressing counterflow equivalence [5].

A particular category of heat exchanger which has small values for K and hydraulic radius must next be chosen. The weight of heat exchanger per unit air side heat transfer area is minimum for a device in which the fin surface area dominates. The plate-fin type heat exchanger typically will have the ideal surface-to-mass ratio. Reference [6], Figures 10-52 through 10-64, illustrates various plate-fin heat exchanger designs. One must select and examine several heat exchanger designs in order to determine the design which optimizes cost and performance.

The selection of a specific heat exchanger type establishes the geometric parameters of the heat exchanger. Then, computations are made to evaluate water travel distance, number of water passes, and the number of water tube columns. An iterative procedure which varies K, E, and F is used to optimize cost and performance for the heat exchanger type selected. The optimized cost and performance results for several heat exchanger types are then compared to establish the optimum heat exchanger type.

### Cumulative Cost Optimization

Next, the total tower cost is optimized by varying the air temperature rise and the air friction losses.

The optimum air temperature rise for which calculations have been made only optimizes air friction losses. In order to minimize true heat exchanger area, the air temperature rise must be smaller than the air friction optimized value [9], see Figure 4A. The dashed lines show the variation of tower size with air temperature rise while the solid lines show the variation of the heat exchanger area.

Thus the air temperature rise value is varied, and the corresponding variations of air friction losses and heat exchanger area are evaluated. This procedure will determine the optimum air temperature rise based on

a cumulative cost criterion.

From Figure 4B, it may be seen that the air friction losses (tower height) approach their minimum value at large values of heat exchanger area. In order to conclude the cost optimization, the ratio of the design tower exhaust area to the tower exhaust area corresponding to the optimum air friction losses is iteratively determined.

#### APPLICATION OF THE METHOD

The application of the dry cooling tower design method presented will be illustrated for the case of a 200 MWe electric generating station with seasonally varying load and ambient conditions. Typical variations of both the system load and the ambient dry bulb temperature during 1976 are illustrated in Figure 5. The peak load may be seen to occur when the ambient temperature is the lowest thus improving the attractiveness of a dry cooling system.

The complete dry cooling tower design optimization procedure will be repeated for each month and the solutions compared. Ultimately, a tower design will be obtained that includes the optimum air temperature rise, the optimum ratio of exhaust area to its minimum value based on air friction losses, and the optimum type of heat exchanger which will minimize the cumulative tower cost.

The numerical results for this case will be presented in detail at the Conference.

## REFERENCES

- [1] J.L. Parker and P.A. Krenkel, Physical and Engineering Aspects of Thermal Pollution (Cleveland, CRC Press, 1970).
- [2] F.K. Moore, "On the Minimum Size of Large Dry Cooling Towers with Combined Mechanical and Natural Draft," Journal of Heat Transfer, Vol. 95, Series C, August 1973, pp. 383-389.
- [3] B.M. Johnson and D.R. Dickenson, "On the Minimum Size for Forced Draft Dry Cooling Towers for Power Generating Plants," Dry and Wet/Dry Cooling Towers for Power Plants (New York, ASME, 1973), pp. 25-34.
- [4] F.K. Moore, "Dry Cooling Towers," Advances in Heat Transfer, Vol. 12 (New York, Academic Press, 1976), pp. 1-75.
- [5] F. Kreith, Principles of Heat Transfer, 3rd Edition (New York, Intext Press, 1973).
- [6] W. Kays and A.L. London, Compact Heat Exchangers, 2nd Edition (New York, McGraw-Hill, 1964).
- [7] F.K. Moore, "Minimization of Air Heat-Exchange Surface Areas in Dry Cooling Towers for Large Power Plants," Dry and Wet/Dry Cooling Towers for Power Plants (New York, ASME, 1973), pp. 13-23.
- [8] P.J. Christopher and V.T. Forster, "Rugeley Dry Cooling Tower System," Proceedings of the Institution of Mechanical Engineers, Vol. 184, Part I, No. 11, 1969-70, pp. 197-222.
- [9] F.K. Moore and T. Hsieh, "Concurrent Reduction of Draft Height and Heat Exchange Area for Large Dry Cooling Towers," Journal of Heat Transfer, Vol. 96, Series C, August 1974, pp. 279-285.
- [10] M.W. Larinoff, "Dry Cooling Power Plant Design Specifications and Performance Characteristics," Dry and Wet/Dry Cooling Towers for Power Plants (New York, ASME, 1973), pp. 57-83.
- [11] J.P. Rossie and E.A. Cecil, "Research on Dry-Type Cooling Towers for Thermal Electric Generation: Part I," Water Quality Office, U.S. EPA Report 16130EES11/70.

NOMENCLATURE

- $A_a$  = Total Heat Exchanger Area  
 $A_c$  = Heat Exchanger Free Flow Area  
 $A_e$  = Cooling Tower Exhaust Area  
 $E$  = A Coefficient Combining Water Side Resistance and Air Side Effectiveness  
 $f$  = Friction Coefficient  
 $F$  = A Coefficient of Counterflow Equivalence  
 $I$  = Initial Temperature Difference  
 $K$  = Ratio of Friction Coefficient to Stanton Number  
 $p$  = Ratio of  $A_e$  to  $A_e$ -Minimum, Based on Air Friction Losses  
 $Q$  = Approach  
 $St$  = Stanton Number  
 $IHX$  = Type of Heat Exchanger  
 $\alpha$  = Air Temperature Rise  
 $\alpha^*$  = Optimum Air Temperature Rise (Optimized for Air Friction Losses)  
 $\psi$  = Tower Size  
 $\psi^*$  = Optimum Tower Size (Optimized for Air Friction Losses)

Superscripts

- $\$$  = Cost Optimized Parameters  
 $*$  = Parameters Optimized for Air Friction Losses

Subscript

- $I$  = Normalized with Respect to Initial Temperature Difference

Table 1

VARIATION OF OPTIMUM, NORMALIZED AIR TEMPERATURE RISE WITH CHANGES IN NORMALIZED APPROACH

| Normalized Approach ( $Q_t$ ) | Optimum, Normalized Air Temperature Rise ( $\alpha_I^*$ ) |
|-------------------------------|---|
| 0.2                           | 0.800   |
| 0.3                           | 0.813   |
| 0.4                           | 0.822   |
| 0.5                           | 0.829   |
| 0.6                           | 0.835   |
| 0.7                           | 0.840   |
| 0.8                           | 0.844   |
| 0.9                           | 0.848   |
| 1.0                           | 0.857   |

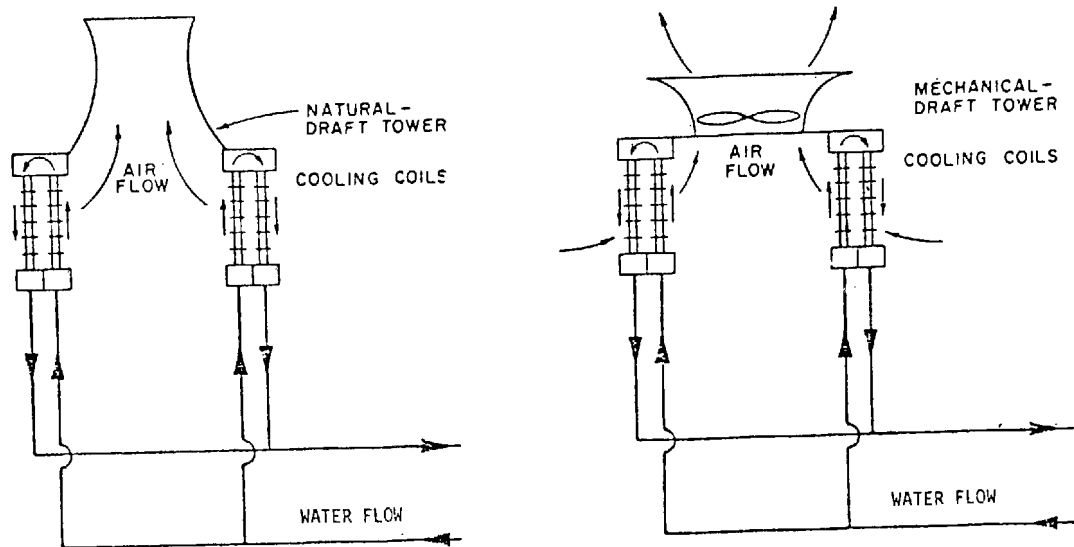


FIGURE 1: TYPICAL DRY COOLING TOWER SCHEMATICS  
(Taken from Reference [11])

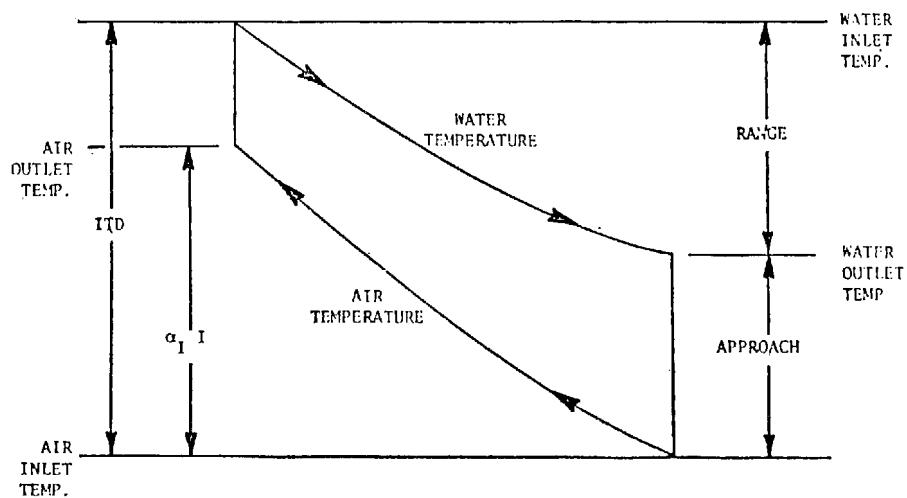


FIGURE 2: TEMPERATURE DIAGRAM OF A TYPICAL DRY  
COOLING TOWER HEAT EXCHANGER

FIGURE 3A- DRY COOLING TOWER DESIGN METHOD:  
HEAT EXCHANGER DESIGN OPTIMIZATION

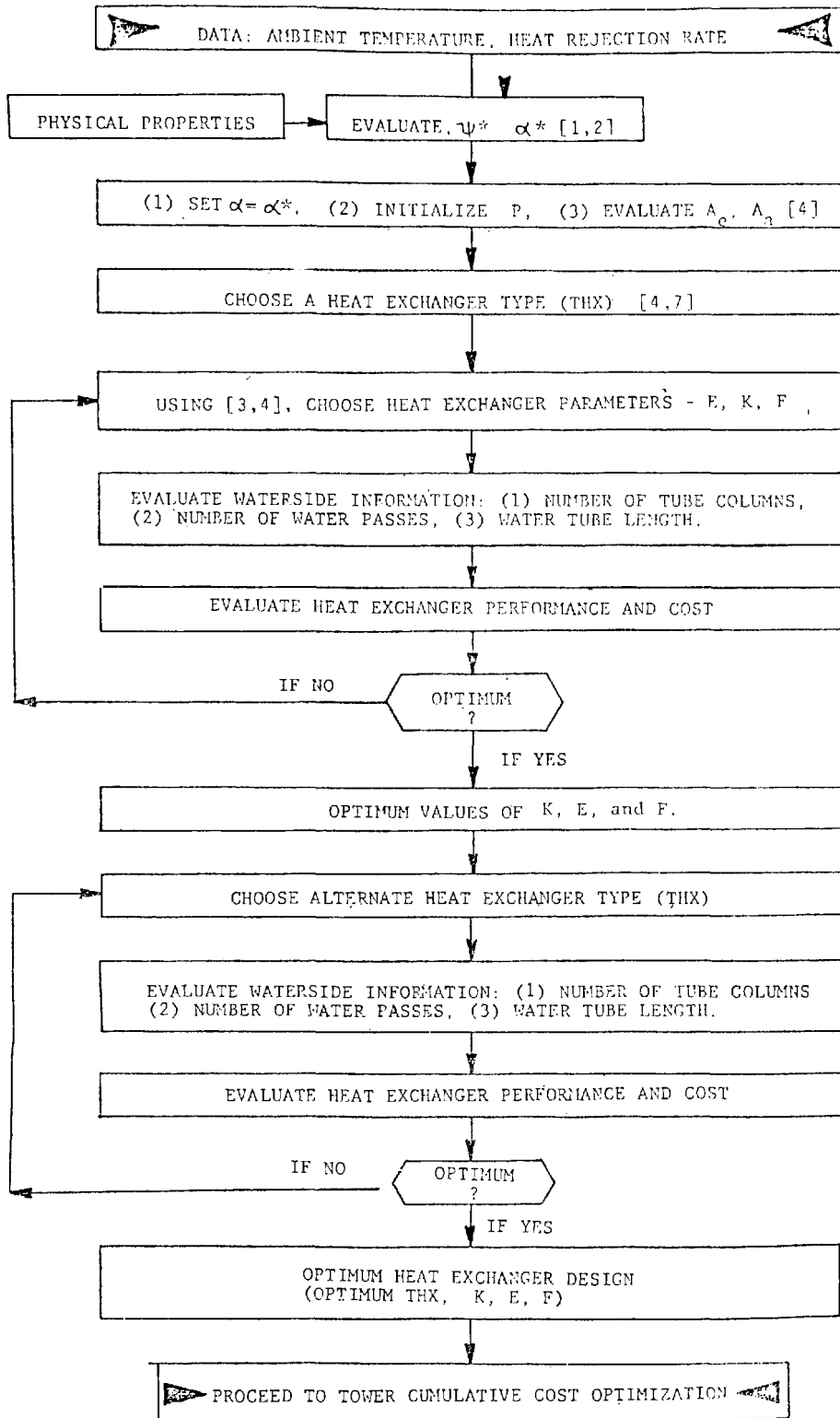
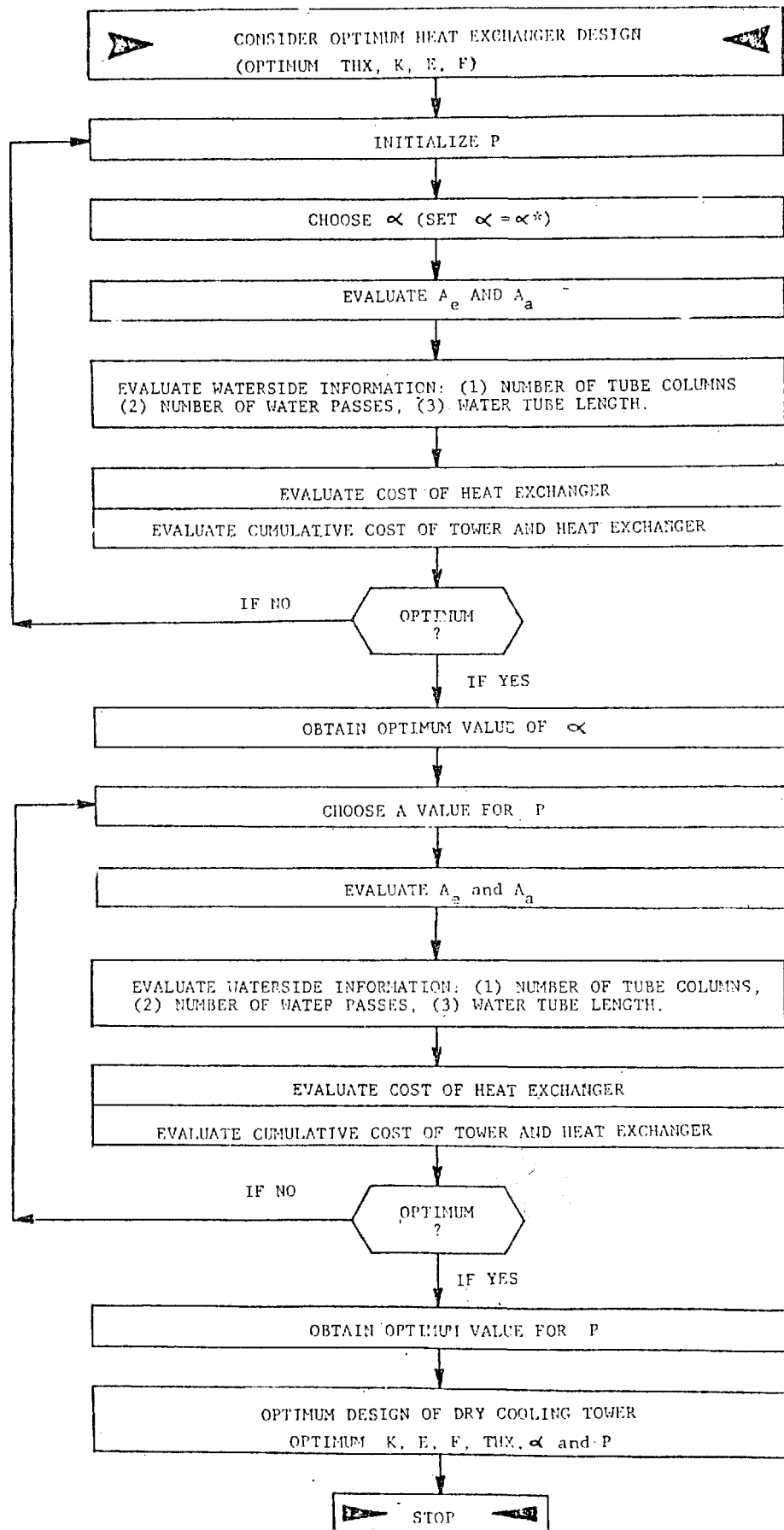


FIGURE 3B: DRY COOLING TOWER DESIGN METHOD:  
TOTAL TOWER COST OPTIMIZATION



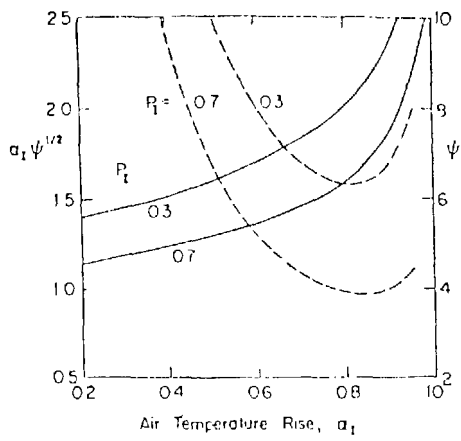


FIG. 4A: TOWER SIZE FUNCTION -  $\psi$  (Dashed Lines) AND HEAT EXCHANGER AREA FUNCTION -  $\alpha_1 \psi^{1/2}$  (Solid Lines)  
(Taken from Reference [7])

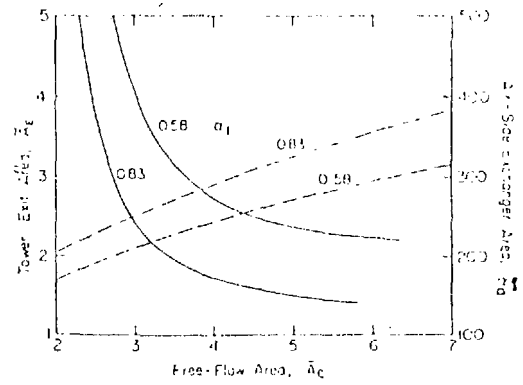


FIG. 4B: INFLUENCE OF FREE-FLOW AREA -  $A_c$  ON TOWER SIZE -  $A_E$  (Solid Lines) AND HEAT EXCHANGER AREA -  $A_a$  (Dashed Lines)  
(Taken from Reference [7])

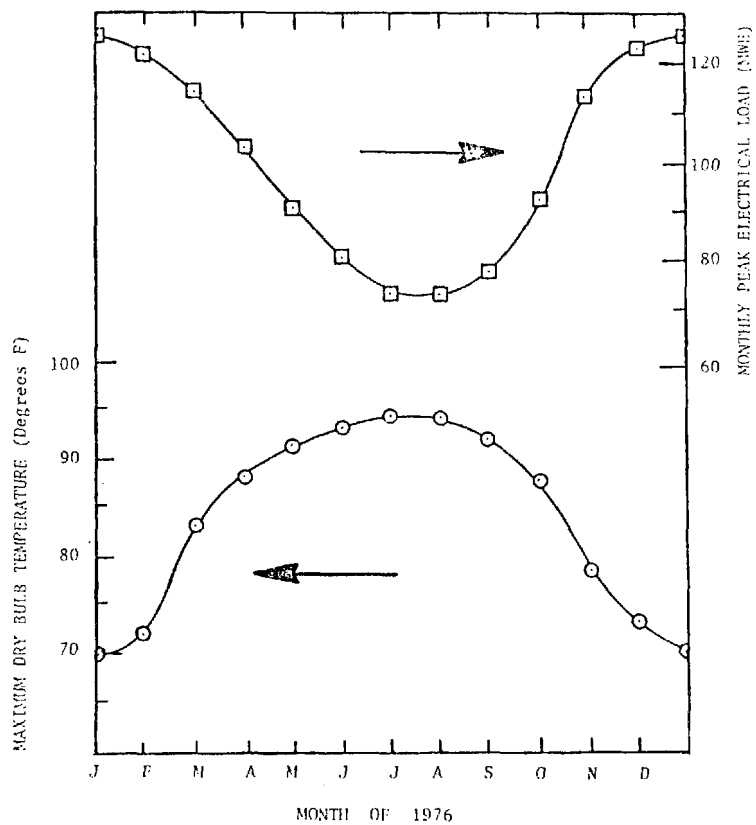


FIGURE 5: SEASONAL VARIATION OF PLANT LOAD AND AMBIENT DRY BULB TEMPERATURE FOR THE DESIGN CASE USED TO ILLUSTRATE THE DRY COOLING TOWER DESIGN METHOD

# EVAPORATIVE HEAT REMOVAL IN WET COOLING TOWERS

by

Thomas E. Eaton  
Mechanical Engineering Department  
University of Kentucky

## ABSTRACT

The ratio of evaporative-to-total (sensible plus evaporative) heat transfer in a wet, cross-flow, mechanical draft cooling tower was analyzed. The ratio was found to vary from 60% to 90% during typical operating conditions. The evaporative heat removal fraction increased as temperature (either wet-bulb or dry-bulb) increased and as relative humidity decreased. Similar results were obtained for a counter-flow, natural draft tower.

## INTRODUCTION

Wet or evaporative cooling towers are commonly used to provide for the cooling of water by direct contact with air. Two heat removal mechanisms dominate in an evaporative cooling tower: evaporative heat removal and sensible heat transfer. Sensible heat transfer refers to heat transferred by virtue of a temperature difference between the water and air. Evaporative heat removal refers to the energy removal from the water as latent heat of evaporation; this heat removal is the result of the evaporation of water into air during the direct-contact cooling process.

The cooling tower industry typically quotes the fraction of energy removed from the water by evaporative cooling as three-fourths or about 75%. As will be shown in this work, the fraction of the heat removed by evaporative cooling in wet cooling towers varies between 60% and 90% during typical operating and ambient conditions. It is of interest to note that under certain conditions, both the water and air are cooled by evaporation so that the evaporative cooling exceeds 100% of the cooling effect on the water alone.

The water evaporation losses from wet cooling towers determine make-up water requirements. Although the literature discusses the calculation of evaporative losses (see Hamilton [1], for example), the specific topic of the fraction of heat removed by evaporation and by sensible heat transfer has not been quantitatively evaluated [2].

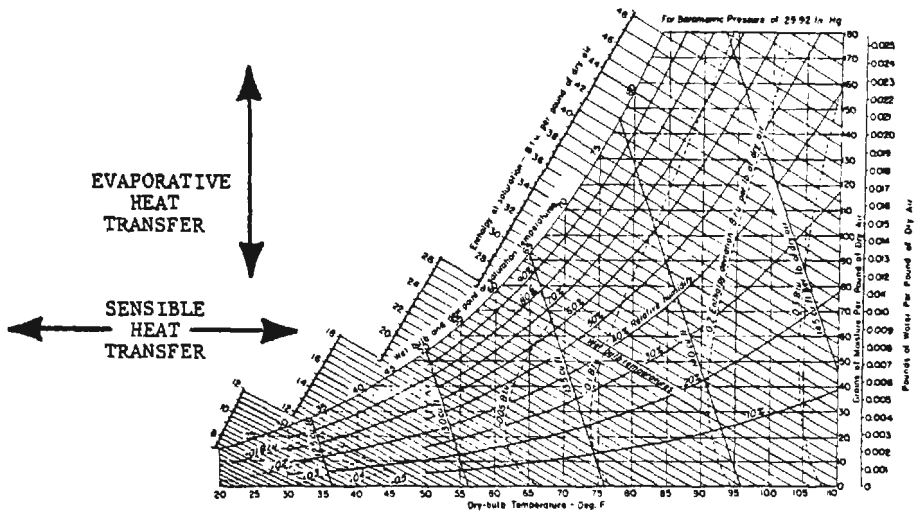


FIGURE 1: TYPICAL PSYCHOMETRIC CHART

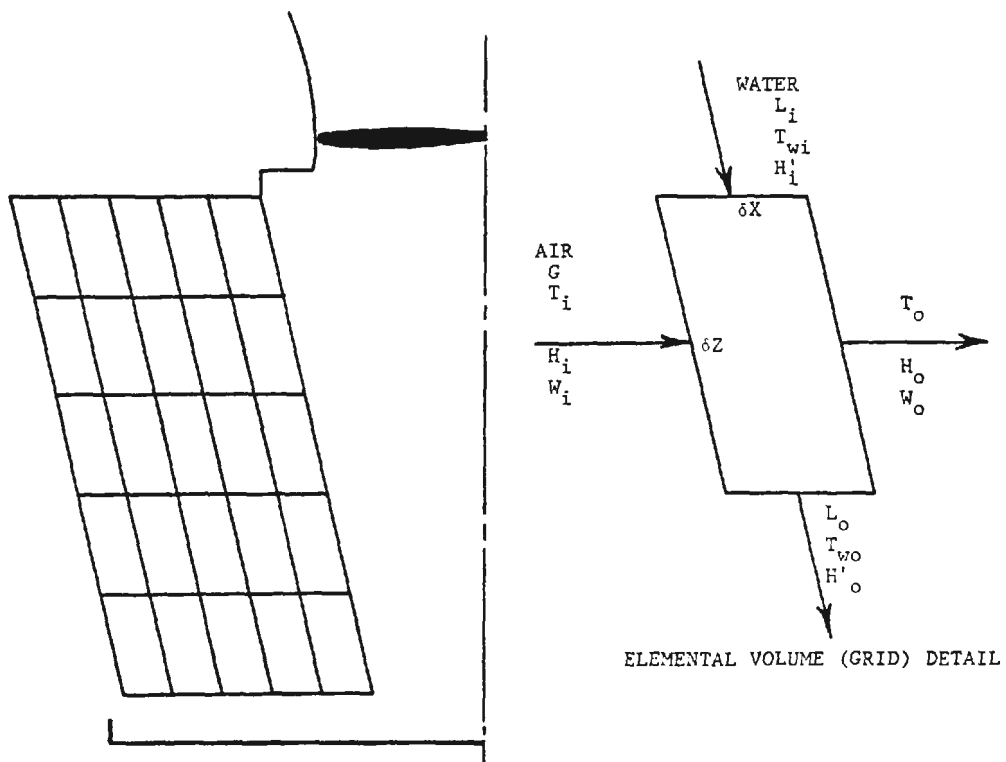


FIGURE 2: SCHEMATIC OF GRID LAYOUT USED TO ANALYZE A CROSS-FLOW, MECHANICAL DRAFT COOLING TOWER

This paper investigates the influence of variations in ambient conditions and changes in cooling tower design parameters on the evaporative cooling-to-total cooling ratio in wet cooling towers. Particular emphasis is given to the commonly-used, mechanical draft cross-flow cooling tower design. Results for a typical natural draft cooling tower of counter-flow design are also given.

### Fundamental Considerations

The enthalpy  $H_m$  of a mixture of air and water vapor is given by

$$H_m = 0.240 T_d + W (1041 + 0.444 T_d)$$

where  $W$  is the humidity ratio (lbm water vapor/lbm dry air) and  $T_d$  is the dry bulb temperature of the mixture. From the psychrometric chart, see Figure 1, it may be readily determined that the enthalpy remains nearly constant at constant wet bulb temperature  $T_w$ .

Sensible heat transfer involves an increase in the dry bulb temperature of the mixture but evaporative heat transfer involves a change in the humidity ratio of the mixture. Thus, a sensible heat transfer from water to air inside a cooling tower involves a horizontal change on the psychrometric chart while evaporative transfer involves a vertical movement as is illustrated in Figure 1.

In a wet cooling tower, where the tower-on temperature is greater than the ambient wet bulb temperature, the air humidity always increases as the air passes through the tower. However, as will be demonstrated later, sensible heat transfer may be either positive or negative. When the tower-on temperature is less than the ambient dry bulb temperature, the sensible heat transfer may be negative and the air dry bulb temperature will be lowered as the air passes through the tower; under these circumstances, the air as well as the water is cooled by evaporative transfer in the cooling tower.

In this paper, the total heat transfer will be taken as the evaporative plus the sensible heat transfer to the air as it passes through the tower. In cases where air cooling occurs in addition to water cooling, the ratio of air-side evaporative and sensible heat transfer to the water-side heat transfer will be greater than 100%.

Consider a counter-flow natural draft cooling tower for example; in this case the exhaust air conditions are usually saturated. If the ambient conditions are known, say 72°F and 50% relative humidity, and the exit conditions are determined as say 96°F (100% RH), then the air dry bulb temperature increases by 24°F (from 72°F to 96°F), the humidity ratio increases by 0.030 lbm-WV/lbm-DA from 0.0084 to 0.0380), and the mixture enthalpy varies by 38.5 BTU/lbm (from 26.5 to 65.0). Based on the air-side information only, the fraction of heat rejected by evaporation can be estimated:  $\Delta W(h_{fg})/\Delta H$ , or  $(0.030)(1040)/38.5 = 80\%$ .

However, because the exit air conditions vary with fill height in a cross-flow tower, the average exhaust conditions must be determined before the evaporative cooling fraction can be estimated.

## CROSS-FLOW COOLING TOWER ANALYSIS

The computer program used for the analysis of cross-flow, evaporative cooling towers was developed using the enthalpy-difference driving force model to calculate the combined effects of heat and mass transfer in the cooling tower. The basic equations are similar to those presented by Kelly [3] or Hallett [4].

The cross-flow cooling tower packing is divided into a grid as shown in Figure 2. In the upper, air inlet corner of the packing, the air and water inlet conditions to the grid are known. With this, the water outlet and air outlet conditions may be calculated for the first grid. The air inlet condition for the next grid element is then known, and the program analysis proceeds across the tower fill. At the end of the grid row, the calculation proceeds to the air inlet of the next row down. In this manner, the entire fill is analyzed. Both air outlet and water outlet conditions along the fill are predicted by the code.

Because the code uses the enthalpy-difference for the driving force, little information about the air inside the cooling tower is known. Typically, only the air enthalpy is calculated. The wet-bulb temperature is nearly constant with air enthalpy over a wide range of relative humidities so that the wet-bulb temperature is also known to a good approximation.

From routine observations, it is apparent that the air entering the tower is usually not saturated and the air leaving the tower is not always saturated. The enthalpy-difference driving force model is only capable of predicting the local enthalpy and wet-bulb temperature inside the tower fill; local air humidity and dry-bulb temperature are not predicted when using this analytical method.

### Calculation of Humidity Inside the Tower Fill

Because the calculation of evaporative cooling was of primary interest in this work, considerable effort was devoted to attempting to calculate the humidity at each grid inside the tower fill. The governing equations based on a "humidity-difference" driving force inside the tower were developed in a manner similar to that of Park and Vance [5,6]. However, the humidity-difference driving force method was abandoned because the appropriate empirical correlations for the tower characteristic ( $K_a$ ) were not available.

Tower characteristics developed using enthalpy-difference methods to analyze data cannot be used to predict cooling tower performance using a humidity-difference driving force.

In order to determine the humidity variations inside a wet cooling tower, the humidity ratio change between successive grid points must be known, i.e., the amount of water evaporated inside the grid

must be calculated. Conventional cross-flow cooling tower analysis methods can not do this. An improved method for cross-flow cooling tower analysis has been developed by Baker and Eaton [7], but was not available for this work.

For this work, the air humidity inside the cooling tower was estimated assuming that the humidity ratio change within a grid was that predicted by the humidity ratio change along the air-water vapor mixture saturation line. That is, the entering and leaving air enthalpies are calculated so that the humidity ratio change along the saturation (100% relative humidity) line could be determined. Since the air humidity at the tower inlet was known and the change in humidity ratio in any calculational increment was determined in the manner described above, the humidity at any point inside the tower could be estimated.

Although this method was not exact, it was felt to be more accurate than the assumption that the air inside the tower is saturated. Occasionally, the above internal humidity calculations predicted supersaturated air conditions; if such calculations occurred, the air was assumed to be saturated at the calculated enthalpy.

The basic equations used to analyze the performance of the cross-flow cooling tower are discussed in detail in Appendix A.

#### Other Computer Code Information

For the analysis of cross-flow cooling towers, the tower characteristic equation developed by Hallett [4] was used throughout this work:

$$K_a = 0.120 G^{0.410} L^{0.525} \quad (\text{Eq. 2})$$

As may be seen in Figure 3, this correlation was found to predict the performance of the reference design cooling tower with  $+2^{\circ}\text{F}$  and  $-0^{\circ}\text{F}$  of the tower manufacturer's performance curves. The details of the reference design cooling tower are given in Table 1. This tower design was the basis for all results reported on cross-flow towers.

Properties of air-water vapor mixtures were calculated using the ideal gas equations, see the ASHRAE Brochure on Psychrometry [8] for details.

Water properties were calculated based on data from the 1967 ASME Steam Tables.

#### Outlet Air and Water Temperature Distributions

For the case of a cross-flow cooling tower, hot water enters the top of the tower fill at a uniform temperature. This water is cooled by air admitted from the side of the tower. Because of the cross-flow cooling arrangement, the temperature of the water at the bottom of the

TABLE I

DESIGN PARAMETERS FOR A TYPICAL INDUSTRIAL CROSS-FLOW COOLING TOWER

|                                     |   |
|-------------------------------------|---|
| Cooling Tower Type . . . . .        | Cross Flow Design,<br>Double Flow Arrangement           |
| Draft . . . . .                     | Mechanical, Induced Draft                               |
| Number of Tower Cells . . . . .     | 12  |
| Dimensions                          |   |
| Overall Length . . . . .            | 432 ft  |
| Air-Travel Distance . . . . .       | 18 ft   |
| Water-Travel Distance . . . . .     | 36 ft   |
| Fan Diameter . . . . .              | 28 ft   |
| Stack Exhaust Diameter . . . . .    | 31.5 ft   |
| Cell Length . . . . .               | 36 ft   |
| Design Operating Conditions         |   |
| Total Air Flow (G*) . . . . .       | 1,410,000 CFM/CELL                                      |
| Total Water Flow (L*) . . . . .     | 190,000 GPM   |
| L*/G* . . . . .                     | 1.44  |
| Wet Bulb Temperature . . . . .      | 76°F  |
| Tower-On Temperature . . . . .      | 117°F   |
| Tower-Off Temperature . . . . .     | 90°F  |
| Range . . . . .                     | 27°F  |
| Approach . . . . .                  | 14°F  |
| Liquid Loading (L) . . . . .        | 6100 lbm/hr-ft <sup>2</sup> (12.3 GPM/ft <sup>2</sup> ) |
| Air Loading (G) . . . . .           | 2150 lbm-DA/hr-ft <sup>2</sup>                          |
| L/G . . . . .                       | 2.88  |
| Velocity at Fan . . . . .           | 2400 ft/sec   |
| Velocity at Stack Exhaust . . . . . | 1800 ft/sec   |
| Tower Characteristic                |   |
| KaX/G . . . . .                     | 2.26  |
| KaY/L . . . . .                     | 1.60  |
| Ka . . . . .                        | 270   |
| Fan Power . . . . .                 | 175 HP  |

747

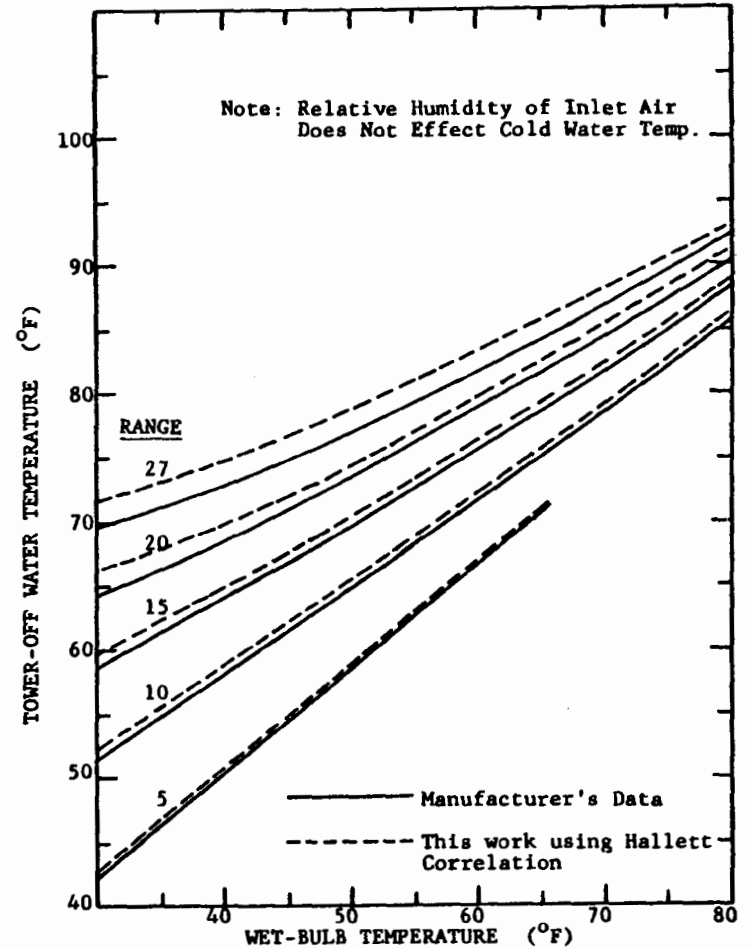


FIGURE 3: COMPARISON OF COOLING TOWER PERFORMANCE CURVES SUPPLIED BY MANUFACTURER VS. CALCULATED IN THIS WORK FOR THE REFERENCE DESIGN COOLING TOWER

fill as well as the temperature and humidity of the air at the inside of the fill varies with position.

It was necessary to determine the fill outlet variations of water temperature, air dry-bulb temperature, and relative humidity in order to adequately assess the heat removal from the water and the total and evaporative transfer to the air. The evaporative heat removal fraction was determined as the average of the ratio of evaporative heat removal-to-total air heat removal for each row of fill calculations:

$$\frac{Q_{ev}}{Q_{tot}} = \frac{1}{N} \sum_{j=1}^N h_{fg} (W_{oj} - W_{ij}) / (H_{oj} - H_{ij}) \quad (\text{Eq. 3})$$

The average outlet water temperature was calculated by averaging the outlet water temperatures:

$$\bar{T}_{wo} = T_{off} = \frac{1}{M} \sum_{j=1}^M T_{wj} \quad (\text{Eq. 4})$$

With this, the total heat removed from the water is

$$Q_{rej} = \dot{m}_{wi} c_{pw} T_{on} - \dot{m}_{wo} c_{pw} T_{off} \quad (\text{Eq. 5})$$

The correction for water evaporation loss has been included in the heat rejection equation.

Typical results of air and water outlet variations are shown in Figures 4 and 5. The cooling tower design parameters are given in Table 1; the results plotted are for a hot water temperature of 119°F with 76°F wet-bulb and 81°F dry-bulb temperatures (80% relative humidity) as the ambient conditions.

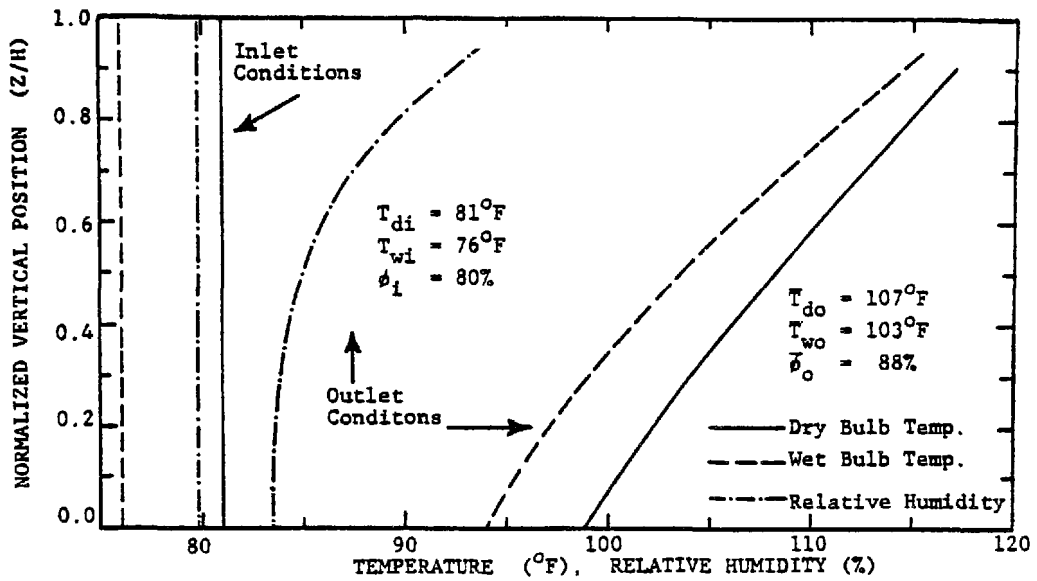


FIGURE 4: VERTICAL VARIATION OF AIR-SIDE CONDITIONS FOR THE REFERENCE DESIGN COOLING TOWER

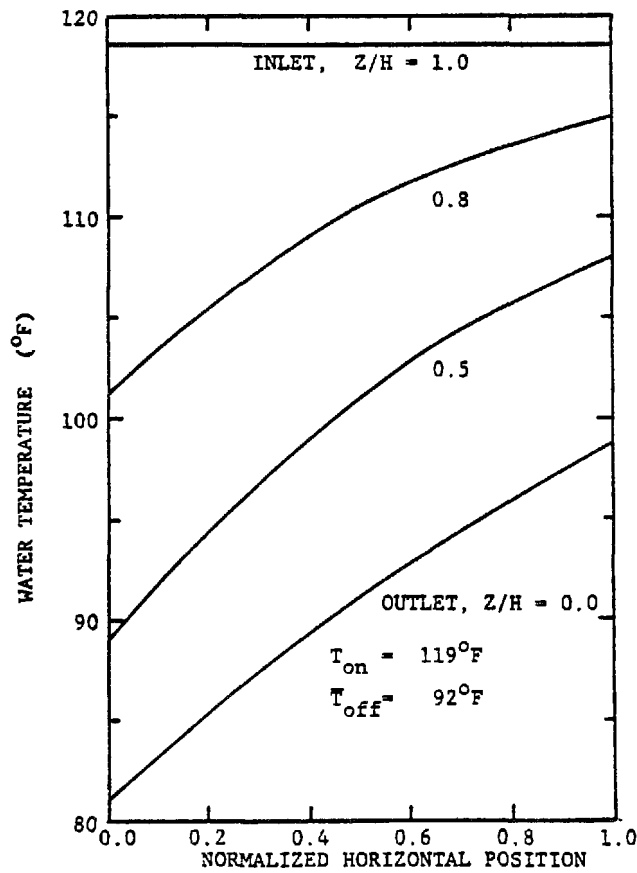


FIGURE 5: WATER TEMPERATURE DISTRIBUTION IN THE REFERENCE DESIGN COOLING TOWER

## THE EVAPORATIVE HEAT REMOVAL FRACTION

### Cross-Flow Cooling Tower Analysis

The evaporative heat removal fraction as influenced by the variation of typical cooling tower operating conditions or design parameters was evaluated using the computational methods described earlier for a cross-flow, mechanical draft tower design.

### Cross-Flow Cooling Tower Parameters

The cross-flow, mechanical draft cooling tower is common throughout the United States. For this reason, the influence of the variation of several parameters on the evaporative cooling fraction was investigated for a typical, large industrial cross-flow tower. The goal in studying the parameter variations was to determine their effect on a cooling tower of fixed design. The parameters varied are listed below:

- (A) Ambient Air Wet-Bulb Temperature
- (B) Ambient Air Relative Humidity
- (C) Hot Water (Tower-On) Temperature
- (D) Cooling Tower Range
- (E) Liquid Loading
- (F) Air Loading
- (G) Cooling Tower Characteristic (Ka)
- (H) Elevation Above Sea Level.

Typically, the cooling tower parametric variations were examined with the total water flow to the cooling tower and the velocity of the water vapor/air mixture specified at the tower exhaust. The water loading and the mixture exhaust velocity were varied only in the above items (E) and (F), respectively.

Recall that the specific cooling tower design parameters used for the reference design cooling tower (cross-flow design) are given in Table 1.

Parametric studies on cooling towers can, in general, be quite involved because many design parameters can be varied. Indeed, there are many variables which can be varied which have not been considered here, e.g., fill height, fill width, and packing design - to name just a few.

### Typical Behavior

The variation of the evaporative heat removal fraction in the reference design cooling tower operating at the design heat rejection rate (2.6 Billion BTU/hr) under varying ambient conditions is shown in Figure 6. The evaporative cooling effect varies from 60% to over 90%

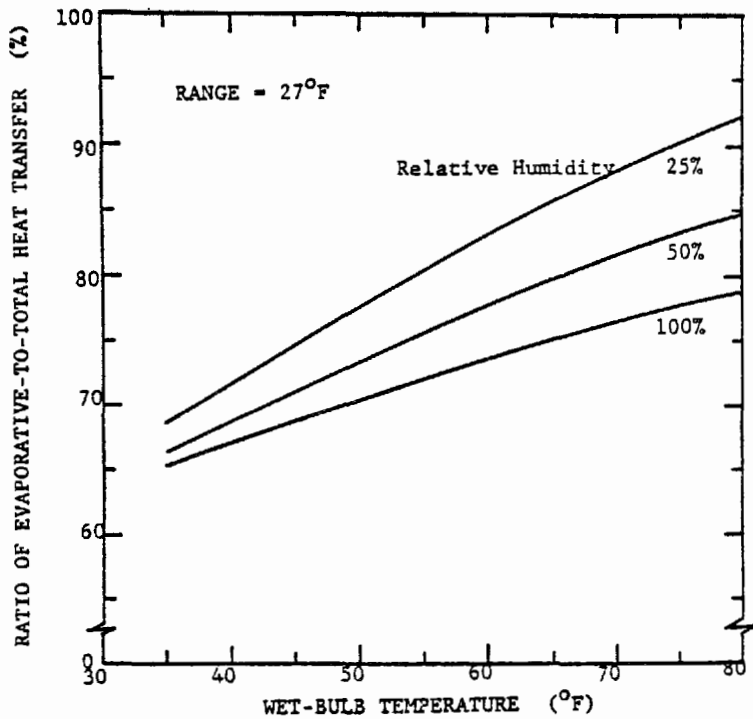
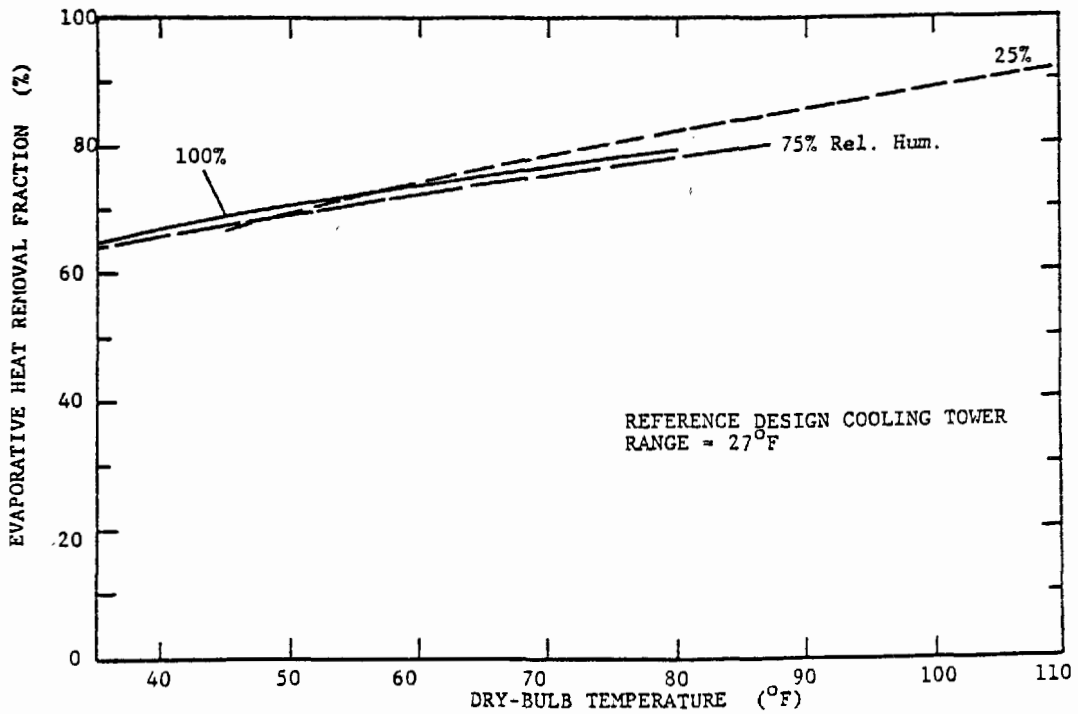


FIGURE 6: INFLUENCE OF AMBIENT CONDITIONS ON THE RATIO OF EVAPORATIVE-TO-TOTAL HEAT TRANSFER IN THE REFERENCE DESIGN COOLING TOWER

FIGURE 7: EVAPORATIVE HEAT REMOVAL FRACTION VS. AMBIENT DRY-BULB TEMPERATURE FOR VARIOUS RELATIVE HUMIDITIES



during normal changes in ambient conditions. The fraction of heat removed by evaporative cooling increases as the wet-bulb temperature increases and increases as the relative humidity decreases (at constant wet-bulb temperature).

The variation of the evaporative heat removal fraction in the reference design tower operating at the design heat rejection rate (range = 27°F) is shown plotted versus ambient dry-bulb temperature in Figure 7. Note that for a fixed dry-bulb temperature, the relative humidity has little influence on the fraction. The evaporative cooling fraction increases about 1% for each 3°F rise in dry-bulb temperature.

### Tower-On Temperature Effect

The evaporative heat removal fraction plotted versus tower-on (hot water) temperature is shown in Figure 8 for wet-bulb temperatures of 40°F, 60°F, and 76°F at 80% relative humidity. For a given hot-water temperature, the evaporative cooling fraction increases as the wet-bulb temperature increases; also, a minimum fractional value can be identified for a given wet-bulb temperature (at 80% relative humidity).

Figure 9 shows the effect of relative humidity on the evaporative fraction versus tower-on temperature for a fixed wet-bulb temperature of 60°F. The evaporative cooling fraction increases with decreasing relative humidity. The minimum evaporative cooling fraction depends on relative humidity at a fixed wet-bulb temperature.

### Cooling Tower Range

The effect of the cooling tower's operating range (hot water temperature minus cold water temperature) is shown in Figure 10A-D for ranges of 30°F, 20°F, 10°F, and 5°F, respectively. As the range increases, the variation in the evaporative cooling fraction due to changes in the wet-bulb temperature becomes less significant. During typical operating conditions, i.e., a range above 20°F and a relative humidity above 50%, the evaporative cooling fraction varies from 60% to 90%.

In general, the evaporative cooling fraction increases over all operating ranges as the wet bulb temperature increases and as the relative humidity decreases (with wet bulb temperature constant). At low ranges, i.e., less than 10°F, the fraction increases rapidly as the relative humidity decreases. On hot dry days with ranges below 10°F, the evaporative cooling fraction will exceed 100%.

Recall that when the evaporative heat removal fraction is greater than 100%, the cooling tower is physically cooling both the water and the air (by evaporative cooling) as it passes through the fill. That is, the sensible heat transfer to the air is negative.

The effect of range variations for relative humidities of 80% and 20% are shown in Figure 11.

The effect of relative humidity on the evaporative heat removal fraction versus range is shown in Figure 12. At ranges below 20°F, the relative humidity has a marked effect on the evaporative cooling fraction.

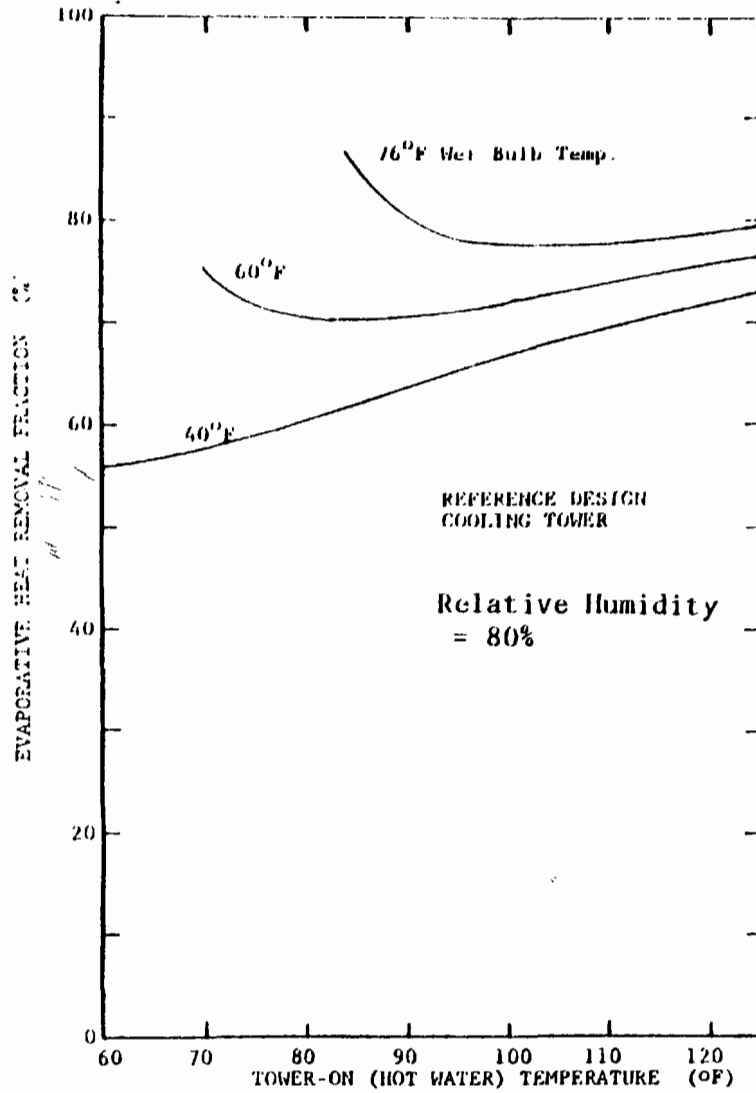


FIGURE 8: EVAPORATIVE HEAT REMOVAL RATIO VERSUS TOWER-ON TEMPERATURE FOR VARIOUS WET-BULB TEMPERATURES.

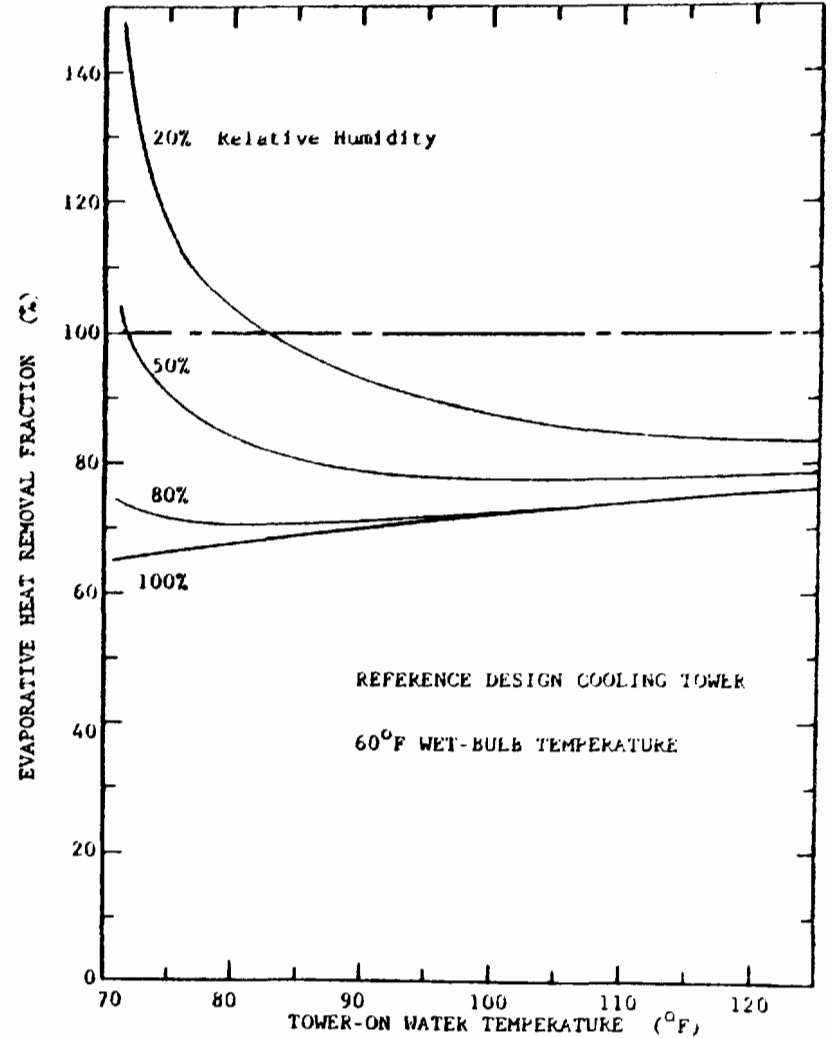


FIGURE 9: INFLUENCE OF RELATIVE HUMIDITY ON EVAPORATIVE HEAT REMOVAL FRACTION VERSUS HOT WATER TEMPERATURE AT 60°F WET-BULB TEMPERATURE

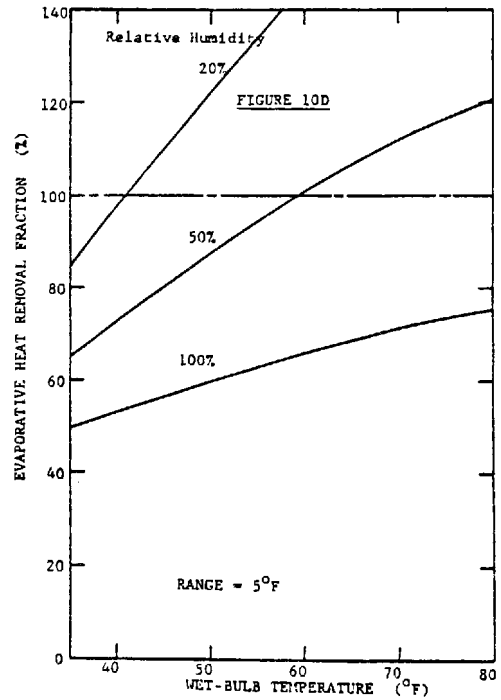
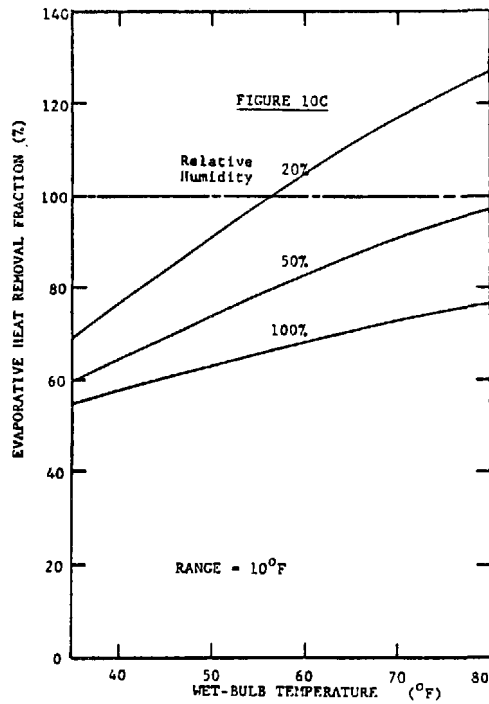
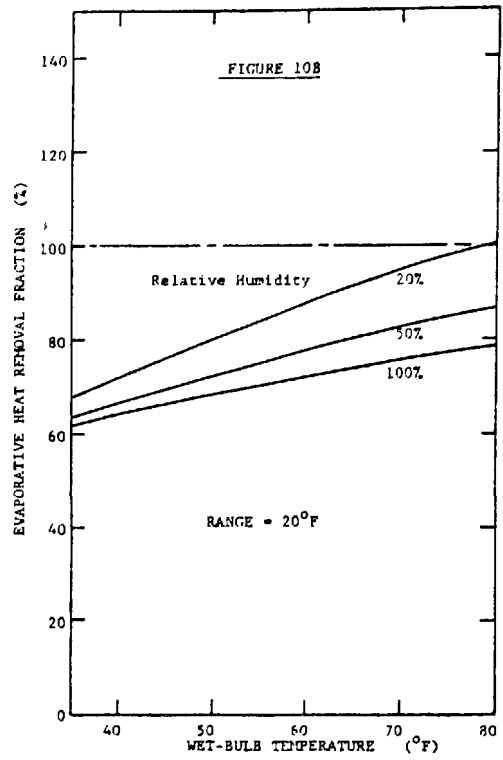
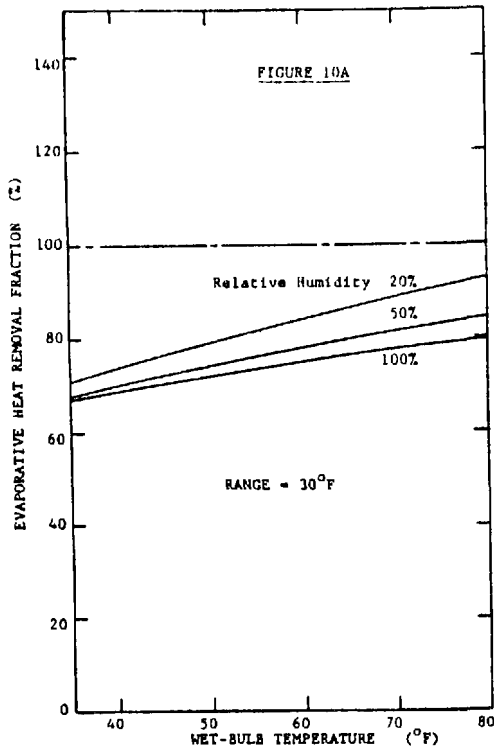


FIGURE 10: EVAPORATIVE HEAT REMOVAL FRACTION  
VERSUS WET-BULB TEMPERATURE FOR  
VARIOUS RANGES

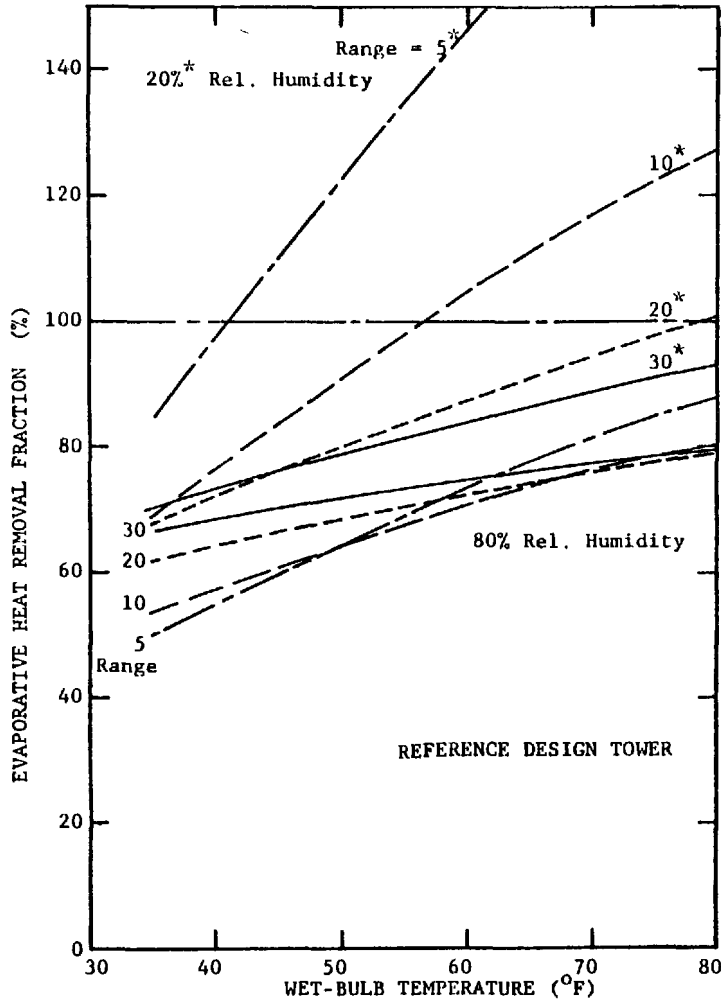


FIGURE 11: THE INFLUENCE OF RANGE ON THE EVAPORATIVE HEAT REMOVAL FRACTION AT 80% and 20% RELATIVE HUMIDITY

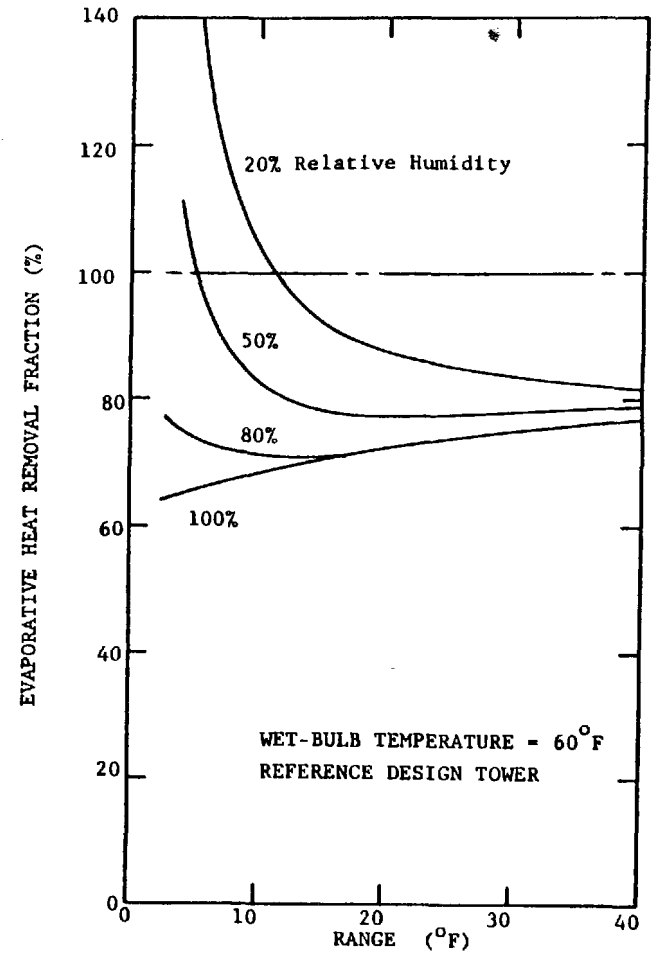


FIGURE 12: VARIATION OF EVAPORATIVE HEAT REMOVAL FRACTION WITH RANGE AT 60°F WET-BULB TEMPERATURE

### Cooling Tower Range (Dry-Bulb Temperature)

The effect of cooling tower range on evaporative cooling fraction versus dry-bulb temperature is shown in Figure 13A-D for ranges of 30°F, 20°F, 10°F, and 5°F, respectively. The effect of relative humidity variations is shown in each figure.

For the typical large, industrial cooling tower considered (operating under routine conditions, i.e., a range over 20°F), the evaporative cooling fraction increases linearly with dry-bulb temperature at a rate of about 1% / 3°F. The fraction varies from 65% at 40°F to about 90% at 100°F; changes in the ambient relative humidity have only a slight influence on the evaporative cooling fraction during normal operating conditions (at constant dry-bulb temperature).

As the range decreases below 20°F, the relative humidity has an increasingly important influence on the variation of the fraction with dry-bulb temperature. At ranges below 10°F, the fraction increases rapidly as the humidity increases. This sensitivity increases as the dry-bulb temperature increases.

The same results of Figure 13A-D, are shown in Figure 14A-C; however, the latter figure shows the effect of range variations at constant relative humidity. Note that the effect of low operating ranges (i.e., less than 20°F) on the evaporative cooling fraction changes markedly as the relative humidity decreases.

### Liquid Loading - L

For the reference design tower, the effect of liquid loading (L) variations on the evaporative-to-total heat removal ratio is shown in Figure 15. Increasing the liquid loading produces a small decrease in the evaporative heat removal fraction. The exhaust air mixture velocity was held constant for this case.

### Gas (Dry Air) Loading - G

The influence of varying the gas or dry air loading in the reference design tower fill is shown in Figure 16. With the liquid loading held constant, the evaporative heat removal fraction slightly decreases as the gas loading increases.

### Cooling Tower Characteristic - Ka

The effect of varying the cooling tower characteristic in the reference design cooling tower is shown in Figure 17. Over the range of interest, i.e.,  $K_a = 100 - 350$ , there is a small effect on the evaporative heat removal fraction.

### Elevation Above Sea Level

The barometric pressure varies with elevation and ambient conditions.

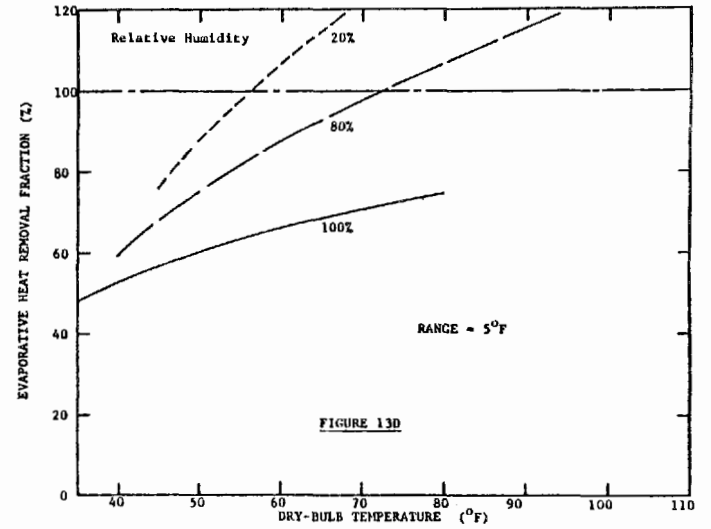
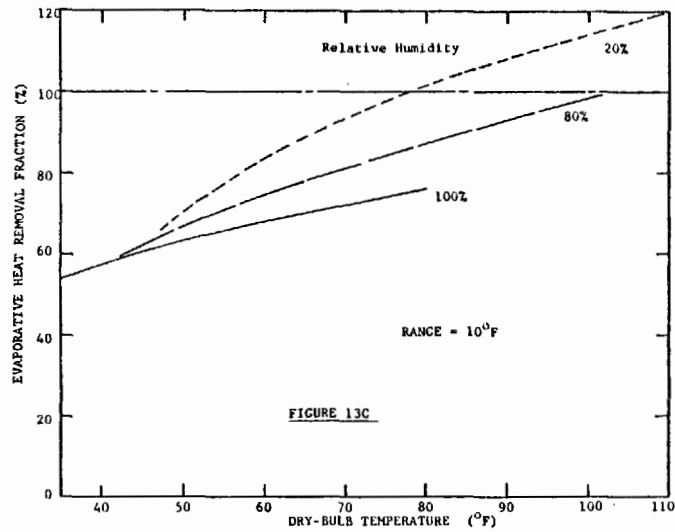
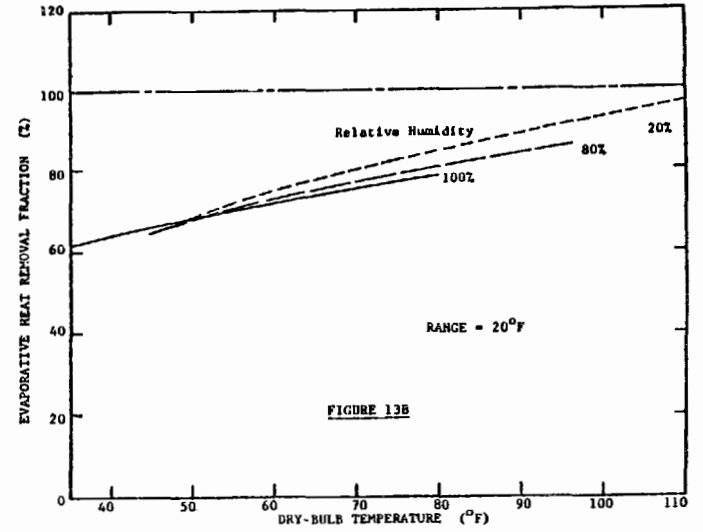
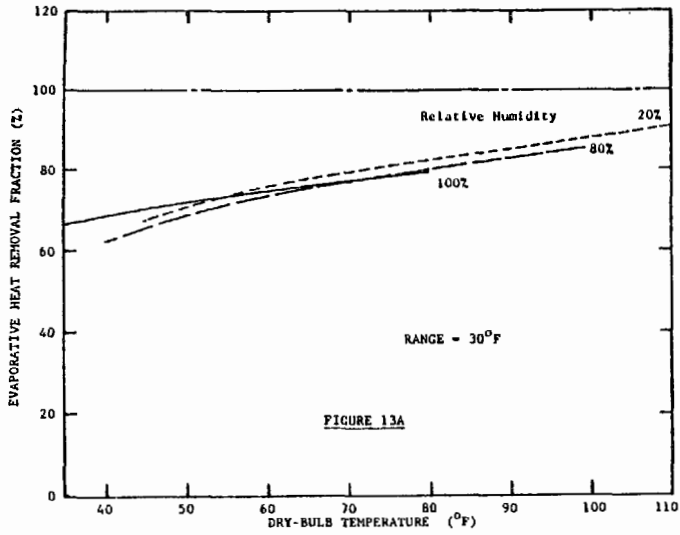


FIGURE 13: EVAPORATIVE HEAT REMOVAL FRACTION  
VERSUS DRY-BULB TEMPERATURE FOR  
VARIOUS RANGES

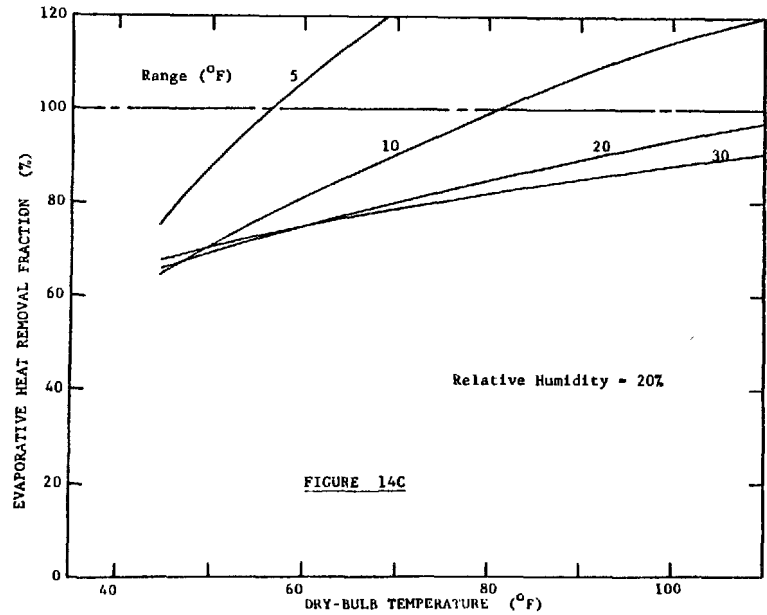
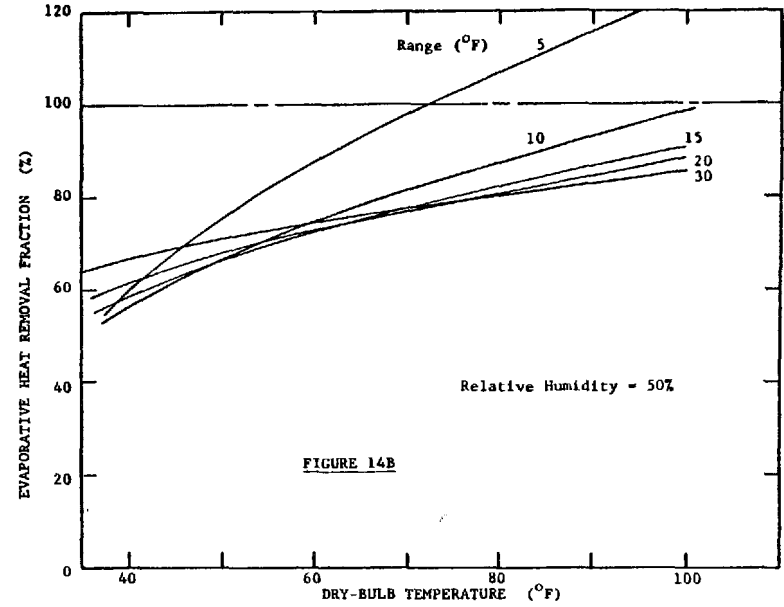
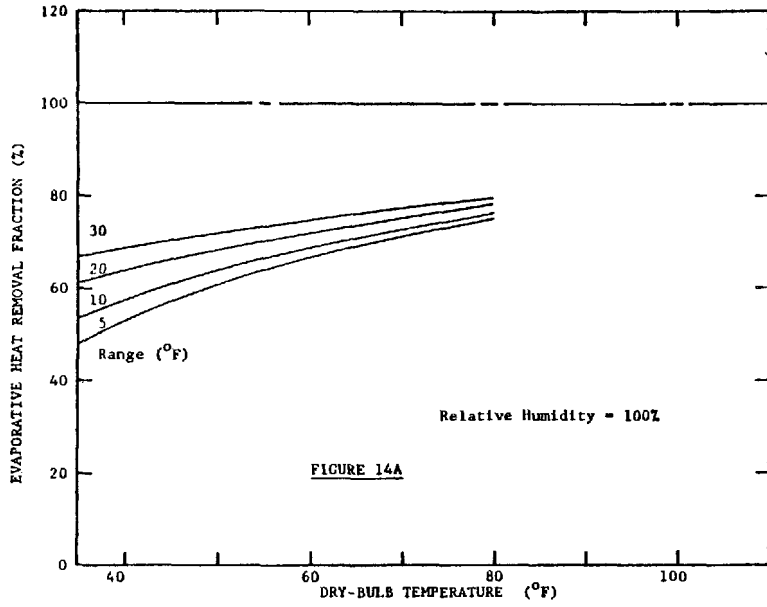


FIGURE 14: EVAPORATIVE HEAT REMOVAL FRACTION  
VERSUS DRY-BULB TEMPERATURE FOR  
VARIOUS RELATIVE HUMIDITIES

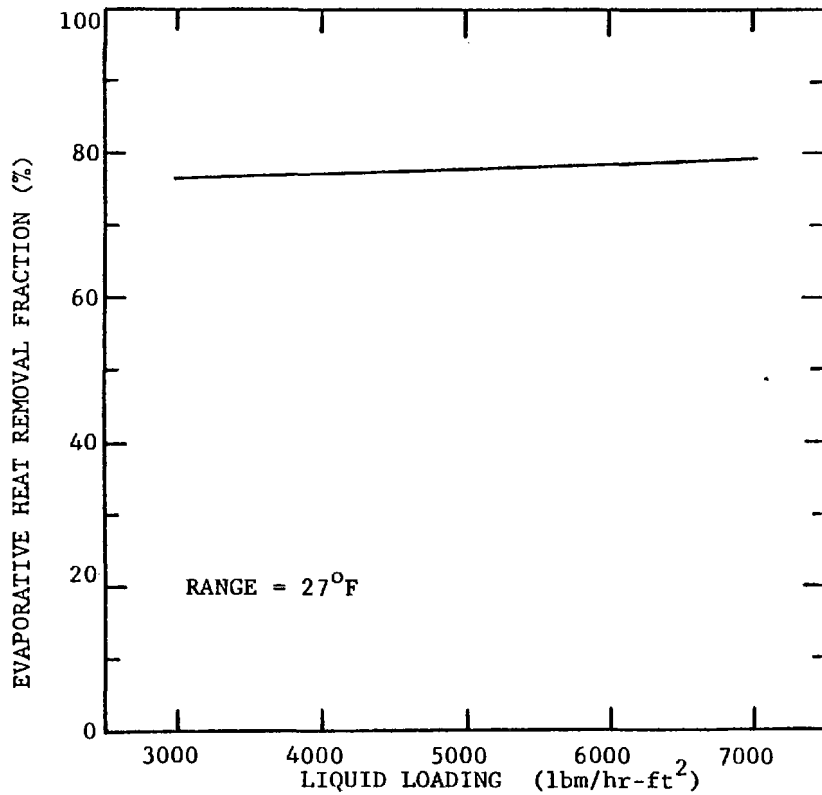


FIGURE 15: EFFECT OF LIQUID LOADING VARIATIONS ON EVAPORATIVE HEAT REMOVAL FRACTION

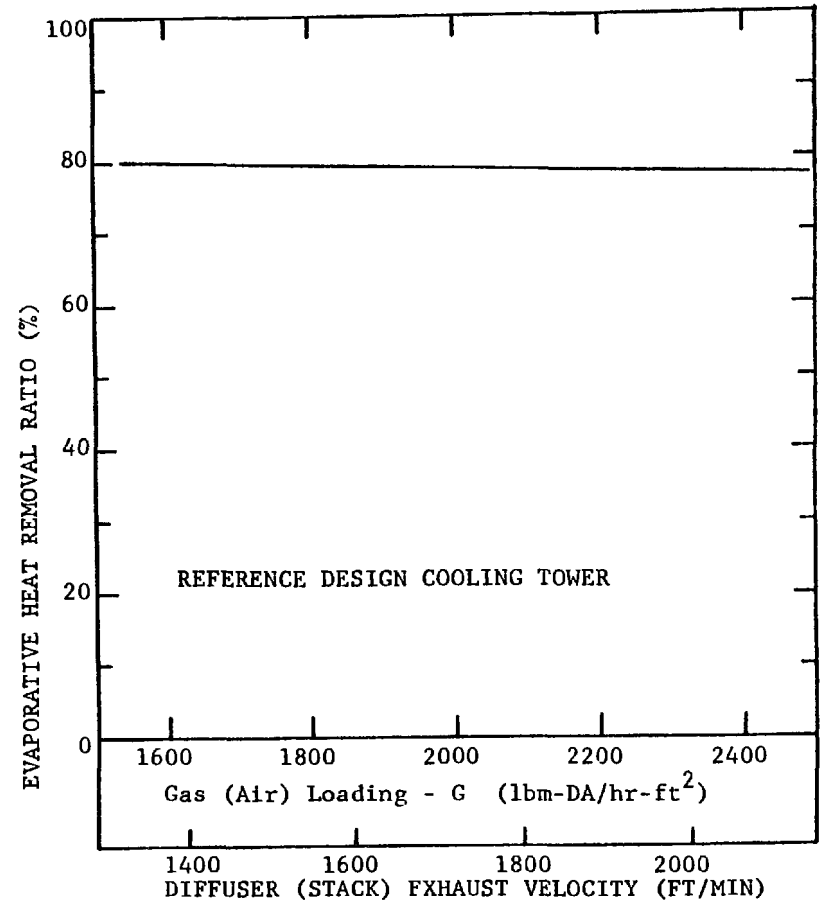


FIGURE 16: INFLUENCE OF GAS LOADING VARIATIONS ON EVAPORATIVE HEAT REMOVAL RATIO

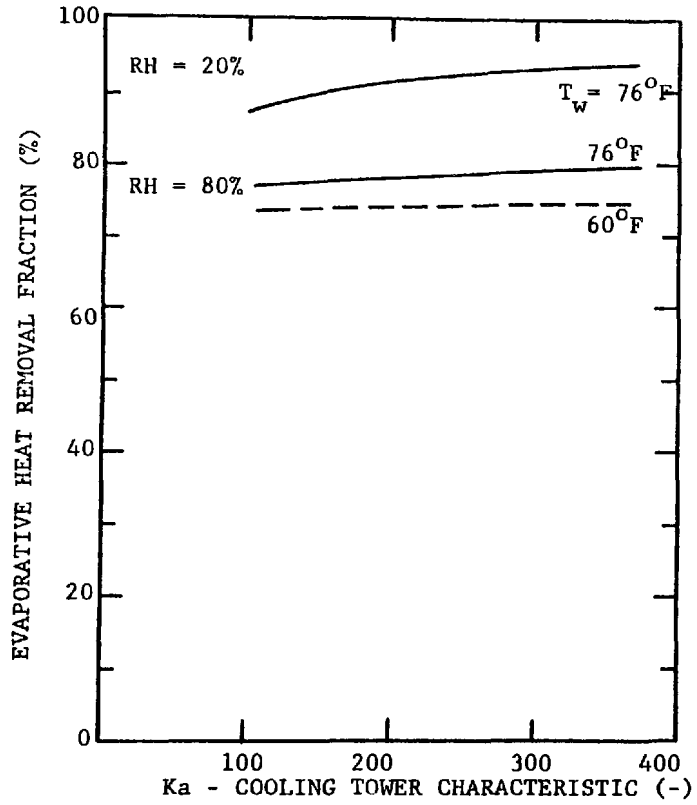


FIGURE 17: INFLUENCE OF COOLING TOWER CHARACTERISTIC ON EVAPORATIVE HEAT REMOVAL

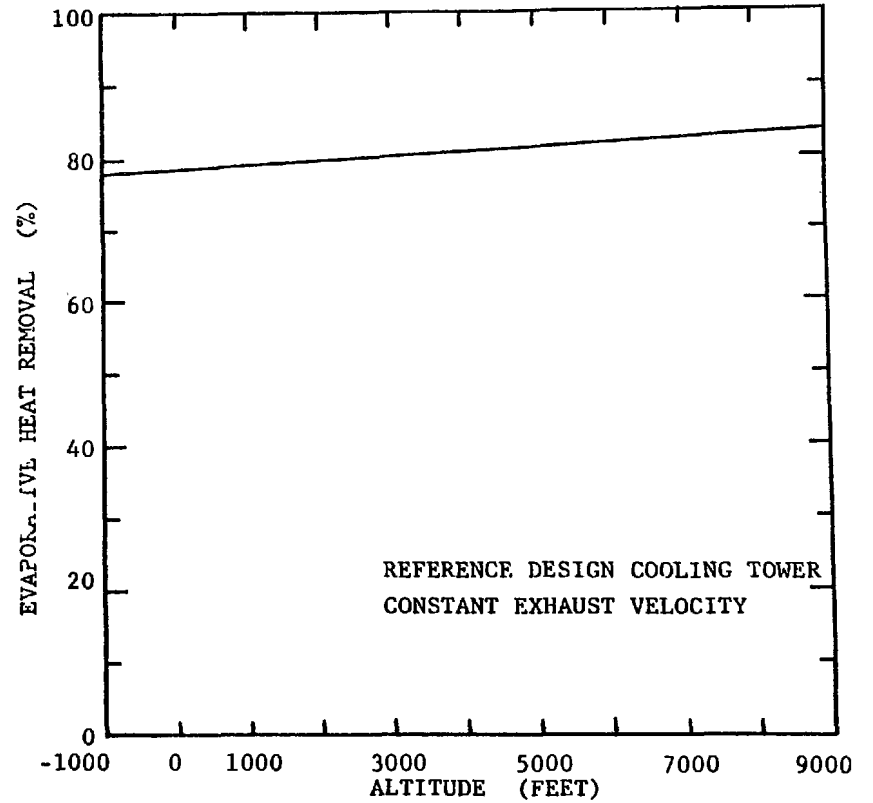


FIGURE 18: EFFECT OF ELEVATION ON EVAPORATIVE HEAT REMOVAL

The effect of barometric pressure (altitude) variations on the evaporative cooling fraction is shown in Figure 18. The barometric pressure may be seen to have a small effect on the fraction.

For this particular study, the air exhaust velocity was held constant so that the effect on a fixed tower design could be examined. Because the air density decreases as the elevation increases, a practical tower design would provide for an increase in the air velocity as the elevation increased.

Barometric pressure as a function of elevation above sea level was calculated using an empirical formula from the ASHRAE Brochure on Psychrometry [8].

### Natural Draft Cooling Tower Analysis

The evaporative heat removal fraction in a typical natural draft cooling tower is shown in Figures 19 and 20. The cooling tower analyzed was of the counter-flow type and used parallel-plate packing. The cooling tower design details are given in Table 2 below.

Table 2

#### NATURAL DRAFT COOLING TOWER DESIGN PARAMETERS

|                               |                          |
|-------------------------------|--------------------------|
| Overall Height . . . . .      | 480 ft.                  |
| Fill Diameter . . . . .       | 340 ft.                  |
| Air Inlet Height . . . . .    | 30 ft.                   |
| Fill Design . . . . .         | Counter-Flow             |
| Packing Type . . . . .        | Parallel-Plate           |
| Packing Height . . . . .      | 12 ft.                   |
| Plate Spacing . . . . .       | 1.0 in.                  |
| Plate Thickness . . . . .     | 0.19 in.                 |
| Heat Rejection Rate . . . . . | $5.5 \times 10^9$ BTU/hr |
| Water Flow Rate . . . . .     | 450,000 GPM              |

The analysis was performed using a computer code which was a modified version of a code written by Winiarski, Tichenor, and Byram [10].

The fraction of heat removed from the natural draft tower by evaporation is shown (versus wet-bulb temperature) in Figure 19 for the case of constant heat rejection. The only parameters varied in the natural draft tower studies were the ambient conditions. The evaporative heat removal fraction varied from 60% to 90% over the range of typical operating conditions. The evaporative heat removal fraction was

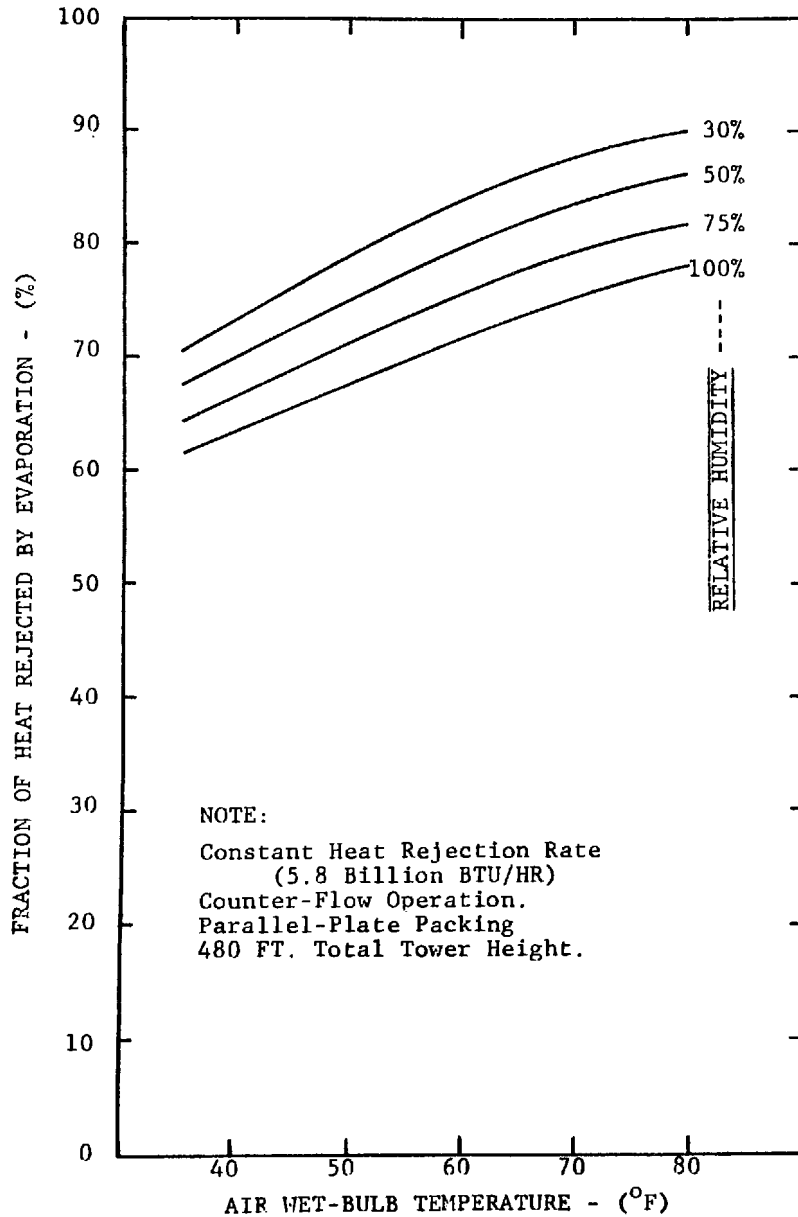


FIGURE 19: EVAPORATIVE HEAT REMOVAL FRACTION VERSUS WET-BULB TEMPERATURE: TYPICAL NATURAL DRAFT COOLING TOWER

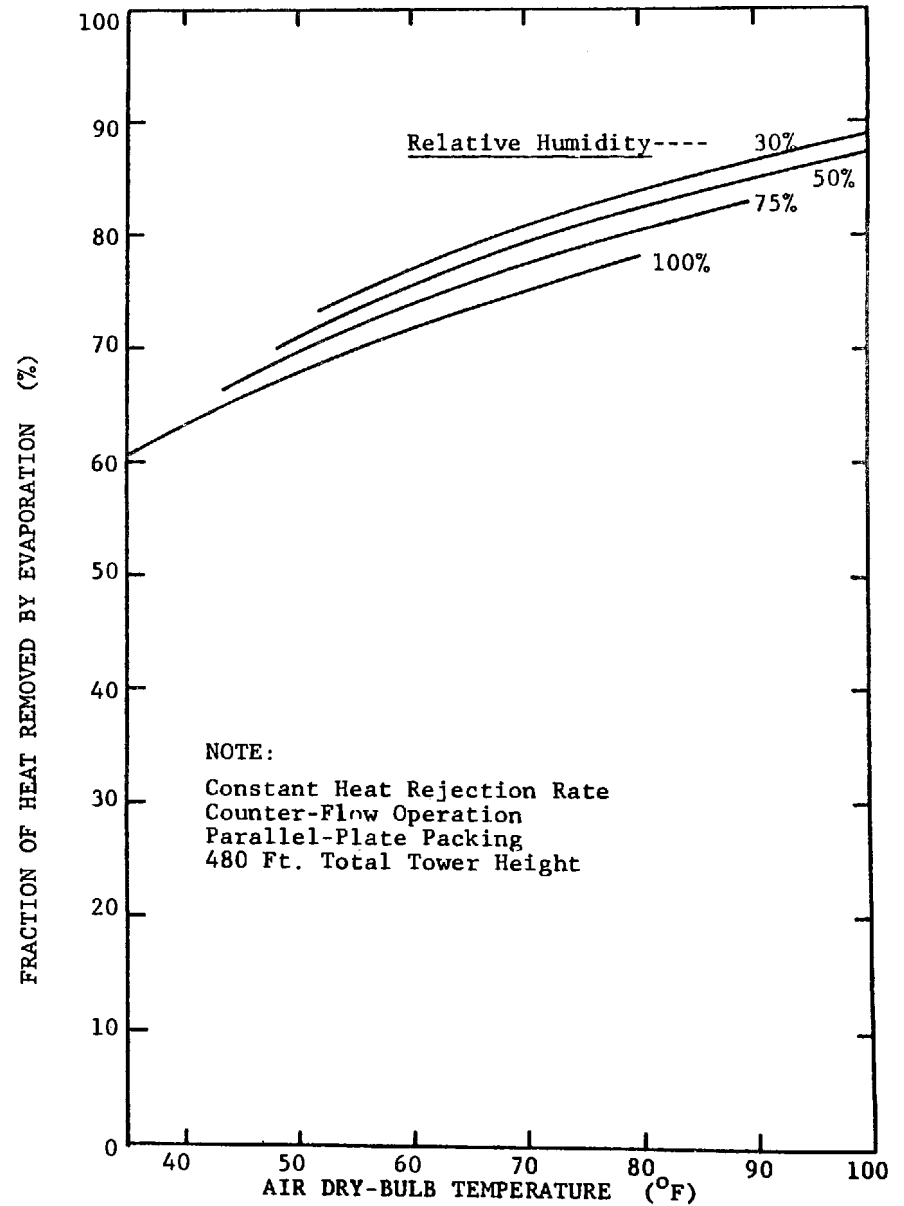


FIGURE 20: EVAPORATIVE HEAT REMOVAL VERSUS DRY-BULB TEMPERATURE FOR A TYPICAL NATURAL DRAFT COOLING TOWER

increased by about 12% of the total heat rejection as the relative humidity was decreased from 100% to 30% at a constant wet-bulb temperature.

Figure 20 shows the evaporative removal fraction plotted versus dry-bulb temperature. The relative humidity is seen to have a more significant effect on the evaporative cooling fraction in the natural draft tower than was the case in the mechanical draft tower. At any dry-bulb temperature, decreasing the relative humidity from 100% to 30% increases the value of the fraction by 6%. As a good approximation, the fraction increases by 1% for each 3°F increase in the dry-bulb temperature.

Because of the difficulties associated with converging the air flow rate and heat rejection rate simultaneously, it was not convenient to examine the effects of varying the natural draft cooling tower design. Nevertheless, the results given are believed to be indicative of natural draft cooling towers using counter-flow, parallel-plate packing.

#### EVAPORATIVE WATER LOSSES

Evaporative cooling results in moisture release into the atmosphere; it is the evaporative water loss that is responsible for the consumption of water in wet cooling towers, i.e., evaporation and the blowdown it necessitates. If all cooling were by evaporation the associated water loss due to evaporative heat removal would be 1% / 10°F range.

Figure 21 shows the water loss due to evaporation in the reference design mechanical draft, cross-flow cooling tower plotted versus dry-bulb temperature. A similar plot for the reference design natural draft cooling tower is shown in Figure 22. Except for the vertical scale, the plots are quite similar to those presented earlier for the evaporative cooling fraction.

The water evaporation rate in wet cooling towers (both mechanical and natural draft) was found to vary typically from 1% / 15°F range at 35°F to 1% / 11°F range at 100°F dry bulb temperature; this behavior reflects an increase in sensible cooling as the ambient dry-bulb temperature decreases. The evaporative water loss (WL) in large wet cooling towers may be estimated as follows for ranges above 20°F and relative humidities above 50%.

$$WL = \{ 0.061 + 0.0004 ( T_d - 35 ) \} \times \text{Range} \quad (\text{Eq. 6})$$

In this equation, the water loss WL is in per cent (%) of the circulating water flow,  $T_d$  is ambient dry-bulb temperature in degrees Fahrenheit, and the range is in degrees F. This equation underpredicts the water evaporation if the range is below 20°F or if the relative humidity is below 50%.

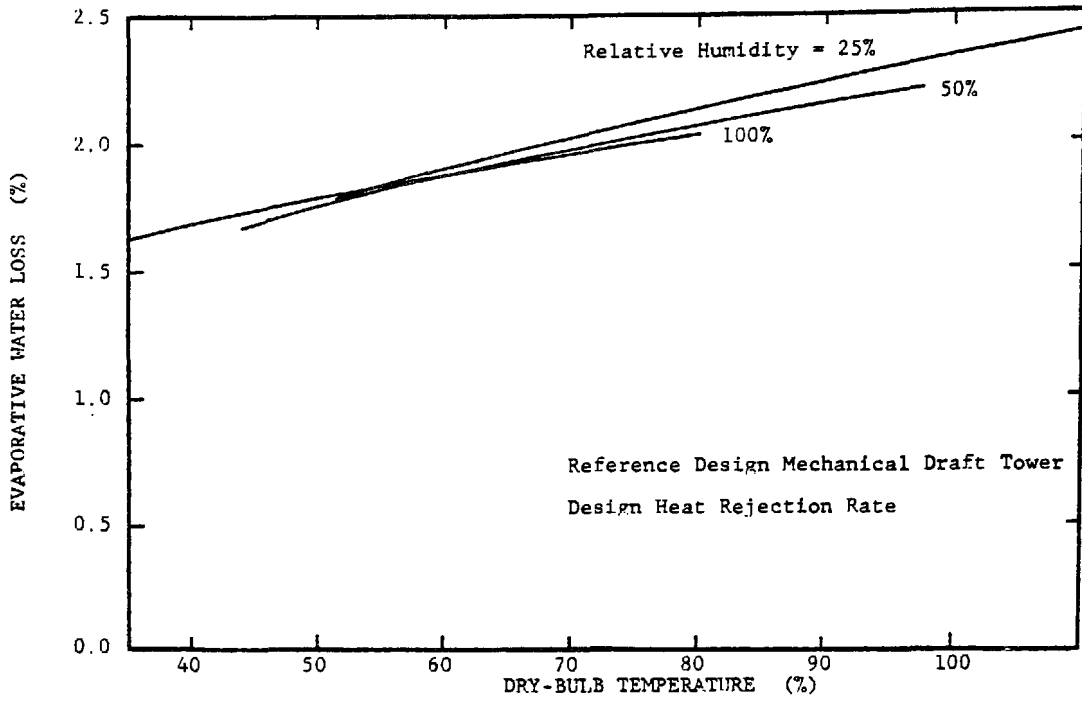


FIGURE 21: EVAPORATIVE WATER LOSS VERSUS DRY-BULB TEMPERATURE IN-A TYPICAL MECHANICAL DRAFT COOLING TOWER

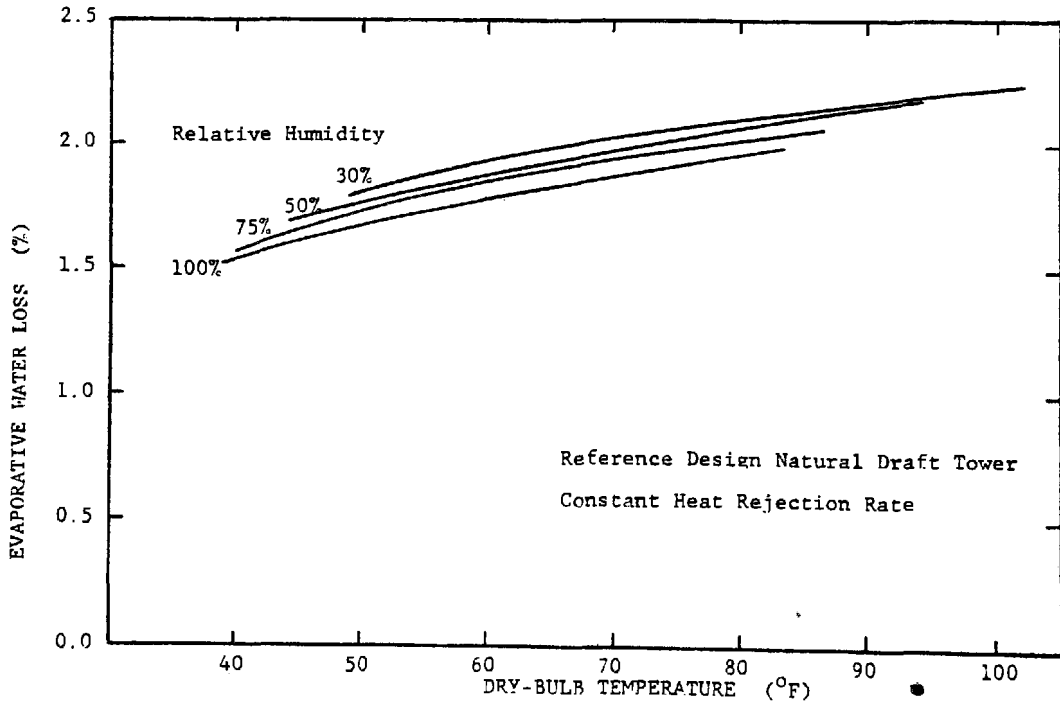


FIGURE 22: EVAPORATIVE WATER LOSS VERSUS DRY-BULB TEMPERATURE IN A TYPICAL NATURAL DRAFT COOLING TOWER

## RECOMMENDATIONS FOR FUTURE WORK

### Analytical Method

The details of the enthalpy-difference driving force method used for this have been discussed earlier. Importantly, however, for future work, it is recommended that a more exact analysis by Baker and Eaton [7] be used to evaluate evaporative heat removal in wet, cross-flow cooling towers.

### Other Tower Designs

This work has reported the evaporative heat removal fraction in a typical mechanical draft, cross-flow cooling tower and in a typical natural draft, counter-flow tower. Although it is expected that the results for a mechanical draft, counter-flow tower and for a natural draft, cross-flow tower will not differ significantly from those reported herein, it would be of interest to do the detailed analysis for those tower designs not considered here, i.e., mechanical draft counter-flow towers and natural draft cross-flow towers.

The analytical method developed by Navahandi, et al. [11] is recommended for evaluating mechanical draft, counter-flow tower designs. It is expected that the results for mechanical and natural draft counter-flow towers will be similar though the draft in a mechanical draft tower is nearly independent of the operating conditions.

The variation of the air humidity and dry bulb temperature at the outlet of the fill of a cross-flow natural draft tower might alter the evaporative cooling fraction somewhat from that in a counter-flow natural draft tower. It will be necessary to develop an iterative procedure to establish the air loading under natural draft conditions when using the Baker and Eaton method for cross-flow tower analysis.

### Field Measurements

In counter-flow tower designs and natural draft cross-flow towers, simple field measurements of inlet and outlet air humidity and dry bulb temperature will rapidly establish the fraction of heat removed by evaporation. Such measurements over an extended period of time will demonstrate the effect of several parameter variations on the evaporative cooling fraction.

For cross-flow mechanical draft towers, vertical air temperature and humidity profiles at the fill outlet would be required; however, five to ten measurement positions should be adequate. Here again, extended measurements would establish the effect of variations in tower operating conditions of evaporative heat removal.

## SUMMARY

Wet or evaporative cooling towers are commonly used to provide for the cooling of water by direct contact with air. Two heat removal mechanisms dominate in an evaporative cooling tower: evaporative heat removal and sensible heat transfer. Sensible heat transfer refers to heat transferred by virtue of a temperature difference between the water and air. Evaporative heat removal refers to the energy removal from the water as latent heat of evaporation; this heat removal is the result of the evaporation of water into air during the direct-contact cooling process.

The ratio of evaporative-to-total (sensible plus evaporative) heat transfer in a wet, cross-flow, mechanical draft cooling tower was analyzed. The ratio was found to vary from 60% to 90% during typical operating conditions. The evaporative heat removal fraction increased as temperature (either wet-bulb or dry-bulb) increased and as relative humidity decreased.

Typically, the fraction of the heat removal from a wet cooling tower due to evaporative cooling increases about one per cent per three degrees F ( 1% / 3°F ) increase in the ambient dry-bulb temperature. For large wet cooling towers (either mechanical or natural draft), the evaporative heat removal fraction can be estimated as follows for operating ranges above 20°F:

$$Q_{ev} / Q_{tot} = 0.65 + 0.0038 ( T_d - 35 ) \quad (\text{Eq. 7})$$

The theoretical maximum evaporative water loss is one per cent of the circulating water flow rate per 10°F operating range, i.e., 1% / 10°F range. For ranges above 20°F, the evaporative water loss WL (as % of circulating water flow) in large wet cooling towers can be estimated by

$$WL = ( 0.061 + 0.0004 ( T_d - 35 ) ) \times \text{Range} \quad (\text{Eq. 8})$$

where the ambient dry-bulb temperature  $T_d$  and the range are in degrees F. The above equations apply at relative humidities above 50%.

Results similar to those obtained above were obtained for a counter-flow natural draft cooling tower. For the mechanical draft, cross-flow tower, it is of interest to note that under certain conditions, both the water and air are cooled by evaporation so that the evaporative cooling exceeds 100% of the cooling effect on the water alone.

## REFERENCES

- (1) Hamilton, Thomas H., "Estimating Cooling Tower Evaporation Rates," Power Engineering, V. 81, No. 3, 1977, pp. 52-54.
- (2) Eaton, Thomas E., "Evaporative Cooling Tower Performance: A Comprehensive Bibliography," Industrial Heat Rejection Project Report, Mechanical Engineering Department, University of Kentucky, December 1978.
- (3) Kelly, Neil W., "A Blueprint for the Preparation of Cross-Flow Cooling Tower Characteristic Curves," Cooling Tower Institute Technical Paper TP-146A, 1976, 30 pp.
- (4) Hallett, G.F., "Performance Curves for Mechanical Draft Cooling Towers," Journal of Engineering for Power, Trans. of the ASME, Vol. 97, October 1975, pp. 503-508, also ASME Paper 74-WA/PTC-3.
- (5) Park, J.E., J.M. Vance, K.E. Cross, and N.H. van Wie, "A Computerized Engineering Model for Evaporative Water Cooling Towers," Proceedings of the Conference on Waste Heat Management and Utilization, May 1976, pp. IV-C-180 to 199; also U.S. DOE (ORNL) Report K/CSD/INF-77/1.
- (6) Park, J.E., and J.M. Vance, "Computer Model of Cross-Flow Towers," Cooling Towers, Vol. 1, AIChE-CEP Technical Manual. 1972, pp. I22-I24.
- (7) Baker, Kenneth L., and Thomas E. Eaton, "An Improved Method for Evaporative Cross-flow Cooling Tower Performance Analysis," Second Conference on Waste Heat Management and Utilization, Miami, December 1978.
- (8) ASHRAE Brochure on Psychrometry (N.Y., American Society of Heating, Refrigerating, and Air-Conditioning Engineers, 1977), 167 pp.
- (9) Croley, Thomas E., II, V.C. Patel, and M.S. Cheng, "The Water and Total Optimizations of Wet and Dry-Wet Cooling Towers for Electric Power Plants," Iowa Institute of Hydraulic Research, The University of Iowa, IIHR Report No. 163, January 1975, 290 pp.
- (10) Winiarski, Lawrence D., Bruce A. Tichenor, and Kenneth V. Byram, "A Method for Predicting the Performance of Natural Draft Cooling Towers," U.S. Environmental Protection Agency, Water Quality Office, Water Pollution Control Research Series Report 16130 GKF 12/70, December 1970, 69 pp.
- (11) Nahavandi, Amir N., and Johann J. Oellinger, "An Improved Model for the Analysis of Evaporative Counterflow Cooling Towers," Nuclear Engineering and Design, Vol. 40, 1977, pp. 327-336.

## NOMENCLATURE

- a - Interfacial air-water contact area per unit fill volume ( $\text{ft}^2/\text{ft}^3$ )
- $c_{pw}$  - Specific heat of water at constant pressure (BTU/lbm $^{\circ}$ F)
- G - Gas (Air) loading (lbm-DA/ $\text{ft}^2$ )
- H - Enthalpy of an air-water vapor mixture (BTU/lbm-Dry Air)
- $H_m$  - Same as H
- H' - Air-Water vapor mixture enthalpy at a specified water temperature (BTU/lbm-DA)
- $h_{fg}$  - Latent heat of vaporization of water (BTU/lbm)
- K - Overall mass transfer coefficient (lbm-WV/(hr- $\text{ft}^2$ -lbm water/lbm DA)
- Ka - Cooling tower characteristic (BTU/hr- $\text{ft}^3$ )/BTU/lbm-DA)
- L - Liquid loading (lbm-water/ $\text{ft}^2$ )
- $\dot{M}_w$  - Total water flow to cooling tower (lbm/hr)
- M - Number of horizontal grid points (-)
- N - Number of vertical grid points (-)
- $Q_{ev}$  - Total evaporative heat removal (BTU/hr)
- $Q_{tot}$  - Total evaporative plus sensible heat removal (BTU/hr)
- $Q_{rej}$  - Heat rejection rate of cooling tower (BTU/hr)
- $T_d$  - Air dry bulb temperature ( $^{\circ}$ F)
- $T_w$  - Water temperature ( $^{\circ}$ F)
- $T_{on}$  - Hot Water Temperature ( $^{\circ}$ F)
- $T_{off}$  - Average cold water temperature ( $^{\circ}$ F)
- W - Humidity ratio (lbm-water vapor/lbm-dry air)
- $\delta X$  - Horizontal grid width (ft)
- $\delta Y$  - Vertical grid height (ft)
- $\phi$  - Relative humidity (%)

### Subscripts

- i - inlet
- o - outlet

## ACKNOWLEDGEMENTS

The author would like to express his sincere gratitude to the Institute for Mining and Minerals Research and to the Mechanical Engineering Department of the University of Kentucky for their partial financial support of this project,

Mr. C.F. Hsu's computational efforts which established the preliminary estimates of the evaporative cooling effect in mechanical draft towers are gratefully acknowledged.

Also, the author would like to thank Ms. Paulette Montross for preparing the final draft of this paper. Professor O.J. Hahn of the University of Kentucky is acknowledged for his assistance in obtaining financial support for this work.

Finally, Professor Norman C. Rasmussen of the Massachusetts Institute of Technology is gratefully recognized for supervising the author's first project on cooling towers which inspired this paper.

## APPENDIX A

### CROSS-FLOW COOLING TOWER ANALYSIS METHOD

#### Basic Enthalpy-Difference Equations

The performance analysis of cross-flow mechanical draft cooling towers was accomplished using the enthalpy-difference driving force method. This method has been used by others, e.g., Kelly [3], Hallett [4], or Croley [9], to analyze cross-flow cooling towers. Further, Hallett has developed an empirical correlation of the unit volume coefficient (Ka) for a typical cross-flow cooling tower packing. Hallett's correlation for Ka is intended to be used in an enthalpy-difference driving force calculational model for cooling tower performance.

The enthalpy-difference driving force model provides a reasonably accurate prediction of water temperatures without calculating the details of the air conditions in the tower. This method is successful principally because the enthalpy of a mixture of air and water vapor is nearly constant for constant wet bulb temperature. The enthalpy-difference driving force model then estimates the heat transfer between the water and air assuming that the air is saturated at the wet bulb temperature and that the air-water vapor mixture near the liquid water surface is saturated at the water temperature; with this, the enthalpy of the air and water vapor near the water surface is readily determined.

The basic equation for the enthalpy change of the air in a differential volume of the tower fill is

$$H_o - H_i = \frac{Ka \delta X}{G} (H_i' - H_i) \quad (\text{Eq. A1})$$

where  $H_i'$  is the enthalpy of saturated air at the entering water temperature and  $H_i$  is the enthalpy of the entering air. While this equation is convenient for an initial estimate of the outlet air enthalpy, the following equation, which averages the entering and leaving enthalpy difference, is more accurate:

$$H_o = \frac{H_i + \frac{Ka \delta X}{2G} [H_i' - H_i + H_o']}{[1 + \frac{Ka \delta X}{2G}]} \quad (\text{Eq. A2})$$

The outlet water temperature  $T_{wo}$  may then be estimated using the following equation:

$$T_{wo} = T_{wi} - \frac{G \delta Z}{C_p L_i \delta X} (H_o - H_i) \quad (\text{Eq. A3})$$

This value of  $T_{wo}$  can be used to determine a new value for enthalpy of air saturated with water vapor at the outlet water temperature,  $H_o'$ . Next, this new estimate for  $H_o'$  is used to reevaluate Eq. A2 for an im-

proved estimate of  $H_o$ . This iterative procedure converges rapidly; typically the values of  $H_o$  and  $T_{wo}$  will converge in less than five iterations.

### Estimation of the Relative Humidity Inside the Tower

The use of the enthalpy difference driving force method allows one to evaluate the local water temperature and air enthalpy inside the cooling tower without regard to the local air relative humidity.

Because the outlet air relative humidity was important in evaluating the evaporative heat removal in the cooling tower, the following procedure was used to estimate the local humidity ratio inside the cooling tower fill.

Since the objective was simply to determine the change in the humidity ratio as the air crossed a differential volume element of fill, and since the change in enthalpy across the volume element was known, the humidity ratio change was estimated as the change in the humidity ratio along the saturation line between the inlet and outlet air enthalpies. This change in the humidity ratio was added to the entering humidity ratio to determine the outlet humidity ratio, i.e.,

$$W_o = W_i + [W_{sat}(H_o) - W_{sat}(H_i)] \quad (\text{Eq. A4})$$

At this point the enthalpy and humidity ratio leaving the grid were known so that the wet-bulb and dry-bulb temperatures could also be determined.

This method for determining the humidity ratio distribution in the tower is not exact; however, for the purposes estimating the outlet air humidity, this method was believed to be better than assuming saturated outlet conditions. Further, this exhaust humidity calculation technique is in better agreement with observed cooling tower exhaust conditions than is the assumption of saturated conditions - particularly on mechanical draft, cross-flow towers.

With the local humidity variation known, the small correction to the liquid loading due to evaporation was made and used in the next row of calculations:

$$L_o = L_i - \frac{G \delta Z}{\delta X} (W_o - W_i) \quad (\text{Eq. A5})$$

Park, et al. [5,6] have developed a humidity difference driving force method for analyzing cross-flow cooling towers. However, because the properly determined tower characteristics ( $Ka$ ) were not available, this method was not used in this work. A method has been developed by Baker and Eaton [7] which accurately predicts the air conditions inside the cooling tower fill; however, it was not available for use in determining the evaporative heat removal fractions reported in this paper.

Prepared for Presentation at a  
Waste Heat Management &  
Utilization Conference

Miami Beach, Florida  
December 4-6, 1978

Comparative Cost Study of Various Wet/Dry Cooling  
Concepts that Use Ammonia as the Intermediate  
Heat Exchange Fluid

B. M. Johnson, R. D. Tokarz, D. J. Braun, R. T. Allemann

1. PURPOSE OF THIS WORK

Dry cooling of thermal power plants, by which the heat from the power cycle is rejected directly to the air, has been used in a few isolated instances throughout the world for the past 15 years. Very few installations are in operation in the U.S. although it is being given increased consideration for new large power stations. Dry cooling is a more costly option than once-through or evaporative cooling, but there are a few locations now, and there will be far more in the future, at which once-through and all-wet evaporative cooling towers cannot be used because of the increased competition for existing water supplies among growing populations, agriculture and industry. Earlier studies at the Pacific Northwest Laboratory, have shown that considerable incentives exist for development of an advanced concept which makes use

of ammonia as an intermediate heat transfer fluid in a process which provides augmented cooling by evaporation.

This paper summarizes the conceptual design and costs of four different configurations for such a system and compares them to a state-of-the-art integrated dry/wet circulating water system.<sup>1</sup> All are mechanical draft systems.

These studies are part of an ongoing effort, supported by both the U. S. Department of Energy and the Electric Power Research Institute, to increase the flexibility of plant siting and reduce the break-even cost of water at which power companies would choose to conserve water through use of some dry cooling.

## 1.2 Incentives for Dry/Wet Cooling

Providing some capability for augmented cooling via water evaporation to dry cooled heat rejection systems has been shown to be highly cost-effective. It is probable that in this country most dry-cooled systems for large power plants will have some evaporative cooling capability included in the system to avoid either of the costly alternatives of (1) building excessively large systems to provide adequate heat rejection for peak power projection during the hottest summer days, or (2) buying power from other sources during peak demand periods on the hottest days. With some evaporative cooling capability the dry/wet system can be built so as to use whatever water is available for cooling and thus minimize the required size of the high-priced dry cooling system. How to best provide this evaporative cooling capability with the ammonia system was one of the purposes of this work.

---

1. R. D. Tokarz, et. al., "Comparative Cost Study of Four Wet/Dry Cooling Concepts that use Ammonia as the Intermediate Heat Exchange Fluid," PNL-2661, Battelle Pacific Northwest Laboratories, May 1978.

at a specific ambient temperature, which was established so as to require a predetermined amount of water each year for augmented cooling.

Capital costs included all engineering, construction and material costs associated with the cooling towers, condenser, water treatment equipment and related piping and pumps. Construction costs included the contractor's profit and overhead, but excluded any escalation or contingencies. Operating costs included the cost of auxiliary power for pumps and fans, maintenance, and water treatment.

Credit was taken for improvements in plant heat rate associated with lower back pressures made possible by the advanced designs. However, no credit was taken for increases in load that would be made possible by back pressures lower than the design values of the reference plant.

To assure the validity of the comparisons, every effort was made to use uniformity in the conceptual designs and cost estimation of each concept.

All estimates were prepared by an architect-engineer subcontractor <sup>(a)</sup> from preconceptual design descriptions prepared for each concept. All design descriptions used a common reference plant location, the San Juan Unit 3 of the Public Service Company of New Mexico. This plant was selected as the reference plant for this study because a plant with integrated dry/wet cooling towers is currently under design and construction at this location. As a result, adequate site data were already available on which to base the preconceptual designs of the advanced alternatives, including

meteorology,

fuel costs,

---

(a) S&Q Engineering Corporation

### 1.3 Incentives for Using Ammonia

The use of ammonia as a heat transfer medium between the steam condenser of the turbine-generator and the air-cooled heat rejection system has been shown to be cost effective in earlier studies which were reported in the previous conference.<sup>1</sup> The use of ammonia offers at least four advantages leading to reduction in system costs. These are:

1. Reduced pumping power in the transport loop;
2. Elimination of the temperature range of the transport loop as a temperature increment between the ambient dry bulb and the condensing steam temperature;
3. The ability to use high performance surfaces on the ammonia side of the steam condenser/ammonia reboiler to reduce the condenser terminal temperature difference, and lastly,
4. No need to prevent freeze up.

## 2. BASIS OF COMPARISON

The comparisons of the various concepts were performed on the basis of "comparable capital cost" defined as the sum of the estimated capital cost of the installation plus the capitalized operating cost. This latter term is just the operating cost divided by the annual-fixed-charge-rate of 18 percent. The designs have not been optimized in the sense that they would yield the lowest bus bar cost of electricity. At the time the study was initiated the dry/wet design optimization code was not completed. Instead, each design satisfies a set of design parameters, particularly with respect to heat rejection capability

<sup>1</sup>"Dry/Wet Cooling Towers with Ammonia as an Intermediate Heat Exchange Medium," Paper 4C-4, Waste Heat Management & Utilization Conference, Miami Beach Florida, May 9-11, 1977.

at a specific ambient temperature, which was established so as to require a predetermined amount of water each year for augmented cooling.

Capital costs included all engineering, construction and material costs associated with the cooling towers, condenser, water treatment equipment and related piping and pumps. Construction costs included the contractor's profit and overhead, but excluded any escalation or contingencies. Operating costs included the cost of auxiliary power for pumps and fans, maintenance, and water treatment.

Credit was taken for improvements in plant heat rate associated with lower back pressures made possible by the advanced designs. However, no credit was taken for increases in load that would be made possible by back pressures lower than the design values of the reference plant.

To assure the validity of the comparisons, every effort was made to use uniformity in the conceptual designs and cost estimation of each concept.

All estimates were prepared by an architect-engineer subcontractor <sup>(a)</sup> from preconceptual design descriptions prepared for each concept. All design descriptions used a common reference plant location, the San Juan Unit 3 of the Public Service Company of New Mexico. This plant was selected as the reference plant for this study because a plant with integrated dry/wet cooling towers is currently under design and construction at this location. As a result, adequate site data were already available on which to base the preconceptual designs of the advanced alternatives, including

- meteorology,
- fuel costs,

---

(a) S&Q Engineering Corporation

- water availability and quality,
- onsite construction costs,
- transportation costs,
- power costs, and
- site characteristics.

Each of the dry/wet systems was conceptually designed and estimated using the same procedure, including the integrated wet/dry concept used in the reference plant. No cost or detail design information was obtained from the utility about the integrated wet/dry concept, so it, too, was designed and costed on the same basis as the other four. This cost comparison study applies only to the reference plant design conditions. Other sites would have different conditions that could markedly affect the resulting comparison.

## 2.1 Conceptual Design Bases

The conceptual designs of the three cooling tower concepts were based on performance requirements established by the Public Service Company of New Mexico for the San Juan Unit 3. These requirements are listed below.

1. The heat rejection capability of the cooling system shall be about  $2.5 \times 10^9$  Btu/hr over a yearly cycle.
2. The cooling system shall accommodate the meteorological profile of Farmington, New Mexico (Table 1).
3. The turbine shall be operated at or below a back pressure of 4.5 in. Hg at an ambient temperature of 95<sup>0</sup>F or below. Above 95<sup>0</sup>F, the turbine back pressure shall be allowed to increase to a maximum of 5.0 in. Hg.

Table 1. Meteorological Profile at Farmington, NM

| <u>Dry Bulb Air<br/>Temperature, °F</u> | <u>Wet Bulb Air<br/>Temperature, °F</u> | <u>Hours per<br/>Year</u> |
|---|---|---------------------------|
| 7                                       | 7                                       | 55                        |
| 12                                      | 11                                      | 98                        |
| 17                                      | 16                                      | 198                       |
| 22                                      | 20                                      | 336                       |
| 27                                      | 25                                      | 553                       |
| 32                                      | 29                                      | 698                       |
| 37                                      | 33                                      | 688                       |
| 42                                      | 36                                      | 708                       |
| 47                                      | 39                                      | 678                       |
| 52                                      | 41                                      | 648                       |
| 55                                      | 44                                      | 388                       |
| 57                                      | 45                                      | 259                       |
| 62                                      | 47                                      | 704                       |
| 65                                      | 49                                      | 411                       |
| 67                                      | 50                                      | 274                       |
| 70                                      | 52                                      | 351                       |
| 72                                      | 53                                      | 234                       |
| 75                                      | 54                                      | 295                       |
| 77                                      | 54                                      | 197                       |
| 80                                      | 55                                      | 245                       |
| 82                                      | 56                                      | 164                       |
| 87                                      | 58                                      | 331                       |
| 92                                      | 61                                      | 179                       |
| 97                                      | 62                                      | 34                        |
| 102                                     | 63                                      | 1                         |

4. The maximum amount of water available annually for consumptive use is 1900 acre-ft or  $5.12 \times 10^9$  lb, which is about 20% that consumed by all-wet tower of similar rating.
5. The maximum instantaneous flow rate of consumptive water due to evaporation shall be  $2.0 \times 10^6$  lb/hr (4000 gpm).

The San Juan River was assumed to be the source of water to the plant. Water treatment requirements for closed-loop recirculating systems associated with dry towers were assumed to include demineralization, vacuum deaeration, corrosion inhibition, and pH control (pH 8.5). Open loop systems used in wet and wet/dry towers were assumed to require lime-soda softening (side stream), scale inhibition and biofouling control. Delugeate treatment to maintain a Langlier saturation index of zero or slightly negative was assumed.

### 3. ALTERNATIVES CONSIDERED

The four cooling concepts principally studied utilize the ammonia liquid-vapor phase change to transfer heat from the steam turbine outlet to the cooling towers. These concepts are compared with the conceptual design of the integrated dry/wet cooling tower of a configuration similar to that being constructed at Farmington, New Mexico. This design and cost estimate were developed without obtaining design details or costs from either the owner or manufacturer of that system. Consequently all systems were estimated by the same method and from similar data base. However, the ammonia systems' designs had not undergone the extent of engineering optimization studies inherent in a commercial system.

### 3.1 Ammonia Heat Transport System

The following is a brief description of the salient features of the ammonia heat transport system.

The ammonia heat transport system for power plant heat rejection is functionally similar in many respects to the "direct" system in which the exhaust steam from the last stage of the turbine is ducted directly to an air-cooled condenser. The principal difference is the existence of a steam condenser/ammonia reboiler in which ammonia is "substituted" for steam as the medium for transporting heat from the turbine to the tower (heat sink). In all respects the ammonia system, with vapor moving from the reboiler to the air-cooled condenser and liquid returning to the reboiler, will function and respond to load changes in the same manner as the direct system. Figure 1 is the process flow sketch.

Exhaust steam from the last stage of the turbine is condensed in the condenser/reboiler located directly below the turbine. Instead of water circulating through the tubes, liquid ammonia is boiled as it is pumped through the tubes under pressure, set by the operating temperature in the condenser. The flow rate of ammonia is set to yield a vapor quality emerging from the tubes varying from 50 to 90%. This two-phase mixture is passed through a vapor-liquid separator from which the vapor is sent to the air-cooled condenser, while the liquid is combined with the ammonia condensate from the dry tower and recycled back through the condenser/reboiler.

Table 2. Design Parameters

| <u>Tower</u>   | <u>Vertical ROTERY</u>                          | <u>Horizontal ROTERY</u>                        | <u>SCAT Tower Design</u>      | <u>Augmenting High Condenser</u> | <u>Integrated Wet/Dry</u>                       |
|--|---|---|-------------------------------|----------------------------------|---|
| Tower size (ft)  | 259 dia x 56 high                               | 205 x 230 x 57 high                             | 225 dia x 56 high             | 170 dia x 56 high                | 402 x 138 x 55 high                             |
| Tower Design Temp.   | 55°F  | 55°F  | 55°F                          | 35°F                             | 35°F  |
| Design ITD, degrees  | 67  | 67  | 67 dry, 32 wet                | 37 dry, 32 wet                   | 30 dry, 30 wet                                  |
| Number of Towers   | 3   | 2   | 2                             | 2                                | 2   |
| Number of Bundles  | 288   | 288   | 122                           | 88                               | 320   |
| Dimensions   | 47.5 ft x 8 ft x 6 in.                          | 47.5 ft x 8 ft x 6 in.                          | 50 ft x 12 ft x 1 ft          | 50 ft x 12 ft x 7.2 in.          | 48 ft x 72 ft x 10 in.                          |
| Total Surface Area, ft <sup>2</sup>                                    | 9.71 x 10 <sup>6</sup>                          | 9.71 x 10 <sup>6</sup>                          | 8.91 x 10 <sup>6</sup>        | 5.41 x 10 <sup>6</sup>           | 7.206 x 10 <sup>6</sup>                         |
| Frontal Area, ft <sup>2</sup>  | 1.072 x 10 <sup>5</sup>                         | 1.072 x 10 <sup>5</sup>                         | 0.732 x 10 <sup>5</sup>       | 0.522 x 10 <sup>5</sup>          | 9.216 x 10 <sup>4</sup>                         |
| Tube OD, inches  | 0.78  | 0.78  | 0.3                           | 0.3                              | 1.07  |
| Fin Design   | Rectangular Plate                               | Rectangular Plate                               | Integral                      | Integral                         | Single Leg Wrapped                              |
| Fin Dimensions   | 6 in. deep<br>7.37 ft high                      | 6 in. deep<br>7.37 ft high                      | 0.707 in. high<br>12 in. deep | 0.707 in. high<br>12 in. deep    | 2.25 round                                      |
| Fins Per Inch  | 9   | 9   | 10.6                          | 10.6                             | 10  |
| Tube Material  | Aluminum  | Aluminum  | Aluminum                      | Aluminum                         | Admiralty                                       |
| Fin Material   | Aluminum  | Aluminum  | Aluminum                      | Aluminum                         | Aluminum  |
| Tube Geometry  | Staggered Rows                                  | Staggered Rows                                  | Rectangular Aligned Channels  | Rectangular Aligned Channels     | Equilateral                                     |
| Transfer Tube Pitch, Inches  | 2.36  | 2.36  | NA                            | NA                               | 2.35  |
| Heat Transfer Coefficient Btu/hr-ft <sup>2</sup> -°F                   | 7.57  | 7.57  | 8                             | 9.1                              | 6.41  |
| Frontal Velocity/<br>Internal Velocity,<br>ft/sec.                     | 3/13.3  | 3/13.3  | 12/16.4                       | 14.0/19.1                        | 10.5/15   |
| Air Flow, lb/hr - <u>Dry</u>   | 1.93 x 10 <sup>8</sup>                          | 1.93 x 10 <sup>8</sup>                          | 1.97 x 10 <sup>8</sup>        | 1.70 x 10 <sup>8</sup>           | 2.196 x 10 <sup>8</sup>                         |
| Air Flow, lb/hr - <u>wet</u>   | 1.3 x 10 <sup>8</sup>                           | 1.3 x 10 <sup>8</sup>                           | 0.45 x 10 <sup>8</sup>        | 0.47 x 10 <sup>8</sup>           | 0.24 x 10 <sup>8</sup>                          |
| Air Mass Flow Rate, - <u>Dry</u><br>lb/hr-ft <sup>2</sup> - <u>wet</u> | 1.79 x 10 <sup>3</sup><br>0.9 x 10 <sup>3</sup> | 1.79 x 10 <sup>3</sup><br>0.9 x 10 <sup>3</sup> | 2.69 x 10 <sup>3</sup>        | 3.25 x 10 <sup>3</sup>           | 2.08 x 10 <sup>3</sup><br>0.5 x 10 <sup>3</sup> |
| Cooling Water Flow, GPM  | 7,000 (80 TDH)                                  | 21,000 (40 TDH)                                 | 170,000 (35 TDH)              | 200,000 (35 TDH)                 | 219,000 (77 TDH)                                |
| Airside Heat Exchange/ΔP/<br>Total ΔP, inches H <sub>2</sub> O         | 0.356/0.464                                     | 0.356/0.464                                     | 0.281/0.384                   | 0.243/0.358                      | 0.345/0.538                                     |
| Fans - <u>Dry</u><br><u>wet</u>  | 57  | 56  | 48<br>9                       | 25<br>3                          | 40<br>10  |
| Fan Diameter, ft - <u>Dry</u><br><u>wet</u>                            | 23  | 28  | 28                            | 22                               | 30<br>24  |
| HP Per Fan - <u>Dry</u><br><u>wet</u>                                  | 22.3  | 82.3  | 50<br>150                     | 105<br>150                       | 145<br>90                                       |
| Number of Blades - <u>Dry</u><br><u>wet</u>                            | 6   | 6   | 5                             | 6                                | 3<br>6  |
| Pitch, degrees - <u>Dry</u><br><u>wet</u>                              | 12  | 12  | 10<br>22                      | 16<br>22                         | 14<br>16  |

The vapor from the vapor-liquid separator flows to the dry tower under the driving force of the pressure difference between these two components created by the temperature difference and the associated vapor pressure of the ammonia.

The steam condenser is composed of horizontal tube bundles, with steam condensation on the shell side, and anhydrous ammonia evaporation on the tube side. Design tube side maximum pressure is 350 psig, 135°F. Tubes are aluminum with the following dimensions:

|                       |         |
|-----------------------|---------|
| tube length           | 50 ft   |
| tube OD               | 1 in.   |
| tube gauge            | 12 BWG  |
| tube pitch            | 1.5 in. |
| total number of tubes | 15,100  |

The tube is enhanced on the outside for condensation and on the inside for boiling with proprietary Union Carbide Company/Linde enhanced condensation surface. The tubesheets are aluminum and the condenser is equipped with impingement protection where necessary.

The air removal section of the condenser is stainless steel.

The performance and cost of this component are significant uncertainties in this study. The cost algorithms developed for computer optimization studies on the basis of laboratory data indicated its cost would be very nearly similar to that of a conventional turbine condenser. The estimate developed by the architectural engineer and used in this study, reflected the lack of firm data from similar equipment. The architectural engineer estimated the equipment to be 50% more costly than a conventional condenser.

The piping for the system consists of vapor transport piping, vapor distribution piping, condensate collection piping, and condensate return piping. Associated with this system are pumps for condensate return and reboiler circulation, a combination vapor separator/reboiler supply tank, and ammonia storage tanks. The vapor separator/reboiler supply tank is located as close to the steam condenser/ammonia reboiler exit as possible. The upper portion of the tank acts as a cyclone separator to remove liquid ammonia carried over in the vapor leaving the reboiler. The lower portion of the tank acts as a reservoir for supplying the reboiler injection pumps and also provides system surge capacity. The lower portion of this tank has sufficient volume to contain the inventory of two tower quadrants if it becomes necessary to evacuate them for maintenance or in case of leaks. The material for all piping and tanks is carbon steel.

Each of the two condensate return pumps would have a capacity of 10,000 gpm at 27 ft  $\text{NH}_3$  TDH. Each of the two condenser recirculation pumps would have a capacity of 20,000 gpm at 30 ft  $\text{NH}_3$  TDH. The drain and fill pump would have a capacity of 2500 gpm at 50 ft  $\text{NH}_3$  TDH.

Excess storage capacity would be provided by ten 7750-gal pressure tanks. These tanks will store the entire quantity of ammonia if it becomes necessary to evacuate the system for maintenance or in case of emergency.

Provision is made for a nitrogen purge system to flush the air from the system before filling it with ammonia to prevent the possibility of stress corrosion cracking of the steel components. The total volume of the system is approximately 50,000  $\text{ft}^3$ . Vents are located at the highest point in each quadrant from which ammonia vapor can be evacuated after the quadrant has been drained and isolated. The vents are piped to a flare station on top of the tower.

### 3.2 HÖTERV Plate Fin Heat Exchanger with Deluge Augmentation

The initial cooling tower arrangement using the HÖTERV plate fin exchangers was round towers with fans across the top and the heat exchangers around the periphery. Previous studies had shown this to be a cost effective configuration for long fin-tube exchangers. However, as the result of the ensuing cost estimate for the towers, it was concluded that it was not a good arrangement for the HÖTERV bundles arranged horizontally to accommodate deluging. A second configuration was scoped out and estimated in which the heat exchangers were arranged as A frames on a plane below the fins. Figures 2 and 3 show these two arrangements.

With the vertical peripheral arrangement, three towers 260 ft in diameter and 56 ft high (to the fan deck) are needed. The cooling tower is designed to operate as a completely dry system when the ambient temperature is below 55°F. Above this temperature, a portion of the heat exchanger surface is deluged with water on the outside of the plate fins to increase heat rejection capability. In this way sensible heating of the air is augmented by heat transfer to the air through evaporation of the deluge water. The tower design temperature is based upon the maximum use of available water for augmentation (1900-acre ft) with minimum amount of heat exchange surface area.

The airflow through each tower is induced by 19 fans (28-ft diameter) mounted at the top of the tower structure. The heat exchanger bundles (240 tubes/bundle) are arranged around the periphery of the towers. No louvers for air control to prevent freezing of the ammonia are required. However, passive louvers are located beneath each fan to prevent back flow of air when a particular fan is off. For airflow control, one or

more fans can be started or stopped. Protection of the heat exchanger surfaces is provided by hail screens mounted directly to the face of each bundle. Table 2 gives specific information on all of the cooling tower systems at design point conditions.

The HÖTERV heat exchangers are 47.6 ft (15 m) long, 7.8 ft (2.3 m) high, and 5.9 in. (15 cm) deep in the direction of airflow. There are 16 bundles/tower quadrant, 96 bundles/tower, and 288 bundles total. The bundles are sloped at a 5 degree angle to promote drainage of the condensed ammonia. They are also canted forward to promote uniform deluging of the plate fins during wet operation.

All of the vapor transport piping lies above grade. The main vapor line transports ammonia vapor from the vapor separator to the general area of the cooling towers through a 48-in. diameter pipe approximately 1000-ft long. The piping then splits into successively small pipes leading to each tower and subsequently to tower quadrants, bundle groups and eventually individual bundles. The condensed ammonia liquid drains to a collection header running around the inside periphery of the tower. The main return line is 18 in. in diameter.

The deluge system is capable of augmenting the entire heat exchanger surface, although the maximum design wet area is probably less than 67%. Augmentation of the plate-fin surfaces is accomplished by allowing an approximate water flow rate of 2 gpm per lineal ft of heat exchanger to run down the plate fins. A small perforated pipe header adds water above each bundle to make up for the deluge water evaporated in the previous bundle. The deluge piping for each tower consists of

- two deluge pumps (vertical sump),
- deluge storage sump,
- distribution piping, and
- deluge distribution headers and splash plates.

The deluge pumps will have a capacity of 1200 gpm at 80 ft of H<sub>2</sub>O (two pumps per tower). The suction side of the vertical sump pump will be immersed in a circular concrete channel that catches all the water falling from the tube bundles and serves as a storage sump when the tower is operating dry. Polyethylene or PVC is used throughout. Maximum instantaneous consumptive use rate is approximately 4000 gpm. The maximum recirculation rate to the top of the towers is 7200 gpm, although the maximum anticipated is about 4500 gpm, with additional makeup being added at each of the five layers of heat exchanger in the vertical arrangement. Water treatment will consist of sulfuric acid addition to control pH to 7.6-7.8 and blowdown (800 gpm) to maintain a sufficiently low dissolved solids concentration. The blowdown will undergo lime softener treatment, and the effluent from the treatment plant will be recycled into the deluge system. Sludge from the softener (85 gpm) will be discarded to the effluent pond.

The horizontal arrangement of the HÖTERV heat exchangers differ essentially only in the tower configuration. Each of the two required towers is 205 ft by 230 ft and 57 ft to the fan deck. The horizontally arranged bundles are 35 ft above the ground to provide adequate area for air flow. Twenty eight fans (28 ft diameter) are used.

The A frames of the heat exchanger bundles are tilted at 5° as in the vertical design to promote drainage of the ammonia.

The total recirculation flow of the deluge system is higher, about 20,000 gpm because the bundles are not vertically stacked to provide a means of water flow down the stack.

The savings in this arrangement accrue from the need for only two towers. Table 2 lists the significant design parameters which are very similar to those of the vertical arrangement.

### 3.3 Separate Channel Augmented Tower

The heat exchanger in this concept is an adaptation of the Curtiss-Wright surface comprising integral fins chipped from an extruded multi-port aluminum tube. Additional cooling is provided by the separate channel augmented tower (SCAT) system, which uses selected channels within each multichannel tube as water channels. (Figure 4) When water is pumped through these channels, increased cooling of the ammonia occurs by heat transfer to the water. The heated water is piped to a wet cooling tower, located either inside the dry tower (this design) or outside. The basic design parameters for the SCAT system are the same as the previous two concepts. The tower can reject the design heat load without the use of any water at a turbine exit temperature of 130°F, an ambient temperature of 55°F, and an 80°F temperature drop across the condenser/reboiler and the ammonia transport lines.

Each of the quadrants of the two towers can be operated all dry or with additional SCAT cooling using the wet tower. The airflow through each tower is induced mechanically with 34 fans (28 ft diameter) mounted at the top of the tower structure. The 50 ft by 12 ft x 1 ft (in the direction of air flow) heat exchanger bundles (80 tubes/bundle) are arranged vertically around the periphery of the towers.

Ammonia vapor enters at the top and saturated liquid ammonia emerges at the bottom. Figure 5 shows the cross-section of the tubes. For the purpose of sizing the tower, the fins over the back portion of the tube where the water channels are located were not included in the calculation of heat transfer to the air during wet operation but were included in the calculation for pressure drop. For enhanced cooling, water is run through five alternating channels in the rear (relative to airflow) of the SCAT tube and then through the wet tower for cooling. The temperature range of this water, the overall heat transfer coefficient, and the effectiveness of this section of the bundle for heat transfer are calculated independently of any interaction with the airflow over the tube. This is justified by the fact that the air and the cooling water would be at approximately the same average temperature in this part of the bundle and the presence of the air would neither add nor subtract from the cooling action of the circulating water. Table 2 lists the significant design parameters of the tower.

The wet tower which provides cooling of the circulating SCAT water is located concentric and within the dry tower structure. A portion of the air drawn through the heat exchanger is taken on through the wet packing and exhausted by the wet tower fans. The rest of the air is exhausted by the dry-only fans arranged in the annular region between the respective peripheries of the wet and dry towers. When the tower is operated at less than fully enhanced cooling capacity, sections of the wet packing are not wetted; none are wetted during all-dry operation (below 55°F). The tower is designed for a 67.5°F wet bulb and 113.6°F

dry bulb for air inside the dry tower. A water range of 17.8°F and an approach of 22.5°F is used with inlet water at 107.8 and outlet at 90°F

Up to 170,000 gpm of circulating water through the SCAT channels is provided by 16 pumps (2 per quadrant in each tower). Very close coupling exists between the heat exchangers and the wet tower. Eight inch polyethylene lines carry water up through heat exchanger and then to the tower. Water treatment is the same as for the integrated wet/dry system although a smaller quantity is needed.

#### 3.4 Augmenting NH<sub>3</sub> Condenser

The concept of using a water-cooled ammonia condenser for augmented cooling, located at the dry tower and close coupled with a wet tower, was selected for the following reasons:

1. Less design uncertainty than with a turbine condenser cooled by both water and ammonia;
2. Close-coupling the ammonia condenser and wet tower was believed to more than offset the increased equipment size and cost resulting from the loss in temperature difference.

The condensers (four for each tower) function in parallel with the dry tower to maintain the pressure in the ammonia. Since the operation of the dry tower is unaffected by the operation of the condenser (unlike the deluge approach), evaporative cooling is not substituted for dry cooling and the dry tower can be somewhat smaller for the same water allotment. Like the integrated tower, described in Section 3.5, it is designed for an ambient temperature of 35°F (ITD=87°F) rather than 55°F (ITD=67°F) for the other three systems.

Placement, spacing, and general configuration is similar to the SCAT towers. However, the higher design ITD and simpler tube configuration result in a smaller tower. The heat exchanger bundles (80 tubes/bundle) are arranged around the periphery of the towers as shown, and the water-cooled condenser (four in each tower) are hung within the annular space between the periphery of the dry and wet towers. The enhancement cooling water is pumped from the center basin to the top header of each of the condensers, passes down and back up through the cooling tubes and out the top header to the wet tower inlet distribution box.

The heat exchangers are bundles of multiport finned channels 50 ft x 12 ft x 7.2 in. (in the direction of airflow) of the integral chipped-fin type manufactured by Curtiss-Wright. Each bundle consists of 80 tubes 50 ft long.

Table 2 summarizes the design parameters for the dry tower.

The eight water-cooled condensers are tube-in-shell pressure vessels designed for 350 psi at 150°F with ammonia on the shell side. Each is 8 ft in diameter and contains 875 U-bend aluminum tubes 1 in. in diameter 50 ft long. Maximum flow through each is 25,000 gpm. The wet tower which provides cooling for the circulating water is integral with the dry tower and is located concentric within this structure essentially the same as with the SCAT concept. The water system is closely similar to SCAT except that slightly more water is used.

### 3.5 Integrated Dry/Wet Cooling Tower Concept

This heat rejection concept is currently planned for use in the San Juan Unit 3. It was included in this study to provide a basis for comparing

these alternative concepts to previous design concepts and to each other. To assure the validity of the comparisons, this system was conceptually designed and estimated using the same bases as the other concepts, i.e., without reference to actual cost figures and design details.

The condenser cooling water is transmitted to the cooling towers via a 96-in diameter concrete piping system and circulated by three 73,000 gpm (77 TDH) vertical well pumps. Two rectangular cooling towers house both the air-cooled heat exchange surface, which is composed of spiral-wrapped finned tubes tilted 25 degrees from horizontal and the wet tower packing. The hot water from the condenser passes first through the dry section and then flows directly into the wet towers. The cooling tower is designed to operate as a completely dry system at temperatures below 35°F by turning off the fans above the wet portion of the tower. A sketch is shown as Figure 6.

There are 10 heat exchanger units per tower, two units in each bay. The spiral-wrapped fin tubes are 1 in. in diameter, of Admiralty metal, with the thin (0.018-in.) aluminum fin wound as a single leg wrap around the tube. They are arranged in a staggered equilateral close-packed spacing three rows deep.

A total of 25 induced draft fans were specified for each tower, 20 in the dry section and 5 in the wet section. Louvers have not been specified although they may be required for airflow control during high winds and for equalizing flow into each bay to avoid local freezing.

The conventional steam condenser contains 28,500 admiralty metal tubes 1 in. in diameter and 35 ft long.

#### 4. BASES FOR COST ESTIMATES

All cost data developed by the architect/engineering firm reflect construction as of mid 1976 and thus include no contingency or escalation.

The preconceptual designs which have been developed and evaluated in this report are not the optimal design for each system, i.e., they are not designs which have been coordinated with the design and sizing of the steam supply to give the lowest cost of busbar electricity. Instead, they are designs which fit a stipulated set of conditions with respect to ambient temperature and heat rejection capability.

Optimization studies of dry (and dry/wet) systems generally compare the "operating costs" of alternative systems in terms of several "penalty costs" which represent the incremental increases in plant operating costs resulting from the use of the dry cooling system in relation to a reference system with a once-through flow of cooling water. Included in the list of penalty costs may be those for (a) an energy penalty because during hot weather the plant cannot export as much energy as the reference plant, (b) a capacity penalty because reserve generating capacity must be available to make up for the deficiencies of the dry cooled plant, (c) a make-up water penalty which reflects the cost of any water treatment unique to the subject plant.

An "optimized" design represents a trade-off between a larger-sized cooling system which has small energy and capacity penalties and a smaller-sized cooling system which has larger penalties.

With the present comparison of five systems there were no such trade-offs involved in the designs. All were sized to meet stipulated parameters

Table 3. Operating Cost Summary  
(dollars)

|   | <u>Vertical<br/>Höterv</u> | <u>Horizontal<br/>Höterv</u> | <u>SCAT<br/>Tower</u> | <u>Augmenting<br/>Ammonia<br/>Condenser</u> | <u>Integrated<br/>Wet/Dry</u> |
|---|----------------------------|------------------------------|-----------------------|---|-------------------------------|
| Hours of Operation                                    | Dry                        | 6 640                        | 6 640                 | 6 640                                       | 6 640                         |
|   | Wet                        | 4 426                        | 4 426                 | 5 146                                       | 5 146                         |
| Circulation Pump<br>Primary Fluid                     | 38 500                     | 38 500                       | 38 500                | 38 500                                      | 694 000                       |
| Circulation Pump<br>Augmenting Cooling<br>Water       | 10 100                     | 19 600                       | 110 900               | 130 900                                     | --                            |
| Water Treatment                                       | 79 000                     | 79 000                       | 89 000                | 105 000                                     | 105 000                       |
| Fan Power   | 588 900                    | 571 600                      | 435 400               | 433 300                                     | 798 000                       |
| Capacity Penalty<br>(Annualized)                      | 83 300                     | 84 700                       | 95 600                | 98 000                                      | 184 000                       |
| Fuel Saving Credit<br>Due to Reduced<br>Back Pressure | -235 000                   | -235 000                     | -235 000              | -55 000                                     | - 55 600                      |
| TOTAL   | <u>564 800</u>             | <u>558 400</u>               | <u>534 400</u>        | <u>750 100</u>                              | <u>1 725 400</u>              |

of inlet temperature difference, heat rejection capability and annual water rate. Thus, the gross plant output is approximately the same from a plant equipped with each cooling system. However, the total penalties would differ with each design, depending on the characteristics of each with respect to: 1) the power required for fans and water/ammonia recirculating, 2) the capacity penalty for this power, and 3) water treatment and pumping power required for the enhanced (evaporative) cooling system.

In addition, there is a negative energy penalty which arises from increased output in cold weather which differs in each case. All plants have been designed to reject the stipulated heat load at a particular design ambient temperature. At temperatures below this, the plant is capable of operating at rated output with lower fuel consumption because of higher turbine efficiency (lower back pressure). Credit is taken for fuel savings from the higher plant efficiency. The three alternatives using deluge cooling are designed to a higher ambient temperature (55°F vis-a-vis 35°F for the other two) because a large dry tower is required to compensate for the dry capability taken out of service as it is converted to evaporative cooling by deluging. This has the compensating effect that the plant can operate at a lower back pressure in the winter and thus use slightly less fuel.

In summary, in this study the differences in "penalties" among the various alternatives are accounted for by evaluating five "operating" cost terms and a sixth capital cost term. Those six cost terms are:

- power for the main circulating system,
- power for the fans,
- water treatment operating costs,
- power for pumping deluge water,
- fuel savings resulting from the capability to operate at lower than the reference turbine back pressure at temperatures below the design ambient, and
- capital cost of peaking reserve capability to provide auxiliary power to the cooling system.

To combine these "operating" and other penalty costs with the capital costs of the plant, the former are "capitalized" by dividing by an annual fixed-charge rate of 18% and adding them to the capital cost.

Water treatment would include scale inhibition by pH adjustment and biofouling control with chlorine. Blowdown would be treated by lime softening to remove dissolved solids with return of the effluent and drying of the sludge. In addition provision would be made to supply demineralized water from zeolite softeners to flush the deluged surfaces. The main differences in cost are due to the cost of biofouling control.

All operating costs are summarized in Table 3.

## 5. RESULTS

To facilitate comparison of the total costs of the five dry/wet systems a "comparative capital cost" was used which is defined as the sum of the estimated basic capital cost (i.e., the estimated cost

Table 4. Capital Cost Estimates

(Thousands of Dollars)

|                                   | <u>Vertical<br/>HOTERV</u> | <u>Horizon<br/>HOTERV</u> | <u>SCAT<br/>Tower</u> | <u>Aug.<br/>Ammonia<br/>Cond.</u> | <u>Integrat<br/>Wet/Dry</u> |
|-----------------------------------|----------------------------|---------------------------|-----------------------|-----------------------------------|-----------------------------|
| STEAM CONDENSER                   | <u>2,653</u>               | <u>2,653</u>              | <u>2,653</u>          | <u>2,653</u>                      | <u>1,740</u>                |
| COOLING TOWER                     |                            |                           |                       |                                   |                             |
| Dry Tower                         |                            |                           |                       |                                   |                             |
| Structures                        | 1,905                      | 998                       | 858                   | 600                               | 2,182                       |
| Piping-NH <sub>3</sub>            | 308                        | 102                       | 213                   | 152                               | --                          |
| Heat Exchangers                   | 5,874                      | 5,387                     | 4,982                 | 2,734                             |                             |
| Pumps/Piping-<br>H <sub>2</sub> O | 305                        | 423                       | 678                   | 703                               | 1,215                       |
| Augmented<br>Ammonia Cond.        | --                         | --                        | --                    | 1,562                             |                             |
| Wet Tower                         | --                         | --                        | 263                   | 309                               | 1,078                       |
| Fans                              | 1,205                      | 1,186                     | 1,070                 | 880                               | 2,646                       |
| Vents & Flair                     | <u>15</u>                  | <u>10</u>                 | <u>10</u>             | <u>10</u>                         | <u>--</u>                   |
| Subtotal                          | <u>9,612</u>               | <u>8,105</u>              | <u>8,073</u>          | <u>6,950</u>                      | <u>10,307</u>               |
| MAIN COOLING SYSTEM               |                            |                           |                       |                                   |                             |
| Pumps/Piping<br>Vapor             | 309                        | 344                       | 342                   | 342                               | --                          |
| Pumps/Piping Liq.                 | 422                        | 264                       | 273                   | 273                               | 1,951                       |
| Pumps-Reboiler                    | 159                        | 159                       | 159                   | 159                               | --                          |
| Vapor/Liq.Sep.                    | <u>310</u>                 | <u>310</u>                | <u>310</u>            | <u>310</u>                        | <u>--</u>                   |
| Subtotal                          | <u>1,200</u>               | <u>1,077</u>              | <u>1,084</u>          | <u>1,084</u>                      | <u>1,951</u>                |
| STORAGE/FILL/DRAIN                | 780                        | 780                       | 780                   | 780                               | 86                          |
| OVER GAS                          | 211                        | 143                       | 143                   | 143                               | --                          |
| WATER TREATMENT                   | 562                        | 628                       | 545                   | 545                               | 451                         |
| ELECT/INST                        | 2,263                      | 1,554                     | 1,633                 | 1,633                             | 1,994                       |
| BUILDINGS                         | <u>52</u>                  | <u>52</u>                 | <u>52</u>             | <u>52</u>                         | <u>52</u>                   |
| COMPLETE SUBTOTAL                 | 17,334                     | 14,994                    | 14,963                | 13,840                            | 16,584                      |
| CONTRACTORS OH & PROFIT           | 3,329                      | 2,998                     | 2,948                 | 2,631                             | 2,921                       |
| ENGRG & COST MGMT                 | <u>4,132</u>               | <u>3,598</u>              | <u>3,582</u>          | <u>3,394</u>                      | <u>3,902</u>                |
| TOTAL CAPITAL COST                | <u>24,795</u>              | <u>21,590</u>             | <u>21,493</u>         | <u>19,765</u>                     | <u>23,407</u>               |
| (Without Contingency)             |                            |                           | 796                   |                                   |                             |

without escalation and contingency) and the capitalized annual operating cost. This latter cost is just the estimated annual operating cost (summarized in Table 3) divided by the annual fixed charge rate of 18 percent.

### 5.1 Capital Costs of Alternatives

The subsystem capital costs of the four ammonia systems and the integrated wet/dry system are listed in Table 4. The integrated dry/wet concept is considered a baseline for comparison because it represents current practice. The San Juan Plant Unit 3 is currently being constructed with a heat dissipation system of this type. The estimate of the integrated dry/wet concept was performed without the benefit of prior knowledge of actual construction costs of San Junit Unit 3 to put all estimates on the same relative basis and may or may not correspond to actual costs.

### 5.2 Comparative Costs

The comparable costs of the four concepts plus the state-of-the-art integrated Wet/Dry are listed in Table 5.

Table 5. Summary of Comparative Capital Costs  
(dollars)

| <u>Cooling Tower Concept</u> | <u>Basic Capital Cost</u> | <u>Capitalized Operating Cost</u> | <u>Comparable Capital Cost</u> |
|------------------------------|---------------------------|-----------------------------------|--------------------------------|
| Integrated dry/wet           | 23,407,000                | 9,586,000                         | 32,993,000                     |
| Vertical HOTERV tower        | 24,795,000                | 3,138,000                         | 27,933,000                     |
| Horizontal HOTERV tower      | 21,590,000                | 3,102,000                         | 24,692,000                     |
| SCAT tower                   | 21,493,000                | 2,969,000                         | 24,462,000                     |
| Augmenting Ammonia Condenser | 19,765,000                | 4,167,000                         | 23,932,000                     |

The costs presented in this paper are approximate in nature. None of the concept designs were fully optimized from the standpoint of all parameters involved. However, all designs and estimates were arrived at utilizing the same bases and uniform procedures. It is not anticipated that exhaustive optimization would change the relative ranking of the concepts with regard to comparative capital costs.

The ammonia systems were found to have potentially lower capital and operating costs than comparable capital cost for the integrated concept considered in this base study. Although the ammonia systems require (1) an ammonia reboiler, which may be somewhat more complex and expensive than a simple condenser, and (2) a complex pressurized ammonia fill and drain system, the ammonia systems have a number of important cost advantages associated with the evaporation-condensation heat transfer system. Among these advantages is the enhanced heat transport from the reboiler to the cooling tower. Only small pumps are required to return the ammonia to the reboiler and to provide forced recirculation. Water treatment costs are also less because of the need for treating smaller quantities of water. Moreover, the cost of the ammonia condenser/reboiler was conservatively estimated to be significantly greater than a conventional turbine condenser but there is reason to question that estimate.

Operating costs for the ammonia systems are substantially less than the integrated concept because 1) less power is required to operate recirculation pumps and fans, and 2) the capacity penalty is lower because less generating capacity must be provided in reserve.

# LAYOUT OF STEAM PLANT WITH AMMONIA

799

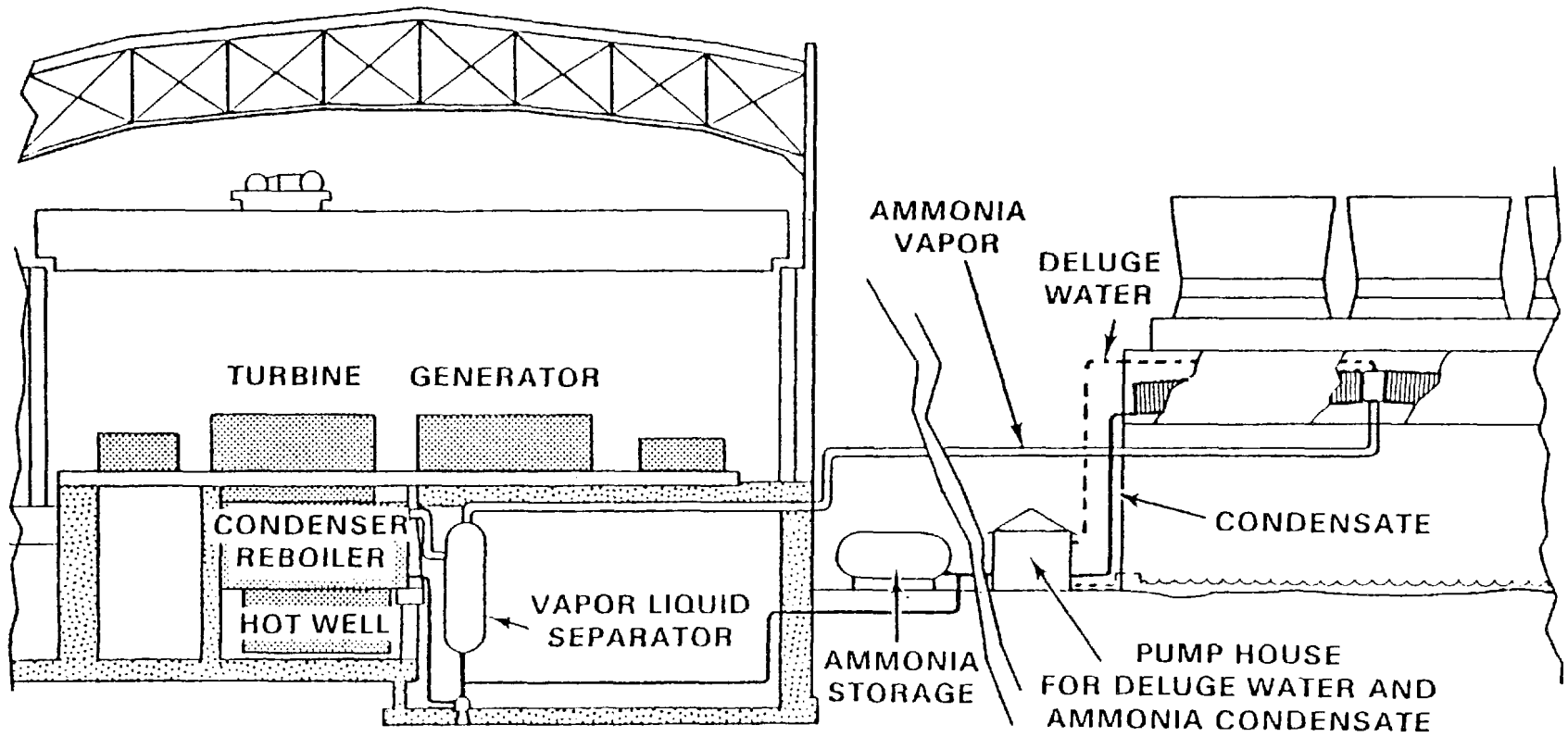


FIGURE 1.

# VERTICAL HOTERV ARRANGEMENT

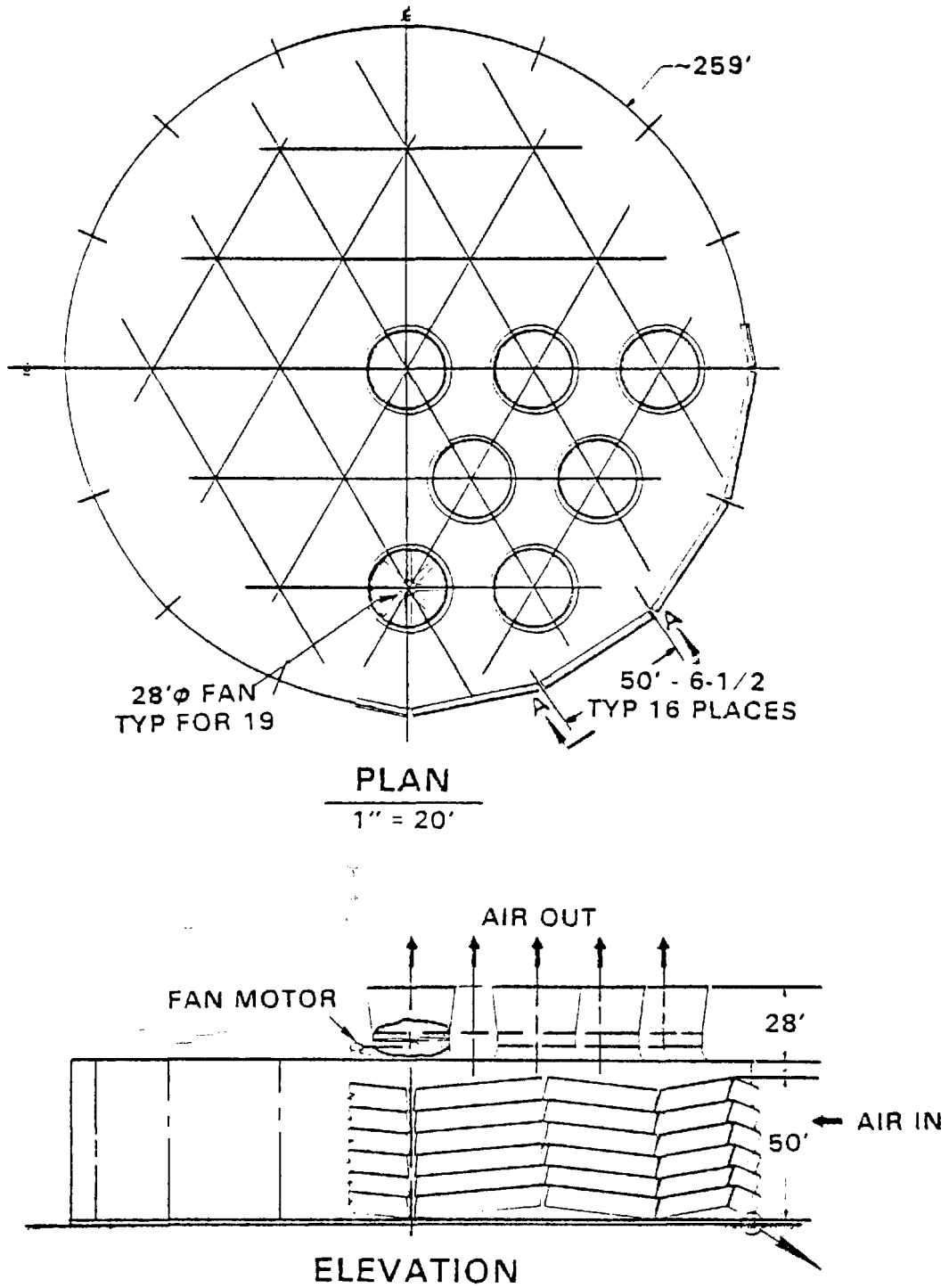


FIGURE 2.

# HORIZONTAL HOTERV ARRANGEMENT

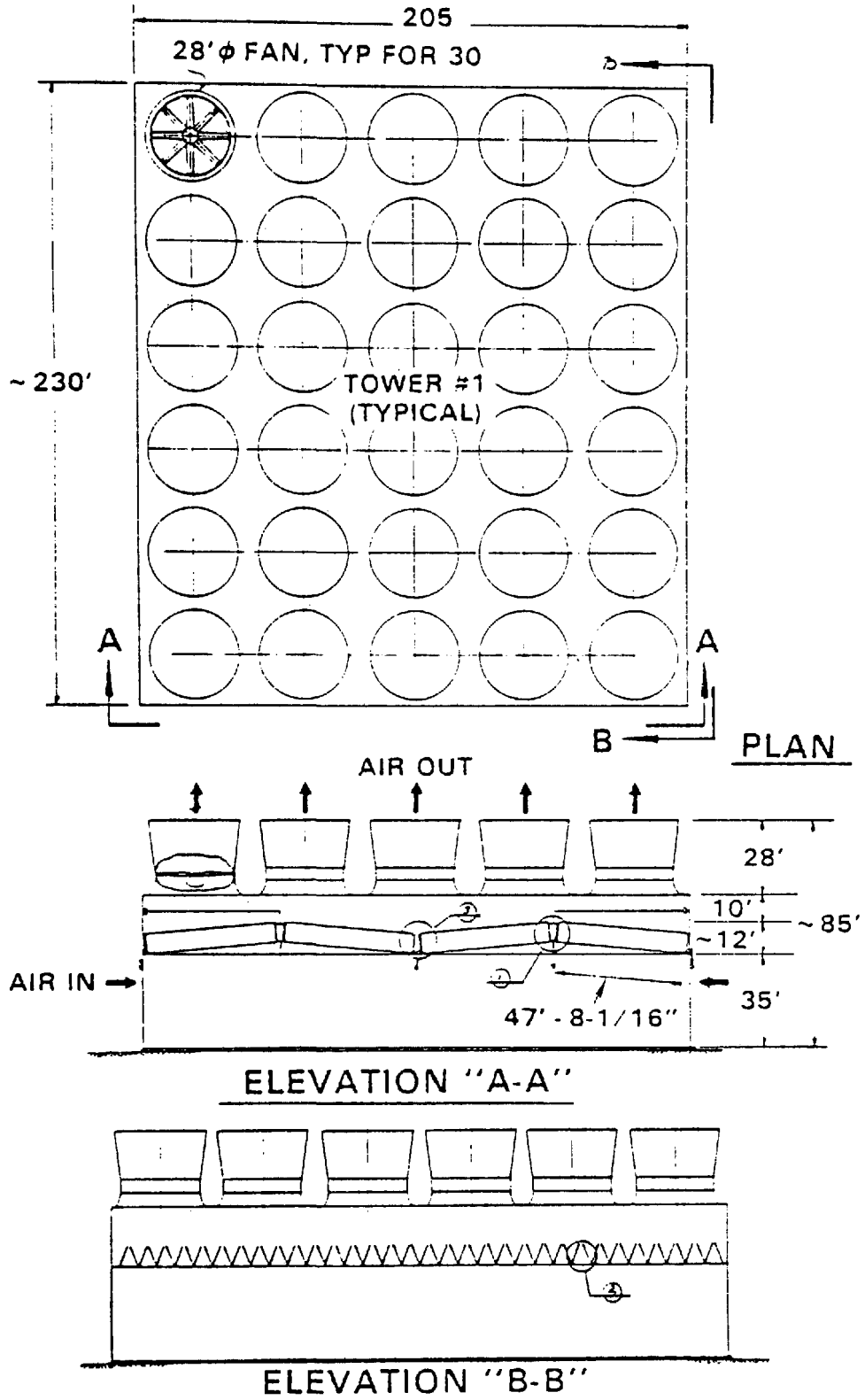


FIGURE 3.

# SCAT TOWER USING CURTISS-WRIGHT HEAT EXCHANGERS

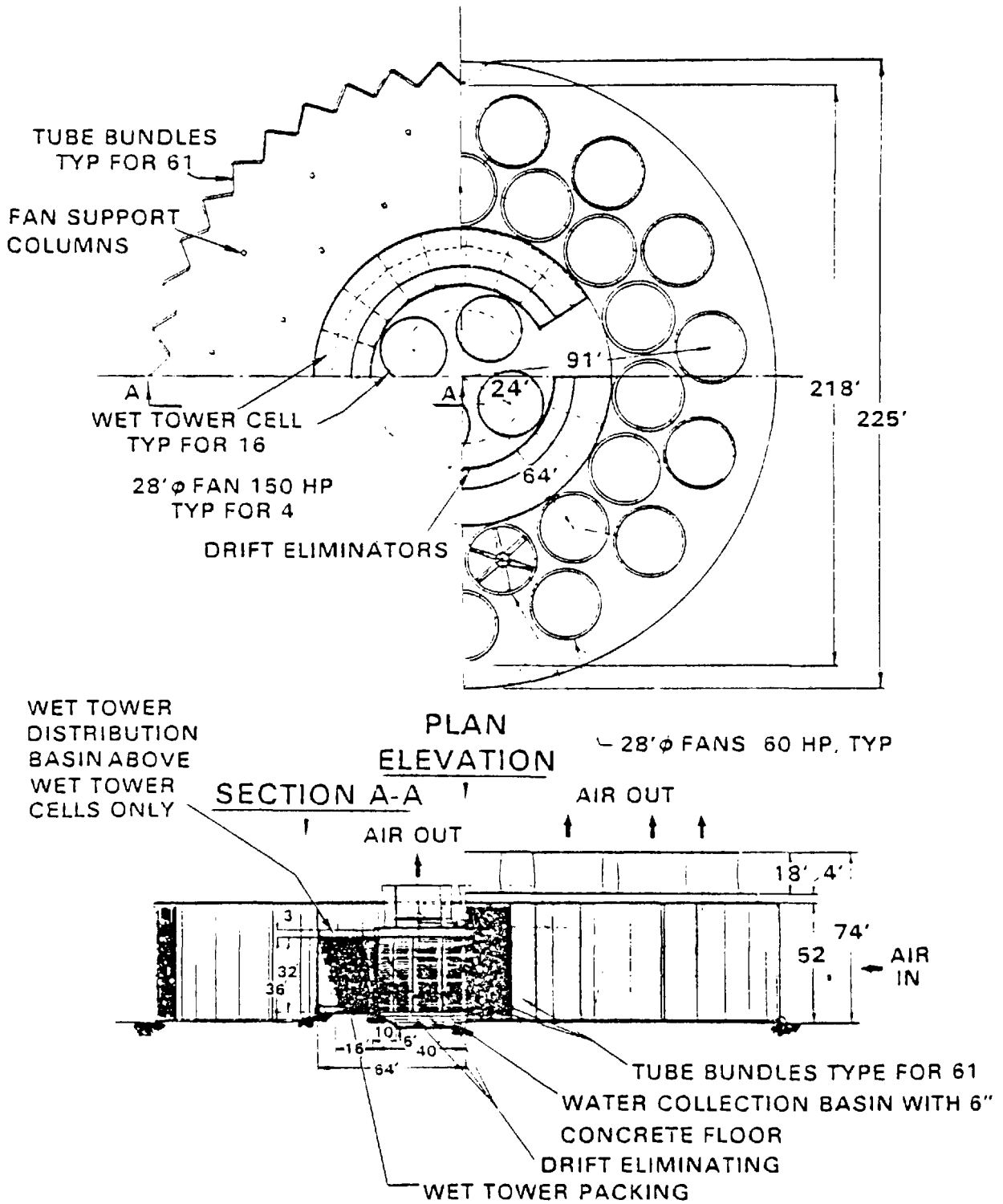


FIGURE 4.

# SCHEMATIC OF CURTISS-WRIGHT EXCHANGER ADAPTED FOR THE SCAT TOWER

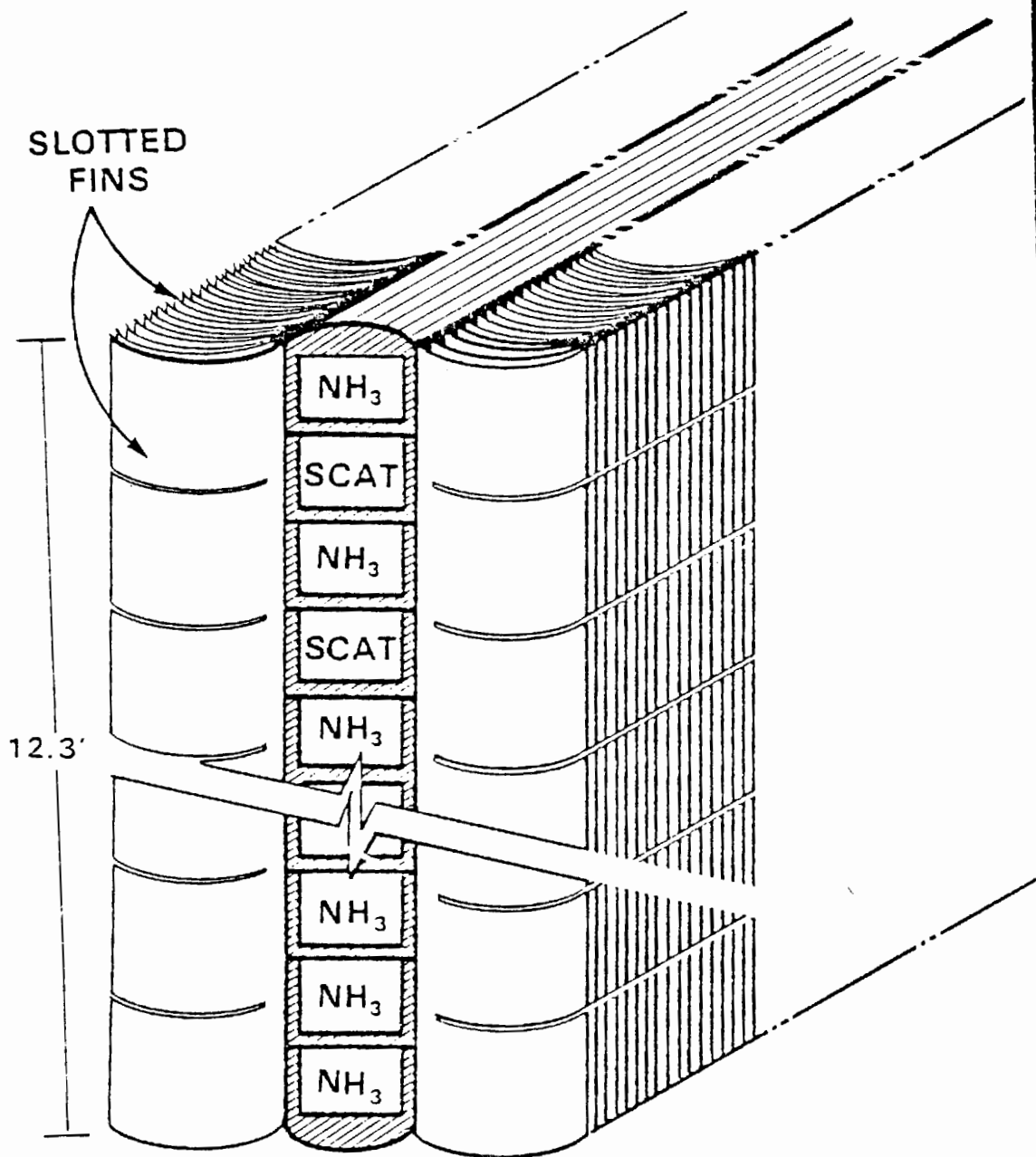
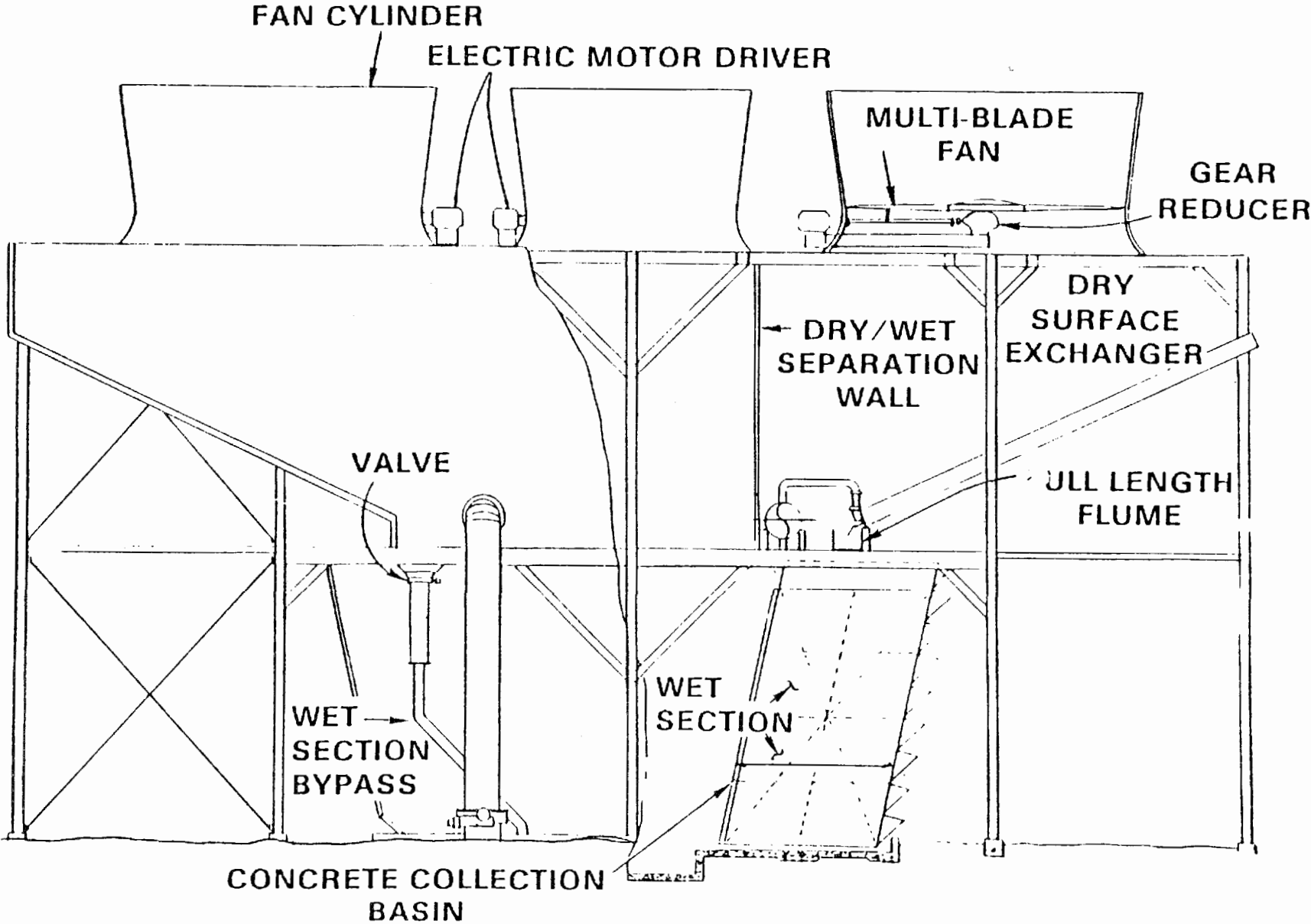


FIGURE 5.

# INTEGRATED DRY/WET COOLING TOWER



CROSS SECTION

FIGURE 6.

804

ENVIRONMENTAL ASPECTS OF EFFECTIVE ENERGY  
UTILIZATION IN INDUSTRY\*

Robert E. Mournighan

U. S. Environmental Protection Agency  
Industrial Environmental Research Laboratory  
Office of Research and Development  
Cincinnati, Ohio

ABSTRACT

This paper presents some of the energy conservation program in which the Power Technology and Conservation Branch, of the EPA's Office of Research and Development, is involved. Initial results of hardware research and development projects are presented.

Examples of combined energy conservation-pollution control projects concerning the glass, steel and textile industries are given. These are research programs funded under a coordinated federal program.

The tentative results of these studies indicate that 30-40% of energy is wasted in industrial manufacturing processes. Effective utilization of energy could provide at least a partial solution to our energy supply problem. At the same time, effort must be made to reduce the pollution associated with the waste streams, or else a great opportunity will pass by, resulting in a waste of economic resources and unnecessary pollution.

Three specific projects are the principal focus for our discussion: (1) preheating of glass furnace batch with waste furnace emission gases; (2) dry quenching of coke in the steel industry; and (3) reverse osmosis recovery of hot textile dye wastes. The technologies being investigated have the combined advantages of improved water or air pollution control with energy, water and/or chemicals recovery.

INTRODUCTION

The U. S. Environmental Protection Agency (EPA) is conducting a research effort in assessing the environmental aspects of efficient energy utilization technologies. A major goal of this program is to

---

\*Presented at the "Second Conference on Waste Heat Management and Utilization," December 1978. Mr. Mournighan is with the Power Technology and Conservation Branch, Energy Systems Environmental Control Division.

foster a reduction in environmental pollution, particularly air pollution, while at the same time making use of energy currently wasted.

The program is managed by the Power Technology and Conservation Branch (PTCB) of EPA's Industrial Environmental Research Laboratory, Cincinnati, Ohio, under EPA's Office of Research and Development. PTCB's activities are concerned with the environmental control problems and benefits of a broad range of energy technologies. Branch interests include: solar and geothermal energy conversion; advanced conversion systems such as high temperature turbines, magnetohydrodynamics and fuel cells; energy management, i.e., conservation and energy recovery in all sectors; and indoor air quality control in homes and public buildings. The results of the PTCB program will provide useful data to other EPA functions, such as, air and water standards development, and will be useful to other federal, state and local agencies concerned with energy environmental issues in developing the most environmentally sound energy technologies.

This paper presents, principally, the results from three industrial projects on improved energy management which have positive energy savings and environmental impacts and whose economics indicate a moderate chance for success.

#### BACKGROUND

The EPA industrial energy research program has three primary areas of activity: (1) assessment of the amount of industrial energy which can be recovered, including, where possible, the amount and types of associated pollutants; (2) assessment of the technologies available; and (3) support of technology research and development.

In the first area, an assessment of the amount of waste heat available is being done by DSS Engineers with field measurements by KVB, Inc. (The project will be reported in the following paper.)

In the second area, an evaluation of technologies for recovering waste heat is the objective of a project now being conducted by Energy and Environmental Analysis, Inc. The results of this project are expected to define the areas of greatest potential and the technologies which have the best energy/environmental tradeoffs.

In the third area of interest, research and development of technologies which have significant energy savings associated with a positive environmental impact, are three projects applicable to the glass, steel, and textile industries, being conducted by PTCB in conjunction with EPA industrial groups and the Industrial Energy Conservation Division of the Department of Energy. On the textile project, the Department of the Interior also has an interest.

## DISCUSSION

Table I shows the estimated energy consumption, wasted energy, and estimated energy savings possible for the container glass industry (Largest segment of glass industry), the coking operation in the steel industry, and in the textile dying and finishing industry.

Table I. Estimates of Energy Consumption, Wasted Energy and Possible Energy Savings<sup>(5)</sup>

|                                | Energy<br>Consumption<br>$10^{15}$ Btu/yr. | Energy Waste<br>$10^{15}$ Btu/yr. | Possible<br>Energy Savings<br>$10^{15}$ Btu/yr. |
|--------------------------------|--|-----------------------------------|---|
| Glass                          | .22  | .140                              | .018 (.052)                                     |
| Steel (Coking)                 | 1.44                                       | .44                               | .14   |
| Textile Dying<br>and Finishing | 0.54                                       | .37                               | .23   |

The table shows that of the 2.2 quads ( $10^{15}$  Btu) consumed, the waste energy for these three categories is 0.95 quads. The third column shows that an estimated 0.4 of the 0.95 quads can be saved by effective and economic technologies. To put the possible savings in perspective, it represents about 14% of the yearly oil needs of the electric utility industry or about 65 million barrels of oil per year.

### GLASS INDUSTRY PROJECT - PREHEATING WITH STACK GASES

The major reasons for undertaking a project in the glass industry are the declining reliability of natural gas as an energy source, the need for reducing stack emissions and a need to find an environmentally and economically acceptable solution to both problems.

Under contract to EPA, Battelle Memorial Institute and Corning Glass Works initiated a bench scale project to study the feasibility of preheating pelletized glass batch raw materials with waste furnace gas. It was theorized that the batch pellets could also capture some of the pollutants from the stack gas. Figure 1 shows a simplified diagram of the process.

The study was recently completed<sup>(7)</sup>, and it was found that without impairing glass quality:

- Soda lime glass batch can be pelletized successfully;

- o The pellets can be heated with the waste gas to 800° C without sticking together or deforming excessively;
- o The melting furnace temperature may be reduced up to 50° C, reducing the furnace energy requirement by about 20% - throughput may also be increased significantly to bring the overall savings to about 40%;
- o Up to 85% of the SO<sub>2</sub> can be absorbed from the waste gases, by the pelletized material;
- o NO<sub>x</sub> from the gas combustion zone can be reduced about 65% by instituting the above mentioned furnace temperature drop and fuel reductions;
- o
- o The pelletized batch may capture as much as 75-80% of the furnace particulate emissions. Further work is necessary to determine exactly how accurate this figure is.

Referring back to Table I, the item in parenthesis under "Possible Energy Savings" represents the energy savings, if this technology could be applied to the whole industry.

There are other advantages to this process modification in that it can be retrofitted on existing furnaces and, through energy efficiency and pollution control, it should prove to be of economic benefit to the industry. Also, it has flexibility and efficiency that are not found in the use of waste heat boilers and a large scale switch to electric melting. Currently, a proposal is under consideration for the construction and operation of a pilot plant for the evaluation of this technology.

#### STEEL INDUSTRY - DRY QUENCHING OF COKE

Most people are aware that the steel industry uses a large amount of energy in the manufacturing processes. Most of the time we picture the white-hot heat of the furnace with sparks of white-hot metal flying through the air; or the incandescent flowing liquid being poured into molds or transfer cars.

There is, however, a less spectacular place in the integrated steel mill where there is a tremendous waste of energy and a considerable source of pollution: the coke batteries and quench tower.

Currently, hot coke (at 1000 to 1100° C) is transported from the coke ovens to a tower where tons of water are sprayed onto the incandescent coke to cool it below ignition temperature. In this process, large quantities of steam and pollutants are vented to the atmosphere. A significant amount of polluted water is also generated.

As shown in Figure 2, a dry quenching system, hot coke is cooled in a closed system by recirculating inert gas. The hot gas, in turn, is used to generate steam in a waste heat boiler or is treated by other heat removal techniques.

In 1977, the Department of Energy (then ERDA) and EPA initiated a contract with National Steel Corporation to determine the economic and technical feasibility and the design for installing a dry quenching unit at one of their locations. Recently, the project was completed<sup>(6)</sup> with the following results:

- Dry quenching of coke, while a huge energy saver would not be economically attractive because of the huge initial investment for equipment - \$21,000,000 per 1,000,000 ton/yr. plant;
- If the pollution abatement benefits must be figured into the economics, the process becomes much more attractive.

The energy benefits are considerable. Referring to Table I, the possible energy savings as seen by Streb<sup>(5)</sup> could be as much as 0.14 quads. Even at that, the economics are poor, with a projected return on investment between 7 and 16%.

However, emissions to the atmosphere are projected to be less than 0.01 grams of particulate/SCF gas at 1 million SCF/hr. or an emission rate of about 1.5 pounds per hour, about 10% that of a large industrial boiler.

Water pollution with this system will be at a minimum. The volume of heavily contaminated water is orders of magnitude less than with the wet quenching system. The only problem, however, is that we don't know what toxics, if any, are present and how much there may be.

In any case, in making a comparison of wet vs. dry quenching, the pollution control estimates for wet quenching must be figured in, and the technology should not be evaluated on energy savings alone.

#### TEXTILE INDUSTRY PROJECT - ENERGY AND WASTE RECOVERY BY REVERSE OSMOSIS

The textile industry in this country consumes about 300 million gallons of process water per day. Approximately 50% of this water is hot (>40° C), and is not reused, thereby wasting a tremendous amount of energy and at the same time causing thermal pollution problems<sup>(1)</sup>.

EPA, the Department of Energy and the Department of Interior have formed a joint effort to develop technology which would (1) conserve as much waste heat as possible, (2) conserve the water resources, and (3) solve the problem of toxic chemical discharges from these plants. A dyeing and finishing plant with a continuous processing unit was chosen for the project.

Figure 3 is a simplified diagram of the washing process, the largest consumer of hot water in the process. Before this project was begun, each section received a separate supply of fresh hot water and the discharge sent to the waste treatment plant.

To meet all the goals of the project, reverse osmosis (RO) was chosen as the water cleanup process. A high temperature membrane, recently developed and tested (serviceable up to 100° C), seems to be the best choice available. Membrane systems are very expensive, so a water conservation program was undertaken to minimize the size and cost of the RO unit. The water conservation effort was very successful, showing it possible to reduce the process flow to a washing section from 300 gpm to about 50 gpm.

The RO unit has been sized to treat the 50 gpm stream and will in effect reduce the discharge to the waste treatment system to a small blowdown of about 4 gpm. Most of the hot water will be directly recycled back to the process. Figure 4 is a diagram of the proposed installation.

Currently, the project is the stage where equipment is being purchased, with construction starting in a few months. After the system is complete, the unit will undergo shakedown testing for a full year to determine the economics, energy savings and pollution control benefits.

The projection is that there will be a return on investment for this system, but will be below 20% energy and water recovery considered alone. In comparison with separate energy and pollution control alternatives, the system looks very attractive indeed, especially when toxics substance control is brought into the picture.

#### A WORD ABOUT RETURN ON INVESTMENT

In a recent article in the Harvard Business Review<sup>(10)</sup>, the point was made that most manufacturers set a high rate of return for energy projects, actually higher than their regular capital projects. This adds to the energy conservationists woes. In the article, the authors point out that if firms would accept lower rates of return and fund energy recovery projects, they would find waste heat recovery systems providing energy at about one-half the cost that the utility itself would charge if it were the supplier.

The point is that if an energy conservation project or waste heat recovery project has any pollution control benefits, it should be looked on by management in this light. We should not look upon these projects as quick expense-cutting programs, but as an investment, guarding against future higher energy and pollution control costs. Conservation projects are probably the least capital intensive way to save our energy resources<sup>(10)</sup>.

## CONCLUSION

In summary, I have given three examples of energy conservation projects that involve our Agency. We are generally trying to encourage the idea of adding in pollution control benefits in the decision-making process in energy conservation projects. We feel that, with all this considered, energy conservation alternatives can help our country through the energy squeeze, maintain the environment and still permit a healthy economy.

## REFERENCES

1. Brandon, C. A., et al. "Hot Textile Process Effluent Recycle by Membrane Separation." Presented at the 85th National Meeting of the American Institute of Chemical Engineers, Philadelphia, PA, June 4-8, 1978.
2. Lee, C. C. "Potential Research Programs in Waste Energy Utilization," Proceedings of Second Waste Heat Management and Utilization Conference, Miami Beach, Florida, May 9-11, 1977.
3. Mournighan, R. E. and Bostian, H. E. "Energy Conservation and Improvement of the Environment," proceedings of Fifth Conference on Energy and the Environment, Cincinnati, Ohio, November 4-7, 1977.
4. Sternlicht, B. "Capturing Energy from Industrial Waste Heat," Mechanical Engineering, p. 30, August 1978.
5. Streb, A. J. "Priority Listing of Industrial Processes by Total Energy Consumption and Potential for Savings," ERDA CONS/50151, 1977.
6. Draft Final Report, DOE Contract EC-77-c-024553. "Dry Coke Quenching," Phase I Engineering.
7. Draft Report, EPA Contract 68-02-2640. "Technology for the Conservation of Energy and Abatement of Emissions in Glass Melting Furnaces."
8. "Environmental Considerations of Selected Energy Conserving Manufacturing Process Options," EPA report, EPA 600/7-76-034k.
9. Steam Electric Plant Factors, 1976, National Coal Association, Washington, DC.
10. Hatsopoulos, G. N., et al. Harvard Business Review, March 1978.

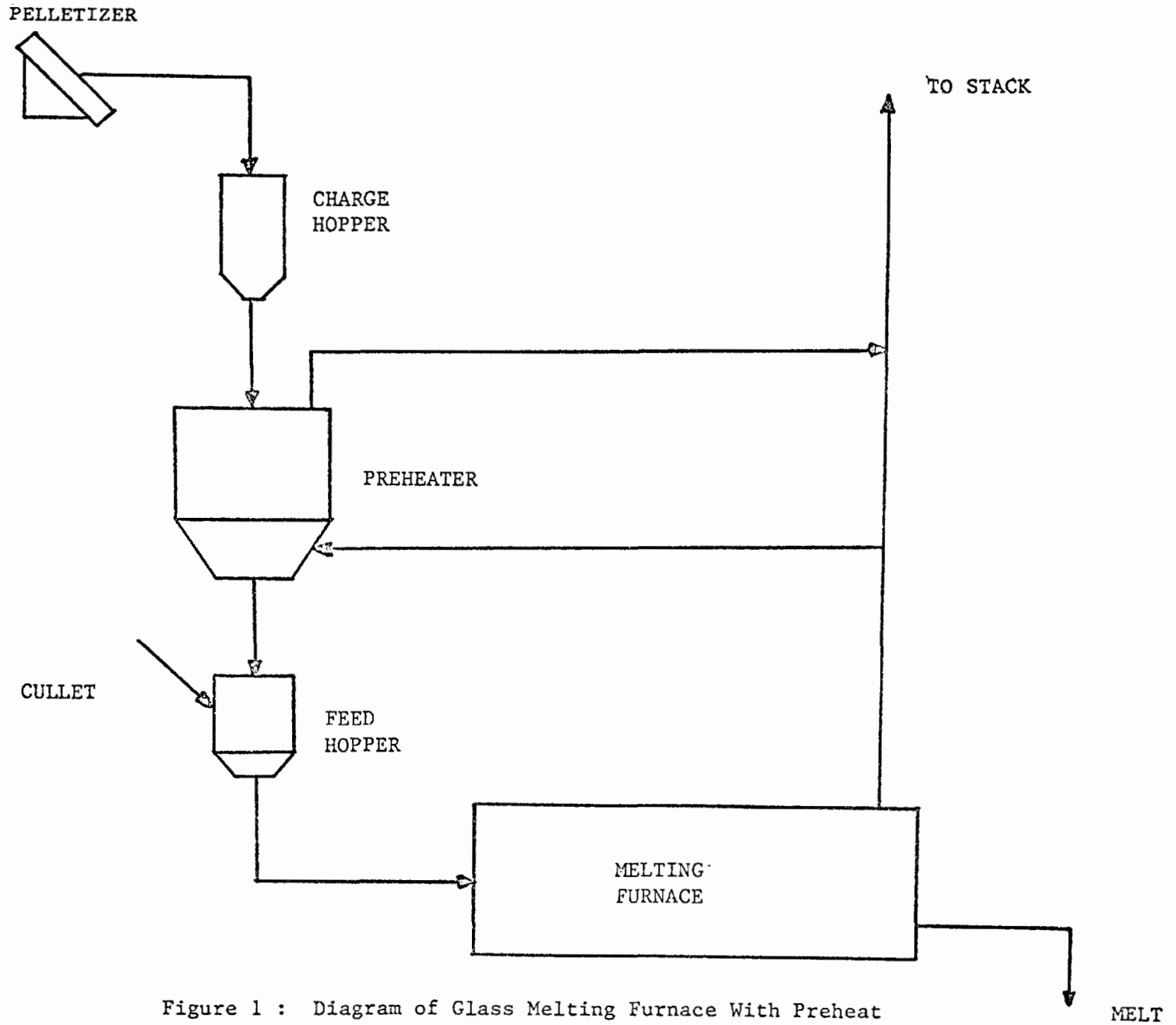


Figure 1 : Diagram of Glass Melting Furnace With Preheat

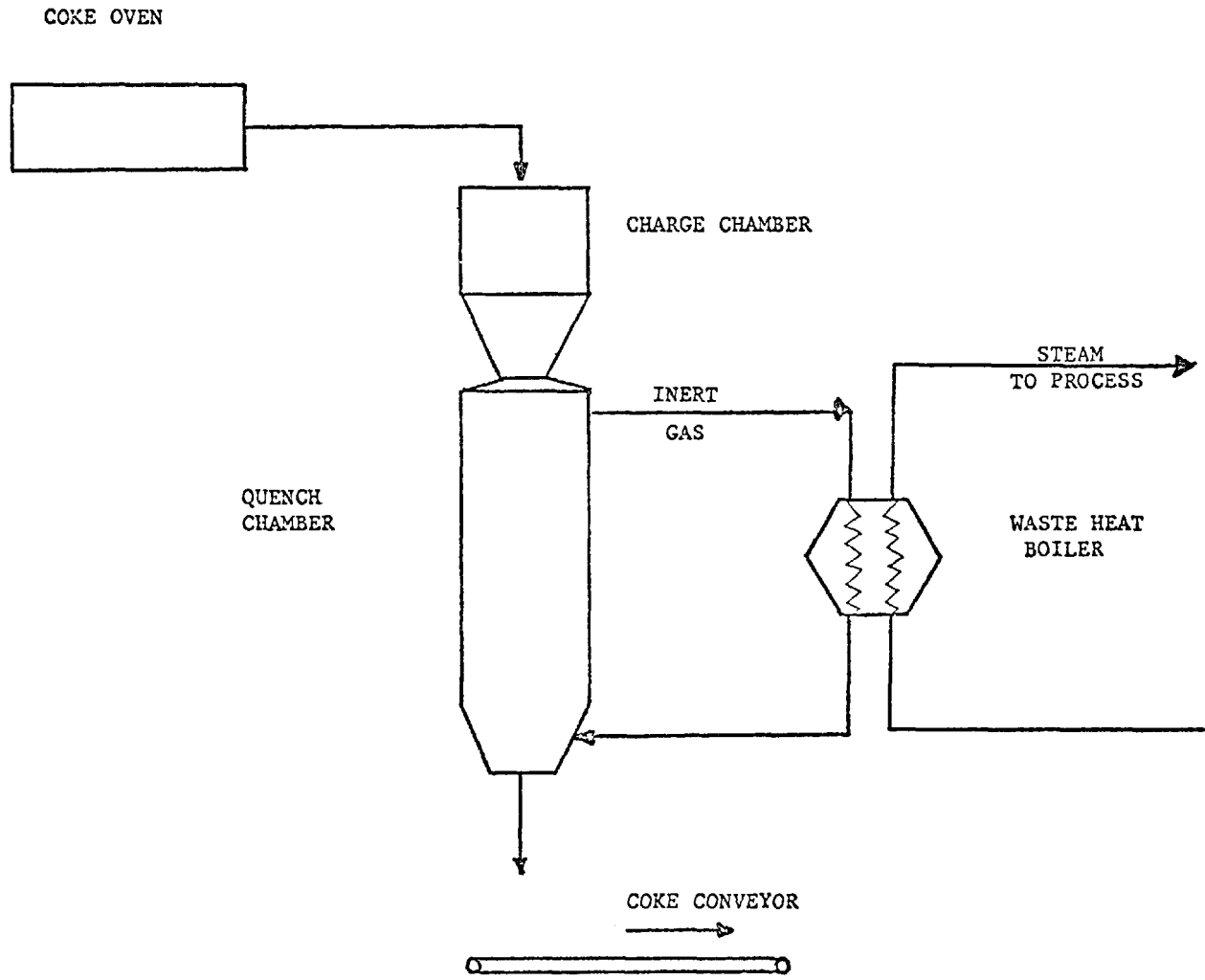


Figure 2: Dry Coke Quenching Process

815

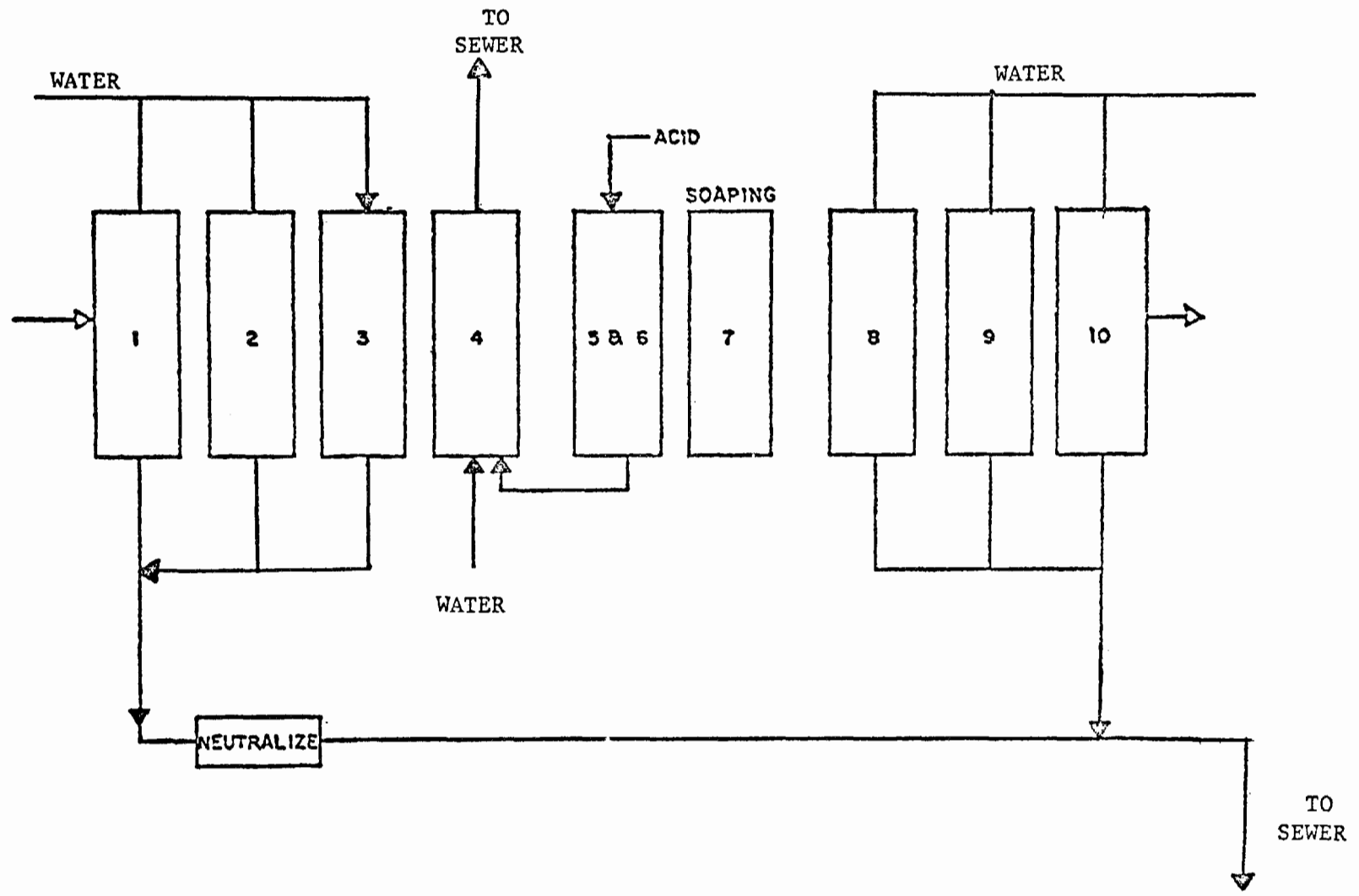


Figure 3: Continuous Dyeing Process - Before changes

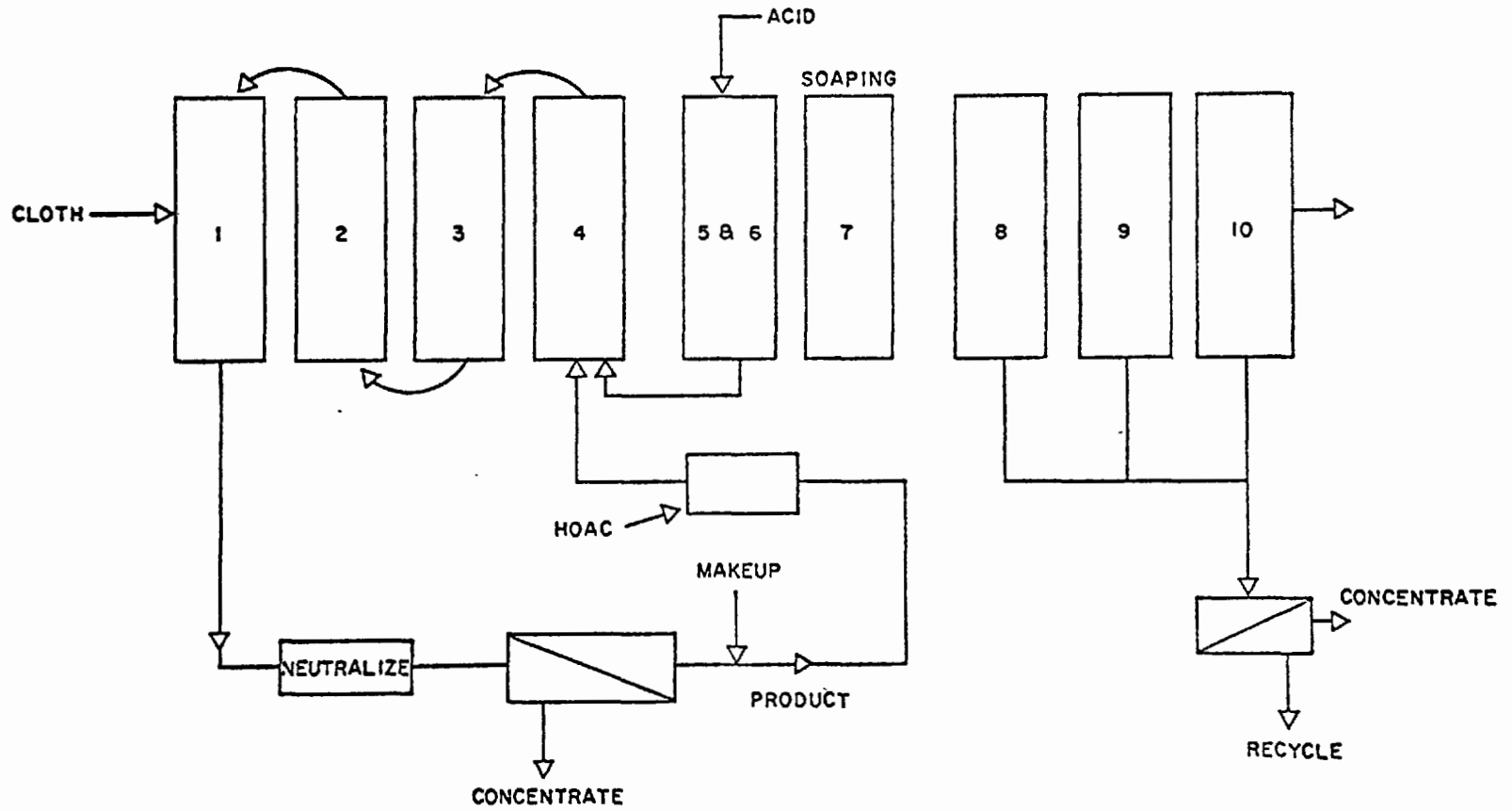


Figure 4: Continuous Dyeing Process - Washing Section Flow Schematic. with recycle

WASTE HEAT RECOVERY POTENTIAL  
FOR  
ENVIRONMENTAL BENEFIT  
IN  
SELECTED INDUSTRIES

Prepared By

S. R. Latour

J. G. Menningmann

DSS Engineers, Inc., Ft. Lauderdale, Fla.

Dr. C. C. Lee

U. S. Environmental Protection Agency

Industrial Environmental Research Laboratories

Cincinnati, Ohio

The power Technology and Conservation Branch of the EPA's Industrial Environmental Research Laboratory in Cincinnati, Ohio, is currently conducting a program intended to assess the relative economic/environmental impacts of waste heat utilization. The reasons for the EPA's involvement in this area are twofold:

- 1) First, increasing the efficiency of energy utilization may be considered a pollution control alternative in that the resulting decrease in fuel consumption will also result in a corresponding decrease in quantity of pollutants discharged.
- 2) Secondly, it is necessary to insure that as these more efficient systems are developed, new pollutants are not generated which would adversely affect the environment.

As a result, the EPA has funded the study title, "Waste Heat Recovery Potential for Environmental Benefit in Selected Industries." The objective of this study is to identify the points, quantity and quality of heat discharged by Energy Intensive Industries and Emerging Technologies for Energy development. Energy Intensive Industries were selected on the premise that those industries which consumed the greatest quantities of energy offered the greatest potential for discharging substantial quantities of waste heat to the environment. Consideration was also given to the thermal intensity and diversification of each industry. Table #1 lists those 4-digit SIC classification included in the study.

TABLE #1  
SELECTED INDUSTRIES

|       |                                 |      |                             |
|-------|---------------------------------|------|-----------------------------|
| SIC # |                                 |      |                             |
| 2611  | Pulp Mills                      | 2911 | Petroleum Refineries        |
| 2621  | Paper Mills (ex Bldg Paper)     | 3211 | Flat Glass                  |
| 2631  | Paperboard Mills                | 3221 | Glass Containers            |
| 2812  | Alkalies and Chlorines          | 3229 | Pressed & Blown Glass       |
| 2813  | Industrial Gases                | 3241 | Cement Hydraulic            |
| 2819  | Industrial Inorganic Chemicals  | 3274 | Lime                        |
| 2865  | Cyclic Crudes and Intermediates | 3312 | Blast Furnace & Steel Mills |
| 2869  | Industrial Organic Chemicals    | 3321 | Grey Iron Foundries         |
| 2873  | Nitrogenous Fertilizers         | 3331 | Primary Copper              |
|       |                                 | 3334 | Primary Aluminum            |

For each of these industries, a study was conducted to document the points, quality, and quantity of all waste heat discharges to the environment. The major source of data collected on flue gases was from the National Emissions Data System's ( NEDS ) Point Source Listings. This data was then verified by discussion with various industry officials and by correlation with other related studies conducted both by the EPA and the DOE.

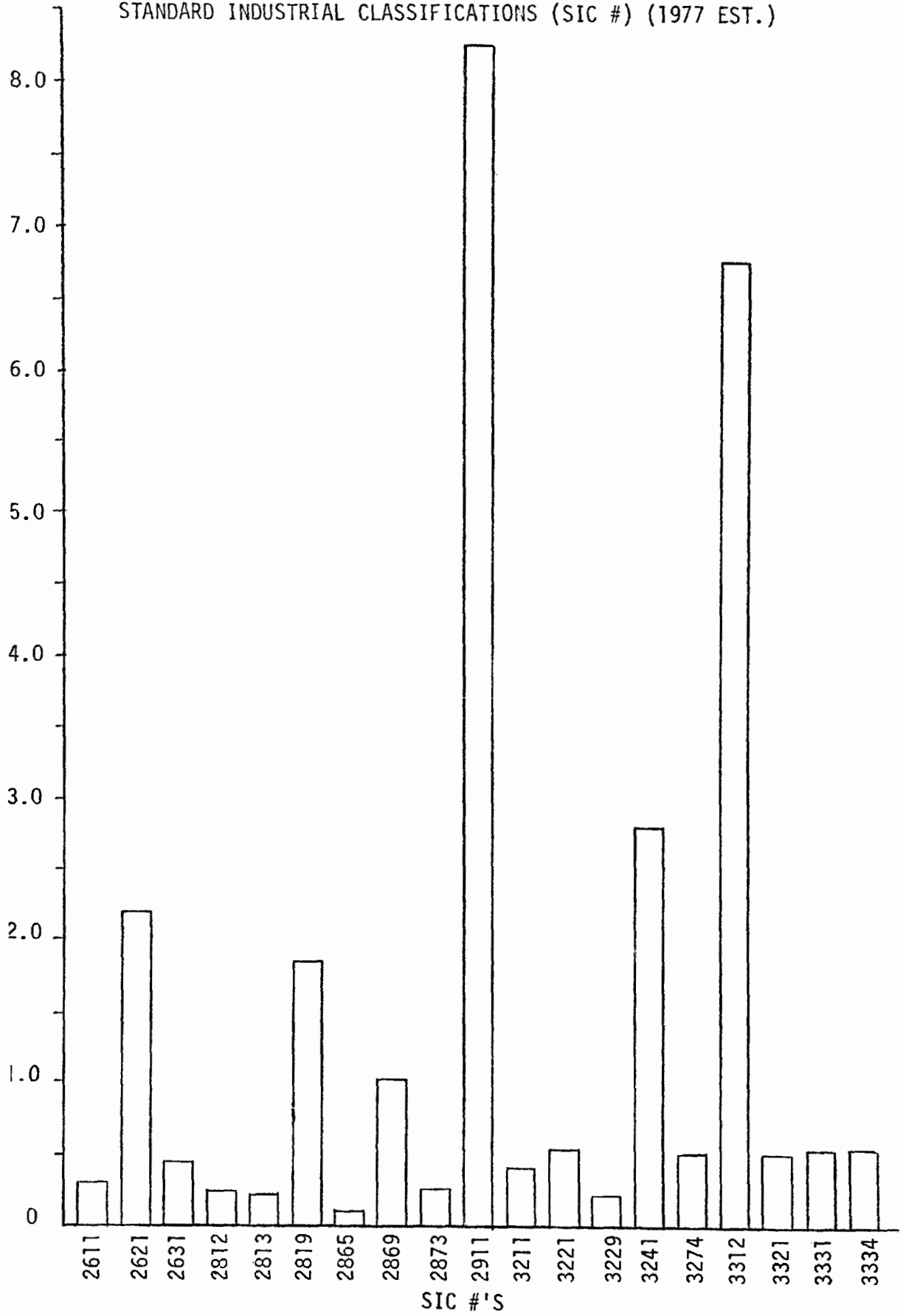
Data on wastewater and non-contact cooling waters containing significant quantities of waste heat were also identified, when possible, from EPA Development Documents for Effluent Limitations, correspondence with Industrial Pollution Control Officers, literature surveys, and various U.S. Government sponsored R & D Reports.

Since it is not possible, within the scope of this presentation, to present the data collected in this study in the detail contained in the final report, and since considerable variations in the accuracy of the data on wastewater discharges exist between each SIC classification, it was decided to present a summary of only the flue gas emission of each industry. This data accounts for about 99% of the total waste heat discharged, from industries such as cement production, to approximately 50% for such industries as petroleum refining and steel production which utilize considerable quantities of both non-contact cooling and process wastewaters.

For this presentation it was decided that four graphs would be adequate to summarize the main findings of the original report.

In Fig. 1, the annual waste heat discharged by flue gasses versus the standard industrial classifications is represented. As mentioned previously, the industries such as petroleum refineries and steel mills (incl blast furnaces) are only represented by about 50% of there total waste heat, the other 50% was contributed by wastewaters, whereas cement and papermills are

.FIGURE #I  
 \* ANNUAL WASTE HEAT DISCHARGED  
 BY  
 STANDARD INDUSTRIAL CLASSIFICATIONS (SIC #) (1977 EST.)



ue Gasses Only

represented by roughly 99% and 96% of their total waste heat because of the minimal amounts of non-contract cooling and process wastewaters utilized within these industries. From these figures and the wastewater data it was determined that approximately 50% of the total waste heat discharged, within these SIC groups, is discharged by petroleum refineries and steel mills. With this in consideration it seems apparent that petroleum refining and steel production should be prime candidates for further research into the potentials for energy recovery.

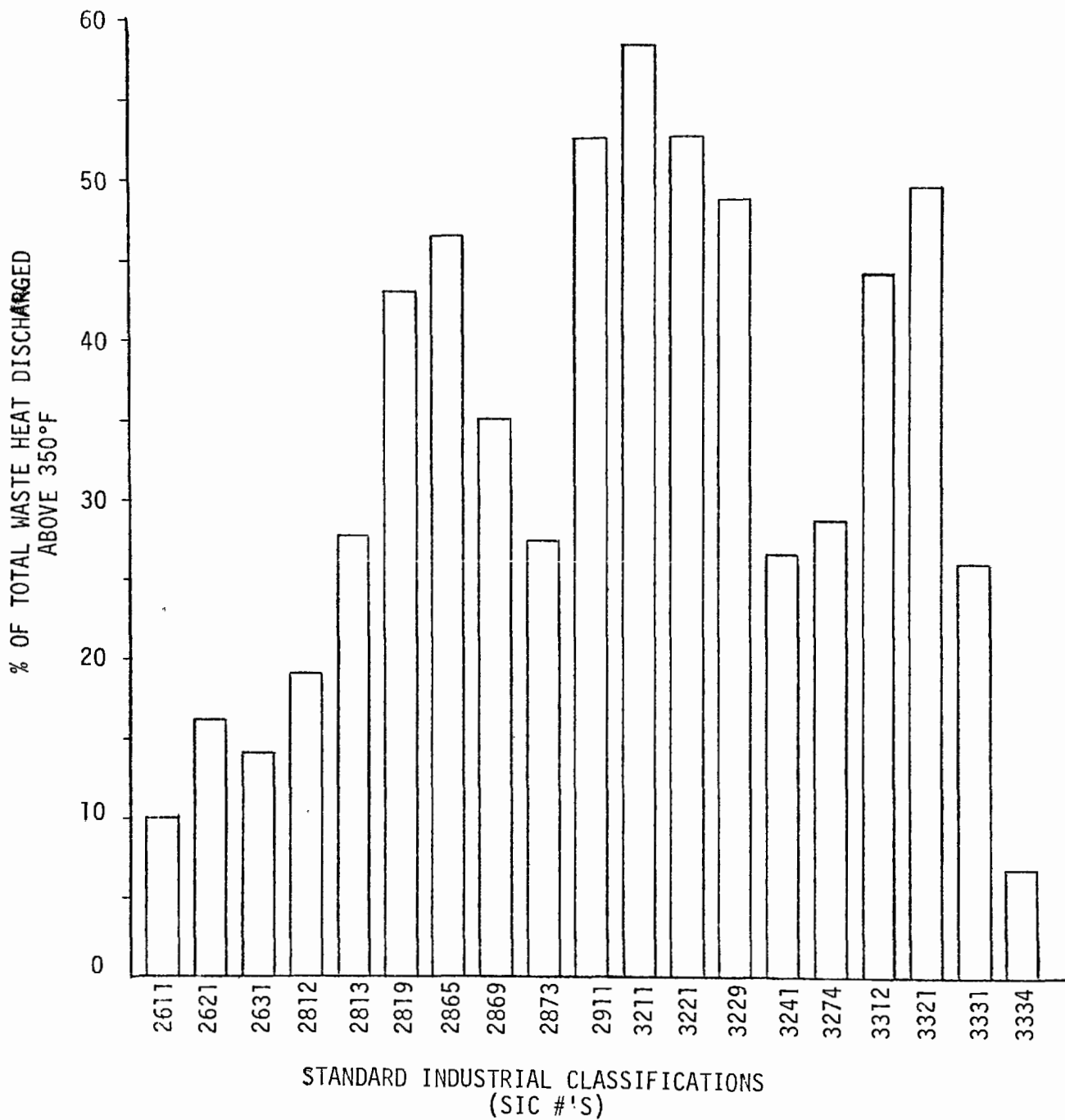
The percentage of waste heat discharged above 350 F is the subject of Fig. 2. Waste heat streams above this temperature were termed BTU's available because of three primary reasons: 1) this is the approximate dew point of sulfuric acid, which is present as an acid gas in most combustion processes, and can deteriorate equipment materials such as baghouse fabrics and stack liners when condensed out of the flue gas; 2) heat recovery tends to reduce the buoyancy of stack plumes thereby reducing plume height and causing an increase in ground level concentrations of sulfur and nitrogen oxides; and 3) temperatures lower than 250 F do not prove advantageous for "heat exchanger devices", however there are systems such as heat pumps, conventional and direct contact organic rankine cycles that do operate in this range.

Fig. 2 illustrates the industries that have the greatest percentages of "waste heat available". These industries show more potential for energy recovery via conventional "heat exchanger devices."

In Fig. 3 we see the percent of purchased fuels and electricity discharged as waste heat by standard industrial classifications. This data was also generated with only flue gas discharges.

It should be noted that in Fig. 3, for example petroleum refining, discharges about 62% of their purchased fuels and elec. by flue gas. This may not

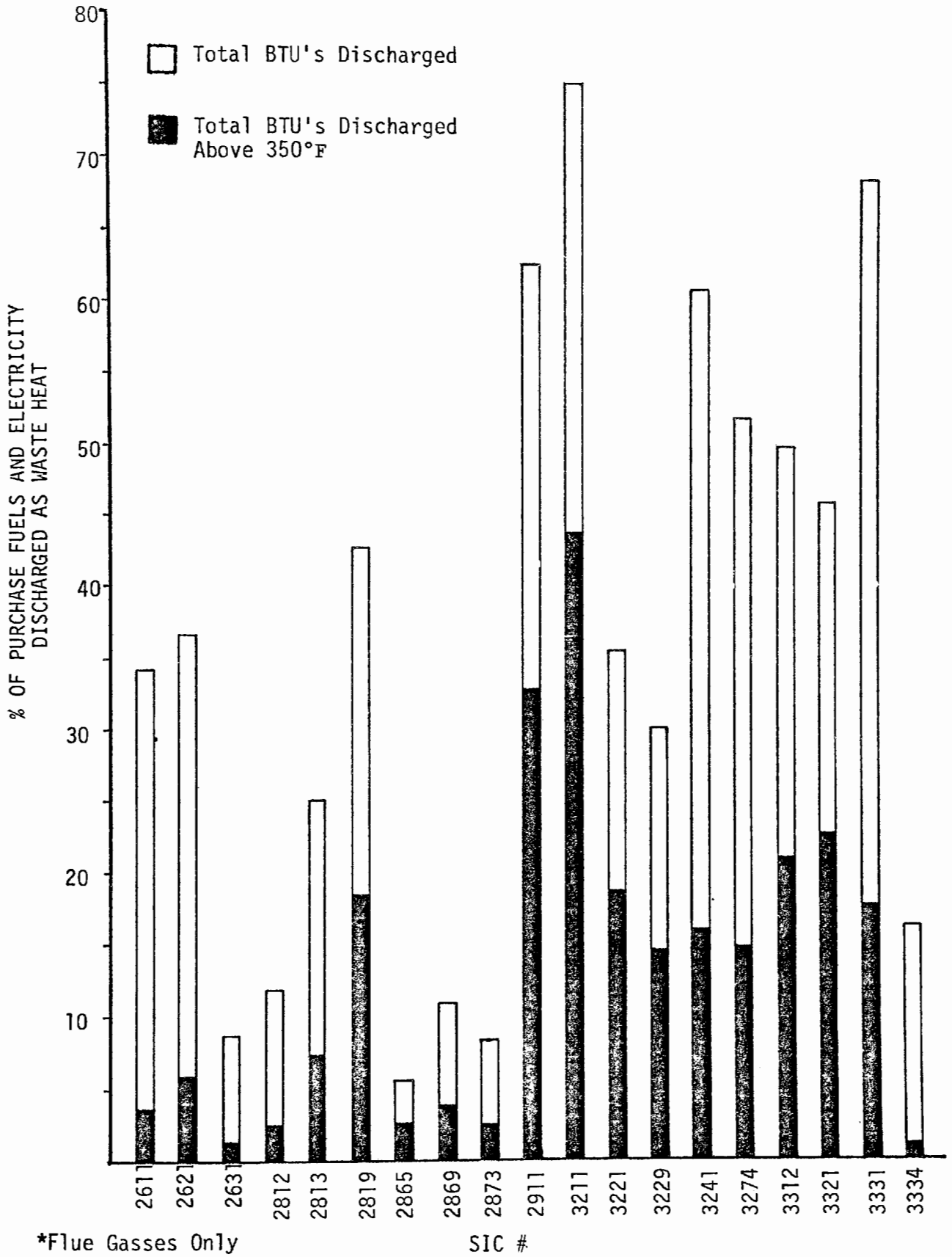
FIGURE #2  
 \* PERCENT WASTE HEAT DISCHARGED  
 ABOVE 350°F  
 BY  
 STANDARD INDUSTRIAL CLASSIFICATION (SIC #)



\*Flue Gasses Only

FIGURE #3

\*  
 PERCENT OF PURCHASED FUELS AND ELECTRICITY  
 DISCHARGED AS WASTE HEAT BY  
 STANDARD INDUSTRIAL CLASSIFICATION (SIC #)  
 (1977 EST.)



seem reasonable at first glance because flue gas only represents about 50% of the waste heat discharged in refineries. This means that 124% of purchased fuels and electricity is discharged by flue gases and waste waters as waste heat. The explanation for this is that 50% or more of the petroleum refineries energy needs are supplied with byproduct refinery gas and coke. Then, with these points considered, petroleum refineries would only discharge roughly 62% of the total energy consumed by that industry. This is the case for steel production and to a much lesser extent for the other industries.

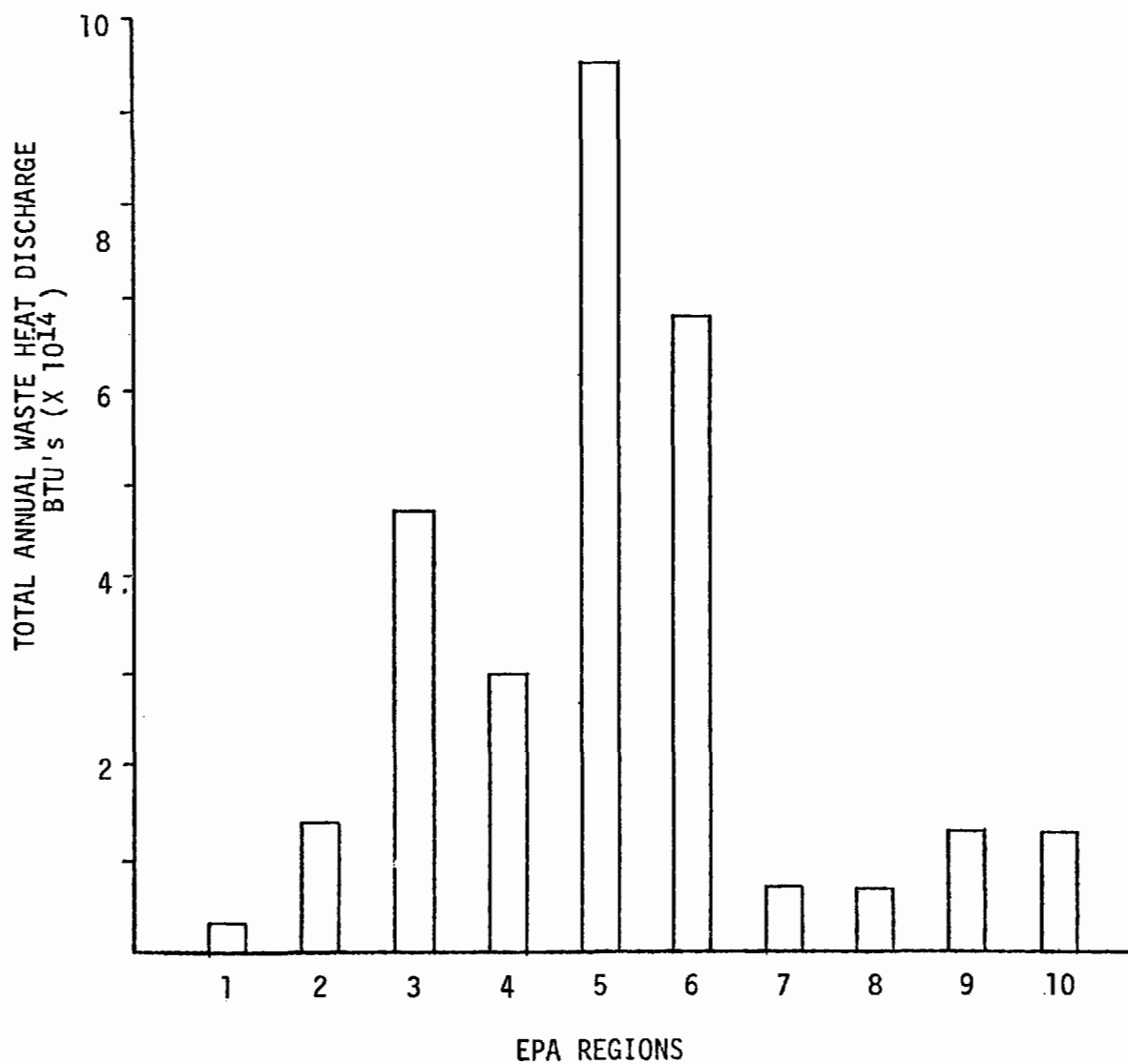
Considering Fig. 3 one can see that some industries which have a high % of purchased fuels and electricity discharged as waste heat do not necessarily have a high % of "BTU's available", the % black area. Keeping in mind the total BTU's discharged annually for each Sic #, this Fig. differentiates industries, which have close to the same percentages of waste heat discharged, by their potential for energy recovery with conventional "heat exchanger devices."

The next graph, Fig. 4, gives annual waste heat discharged in the 10 EPA regions. For the individual Sic #'s, we assessed the BTU's discharged in each region. With this data we could attribute the high percentage of waste heat in region 5 to primarily steel, petroleum and industrial inorganic chemicals N.E.C. productions; region 6 to petroleum, industrial organic chemicals N.E.C., cement, industrial inorganic chemicals N.E.C. and papermills (excl. Bldg. paper) productions; region 3 to industrial gases, steel, petroleum and cement productions; region 4 to papermills, petroleum, cement paperboard mills and steel productions.

This data reflects the regional potentials for commercial use of waste heat in the fields of space heating, soil warming, aquaculture farming and other potential uses of low grade waste heat.

FIGURE #4  
\* ANNUAL WASTE HEAT DISCHARGED

BY  
EPA REGIONS  
(1977 EST.)



\*Flue Gasses Only

FIGURE #5  
**EPA REGIONS**



## POSSIBLE ENVIRONMENTAL IMPACTS

Waste heat discharged by industry can create undesirable thermal loading of the local environment. The impact of these heat additions is dependent upon both the concentration and route by which this heat energy is discharged.

While a variety of pollutants are often directly related to waste heat discharge, this discussion will focus primarily on the impact of the thermal discharges to the environment.

Heat is unlike most "pollutants" which can be readily collected, concentrated, and disposed of under controlled conditions. Conversely, heat energy must be disposed of through retention with controlled dissipation so as to minimize its effects on the surrounding biosphere.

Heat rejection by cooling and process waters can be a significant amount of the overall waste heat discharged in some industries. Until recently, a common method of waste heat disposal was to discharge once through cooling water into a nearby waterway, this has proven to be both efficient and economical. However, public concern over the potential adverse environmental impacts caused by the addition of this waste heat to natural waterways has promoted considerable research in an attempt to define these impacts in order to determine "acceptable" levels of thermal pollution.

Temperature is one of the most important single factors governing the occurrence and behavior of life. The discharge of waste heat into a natural body of water can cause a number of physical, biological and chemical effects. Raising the temperature of water reduces the oxygen retaining capacity of the water, reduces the reaeration rate, changes the density which may in turn result in stratification, increases the rate of evaporation, increases the rate of many biological, chemical and physical reactions,

and decreases the viscosity thereby reducing the sediment transporting ability of the water.

The impacts of these changes can be detrimental, beneficial, or insignificant depending upon the extent of these changes and the intended use of the receiving body of water. Heat inputs into a receiving body of water increases the rate of BOD exertion which, when coupled with the accompanying reduced reaeration rate, may reduce its organic waste assimilation capacity. On the other hand, the addition of waste heat during winter months may significantly lengthen the shipping season of a waterway by shortening the period of ice cover in the shipping lanes.

However, the greatest potential impact of waste heat discharges to natural bodies of water is upon the aquatic ecosystem. Although a large number of studies have been and are being conducted in attempts to further define these cause and effect relationships, considerable data is still lacking. Some of the known and reported effects associated with temperature increases of natural waterways are: decreasing gas (oxygen) solubilities; changes in species diversity, metabolic rates, reproductive cycles, digestive and respiration rates, behavior of the aquatic organisms; and increasing the parasitic bacterial populations. All of these have the potential of creating an unbalanced, unchecked aquatic ecosystem.

Although the potential adverse environmental impacts of discharging waste heat into the aquatic environments are quite numerous and diversified the direct release of this waste heat to the atmosphere is not without its own potential for adverse environmental impact.

It is becoming increasingly apparent that man affects the climatic conditions of the earth by the release of heat and materials to the atmosphere.

For this reason, stack gases and cooling tower plumes are of considerable concern to investigators from an environmental and energy standpoint.

Several studies have suggested that possible intensification of convective activity and associated concentration of vorticity may be caused by the release of large quantities of heat in relatively small areas, resulting in severe thunderstorms and tornadoes. On a smaller scale, the release of this heat, and contained moisture, can increase or change the spatial and temporal pattern of precipitation, cloud cover, and mean temperatures.

Cooling towers, either wet-or-dry, are frequently used to dissipate waste heat to the atmosphere. The major complaint from the public concerning these towers has been the appearance of these devices and, at close range, the noise generated by them. They are, however, several environmental impacts directly related to the operations of these towers. Some of these are 1) the restriction of sunlight caused by visible plumes ("shaddowing") 2) restriction of visibility when plumes reach ground level (fogging) 3) deposition of detrimental chemicals contained in cooling waters onto surrounding areas ("drift") 4) atmospheric changes. For most sites these impacts are rather small and local, and usually environmentally acceptable.

Since proven mathematical models are not yet available for accurately predicting the extent and frequency of these atmospheric effects for a particular site and heat-dissipation system, considerable field research will be required to develop these models before accurate determinations of "critical heat loads" may be projected.

## WASTE HEAT UTILIZATION AND THE ENVIRONMENT

M.E. Gunn, Jr., Program Manager  
Division of Fossil Fuel Utilization  
U.S. Department of Energy  
Washington, D.C. U.S.A.

### ABSTRACT

One way of reducing the national energy needs and conserving valuable fossil fuels in the near and long term is the recovery of waste heat energy. Industrial processes, residential and commercial heating, transportation systems, and electric power generation efficiently utilize only a small percentage of the energy fed into them. Much of this energy can be recovered by using the new technologies now being developed. This recoverable energy amounts to 20 to 30 percent of the forecast national energy consumption.

Waste heat recovery also has a beneficial impact on the environment when the rejected energy is harnessed and used; thermal as well as air pollution is significantly reduced. In particular, thermal pollution is reduced to the atmosphere and to waterways, as applicable, and the pollution to the atmosphere is reduced when the use of waste heat recovery decreases the quantity of fossil fuel that would be burned to achieve given performance levels.

In late 1978, a significant number of preproduction prototype waste heat recovery systems will be in operation at selected electric utility and industrial generation stations located throughout the U.S. They represent modern versions of technology dating back to the 1930's and more recently used in aerospace applications. DOE is supporting the development of several unique concepts of packaged Rankine cycle systems using different working fluids ranging from steam to Freon. Each system will be rated under one megawatt and will be ideal for recovering waste heat from the diesel engines used by many small municipal electric utilities as well as other waste heat recovery opportunities in industrial applications. The systems will recover the waste heat from the prime mover exhaust streams and convert it to additional useful shaft power at efficiency levels of 18-20 percent.

This paper will describe the technology as it is characterized in the DOE sponsored concepts and will address the impacts, pro and con, on the environment as a result of their implementation. The conditions of using the organic fluids as working fluids will be discussed and an attempt will be made to quantify selected thermal and air pollution improvements.

## INTRODUCTION

A most important principle of the President's National Energy Plan (NEP) is seen as the "Cornerstone of National Energy Policy." This principle states that the growth energy demand must be restrained through conservation and improved energy efficiency. Conservation represents practice that is cheaper than production of new energy supplies, and a most effective means for protecting the environment. See Figure 1.

The level of imported fuels can be substantially reduced by pursuing attractive energy efficient technologies. Studies have estimated that overall economy of the U.S. operates at less than 10 percent energy efficiency. A recent analysis determined that the U.S. could expend between 20 and 40 percent less energy and still maintain overall economic growth into the 1990's. Much of the required energy is lost as waste heat and can be recovered by using new technologies. This recoverable energy can amount to 20 to 30 percent of the forecast national energy consumption.

If the waste heat recovery program currently underway via Federal support and sponsorship were carried through to completion, potentially, the Nation's annual expenditure for imported oil can be reduced by \$15 billion in 1985 and by \$48 billion in the year 2000. Full utilization of recoverable waste heat energy would result in potential savings of \$57 billion in 1985 and by \$68 billion in 2000. See Figure 2.

By reducing the need for additional oil imports by recovering and making use of waste energy, conservation and improved efficiency in the use of energy can contribute to national security and international stability. This leads to the possible reduction of the need for additional domestic energy production, thereby contributing to environmental protection.

To achieve these savings and ultimate improvements for the environment, DOE has been supporting waste heat recovery and utilization projects since 1975.

In the High Temperature Heat Recovery program at DOE (Figure 3) a goal was established to develop heat recovery technology as an alternate source of energy by developing the necessary technology base for recovering and using waste heat and by demonstrating the technical and economic feasibility of the technological components. As shown in Figure 4, specific projects of this program include the development of several unique concepts of organic Rankine cycle systems. These systems are ideal for recovering waste heat from diesel engines used by many small municipal electric utilities and

are suitable for recovering waste heat in industrial processes. The shear implementation of these systems will significantly reduce thermal and air pollution typically characteristic of the respective prime movers, and the impact on the environment may even be considered negligible when one takes into account the system performance and reliability aspects.

## THE TECHNOLOGY

The organic Rankine cycle system technology being developed in the DOE program represents modern versions of technology dating back to the 1930's and more recently used in aerospace applications. Basically, a Rankine cycle system, depicted in Figure 5, is a thermally driven engine that converts heat energy into the mechanical energy by alternately evaporating a working fluid at high pressure and producing shaft power which operates at low pressure.

The Rankine cycle system can be readily identified as the thermodynamic cycle that characterizes a steam generation system used to produce electricity. The use of organic fluids instead of steam offers advantages as well as the disadvantages listed in Figure 6. As indicated in Figure 7, organic fluids typically have low heats of vaporization, thereby allowing for sensible heat use at the lower temperature conditions. Therefore, the systems being developed are suitable for low or middle temperature heat utilization.

Before the end of 1979, at least four preproduction prototype organic Rankine cycle waste heat recovery systems will be in operation at selected electric utility generation stations in the United States. The units will produce additional electric power from the exhausts of stationary diesel engines.

Three of the units are products of a DOE/Sundstrand Energy Systems Cooperative Agreement. Under this agreement, Sundstrand has designed and developed a system which uses toluene as a working fluid to generate 600 Kw of electric power. The fourth unit was developed by Mechanical Technology Incorporated (MTI), and employs two safe and well accepted power fluids, steam and Freon to generate 500 Kw of electric power.

As illustrated in Figure 8, the Sundstrand system uses a single stage supersonic high-work impulse turbine, and a vaporizer which uses a compact centrifugal separator to remove liquid from the vapor stream at the outlet of its natural circulation boiler. A modular packaging concept (Figure 9) is employed so that the power conversion system may be easily transported and set up without special foundations. One organic Rankine cycle loop is entirely sealed with exception of the turbine output

shaft. The regenerator, condenser and hotwell are combined in a single vessel. Sundstrand units will be in operation at municipal utility plants located at Beloit, Kansas, Easton, Maryland, and Homestead, Florida.

The MTI unit is characterized by the cycle shown in Figure 10. In this system basically, two Rankine cycles are employed. The steam topping cycle buffers the Freon bottoming cycle enabling the system to be applicable over a wider range of gas temperatures. The machinery arrangement consists of two radial in-flow turbines that drive a common output gear. The system is designed to use exhaust gases at 520°F to generate steam at 430°F which is expanded across the Freon turbine. Each turbine is independently optimized. The system is low pressure in character and conventional process and refrigeration industry heat exchange components have been adapted for use. The system is neatly packaged for simplicity in transportation and installation. The MTI unit will be recovering exhaust gases from two turbocharged diesels in operation at the Municipal Power Plant in the Village of Rockville Centre, New York (Figure 11)

#### INSTALLATIONS AND ENVIRONMENTAL CONSIDERATIONS

Unlike nuclear and fossil fuel cycles, the basic fuel cycle for these waste heat power conversion systems is located at the source of fuel, which is, in this case, exhaust gases from stationary diesel engines. Therefore, environmental effects occur mainly during the operation phase of these systems, and are very site specific. This operating phase consists of power generation under specific load conditions and constraints that might be imposed by the system users. Typically, the environmental factors normally considered for power generation plants include but are not limited to land use, noise, seismic effects, thermal discharges, and gaseous and liquid effluents. Figures 12a through c provides illustrations of the site plans for the Sunstrand installations. It is readily apparent that adequate land area is available at each installation. This is also true for the MTI installation shown in Figure 13. Perhaps, the most significant aspect of this installation is the location of the steam boiler. This component is mounted between the exhaust stacks of the two diesel engines supplying the recovery system "fuel", on the top of the diesel engine building.

These initial installations are retrofits to existing facilities. The main disturbance of the land area takes place at the Sundstrand installations where toluene sumps are made available to contain any major leakage of the toluene inventory. The system contains ~900 gallons of toluene when fully charged. The tank is designed to prevent any leakage into

into the earth and is buried well above water table levels at each site. Aside from this, no significant land modifications are required, i.e., mining, well digging, etc.

Seismic problems are not seen to pose any significant concerns. Structural integrity for each installation will be consistent with the existing powerplant requirements and will be at least as safe as the primary systems.

Noise problems are centered around the turbomachinery or power conversion components of each unit. Considering the noise level of the muffled diesel engines operating in the existing facilities, the turbomachinery noise cannot be detected during operation. Since the waste heat recovery system only operates when the diesels are running, noise pollution can be considered negligible for the additional systems.

The discussion of thermal pollution is concentrated mainly at two interfaces -- the vaporizers at the heat source and the cooling towers at the heat sink. The Sundstrand system is designed for vaporizer application in heat sources between 800°F and 330°F; the MTI unit is designed for exhaust (heat source) temperatures of 520°F with the heat source exit temperature at 333°F. Considering that typical exhaust temperatures for large stationary diesels range as high as 1200°F, it is readily apparent that when the entire exhaust streams are captured by the systems in question, or when the available heat source exceeds  $\sim 10 \times 10^6$  Btu/hr., above the 330°F temperature, there is a substantial reduction in thermal pollution as a result of waste heat recovery system implementation. Even if the systems recover only a portion of the available waste heat, the thermal impact on the environment is reduced. Although no thermal discharge measurements have been recorded as of yet for either the Sundstrand or MTI unit under actual operation, one can expect that the above drawn conclusion will be substantiated.

For the installations discussed in this writing, cooling towers are utilized to reject the energy transferred at the condensing systems for each unit. The MTI unit is designed to reject energy at 67°F to the cooling tower. The Sundstrand system has a liquid (cooling water) side condenser exit temperature of 100°F. Of course, the cooling water temperature from each system is reduced via the cooling towers by some 6°F to 15°F. Therefore, thermal pollution at the cooling towers of these waste heat systems is minimal.

When considering gaseous effluents to the environment, basically two areas of concern come to mind. The first area is at the diesel exhaust stacks. A question raised here is with respect

to any change in the exhaust stream of the diesel engines as a result of heat extraction. The mere fact that implementation of these organic systems to generate power from expended energy sources leads to the analogous situation that would exist to, say, generate that same power using a prime mover, such as another diesel. Figure 14 shows a plot depicting the impact on emissions from fuel combustion relative to the efficiency of utilization of fossil fuel. The 20 percent efficient bottoming plants improve fuel utilization efficiency by up to 10 points. This corresponds to significant reduction in emissions and represents the emissions impact on the environment that does not occur as a result of using waste heat as a fuel source.

The extraction of heat from the diesel exhaust stream does raise possible concern for sulphuric acid formation in the stacks and subsequent acid mist introduced to the atmosphere. In each installation the fuel for the prime movers is relatively clean #2 fuel oil. Thermal conditions, however, are related to the formation of sulphuric acid. In a recently completed report that included diesel exhaust gas analysis, the exhausts from five large diesel engines were sampled over a range of engine operating conditions using fuels with sulphur contents varying from 0.05 percent to 1.8 percent (Figure 15). The exhausts were characterized via measurements of SO<sub>2</sub>, SO<sub>3</sub>, CO, H<sub>2</sub>O, NO, chloride, acid dew point, peak rate temperature of acid deposition, particulate loading, particle sizing, particulate composition and smoke number. The results of the analysis were used to determine that the temperature where the peak acid deposition rate was approximately 20°F lower than the determined acid dew point temperature of ~240°F. The peak acid deposition rate corresponds to the point of maximum corrosive environment for the vaporizer. Therefore, if acid formation is avoided, problems with regard to acid mist and corrosion can be mitigated.

Recall that in the Sundstrand system the lowest allowable exhaust temperature after heat extraction is 330°F, while in the MTI system the steam boiler is designed so that the diesel exhaust temperature never drops below 333°F. Both are safely above the acid dew point limit suggested by the analysis.

The other area of concern when discussing gaseous effluents is the possible leak of organic vapors or liquids into the environment. The use of organic fluids raises serious concerns, at times more emotional than actually hazardous. As indicated in Figure 16, characteristics of organic fluids typically include toxicity and flammability limits. The designs employed by Sundstrand and MTI have taken these limits into consideration, but despite this, one might speculate that leakages may

occur that could prove to be hazardous to the health and safety of workers, and toxic substances may escape.

As mentioned before, Sundstrand uses toluene as a working fluid which is moderately toxic. It has a National Fire Protection Association (NFPA) health hazard rating of 2. A threshold limit value (TLV) of 200 ppm (750 mg/m<sup>3</sup>) has been assigned to toluene. The recommended average TLV is 100 ppm with a peak of 200 ppm for no more than 10 minutes.

The operation of the Sundstrand units at each installation will be without the need of an operator, and each installation will have adequate ventilation to guard against excessive accumulation of toluene leaks into the atmosphere. Sufficient fire protection is also included. As mentioned before, toluene sump tanks are supplied with each system installation. These tanks are designed to protect the environment from leaks of the fluid. Since the temperature and pressure of the toluene in the system is never expected to exceed 465°F and 200 psia respectively, there is no apparent concern for autoignition. Toluene decomposes at 750°F.

The MTI unit employs Freon-11 in its bottom cycle. A TLV of 1000 ppm has been assigned to Freon-11 (CFCl<sub>3</sub>). In animal tests, closely related chemical species such as Freon-112 (CGCl<sub>2</sub> CFCl<sub>2</sub>), chloroform (CHCl<sub>3</sub>), and carbon tetrachloride (CCl<sub>4</sub>) have been shown to be carcinogenic. However, no such conclusion has been drawn regarding Freon-11. In the MTI design, Freon-11 will be heated to 190°F at 90 psia, thereby mitigating the possibility of decomposition. Decomposition of R-11 occurs between 350°F and 400°F.

Freon-11 has been reported to catalyze the breakdown of the ozone layer, Design conditions will not permit leaks of Freon-11 during normal operation and barring any unforeseen failures, it is not expected that Freon-11 leaks will be a problem. The mere fact that there is significant handling experience via the refrigeration industry will enhance the acceptability of the fluid.

#### SUMMARY AND CONCLUSION

After considering some of the typical environmental effects pertinent to power generation plants, it can be safe to assume based upon this somewhat simplified assessment that the implementation of organic Rankine cycle waste heat recovery systems in municipal utilities will benefit rather than impair the environment. The critical area of concern will continue to center around the organic fluids themselves and the character of the respective Sundstrand and MTI designs. Each

has taken into account the seriousness of catastrophic failures and has taken the necessary precautions in design to mitigate their occurrence.

It can therefore, be concluded that implementation of waste heat recovery devices can, in fact, serve to protect the environment from adverse influences.

# **Heat Engine and Heat Recovery R&D Supports NEP and Supply Strategy Policy**

- **Enhance Conservation and Lower the Rate of Growth of Total U.S. Energy Demand**
- **Shift Industrial and Utility Consumption of Natural Gas and Oil to Coal and Other Abundant Resources**
- **Develop Synthetic Substitutes for Oil and Gas**
- **Reduce Dependence on Oil Imports and Vulnerability to Interruptions of Foreign Oil Supply**



## Potential Savings in Oil Imports

| Category                       | Estimated Energy Savings |       |                          |       |
|--------------------------------|--------------------------|-------|--------------------------|-------|
|                                | Ongoing Projects         |       | Total Recoverable Energy |       |
|                                | 1985                     | 2000  | 1985                     | 2000  |
| Total Savings of Oil (MBDOE)   | 2.7                      | 8.7   | 10.4                     | 12.5  |
| Total Savings of Oil (Quads)   | 5.4                      | 17.4  | 20.8                     | 25.0  |
| % Reduction in Oil Imports     | 23                       | 76    | 66                       | 79    |
| \$/Yr. Savings on Oil Imports* | 14.8B                    | 47.6B | 56.9B                    | 68.4B |

\*Based on an estimated value of \$15 per barrel, which appears quite conservative for the 1985-2000 time frame.

FIGURE 2



# The Goals

**To Develop Heat-Recovery Technology as an Alternative Source of Energy by:**

- **Developing the Necessary Technology Base for Recovering and Using Waste Heat**
- **Demonstrating the Technical and Economic Feasibility of the Technological Components**

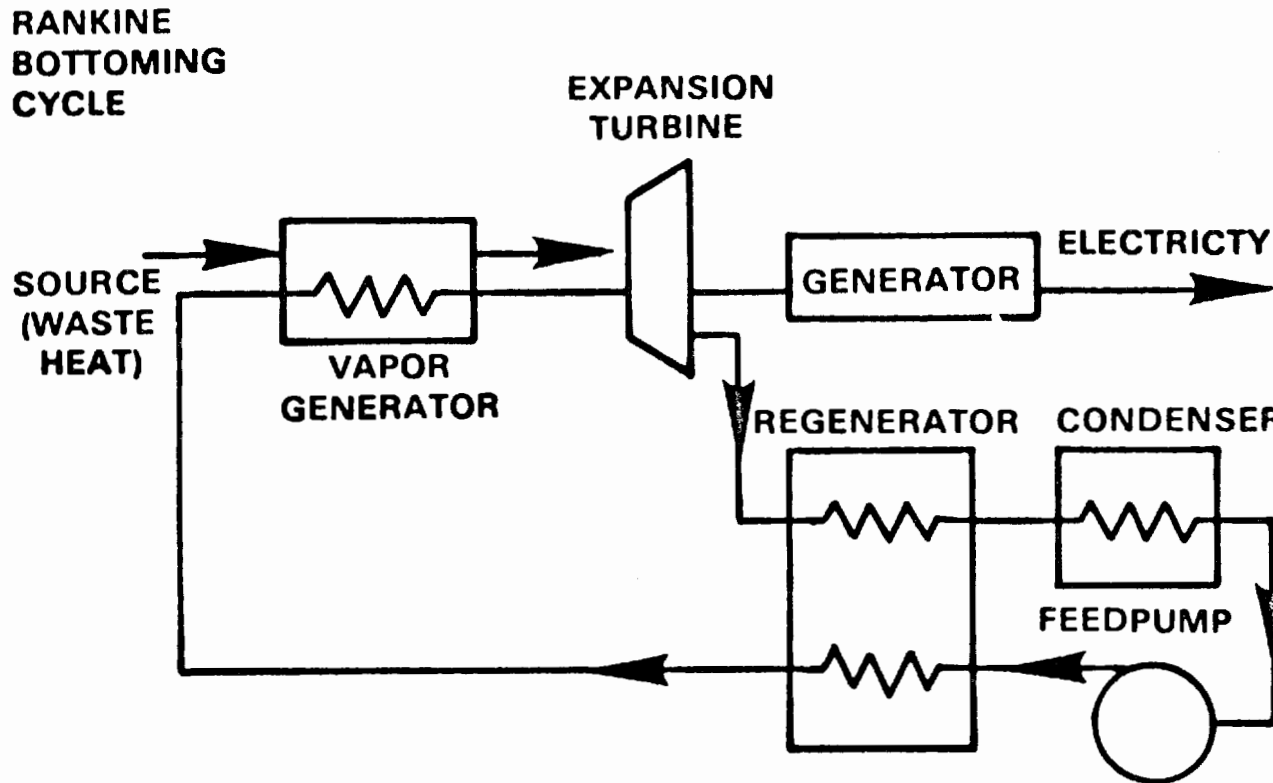
# **Bottoming Cycle Systems for Waste Heat Recovery and Cogeneration**

- **Four Unique Concepts in Organic Rankine Cycle System Technology**



- **Mechanical Technology Inc. — 500 KW Binary-Rankine Cycle System**
- **Sundstrand Energy Systems — 600 KW Toluene Rankine Cycle System**
- **Thermo Electron Corporation — 440 KW Fluorinol Rankine Cycle System**
- **Biphase Energy Systems — 400-600 KW Two Phase Heat Engine Cycle System**

# Rankine Bottoming Cycle Concept



842

FIGURE 5

# Organic Vs Steam Comparison

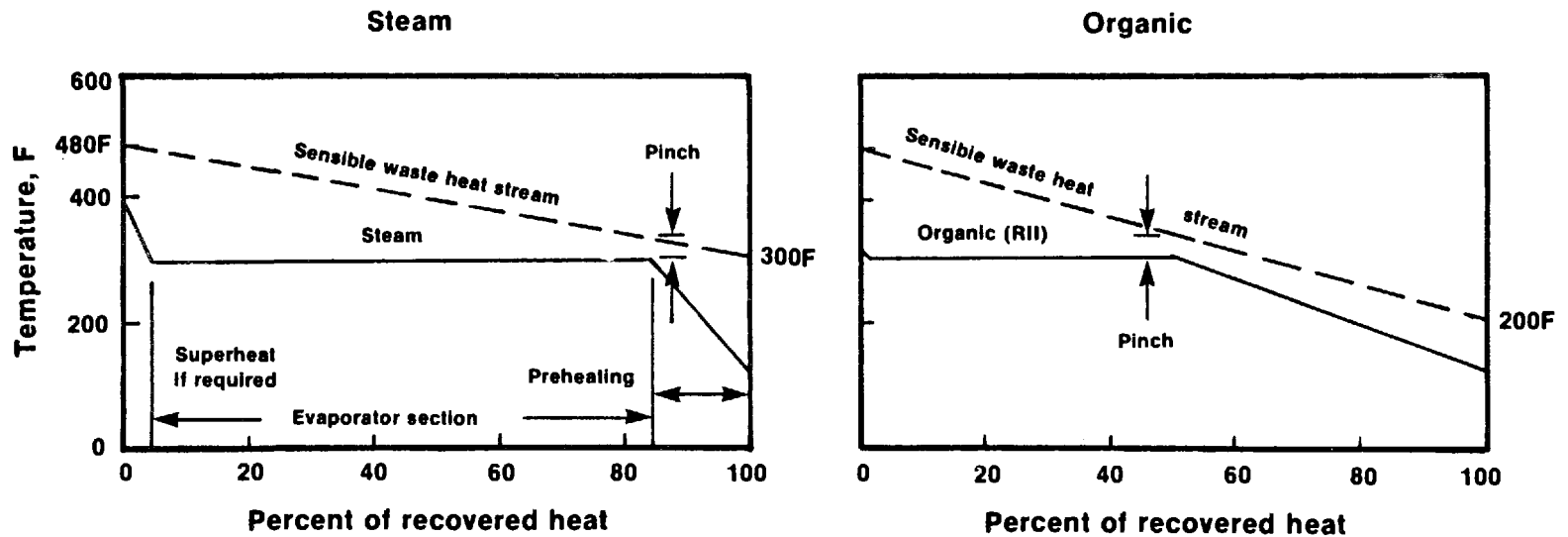
## Advantages Of Organics

- High Efficiency With Single-Stage Turbine
- High Efficiency In Small Sizes
- Little Or No Superheating And/Or Desuperheating Required
- Condenser Pressures Near Atmospheric Reduces Leakage Problems
- Compact And Lightweight Turbomachinery
- Low System Cost
- Wide Variety Of Fluids Possible

## Disadvantages

- Maximum Temperature Limited By Chemical Stability
- Fluids Can Be Expensive
- Expensive Materials Required To Avoid Decomposition At Elevated Temperatures
- Lower Heat Transfer Coefficients Require Larger And More Expensive Heat Exchangers
- Fluids Can Be Toxic, Flammable
- Very Limited Availability Of Off-The-Shelf Hardware Specifically Designed For Fluids

# For Same Pinch Temperature Organic Fluids Can Extract More Heat Than Steam

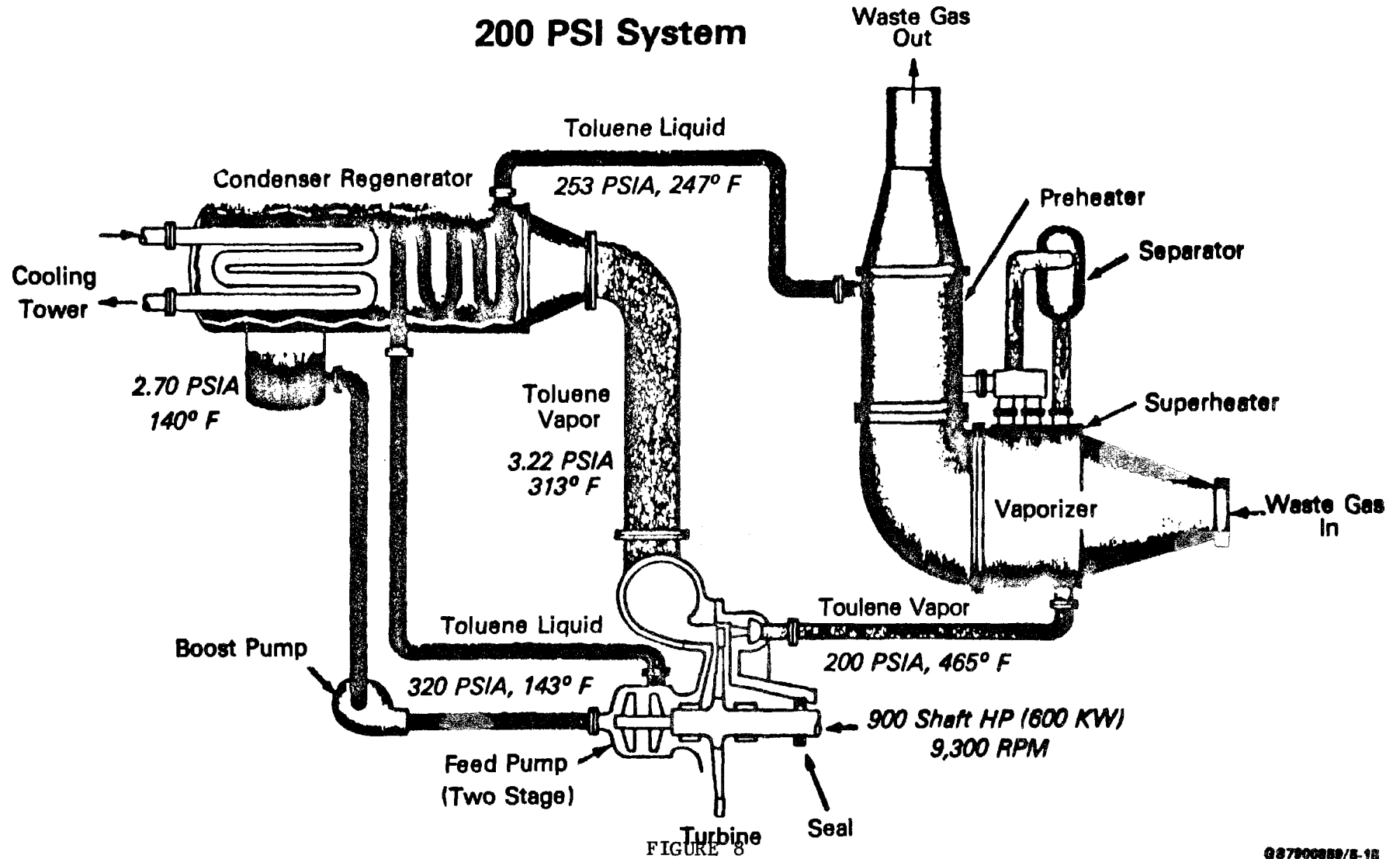


844

FIGURE 7

# 600 KW ORC Schematic

## 200 PSI System

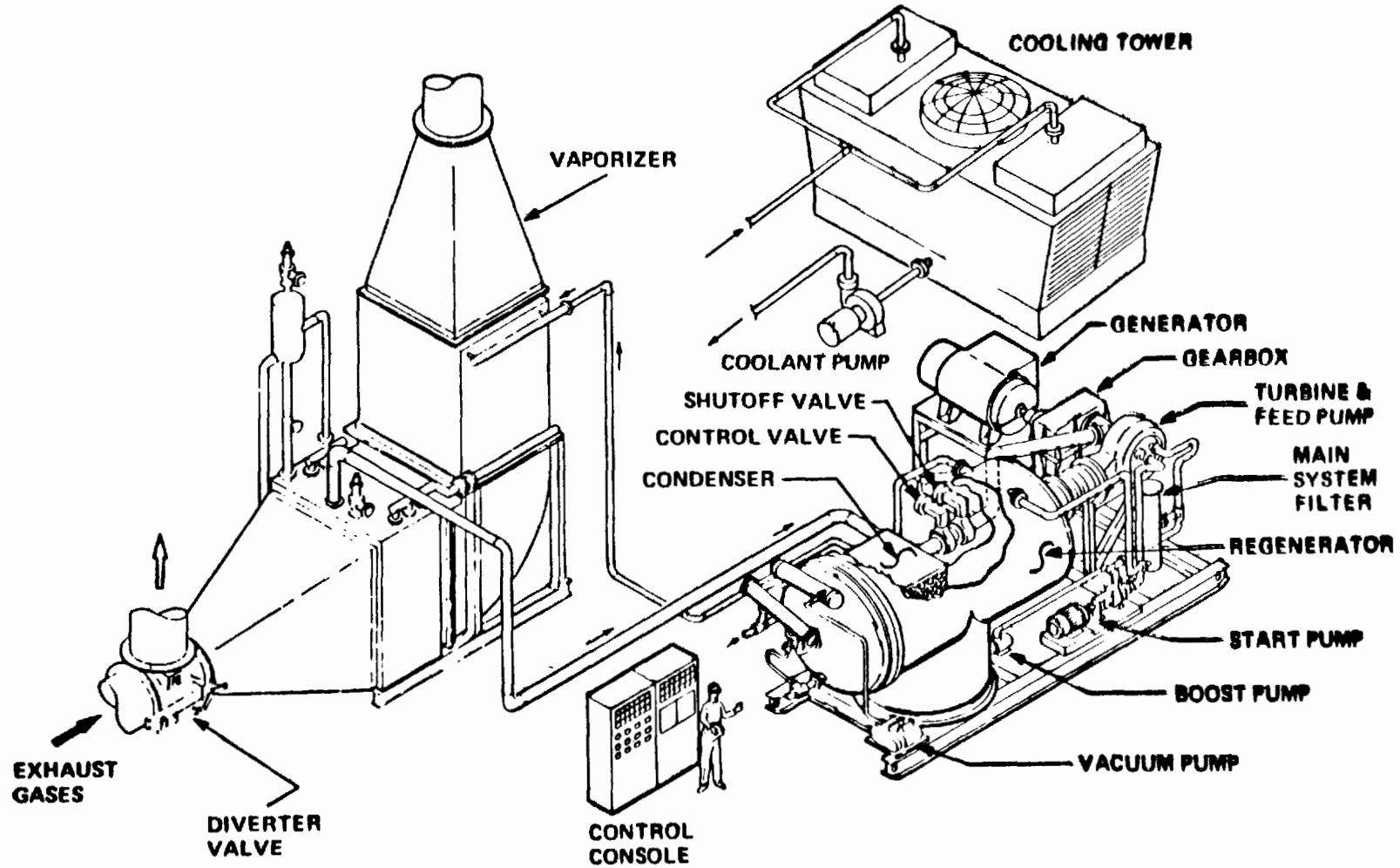


845

FIGURE 8

GS7900889/8-18

# 600 KW ORC Bottoming System



846

FIGURE 9

# Cycle Schematic For Binary System

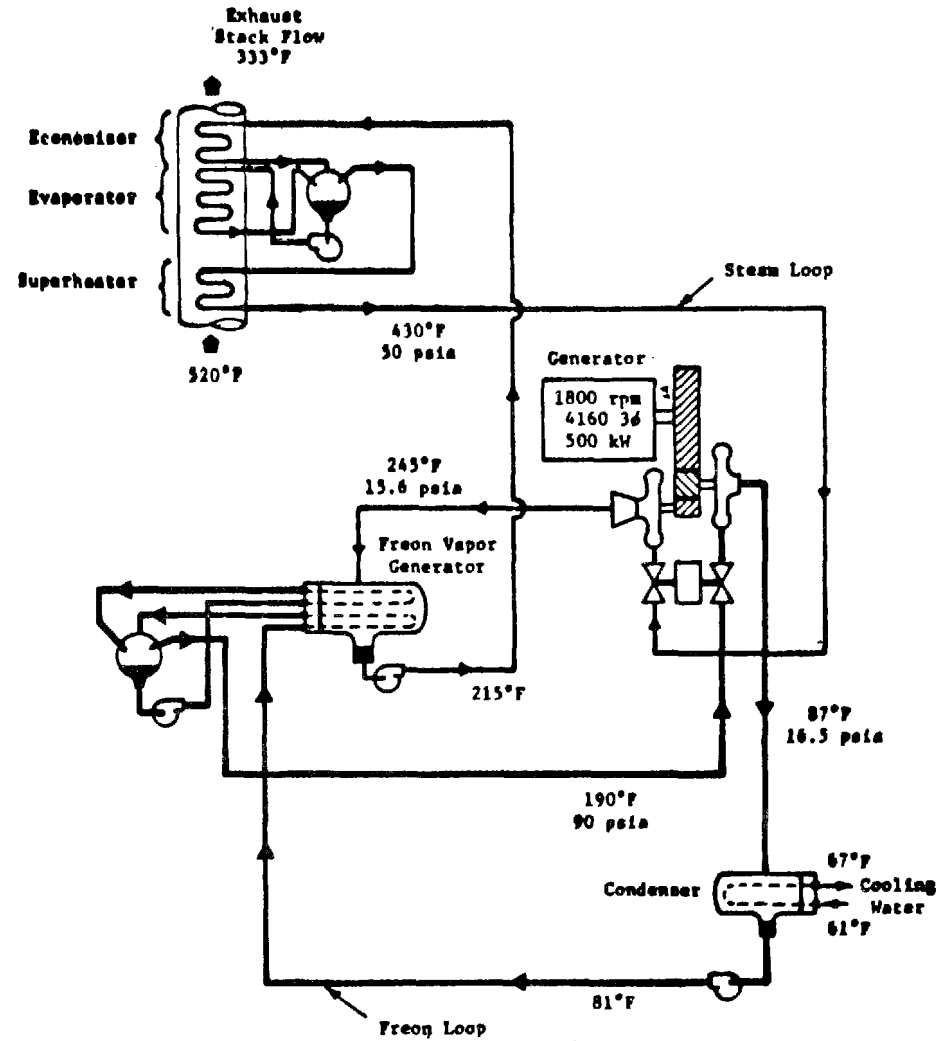
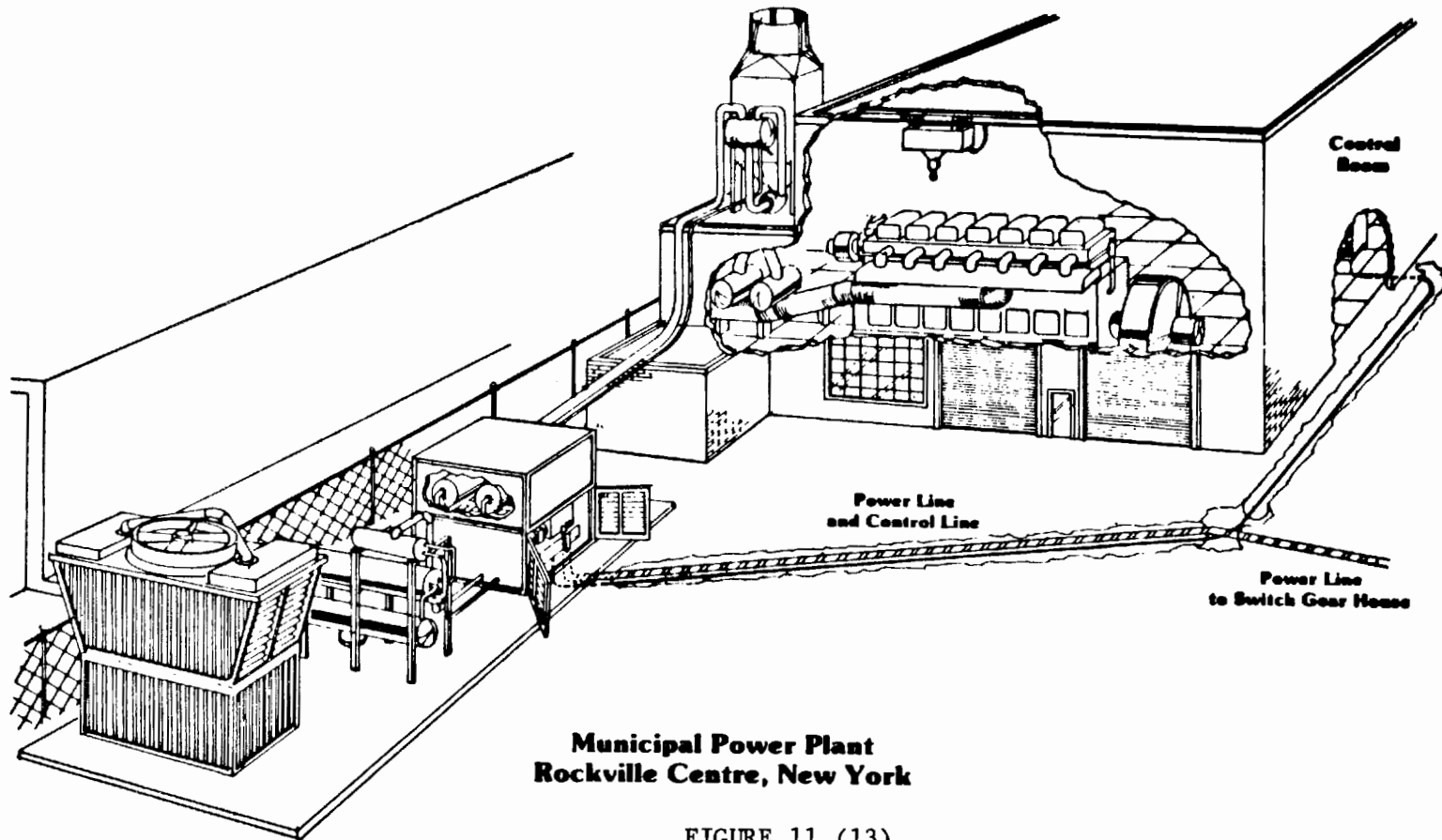


FIGURE 10

847

# General Arrangement of MTI Binary Rankine Cycle System for Waste Heat Recovery/Electric Power Generator

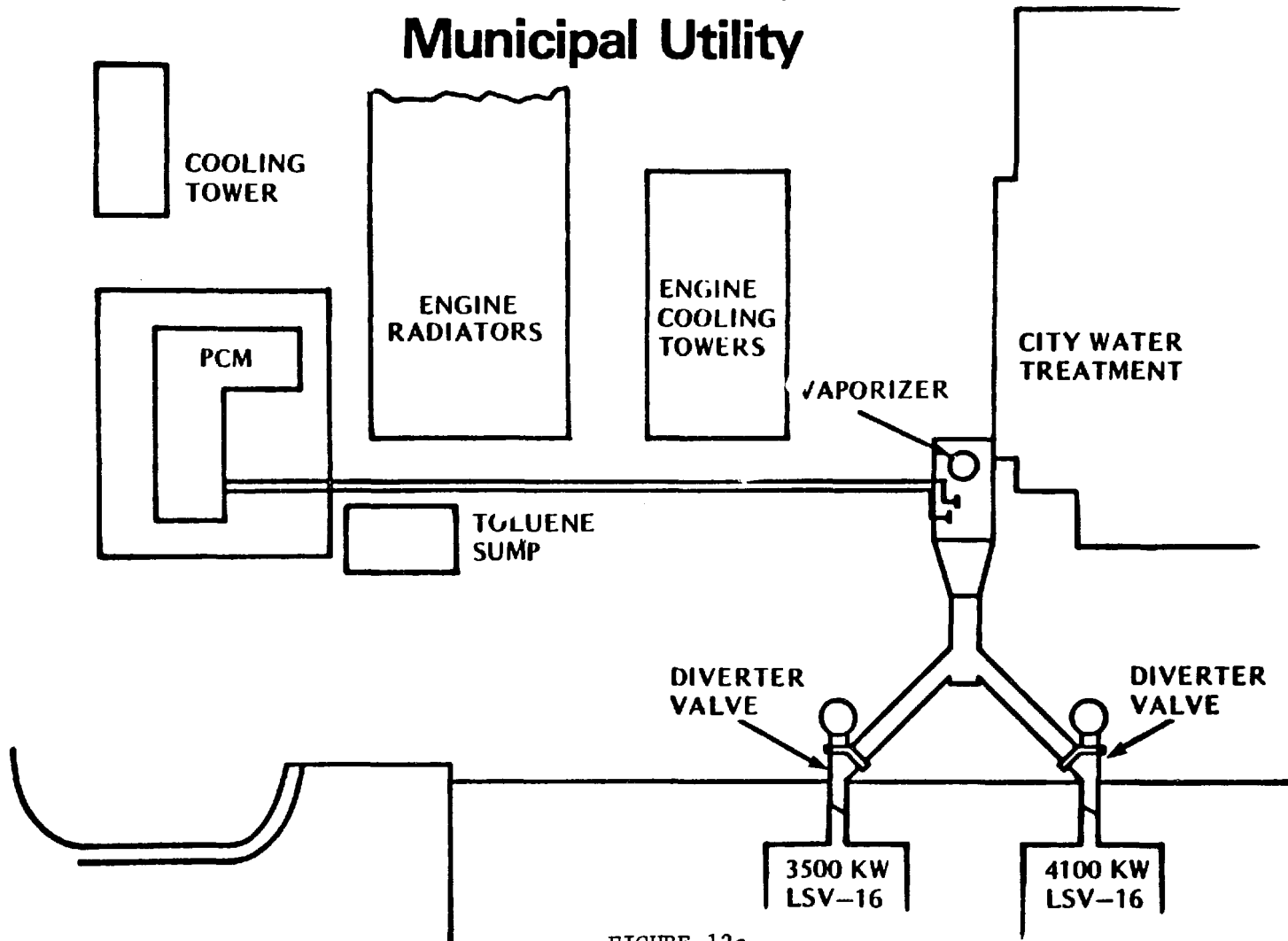
848



**Municipal Power Plant  
Rockville Centre, New York**

FIGURE 11 (13)

# Installation Schematic 600 KW ORC at Beloit, Kansas Municipal Utility



849

FIGURE 12a

G87900668/12-18

# Installation Schematic 600 KW ORC at Easton, Maryland Municipal Utility

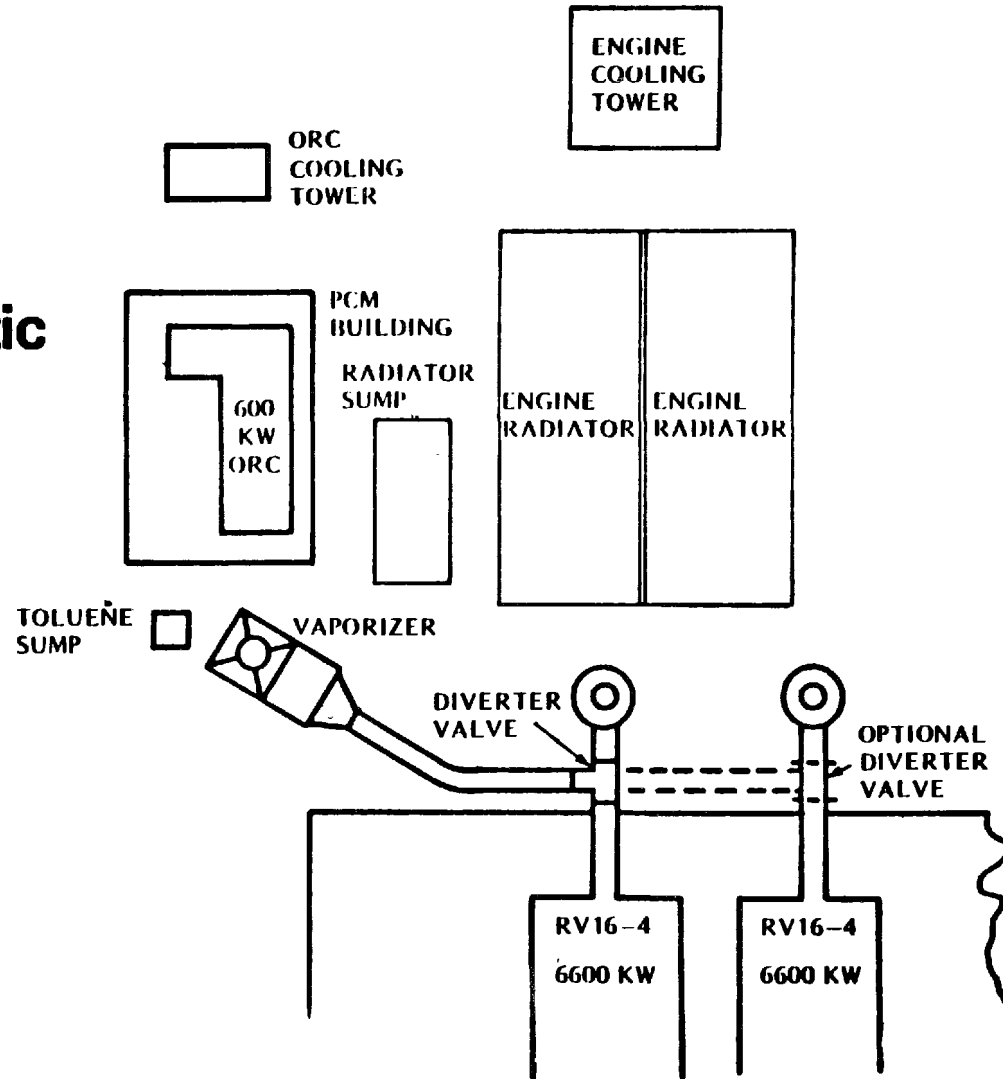


FIGURE 12b

**Installation Schematic  
600 KW ORC at  
Homestead, Florida  
Municipal Utility**

851

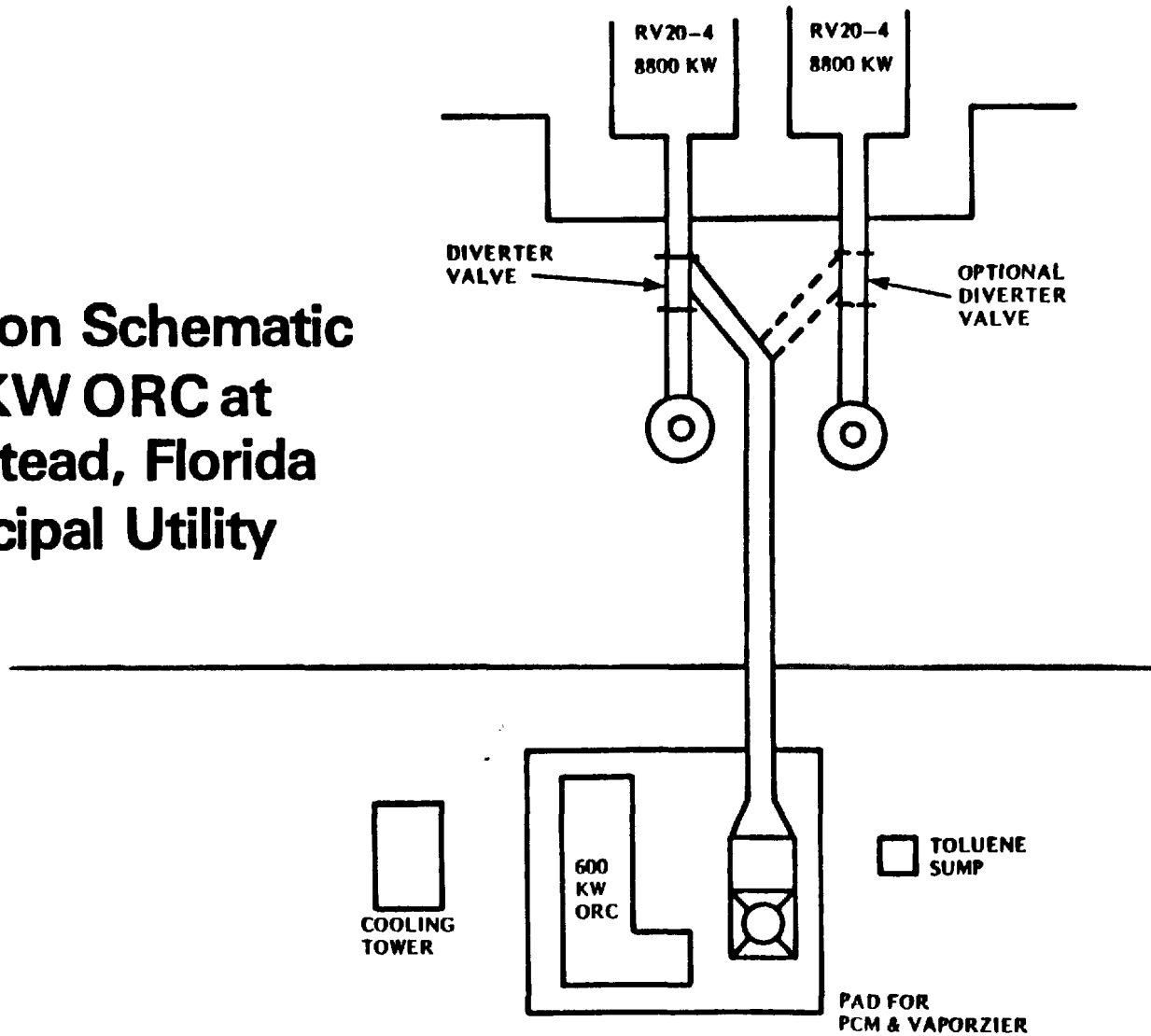


FIGURE 12c

# The Impact of Advanced Cogeneration on Emissions

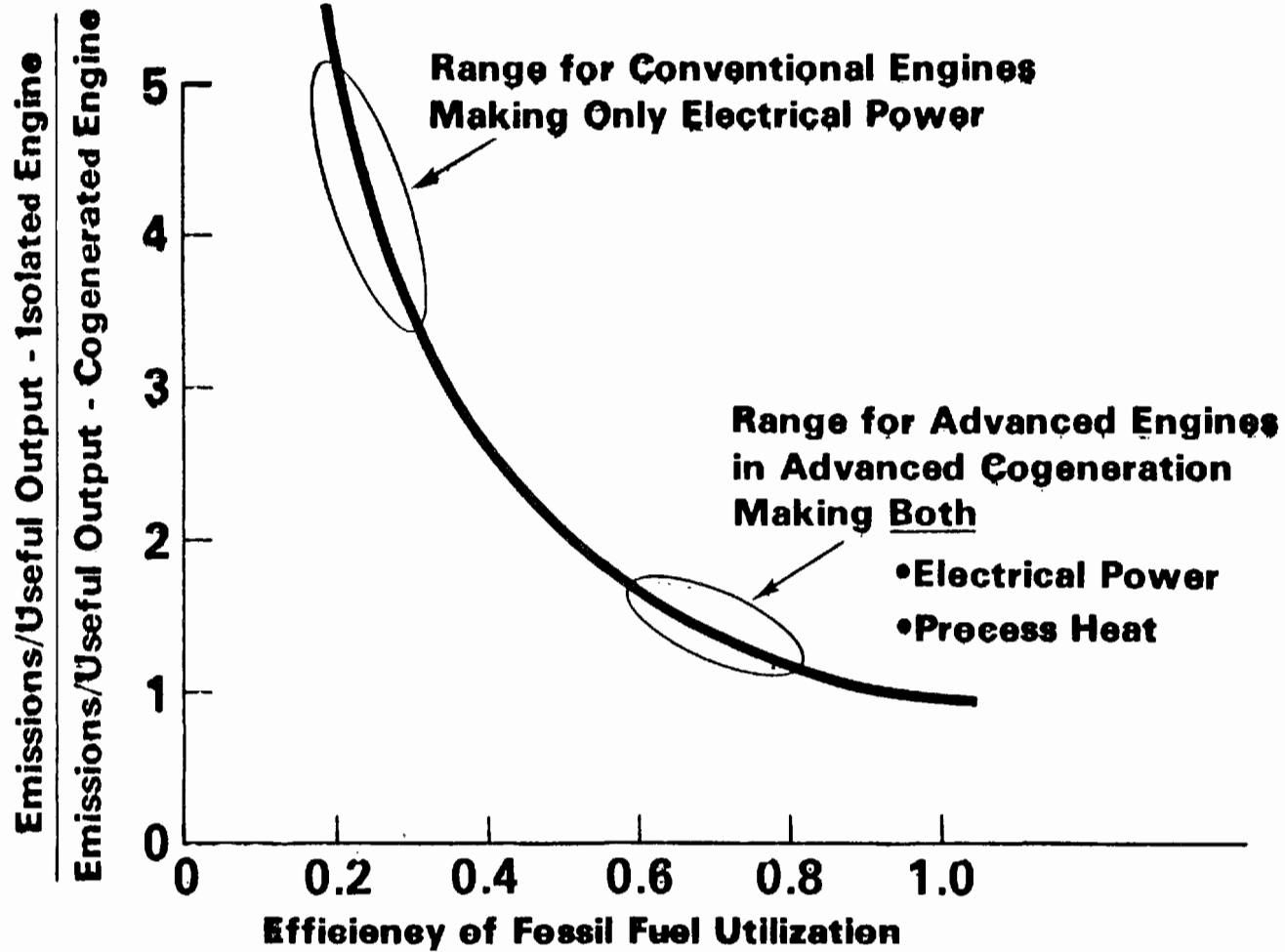


FIGURE 14

# Diesel Exhaust Analysis Summary

| Site   | Unit No. | Engine | Cycl | Load <sup>†</sup><br>kw | Exhaust <sup>†</sup><br>Temp.<br>°C (°F) | O <sub>2</sub> <sup>†</sup><br>(%) | CO <sub>2</sub> <sup>†</sup><br>(%) | H <sub>2</sub> O <sup>†</sup><br>(%) | Dupont   |  | Wet Chemistry  |  | Predicted<br>SO <sub>x</sub><br>Dry @<br>3% O <sub>2</sub> | Dew Point        |                               | P.R.T.<br>Meas. <sup>†</sup><br>°C (°F) | Chlorides <sup>†</sup><br>ppm | Smoke <sup>†</sup> | Solid<br>Part. <sup>†</sup><br>ng/J<br>(lb/MMBtu) |     |                |
|--|----------|--------|------|-------------------------|--|------------------------------------|-------------------------------------|--------------------------------------|--|--|--|--|--|------------------|-------------------------------|---|-------------------------------|--------------------|---|-----|----------------|
|  |          |        |      |                         |  |                                    |                                     |                                      | SO <sub>2</sub><br>ppm<br>Dry @<br>3% O <sub>2</sub> | SO <sub>2</sub><br>ppm<br>Dry @<br>3% O <sub>2</sub> | SO <sub>3</sub><br>ppm<br>Dry @<br>3% O <sub>2</sub> | SO <sub>3</sub><br>ppm<br>Dry @<br>3% O <sub>2</sub> |  | Calc.<br>°C (°F) | Meas. <sup>†</sup><br>°C (°F) |   |                               |                    |   |     |                |
|  |          |        |      |                         |  |                                    |                                     |                                      |  |  |  |  |  |                  |                               |   |                               |                    |   |     |                |
| 1.<br>Fuel No. 2<br>Ash<br>< 0.001%<br>Sulfur<br>0.40% | 12       | EMD    | 12   | 950                     | 327<br>(620)                             | 14.8                               | 4.3                                 | 5.5                                  | 605  | (172)  | 2.8  | 8.   | 236  | 117<br>(243)     |                               |   | 0.16                          | 4.5                | 12.6<br>(0.029)                                   |     |                |
|  |          |        |      | 1450                    | 382<br>(720)                             | 12.6                               | 5.7                                 | 5.2                                  | 394  | (182)  | 2.7  | 5.6 <sup>•</sup>                                     | 237  | (242)            |                               |   | 0.91                          | 6.5                | 18.2<br>(0.042)                                   |     |                |
|  | 8        | EMD    | 16   | 1378                    | 360<br>(680)                             | 9.4                                | 7.5                                 | 7.0                                  | 315  | -  | 0.89   | 2.9  | 236  | 113<br>(236)     | Ambient Chlorides             |   | 1.0                           | 9.5                | 36.7<br>(0.091)                                   |     |                |
| 2.<br>Fuel No. 6<br>Ash<br>0.002%<br>Sulfur<br>0.80%   | 6        | DE     | 16   | 5830                    | 462<br>(845)                             | 11.0                               | 6.5                                 | 5.2<br>(4.2*)                        | 483  | 456  | 5.3  | 13.4   | 472  | 120<br>(249)     | 177<br>(242)                  | 104<br>(220)                            |                               | 5.5                | 59.0<br>(0.14)                                    |     |                |
|  |          |        |      | 3000                    | 421<br>(790)                             | 12.4                               | 5.6                                 | 4.5<br>(3.9*)                        | 487  | 494  | 3.5  | 9.1  | 467  | 116<br>(241)     | 112<br>(234)                  | 93-102<br>(200-215)                     | 5.4                           | 8.0                | 73.8<br>(0.17)                                    |     |                |
|  | 5        | DE     | 16   | 5870                    | 416<br>(780)                             | 11.8                               | 6.3                                 | 4.9<br>(4.2*)                        | 449  | 444  | 3.7  | 8.8  | 471  | 117<br>(242)     | 114<br>(238)                  | 102<br>(215)                            | 2.9                           | 5.0                | 80.6<br>(0.19)                                    |     |                |
|  |          |        |      | 5870                    | 241<br>(465)                             | 12.2                               | 5.9                                 | 4.8                                  | 503  | 438  | 3.1  | 6.6  | 470  | 117<br>(242)     | 118<br>(240)                  | 102<br>(215)                            | Ambient Chlorides             |                    | 1.2   | 5.0 | 28.4<br>(0.07) |
| 3.<br>Fuel No. 2<br>Ash<br>< 0.001%<br>Sulfur 0.05%    | 7        | CB     | 20   | 6600                    | 442<br>(830)                             | 11.3                               | 6.4                                 | 7.2                                  | 261  | 36   | 0.98   | 1.86   | 44   | 113<br>(235)     | 96<br>(209)                   | -                                       | 4.3 <sup>§</sup>              | 5.0                | 9.8<br>(0.023)                                    |     |                |
|  |          |        |      | 3500                    | 407<br>(765)                             | 12.3                               | 6.7                                 | 6.3                                  | 226  | 43   | 1.7  | 3.6  | 44   | 113<br>(236)     | 97<br>(207)                   | -                                       | 1.6 <sup>§</sup>              | 4.5                | 7.4<br>(0.017)                                    |     |                |

( ) Shell-Emeryville Method.

† Measured values.

§ Corrected for ambient.

• Corrected moisture.

FIGURE 15

# Fluid Study Bottoming Cycle

| Characteristic  | 2-Methyl Pyridine                       | Fluorinal 85                               | Fluorozene M              | Pentafluorobenzene Hexafluorobenzene | Toluene (Methyl Benzene)                                   |
|---|---|--|---------------------------|--------------------------------------|--|
| <b>Toxicity TLV OSHA/NIOSH Class</b>  | 5PPM Toxic                              | 10PPM Toxic                                | N.A. Toxic                | <20PPM Toxic                         | 200PPM Toxic   |
| <b>Availability Quantity</b>  | Large                                   | Medium (22,000 lbs/yr)                     | Large                     | 3500 Lb                              | Unlimited  |
| <b>Cost - \$/Gal</b>  | 4.80                                    | 35.00                                      | 25.00                     | 233.00                               | 2.50   |
| <b>Materials Vessels</b>  | No copper mixture                       |  |                           | Stainless Steel                      |  |
| <b>Seals</b>  | EPR, ECD-008                            | EPR  | Fluorocarbon              | Fluorocarbon                         | Fluorocarbon   |
| <b>Flammability Flash Point Fire Point Auto Ignition Point Products of Combustion</b>   | 88°F<br>145-150°F<br>900°F<br>Non-toxic | 105°F<br>180°F<br>900°F<br>Toxic           | 110°<br>227°F<br>Toxic    | None<br>None<br>None<br>Toxic        | 40°F<br>40°F<br>1025°F<br>Non-toxic                        |
| <b>Vapor Pressure PSIA @ 70°F</b>   | 1.59                                    | 1.0  | 0.28                      | 3.28                                 | 0.4588   |
| <b>Max. Operating Temp °F</b>   | 675-750                                 | 550-575                                    | 650-700                   | 900-1000                             | 750-800  |
| <b>System Efficiency Heat Source Exh. Temp °F Turbine Inlet Temp °F Condenser Temp °F <math>\eta</math> = Elect. Power Sys mCphs (755-240)*</b> | 248<br>675<br>167<br>.192               | 248 300<br>550 550<br>181 140<br>.188 .151 | 390<br>600<br>190<br>.161 | 315<br>600<br>189<br>.170            | 300 300 342<br>650 465 550<br>150 140 140<br>188 1621 1638 |
| <b>Total Heat Exchanger Volume - Cu.Ft.</b>   | 200                                     | 185 226                                    | 209                       | 277                                  | 255 225 271  |

\*Based on optimized single stage turbine:  $\eta$  Feed Pump - 0.6,  $\eta$  Generator - 0.95,  $\eta$  Gearbox - 0.96

FIGURE 16

## THERMAL STORAGE FOR INDUSTRIAL PROCESS AND REJECT HEAT

R. A. Duscha and W. J. Masica  
NASA Lewis Research Center  
Cleveland, Ohio U.S.A.

### ABSTRACT

Industrial production uses about 40% of the total energy consumed in the United States. The major share of this is derived from fossil fuel. Potential savings of scarce fuel is possible through the use of thermal energy storage (TES) of reject or process heat for subsequent use. Results of study contracts awarded by the Department of Energy (DOE) and managed by the NASA Lewis Research Center have identified three especially significant industries where high temperature TES appears attractive - paper and pulp, iron and steel, and cement. Potential annual fuel savings with large scale implementation of near-term TES systems for these three industries is nearly  $9 \times 10^6$  bbl of oil.

### INTRODUCTION

One of the many responsibilities of the Department of Energy (DOE) is administering the Voluntary Business Energy Conservation Program. This program, under the guidelines of the 1975 Energy Policy and Conservation Act, requires major energy consuming firms within industries for which energy efficiency improvement targets have been set to report directly to DOE on their energy efficiency. The fact that industrial production uses about 40% of the total energy consumed in the United States indicates the tremendous potential that exists for significant energy savings through a concerted effort by all concerned.

Major energy consuming industries, arranged by the two-digit Standard Industrial Classification (SIC) Code, were assigned 1980 goals for improvement in energy efficiency over their 1972 base level. As of the first six months of 1977, the index of energy efficiency was at an estimated 9.2 per cent above the 1972 base level [1]. Although very encouraging in regards to the overall energy savings implicit in this index, the decline in the use of natural gas was offset by an increase in the use of fuel oil.

As with every major problem, the solution for achieving maximum energy savings lies in many approaches. One approach, known for decades but relegated to the sidelines because of the past availability of relatively cheap energy in the United States, is the recovery and use of industrial waste heat. Recognizing the increased importance of waste heat

recovery and use, the former Energy Research and Development Administration (ERDA) funded a study to determine the economic and technical feasibility of thermal energy storage (TES) in conjunction with waste heat recovery [2]. This study was directed toward identifying industrial processes characterized by fluctuating energy availability and/or demand, a key criterion for TES applicability.

At least 20 industries were identified as areas where thermal energy storage had potential application to some degree. Responses to a Program Research and Development Announcement (PRDA) issued by ERDA shortly after the conclusion of the feasibility study program resulted in contract awards to study three industries in the high temperature (>250°C) TES area with potential significant energy savings. These industries were paper and pulp, iron and steel, and cement. DOE's Division of Energy Storage Systems awarded the contracts, and the NASA Lewis Research Center provided the technical management. Major emphasis was given to TES systems and applications that have potential for early commercialization within each specific industry.

#### PAPER AND PULP

The forest products industry, as a whole, is one of the largest users of fossil fuels for in-plant process steam generation. Boeing Engineering and Construction, with team members Weyerhaeuser Corp. and SRI International, investigated the application of process heat storage and recovery in the paper and pulp industry [3]. For this investigation, Weyerhaeuser's paper and pulp mill at Longview, Washington [4] was selected to assess the potential energy savings and to evaluate the effectiveness of thermal energy storage in achieving these savings.

The paper and pulp operation at Longview consists of process systems and a power plant which supplies steam to the processes and the power generation turbines. Figure 1 shows schematically the energy supply characteristics without energy storage. The recovery (liquor-kraft black and sulfite from conventional chemical wood pulping) and waste (hog fuel-wood waste produced by the various machining processes) boilers provide a base load of steam generation while the oil/gas boilers provide the time dependent load. The primary goal of using thermal energy storage at Longview (and similar paper and pulp mills throughout the industry) is to substitute usage of more hog fuel for the oil/gas fossil fuels.

The inability to follow rapidly changing steam demands with hog fuel boilers requires the reduction of hog fuel firing in favor of increased fossil fuel firing. However, this can be overcome by the use of thermal energy storage. The hog fuel boiler would be operated at a higher base

load, the excess steam would be stored when the demand is low, and storage would be discharged when the demand is high. The economics of steam swing smoothing in the paper and pulp industry depends on the capacity of the swing smoothing system and the number of hours per year the system will allow hog fuel substitution for fossil fuel.

Daily operational data from the Longview plant was used to evaluate the effectiveness of thermal energy storage. This plant was considered representative of paper and pulp mills where the potential exists for the economic use of thermal energy storage. The analyses using this typical mill data indicated that for a system as shown on Figure 2, a storage time of about 0.5 hours with a steaming rate capacity of 100,000 lb/hr would result in 60,000 lb/hr of steam load transfer from fossil fuel boilers to the hog fuel boiler. This corresponds to about a 50% reduction in fossil fuel consumption for load following.

Initial sizing and cost estimates for storage system concepts were generated for a range of steaming rates and storage times. The results indicated that for storage times less than one hour, direct storage of steam using a variable pressure steam accumulator was more economically attractive than indirect sensible heat storage using media such as rock/oil or rock/glycol combinations.

Figure 3 shows the variable pressure accumulator TES concept. Steam used for charging storage from either the high pressure or intermediate pressure header bubbles through the saturated water contained under pressure in the vessel. The steam condenses and transfers energy to the water, raising the water's temperature and pressure. Upon discharging to the low pressure header, the steam pressure above the water surface is reduced causing the water to evaporate, supplying steam but lowering the water's temperature and pressure.

Oil savings estimated for the Longview plant is 100,000 bbl/yr based on the transfer of 60,000 lb/hr of steam load from the fossil fuel boilers to the hog fuel boiler. A survey performed using data supplied by the American Paper Institute indicated that there are 30 candidate mills that either have now or will have by 1980, operating characteristics similar to the Longview plant. Therefore, potential near-term (1985) fossil fuel savings are projected as being  $3 \times 10^6$  bbl/yr.

Energy resource and environmental impact studies completed by SRI International indicates potential long-term (2000) fuel savings of  $18 \times 10^6$  bbl/yr based on a 10% shift in steam generation from gas and oil to hog fuel and coal due to TES use. This also takes into account the additional cogeneration accompanying this shift and the resultant decrease in purchased electricity. This displacement of gas and oil will decrease the national sulfur dioxide emissions but will result in an increase in the nation's particulate emissions - roughly two pounds of SO<sub>2</sub> removed for each pound of particulate added.

Preliminary economic evaluation shows a potential return on investment (ROI) for this TES system in excess of 30% over a 15-year return and depreciation period. The conceptual system using a steam accumulator appears technically and economically feasible. Because of the availability of all the required technology, implementation would not require technology development or a reduced scale technology validation. Installation at full scale in one of the candidate mills utilizing commercially available equipment could be accomplished within a two-year time period for a cost of less than one million dollars.

## IRON AND STEEL

The primary iron and steel industry accounts for about 11% of the total national industrial energy usage. Rocket Research, with team members Bethlehem Steel Corporation and Seattle City Light, investigated the use of thermal energy storage with recovery and reuse of reject heat from steel processing in general and electric arc steel plants specifically [5]. Thermal analysis of the complex heat availability patterns from steel plants indicates significant potentially recoverable energy at temperatures of 600 to 2800°F.

A detailed assessment for Bethlehem's Seattle scrap metal refining plant was made of the energy sources, energy end uses, thermal energy storage systems, and system flow arrangements. This plant is typical of electric arc furnace installations throughout the United States, allowing results of this site-specific study to be extrapolated to a national basis.

The hot gas in the primary fume evacuation system from a pair of electric arc steel remelting furnaces was selected as the best reject energy source. Presently, the dust laden fume stream is water quenched and then ducted to the dust collection system prior to discharge to the atmosphere. The new flow arrangement shown in Figure 4 would have the unquenched fume stream flowing through the energy storage media prior to discharge. The solid sensible heat storage media would have to be able to withstand the hot gas temperature which could be as high as 3000°F while averaging about 1750°F. Potential materials are refractory brick, slag or scrap steel.

Two energy storage beds are required. The operational storage bed serves to time average the widely fluctuating temperature of the energy source. The peaking storage bed serves to hold energy until the demand arises. During charging, all of the furnace-gas discharge flow goes through both storage beds and is exhausted through the baghouse, the dust collection system.

During peak demand periods, the combined streams from the furnace (through the operational storage) and the peaking storage (in a

reversed flow direction) would flow through the heat exchanger to create steam to drive the turbogenerator. Upon initial discharge of the peaking store, ambient air is drawn in through the lower fan/valve arrangement. When the required flow rate through the peaking bed is established, the ambient air valve is closed. At the exit of the heat exchanger, gas flow is divided, with a portion going to the baghouse and the rest providing the peaking storage discharge gas stream.

To complement the assessment, Seattle City Light provided data on electricity costs. The economic benefits to be derived from the use of energy storage to provide peak power generation is a direct function of either a demand charge, time of day pricing, or a combination of both. The conceptual system proposed for the Bethlehem plant would result in a payback period of about five years depending on the combination of electricity costs and size of the power generation equipment. For example, a system providing a four-hour peak storage capability and generating 7MW of peak demand electricity would result in a five-year payback period if it were displacing peak power at a cost of 10¢/kwh.

Assuming fossil fuel is required to produce peak power, annual oil savings attributed to TES at a plant with a daily production of 1200 tons for 300 days/yr would be about 16,000 bbl. The potential electric arc steel industry annual oil savings could approach  $2 \times 10^6$  bbl based on a projected annual production of  $50 \times 10^6$  tons by 1985. In this case, there would be a direct reduction in sulfur dioxide emissions without an associated increase in particulates as for the paper and pulp projections.

The TES concept development in this study yielded favorable predictions of fossil fuel displacement and investment returns. However, the approach isn't ready to be applied directly to a full scale demonstration without an interim concept development period. Experimental scale studies of large, granular masses in the high temperature region (up to 1500°F) are required. Data from these studies would provide design criteria needed to verify analytical models for high temperature applications. The effect of the particulates in the furnace exhaust stream on the heat storage media must also be determined and resolved if detrimental. Successful completion of such a development phase could lead to a small scale demonstration followed by a full-scale system demonstration in an operating electric arc steel plant. Such a program would take about 8 years and cost between 5 and 10 million dollars.

## CEMENT

The cement industry is the sixth largest user of energy in the United States. Eighty percent of the energy used is consumed as fuel for the kiln operation. Martin Marietta Aerospace, with team members Martin Marietta Cement and the Portland Cement Association, investigated the

use of thermal energy storage in conjunction with reject heat usage in the cement industry [6]. Thermal performance and economic analyses were performed on candidate storage systems for four typical cement plants representing various methods of manufacturing cement. Basically, plants with long, dry-process kilns and grate-type clinker coolers offer the best choice for reject energy recovery.

An assessment of potential uses of the recovered energy determined that the best use for it would be in a waste heat boiler to produce steam for driving a turbogenerator to produce electricity for in-process use. Approximately 75% of a plant's electrical requirements could be met with on-site power generation. However, this reject heat source for the steam boiler is not available when the kiln is down for maintenance of either the clinker cooler grate or the kiln. At this time, the power demand for other cement plant operations must be obtained from a utility. This would require demanding large amounts of utility power for short periods of time, e.g. 5 to 10 MW for 2 to 24 hours. The cost to the plant in peak power rates and to the utility in maintaining excess peaking capacity is significant. The other alternative is to curtail other plant operations such as raw or finish milling.

This problem could be alleviated by using thermal energy storage to reduce the utility load demand. By charging the storage unit while the kiln is operating, the stored thermal energy would be available when the kiln is down. The storage concept proposed in conjunction with dry-process kilns uses a solid sensible heat storage material such as magnesia brick, granite, limestone, or even cement clinker. The storage system would use two separate thermal stores as shown on Figure 5. One would store high temperature (1500°F) reject heat from the kiln exit gas. The other would store low temperature (450°F) heat from the clinker cooler excess air. These two separate storages would be charged independently but discharged in series. Ambient air would be passed through the low temperature TES units and heated to about 400°F. It would then be heated to about 1200°F while passing through the high temperature TES units. The heated air would then flow through the waste heat boiler and generate steam to produce electricity.

Storage system sizing for typical cement plants indicates that provision for 24 hours of power production at about 10 MW would be a beneficial size in relation to normal plant operation. During kiln operation 80-90% of the kiln exit gas would go directly to the waste heat boiler to produce electricity while the rest would pass through the high temperature storage unit. Therefore, it would take roughly one week to charge the system to its full 24 hour withdrawal capacity.

An economic evaluation of the system indicates that a 10 MW waste heat boiler/power plant/TES installation would cost about 10 million dollars. A 90% ROI was calculated for a 30-yr system life and an average energy cost of 2.8¢/kwh. About 15% of this ROI can be attributed to the TES

system. Again, assuming fossil fuel is originally required to produce this waste-heat derived power, a potential energy savings of about  $4 \times 10^6$  bbl of oil per year is projected. This is based on utilizing the cement industry's current installations of about 120 long dry kilns. As with the steel industry storage/generation systems, this represents a potential direct reduction of sulfur dioxide emissions.

There is another similarity between the cement plant and steel plant systems. The necessity for a phased technology development and validation program through full scale demonstration also exists for the cement plant system. Estimates of 8 years and 5 to 10 million dollars appear to be valid for such a program.

#### SUMMARY

From the response to ERDA's FY 77 Industrial Applications PRDA, three attractive industries which could utilize high temperature thermal energy storage were selected for study. These industries are paper and pulp, iron and steel, and cement which account for 25% of the total national industrial energy usage. Potential annual fuel savings with large scale implementation of near-term thermal energy storage systems for these industries is nearly  $9 \times 10^6$  bbl of oil. This savings is due to both direct fuel substitution in the paper and pulp industry and reduction in electric utility peak fuel use through in-plant production of electricity from utilization of reject heat in the steel and cement industries. Economic analyses for all of these systems indicate potential return on investments from 30 to 90%.

#### CONCLUDING REMARKS

The results of these three studies appear to be so attractive that the question immediately arises - "If it looks so good, why aren't the industries involved already doing it on their own?" Perhaps the answer to this question can be found in a recent article on energy related capital investment [7]. The point being made in this article is primarily that most companies set the rate of return from energy-saving investments at a level about twice as high as that for mainstream business investments. Discretionary investments that do not increase productivity have a low priority. In addition, paper studies without the visible proof of a working demonstration do not stimulate the flow of working capital that is already in limited supply.

The ultimate objective of the effort summarized in this paper is the demonstration of cost-effective thermal energy storage systems capable of contributing significantly to energy conservation. To achieve this the Department of Energy's role is that of a catalyst to bring these

systems to the point that they will be accepted and widely implemented throughout the various industries. This effort has shown that a full scale working system for the paper and pulp industry could be available in the very near term at moderate cost. Other systems, although dependent on further technology development and significant capital investment, appear capable of being implemented within the next eight years.

#### REFERENCES

1. Voluntary Business Energy Conservation Program, Progress Report No. 6. U.S. Department of Energy (DOE/CS-0018/6), April, 1978.
2. Glenn, D. R.: Technical and Economic Feasibility of Thermal Energy Storage. General Electric Co., (COO-2558-1), 1976.
3. Carr, J. H.: Application of Thermal Energy Storage to Process Heat Storage and Recovery in the Paper and Pulp Industry. Boeing Engineering and Construction (CONS/5082-1), 1978.
4. Nanney, W. M.; and Gustafson, F. C.: Large Bark and Wood Waste-Fired Boiler - A Case History. Tappi, Journal of the Technical Association of the Paper and Pulp Industry, pp 94-97, Vol. 60, No. 8, August, 1977.
5. Katter, L. B.; and Peterson, D. J.: Applications of Thermal Energy Storage to Process Heat and Waste Heat Recovery in the Iron and Steel Industry. Rocket Research Co. (CONS/5081-1), 1978.
6. Jaeger, F. M.; Beshore, D. G.; Miller, F. M.; and Gartner, E. M.: Applications of Thermal Energy Storage in the Cement Industry. Martin Marietta Aerospace. (CONS/5084-1), 1978.
7. Hatsopoulos, G. N.; Gyftopoulos, E. F.; Sant, R. W.,; and Widmer, T. F.: Capital Investment to Save Energy, pp 111-122, Harvard Business Review, March-April, 1978.

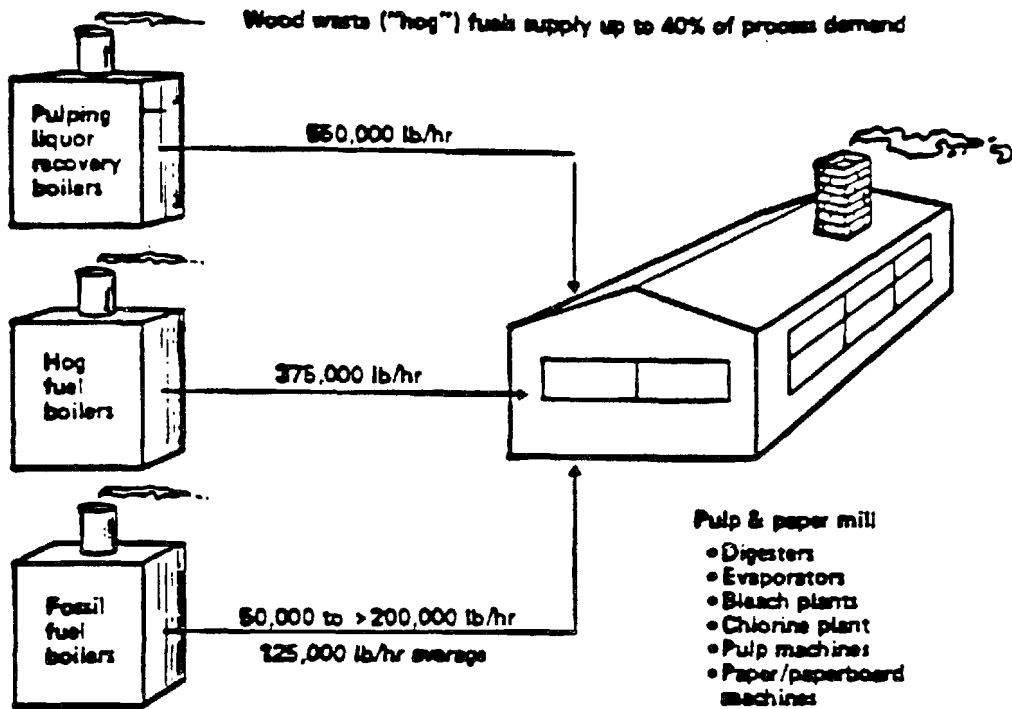


Figure 1. Paper and Pulp Energy Supply Characteristics

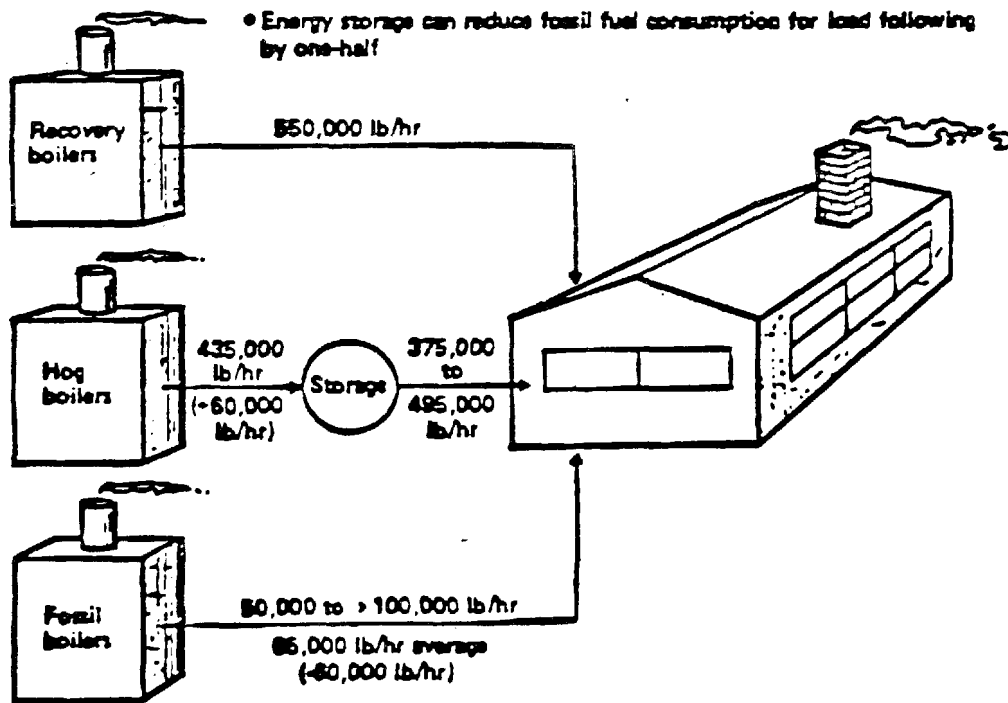


Figure 2. - Energy Supply With Thermal Energy Storage

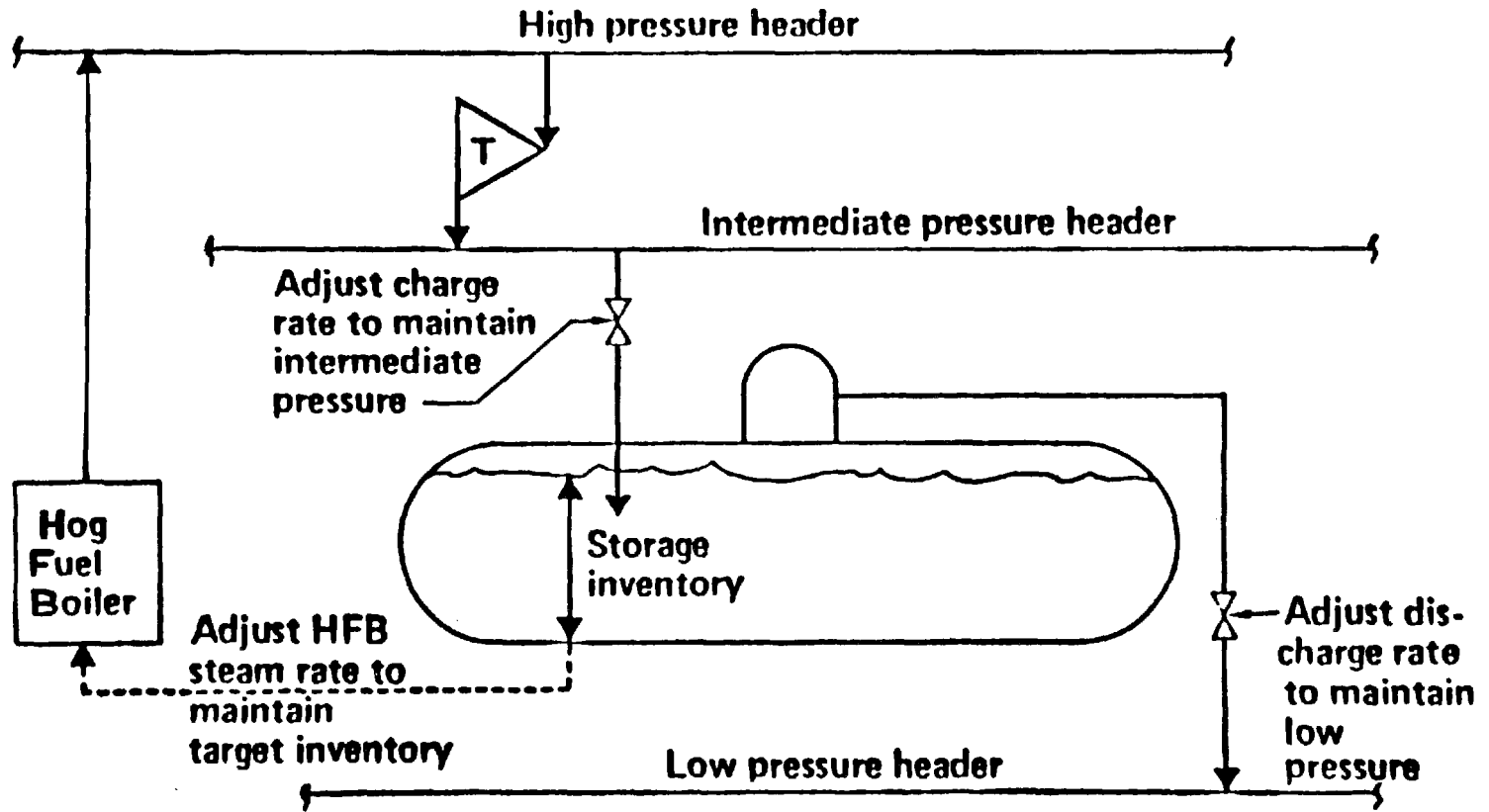


Figure 3. - Variable Pressure Accumulator TES Concept

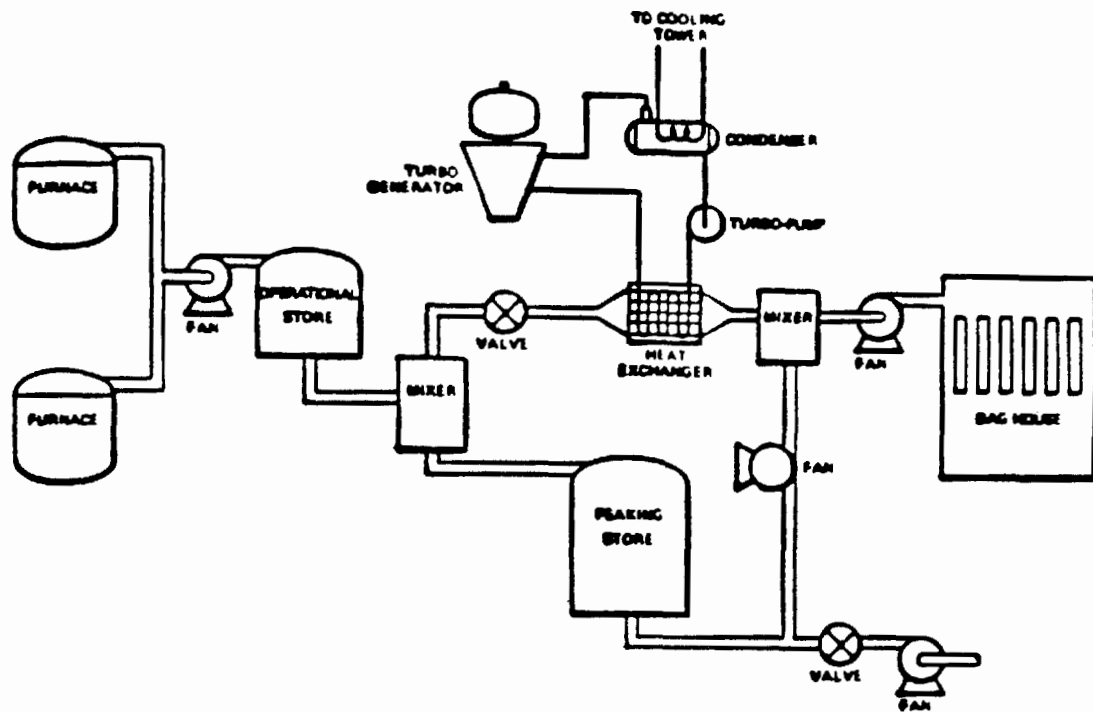


Figure 4. - Steel Arc Furnace Energy Recovery and Storage System

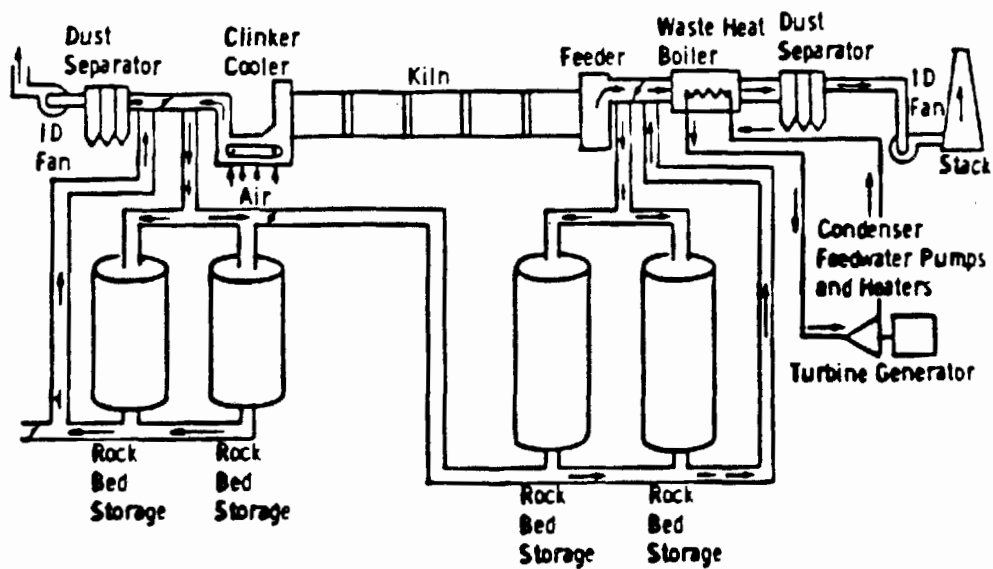


Figure 5. - Cement Plant Energy Recovery and Storage System

## PERFORMANCE AND ECONOMICS OF STEAM POWER SYSTEMS UTILIZING WASTE HEAT

J. P. Davis  
Thermo Electron Corporation  
Waltham, Massachusetts U.S.A.

### ABSTRACT

The performance and economics of steam systems for electric power generation from waste heat sources are discussed. A simple method for determining after-tax discounted return-on-investment is presented. General performance data for steam power systems utilizing waste heat are shown.

### INTRODUCTION

The majority of steam turbine systems utilized in industry for in plant electric power generation are of the back-pressure type, 600-1200 psig inlet steam, with or without intermediate pressure extraction as shown in Figure 1. Where condensing is employed, it is often for the purpose of affording some degree of flexibility over the power/steam ratio rather than a desire for substantial continuous power generation from condensing steam. This approach is usually correct when the steam is being generated by purchased fuel. The portion of the system which is in the condensing mode is essentially duplicating what the electric power utility is doing - and less efficiently than the utility.

However, when the heat source is combustion of waste materials, or lower temperature waste heat from process operations, or low pressure waste steam itself, the economics of condensing power are altered dramatically. Whereas combustion of purchased fuel to generate power exclusively, i.e. no process steam, is almost never competitive with purchased power; use of waste energy almost always results in a positive return-on-investment. Of course, whether or not that positive return is sufficiently high to warrant the investment is another story.

### ECONOMICS

Simple payback, i.e. the ratio of initial investment to pre-tax annual savings, is often used as a criteria for investment. Paybacks of 3 years or less are generally considered by industry to be reasonably attractive and worthy of further consideration. While this rule-of-thumb is a rough indication of economic desirability, it obviously does not give a true picture of worth for comparison to various other investment opportunities.

However, using this readily calculable parameter of payback based on first years's pre-tax savings it is possible to calculate equivalent after-tax discounted return-on-investment for a specific set of assumptions. Figure 2 shows the results for the following set of assumptions.

- . 50% tax rate
- . 20 year plant life
- . 15 year sum-of-digits depreciation
- . 10% investment tax credit
- . 6% savings escalation rate
- . Continuous cash flow model

It is interesting to note that, for this set of assumptions, the after-tax discounted return is approximately equal to the reciprocal of the pre-tax simple payback based on first year's savings.

Maintaining the above assumptions except for investment tax credit and assumed escalation rate, additional calculations yield the results shown in Figure 3.

The example shown in Figure 4 will show how these results are utilized.

Installed costs for steam power systems vary depending on the plant-specific situation, particularly power level, waste heat temperature, and retrofit installation requirements. Typical installed costs for (a) a 600°F gaseous waste heat source (with waste heat boiler), and (b) 15 psig waste steam (without waste heat boiler) are shown in Figure 5 for condensing non-extraction systems.

For those situations where waste heat can be utilized for both electric power and process steam, in either of the configurations shown in Figure 1, the economics can be extremely favorable, in some cases yielding paybacks in the 1-2 year range. Installed costs for such systems are highly application-specific and cannot readily be generalized.

#### PERFORMANCE

Typical steam rates for a 1500 kWe system condensing at 3" HgA (115°F) are shown in Figure 6. Performance is improved for higher power systems and/or lower condensing temperatures, and conversely for lower power systems and/or higher condensing temperatures.

The range of frame sizes and maximum output capabilities available are shown in Figure 7. A typical condensing system, fully integrated and skid mounted, is shown in Figure 8. All systems can be substantially derated with small loss in efficiency for lower power applications, although 500 kWe is roughly the lower limit for reasonable turbines.

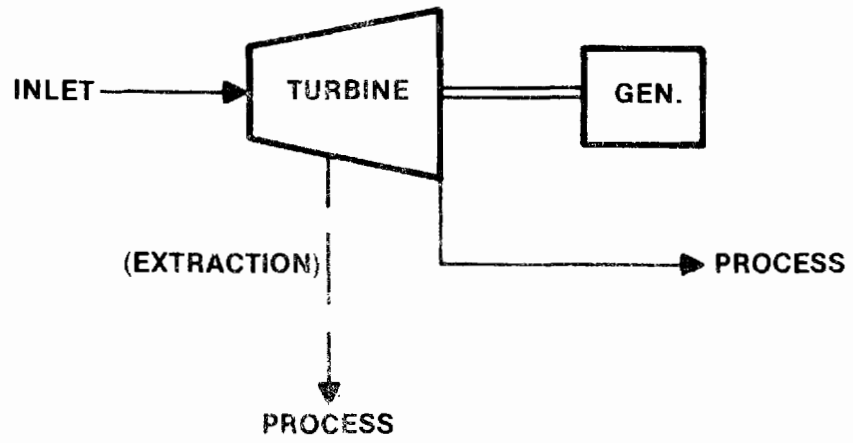
Smaller back-pressure turbines are available from others down to outputs of under 100 kWe.

For gaseous waste heat sources, approximate power generation capabilities for condensing non-extraction systems are estimated and shown in Figure 9. Calculations assume a 3" HgA condensing pressure and a fixed waste heat exhaust temperature of 350°F from the heat recovery boiler.

#### SUMMARY

The utilization of waste heat for electric power generation or combined process steam/electric power often results in attractive after-tax rates of return, particularly when anticipated escalation of costs of power and fuels is included in the analysis. In particular, condensing steam systems not competitive with purchased utility power when fired with conventional fuels become highly competitive in many situations. Economics generally dictate the lower limit of power output for these condensing systems in the range of 500-1000 kWe.

**BACK-PRESSURE STEAM TURBINE**



**CONDENSING STEAM TURBINE**

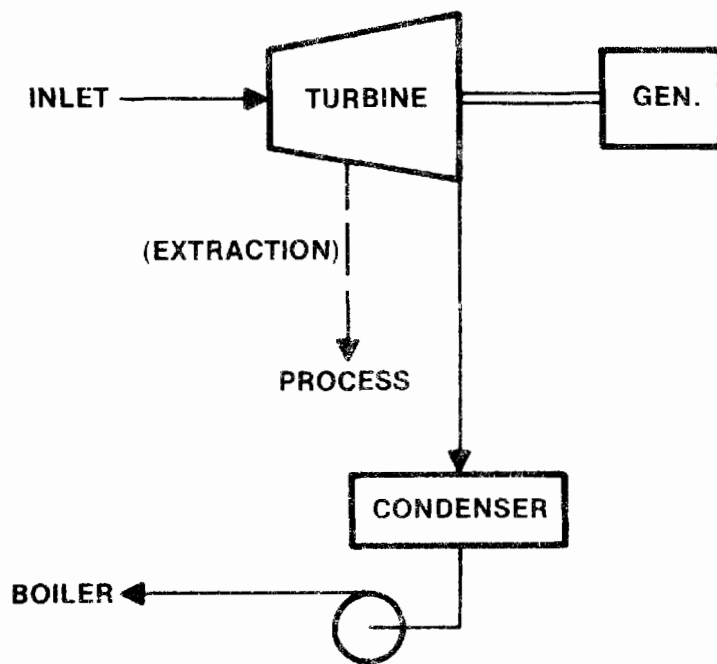


Fig. 1. Back-Pressure Steam Turbine

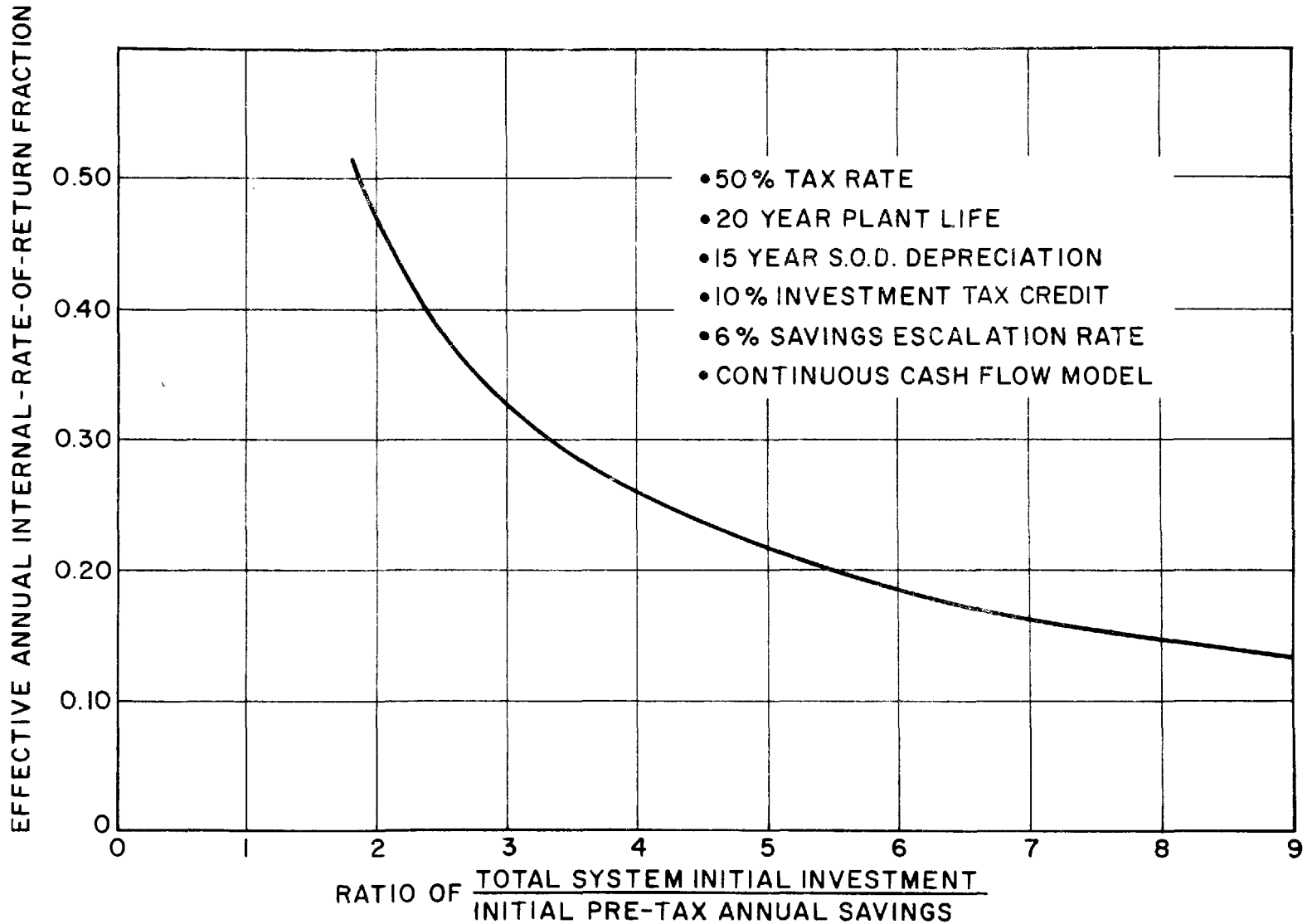


Fig. 2. Effective Annual Internal-Rate-Of-Return vs. Gross Payback Computed Based on First Year's Savings

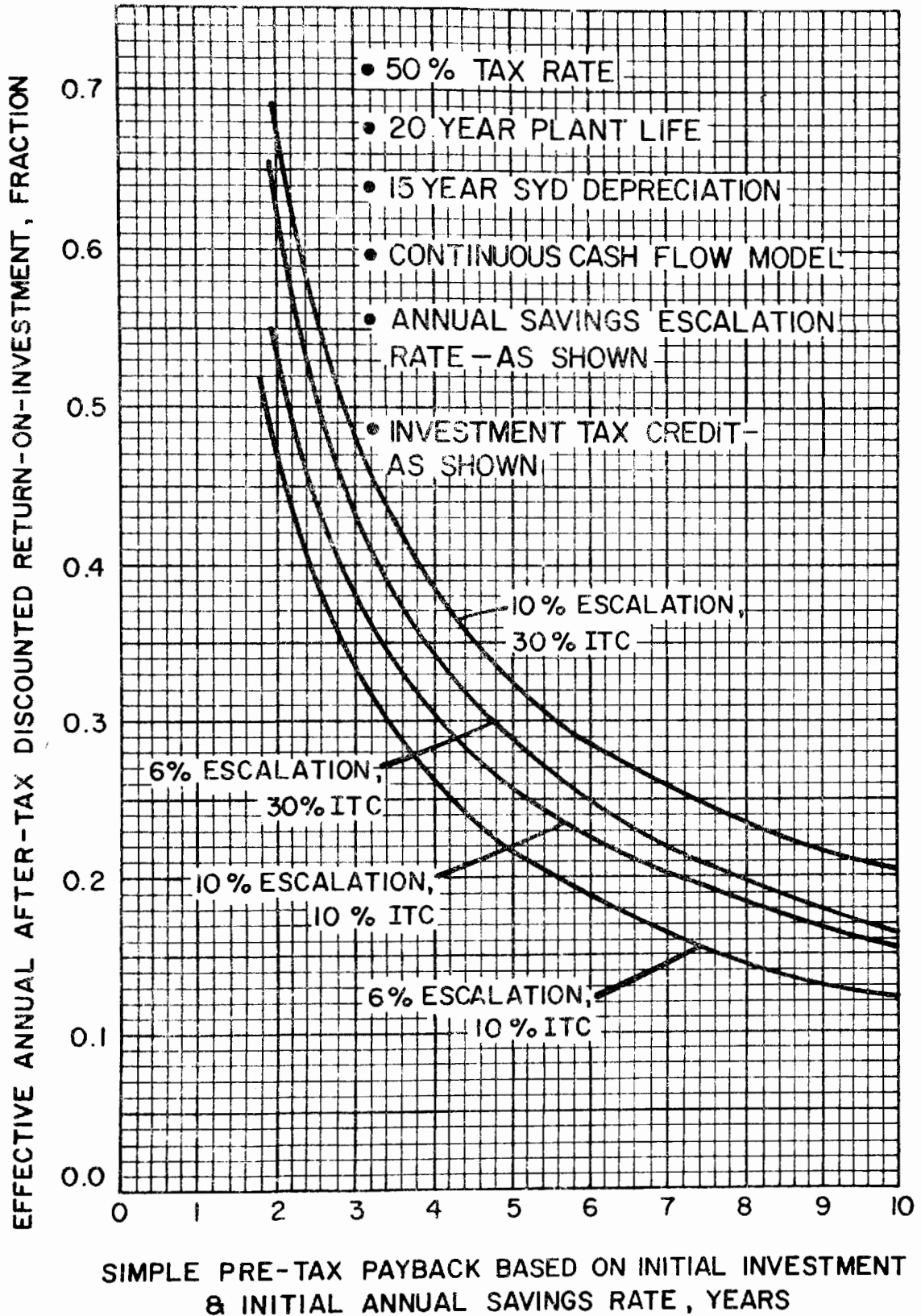


Fig. 3. Effective Annual After-Tax Discounted Return-On-Investment vs. Simple Pre-Tax Payback

|   |   |                             |
|---|---|-----------------------------|
| Thermal Source  | : | Waste Heat                  |
| Initial Investment  | : | \$650/kW                    |
| Electric Power Savings  | : | 3¢/kWh                      |
| First Year Full Power Hours   | : | 6000 hrs/yr                 |
| First Year Local Taxes, Insurance, Maintenance, Incremental Operating Labor | : | 5% of initial investment/yr |
| First Year Pre-tax Savings  | = | .03 x 6000 - .05 x 650      |
|   | = | 180 - 32.50                 |
|   | = | 147.50 \$/kW-yr             |
| Payback Based on First Year Savings   | = | $\frac{650}{147.50}$        |
|   | = | 4.41 years                  |

Assuming the assumptions shown in Figure 1 apply:

After-tax Discounted Return-on-Investment = 24%

Fig. 4. Sample Analysis

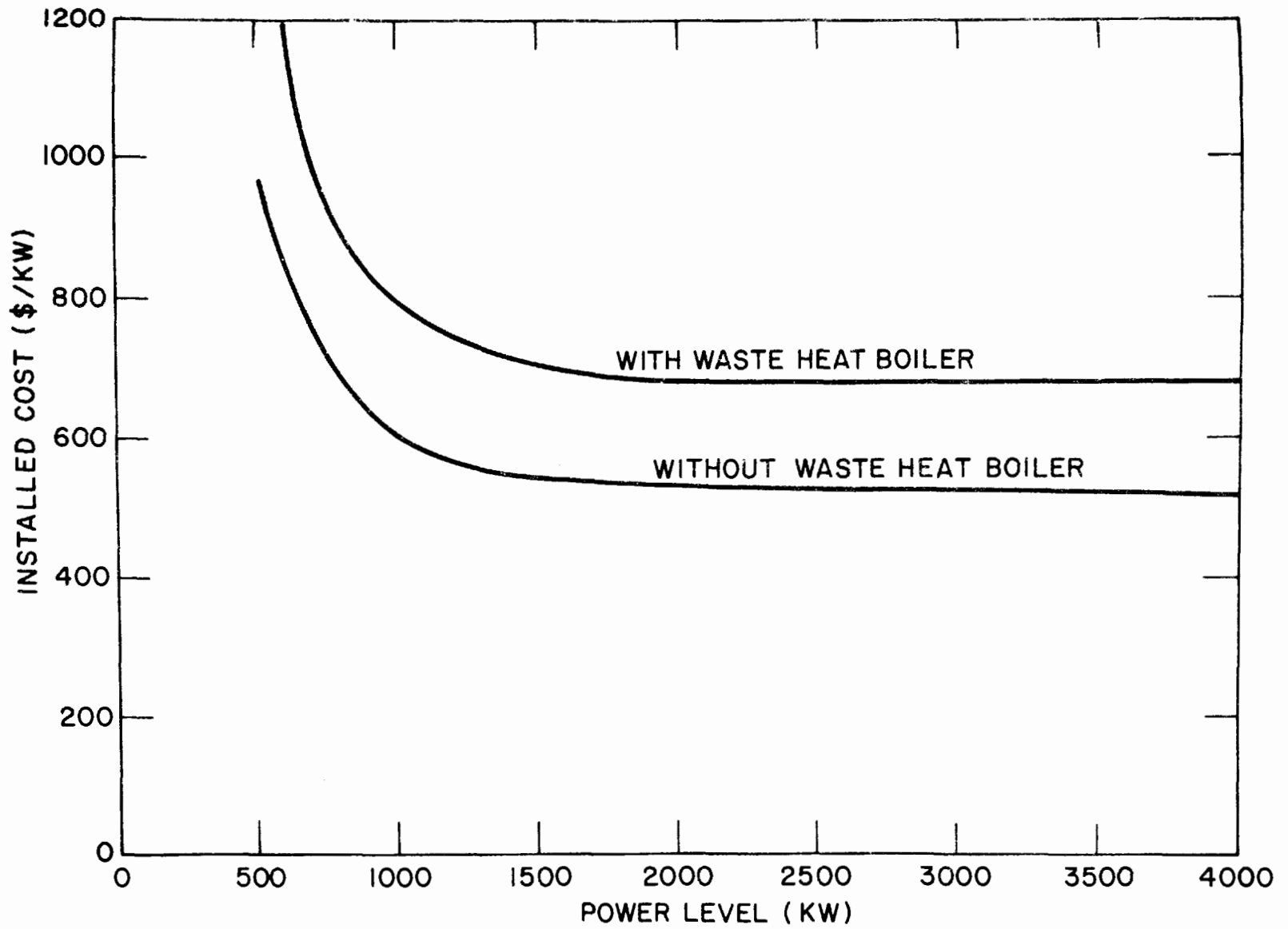


Fig. 5. Installed Power System Costs

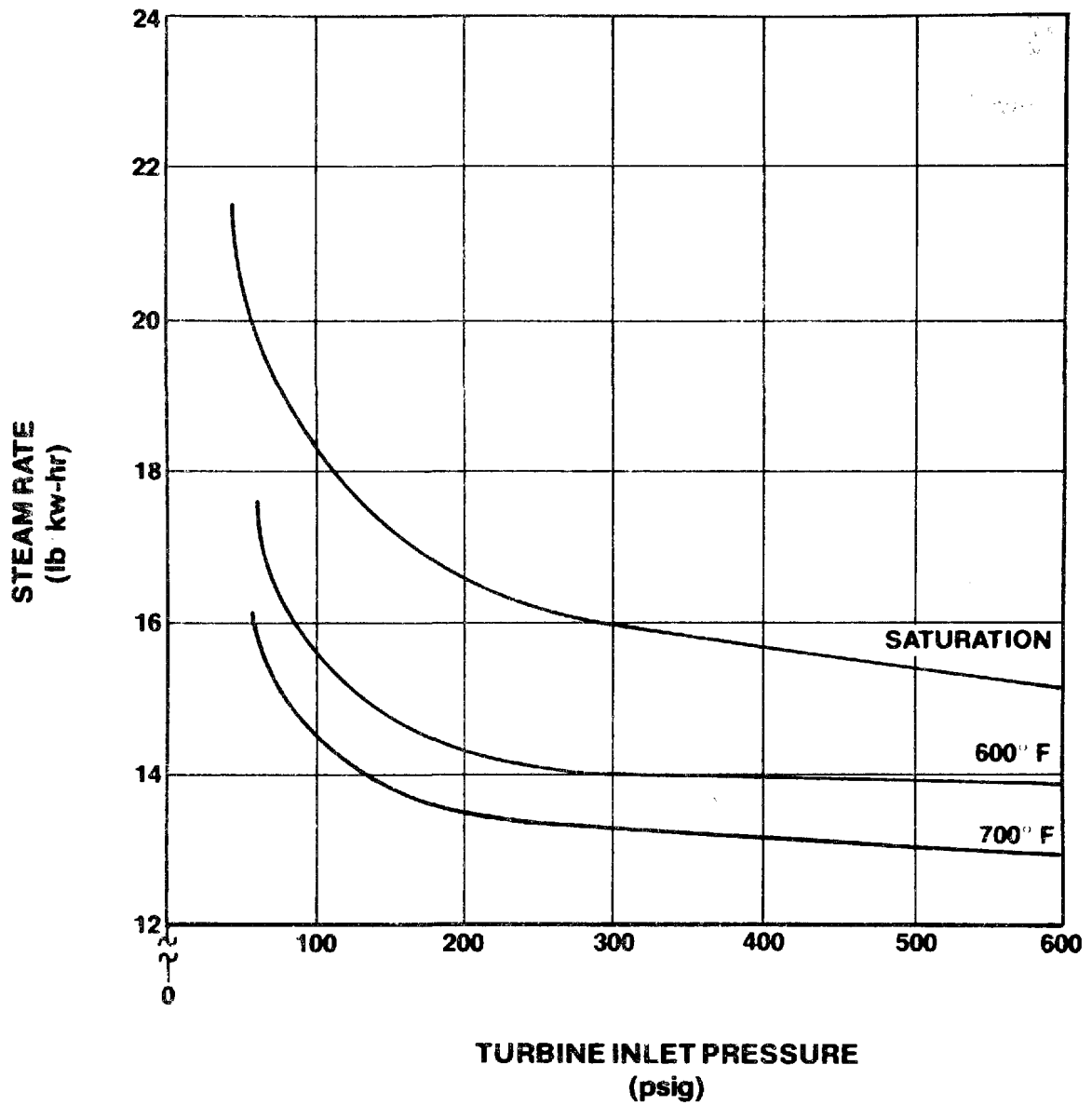


Fig. 6. Performance Data for Nominal 1500 kwe Thermo Electron Steam Power System ( $T_{\text{Condenser}} = 115^{\circ}\text{F}$ )

# Thermo Electron Corporation

## ENERGY SYSTEMS

### MAXIMUM CAPABILITIES OF MULTI-STAGE TURBINE FRAMES

| GEARED BACK PRESSURE TURBINES |               |            |             |                                  |                                 |
|-------------------------------|---------------|------------|-------------|----------------------------------|---------------------------------|
| Frame No.                     | Size (inches) | Power (MW) | Speed (rpm) | Inlet Steam Conditions (psig/°F) | Exhaust Steam Conditions (psig) |
| 9                             | 12            | 3          | 12,000      | 900/950                          | 60                              |
| 14(A)                         | 18/20         | 3          | 10,000      | 300/750                          | 30                              |
| 14(B)                         | 18/20         | 5          | 10,000      | 450/750                          | 50                              |
| 3                             | 18            | 5          | 10,000      | 900/950                          | 350                             |
| 4B                            | 18            | 7          | 8,500       | 350/650                          | 150                             |
| 4A                            | 18            | 10         | 8,500       | 900/950                          | 150                             |
| 1B                            | 24            | 11         | 6,600       | 350/650                          | 50                              |
| 1A                            | 24            | 15         | 6,600       | 900/950                          | 150                             |

| BACK PRESSURE/EXTRACTION TURBINES |               |            |             |                                  |                                 |                   |
|-----------------------------------|---------------|------------|-------------|----------------------------------|---------------------------------|-------------------|
| Frame No.                         | Size (inches) | Power (MW) | Speed (rpm) | Inlet Steam Conditions (psig/°F) | Exhaust Steam Conditions (psig) | Extraction (psig) |
| 2                                 | 18            | 8          | 8,500       | 900/950                          | 100                             | 250               |

| GEARED CONDENSING TURBINES |               |            |             |                                  |                 |
|----------------------------|---------------|------------|-------------|----------------------------------|-----------------|
| Frame No.                  | Size (inches) | Power (MW) | Speed (rpm) | Inlet Steam Conditions (psig/°F) | Vacuum (in. Hg) |
| 7A (IC)                    | 18/22         | 2          | 10,000      | 500/650                          | 1 ½             |
| 7B(SC)                     | 18/22         | 2          | 10,000      | 500/650                          | 1 ½             |
| 15A(IC)                    | 18/22         | 3          | 10,000      | 900/950                          | 1 ½             |
| 15B(SC)                    | 18/22         | 3          | 10,000      | 900/950                          | 1 ½             |
| 12(SC/DF)                  | 18            | 5          | 10,200      | 900/950                          | 1 ½             |

| DIRECT DRIVE CONDENSING TURBINES |               |            |             |                                  |                 |
|----------------------------------|---------------|------------|-------------|----------------------------------|-----------------|
| Frame No.                        | Size (inches) | Power (MW) | Speed (rpm) | Inlet Steam Conditions (psig/°F) | Vacuum (in. Hg) |
| 16(SC)                           | 18/22         | 3          | 10,250      | 900/950                          | 1 ½             |
| 12A(SC/DF)                       | 18            | 5          | 10,200      | 900/950                          | 1 ½             |

| GEARED CONDENSING/EXTRACTION TURBINES |               |            |             |                                  |                 |                   |
|---------------------------------------|---------------|------------|-------------|----------------------------------|-----------------|-------------------|
| Frame No.                             | Size (inches) | Power (MW) | Speed (rpm) | Inlet Steam Conditions (psig/°F) | Vacuum (in. Hg) | Extraction (psig) |
| 13(DF)                                | 18            | 5          | 10,000      | 900/950                          | 1 ½             | 100               |
| 17(DF)                                | 24/30         | 15         | 6,600       | 900/950                          | 1 ½             | 100               |
| 17A(DF)                               | 24/30         | 15         | 6,600       | 900/950                          | 1 ½             | 250               |

IC = Integral Condenser  
 SC = Separate Condenser  
 DF = Double Flow last stage

Fig. 7

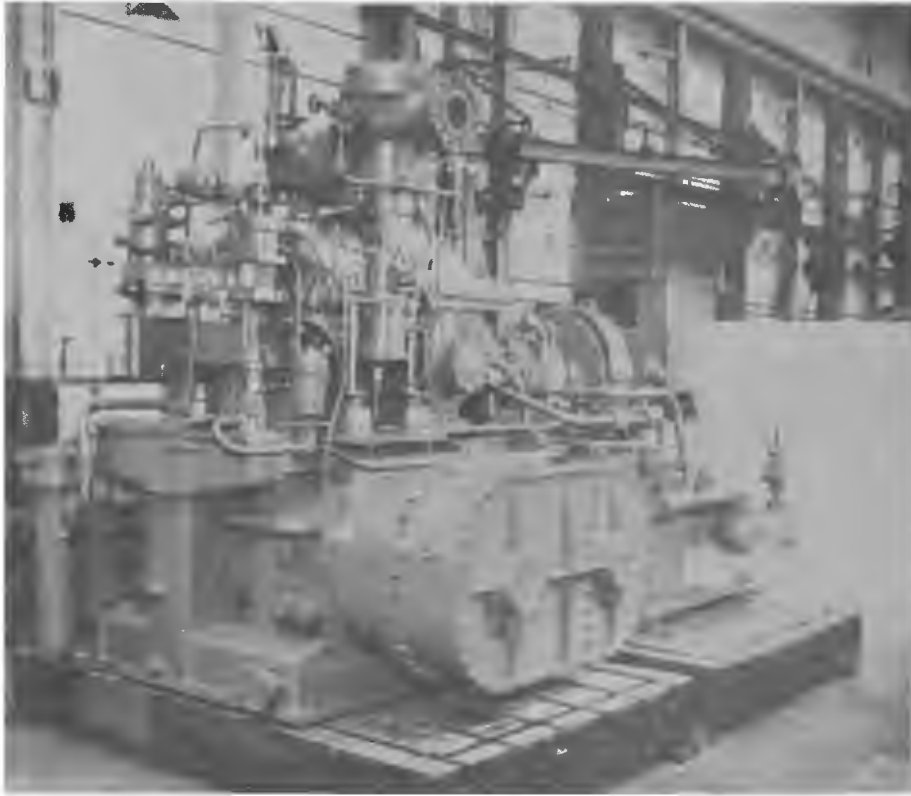


Fig. 8. Packaged Steam Power System

| Waste Heat<br>Inlet Temp.<br>(°F) | Steam<br>Pressure<br>(psig) | Steam<br>Temp.<br>(°F) | Power<br>Heat Recovered<br>(kWh/10 <sup>6</sup> Btu) | Heat Recovered*<br>Heat Available |
|-----------------------------------|-----------------------------|------------------------|--|-----------------------------------|
| 1000                              | 600                         | 900                    | 75.7   | 0.69                              |
| 800                               | 250                         | 700                    | 55.3   | 0.61                              |
| 600                               | 125                         | 500                    | 47.5   | 0.47                              |
| 400                               | 50                          | 298 (sat)              | 39.1   | 0.15                              |

$$\frac{\text{Heat Recovered}}{\text{Heat Available}} = 0.98 \left( \frac{T_o - 350}{T_o - 80} \right)$$

(Heat available above 80°F - no condensation)

Fig. 9. Power Generation Capability

A ONE-DIMENSIONAL VARIABLE CROSS-SECTION  
MODEL FOR THE SEASONAL THERMOCLINE

S. Sengupta, S. S. Lee and E. Nwadike  
University of Miami  
Coral Gables, Florida 33124

ABSTRACT

A 1-D model which assumes lateral uniformity is developed to study the seasonal temperature variations in a lake. The model includes the effects of variation of horizontal cross-sectional area with depth. The surface heating due to solar-radiation absorbed at the surface layer and the internal heating due to the transmission of the unabsorbed solar radiation to the deeper layers of the lake are also included. The exchange of mechanical energy between the lake and the atmosphere is accounted for through the friction velocity and eddy diffusivity under neutral conditions. The effects of power plant discharge and intake are also considered.

The equations describing the above model were solved by explicit finite-difference methods. The effects of thermal discharges on the turbulent diffusivity and thermocline formation are studied. The effects of the non-linear behavior of the eddy diffusivity on the overall stratification are also studied qualitatively and quantitatively. Model simulations have been compared to data acquired to Lake Cayuga. It is demonstrated that the inclusion of area change with depth has significant effect on temperature distributions at mid-depth. All prior models neglect this parameter.

A ONE-DIMENSIONAL VARIABLE CROSS-SECTION  
MODEL FOR THE SEASONAL THERMOCLINE

S. Sengupta, S. S. Lee and E. Nwadike  
University of Miami  
Coral Gables, Florida 33134

INTRODUCTION

In temperate regions most deep bodies of water develop a thermocline during their annual heating cycle. A warmer epilimnion at the top is isolated from a cooler hypolimnion below by severe stable thermal gradients. This stratification has a seasonal cycle, and is an important natural characteristic of a water body. The formation time phasing and the depth and severity of the thermocline are crucial factors affecting the bio-chemical processes in an aquatic ecosystem. The nutrient levels, species spectra and physical characteristics are quite different in the two distinct domains below and above the thermocline.

Convective transport and heat addition caused by power plant discharges result in disturbances in the thermocline. The seasonal phasing of thermocline formation and decay is affected by thermal discharge.

The formation of this stratification is caused by non-linear interaction between the wind generated turbulence and stable buoyancy gradients. While being heated from above, a basin forms stable stratification thereby inhibiting wind generated turbulence. The thermocline is a region of very stable buoyancy gradients and consequently low turbulence levels. Therefore, turbulent diffusion through the thermocline is minimal. Further heating merely

accentuates the warming of the upper layer and enhances the thermocline gradients. The temperature of the hypolimnion, therefore, remains almost constant. With the beginning of the cooling process in winter, unstable buoyancy gradients in the epilimnion augment the turbulent mixing caused by wind stress. Thus, the thermocline recedes downwards as the epilimnion cools finally resulting in overturn of the water in the lake. Near homothermal conditions result. The present paper presents a one-dimensional numerical model that simulates thermocline behavior and the impact of thermal discharges.

#### Previous Thermocline Studies

Numerous attempts in modeling the thermocline have been attempted. Most of these are one-dimensional time-dependent models. One of the earliest theories was presented by Munk and Anderson (1948). They formulated the vertical transport of heat and momentum as functions of shear generated turbulence and buoyancy effects. They proposed functional relationships between eddy transport co-efficients and Richardson number. They used these co-efficients in the steady state Ekman spiral formulation. The time-dependent features of the thermocline could not, therefore, be investigated. Kraus and Rooth (1961), studied the well-mixed layer above the thermocline for oceanic problems. They assumed exponential radiative flux with depth. They concerned themselves with the steady state energy balance in this layer. The surface temperature and the depth of the surface layer were numerically predicted with variations in atmospheric conditions. Some qualitative

transient analysis was also presented.

Kraus and Turner (1967), developed a one-dimensional model of the seasonal thermocline. They accounted for interaction of stratification and wind-generated turbulence by using the zeroth and first moments of the one-dimensional, time-dependent conduction equation and the equation for global conservation of turbulent energy. They assumed two well-mixed layers below and above the thermocline. They assumed that the temperature profiles could be represented by two parameters, namely the depth of the upper well-mixed layer and its temperature. Detailed analysis of the formation and destruction of the temperature profile over the season could not be adequately studied.

Dake and Harleman (1969), developed a theory for the thermocline based on exponentially decaying absorption of solar radiation with depth. Adequate representation of the turbulent transport and interaction with buoyancy field was not modeled. They predicted the formation of a thermocline only after the onset of cooling of the upper layers and consequent static instability and rapid mixing. In reality the thermocline forms sometime after the start of heating in spring and before the peak heating periods of summer.

Sundaram et al (1970, 1971, 1973), in a series of papers have presented a theory for the formation and sustenance of the seasonal thermocline. They also investigated the effects of thermal discharges. They solved the one-dimensional energy equation of the form:

$$\frac{\partial T}{\partial t} = \frac{\partial}{\partial z} \left( K_z \frac{\partial T}{\partial z} \right)$$

with  $K_z = K_{z0} (1 + \sigma_1 R_1)^{-1}$

and  $R_1 = \alpha_v g z^2 \frac{\partial T}{\partial z} / W^{*2}$

where T is the temperature, t is the time, z is the vertical distance from the surface,  $K_z$  is the vertical eddy transport coefficient.  $K_{z0}$  is the eddy diffusivity without stratification,  $\sigma_v$  is the volumetric coefficient of thermal expansion of water, g is the acceleration due to gravity and  $W^* = \sqrt{(\tau_s/\rho)}$  the friction velocity due to surface wind stress  $\tau_s$ ,  $\rho$  is the density and  $\sigma_1$  is an empirical constant. They compared their numerical results with observations in Lake Cayuga. The agreement was good. The positive feature of this model is the adequate formulation of the shear-generated turbulence and buoyancy effects. However, there are two aspects where improvement is essential. The surface boundary condition is taken similar to that suggested by Edinger and Geyer (1967), where the surface heat flux

$$q_s = K_s (T_E - T_s)$$

$q_s$  is the surface heat flux (downwards)  $K_s$  is the surface heat transfer coefficient,  $T_s$  is the surface temperature and  $T_E$  is the equilibrium temperature, or the temperature of the surface at which no heat flux occurs. The differential absorption of solar radiation with depth has been completely ignored.

Moore and Jaluria (1972), have studied the effects of thermal discharges on the vertical temperature profiles in lakes. They

assumed two well-mixed layers with the upper layer having a linear temperature gradient. This model is not adequate to study the temporal variation of temperature profiles during the formation of the thermocline.

More recently Roberts et al (1976), has used a higher order turbulent closure to study the effect of discharges on the oceanic thermocline. They developed a two dimensional model for an ocean thermal power plant. They ignored solar radiation absorption and were primarily concerned with the effect of discharges on a developed oceanic temperature profile.

Mitry and Ozisik (1976) have developed a two layer model for the thermocline. They applied their model to Lake Cayuga.

No single model to date includes all the pertinent effects viz.

- a) The effects of area change with depth.
- b) Nonlinear interaction of wind generated turbulence and buoyancy.
- c) Absorption of radiative heat flux below the surface.
- d) Thermal discharges.
- e) Effect of vertical convection caused by discharge.

The model presented in this paper includes all these effects.

### Model Formulation

The basic balance equations of mass and heat are:

$$\frac{\partial \rho}{\partial t} = -\bar{\nabla} \cdot \rho \bar{V} \quad (1)$$

$$\frac{\partial}{\partial t} (\rho C_p T) = \bar{\nabla} \cdot \rho C_p \bar{K} \cdot \bar{\nabla} T - \bar{\nabla} \cdot \rho C_p T \bar{V} + H \quad (2)$$

where

- $\rho$  is the density
- $t$  time
- $I$  velocity of flow
- $C_p$  the heat capacity
- $T$  the temperature
- $K$  heat diffusivity tensor (including turbulent diffusivity)
- $H$  source of heat per unit volume.

There are at least two reasons for the existence of horizontal divergence in real lakes.

- a) The variation of horizontal cross-sectional area of the lake with depth.
- b) The existence of sources of heat and matter efflux at depths above the deepest point.

The need to include these in the diffusion equations of lakes was already felt by Lerman and Stiller (1969), Dutton and Bryson (1962) and Tzur (1973). Only Tzur (1973) formulated a corrected diffusion equation. The effects of area change with depth are included by the following treatments of equations (1) and (2). Integrating equation (1), over the volume of water below height  $h$ , measured from the deepest point in the lake;

$$\int_V \frac{\partial \rho}{\partial t} dV = - \int_V \bar{\nabla} \cdot \rho \bar{V} dV$$

Using Gauss theorem on left hand side;

$$\int \frac{\partial \rho}{\partial t} dV = -\rho \int \hat{n} \cdot \bar{V} dS$$

where  $S$  is a surface completely surrounding the volume  $V$ , hence  $dS=dc + dA$

where  $c$  is the surface area of the part of the bottom of the lake that is bounded by the contour at height  $z$ . As  $s$  subscript it marks a variable at the contour.

Using,  $dV=Adz$  in equation (3),

$$\int_0^h \frac{\partial \rho}{\partial t} Adz = - \rho \int \hat{n} \cdot \bar{V} dc - \rho \int_A \hat{n} \cdot \bar{V} dA$$

or

$$\int_0^h \frac{\partial \rho}{\partial t} Adz = - \rho V_z A(h) - \int_0^h \rho V_n dc \quad (4)$$

Integrating equation (2), over the volume of water below height  $h$ , measured from the deepest point of the lake,

$$\int_V \frac{\partial}{\partial t} \rho C_p T dV = \int_V (\bar{v} \cdot \rho C_p \bar{K} \cdot \bar{v} T) dV - \int_V \bar{v} \cdot \rho C_p T \bar{V} dV + \int_V H dV$$

Applying the divergence theorem to the first two terms on the right,

$$\int_0^h A(z) \frac{\partial}{\partial t} \rho C_p T dz = \int_S \hat{n} \cdot (\rho C_p \bar{K} \cdot \bar{v} T) dS - \int_S (\hat{n} \cdot \rho C_p T \bar{V}) dS + \int_0^h A(z) H(z) dz$$

Using  $dS=dA + dc$

$$\int_0^h A(z) \frac{\partial}{\partial t} \rho C_p T dz = \int_0^h (\rho C_p \bar{K} \cdot \bar{v} T)_z dA + \int_0^h (\rho C_p \bar{K} \cdot \bar{v} T)_n dc - \int_0^h (\rho C_p T \bar{V})_z dA - \int_0^h (\rho C_p T \bar{V})_n dc + \int_0^h A(z) H(z) dz$$

i.e.

$$\int_0^h A(z) \frac{\partial}{\partial t} \rho C_p T dz = \rho C_p A(h) \{ \bar{K} \cdot \bar{\nabla} T \}_z + \int_0^h \rho_c C_{p_c} \{ \bar{K} \cdot \bar{\nabla} T \}_n dc - \rho C_p A(h) T V_z - \int_0^h \rho_c C_{p_c} T V_n dc + \int_0^h A(z) H(z) dz \quad (5)$$

where

$z$  is the vertical coordinate, measured upward from the deepest point of the lake. As a subscript it marks the vertical component of a vector.

$n$  subscript, marks the component of a vector that is perpendicular to the lake-bottom, positive outwards.

$A(z)$  is the horizontal cross-section of the lake at height  $z$ .

Differentiating equations (4) and (5) with respect to the height, a set of 1-D equations are obtained,

$$A \frac{\partial \rho}{\partial t} = - \frac{\partial}{\partial z} A \rho V_z - \rho_c V_n \frac{\partial c}{\partial z}$$

$$\text{or } A \frac{\partial \rho}{\partial t} = - \frac{\partial}{\partial z} A \rho V_z + I A' \quad (6)$$

where  $I \equiv$  the bottom-surface source of mass per unit area.

$$\text{and } A' = \frac{dA}{dz} \approx \eta \frac{dc}{dz}$$

Where  $\eta \approx 1$ , is the average of the cos-arc-tan (gradient) of the bottom surface at that depth

$$\text{i.e. } A' = \frac{dc}{dz}$$

From equation (5), and noting that  $A=A(z)$  and  $H=H(z)$ ;

$$A \frac{\partial}{\partial t} (\rho C_p T) = \frac{\partial}{\partial z} \rho C_p A (K \cdot \nabla T)_z - \frac{\partial}{\partial t} \rho C_p A T V_z + [\rho_c C_{p_c} (\bar{K} \cdot \bar{\nabla} T)_n - \rho_c C_{p_c} T V_n] \frac{dc}{dz} + A H \quad (7)$$

The terms in the square brackets are the heat addition terms. Because the horizontal gradients vanish, equation (7) can be simplified further by noting that:

$$(\bar{K} \cdot \bar{\nabla}T)_z = K_z \frac{\partial T}{\partial z}$$

$$A \frac{\partial}{\partial t} (\rho C_p T) = \frac{\partial}{\partial z} (\rho C_p A K_z \frac{\partial T}{\partial z}) - \frac{\partial}{\partial z} (\rho C_p A T V_z) + Q A' + A H \quad (8)$$

where,  $Q$  = the bottom-surface source of heat per unit area.

Equations (6) and (8) are the equations to be solved. Before attempting to solve these equations numerically, the relevant terms and parameters will be discussed.

The numerical values represent the Lake Cayuga application presented in subsequent sections.

1. Density,  $\rho$  is assumed to vary with temperature in the form

$$\rho = A' + B'T + C'T^2$$

where  $A'$  = Density at  $0^\circ\text{C}$

$$= 1.02943 \text{ gm/cc}$$

$$B' = -0.00002$$

$$C' = -0.0000048$$

This is the form given by Sengupta and Lick (1974).

2. Eddy diffusivity,  $K_z$  is a function of both thermal and current structure of a lake. The form used in this study was deduced by Rossby and Montgomery (1935).

$$K_z = K_{z0} (1 + \sigma_1 R_i)^{-1} \quad (9)$$

Where  $R_i$  is the Richardson number which characterizes the interaction between the mechanically generated turbulence and the thermal structure is defined as

$$R_i = \frac{\alpha_v g z^2}{W^{*2}} \frac{\partial T}{\partial z} \quad (10)$$

$\sigma_1 = .1$ , is an empirical constant, estimated in this study by comparing the values used by Sundaram et al (1971), the original value of Monin and Obukhov (1954).

3.  $\alpha_v$  is the volumetric coefficient of expansion of water and varies as shown below

$$\alpha_v = A_1 + B_1(T-4) + C_1(T-4)^2 \quad (11)$$

where  $A_1 = 0$  is  $\alpha_v$  at  $4^\circ\text{C}$

$$B_1 = 1.538 \times 10^{-5}$$

$$C_1 = -2.037 \times 10^{-7}$$

4.  $W^*$  is the friction velocity given by the surface shear stress,  $\tau_s$ , induced by the wind, and the density

$$W^* = \sqrt{(\tau_s/\rho)} \quad (12)$$

An empirical form of  $W^*$  which has been widely used is also used in this study;

$$W^* = A_2 + B_2 \sin\left(\frac{2\pi}{365} t + C_2\right) \quad (13)$$

where  $A_2$  = Average value of  $W^*$

$$= 3.048 \text{ cm/sec}^2$$

$B_2$  = Half annual variation of  $W^*$

$$= 0.762 \text{ cm/sec}^2$$

$C_2$  = Phase angle (chosen in such a way that at time,

$t=0$ ,  $W^*$ =initial value of the friction velocity).

$$= 2.61$$

5. It has also been assumed that the eddy diffusivity under neutral conditions,  $K_{z0}$  varies as

$$K_{z0} = A_3 + B_3 \sin \left( \frac{2\pi}{365} t + C_3 \right) \quad (14)$$

where  $A_3$  = Average value of  $K_{z0} = 0.21 \text{ cm}^2/\text{sec}$

$B_3$  = Half annual variation of  $K_{z0} = 0.052 \text{ cm}^2/\text{sec}$

$C_3$  = Phase angle (chosen such that at  $t=0$ ,  $K_{z0}$  = initial value of  $K_{z0}$ )  
 $= 2.61$

6. The heat source,  $H$ , is that part of the solar radiation transmitted exponentially through the depths of the lake. (In this study  $H$ , is not included in the equilibrium temperature estimation since  $H$ , is not absorbed at the surface).

$$H = \eta(1-\beta)A(z)\phi_0 \exp(-\eta(Z-h)) \quad (15)$$

$\beta = 0.5$ , is the fraction of the solar radiation absorbed at the surface

$\eta = 0.75$ , is the solar radiation absorption coefficient

$\phi_0$ , is the net solar radiation reaching the water surface.

An empirical relation has been used in this study to describe  $\phi_0$ ;

$$\phi_0 = A_4 + B_4 \sin \left( \frac{2\pi}{365} t + C_4 \right) \quad (16)$$

where  $A_4$  = Average value of  $\phi_0$

$$= 6.14 \times 10^{-3} \text{ cal/cm}^2\text{S}$$

$B_4$  = Half the annual variation of  $\phi_0$

$$= 3.52 \times 10^{-3} \text{ cal/cm}^2\text{S}$$

$$C_4 = \text{Phase angle (chosen in the same way as } C_3 \text{ or } C_2) \\ = 0.049$$

7. The discharge from the power plant is included in two ways.

(i) The heat flux  $Q$  in equation (8) is defined as

$$Q = (\rho C_p \Delta T Q_p) / A(z) \quad (17)$$

Where  $Q_p$  is the volumetric discharge from the power plant.

In this study  $Q_p = 1.508 \times 10^8 \text{ cm}^3/\text{sec}$ , this value is chosen to correspond to Sundaram et al pumping velocity of  $\frac{1}{4}$  ft/day.  $\Delta T = 10^\circ\text{C}$  is the assumed temperature change through the condensers of the power plant.

(ii) The pumping velocity term is  $\left\{ \frac{\partial}{\partial z} C_p A(z) T V_z \right\}$

$$\text{where } V_z = \frac{Q_p}{A(z)} \quad (18)$$

The pumping velocity term effects are only felt between the intake and the level at which the heated effluent becomes neutrally buoyant (effective discharge level).

#### Numerical Integration of the Governing Equations

A forward time - Dufort Frankel scheme is used to solve the governing equations. The solution of equations (6) and (8) requires one initial condition and two boundary conditions.

The temperature of the lake at spring homothermy is taken as the initial temperature. For Cayuga Lake the spring homothermy occurs around March and the temperature at spring homothermy is  $2.9^\circ\text{C}$ .

(i) The first boundary condition is

$$q_s = K_z \left. \frac{\partial T}{\partial z} \right|_{z=h} = K_s (T_E - T_s) \quad (19)$$

The equilibrium temperature,  $T_E$ , surface heat exchange coefficient,  $K_s$  are both functions of wind speed, air temperature and humidity, and net incoming (sky and solar) radiation.

Methods of evaluating  $T_E$  and  $K_s$  are fully described by Edinger and Geyer (1967) and Sundaran et al. In this study  $T_E$  is defined as

$$T_E = A_5 + B_5 \times \text{Sin}\left(\frac{2\pi}{365} t + C_5\right) \quad (20)$$

where the constants  $A_5$ ,  $B_5$  and  $C_5$  are chosen in such a way that at spring homothermy  $T_E =$  initial temperature,  $A_5=11^\circ\text{C}$ ,  $B_5=16^\circ\text{C}$  and  $C_5=0.531$ .

(ii) The second boundary condition is at the bottom of the lake which is assumed to be perfectly insulated,

$$\left. \frac{\partial T}{\partial z} \right|_{z=0} = 0 \quad (21)$$

During the heating portion of the annual cycle once the thermocline is formed, the values of  $K_z$  below the thermocline do not represent a correct thermal diffusivity since nonlinear effects are now dominant. A cut-off procedure is used to eliminate this problem. After thermocline formation (defined by the condition that  $\frac{\partial T}{\partial z}$  reaches a minimum value which is not at the surface of the lake  $z=h$ ), the minimum value of  $K_z$  is determined. This value is denoted by  $K_{z_{\min}}$  and the position is  $z_{\min}$ . Similarly during cooling, convective mixing becomes important within the epilimnion, again another cut-off procedure is used, the local maximum  $K_{z_{\max}}$  and  $z_{\max}$  are calculated.

Thus the following limits on diffusivity are used.

$$K_z = K_z \text{ for all } z \leq z_{\min} \quad \text{heating}$$

$$K_z = K_{z_{\min}} \text{ for all } z \geq z_{\min}$$

$$K_z = K_z \text{ for all } z \geq z_{\max} \quad \text{cooling}$$

$$K_z = K_{z_{\max}} \text{ for all } z \leq z_{\max}$$

The conditions applicable to Lake Cayuga are taken from Sundaram and Rehm (1973).

The depth of the lake (Cayuga) = 200 ft (60.96 m.)

$$K_s = 180 \text{ Btu/ft}^2 \text{ day } ^\circ\text{C} \quad (5.65 \times 10^{-4} \text{ cal/cm}^2 \text{ - S - } ^\circ\text{C})$$

$$\phi_o = 6.14 \times 10^{-3} + 3.52 \times 10^{-3} \times \sin\left(\frac{2}{365} t - 0.049\right) \text{ cal/cm}^2 \text{ S.}$$

$$T_E = 11 + 16 \sin\left(\frac{2\pi}{365} t - 0.531\right), \text{ } ^\circ\text{C}$$

$$\text{Initial Temp.} = 2.9^\circ\text{C}$$

For a postulated 3500 mW plant for Cayuga Lake a  $8.79 \times 10^{-4} \text{ cal/cm}^2 \text{ S}$  of waste heat will have to be rejected.

$$\Delta T = 10^\circ\text{C}$$

The intake to the power plant is fixed at 125 ft (38.1 m) from the surface of the lake.

Two topographies were considered for Cayuga Lake:

1. Cylindrical Topography

The area of the lake is constant throughout.

The term  $A'$  or  $\frac{dA}{dz} = 0$  (see equations (1) and (2)).

2. Circular Paraboloid Topography

The lake is assumed to be a circular paraboloid, with surface radius,  $B = 7.38 \times 10^5 \text{ cm}$ . (Surface area of Cayuga Lake 66 sq. mls.) The area at any depth  $z$  (measured from the deepest point

of the lake) is given by

$$A = \frac{\pi B^2 z}{h} \quad (22)$$

where  $h$  is the depth of the lake.

Thus  $A'$  becomes a constant:

$$A' = \frac{\pi B^2}{h} \quad (23)$$

## Results

Computations for a yearly cycle for Lake Cayuga are presented. The verification data base consists of vertical temperature profiles compiled by Henson et al (1961). The comparison of simulated and observed vertical temperature profiles are shown in Figs. 1, 2, and 3. Each figure shows five profiles representing observed, and the four cases of discharge, no-discharge, parabolic and cylindrical domains. The no-discharge simulations are in good agreement with the data. (The data was for no-discharge condition). The parabolic case has somewhat better agreement since it represents qualitatively, the decrease in area with depth. However, the closeness of the simulated results for the two cases is surprising. Most lakes have the rate of decrease in area with depth greater than a paraboloid, which has a linear decrease. Thus, when realistic area changes are used a greater difference between cylindrical and paraboloid cases can be expected. The discharge from the power plant is treated as a plane source and is injected into the lake at the level where the discharge temperature equals the local level temperature. The effects of the pumping velocity term are applied from this level to the intake

level (also considered as a plane sink) which for this study is 125 ft. (38.1 m) from the surface of the lake.

A pumping velocity  $V_z$  of  $\left(\frac{1.62 \times 10^5}{A_z}\right)$  cm/sec was assumed corresponding to the value of  $\frac{1}{4}$  ft/day assumed by Sundaram et al in one of their calculations for Cayuga Lake. A temperature rise of  $10^\circ\text{C}$  through the condensers was also assumed between the intake and discharge levels, a situation which calls for the use of density as a function of temperature. The effect of discharge is significant only in the top layers until July. This is because the heated discharge rises to the surface. For the later months the discharge temperature is lower than the surface temperature causing the discharge to reach static equilibrium somewhere below the surface. Thus significant thermal effects of discharge are seen at mid-depths until December. The temperatures were higher at these depths for the paraboloid topography. In general, a temperature difference of the order of  $3^\circ\text{C}$  over no-discharge case, can be seen. At the end of the annual cycle a residual temperature increase of  $1.75^\circ\text{C}$  is detected. Figs. 4 and 5 show the annual stratification cycle. It is evident that the surface temperature difference between the four cases is less than  $2^\circ\text{C}$  over the yearly cycle. However, at mid-depth the paraboloid discharge case shows a  $5^\circ\text{C}$  difference compared to no-discharge case. The cylindrical-discharge case at mid-depth shows a  $3^\circ\text{C}$  difference from observed no-discharge data and simulation. The highest surface temperatures are reached after 150 days. It is noted that the highest equilibrium temperature

occurs after 120 days. Thus there is approximately a 30 day lag in surface temperature response. The maximum temperatures at mid-depth occur after 240 days for the no-discharge case. For the discharge case maximum temperatures at mid-depth occur after 210 days. No significant phase lag between cylindrical and paraboloid cases are observed.

Figs. 6 and 7 show the eddy diffusivity variation with depth and time for cylindrical and paraboloid cases. It is observed that thermal discharge causes increase in eddy diffusivity in the epilimnion owing to increased mixing. No significant changes are seen in the hypolimnion. The difference between discharge and no-discharge cases increase with time. The effect of discharge is also seen as an increase in epilimnetic depth or lowering of the thermocline. These observations apply to both the cylindrical and paraboloid cases. Comparison of cylindrical and paraboloid cases indicate that the diffusivity values are larger for the paraboloid cases. Also at any given time the paraboloid case shows deeper thermoclines.

### Conclusions

A one-dimensional model which includes area-change with depth, vertical convection, varying diffusivity, thermal discharges, and internal absorption of radiation has been formulated. Its application to Lake Cayuga indicates excellent performance. A comparison of cylindrical and paraboloid cases indicate that significant differences in thermocline depth, eddy-diffusivity, and temperature at mid-depths are observed. This indicates

the effects of area change with depth are not negligible. These effects will be more pronounced in real basins where decrease in area with depth is more severe than the linear variation for the paraboloid case.

#### Acknowledgements

This work was conducted under funding from National Aeronautic and Space Administration, Kennedy Space Center and Environmental Protection Agency.

## Nomenclature.

- $z$  Vertical coordinate measured upward from deepest point of the lake. As a subscript it marks the vertical component of a vector.
- $h$  Depth of lake
- $A(z)$  Horizontal cross-sectional area at height  $Z$ .
- $I(z)$  Bottom-surface source of mass per unit area.
- $Q(z)$  Bottom-surface source of heat per unit area.
- $T$  Temperature ( $^{\circ}\text{C}$ )
- $\rho$  Density of water
- $V_z$  Vertical velocity
- $K_z$  Eddy diffusivity
- $K_{z0}$  Eddy diffusivity under neutral condition
- $W^* = \sqrt{(\tau_s/\rho)}$  Friction Velocity
- $\sigma_1$  Empirical constant
- $R_i$  Richardson number
- $\alpha_v$  Volumetric coefficient of expansion of water
- $\tau_s$  Surface shear stress
- $C_p$  Heat capacity
- $H(z)$  Heat source/unit vol.
- $A'$  Density at  $0^{\circ}\text{C}$
- $B, C'$  Density variation constants
- $A_1$  Volumetric coefficient of expansion at  $4^{\circ}\text{C}$
- $B_1, C_1$  Volumetric Coefficient of expansion variation constants
- $A_2$  Average value of  $W^*$
- $B_2$  Half of the annual variation  $W^*$

|                      |   |
|----------------------|---|
| $C_2, C_3, C_4, C_5$ | Phase angles                                  |
| $A_3$                | Average value of $K_{z0}$                     |
| $B_3$                | Half the annual variation of $K_{z0}$         |
| $\phi_0$             | Solar radiation incident on the water surface |
| $A_4$                | Average value of $\phi_0$                     |
| $B_4$                | Half the annual variation of $\phi_0$         |
| $\eta$               | Extinction coefficient (equation 10)          |
| $\beta$              | Absorption coefficient (equation 10)          |
| $Q_p$                | Volumetric discharge (equation 12)            |
| $\Delta T$           | Condenser Temperature change (equation 12)    |
| $T_D$                | Discharge temperature                         |
| $q_s$                | Surface heat flux                             |
| $K_s$                | Surface heat exchange coefficient             |
| $T_E$                | Equilibrium temperature                       |
| $A_5$                | Average value of $T_E$                        |
| $B_5$                | Half annual variation of $T_E$                |
| $T_s$                | Surface temperature                           |
| $q_B$                | Bottom surface heat flux                      |
| $B$                  | Lake surface radius                           |
| $\frac{dA}{dz}$      | Area variation with depth,                    |

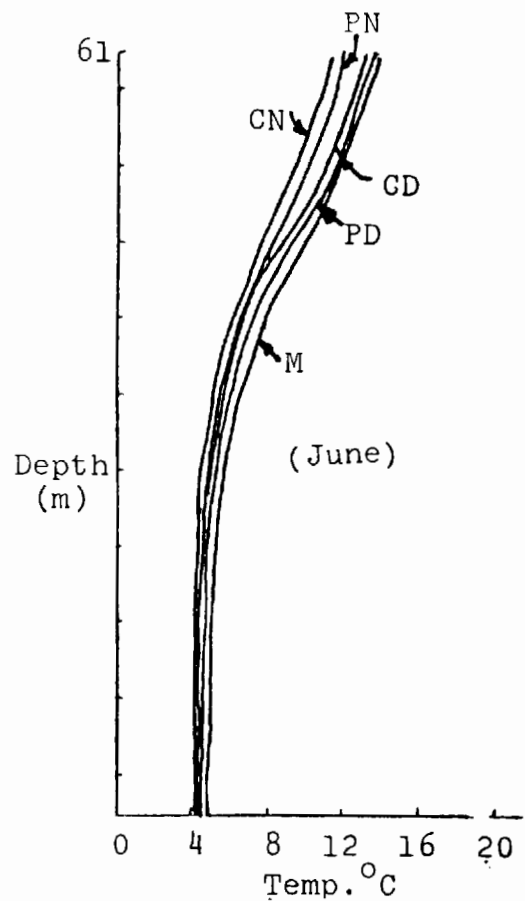
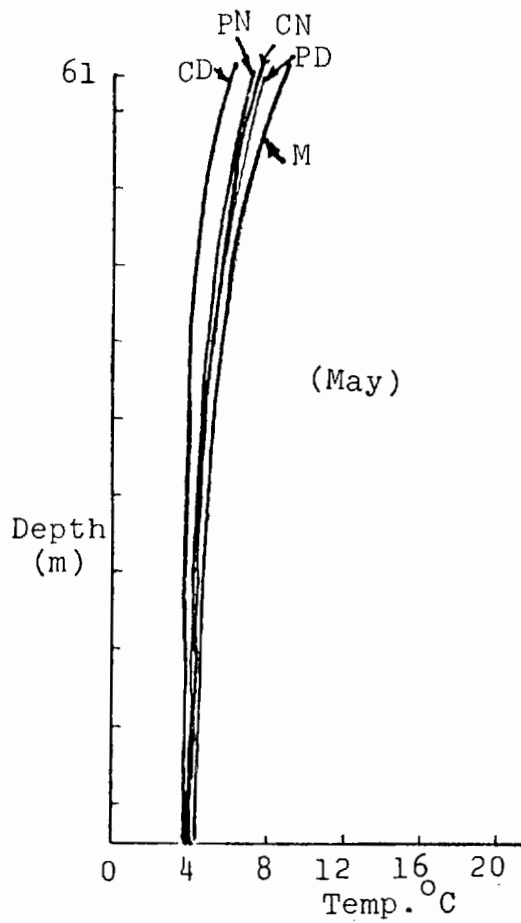
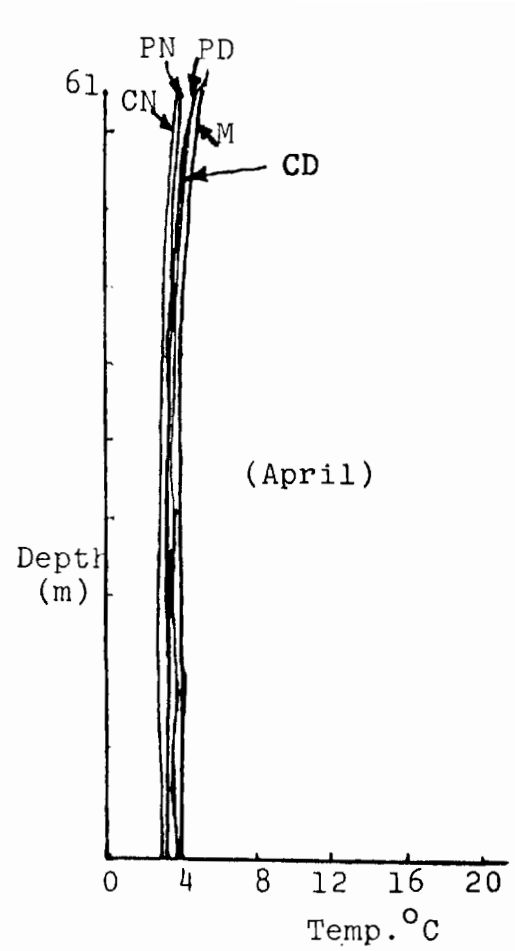
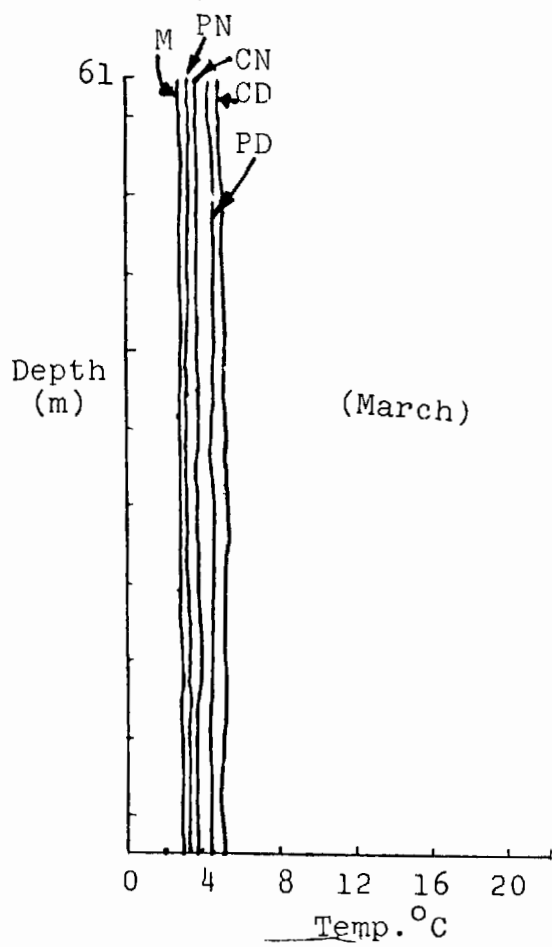


Fig.1 Vertical Temperature Profile (0 to 90 Days)  
 (PN=Paraboloid, No-Discharge; CN=Cylindrical  
 No-Discharge; PD=Paraboloid + Discharge;  
 CD=Cylindrical + Discharge; M=Measured)

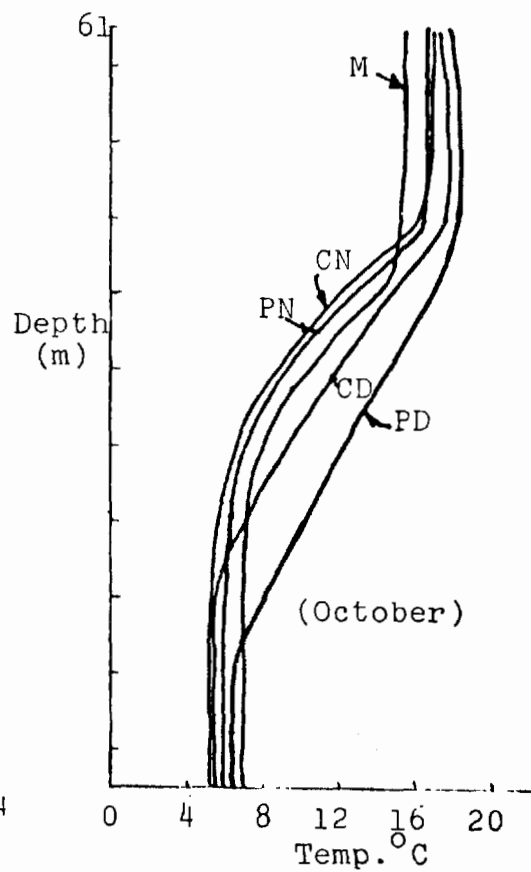
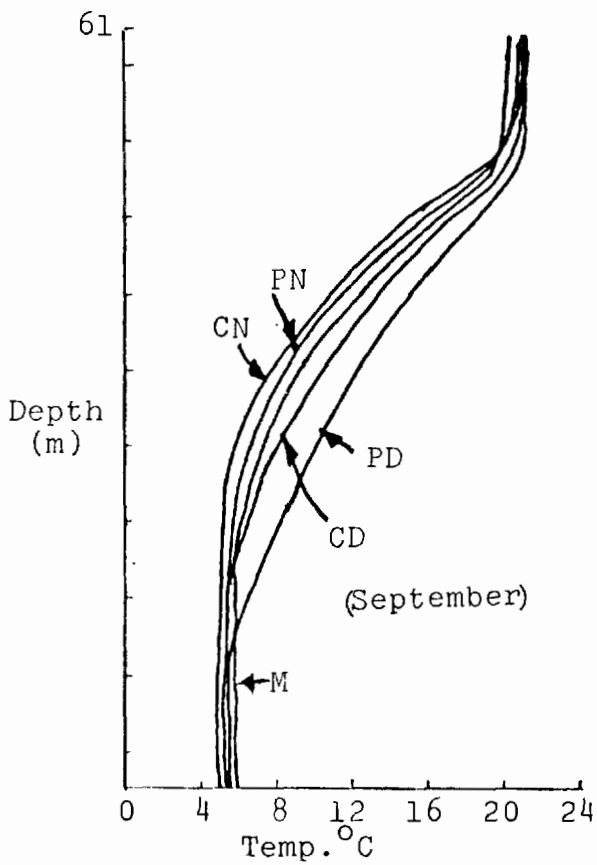
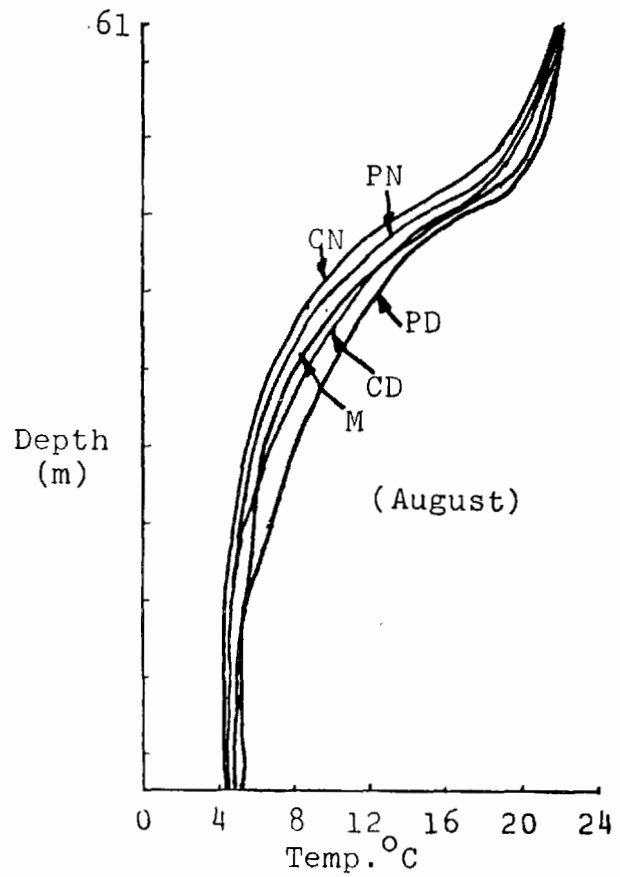
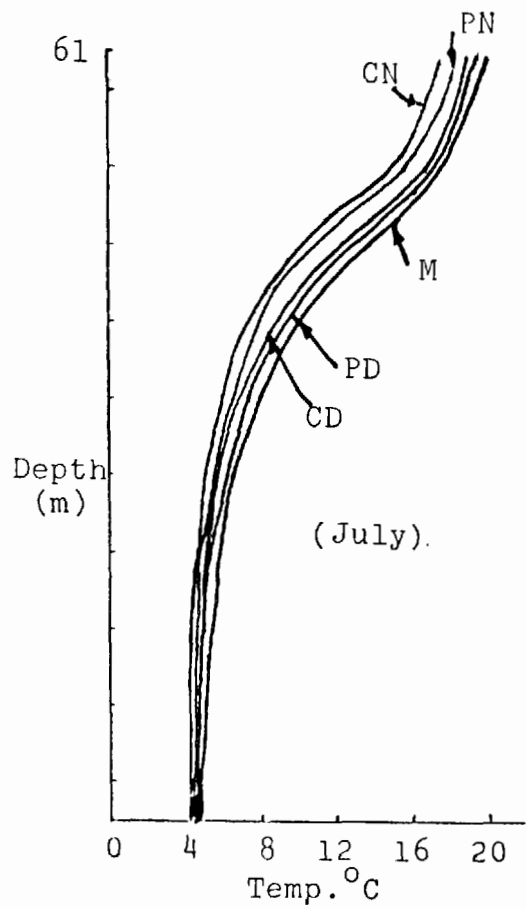


Fig.2 Vertical Temperature Profiles (from 120 to 210 days)

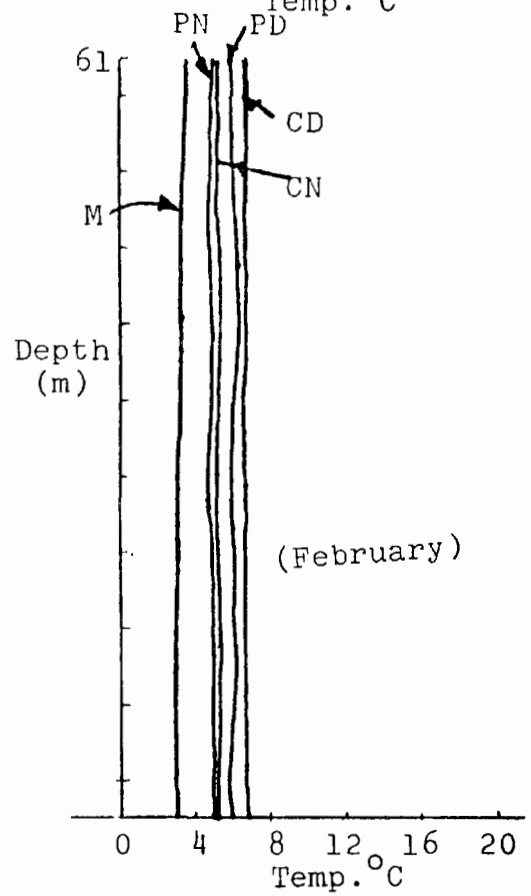
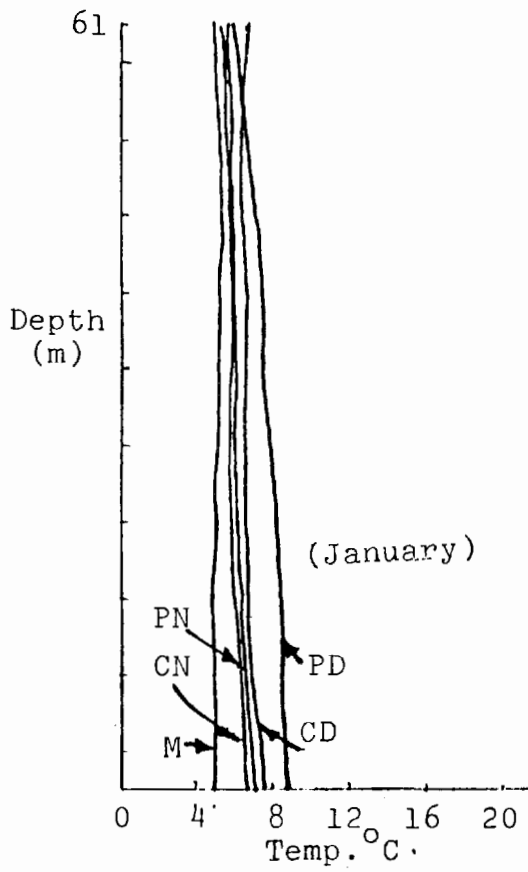
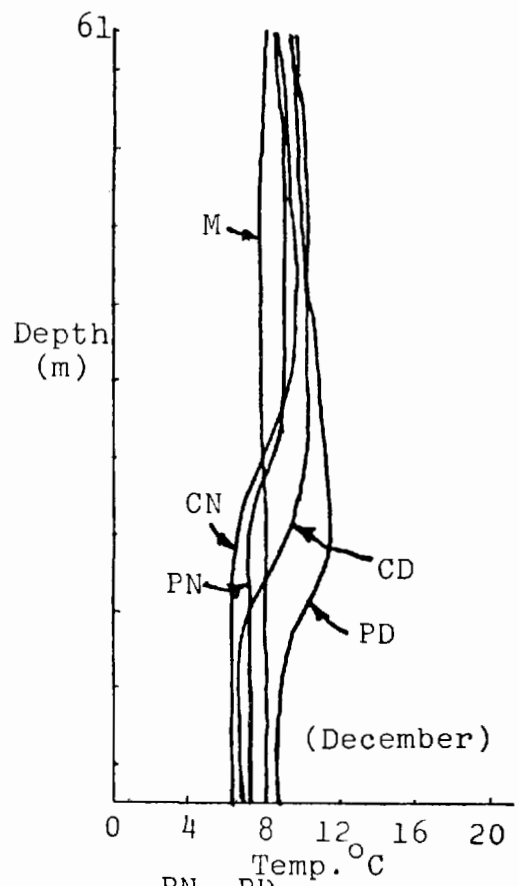
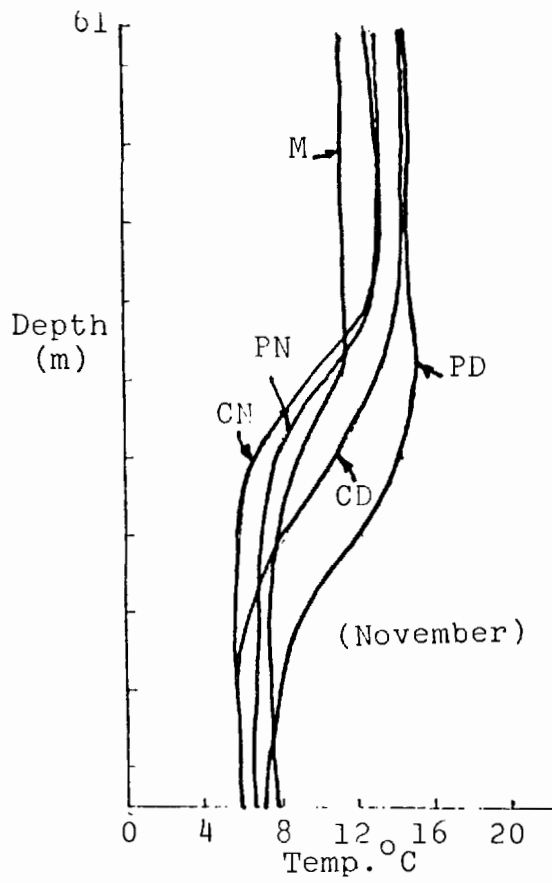
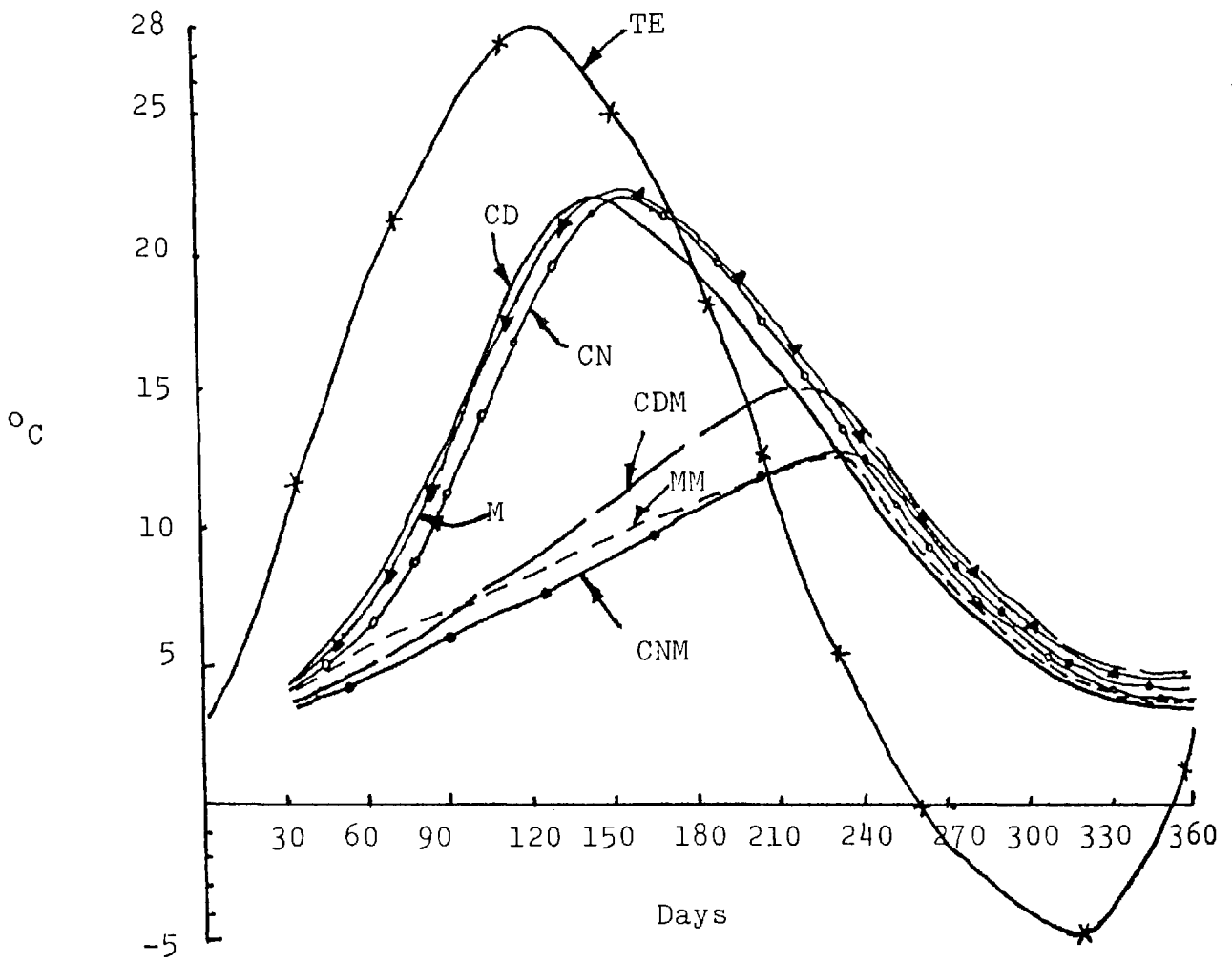


Fig.3 Vertical Temperature Profile (from 240 to 330 days)



TE      Equilibrium temperature

SURFACE TEMPERATURES

M        Measured

CN       Cylindrical, no discharge

CD       Cylindrical + discharge

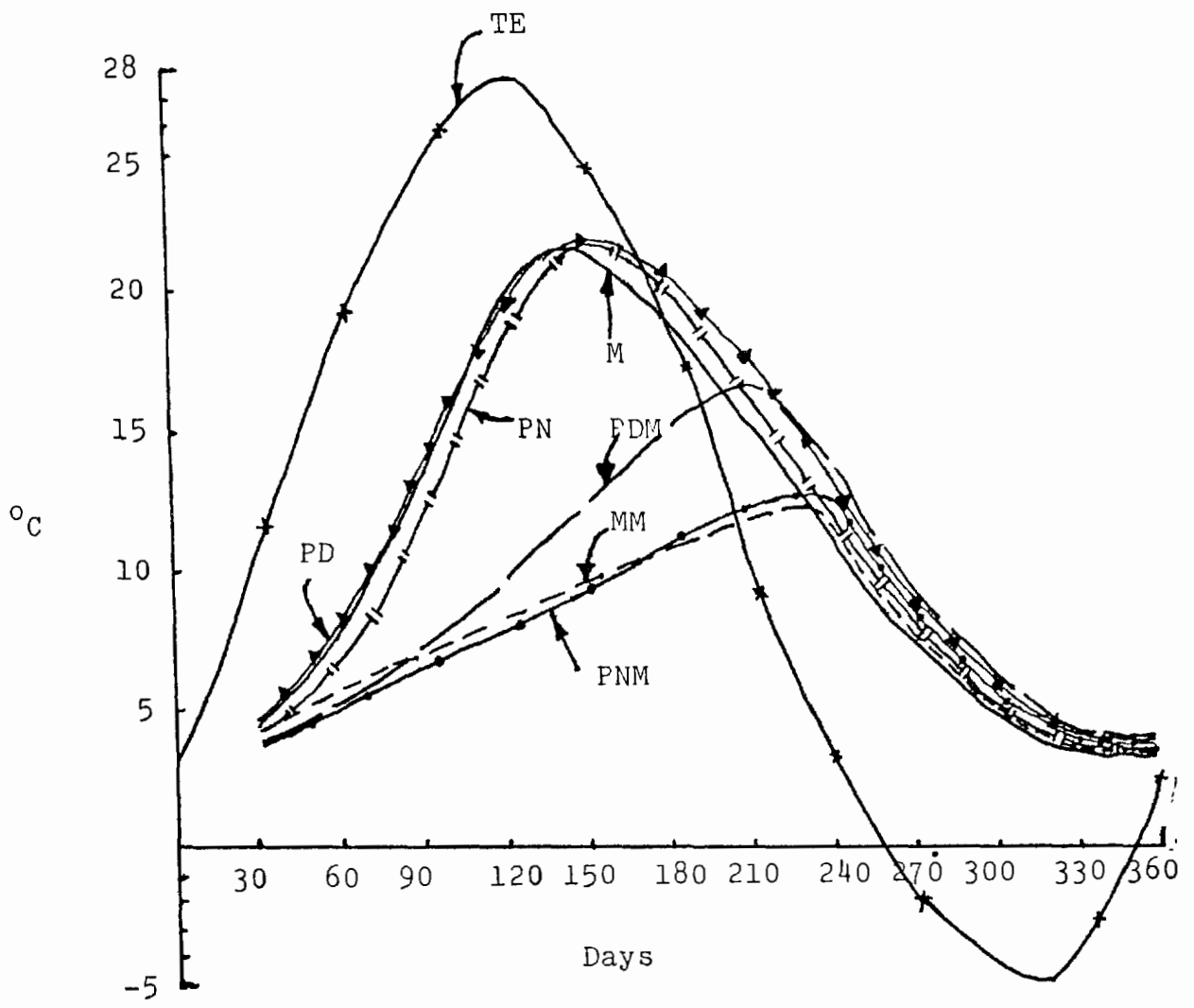
MIDLAYER TEMPERATURES

MM       Measured

CNM      No discharge

CDM      Discharge

Fig.4 Stratification Cycle (Cylindrical Domain)



|                              |                         |
|------------------------------|-------------------------|
| TE                           | Equilibrium temperature |
| <u>SURFACE TEMPERATURES</u>  |                         |
| M                            | Measured                |
| PN                           | No discharge            |
| PD                           | Discharge               |
| <u>MIDLAYER TEMPERATURES</u> |                         |
| MM                           | Measured                |
| PNM                          | No discharge            |
| PDM                          | Discharge               |

Fig.5 Stratification Cycle (Parabolic Domain)

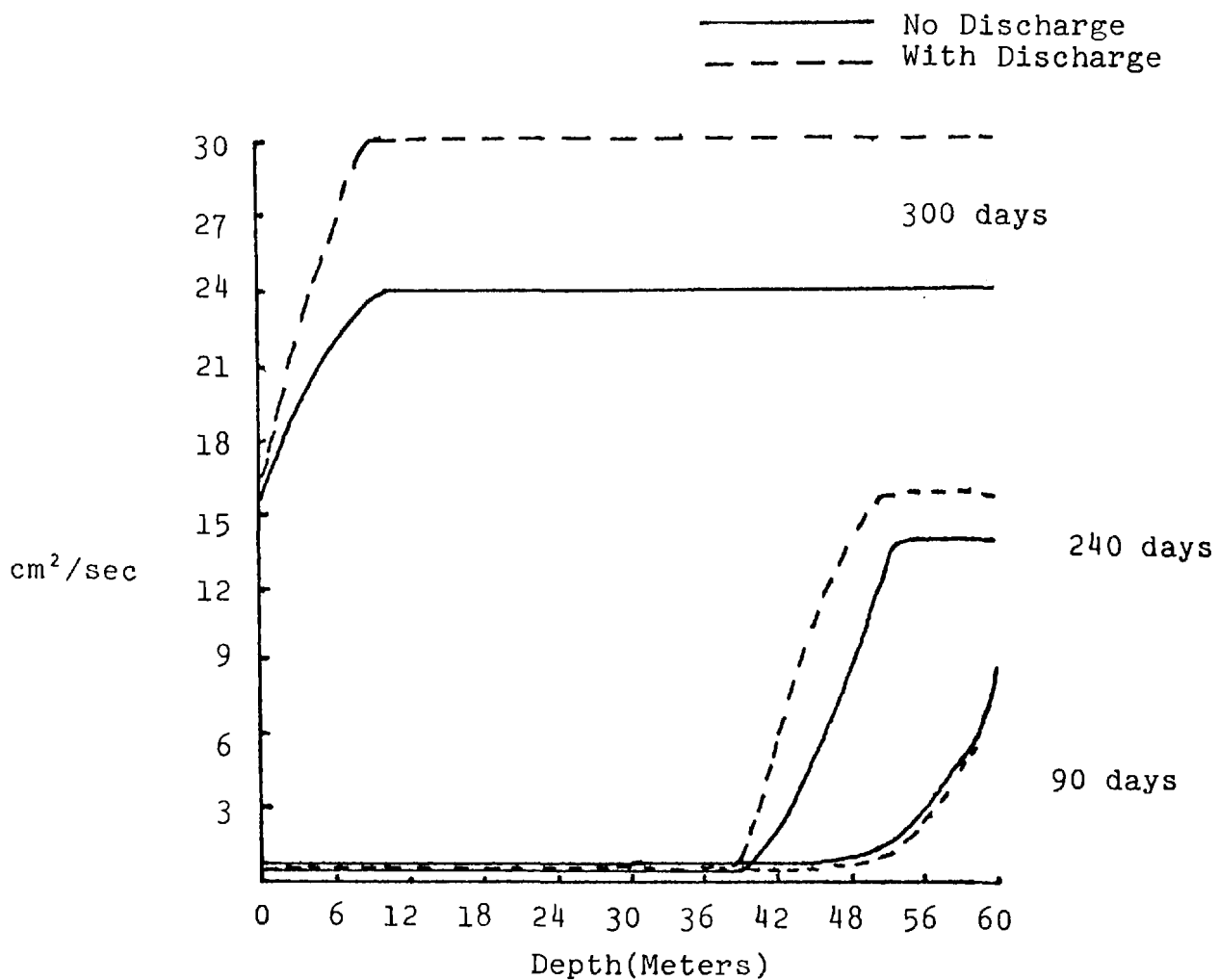


Fig.6 Variation of Eddy Diffusivity with Depth (Cylindrical Domain)

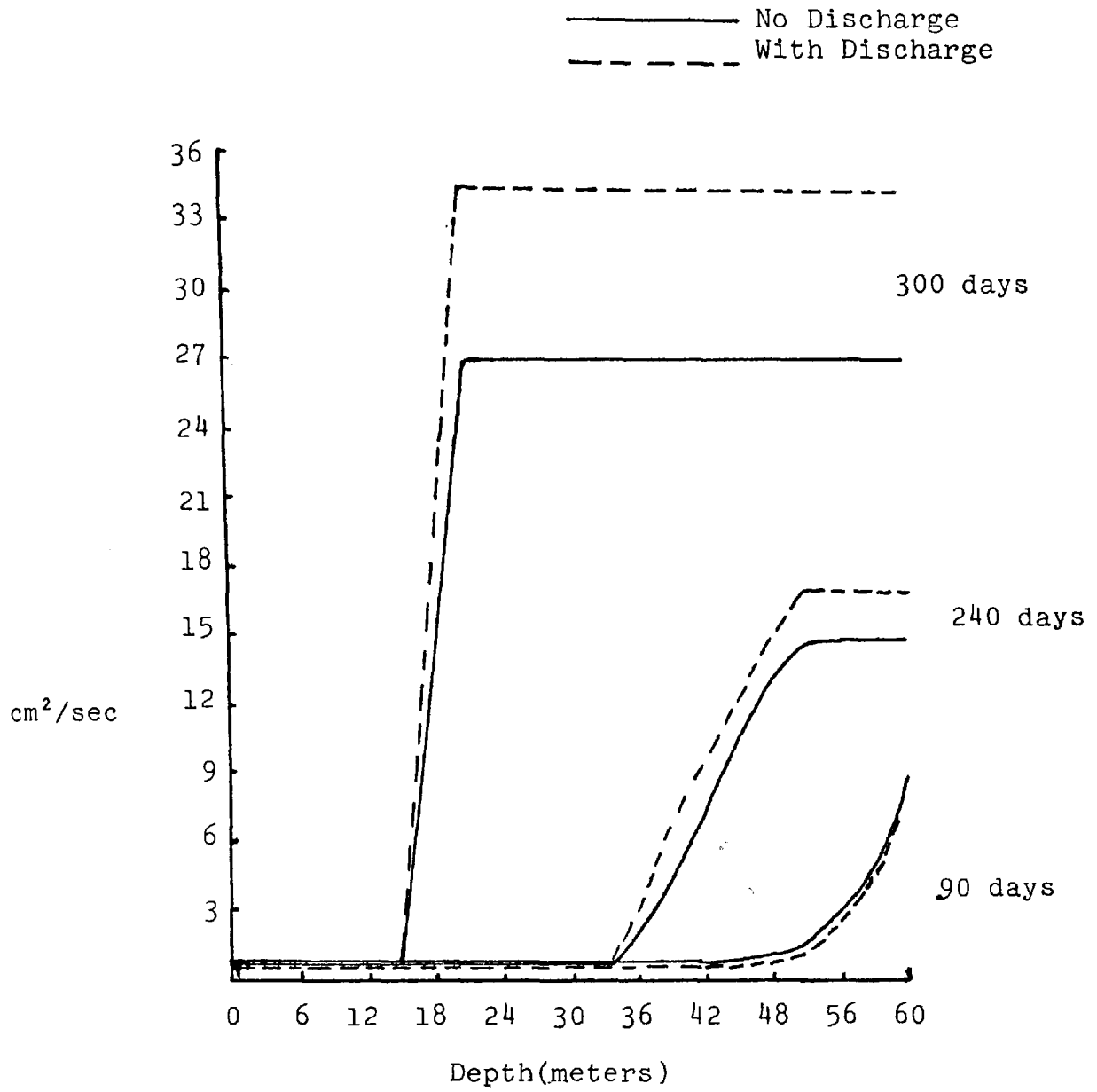


Fig.7 Variation of Eddy Diffusivity with Depth (Parabolic Domain)

## REFERENCES

- Dake, J. M. K., and D. R. F. Harleman, An Analytical and Experimental Investigation of Thermal Stratification in Lakes and Ponds, MIT Hydrodynamics Lab. Tech. Rept. 99, Cambridge, Massachusetts, September 1966.
- Dake, J. M. K. and Harleman, D. R. F., "Thermal Stratification in Lakes: Analytical and Laboratory Studies," Water Resources Research Vol. 5, No. 2, April 1969, pp 484-495.
- Dutton, J. A., and Bryson, R. A. 1962, Heat Flux in Lake Mendota, Limnol Oceanog. 7,80.
- Edinger, J. E. and Geyer, J. C., "Heat Exchange in the Environment." Sanitary Eng. and Water Resources Report, 1967.
- Henson, E. B., Bradshaw, A. S., and Chandler, D. C., "The Physical Limnology of Cayuga Lake, New York," Memoir 378, 1961, Agricultural Experimental Station, Cornell University, Ithaca, New York.
- Kraus, E. B., and Rooth, C., 1961. Temperature and Steady State Vertical Heat Flux in the Ocean Surface Layers. Tellus, 13, pp. 231-238.
- Kraus, E. B. and Turner, J. S., "A One-Dimensional Model for the Seasonal Thermocline II. The General Theory and Its Consequences," Tellus, Vol. 19, No. 1, 1967, pp 98-105.
- Lerman, A. and Stiller, M. 1969 Vertical Eddy Diffusivity in Lake Tiberias Verh. Internat. Verein. Limnol. 17, 323.
- Mitry, A. M. and Ozisik, M. N., A One-Dimensional Model for Seasonal Variation of Temperature Distribution in Stratified Lakes, International J. Heat Mass Transfer Vol. 19, pp. 201-205, 1976.
- Monin, A. S., Obukhov, A. M., Basic Regularity in Turbulent Mixing in the Surface Layer of the Atmosphere, USSR Acad. Sci. Works of Geophys. Met. No. 24, 163 (1954).
- Moore, F. K. & Jaluria, Y. 1972. Thermal Effects of Power Pla on Lakes Journal of Heat Transfer, Transactions of the ASME, pp. 163-8.
- Munk, W. H. and Anderson, E. R., "Notes on the Theory of the Thermocline," Journal of Marine Research 1, Vol. 7, No. 3, March 1948, pp 276-295.
- Roberts, G. O., Piacsek and Toome, J.; Two Dimensional Numerical Model of the Near-Field Flow for an Ocean Thermal Power Plant. Part I. The Theoretical Approach and a Laboratory Simulation,

NRL-GFO/OTEC, 5/76, Naval Research Laboratory 1976.

Rosby, C. C.; and Montgomery, B. R., "The Layer of Frictional Influence in Wind and Ocean Currents, Papers in Physical Oceanography, Vol. 3, No. 3, 1935, p. 101.

Sengupta, S. and Lick, W., A Numerical Model for Wind-Driven Circulation and Heat Transfer in Lakes and Ponds. FTAS/TR-74-98.

Sundaram, T. R., Rehm, R. G., Rudinger, G., and Merritt, G. E., "A Study of Some Problems on the Physical Aspects of Thermal Pollution," VT-2790-A-1, 1970. Cornell Aeronautical Laboratory, Buffalo, New York,

Sundaram, T. R., and Rehm, R. G., Formulation and Maintenance of Thermoclines in Stratified Lakes Including the Effects of Power Plant Thermal Discharges, AIAA Paper No. 70-238, 1970.

Sundaram, T. R., Easterbrook, C. C.; Piech, K. R. and Rudinger, G., "An Investigation of the Physical Effects of Thermal Discharges into Cayuga Lake," Report VT-2616-0-2, Cornell Aeronautical Laboratory, Buffalo, N.Y. (Nov. 1969).

Tzur, Y. "One-Dimensional Diffusion Equations for the Vertical Transport in An Oscillating Stratified Lake of Varying Cross-Section, Tellus XXV, 1973.

ABSTRACT

Hydrothermal Structure of Cooling Impoundments\*

by Gerhard H. Jirka

School of Civil and Environmental Engineering

Cornell University

Ithaca, NY 14853

Cooling impoundments, such as on-stream reservoirs and off-stream perched cooling ponds, can exhibit a highly complex and variable temperature and circulation structure. The understanding of this structure and its dependence on governing parameters is of crucial importance for the formulation and application of predictive mathematical models for cooling pond design and impact prediction. Proceeding from an analysis of two-layer stratified flow with variable density, a characteristic "pond number" is defined which accounts for the effects of pond shape, depth, condenser flow rate and temperature rise, entrance mixing, and internal friction. Use of the "pond number" allows to distinguish cooling ponds into the vertically well stratified, partially mixed and vertically fully mixed type. The partially mixed and fully mixed types can be further classified in terms of their internal circulation pattern as a recirculating pond or a dispersive pond. Comparisons with available field and laboratory data are given. The application of mathematical models to these pond types is discussed.

\* A revised version of this paper has been submitted under the title "Thermal Structure of Cooling Ponds" by G.H. Jirka and M. Watanabe for publication in the Journal of the Hydraulic Division, American Society of Civil Engineers.

## HYDROTHERMAL PERFORMANCE OF SHALLOW COOLING PONDS

E. Adams  
A. Koussis  
M. Watanabe  
G. Jirka  
D. Harleman

R.M. Parsons Laboratory for Water Resources and Hydrodynamics  
Massachusetts Institute of Technology  
Cambridge, MA 02139, USA

### ABSTRACT

The hydrothermal performance of shallow-dispersive cooling ponds is analyzed for the purpose of facilitating pond design. In the first part of the paper, plant performance is simulated with a transient mathematical model for a variety of pond configurations including variation of surface area, depth, length-to-width ratio, condenser flow rate and temperature rise. In the second part, a quasi-steady model is developed and compared with the results of the transient simulation. Together with pertinent cost information, these models should be useful in establishing trade-offs among the various parameters which characterize pond design.

### INTRODUCTION

Cooling ponds are large, artificially constructed bodies of water used for closed cycle cooling of steam power plants. In regions where land use permits, ponds offer a number of advantages over other forms of closed cycle cooling (e.g. mechanical or natural draft evaporative towers) including lower operation and maintenance cost and higher thermal inertia.

One disadvantage, however, is the relative difficulty in predicting pond performance. Unlike wet towers, ponds respond to a complex combination of meteorological parameters, and because of their heat capacity, their response is transient with a time constant on the order of days rather than minutes as is the case with towers. This thermal inertia helps filter out peak temperatures caused by fluctuating meteorology and plant operation but requires that some sort of transient analysis be adopted to obtain the correct response. Further difficulty lies in the complex circulations, both lateral and vertical, which may result from discharge momentum, buoyancy or surface shear stress from wind.

In order to learn more about pond behavior, an effort has been made to classify ponds with respect to their basic hydrodynamic circulation. Jirka [1] for example, has described a classification scheme based on relative depth of the pond and the extent of horizontal circulation.

It was found that the relative depth of a cooling pond is dependent on the pond number

$$P = \left( \frac{f_i Q_o^2}{4\beta\Delta T_o g H^3 W^2} D^3 \frac{L}{H} \right)^{1/4} \quad (1)$$

where L, W and H are the pond length, width and depth,  $Q_o$  and  $T_o$  are the condenser flow rate and temperature rise, D is the dilution produced by entrance mixing,  $f_i$  is an interfacial friction factor,  $\beta$  is a coefficient of thermal expansion and g is acceleration of gravity. Ponds for which  $P < 0.3$  are classified as deep and exhibit a definite two layer structure with a warm surface layer and a cooler, horizontally uniform, lower layer. Ponds for which  $P > 0.3$  are classified as shallow and do not possess a distinct surface layer. For  $0.3 < P < 1.0$  some stratification is observed while for  $P > 1.0$  only horizontal temperature gradients are present. The tendency for horizontal circulation depends on the relative pond depth and its length to width ratio (computed along the flow path). In shallow ponds for which  $L/W < 3$  to 5 horizontal circulation takes place in the form of large eddies while for  $L/W > 3$  to 5 the flow is essentially one-dimensional, and dispersive in character. For deep ponds, density-induced spreading promotes utilization of the entire pond area, thereby decreasing the tendency for horizontal eddies.

Of the three classes of ponds - shallow-dispersive, shallow-recirculating, and deep-stratified - it appears that the shallow-dispersive pond offers a number of general advantages for artificially constructed ponds. These advantages include avoidance of short-circuiting associated with adverse wind conditions, reduction of destructive entrance mixing due to the absence of horizontal or vertical circulation, and relatively low diking costs due to shallow depth.

The object of this paper has been to study the performance of shallow-dispersive ponds with the aim of facilitating pond design. This effort has included two parts. In the first, a transient mathematical model has been used to simulate the annual performance of various pond configurations. The results, in terms of plant intake temperature and associated power production can be used to help evaluate the cost effectiveness of various pond designs (pond area, baffle density, etc). In the second part a quasi-steady model has been developed and compared with the transient analysis. Because of its simplicity, it can serve as a design tool in the preliminary screening of cooling pond designs.

#### TRANSIENT SIMULATION

A transient, mathematical model for shallow-dispersive cooling ponds has been developed by Watanabe and Jirka [2]; the essential features are indicated in Figure 1. The pond is characterized by the variables L, W, H,  $Q_o$  and  $\Delta T_o$ . The jet entrance mixing region is a small fraction of the total pond area with the major throughflow portion of the pond being characterized by a longitudinal dispersion process. Temperatures within the pond are governed by a one-dimensional bulk diffusion equation with cross-sectionally averaged variables;

$$\frac{\partial T}{\partial t} + U \frac{\partial T}{\partial x} = E_L \frac{\partial^2 T}{\partial x^2} - \frac{\phi_n}{\rho c H} \quad (2)$$

where T is the cross-sectional mean temperature, U is the cross-sectional mean velocity  $Q_0/WH$ , x is longitudinal distance, t is time,  $E_L$  is longitudinal dispersion coefficient,  $\phi_n$  is net heat flux across the surface and  $\rho c$  is the heat capacity of water per unit volume.  $E_L$  is based on Fischer [3] and is given by

$$E_L = \frac{0.3\sqrt{f/8} U (\frac{W}{2})^2}{\kappa^2 H} \quad (3)$$

where  $\kappa$  is von Karman's constant (0.4) and f is a bottom friction factor. The surface heat transfer includes short and long wave net radiation, evaporation, conduction, and back radiation and is given by Ryan and Harleman [4]. Boundary conditions are specified at either end of the pond to ensure conservation of thermal energy, and the equation is solved with an implicit numerical scheme. A comparison of predicted and observed temperatures at the Dresden cooling pond (Watanabe and Jirka, [2]) indicated good agreement.

This model was used to simulate pond performance for a generic-shaped pond under variation of a number of its parameters. For a base case, a pond of area  $A=1000$  acres, length to width aspect ratio  $L/W=12$ , and depth  $H=9$  feet was used for a plant with condenser flow rate  $Q_0=1800$  cfs and temperature rise  $\Delta T=20^\circ$  F (heat rejection  $J=8.09 \times 10^9$  Btu/hr, corresponding roughly to a 1200 MWe nuclear power plant). Note that these parameters result in relatively high loading (approximately 1.2 nuclear MWe per acre) in order to highlight the sensitivities. For sensitivity, values of  $A=750, 1500, 2000$  and  $3000$  acres,  $L/W=36$ ,  $H=6$  and  $12$  feet and  $\Delta T=10$  and  $30^\circ$  F ( $Q_0=3600$  and  $1200$  cfs) were considered. In addition, an extra test with  $L/W=3$  was performed with a shallow recirculating pond model assuming that  $D=2$  for entrance mixing. Only one variable was changed for each run and  $J_0$  was assumed constant at  $8.09 \times 10^9$  Btu/hr. The pertinent information for each run is summarized in Table 1. Also tabulated are the dimensionless dispersion coefficient (see below) and the pond number  $IP$ . Values of the latter indicate that, while some vertical temperature gradient would exist, each pond is well within the shallow category.

Simulations were performed for the year 1970 using three-hour time steps with three-hour meteorological data (air temperature, wind speed, relative humidity and cloud cover) obtained from the NWS station at Moline, Illinois. The 2920 values of plant intake temperature (pond outlet temperature) for each run were compiled into cumulative distribution functions for the year as shown in Figures 2a-d. Associated with each temperature is the gross power, which could have been produced from a conventional 1200 MWe nuclear turbine-generator. The cumulative distribution function for power production shown in Figures 3a-d allows easier comparison of the cost effectiveness of various pond designs. In order to illustrate more of the short range performance of the ponds, the mean and standard deviations of the

intake temperatures were computed for the month of July and are listed in Table 1. Since the governing meteorology was more or less stationary over this period, this table allows one to identify differences in gross efficiency (given by variation in the mean temperature) and thermal inertia (given by variation in the standard deviation).

It is clear from the figures and table, as well as from a steady state analysis, that surface area and condenser flow rate (temperature rise) are the primary variables affecting pond performance. Increasing pond area or flow rate both result in higher plant efficiencies at the expense of greater land purchase and preparation costs on the one hand, and greater pumping and condenser costs on the other. The effect of baffling (aspect ratio) and pond depth show secondary effects. The aspect ratio influences performance through its effect on the dispersion coefficient. (The non-dimensional coefficient  $E_L^* = E_L / UL$  decreases with the  $3/2$  power of  $L/W$ ). Thus as  $E_L^*$  decreases ( $L/W$  increases) plant intake temperatures decrease towards the ideal limit of plug flow, while as  $E_L^*$  increases ( $L/W$  decreases) fully mixed conditions are approached. In addition, by comparing the results for  $L/W=12$  and  $36$  with those for  $L/W=3$ , it is clear that the achievement of one-dimensional flow (suppression of horizontal eddying) results in a significant decrease in intake temperature. The fourth variable, pond depth, shows modest sensitivity within the parameter range tested.  $E_L^*$  is inversely proportional to  $H$ , implying some improvement in steady state performance as depth is increased. Furthermore, increasing depth slows the response to fluctuating meteorological conditions leading to a decrease in variation (standard deviation) of the plant intake temperatures (see Table 1).

#### QUASI-STEADY MODEL

In order to evaluate the performance of a cooling pond, it is necessary to cover a wide range of meteorological conditions which might occur during the pond's lifetime. One way to do this would be to run a transient model with time-varying meteorological conditions for a number of years. A disadvantage of this type of simulation, however, is the considerable computation and effort which is involved; at the design stage, where a number of alternative designs must be evaluated, such a simulation is impractical. Therefore it is desirable to develop a simpler, approximate model to be used for the purpose of initial pond design. In particular it is desirable to use a steady state model so that, as with the design of cooling towers, a frequency distribution of meteorological data, rather than a long time series, can be used as model input. The more accurate transient simulation can then be used to evaluate the chosen design.

The quasi-steady model uses the following differential equation

$$U \frac{\partial T}{\partial x} = E_L \frac{\partial^2 T}{\partial x^2} - \frac{K}{\rho ch} (T - T_E) \quad (4)$$

where  $T_E$  is the equilibrium temperature. Equation (4) requires the same boundary conditions as those used with Equation (2) and differs from

Equation (2) only in the use of a linearized excess temperature representation for surface heat transfer and the fact that the time-dependent term is missing. The model is quasi-steady in the sense that the input parameters governing pond performance (plant operating condition and meteorology) are assumed to be constant over a period of time and the pond temperature is assumed to be in instantaneous equilibrium with these parameters. The constant input parameters are derived by averaging the real time parameters over the time interval. Clearly this procedure is an approximation of true pond behavior. By averaging the input data one is filtering high frequency fluctuations and by assuming "instant response" one is ignoring the "thermal inertia" known to characterize ponds. The intent is to adjust the averaging interval such that the two effects cancel as much as possible in their influence on the cumulative distribution of intake temperatures.

The solution to Equation (4) was obtained by Wehner and Wilhelm [5]. The resulting plant intake temperature is given by

$$\frac{T_i - T_E}{\Delta T_o} = \frac{4a \exp\{1/2E_L^*\}}{(1+a)^2 \exp\{a/2E_L^*\} - (1-a)^2 \exp\{-a/2E_L^*\} - 4a \exp\{1/2E_L^*\}} \quad (5)$$

where  $a = \sqrt{1+4rE_L^*}$

$$r = \frac{KA}{\rho c Q_o}$$

and  $E_L^* = \frac{E_L}{UL}$

In order to predict the intake temperature  $T_i$ , the equilibrium temperature  $T_E$  and the heat exchange coefficient  $K$  have to be defined. The former is defined as the water temperature at which the net heat flux  $\phi_n = 0$  and can be found by an iterative procedure. The linearized surface heat exchange coefficient is defined by  $\phi_n = K(T_s - T_E)$  where  $T_s$  is a characteristic surface temperature. For this analysis  $T_s = T_E + \Delta T_o / 2r$ , where  $r$  is determined by iteration.

Cumulative distributions of predicted intake temperatures using both the quasi-steady and the transient models were compared using the base case pond described in the previous section. The transient model was run for one year using three-hour time steps with three-hour meteorological data. The cumulative distribution of predicted intake temperature and power using this model are shown in Figures 4 and 5 as solid lines. Quasi-steady calculations were also made for the same pond and time period by averaging the meteorological data over different averaging intervals, computing values of  $K$  and  $T_E$  for each time interval, and then using Equation (5) to compute intake temperatures. Distribution of intake temperature and power production are plotted in Figures 4 and 5 for averaging intervals of 1, 3, 5, 10 and 30 days.

Comparison of the various curves suggests that reasonably good agreement is obtained between the transient model and both the 3 day and 5 day averaged model. By contrast, results for one day averaging show greater extremes in temperature suggesting that the averaging has not adequately filtered the high frequency fluctuations, while the distributions resulting from the 10 and 30 day averaging are the flattest, suggesting that the averaging of input data provides more filtering than the transient model. These results indicate that, for this site and pond, an averaging of between 3 and 5 days is appropriate. This figure is reasonable because it corresponds approximately to the time constant  $\rho H/K$  which governs the response of a shallow water body to a step change in  $T_E$ .

#### REFERENCES

- [1] Jirka, G., "Hydrothermal Structure of Cooling Impoundments," presented at this conference.
- [2] Watanabe, M., and G. Jirka, "A Longitudinal Dispersion Model for Shallow Cooling Ponds," Proc. of First Conference on Waste Heat Management and Utilization, Miami Beach, May 1977.
- [3] Fischer, H., "The Mechanics of Dispersion in Narrow Streams," Proc. of ASCE, Vol. 93, No. HY 6, 1967.
- [4] Ryan, P., and D. Harleman, "An Analytical and Experimental Study of Transient Cooling Pond Behavior," R.M. Parsons Laboratory for Water Resources and Hydrodynamics, Technical Report No. 161, Dept. of Civil Engineering, MIT, January 1973.
- [5] Wehner, J., and R. Wilhelm, "Boundary Conditions of Flow Reactor," Chemical Engineering Science, Vol. 6, 1956.

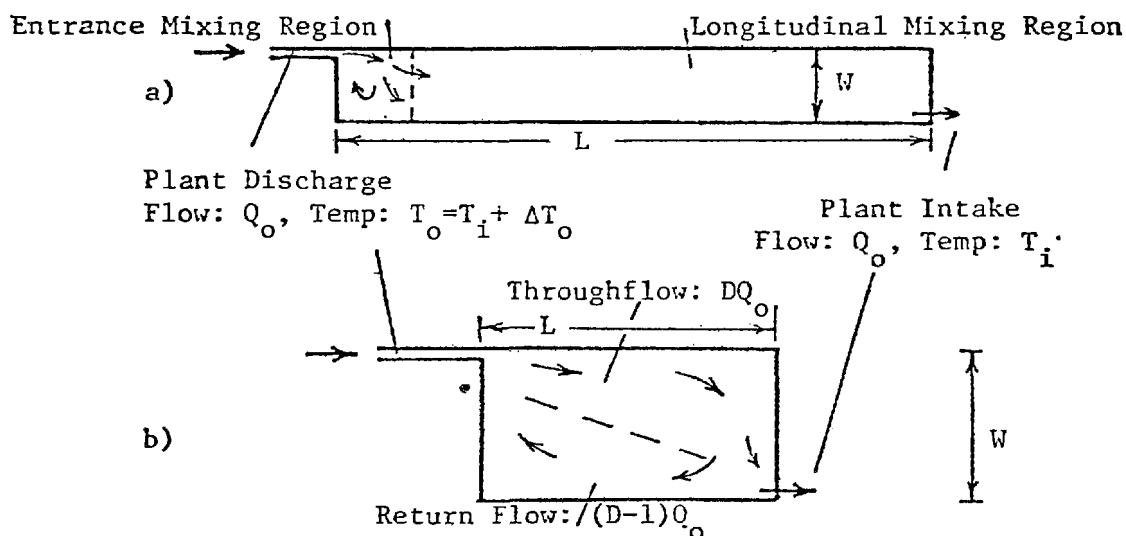


Figure 1 Mathematical Schematization for a) Shallow-Dispersive Cooling Pond b) Shallow-Recirculating Cooling Pond (Plan Views)

| STUDY CASES       |                 |                        |  |                         |       |            | STATISTICS OF INTAKE TEMPERATURE<br>Month of July |                            |
|-------------------|-----------------|------------------------|--|-------------------------|-------|------------|---|----------------------------|
| Area A<br>(acres) | Depth H<br>(ft) | Aspect<br>Ratio<br>L/W | Temperature<br>Rise $\Delta T_o$<br>(°F) | Flow<br>Rate Q<br>(cfs) | $P^3$ | $E_L^{*4}$ | Mean<br>(°F)                                      | Standard Deviation<br>(°F) |
| 750               | 9               | 12                     | 20                                       | 1800                    | 0.53  | 0.36       | 94.6  | 3.0                        |
| 1000 <sup>1</sup> | 9               | 12                     | 20                                       | 1800                    | 0.51  | 0.41       | 90.7  | 2.9                        |
| 1500              | 9               | 12                     | 20                                       | 1800                    | 0.49  | 0.51       | 86.4  | 2.8                        |
| 2000              | 9               | 12                     | 20                                       | 1800                    | 0.47  | 0.58       | 84.1  | 2.8                        |
| 3000              | 9               | 12                     | 20                                       | 1800                    | 0.44  | 0.72       | 81.7  | 2.7                        |
| 1000              | 6               | 12                     | 20                                       | 1800                    | 0.77  | 0.62       | 91.5  | 3.5                        |
| 1000 <sup>1</sup> | 9               | 12                     | 20                                       | 1800                    | 0.51  | 0.41       | 90.7  | 2.9                        |
| 1000              | 12              | 12                     | 20                                       | 1800                    | 0.38  | 0.31       | 90.1  | 2.5                        |
| 1000 <sup>2</sup> | 9               | 3                      | 20                                       | 1800                    | 0.51  | 0.83       | 97.3  | 2.8                        |
| 1000 <sup>1</sup> | 9               | 12                     | 20                                       | 1800                    | 0.51  | 0.41       | 90.7  | 2.9                        |
| 1000              | 9               | 36                     | 20                                       | 1800                    | 0.77  | 0.08       | 87.4  | 3.0                        |
| 1000              | 9               | 12                     | 10                                       | 3600                    | 0.86  | 0.41       | 92.6  | 2.8                        |
| 1000 <sup>1</sup> | 9               | 12                     | 20                                       | 1800                    | 0.51  | 0.41       | 90.7  | 2.9                        |
| 1000              | 9               | 12                     | 30                                       | 1200                    | 0.38  | 0.41       | 89.2  | 3.0                        |

1 base case

2 computed as shallow-recirculating pond using entrance dilution of 2.

3 based on  $f_1 = 0.01$ , and  $\beta = .00018 \text{ } ^\circ\text{F}^{-1}$

4 based on  $f = 0.02$

TABLE 1: SUMMARY OF SENSITIVITY STUDY

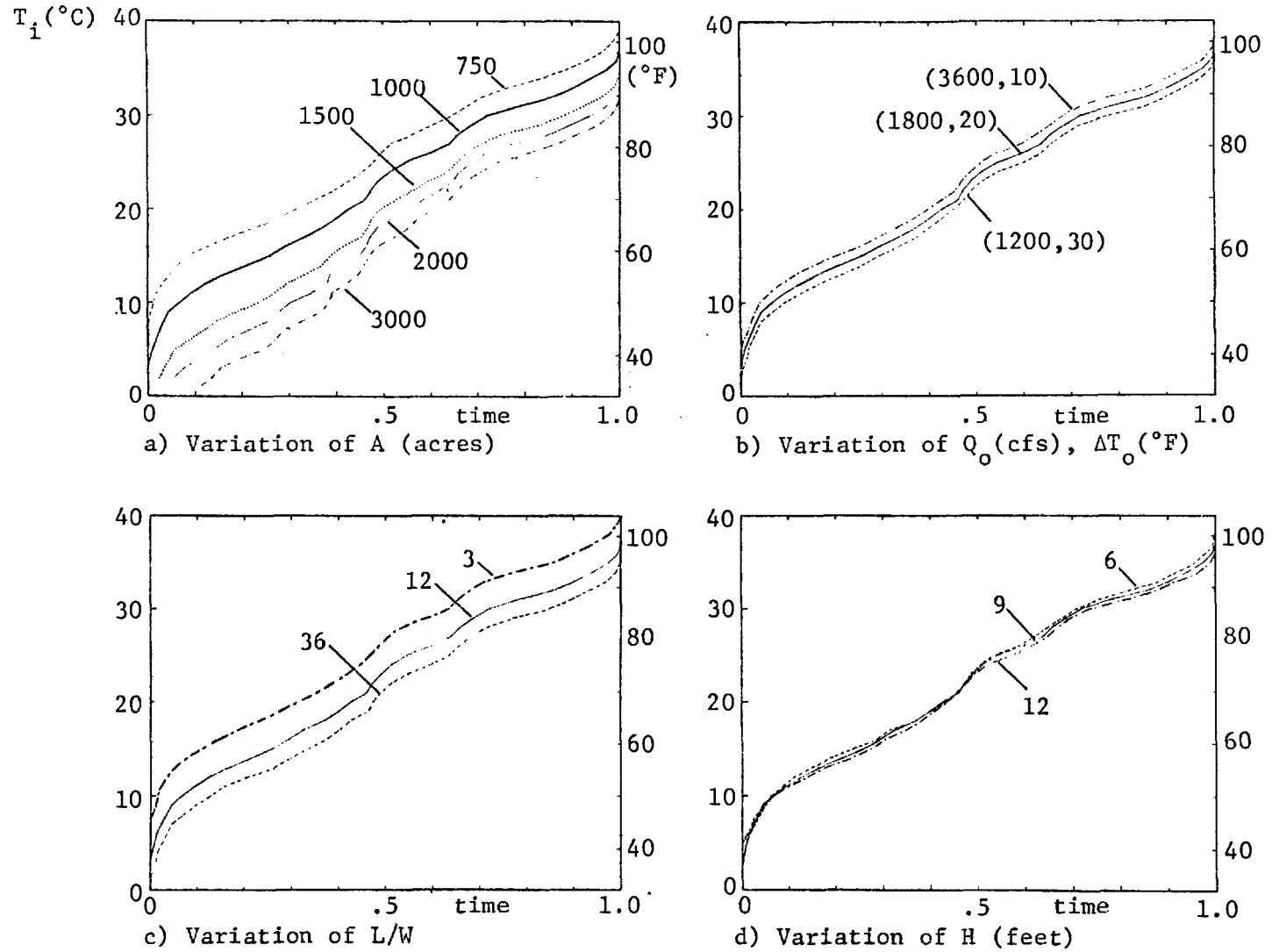


Figure 2 Cumulative Distributions of Predicted Plant Intake Temperature

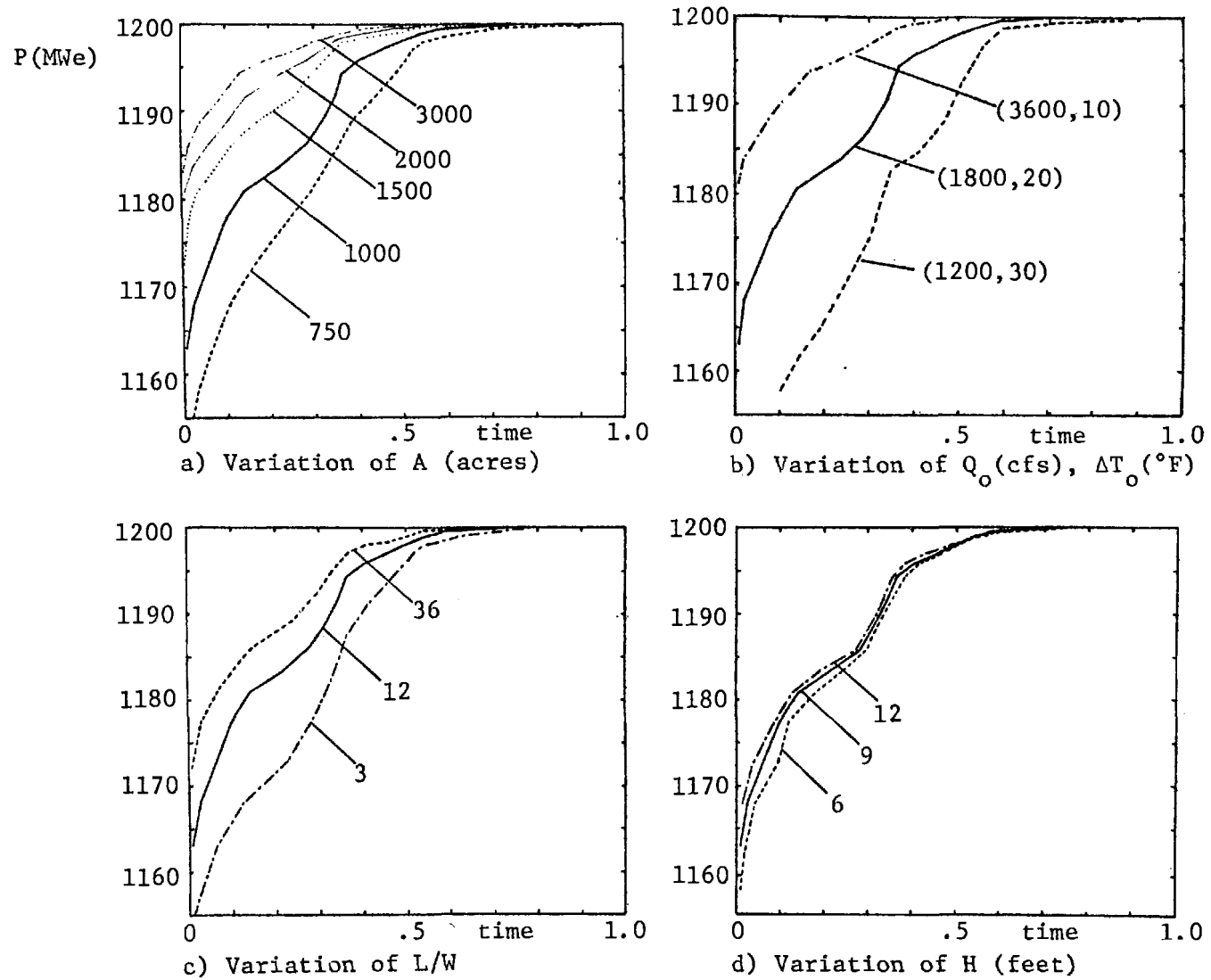


Figure 3 Cumulative Distributions of Predicted Power Production

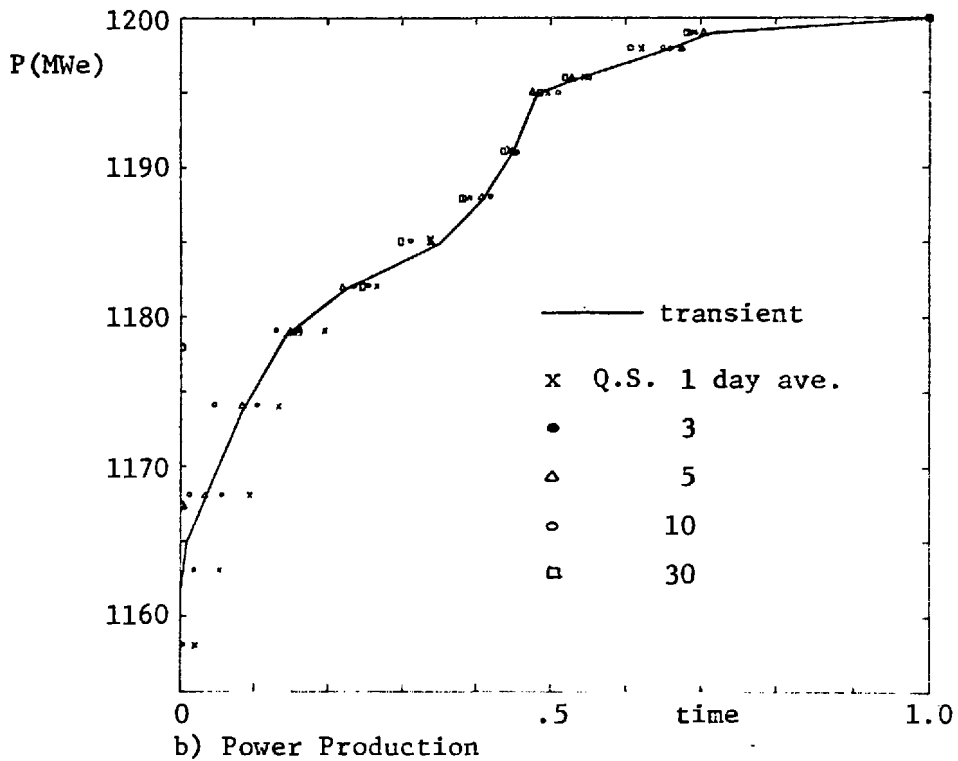
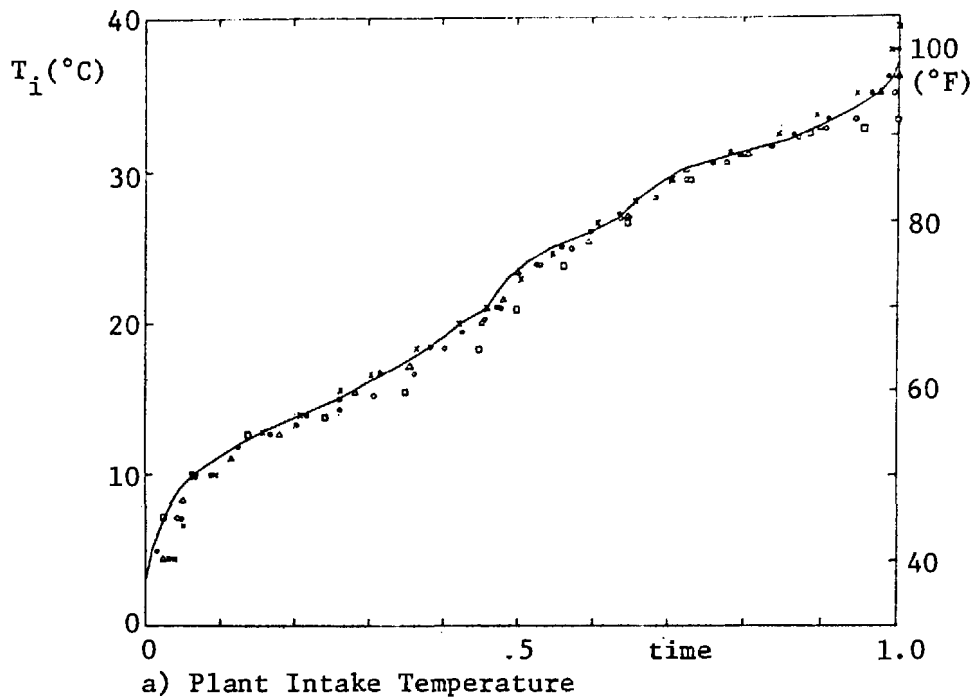


Figure 4 Cumulative Distributions of Plant Intake Temperature and Power Production using Transient and Quasi-Steady Models

TRANSIENT SIMULATION OF COOLING LAKE PERFORMANCE  
UNDER HEAT LOADING FROM THE NORTH ANNA POWER STATION

D. R. F. Harleman, G. H. Jirka, D. N. Brocard,  
K. Hurley-Octavio, and M. Watanabe  
R. M. Parsons Laboratory for Water Resources and Hydrodynamics  
Department of Civil Engineering  
Massachusetts Institute of Technology  
Cambridge, Massachusetts U.S.A.

ABSTRACT

The North Anna Power Station of the Virginia Electric and Power Co. (4 nuclear units with a combined capacity of 3800 MWe) is located North-West of Richmond. The heat dissipation system includes a Waste Heat Treatment Facility consisting of a series of lagoon cooling ponds with attached dead-end side arms, discharging into Lake Anna, on which the intake is located.

An experimental and analytical study of the buoyancy-driven circulations in long, dead-end side arms of cooling lakes was carried out. Results were utilized in the subsequent simulations to demonstrate the relative effectiveness of cooling lake side arms in dissipating heat.

A transient, segmented cooling pond model was developed which links the mathematical models applicable to the components of the Waste Heat Treatment Facility (WHTF) and the main lake. To provide additional information on the isotherm and velocity patterns in the main lake, a finite element model for the surface layer in a stratified cooling lake was developed.

The above models were utilized in long-term (10 year) simulations to evaluate the effect of the power plant operation on Lake Anna. The natural (ambient) temperature regime was predicted using the MIT Lake and Reservoir Model. The segmented cooling pond model was used to simulate one-, two-, three- and four-unit power plant operation.

INTRODUCTION

This paper summarizes the development of mathematical models for predicting the performance of a cooling lake used as the condenser heat dissipation system for the North Anna Nuclear Power Station of the Virginia Electric and Power Company. The performance of a cooling lake is determined by both its effectiveness and its thermal inertia. "Effectiveness" relates to the ability of cooling lakes to dissipate the artificial heat load with the lowest possible intake temperature. This is governed by the geometric configuration of the lake and by the design of inlet and outlet structures. One of the interesting features of Lake Anna is the existence of several long, isolated side arms which required a detailed investigation

of their role in the heat dissipation process. "Thermal inertia" is the ability of cooling lakes to damp out meteorological transients and fluctuations in the power plant operation. Cooling lakes are practically never in a steady-state condition, hence an evaluation under realistic transient conditions is necessary.

The optimal approach to assess cooling lake performance - whether environmental impacts or technical parameters - is to consider long-term behavior, over a period of the order of ten years, so as to form representative statistical measures, such as average or extreme thermal conditions.

A portion of the lake, into which the condenser water is discharged, is separated from the main body of the lake by dikes. A major fraction of the waste heat is dissipated in this portion, known as the Waste Heat Treatment Facility (WHTF). Its purpose is to minimize the thermal impact on the main lake and on the stream below the dam forming the impoundment.

The results of the analysis are presented as induced temperatures or temperature rises above natural conditions at various points of interest. During operation of the power station it will not be possible to measure "natural" lake temperatures. Therefore, it is necessary to predict transient natural lake temperature under the meteorological conditions prevailing during operation. The predictions of the natural lake temperature model were compared with pre-operational observations during several years of record. Surface isotherms and longitudinal temperature profiles have been prepared for operating conditions of one to four units. The results are intended to be used in subsequent analyses by biologists and engineers to assess the potential environmental impact of the North Anna cooling system and to compare to applicable thermal regulations. However, no such assessments and/or comparisons are made in this paper.

#### PLANT CHARACTERISTICS

The North Anna Power Station is located in central Virginia, between Richmond and Charlottesville. The station is situated on the south bank of Lake Anna formed by a dam on the North Anna River (Fig. 1) which was closed in January 1972.

The station will ultimately consist of four nuclear units of a combined capacity of 3760 MWe (about 940 MWe per unit). The waste heat load rejected in the condensers is  $6.5 \times 10^9$  BTU/hr per unit or  $25.9 \times 10^9$  BTU/hr total. The condenser cooling water flow rate is about 2,100 cfs per unit (8,400 cfs total) and the temperature rise through the condensers is about 14°F.

#### Lake Anna and Waste Heat Treatment Facility

The construction of three dikes and the dredging of channels formed a separate series of ponds, the Waste Heat Treatment Facility (WHTF). Both the WHTF and the lake participate in the dissipation to the atmosphere of the

waste heat loading, but the WHTF dissipates the major portion. Lake Anna has a surface area of 9,600 acres, a volume of  $10.6 \times 10^9 \text{ ft}^3$ , and an average depth of 25 ft. The maximum depth at the dam is 70 ft. The lake receives an average annual inflow of about 270 cfs. The lake elevation is maintained by radial gates at the dam. The outflow rate equals the inflow minus the rate of evaporation from the lake surface (estimated at about 60 cfs average).

The WHTF has a surface area of 3,400 acres, a volume of  $2.66 \times 10^9 \text{ ft}^3$  and an average depth of 18 ft. The maximum depth is 50 ft in the vicinity of the dikes. As shown in Fig. 1, Dike I forms Pond 1 of the WHTF which receives the cooling water via the discharge canal from the power plant. Connecting channels have been dredged between Pond 1 and Pond 2 (formed by Dike II) and between Pond 2 and Pond 3 (formed by Dike III). These channels have a constant trapezoidal cross-section of 25 ft depth and 160 ft average width. After passing through Ponds 2 and 3, the cooling water is discharged into the main lake through a submerged discharge structure in Dike III. After residence in the main lake, cooling water is withdrawn through near-surface intakes in the vicinity of the station. A major characteristic of the system is the existence of the long narrow side arms in the WHTF. These arms comprise about 1530 acres or 45% of the area of the WHTF.

The North Anna heat dissipation system has a low heat loading per unit surface area. Using the combined surface area for the main lake and the WHTF, the loading ranges between 0.15 and 0.6  $\text{MW}_t$  (waste heat) per acre for 1 and 4 units, respectively. Frequently, cooling pond designs have a much higher thermal loading, between 0.5 and 3  $\text{MW}_t$  per acre. The loading on the area of the WHTF along corresponds to 2.2  $\text{MW}_t/\text{acre}$  for four units.

#### CHARACTERISTICS OF COOLING LAKES

Experimental and theoretical studies on cooling lake behavior have been conducted by Ryan and Harleman [1] and Watanabe, Harleman and Connor [2]. The major results of earlier studies have been summarized by Jirka, Abraham and Harleman [3] and a detailed report on the North Anna cooling lake study has been prepared [4].

The temperature differential which exists in a cooling lake between the discharge and the intake of the power plant is, if transient fluctuations are averaged, equal to the condenser temperature rise. As density changes are associated with temperature changes, buoyant forces arise which tend to cause spreading of lighter (warmer) water over heavier (cooler) water. The paramount role of these density currents has been observed in laboratory experiments [1]. In deep ponds it was found that density currents effectively spread the heated water over the entire surface of the pond, even if there are distinct backwater ("dead") areas. Thus, deep cooling ponds are characterized by a heated, thin surface layer, in which predominately horizontal temperature variations occur due to cooling to the atmosphere, and an underlying subsurface layer, in which only vertical temperature variations occur due to the gradual advective flow to the

submerged intakes. Ryan and Harleman [1] also established the importance of discharge channel design to minimize entrance mixing and of a submerged skimmer wall intake structure and formulated a transient predictive model consisting of two parts:

- a) the surface layer model, which assumes a constant surface layer thickness and computes transient areal temperature distribution resulting from heat loss to the atmosphere; account is also taken of an entrance mixing region,
- b) the subsurface model, which calculates the vertical temperature variation due to downwelling from the end of the surface region; the subsurface region may be weakly or strongly stratified. This model is an adaptation of the M.I.T. Deep Reservoir Model [5],[6]. The cooling pond model has been applied to several field cases of deep cooling lakes and excellent results have been obtained in the calculation of the transient annual behavior.

An accurate prediction of temperatures induced by heated discharges hinges on the correct specification of the heat transfer from the water surface to the atmosphere. The heat dissipation of artificially heated water surfaces has been addressed by Ryan et al [7] and heat dissipation formulae have been developed which specifically account for the evaporative heat transfer due to free buoyant convection which arises from the virtual temperature difference between the moist air at the water surface and a certain distance above the water surface.

#### DEVELOPMENT OF PREDICTIVE MODELS FOR THE NORTH ANNA COOLING SYSTEM

The preceding discussion has stressed that the applicability of available mathematical models for cooling lake prediction is strongly tied to the thermal structure of a cooling lake. In turn, the thermal structure depends on geometric features of the lake and discharge and intake structures. The North Anna cooling system, consisting of a series of ponds in the WHTF with attached side arms and connecting channels and of the main lake, is expected to have a particularly complex thermal structure. For example, while the individual ponds of the WHTF will be distinctly stratified, there is a tendency for destratification in the connecting channels of the WHTF. Also, the role of buoyant convective circulations into the isolated side arms of the WHTF is expected to be important. None of the existing models encompass all of these features.

The following approach was taken in the development of predictive models for the North Anna cooling system:

##### Side Arm Heat Dissipation

An experimental and analytical study of the buoyant convection which occurs due to surface cooling in long side arms of cooling ponds was carried out by Brocard, et al. [8]. As shown in Fig. 2, the salient features are the

length and depth of the side arm, the thickness and temperature of the stratified layer at the entrance to the side arm and the surface cooling rate. In addition, the special features of the lateral constructions within the side arm and of bottom slopes were investigated. The results of the side arm investigation are represented in design graphs, which give the flow rate and associated temperature drop as a function of the governing parameters.

In order to analyze the complex structure of the North Anna heat dissipation system, a "segmented model" was developed which links different mathematical models applicable for each of the components of the WHTF and the main lake. A schematic diagram of the segmented model is shown in Fig. 3. For the three ponds of the WHTF which are of shallow average depth, a two-layer model was developed in which each of the layers is assumed to be vertically uniform and which includes the inflows into and outflows from the side arms. Stability criteria describe the mixing of the layers at the connecting channels between the individual ponds. The residence times in each WHTF pond is of the order of two days and thus larger than the computational time step of one day. Therefore, the transient characteristics were accounted for through a delay in the computed temperature at the end of each pond which is equal to the residence time of each pond.

#### WHTF Model

Pond 1 of the WHTF does not include any major side arm and is schematized as shown in Fig. 4. The condenser discharge  $Q_0$  at temperature  $T_0$  undergoes some mixing at the entrance. The dilution ratio  $D_s = (Q_0 + Q_e)/D_0$  is obtained from the buoyant surface jet model of Stolzenbach and Harleman [9] corrected for the interference of the jet with the bottom of the receiving water [3].  $Q_e$ , the entrained flow, is a function of the densimetric Froude number of the surface jet and the geometry of the discharge channel.  $T_1$  is the temperature after mixing and  $T_2$  is the temperature in the canal leading to pond 2. The heat flux to the atmosphere,  $\phi_n$ , is linearized in the usual way,  $\phi_n = -K(T - T_E)$  where  $K$  is the surface heat transfer coefficient and  $T$  and  $T_E$  are the surface and equilibrium temperatures. The temperature distribution in the reach is treated in a one-dimensional fashion with respect to surface area. Since  $D_s$  depends on the entrance densimetric Froude number which itself depends on  $T_2$  (the temperature in the counterflowing lower layer), the solution involves iterations.

Pond 2 of the WHTF has two side arms and is shown schematically in Fig. 5. Three possible flow configurations must be considered: (a) the entrance jet entrainment flow is greater than the sum of the flows entering the side arms, (b) the entrainment flow is smaller than the sum of the side arm flows and (c) the entrainment is smaller than the flow entering the first side arm. Figure 5 shows the counter flow conditions for case (b).

The model for pond 3 is similar to that for pond 2. The final consideration for the WHTF is the submerged discharge of the condenser flow, at temperature  $T_4$ , into the main lake through dike III (see Fig. 3). As shown in Fig. 6, the lake in front of the dike is rather shallow and is constrained

laterally. Therefore, the lake water for entrainment and mixing with the dike III jet must come through a restricted section. It is assumed that the limiting entrainment flow,  $Q_e$ , is reached when the lower layer flow at section "A" is critical.

### Main Lake Model

The maximum depth of the main lake is 70 ft near the downstream dam and 50 ft near the plant intake, while the computed upper layer depth is of the order of 15 ft for all cases of plant operation. The main lake can therefore be considered as a deep cooling lake for which the model of Ryan and Harleman [1] is applicable. The lake is separated in two regions: - a surface layer assumed to be of uniform temperature vertically. Its horizontal temperature distribution is solved as a function of surface area on a transient basis. The shape and location of the isotherms is therefore not determined, but the model gives the surface area inside each isotherm; - a subsurface pool assumed to be vertically stratified, but of uniform horizontal temperature. The vertical temperature profiles in this region are computed following the assumptions and method of the M.I.T. Lake and Reservoir Model described in [10].

A side arm reach is attached to the end of the main lake. This reach represents the regions of Lake Anna (4231 acres) which are located upstream of a lateral construction about two miles to the northeast of the power plant. The amount of side arm flow, its temperature drop and the return flow in the lower layer are calculated using the techniques discussed for the WHTF.

### Finite Element Model for Velocity and Temperature Distributions in Surface Layer of Lake Anna

A transient finite element model has been developed by Watanabe, et al. [2] which predicts the two-dimensional temperature and velocity distributions in the surface layer of the main lake. The FEM model is an extension of the main lake model which predicts surface temperatures only as a function of area fractions. Because of the expense of running the two-dimensional FEM (215 mesh points), it was used only for short period (2 week) studies for detailed temperature distribution in the main lake. The FEM grid is shown in Fig. 1 and representative velocity and temperature distributions are shown in Figs. 7 and 8.

### Prediction of Natural Lake Temperatures

Any lake temperatures which are induced by the power plant operation must be considered relative to the naturally occurring conditions (in the absence of plant operation). The M.I.T. Lake and Reservoir Model (Octavio et al. [10] was used to provide the predictions on a long-term basis. The model was verified using meteorological and hydrological input data collected on the North Anna site during 1974-76 by comparing the predictions with measured pre-operational lake temperatures.

Many lakes and reservoirs exhibit horizontal temperature homogeneity and thus a time-dependent, one-dimensional model which described the temperature variation in the vertical direction is adequate to describe their thermal structure. The M.I.T. Lake and Reservoir Model is a time-dependent, one-dimensional, variable area, discretized mathematical model based on the absorption and transmission of solar radiation, convection due to surface cooling, advection due to inflows and outflows and wind mixing. The model contains provisions for simultaneous or intermittent withdrawal from multi-level outlets and time of travel for inflows within the reservoir. Turbulent entrainment at the thermocline is treated by the wind mixing representation. The wind mixing algorithm is based on the rule that the rate of change of potential energy of the water column due to entrainment is equal to the rate of input of kinetic energy by the wind. An iterative procedure minimizes the accumulation of errors in the computation of the heat input. The model inputs include daily averaged values of air temperature, relative humidity, wind speed, cloud cover, and total short wave solar radiation. The model time-step is one day. The absorption coefficient for short wave solar radiation,  $\eta$ , was computed from Secchi disk depths.

A comparison of measured and predicted water surface temperature during 1976 is shown in Fig. 9, good agreement is obtained with respect to both absolute value and transient behavior. Vertical temperature distributions for two days in May and July for which detailed measurements were performed are compared with predicted values in Fig. 10.

#### LONG TERM SIMULATIONS

A long term simulation of the natural surface temperature of Lake Anna was made for a ten year period using meteorological data for 1957-1966. The ten year average and standard deviation above and below the mean are shown in Fig. 11. Similar ten year simulation runs were made for operational conditions corresponding to one through four units. A comparison of surface temperatures at the dam for meteorological conditions corresponding to year 1962 (an average year in the 10 year sequence) with 2 units operational is shown in Fig. 12. Changes in the vertical temperature structure of the lake were also computed. Figure 13 shows the ten year average for 3 operating units in comparison with the natural temperatures. The relative heat losses in the WHTF and in the main lake are indicated by the longitudinal temperature profile shown in Fig. 14 for 4 units in operation. Seventy percent of the total induced temperature change of 14°F occurs between the plant discharge into the WHTF and the end of the jet mixing zone downstream of dike III.

#### CONCLUSIONS AND ACKNOWLEDGEMENTS

The North Anna heat dissipation system is an example of an effective combination of a highly loaded, stratified cooling pond (the WHTF) and a lightly loaded cooling lake. It has also been demonstrated that in stratified systems, dead-end, side arms are effective in dissipating heat

through buoyancy induced circulation. The hydrothermal model developed for North Anna is computationally efficient, thereby making possible long-term simulation runs covering a wide range of meteorological and plant operating conditions.

This study was supported by Virginia Electric and Power Company, Richmond, Virginia, and by Stone and Webster Engineering Corporation, Boston, Mass. We gratefully acknowledge the close cooperation and assistance of the following individuals: Morris Brehmer, Carl Pennington and Robert Rasnic at VEPCO and David Knowles, David McDougall, Fred Mogolesko and Robert Taylor at Stone and Webster.

#### REFERENCES:

1. Ryan, P.J. and Harleman, D.R.F., "An Analytical and Experimental Study of Transient Cooling Pond Behavior", M.I.T., Department of Civil Engineering, R.M. Parsons Laboratory for Water Resources and Hydrodynamics Technical Report No. 161, Cambridge, Massachusetts, 1973. (Subsequent reports of this laboratory are referred to as M.I.T., R.M. Parsons T.R. No. \_\_\_.)
2. Watanabe, M., Harleman, D.R.F. and Connor, J.J., "Finite Element Model for Transient Two-Layer Cooling Pond Behavior", M.I.T., R.M. Parsons T.R. No. 202, 1975.
3. Jirka, G.H., Abraham, G. and Harleman, D.R.F., "An Assessment of Techniques for Hydrothermal Predictions", M.I.T., R.M. Parsons T.R. No. 203, 1975.
4. Jirka, G.H., Brocard, D.N., Hurley Octavio, K.A., Watanabe, M. and Harleman, D.R.F., "Analysis of Cooling Effectiveness and Transient Long-Term Simulations of a Cooling Lake (with application to the North Anna Power Station)", M.I.T., R.M. Parsons T.R. No. 232, 1977.
5. Huber, W.C. and Harleman, D.R.F., "Laboratory and Analytical Studies of Thermal Stratification of Reservoirs", M.I.T., R.M. Parsons T.R. No. 112, 1968.
6. Ryan, P.J. and Harleman, D.R.F., "Prediction of the Annual Cycle of Temperature Changes in a Stratified Lake or Reservoir: Mathematical Model and User's Manual", M.I.T., R.M. Parsons T.R. No. 137, 1971.
7. Ryan, P.J., Harleman, D.R.F. and Stolzenbach, K.D., "Surface Heat Loss from Cooling Ponds", Water Resources Research, Vol. 10, No. 5, 1974.
8. Brocard, D.N., Jirka, G.H. and Harleman, D.R.F., "A Model for the Convective Circulation in Side Arms of Cooling Lakes", M.I.T., R.M. Parsons T.R. No. 223, 1977.
9. Stolzenbach, K.D. and Harleman, D.R.F., "An Analytical and Experimental Investigation of Surface Discharges of Heated Water", M.I.T., R.M. Parsons T.R. No. 135, 1971.
10. Hurley Octavio, K.A., Jirka, G.H. and Harleman, D.R.F., "Vertical Heat Transport Mechanisms in Lakes and Reservoirs", M.I.T., R.M. Parsons T.R. No. 227, 1977.

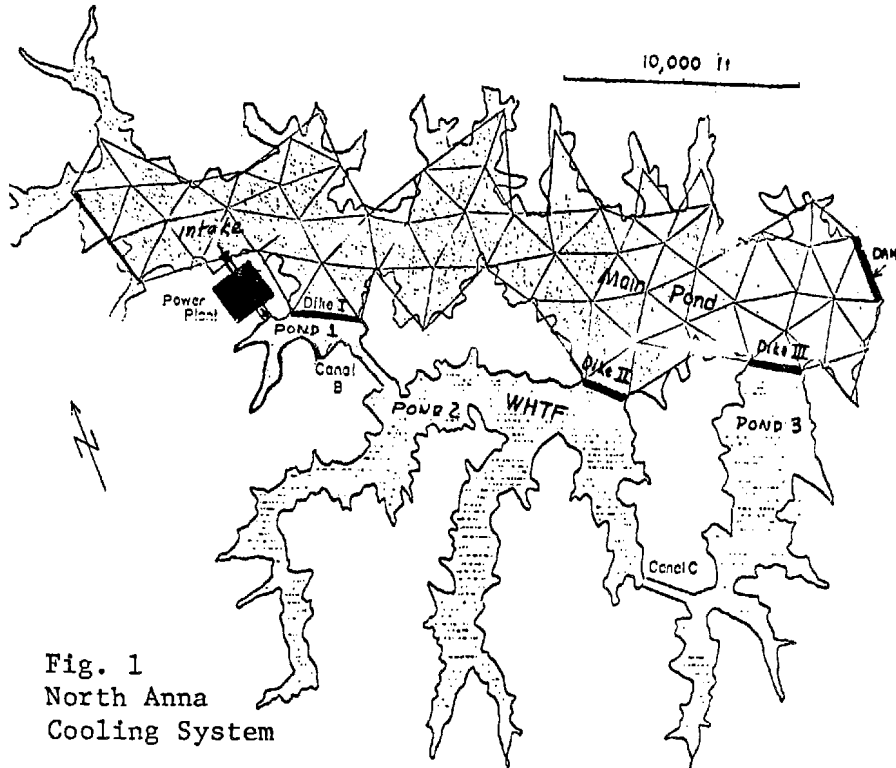


Fig. 1  
North Anna  
Cooling System

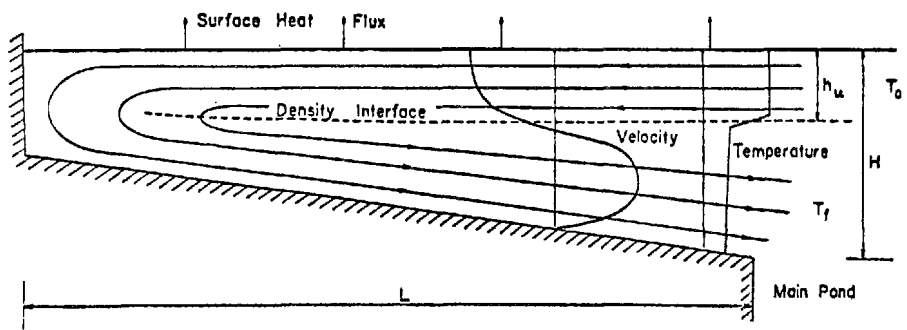


Fig. 2 Schematic of Side Arm Convective Circulation

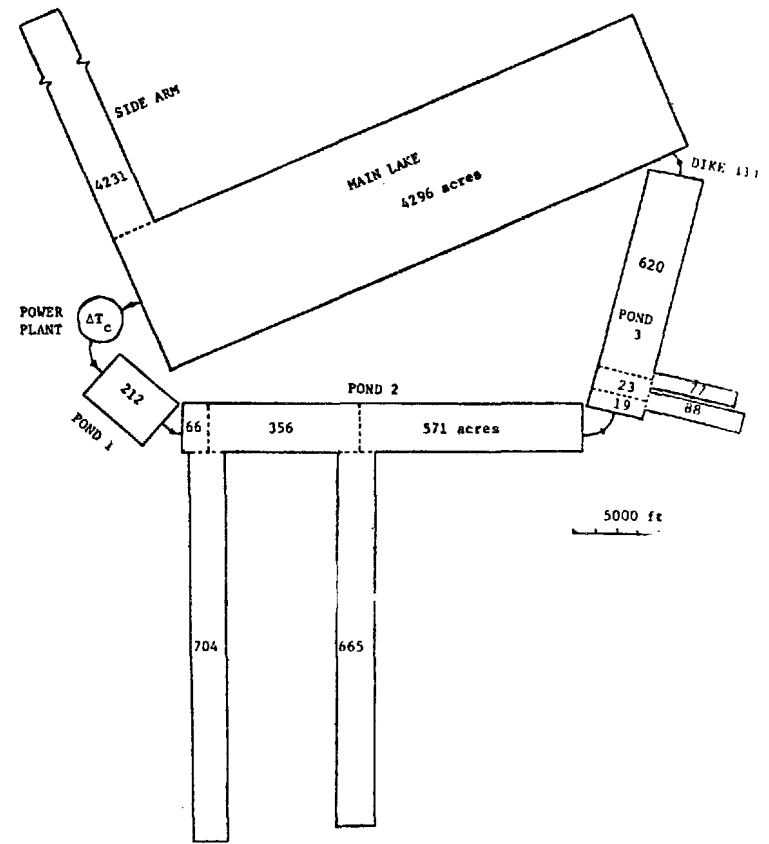


Fig. 3 Schematic of Segmented Model  
for North Anna

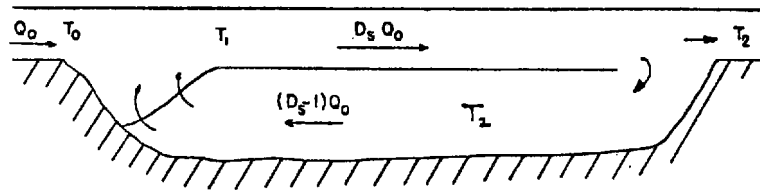


Fig. 4 Schematic of Pond 1 of WHTF

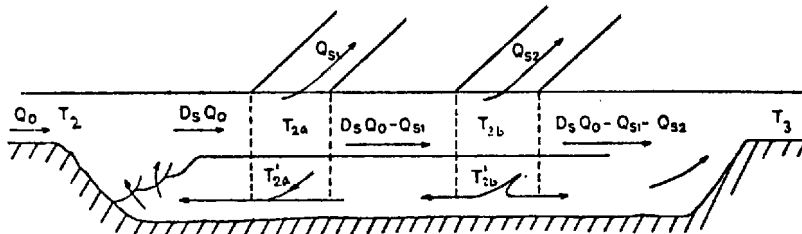


Fig. 5 Flow Configuration of Pond 2 of WHTF, with Two Side Arms

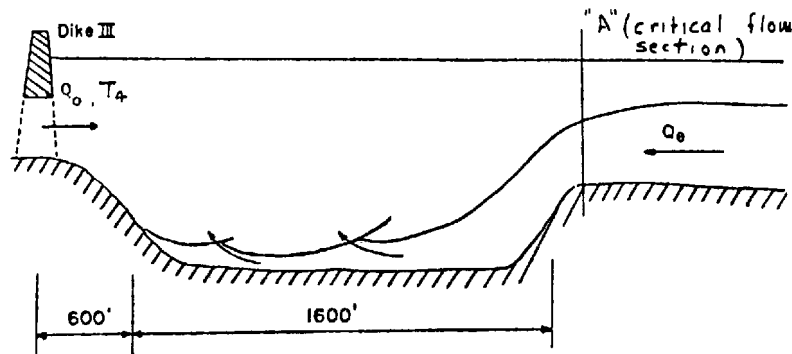


Fig. 6 Cross Section Along Axis of the Dike III Jet

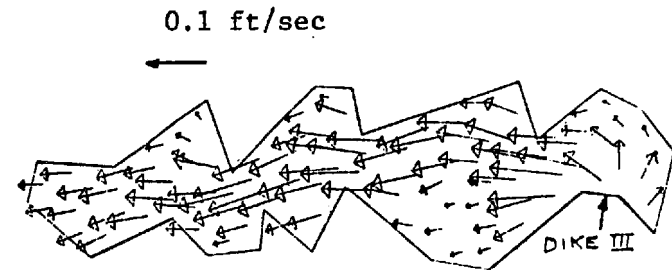


Fig. 7 Velocity Distribution in the Surface Layer for 50% Downwelling Flow at the End of the Lake and the Remaining 50% Distributed Along Both Sides

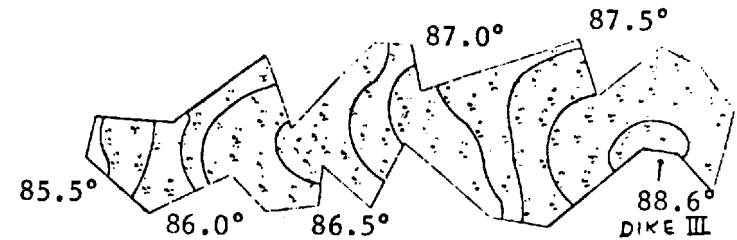


Fig. 8 Temperature Distribution in the Surface Layer Computed from FEM

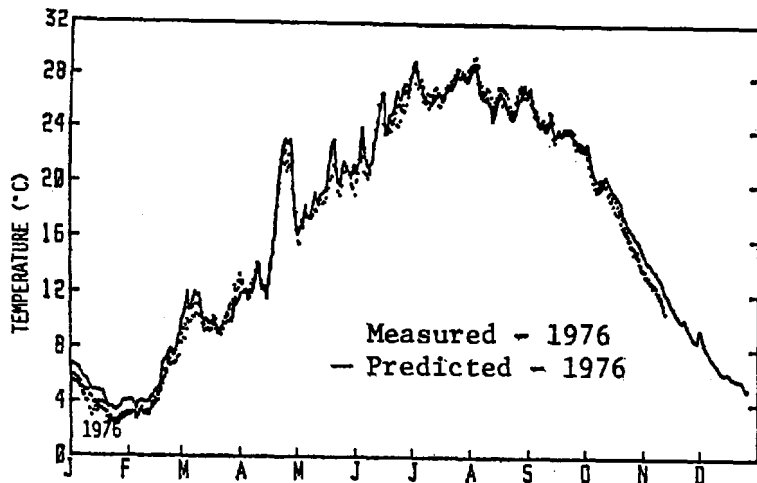


Fig. 9 Measured and Predicted Natural Surface Temperature

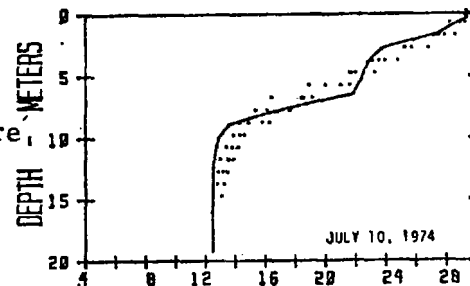
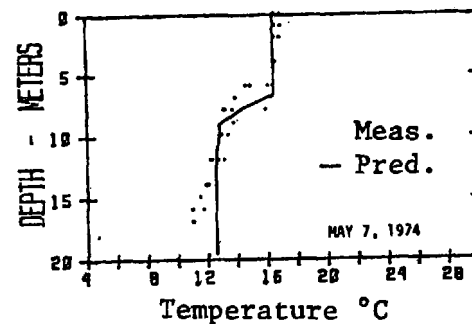


Fig. 10 Measured and Predicted Vertical Temperature Profiles

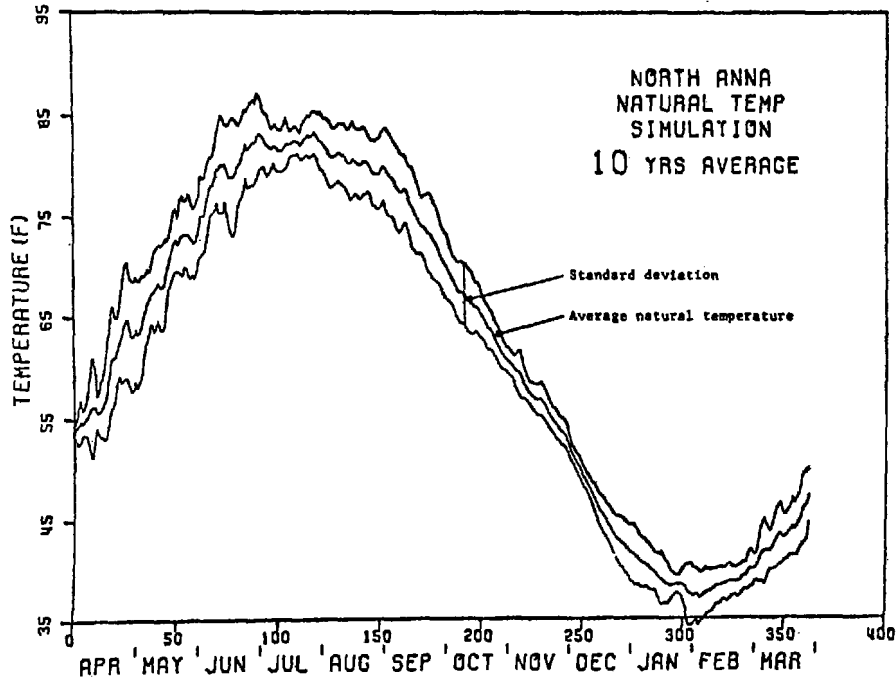


Fig. 11 Ten Year Average Natural Surface Temperatures and Standard Deviations

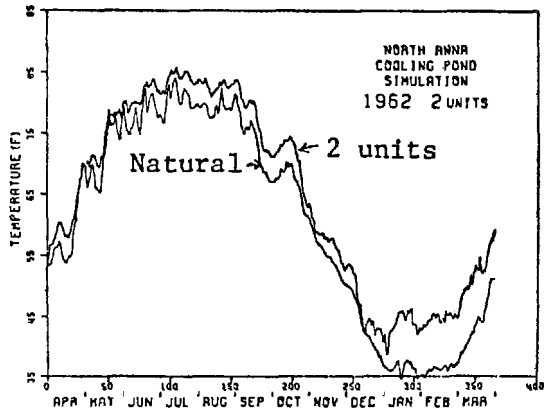


Fig. 12 Loaded and Unloaded Temps. in 1962, with 2 Units Operational

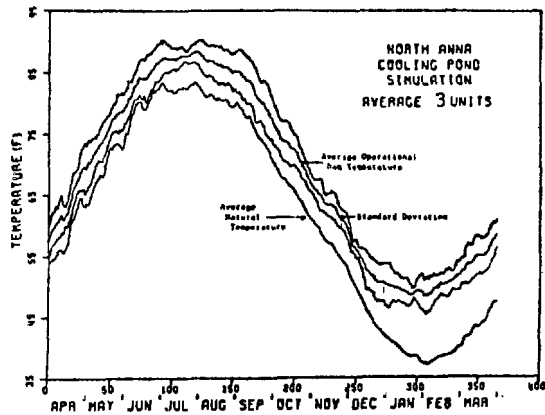


Fig. 13 10 Year Averaged Loaded and Unloaded Temperatures, with 3 Units Operational

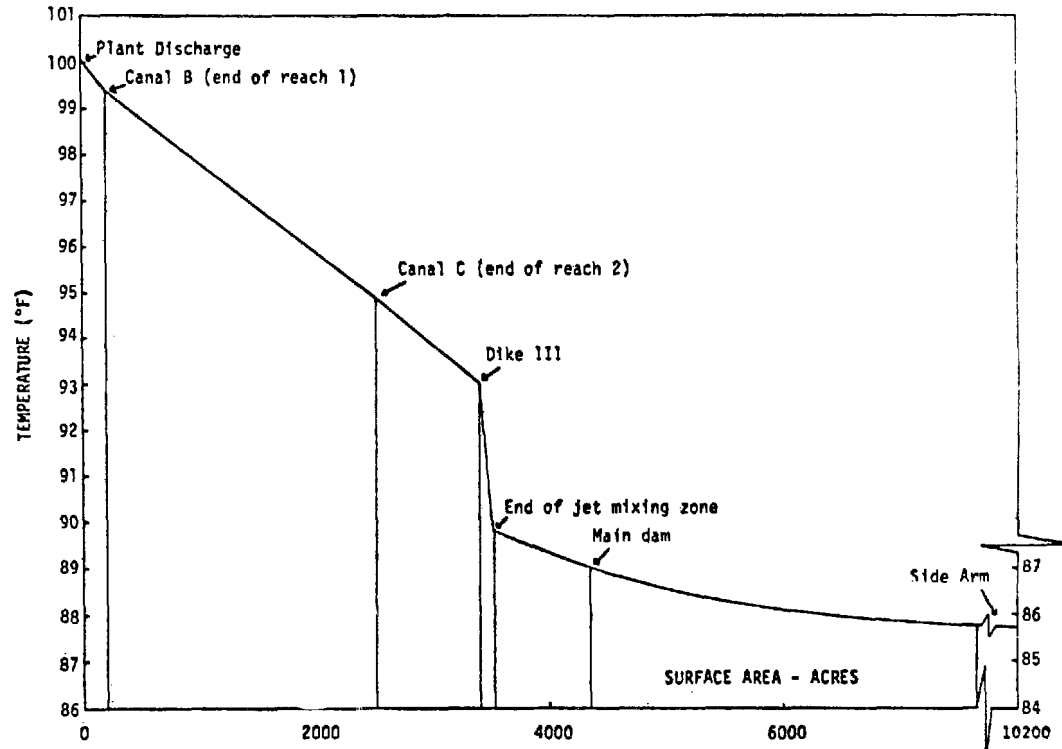


Fig. 14 Average Temperature Profile for North Anna Cooling System during Month of July 1962, with 4 Units Operating

COMPARISON OF THE SURFACE AREA REQUIREMENTS OF A  
SURFACE TYPE CONDENSER FOR A PURE STEAM  
CYCLE SYSTEM, A COMBINED CYCLE SYSTEM AND A  
DUAL-FLUID CYCLE SYSTEM

M.H. Waters  
VP Engineering  
International Power Technology  
California, U.S.A.

Dr. E.R.G. Eckert  
Regents Professor Emeritus  
University of Minnesota, U.S.A.

ABSTRACT

A recently issued patent to International Power Technology (IPT) on the Dual-Fluid cycle (DFC) and analysis by Kinney, et.al., on steam injected gas turbine cycles has demonstrated significant benefits for engines which use steam as a second working fluid in a gas turbine engine. These benefits include high thermal efficiency which is comparable to or better than that for combined cycle powerplants, and reduced system mechanical complexity and initial cost when compared with combined cycle powerplants.

The objective of this paper is to provide a quantitative evaluation of the condenser requirements for DFC engines. A very important feature of such an engine is that the exhaust gas at the condenser inlet is approximately at atmospheric pressure and is between 300<sup>o</sup>-400<sup>o</sup>F depending upon the cycle parameters. This contrasts dramatically with the condenser for either a pure steam system or a combined cycle system which is at low vacuum pressures (0.5-1.5 psia) and thus low temperature (80<sup>o</sup>-115<sup>o</sup>F).

INTRODUCTION

A recently issued patent to International Power Technology (IPT) on the Dual-Fluid Cycle (DFC) and analysis by Kinney, et. al., on steam injected gas turbine cycles has demonstrated significant benefits for engines which use steam as a second working fluid in a gas turbine engine (References 1 and 2). These benefits include high thermal efficiency which is comparable to or better than that for combined cycle powerplants provided the mixture of steam-air in the gas turbine is carefully controlled. Figure 1 is a schematic drawing of a DFC engine. A detailed description of the cycle is given later in the report, but the main feature is that the steam generated in the waste heat boiler is injected into the gas turbine ahead of the turbine section. In contrast,

a combined cycle powerplant uses a separate steam turbine system. There is an excellent potential for reduced system mechanical complexity and thus initial cost for DFC powerplants because of the single shaft output and no requirement for a separate steam turbine.

An obvious concern for the DFC is the performance of the condenser since the exhaust gas is a mixture of water vapor and non-condensable gases (typically the steam-air ratio is .15). A very important feature of a DFC engine is that the exhaust gas at the condenser inlet is approximately at atmospheric pressure and is between 300°-400°F depending upon cycle parameters. Condensing will begin at 130-180°F depending upon the amount of vapor in the exhaust and thus relatively high temperature differences exist across the heat exchanger surfaces. This contrasts dramatically with the condenser for either a pure steam system or a combined cycle system which is at low vacuum pressure (0.5-1.5psi) and thus low saturation temperatures (80°F-115°F).

The condenser surface area requirements for steam cycle powerplants are relatively easy to compute since the condensing fluid is a pure vapor and the equivalent heat transfer coefficient is a constant throughout the condenser. However, if the fluid is a mixture of water vapor and non-condensable gases, the heat transfer coefficient varies from point to point in the heat exchanger as the composition of the gas mixture changes due to removal of water vapor as condensate. The flow of vapor towards the condensing surface is diffusion controlled in a pure steam condenser since the vapor migrates to the cool tube surface as a sink. In a mixture of gases which contains vapor and non-condensable gases, both migrate to the cool tubes but the non-condensable gases would have to diffuse away from the surface. This can severely reduce the condensation heat transfer coefficient. In general for a DFC engine, there is a much larger quantity of non-condensable gases than there is water vapor, and the rate of condensation is a function of the vapor concentration in the mixture. Thus, the surface area calculation becomes a step wise process through the condenser as both the bulk fluid temperature and the fraction of water vapor in the gas mixture is reduced.

The condensation process is also controlled by convection because of the large fraction of non-condensable gases. Higher velocities through the tube banks thin the boundary layer thus increasing the condensing heat transfer coefficient. However, this also increases the pressure drop through the condenser which degrades engine performance thus creating a trade off situation.

The objective of this paper is to compute the condenser surface area requirements for a given DFC engine and make direct size comparisons with condensers for power equivalent steam and combined cycle powerplants. A condenser for a DFC engine can either be a contact type as in boiler scrubbers or be a surface type

with a bundled tube arrangement. The latter type is used in this paper as a basis for comparison.

#### NOMENCLATURE

|                 |  |
|-----------------|--|
| F               | Equivalent temperature driving force (defined by equation 9) |
| g               | Gravity constant   |
| G <sub>a</sub>  | Mass flow of air   |
| G <sub>s</sub>  | Mass flow of steam   |
| h <sub>c</sub>  | Equivalent heat transfer coefficient of condenser vapor film |
| h <sub>f</sub>  | Heat transfer coefficient in cooling water film              |
| h <sub>fg</sub> | Enthalpy of condensation                                     |
| h <sub>g</sub>  | Heat transfer coefficient in flowing gas film                |
| h <sub>w</sub>  | Conductivity of the tube well                                |
| ID              | Tube inside diameter   |
| k <sub>g</sub>  | Gas film mass transfer coefficient                           |
| k <sub>t</sub>  | Thermal conductivity of the tube well                        |
| k <sub>w</sub>  | Thermal conductivity of liquid film                          |
| MTD             | Mean temperature difference (defined by equation 5)          |
| n <sub>r</sub>  | Number of tube rows in a bank                                |
| Nu <sub>w</sub> | Nusselt number of flowing water                              |
| OD              | Tube outside diameter  |
| P               | Total pressure   |
| p <sub>c</sub>  | Steam partial pressure at film interface temperature         |
| Pr <sub>w</sub> | Prandtl number of water                                      |
| p <sub>s</sub>  | Steam partial pressure at steam bulk temperature             |
| Q               | Heat flow rate   |
| Re <sub>w</sub> | Reynolds number of flowing water                             |
| S               | Heat exchanger surface area                                  |
| T <sub>c</sub>  | Film interface temperature                                   |
| T <sub>s</sub>  | Bulk temperature of vapor or vapor-gas mixture               |
| T <sub>w</sub>  | Water temperature  |
| U               | Overall heat transfer coefficient defined by equation 1      |
| U <sub>c</sub>  | Overall heat transfer coefficient defined by equation 11     |
| ΔT'             | Temperature difference (T <sub>s</sub> -T <sub>w</sub> )     |
| ρ <sub>w</sub>  | Density of water   |
| μ <sub>w</sub>  | Dynamic viscosity of water                                   |

## METHODOLOGY

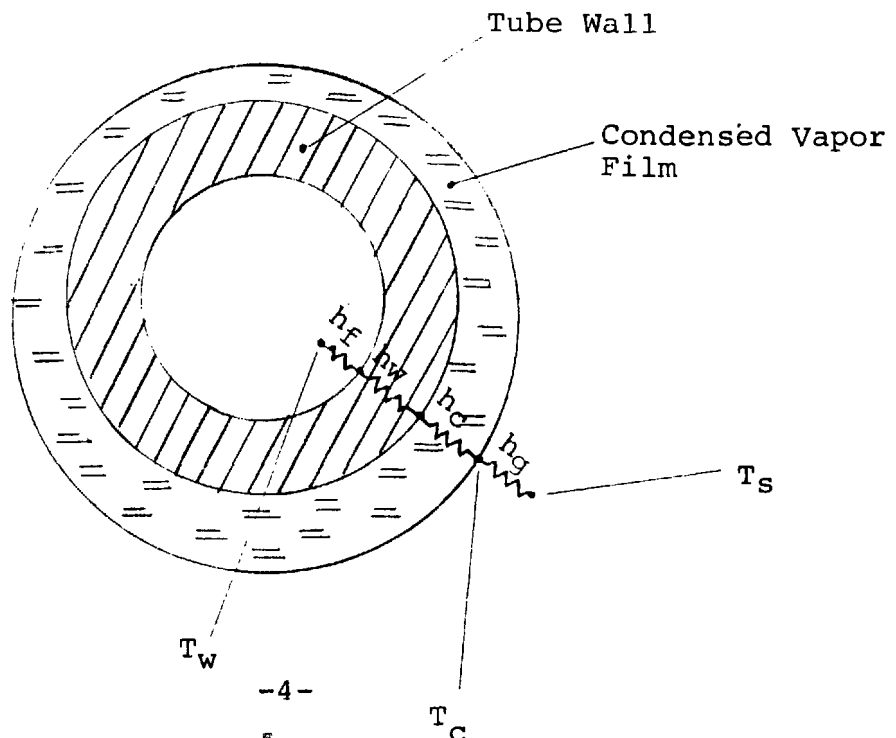
Condenser surface areas are designed by general procedures of heat exchanger design with the particular problem being the calculation of heat transfer coefficients with condensation. In the case of steam systems - either a conventional steam cycle or a combined cycle - the overall heat transfer coefficient is calculated from straight forward formulas and is essentially constant throughout the exchanger. However, for the Dual-Fluid Cycle condensation proceeds from a mixture of gases - the combustion products of air and steam. For this reason, the flow of vapor towards the condensing surface is diffusion controlled only across a thin boundary layer. This can be designed as a trade-off against the pressure drop across the tube bank. The non-condensable gases also flow towards the condensing surface and then diffuse away after they cool to preserve a local mass balance at the condensing surface. Thus, the heat transfer coefficient varies from point to point in the condenser as the composition of the mixture varies due to the removal of water vapor.

The cooling medium in the condenser is specified to be water, and the following two sub-sections describe the computational methods in some detail.

### Condensing from Pure Vapor

The sketch below demonstrates the mechanisms of heat transfer that take place in the pure vapor condenser;

- \* Forced convection between the flowing saturated vapor and the condensed vapor film
- \* Conduction across the condensed vapor film
- \* Conduction across the tube well
- \* Forced convection in the cooling water film



The overall heat transfer coefficient is given by:

$$\frac{1}{U} = \frac{(OD/ID)}{h_f} + \frac{OD}{h_w \left( \frac{OD+ID}{2} \right)} + \frac{1}{h_c} + \frac{1}{h_g} \quad (1)$$

For pure vapor,  $1/h_g \cong 0$ , so that the last term disappears from equation (1) and the outside film temperature,  $T_c$ , is equal to the saturated vapor temperature,  $T_s$ . The thermal conductivity of the tube,  $k_t$ , is constant, and thus the heat transfer coefficient,  $h_w$ , is constant.

$$h_w = \frac{k_t}{\left( \frac{OD - ID}{2} \right)} = 11800 \text{ BTU/hft}^2\text{F} \quad (2)$$

The equivalent heat transfer coefficient of the condensed vapor film,  $h_c$ , for a bank of tubes is given by the formula from reference 3:

$$h_c = .728 \left[ 1 + 0.2 \frac{c_w \Delta T'}{h_{fg}} (n_r - 1) \right] \left[ \frac{g \rho_w^2 k_w^3 h_{fg}}{n_r (OD) \mu_w \Delta T'} \right]^{1/4} \quad (3)$$

The cooling water film heat transfer coefficient is found from MacAdams Formula:

$$\frac{h_f (ID)}{k_w} = Nu_w = .023 Re_w^{.8} Pr_w^{.33} \quad (4)$$

The temperature difference MTD, to be used with  $U$ , is the average between the temperature difference at inlet and at outlet. We shall use the arithmetic average:

$$MTD = \frac{\Delta T_{inlet} + \Delta T_{outlet}}{2} \quad (5)$$

The total exchange surface required is:

$$S = \frac{Q}{U (MTD)} \quad (6)$$

## Condensing From a Mixture of Gases

The heat transfer coefficient  $U$  is not constant throughout the exchanger so that the previous method cannot be applied. A procedure developed by Colburn and Hougen is used, in the form presented by Votta (See references 4 and 5).

The condenser is divided in several sections for each of which  $U$  is calculated and assumed constant. The exchange surface for each section is:

$$dS = \frac{dQ}{U(\Delta T)}$$

The total exchange surface is:

$$S = \int \frac{dQ}{U(\Delta T)}$$

In this procedure, instead of calculating  $U$  and  $\Delta T$  separately, their product is used, as determined from a local heat balance (reference 5):

$$\frac{dQ}{dS} = h_g (T_s - T_c) + k_g h_{fg} (P_s - P_c) = u_c (T_c - T_w) = U(\Delta T) \quad (7)$$

The steam partial pressure is computed from  $G_s$  the steam flow rate,  $G_a$  the air flow rate, and  $P$  the total pressure of the mixture.

$$P_s = \frac{(G_s/G_a) P}{0.623 + (G_s/G_a)} \quad (8)$$

In the modification by Votta, the first equality in the string of equations (7) is written as:

$$\frac{dQ}{dS} = h_g (F_s - F_c) \quad (9)$$

where  $F(T)$  is a function of temperature and represents a single potential for both heat and mass transfer at the film interface. Table 1 is taken from reference 5 for a steam air mixture.

Table 1

| Temperature<br>°F | F at 1 ata<br>°F | F at 2 ata<br>°F |
|-------------------|------------------|------------------|
| 32                | 0                |                  |
| 40                | 15               |                  |
| 50                | 37               |                  |
| 60                | 62               |                  |
| 80                | 132              | 90               |
| 100               | 239              | 154              |
| 120               | 400              | 242              |
| 140               | 679              | 381              |
| 160               | 1138             | 597              |

In eqns (9) the interface temperature  $T_c$  to be used in finding  $F_c$  is determined by trial and error from the second equality in the string (9):

$$h_g (T_s - T_c) + k_g h_{fg} (P_s - P_c) = U_c (T_c - T_w) \quad (10)$$

For each condenser section, first the interface temperature is found, then  $F_s$  and  $F_c$  from the table, then equation (9) to find the area  $dS$ . Then the surfaces of the different sections are added up to give the total exchange surface  $S$ . The equivalent heat transfer coefficient between the cooling water and the outer face of the condensed steam film,  $U_c$ , is given by the equation:

$$\frac{1}{U_c} = \frac{(OD/ID)}{h_f} + \frac{OD}{h_w \left( \frac{OD+ID}{2} \right)} + \frac{1}{h_c} \quad (11)$$

where the calculation of  $h_w$ ,  $h_c$ , and  $h_t$  is as given in equation (2), (3) and (4) respectively.

#### Pressure Drop Across a Tube Bank

The pressure drop across a tube bank having a staggered arrangement is as follows (reference 6):

$$\Delta p = (n_r)(f) \frac{\rho_g V_g^2}{2} \quad (12)$$

where  $n$  is the number of tubes,  $f$  is the friction factor (a function of Reynolds number),  $\rho_g$  is the density and  $V_g$  the velocity of the gas.

## POWERPLANT DEFINITION

For purposes of comparison a 10,000 horsepower powerplant for marine propulsion is assumed. The steam cycle powerplant is typical for modern marine powerplants, whereas both the combined cycle and Dual-Fluid Cycle powerplants are based on the cycle of the General Electric LM 5000 gas turbine.

Sea water is the condenser coolant, and to provide for operations in tropical seas, it is assumed that the inlet temperature of the sea water to the condenser is 85°F. The condenser cooling water discharge temperature is assumed to be 88°F.

### Steam Cycle

The steam cycle power selected for this study is a regenerative-reheat single unit which is typical of steam powerplants for marine application. The engine has the following characteristics taken from Babcock and Wilcox (reference 7).

|                           |   |      |
|---------------------------|---|------|
| Throttle Pressure (psia)  | - | 1465 |
| Throttle Temperature (°F) | - | 1000 |
| Reheat Temperature (°F)   | - | 1000 |
| Condenser Pressure (psia) | - | 0.7  |
| Boiler Efficiency (%)     | - | 90   |

The system has a best heat rate of 7460 Btu/hp-hr, and thus the overall efficiency is given by:

$$\eta_{\text{overall}} = \eta_{\text{thermal}} \eta_{\text{boiler}} = \frac{(2545)}{7460} (0.90) = .307$$

Therefore, the heat rejected by the condenser is given by:

$$\text{Rejected Heat} = 2545 \left( \frac{1}{.307} - 1 \right) (0.90) = 5170 \text{ Btu/hp-hr}$$

At 0.7 psia condenser pressure, the latent heat is 1043 Btu/lb. Thus, the flow rate of steam for a 10,000 hp engine is given by

$$\text{Steam flow} = \frac{(\text{Heat rejected})}{(\text{Latent heat})} (\text{engine power}) =$$
$$\frac{(5170)}{1043} (10,000) = 49,569 \text{ lb/hr}$$

The condensing temperature at 0.7 psia condenser pressure is quite low (90°F). Thus, the temperature differences in the condenser are quite small since the cooling water is 85-88°F. This results in very large surface areas. Higher condensing pressures should also be considered even though the thermal efficiency of the steam system will suffer. Table 2 summarizes the pertinent data for three condensing pressures 0.7, 1.0 and 2.0 psia.

Table 2  
Steam Cycle 10,000 hp Engine

|                        |             |        |        |        |
|------------------------|-------------|--------|--------|--------|
| Condensing Pressure    | (psia)      | 0.7    | 1.0    | 2.0    |
| Condensing Temperature | (°F)        | 90     | 102    | 126    |
| Overall Efficiency     | (%)         | 30.7   | 30.3   | 29.3   |
| Rejected Heat          | (Btu/hp-hr) | 5170   | 5269   | 5526   |
| Steam Flow             | (lb/hr)     | 49,569 | 50,859 | 54,070 |

These data will be used in computing the condenser surface areas later in the report.

### Combined Cycle

The combined cycle powerplant used in this study is based on the Curtiss Wright Mod Pod 35A gas turbine which uses the LM5000 gas generator. This cycle has high efficiency, and it was selected because it would represent a very high performance combined cycle powerplant. The heat rate and the exhaust temperature of the Mod Pod 35A are as follows:

$$\begin{aligned} \text{Heat rate} &= 7050 \text{ Btu/hp-hr} \\ \text{Turbine exhaust temperature} &= 786^{\circ}\text{F} \end{aligned}$$

Although it is not in production, the Curtiss Wright Corporation has proposed a combined cycle powerplant with the LM 5000 as the gas turbine (reference 8). The stated heat rate for this combined cycle conversion for the LM 5000 is 5513 Btu/hp-hr (thermal efficiency = 46.2%).

A brief evaluation was made for both single pressure and two pressure steam turbine systems based on the LM 5000 cycle. Details of this evaluation are given in the Appendix. For the computation of condenser requirements of a 10,000 horsepower combined cycle powerplant, the following engine characteristics are defined:

Table 3  
LM 5000/Combined Cycle 10,000 hp Engine

|                         |             |       |       |       |
|-------------------------|-------------|-------|-------|-------|
| Condensing Pressure     | psia        | 0.7   | 1.0   | 2.0   |
| Condensing Temperature  | °F          | 90    | 102   | 126   |
| Single Pressure System  |             |       |       |       |
| Thermal Efficiency      | (%)         | 46.9  | 46.3  | 45.5  |
| Power Split (steam/gas) |             | .301  | .287  | .275  |
| Rejected Heat Flow      | (Btu/hp-hr) | 5910  | 6322  | 6710  |
| Steam Flow              | (lb/hr)     | 13106 | 13608 | 14161 |

## Two Pressure System

|                         |             |       |       |       |
|-------------------------|-------------|-------|-------|-------|
| Thermal Efficiency      | (%)         | 49.0  | 48.2  | 47.0  |
| Power Split (steam/gas) |             | .357  | .334  | .301  |
| Rejected Heat Flow      | (Btu/hp-hr) | 4583  | 5074  | 5910  |
| Steam Flow              | (lb/hr)     | 11560 | 12263 | 13379 |

Although the thermal efficiencies shown in the table are greater than that of the LM 5000 combined cycle quoted above, the difference is not great and is probably the result of not accounting for any degradation in the gas turbine performance due to back pressure from the waste heat boiler. For comparison purposes, the results in Table 3 are representative of the best in combined cycle engine performance, and these data will be used in computing the condenser surface areas later in this report.

## Dual Fluid Cycle

As with the combined cycle, the Dual-Fluid Cycle (DFC) makes use of two separate working fluids. In either cycle, each fluid is compressed separately; but in the DFC the two fluids are combined in a single mixture for expansion through the turbines and heat regeneration in the waste heat boiler.

The Dual Fluid Cycle essentially combines a regenerative Brayton cycle and a regenerative Rankine cycle system in parallel. Thus, both cycles are operating at the specific turbine inlet temperature. In contrast, combined cycle engines combine the Brayton and Rankine cycles in series and the maximum temperature of the Rankine cycle fluid is the turbine discharge temperature.

To describe the operation of a DFC engine, the following subparagraphs outline the thermodynamic cycle in more detail.

1. Compression of the two fluids takes place separately. Air is compressed from atmospheric pressure up to the maximum cycle pressure in a conventional axial or centrifugal flow compressor. Water is pumped at ambient temperature to a pressure somewhat greater than the compressor discharge air pressure.
2. Combustion takes place in a mixture of air and a suitable fuel in a conventional gas turbine combustor. Water, in the form of steam, is then mixed with the combustion products of air. This steam is the result of water being preheated by the regenerative heat exchanger (see No. 4 below) and is at a somewhat higher pressure than the combustion gas to promote proper mixing.
3. The resultant mixture of combustion products of air and steam, hereafter called the gas mixture, is at a specified maximum turbine inlet temperature which dictates the combination of water-air ratio and fuel-air ratio selected. Expansion of this gas mixture takes place in two conventional axial flow turbines.

The first or high temperature turbine drives the air compressor through a connecting shaft. The second turbine is a free turbine which provides the useful output work.

4. The gas mixture discharging from the power turbine is then passed through a counter flow regenerative heat exchanger. This heat exchanger uses steam which is then injected into the combustor (see No. 2 above). Thus the heat in the cycle is being "regenerated".

5. The gas mixture leaves the heat exchanger at or above the saturation temperature of the steam in the gas mixture as determined by the partial pressure of the steam, and it then passes through a condenser. In general, no condensation is desirable from a design consideration in the heat exchanger, but in the condenser steam condenses to water and is separated from the mixture. The remaining products of the combustion of air are exhausted to the atmosphere. The condensed water is purified pumped to high pressure and recycled to the regenerative heat exchanger.

It must be pointed out that steam injection into gas turbine engines is not a new concept. However, almost without exception the objective has been to increase power for short periods of operation. Extensive work by IPT over the past 5 years has demonstrated that extremely high efficiencies can be achieved in the DFC described above. However, peak efficiency can only be obtained at a particular balance of air-steam ratio and air-fuel ratio. Reference 1 describes in some detail how this balance is linked to the cycle pressure ratio and the turbine inlet temperature of the gas turbine engine.

The Dual Fluid Cycle does lend itself to a retrofit of existing engines. Mechanical design modifications must be carefully assessed for a particular engine, but for purposes of this paper which is to compare condenser surface area requirements - it is presumed that a LM 5000/DFC engine can be accomplished. Thermodynamic cycle calculations give the following peak performance characteristics for such an engine.

Table 4  
LM 5000/DFC Engine

|                            |          |      |
|----------------------------|----------|------|
| Overall Thermal Efficiency | (%)      | 48   |
| Power per Unit Air Flow    | (hp/pps) | 291  |
| Steam Flow/Air Flow        |          | .113 |
| Air Flow/Fuel Flow         |          | 43   |

As described in the Methodology section, condensing from a mixture of gases poses a different computational problem because the heat transfer coefficient is not constant through the ex-

changer.

The gas mixture temperature at the discharge of the waste heat boiler is 400°F, and thus the condenser is a gas cooler from this temperature down to the temperature at which vapor begins to condense. This will be outlined in more detail in the following section on condenser surface areas.

CONDENSER SURFACE AREA REQUIREMENTS

Steam Cycle and Combined Cycles

Using the methodology outlined in a previous section, the overall heat transfer coefficient is relatively easy to compute for pure steam systems - both the steam cycle engine and the combined cycle engine. Several assumptions were made concerning the heat exchanger:

|   |       |     |
|---|-------|-----|
| Incoming Temperature of the Cooling Water | (°F)  | 85  |
| Cooling Water Temperature Rise            | (°F)  | 3   |
| Outside Diameter of Condenser Tubes       | (in)  | .75 |
| Inside Diameter of Condenser Tubes        | (in)  | .62 |
| Water Flow Velocity in the Tubes          | (fps) | 5   |

The following equations are used to derive the the number of condenser tubes:

$$\text{Cooling Water Flow Rate} = \text{Heat Exchanger Duty} / \text{Temperature Rise}$$

$$\text{Total Cross Sectional Area for Water Flow} = \text{Cooling Water Flow Rate} / \text{Density} / \text{Velocity}$$

$$\text{Number of Tubes} = \text{Cross Sectional Area} / \left( \frac{\pi}{4} \text{ID}^2 \right)$$

Tables 5, 6 and 7 summarize the pertinent data for the steam cycle engine, the single pressure combined cycle engine and the two pressure combined cycle engine respectively. Recall that each powerplant is rated at 10,000 hp and that the combined cycle steam system is relatively small because of the split in power between the gas turbine and the steam turbine.

Table 5  
Steam Cycle System

|                           |                             |      |      |      |
|---------------------------|-----------------------------|------|------|------|
| Condensing Pressure       | (psia)                      | 0.7  | 1.0  | 2.0  |
| Condensing Temperature    | (°F)                        | 90   | 102  | 126  |
| Cooling Water Flow Rate   | (lb/hr x 10 <sup>-7</sup> ) | 1.72 | 1.76 | 1.84 |
| Number of Condenser Tubes |                             | 7319 | 7491 | 7830 |

|                                   |                              |       |      |      |
|-----------------------------------|------------------------------|-------|------|------|
| Overall Heat Transfer Coefficient | (Btu/hr ft <sup>2</sup> °F)  | 543   | 674  | 742  |
| Mean Temperature Difference       | (°F)                         | 3.5   | 13.5 | 39.5 |
| Duty                              | (Btu/hr x 10 <sup>-7</sup> ) | 5.17  | 5.27 | 5.53 |
| Condenser Surface Area            | (ft <sup>2</sup> )           | 27923 | 5791 | 1887 |

Table 6  
Single Pressure Combined Cycle

|                                   |                              |       |      |      |
|-----------------------------------|------------------------------|-------|------|------|
| Condensing Pressure               | (psia)                       | 0.7   | 1.0  | 2.0  |
| Condensing Temperature            | (°F)                         | 90    | 102  | 126  |
| Cooling Water Flow Rate           | (lb/hr x 10 <sup>-7</sup> )  | .593  | .605 | .615 |
| Number of Condenser Tubes         |                              | 2522  | 2575 | 2618 |
| Overall Heat Transfer Coefficient | (Btu/hr ft <sup>2</sup> °F)  | 444   | 577  | 677  |
| Mean Temperature Diff.            | (°F)                         | 3.5   | 13.5 | 39.5 |
| Duty                              | (Btu/hr x 10 <sup>-7</sup> ) | 1.78  | 1.81 | 1.85 |
| Condenser Surface Area            | (ft <sup>2</sup> )           | 11454 | 2328 | 690  |

Table 7  
Two-Pressure Combined Cycle

|                                   |                              |       |      |      |
|-----------------------------------|------------------------------|-------|------|------|
| Condensing Pressure               | (psia)                       | 0.7   | 1.0  | 2.0  |
| Condensing Temperature            | (°F)                         | 90    | 102  | 126  |
| Cooling Water Flow Rate           | (lb/hr x 10 <sup>-7</sup> )  | .547  | .565 | .593 |
| Number of Condenser Tubes         |                              | 2326  | 2403 | 2522 |
| Overall Heat Transfer Coefficient | (Btu/hr ft <sup>2</sup> °F)  | 440   | 570  | 674  |
| Mean Temperature Difference       | (°F)                         | 3.5   | 13.5 | 39.5 |
| Duty                              | (Btu/hr x 10 <sup>-7</sup> ) | 1.64  | 1.69 | 1.78 |
| Condenser Surface Area            | (ft <sup>2</sup> )           | 10649 | 2201 | 668  |

The condenser surface areas for the three different systems are shown in figure 2. It is fairly obvious that the need for low condensing pressures to achieve a high thermal efficiency will result in a very large condenser. Note that the data in figure 1 are plotted on semi-log paper and the reduction in condenser surface area with higher condenser pressures is quite significant.

The combined cycle condenser exhibits an identical trend, but at significantly lower areas since the steam turbine handles only a fraction of the total engine power.

### Dual-Fluid Cycle

As outlined in the Methodology section, the calculation of condenser surface area for a mixture of gases is a step wise process. The heat exchanger may be considered to be formed of two sections with different heat transfer regimes:

Section 1 - Single phase heat transfer, from inlet to point of saturation

Section 2 - Two phase heat transfer from the point of saturation to the outlet.

The exhaust temperature from the waste heat boiler of an LM 5000/DFC engine is 400°F, and the temperature in section 1 drops to 133°F before condensation begins to take place. For section 2, the temperature difference from inlet to outlet is divided into intervals and the heat exchange duty and surface is computed for each interval. Table 8 summarizes the pertinent data for each of the intervals. The total condenser surface area for the 10,000 hp engine is calculated to be 3823 ft<sup>2</sup>.

The final temperature (not shown on table 8) is 93°F, and it was chosen so that the water remaining as vapor in the gas mixture was balanced by the water formed in the combustion process, i.e., there is no water lost or gained by the system. If it is acceptable to provide makeup water, then the final condensing temperature can be higher, and thus the condenser will be smaller. This is shown in figure 3. Also shown in the figure is the effect of water vapor from the atmosphere. For example if the water break-even point was designed for an ambient temperature of 80°F with a relative humidity of 0.6 the final condenser temperature would be approximately 101°F and the required condenser surface area would be 3080 ft<sup>2</sup>.

It should be noted that a larger portion of the condenser areas (1436 ft<sup>2</sup>) is actually a gas cooler - not a condenser. It is entirely feasible to use this waste heat for other purposes in a separate heat exchanger. For example, it can be used for stack gas heating or for feed water heating if necessary or desirable.

Table 8  
 Calculation of Required Exchange Surfaces  
 for the LM 5000/DFC 10,000 hp engine

|                           | Gas *<br>temper-<br>ature<br>°F | Heat<br>exchange<br>Btu/h | Gas heat<br>transfer<br>coeff.<br>Btu/hFft <sup>2</sup> | Interface<br>temper-<br>ature<br>°F | Overall<br>heat trans.<br>coeff.<br>Btu/hFft <sup>2</sup> | Heat<br>exchange<br>surface<br>ft <sup>2</sup> |
|---------------------------|---------------------------------|---------------------------|---|-------------------------------------|---|--|
| Section 1<br>(gas cooler) | 400                             | 9.7 x 10 <sup>6</sup>     | 38.2  |                                     | 38  | 1436   |
| Section 2<br>(condenser)  | 133                             | 3.559 x 10 <sup>6</sup>   | 34.9  | 105                                 | 216   | 383  |
|                           | 125                             | 1.773 x 10 <sup>6</sup>   | 34.4  | 101                                 | 210   | 240  |
|                           | 120                             | 1.514 x 10 <sup>6</sup>   | 34.3  | 98                                  | 205   | 252  |
|                           | 115                             | 1.353 x 10 <sup>6</sup>   | 34.2  | 96                                  | 200   | 260  |
|                           | 110                             | 1.160 x 10 <sup>6</sup>   | 34.1  | 95                                  | 195   | 272  |
|                           | 105                             | 2.292 x 10 <sup>6</sup>   | 34.0  | 91                                  | 190   | 980  |
|                           | TOTAL                           | 2.135 x 10 <sup>7</sup>   |   |                                     | TOTAL   | 3823   |

\* at the beginning of the interval

## CONCLUDING REMARKS

The objective of this paper was to provide a quantitative evaluation of the condenser surface area requirements for a Dual-Fluid Cycle engine and to compare these results with those for pure steam condensers - both conventional steam cycle and combined cycle. The evaluation summarizes the choice of parameter tradeoffs for all three engine systems, and it is safe to state that at a constant rated power the condenser for a DFC engine will have a surface area which is smaller than a steam cycle engine and comparable to the combined cycle engine.

The original concern was that the DFC engine condenser would be significantly larger because the heat transfer rate from the gas mixture was greatly reduced due to the presence of non-condensable gases. However, the heat transfer is no longer completely diffusion controlled. The temperature and concentration gradients can be controlled by the forced convection process in the flow of gases over the condenser tubes. Although the heat transfer coefficient is much reduced, the large temperature differences available through most of the condenser compensate for this deficiency.

It is worth noting that the DFC engine condenser is essentially operating at atmospheric pressure. Thus, light weight materials, even plastics, and units having rectangular cross sections can be employed. In contrast the low vacuum pressures typical of a steam system requires heavier metals with cylindrical cross sections to overcome buckling stress. Thus, the DFC engine condenser offers the potential for design flexibility and cost reduction.

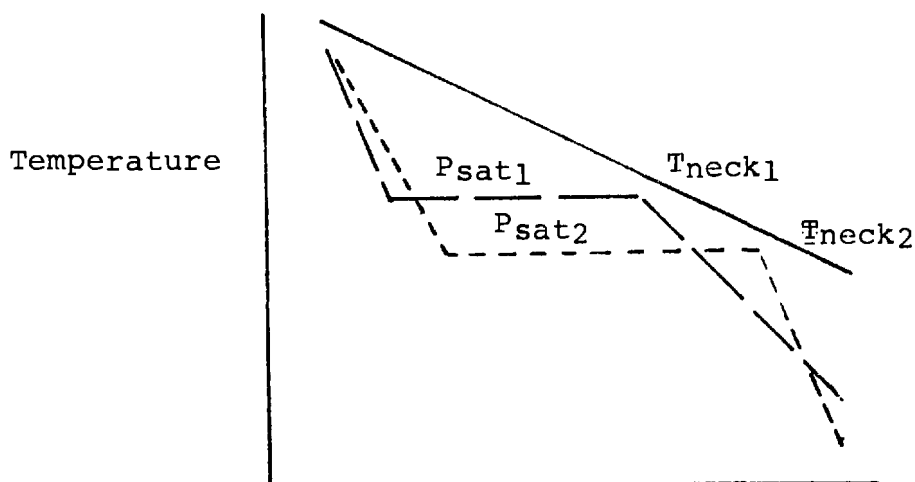
There are many aspects to consider in optimizing either of these systems, and they should be evaluated on the basis of powerplant operating costs taking into account the heat rate of the total combined cycle powerplant and the initial cost and required maintenance of the steam cycle equipment. This is beyond the scope of this paper, but these considerations should be kept in mind when evaluating the tradeoffs. Reference 9 is a good example of a tradeoff study for a combined cycle steam system.

### Single Pressure System - Power Output

It is assumed that the state-of-the-art in steam turbine isentropic efficiency is approximately 80%. Obviously the power rating of the turbine will have an effect on isentropic efficiency. Smaller turbines result in a reduced Reynolds number in the steam turbine and thus reduced efficiency. However, this effect is considered to be a second order effect and is ignored here.

For the single pressure system, the condensing pressure (and thus temperature) is specified and expansion is presumed to take place down to the Wilson line (96% quality for a given pressure). In addition, the maximum steam temperature is assumed to be 736°F (50 degrees below the LM 5000 turbine discharge temperature). Thus, the only unknown in the system is the maximum steam pressure, and this is easily determined from the steam tables.

The results shown in figures A1 and A2 demonstrate the expected result. The maximum steam pressure is reduced for reduced condensing pressures; however, the thermal efficiency based on heat input to the waste heat boiler and the power per unit steam flow both increase at the reduced condensing pressures. The sketch below demonstrates how the reduced steam pressure is beneficial to the waste heat boiler.



The lower pressure results in a lower pinch point temperature, and thus more heat is transferred from the gas turbine exhaust. This results in a greater quantity of steam flow and an increase in steam turbine power per unit flow of the gas turbine exhaust. This has a direct impact on the overall thermal efficiency of the combined cycle powerplant as discussed later in this Appendix.

#### Two Pressure System - Power Output

A different approach is taken for the two pressure system. To specify the system, both the condensing pressure and the maximum steam pressure of the system are specified. Expansion through the first turbine proceeds to the Wilson line. This determines the pressure for the second turbine and a second pass through the boiler elevates the steam temperature back to 736<sup>o</sup>F. The expansion through the second turbine is down to the specified condensing pressure or to the Wilson line if it is encountered at higher pressures. More typically the specified pressure will be reached while still in the superheat region.

Results for the two pressure system are shown in figures A3 and A4. Based on the heat input from the waste heat boiler to the steam, the results in figure A3 suggest that increased steam pressure for the first turbine is desirable since both the steam thermal efficiency and the power per unit steam flow increase as this pressure increases. Again low condensing pressures improve the system performance significantly. However, the quantity of steam which can be generated is increased at reduced maximum steam pressures just as it is for the single pressure system (see figure A4). Thus, there is a tradeoff, and the upper portion of figure A4 shows there is a well defined optimum in terms of power from the steam turbine per unit flow in the gas turbine exhaust.

#### Overall Thermal Efficiency of the Combined Cycle Powerplant

The Curtiss-Wright Mod Pod 35A mechanical drive gas turbine is derived from the LM 5000 gas generator, and its thermal efficiency and power per unit air flow as stated in reference 10 are 36.1% and 153 hp/p<sub>pps</sub> respectively.

Integration of a waste heat boiler for the combined cycle will affect this performance somewhat due to the back pressure at the gas turbine. For purposes of comparison, this effect is ignored for the results shown in figures A5 and A6.

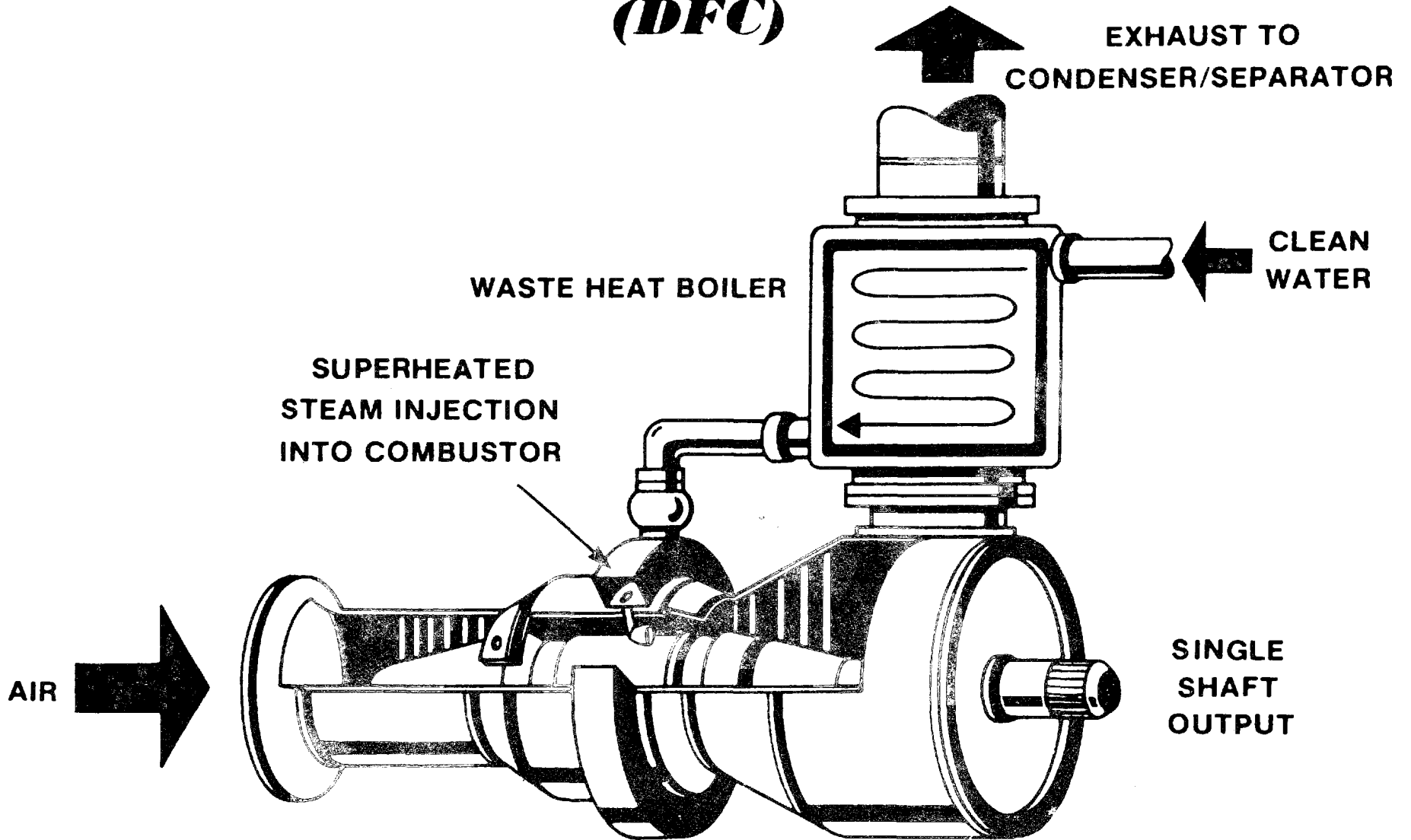
The data presented in figures A5 and A6 summarize the results for the single pressure and two-pressure systems respectively. As expected, a reduced condensing pressure increases the power split (steam turbine power/gas turbine power) and thus the overall efficiency of the combined cycle powerplant. For the two pressure system, note that the peak efficiency shifts to

maximum steam pressures as the condensing pressure is reduced.

These results are those used in the main body of the report to compute condenser surface areas.

1. Anon., Regenerative Parallel Compound Dual Fluid Heat Engine, U.S. Patent 4,128,994, (12 December 1978).
2. Fraise, W.E. and Kinney, C.; Effects of Steam Injection on the Performance of Gas Turbine Power Cycles, ASME Paper No. 78-GT-11, April, 1978.
3. Chen, M.M., J. Heat Transfer, Trans ASME, C 83:55 (1961).
4. Colburn, A.P., and Hougen, O.A., Ind. Eng. Chem., 26:1178 (1934).
5. Votta Jr., F., Condensing from Vapor Gas Mixtures, Chem. Engrg., 71:223 (1964).
6. Eckert, E.R.G., Analysis of Heat and Mass Transfer, McGraw Hill Book Company (1972).
7. Anon, Steam Its Generation and Use, The Babcock and Wilcox Company, 37th Edition.
8. Anon, "Mod Pod LM 5000's offer lowest plant heat rates", Gas Turbine World, September, 1976, pp26-30.
9. Bernstein, E., and Cashman, J.; The Energy Saver Combined Cycle, ASME paper 78-GT-127, presented at the Gas Turbine Conference, London, April 9-13, 1978.
10. Anon, Gas Turbine World Handbook, 1977-78, Pequot Publications, Inc.

# CONCEPT OF THE DUAL-FLUID CYCLE ENGINE (DFC)



951

Figure 1

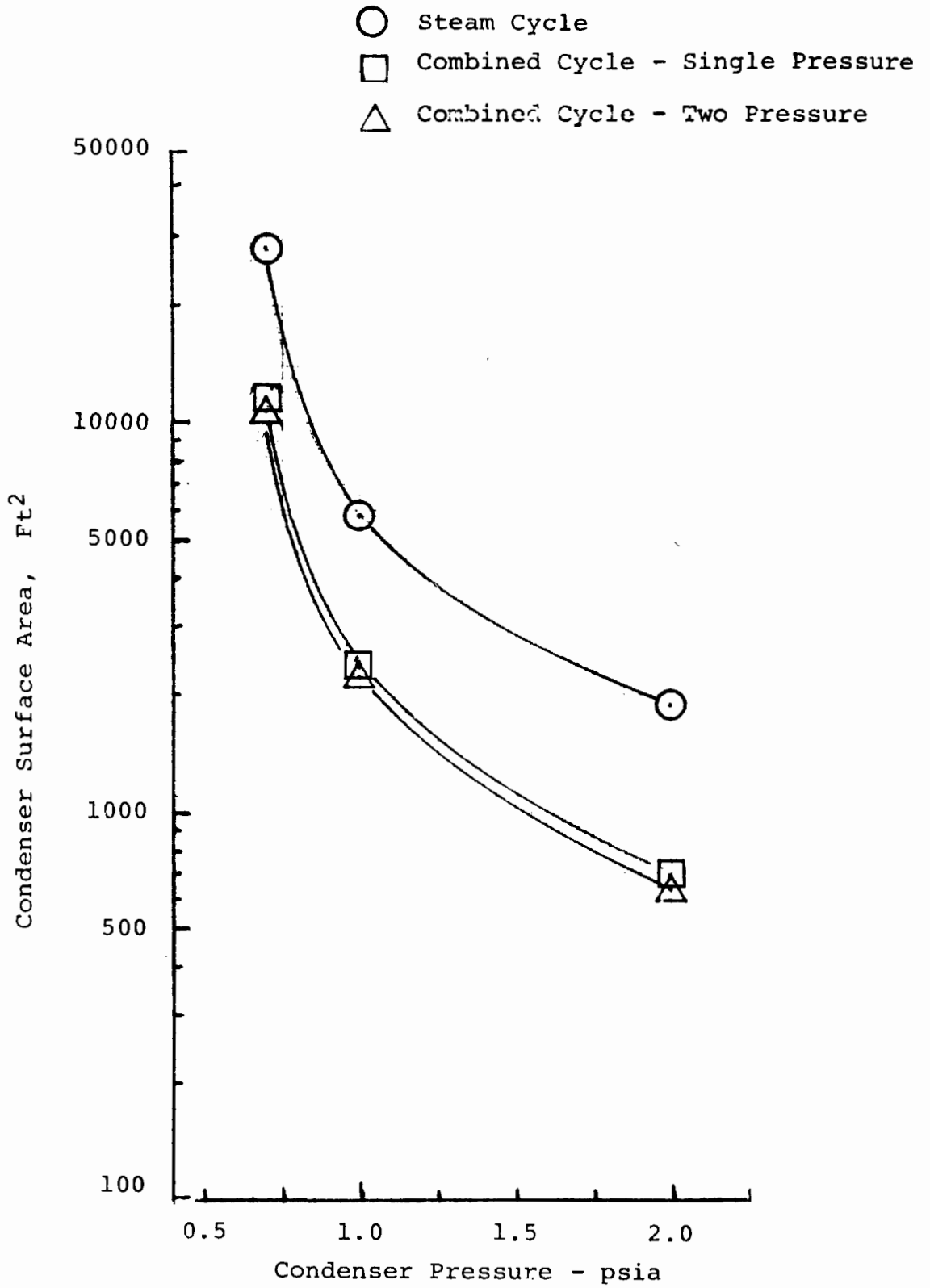


Figure 2 Effect of Condenser Pressure on Vapor Condenser Surface Area

Ambient Temperature = 80°F

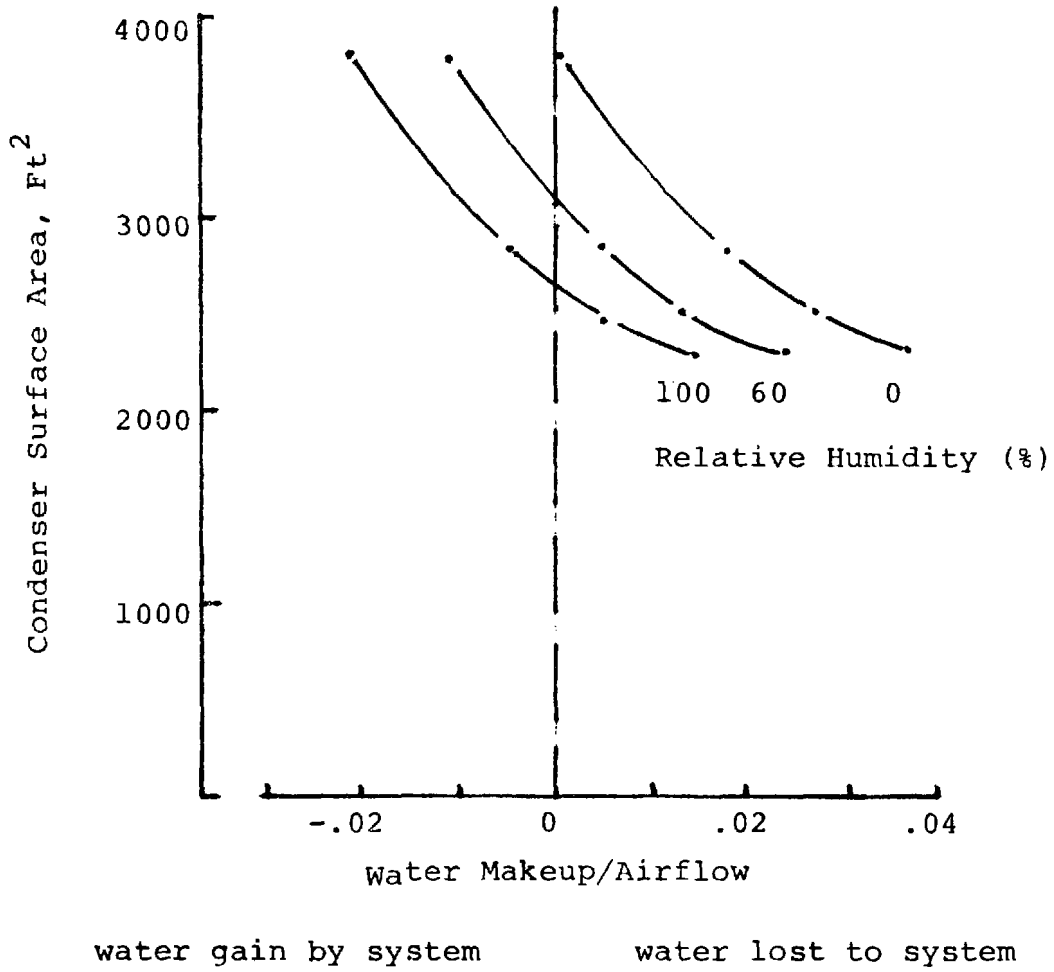


Figure 3 Relation between Condenser Size and Water Gained/Lost to the System for a LM 5000/DFC Engine Rated at 10000 hp

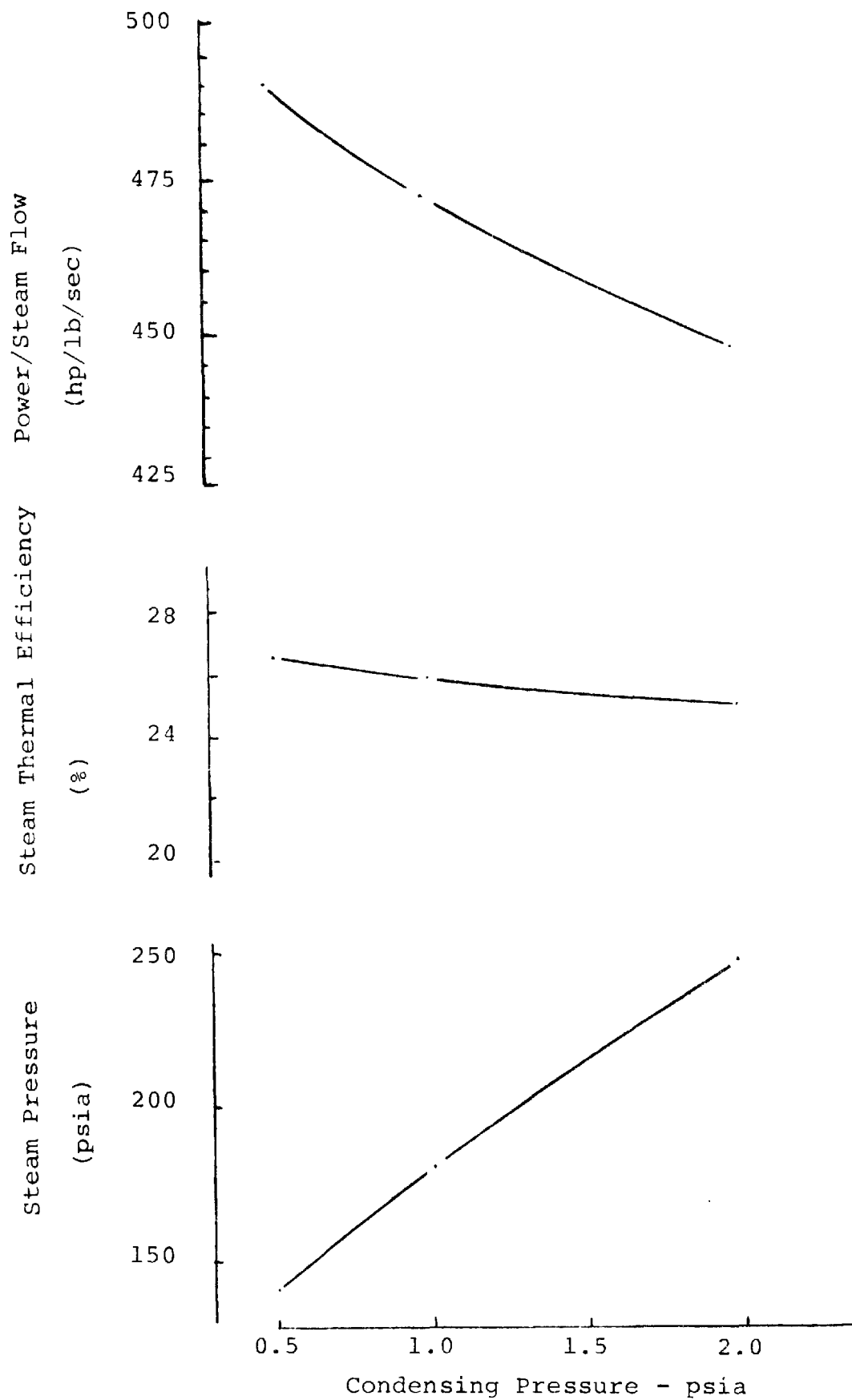


Figure A-1 Effect of Condensing Pressure on the Performance of a Single Pressure Steam Turbine System

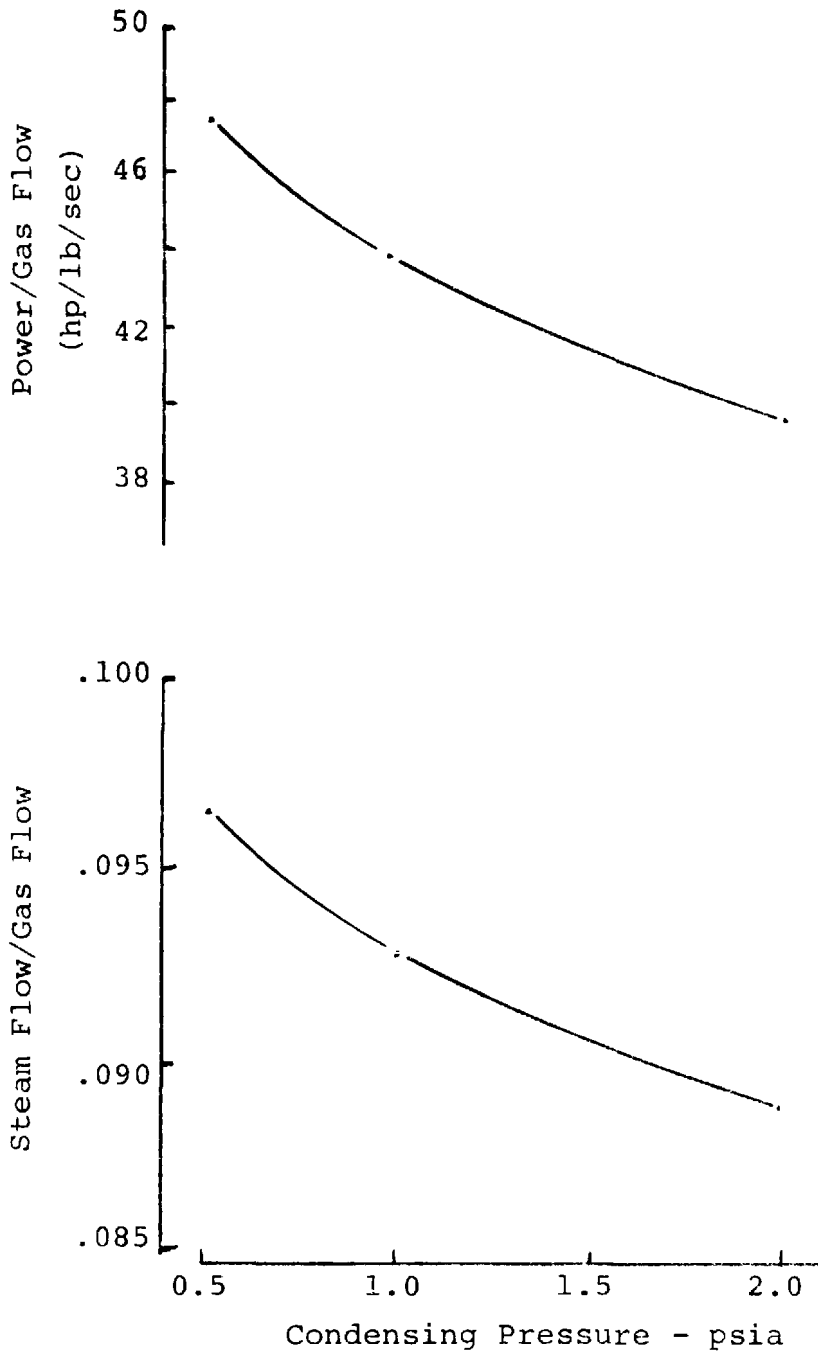


Figure A-2 Effect of Condensing Pressure on the Performance of a Single Pressure Combined Cycle System

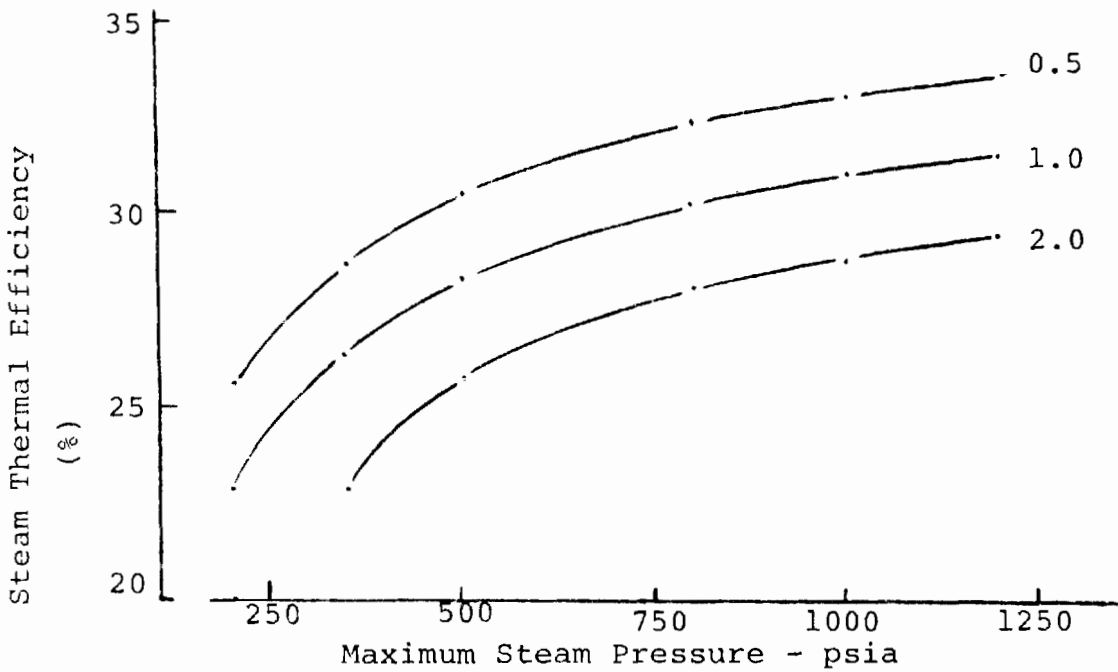
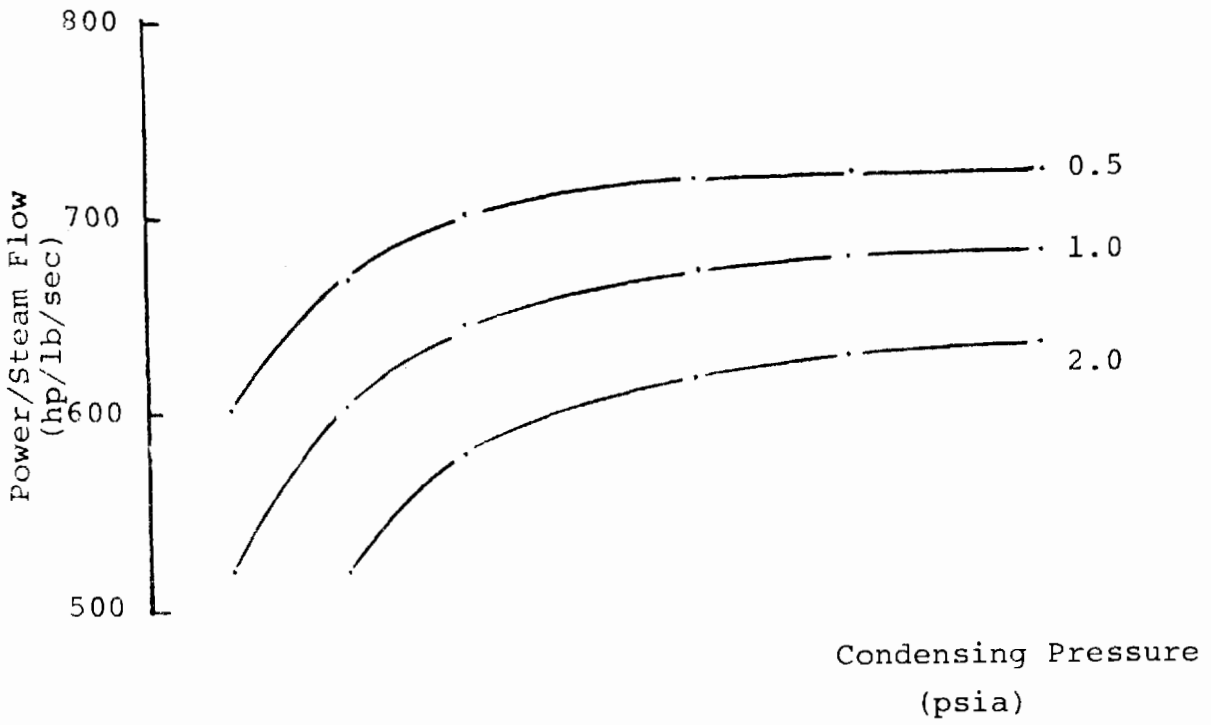


Figure A-3 Effect of the Maximum Steam Pressure and the Condensing Pressure on the Performance of a Two-Pressure Steam Turbine System

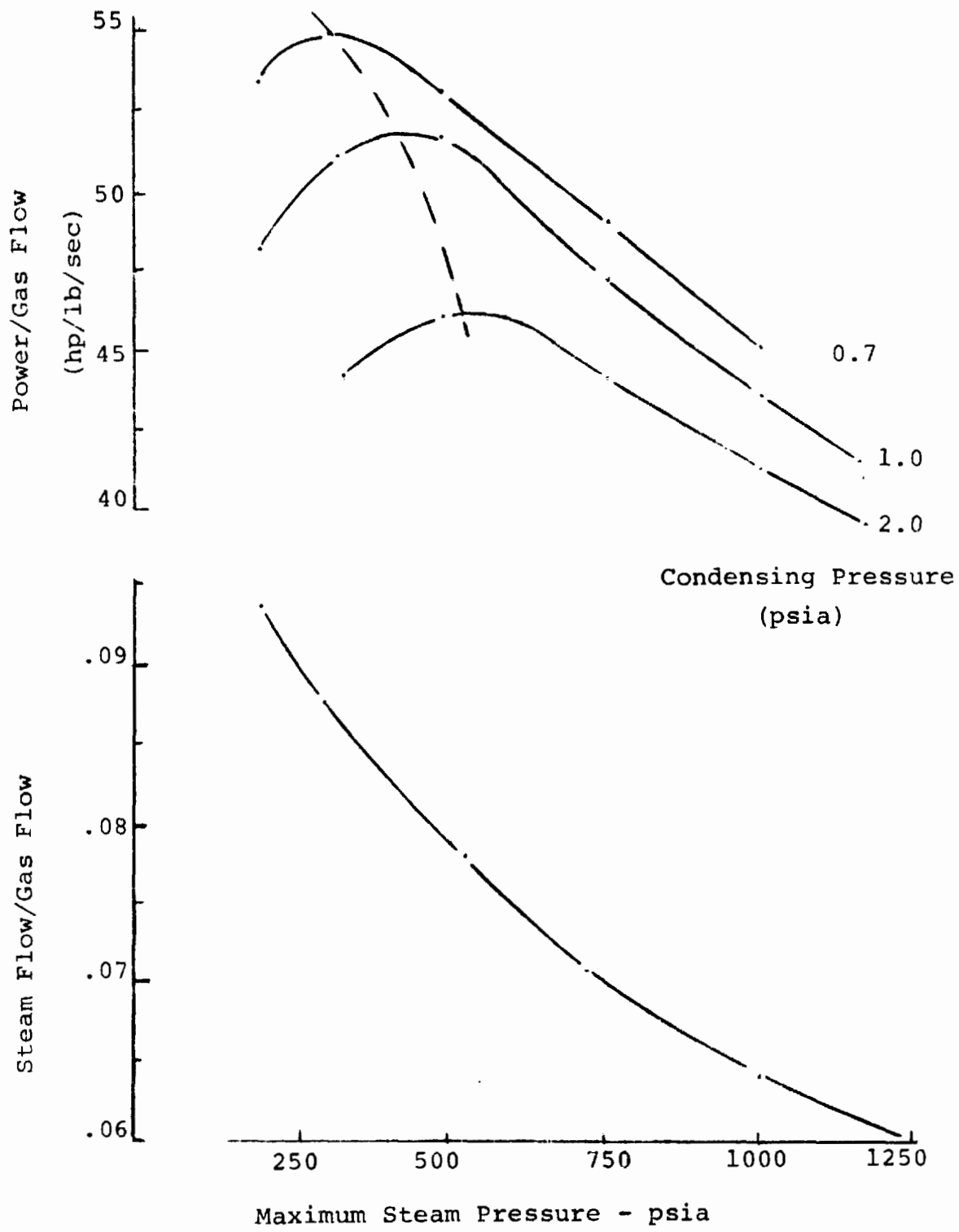


Figure A-4 Effect of the Maximum Steam Pressure and the Condensing Pressure on the Performance of a Two-Pressure Combined Cycle System

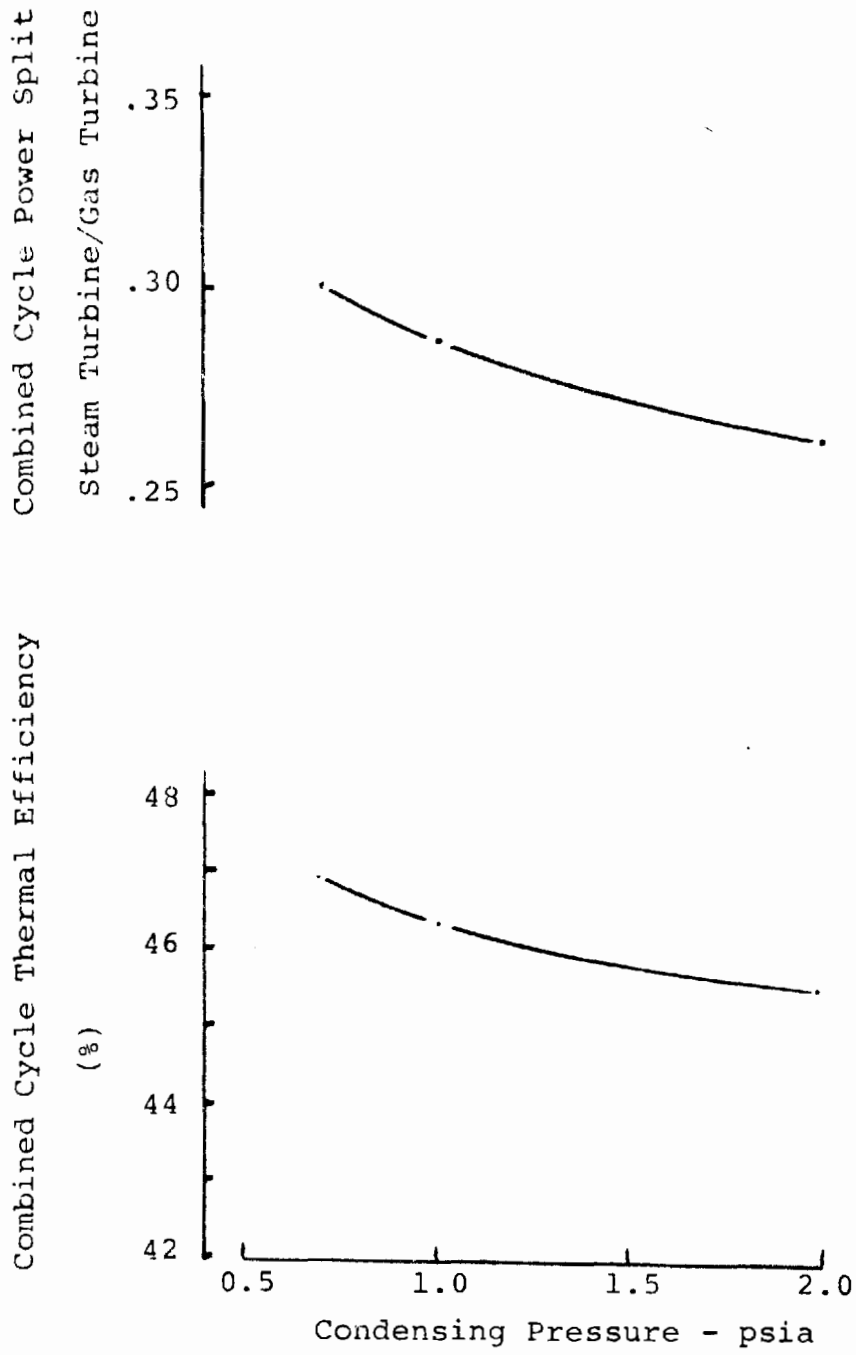


Figure A-5 Performance of a Single Pressure Combined Cycle System

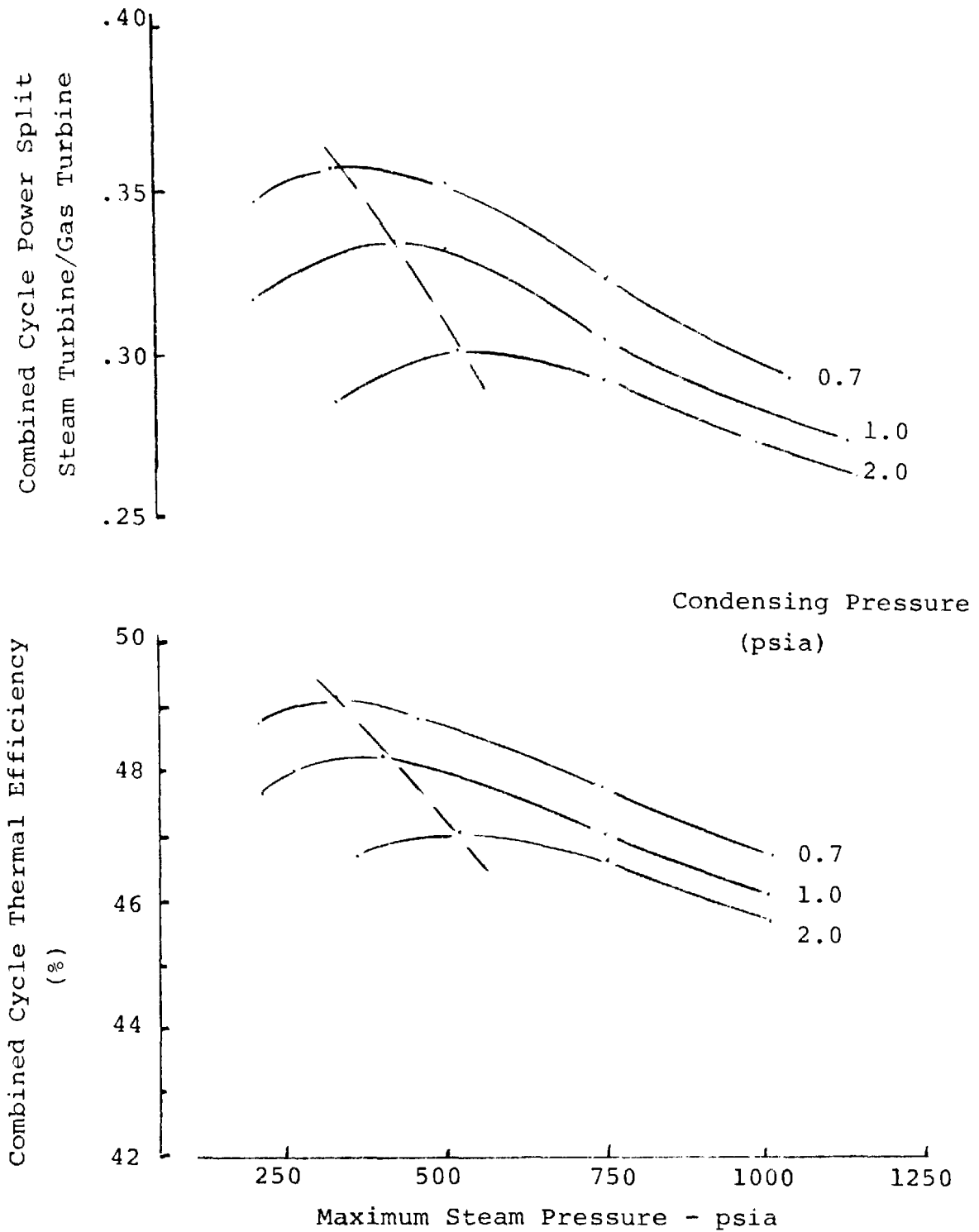


Figure A-6 Performance of a Two-Pressure Combined Cycle System

## UTILIZATION OF TRANSFORMER WASTE HEAT

D. P. Hartmann  
Bonneville Power Administration  
U.S. Department of Energy  
Portland, Oregon

H. H. Hopkinson  
Energy Systems Division  
Carrier Corporation  
Syracuse, New York

### ABSTRACT

Bonneville Power Administration has installed a Carrier Corporation specially designed heat pump system to utilize transformer waste heat for heating a substation control house at the J. D. Ross Substation in Vancouver, Washington. The source of waste heat is a 250 MVA transformer. It has 90 kW of iron losses present whenever the transformer is energized. It also has variable or load dependent copper losses which range up to 300 kW at rated load. Because of the heat sensitivity of the oil/paper electrical insulation, the hottest spot in the transformer is limited to less than 55° C rise above ambient.

Because only a fraction of the available waste heat from the transformer can be used at the control house, and because of possible problems with interruption of the existing oil to air cooling system, an innovative air to freon heat recovery system was implemented. This allowed installation with minimum equipment connection to the transformer, thus preserving the high electrical reliability required of the transformer service. Freon 22 serves as the transformer medium because it can go directly into the heat pump eliminating heat exchanger losses and potential freezing and water line heat losses which would have resulted in a lower coefficient of performance for the heat pump.

This paper describes the heat pump size in terms of the original building load, and the building modifications; insulation and storm windows, which reduced the required heat pump size. The components and system along with its controls are also described. A special accumulator is required to separate crankcase oil from the vaporized freon as it comes to the heat pump.

This project was initiated several years ago. The heat pump was installed in October 1977. This paper summarizes the test results and operating data collected to date, along with the anticipated annual performance, which is expected to yield a quite satisfactorily high coefficient of performance for the heat pump.

The paper concludes with recommendations for future transformer heat retrieval systems.

## INTRODUCTION

The impetus for the Prototype Energy Retrieval and Solar (PERS) system arose in the autumn of 1973. Rainfall and snowfall in the Columbia Basin was very low due to a drought. The conservation measures instituted at that time were successful in limiting electric power demand (1). Also the boycott of oil, while not directly influencing the Pacific Northwest's Hydro based electric generating system did reemphasize the need to conserve energy. The PERS was developed in an attempt to use locally available energy other than electricity for heating and cooling control houses at BPA substations. This first system is intended as a test bed to try various alternatives for retrieving energy for the substation environment.

Figure 1 is a block diagram showing the overall system. During the winter heating season, the power transformer has its highest load, and losses. This is because widespread air-conditioning is not required west of the Cascade Mountains but electric heating is widely used. Thus the peak load occurs in winter in the Pacific Northwest. Utilization of transformer waste heat looked attractive since the potential source is near the control house (See Figure 2). Electric power transformers have been designed and built for nearly 100 years so they are very efficient; above 99.98 percent. However, even a 250,000 kVA transformer, 0.15 percent losses are significant in that nearly 400 kW are lost when the transformer is at rated load. By connecting a Freon 22 evaporator into the transformer oil-cooling air stream, a portion of the transformer's waste heat is captured in vaporized freon to give a boost to the electric heat pump which heats the control room.

During the summer cooling season, 840 tubular glass vacuum insulated solar collectors, in 35 panels, inclined at  $30^{\circ}$  facing south, for a total of 89 sq. meters (959 sq. ft), in four rows, (Figure 3) gather the sun's heat to drive a lithium bromide absorption chiller (Figure 4) to provide chilled water to cool the control house space. In spring and fall, intermediate heating is obtained from the solar energy stored in an insulated 16,200 liter (4300 gallon) storage tank (Figure 5). The lithium bromide absorption cooler is described in another paper (2). The heat pump, absorption chiller, and associated pumps and controls are housed in an auxiliary building adjacent to the control house (Figure 6).

## DESIGN PARAMETERS

The transformer, whenever it is excitable by voltage on the primary, has constant iron losses of 90 kW. This is due to hysteresis losses in the core material. Copper losses are a function of load and range up to 300 kW at a rated load of 250 MVA. Figure 7 shows a typical month's analysis, from existing records, of how the average daily load on the

transformer, the ambient temperature and the top oil temperature are related. The temperature of the cooling air coming out of the transformer oil cooler averages about 13°C warmer than the ambient temperature for this particular transformer during the winter months. Figure 8 shows a typical actual days temperature performance for November 9, 1978. Table I lists the heating design conditions for the Ross Control House. Our first winter's experience shows that with the building's new storm windows, if no outside air makeup is provided, the indoor humidity becomes too low for comfort; well into the lower 20 percent R.H. range.

Preliminary heat loss evaluation of the building showed an estimated 27 kW heat loss. In 1938, 35 kW of electric resistance heaters had been installed during original construction. After application of storm windows (Figure 9) and roof insulation plus removal of the original glass skylight (Figure 10) and the replacement by precast concrete and an insulated roof reduced the control room heat needs to about 6 kW.

#### EQUIPMENT LOCATION

The option of placing the heat pump at the transformer vs in the control building were explored. The transformer area is under 230-kV power lines and access to the transformer for maintenance precluded placement of the heat pump at the transformer. The control house, upon casual inspection, appears to have space available, but most of this space is required for instrument carts used during maintenance. Thus, it was decided to erect a separate Armco type building on the north side of the existing control house. In a new construction program, before power lines are energized, better location of the heat pump nearer to the transformer would be included in the construction plan. As it is, the separate location eased construction since all of the equipment was in one place away from the hazards of construction near the 230-kV power lines. The result is that a loss in booster temperature due to extra line length was traded for ease during construction and for continuing operation and maintenance. Service personnel can enter the separate auxiliary building without access to the secured electrical substation area, and without interference with substation control room operations and maintenance.

#### HEAT PUMP COMPONENT AND SYSTEM DESCRIPTION

##### EVAPORATOR

The evaporator is a specially constructed 1.22 m (4 foot) square, 7.6cm (3-inch) thick plate fin coil arrangement manufactured by Carrier Corporation. It is placed directly above the existing transformer to air cooler and extracts heat from the cooling air stream by vaporization of Freon 22. The evaporator is shown in Figure 10. Two evaporators are

required since alternate weekly operation of the two existing transformer cooling units is required to assure reliable availability of both cooling units should the transformers partner bank be out for maintenance. At that time rated load would be placed on the transformer and simultaneous operation of both cooling units would be automatically started by control thermostats.

#### COMPRESSOR

Figure 11 shows the compressor as installed in the auxiliary building. It is a Carrier Model MD24/3HP with special oil level indicators and a welded shell which is hermetically sealed. This is an air to water heating unit.

#### CONTROLS

The heat pump is set to operate in a heating mode, a cooling mode for backup for the solar lithium-bromide absorption chiller and a heat pump down mode.

Refrigerant gas will condense at the coldest point in the refrigerant system causing a local low pressure area which induces more refrigerant gas to flow towards the system cold point. Since this system has two remote refrigerant evaporators, it is necessary to prevent these components from collecting the total refrigerant charge leaving insufficient charge in the operating circuit. In the cooling mode, the 100 meters of (328 ft) of return gas refrigerant line, up to 35.7 kg (78.7 lbs.) of refrigerant could be held.

Check valves have been added at the outlets of each evaporator and also at the outlet of the return gas line to prevent this refrigerant migration. However, since solenoid and check valves can leak refrigerant long periods of time, a heat pump down mode was incorporated into the controls for the heat pump. This mode is controlled by the liquid level in the accumulator (receiver).

#### ACCUMULATOR (RECEIVER)

This is a tank in the heat pump suction line which separates oil and any liquid freon from the evaporator generated freon vapor. A small hole in the suction line pickup is provided to return oil to the compressor. Initially, a small accumulator of about .94 liter (1 qt.) was used. During cold start, the capacity was exceeded by liquid freon in the return from the evaporators. One compressor required replacement due to failure induced by liquid freon entry to the compression chamber. Replacement of the original accumulator with a 15 liter (3 gallon) unit solved this problem. Also, a small heater is incorporated into the accumulator to provide some vapor during cold start conditions.

#### DOWNSTREAM PRESSURE REGULATOR

This pressure regulator located in the return gas line to the compressor senses pressure entering the compressor and is set to restrict refrigerant flow to the compressor such that a suction pressure above 717kPa (104 Psig) is not reached. This is to protect the compressor from overloading caused by excessive energy absorbed by the remote transformer evaporators.

#### PERS HEAT PUMP HEATING SYSTEM

##### FAN COIL

The fan coil unit is shown in Figure 12. This is a 15-ton carrier packaged chilled water air handling unit of the 408 RS series. It delivers heated or cooled air to the room through plenum space ducting at 200 CFM. Adjustable dampers are available to modulate this air flow from control room requirements, i.e., eliminate drafts, but assure adequate air circulation for delivery of heating and cooling.

##### WATER PIPING - CONTROL VALVES

Water pipes are connected from the heat pump to the fan coil unit for use in heating or as a backup cooling for the lithium bromide absorption chiller. There also is a connection which allows use of solar heated water to be sent to the fan coil unit for solar heating. All water piping is simulated with a 11.4 cm (4.5 inch) radial thickness of performed urethane foam insulation. The heat pump cooler uses water cooling. To prevent water from freezing in the cooler under certain conditions of the "pump down" cycle, a solenoid valve has been added to the heat pump's refrigeration circuit. This solenoid valve is de-energized any time the pressure in the cooler drops below 400 kPa (51Psig). It will remain off until the pressure increases to 448 kPa (65 Psig). The cut off point of the pressure switch (58 Psig) corresponds with a refrigerant saturation temperature of 0°C (32°F).

#### INSTRUMENTATION

The overall system has 49 analog and 9 discrete (contact closure) inputs to gather thermal insulation wind condition fluid flow, pressure and one control room relative humidity data for the PERS system. In order to obtain a heat balance for the heat pump precision, several thermopiles capable of measuring temperature to within  $\pm 0.1^\circ\text{C}$  were installed. Fluid flow is measured with Brookes Instrument turbine flow meters which utilize frequency to analog voltage converters to provide inputs to the BPA supplied PPP1135 data formulating computer. A microwave channel sends

accumulated data to Portland headquarters where the CDC CYBER is utilized for data reduction calculations. Professor Gordon Reistad of the Mechanical Engineering Department of Oregon State University of Corvallis, Oregon, has a contract for system data evaluation.

#### HEAT PUMP HEATING SYSTEM PERFORMANCE

There were problems initially with too small a suction line accumulator. Upon replacement of the accumulation with a larger size, the heat pump unit has worked well. In the fall of 78, after one year's service, a freon leak was detected. After refilling the heat pump system with additional freon, and repairing the leak, the heat pump heating system has again been providing excellent performance. The data for the 78-79 heating season is being gathered and analyzed. A report will be made available for NTIS Distribution in 1979. If the transformer were near rated load capacity for most of the heating season, the expected heat pump COP might rise to near 6. However, the transformer usually shares load with a sister unit and is only operating at about one-half of normal name plate rating. Thus, the heat pump COP on November 9, 1978, was calculated at 2.8 average for the hour ending at 1700 PST, and the COP was calculated at 2.3 overage for the hours ending at 2200 PST. Use of a higher fraction of the transformer's waste heat would lead to larger, better insulated freon tubing with a better resultant COP for the heat pump.

#### OTHER APPLICATIONS OF TRANSFORMER WASTE HEAT

Commonwealth Edison of Chicago (3) has a number of substations inside the Sears tower in downtown Chicago. Portable service water is used to cool these transformers with double wall oil to water heat exchanges. Thus the Sears' building waste transformer heat is used to preheat the building's service water year around.

Hydro Quebec (4) in their downtown headquarters building use the air from their transformer cooling system on the building makeup air source for the winter heating season. In summer, the transformer waste heat is vented to the environment.

Seattle City Light (5) in cooperation with the Electric Power Research Institute (EPRI) and a contractor, Rocket Research, are surveying the United States utility industry as to the extent of the available resource in the transformer waste heat. The contractor is also studying the feasibility of heating the Pacific Science Center in downtown Seattle with waste heat from a large transformer of Seattle City Light located about 1,000 feet from the center.

## RECOMMENDATIONS FOR FUTURE TRANSFORMER HEAT RETRIEVAL SYSTEMS

The method of reclaiming waste energy from the transformer described in this paper is based on a direct expansion evaporator coil mounted above the transformer oil cooling coil. This method transfers energy from the cooling oil to the air and in turn energy is transferred from the cooling air to the refrigerant system by means of the evaporator coil. Using the air side transfer approach removed any potential problems of coolant oil contamination or restrictions to oil flow rates.

Figure 13 is a diagram showing the application of a specially designed "three-way" coil. This "three-way" coil makes it possible to obtain waste energy from the transformer or if waste energy is not available from the transformer, then energy can be obtained from the outdoor cooling air. Under certain operational conditions, energy for the heat pump may come from both sources. Modulation of either the oil or air flow rates or both provides a means of optimizing the transformer and heat pump operation.

This approach has all the advantages of the present PER System plus an improvement in heat pump COP. The improved COP results from the elimination of air as the energy transfer medium and transferring energy directly to the refrigerant by way of the coil fins. It maintains a separation of transformer oil and refrigerant - an oil leak would not contaminate the refrigerant system; either system can operate independently of the other; and installation requires only that the oil cooling coil be changed - no modifications to the transformer proper are required. In addition to an improved COP, a savings in heat transfer surface costs can be realized on new installations. Two individual coils are replaced by one three-way coil.

While this approach can be utilized to provide space heating in accessory buildings associated with a power distribution center, as was done in the PER program, the total potential of the available waste energy will usually exceed the requirement for space heating. Therefore, to be successful in fully using the available energy, some combination of a power distribution center matched with a manufacturing facility requiring large amounts of heated process water and space heating should be investigated. A combination of this type offers economies for both the utility and its customer.

A conventional heat pump such as used on the PER system can successfully be used to heat water to a 50°C level which is satisfactory for space heating. For the higher temperature levels required for process water, a different type of heat pump is required.

Refrigerant R-12 and R-22 are "dry" compression types and result in discharge gas temperatures higher than those obtained by using so-called "wet" compression types of refrigerant. Refrigerant R-113 is an example of a "wet" compression refrigerant. A centrifugal compressor using R-113, for example, could supply process water heated up to 90°C without exceeding the discharge gas temperature limits for reliable operation.

The COP for all heat pump systems falls as the condensing temperature level increases; therefore, any pricing structure for heated process water should increase with the required temperature level.

Figure 14 is a line diagram for a system which could meet the energy requirements for both heating process water and space heating. In a system of this type, it would be possible to operate the heat pump only during "off-peak" hours storing energy for later "peak" time use. This helps to balance the load with available power generating capacity, but would substantially reduce the amount of waste energy available.

In certain areas of the country, it may be economically feasible to add a solar collection system to operate in parallel with the heat pump system.

TABLE I

ENERGY RECOVERY SYSTEMS

INPUT DATA FOR DESIGN POINT

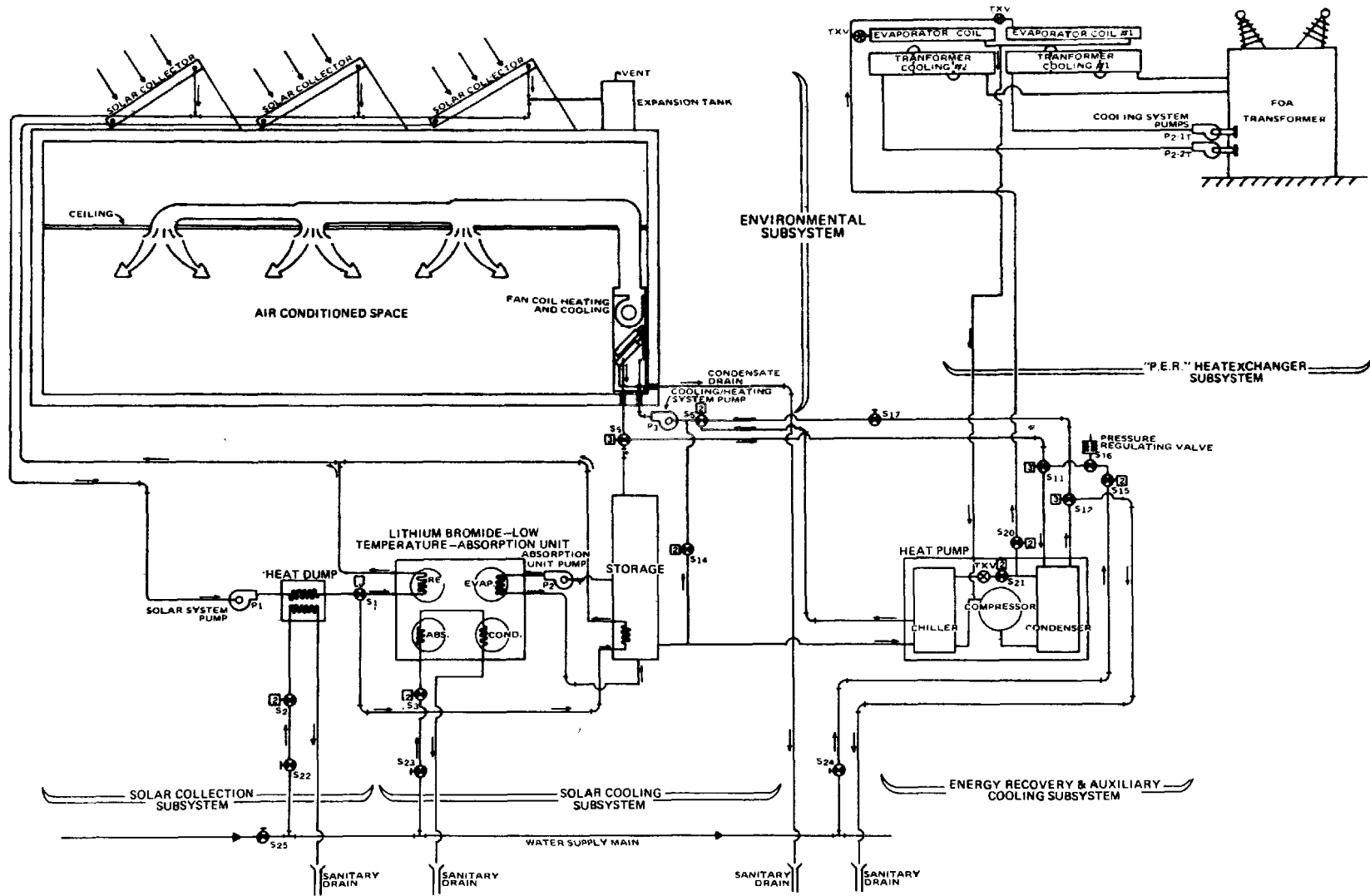
|                                   |                     |
|-----------------------------------|---------------------|
| Ambient Air Temperature           | 21 <sup>o</sup> F   |
| Transformer Load                  | 67%                 |
| Oil Temperature                   | 68.5 <sup>o</sup> F |
| Heat Rejection, Oil Radiator      | 361,500 BTU/HR      |
| Air Temperature, Leaving Radiator | 54.5 <sup>o</sup> F |
| Air Flow Rate                     | 10,000 CFM          |

AIR COIL DATA

|                         |                          |
|-------------------------|--------------------------|
| Coil Dimensions         | 58' x 58' x 3 1/2        |
| Rows                    | 2                        |
| Spacing, Face           | 2 Inches                 |
| Row                     | 1.5 Inches               |
| Fins                    | 12.95 Inch <sup>-1</sup> |
| Saturated Suction Temp. | 42.1 <sup>o</sup> F      |
| Capacity                | 55,000 BTU/HR            |

## REFERENCES

1. D. Davey, "The Pacific Northwest Energy Conservation Program"  
9th Interagency Energy Conversion Engineering Conference,  
San Francisco, August 1974, IEEE publication No. 74CHO8T4-8 pp 560-566
2. Dr. Wendell Biermann, "An Absorption Machine for Solar Cooling"  
to be presented at the 1979 ASHRAE meeting on January 28 in  
Philadelphia, PA.
3. Private Communication with Mr. Aldo Zanona of Commonwealth  
Edison Company, Maywood, Illinois.
4. Private Communication with Dr. Jacque Bonneville of Hydro Quebec,  
Electrical Research Institute, IREQ, Varannes, Quebec.
5. Private Communication with Mr. Eldon Ehlers of the Electric  
Power Research Institute, (EPRI).



PROTOTYPE ENERGY RETRIEVAL SYSTEM BLOCK DIAGRAM

Figure 1 System Diagram

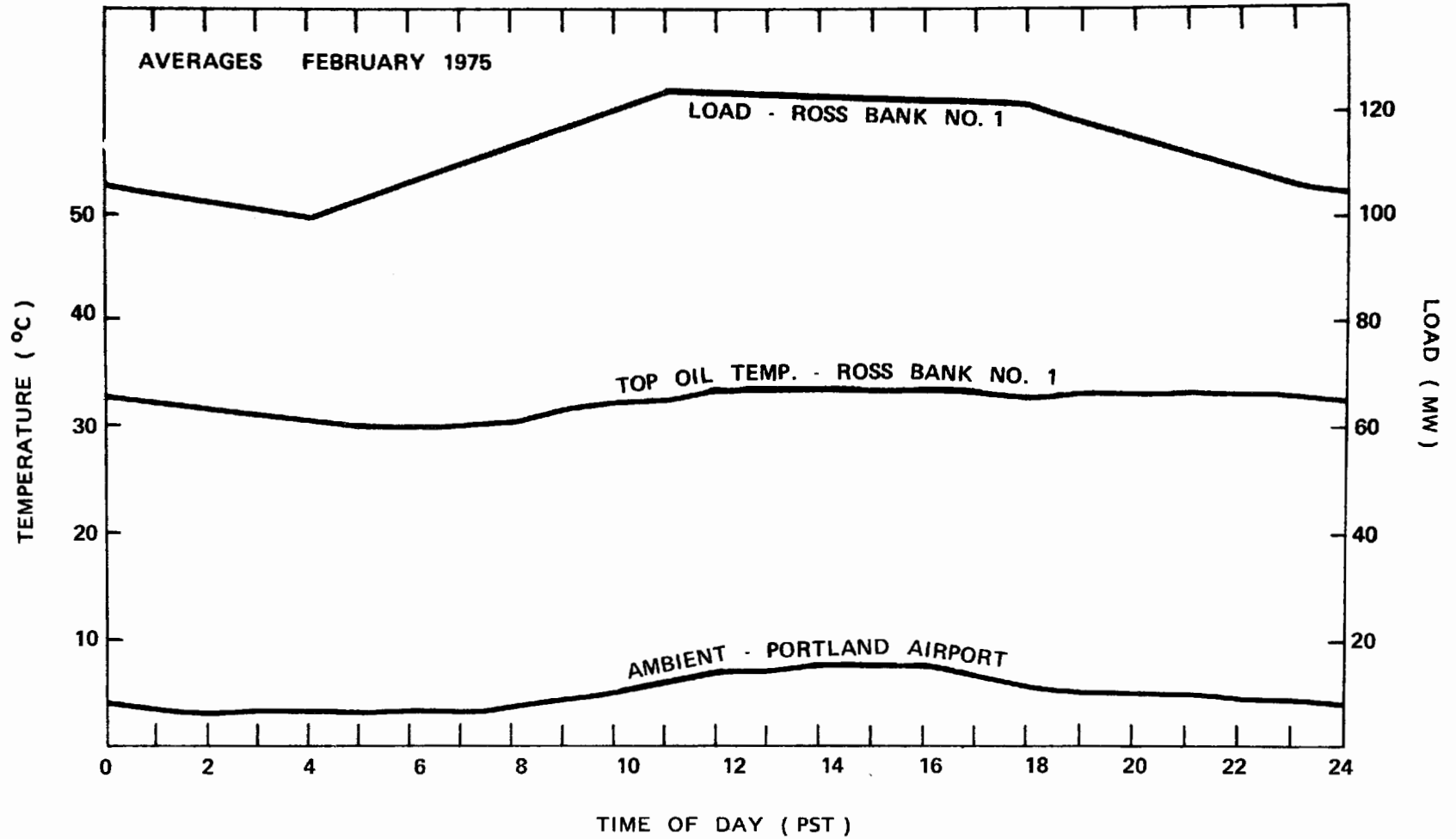


FIGURE 7 HOURLY AVERAGE TEMPERATURES AND TRANSFORMER LOAD PROFILE FOR FEBRUARY, 1975 FOR A 24-HOUR PERIOD.

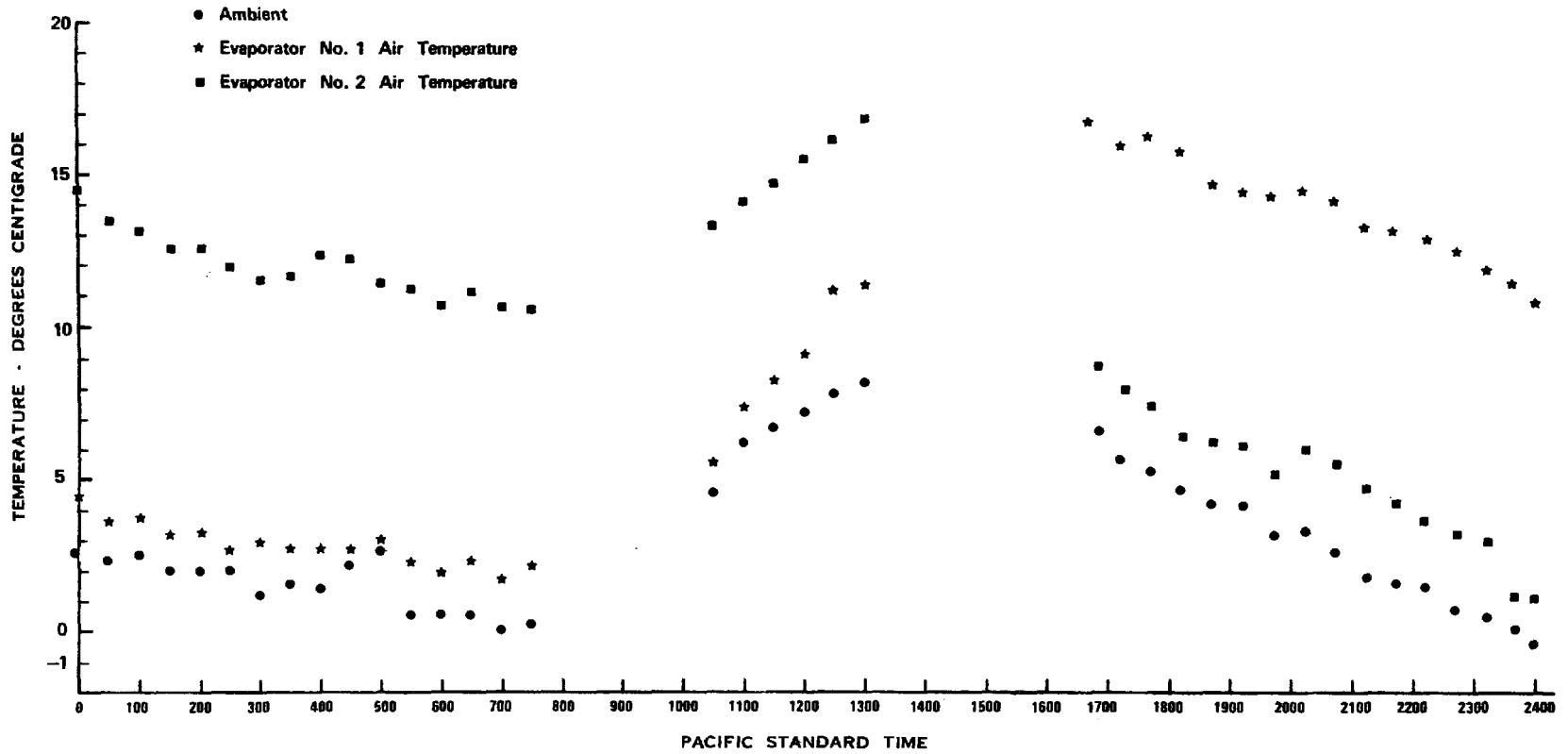
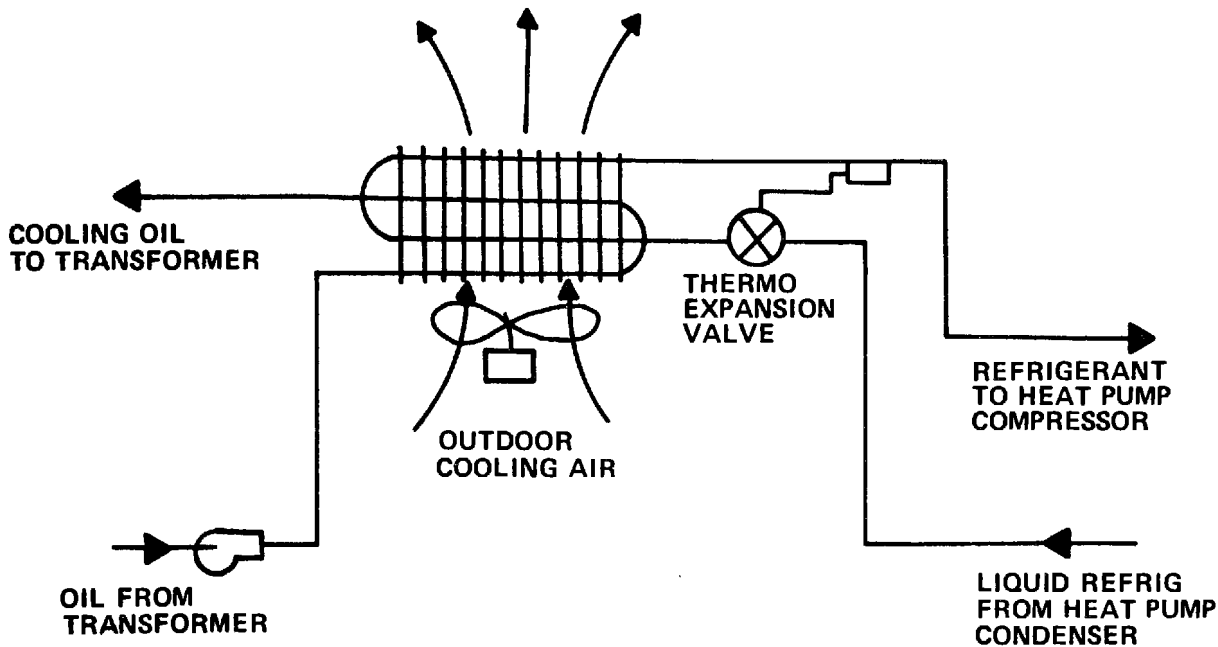


FIGURE 8. J. D. ROSS SUBSTATION, TEMPERATURES FOR NOVEMBER 9, 1978



**THREE-WAY-COIL**

1. Oil cooled by energy transfer from oil to outside air (oil to fins to air), heat pump off.
2. Oil cooled by heat pump evaporator by energy flow from oil to refrigerant (oil to fins to refrigerant), heat pump on.
3. Transformer off, energy flow from air to refrigerant (air to fins to refrigerant), heat pump on.

**Figure 13**

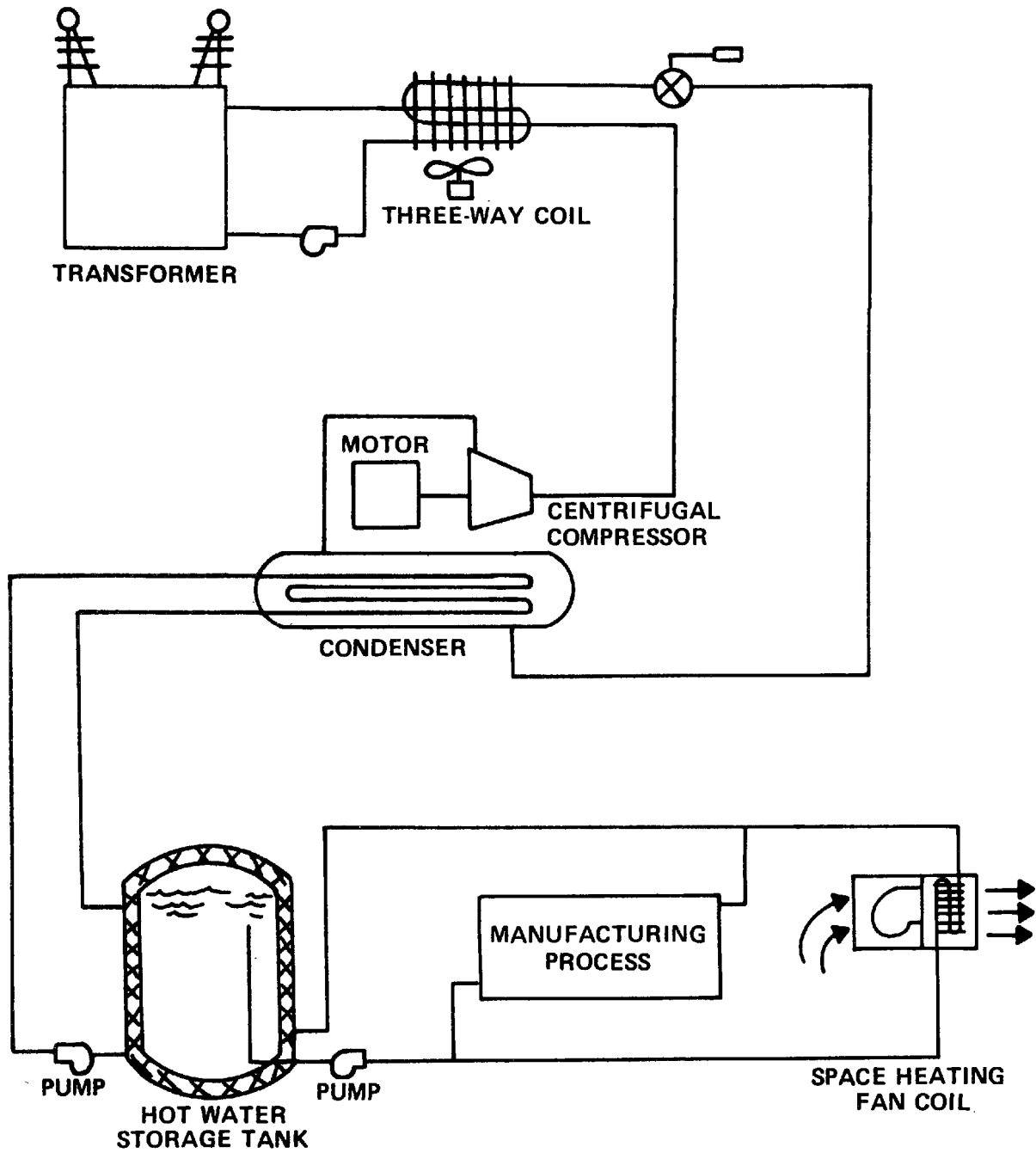


Figure 14

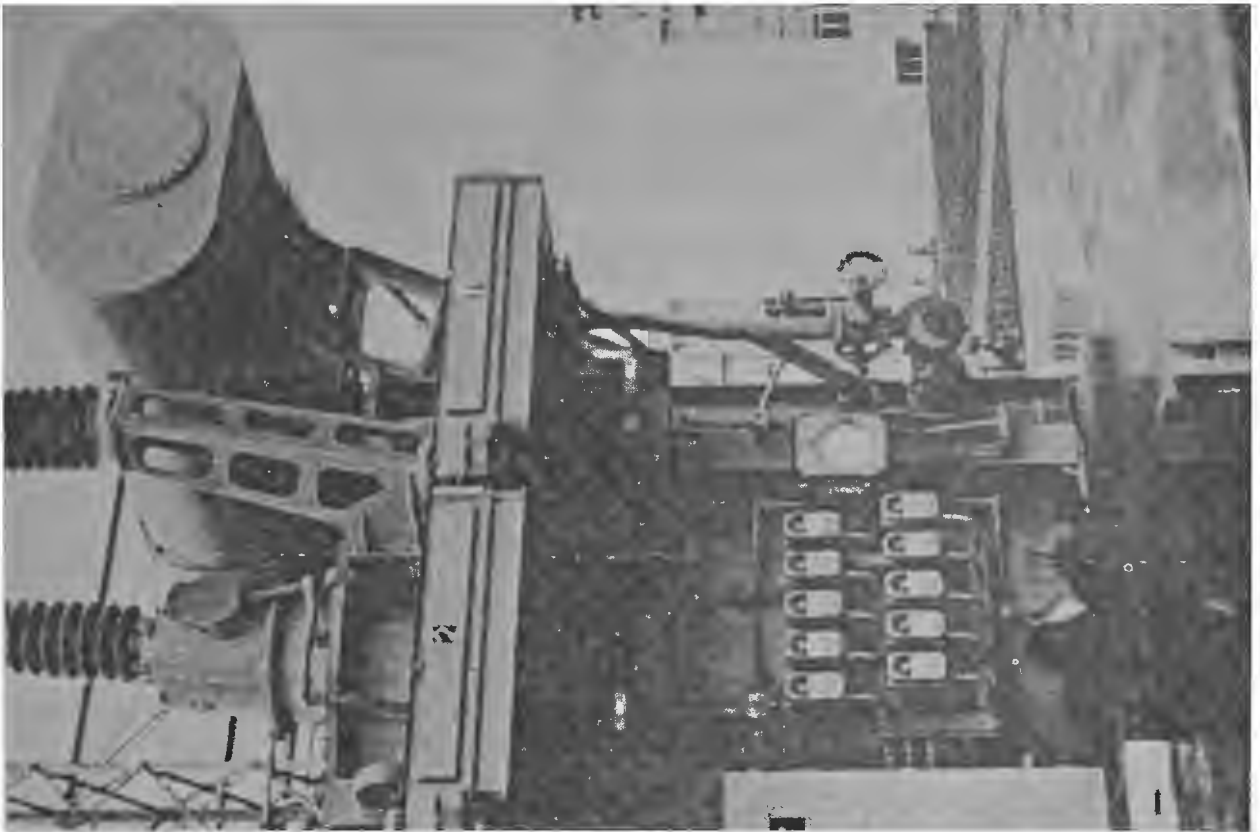


Fig. 2 Transformer near Control House



Fig. 3 Solar Collector

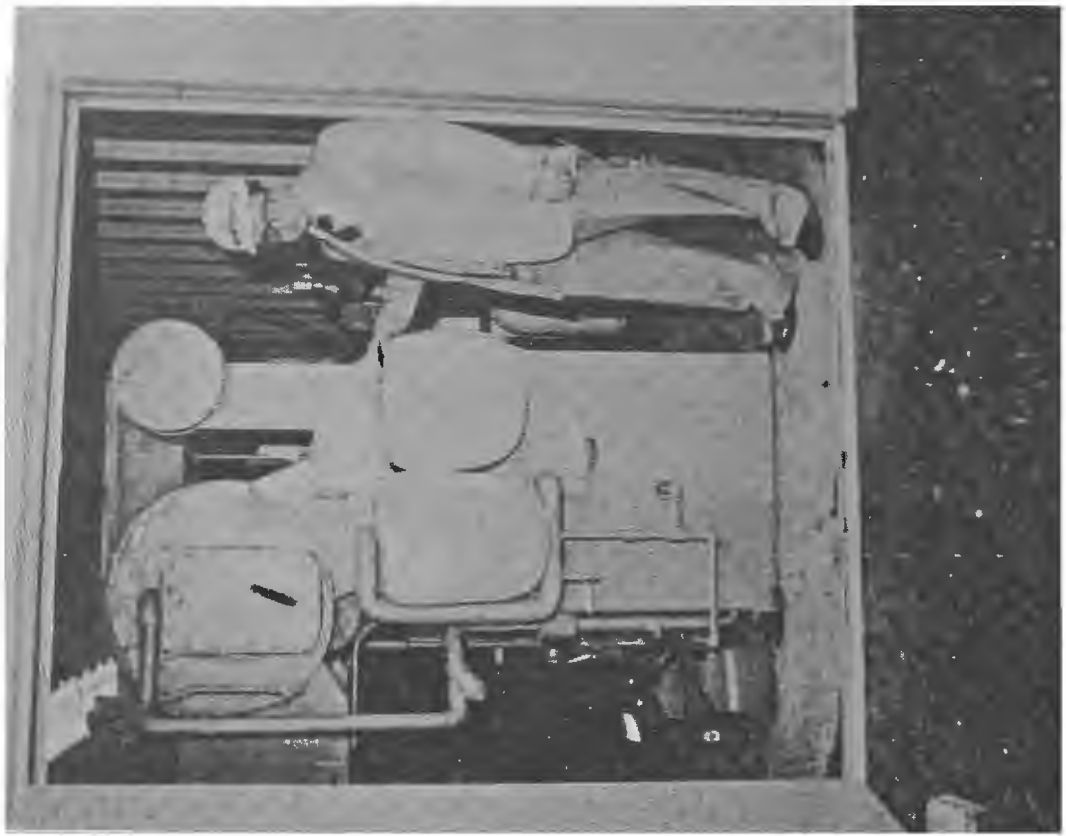


Fig. 4 Lithium Bromide Absorption Chiller

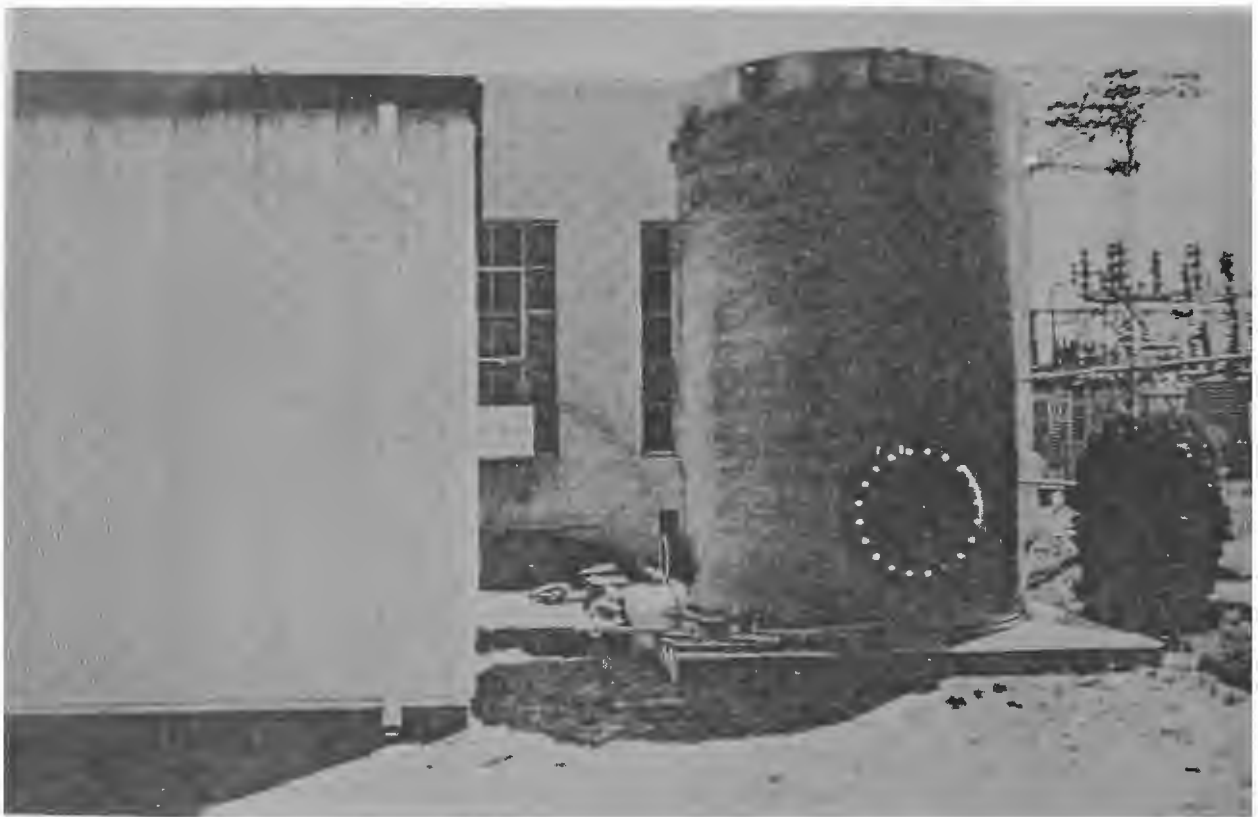


Fig. 5 Storage Tank

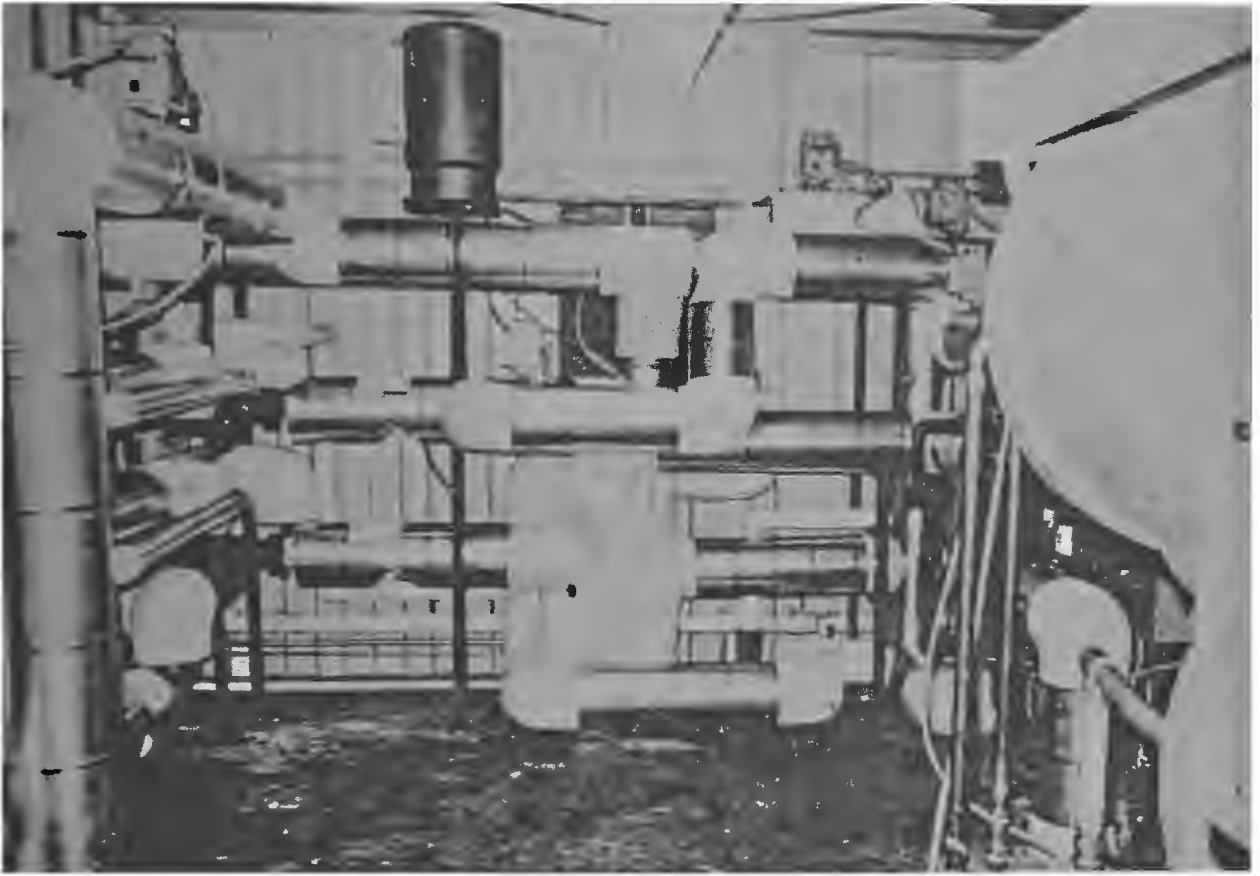


Fig. 6 Equipment Building

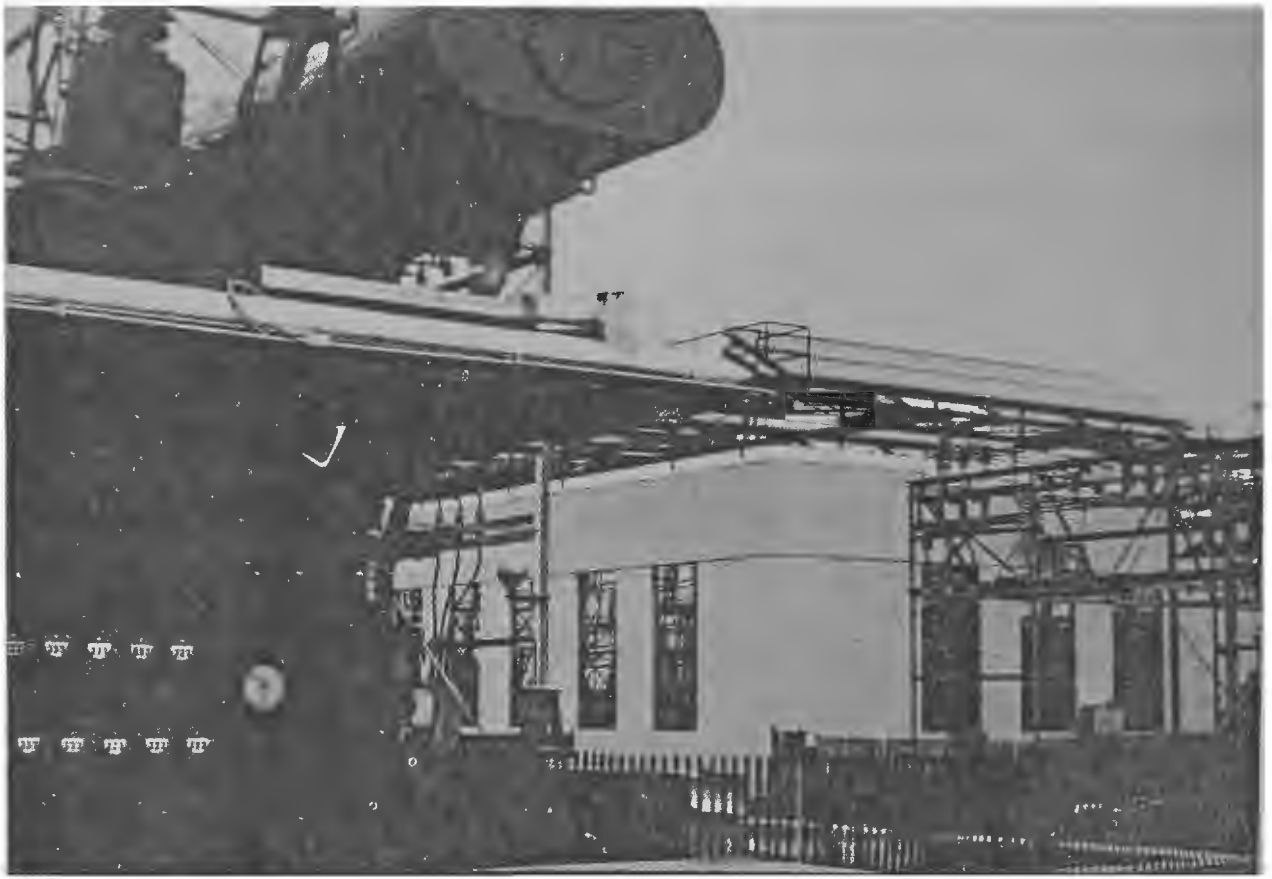


Fig. 9 Storm Window picture



Fig. 10 Evaporator

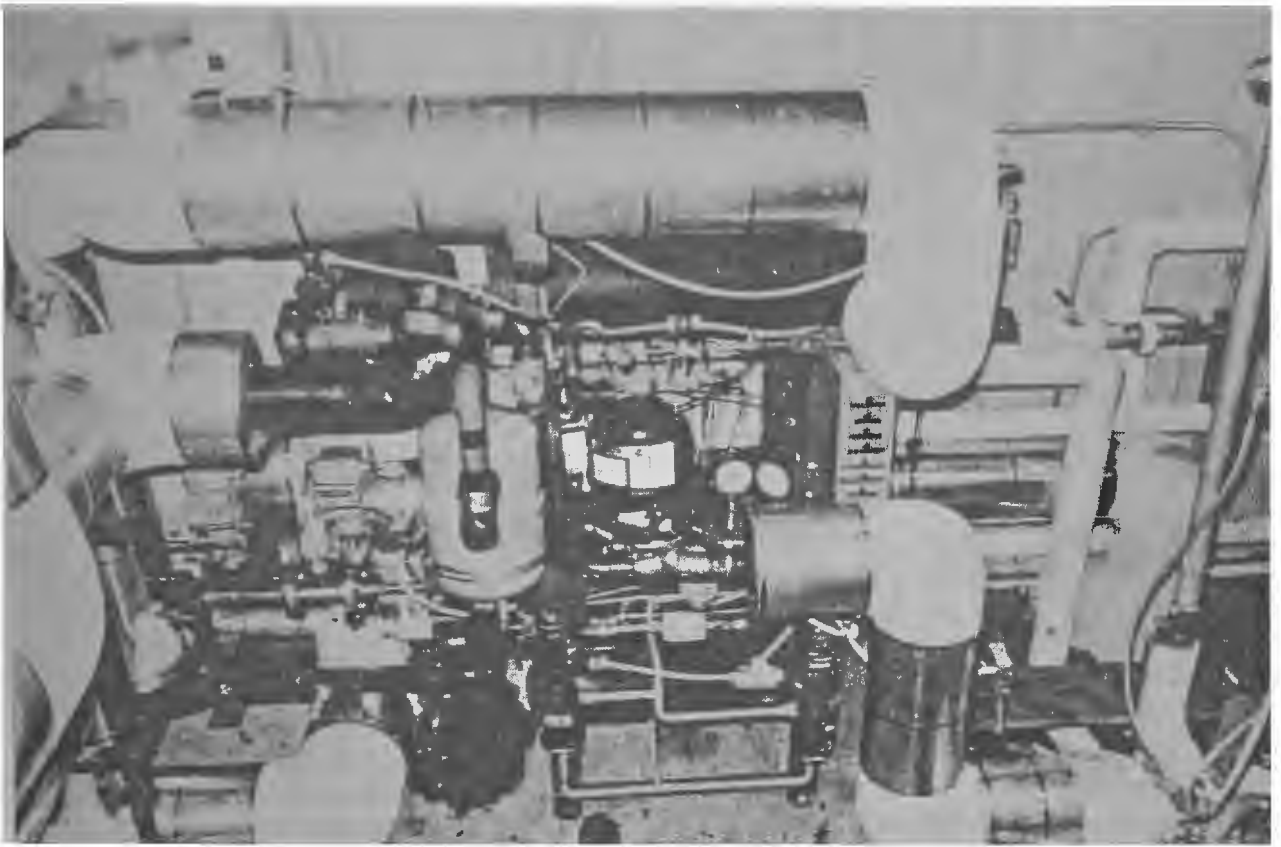


Fig. 11 Heat Pump Compressor

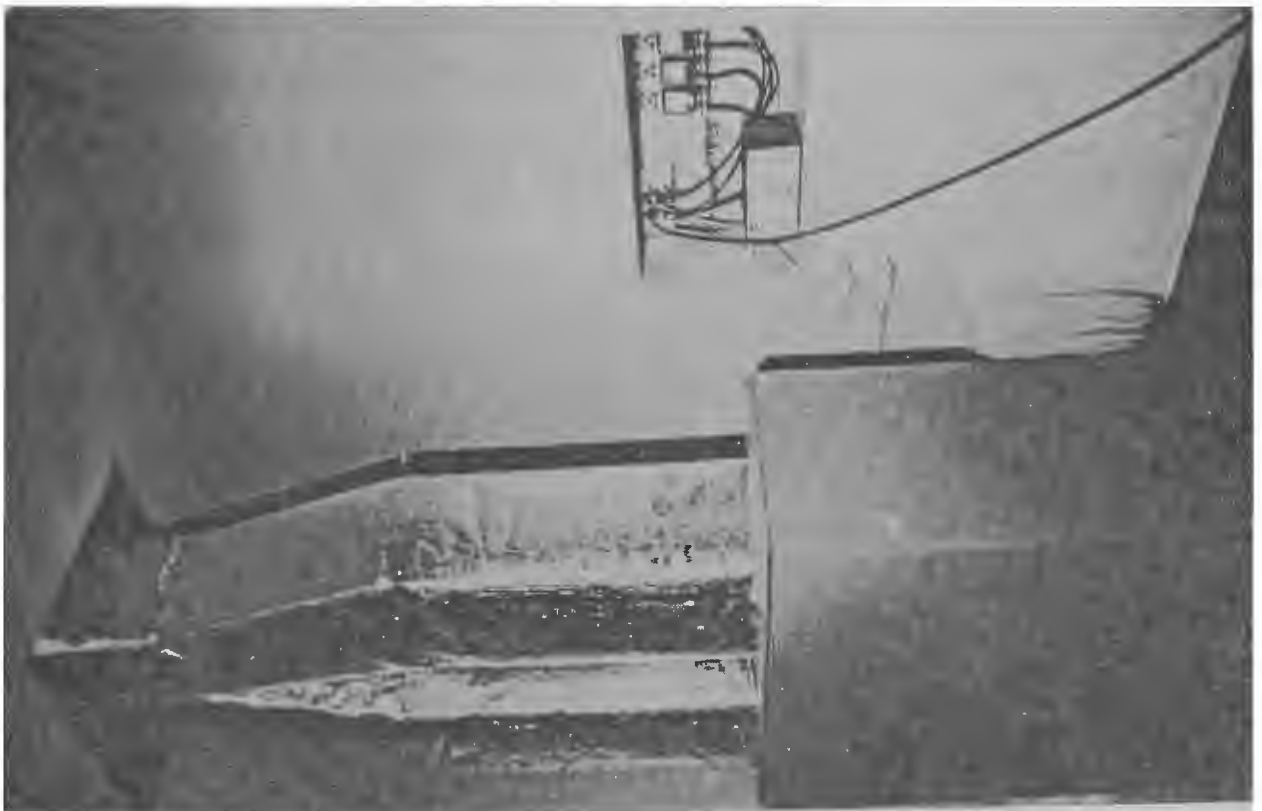


Fig. 12 Air Handler

THE APPLICATION OF PRESSURE-STAGED  
HEAT EXCHANGERS TO THE GENERATION  
OF STEAM IN WASTE HEAT RECOVERY SYSTEMS

Dr. Dah Yu Cheng  
President  
International Power Technology  
California, U.S.A.

Mark H. Waters  
VP Engineering  
International Power Technology  
California, U.S.A.

ABSTRACT

The objective of this paper is to describe an improved system of transferring heat energy from a high temperature fluid to a low temperature fluid which undergoes a thermodynamic transition from the liquid phase to the vapor phase. A counter current heat exchanger is employed and the cool fluid may undergo thermodynamic transition at more than one pressure. This requires additional mechanical components. It will be shown that with this heat exchanger either a greater amount of heat energy can be transferred per unit surface area or a greater amount of fluid will undergo the thermodynamic transition than is possible by conventional techniques.

INTRODUCTION

Heat exchangers are employed in various chemical engineering processes such as powerplants, heating and cooling systems and energy retrieval systems. Generally, heat exchange design has focused upon means to transfer the greatest amount of heat per unit surface area of the exchanger. However, with the recent interest in co-generation, which makes use of gas turbine waste heat to generate steam, there is also incentive to increase the amount of steam generated from a fixed quantity of waste heat.

In conventional heat exchangers, the fluid to be heated is supplied at a certain pressure. The temperature of the fluid begins to rise generally under a continuously smooth temperature profile unless thermodynamic transition occurs. If such a transition does in fact occur, the heated fluid would for a period have a constant or flat temperature profile until all of the liquid has been converted into vapor. The limiting variable is the temperature difference between the heating and heated fluid

for when this temperature difference is small, very little energy is transferred between the two fluids. If the temperature difference between the two fluids is small, a heat exchanger must have a correspondingly large surface area in order to transfer a given amount of energy. An optimum situation would exist if one could maintain the temperature difference between the fluids at a maximum so that the heat exchanger surface area could be kept at a minimum and thus reduce the equipment costs involved in the energy transfer.

The objective of this paper is to describe a novel heat exchanger design which maintains a greater temperature difference between the two fluids by having multiple evaporators which operate at different pressures. This paper is abstracted from the patent described in reference 1.

#### DESCRIPTION OF A PRESSURE-STAGED HEAT EXCHANGER

A pressure staged heat exchanger has at least two evaporators which are separated by staged pumps. As the fluid to be heated enters the heat exchanger, it increases in temperature until it reaches its thermodynamic transition point at a pressure below the final exit pressure of the fluid. During thermodynamic transition, the fluid is partially vaporized. The two-phase fluid is then pressurized to a pressure which is substantially equivalent to the exit pressure of the heated fluid. At this point, the thermodynamic transition temperature is raised and the heated fluid begins to increase in temperature until it reaches a second, higher, thermodynamic transition point. The fluid enters into thermodynamic transition in a second high temperature evaporator and continues thermodynamic transition until the fluid in a liquid state is vaporized. Once vaporized, the temperature of the vapor begins to increase and, in the case of water, superheated steam exits the evaporator.

The pressure staged heat exchanger described in the previous paragraph was described as having two evaporators separated by a single stage pump. As will be explained later, however, a pressure staged heat exchanger can be designed with a multitude of evaporators separated by a multitude of stage pumps. The number of such stages depends upon design characteristics such as energy costs in operating multiple pumps, the surface area of the exchanger, and the nature of the fluids employed in the energy transfer and the payoff in weight cost and energy recovery efficiency.

#### Conventional Heat Exchanger Constraints

Figure 1 represents conventional heat exchangers in which the heated and heating liquids travel in countercurrent paths.

If thermodynamic transition occurs, the liquid to be heated enters the heat exchanger at temperature  $T_{14}$  and progresses to  $T_{15}$  at which time spontaneous thermodynamic transition occurs. If the heated liquid which has been converted into a vapor exits the heat exchanger during or after thermodynamic transition without further heating, this fluid would thus exit at temperature  $T_{15}$ . If, however, the heated fluid remains in the heat exchanger after thermodynamic transition has occurred, then the vapor becomes superheated and exits at temperature  $T_{13}$ .

As stated previously, a limiting factor in conventional heat exchangers is the temperature difference between the heating and heated liquids. As this temperature difference becomes smaller, a greater surface area is needed to transfer a specific quantity of heat energy. Thus, for a heat exchanger of a given surface area, the amount of heat that can be transferred is directly affected by the temperature difference  $T_n$  which is called the temperature "neck". Referring again to figure 1, one would like a maximum  $T_{15}$  or  $T_{13}$ . However, the limiting factor is  $T_n$ . As  $T_n$  grows smaller, the heat transfer per unit area becomes less, thus limiting the amount of heated fluid to reach  $T_{15}$  or  $T_{13}$ .

#### Tradeoffs in Using the Pressure-Staged Heat Exchanger

The thermodynamic transition temperatures of a fluid can be controlled by the pressure to which the fluid is exposed. To pressurize a fluid in liquid form requires relatively little pump work, but a much larger amount is required to compress a vapor. Thus, a pressure staged heat exchanger requires more pump work than conventional techniques in which only a fluid in liquid state is compressed. The tradeoff is between increased pump work and the savings in heat exchanger surface area.

The pressure-staged heat exchanger can better be appreciated by studying figures 2 and 3. The fluid to be heated enters the heat exchanger at temperature  $T_{24}$  and is heated in a section called a preheater shown in figure 2, 3. At this point, the fluid is at a pressure lower than the final exit pressure and thus has a lower thermodynamic transition temperature. As the liquid raises in temperature to point A, thermodynamic transition occurs and continues to a predetermined point B. At point B, the fluid is in a liquid/gaseous state, the percentage of each phase being a design variable which will be discussed later. At point B, a staged pump raises the pressure of the heated fluid to the final exit pump pressure desired. Because of the increased pressure, the two-phase fluid again increases in liquid content and enters thermodynamic transition at C. Thermodynamic transition continues until the heated fluid is all vapor, at E. At point E, all of the fluid has been converted to a vapor state and the temperature again begins to rise as superheated vapor is produced. The heated fluid exits the heat exchanger at temperature  $T_{23}$ .

The dotted line A-C in figure 2 represents the temperature profile for the heating of a fluid which undergoes thermodynamic transition carried out in a conventional heat exchanger, i.e., without multiple evaporators and a staged pump. In order to appreciate the advantages of the pressure-staged heat exchanger, one need only compare the differences between necks A/A<sub>0</sub>, C/C<sub>0</sub> and T'. The necks are orders of magnitude larger than the single neck of the prior art and, thus, the heat transfer achieved is much greater than in conventional heat exchangers.

### Operation of a Two-Evaporator Pressure-Staged Heat Exchanger

Among the variables which can be used to determine the overall characteristics of the pressure staged heat exchanger is the fluid quality, hereafter referred to as  $Z_1$ , which is the percentage of liquid which has been converted to a vapor in the first fluid evaporator before the staged pump acts to increase the pressure of the heated fluid. When  $Z_1$  is between approximately 0 and 10% or within the range of approximately 85 to 100%, a single pump can adequately be used to pressurize the heated fluid. However, when  $Z_1$  is in the range of approximately 10 to 85%, it has been found that the liquid-vapor mixture is difficult to compress using a single stage pump. The pump generally suffers from "cavitation" which is a phenomenon which occurs when the bubbles of vapor within the liquid collapse. If the pressure ratio is not particularly high, a standard positive displacement pump can be used. However, the cavitation problem can also be greatly reduced by using a liquid-vapor separator followed by separate pumps to compress different fractions of the liquid-vapor mixture. Once the separate fractions are compressed, they are remixed before being added to the next evaporator.

Such a configuration is shown in figure 4 wherein heated fluid S enters primary pump 40 and travels through coils 45. Heated fluid S travels through the preheat section and then enters evaporator 1 at which time the fluid enters into a state of thermodynamic transition. Once the fluid has partially vaporized, it enters liquid-vapor separator 41 at which time the liquid is pumped separately through stage pump 42 while the vapor is drawn off and pumped through stage pump 43. Once each component has been compressed to the desired pressure, the fluids are remixed in mixer 44 and passed into the second evaporator wherein a second thermodynamic transition occurs. Upon exit from the second evaporator, the heated fluid is now entirely vaporous and is superheated in the superheat section and exits from the heat exchanger at T.

The diagram in figure 5 depicts a further advantage of the pressure staged heat exchanger. Naturally, one would seek to maximize the final exit temperature of the heated fluid and thus would strive to achieve a maximum  $T_{33}$ . Once the temperature of the heating fluid  $T_{31}-T_{32}$  is set, a temperature profile of the

heated fluid cannot rise above the heating fluid temperature and thus the temperature  $T_{33}$  is limited under conventional heat exchanger designs. The dotted line in figure 5 shows that under conventional techniques, if one were to start with a fluid temperature  $T_{34}$  and end at a temperature  $T_{33}$ , an impossible situation would occur in which the "neck" temperature  $T^n$  would be negative (i.e., the temperature of the heated fluid would be greater than that of the heating fluid). This violates the second law of thermodynamics which prevents heat flowing from a low temperature source to a high temperature source spontaneously. This is prevented by the use of the design of this new heat exchanger which uses a multi-evaporator system separated by a staged pump, the profile which is shown by solid lines D' - A' - B' - C' - E'.

### Application of Multiple Evaporators

Another variable is the use of multiple evaporators. For example, figure 6 shows a temperature profile employing three evaporators and two stage pumps. Under conventional systems, the heated fluid would follow the temperature profile shown by the dotted line which results in a "neck" of  $T^n$ . However, by employing a triple evaporator system, the heated fluid would preheat in sections D"-A", enter transition between A"-B", be compressed at B"-C", enter second phase transition at C"-E", be recompressed by a second stage pump at E"-F", enter a third phase transition at F"-G" and exit the exchanger at  $T_{43}$ . A number of temperature "necks" are formed at A"-A<sup>o</sup>", C"-C<sup>o</sup>" and F"-F<sup>o</sup>". One can see by this figure that the "necks" are greatly increased over  $T^n$ , the "neck" of a conventional system. Thus, the log-mean temperature difference is increased and the heat transition rate is improved.

### Use of Superheated Steam to Drive the Stage Pumps

Figure 7 shows a further modification of the present system. Schematically, heated fluid enters primary pump 71 and passes through heating coils 73 in the preheater section. The temperature of the fluid increases until evaporator 1 is reached, at which time thermodynamic transition occurs and the fluid partially vaporizes. Instead of simply increasing the pressure of the heated fluid and causing the fluid to immediately enter the second evaporator, the fluid is separated into its liquid and vapor states in order to minimize pump work. As stated previously, this is particularly advantageous when the fluid has been converted into a vapor state such that the fluid contains between approximately 10 and 85% vapor. Thus, the liquid phase is fed into stage pump 76 while the vapor phase is pumped through stage pump 75. Both phases are then mixed in mixer 78 and fed into the second evaporator section. The pressure within the second evaporator can be controlled by means of throttle valve 79 in order to gain further flexibility within the system.

Upon exit from the second evaporator, the fluid, now entirely in a vapor state, is superheated in the final section of the exchanger. At this point, the majority of the superheated vapor is drawn off at Y although a quantity of such vapor can be bled by means of throttle valve 80 and fed into turbine 77 which can drive stage pumps 75,76. In this way, much of the pumping work can be performed by the latent heat of condensation of the heated fluid. Once the heat of condensation is exhausted within turbine 77, the liquid can be drained and fed into preregenerator 70 together with make-up fluid 72. This has the further advantage of preheating the entering fluid.

#### EXAMPLE OF THE APPLICATION OF A PRESSURE-STAGED HEAT EXCHANGER

A waste heat boiler is employed where hot gases consisting mostly of air and petroleum combustion products at one atmosphere pressure were employed to heat water from an arbitrary starting temperature of  $59^{\circ}\text{F}$  to superheated steam at high pressure. For the purposes of these calculations, the heating gases were assumed to have a flow rate of  $100\text{ lb/sec}$  and a specific heat at constant pressure of  $0.25\text{ Btu/}^{\circ}\text{F/lb}$  on the average during the entire heat exchanging process. Water, being the fluid to be heated, is assumed to have a specific heat of  $1\text{ Btu/lb/}^{\circ}\text{F}$ . It is assumed that the average heat transfer coefficient within the boiler is  $20\text{ Btu/}^{\circ}\text{F/hr/ft}^2$  which is a realistic value governed by the gas coefficient of the air-petroleum gas mixture.

The water at  $59^{\circ}\text{F}$  enters the heat exchanger precompressed to a certain pressure below the final exit pressure. After the water is boiled to a quality  $Z_1$ , the mixture of vapor and liquid is compressed again to a final pressure and quality  $Z_2$ . The ratio of the final pressure to the precompressed pressure,  $R$ , together with the first thermodynamic transition temperature, specific heat ratio  $\lambda$  and  $Z_1$  are design variables.

The steam's final temperature is chosen as a required condition as the temperature is important for steam turbine operation and various chemical processes. The amount of steam that can be generated is calculated as a function of the "neck" temperature  $T_n$ . The steam flow rate  $M_2$  is then a direct measure of the amount of heat being recovered. In this example, the hot gas temperature at the heat exchanger inlet is  $950^{\circ}\text{F}$ , and the steam is assumed to be  $900^{\circ}\text{F}$  at a pressure of  $400\text{psia}$ .

Reference 1 describes the analytical equations used to compute heat exchanger performance. The calculation process is a standard one and is not repeated here.

Assuming a  $50^{\circ}\text{F}$  temperature differential at the neck ( $T_n$  in

figure 1), a conventional heat exchanger is required to have a surface area of 18,443 ft<sup>2</sup> and will generate steam at a rate of 10.88 lb/sec. The average heat flux is 3040 Btu/ft<sup>2</sup>/hr.

The same problem is calculated parametrically for a two evaporator pressure-staged heat exchanger using stage pressure ratios, R, of 2, 4 and 8 and varying the quality at the staging point, Z<sub>1</sub>, from 0 to 1. The results are shown in figure 8, and the advantages of the system can be summarized as follows:

1. The use of the staged evaporative heat transfer system results in a significant reduction in heat transfer surface area because the constraint of the apparent "neck" temperature is removed.
2. High values of Z<sub>1</sub> and high compression ratios R give maximum heat flux values; that is, greater reductions in heat transfer area or equipment costs.
3. At higher values of R, there are regions of Z<sub>1</sub> where the heat exchanger cannot operate because of a negative "neck" and sometimes the mixture cannot reach the boiling temperature at final pressure. This region is labeled "forbidden zone" on figure 8.

One can see that using a "neck" of 50°F with an M<sub>2</sub> of 10.88 lb/sec, a conventional heat exchanger<sub>2</sub> having a Z<sub>1</sub> equal to 0 would have a heat flux of 3040 Btu/hr/ft<sup>2</sup>. By using the pressure-staged heat exchanger in which Z<sub>1</sub> could be selected, to .95, the heat flux would be in the vicinity of 4000 Btu/hr/ft<sup>2</sup>. Thus, by use of a staged pressure heat exchanger, the heat transfer area can be reduced by 25% as compared to a conventional heat exchanger while yielding the same energy transfer.

Similar results are shown in figure 9 for a neck temperature of -20°F. This, of course, is a fictitious condition for a conventional heat exchanger, but has meaning for a properly designed pressure-staged heat exchanger. Results from figure 8 are reproduced on figure 9 to show the effect of reducing the neck temperature. The heat flux is reduced because of the smaller temperature differences. However, the neck occurs at a lower absolute temperature which allows an increase in the steam rate from 10.88 lb/sec to 12.56 lb/sec - an increase in energy recovery of 15%.

Figure 10 was generated in a similar manner except that the steam pressure was dropped to 100 psia. This condition corresponds to the typical operation of a heating plant. One can see by comparing figure 10 to figure 9 that the graphs are quite similar except that the "forbidden zone" of figure 10 is some-

what narrower. Also, the effects of the compression ratios are not as large for a large "neck" as it is when the "neck" is small or negative.

#### COST EFFECTIVENESS OF THE PRESSURE-STAGED HEAT EXCHANGER

The advantages of the staged counterflow heat exchanger are four-fold. First, its use results in cost reductions by reducing the surface area of the heat exchanger. Second, one can achieve the highest possible temperature in the heat receiving fluid so that the equipment associated with the system can be designed more efficiently. Third, energy requirements are reduced which, in turn, saves operating costs. Fourth, the weight can be further reduced by using thinner walls in the pre-heater and low temperature evaporator sections within the bounds of the ASME Boiler Code.

In order to dramatize the actual savings, a "Figure of Merit",  $\eta$ , has been devised. This Figure of Merit can best be appreciated by citing actual estimated cost savings. Generally, boilers cost in the range of \$5.00 to \$10.00 per square foot of surface area. The pump, compressor and accessories are estimated to cost between \$10.00 and \$30.00 per pumping horsepower depending on the value of  $Z_1$ . The Figure of Merit is defined as the surface Area  $A_0$  without staging minus the surface area  $A$  with staging times  $C_1$ , the cost/ft<sup>2</sup> of the heat exchanger, minus the pump costs expressed in horsepower,  $M_2W$ , times the cost per horsepower,  $C_2$ . The difference is divided by the surface area times cost  $C_1$  without staging.

$$\eta = \frac{(A_0 - A)C_1 - M_2WC_2}{A_0C_1}$$

Thus,  $\eta$  is really a fraction which is achieved by subtracting the pump cost from the cost difference between a heat exchanger without and with staging divided by the cost of a heat exchanger without staging. Thus, the greater this fraction, the greater are the economies of using a pressure-staged heat exchanger.

In order to present the fairest comparison, figures were chosen which would least point out the advantages of this heat exchanger. For example,  $C_1$  was chosen at \$5.00/ft<sup>2</sup> and  $C_2$  at \$30.00/hp. The Figure of Merit in terms of capital cost for compression ratios of 2 and 4 are shown in figure 11. The greatest advantage occurs when  $Z_1$  is between 0.2 and 0.4.

To optimize a pressure-staged heat exchanger, operation in the "negative neck" region is preferred. Although a mathematical comparison between the pressure staged heat exchanger and one of conventional design can be made, in actuality a conventional heat exchanger cannot operate in a negative neck area. If a negative neck temperature of -20°F is chosen, Figures of Merit

for pressure ratios of 2 and 4 are shown in figure 12. For a compression ratio of 4, the synthesized Figure of Merit has a peak at  $Z_1$  between 0.5 and 0.7. At a compression ratio of 2, the Figure of Merit increases with  $Z_1$ . Thus, design parameter selection indicates that complete evaporation should be employed at low compression ratios.

#### CONCLUDING REMARKS

The pressure-staged heat exchanger is a novel method to improve the performance of heat exchangers where the cool fluid being heated undergoes a phase change. The advantages can be realized either as reduced surface area for the heat exchanger or as an increase in the mass flow of the fluid being heated.

The pressure staging of the evaporative process requires an increase in mechanical complexity with the addition of pumps, separators and mixers. In addition, the work input to the pumps must be evaluated. However, even with this complexity, the pressure staged heat exchanger appears to be cost effective for many thermodynamic conditions in light of potential performance gains and weight reductions.

#### REFERENCES

1. Anon, Pressure Staged Heat Exchanger, U.S. Patent No.4,072,182, 7 February 1978.

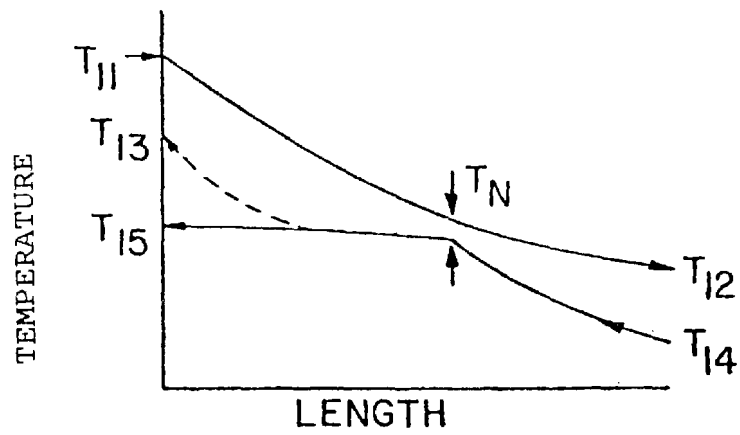


Figure 1 Temperature Profile for a Conventional Heat Exchanger

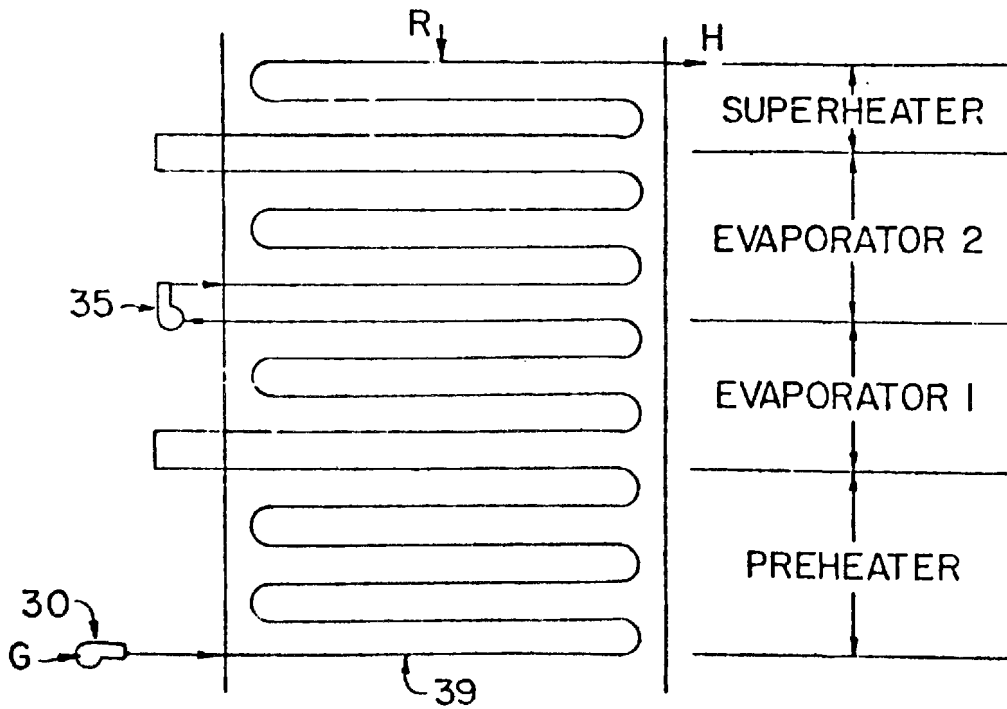


Figure 3 Mechanical Concept of a Pressure-Staged Heat Exchanger having 2 Evaporators

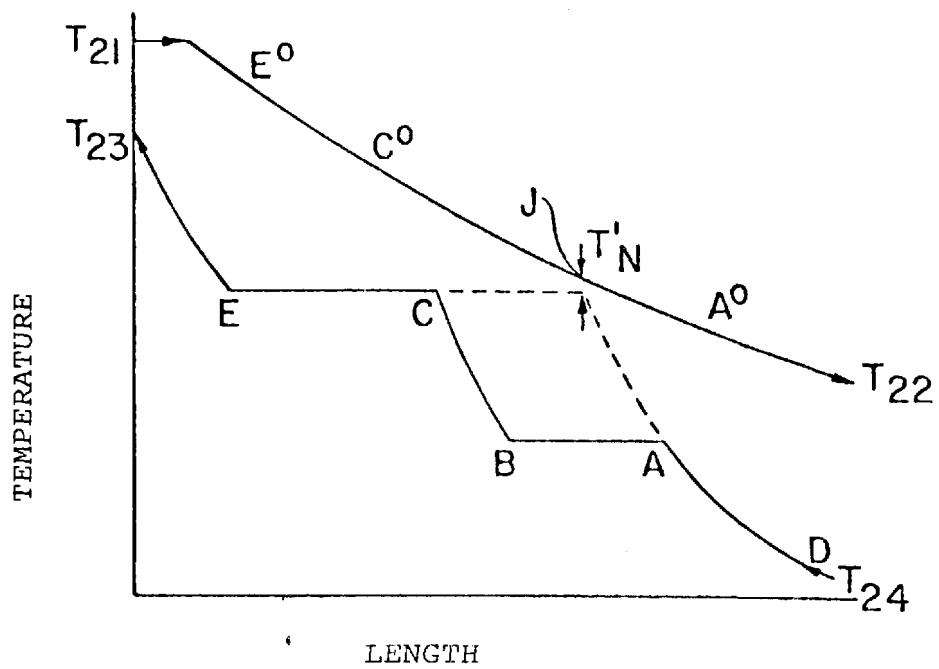


Figure 2 Temperature Profile for a Pressure-Staged Heat Exchanger having 2 Evaporators

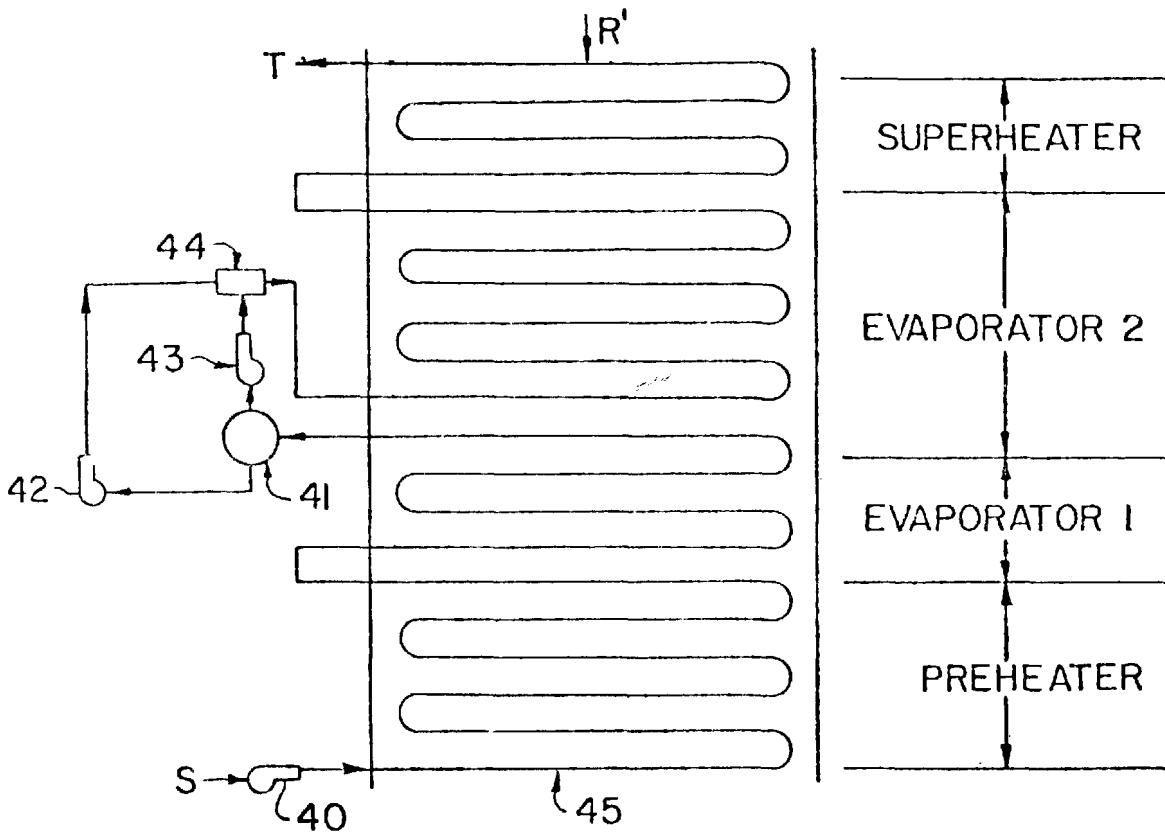


Figure 4 Concept for Separating and Pumping Liquid and Vapor in a Pressure-Staged Heat Exchanger

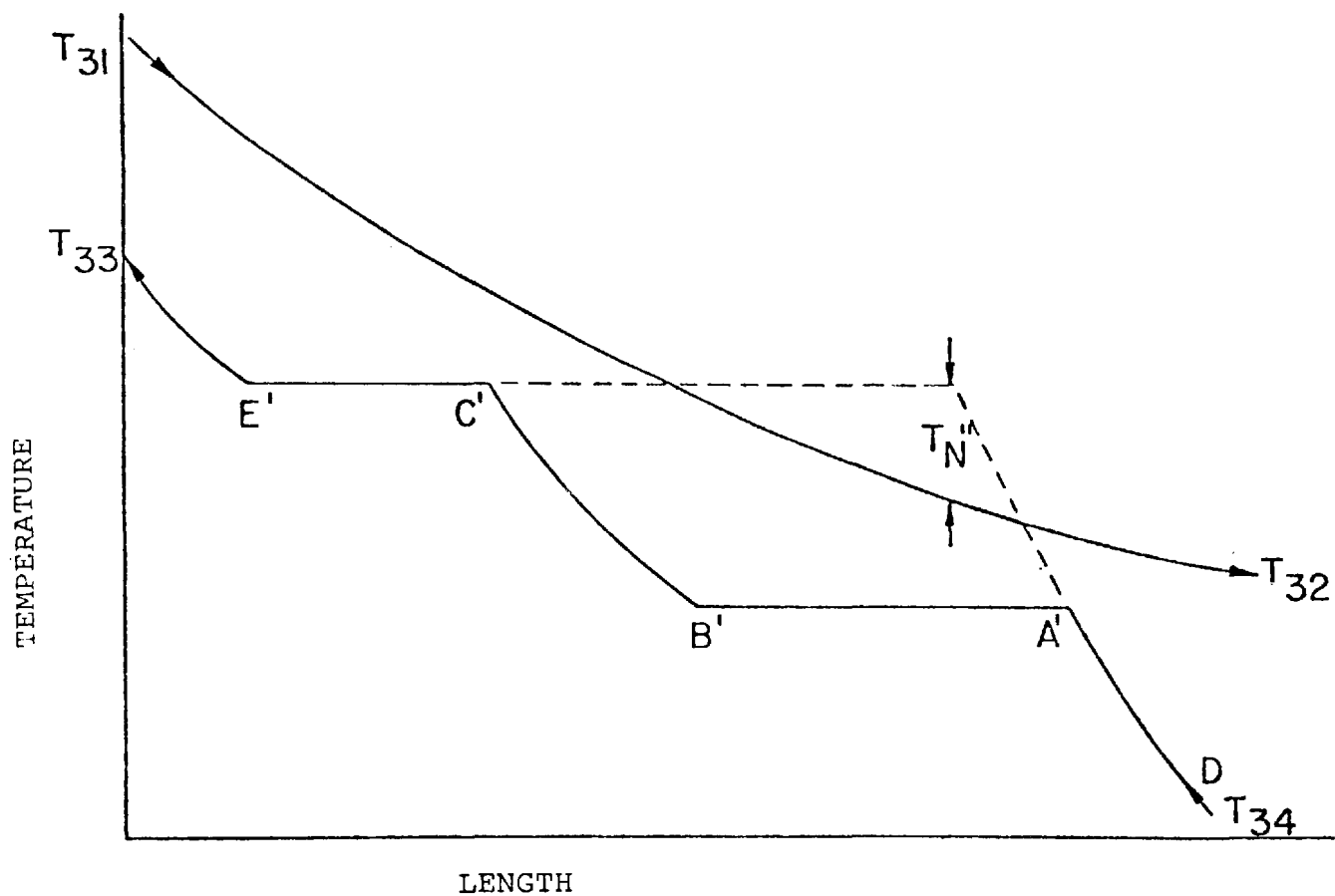


Figure 5 Avoiding the Limiting Condition of the Neck through the use of a Pressure-Staged Heat Exchanger

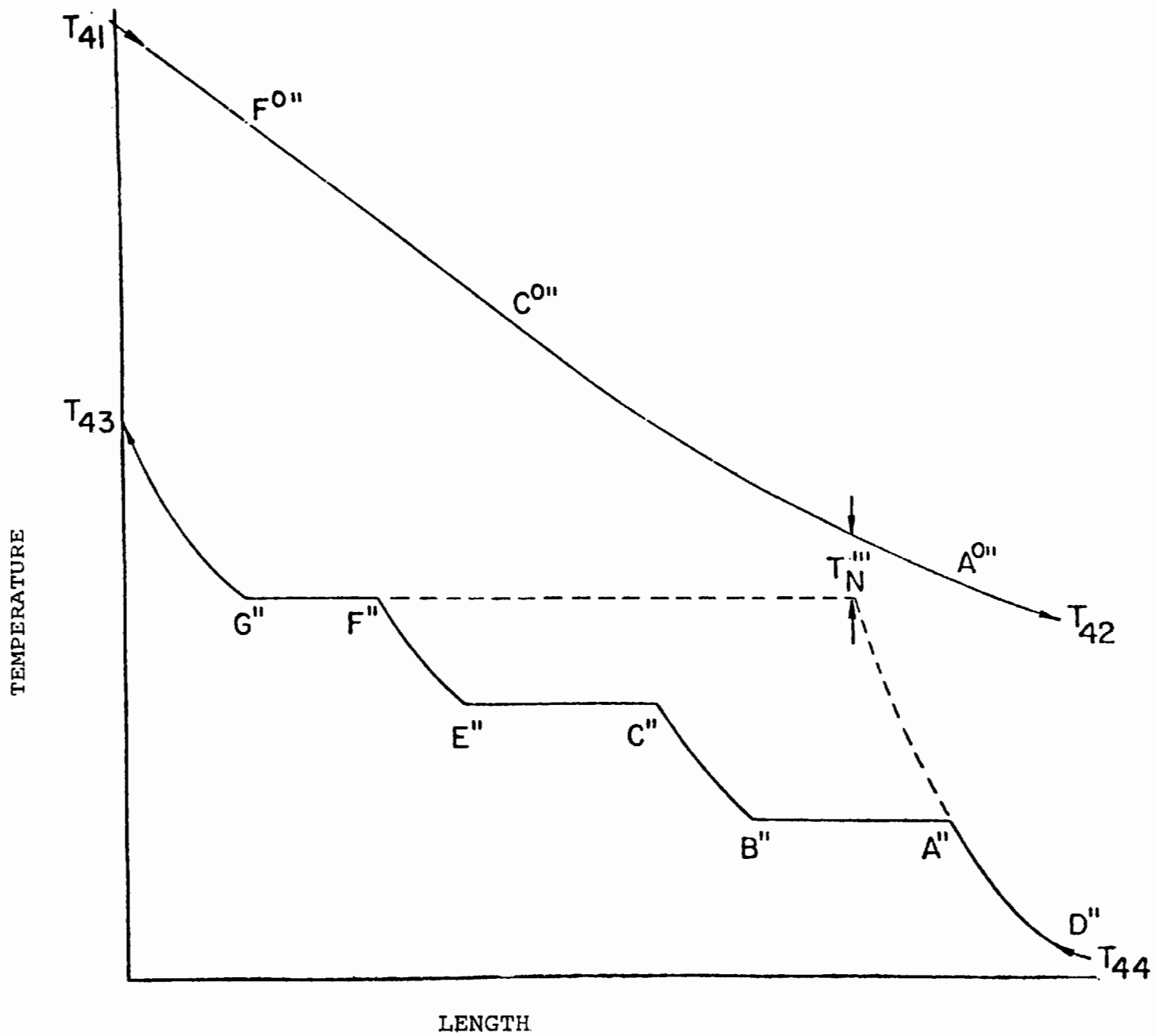


Figure 6 Multiple Evaporators in a Pressure-Staged Heat Exchanger

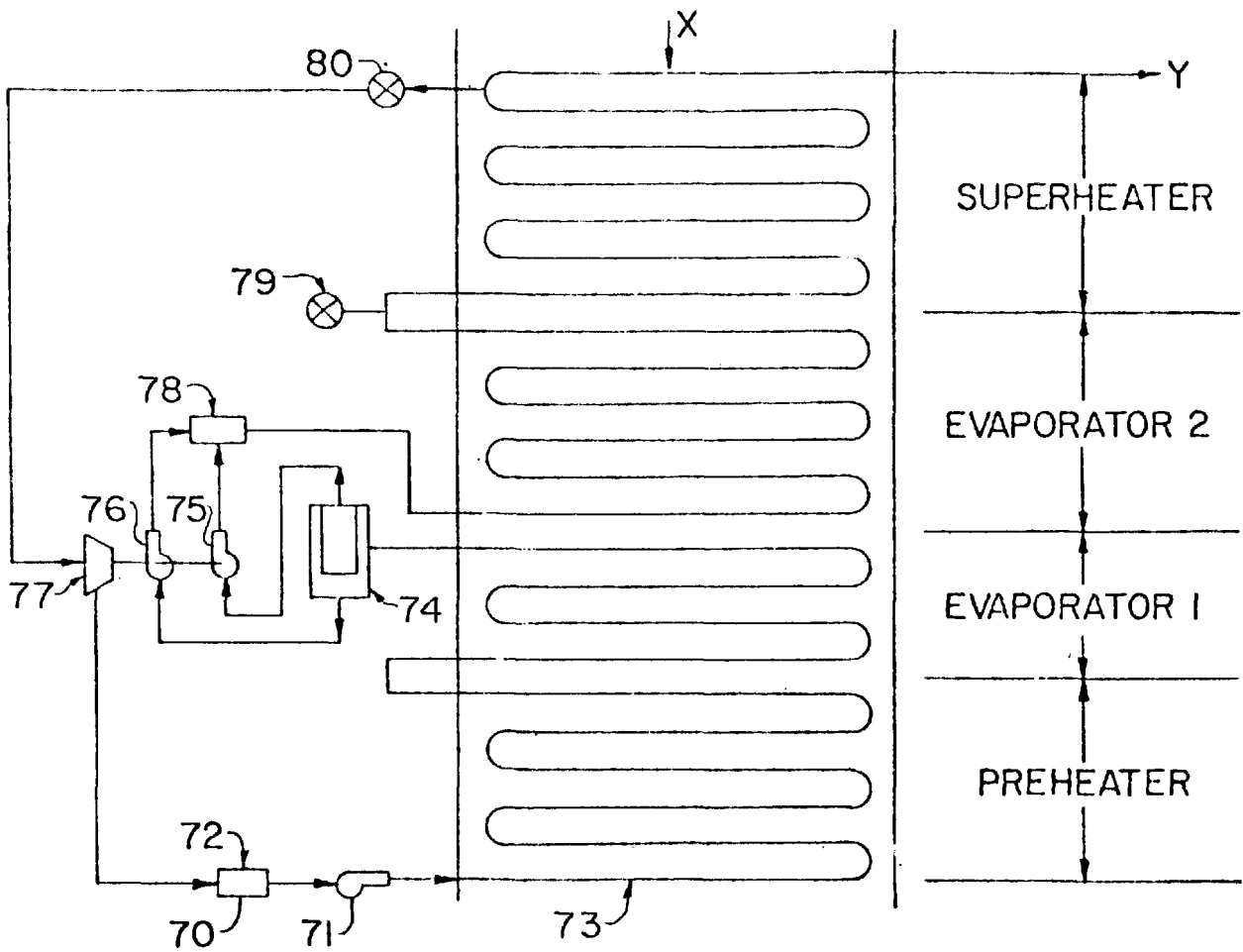


Figure 7 Use of Superheated Steam to Drive the Stage Pumps in a Pressure-Stage Heat Exchanger

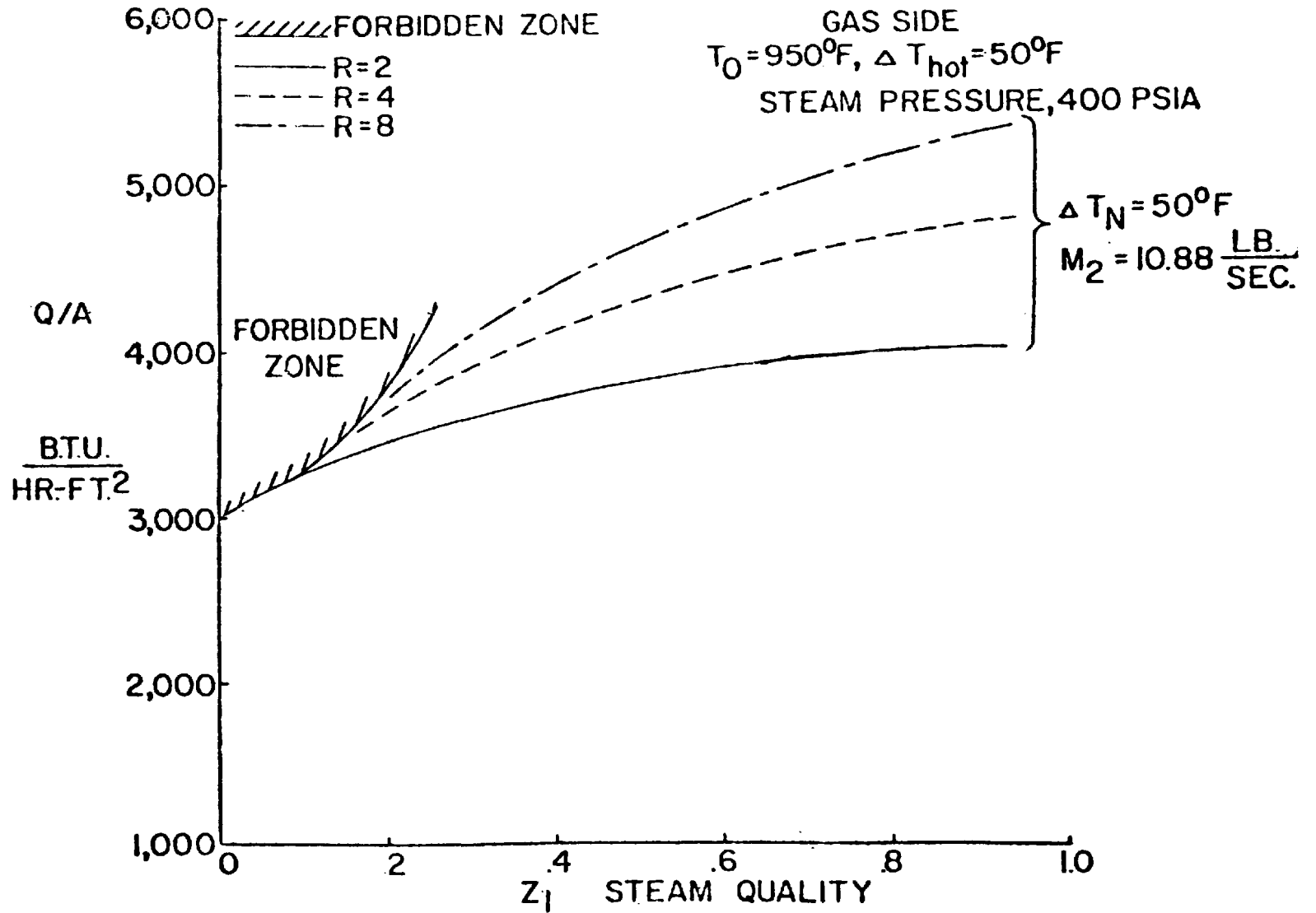


Figure 8 Increase in the Heat Flux Available with a Pressure-Staged Heat Exchanger  
 Steam Pressure = 400 psia

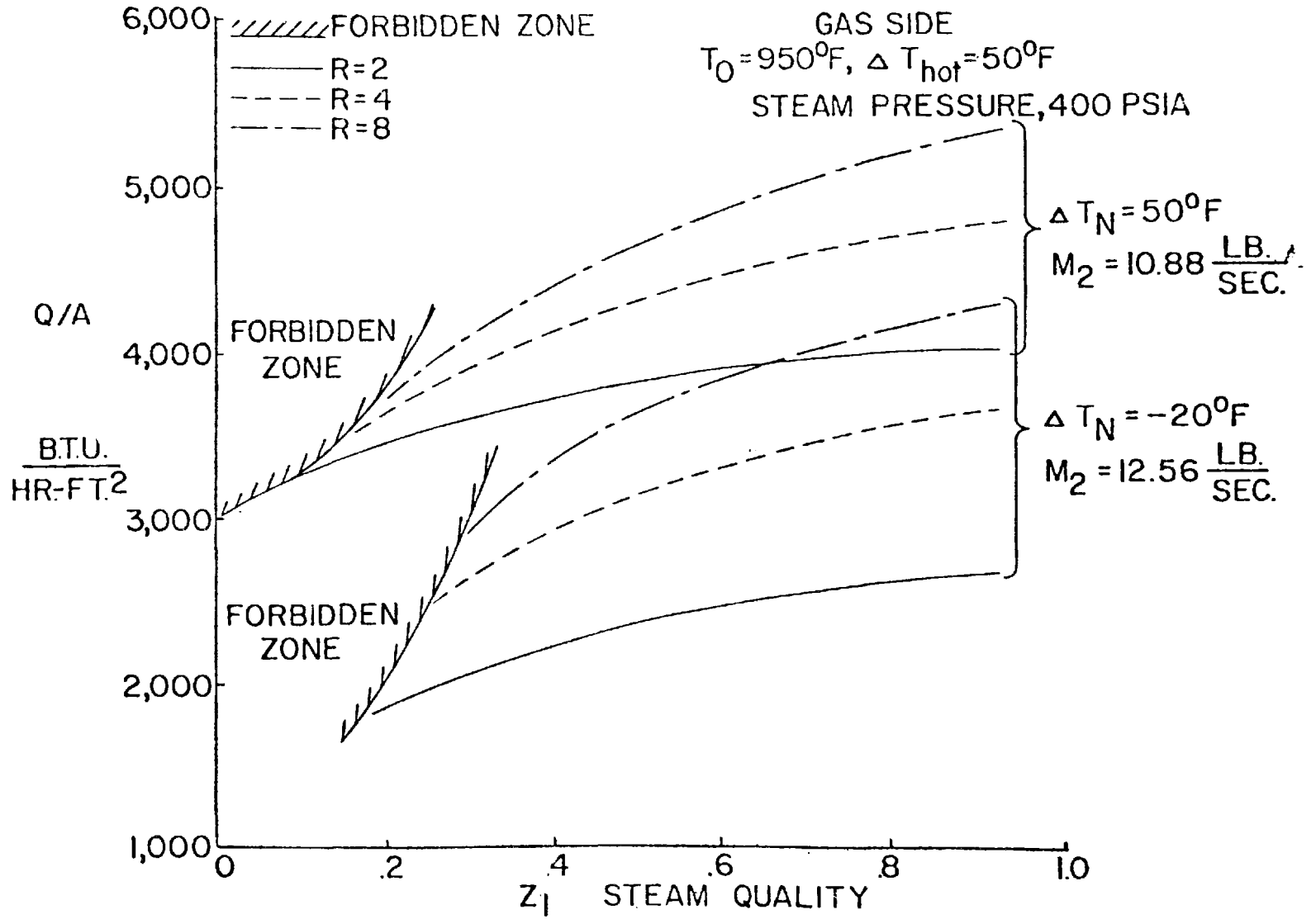
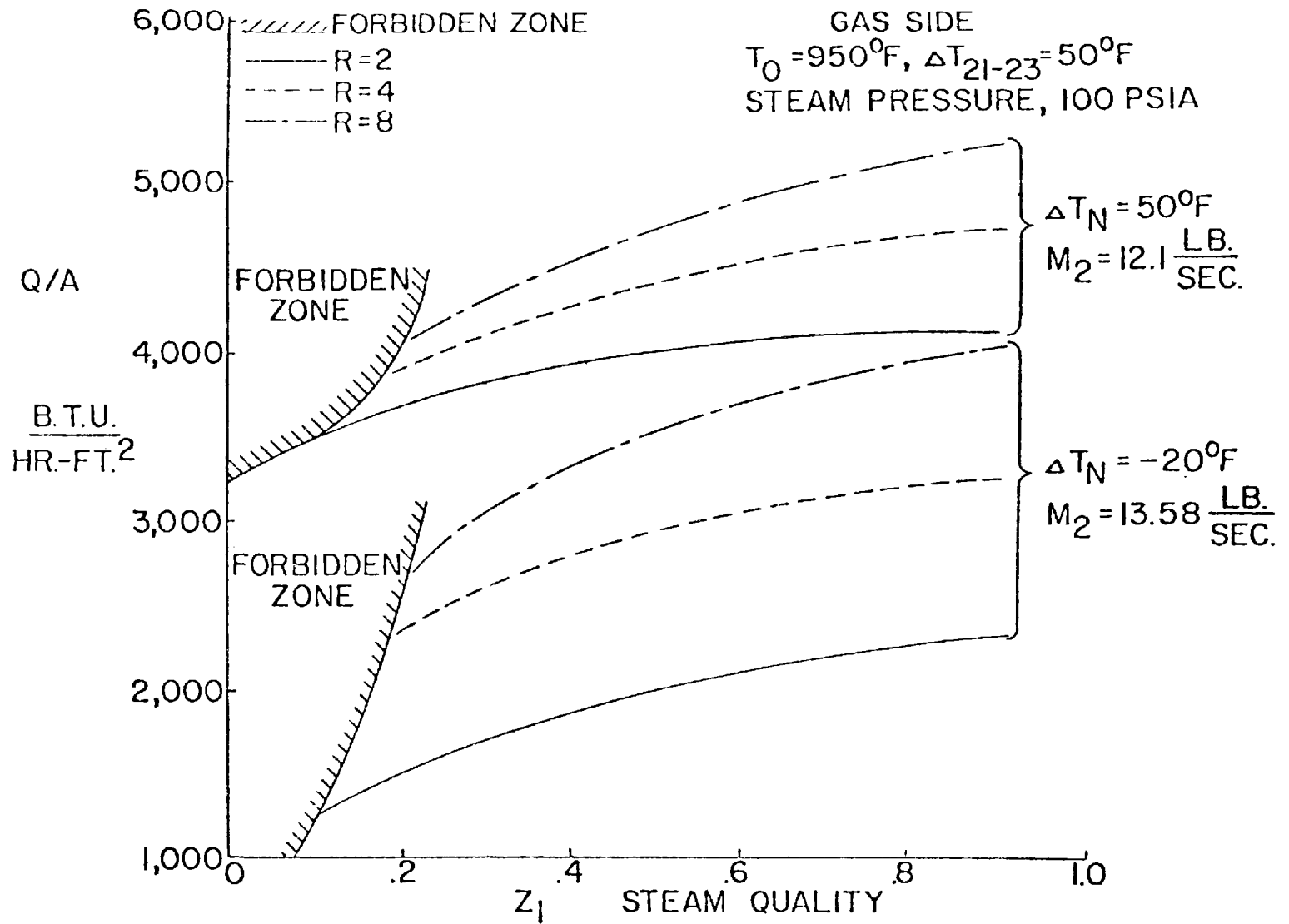


Figure 9 Increase in Steam Mass Flow Available with a Pressure-Stage Heat Exchanger  
 Steam Pressure = 400 psia



997

Figure 10 Increase in Heat Flux and/or Steam Mass Flow Available with a Pressure-Stage Heat Exchanger - Steam Pressure = 100 psia

$$\eta = \frac{(\text{Surface Area Reduction}) (\text{Cost/Area}) - (\text{Pump Power}) (\text{Cost/Power})}{(\text{Conventional Heat Exchanger Area}) (\text{Cost/Area})} \times 100$$

GAS 950<sup>0</sup>F,  $\Delta T_{HOT} = 50^0F$

STEAM 400 PSIA,  $\Delta T_N = 50^0F$

$M_1 = 100 \frac{LB.}{SEC.}$ ,  $M_2 = 10.88 \frac{LB.}{SEC.}$

$A_0 = 18,443 \text{ FT.}^2$

$C_1 = \$5/\text{FT}^2$

$C_2 = \$30/\text{H.P.}$

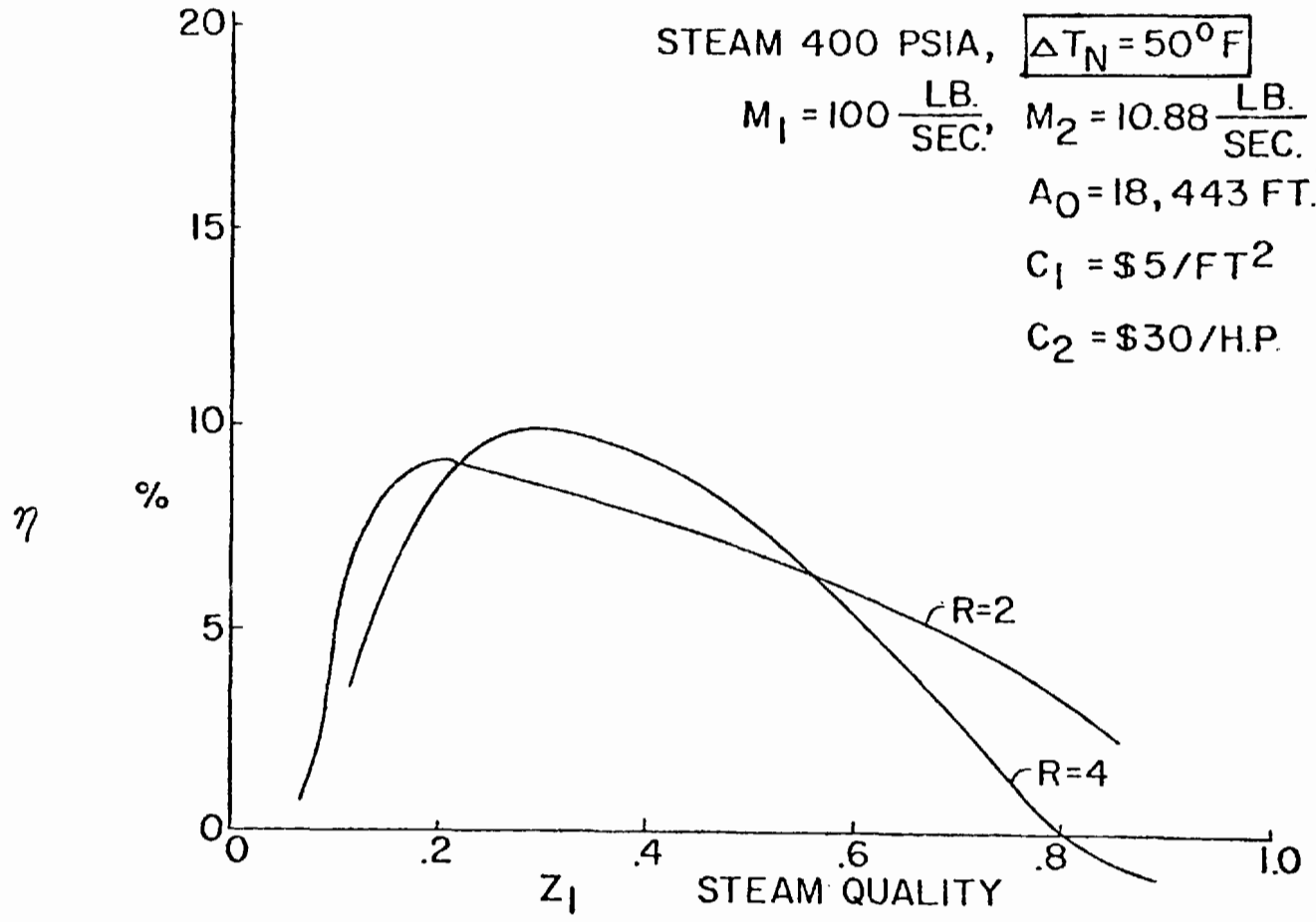


Figure 11 Cost Effectiveness of the Pressure-Staged Heat Exchanger

$$\eta = \frac{(\text{Surface Area, Reduction}) (\text{Cost/Area}) - (\text{Pump Power}) (\text{Cost/Power})}{(\text{Conventional Heat Exchanger Area}) (\text{Cost/Area})} \times 100$$

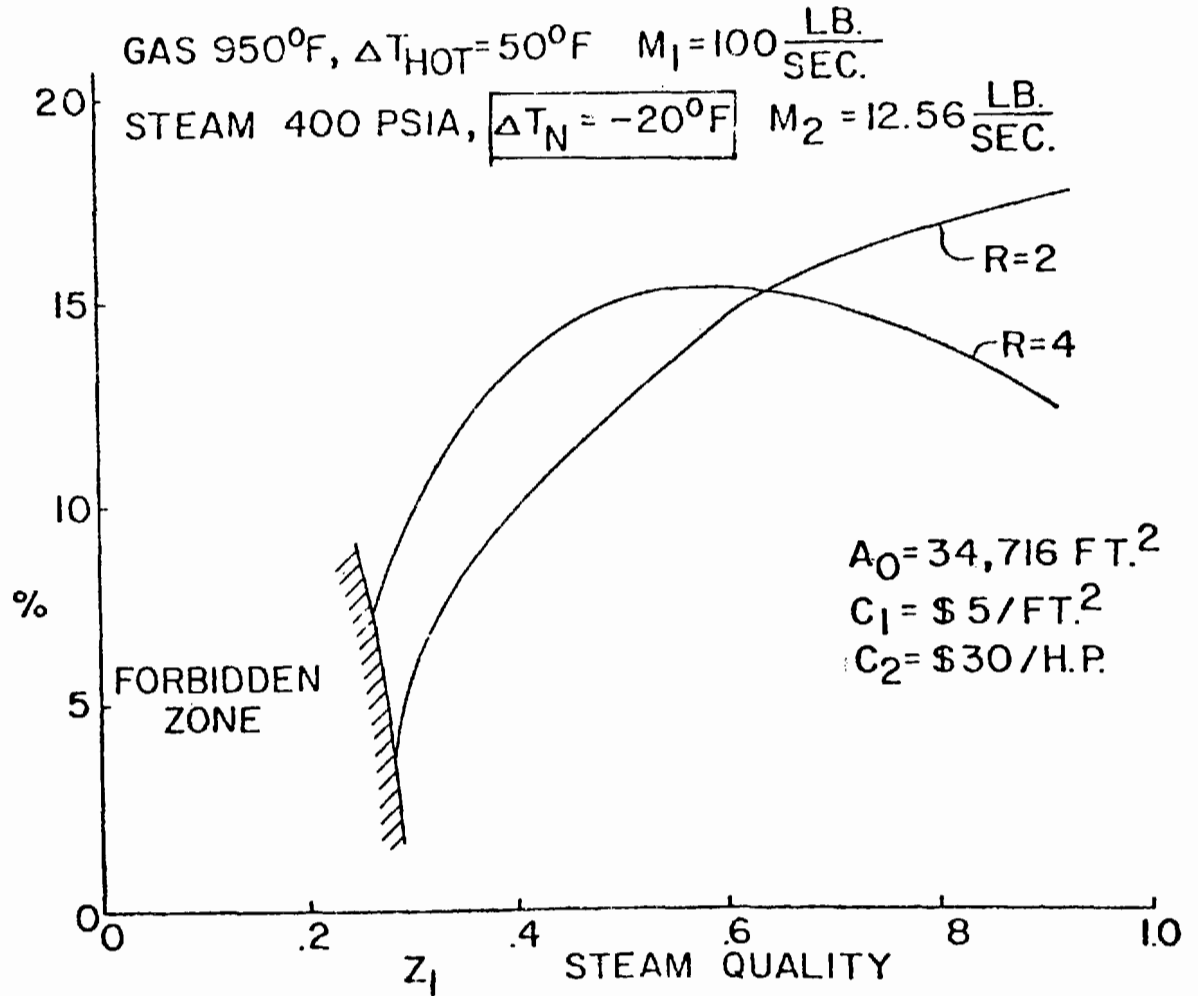


Figure 12 Cost Effectiveness of the Pressure-Stage Heat Exchanger

## HEAT RECOVERY FROM WASTE FUEL

Y. H. Kiang  
Trane Thermal Company  
Conshohocken, Pa. 19428, U.S.A.

### ABSTRACT

The attention of industry has been focused on fuel shortages and the high costs of available fuels. Recovery of available energy from sources once considered as only waste is in practice in many plants and processes today. Industrial wastes which have fuel value can be in any form - solid, liquid or gaseous. Many presentations and discussions have centered the utilization of heat available from solid waste materials. In this paper, the possibility of recovering heat from waste liquid and gaseous materials will be discussed. This paper will present the problems of handling these various wastes, combustion equipment, and the effect of waste properties on combustion and heat transfer. Case histories of installations where systems have been applied in industry to recover waste fuel value will also be presented.

## HEAT RECOVERY FROM WASTE FUEL

by Yen-Hsiung Kiang, Trane Thermal Company, Pa. 19428, U.S.A.

Industrial waste materials which have fuel values are defined as the waste fuel. This paper will discuss the heat recovery from liquid and gaseous waste fuels.

### LIQUID WASTE FUEL

In many types of process plants, whether they be chemical, petrochemical, metallurgical, automotive, paper, food, pharmaceutical, etc., there are liquid wastes generated that contain heating values. The ultimate solution to these waste problems is combustion.

The following are some of the problems involved in the combustion of liquid waste fuels:

- (1) Low heat of combustion: High water content or high ash and halogen content makes a waste liquid less liable to sustain combustion in conventional burners.
- (2) High viscosity or mixture of solid particles: These factors adversely affect the atomizing of the liquid. A proper selection of injector is required to ensure trouble free operation.
- (3) Polymerization or decomposition: In some cases, the waste undergoes polymerization in the pipe line or in the nozzle before atomization. Some times, thermal decomposition takes place and corrosive substances are formed. This can be corrected by properly designing the piping and injectors.
- (4) Contaminated combustion product gases: The contaminants in the fuel will become contaminants in the combustion product gases. Properties of the product gases will determine the selection of heat recovery equipment. A pollution control system is also required to ensure clean exhaust gases.

In order to ensure an optimal combustion-heat recovery system, certain data has to be generated on the waste fuels. They are:

1. Chemical Composition
2. Heat of Combustion

3. Viscosity
4. Corrosive problems to be considered for pumps, piping, valves and injectors.
5. Chemical reaction with other compounds (e.g. steam to waste reaction in the injector).
6. Polymerization
7. Solid content (solids tend to plug valves, orifices, etc. in the piping system).
8. Ash reaction with refractories at high temperatures.
9. Slag formation (its reaction with plugging of tubes).
10. Analysis of combustion gases and their effect on heat exchange surfaces.
11. Nitrogen composition ( $\text{NO}_x$  formation)

These are critical data to be reviewed. Typical application of some waste fuels is shown in Table 1.

Liquid Waste Fuel Injector - In liquid waste fuel combustion, the atomizers used to inject waste into the combustion zone are critical equipment. For relatively clean waste fuel, a conventional burner injector can be used<sup>(1,2)</sup>. For high viscosity or highly undissolved solid content liquids, specially designed injectors are required. The TEAT atomized tip, Figure 1a, as developed at Trane Thermal Company has been used successfully for this type of application. This design operates at low pressures, thereby avoiding the problems of high pressure pumping. These nozzles have been used on materials with viscosities as high as 4500 ssu at 300°F. For two non-compatible waste fuels, a dual liquid TEAT atomizer can be used, as illustrated in Figure 1b. The TEAT design generates a solid cone. Combustion rates slow down because of poor fuel air mixing in the center fuel mass. Increased residence time or a high intensity burner is usually required for a TEAT nozzle application.

The heat atomizer is another externally atomized tip developed by the Trane Thermal Company. Figure 1c illustrates the schematics of the heat tip. The spray generated by heat nozzle is hollow cone, improving fuel air mixing.

Combustion Equipment - Liquid waste fuels, in general, do not combust efficiently. A special burner is needed to increase the combustion

efficiency. The requirement of the special burner is high heat release. The Vortex burner developed by Trane Thermal Company, Figure 2, has been used effectively in waste liquid combustion.

In the vortex design, waste fuel is introduced through a nozzle at the centerline of the burner. Combustion air is brought in tangentially and passes through swirl vanes which impart rotational energy. A twisting, high velocity vortex action results in complete mixing with the fuel spray at its point of injection, and at the same time creates a low pressure zone immediately downstream from this point. As the highly turbulent air-fuel mixture enters the flame zone, the low pressure area causes a recycling of the hot gases of combustion back into the mixture. Thus, the mixture is preheated, vaporized and raised to ignition temperature almost instantaneously. The flame rotates tangentially within the combustion chamber. This high intensity combustion allows the combustion chamber to be considered as a reaction chamber.

Flame length is short, about one to one-and-a-half times the chamber length, with heat release rates upwards of a million BTU per hour per cubic foot in the standard unit. This vortex action provides most efficient oxidation reaction for waste disposal.

The Vortex burner can be used to burn waste fuels with heating values 4500 Btu/lb. and up. For waste fuels having heating values lower than 4500 Btu/lb., two-stage combustion is necessary. The two-stage combustion equipment can be either a modified Vortex burner or a standard two-stage combustion equipment. Details are illustrated in Reference 2.

Secondary Chamber - It is important in any conversion to a waste fuel fired burner that a proper review of the burner location be made. Its relationship to tube surface is most important. One must be sure that the waste is first completely oxidized to its final products and that there is no chance of unburned materials getting into the stack and exhausting to atmosphere. With some slower burning waste fuels, increased residence time is necessary. A secondary combustion chamber is usually required prior to entry into the heat exchange device. The secondary chamber will ensure the complete oxidation. This will prevent the deposit of unburned hydrocarbons which could condense and attack the heat exchanger surfaces.

Combustion and Heat Transfer - In order to illustrate and analyze the effect of waste fuels, two waste fuels - as listed in Table 2 - are used for study.<sup>(3)</sup> No. 2 oil is used as the reference.

The data presented in Table 3 are the fuel composition, stoichiometric products and heat transfer coefficients for these three fuels. The emissivity values of the various fuel products of combustion are related to the water vapor, carbon dioxide values and the gas temperature. The radiation heat transfer coefficients are determined for the fuels tabulated.

The mass flow of products of combustion per million Btu of heat release generally increases in value as the heating value drops off.

The decrease in combustion temperature as the excess air rate increases is illustrated in Figure 3. The gas emissivities and radiation heat transfer coefficients as a function of gas temperature (thus, excess air) are illustrated in Figures 4 and 5. At the same temperature, methanol has the highest radiation heat transfer coefficients and No. 2 oil the lowest. The convective heat transfer coefficients are shown in Figure 6. The convective heat transfer coefficients are lowest for methanol and highest for No. 2 oil.

The data used in this section are limited to the special geometrical configurations (identical for all fuels), temperature, fuels, and other parameters of the cases examined. This can only be used as a general guide line for waste fuel application. It is advisable to study the theoretical combustion and heat transfer analysis before the designing of a system.

### Discussion

Before any waste material is burned in a heat recovery unit, it is recommended that a test run be made to determine the composition of the products of combustion and if a particulate problem exists. This information is necessary so that the designer of the heat exchanger will be able to determine the effectiveness of the surface, and also if any problems will exist in fouling of the surface. This will also indicate whether any clean-up equipment is necessary prior to discharge to atmosphere.

The physical and chemical properties are also necessary for the designer. The physical properties are necessary to design waste fuel handling systems. The chemical properties are the key to a successful combustion-heat transfer system. Besides heat transfer, the selection of equipment is determined by waste chemistry.<sup>(4,5,6)</sup> One example is the chlorinated hydrocarbons. A gas to gas heat exchanger cannot be used and special characteristics must be built into the boiler design. References 4 to 6 give illustrations of the selection of heat transfer equipment as the waste chemistry changes.

Another problem often encountered in the waste fuel application is the changing of composition, heating values, etc. It is necessary to provide a day tank to mix the wastes so that the change in composition is gradual and the control scheme can compensate for the gradual changes.

### GASEOUS WASTE FUEL

In many areas of the process industries, gases from the process must be vented in order to:

1. Prevent pressure build-up in the system
2. Purge undesirable constituents in the reaction
3. Purge a vessel of residual products after emptying the vessel.

If the gases contain combustibles, combustion may be used to recover waste heat.

Combustion Equipment - The Vortex burner, described before, has been used successfully to burn waste gases with a heating value as low as 100 Btu/CF.

Combustion & Heat Transfer - The gases used for comparison are listed in Table 4. The properties of the stoichiometric combustion products are shown in Table 5. The combustion temperature, emissivity, radiation and convective heat transfer coefficients are illustrated in Figures 7, 8, 9, and 10.

Case History<sup>(7,8)</sup> - A case in point is a waste gas with the following composition by volume:

|                 |   |              |
|-----------------|---|--------------|
| CO <sub>2</sub> | - | 0.9 percent  |
| O <sub>2</sub>  | - | 0.2 percent  |
| H <sub>2</sub>  | - | 26.2 percent |
| CO              | - | 5.3 percent  |
| CH <sub>4</sub> | - | 0.4 percent  |
| N <sub>2</sub>  | - | 67 percent   |

This waste gas is defined as WAG in Tables 5 and 6.

The average heating value varies between 88 and 100 Btu/cu.ft. This value is 10 percent of that for natural gas. The available heat from this vent gas is on the order of 75 MM Btu/hr. In this particular process, 40 MM Btu/hr. was needed for gas preheating. A test burner was set up to determine whether there would be problems in burning this waste gas in a standard combustion chamber configuration. One of these problems was the high mass flow of combustion products that would result from the combustion reaction at a specific heat release.

Since the waste gas contained 67 percent nitrogen, this acts as a diluent and at the same time increases the total nitrogen in the combustion products. The fuel-air ratio, in this case, is approximately 1 part of air to 1 part of fuel. Normally, when burning natural gas, 10 parts of air is required for 1 part of natural gas. The exact requirements for this waste gas is covered in Table 5. The waste gas has almost 150 percent as much product resulting from the combustion reaction as compared with natural gas. This increase in mass flow would have to be reviewed for both heat transfer and pressure drop in an existing heater design.

A heat transfer analysis, in this case, indicated that the waste gas could be burned in an existing heater design without causing any problems from a pressure drop or overall heat transfer design. In fact, it provided an additional margin of safety from a temperature standpoint. With natural gas, the maximum flame temperature that could be reached at theoretical conditions would be 3450°F. In this case, the maximum flame temperature possible was 2412°F. This was a benefit since in this particular application, a heat sensitive material was flowing inside the tubes of the heat exchanger and tube metal temperature was critical. The lower temperature level of the combustion products added an additional margin of safety.

Burner tests were run with a burner 25 percent of the size necessary in the full scale unit. These tests were necessary to determine optimum gun size for the waste gas, optimum gun position and optimum combustion chamber dimensions. It was found that the gun position was critical to prevent flashback and also to insure uniform mixing of the waste fuel with the combustion air. It was also determined that if this waste were injected directly into the burner throat section without thorough mixing with combustion air, a rumble or vibrating resulted. This was due to fuel being injected into a zone of combustion products deficient in oxygen. Proper mixing of both the combustion gas and oxygen is necessary to provide smooth burning without vibrations and instability.

Due to the lower flame temperature, a decrease in the combustion chamber diameter could be made without deterioration of the burner efficiency. The smaller volume aided in having the reaction temperature very close to the theoretical flame temperature. At the same time, this provides more complete combustion in the reduced combustion chamber volume.

These modifications were made to the full size burner (LV-24) and installed in three units. These units have been operating in this application since 1964. These units operate continuously, 24 hours a day, 7 days a week, and are shut down once per year for maintenance turnaround. By using this waste gas, approximately 75,000 standard cu.ft./hr. of natural gas is saved and over a ten year period has resulted in a saving of \$3.6 Million (based on average cost of 0.60/1000 cu.ft.). The only natural gas that is used in this particular heater is the operation of a constant pilot which requires approximately 250 SCFH of natural gas. This is used for safety reasons in the event that there is an interruption in the flow of waste gas or instantaneous drop of the hydrogen content in the waste gas. The pilot will permit re-ignition if this occurs, prior to shutdown by the flame-out controls.

The waste gas is burned in three separate fired heaters. The units are constructed as shown in Figure 11. The burner fires directly into a secondary chamber where the gases are tempered to 1600°F. This is necessary due to the critical tube metal temperature limitations and maximum heat flux permitted on the material being heated within the tubes; however, in another application this has been fired directly at a flame

temperature of 2200°F. The short flame characteristics of the vortex combustor permits a short mixing chamber to be used to dilute these products from flame temperature to design temperature. Normally, a chamber five to six times this size would be required with a conventional burner system to enclose the flame which might be as long as 20 ft. at a firing rate of 24 MM Btu/hr. In this case, the flame was approximately 5 ft. long downstream of the burner exit. Complete combustion in the burner also permitted the unit to be installed adjacent to the heat transfer surface without fear of high radiant losses causing incomplete combustion of the waste gas. This also saved in the total installed cost of the burner system necessary for these waste gases.

Discussion - If a fume contains at least 16 percent oxygen, it may be used as combustion air for the main burner. A savings of 745 SCFH of natural gas per thousand SCFM of fume may be realized over the use of outside combustion air. This should be reviewed carefully to determine what problems may result. Some fumes contain condensible materials which could deposit on blower wheels, control valves, and burner internals. Figure 12 shows schematics of typical fume systems.

One problem associated with gaseous waste fuel is the cyclic properties of both flow rates and composition. A well designed control system is required to ensure trouble free operation. The control system usually keeps the oxidation temperature and stack oxygen content relatively constant by adjusting the flow of air and auxiliary fuel. An alternate approach is to base load the system with auxiliary fuel. The latter approach usually gives a more stable system.

#### REFERENCES

1. Santoleri, J.J., "Spray Nozzle Selection", CEP, 70,9,p.84,1974.
2. Kiang, Y.H., "Total Hazardous Waste Disposal Through Combustion", Industrial Heating, December 1977.
3. Ashburn, L., "Techniques of Energy Recovery from the Combustion of Low Heating Value Fuels and Industrial Fluid Wastes", presented to Ass. of Iron and Steel Engineer 1977 Convention, Cleveland, 1977.
4. Hung, W., "Results of a Five Tube Test Boiler in Flue Gas with Hydrogen Chloride and Fly Ash", ASME WAM, Houston, Nov. 1975.
5. Kiang, Y.H., "Prevent Shell Corrosion for Chlorinated Hydrocarbon Incineration", Presented to Seminar on Corrosion Problems in Air Pollution Control Equipment, sponsored by AQCA, IGCZ, and NACE, Atlanta, Jan. 1978.
6. Kiang, Y.H., "Technology for the Utilization of Waste Energy", presented to IEC 23rd Annual Meeting, L.A., April 1977.
7. Santoleri, J.J., "Energy Recovery from Low Heating Value Industrial Waste", presented to ASME Industrial Power Conference, Pittsburgh, May 1975.
8. Santoleri, J.J., "Waste Energy - The New Source of Plant Profits", presented to AIChE 85th Annual Meeting, Philadelphia, June 1978.

# ACKNOWLEDGMENT

The author wants to acknowledge his gratitude to Mr. J. J. Santoleri and Len Ashburn of Trane Thermal Company for providing reference materials and assistance in preparing this manuscript.

TABLE 1  
LIQUID WASTE FUEL APPLICATION

| Waste Fuel  | Equipment                        | Firing Rate, Btu/hr |
|---|----------------------------------|---------------------|
| 1. Diethylene Triamine Tar  | Petroleum Heater                 | $3 \times 10^6$     |
| 2. Irradiated organic moderator from nuclear reactor              | Packaged Boiler                  | $3 \times 10^6$     |
| 3. Tar, Water, Misc. Organics, Ammonium Sulfate, Ammonium Nitrate | Poncor-Wheeler Waste Heat Boiler | $98 \times 10^6$    |
| 4. Phenolic Tar   | Steam Superheater                | $7 \times 10^6$     |
| 5. Thiourea di-isocyanate Oxidus (viscosity 1500 ssu at 300°F)    | Babcock & Wilcox Boilers         | $80 \times 10^6$    |
| 6. Alpha Methyl Styrene   | Thermal Boiler                   | $7 \times 10^6$     |

TABLE 2  
LIQUID WASTE FUELS

|                 | Btu/lb.              | HHV    | LHV    | Air/Fuel Ratio |
|-----------------|----------------------|--------|--------|----------------|
| NO <sub>2</sub> | No. 2 oil            | 19,800 | 18,680 | 14.4           |
| NET             | Methanol             | 10,300 | 9,078  | 6.52           |
| LRL             | Low Btu Waste Liquid | 3,050  | 7,039  | 5.96           |

TABLE 3  
LIQUID WASTE FUEL-STOICHIOMETRIC

| FUEL            | HHV<br>Btu/lb. | Composition, Wt. % |                |     |                |                |                  |     | A<br>F | Stoichiometric Products  |                 |                  |             |                      |                |                |                |
|-----------------|----------------|--------------------|----------------|-----|----------------|----------------|------------------|-----|--------|--------------------------|-----------------|------------------|-------------|----------------------|----------------|----------------|----------------|
|                 |                | C                  | H <sub>2</sub> | S   | O <sub>2</sub> | H <sub>2</sub> | H <sub>2</sub> O | Ash |        | Vol. %<br>N <sub>2</sub> | CO <sub>2</sub> | H <sub>2</sub> O | LB<br>Moles | T <sub>f</sub><br>°F | α <sub>G</sub> | h <sub>r</sub> | h <sub>c</sub> |
| NO <sub>2</sub> | 19,860         | 87.0               | 12.4           | 0.5 | 0              | 0.1            | 0                | 0   | 14.4   | 72.4                     | 13.2            | 14.4             | 792         | 3659                 | 0.083          | 12.3           | 14.3           |
| NET             | 10,260         | 37.5               | 12.5           | 0   | 50             | 0              | 0                | 0   | 6.52   | 61.9                     | 10.8            | 37.3             | 759         | 3443                 | 0.134          | 14.4           | 14.4           |
| LRL             | 8,046          | 38.2               | 4.3            | 0.9 | 0              | 0              | 56.1             | 0.5 | 5.96   | 65.8                     | 12.8            | 21.4             | 865         | 3353                 | 0.13           | 13.9           | 15.4           |

T<sub>f</sub>: flame temperature, °F; α<sub>G</sub>: gas emissivity;  
h<sub>r</sub>: radiation heat transfer coefficient (Btu/hr.-ft<sup>2</sup>-°F)  
h<sub>c</sub>: convective heat transfer coefficient (Btu/hr.-ft<sup>2</sup>-°F)

TABLE 4  
GASEOUS WASTE FUEL

|     | Btu/SCF           | Btu/lb. | HHV    | LHV    | Air/Fuel Ratio |
|-----|-------------------|---------|--------|--------|----------------|
| NG  | Natural Gas       | 1,036   | 22,970 | 20,790 | 14.56          |
| COG | Coke Oven Gas     | 767     | 22,070 | 19,650 | 14.40          |
| LBG | Low Btu Gas       | 178     | 2,804  | 2,022  | 1.07           |
| WAG | Waste Gas         | 106     | 1,878  | 1,638  | 1.07           |
| BFG | Blast Furnace Gas | 81      | 1,025  | 1,013  | 0.59           |

TABLE 5  
GASEOUS WASTE FUEL-STOICHIOMETRIC

| FUEL | HHV<br>Btu/lb. | Composition, Vol. % |                |                 |       |                |                 |     | A<br>F | Stoichiometric Products  |                 |                  |             |                      |                |                |                |
|------|----------------|---------------------|----------------|-----------------|-------|----------------|-----------------|-----|--------|--------------------------|-----------------|------------------|-------------|----------------------|----------------|----------------|----------------|
|      |                | CO                  | H <sub>2</sub> | CH <sub>4</sub> | Other | H <sub>2</sub> | CO <sub>2</sub> | Ash |        | Vol. %<br>N <sub>2</sub> | CO <sub>2</sub> | H <sub>2</sub> O | LB<br>Moles | T <sub>f</sub><br>°F | α <sub>G</sub> | h <sub>r</sub> | h <sub>c</sub> |
| NG   | 22,970         | 0                   | 0              | 93.3            | 4.9   | 1.9            | 0               | 0   | 14.6   | 72.1                     | 9.8             | 18.1             | 770         | 3741                 | 0.091          | 12.7           | 13.9           |
| COG  | 22,070         | 4.5                 | 37.9           | 30.3            | 3.3   | 2.2            | 1.8             | 0   | 14.6   | 70.0                     | 7.9             | 22.1             | 707         | 3851                 | 0.098          | 13.6           | 13.4           |
| LBG  | 2,804          | 28.1                | 17.0           | 1.7             | 0.1   | 67.2           | 6.5             | 0   | 1.67   | 72.8                     | 16.7            | 10.5             | 953         | 3217                 | 0.104          | 12.1           | 14.9           |
| WAG  | 1,878          | 5.3                 | 26.2           | 0.4             | 0.2   | 67.0           | 0.9             | 0   | 1.07   | 78.4                     | 4.0             | 16.6             | 1101        | 2400                 | 0.159          | 12.2           | 16.1           |
| BFG  | 1,025          | 23.4                | 1.6            | 0.1             | 0     | 59.3           | 15.6            | 0   | 0.59   | 77.5                     | 26.1            | 1.2              | 1549        | 2702                 | 0.143          | 9.8            | 17.8           |

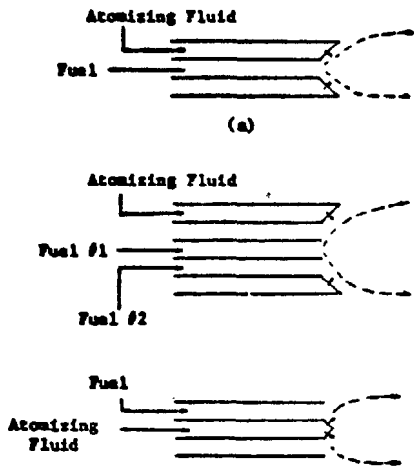


Figure 1  
External Atomized Tips

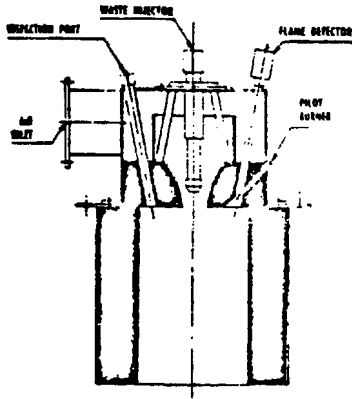


Figure 2  
Trane Thermal Vortex Burner

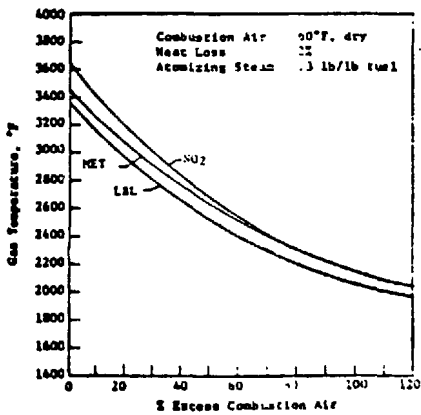


Figure 3  
Combustion Temperature of Liquids

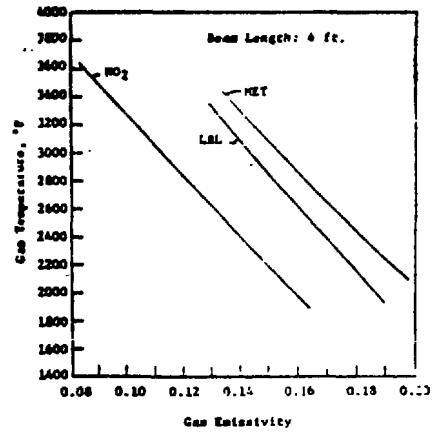


Figure 4  
Sensitivity of Liquid Combustion

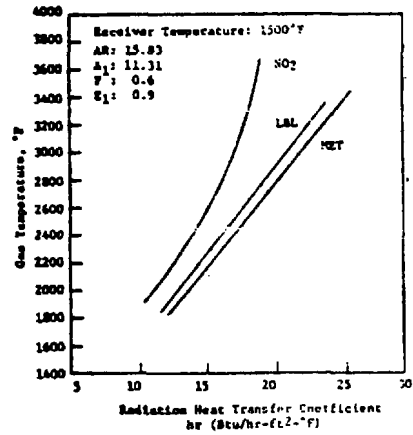


Figure 5  
Radiation Heat Transfer Coefficient  
of Liquid Combustion

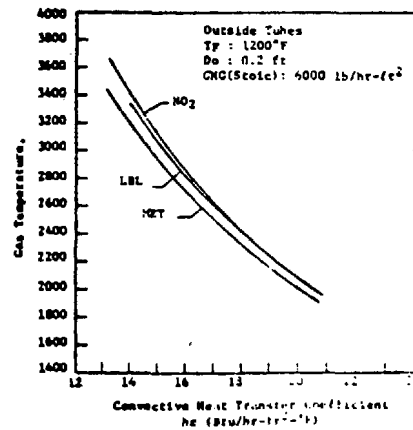


Figure 6  
Convective Heat Transfer Coefficients  
of Liquid Combustion

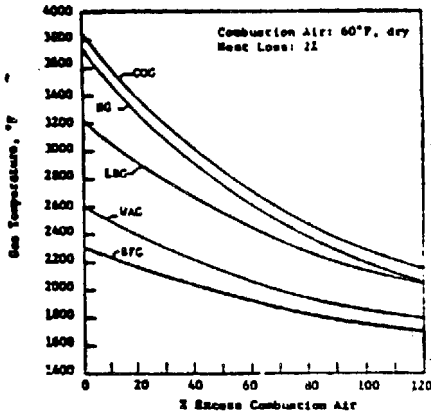


Figure 7  
Combustion Temperature of Gases

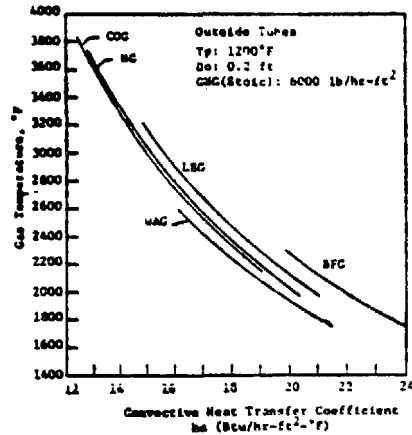


Figure 10  
Convective heat transfer coefficient of gas combustion

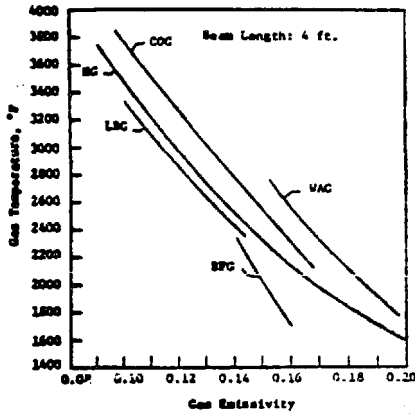


Figure 8  
Emisivity of Gas Combustion

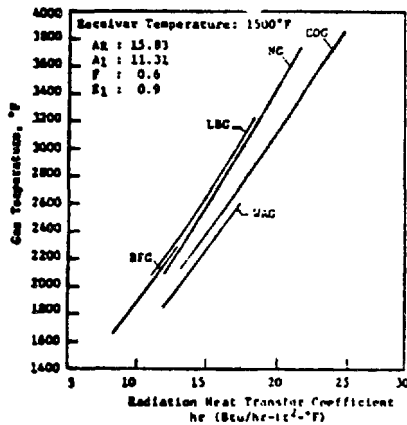


Figure 9  
Radiation heat transfer coefficient of gas combustion

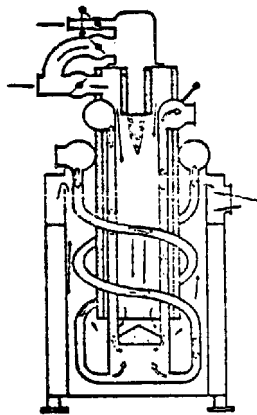
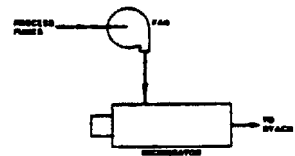
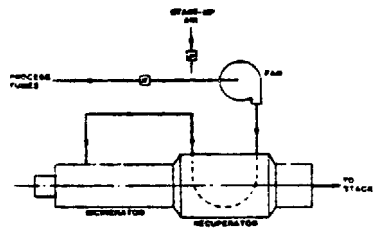


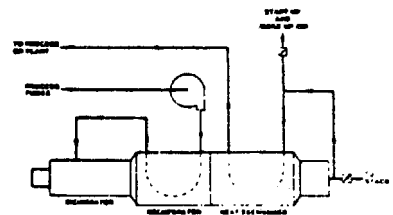
Figure 11  
Direct fired heater



1. Direct fume incineration without heat recovery. Alternately, incinerator exhaust may be fired into boiler to produce steam or hot water.



2. Basic heat recovery scheme with hot exhaust gases from incinerator used to preheat the incoming process fumes. Temperatures up to 1200 F are achieved.



3. Hot exhaust from incinerator passes through recuperator to preheat process waste fumes and then through second heat exchanger to recover additional heat which may be returned to process or other plant uses.

Figure 12  
Schematics of fume system

# SURFACE-SKIN TEMPERATURE GRADIENTS IN COOLING LAKES

S. S. Lee, S. Sengupta, C. R. Lee  
University of Miami  
Coral Gables, Florida 33124

The thermal structure at the air-water interface indicates the direction of heat transfer. Detailed understanding of the temperature profile at the interface is imperative for formulating boundary conditions and determining the relationship of radiometric measurements of surface skin temperature and the bulk temperature in the mixed region immediately below. When heat flow is from water to air the skin temperature is cooler than the bulk temperature. Roll (1965) provides a summary of measurements of skin temperature anomalies.

## THEORETICAL BACKGROUND

The surface heat flux  $Q$  is a sum of sensible heat flux from water to air, flux of latent heat due to evaporation and net flux of long-wave radiation from water to air. Fig.1 taken from Hasse (1971) shows the individual heat transfer components.

In general environmental flows are turbulent. However, a thin layer just below the air-water interface may be assumed to be laminar. This implies that the transport processes in this layer are molecular. Saunders (1967) through dimensional arguments derived that

$$\delta \sim \nu / \left( \frac{\tau'}{\rho_w} \right)^{1/2} \quad (1)$$

Where  $\delta$  is the thickness of the molecular layer,  $\tau'$  is the viscous stress.  $\nu$  is the kinematic viscosity of water and  $\rho_w$  is the density. Saunderson's, also assumed that the major part of the difference between the surface temperature and bulk temperature occurred in the molecular layer, such that

$$Q \sim \frac{K \Delta T}{\delta} \quad (2)$$

Where  $K$  is the thermal conductivity. A combination of (1) and (2) yields

$$\Delta T = \frac{\lambda Q \nu}{K (\tau / \rho_w)^{1/2}} \quad (3)$$

Where  $\tau$  is the surface wind stress and  $\lambda$  is a numerical coefficient.

Hasse (1971) developed a similar relationship from data analysis and theoretical considerations. For negligible solar radiation be derived

$$\Delta T = C_1 \frac{Q(ly/min)}{U_{10}(m/sec)} \quad (4)$$

Where  $C_1$  is a parameter varying slowly with  $\delta$  and  $U_{10}$  is wind speed 10 meters above the surface.

If the wind stress is represented as  $\rho C_D U_{10}^2$ , where  $C_D$  is the drag coefficient.

$$\Delta T = \frac{\lambda v \rho_w^{3/2}}{K \rho^{1/2} C_D^{1/2}} \frac{Q}{U_{10}} \quad (5)$$

Using coefficients provided by Hasse we find that  $\lambda=8$ . Thus the relationships of Hasse and Saunders are quite similar. Paulson and Parker (1972) discusses these two relations.

It has been conjectured that  $\lambda$  is independent of  $Q$  and  $U$ . The implication of such an independence is profound since it would allow computation of  $Q$  using only wind speed and  $\Delta T$ . Further, usefulness of this method would be to compute water loss through evaporation. Solar radiative fluxes are measured directly. The purpose of this paper is to utilize field measurements taken in Lake Belews North Carolina to investigate the constancy of  $\lambda$ . This will bridge the gap between data available for laboratory scale experiments and ocean data.

## PREVIOUS STUDIES

Several investigations have been made in the past few years using field and laboratory data. Table I shows a summary of some of these studies. Hasse used oceanographic field data for his investigations. From his data the values of  $\lambda$  calculated is about 8. Wind speed varied from 1.45 m/sec to 11.35 m/sec. Saunders also used oceanographic data and found  $\lambda$  to lie between 5-10. Laboratory experiments by McAllister and Mcleish (1969) indicate a value of  $\lambda=4.5$  which is considerably smaller than the values obtained by field measurements. (The values of  $L$  in the chart indicate the characteristic horizontal length of experimental basin). Paulson and Parker (1972) conducted laboratory experiments on a relatively small basin with no wave generation. They varied wind speed from 1.39 m/sec to 3.64 cm/sec. They calculated  $\lambda=15 \pm 1$ . This is significantly larger than those obtained from field observations. Hill (1972) conducted a series of experiments in laboratory scale with and without surface waves. He obtained for the no wave case a value of  $\lambda$  equal to 4 with wave he obtained  $\lambda$  equal to 11. Paulson et al suggests that the variation in  $\lambda$

is primarily caused by the wave state, the effect of surface waves on  $\lambda$  being more pronounced in the laboratory than in field conditions. This conjecture was emphasized by noting that capillary waves are more dominant in laboratory water-tables than in the field. Witting (1972) has conducted an analytical investigation of wave effects on surface temperatures. He concluded that waves particularly steep capillary waves decrease  $\Delta T$  and thereby  $\lambda$ . Waves also reduce the shear stress  $\tau$  thereby increasing  $\lambda$ . However, the first effect dominates especially in laboratory experiments since capillary waves are more prevalent in the laboratory tanks than in the open ocean conditions. Saunders (1973) provides a review of the existing literature on this topic.

## FIELD MEASUREMENTS

The field observations were made at Lake Belews North Carolina during May 18 and 19, 1976. This is a cooling lake for a thermal power plant of the Duke Power Co. It has two basins connected by a connecting canal. The smaller basin is well mixed and receives the heated effluent. The larger basin is seasonally stratified and the intake to the plant is located there. The measurements of skin temperature gradients were made in the smaller pond. A Barnes model PRT-5 radiometer was used to measure surface temperature. A thermistor attached to a float measured temperatures approximately 3 centimeters below the surface. Since the thickness of the surface skin layer is of the order of 1 mm, the thermistor reading is the bulk temperature. These readings were made from a boat. Wind speed, solar insolation, humidity and air-temperature were recorded at a meteorological tower in the larger lake. Fig.2 shows the configuration of Lake Belews. Details of the field experiment are provided by Lee et al (1976).

## CALCULATION PROCEDURE AND RESULTS

The objective of the present investigation is to calculate  $Q$  using existing formulae and measured meteorological parameters and obtain values for  $\lambda$  and  $C_1$ . The motivation for this is to establish what effect length scale of the domain has on these constants. Since studies on oceanographic scales and laboratory scales have been made, this study on an intermediate length scale domain is important. This study is also directed to determine what degree of variation of  $\lambda$  and  $C_1$  is observed for a single basin.

### General Description of Heat Flux Across the Air-Water Interface

The net heat transfer through a water surface is composed of radiation penetrating the water surface from above, radiation out of the water surface, evaporation, and conduction transfer.

These are indicated schematically in the Fig.3.

$$Q_{net} = (Q_s - Q_{sr} + Q_a - Q_{ar}) - (Q_{br} \pm Q_e \pm Q_c)$$

$$= Q_{sn} + Q_{an} - (Q_{br} \pm Q_e \pm Q_c)$$

Where  $Q_{sn}$  = net absorbed solar radiation

$Q_{an}$  = net absorbed atmospheric radiation

Each of these terms is discussed below.

### 1. Short-Wave Solar Radiation

The total incident solar radiation impinging on the water surface  $Q_{si}$  was recorded by pyrheliometer at the weather island at Lake Belews, operated by Duke Power Company. Dake and Harleman (1969) estimate that about 40% of the solar radiation arriving at the air-water interface is absorbed in a thin layer of water at the surface, and the reflected solar radiation is typically 6% of incident solar radiation. Hence the net solar radiation absorbed by the water surface is

$$Q_{sn} = Q_s - Q_{sr} \approx 0.94 \times 0.4 \times Q_{si} \left\{ \frac{\text{cal}}{\text{cm}^2 \text{sec}} \right\}$$

### 2. Long-Wave Atmospheric Radiation

Clear sky incident atmospheric radiation,  $Q_{ac}$ , may be expressed as,

$$Q_{ac} = 1.2 \times 10^{-13} (T_a^*)^6 \quad \{B/\text{ft}^2 \text{ day}\}$$

Where  $T_a^*$  = absolute air temperature ( $^{\circ}\text{R}$ )

The presence of clouds tends to increase the average radiation received at the ground from atmosphere. Harleman et al (1975) recommend an equation of the form

$$Q_a = Q_{ac}(1 + 0.17C^2)$$

Where  $Q_a$  = heat flux at the surface. (B/ft<sup>2</sup>day)

$C$  = fraction of the sky covered by clouds.

A figure of 3% is usually accepted as reflectance of a water surface to long-wave radiation. Thus the net atmospheric radiation absorbed by the surface is

$$Q_{an} = Q_a - Q_{ar} = 0.97 Q_a$$

and, therefore, we have

$$Q_{an} = 1.16 \times 10^{-13} (T_a^*)^6 (1 + 0.17C^2) \left\{ \frac{B}{ft^2 day} \right\}$$

or

$$Q_{an} = 1.16 \times 3.14 \times 10^{-19} (T_a^*)^6 (1 + 0.17C^2) \left\{ \frac{cal}{cm^2 sec} \right\}$$

### 3. Long-Wave Back Radiation

Harleman et al (1975) note that the emmissivity of a water surface is independent of temperature and salt or colloidal concentrations, and gives a value of 0.97. Thus we obtain

$$Q_{br} = 0.97\sigma (T_{s1}^*)^4 \left\{ \frac{cal}{cm^2 sec} \right\}$$

Where  $T_{s1}$  = water surface temperature ( $^{\circ}K$ )

$$\sigma = 1.354 \times 10^{-12} (cal/cm^2 sec \text{ } ^{\circ}K^4)$$

### 4. Evaporation Heat Loss

Following the recommendation of Harleman et al (1975) the "Lake Hefner" formula is used in this study to estimate heat loss due to evaporation. The formula is

$$Q_e = f(w)(e_s - e_z) \left\{ \frac{cal}{cm^2 sec} \right\}$$

Where  $f(w)$  = wind speed function

$e_s$  = saturated vapor pressure of air at  $T_{s1}$  (mbar)

$e_z$  = vapor pressure at height 2 m above the surface (mbar)

$w$  = wind speed ( $cm/sec$ )

The wind speed function can be written as

$$f(w) = 0.9 \times 10^{-6} W \left\{ \frac{cal}{cm^2 sec} \left( \frac{cm}{sec} \right) mbar \right\}$$

To facilitate calculations, the saturated vapor pressure of air is computed as

$$e_s = 0.0435 T_{s1}^2 - 0.0917 T_{s1} + 7.80$$

Where  $T_{s1}$  = water surface temperature ( $^{\circ}C$ )

and the unsaturated vapor pressure is

$$e_z = \phi e_s'$$

Where  $\phi$  = relative humidity

$e_{s'}$  = saturated vapor pressure of air at the temperature existing 2 m above the surface.

## 5. Conduction Heat Loss

Bowen's ratio is used to estimate the heat flux across the air-water interface by conduction. The equation is

$$Q_c = 0.639 \left( \frac{T_{s1} - T_a}{e_s - e_z} \right) Q_e \quad \{\text{cal/cm}^2 \text{ sec}\}$$

Where  $T_a$  = air temperature at a height of 2 m ( $^{\circ}\text{C}$ )

## Heat Transfer Calculations

The data measured in Lake Belews, North Carolina for this study are presented in Table II.

According to the formuluses described in previous sections, each of the heat flux components calculated are shown in Table III.

Where  $Q_{\text{net}}$  is negative, which means the heat flux is directed upward away from the water surface. This is expected for the smaller mixing lake since it receives the heated effluent from the power plant.

## The Values of $\lambda$ and $C_1$

The temperature difference  $\Delta T$  between the surface and a lower well mixed region of nearly constant temperature is

$$\Delta T = \frac{\lambda \nu \rho_w^{1/2} Q_{\text{net}}}{K \rho^{1/2} C_D^{1/2} W} \quad \text{according to Saunders (1967)}$$

$$\text{or } \lambda = \frac{K C_D^{1/2} \rho^{1/2}}{\nu \rho_w^{1/2}} \frac{W \Delta T}{Q_{\text{net}}}$$

Where  $\lambda$  = dimensionless constant

$K$  = thermal conductivity of water

$\nu$  = kinematic viscosity of water

$\rho$  = density of air

$\rho_w$  = density of water

$$\Delta T = T_{s1} - T_{s2}$$

with  $C_D = 1.21 \times 10^{-3}$ , we have

$$\lambda = 1.73 \times 10^{-4} \frac{W \cdot \Delta T}{Q_{\text{net}}}$$

Hasse (1971) examined  $\Delta T$  as a function of mean wind speed at a height of 10 meters, and  $Q_{\text{net}}$ , he finds

$$\Delta T = C_1 \frac{Q_{\text{net}} (\text{ly/min})}{W (\text{m/sec})}$$

$$\text{or } C_1 = \frac{1}{6000} \frac{W (\text{cm/sec}) \times \Delta T (^\circ\text{C})}{Q_{\text{net}} (\text{cal/cm}^2\text{sec})} = \frac{1}{1.038} \lambda$$

Using  $Q_{\text{net}}$  obtained from above calculations,  $C_1$  and  $\lambda$  are calculated. They are shown in Table IV.

#### DISCUSSION AND CONCLUSIONS

From Table IV it is seen that the value of  $\lambda$  lies between 10.4 and 5.6. The value 10.4 is significantly larger than its nearest value 8.4 and may be an isolated data point involving error in observation. Without neglecting this point the average value for  $\lambda$  is 7.1. This value lies between the range calculated from Saunders data ie 5-10. The value of  $\lambda$  calculated in this study is in agreement with Hasse's value of 8. It is considerably smaller than the Paulson and Parker's calculated value of near constant 15. The value of 7.1 is also quite different from Hill's with wave result of  $\lambda=4$ . The value of  $C_1$  shown in Table IV is between 5.4 and 10.4. This compares with Hasse's value of 9.4.

The following conclusion can be made from the calculated values for  $\lambda$ .

- a). From the calculations of Saunders, Hasse and the present study a value of  $\lambda$  between 7 and 8 is a reasonable estimate for field situations.
- b). There is no apparent relationship between  $\lambda$  and length scale in field conditions, since oceanographic and lake data yielded approximately the same range for  $\lambda$ .
- c). Calculations using laboratory measurements yield much larger values of  $\lambda$  for no wave condition eg. 15. The effect of waves reduce this value to 4-4.5.

- d). The effect of waves is to reduce the value of  $\lambda$  with maximum effect on laboratory scale conditions owing to predominance of capillary waves.

The direction of investigation presented provides encouraging results since a near constant value of  $\lambda$  implies the net heat flux may be estimated by measuring  $\Delta T$  and wind speed only. Thus the empirical relations for obtaining  $Q$  may be avoided. It is imperative however to conduct parametric studies both in laboratory and field length scales to understand further the variations in  $\lambda$  that have been observed to date.

#### ACKNOWLEDGEMENTS

This work was conducted under funding from National Aeronautic and Space Administration, Kennedy Space Center.

## REFERENCES

1. Dake, J.M.K., and Harleman, D.R.F., "Thermal Stratification in Lakes: Analytical and Laboratory Studies," *Water Resour. Res.*, 5(2), 484-495, 1969.
2. Harleman, D.R.F., and Stolzenback, K.D., "Engineering and Environmental Aspects of Heat Disposal from Power Generation," Dept. of Civil Engineering, M.I.T., Jun., 1975.
3. Hasse, L., "The Sea Surface Temperature Deviation and the Heat Flow at the Sea-Air Interface," *Boundary-Layer Meteorol.*, 1, 368-379, 1971.
4. Hill, R.H., "Laboratory Measurement of Heat Transfer and Thermal Structure Near an Air-Water Interface," *J. Physical Oceanography*, Vol.2, pp.190, 1972.
5. Lee, S.S., Sengupta, S., and Mathavan, S.K., "Three Dimensional Numerical Model for Lake Belews," Final Report NASA Contract NAS 10-9005, June, 1977.
6. McAlister, E.D., and McLeish, W., "Heat Transfer in the Top Millimeter of the Ocean," *J. Geophys. Res.*, 74, 3408-3414, 1969.
7. Paulson, C.A., and Parker, T.W., "Cooling of a Water Surface by Evaporation, Radiation, and Heat Transfer," *J. Geophys. Res.*, Vol.77, No.3, pp.491, Jan. 1972.
8. Roll, H.U., "Physics of the Marine Atmosphere," pp.227-247, Academic, New York, 1965.
9. Saunders, P.M., "The Temperature at the Ocean-Air Interface," *J. Atmos. Sci.*, 24, 269-273, 1967.
10. Saunders, P.M., "The Skin Temperature of the Ocean," Contribution No.3148 from the Woods Hole Oceanographic Institution, 1973.
11. Witting, J., "Temperature Fluctuations at an Air-Water Interface Caused by Surface Waves," *J. Geophys. Res.*, Vol.77, No.18, pp.3265, June 1972.

TABLE I

CHART SHOWING  $\lambda$  FOR DIFFERENT INVESTIGATORS

|                      | $\lambda$ | CONDITION  | LENGTH SCALE                       |
|----------------------|-----------|--|------------------------------------|
| HASSE                | 8         | Wind speed 1.45-11.35 m/sec, $v$ is used at temperature = 15 °C<br>neglect solar radiation | Field measurement                  |
| SAUNDERS             | 5-10      | Wind speed > 2 m/sec,<br>neglect the divergence<br>of solar radiation                      | Field measurement                  |
|                      | 7         | In middle latitude<br>winter $\Delta T$ reaches to<br>1 °C.                                |                                    |
| PAULSON<br>PARKER    | 15        | Neglect wave generation,<br>$v$ is used at temperature = 25 °C                             | Laboratory measurement<br>L=13 cm  |
| HILL                 | 4         | With wave  | Laboratory measurement<br>L=90 cm  |
|                      | 11        | Without wave   |                                    |
| MCALISTER<br>MCLEISH | 4.5       | Wind speed 4.5 m/sec<br>With wave  | Laboratory measurement<br>L=220 cm |

TABLE II  
LAKE BELEWS DATA

| No. | Station | Date    | Time  | T <sub>a</sub><br>(°C) | T <sub>a</sub><br>(°F) | T <sub>s1</sub><br>(°C) | T <sub>s2</sub><br>(°C) | ΔT<br>=T <sub>s1</sub> -T <sub>s2</sub> | W<br>( $\frac{\text{cm}}{\text{sec}}$ ) | φ<br>(%) | C   | Q <sub>sl</sub><br>(cal/cm <sup>2</sup> sec) |
|-----|---------|---------|-------|------------------------|------------------------|-------------------------|-------------------------|---|---|----------|-----|--|
| 1   | A       | 5/18/76 | 8:45  | 20.6                   | 69                     | 28.9                    | 29.8                    | -0.9                                    | 232.4                                   | 67       | 0.7 | 7.7x10 <sup>-3</sup>                         |
| 2   | A       | "       | 8:52  | 20.6                   | 69                     | 29.0                    | 29.8                    | -0.8                                    | 223.5                                   | 67       | 0.7 | 8.0  |
| 3   | A       | "       | 9:19  | 21.1                   | 70                     | 29.0                    | 29.8                    | -0.8                                    | 245.9                                   | 67       | 0.6 | 9.0  |
| 4   | H       | "       | 10:00 | 21.1                   | 70                     | 29.0                    | 30.2                    | -1.2                                    | 290.6                                   | 61       | 0.4 | 13.0   |
| 5   | G       | "       | 10:40 | 21.7                   | 71                     | 29.2                    | 30.2                    | -1.0                                    | 335.3                                   | 61       | 0.6 | 12.7   |
| 6   | B       | "       | 11:10 | 21.7                   | 71                     | 28.9                    | 29.8                    | -0.9                                    | 393.4                                   | 60       | 0.6 | 11.0   |
| 7   | C       | "       | 11:35 | 21.7                   | 71                     | 28.8                    | 29.7                    | -0.9                                    | 420.2                                   | 60       | 0.7 | 8.3  |
| 8   | D       | "       | 12:30 | 22.2                   | 72                     | 29.0                    | 29.8                    | -0.8                                    | 447.0                                   | 59       | 0.9 | 8.0  |
| 9   | A       | 5/19/76 | 13:50 | 19.0                   | 66                     | 27.2                    | 28.0                    | -0.8                                    | 662.0                                   | 62       | 0.3 | 16.8   |
| 10  | F       | "       | 14:00 | 19.1                   | 66                     | 26.1                    | 26.8                    | -0.7                                    | 635.7                                   | 61       | 0.3 | 16.8   |
| 11  | F       | "       | 15:05 | 20.0                   | 68                     | 27.0                    | 27.9                    | -0.9                                    | 657.0                                   | 61       | 0.3 | 15.8   |

TABLE III  
HEAT FLUX COMPONENTS

| No. | $Q_{sn} \times 10^3$ | $Q_{an} \times 10^3$ | $Q_{br} \times 10^3$ | $Q_e \times 10^3$ | $Q_c \times 10^3$ | $Q_{net} \times 10^3$ ( $\frac{\text{cal}}{\text{cm}^2 \text{sec}}$ ) |
|-----|----------------------|----------------------|----------------------|-------------------|-------------------|---|
| 1   | 2.9                  | 8.6                  | 10.9                 | 5.3               | 1.1               | -5.8  |
| 2   | 3.0                  | 8.6                  | 10.9                 | 5.1               | 1.1               | -5.5  |
| 3   | 3.4                  | 8.6                  | 10.9                 | 5.7               | 1.1               | -5.7  |
| 4   | 4.9                  | 8.4                  | 10.9                 | 6.9               | 1.3               | -5.8  |
| 5   | 4.8                  | 8.6                  | 11.0                 | 7.9               | 1.4               | -6.9  |
| 6   | 4.1                  | 8.6                  | 10.9                 | 9.1               | 1.6               | -8.9  |
| 7   | 3.1                  | 8.8                  | 10.9                 | 9.6               | 1.7               | -10.3   |
| 8   | 3.0                  | 9.4                  | 10.9                 | 10.3              | 1.7               | -10.5   |
| 9   | 6.3                  | 8.1                  | 10.6                 | 14.3              | 3.1               | -13.6   |
| 10  | 6.3                  | 8.1                  | 10.5                 | 12.4              | 2.6               | -11.1   |
| 11  | 6.0                  | 8.3                  | 10.6                 | 13.5              | 2.7               | -12.5   |

TABLE IV  
VALUES OF  $C_1$  AND  $\lambda$  CALCULATED FOR LAKE BELEWS

| No. | $Q_{\text{net}} \times 10^3 \left( \frac{\text{cal}}{\text{cm}^2 \text{sec}} \right)$ | $W \left( \frac{\text{cm}}{\text{sec}} \right)$ | $\Delta T$ | $\lambda$ | $C_1$ |
|-----|---|---|------------|-----------|-------|
| 1   | -5.8  | 232.4   | -0.9       | 6.2       | 6.0   |
| 2   | -5.5  | 223.5   | -0.8       | 5.6       | 5.4   |
| 3   | -5.7  | 245.9   | -0.8       | 6.0       | 5.8   |
| 4   | -5.8  | 290.6   | -1.2       | 10.4      | 10.0  |
| 5   | -6.9  | 335.3   | -1.0       | 8.4       | 8.1   |
| 6   | -8.9  | 393.4   | -0.9       | 6.9       | 6.6   |
| 7   | -10.3   | 420.2   | -0.9       | 6.4       | 6.2   |
| 8   | -10.5   | 447.0   | -0.8       | 5.9       | 5.7   |
| 9   | -13.6   | 662.0   | -0.8       | 6.7       | 6.5   |
| 10  | -11.1   | 635.7   | -0.7       | 6.9       | 6.6   |
| 11  | -12.5   | 657.0   | -0.9       | 8.2       | 7.9   |

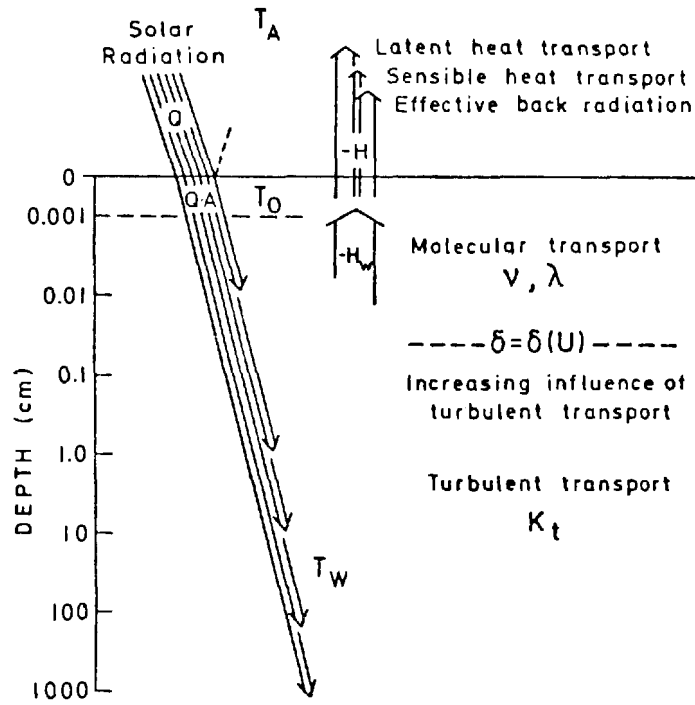


Fig.1 Schematic Diagram of Heat Flow at the Sea-Air Interface.

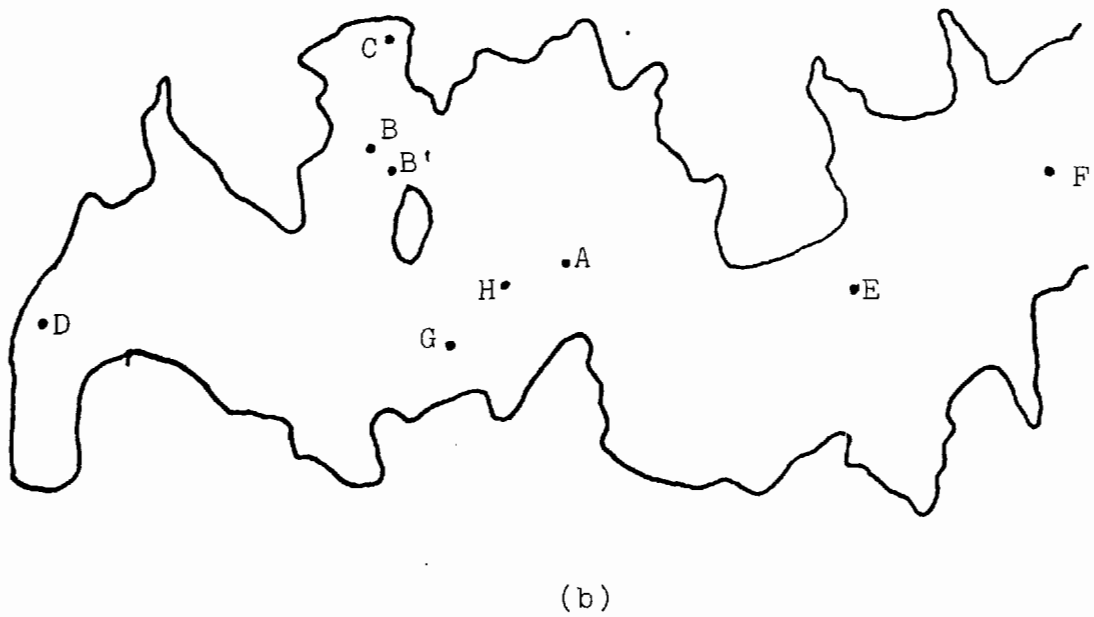
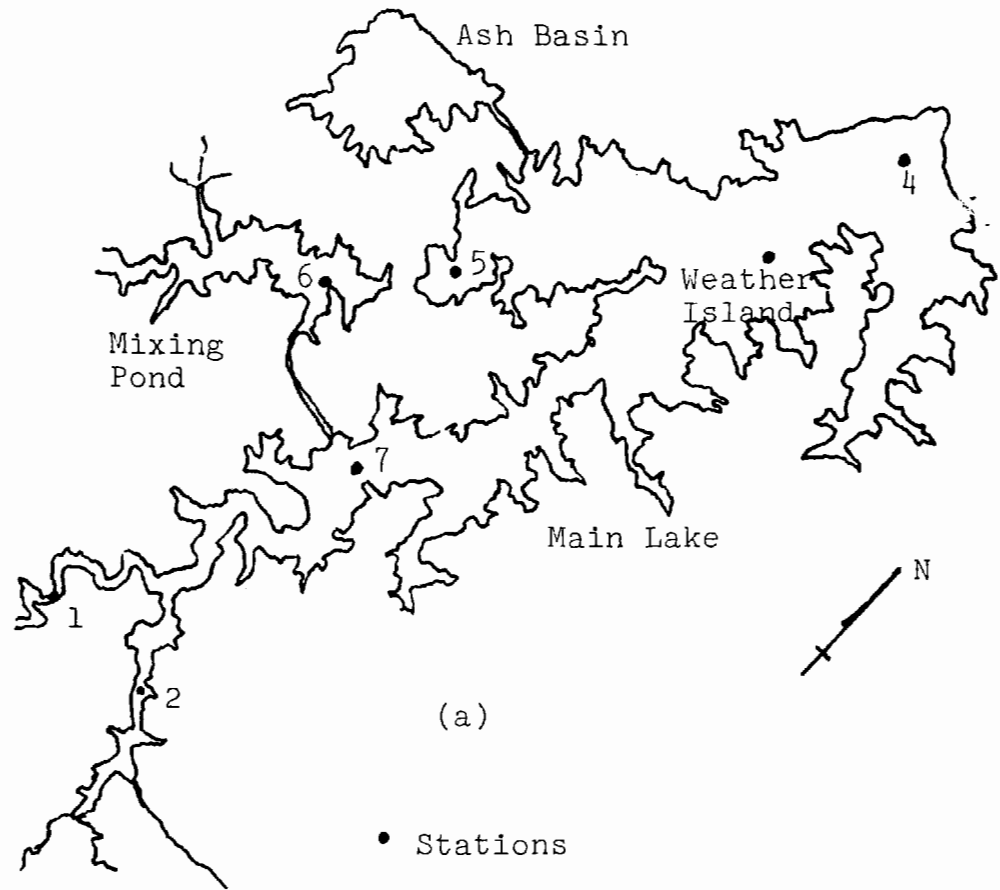


Fig.2 Map of Lake Belews Showing (a) Location of Meteorological Towers (b) Mixing Pond Station Locations on May 18, 19 of 1976.

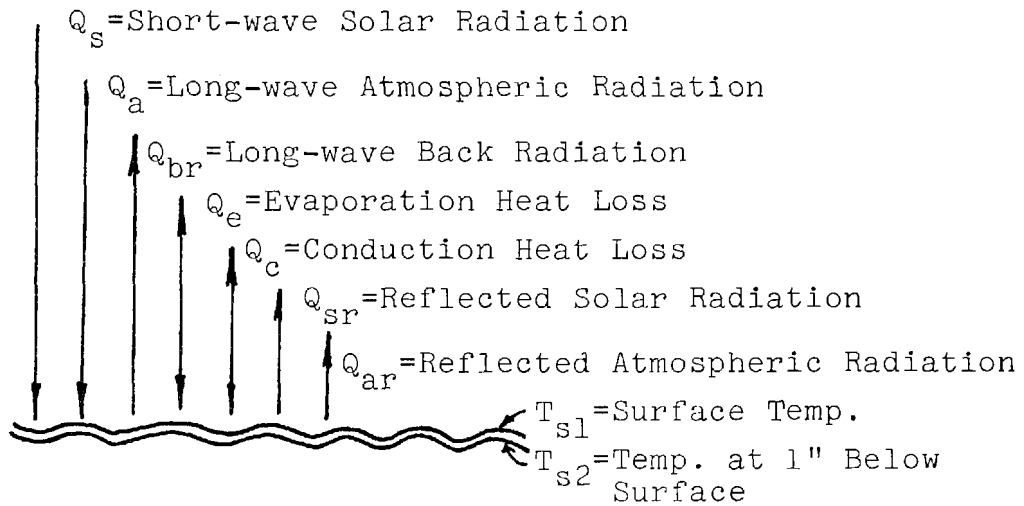


Fig.3 Net Rate at Which Heat Crosses Water Surface

# FOUR THERMAL PLUME MONITORING TECHNIQUES: A COMPARATIVE ASSESSMENT\*

ROBERT S. GROVE, RONALD W. PITMAN, AND JACK E. ROBERTSON<sup>1</sup>

## ABSTRACT

Four different methods of monitoring thermal plumes were compared: two from a vessel and two from an airplane. The study area was the Pacific Ocean offshore of the 450 MW San Onofre Nuclear Generating Station in southern California. The ocean provides the once-through cooling water which is discharged through a submerged, single port, twelve foot diameter conduit. Water temperature data were taken along with other oceanographic and meteorological data on four separate days, and three of the four different plume monitoring techniques were conducted simultaneously.

The plume monitoring methods consisted of: 1) an in-hull solid state thermistor recording surface temperature while the survey vessel traversed the area of the thermal plume for approximately one hour with vessel position recorded continuously using an electronic range positioning system, 2) an airplane traversing the thermal field for approximately one hour at an altitude of 1000 feet using a narrow beam infrared radiometer calibrated by ground truth temperature measurements, 3) an airplane traversing the thermal field for approximately 15 minutes at an altitude of 1000 feet using an infrared thermal scanner that photographically recorded the configuration of the thermal plume, and 4) vertical temperature profiles taken from a vessel at pre-determined positions in the area of the thermal plume over a three to four hour period.

Assessment of the study methods revealed that each had certain advantages depending on what plume characteristics were being determined. Comparison of plume configuration indicates good general agreement among methods. The infrared scanner provided the best picture of the surface plume but the least degree of absolute isotherm definition, while the vertical temperature profiling method provided accurate absolute temperatures but produced comparatively distorted plume configurations due to the duration required for monitoring.

\*This paper was not presented.

---

<sup>1</sup> Respectively: Research Engineer, Southern California Edison Company, Rosemead, California; Project Oceanographer, Brown and Caldwell, Pasadena, California; and Project Manager, Brown and Caldwell, Pasadena, California.

# EXPERIMENTAL RESULTS OF DESTRATIFICATION BY BUOYANT PLUMES

D. S. Graham  
Dept. of Civil Engineering  
University of Florida  
Gainesville, Florida U.S.A.

## ABSTRACT

The effects of ambient stratification upon buoyant plumes have been studied in detail, but the converse case has received little attention. A literature review of destratification experiments in the laboratory and field tends to show a rapid decrease in mixing efficiency of plumes associated with an apparent change from overall mixing to interfacial formation and descent (ascent). A rigorous dimensionless scheme for interpretation of the results of such experiments is given, and an analogy to the Fourier equation for one of the mixing regimes is outlined. Finally, sample results of experiments are presented which show that two distinctive mixing regimes termed "diffusive" and "interfacial" can be identified. The former is associated with high Richardson numbers and the latter with low. The latter is especially pronounced near the orifice. The point of change from one to the other can be predicted from dimensionless criteria for the particular experimental geometry used.

## INTRODUCTION

Ejection of waste heat to the environment by means of outfall diffusers (line or source) into lakes, reservoirs and coastal seas can be expected to continue to increase. While use of evaporative cooling towers is currently being encouraged by the EPA, once-thru cooling systems usually have substantially lower cost and cause minimal disturbances to the atmosphere in warm humid locations like Florida. Usual diffuser locations are either near the water surface for rapid radiation of heat to the atmosphere, or at depth for efficient mixing of the plume with the ambient water.

Many bodies of water into which the outfalls discharge are density-stratified by temperature, salinity, or both. Stratification may be temporally intermittent (eg., diurnally, seasonally, or over a portion of a tidal cycle) or persistent. Two types of stratification commonly occur—linear and interfacial. The former is characterized by an approximately linear density gradient and has received more intensive study because several closed-form solutions are possible (see (1) and (24), for a partial review). The latter type of stratification has a readily identifiable interface between almost homogeneous masses of water of different density. The interface location and sharpness are functions of both environmental conditions and mixing induced by the usually

less dense thermal plume. While plume rise and entrainment properties have been well studied, interaction of a buoyant plume with ambient interfacial-type stratification has not received the same thorough experimental investigation.

The orientation of this study should not be confused with the many excellent studies of the effects of ambient stratification upon plume or jet behavior (see, for instance (1), (2), and (24)). For small receiving bodies, and locally, the plume and ambient stratification are linked to one another and it is the effect of the plume upon the ambient stratification that is investigated here.

#### PREVIOUS STUDIES

Studies by Rouse and Dodu (3), Turner (4), and others, which were reviewed by Turner (5) and Long (6), showed destratification due to interfacial entrainment without shear to be proportional to a Richardson number based on overall length scales and a Péclet number based on molecular diffusivity despite the fact that Reynolds numbers were high away from the interface. The entrainment velocity could be expressed as a power of the Richardson number (about -1.5 to -1) which was dependent upon the Péclet number for destratification without shear (i.e., all destratification accrued from the energy flux divergence term of the turbulent kinetic energy equation) and a constant (-1) for shear-induced entrainment. Kantha (14) notes that the range of Péclet influence appears to be dependent upon the Reynolds number. Subsequent experimentation has been ongoing to better define these processes, but the relevant dimensionless parameters have been identified. Prior to these experiments most mixing studies by chemical engineers had tried (incorrectly) to relate mixing time to a Reynolds criterion (see Uhl and Gray (7)).

For the case of a jet or plume aimed at an interface, the literature may be divided into several categories - 1) small scale laboratory investigations, 2) chemical engineering studies using intermediate-sized containers, and 3) large scale destratification experiments in lakes and reservoirs. The orientation and utility of each of these groups differs greatly. The chemical engineer or reservoir manager often wants to know time until complete mixing, while the fluid mechanics scientist is more interested in defining entrainment velocities.

Baines (8) describes experiments in which a dense salt plume is allowed to fall to an interface, but not penetrate it. He found

$$\text{Entrainment flux} = \text{const.} * (\text{Jet Richardson No.})^{-3/2} \quad (1)$$

Sullivan (9) described similar experiments with the exception that 1) finite quantities of liquid were used, and 2) some cases were forced plumes. These are reviewed by Brooks (1). Linden (10) shot vortices of freshwater at a salt-fresh interface and found the depth of maximum penetration to be inversely proportional to a Froude-type number while

the entrainment rate was proportional to the cube of a Froude number [or to the -1.5 power of a Richardson number, again].

A series of experiments by Brush, et al., (11), Brush (12) and Neilson (13) attempted to relate mixing of different scales thru a dimensionless format. In the more sophisticated 1970 experiment Brush (12) varied both density difference and jet discharge. His results have some computational (and likely typographical) errors as reported, but after recalculation they are presented as Figure 1. It can be seen that dimensionless entrainment velocity is a function of Richardson, Péclet, and perhaps Reynolds, effects. At lower Richardson (higher Reynolds and Péclet) numbers, the molecular effects disappear and the data follow a -1 slope as energy considerations alone would imply. This is consistent with many other results (Kantha (14)). These results are based upon jetting one layer into the other, and measuring the difference in density to compute the entrainment coefficient.

Neilson (13) repeated Brush's (1970) experiments with an air plume. He found the air plume destratified the system, that a Péclet influence was again evident, and that the interface approached the nozzle almost asymptotically with time making computation of the entrainment velocity by density measurements very difficult. Again, the shape of the density profile during destratification was not measured.

An interesting result of this set of experiments, which was not discussed in detail by the authors, was the apparent nonlinearity of the destratification process. As shown in Figure 2, two apparent mixing regimes were found by Neilson. In one the mixing time decreased rapidly with increasing Richardson number (air flow rate), while it decreased only very slowly for the second. Similarly Brush, et al., (11) state (p.49): "The mixing time [for liquid jets or plumes] decreases with increasing distance from the interface and for a reason not apparent, the mixing time is less when the outlet is placed in the lighter fluid."<sup>1</sup> In the 1970 experiments (12) with air plumes, Brush found a dimensionless mixing time

$$t_m^* = \frac{(t_m V_{jair}^*)}{\text{Depth}}$$

decreased much more rapidly with increasing  $V_{jair}$  (and hence inverse Richardson number) when depth (and hence volume) and distance to the interface from the nozzle were greater. As the latter two parameters were kept as a constant ratio with only  $V_{jair}$  varying, differing effects of each were not isolated.

---

<sup>1</sup> sic, the comma may be misplaced here.

\* $V_{jair}$  = velocity of the air jet based on orifice discharge divided by area.

In none of the experiments reviewed thus far has the change in the density-depth function been related to the mixing process. The mixing process was described either by measurement of density in one, or both, layers, or as a time to complete mixing. Few observations have been made of the actual destratification process, but a comparison of those available sheds light on several properties including the apparent change of plume-mixing efficiency. Crapper and Linden (15) measured changes in density profiles for salt and heat from mechanical mixing (grids). In particular they found that 1) the interface thickness decreased with increasing agitation (i.e., lower Richardson number) and 2) the destratification process appears, at times, to be "diffusive" [that is, the interface does not descend distinctly as most mechanical mixing models implied, but the density-related scalar appears to propagate across a plane of constant density at the position of the initial interface in a manner analogous to an error function solution of the Fourier equation] at "high" Richardson numbers. An illustration of the mixing process from their article is provided as Figure 2. Because they assumed the turbulence to be homogeneous, Crapper and Linden's analysis is suspect however.

Finally, several lake or reservoir destratification experiments using air plumes have been reported in the literature. Many of these are of no utility at all since either incremental volume was not calculated or only the time to complete mixing irrespective of initial stratification was measured. A few papers report results of interest however. Knoppert, Rook and Oskam (16) destratified a lake of  $8.02 H_m^3$  volume and 30 m depth with an air plume. The progress of destratification is shown in Figure 4. Note that an initial linear density profile sharpened to an interface as the nozzle was approached. Furthermore the efficiency of mixing dropped quickly as the interface sharpened. After measuring data from their figure, the depth of the lower layer (hypolimnion) was found (Graham (17)) to be described well by the empirical equation

$$h_2 = 63 - 41.7 (\Sigma q_{air} * E^{-4})^{0.686} \quad (2)$$

where  $h_2$  - distance from nozzle to thermocline in feet

$$\Sigma q_{air} - \text{cumulative air discharge, in ft}^3/\text{s}^1$$

Graham (17) also calculated the mixing efficiency,  $E_m$ , defined as volume of water raised per unit volume of air released, from Knoppert, et al.'s data to increase with  $h_2$ :

$$E_m = 3.316 \exp(+0.204 h_2) \quad (3)$$

empirically, based on a best-fit criterion.

---

<sup>1</sup> U.S. customary units were used in the original paper.

From a now-classic set of experiments by Koberg and Ford (18) it is possible to use their data to show that the change lake stability (in Kg - mE6) decreased rapidly as compressor operation time increased. A good fit is provided by

$$\text{Stability} = 50.1 t_{op}^{-1.083} \quad (4)$$

where  $t_{op}$  is duration of compressor operation, in hours. These results correspond with these of Knoppert, et al.

A very recent paper by Moretti and McLaughlin (19) shows even more clearly some aspects of the destratification process previously described. Their figures 11 and 13 (\*) show a "diffusive" type of destratification with some evidence of interface sharpening in the prototype (an Oklahoma lake), and a very clear interfacial re-sharpening as the thermocline approached the jet (liquid, not air) in the model. A plot of stability index vs. time (or cumulative discharge) is almost identical to those of Neilson, Knoppert et al., and Koberg and Ford in form.

While there are many papers on the subject in the literature (20, 21 for instance), this brief review has been adequate to define the problem. It appears that plumes, jets, and forced plumes affect, as well as are affected by, the ambient stratification. While numerous investigators have studied plume behavior in stratified environments (particularly linear ones), and interfacial entrainment velocities under laboratory conditions, very little attention has been paid to the actual shape of the vertical density profile as a plume or jet acts upon it. It appears that two distinct "regimes" characterize the mixing process - a more efficient "diffusive" regime occurring far from the orifice and in "High Richardson No." cases and paradoxically, interfacial formation close to the orifice or with "high" degrees of agitation. A series of simple experiments was devised to test this hypothesis in a dimensionally rigorous format.

#### DIMENSIONAL ANALYSIS

From geometrical and physical reasoning it may be postulated that the following function defines the mixing process.

$$\Phi_1 [t_H, \rho_1, \rho_2, \rho_3, K_{12}, K_{13}, K_{23}, h_1, h_2, d_0, R_0, g, \mu_1, \mu_2, \mu_3, a_e, r, \phi, z] = 0 \quad (5)$$

where  $t_H$  - time until the fluid is H% mixed locally  
 $\rho_1$  - density of the lower (denser) fluid  
 $\rho_2$  - density of the upper (lighter) fluid

---

\* These cannot be reproduced for copyright reasons. The journal is readily available however.

- $\rho_3$  - density of the plume  
 $\kappa_{ij}$  - molecular diffusion between fluids i and j at different concentrations of heat where 1 - lower fluid; 2 - upper fluid; 3 - plume  
 $h_1$  - depth of upper layer (see Figure 5)  
 $h_2$  - depth of lower layer (see Figure 5)  
 $d_0$  - orifice diameter (see Figure 5)  
 $R_0$  - vessel radius (see Figure 5)  
 $g$  - gravitational acceleration constant =  $9.81 \text{ ms}^{-2}$  (6)  
 $\mu_i$  - molecular viscosity of fluid i  
 $a_e$  - bubble radius  
 $r$  - radial coordinate (see Figure 5)  
 $z$  - vertical coordinate (see Figure 5)  
 $\phi$  - azimuthal coordinate (see Figure 5)

The geometrical parameters are illustrated in Figure 5.

The presence of the third reference fluid of the plume (or jet) makes solution of equation 5 nearly intractable. A simplification can be made if an air plume be used since 1) almost no mass is introduced into the system (since  $\rho_{\text{air}} \ll \rho_{\text{water}}$ ), 2) the density and viscosity of air are much less than water, and 3) density and viscosity differences between the air and water are much greater than between those of the water layers themselves. If an air plume is used as an agitator, equation 5 can be reduced to

$$\Phi_2 [t_H, \rho_0, \Delta\rho, \kappa_{12}, h_1, h_2, d_0, R_0, g, \mu, a_e, r, z, \phi] = 0 \quad (7)$$

where  $\rho_0$  - reference (Boussinesq) density for  $\rho_1$  and  $\rho_2$

$$\mu - \text{reference mol. viscosity, i.e., } \mu_1 \approx \mu_2 \quad (8)$$

$$\Delta\rho = \rho_2 - \rho_1$$

$$\text{Let } \kappa_{12} = \kappa$$

It is assumed that  $\rho_{\text{air}}$ ,  $g$ ,  $\mu$  may be considered constant.  $\rho_{\text{air}}$  is deleted as a parameter if the bubbles are large and not concentrated since it can be neglected in the momentum terms because  $\rho_{\text{air}} \ll \rho_0$ .

$$\text{If } a_e = \Phi_3 [d_0, \rho_0, q_{\text{air}}, \rho_{\text{air}}, D, g, \mu] \quad (9)$$

$$\text{where } D = h_1 + h_2 \quad (10)$$

$q_{\text{air}}$  = air discharge rate

as found from the literature, then in the experiments

$$a_e = \Phi_4 [q_{\text{air}}, D] \quad (11)$$

only since all other effects are fixed. Since, over  $D_{\text{max}} = 38.735 \text{ cm}$ , differences in  $D$  account for a volume change of about 3% at most, then

$$a_e = \Phi_5 [q_{\text{air}}] \quad (12)$$

approximately.

Using equations (10) and (12), and holding  $d_0$ , and  $R_0$ , and  $\kappa$  constant in the experiments (see Figure 5) equation 7 reduces to:

$$\Phi_6 [t_H, \rho_0, \Delta\rho, q_{air}, h_1, D, r, \phi, z] = 0 \quad (13)$$

Due to the measuring technique, to be described presently, variation of density with  $r$  and  $\phi$  is small. While  $R_0$  is not varied in the experiments, it is retained since common sense and a literature review by Graham (17) indicates  $t_H$  is inversely proportional to volume and not depth cubed.  $d_0$  is also retained, although not varied, in order to scale the plume. Nine terms remain which may be formed into six dimensionless groups:

$$\Phi_7 \left[ \frac{t_H q_{air}}{D R_0^2}, \frac{\Delta\rho}{\rho_0}, \frac{h_1}{D}, \frac{R_0}{D}, \frac{z}{D}, \frac{D}{d_0} \right] = 0 \quad (14)$$

These are the simplest forms of the parameters - the experiments attempted to relate all but  $R_0/D$  which had to be left fixed, unfortunately.

It may be enlightening to show that more classical dimensionless parameters may be defined if  $g$ ,  $\kappa$ , and  $\mu$  be reintroduced so that  $12 - 3 = 9$  dimensionless parameters exist -

$$\Phi_8 \left[ \frac{t_H q_{air}}{D R_0^2}, \frac{\Delta\rho}{\rho_0}, \frac{gD^5}{q_{air}^2}, \frac{\mu t_H}{\rho_0 R_0^2}, \frac{D}{d_0}, \frac{z}{d_0}, \frac{h_1}{d_0}, \frac{\kappa t_H}{R_0^2}, \frac{R_0}{D} \right] = 0 \quad (15)$$

$$\text{Now } \frac{h_1}{D} \cdot \frac{\Delta\rho}{\rho_0} \cdot \frac{gD^5}{q_{air}^2} \cdot \left(\frac{d_0}{D}\right)^4 = \frac{\Delta\rho}{\rho_0} \frac{gh_1}{(q_{air}/d_0^2)^2} \quad (16)$$

$$= Ri_p \quad (17)$$

$$\frac{R_0^2}{\mu t_H} \cdot \frac{t_H q_{air}}{R_0^2 D} \cdot \frac{D}{d_0} = \frac{\rho_0 q_{air}}{\mu d_0} \quad (18)$$

$$= Re_p \quad (19)$$

$$\frac{R_0^2}{\kappa t_H} \cdot \frac{t_H q_{air}}{R_0^2 D} \cdot \frac{D}{d_0} = \frac{q_{air}}{\kappa d_0} = Pe_p \quad (20)$$

and

$$\frac{\kappa t_H}{R_0^2} \cdot \frac{R_0^2 \rho_0}{\mu t_H} = \frac{\kappa \rho_0}{\mu} = Sc_p \quad (21)$$

where  $Ri_p$ ,  $Re_p$ ,  $Pe_p$  and  $Sc_p$  are plume Richardson, Reynolds, Péclet and Schmidt numbers respectively. Equation 15 may thus be rewritten as

$$\Phi_g \left[ \frac{t_H q_{air}}{D R_0^2}, Ri_p, Re_p, Pe_p, Sc_p, \frac{D}{d_0}, \frac{h_1}{D}, \frac{z}{d_0}, \frac{R_0}{D} \right] = 0 \quad (22)$$

Since  $\kappa$ ,  $\mu$ ,  $R_0$ ,  $d_0$  were not experimentally varied, then effects of  $Pe_p$ ,  $Sc_p$ , and  $R_0/d_0$  were not analysed; and analysis of  $Re_p$  is redundant if  $Ri_p$  be examined since the parameters which were varied -  $\rho_0$ ,  $q_{air}$  and  $D$  - are common to both. If  $D$  and  $q_{air}$  be kept constant, then the relation between  $t_H q_{air} D^{-1} R_0^{-2}$  ( $\equiv \Phi t_H$  henceforth) and  $Ri_p$  is the same as that with  $\Delta\rho/\rho_0$  (hence the validity of equation 14) provided  $t_H$  is not sensitive to  $Re_p$  which is usually the case in turbulent conditions. Note in comparing equations 15, 16 and 22 that the Richardson function should be derivable by varying either  $\Delta\rho/\rho_0$  or  $q_{air}$  for constant geometry.

#### A. DIFFUSION ANALOGY

Harleman, *et al.*, (23) suggested in 1962 that the decoupling and mixing action at an interface could be described by a turbulent diffusion equation. Their arguments were based upon the equation of continuity of mass which implied a convective - diffusive equation would describe the process. Experimental results of Crapper and Linden (Figure 3) and Graham (Figure 7) indicate that a boundary condition of constant density over time near or at the initial interface location, and the associated symmetry of the density transects about this level, would be amenable to description with an error solution of the heat equation.

The fundamental conservation equation may be stated as

$$\frac{D\rho}{Dt} = 0 = \frac{1}{r} (\rho u) + \frac{\partial}{\partial r} (\rho u) + \frac{1}{r} \frac{\partial}{\partial \phi} (\rho v) + \frac{\partial}{\partial z} (\rho w) \quad (23)$$

where  $(u,v,w)$  are instantaneous velocities in the coordinate directions  $(z,r,\phi)$ , (see figure 5). While space is not available to include the derivation here, Graham (17) averaged fluctuations of  $u(z,r,\phi,t)$ ,  $v(z,r,\phi,t)$ ,  $w(z,r,\phi,t)$  and  $\rho(z,r,\phi,t)$  over  $r,\phi$ , and  $t$ , and used mass continuity, to derive

$$\frac{\partial}{\partial t} (\tilde{\rho}') + \frac{\partial}{\partial y} (\tilde{\rho}' u') = 0 \quad (24)$$

where the tilde is a time average, and a prime indicates a time fluctuation. The  $y$ -variable is just  $y = z-h_2$  which centers the coordinates at the interface at  $t=0$ .

Equation 24 results when variations in  $r$  and  $\phi$  are removed by turning off the plume and allowing the fluid system to equilibrate. What equation 24 describes then is the effect of the plume agitation, not the plume dynamics.

Traditional phenomenological arguments based on the Prandtl mixing-length concept and Reynolds' analogy allow equation 24 to be altered to

$$\frac{\partial}{\partial t} (\tilde{\rho}') = \frac{\partial}{\partial y} [E_y \frac{\partial}{\partial y} (\tilde{\rho}') ] \quad (25)$$

Since  $E_y(y)$  because  $h_2/d_0$  is not scaled to  $h_1/h_2$  in the experiments,  $E_y$  should not be placed inside a  $\nabla^2$  operator. Solution for  $E_y$  has been done numerically from experimental data. Finally, equation (25) has the same form if the parameters are nondimensionalized. Further discussion of this concept may be found in reference (17).

#### SOME EXPERIMENTAL RESULTS

The experimental apparatus is illustrated in Figure 6. It consisted of a plexiglas cylinder (to provide radial symmetry) 38.74 cm high and 12.17 cm in diameter. The orifice was 0.476 cm in diameter and centered. A plate above the bottom and 2 side outlets allowed sharp interfaces to be made. Only saline solutions were used so that no conservation problems would arise, and  $\kappa = \text{constant}$ . (Temperature losses or gains to the atmosphere during an experiment would alias the results). Air discharge rate ( $Q_{\text{air}}$ ), total depth ( $D$ ), buoyancy difference ( $\Delta\rho/\rho_0$ ), and initial interfacial height ( $h_2$ ) were systematically varied. The experimental values are given in Table 1.

In general, the rather small volume of the cylinder resulted in the liquid being very agitated at high air flow rates. Because  $Ro$  could not be varied, the results cannot be generalized to other geometric configurations since volume-dependency has not been removed from the coefficients. On the other hand, a very clear picture of the sequential destratification process adumbrated in the various references could be discerned. A detailed description of the experimental results is not possible within the length constraints of this article, but some selected results will be given in the hope that it might encourage some prototype-scale experiments along these lines.

Figures 7 and 8 are actual reduced reproductions of conductivity-depth X-Y recordings for experiments (6-2) and (8-4) respectively. After the air plume had been passed through the system for a period of time it was turned off and the liquid allowed to come to rest. A transect was then made with a very sensitive salinity recorder and a depth-conductivity signal was fed into an X-Y recorder. These figures have not been adjusted for density calibration so that the final "fully-mixed" trace does not lie at an appropriate proportional distance from the initial upper and lower density tracings. The patterns on the figures selected are quite clear nevertheless however.

All features of the full "classic" destratification process can be seen in Figure 7. First, note that the density at the interface did not change during the first few transects. This is the so-called "diffusive" regime.

Note also that the rate of change of density at locations remote from the interface occurred rapidly in this regime. After transect 4 (45 sec.) the stratification changed to one being progressively more interfacial and which approached the nozzle only very slowly. The upper layer became rapidly homogeneous while material from the upper layer did not seem to mix into the lower so easily. A zone just below the initial interface location actually became more saline.

If the traces represented some density-associated water-quality parameter, such as DO, it is easy to see that DO could reach locations below the thermocline much more readily and efficiently if a "diffusive" regime prevailed. In light of the dimensional arguments given previously, particularly in the discussion regarding  $Ri_p$  (equation 17) it was found that interfacial destratification occurred sooner (dimensionless time  $\phi t_H$ ) at a lower Richardson number, that is, at higher air discharge rates or lower initial buoyancy differences. The slower (in terms of nondimensional time  $\phi t_H$ ) mixing after a change from "diffusive" to "interfacial" regimes results in graphs similar to Figure 2, and Figure 12 of reference (19).

It was possible to demarcate the point of transition from one regime to the other in all the experiments. This dimensionless time was termed  $\phi t_D$  and an empirical equation describing its occurrence was found, by best fit, to be

$$\phi t_D = \text{constant} * \left(\frac{\Delta\rho}{\rho_0}\right)^{1.07} * \left(\frac{h_2}{d_0}\right)^{0.65} * \phi_{10} \left(\frac{h_1}{h_2}\right) \quad (26)$$

where  $h_1$ ,  $h_2$  represent the initial values of these parameters (see Figure 5). Note that in equation (26)  $t_H \propto q_{air}^{-1}$ , and the exponent for the buoyancy difference is also close to 1, while the relations with respect to  $h_1/d_0$  and  $h_1/h_2$  are nonlinear, as hypothesized in equations (2,3,4). Additional analysis and the form of  $\phi_{10}$  can be found in Graham (17).

Finally, the dominance of the 'interfacial' regime at small  $h_2/d_0$  (near the orifice) can be seen in Figure 8. This appears to be a local scaling phenomenon since it occurred for all  $D/d_0$ , and near the end of all experiments. Paradoxically the interface is most distinct where the local agitation is greatest (measured by jet velocity), but the jet width is least. Entrainment at this location is very weak and destratification occurs very slowly.

#### SUMMARY AND CONCLUSIONS

As mentioned, many studies have been made of the effects of local stratification upon plume behavior (7,2,24) but very few of the opposite case. Thermal plumes and jets obviously affect local stratification, particularly in smaller lakes and reservoirs. It has been shown that similar distinct

mixing sequences seem to occur in both the field and in laboratory studies. A more 'efficient' overall type of mixing (diffusive) is characteristic of high initial stability and low jet agitation; while classic interfacial descent occurs where there is low initial stability and/or high jet agitation, and especially when the interface is near the diffuser. While greater analysis of the results appears in (17), experiments at a prototype scale are needed to extrapolate these results to different geometries (25). Such experiments should also follow a rigorous dimensional format such as the one presented. Additional laboratory and field experiments are necessary to 1) determine the validity of the Fourier analogy, and 2) properly understand the cause of the change from one mixing phase to the other.

If this plume mixing process is more clearly understood, then thermocline location and sharpness (and other associated water quality parameters) can be better modeled and predicted.

#### ACKNOWLEDGEMENTS

This study was conducted as private research. Laboratory space and equipment were provided by the Johns Hopkins University, Baltimore. Assistance with drafting was provided by Carol Dillard, engineering student at UF. Thanks are also due to Irene Urfer of the Department of Geography, Brandon University for typing the manuscript.

#### REFERENCES

1. Brooks, Norman H. (1972) Dispersion in Hydrologic and Coastal Environments. CIT Keck Lab. Rpt. KH-12-22. 203 pp.
2. Harleman, Donald R.F. (1972) "Thermal stratification due to heated discharges", Proc. Int'l. Symp. on Stratified Flows, ASCE, Novosibirsk, 35-68.
3. Rouse, H. and J. Dodu (1955) "Turbulent diffusion across a density interface". La Houille Blanche, 10, 405-410.
4. Turner, J. S. (1968) "The influence of molecular diffusivity on turbulent entrainment across a density interface". JFM, 33, 639-656.
5. Turner, J.S. (1973) Buoyancy Effects in Fluids. Cambridge Univ. Press.
6. Long, Robert R., (Oct. 1974) Lectures on Turbulence and Mixing Processes in Stratified Fluids. Tech. Rpt. No. 6 (Series C). Dept. of Earth and Planetary Sciences, the Johns Hopkins Univ., Baltimore, MD.
7. Uhl, Vincent and Joseph B. Gray (1966), Mixing, Theory and Practise Vol. 1, Academic Press, N.Y.
8. Baines, W.D. (1975) "Entrainment by a jet in plume at a density interface". JFM, 68, (2), 307-320.

9. Sullivan, Paul J. (1972). The penetration of a density interface by heavy vortex rings. Air, Water and Soil Pollution, 1, (3), 322-336.
10. Linden, P.F. (1973). "The interaction of a weak vortex ring with a sharp density interface: a model for turbulent entrainment" JFM, 60, 467-480.
11. Brush, Lucien M. Jr., Francis, C. McMichael and Chen Y. Kuo (1968). Artificial Mixing of Density-Stratified Fluids: A Laboratory Investigation - Princeton Univ., Moody Hydrodynamics Laboratory Rpt. MH-R-2. 80 pp.
12. Brush, Lucien M. Jr., (1970) Artificial Mixing of Stratified Fluids Formed by Salt and Heat in a Laboratory Reservoir. N.J. Nat. Res. Instit., Rutgers Univ. 33 pp.
13. Neilsen, Bruce J. (1972) Mechanism of Oxygen Transport and Transfer by Bubbles. Ph.D. Diss., the Johns Hopkins Univ., Baltimore, MD. 131 pp.
14. Kantha, Lakshmi H. (August, 1975) Turbulent Entrainment at the Density Interface of a Two-Layer Stability Stratified System. Publ. of Dept. Earth and Planetary Science, The Johns Hopkins Univ., Baltimore, MD. 161 pp.
15. Crapper and Linden (1974), "The structure of turbulent density interfaces." JFM, 65, (1), 45-63.
16. Knoppert, P.L., J.J. Rook and G. Oskam (1970). "Destratification experiments at Rotterdam", Jrl. AWWA, 62, 448-454.
17. Graham, Donald S. (Sept. 1976) An Experimental Study of the Mixing of 2-layer Density-Stratified Liquids by an Air Plume in a Small Cylindrical Container. Submitted to The Johns Hopkins Univ. in partial fulfillment of the requirements for the Ph.D. degree, Oct. 6, 1976. 872 pp. Draft.
18. Koberg, Gordon E. and Maurice E. Ford, Jr. (1965) Elimination of Thermal Stratification in Reservoirs and Resulting Benefits. U.S.G.S. Water Supply Paper 1807-M. 28 pp.
19. Moretti, Peter M. and Dennis K. McLaughlin (Apr. 1977). "Hydraulic modeling of mixing in stratified lakes". Proc. ASCE, 103, HY4, 367-380.
20. Henderson - Sellers, Brian (June 1976). "Role of eddy diffusivity in thermocline formation". Proc. ASCE, 102, (EE6), 517-531. With British references.

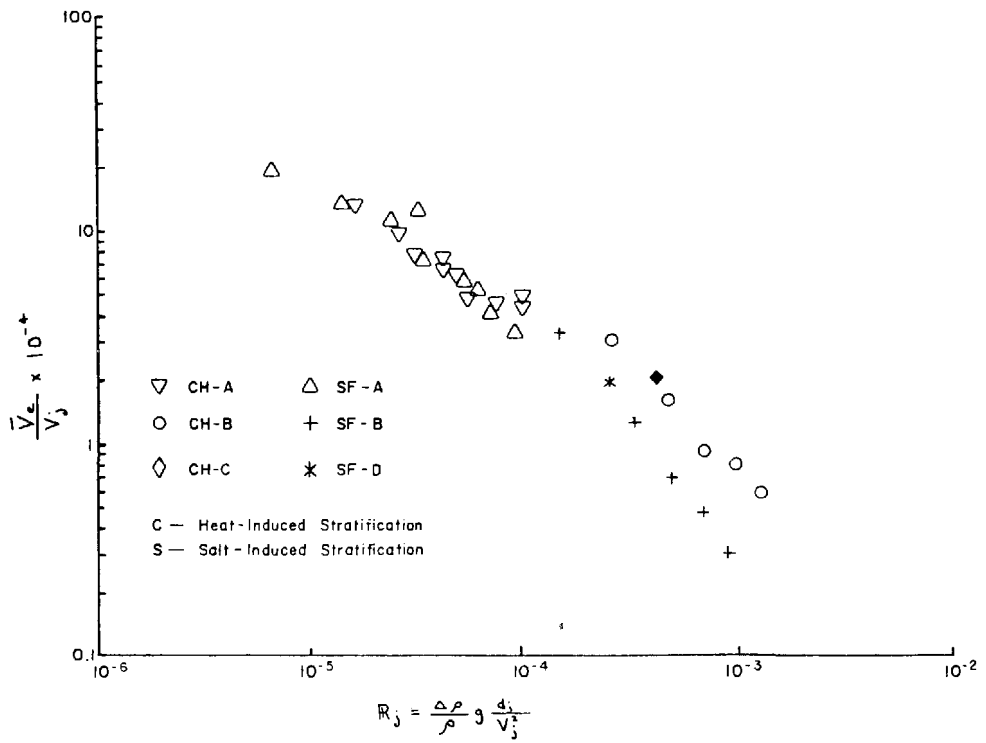
21. Ito, Takeshi (1972), "Mixing method of stratified water layer in reservoirs" (sic). In International Symp. on Strat. Fluids, Novosibirsk, USSR. ASCE Publ. 567-577.
22. Gebhart, Glen E. and Robert C. Summerfelt (Dec. 1976). "Effects of destratification on depth distribution of fish". Proc. ASCE, 102, (EE12), 1215 - 1228.
23. Harleman, D.R.F., J.A. Hoopes, D. McDougall and D. A. Goulis (1962) Salinity Effects on Velocity Distributions in an Idealized Estuary. MIT Parsons Lab. Tech. Rpt. No. 50. 45 pp.
24. Wright, Steven Jay (May, 1977). Effects of Ambient Crossflows and Density Stratification on the Characteristic Behavior of Round Turbulent Buoyant Jets. CIT Keck Lab. Rept. KH-R-36. 254 pp.
25. Graham, Donald Steven (June, 1978). Disc. of "Aeration of hydro releases at Ft. Patrick Henry Dam". Proc. ASCE, 104, (HY6), 943-945.

TABLE I

## VALUES OF EXPERIMENTAL PARAMETERS

| Experiment<br>Number | Abbr. | $q_{air}$<br>$cm^3$ | D<br>cm | $\Delta\rho$<br>$\frac{\cdot}{\text{(Initial)}}$ | $\rho_0$<br>$\frac{\cdot}{\text{(Initial)}}$ | $h_1/D$<br>$\frac{\cdot}{\text{(Initial)}}$ |
|----------------------|-------|---------------------|---------|--|--|---|
| 10.5.1.-(5-1)        | 5-1   | 35                  | 38.735  | 0.0130   | 1.0154                                       | 1/2   |
| 10.5.1.-(5-2)        | 5-2   | 80                  | do.     | do.  | 1.0154                                       | do.   |
| 10.5.1.-(5-3)        | 5-3   | 120                 | do.     | do.  | 1.0154                                       | do.   |
| 10.5.1.-(5-4)        | 5-4   | 210                 | do.     | do.  | 1.0154                                       | do.   |
| 10.5.1.-(6-1)        | 6-1   | 49                  | do.     | .0124  | 1.0130                                       | do.   |
| 10.5.1.-(6-2)        | 6-2   | 49                  | do.     | .0124  | 1.0130                                       | do.   |
| 10.5.1.-(6-3)        | 6-3   | 49                  | do.     | .0062  | 1.0161                                       | do.   |
| 10.5.1.-(6-4)        | 6-4   | 49                  | do.     | .0034  | 1.0175                                       | do.   |
| 10.5.1.-(6-5)        | 6-5   | 49                  | do.     | .0014  | 1.0185                                       | do.   |
| 10.5.1.-(7-1)        | 7-1   | 49                  | 38.735  | .0141  | 1.0114                                       | 1/2   |
| 10.5.1.-(7-2)        | 7-2   | 49                  | do.     | do.  | 1.0078                                       | 3/4   |
| 10.5.1.-(7-3)        | 7-3   | 49                  | do.     | do.  | 1.0164                                       | 0.148                                       |
| 10.5.1.-(8-1)        | 8-1   | 49                  | 38.735  | .0080  | 1.0103                                       | 1/2   |
| 10.5.1.-(8-2)        | 8-2   | 49                  | 29.05   | do.  | 1.0103                                       | 1/2   |
| 10.5.1.-(8-3)        | 8-3   | 49                  | 19.37   | do.  | 1.0103                                       | 1/2   |
| 10.5.1.-(8-4)        | 8-4   | 49                  | 19.37   | do.  | 1.0103                                       | 1/2   |
| 10.5.1.-(8-5)        | 8-5   | 49                  | 10.80   | do.  | 1.0103                                       | 1/2   |

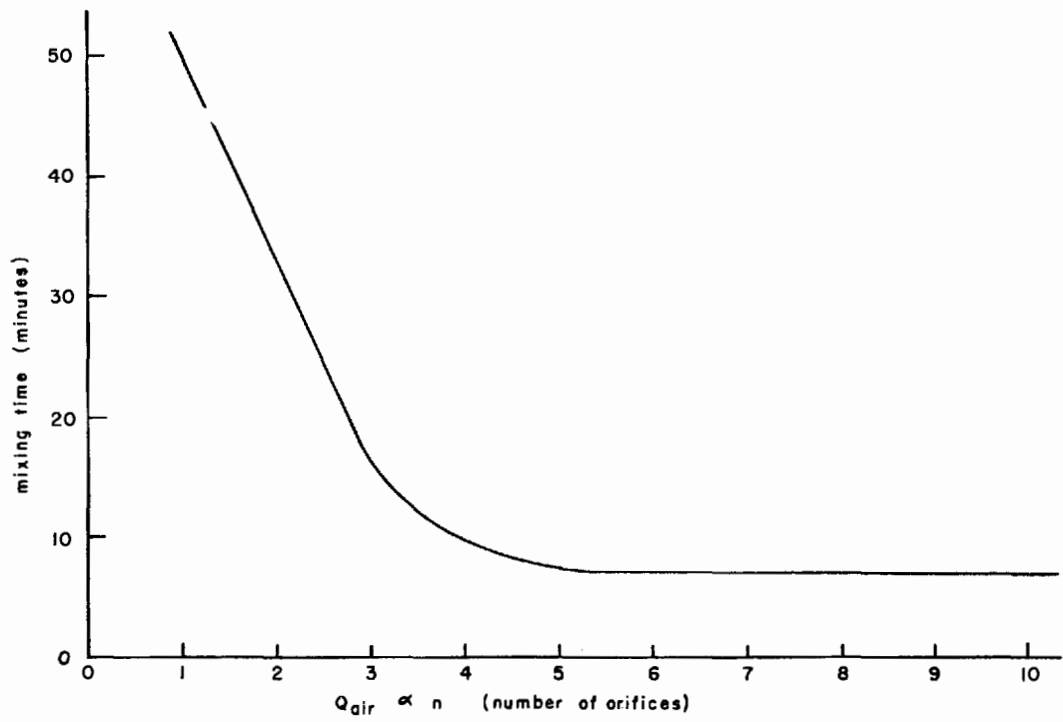
Figure 1



Jet Entrainment Velocity v. Richardson Number

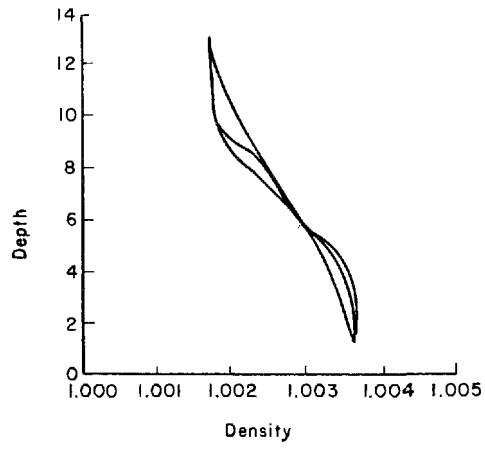
Source: Brush (12), modified by Graham (17)

Figure 2



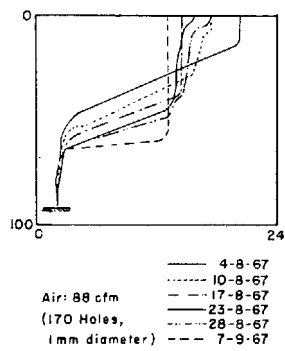
Mixing Time as a Function of Air Flow Rate According to Neilsen  
Source: Neilsen (13)

Figure 3

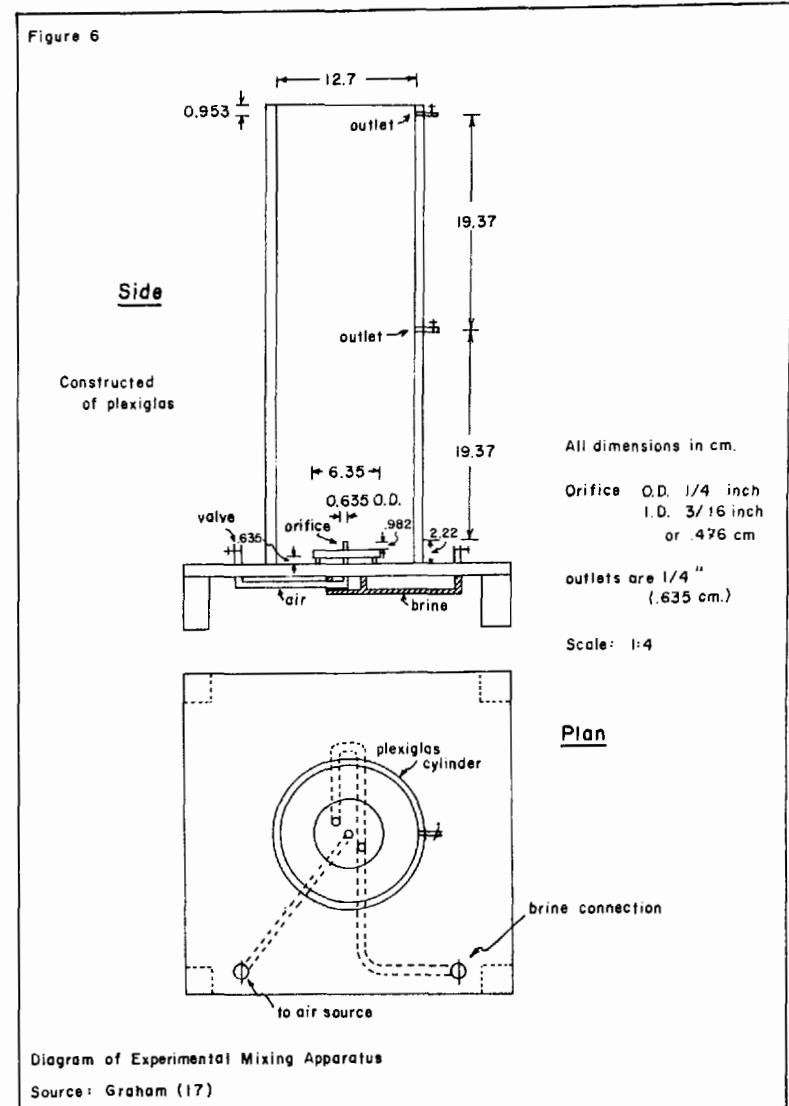
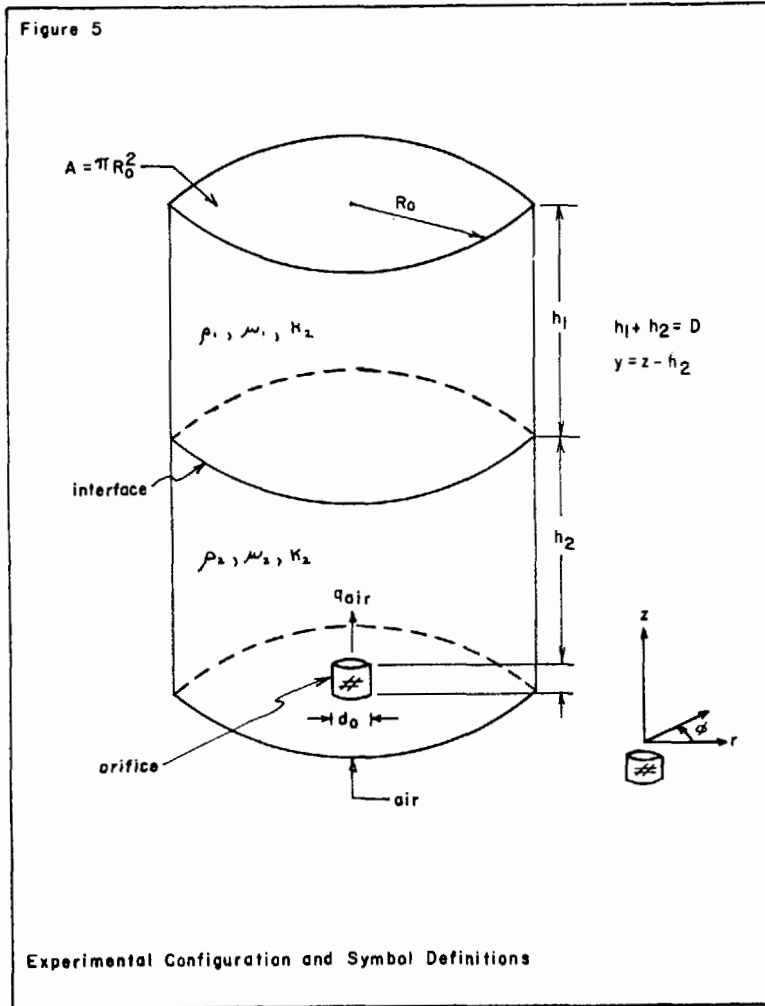


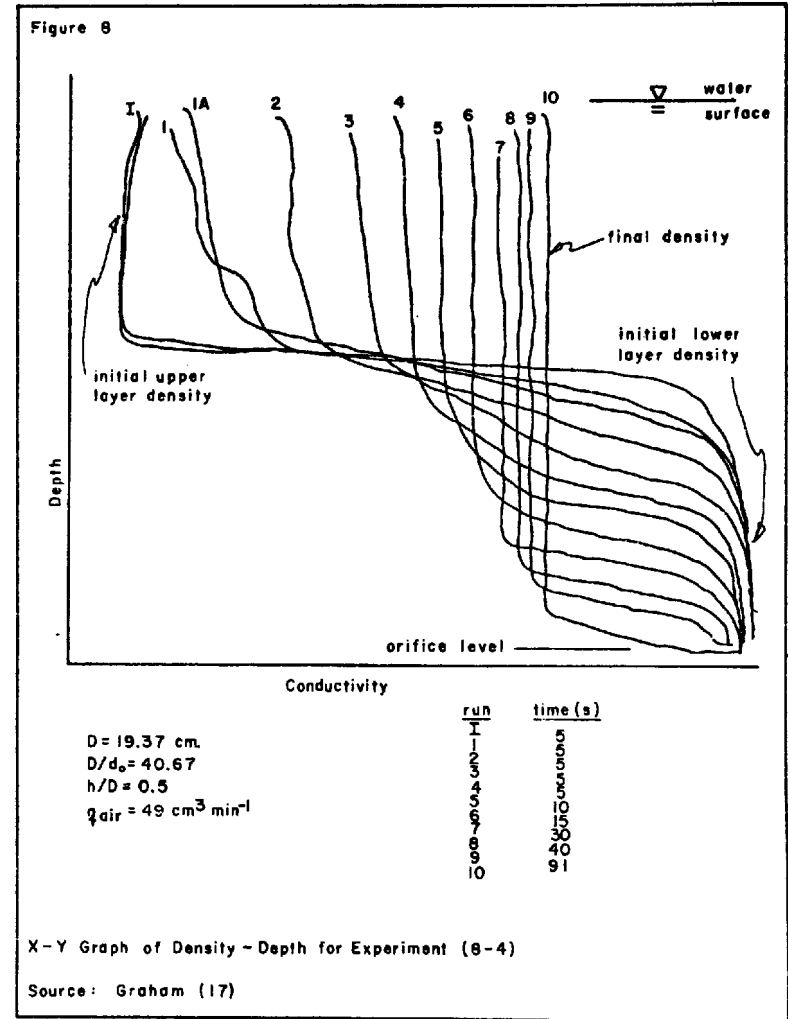
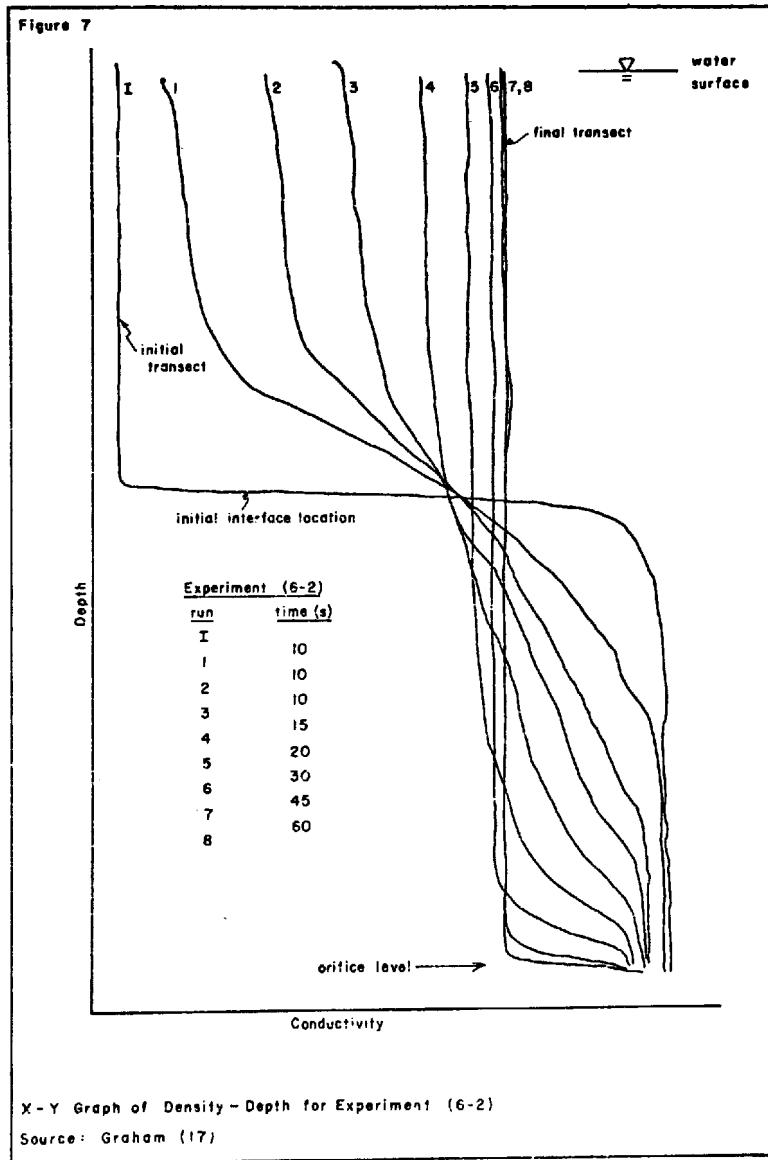
A Series of Depth-Density Transects From Crapper and Linden  
Source: Modified from Crapper and Linden (15)

Figure 4



Progress of Destratification of Lake Maarsseveen  
Source: Knoppers, *et al.*, (16).





## THREE-DIMENSIONAL FIELD SURVEYS OF THERMAL PLUMES FROM BACKWASHING OPERATIONS AT A COASTAL POWER PLANT SITE IN MASSACHUSETTS

A.D. Hartwell, Normandeau Associates, Inc., Bedford, NH 03102 and  
F.J. Moglelesko, Boston Edison Company, Boston, MA 02199, U.S.A.

### ABSTRACT

Using specially designed temperature profiling equipment, two surveys were conducted during thermal backwashing operations at Pilgrim Nuclear Power Station to determine the spatial and temporal extent of temperature rises above ambient. Backwashing formed a thermal plume about 5 to 6-ft thick (1.5 to 1.8 m) in front of the intake screenwall. Maximum observed surface temperatures were 101.0 F (38.3 C), representing a  $\Delta T$  of 43.4 F (24.1 C) above ambient. The frontal zone of the plume spread gradually seaward at about 0.2 kn. Its outer edge became thinner and rapidly cooled, presumably by advection and turbulent diffusion associated with currents from the reverse pumping and local changes from dissipation to the atmosphere. Along the intake shoreline, the plume was often less than 1 ft (0.3 m) thick. Most of the hot water was dissipated within several hundred feet of the intake with  $\Delta T$ 's of about 10.0 to 15.0 F (5.6 to 8.3 C) above ambient. Under the influence of strong southwesterly winds during the second survey, some warmed water was apparently carried beyond the outer breakwaters into Cape Cod Bay. These surveys provided real-time data indicating that the backwashing operation caused a relatively thin thermal plume, which spread rapidly from the intake out across the study area and along the seaward breakwater. Within a few hours these backwash thermal plumes were completely dissipated.

### INTRODUCTION

Although thermal backwashing is a commonly used technique for control of biofouling in condenser tubes and intake structures of operating power plants, only limited published information is available on the receiving water temperature structure caused by such operations. Boston Edison Company, Boston, Massachusetts, conducted two thermal surveys of actual mid-summer backwashing operations under varying tidal conditions at Pilgrim Nuclear Power Station during 1977 to establish a synoptic picture of the plume's three-dimensional structure [1].

The Pilgrim Nuclear Power Station, located on the shore of Cape Cod Bay in Plymouth, Massachusetts, is a 655 MW light-water moderated, boiling water nuclear reactor with a once-through condenser cooling water system. Water used for cooling the condenser is removed from Cape Cod Bay through a shoreline intake (Fig. 1). It enters the intake between two breakwaters via a dredged channel which is about 18 to 24 ft deep (5.5 to 7.3 m) at mean low water (MLW).

Under normal operating conditions, the water is drawn into the intake by two pumps (designated herein as east and west), circulated through the condenser system and discharged via a surface canal at a rate of about 510 million gallons/day and a  $\Delta T$  (difference between the discharge and intake temperatures) averaging 30.0 F (16.7 C). Condenser tubes are cleaned by backwashing on a 1 to 2-week interval, depending upon bio-fouling severity. Generally 45 to 60 min are required to treat each of the two circulating water pumps, with elevated temperatures averaging around 100.0 F (37.8 C). Occasionally the temperatures peak at from 110.0 F (43.3 C) to 120.0 F (48.9 C), depending upon the amount of heat treating necessary. Because plant load must be reduced during backwashing, the operation is generally conducted at night during off-peak hours.

## METHODS

This study conducted by Normandeau Associates, Inc. (NAI), of Bedford, New Hampshire, consisted of overnight three-dimensional temperature and current surveys, supplemented by continuous thermal monitoring. For the first survey on July 9 and 10, 1977, backwashing began at low water and continued into early flood tide. During the second survey on July 16 and 17, 1977, backwashing began at high water and continued into early ebb tide. Both surveys concentrated on the time history of plume build-up and dissipation.

Temperature and depth data were collected at selected stations (Fig. 1) and plotted on board the survey boat using a Naico Model 3100-TD Profiling System (Fig. 2). Current velocity profiles were acquired using Bendix Model Q-15 current meters and Model 270 recorders. Precise location was continuously recorded using a Motorola MiniRanger III System with two shore based transponders.

Two Naico Model 200 Digital Field Temperature Recorders were utilized to periodically measure temperature profiles from water surface to bottom at two stations in the intake channel. The arrays were assembled so they could be moved quickly within the survey area to check thermal anomalies. In addition, two Naico Model 1001-T Temperature Recorders were installed to monitor water temperatures 1) inside the intake screenwall and the discharge canal, and 2) in ambient receiving waters of adjacent Cape Cod Bay.

Observed temperatures were transformed to true temperatures using regression equations based on calibration data for each respective field instrument. From measurements of ambient near-bottom waters mid channel between the two intake breakwaters (Fig. 1), a  $\Delta T$  or approximate temperature rise above ambient was calculated for each temperature observation.

## FIELD SURVEYS

### Low-Water Backwash Survey

The July 9 and 10 low-water backwash survey consisted of five sampling runs keyed to actual plant operations. For this survey, NAI's ambient temperature measurements along the bottom of the intake channel started around 49.0 to 50.0 F (9.4 to 10.0 C) and then gradually rose to about 58.0 F (14.4 C) by the time of low water. Throughout the rest of the night, ambient temperatures continued to rise slowly, reaching about 60.0 F (15.6 C) by the end of the survey. This rise may represent some recirculation of the discharge plume toward the intake area because of local winds and coastal currents.

As backwashing was initiated, plant load was gradually brought down. NAI's readings of discharge canal temperatures showed a drop from 87.0 F (30.6 C) to 74.6 F (23.6 C; Fig. 3). Next, the west pump was backwashed from about 0030 to 0119 EST. The *in situ* temperature monitors recorded a sudden rise in discharge temperature to about 83.0 F (28.3 C), followed by a sharp drop to about 65.3 F (18.5 C). Simultaneously water box temperatures rose quickly to about 104.0 F (40.0 C) and remained at this level for much of the backwashing period (Fig. 3). As backwashing of the first pump neared completion, discharge temperatures rose again to 83.2 F (28.4 C) and water box temperatures dropped back down to below 70.0 F (21.1 C). From about 0150 to 0227 EST the east pump was backwashed in the same way with similar backwash temperatures observed for both pumps. During this backwashing period, discharge temperatures dropped to about 70.6 F (21.4 C), then rose to 87.0 F (30.6 C) for a short time, dropped back down to about 75.0 F (23.9 C), and finally rose back toward normal operational levels (Fig. 3).

A prebackwash survey conducted during late-ebb showed surface temperature rises ( $\Delta T$ ) ranging from 9.1 F (4.1 C) near the offshore discharge to 4.9 F (2.7 C) near the plant intake.

As backwashing started, the first visible evidence was a sudden rush of hot, turbulent water marked by foam and a steamy vapor right in front of the intake. With continuing backwashing, the hot water formed a surface layer about 5-ft (1.5 m) thick, which reached temperatures as high as 100.0 F (37.8 C) in front of the intake screenwall. A distinct frontal zone moved slowly northward (or seaward) away from the intake, bulging in the middle and slightly restrained along shore due to frictional effects. The water temperatures in the near-surface thermal plume gradually decreased with both distance away from the intake and time, presumably due to evaporative heat loss and dilution (mixing with ambient waters).

At the surface,  $\Delta T$ 's of 42.1 F (23.4 C) in front of the west pump and 24.8 F (13.8 C) in front of the east pump were observed (Fig. 4). Within less than 100 ft (30.5 m), the  $\Delta T$  from the western pump was 28.0 F (18.6 C) or less. High  $\Delta T$  water hugged the outer breakwater, apparently because of momentum effects and southwesterly winds during the night. Surface  $\Delta T$ 's of 10.0 F (5.6 C) and higher were confined to the western third of the intake area between the breakwaters (Fig. 4). The remainder of the area experienced  $\Delta T$ 's equal to or colder than observed prior to backwashing.

At the 3.3 ft (1.0 m) depth level, observed  $\Delta T$ 's were 23.4 to 24.3 F (13.0 to 13.5 C) in front of the intake. Within less than 200 ft (61.0 m),  $\Delta T$ 's were down to 18.2 F (10.1 C). Beyond that distance they dropped from 14.8 to 6.7 F (8.2 to 3.7 C). Near the outer end of the breakwaters,  $\Delta T$ 's were only 2.4 to 3.3 F (1.3 to 1.8 C).

At the 9.8 ft (3.0 m) level,  $\Delta T$ 's were 4.6 F (2.6 C) or less in front of the intake and 1.2 to 2.1 F (0.7 to 1.2 C) along the dredged channel. Along the bottom all of the  $\Delta T$ 's were negative, or colder than conditions at the outer end of the breakwaters. At Station 6 minimum values were -4.4 F or -2.4 C (Fig. 5).

The detailed profiles at Station 6 showed that the backwashing from the western pump formed a distinct slug or pulse of hot water along the surface, which eventually extended down to about 7 ft (2.1 m). The heated effluent apparently took about 15 min to reach and about 75 min to pass the anchored boat in its seaward progression (Fig. 5). Maximum observed  $\Delta T$  at the surface was 22.6 (12.5 C), which represented an actual temperature of 79.0 F (26.1 C). Near-bottom temperatures were 53.4 to 56.2 F (11.9 to 13.4 C) which represented negative  $\Delta T$ 's of up to -4.7 F (-2.6 C). By about 0119 EST backwashing of the west pump was complete.

At about 0150 EST backwashing of the east circulating water pump started. As before, there was a sudden surge of hot, turbulent and steamy water at the surface. Within minutes a thin thermal plume and a distinct seaward-moving frontal zone was observed. At the surface,  $\Delta T$ 's were essentially the same as during backwashing of the west pump, averaging 20.0 F (11.1 C) and more across the western third of the study area, 10.0 to 20.0 F (5.6 to 11.1 C) in the middle, and 5.0 to 10.0 F (2.8 to 5.6 C) across the eastern third. As before, the highest temperatures were along the outer breakwater. At 3.3 ft (1.0 m)  $\Delta T$ 's were 15.5 to 23.4 F (8.6 to 13.0 C) next to the intake and gradually decreased seaward. Below this level there was no evidence of the backwash plume, whereas along the bottom  $\Delta T$ 's remained negative.

At Station 6 the second backwash manifested itself as another pulse of hot water, which was warmer than before (up to 81.1 F or 27.3 C) but slightly thinner and shorter-lived (Fig. 5). This plume had surface  $\Delta T$ 's of up to 23.5 F (13.1 C). Apparently it took about 10 to 15 min for this

second plume to reach the anchored boat, but its effects were only evident for about 60 min. By the time the plume had passed, it was only about 1 to 2 ft (0.3 to 0.6 m) thick. Near-bottom temperatures showed little change, ranging from 54.1 to 56.2 F (12.3 to 13.4 C) and representing negative  $\Delta T$ 's (down to -3.4 F or -1.9 C). By about 0227 EST backwashing of the east pump was complete and the plant began to return to normal operation.

Subsequent surveys for the rest of the night showed that the elevated surface temperatures from the backwashing operation persisted for only about 2 to 2.5 hrs in the western portion of the study area and even less in the eastern portion, before being completely dissipated.

#### High-Water Backwash Survey

One week later on July 16 and 17, a second survey was conducted under high-water tidal conditions. Throughout this survey ambient temperature measurements along the bottom of the intake channel showed very little variation, ranging from 52.0 to 55.0 F (11.1 to 12.8 C). Backwash temperatures were about the same for both pumps (peak of 107.0 F or 41.7 C); however, this series of backwashes lasted 20 to 25 min longer than respective ones the week before because of increased fouling of the condenser tubes.

At about 2354 EST on July 16, backwashing started on the west pump. This time, in sharp contrast to the low-water backwashing, the surface appearance of the backwash waters was much less dramatic. The thermal plume was somewhat turbulent and steamy, but the thermal front along the interface with Cape Cod Bay waters was much less distinct than it had been the week before. Apparently this was because more dilution or "receiving" water was available at high tide.

The observed surface  $\Delta T$ 's were 28.2 F (15.7 C) in front of the west pump and 17.1 F (9.5 C) in front of the east pump (Fig. 6). Warmest temperatures were along the west side of the study area with  $\Delta T$ 's from 28.0 F down to about 14.8 F (15.6 to 8.2 C). Across the middle portion of the study area,  $\Delta T$ 's ranged from 15.0 to 10.0 F (18.3 to 15.6 C), with most of the warmed water apparently being blown against the outer breakwater by the strong southwesterly winds which persisted throughout the survey. Much lower  $\Delta T$ 's were seen along the shore in front of the power plant (6.1 to 9.1 F or 3.4 to 5.1 C). In the eastern portion of the study area, some warm water was observed along the outer breakwater (8.7 to 11.8 F or 4.8 to 6.6 C); but, close to shore temperatures remained unchanged. At the discharge the temperature rise was 14.8 F (8.2 C). At the 3.3 ft (1.0 m) level,  $\Delta T$ 's were lower than at the surface, but the general distribution of the backwash plume was about the same. At 9.8 ft (3.0 m)  $\Delta T$ 's were small, while near-bottom  $\Delta T$ 's were negative apparently due to cold water being drawn into the intake area.

Temperature measurements from the boat anchored at Station 6 showed that the west pump's backwash plume arrived within 5 to 10 min of the start of backwashing (Fig. 7). The  $\Delta T$ 's rose sharply to 14.4 F (8.0 C) or an actual temperature of 69.1 F (20.6 C). The resulting thermal plume seemed to be about 2 to 3 ft (0.6 to 0.9 m) thick and persisted for almost 90 min. Actual backwashing of the west pump was completed around 0113 EST.

At about 0159 EST backwashing of the east pump started. Surface  $\Delta T$ 's were 43.2 F (24.0 C) in front of the east pump and 25.2 F (14.0 C) in front of the west pump. Elsewhere  $\Delta T$ 's were generally higher than during the previous sampling run. Temperature rises of 20.0 F (11.1 C) and more were found across the channel to the outer breakwater. As before the elevated  $\Delta T$ 's were observed along the outer breakwater ( $\Delta T$ 's of 15.0 to 20.0 F or 8.3 to 11.1 C), possibly due to continuing wind influence. Slightly deeper at 3.3 ft (1.0 m), the temperature distribution was about the same as at the surface; but deeper down and along the bottom, temperatures were much warmer than earlier in the evening.

At Station 6 the passage of the east pump thermal plume was very evident (Fig. 7). It took less than 10 min for the backwash water to arrive and, as before, it persisted for about 90 min. The temperatures were slightly higher this time, with the greatest rise occurring after backwashing was complete. At about 0307 EST backwashing of the east pump was completed and the plant started to return to normal operation.

Subsequent surveys during the rest of the night showed that the elevated surface temperatures and thermal backwashing plumes persisted for almost 4 hrs in the western portion of the study area and somewhat less in the eastern portion, before dissipating. Backwashing momentum effects, as well as local winds, seemed to play a role in forcing the warmed water along the outer breakwater and keeping it away from the shore in front of Unit 1 (Fig. 6).

## DISCUSSION

Each backwashing was first evidenced by a pulse of warmed water at depth from the intake (Fig. 8). As the pumping continued, the hot buoyant water rose to the surface and within a few minutes formed a warm thermal plume averaging 3 to 5 ft (0.9 to 1.5 m) thick. Below the plume was a steep gradient to the colder near-ambient waters along the bottom of the intake channel. During the first weekend survey, the thermal plume formed a distinct frontal zone of foam and turbulent, steaming water which could be easily tracked by eye. Under the influence of the reverse intake flows, the initial jet momentum, the plume buoyancy effect and the localized hydrostatic head in front of the screenwall, the frontal zone moved slowly across the study area. Along shore and in shallow water,

frictional effects slowed the frontal zone, causing the plume to bulge in the center. The hot water propagated toward the western portion of the study area and the outer breakwater; but relatively little hot water contacted the shoreline area in front of Unit 1 during both of the surveys (Figs. 4 and 6). During the second survey the frontal zone behaved in a similar manner; but was much less distinct, probably because of the increased volume of receiving water (high-water condition).

Because of the relative thinness of the thermal plume and the pronounced stratification it created, it appeared to be highly susceptible to wind-shear effects. During both weekend surveys, momentum effects and south-westerly winds apparently forced much of the plume against the outer breakwater, leaving the shoreline area much less affected. During the second weekend some warmed water was apparently forced out into Cape Cod Bay beyond the outer breakwater by transient wind effects (estimated to be only a small percentage of the surface backwash thermal plume). In general, the eastern portion of the study area remained relatively unaffected by the hot water during both studies. Where the thermal plume impinged the shoreline, such as along the breakwaters, it was generally less than 2 ft (0.6 m) thick.

#### SUMMARY AND CONCLUSIONS

These surveys showed that backwashing operations at Pilgrim Station form a relatively thin thermal plume averaging 3 to 5 ft (0.9 to 1.5 m) thick. Higher temperatures were observed during the low-water backwashing than during the high-water backwashing, presumably due to lesser amounts of available entrainment water. During the first survey the thermal plume persisted for about 2 to 2.5 hrs before being completely dissipated. The second weekend more heat treatment was required due to accumulated bio-fouling and the thermal plume persisted for almost 4 hrs. Initial momentum effects of the backwashing flows apparently tend to carry the thermal plume northward and along the outer breakwater, with little tendency for warmed water to impinge the shoreline in front of Unit 1. During both surveys local winds also appeared to play a role in pushing the thermal plume seaward. Finally, observed near-bottom ambient temperature variations suggest that some water from the plant discharge can recirculate into the intake area.

#### REFERENCE

Normandeau Associates, Inc. 1977. Thermal surveys of backwashing operations at Pilgrim Station during July 1977. Conducted for Boston Edison Company, Boston, Massachusetts. 73 pp.

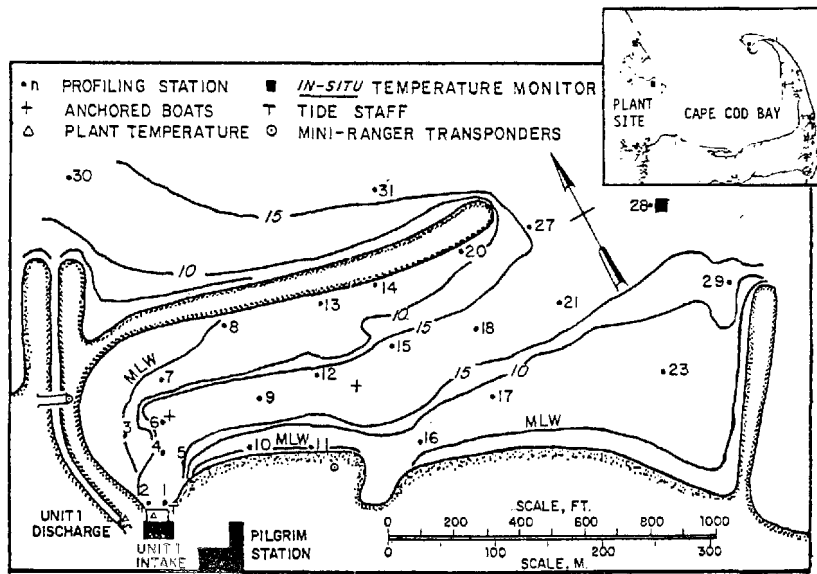


Fig. 1 Location map showing approximate sampling stations and *in situ* instrumentation for the July 1977 Pilgrim Station backwashing studies.

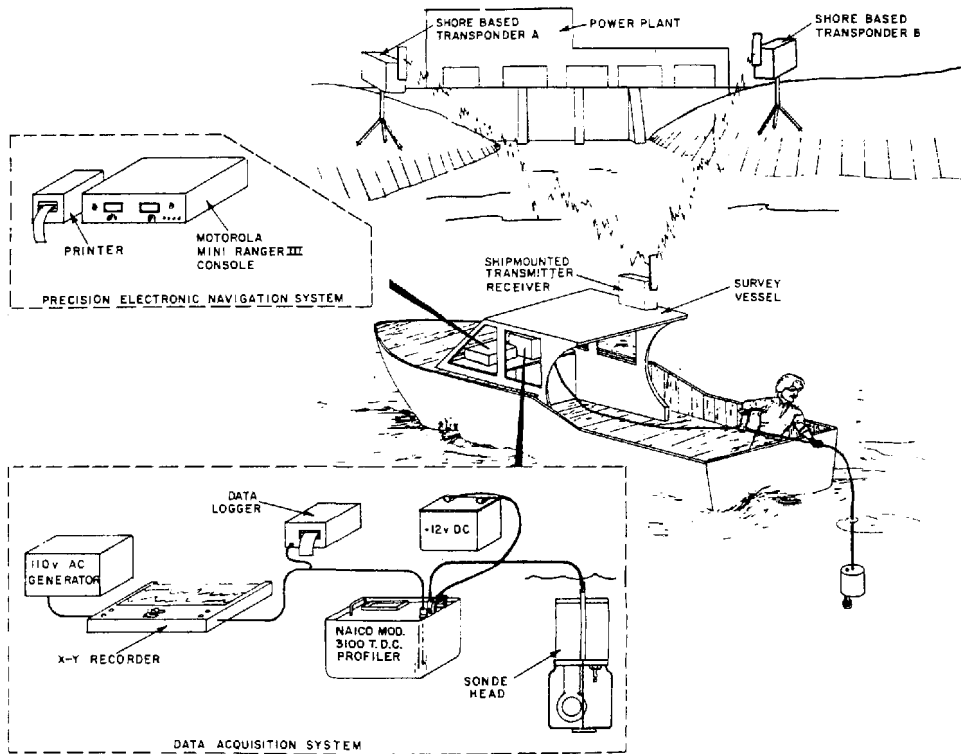


Fig. 2 Instrumentation set up for field surveys.

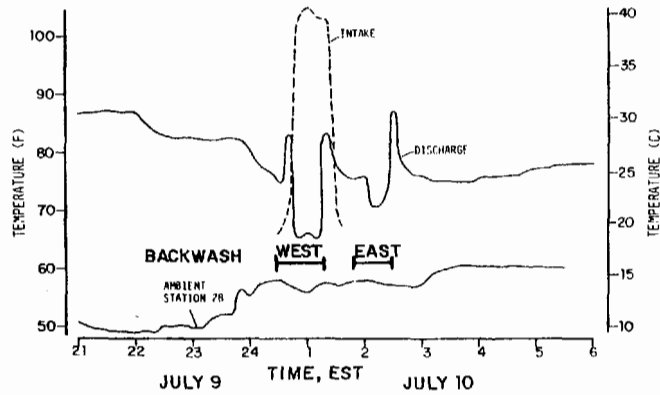


Fig. 3 Temperature monitor data from the west pump waterbox, the discharge canal and the ambient *in situ* unit at Station 28 during backwashing operations on July 9 and 10, 1977.

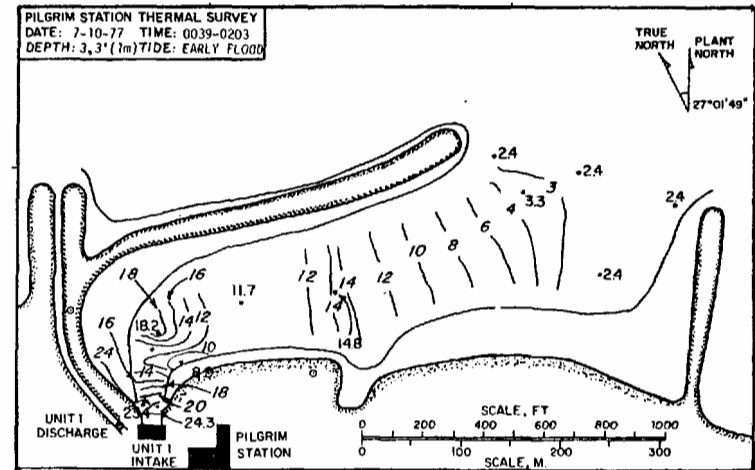
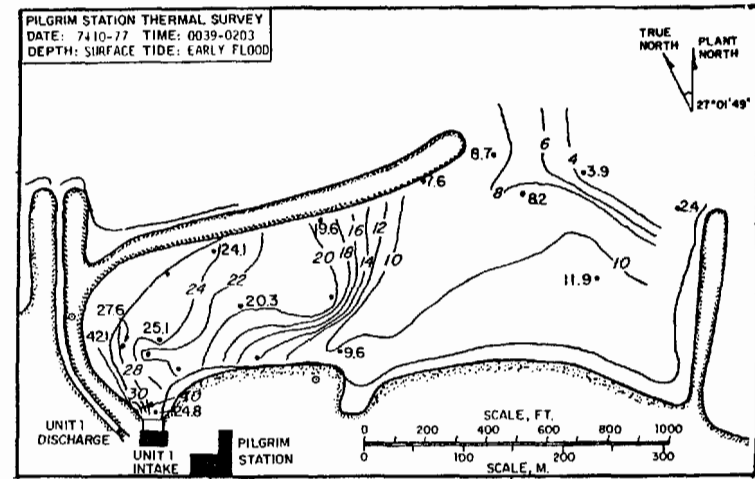


Fig. 4 Contour maps of observed temperature rises ( $\Delta T$ ) in degrees F above ambient during early flood (backwash west pump) at surface and 3.3 ft (1.0m) on July 10, 1977.

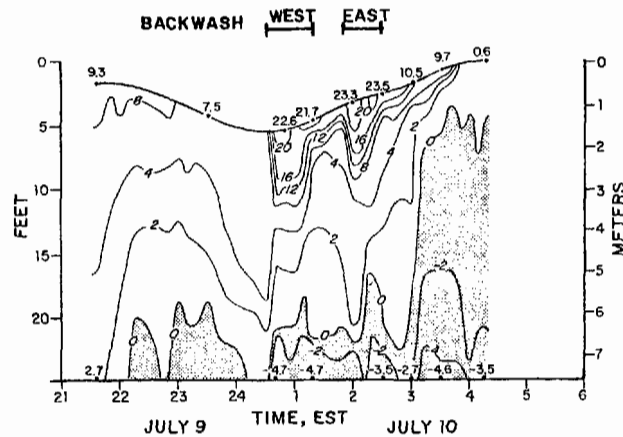


Fig. 5 Temperature data from an anchored survey boat at Station 6 on July 9 and 10, 1977 showing actual temperatures and corresponding  $\Delta T$ 's above ambient in degrees F.

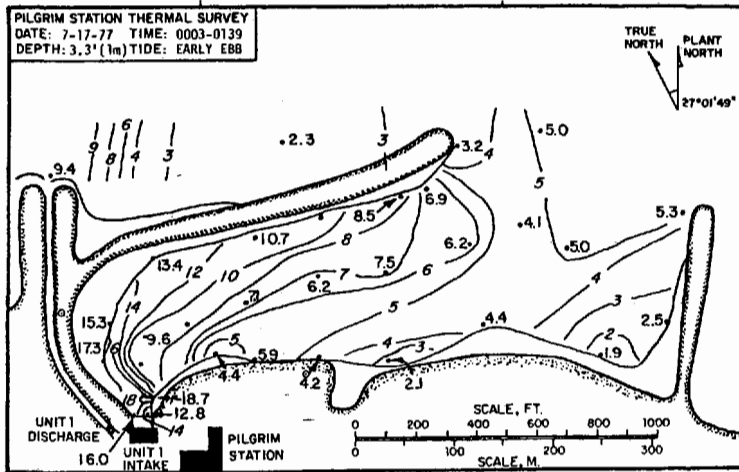
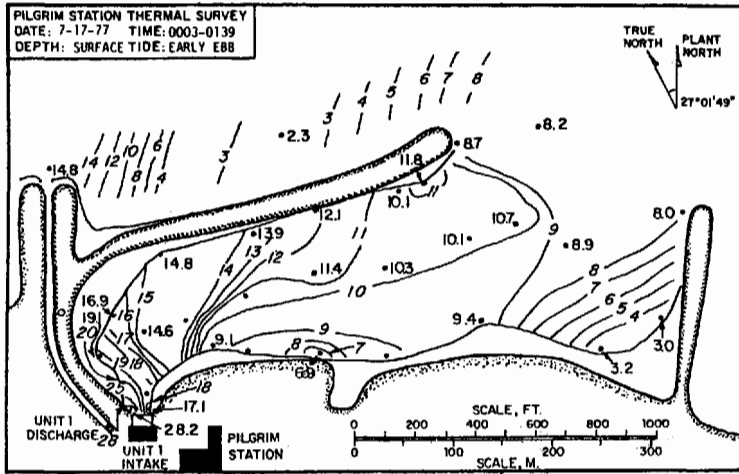


Fig. 6 Contour maps of observed temperature rises ( $\Delta T$ ) in degrees F above ambient during early ebb (backwash west pump) at surface and 3.3 ft. (1.0m) on July 17, 1977.

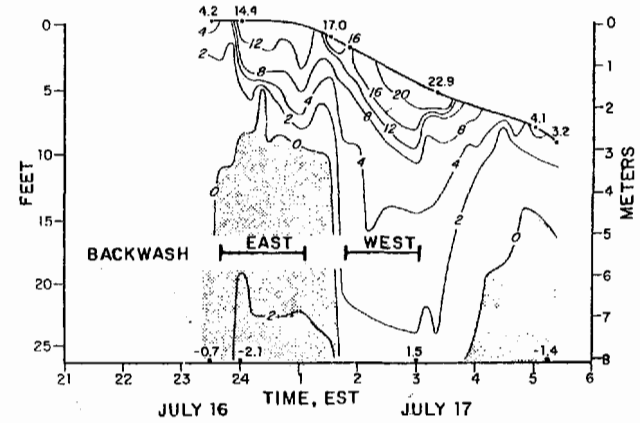


Fig. 7 Temperature data from an anchored survey boat at Station 6 on July 16 and 17, 1977 showing actual temperatures and corresponding  $\Delta T$ 's above ambient in degrees F.

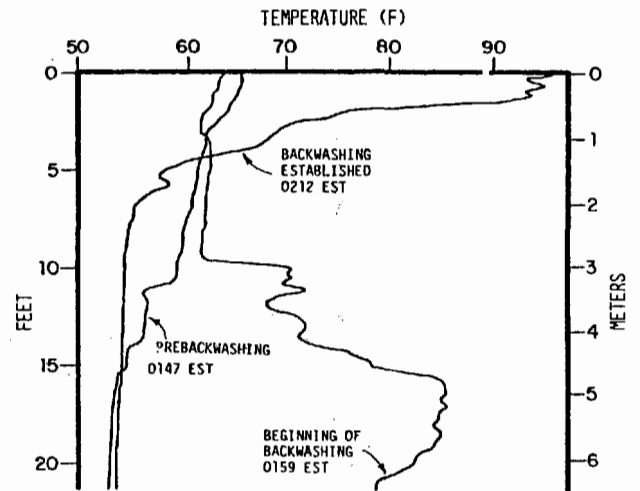


Fig. 8 Temperature profiles from Station 1 during the start of backwashing of the east circulating water pump on July 17, 1977.

# SHORT-TERM DYE DIFFUSION STUDIES IN NEARSHORE WATERS

D.E. Frye\* and S.M. Zivi\*\*

## ABSTRACT

Short-term dye diffusion studies were conducted in the nearshore waters of Lake Michigan and Massachusetts Bay. Measurements of horizontal and vertical diffusion of continuous and batch dye releases were made using a combination of fluorometric and aerial photographic techniques. Results of experiments performed in summer of 1973 on Lake Michigan and fall of 1974 on Massachusetts Bay showed a similar range of values for diffusion coefficients. Horizontal diffusivities ranged over about 2 orders of magnitude with most values falling between 500 and 5000 cm<sup>2</sup>/sec.

An efficient and practical method of using aerial photography for quantitative diffusion studies was developed following work of Ichiye and Plutchak (1966).<sup>[1]</sup> Comparison between the photographic method and standard boat-based fluorometry indicates good agreement between the methods.

## 1. INTRODUCTION

Studies of diffusion in nearshore waters, conducted in Lake Michigan and in Massachusetts Bay, were motivated by a need to forecast the behavior of thermal plumes from power plants. The Lake Michigan experiments were conducted in the summer of 1973 at three sites: the Point Beach Nuclear Generating Station, Two Rivers, Wisconsin; the J.H. Campbell Generating Station, Holland, Michigan; and the D.C. Cook Nuclear Generating Station, Bridgman, Michigan. These sites are located on long, straight shorelines with gently sloping, sandy bottoms, typical of much of the east and west shores of Lake Michigan. Currents at the sites typically flow shore-parallel and are primarily wind-driven. The lake is strongly stratified in summer, and periods of upwelling (particularly on the western shore) and downwelling (particularly on the eastern shore) are common occurrences. Diffusion measurements were made in water 7 to 10 meters deep between 0.5 and 1.0 km offshore.

In the fall of 1974, a similar series of diffusion studies were conducted near the Pilgrim Nuclear Generating Station, Plymouth, Massachusetts. The study site is located just south of Plymouth Harbor on the western shore of the Bay at a point separating Massachusetts Bay in its entirety from Cape

---

\*EG&G, Environmental Consultants, Waltham, Massachusetts, U.S.A.

\*\*Argonne National Laboratory, Argonne, Illinois, U.S.A.

Cod Bay. The waters are semi-enclosed; open to the ocean to the north-east. Currents are primarily shore-parallel and wind-driven. Semidiurnal tidal currents of the order of 5 to 10 cm/sec result from tides whose range is about 3 meters (EG&G, 1976).[2] The bottom gently slopes from shore, and waters are vertically well-mixed during the fall.

At both sites, similar data collection and analysis techniques were used to obtain estimates of horizontal and vertical eddy diffusion coefficients. The Lake Michigan experiments were performed using sodium fluorescein as a tracer (due to an EPA ban on Rhodamine at that time). Rhodamine WT was used in the Massachusetts Bay studies.

Dye dispersion studies in natural water bodies have been performed by a number of investigators including Csanady (1973),[3] Murthy (1972),[4] Huang (1971),[5] Ichiye and Plutchak (1966), [1] Eliason, et al. (1971)[6] and others. However, due to the complex nature of the diffusion phenomenon, neither an adequate theoretical model nor a well-founded engineering approximation exists to describe the range of turbulent diffusion in the ocean or large lakes. In defining an eddy diffusivity, it is assumed that turbulent diffusion is analogous to molecular diffusion with the coefficient of molecular diffusivity replaced by an equivalent, but much larger, coefficient of eddy diffusivity. Studies conducted over a variety of conditions indicate a broad range of diffusion coefficients governed in part by the complex interaction of current shears, thermal stratifications, wave action, wind effects, and topography. The data presented here add to the base of information on diffusion processes in nearshore waters in both large lakes and in semi-enclosed oceanic waters, and suggest diffusion rates similar to those found in previous oceanic studies. The methods described represent techniques for measuring the spread of fluorescent dye tracers in nearshore waters in a more efficient and comprehensive manner than is generally used.

## 2. METHODS

Several experimental techniques were employed in these investigations of nearshore diffusion. These techniques included the use of continuous and instantaneous dye releases measured by continuous-pumped-fluorometry, discrete water sampling, and quantitative aerial photographic dye measurements. A brief discussion of each of the measurement techniques is presented below.

For those measurements where a continuous point-source of dye was used to produce a continuous plume, the dye (as a 5 or 10% solution) was pumped from a 15-gallon drum located on a moored raft. A continuous flow rate of 5 cm<sup>3</sup>/sec was maintained by a peristaltic metering pump injecting the dye 1.5 meters below the surface. Density of the dye solution was adjusted, using ethyl alcohol, to match the density of the water.

Batch dye releases consisted of either 1 gallon of 5% dye solution, adjusted for density, pumped into the water at a depth of 1.5 meters at a single point, or "T" shaped patches deployed from a fast-moving boat. These "T's" were about 300 meters on a side, with an initial width of about 3 meters (see Figure 1). Diffusion of each leg of the "T's" provided information on the smaller scales of turbulent diffusion (3 to 100 meters), while gross distortion of the "T's" indicated the presence of larger scale motions.

In those experiments where the absolute dye concentration was measured, it was sampled using a small boat equipped with a pumping system coupled to a Turner Model 111 fluorometer having a flow-through door. Water was drawn from a single depth through the fluorometer while the boat traversed the dye at a constant speed. The boat position was obtained using a microwave navigation system. Dye concentration and position information (and temperature, when appropriate) were recorded on a strip chart recorder or on an automatic digital data acquisition system. Vertical profiles of dye concentration were obtained by either taking bottle samples from several depths or by lowering the water intake hose and recording the fluorometer output for a series of intake depths.

Relative dye concentration was measured using an aerial photographic technique developed by Ichiye and Plutchak (1966).<sup>[1]</sup> With this technique, aerial photographs of the diffusing dye were taken at frequent intervals using a standard 9 inch format aerial camera with either black and white or color film (both were used). In the Lake Michigan experiments, Kodak Tri-X Aerographic film No. 2403 was used with a Wratten No. 61 filter to enhance the contrast between the fluorescein dye and the lake water. Flight altitudes of 4000 to 5500 feet were used. In the Massachusetts Bay experiments, Kodak Aerocolor No. 2445 negative color film was used at altitudes of 2000 and 4000 feet.

Relative dye concentration is proportional to the intensity of the light in the wave band emitted by the fluorescent dye, assuming low background levels at that wavelength and uniform vertical structure of the dye. For dye released near the surface and initially uniformly mixed to some depth, these assumptions are reasonably accurate. The optical density recorded on the film negative is related to the intensity of the fluorescent emission (or the relative dye concentration) through the characteristic curve for the film. From this curve, the relationship between optical film density and relative dye concentration was determined. Film density was then measured densitometrically using precision microdensitometers (a color microdensitometer was used for the color photography).

The microdensitometers automatically scanned across the film negative and recorded a signal proportional to the film density. Aperture size of the densitometer was chosen such that a rectangle approximately 0.5 meter x 2 meters (on the water surface) was viewed at any one time. This rectangle was oriented such that the larger dimension was along the axis of the dye patch, resulting in a smoothed densitometer trace. Between 10 and 25

scans across each segment of dye were averaged together to obtain a single representative measure of dye spread.

In addition to measuring dye concentration, ambient conditions at each of the study sites were recorded. The results of the ambient measurements are summarized in Table 1.

### Data Analysis

Distribution of a diffusing substance, assuming a uniform flow field with a constant diffusivity, is described by Csanady (1973)[3]

$$\psi = \frac{A}{\sqrt{t}} e^{-x^2/4Kt} \quad (1)$$

where  $\psi$  is the concentration of the diffusing substance, A is a constant, x is the distance from the origin, K is the eddy diffusivity coefficient, and t is time. Equation 1 describes a Gaussian distribution with its mean at the origin of the diffusing substance (assumed to be a point source), and its standard deviation,  $\sigma$ , equal to  $\sqrt{2Kt}$ . It is thus possible to calculate a coefficient of eddy diffusivity from knowledge of the concentration distribution of the diffusing substance and Equation 1.

Calculation of diffusion coefficients from the data collected by the aerial photograph and boat-based fluorometric techniques is outlined below (following Tokar, et al., 1975).[7] Densitometric reduction of photographic data and digitization of boat fluorometric data provided dye concentration as a function of position. Background fluorescence was removed from the records. The center of gravity  $M_1$  (first moment) of each transect across the dye patch was calculated from:

$$M_1 = \frac{\sum_i x_i \psi(x_i)}{\sum_i \psi(x_i)} \quad (2)$$

Those transects taken at about the same time and on the same leg of the "T" were averaged together to produce an average concentration distribution across the leg. From this average concentration distribution, the variance,  $M_2$  (second moment), was calculated from:

$$M_2 = \frac{\sum_i (x_i - M_1)^2 \psi(x_i)}{\sum_i \psi(x_i)} \quad (3)$$

Theoretically, if enough dye patch transects were synoptically recorded, the average concentration curve would approach a Gaussian distribution. In practice, this was approached in the aerial photographic results, unless strong current shears distorted the dye motion. Fluorometric measurement of dye patches, however, was limited by the time necessary to make the measurements, and only a limited number of transects could be made in a short period of time; therefore, the Gaussian assumption was less reliable. After the second moment was calculated, the eddy diffusion coefficient,  $K$ , was calculated as

$$K = \frac{\sigma_1^2 - \sigma_0^2}{2(t_1 - t_0)} \quad (4)$$

where  $\sigma_1^2 = M_2(t_1)$  is the variance of the distribution at time,  $t_1$ , and  $\sigma_0^2$  is the variance of the distribution at time  $t_0$ .

### Results and Conclusions

Results of horizontal measurements of nearshore dye diffusion spanning time periods up to 6 hours and space scales up to several hundred meters are shown in Table 2. Observed values for the eddy diffusion coefficients calculated from Equation 4 ranged from about 100 cm<sup>2</sup>/sec to about 5000 cm<sup>2</sup>/sec for both the lateral and longitudinal directions. No strong evidence for a significant difference between these two directions was observed in those experiments which yielded data on both directions (those studies using the "T" shaped dye patches).

Both the Lake Michigan studies and the Massachusetts Bay studies resulted in a similar range of values for eddy diffusion coefficients. No significant difference between the data sets is distinguishable, although lateral diffusivities seen on the lake were slightly lower than those observed at the oceanic site. Comparison between diffusing dye released in the far-field thermal plume and dye released in nearby ambient waters showed no coherent difference in calculated eddy diffusivities.

The effects of existing oceanic and meteorological conditions on the observed diffusivities are not apparent in the data. In general, the range of wind speeds, wave conditions, and current speeds seen during the studies do not correlate in any obvious way with the measured diffusion coefficients. On October 27, 1974, in the Massachusetts Bay studies, conditions of strong winds and high waves (~2 meters) forced a halt to the boat measurements, and aerial measurements were cut short due to rapid disappearance of the dye. This was apparently attributable to increased vertical mixing due to wave action; even though horizontal diffusivities were at the high end of the measured range, they were not large enough to account for the rapid dispersal of the dye. Similar horizontal diffusivities were observed on October 29 and 30, 1974, when winds were light and wave heights were minimal.

Figure 2 contains diffusion diagrams (after Okubo, 1971)[8] showing eddy diffusivity plotted against a length scale,  $L$ , defined as  $4\sigma$ . The line labeled Okubo on these figures shows the results of a large number of oceanic dye diffusion studies.

In general, the eddy diffusivity measurements made in Lake Michigan and Massachusetts Bay produced results similar to these oceanic measurements with respect to the rate of increase of the diffusion coefficient as a function of patch size. At a particular patch size, however, the near-shore measurements show higher diffusion rates than the oceanic data indicates. The results of Murthy (1970)[8] and Huang (1971)[5] taken in the Great Lakes indicate diffusivities as a function of size very similar to the nearshore results shown here.

Vertical dye measurements made in Lake Michigan indicate values of vertical diffusivity ranging from 0.3 to 2.7  $\text{cm}^2/\text{sec}$ . A single set of profiles obtained in Massachusetts Bay indicates little or no vertical mixing following an initial mixing to a depth of several meters and most of the Lake Michigan data are amenable to this interpretation also. Thus, our conclusions are that vertical diffusion under conditions described here does not exceed 3  $\text{cm}^2/\text{sec}$  after an initial mixing period and may actually be less than this value. This result has been observed previously on the Great Lakes (Csanady, 1973).[3]

Table 3 summarizes the comparison between fluorometric and photographic measurement techniques employed in the Massachusetts Bay experiments. Fluorometric and aerial photographic determinations of the standard deviation of the dye distribution correspond well for most of the measurements. Inconsistencies in the measured values such as at 1048 on October 28, 1974, were probably the result of distortion of the "T," resulting in fluorometric measurements at inappropriate locations. The aerial data collection method has much to recommend it, including ease of data collection and comprehensive spatial results, though it does lack the sensitivity of the fluorometric technique.

### Summary

Results of short-term, nearshore dye studies in Lake Michigan and Massachusetts Bay indicate a range of horizontal diffusivities between about 100  $\text{cm}^2/\text{sec}$  and 5000  $\text{cm}^2/\text{sec}$  over time scales of 0.1 to 6 hours. These results were obtained under calm to moderate conditions, about 1 km offshore in waters about 10 meters deep. They agree well with previous data taken on the Great Lakes, but indicate slightly higher diffusivities at a particular scale size than are generally seen at oceanic sites. The increase in eddy diffusion coefficients as a function of scale size is similar to that observed at oceanic sites. While the short time period of these observations limits their usefulness, the measured values indicate a range of diffusion coefficients applicable to nearshore waters under calm to moderate conditions.

Vertical diffusivity of less than  $3 \text{ cm}^2/\text{sec}$  was observed on several days; but a meaningful numerical result was not obtained, since most of the data are also amenable to an interpretation invoking rapid vertical mixing throughout a well-mixed layer of some depth followed by an extremely low rate of vertical mixing. This well-mixed depth was of the order of 2 meters, but is probably a function of the wind and wave conditions present during the study.

The use of aerial photography to obtain quantitative results for diffusion processes appears to be a valuable technique. Limited time periods and sensitivity may reduce its usefulness, but in some nearshore applications it can result in significantly better and more easily obtained results than boat-based fluorometric techniques. One of the common problems in making fluorometric measurements from small boats is the lack of a visualization of the gross nature of the dye motion. This often results in poorly run experiments and inaccurate results, which the aerial technique can help eliminate. In practice, a combination of the two techniques results in the most accurate and convincing measure of dye mixing.

#### Acknowledgments

The authors are pleased to acknowledge the members of the Argonne National Laboratory Great Lakes Project for support and assistance in the Lake Michigan measurements, and members of the EG&G, Environmental Consultants staff on the Massachusetts Bay program. The Lake Michigan portion of the work was sponsored by the U.S. Energy Research and Development Agency (ERDA). The Massachusetts Bay portion was sponsored by ERDA, Public Service Electric and Gas Company, Electric Power Research Institute, Boston Edison Company, New England Power Company, and the Commonwealth of Massachusetts Division of Water Pollution Control.

#### REFERENCES

1. Ichiye, T. and Plutchak, N.B., "Photodensitometric Measurement of Dye Concentration in the Ocean," *Limnology and Oceanography*, 11(3): 364, July 1966.
2. EG&G, Environmental Consultants, "Phase II Final Report, Forecasting Power Plant Effects on the Coastal Zone." Report B-4441, Waltham, Mass., 1976.
3. Csanady, G.T., "Turbulent Diffusion in the Environment," D. Reidel Publishing Company, Boston, 1973.
4. Murthy, C.R., "Complex Diffusion Processes in Coastal Currents of a Lake," *Journal of Physical Oceanography*, 2:80, 1972.
5. Huang, J.C.K., "Eddy Diffusivity in Lake Michigan," *Journal of Geophysical Research*, 76(33): 8147, November 1971.

6. Eliason, J.R., Daniels, D.G., and Foote, H.P., "Remote Sensing Acquisition of Tracer Dye and Infrared Imagery Information and Interpretation for Industrial Discharge Management," Pacific Northwest Laboratories of Battelle Memorial Institute, March 1971.
7. Tokar, J., et al., "Measurements of Physical Phenomena Related to Power Plant Waste Heat Discharges: Lake Michigan, 1973 and 1974," Argonne National Laboratory, ANL/WR-75-1, 1975.
8. Okubo, A., "Oceanic Diffusion Diagrams," Deep Sea Research 18:789-802, 1971.
9. Murthy, C.R., "An Experimental Study of Horizontal Diffusion in Lake Ontario," Thirteenth Conference on Great Lakes Research, Buffalo, New York, March 31 - April 3, 1970.

TABLE 1. AMBIENT CONDITIONS DURING DIFFUSION MEASUREMENTS.

| Site          | Date     | Time      | Tide Stage | Wind Velocity<br>(m/s) | Wave Height<br>(m) | Current Velocity<br>(Near-surface)<br>(cm/s) | Water Temp.<br>(Near-surface)<br>(°C) | Air Temp.<br>(°C) |
|---------------|----------|-----------|------------|------------------------|--------------------|--|---------------------------------------|-------------------|
| Point Beach 1 | 8-9-73   | 1700-2000 | ----       | 5 at 225°              | ---                | 5 at 240°                                    | 10                                    | 24                |
| Point Beach 2 | 8-23-73  | 1430-1700 | ----       | 5 at 175°              | ---                | 13 at 045°                                   | 18                                    | 16                |
| Point Beach 3 | 8-24-73  | 1000-1200 | ----       | 3 at 120°              | 0.5                | 8 at 015°                                    | 18                                    | 20                |
| Campbell 1    | 9-12-73  | 1356-1444 | ----       | 2 at 195°              | 0.2                | 13 at 200°                                   | 11                                    | 14                |
| Cook 1        | 10-23-73 | 1345-1520 | ----       |                        | ---                | 5 at 200°                                    | 14                                    | 18                |
| Pilgrim 1     | 10-25-74 | 1330-1430 | Ebb        | 8 at 210°              | 0.3                | 7 at 280°                                    | 10                                    | 16                |
| Pilgrim 2     | 10-27-74 | 0935-1309 | High-Ebb   | 6 at 300°              | 1.5                | 3 at 255°                                    | 11                                    | 13                |
| Pilgrim 3     | 10-28-74 | 1000-1603 | Ebb-Low    | Variable               | ---                | 7 at 150°                                    | 10                                    | 8                 |
| Pilgrim 4     | 10-29-74 | 0915-1045 | High       | 4 at 215°              | ---                | 8 at 300°                                    | 10                                    | 15                |
| Pilgrim 5     | 10-30-74 | 0940-1040 | High       | 2 at 200°              | ---                | 11 at 310°                                   | 10                                    | 17                |

TABLE 2. RESULTS OF DIFFUSIVITY MEASUREMENTS.

| Site          | Diffusion Time (s) | K <sub>x</sub> (cm <sup>2</sup> /s) | K <sub>y</sub> (cm <sup>2</sup> /s) | K <sub>z</sub> (cm <sup>2</sup> /s) | Technique  | Comments  |               |      |      |      |     |                                      |                                  |      |      |      |     |      |      |        |     |      |      |      |     |               |      |      |     |     |                                 |                                  |      |      |      |     |      |      |    |     |      |      |      |     |            |      |     |      |     |                                   |  |      |     |      |     |      |      |      |     |        |      |     |     |     |                                   |  |      |      |      |     |      |      |      |     |           |      |      |      |     |                                   |  |      |      |     |     |      |     |      |     |      |     |      |     |           |      |      |      |     |  |  |      |      |      |     |      |      |      |     |       |      |      |     |       |      |      |     |           |     |     |     |     |  |   |      |     |      |     |      |      |     |     |      |      |     |     |      |      |      |     |      |      |     |     |      |      |     |     |      |     |     |     |       |      |      |     |       |      |      |     |       |      |      |     |       |      |      |     |       |      |      |     |       |      |      |     |       |      |      |     |           |      |      |    |     |                                       |  |      |      |     |     |      |      |     |     |           |     |     |      |     |  |  |      |      |      |     |      |      |      |     |      |
|---------------|--------------------|-------------------------------------|-------------------------------------|-------------------------------------|--|---|---------------|------|------|------|-----|--------------------------------------|----------------------------------|------|------|------|-----|------|------|--------|-----|------|------|------|-----|---------------|------|------|-----|-----|---------------------------------|----------------------------------|------|------|------|-----|------|------|----|-----|------|------|------|-----|------------|------|-----|------|-----|-----------------------------------|--|------|-----|------|-----|------|------|------|-----|--------|------|-----|-----|-----|-----------------------------------|--|------|------|------|-----|------|------|------|-----|-----------|------|------|------|-----|-----------------------------------|--|------|------|-----|-----|------|-----|------|-----|------|-----|------|-----|-----------|------|------|------|-----|--|--|------|------|------|-----|------|------|------|-----|-------|------|------|-----|-------|------|------|-----|-----------|-----|-----|-----|-----|--|---|------|-----|------|-----|------|------|-----|-----|------|------|-----|-----|------|------|------|-----|------|------|-----|-----|------|------|-----|-----|------|-----|-----|-----|-------|------|------|-----|-------|------|------|-----|-------|------|------|-----|-------|------|------|-----|-------|------|------|-----|-------|------|------|-----|-------|------|------|-----|-----------|------|------|----|-----|---------------------------------------|--|------|------|-----|-----|------|------|-----|-----|-----------|-----|-----|------|-----|--|--|------|------|------|-----|------|------|------|-----|------|
| Point Beach 1 | 6000               | ----                                | 390                                 | 0.5                                 | fluorometry-<br>continuous injection                 | thermal plume,<br>ambient waters  |               |      |      |      |     |                                      |                                  |      |      |      |     |      |      |        |     |      |      |      |     |               |      |      |     |     |                                 |                                  |      |      |      |     |      |      |    |     |      |      |      |     |            |      |     |      |     |                                   |  |      |     |      |     |      |      |      |     |        |      |     |     |     |                                   |  |      |      |      |     |      |      |      |     |           |      |      |      |     |                                   |  |      |      |     |     |      |     |      |     |      |     |      |     |           |      |      |      |     |  |  |      |      |      |     |      |      |      |     |       |      |      |     |       |      |      |     |           |     |     |     |     |  |   |      |     |      |     |      |      |     |     |      |      |     |     |      |      |      |     |      |      |     |     |      |      |     |     |      |     |     |     |       |      |      |     |       |      |      |     |       |      |      |     |       |      |      |     |       |      |      |     |       |      |      |     |       |      |      |     |           |      |      |    |     |                                       |  |      |      |     |     |      |      |     |     |           |     |     |      |     |  |  |      |      |      |     |      |      |      |     |      |
|               | 5000               | ----                                | 75                                  | 2.7                                 |  |   | Point Beach 2 | 2500 | ---- | 3500 | 1.4 | fluorometry-<br>continuous injection | thermal plume,<br>ambient waters | 4600 | ---- | 2500 | 0.4 | 3100 | ---- | 12,000 | --- | 3500 | ---- | ---- | 1.4 | Point Beach 3 | 4300 | ---- | 130 | --- | fluorometry-<br>batch injection | thermal plume,<br>ambient waters | 4900 | ---- | ---- | 0.3 | 5200 | ---- | 65 | --- | 6000 | ---- | ---- | 0.3 | Campbell 1 | 1260 | 290 | ---- | --- | photography/T-shaped<br>injection |  | 2280 | 480 | ---- | --- | 2880 | 1130 | ---- | --- | Cook 1 | 1500 | 600 | 470 | --- | photography/T-shaped<br>injection |  | 4500 | 2160 | 1260 | --- | 5700 | 5000 | 2600 | --- | Pilgrim 1 | 1200 | ---- | ---- | --- | photography/T-shaped<br>injection |  | 1500 | ---- | 473 | --- | 1680 | 302 | 1798 | --- | 3600 | 487 | 3740 | --- | Pilgrim 2 | 1560 | ---- | ---- | --- | photography and<br>fluorometry/T-shaped<br>injection |  | 4860 | ---- | 2286 | --- | 6180 | 3983 | ---- | --- | 11640 | 3524 | ---- | --- | 12840 | ---- | 5026 | --- | Pilgrim 3 | 840 | 481 | 747 | --- | photography and<br>fluorometry/T-shaped<br>injection | after an initial<br>mixing period,<br>no changes in<br>vertical dye<br>distribution<br>were observed. | 1800 | 770 | 1782 | --- | 3600 | ---- | 284 | --- | 5700 | 1167 | 691 | --- | 6240 | 1096 | ---- | --- | 7200 | 1326 | 624 | --- | 7560 | ---- | 343 | --- | 9000 | 841 | 872 | --- | 10200 | 3052 | ---- | --- | 10620 | ---- | 1520 | --- | 10800 | 1108 | ---- | --- | 11880 | 2579 | ---- | --- | 18300 | 5864 | ---- | --- | 19980 | 3734 | ---- | --- | 21780 | 5153 | ---- | --- | Pilgrim 4 | 2880 | 5323 | 14 | --- | photography of T-<br>shaped injection |  | 3420 | 2763 | 110 | --- | 5400 | 3778 | 280 | --- | Pilgrim 5 | 960 | 137 | ---- | --- |  |  | 1740 | 2002 | 1621 | --- | 2940 | 2055 | 2487 | --- | 3660 |
| Point Beach 2 | 2500               | ----                                | 3500                                | 1.4                                 | fluorometry-<br>continuous injection                 | thermal plume,<br>ambient waters  |               |      |      |      |     |                                      |                                  |      |      |      |     |      |      |        |     |      |      |      |     |               |      |      |     |     |                                 |                                  |      |      |      |     |      |      |    |     |      |      |      |     |            |      |     |      |     |                                   |  |      |     |      |     |      |      |      |     |        |      |     |     |     |                                   |  |      |      |      |     |      |      |      |     |           |      |      |      |     |                                   |  |      |      |     |     |      |     |      |     |      |     |      |     |           |      |      |      |     |  |  |      |      |      |     |      |      |      |     |       |      |      |     |       |      |      |     |           |     |     |     |     |  |   |      |     |      |     |      |      |     |     |      |      |     |     |      |      |      |     |      |      |     |     |      |      |     |     |      |     |     |     |       |      |      |     |       |      |      |     |       |      |      |     |       |      |      |     |       |      |      |     |       |      |      |     |       |      |      |     |           |      |      |    |     |                                       |  |      |      |     |     |      |      |     |     |           |     |     |      |     |  |  |      |      |      |     |      |      |      |     |      |
|               | 4600               | ----                                | 2500                                | 0.4                                 |  |   |               |      |      |      |     |                                      |                                  |      |      |      |     |      |      |        |     |      |      |      |     |               |      |      |     |     |                                 |                                  |      |      |      |     |      |      |    |     |      |      |      |     |            |      |     |      |     |                                   |  |      |     |      |     |      |      |      |     |        |      |     |     |     |                                   |  |      |      |      |     |      |      |      |     |           |      |      |      |     |                                   |  |      |      |     |     |      |     |      |     |      |     |      |     |           |      |      |      |     |  |  |      |      |      |     |      |      |      |     |       |      |      |     |       |      |      |     |           |     |     |     |     |  |   |      |     |      |     |      |      |     |     |      |      |     |     |      |      |      |     |      |      |     |     |      |      |     |     |      |     |     |     |       |      |      |     |       |      |      |     |       |      |      |     |       |      |      |     |       |      |      |     |       |      |      |     |       |      |      |     |           |      |      |    |     |                                       |  |      |      |     |     |      |      |     |     |           |     |     |      |     |  |  |      |      |      |     |      |      |      |     |      |
|               | 3100               | ----                                | 12,000                              | ---                                 |  |   |               |      |      |      |     |                                      |                                  |      |      |      |     |      |      |        |     |      |      |      |     |               |      |      |     |     |                                 |                                  |      |      |      |     |      |      |    |     |      |      |      |     |            |      |     |      |     |                                   |  |      |     |      |     |      |      |      |     |        |      |     |     |     |                                   |  |      |      |      |     |      |      |      |     |           |      |      |      |     |                                   |  |      |      |     |     |      |     |      |     |      |     |      |     |           |      |      |      |     |  |  |      |      |      |     |      |      |      |     |       |      |      |     |       |      |      |     |           |     |     |     |     |  |   |      |     |      |     |      |      |     |     |      |      |     |     |      |      |      |     |      |      |     |     |      |      |     |     |      |     |     |     |       |      |      |     |       |      |      |     |       |      |      |     |       |      |      |     |       |      |      |     |       |      |      |     |       |      |      |     |           |      |      |    |     |                                       |  |      |      |     |     |      |      |     |     |           |     |     |      |     |  |  |      |      |      |     |      |      |      |     |      |
|               | 3500               | ----                                | ----                                | 1.4                                 |  |   |               |      |      |      |     |                                      |                                  |      |      |      |     |      |      |        |     |      |      |      |     |               |      |      |     |     |                                 |                                  |      |      |      |     |      |      |    |     |      |      |      |     |            |      |     |      |     |                                   |  |      |     |      |     |      |      |      |     |        |      |     |     |     |                                   |  |      |      |      |     |      |      |      |     |           |      |      |      |     |                                   |  |      |      |     |     |      |     |      |     |      |     |      |     |           |      |      |      |     |  |  |      |      |      |     |      |      |      |     |       |      |      |     |       |      |      |     |           |     |     |     |     |  |   |      |     |      |     |      |      |     |     |      |      |     |     |      |      |      |     |      |      |     |     |      |      |     |     |      |     |     |     |       |      |      |     |       |      |      |     |       |      |      |     |       |      |      |     |       |      |      |     |       |      |      |     |       |      |      |     |           |      |      |    |     |                                       |  |      |      |     |     |      |      |     |     |           |     |     |      |     |  |  |      |      |      |     |      |      |      |     |      |
| Point Beach 3 | 4300               | ----                                | 130                                 | ---                                 | fluorometry-<br>batch injection                      | thermal plume,<br>ambient waters  |               |      |      |      |     |                                      |                                  |      |      |      |     |      |      |        |     |      |      |      |     |               |      |      |     |     |                                 |                                  |      |      |      |     |      |      |    |     |      |      |      |     |            |      |     |      |     |                                   |  |      |     |      |     |      |      |      |     |        |      |     |     |     |                                   |  |      |      |      |     |      |      |      |     |           |      |      |      |     |                                   |  |      |      |     |     |      |     |      |     |      |     |      |     |           |      |      |      |     |  |  |      |      |      |     |      |      |      |     |       |      |      |     |       |      |      |     |           |     |     |     |     |  |   |      |     |      |     |      |      |     |     |      |      |     |     |      |      |      |     |      |      |     |     |      |      |     |     |      |     |     |     |       |      |      |     |       |      |      |     |       |      |      |     |       |      |      |     |       |      |      |     |       |      |      |     |       |      |      |     |           |      |      |    |     |                                       |  |      |      |     |     |      |      |     |     |           |     |     |      |     |  |  |      |      |      |     |      |      |      |     |      |
|               | 4900               | ----                                | ----                                | 0.3                                 |  |   |               |      |      |      |     |                                      |                                  |      |      |      |     |      |      |        |     |      |      |      |     |               |      |      |     |     |                                 |                                  |      |      |      |     |      |      |    |     |      |      |      |     |            |      |     |      |     |                                   |  |      |     |      |     |      |      |      |     |        |      |     |     |     |                                   |  |      |      |      |     |      |      |      |     |           |      |      |      |     |                                   |  |      |      |     |     |      |     |      |     |      |     |      |     |           |      |      |      |     |  |  |      |      |      |     |      |      |      |     |       |      |      |     |       |      |      |     |           |     |     |     |     |  |   |      |     |      |     |      |      |     |     |      |      |     |     |      |      |      |     |      |      |     |     |      |      |     |     |      |     |     |     |       |      |      |     |       |      |      |     |       |      |      |     |       |      |      |     |       |      |      |     |       |      |      |     |       |      |      |     |           |      |      |    |     |                                       |  |      |      |     |     |      |      |     |     |           |     |     |      |     |  |  |      |      |      |     |      |      |      |     |      |
|               | 5200               | ----                                | 65                                  | ---                                 |  |   |               |      |      |      |     |                                      |                                  |      |      |      |     |      |      |        |     |      |      |      |     |               |      |      |     |     |                                 |                                  |      |      |      |     |      |      |    |     |      |      |      |     |            |      |     |      |     |                                   |  |      |     |      |     |      |      |      |     |        |      |     |     |     |                                   |  |      |      |      |     |      |      |      |     |           |      |      |      |     |                                   |  |      |      |     |     |      |     |      |     |      |     |      |     |           |      |      |      |     |  |  |      |      |      |     |      |      |      |     |       |      |      |     |       |      |      |     |           |     |     |     |     |  |   |      |     |      |     |      |      |     |     |      |      |     |     |      |      |      |     |      |      |     |     |      |      |     |     |      |     |     |     |       |      |      |     |       |      |      |     |       |      |      |     |       |      |      |     |       |      |      |     |       |      |      |     |       |      |      |     |           |      |      |    |     |                                       |  |      |      |     |     |      |      |     |     |           |     |     |      |     |  |  |      |      |      |     |      |      |      |     |      |
|               | 6000               | ----                                | ----                                | 0.3                                 |  |   |               |      |      |      |     |                                      |                                  |      |      |      |     |      |      |        |     |      |      |      |     |               |      |      |     |     |                                 |                                  |      |      |      |     |      |      |    |     |      |      |      |     |            |      |     |      |     |                                   |  |      |     |      |     |      |      |      |     |        |      |     |     |     |                                   |  |      |      |      |     |      |      |      |     |           |      |      |      |     |                                   |  |      |      |     |     |      |     |      |     |      |     |      |     |           |      |      |      |     |  |  |      |      |      |     |      |      |      |     |       |      |      |     |       |      |      |     |           |     |     |     |     |  |   |      |     |      |     |      |      |     |     |      |      |     |     |      |      |      |     |      |      |     |     |      |      |     |     |      |     |     |     |       |      |      |     |       |      |      |     |       |      |      |     |       |      |      |     |       |      |      |     |       |      |      |     |       |      |      |     |           |      |      |    |     |                                       |  |      |      |     |     |      |      |     |     |           |     |     |      |     |  |  |      |      |      |     |      |      |      |     |      |
| Campbell 1    | 1260               | 290                                 | ----                                | ---                                 | photography/T-shaped<br>injection                    |   |               |      |      |      |     |                                      |                                  |      |      |      |     |      |      |        |     |      |      |      |     |               |      |      |     |     |                                 |                                  |      |      |      |     |      |      |    |     |      |      |      |     |            |      |     |      |     |                                   |  |      |     |      |     |      |      |      |     |        |      |     |     |     |                                   |  |      |      |      |     |      |      |      |     |           |      |      |      |     |                                   |  |      |      |     |     |      |     |      |     |      |     |      |     |           |      |      |      |     |  |  |      |      |      |     |      |      |      |     |       |      |      |     |       |      |      |     |           |     |     |     |     |  |   |      |     |      |     |      |      |     |     |      |      |     |     |      |      |      |     |      |      |     |     |      |      |     |     |      |     |     |     |       |      |      |     |       |      |      |     |       |      |      |     |       |      |      |     |       |      |      |     |       |      |      |     |       |      |      |     |           |      |      |    |     |                                       |  |      |      |     |     |      |      |     |     |           |     |     |      |     |  |  |      |      |      |     |      |      |      |     |      |
|               | 2280               | 480                                 | ----                                | ---                                 |  |   |               |      |      |      |     |                                      |                                  |      |      |      |     |      |      |        |     |      |      |      |     |               |      |      |     |     |                                 |                                  |      |      |      |     |      |      |    |     |      |      |      |     |            |      |     |      |     |                                   |  |      |     |      |     |      |      |      |     |        |      |     |     |     |                                   |  |      |      |      |     |      |      |      |     |           |      |      |      |     |                                   |  |      |      |     |     |      |     |      |     |      |     |      |     |           |      |      |      |     |  |  |      |      |      |     |      |      |      |     |       |      |      |     |       |      |      |     |           |     |     |     |     |  |   |      |     |      |     |      |      |     |     |      |      |     |     |      |      |      |     |      |      |     |     |      |      |     |     |      |     |     |     |       |      |      |     |       |      |      |     |       |      |      |     |       |      |      |     |       |      |      |     |       |      |      |     |       |      |      |     |           |      |      |    |     |                                       |  |      |      |     |     |      |      |     |     |           |     |     |      |     |  |  |      |      |      |     |      |      |      |     |      |
|               | 2880               | 1130                                | ----                                | ---                                 |  |   |               |      |      |      |     |                                      |                                  |      |      |      |     |      |      |        |     |      |      |      |     |               |      |      |     |     |                                 |                                  |      |      |      |     |      |      |    |     |      |      |      |     |            |      |     |      |     |                                   |  |      |     |      |     |      |      |      |     |        |      |     |     |     |                                   |  |      |      |      |     |      |      |      |     |           |      |      |      |     |                                   |  |      |      |     |     |      |     |      |     |      |     |      |     |           |      |      |      |     |  |  |      |      |      |     |      |      |      |     |       |      |      |     |       |      |      |     |           |     |     |     |     |  |   |      |     |      |     |      |      |     |     |      |      |     |     |      |      |      |     |      |      |     |     |      |      |     |     |      |     |     |     |       |      |      |     |       |      |      |     |       |      |      |     |       |      |      |     |       |      |      |     |       |      |      |     |       |      |      |     |           |      |      |    |     |                                       |  |      |      |     |     |      |      |     |     |           |     |     |      |     |  |  |      |      |      |     |      |      |      |     |      |
| Cook 1        | 1500               | 600                                 | 470                                 | ---                                 | photography/T-shaped<br>injection                    |   |               |      |      |      |     |                                      |                                  |      |      |      |     |      |      |        |     |      |      |      |     |               |      |      |     |     |                                 |                                  |      |      |      |     |      |      |    |     |      |      |      |     |            |      |     |      |     |                                   |  |      |     |      |     |      |      |      |     |        |      |     |     |     |                                   |  |      |      |      |     |      |      |      |     |           |      |      |      |     |                                   |  |      |      |     |     |      |     |      |     |      |     |      |     |           |      |      |      |     |  |  |      |      |      |     |      |      |      |     |       |      |      |     |       |      |      |     |           |     |     |     |     |  |   |      |     |      |     |      |      |     |     |      |      |     |     |      |      |      |     |      |      |     |     |      |      |     |     |      |     |     |     |       |      |      |     |       |      |      |     |       |      |      |     |       |      |      |     |       |      |      |     |       |      |      |     |       |      |      |     |           |      |      |    |     |                                       |  |      |      |     |     |      |      |     |     |           |     |     |      |     |  |  |      |      |      |     |      |      |      |     |      |
|               | 4500               | 2160                                | 1260                                | ---                                 |  |   |               |      |      |      |     |                                      |                                  |      |      |      |     |      |      |        |     |      |      |      |     |               |      |      |     |     |                                 |                                  |      |      |      |     |      |      |    |     |      |      |      |     |            |      |     |      |     |                                   |  |      |     |      |     |      |      |      |     |        |      |     |     |     |                                   |  |      |      |      |     |      |      |      |     |           |      |      |      |     |                                   |  |      |      |     |     |      |     |      |     |      |     |      |     |           |      |      |      |     |  |  |      |      |      |     |      |      |      |     |       |      |      |     |       |      |      |     |           |     |     |     |     |  |   |      |     |      |     |      |      |     |     |      |      |     |     |      |      |      |     |      |      |     |     |      |      |     |     |      |     |     |     |       |      |      |     |       |      |      |     |       |      |      |     |       |      |      |     |       |      |      |     |       |      |      |     |       |      |      |     |           |      |      |    |     |                                       |  |      |      |     |     |      |      |     |     |           |     |     |      |     |  |  |      |      |      |     |      |      |      |     |      |
|               | 5700               | 5000                                | 2600                                | ---                                 |  |   |               |      |      |      |     |                                      |                                  |      |      |      |     |      |      |        |     |      |      |      |     |               |      |      |     |     |                                 |                                  |      |      |      |     |      |      |    |     |      |      |      |     |            |      |     |      |     |                                   |  |      |     |      |     |      |      |      |     |        |      |     |     |     |                                   |  |      |      |      |     |      |      |      |     |           |      |      |      |     |                                   |  |      |      |     |     |      |     |      |     |      |     |      |     |           |      |      |      |     |  |  |      |      |      |     |      |      |      |     |       |      |      |     |       |      |      |     |           |     |     |     |     |  |   |      |     |      |     |      |      |     |     |      |      |     |     |      |      |      |     |      |      |     |     |      |      |     |     |      |     |     |     |       |      |      |     |       |      |      |     |       |      |      |     |       |      |      |     |       |      |      |     |       |      |      |     |       |      |      |     |           |      |      |    |     |                                       |  |      |      |     |     |      |      |     |     |           |     |     |      |     |  |  |      |      |      |     |      |      |      |     |      |
| Pilgrim 1     | 1200               | ----                                | ----                                | ---                                 | photography/T-shaped<br>injection                    |   |               |      |      |      |     |                                      |                                  |      |      |      |     |      |      |        |     |      |      |      |     |               |      |      |     |     |                                 |                                  |      |      |      |     |      |      |    |     |      |      |      |     |            |      |     |      |     |                                   |  |      |     |      |     |      |      |      |     |        |      |     |     |     |                                   |  |      |      |      |     |      |      |      |     |           |      |      |      |     |                                   |  |      |      |     |     |      |     |      |     |      |     |      |     |           |      |      |      |     |  |  |      |      |      |     |      |      |      |     |       |      |      |     |       |      |      |     |           |     |     |     |     |  |   |      |     |      |     |      |      |     |     |      |      |     |     |      |      |      |     |      |      |     |     |      |      |     |     |      |     |     |     |       |      |      |     |       |      |      |     |       |      |      |     |       |      |      |     |       |      |      |     |       |      |      |     |       |      |      |     |           |      |      |    |     |                                       |  |      |      |     |     |      |      |     |     |           |     |     |      |     |  |  |      |      |      |     |      |      |      |     |      |
|               | 1500               | ----                                | 473                                 | ---                                 |  |   |               |      |      |      |     |                                      |                                  |      |      |      |     |      |      |        |     |      |      |      |     |               |      |      |     |     |                                 |                                  |      |      |      |     |      |      |    |     |      |      |      |     |            |      |     |      |     |                                   |  |      |     |      |     |      |      |      |     |        |      |     |     |     |                                   |  |      |      |      |     |      |      |      |     |           |      |      |      |     |                                   |  |      |      |     |     |      |     |      |     |      |     |      |     |           |      |      |      |     |  |  |      |      |      |     |      |      |      |     |       |      |      |     |       |      |      |     |           |     |     |     |     |  |   |      |     |      |     |      |      |     |     |      |      |     |     |      |      |      |     |      |      |     |     |      |      |     |     |      |     |     |     |       |      |      |     |       |      |      |     |       |      |      |     |       |      |      |     |       |      |      |     |       |      |      |     |       |      |      |     |           |      |      |    |     |                                       |  |      |      |     |     |      |      |     |     |           |     |     |      |     |  |  |      |      |      |     |      |      |      |     |      |
|               | 1680               | 302                                 | 1798                                | ---                                 |  |   |               |      |      |      |     |                                      |                                  |      |      |      |     |      |      |        |     |      |      |      |     |               |      |      |     |     |                                 |                                  |      |      |      |     |      |      |    |     |      |      |      |     |            |      |     |      |     |                                   |  |      |     |      |     |      |      |      |     |        |      |     |     |     |                                   |  |      |      |      |     |      |      |      |     |           |      |      |      |     |                                   |  |      |      |     |     |      |     |      |     |      |     |      |     |           |      |      |      |     |  |  |      |      |      |     |      |      |      |     |       |      |      |     |       |      |      |     |           |     |     |     |     |  |   |      |     |      |     |      |      |     |     |      |      |     |     |      |      |      |     |      |      |     |     |      |      |     |     |      |     |     |     |       |      |      |     |       |      |      |     |       |      |      |     |       |      |      |     |       |      |      |     |       |      |      |     |       |      |      |     |           |      |      |    |     |                                       |  |      |      |     |     |      |      |     |     |           |     |     |      |     |  |  |      |      |      |     |      |      |      |     |      |
|               | 3600               | 487                                 | 3740                                | ---                                 |  |   |               |      |      |      |     |                                      |                                  |      |      |      |     |      |      |        |     |      |      |      |     |               |      |      |     |     |                                 |                                  |      |      |      |     |      |      |    |     |      |      |      |     |            |      |     |      |     |                                   |  |      |     |      |     |      |      |      |     |        |      |     |     |     |                                   |  |      |      |      |     |      |      |      |     |           |      |      |      |     |                                   |  |      |      |     |     |      |     |      |     |      |     |      |     |           |      |      |      |     |  |  |      |      |      |     |      |      |      |     |       |      |      |     |       |      |      |     |           |     |     |     |     |  |   |      |     |      |     |      |      |     |     |      |      |     |     |      |      |      |     |      |      |     |     |      |      |     |     |      |     |     |     |       |      |      |     |       |      |      |     |       |      |      |     |       |      |      |     |       |      |      |     |       |      |      |     |       |      |      |     |           |      |      |    |     |                                       |  |      |      |     |     |      |      |     |     |           |     |     |      |     |  |  |      |      |      |     |      |      |      |     |      |
| Pilgrim 2     | 1560               | ----                                | ----                                | ---                                 | photography and<br>fluorometry/T-shaped<br>injection |   |               |      |      |      |     |                                      |                                  |      |      |      |     |      |      |        |     |      |      |      |     |               |      |      |     |     |                                 |                                  |      |      |      |     |      |      |    |     |      |      |      |     |            |      |     |      |     |                                   |  |      |     |      |     |      |      |      |     |        |      |     |     |     |                                   |  |      |      |      |     |      |      |      |     |           |      |      |      |     |                                   |  |      |      |     |     |      |     |      |     |      |     |      |     |           |      |      |      |     |  |  |      |      |      |     |      |      |      |     |       |      |      |     |       |      |      |     |           |     |     |     |     |  |   |      |     |      |     |      |      |     |     |      |      |     |     |      |      |      |     |      |      |     |     |      |      |     |     |      |     |     |     |       |      |      |     |       |      |      |     |       |      |      |     |       |      |      |     |       |      |      |     |       |      |      |     |       |      |      |     |           |      |      |    |     |                                       |  |      |      |     |     |      |      |     |     |           |     |     |      |     |  |  |      |      |      |     |      |      |      |     |      |
|               | 4860               | ----                                | 2286                                | ---                                 |  |   |               |      |      |      |     |                                      |                                  |      |      |      |     |      |      |        |     |      |      |      |     |               |      |      |     |     |                                 |                                  |      |      |      |     |      |      |    |     |      |      |      |     |            |      |     |      |     |                                   |  |      |     |      |     |      |      |      |     |        |      |     |     |     |                                   |  |      |      |      |     |      |      |      |     |           |      |      |      |     |                                   |  |      |      |     |     |      |     |      |     |      |     |      |     |           |      |      |      |     |  |  |      |      |      |     |      |      |      |     |       |      |      |     |       |      |      |     |           |     |     |     |     |  |   |      |     |      |     |      |      |     |     |      |      |     |     |      |      |      |     |      |      |     |     |      |      |     |     |      |     |     |     |       |      |      |     |       |      |      |     |       |      |      |     |       |      |      |     |       |      |      |     |       |      |      |     |       |      |      |     |           |      |      |    |     |                                       |  |      |      |     |     |      |      |     |     |           |     |     |      |     |  |  |      |      |      |     |      |      |      |     |      |
|               | 6180               | 3983                                | ----                                | ---                                 |  |   |               |      |      |      |     |                                      |                                  |      |      |      |     |      |      |        |     |      |      |      |     |               |      |      |     |     |                                 |                                  |      |      |      |     |      |      |    |     |      |      |      |     |            |      |     |      |     |                                   |  |      |     |      |     |      |      |      |     |        |      |     |     |     |                                   |  |      |      |      |     |      |      |      |     |           |      |      |      |     |                                   |  |      |      |     |     |      |     |      |     |      |     |      |     |           |      |      |      |     |  |  |      |      |      |     |      |      |      |     |       |      |      |     |       |      |      |     |           |     |     |     |     |  |   |      |     |      |     |      |      |     |     |      |      |     |     |      |      |      |     |      |      |     |     |      |      |     |     |      |     |     |     |       |      |      |     |       |      |      |     |       |      |      |     |       |      |      |     |       |      |      |     |       |      |      |     |       |      |      |     |           |      |      |    |     |                                       |  |      |      |     |     |      |      |     |     |           |     |     |      |     |  |  |      |      |      |     |      |      |      |     |      |
|               | 11640              | 3524                                | ----                                | ---                                 |  |   |               |      |      |      |     |                                      |                                  |      |      |      |     |      |      |        |     |      |      |      |     |               |      |      |     |     |                                 |                                  |      |      |      |     |      |      |    |     |      |      |      |     |            |      |     |      |     |                                   |  |      |     |      |     |      |      |      |     |        |      |     |     |     |                                   |  |      |      |      |     |      |      |      |     |           |      |      |      |     |                                   |  |      |      |     |     |      |     |      |     |      |     |      |     |           |      |      |      |     |  |  |      |      |      |     |      |      |      |     |       |      |      |     |       |      |      |     |           |     |     |     |     |  |   |      |     |      |     |      |      |     |     |      |      |     |     |      |      |      |     |      |      |     |     |      |      |     |     |      |     |     |     |       |      |      |     |       |      |      |     |       |      |      |     |       |      |      |     |       |      |      |     |       |      |      |     |       |      |      |     |           |      |      |    |     |                                       |  |      |      |     |     |      |      |     |     |           |     |     |      |     |  |  |      |      |      |     |      |      |      |     |      |
|               | 12840              | ----                                | 5026                                | ---                                 |  |   |               |      |      |      |     |                                      |                                  |      |      |      |     |      |      |        |     |      |      |      |     |               |      |      |     |     |                                 |                                  |      |      |      |     |      |      |    |     |      |      |      |     |            |      |     |      |     |                                   |  |      |     |      |     |      |      |      |     |        |      |     |     |     |                                   |  |      |      |      |     |      |      |      |     |           |      |      |      |     |                                   |  |      |      |     |     |      |     |      |     |      |     |      |     |           |      |      |      |     |  |  |      |      |      |     |      |      |      |     |       |      |      |     |       |      |      |     |           |     |     |     |     |  |   |      |     |      |     |      |      |     |     |      |      |     |     |      |      |      |     |      |      |     |     |      |      |     |     |      |     |     |     |       |      |      |     |       |      |      |     |       |      |      |     |       |      |      |     |       |      |      |     |       |      |      |     |       |      |      |     |           |      |      |    |     |                                       |  |      |      |     |     |      |      |     |     |           |     |     |      |     |  |  |      |      |      |     |      |      |      |     |      |
| Pilgrim 3     | 840                | 481                                 | 747                                 | ---                                 | photography and<br>fluorometry/T-shaped<br>injection | after an initial<br>mixing period,<br>no changes in<br>vertical dye<br>distribution<br>were observed. |               |      |      |      |     |                                      |                                  |      |      |      |     |      |      |        |     |      |      |      |     |               |      |      |     |     |                                 |                                  |      |      |      |     |      |      |    |     |      |      |      |     |            |      |     |      |     |                                   |  |      |     |      |     |      |      |      |     |        |      |     |     |     |                                   |  |      |      |      |     |      |      |      |     |           |      |      |      |     |                                   |  |      |      |     |     |      |     |      |     |      |     |      |     |           |      |      |      |     |  |  |      |      |      |     |      |      |      |     |       |      |      |     |       |      |      |     |           |     |     |     |     |  |   |      |     |      |     |      |      |     |     |      |      |     |     |      |      |      |     |      |      |     |     |      |      |     |     |      |     |     |     |       |      |      |     |       |      |      |     |       |      |      |     |       |      |      |     |       |      |      |     |       |      |      |     |       |      |      |     |           |      |      |    |     |                                       |  |      |      |     |     |      |      |     |     |           |     |     |      |     |  |  |      |      |      |     |      |      |      |     |      |
|               | 1800               | 770                                 | 1782                                | ---                                 |  |   |               |      |      |      |     |                                      |                                  |      |      |      |     |      |      |        |     |      |      |      |     |               |      |      |     |     |                                 |                                  |      |      |      |     |      |      |    |     |      |      |      |     |            |      |     |      |     |                                   |  |      |     |      |     |      |      |      |     |        |      |     |     |     |                                   |  |      |      |      |     |      |      |      |     |           |      |      |      |     |                                   |  |      |      |     |     |      |     |      |     |      |     |      |     |           |      |      |      |     |  |  |      |      |      |     |      |      |      |     |       |      |      |     |       |      |      |     |           |     |     |     |     |  |   |      |     |      |     |      |      |     |     |      |      |     |     |      |      |      |     |      |      |     |     |      |      |     |     |      |     |     |     |       |      |      |     |       |      |      |     |       |      |      |     |       |      |      |     |       |      |      |     |       |      |      |     |       |      |      |     |           |      |      |    |     |                                       |  |      |      |     |     |      |      |     |     |           |     |     |      |     |  |  |      |      |      |     |      |      |      |     |      |
|               | 3600               | ----                                | 284                                 | ---                                 |  |   |               |      |      |      |     |                                      |                                  |      |      |      |     |      |      |        |     |      |      |      |     |               |      |      |     |     |                                 |                                  |      |      |      |     |      |      |    |     |      |      |      |     |            |      |     |      |     |                                   |  |      |     |      |     |      |      |      |     |        |      |     |     |     |                                   |  |      |      |      |     |      |      |      |     |           |      |      |      |     |                                   |  |      |      |     |     |      |     |      |     |      |     |      |     |           |      |      |      |     |  |  |      |      |      |     |      |      |      |     |       |      |      |     |       |      |      |     |           |     |     |     |     |  |   |      |     |      |     |      |      |     |     |      |      |     |     |      |      |      |     |      |      |     |     |      |      |     |     |      |     |     |     |       |      |      |     |       |      |      |     |       |      |      |     |       |      |      |     |       |      |      |     |       |      |      |     |       |      |      |     |           |      |      |    |     |                                       |  |      |      |     |     |      |      |     |     |           |     |     |      |     |  |  |      |      |      |     |      |      |      |     |      |
|               | 5700               | 1167                                | 691                                 | ---                                 |  |   |               |      |      |      |     |                                      |                                  |      |      |      |     |      |      |        |     |      |      |      |     |               |      |      |     |     |                                 |                                  |      |      |      |     |      |      |    |     |      |      |      |     |            |      |     |      |     |                                   |  |      |     |      |     |      |      |      |     |        |      |     |     |     |                                   |  |      |      |      |     |      |      |      |     |           |      |      |      |     |                                   |  |      |      |     |     |      |     |      |     |      |     |      |     |           |      |      |      |     |  |  |      |      |      |     |      |      |      |     |       |      |      |     |       |      |      |     |           |     |     |     |     |  |   |      |     |      |     |      |      |     |     |      |      |     |     |      |      |      |     |      |      |     |     |      |      |     |     |      |     |     |     |       |      |      |     |       |      |      |     |       |      |      |     |       |      |      |     |       |      |      |     |       |      |      |     |       |      |      |     |           |      |      |    |     |                                       |  |      |      |     |     |      |      |     |     |           |     |     |      |     |  |  |      |      |      |     |      |      |      |     |      |
|               | 6240               | 1096                                | ----                                | ---                                 |  |   |               |      |      |      |     |                                      |                                  |      |      |      |     |      |      |        |     |      |      |      |     |               |      |      |     |     |                                 |                                  |      |      |      |     |      |      |    |     |      |      |      |     |            |      |     |      |     |                                   |  |      |     |      |     |      |      |      |     |        |      |     |     |     |                                   |  |      |      |      |     |      |      |      |     |           |      |      |      |     |                                   |  |      |      |     |     |      |     |      |     |      |     |      |     |           |      |      |      |     |  |  |      |      |      |     |      |      |      |     |       |      |      |     |       |      |      |     |           |     |     |     |     |  |   |      |     |      |     |      |      |     |     |      |      |     |     |      |      |      |     |      |      |     |     |      |      |     |     |      |     |     |     |       |      |      |     |       |      |      |     |       |      |      |     |       |      |      |     |       |      |      |     |       |      |      |     |       |      |      |     |           |      |      |    |     |                                       |  |      |      |     |     |      |      |     |     |           |     |     |      |     |  |  |      |      |      |     |      |      |      |     |      |
|               | 7200               | 1326                                | 624                                 | ---                                 |  |   |               |      |      |      |     |                                      |                                  |      |      |      |     |      |      |        |     |      |      |      |     |               |      |      |     |     |                                 |                                  |      |      |      |     |      |      |    |     |      |      |      |     |            |      |     |      |     |                                   |  |      |     |      |     |      |      |      |     |        |      |     |     |     |                                   |  |      |      |      |     |      |      |      |     |           |      |      |      |     |                                   |  |      |      |     |     |      |     |      |     |      |     |      |     |           |      |      |      |     |  |  |      |      |      |     |      |      |      |     |       |      |      |     |       |      |      |     |           |     |     |     |     |  |   |      |     |      |     |      |      |     |     |      |      |     |     |      |      |      |     |      |      |     |     |      |      |     |     |      |     |     |     |       |      |      |     |       |      |      |     |       |      |      |     |       |      |      |     |       |      |      |     |       |      |      |     |       |      |      |     |           |      |      |    |     |                                       |  |      |      |     |     |      |      |     |     |           |     |     |      |     |  |  |      |      |      |     |      |      |      |     |      |
|               | 7560               | ----                                | 343                                 | ---                                 |  |   |               |      |      |      |     |                                      |                                  |      |      |      |     |      |      |        |     |      |      |      |     |               |      |      |     |     |                                 |                                  |      |      |      |     |      |      |    |     |      |      |      |     |            |      |     |      |     |                                   |  |      |     |      |     |      |      |      |     |        |      |     |     |     |                                   |  |      |      |      |     |      |      |      |     |           |      |      |      |     |                                   |  |      |      |     |     |      |     |      |     |      |     |      |     |           |      |      |      |     |  |  |      |      |      |     |      |      |      |     |       |      |      |     |       |      |      |     |           |     |     |     |     |  |   |      |     |      |     |      |      |     |     |      |      |     |     |      |      |      |     |      |      |     |     |      |      |     |     |      |     |     |     |       |      |      |     |       |      |      |     |       |      |      |     |       |      |      |     |       |      |      |     |       |      |      |     |       |      |      |     |           |      |      |    |     |                                       |  |      |      |     |     |      |      |     |     |           |     |     |      |     |  |  |      |      |      |     |      |      |      |     |      |
|               | 9000               | 841                                 | 872                                 | ---                                 |  |   |               |      |      |      |     |                                      |                                  |      |      |      |     |      |      |        |     |      |      |      |     |               |      |      |     |     |                                 |                                  |      |      |      |     |      |      |    |     |      |      |      |     |            |      |     |      |     |                                   |  |      |     |      |     |      |      |      |     |        |      |     |     |     |                                   |  |      |      |      |     |      |      |      |     |           |      |      |      |     |                                   |  |      |      |     |     |      |     |      |     |      |     |      |     |           |      |      |      |     |  |  |      |      |      |     |      |      |      |     |       |      |      |     |       |      |      |     |           |     |     |     |     |  |   |      |     |      |     |      |      |     |     |      |      |     |     |      |      |      |     |      |      |     |     |      |      |     |     |      |     |     |     |       |      |      |     |       |      |      |     |       |      |      |     |       |      |      |     |       |      |      |     |       |      |      |     |       |      |      |     |           |      |      |    |     |                                       |  |      |      |     |     |      |      |     |     |           |     |     |      |     |  |  |      |      |      |     |      |      |      |     |      |
|               | 10200              | 3052                                | ----                                | ---                                 |  |   |               |      |      |      |     |                                      |                                  |      |      |      |     |      |      |        |     |      |      |      |     |               |      |      |     |     |                                 |                                  |      |      |      |     |      |      |    |     |      |      |      |     |            |      |     |      |     |                                   |  |      |     |      |     |      |      |      |     |        |      |     |     |     |                                   |  |      |      |      |     |      |      |      |     |           |      |      |      |     |                                   |  |      |      |     |     |      |     |      |     |      |     |      |     |           |      |      |      |     |  |  |      |      |      |     |      |      |      |     |       |      |      |     |       |      |      |     |           |     |     |     |     |  |   |      |     |      |     |      |      |     |     |      |      |     |     |      |      |      |     |      |      |     |     |      |      |     |     |      |     |     |     |       |      |      |     |       |      |      |     |       |      |      |     |       |      |      |     |       |      |      |     |       |      |      |     |       |      |      |     |           |      |      |    |     |                                       |  |      |      |     |     |      |      |     |     |           |     |     |      |     |  |  |      |      |      |     |      |      |      |     |      |
|               | 10620              | ----                                | 1520                                | ---                                 |  |   |               |      |      |      |     |                                      |                                  |      |      |      |     |      |      |        |     |      |      |      |     |               |      |      |     |     |                                 |                                  |      |      |      |     |      |      |    |     |      |      |      |     |            |      |     |      |     |                                   |  |      |     |      |     |      |      |      |     |        |      |     |     |     |                                   |  |      |      |      |     |      |      |      |     |           |      |      |      |     |                                   |  |      |      |     |     |      |     |      |     |      |     |      |     |           |      |      |      |     |  |  |      |      |      |     |      |      |      |     |       |      |      |     |       |      |      |     |           |     |     |     |     |  |   |      |     |      |     |      |      |     |     |      |      |     |     |      |      |      |     |      |      |     |     |      |      |     |     |      |     |     |     |       |      |      |     |       |      |      |     |       |      |      |     |       |      |      |     |       |      |      |     |       |      |      |     |       |      |      |     |           |      |      |    |     |                                       |  |      |      |     |     |      |      |     |     |           |     |     |      |     |  |  |      |      |      |     |      |      |      |     |      |
|               | 10800              | 1108                                | ----                                | ---                                 |  |   |               |      |      |      |     |                                      |                                  |      |      |      |     |      |      |        |     |      |      |      |     |               |      |      |     |     |                                 |                                  |      |      |      |     |      |      |    |     |      |      |      |     |            |      |     |      |     |                                   |  |      |     |      |     |      |      |      |     |        |      |     |     |     |                                   |  |      |      |      |     |      |      |      |     |           |      |      |      |     |                                   |  |      |      |     |     |      |     |      |     |      |     |      |     |           |      |      |      |     |  |  |      |      |      |     |      |      |      |     |       |      |      |     |       |      |      |     |           |     |     |     |     |  |   |      |     |      |     |      |      |     |     |      |      |     |     |      |      |      |     |      |      |     |     |      |      |     |     |      |     |     |     |       |      |      |     |       |      |      |     |       |      |      |     |       |      |      |     |       |      |      |     |       |      |      |     |       |      |      |     |           |      |      |    |     |                                       |  |      |      |     |     |      |      |     |     |           |     |     |      |     |  |  |      |      |      |     |      |      |      |     |      |
|               | 11880              | 2579                                | ----                                | ---                                 |  |   |               |      |      |      |     |                                      |                                  |      |      |      |     |      |      |        |     |      |      |      |     |               |      |      |     |     |                                 |                                  |      |      |      |     |      |      |    |     |      |      |      |     |            |      |     |      |     |                                   |  |      |     |      |     |      |      |      |     |        |      |     |     |     |                                   |  |      |      |      |     |      |      |      |     |           |      |      |      |     |                                   |  |      |      |     |     |      |     |      |     |      |     |      |     |           |      |      |      |     |  |  |      |      |      |     |      |      |      |     |       |      |      |     |       |      |      |     |           |     |     |     |     |  |   |      |     |      |     |      |      |     |     |      |      |     |     |      |      |      |     |      |      |     |     |      |      |     |     |      |     |     |     |       |      |      |     |       |      |      |     |       |      |      |     |       |      |      |     |       |      |      |     |       |      |      |     |       |      |      |     |           |      |      |    |     |                                       |  |      |      |     |     |      |      |     |     |           |     |     |      |     |  |  |      |      |      |     |      |      |      |     |      |
|               | 18300              | 5864                                | ----                                | ---                                 |  |   |               |      |      |      |     |                                      |                                  |      |      |      |     |      |      |        |     |      |      |      |     |               |      |      |     |     |                                 |                                  |      |      |      |     |      |      |    |     |      |      |      |     |            |      |     |      |     |                                   |  |      |     |      |     |      |      |      |     |        |      |     |     |     |                                   |  |      |      |      |     |      |      |      |     |           |      |      |      |     |                                   |  |      |      |     |     |      |     |      |     |      |     |      |     |           |      |      |      |     |  |  |      |      |      |     |      |      |      |     |       |      |      |     |       |      |      |     |           |     |     |     |     |  |   |      |     |      |     |      |      |     |     |      |      |     |     |      |      |      |     |      |      |     |     |      |      |     |     |      |     |     |     |       |      |      |     |       |      |      |     |       |      |      |     |       |      |      |     |       |      |      |     |       |      |      |     |       |      |      |     |           |      |      |    |     |                                       |  |      |      |     |     |      |      |     |     |           |     |     |      |     |  |  |      |      |      |     |      |      |      |     |      |
|               | 19980              | 3734                                | ----                                | ---                                 |  |   |               |      |      |      |     |                                      |                                  |      |      |      |     |      |      |        |     |      |      |      |     |               |      |      |     |     |                                 |                                  |      |      |      |     |      |      |    |     |      |      |      |     |            |      |     |      |     |                                   |  |      |     |      |     |      |      |      |     |        |      |     |     |     |                                   |  |      |      |      |     |      |      |      |     |           |      |      |      |     |                                   |  |      |      |     |     |      |     |      |     |      |     |      |     |           |      |      |      |     |  |  |      |      |      |     |      |      |      |     |       |      |      |     |       |      |      |     |           |     |     |     |     |  |   |      |     |      |     |      |      |     |     |      |      |     |     |      |      |      |     |      |      |     |     |      |      |     |     |      |     |     |     |       |      |      |     |       |      |      |     |       |      |      |     |       |      |      |     |       |      |      |     |       |      |      |     |       |      |      |     |           |      |      |    |     |                                       |  |      |      |     |     |      |      |     |     |           |     |     |      |     |  |  |      |      |      |     |      |      |      |     |      |
| 21780         | 5153               | ----                                | ---                                 |                                     |  |   |               |      |      |      |     |                                      |                                  |      |      |      |     |      |      |        |     |      |      |      |     |               |      |      |     |     |                                 |                                  |      |      |      |     |      |      |    |     |      |      |      |     |            |      |     |      |     |                                   |  |      |     |      |     |      |      |      |     |        |      |     |     |     |                                   |  |      |      |      |     |      |      |      |     |           |      |      |      |     |                                   |  |      |      |     |     |      |     |      |     |      |     |      |     |           |      |      |      |     |  |  |      |      |      |     |      |      |      |     |       |      |      |     |       |      |      |     |           |     |     |     |     |  |   |      |     |      |     |      |      |     |     |      |      |     |     |      |      |      |     |      |      |     |     |      |      |     |     |      |     |     |     |       |      |      |     |       |      |      |     |       |      |      |     |       |      |      |     |       |      |      |     |       |      |      |     |       |      |      |     |           |      |      |    |     |                                       |  |      |      |     |     |      |      |     |     |           |     |     |      |     |  |  |      |      |      |     |      |      |      |     |      |
| Pilgrim 4     | 2880               | 5323                                | 14                                  | ---                                 | photography of T-<br>shaped injection                |   |               |      |      |      |     |                                      |                                  |      |      |      |     |      |      |        |     |      |      |      |     |               |      |      |     |     |                                 |                                  |      |      |      |     |      |      |    |     |      |      |      |     |            |      |     |      |     |                                   |  |      |     |      |     |      |      |      |     |        |      |     |     |     |                                   |  |      |      |      |     |      |      |      |     |           |      |      |      |     |                                   |  |      |      |     |     |      |     |      |     |      |     |      |     |           |      |      |      |     |  |  |      |      |      |     |      |      |      |     |       |      |      |     |       |      |      |     |           |     |     |     |     |  |   |      |     |      |     |      |      |     |     |      |      |     |     |      |      |      |     |      |      |     |     |      |      |     |     |      |     |     |     |       |      |      |     |       |      |      |     |       |      |      |     |       |      |      |     |       |      |      |     |       |      |      |     |       |      |      |     |           |      |      |    |     |                                       |  |      |      |     |     |      |      |     |     |           |     |     |      |     |  |  |      |      |      |     |      |      |      |     |      |
|               | 3420               | 2763                                | 110                                 | ---                                 |  |   |               |      |      |      |     |                                      |                                  |      |      |      |     |      |      |        |     |      |      |      |     |               |      |      |     |     |                                 |                                  |      |      |      |     |      |      |    |     |      |      |      |     |            |      |     |      |     |                                   |  |      |     |      |     |      |      |      |     |        |      |     |     |     |                                   |  |      |      |      |     |      |      |      |     |           |      |      |      |     |                                   |  |      |      |     |     |      |     |      |     |      |     |      |     |           |      |      |      |     |  |  |      |      |      |     |      |      |      |     |       |      |      |     |       |      |      |     |           |     |     |     |     |  |   |      |     |      |     |      |      |     |     |      |      |     |     |      |      |      |     |      |      |     |     |      |      |     |     |      |     |     |     |       |      |      |     |       |      |      |     |       |      |      |     |       |      |      |     |       |      |      |     |       |      |      |     |       |      |      |     |           |      |      |    |     |                                       |  |      |      |     |     |      |      |     |     |           |     |     |      |     |  |  |      |      |      |     |      |      |      |     |      |
|               | 5400               | 3778                                | 280                                 | ---                                 |  |   |               |      |      |      |     |                                      |                                  |      |      |      |     |      |      |        |     |      |      |      |     |               |      |      |     |     |                                 |                                  |      |      |      |     |      |      |    |     |      |      |      |     |            |      |     |      |     |                                   |  |      |     |      |     |      |      |      |     |        |      |     |     |     |                                   |  |      |      |      |     |      |      |      |     |           |      |      |      |     |                                   |  |      |      |     |     |      |     |      |     |      |     |      |     |           |      |      |      |     |  |  |      |      |      |     |      |      |      |     |       |      |      |     |       |      |      |     |           |     |     |     |     |  |   |      |     |      |     |      |      |     |     |      |      |     |     |      |      |      |     |      |      |     |     |      |      |     |     |      |     |     |     |       |      |      |     |       |      |      |     |       |      |      |     |       |      |      |     |       |      |      |     |       |      |      |     |       |      |      |     |           |      |      |    |     |                                       |  |      |      |     |     |      |      |     |     |           |     |     |      |     |  |  |      |      |      |     |      |      |      |     |      |
| Pilgrim 5     | 960                | 137                                 | ----                                | ---                                 |  |   |               |      |      |      |     |                                      |                                  |      |      |      |     |      |      |        |     |      |      |      |     |               |      |      |     |     |                                 |                                  |      |      |      |     |      |      |    |     |      |      |      |     |            |      |     |      |     |                                   |  |      |     |      |     |      |      |      |     |        |      |     |     |     |                                   |  |      |      |      |     |      |      |      |     |           |      |      |      |     |                                   |  |      |      |     |     |      |     |      |     |      |     |      |     |           |      |      |      |     |  |  |      |      |      |     |      |      |      |     |       |      |      |     |       |      |      |     |           |     |     |     |     |  |   |      |     |      |     |      |      |     |     |      |      |     |     |      |      |      |     |      |      |     |     |      |      |     |     |      |     |     |     |       |      |      |     |       |      |      |     |       |      |      |     |       |      |      |     |       |      |      |     |       |      |      |     |       |      |      |     |           |      |      |    |     |                                       |  |      |      |     |     |      |      |     |     |           |     |     |      |     |  |  |      |      |      |     |      |      |      |     |      |
|               | 1740               | 2002                                | 1621                                | ---                                 |  |   |               |      |      |      |     |                                      |                                  |      |      |      |     |      |      |        |     |      |      |      |     |               |      |      |     |     |                                 |                                  |      |      |      |     |      |      |    |     |      |      |      |     |            |      |     |      |     |                                   |  |      |     |      |     |      |      |      |     |        |      |     |     |     |                                   |  |      |      |      |     |      |      |      |     |           |      |      |      |     |                                   |  |      |      |     |     |      |     |      |     |      |     |      |     |           |      |      |      |     |  |  |      |      |      |     |      |      |      |     |       |      |      |     |       |      |      |     |           |     |     |     |     |  |   |      |     |      |     |      |      |     |     |      |      |     |     |      |      |      |     |      |      |     |     |      |      |     |     |      |     |     |     |       |      |      |     |       |      |      |     |       |      |      |     |       |      |      |     |       |      |      |     |       |      |      |     |       |      |      |     |           |      |      |    |     |                                       |  |      |      |     |     |      |      |     |     |           |     |     |      |     |  |  |      |      |      |     |      |      |      |     |      |
|               | 2940               | 2055                                | 2487                                | ---                                 |  |   |               |      |      |      |     |                                      |                                  |      |      |      |     |      |      |        |     |      |      |      |     |               |      |      |     |     |                                 |                                  |      |      |      |     |      |      |    |     |      |      |      |     |            |      |     |      |     |                                   |  |      |     |      |     |      |      |      |     |        |      |     |     |     |                                   |  |      |      |      |     |      |      |      |     |           |      |      |      |     |                                   |  |      |      |     |     |      |     |      |     |      |     |      |     |           |      |      |      |     |  |  |      |      |      |     |      |      |      |     |       |      |      |     |       |      |      |     |           |     |     |     |     |  |   |      |     |      |     |      |      |     |     |      |      |     |     |      |      |      |     |      |      |     |     |      |      |     |     |      |     |     |     |       |      |      |     |       |      |      |     |       |      |      |     |       |      |      |     |       |      |      |     |       |      |      |     |       |      |      |     |           |      |      |    |     |                                       |  |      |      |     |     |      |      |     |     |           |     |     |      |     |  |  |      |      |      |     |      |      |      |     |      |
|               | 3660               | 3142                                | ----                                | ---                                 |  |   |               |      |      |      |     |                                      |                                  |      |      |      |     |      |      |        |     |      |      |      |     |               |      |      |     |     |                                 |                                  |      |      |      |     |      |      |    |     |      |      |      |     |            |      |     |      |     |                                   |  |      |     |      |     |      |      |      |     |        |      |     |     |     |                                   |  |      |      |      |     |      |      |      |     |           |      |      |      |     |                                   |  |      |      |     |     |      |     |      |     |      |     |      |     |           |      |      |      |     |  |  |      |      |      |     |      |      |      |     |       |      |      |     |       |      |      |     |           |     |     |     |     |  |   |      |     |      |     |      |      |     |     |      |      |     |     |      |      |      |     |      |      |     |     |      |      |     |     |      |     |     |     |       |      |      |     |       |      |      |     |       |      |      |     |       |      |      |     |       |      |      |     |       |      |      |     |       |      |      |     |           |      |      |    |     |                                       |  |      |      |     |     |      |      |     |     |           |     |     |      |     |  |  |      |      |      |     |      |      |      |     |      |

TABLE 2. RESULTS OF DIFFUSIVITY MEASUREMENTS.

| Site          | Diffusion Time (s) | K <sub>x</sub> (cm <sup>2</sup> /s) | K <sub>y</sub> (cm <sup>2</sup> /s) | K <sub>z</sub> (cm <sup>2</sup> /s) | Technique  | Comments  |
|---------------|--------------------|-------------------------------------|-------------------------------------|-------------------------------------|--|---|
| Point Beach 1 | 6000               | ----                                | 390                                 | 0.5                                 | fluorometry-<br>continuous injection                 | thermal plume,<br>ambient waters  |
|               | 5000               | ----                                | 75                                  | 2.7                                 |  |   |
| Point Beach 2 | 2500               | ----                                | 3500                                | 1.4                                 | fluorometry-<br>continuous injection                 | thermal plume,<br>ambient waters  |
|               | 4600               | ----                                | 2500                                | 0.4                                 |  |   |
|               | 3100               | ----                                | 12,000                              | ---                                 |  |   |
|               | 3500               | ----                                | ----                                | 1.4                                 |  |   |
| Point Beach 3 | 4300               | ----                                | 130                                 | ---                                 | fluorometry-<br>batch injection                      | thermal plume,<br>ambient waters  |
|               | 4900               | ----                                | ----                                | 0.3                                 |  |   |
|               | 5200               | ----                                | 65                                  | ---                                 |  |   |
|               | 6000               | ----                                | ----                                | 0.3                                 |  |   |
| Campbell 1    | 1260               | 290                                 | ----                                | ---                                 | photography/T-shaped<br>injection                    |   |
|               | 2280               | 480                                 | ----                                | ---                                 |  |   |
|               | 2880               | 1130                                | ----                                | ---                                 |  |   |
| Cook 1        | 1500               | 600                                 | 470                                 | ---                                 | photography/T-shaped<br>injection                    |   |
|               | 4500               | 2160                                | 1260                                | ---                                 |  |   |
|               | 5700               | 5000                                | 2600                                | ---                                 |  |   |
| Pilgrim 1     | 1200               | ----                                | ----                                | ---                                 | photography/T-shaped<br>injection                    |   |
|               | 1500               | ----                                | 473                                 | ---                                 |  |   |
|               | 1680               | 302                                 | 1798                                | ---                                 |  |   |
|               | 3600               | 487                                 | 3740                                | ---                                 |  |   |
| Pilgrim 2     | 1560               | ----                                | ----                                | ---                                 | photography and<br>fluorometry/T-shaped<br>injection |   |
|               | 4860               | ----                                | 2286                                | ---                                 |  |   |
|               | 6180               | 3983                                | ----                                | ---                                 |  |   |
|               | 11640              | 3524                                | ----                                | ---                                 |  |   |
|               | 12840              | ----                                | 5026                                | ---                                 |  |   |
| Pilgrim 3     | 840                | 481                                 | 747                                 | ---                                 | photography and<br>fluorometry/T-shaped<br>injection | after an initial<br>mixing period,<br>no changes in<br>vertical dye<br>distribution<br>were observed. |
|               | 1800               | 770                                 | 1782                                | ---                                 |  |   |
|               | 3600               | ----                                | 284                                 | ---                                 |  |   |
|               | 5700               | 1167                                | 691                                 | ---                                 |  |   |
|               | 6240               | 1096                                | ----                                | ---                                 |  |   |
|               | 7200               | 1326                                | 624                                 | ---                                 |  |   |
|               | 7560               | ----                                | 343                                 | ---                                 |  |   |
|               | 9000               | 841                                 | 872                                 | ---                                 |  |   |
|               | 10200              | 3052                                | ----                                | ---                                 |  |   |
|               | 10620              | ----                                | 1520                                | ---                                 |  |   |
|               | 10800              | 1108                                | ----                                | ---                                 |  |   |
|               | 11880              | 2579                                | ----                                | ---                                 |  |   |
|               | 18300              | 5864                                | ----                                | ---                                 |  |   |
|               | 19980              | 3734                                | ----                                | ---                                 |  |   |
| 21780         | 5153               | ----                                | ---                                 |                                     |  |   |
| Pilgrim 4     | 2880               | 5323                                | 14                                  | ---                                 | photography of T-<br>shaped injection                |   |
|               | 3420               | 2763                                | 110                                 | ---                                 |  |   |
|               | 5400               | 3778                                | 280                                 | ---                                 |  |   |
| Pilgrim 5     | 960                | 137                                 | ----                                | ---                                 |  |   |
|               | 1740               | 2002                                | 1621                                | ---                                 |  |   |
|               | 2940               | 2055                                | 2487                                | ---                                 |  |   |
|               | 3660               | 3142                                | ----                                | ---                                 |  |   |

TABLE 3. FLUOROMETRIC METHOD VERSUS AERIAL PHOTOGRAPHIC METHOD.

| Date     | Time | $\sigma_x$ -Aerial | $\sigma_x$ -Boat | $\sigma_y$ -Aerial | $\sigma_y$ -Boat |
|----------|------|--------------------|------------------|--------------------|------------------|
| 10-27-74 | 1001 |                    |                  |                    | 10.0             |
|          | 1015 | 17.9               |                  | 14.9               |                  |
|          | 1030 |                    | 36.8             |                    |                  |
| 10-28-74 | 1027 |                    |                  |                    | 28.1             |
|          | 1030 | 16.9               |                  | 25.8               |                  |
|          | 1033 |                    | 19.7             |                    |                  |
|          | 1048 |                    |                  |                    | 22.1             |
|          | 1100 |                    |                  | 43.0               |                  |
|          | 1135 | 36.6               |                  | 41.6               | 53.0             |
|          | 1144 |                    | 36.4             |                    |                  |
|          | 1200 | 44.4               |                  | 34.8               |                  |
|          | 1206 |                    |                  |                    | 34.7             |
|          | 1250 |                    | 73.5             |                    |                  |
|          | 1257 |                    |                  |                    | 59.4             |
|          | 1300 |                    |                  | 49.2               |                  |

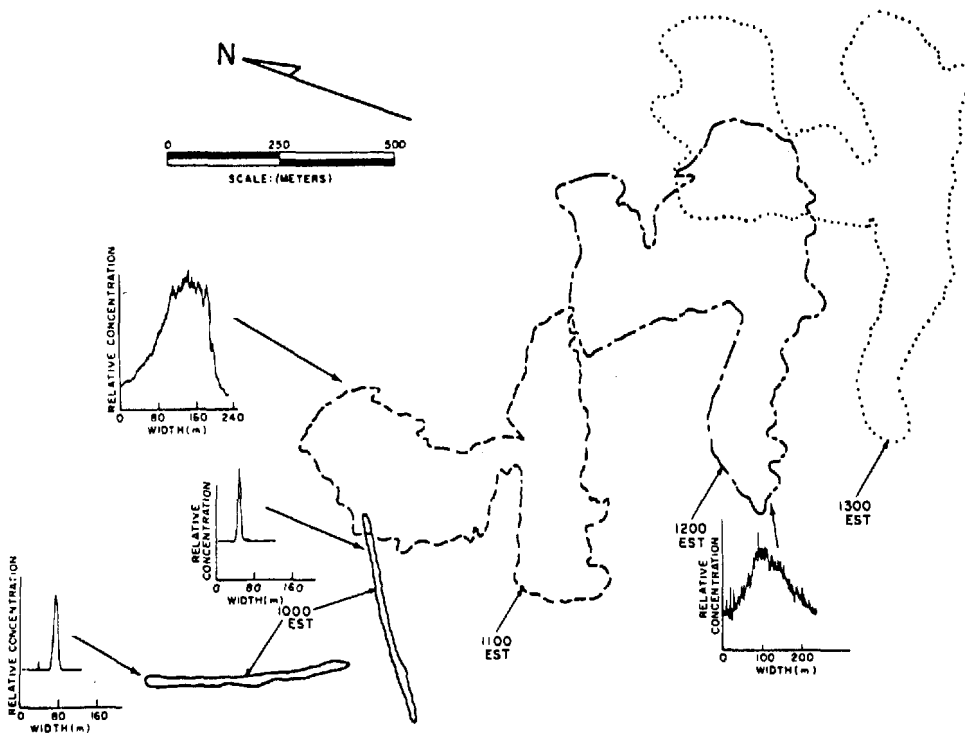


Figure 1. Results of Photography of a T-shaped Dye Patch. Motion, Diffusion, and Distortion of the "T" as a Function of Time is Shown in This Figure. Graphs Show Relative Dye Concentration (Averaged Over 10 Densitometer Scans) For Each Leg of the "T."

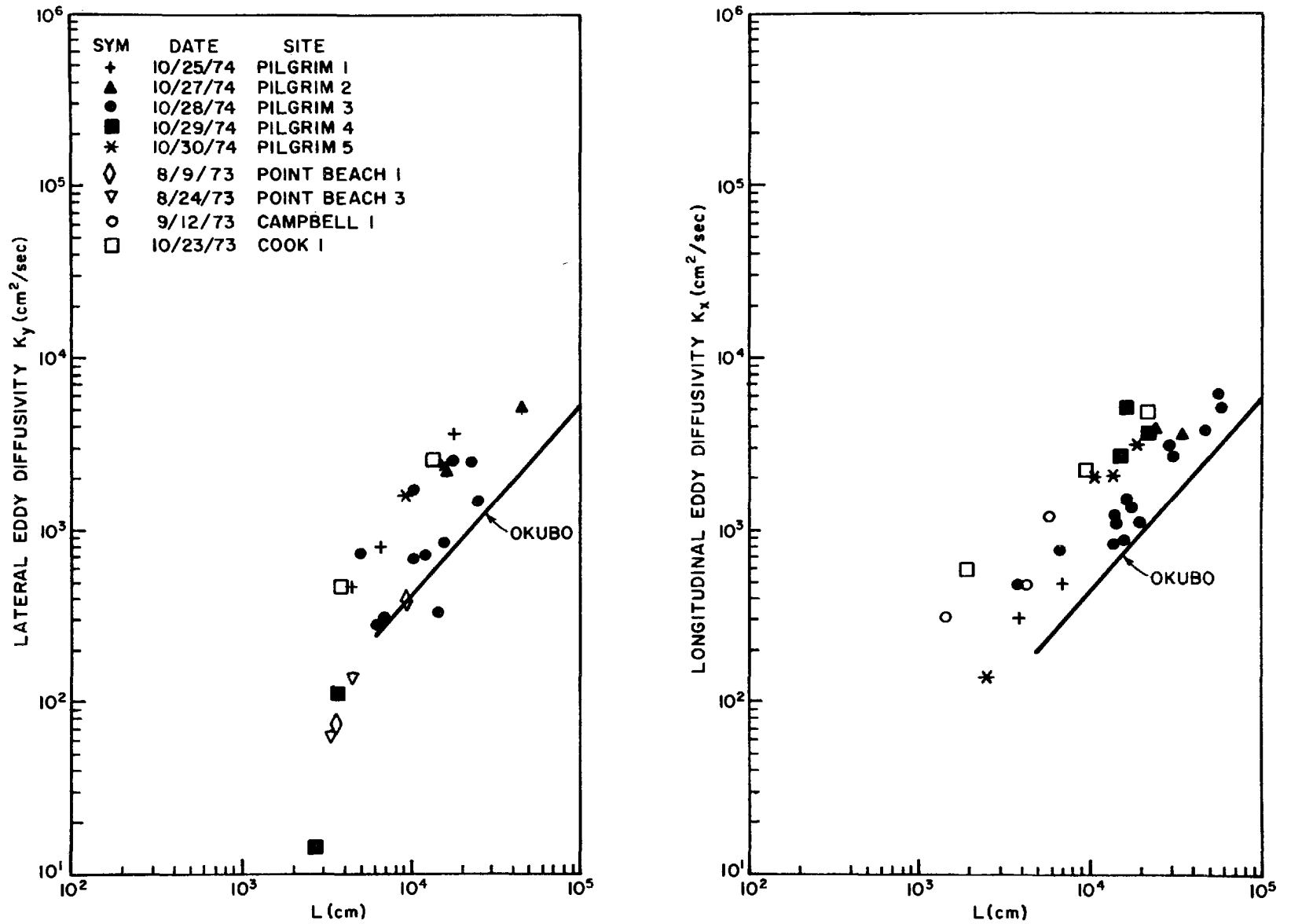


Figure 2. Dye Diffusion Coefficient as a Function of Dye Patch Size " $L$ " =  $4\sigma$ . Line Labeled Okubo Shows Results of Numerous Oceanic Studies.

EFFECTS OF BOTTOM SLOPE, FROUDE NUMBER, AND REYNOLDS  
NUMBER VARIATION ON VIRTUAL ORIGINS OF SURFACE JETS:  
A NUMERICAL INVESTIGATION.

by

J. Venkata, S. Sengupta, S. S. Lee  
University of Miami  
Coral Gables, Florida U.S.A.

(ABSTRACT)

A 3 dimensional numerical model which was developed to predict the behaviour of thermal discharges is used to investigate the effects of variation of bottom slope, Reynolds number and Froude number on the virtual origins of surface jets. Two types of virtual origins, one based on the jet width and the other based on the centerplane velocity and temperature decay are considered. The results indicate that jet width is independent of bottom Slope. Increasing Reynolds number moves the virtual origins upstream of the discharge point.

## INTRODUCTION

Some of the three dimensional numerical models which have been developed recently for velocity and temperature predictions are those of Brady & Geyer (1972), Till, J. (1973), Waldrop & Farmer (1974), Sengupta & Lick (1974), Paul & Lick (1974), and Markham (1975). An excellent review of numerical models is given by Policastro et al (1975). The model that was used to obtain results in this paper is the modified version of the model developed by Sengupta & Lick (1974). The modified version of the model was successfully applied and verified by the authors (Venkata, J & Sengupta, 1977; Mathavan & Lee, 1977 and Sengupta & Lee 1976).

This paper is concerned with the numerical investigation of the effects of bottom slope, Froude number and Reynolds number variation on the virtual origins, therefore, so the details of the verification of the model will not be discussed here. For the verification of the model details the reader is advised to look into the references (7,8 and 12),

Two types of virtual origins have been defined for free jets. One is based on the widening of the jet and is known as geometric virtual origin, and the second, based on the centerplane velocity decay, is known as kinematic virtual origin (Flora & Goldschmidt, 1969). It was found experimentally that the two origins of similarity do not coincide and do not depend on the discharge channel aspect ratio ( $\frac{b}{D}$ ) but, found to depend on the turbulence intensity (Flora & Goldschmidt, 1969; Jenkins & Goldschmidt, 1973 and Kostovinos, 1975). In the present investigation it was attempted numerically to see the possible influence of bottom slope, Froude number and Reynolds number variation on the geometric and kinematic virtual origins for incompressible surface jets.

## THEORY

The flow of an incompressible surface jet entering into a quiescent atmosphere of the same fluid is considered. Fig.(1) shows the discharge canal and receiving basin geometry considered along with the boundary conditions which are discussed elsewhere in this paper. The equations that describe the motion of the fluid and heat transfer for incompressible fluids are the three Navier-Stokes equations of momentum, conservation of mass, conservation of energy and equation of state, which couples energy equation to momentum equations. These equations are stretched in the vertical direction using the relation  $\gamma=Z/h(x,y)$ . The details of the stretching are discussed in reference (12). The advantage of this stretching is that it allows the same number of grid points at shallow and deeper parts of the basin without variable grid spacing. The other approximations that are made before the final set of equations obtained are:

- (1) The vertical equation is replaced by the hydrostatic equation,

(2) A rigid-lid is placed on the top of the surface which allows horizontal velocities but not vertical velocities. In order to determine the pressure on the surface, a Poisson equation is derived from the two horizontal momentum equations. (3) The fluid is treated as incompressible; the coupling between momentum and energy exists through the equation of state. (4) The effect of turbulence is modelled using eddy transport coefficients. The final set of non-dimensional, stretched equations which are similar to Sengupta (1974) are given below.

Continuity:

$$\frac{\partial(hu)}{\partial\alpha} + \frac{\partial(hv)}{\partial\beta} + h\frac{\partial\Omega}{\partial\gamma} = 0 \quad (1)$$

u-Momentum:

$$\begin{aligned} \frac{\partial(hu)}{\partial t} + \frac{\partial(huu)}{\partial\alpha} + \frac{\partial(huv)}{\partial\beta} + h\frac{\partial(\Omega u)}{\partial\gamma} - \frac{h}{R_B} v \\ = -h\frac{\partial P_s}{\partial\alpha} - hB_x + \frac{1}{Re}\frac{\partial}{\partial\alpha}(h\frac{\partial u}{\partial\alpha}) + \frac{1}{Re}\frac{\partial}{\partial\beta}(h\frac{\partial u}{\partial\beta}) \\ + \frac{1}{\epsilon^2 Re}\frac{1}{h}\frac{\partial}{\partial\gamma}(A_V^* \frac{\partial u}{\partial\gamma}) \end{aligned} \quad (2)$$

v-Momentum:

$$\begin{aligned} \frac{\partial(hv)}{\partial t} + \frac{\partial(huv)}{\partial\alpha} + \frac{\partial(hvv)}{\partial\beta} + h\frac{\partial(\Omega v)}{\partial\gamma} + \frac{h}{R_B} u \\ = -h\frac{\partial P_s}{\partial\beta} - hB_y + \frac{1}{Re}\frac{\partial}{\partial\alpha}(h\frac{\partial v}{\partial\alpha}) + \frac{1}{Re}\frac{\partial}{\partial\beta}(h\frac{\partial v}{\partial\beta}) \\ + \frac{1}{\epsilon^2 Re}\frac{1}{h}\frac{\partial}{\partial\gamma}(A_V^* \frac{\partial v}{\partial\gamma}) \end{aligned} \quad (3)$$

Hydrostatic Equation:

$$\frac{\partial P}{\partial\gamma} = E u (1 + p) h \quad (4)$$

ENERGY EQUATION:

$$\begin{aligned} & \frac{\partial(hT)}{\partial t} + \frac{\partial(huT)}{\partial \alpha} + \frac{\partial(hvT)}{\partial \beta} + h \frac{\partial(\Omega T)}{\partial \gamma} \\ &= \frac{1}{Pe} \frac{\partial}{\partial \alpha} (h \frac{\partial T}{\partial \alpha}) + \frac{1}{Pe} \frac{\partial}{\partial \beta} (h \frac{\partial T}{\partial \beta}) + \frac{1}{Pe \epsilon^2} \frac{1}{h} \frac{\partial}{\partial \gamma} (B_v^* \frac{\partial T}{\partial \gamma}) \end{aligned} \quad (5)$$

EQUATION OF STATE:

$$\rho = 1.029431 - .000020T - .0000048T^2 \quad (6)$$

The Poisson equation for pressure is of the form

$$\begin{aligned} \frac{\partial^2 p_s}{\partial \alpha^2} + \frac{\partial^2 p_s}{\partial \beta^2} &= \frac{1}{h} \frac{\partial}{\partial \alpha} (-A_{x1} + A_{x2} + C_x - X_p) \\ &+ \frac{1}{h} \frac{\partial}{\partial \beta} (-A_{y1} - A_{y2} + C_y - Y_p) \\ &- \frac{1}{h} \left\{ \frac{\partial h}{\partial \alpha} \frac{\partial p_s}{\partial \alpha} + \frac{\partial h}{\partial \beta} \frac{\partial p_s}{\partial \beta} \right\} - \frac{\partial(\Omega)}{\partial t} (z = 0) \end{aligned} \quad (7)$$

where

$$A_{x1} = \int_0^h \left\{ \frac{\partial}{\partial x} (uu) + \frac{\partial}{\partial y} (uv) + \frac{\partial}{\partial z} (uw) \right\} dz$$

$$A_{x2} = \frac{1}{RB} \int_0^h udz$$

$$C_x = \frac{1}{Re} \int_0^h \left\{ \frac{\partial}{\partial x} \left( A_H^* \frac{\partial u}{\partial x} \right) + \frac{\partial}{\partial y} \left( A_H^* \frac{\partial u}{\partial y} \right) + \frac{1}{\epsilon^2} \right.$$

$$\left. \left( A_V^* \frac{\partial u}{\partial z} \right) \right\} dz$$

$$X_p = E_u \int_0^h \left\{ \frac{\partial}{\partial x} (\rho dz) \right\} dz$$

and

$$Ay_1 = \int_0^h \left\{ \frac{\partial}{\partial x} (uv) + \frac{\partial}{\partial y} (vv) + \frac{\partial}{\partial z} (vw) \right\} dz$$

$$Ay_2 = \frac{1}{RB} \int_0^h u dz$$

$$C_y = \frac{1}{Re} \int_0^h \left\{ \frac{\partial}{\partial x} \left( A_H^* \frac{\partial v}{\partial x} \right) + \frac{\partial}{\partial y} \left( A_H^* \frac{\partial u}{\partial y} \right) + \frac{1}{\epsilon^2} \frac{\partial}{\partial z} \right.$$

$$\left. \left( A_V^* \frac{\partial u}{\partial z} \right) \right\} dz$$

$$Y_p = Eu \int_0^h \left\{ \frac{\partial}{\partial y} \left( \int_0^z \rho dz \right) \right\} dz$$

WHERE

$$u = \frac{\bar{u}}{U_{ref}} ; v = \frac{\tilde{v}}{U_{ref}} ; w = \frac{\tilde{w}}{E U_{ref}} ; t = \frac{\tilde{t}}{t_{ref}}$$

$$x = \frac{\bar{x}}{L} ; y = \frac{\bar{y}}{L} ; Z = \frac{\bar{z}}{H} ; \epsilon = \frac{H}{L}$$

$$\rho = \frac{\tilde{\rho}}{\rho_{ref}} \frac{U_{ref}}{U_{ref}} ; T = \frac{\tilde{T} - T_{ref}}{T_{ref}} ; \rho = \frac{\tilde{\rho} - \rho_{ref}}{\rho_{ref}}$$

$$A_H^* = \frac{A_H}{A_{ref}} ; A_V^* = \frac{A_V}{A_{ref}} ; B_H^* = \frac{B_H}{B_{ref}} ; B_V = \frac{B_V}{B_{ref}}$$

$$t_{ref} = \frac{L}{U_{ref}}$$

This set of equations are to be solved with appropriate initial and boundary conditions. The initial conditions used on the velocity are, at time  $t=0$ , all velocities are zero. The temperature at  $t=0$  is equal to the reference temperature. The boundary conditions are schematically presented in Figure (1). The conditions on solid walls and bottom are no slip and no normal velocity for all time, except  $w$  is not equal to zero due to the hydrostatic approximation. The temperature boundary condition at solid walls is handled by assuming the walls and bottom as adiabatic i.e.

$$\frac{\partial T}{\partial \bar{n}} = 0. \text{ Where } \bar{n} \text{ is in the direction normal to the wall or bottom.}$$

The boundary condition at the open boundaries used in this investigation is  $\frac{\partial v}{\partial \bar{n}} = 0$  where  $v$  is velocity in the direction normal to the boundary. The boundary conditions in summary for the vertically stretched co-ordinate system are

Boundary Conditions:

On solid lateral wall:

$$u = 0$$

$$v = 0$$

$$\Omega \neq 0$$

$$\frac{\partial T}{\partial y} = \frac{\partial T}{\partial \beta} - \frac{\gamma}{h} \frac{\partial h}{\partial \beta} \frac{\partial T}{\partial \gamma} = 0$$

At the bottom of the basin ( $\gamma=1$ ):

$$\Omega = 0$$

$$u = 0$$

$$v = 0$$

$$\frac{\partial T}{\partial \gamma} = 0$$

Along free boundaries:

At ( $\alpha = 0, \beta, \gamma$ )

$$U_{I=1}, K = U_{I=2}, K$$

$$v = 0$$

$$w \neq 0$$

$$T_{I=1}, K = T_{I=2}, K$$

$$P_s = \text{constant}$$

$$\text{At } (\alpha = \alpha_L, \beta, K)$$

$$U_{I=IN}, K = U_{I=IN-1}, K$$

$$v = 0$$

$$w \neq 0$$

$$T_{I=IN}, K = T_{I=IN-1}, K$$

$$P_s = \text{constant}$$

$$\text{At } (\alpha, \beta = \beta_L, \gamma)$$

$$U_{JN}, K = U_{JN-1}, K$$

$$v = 0$$

$$w \neq 0$$

$$P_s = \text{constant}$$

At the air water interface

$$\Omega = 0 \quad (\text{Rigid lid})$$

$$\frac{\partial u}{\partial \gamma} = \left( \frac{hH}{U_{\text{ref}} A_V} \right) \tau_{zx}$$

$$\frac{\partial v}{\partial \gamma} = \left( \frac{hH}{U_{\text{ref}} A_V} \right) \tau_{zy}$$

$$\frac{\partial T}{\partial \gamma} = \left( \frac{hHK_s}{B_z} \right) (T_E - T_s)$$

The equations 1 to 7 are solved with the above boundary conditions using finite difference approximations on a UNIVAC 1106 computer.

### Computer Simulations

The list of cases run is given in Table (1). First a constant density jet entering a constant depth basin is studied for a Reynolds number equal to 100. Then for the same Reynolds number the bottom is changed from constant depth to smoothly sloping bottom ( $\tan \theta = 0.004$ ) and is studied for a constant density jet. The slope is then doubled ( $\tan \theta = 0.008$ ) and the above case is repeated for a constant density jet at  $Re = 100$ . All the above cases are run until steady state is reached. It took approximately 65 minutes to reach steady state. The jet width ( $b/D$ ) and centerline velocity in the form  $(\frac{U_0}{U_x})^2$  are plotted against centerline distance  $(\frac{X}{D})$  for the above three cases and are shown in Figures (2 to 7). The geometric and kinematic virtual origins are obtained in the following manner. A straight line is fitted in the near region of the jet and the straight line is extended to cut the x-axis. The intercept gives the geometric virtual origin for the jet width diagram and kinematic virtual origin for the centerplane velocity decay diagram.

What is interesting from these figures is that the geometric virtual origin, and, hence, jet width, do not seem to depend on the bottom slope. Whereas kinematic virtual origin is increasing (moving upstream of the discharge point) indicating that the surface centerline velocity decreases more rapidly with increase in slope. As the bottom slope increases there is more bottom entrainment causing the jet velocity to decay at a more rapid rate.

The next step was to consider how the jet behaves when density effects are included. The above three cases are repeated including the effects of density (i.e. Froude number is changed) and keeping the Reynolds number the same. The results of these cases are shown in Figures (8 to 13). Again it can be seen that for the same Reynolds number the geometric virtual origin and hence the jet width is independent of bottom slope. The kinematic virtual origin increased as before indicating that surface centerplane velocity decreased more rapidly with increased bottom slope. But, an important effect of including density can be found by comparing the cases with variable density, to that of cases with constant density. The geometric virtual origin increased (i.e. moved towards the discharge point) for variable density cases. This is because the jet is spreading in the lateral direction more rapidly because of density differences between the discharged fluid and ambient fluid and consequent spreading in a thinner layer at the surface. The kinematic virtual origin decreased (i.e. moved upstream) for cases with variable density indicating that the surface center plane velocity decay is slower than that of the

case with constant density. This is because the fluid is rising due to buoyancy in the cases where density effects are included, causing flow through a smaller effective cross-section.

In all the above six cases, the Reynolds number ( $Re$ ) is kept constant equal to 100. Its effects are studied by increasing  $Re$  from 100 to 285 by decreasing the reference eddy viscosity. The results are plotted and are shown in Figures (14 to 19). It can be again observed here that the geometric virtual origin is independent of bottom slope, and kinematic virtual origin is dependent on bottom slope. The important effect of Reynolds number on virtual origins, as can be seen from Table (1) is, geometric and kinematic virtual origins moved upstream with the increase in Reynolds number. The results of all the above nine cases are summarized in Figures (20 to 23).

## CONCLUSIONS

From the different cases studied, the following conclusions can be drawn:

- (1) From the constant depth and two bottom slope cases, it is concluded that for increasing bottom slope, the decay of centerplane velocity and temperature is faster due to increased entrainment, where as jet width would be independent of bottom slope. Also, it is noticed that geometric virtual origin is independent of bottom slope, and kinematic virtual origin decreases with increase of slope.
- (2) Comparison between non-buoyant and buoyant jets indicate that geometric virtual origin for non-buoyant jets is more upstream than for buoyant jets. The kinematic virtual origin moves further upstream when density effects are included.
- (3) It is found that increasing the Reynolds number moves the geometric and kinematic virtual origins further upstream of the discharge point.

## ACKNOWLEDGEMENTS

This work was conducted under funding from National Aeronautic and Space Administration, Kennedy Space Center.

## REFERENCES

1. Abramovich, G.N., "The Theory of Turbulent Jets", The M.I.T. Press, Cambridge, Mass., 1963.
2. Brady, D., and Geyer, J., "Development of General Computer Model for Simulating Thermal Discharges in Three Dimensions". Report No.7, Dept. of Geography and Environmental Eng., Johns Hopkins University, Baltimore, Md., (1972).
3. Dunn, W.E., Policastro, A.J., and Paddock, R.A., "Surface Thermal plumes: Evaluation of Mathematical Models for the Near and Complete Field", Water Resources Research Program, Energy and Environmental Systems Division, Argonne National Laboratory, Argonne, Illinois (Part one and two), 1975.
4. Flora, J., and Goldschmidt, V., "Virtual Origins of a Free Plane Turbulent Jet", A.I.A.A. Journal 7, pp 2344-2346.
5. Jenkins, P.E., and Goldschmidt, V., "Mean Temperature and Velocity in a Plane Turbulent Jet", A.S.M.E., Journal of Fluids Engineering, 95, pp 581-584.
6. Katsovinos, N.E., "A Note on the Spreading Rate and Virtual Origin of a Plane Turbulent Jet:", Journal of Fluid Mechanics, 1967, Vol.77, Part 2, pp 305-311.
7. Lee, S.S., and Sengupta, S., "Proceedings of the Conference on Waste Heat Manatement and Utilization", Miami Beach, Fla., 9-11 May 1977.
8. Mathavan, S.K.M., "Experimental and Numerical Study of Current and Temperature Fields in Lake Belews an Artificial Cooling Lake", Ph.D. Thesis Submitted to the Department of Mechanical Engineering, University of Miami, Coral Gables, Florida, August 1977.
9. Paul, J., and Lick, W.J., "A Numerical Model for a Three Dimensional Variable Density Jet", FTAS/TR 73-92, Case Western Reserve University (1974).
10. Sengupta, S., and Lick, W.J., "A Numerical Model for Wind Driven Circulation and Temperature Fields in Lakes and Ponds", FTAS/TR-74-79, Case Western Reserve University (1974).
11. Sengupta, S., Lee, S.S., Venkata, J., and Carter, C.,

"A Three Dimensional Rigid Lid Model for Thermal Predictions", presented at the Waste Heat Management and Utilization, Miami Beach, Florida, May 9-11, 1977.

12. Venkata, J., "A Numerical Investigation of Thermal Plumes", Ph.D. Thesis Submitted to the Department of Mechanical Engineering, University of Miami, Coral Gables, Florida, August 1977.
13. Waldrop, W.R., and Farmer, R., "Three Dimensional Computation of Buoyant Plumes", Journal of Geophysical Research, Vol.74, No.9, (March, 1974).

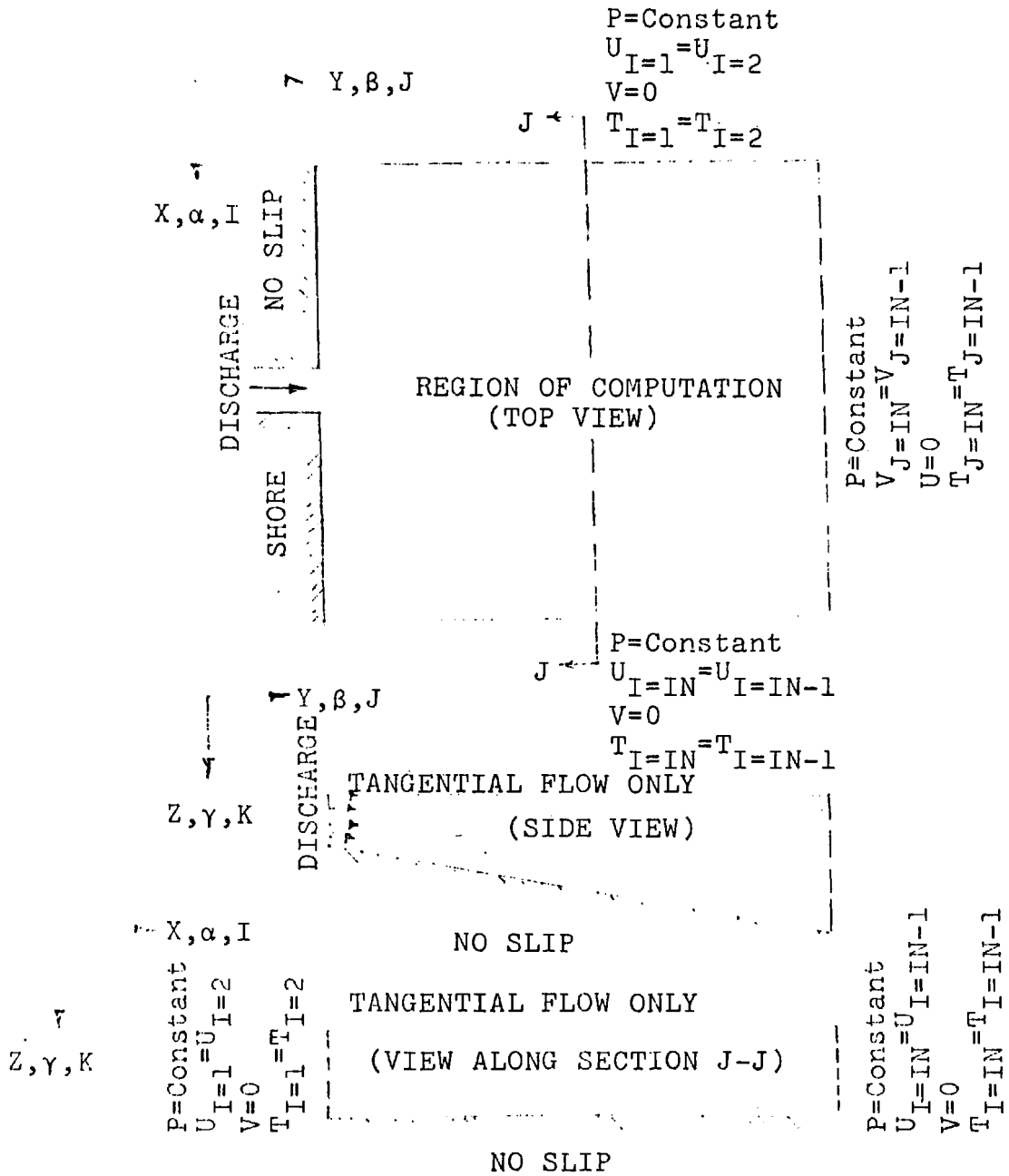


Fig.1 Boundary Conditions for the Region of Computation

LIST OF CASES STUDIED AND VIRTUAL ORIGIN RESULTS OBTAINED

| Case No<br>or Run<br>No | Slope                         | Froude Number<br>(Fr) = $\frac{U_o}{\sqrt{\frac{\Delta\rho}{\rho} g h_o}}$ | Reynolds Number<br>(Re)<br>= $\frac{U_{ref} L}{A_{ref}}$ | Geometric Virtual<br>Origin<br>(C <sub>1</sub> ) | Kinematic Virtual<br>Origin<br>(C <sub>2</sub> ) |
|-------------------------|-------------------------------|--|--|--|--|
| 1                       | Constant Depth<br>(Slope=0.0) | 0.058<br>(Const Density)   | 100  | 1.8  | 3.0  |
| 2                       | Low Slope<br>(Tanθ=0.004)     | 0.058<br>(Const Density)   | 100  | 1.8  | 2.8  |
| 3                       | High Slope<br>(Tanθ=0.008)    | 0.058<br>(Const Density)   | 100  | 1.8  | 2.2  |
| 4                       | Constant Depth<br>(Slope 0.0) | 0.0208<br>(Variable<br>Density)  | 100  | 0.8  | 4.0  |
| 5                       | Low Slope<br>(Tanθ=0.004)     | 0.0208<br>(Variable<br>Density)  | 100  | 0.8  | 3.5  |
| 6                       | High Slope<br>(Tanθ=0.008)    | 0.0208<br>(Variable<br>Density)  | 100  | 0.78   | 3.0  |
| 7                       | Constant Depth<br>(Slope 0.0) | 0.058<br>(Const Density)   | 285  | 11.0   | 14.4   |
| 8                       | Low Slope<br>(Tanθ=0.004)     | 0.058<br>(Const Density)   | 285  | 11.0   | 5.5  |
| 9                       | High Slope<br>(Tanθ=0.008)    | 0.058<br>(Const Density)   | 285  | 11.0   | 3.0  |

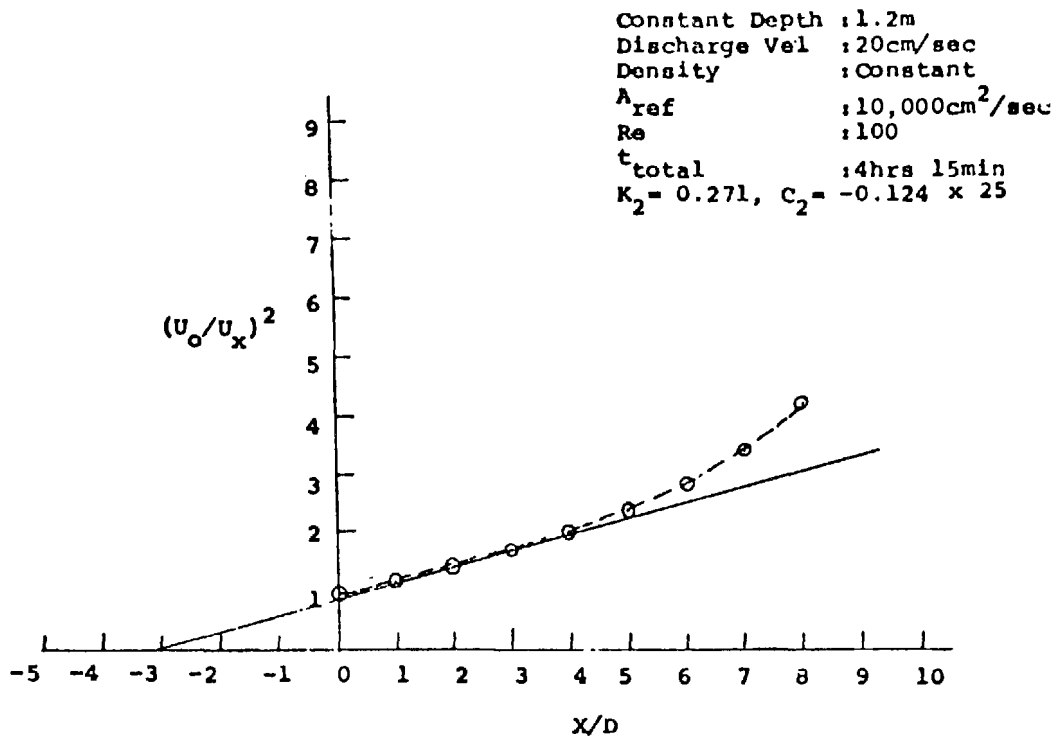


Fig.2 Kinematic Virtual Origin (Constant Depth)

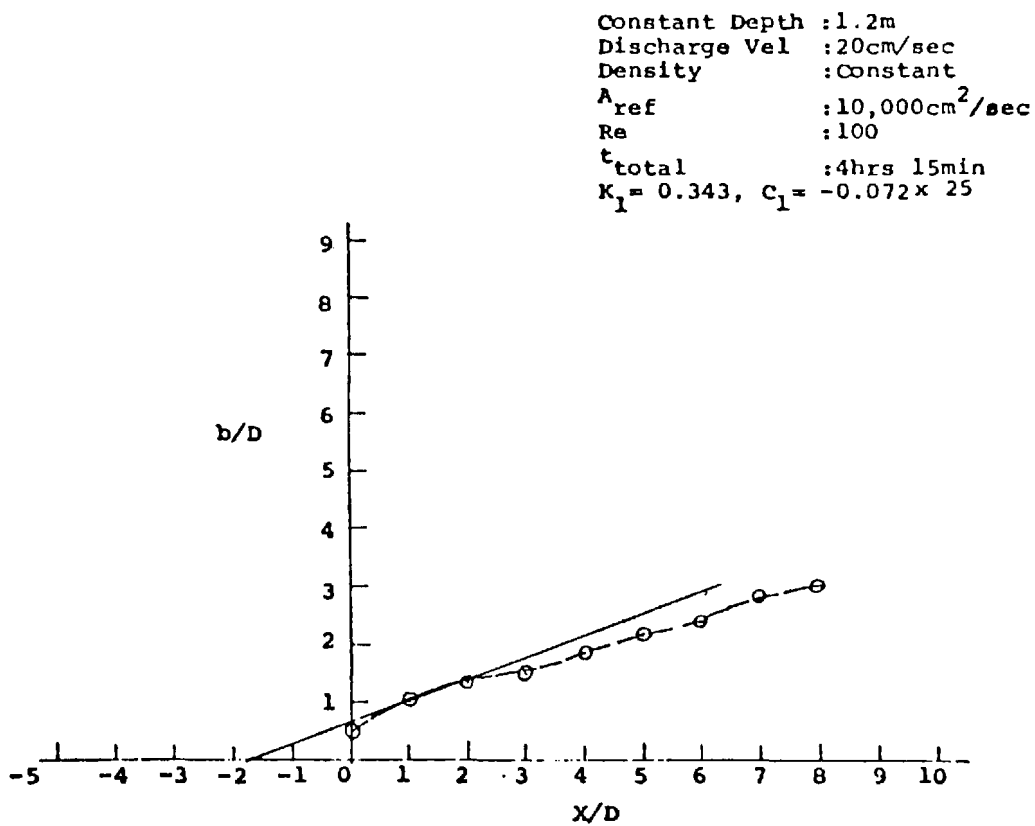


Fig.3 Geometric Virtual Origin (Constant Depth)

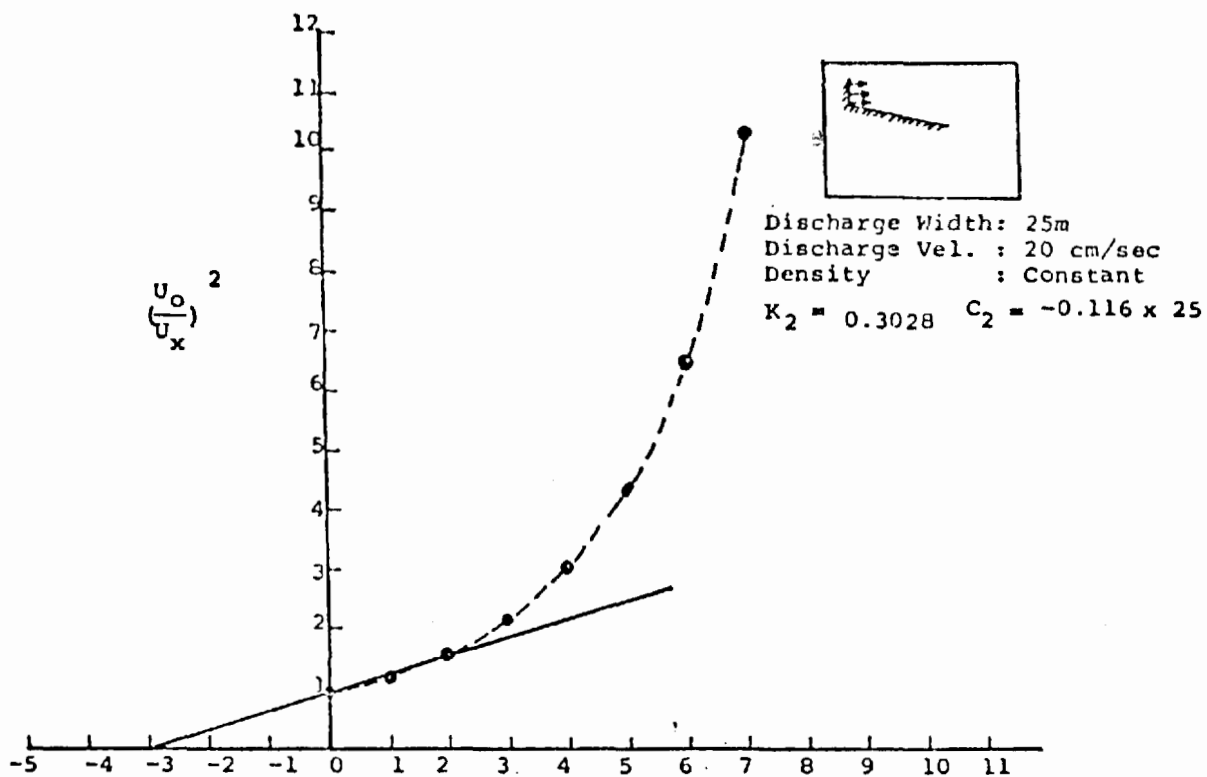


Fig.4 Kinematic Virtual Origin (For Sloping Bottom  $\tan \theta = 0.004$ )

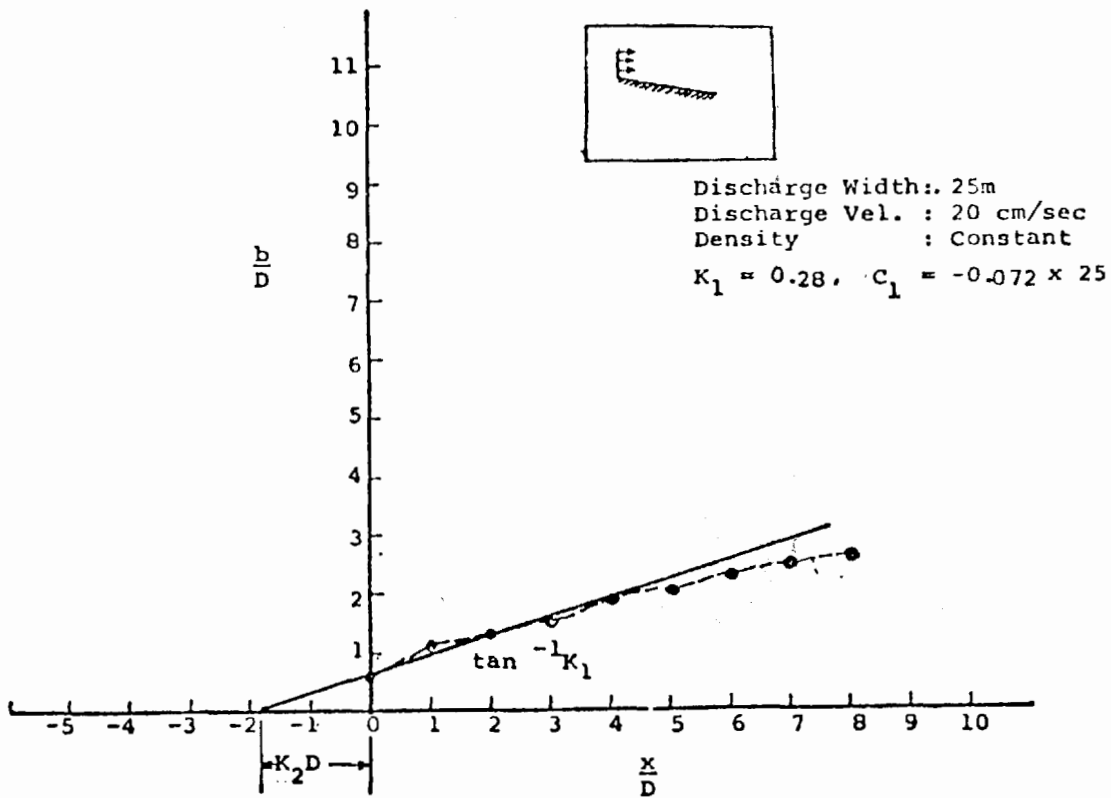


Fig.5 Geometric Virtual Origin (For Sloping Bottom  $\tan \theta = 0.004$ )

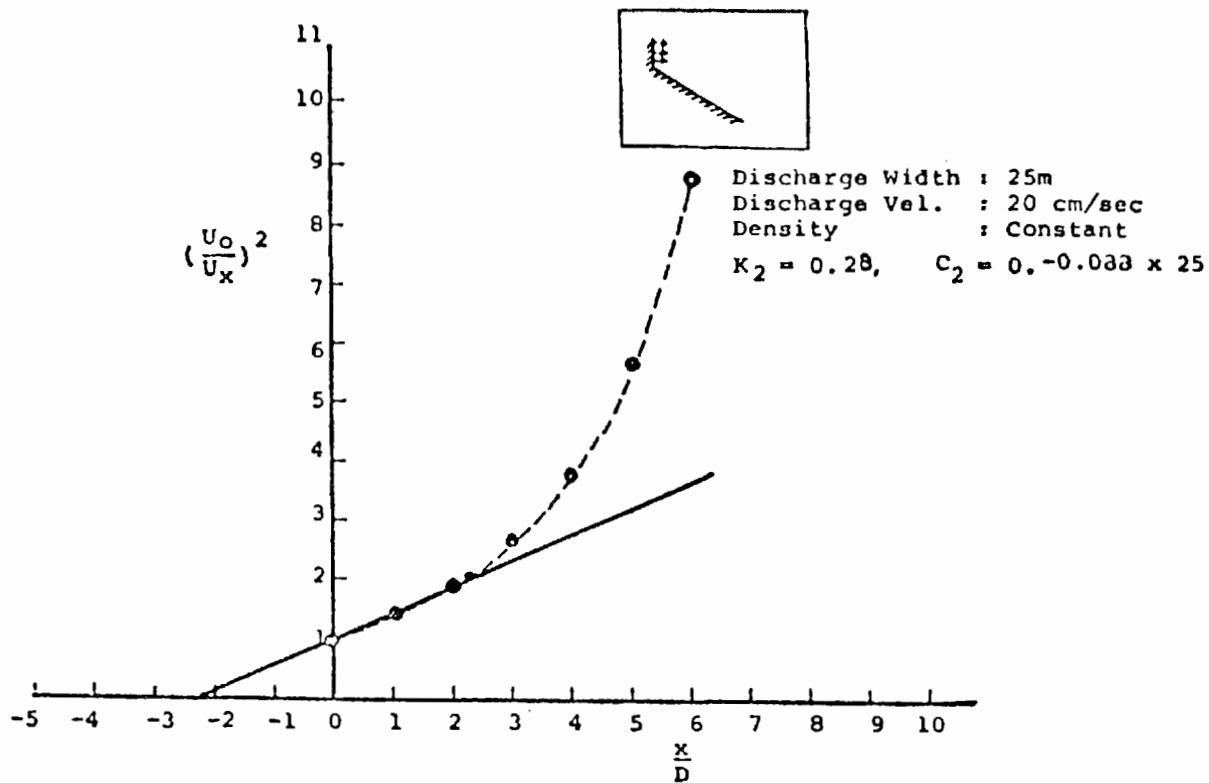


Fig.6 Kinematic Virtual Origin (For Sloping Bottom  $\tan \theta = 0.008$ )

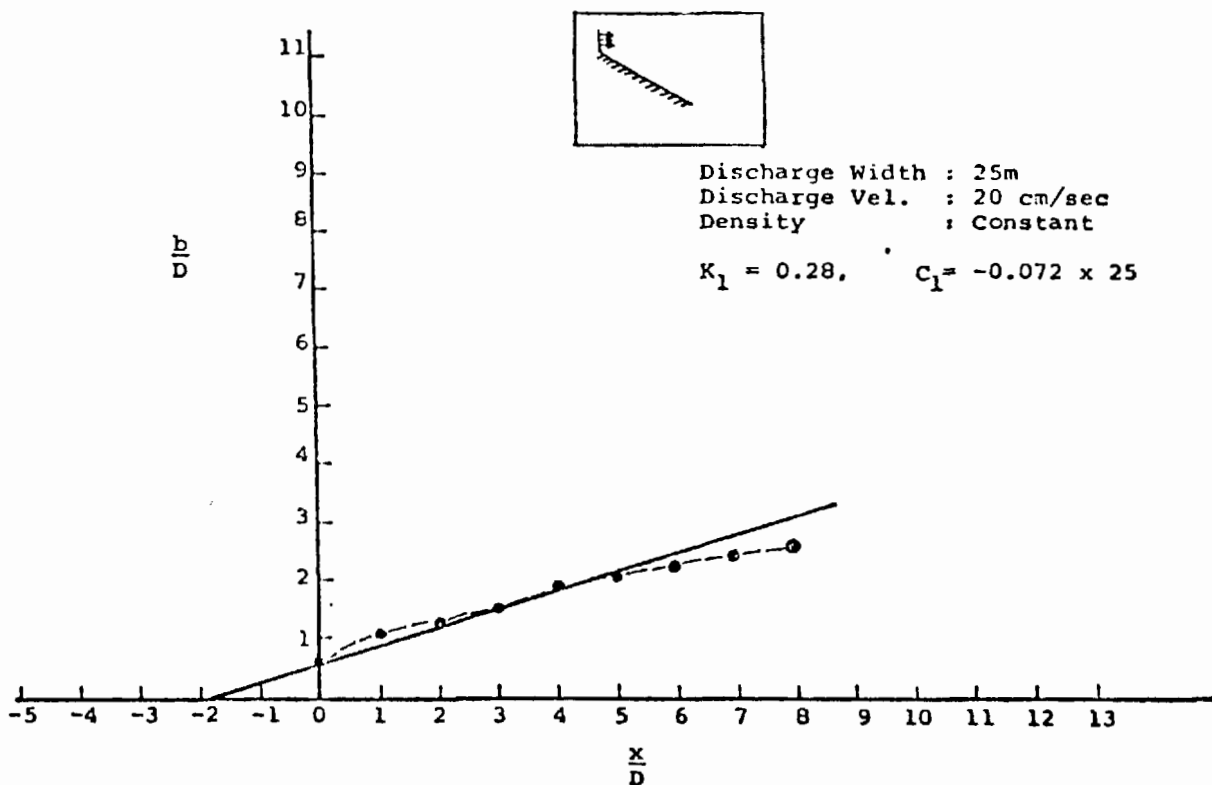


Fig.7 Geometric Virtual Origin (For Sloping Bottom  $\tan \theta = 0.008$ )

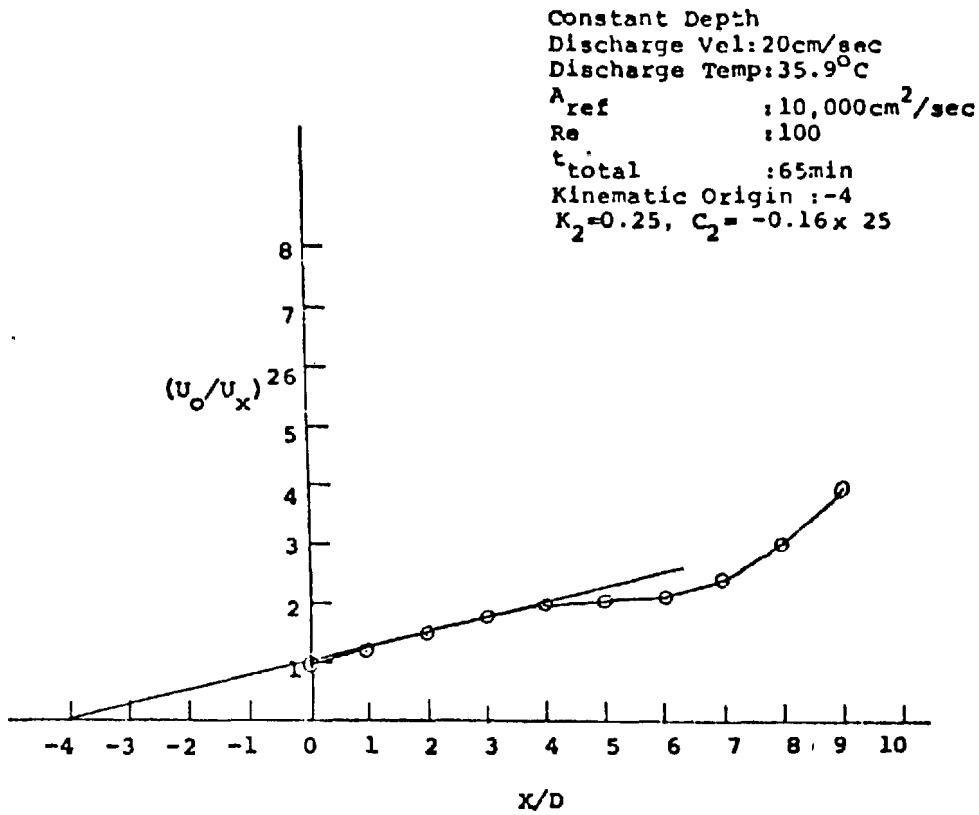


Fig.8 Kinematic Virtual Origin (Constant Depth)

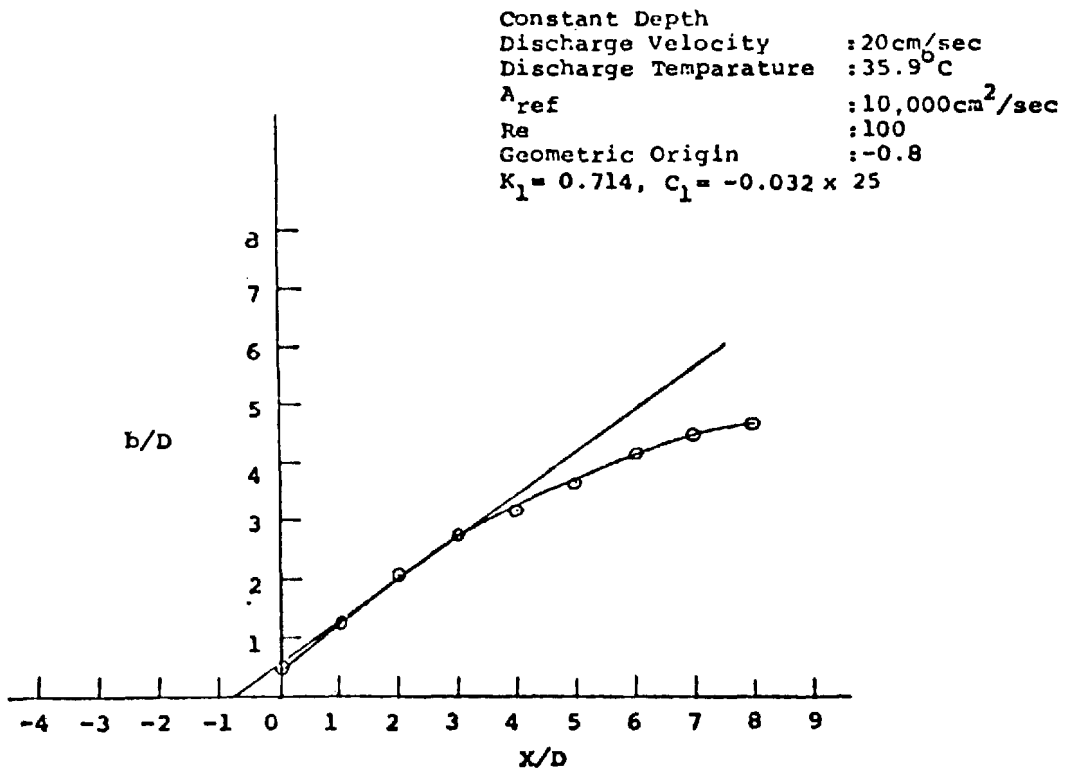


Fig.9 Geometric Virtual Origin (Constant Depth)

Low Slope Case  
 Discharge Velocity : 20cm/sec  
 Discharge Temperature : 35.9°C  
 $A_{ref}$  : 10,000cm<sup>2</sup>/sec  
 $Re$  : 100  
 $t_{total}$  : 65min  
 Kinematic Origin : -3.4  
 $K_2 = 0.294, C_2 = -0.136 \times 25$

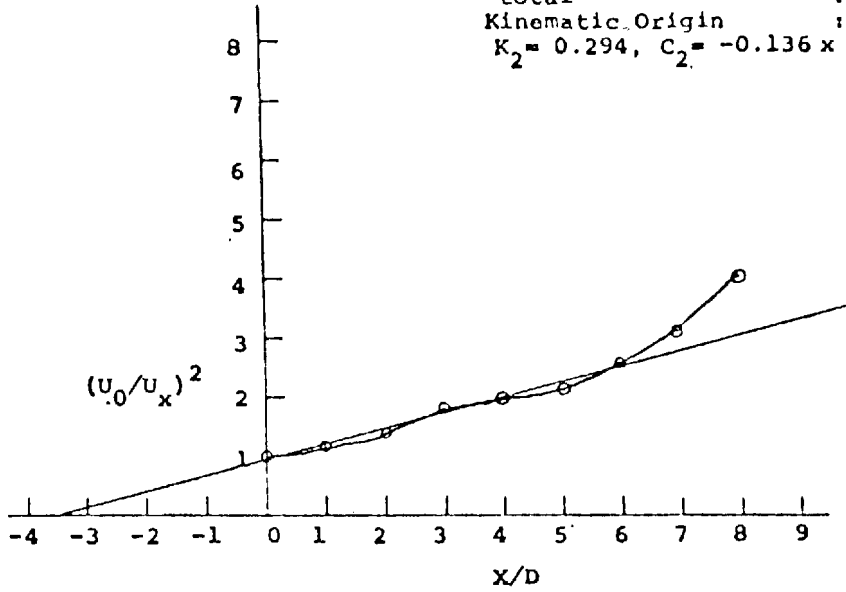


Fig.10 Kinematic Virtual Origin (For Sloping Bottom Tan  $\theta=0.004$ )

Low Slope Case  
 Discharge Velocity : 20cm/sec  
 Discharge Temperature : 35.9°C  
 $A_{ref}$  : 10,000cm<sup>2</sup>/sec  
 $Re$  : 100  
 $t_{total}$  : 65min  
 Geometric Origin : -0.8  
 $K_1 = 0.714, C_1 = -0.032 \times 25$

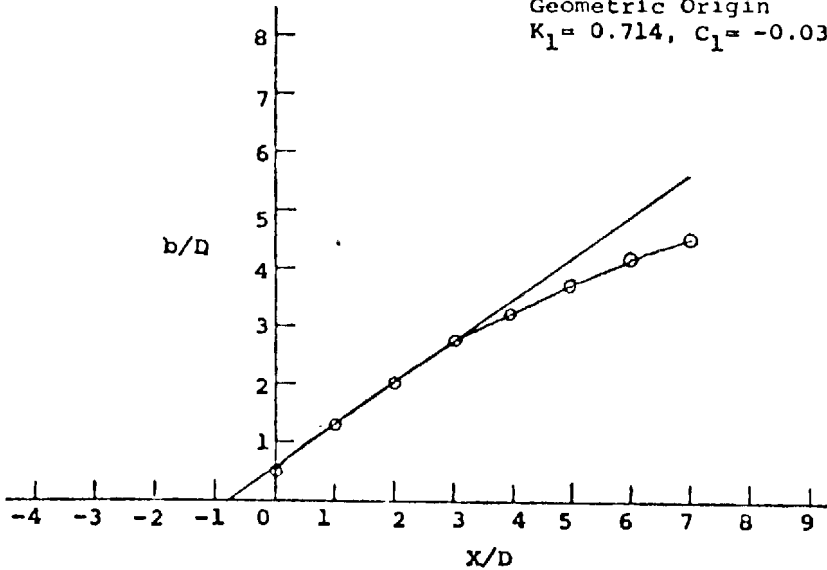


Fig.11 Geometric Virtual Origin (For Sloping Bottom Tan  $\theta=0.004$ )

High Slope Case  
 Discharge Velocity : 20cm/sec  
 Discharge Temperature : 35.9°C  
 $A_{ref}$  : 10,000cm<sup>2</sup>/sec  
 $Re$  : 100  
 $t_{total}$  : 65min  
 Kinematic Origin : -3  
 $K_2=0.33, C_2=-0.12 \times 25$

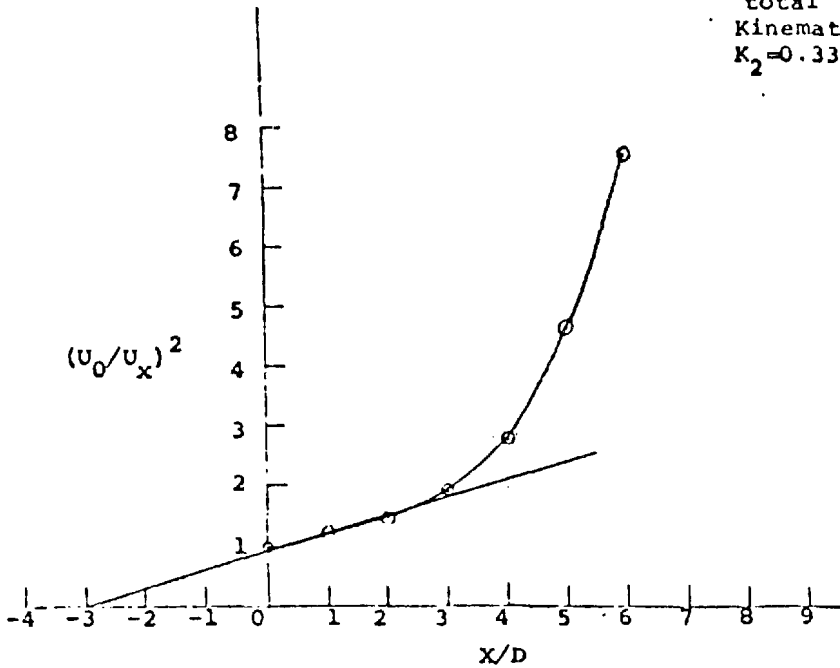


Fig.12 Kinematic Virtual Origin (For Sloping Bottom  
 Tan  $\theta=0.008$ )

High Slope Case  
 Discharge Velocity : 20cm/sec  
 Discharge Temperature : 35.9°C  
 $A_{ref}$  : 10,000cm<sup>2</sup>/sec  
 $Re$  : 100  
 $t_{total}$  : 65min  
 Geometric Origin : -0.78  
 $K_1=0.714, C_1=-0.032 \times 25$

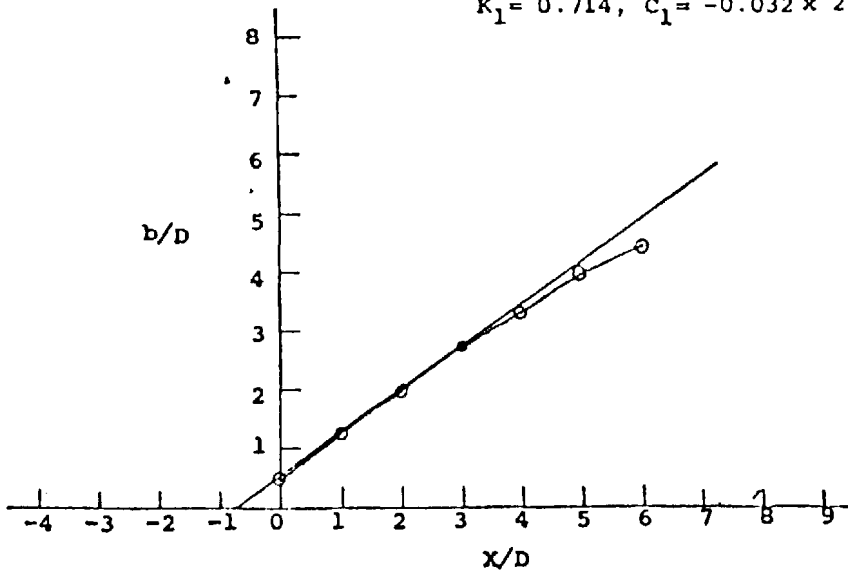


Fig.13 Geometric Virtual Origin (For Sloping Bottom  
 Tan  $\theta=0.008$ )

CONSTANT DEPTH : 1.2m  
 Discharge Vel : 20 cm/sec  
 Discharge Width : 25 m  
 $L_{max}$  : 500 m  
 $L_{min}$  : 425 m  
 $A_{ref}$  : 3,500 cm<sup>2</sup>/sec  
 Reynolds No (Re) : 285  
 $t_{total}$  : 65min  
 $K_2 = 0.069, C_2 = -0.576 \times 25$

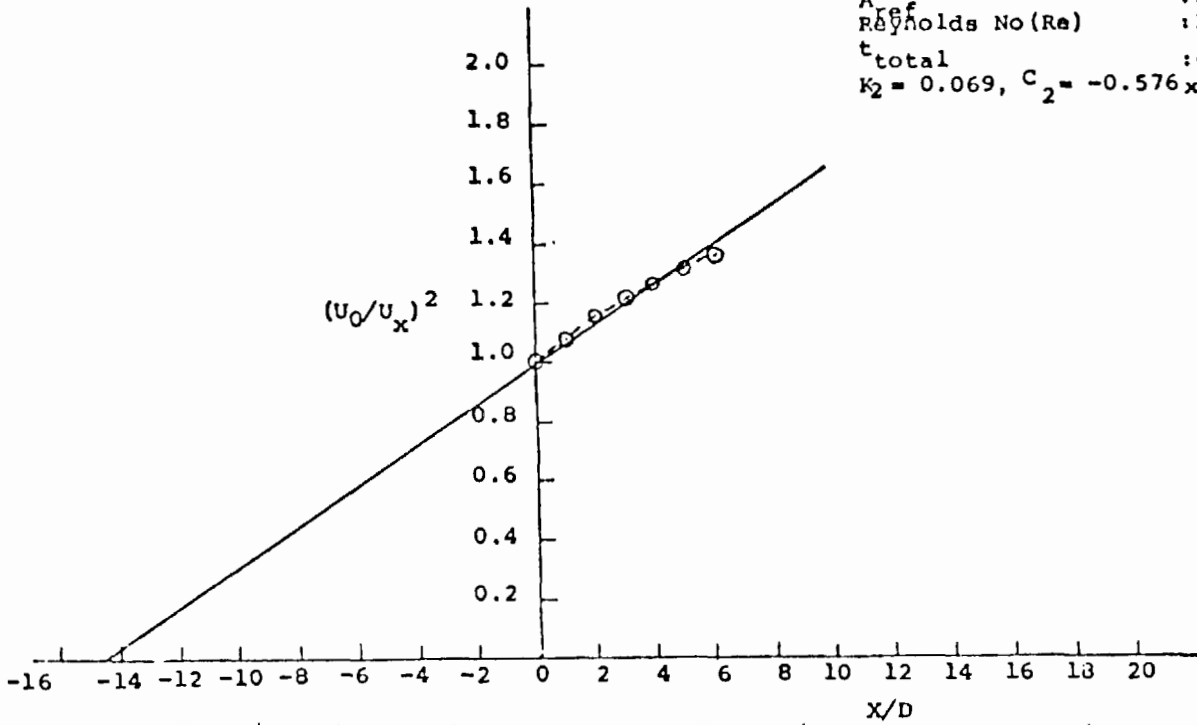


Fig.14 Kinematic Virtual Origin (Constant Depth)

CONSTANT DEPTH : 1.2 m  
 Discharge Vel : 20 cm/sec  
 Discharge Width : 25 m  
 $L_{max}$  : 500 m  
 $L_{min}$  : 425 m  
 $A_{ref}$  : 3,500 cm<sup>2</sup>/sec  
 Reynolds No (Re) : 285  
 $t_{total}$  : 65 min  
 $K_1 = 0.09, C_1 = -0.44 \times 25$

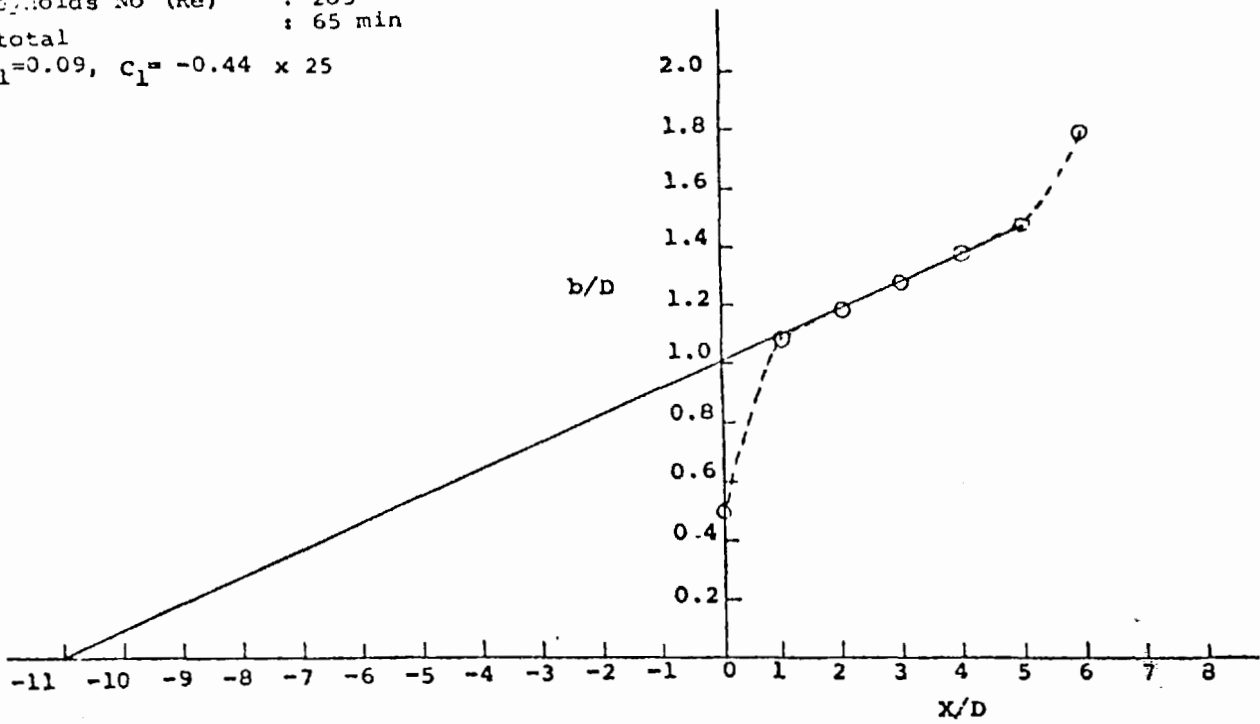


Fig.15 Geometric Virtual Origin (Constant Depth)

LOW SLOPE  
 Discharge Vel : 20 cm/sec  
 Discharge Width : 25 meters  
 $L_{max}$  : 500meters  
 $L_{min}$  : 425 meters  
 $A_{ref}$  : 3500 cm<sup>2</sup>/sec  
 Reynolds No (Re) : 285  
 $t_{total}$  : 65 minutes  
 $K_2=0.18$  ,  $C_2 = -0.22 \times 25$

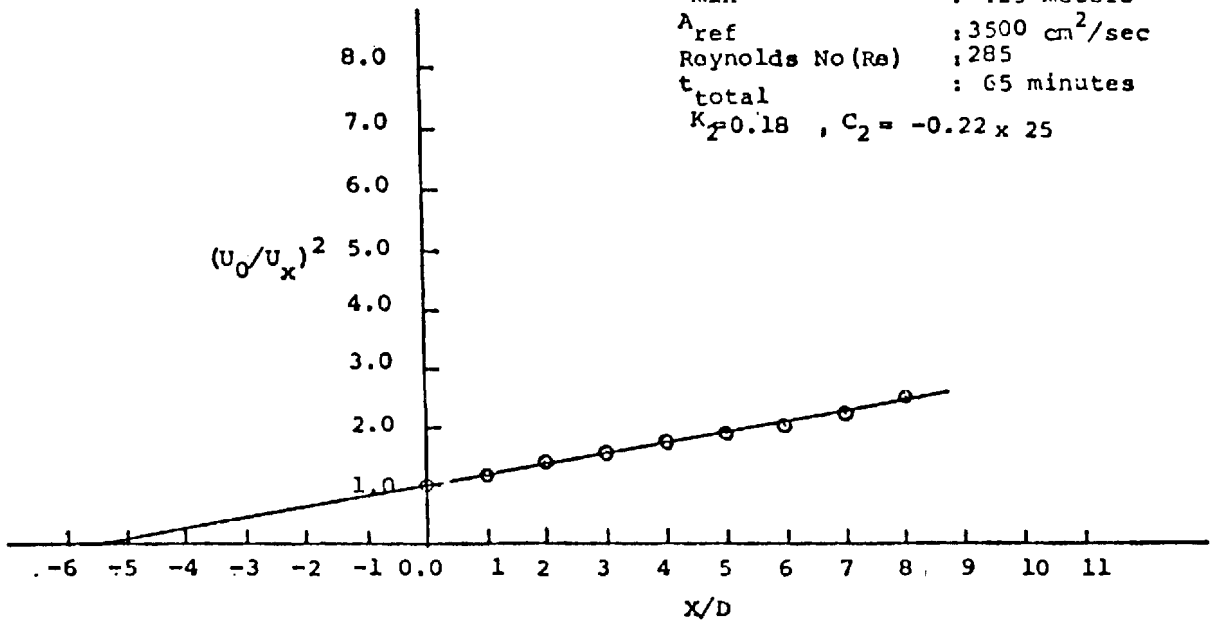


Fig.16 Kinematic Virtual Origin (For Sloping Bottom Tan  $\theta=0.004$ )

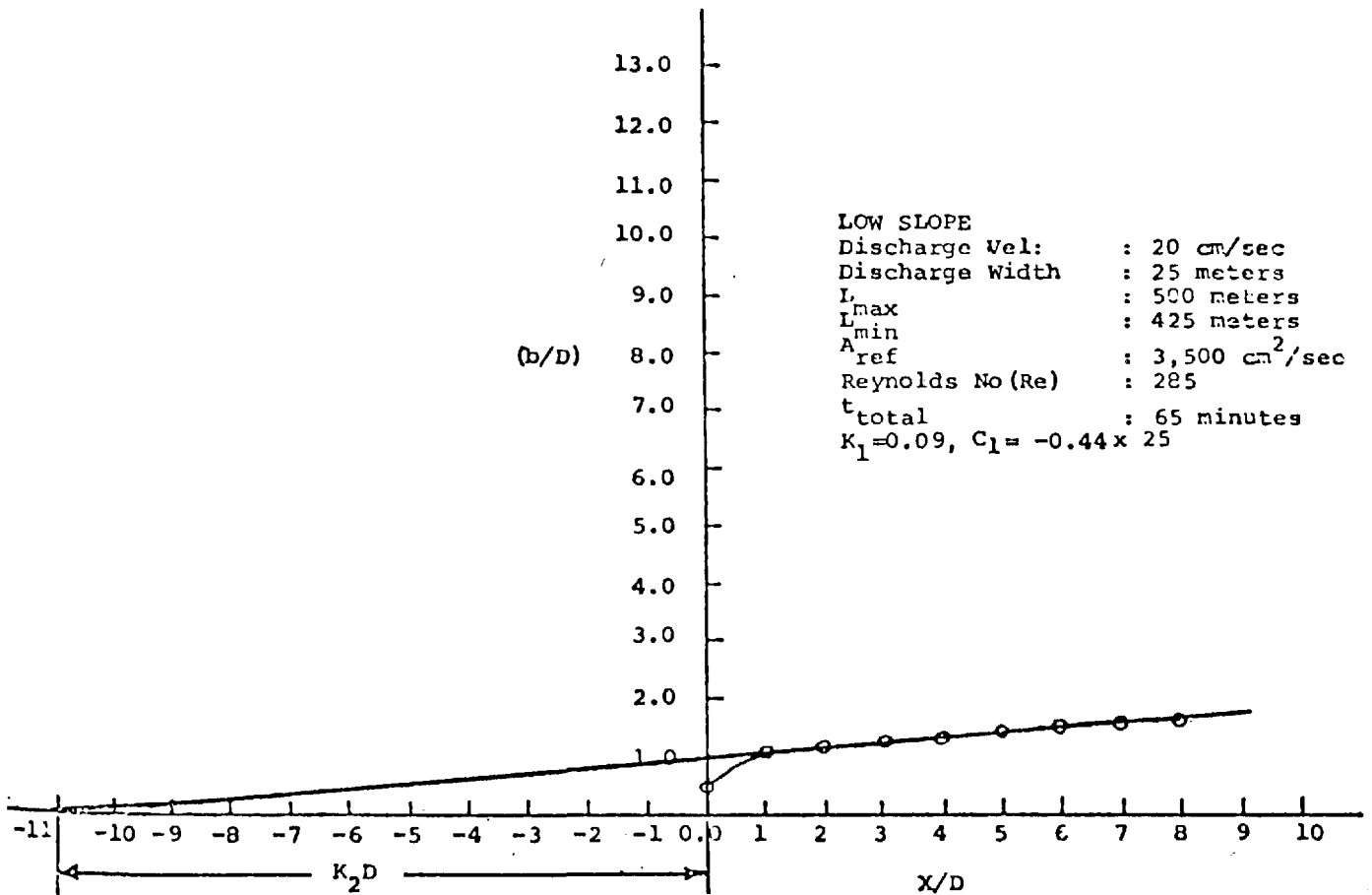


Fig.17 Geometric Virtual Origin (For Sloping Bottom Tan  $\theta=0.004$ )

Severe Slope  
 Discharge Velocity: 20 cm/sec  
 Discharge Width, D: 25 m  
 $A_{ref}$  : 3,500 cm<sup>2</sup>/sec  
 Reynolds No : 285  
 $t_{total}$  : 65 minutes  
 $K_2 = 0.3, C_F = -0.12 \times 25$

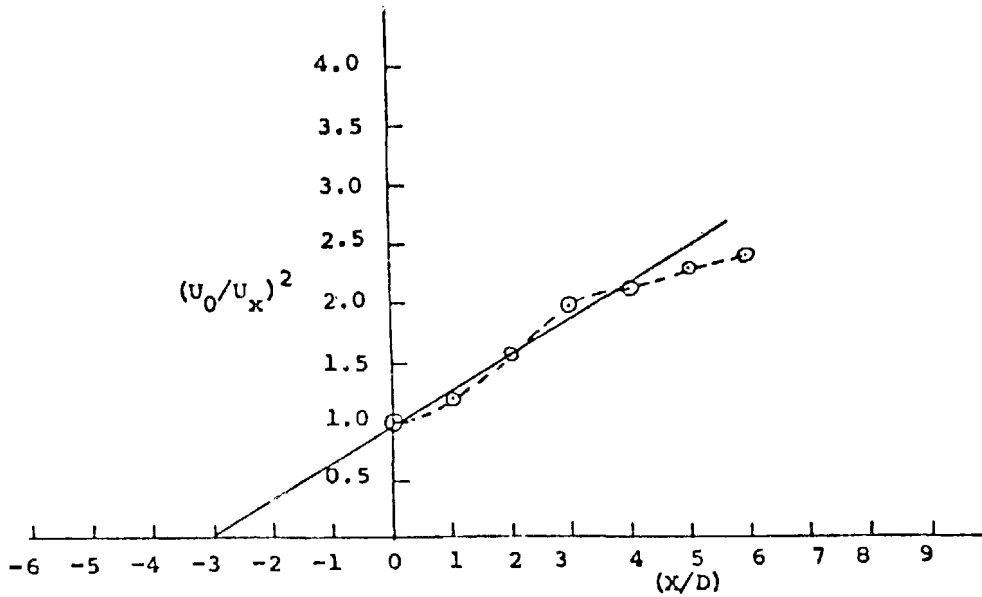


Fig.18 Kinematic Virtual Origin (For Sloping Bottom  
 Tan  $\theta=0.008$ )

Severe Slope  
 Discharge Velocity : 20 cm/sec  
 Discharge Width : 25 m  
 $A_{ref}$  : 3,500 cm<sup>2</sup>/sec  
 Reynolds No (Re) : 285  
 $t_{total}$  : 65 minutes  
 $K_1 = 0.087, C_F = -0.44 \times 25$

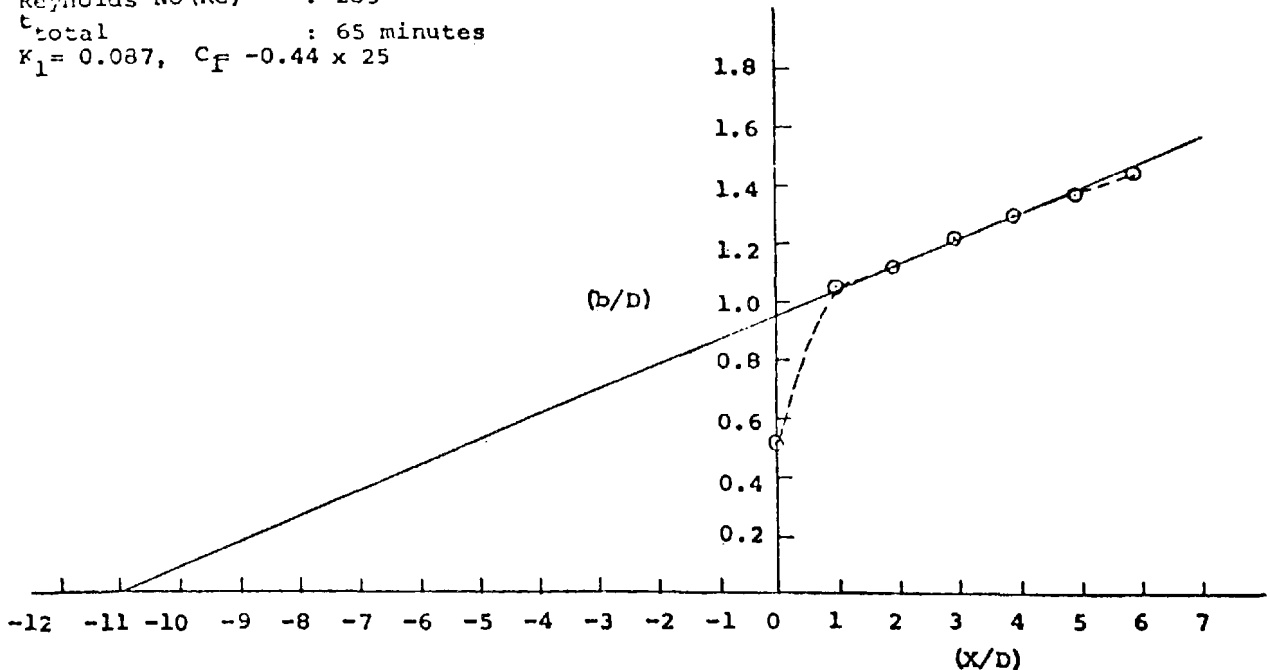


Fig.19 Geometric Virtual Origin (For Sloping Bottom  
 Tan  $\theta=0.008$ )

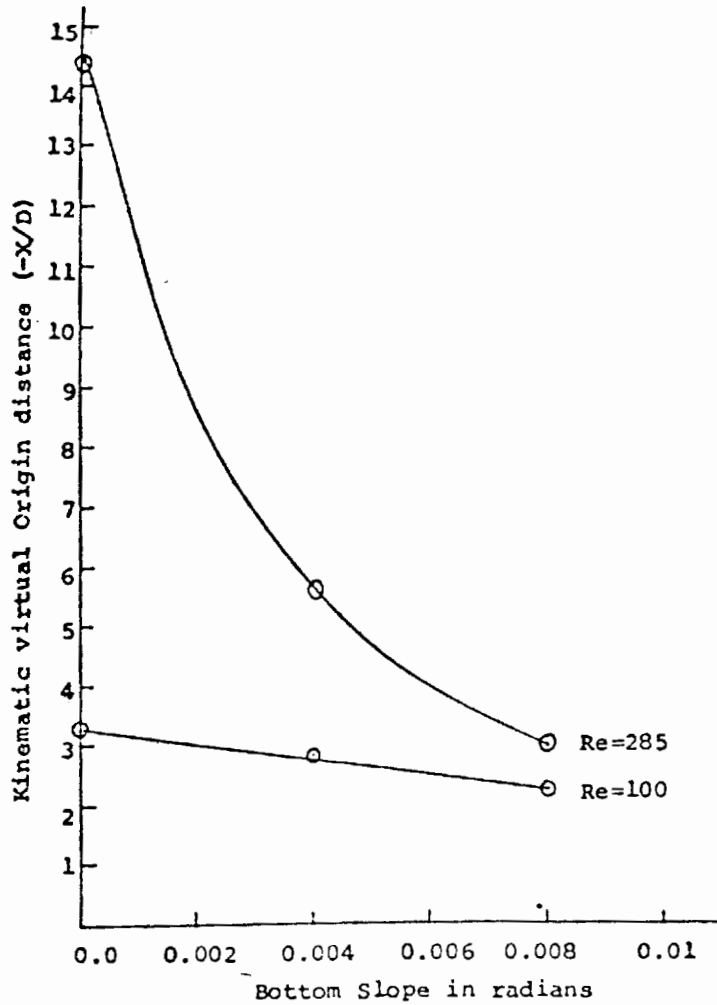


Fig.20 Figure Showing the Relation Between Bottom Slope and Kinematic Virtual Origin for Two Reynolds Numbers (Constant Density Jet)

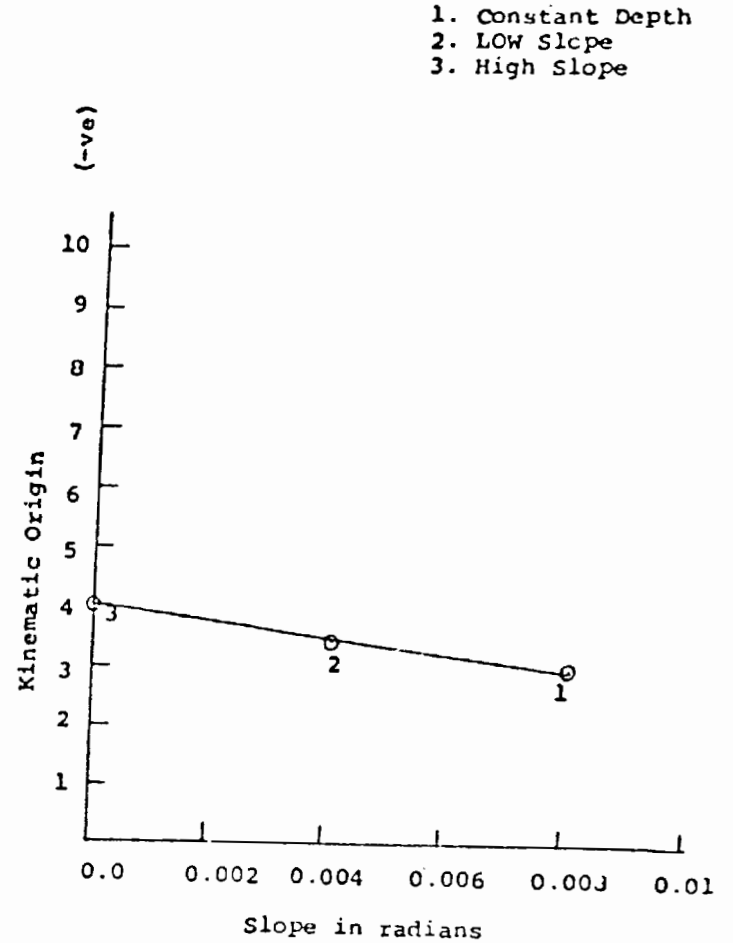


Fig.21 Figure Showing the Relation Between Bottom Slope and Kinematic Virtual Origin for  $Re=100$  (Variable Density Jet)

APPENDIX

|           |   |
|-----------|---|
| $A_H$     | horizontal kinematic eddy viscosity             |
| $A_V$     | vertical kinematic eddy viscosity               |
| $A_z$     | vertical eddy viscosity                         |
| $A_{ref}$ | reference kinematic eddy viscosity              |
| $A_V^*$   | $A_V/A_{ref}$                                   |
| $B_H$     | horizontal diffusivity                          |
| $B_V$     | vertical diffusivity                            |
| $B_{ref}$ | reference diffusivity                           |
| $B_V^*$   | $B_V/B_{ref}$                                   |
| $B_z$     | vertical conductivity $\rho C_p B_V$            |
| $C_p$     | specific heat at constant pressure              |
| Eu        | Euler number                                    |
| f         | Coriolis parameter                              |
| Fr        | Froude number                                   |
| g         | acceleration due to gravity                     |
| h         | depth at any location in the basin              |
| H         | reference depth                                 |
| I         | grid index in x-direction or $\alpha$ direction |
| J         | grid index in y-direction or $\beta$ direction  |
| K         | grid index in z-direction or $\gamma$ direction |
| k         | thermal conductivity                            |
| $K_s$     | surface heat transfer coefficient               |
| L         | horizontal length scale                         |
| P         | pressure  |

|           |  |
|-----------|--|
| $P_s$     | surface pressure                                     |
| $Pr$      | turbulent Prandtl number $(\frac{A_{ref}}{B_{ref}})$ |
| $Pe$      | Peclet number  |
| $Q^*$     | heat sources or sinks                                |
| $Re$      | Reynolds number (turbulent)                          |
| $T$       | temperature  |
| $T_{air}$ | air temperature                                      |
| $T_{ref}$ | reference temperature                                |
| $T_E$     | equilibrium temperature                              |
| $t$       | time   |
| $t_{ref}$ | reference time                                       |
| $u$       | velocity in x-direction                              |
| $v$       | velocity in y-direction                              |
| $w$       | velocity in z-direction                              |
| $x$       | horizontal coordinate                                |
| $y$       | horizontal doordinate                                |
| $z$       | vertical coordinate                                  |

#### Greek Letters

|             |   |
|-------------|---|
| $\alpha$    | horizontal coordinate in stretched system |
| $\beta$     | horizontal coordinate in stretched system |
| $\gamma$    | vertical coordinate in stretched system   |
| $\mu$       | absolute viscosity                        |
| $\rho$      | density                                   |
| $\Phi$      | dissipation terms in energy equation      |
| $\tau_{xy}$ | surface shear stress in x-direction       |

$\tau_{yz}$  surface shear stress in y-direction

Superscripts

- ( ) dimensional quantity
- ( $\sim$ ) dimensional mean quantity
- ( $\hat{\quad}$ ) dimensional fluctuating quantity
- ( ) dimensional quantity
- ( )<sub>ref</sub> reference quantity

The relation between  $K_1$ ,  $K_2$ , jet width and centerplane velocity decay are given by the following relation

$$\frac{b}{D} = K_1 \left( \frac{x}{d} - C_1 \right)$$

$$\left( \frac{U_m}{U_0} \right)^2 = K_2 \left( \frac{x}{d} - C_2 \right)$$

where

$K_1$  = rate of widening of the jet

$K_2$  = slope of centerline velocity decay

$C_1$  = location of the geometric virtual origin from the discharge canal made dimensionless by discharge canal width

$C_2$  = location of the kinematic virtual origin from the discharge canal made dimensionless by discharge canal width

$b$  = jet width

$d$  = discharge canal width

$U_m$  = velocity at the axis of the jet

$U_0$  = discharge velocity

$x$  = distance along the axis measured from the mouth of the jet

## METEOROLOGICAL EFFECTS FROM LARGE COOLING LAKES

F. A. Huff and J. L. Vogel  
Illinois State Water Survey  
Urbana, Illinois U.S.A.

### ABSTRACT

A 30-month field program to evaluate atmospheric effects from waste heat dissipation by large cooling lakes was recently completed in Illinois. Extensive meteorological instrumentation was employed along with radar and satellite data in the evaluation. Results indicated that meteorological effects perpetrated by single power plants are usually insignificant with respect to initiation or enhancement of clouds, precipitation, and fog under the climatic and topographic conditions prevalent in Illinois. Although fog initiation and enhancement are not infrequent in the cold season, the induced visibility restrictions are seldom severe and the downwind extent of the lake effect is usually less than 0.8 km.

### INTRODUCTION

As the demand for electrical energy increases, many more power plants will use auxiliary cooling methods, such as cooling lakes and cooling towers, for the disposal of waste heat. The effect these auxiliary cooling methods have upon the atmosphere are largely unknown [1]. To measure the atmospheric effects associated with waste heat disposal from large cooling lakes, an extensive field program was conducted by the Illinois State Water Survey under contract with the Electric Power Research Institute (EPRI). The program was carried out at Baldwin Lake in southwestern Illinois where an 1800 MW<sub>e</sub> power plant is operated by the Illinois Power Company. The investigation centered on the 2200-acre cooling lake and the surrounding region to determine possible effects on the initiation and enhancement of steam fog, cloudiness, and rainfall. Some results from this recently completed 30-month program are presented here.

Baldwin is situated 72 km (45 miles) SSE of St. Louis, Mo., in a temperate climate characterized by frequent intrusions of cold air, especially in winter. Most of the instruments were installed by the summer of 1976 and the field program ran until March 1978.

Within the instrument network (Fig. 1), temperature and humidity were measured at ground level at 21 locations within an area of approximately 50 km<sup>2</sup>. At five sites, wind was measured at a single level. At five instrumented towers, three levels of temperature and humidity and two levels of wind were recorded. Water temperatures were measured at six sites. Two net radiometers, a recording evaporimeter, recording raingage,

microbarograph, and transmissometer were operated to provide a complete array of meteorological measurements. A non-recording raingage network extending within and beyond the basic instrument network was operated also. Routine visibility measurements and photographs of weather conditions were made by the project observer. Satellite data from the summer of 1975 were used to help assess cloud conditions.

## STEAM FOG

A major atmospheric effect and one of the most visible effects associated with cooling lakes is the initiation and/or the enhancement of steam fog [1, 2, 3, 4]. During the 20-month period from September 1976 to March 1978, 185 steam fog days were recorded by the Baldwin observer (Table 1). The frequency of these events by season and visibility (intensity) were further divided into initiation and enhancement days. Enhancement days were defined as those when natural fog and steam fog occurred simultaneously and the steam fog significantly reduced the visibility. Initiation days were those having steam fog with no natural fog present. The maximum frequency of all steam fog events occurred in winter with a secondary maximum in fall. The frequency of steam fog was at a minimum in both spring and summer.

For this study, dense fog was considered to have a visibility of 0.4 km (0.25 mile) or less. It was felt that such visibilities would be intense enough to impair normal driving. The Transportation Research Board of the National Research Council [5] indicates that the performance of a driver is not affected seriously until the visibility drops below 0.2 km (600 feet). Thus, the dense fog definition for Baldwin provides a conservative estimate of the number of times this event could impair normal road traffic, if the steam fog moved from the lake across a road surface.

Dense fog maximized over Baldwin during winter with twice as many occurrences than any other season. During the winter of 1976-1977 all dense fogs but one were due to the initiation of steam fog over the cooling lake. During the winter of 1976-1977 little natural fog formed, although it tends to maximize during this season [2]. However, during the winter of 1977-1978 natural fog formed more frequently. Winter enhancement was observed on 10 days, and seven of these were associated with dense fog. Dense fog over the cooling lake in the other seasons was associated usually with fog enhancement, rather than initiation.

The frequency and intensities of steam fog initiation maximized during fall and winter and decreased markedly during spring. Only five incidents of steam fog initiation were noted during the summer, all with visibilities of 1.6 km (1 mile) or greater. Although the enhancement of natural fog by steam fog occurred in all seasons, it maximized (unexpectedly) during the summer of 1977. Normally, the enhancement effect will maximize during fall and winter, when the climatic maximum of fog days occurs over

Illinois [2]. However, it will have temporal variance since it is strongly related to the frequency and intensity of natural fog events.

Steam fog over the cooling lake will have only minor impacts upon the movement of vehicles if it is confined to the boundaries of the lake, and no roads are built over or immediately adjacent to the lake. However, if steam fog moves off the lake it can reduce significantly the visibility across roads and cause problems for motor-vehicle traffic. Only 38% of all the steam fog events (71 of 185) were observed to travel beyond the boundaries of the lake, and 78% (55 of 71) did not extend more than 0.2 km (Table 2). On days when steam fog was initiated over the cooling lake only 25% of these fogs moved beyond the boundary of the lake, while nearly 50% (23 of 48) of the enhancement days experienced some horizontal movement from the lake.

In general, the more intense the steam fog the farther it moved beyond the lake. All fogs which moved 1.6 km (1 mile) or more were associated with steam fog that initiated over the lake and the lowest visibility associated with these steam fog events was 0.4 km (0.25 mile) or less. On enhancement days no visibility reductions due to steam fog were noted beyond 0.8 km (0.5 mile). However, it is possible that steam fog could reduce the visibility farther downwind under certain conditions, especially if the natural fog formed with nearly calm wind conditions and the steam fog traveled along natural low-lying areas adjacent to the cooling lake. Such a situation was not observed with natural fog present, but it was observed to occur on two days when steam fog was initiated over the cooling lake. The fog on these days drifted from the lake and traveled by gravity flow along dry creek beds up to distances of 6.5 km (4 miles) from the lake, with much reduced visibilities.

The relation between the intensity of steam fog and the horizontal extent is quite strong. Of the 24 steam fog events which initiated over the cooling lake with visibility of 0.4 km (0.25 mile) or less, 22 experienced some horizontal movement. Similarly, 13 of the 21 dense fog cases with enhancement experienced some horizontal movement from the lake when visibility was 0.4 km or less.

The initiation of steam fog has been linked to the difference between the water and air temperatures and the saturation deficit of the ambient air [2]. The water-air temperature difference for initiation days was greater than on days when the natural fog was present for the same fog intensity. This is due to the greater saturation deficit of the air on initiation days. More water vapor has to be evaporated before condensation in the air is reached on initiation than on enhancement days. The more intense steam fogs that initiated during winter formed with ambient saturation deficits of 1 gm/kgm or less, and the water-air temperature difference was generally 19.4°C (35°F) or greater.

Synoptically, many of the steam fogs formed when a cold air mass was over the cooling lake. The formation was not often associated with frontal

activity. Typically, it occurred with cold, stable air when the water temperature was much warmer than the air temperature. Comparisons with steam fog observations over the Dresden cooling lake in the colder winter climate of northern Illinois showed similar steam fog distributions [6].

#### ENHANCEMENT OF CLOUDINESS

Satellite photographs taken during the summer of 1975 were used to investigate cooling lake effects on the time-space distribution of cloudiness. Analyses were made for two cooling lakes in southern Illinois (Baldwin and Coffeen) and for a much larger, control lake (Carlyle). No evidence was found that the cooling lakes or control lake had any significant effect upon the summer cloud frequencies, and, consequently, upon precipitation. There was some evidence, however, that local terrain features in the study region, ridges and river valleys, do influence the spatial distribution of clouds, primarily cumulus and cumulonimbus.

The potential cooling lake effect was investigated further through use of available radar data for summer during 1971 to 1975. Results supported the satellite findings with respect to the two cooling lakes. However, the larger control lake (Carlyle) appeared to have some influence on the initiation of convective precipitation when atmospheric motions were parallel to the major axis of this elongated lake.

Thus, it was concluded from the satellite and radar evidence that cooling lakes the size of Baldwin and Coffeen have little or no effect upon the initiation of convective cloudiness or precipitation. However, much larger cooling lakes, as indicated by the Carlyle findings, could enhance convective activity when the low-level air and clouds have a relatively long travel time over the lake. Otherwise, most cooling lakes have a minimal impact upon the initiation and enhancement of convective cloudiness and should produce no environmental problems of significance in this direction.

#### RAINFALL

A dense raingage network was operated in the Baldwin area during July-November 1976 and March-November 1977. The objective was to investigate potential effects upon the regional rainfall pattern resulting from waste heat discharges into the cooling lake associated with the Baldwin power plant. Analyses were performed to determine the seasonal distributions of total rainfall, frequency of rainfall events, effect of storm movements on network rainfall patterns, and the relation between rainfall and synoptic weather types.

Results of the 2-year study were inconclusive. There was a persistent high in the Baldwin network located 10-15 km E-ENE of the center of the lake when rainfall for the two years was combined, and this apparent

anomaly was especially prominent with storms moving from the SW quadrant, which place the lake directly upwind of the observed maximum. However, the rainfall maxima within the network were in agreement with the natural rainfall distribution for southern Illinois during the sampling periods, as revealed by the National Weather Service climatic network data.

The most positive evidence of a localized anomaly was its persistence in location during the sampling period. If this is a localized anomaly, it could also be related to topographic features to the west (upwind) of the network where ridges and bluffs apparently stimulate the development of cumulus and cumulonimbus, as indicated in the previous discussion on enhancement of convective clouds. Since no evidence was found of convective cloud stimulation downwind of the lake, it appears unlikely that the relatively high rainfall in the eastern part of the Baldwin Network in 1976-1977 can be attributed to a cooling lake effect on the environment. On the basis of presently available information, it is concluded that cooling lakes of the size of Baldwin (2200 acres) will not significantly modify the precipitation regime in the surrounding area.

#### CONCLUSIONS

Meteorological effects from cooling lakes associated with single power plants are usually insignificant in Illinois and other areas of similar climate and topography. There was no evidence in the Baldwin study of significant lake effects upon clouds and precipitation. Most cases of fog initiation or enhancement occurred in the cold season, and the downwind extent of lake-influenced fog was usually less than 0.8 km (0.5 mi). Dense fog (visibility  $\leq 0.4$  km) occurred in less than 25% of the fog events.

#### REFERENCES

1. Ackermann, William C. Research Needs on Waste Heat Transfer from Large Sources in the Environment. Urbana, Ill.: Report to National Science Foundation, Grant GI-30971, Illinois State Water Survey, 1971.
2. Huff, F. A., and J. L. Vogel. Atmospheric Effects from Waste Heat Transfer Associated with Cooling Lakes. Urbana, Ill.: Report to National Science Foundation, Grant GI-35841, 1973.
3. Vogel, J. L., and F. A. Huff. "Fog Effects from Power Plant Cooling Lakes." J. Appl. Meteor., Vol. 14, 1975, 868-872.
4. Murray and Trettel, Inc. Report on Meteorological Aspects of Operating the Man-Made Cooling Lake and Sprays at Dresden Nuclear Power Station, Chicago, Ill.: Prepared for Commonwealth Edison Company, 1973.

5. Heiss, W. H. Highway Fog Visibility Measures and Guidance Systems. Washington, D.C.: Transportation Research Board, National Research Council, 1976. National Cooperative Highway Research Program Report 171.
6. Vogel, J. L., and F. A. Huff. "Steam Fog Occurrences over Cooling Lakes." Boston, Mass.: Preprints Sixth Conference on Planned and Inadvertent Weather Modification. American Meteorological Society, 1977, 69-72.

Table 1  
 FREQUENCY OF BALDWIN COOLING LAKE STEAM FOGS AND VISIBILITIES

| <u>Season</u> | <u>Initiations</u><br><u>Visibilities (km)</u> |                                |                                |              |              | <u>Enhancements</u><br><u>Visibilities (km)</u> |                                |                                |              |              |
|---------------|--|--------------------------------|--------------------------------|--------------|--------------|---|--------------------------------|--------------------------------|--------------|--------------|
|               | <u>≤0.4</u>                                    | <u>&gt;0.4-</u><br><u>≤1.6</u> | <u>&gt;1.6-</u><br><u>≤8.0</u> | <u>&gt;8</u> | <u>Total</u> | <u>≤0.4</u>                                     | <u>&gt;0.4-</u><br><u>≤1.6</u> | <u>&gt;1.6-</u><br><u>≤8.0</u> | <u>&gt;8</u> | <u>Total</u> |
| Fall 76       | 2  | 5                              | 7                              | 8            | 22           | 3   | 3                              | 1                              | 0            | 7            |
| Winter 76-77  | 10   | 5                              | 4                              | 10           | 29           | 1   | 0                              | 0                              | 0            | 1            |
| Spring 77     | 0  | 1                              | 6                              | 9            | 16           | 0   | 1                              | 0                              | 0            | 1            |
| Summer 77     | 0  | 0                              | 4                              | 1            | 5            | 4   | 6                              | 4                              | 0            | 14           |
| Fall 77       | 2  | 1                              | 4                              | 16           | 23           | 4   | 5                              | 0                              | 0            | 9            |
| Winter 77-78  | 9  | 2                              | 8                              | 20           | 39           | 7   | 2                              | 1                              | 0            | 10           |
| March 78      | <u>1</u>                                       | <u>0</u>                       | <u>1</u>                       | <u>1</u>     | <u>3</u>     | <u>2</u>  | <u>2</u>                       | <u>2</u>                       | <u>0</u>     | <u>6</u>     |
| Total         | 24   | 14                             | 34                             | 65           | 137          | 21  | 19                             | 8                              | 0            | 48           |

Table 2  
 FREQUENCY OF BALDWIN COOLING LAKE STEAM FOGS WITH HORIZONTAL EXTENT

| <u>Visibility</u> | <u>Initiation Days</u><br><u>Horizontal Extent (km)</u> |                          |                          |                |              | <u>Enhancement Days</u><br><u>Horizontal Extent (km)</u> |                          |                          |                |              |
|-------------------|---|--------------------------|--------------------------|----------------|--------------|--|--------------------------|--------------------------|----------------|--------------|
|                   | <u>≤0.2</u>   | <u>&gt;0.2-<br/>≤0.8</u> | <u>&gt;0.8-<br/>≤1.6</u> | <u>&gt;1.6</u> | <u>Total</u> | <u>≤0.2</u>  | <u>&gt;0.2-<br/>≤0.8</u> | <u>&gt;0.8-<br/>≤1.6</u> | <u>&gt;1.6</u> | <u>Total</u> |
| ≤0.4              | 11  | 6                        | 2                        | 3              | 22           | 10   | 3                        | 0                        | 0              | 13           |
| >0.4-≤1.6         | 4   | 2                        | 0                        | 0              | 6            | 8  | 1                        | 0                        | 0              | 9            |
| >1.6 ≤8.0         | 8   | 0                        | 0                        | 0              | 8            | 1  | 0                        | 0                        | 0              | 1            |
| >8.0              | <u>12</u>   | <u>0</u>                 | <u>0</u>                 | <u>0</u>       | <u>12</u>    | <u>0</u>   | <u>0</u>                 | <u>0</u>                 | <u>0</u>       | <u>0</u>     |
| Total             | 35  | 8                        | 2                        | 3              | 48           | 19   | 4                        | 0                        | 0              | 23           |

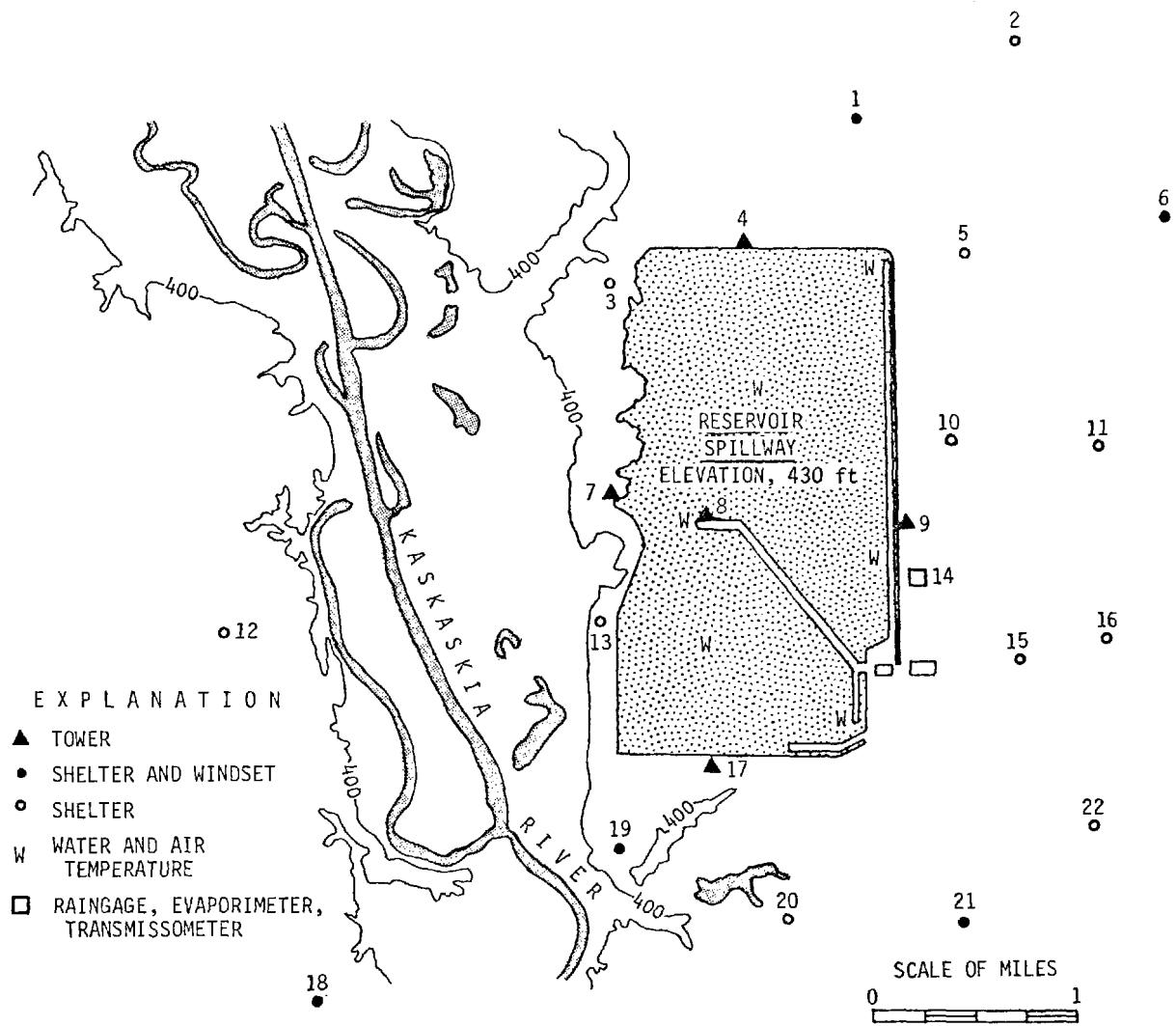


Figure 1. Baldwin instrument network

COMPUTER SIMULATION OF MESO-SCALE METEOROLOGICAL EFFECTS OF  
ALTERNATIVE WASTE-HEAT DISPOSAL METHODS

J.P. Pandolfo and C.A. Jacobs  
The Center for the Environment and Man, Inc.  
Hartford, Connecticut U.S.A.

ABSTRACT

The preliminary use of a physically complete land-sea-air boundary layer model is described in the simulation of the meteorological effects of artificial heat inputs. The model provides solutions obtained by temporal integration of the Eulerian conservation equations. Taken into account are stability-(Richardson number)-dependent mixing, complex topography, spatially varying interface properties, and cloud-dependent radiative heating (cooling). Clouds may be externally specified, or internally generated in the model by exercising a model input option. In the example described, simulation of the effects of hypothetically arranged dry cooling towers in the Rhine valley of Switzerland was carried out (in cooperation with the Institute of Reactor Research of Switzerland). Simulated effects on the mesoscale temperature structure of the atmosphere's lowest kilometer, as well as on the slope-valley circulation as resolved on a 3-km horizontal grid, are presented for a clear summer day.

INTRODUCTION

A physically complete land-sea-air boundary layer model has been used in the simulation of the meteorological effects of artificial heat inputs. The model provides solutions obtained by temporal integration of the Eulerian conservation equations on a relatively fine (1- to 10-km horizontal, 1- to 100-m vertical) spatial mesh, with complex momentum, heat, and moisture sources.

Taken into account are stability-(Richardson number)-dependent mixing, complex topography, spatially varying interface properties, and cloud-dependent radiative heating (cooling). Clouds may be externally specified, or internally generated in the model by exercising a model input option. The model's physical equations, and a previous application in studying inadvertent weather modification, are described by Atwater [1].

In the study described in this paper, the overall objective was defined by the Institute for Reactor Research (EIR) of Switzerland. It is

"to identify and quantify the impact of man's industrialization on the climate of the Rhine River Valley in the region about Basel. In particular, the climatic effects resulting from alternative scenarios involving the size and locations of new electric power generating facilities will be explored."

The reason for this objective becomes apparent when it is pointed out that with present and projected power generating facilities, the man-made heat input to the atmosphere over the region will amount to 50 percent or more of the solar heat input to the region in the winter-time.

The initial phases of this study involved extensive data gathering efforts in the region, including the construction of a pilot-test cooling tower, and the derivation of a general numerical model of the cooling tower plume [2]. This work was begun, and continues, at EIR (Switzerland).

Later in the project, the preparation and use of a valley-scale meteorological model to be used in conjunction with the research products of these activities was begun in a joint CEM-EIR project. A series of numerical experiments was defined to assess the feasibility of using such a general meteorological model in this study. These began with one-dimensional (horizontal variation terms of the Eulerian equations prespecified from observations) simulations of the diurnally varying vertical structure of the atmospheric boundary layer [3]. They continued with two-dimensional (along-valley variations specified from observations) simulations of the diurnally varying atmospheric structure in a cross-valley section. We have now completed the first of our three-dimensional simulation experiments, which is described here.

In this experiment, we wished to determine whether practically obtainable initial three-dimensional data sets (derived from scattered observations integrated into one- and two-dimensional model simulations) could be used in a usefully detailed three-dimensional spatial grid, and integrated over useful periods of time (a few days per simulation), without generating computational errors so large as to make the three-dimensional simulation results uselessly unrealistic. Furthermore, this was to be carried out within practical limitations on computer size and availability.

#### THE FIRST THREE-DIMENSIONAL SIMULATION EXPERIMENT

The scenario used for this feasibility experiment introduced 2000 MW of waste sensible heat at each of three ("dry tower") locations spaced approximately at equal intervals along the main valley floor (grid-square centers marked with the symbol  $\infty$  on Fig. 1a). Figure 1a also shows the smoothed topography on the basic 3km $\times$ 3km horizontal grid. The main Rhine valley is generally oriented E-W, but turns sharply to the north at the west end of the region (in grid columns 1-4). A side valley branches generally north at grid column 12. Three other side valleys branch generally south at grid columns 4, 8, and 15. Features apparently associated with these secondary valleys are evident in the solution temperature and flow patterns shown in later figures.

The boundary ridge elevations are highly asymmetric. The most pronounced ridge lies on the eastern half of the northern boundary, with a much lower, interrupted, ridge along the southern and southwestern boundary. The most intense slope is oriented N-S, east of grid column 12, and north of the main valley. Features of the solution temperature and flow fields apparently related to this topographic feature are also evident in later solutions.

The large-scale weather situation specified for this experiment was one of clear, early-summer (near-solstice) conditions with weak synoptic-scale flow. The integration was carried out on a three-dimensional spatial mesh containing 7(north-south)  $\times$  20(east-west)  $\times$  27(vertical) points. It was found experimentally that 36-second time steps were required to ensure numerical stability. As a consequence, it was found that almost exactly one hour of CRAY-1 CPU time (or about two hours of CDC-7600 time) was required for each simulation day of real time.\*

#### SOLUTION FIELDS FOR THE FIRST EXPERIMENT

Solution features are shown for two times of day--viz., 1707 sun time (ST) June 23rd, and 0507 ST June 24th. There are presented for each of the two times of day the basic ("CONTROL") unperturbed temperature and horizontal flow fields at 8-m and 300-m elevation (above terrain). There are also shown difference fields in which the temperature and horizontal flow vector differences ("DRY TOWER MINUS CONTROL") are plotted at 8-m (above terrain) elevation.

Only a cursory discussion of these results is justified at this time. We point out that generally reasonable "CONTROL RUN" results have been obtained. Results at 1900 and 3100 time steps of integration are shown. These results are reasonable in that they show:

- 1) a general, relatively deep, upslope and upvalley daytime flow (Fig. 2a,b);
- 2) a generally shallow downslope, downvalley flow at night (Fig. 4a,b);
- 3) relatively weak, deep, daytime temperature maxima over the valley in terrain-parallel surfaces (not shown); and
- 4) relatively intense, shallow night-time temperature minima over the valley in terrain-parallel surfaces (Fig. 3a,b).

In addition, the general correspondence between the scattered wind measurements (Fig. 1b) and the solution wind fields (Fig. 4a) is to be noted.

Details in these general fields require more investigation. For example, the ridge-parallel jet-like detail at 300 m found to be:

- 1) N-S in the daytime flow pattern along grid columns 2, 3, 4, and W-E at grid columns 17-20, rows 3-5 (Fig. 2b);
- 2) N-S in the night flow pattern along grid columns 4-9 (Fig. 4b);

is similar in general intensity, orientation, and vertical structure to that found in the much more highly idealized models of Mason and Sykes [4]. A sequence of stepped idealizations from our model to their model will serve to investigate the underlying physics of the apparent similarity. Though this sequence of experiments is easy to formulate, it will require a few hours of computer time to carry out.

The temperature perturbations by the intense waste-heat sources are qualitatively reasonable. Relatively weak (against a strong solar radiation background) daytime maximum differences are evident (Fig. 5a). More intense night-time maxima are evident in Fig. 6a. The wind disturbance is less

---

\* Acknowledgement is made to the NCAR, which is sponsored by the NSF, for the computing time used in this research.

systematic. The daytime flow at 8 m is generally countered, and locally reversed, with wide-spread vector differences as large as and opposing the control run winds (Figs. 2a, 5b). The night-time flow is perturbed strongly only locally in the S-W portion of the region (Figs. 4a, 6b).

#### SUMMARY AND PLANS FOR FURTHER INVESTIGATION

The first experimental results exhibit significant disturbance of the control run daytime meso-scale slope-valley circulation. They also show wide-spread temperature increases of about 1°C in clear, summer, daytime in-valley temperature and 3°C increases in clear, summer, night-time temperatures.

The large-scale weather situation dealt with in this experiment constitutes a "near-worst" case in terms of the computational requirements, a "far-from-worst" case in terms of the relative magnitude of waste-heat to natural solar heat input (about 4% over the total area, and for the day of the year, and the clear conditions considered) and perhaps a "semi-worst" case in terms of natural flow disruption because of the weak large-scale flow component and the strong solar input.

These characterizations remain to be more precisely defined by carrying out other experiments in other weather (particularly cloudy-winter) conditions.

There also remains to be more precisely assessed the level of "computational noise" still present in the solutions. A two-pronged approach to this assessment is planned: one branch obtaining more detailed observations scheduled and placed in accordance with previously obtained model solutions; the other, more theoretical, branch studying stepwise physical idealizations, and applied mathematical questions (e.g., the influence of the finite-difference schemes and the lateral boundary conditions chosen).

Finally, and to some extent, concurrently, alternative waste-heat disposal methods must be simulated, including variation of type (wet cooling towers) and location (e.g., ridge or on-slope rather than in-valley location).

#### REFERENCES

- [1] M.A. Atwater, "Urbanization and Pollutant Effects on the Thermal Structure in Four Climatic Regimes," *J. Appl. Meteor.*, 16, 1977 (Sep).
- [2] F. Gassman, D. Burki, D. Haschke, R. Morel, *Flugmessungen in der atmosphärischen Grenzschicht*, EIR-Bericht Nr. 334, Eidg. Inst. für Reaktorforschung Würenlingen, Schweiz (Switzerland), 1978.
- [3] D. Haschke, F. Gassman, F. Rudin, *Eindimensionale, zeitabhängige Simulation der planetarischen Grenzschicht über eine 48-Stunden Periode*, EIR-Bericht Nr. 337, Eidg. Institut für Reaktorforschung Würenlingen, Schweiz (Switzerland), 1978.
- [4] P.J. Mason and R.I. Sykes, "On the interaction of topography and Ekman boundary layer pumping in a stratified atmosphere," *Quart. J. Roy. Meteor. Soc.*, 104, 475-490, 1978.

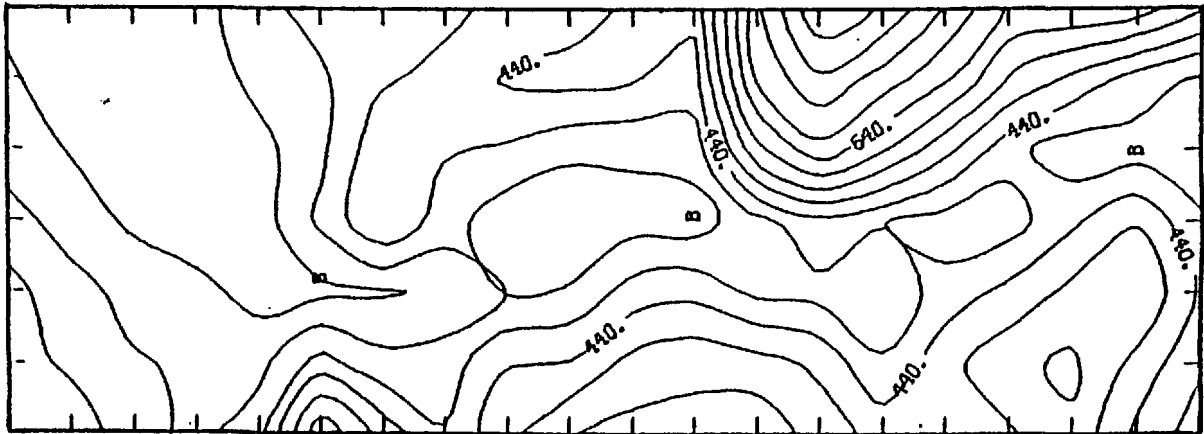


FIGURE 1a. Basic topography with dry cooling tower locations. Elevation is in meters.

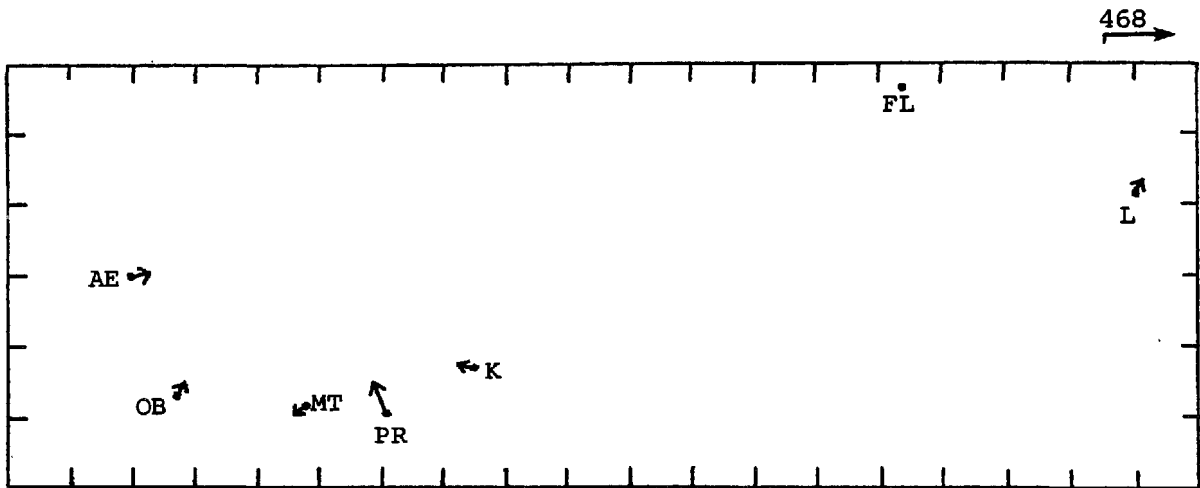


FIGURE 1b. Observed hourly mean wind at 10 meters, 0500-0600 sun time, 23 June 1976. The magnitude of the maximum wind vector (cm/s) in the field is shown in the upper right-hand corner.

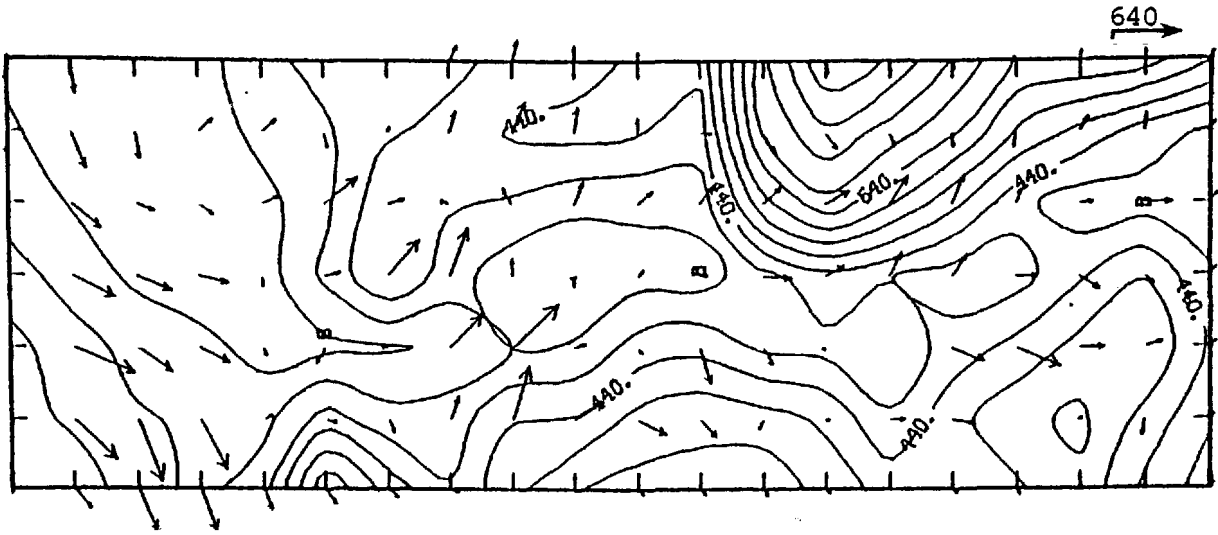


FIGURE 2a. Control run horizontal wind at 8 meter elevation at 1707 sun time. The magnitude of the maximum wind vector (cm/s) in the field is shown in the upper right-hand corner.

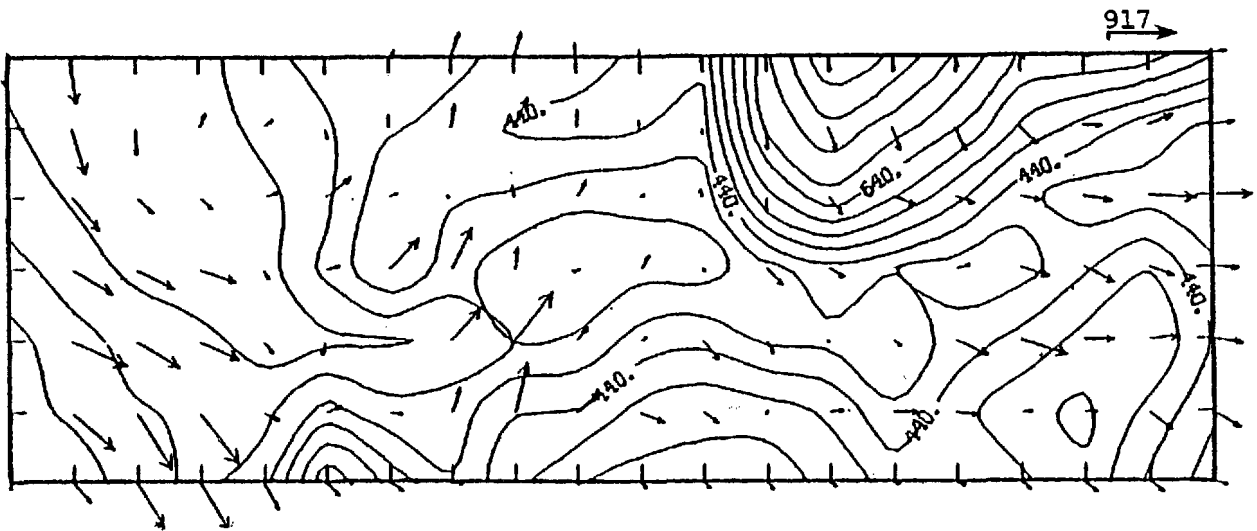


FIGURE 2b. Control run horizontal wind at 300 meter elevation at 1707 sun time. The magnitude of the maximum wind vector (cm/s) in the field is shown in the upper right-hand corner.

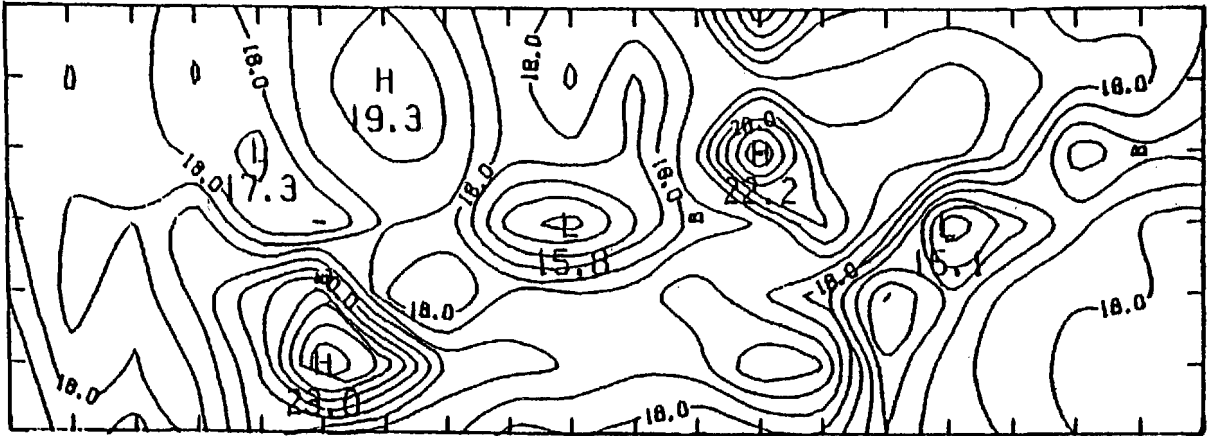


FIGURE 3a. Control run temperature at 8 meter elevation at 0507 sun time.

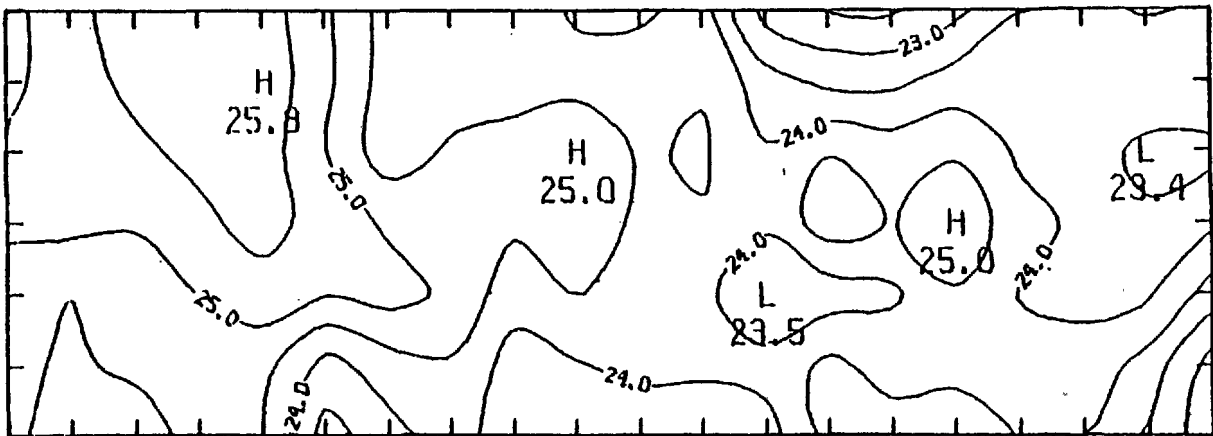


FIGURE 3b. Control run temperature at 300 meter elevation at 0507 sun time.

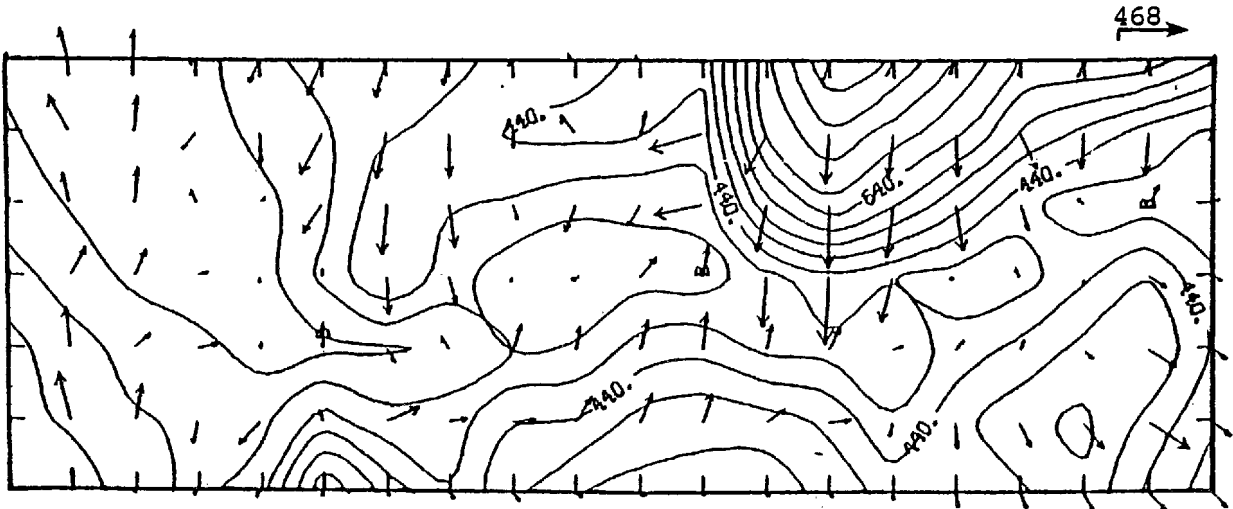


FIGURE 4a. Control run horizontal wind at 8 meter elevation at 0507 sun time. The magnitude of the maximum wind vector (cm/s) in the field is shown in the upper right-hand corner.

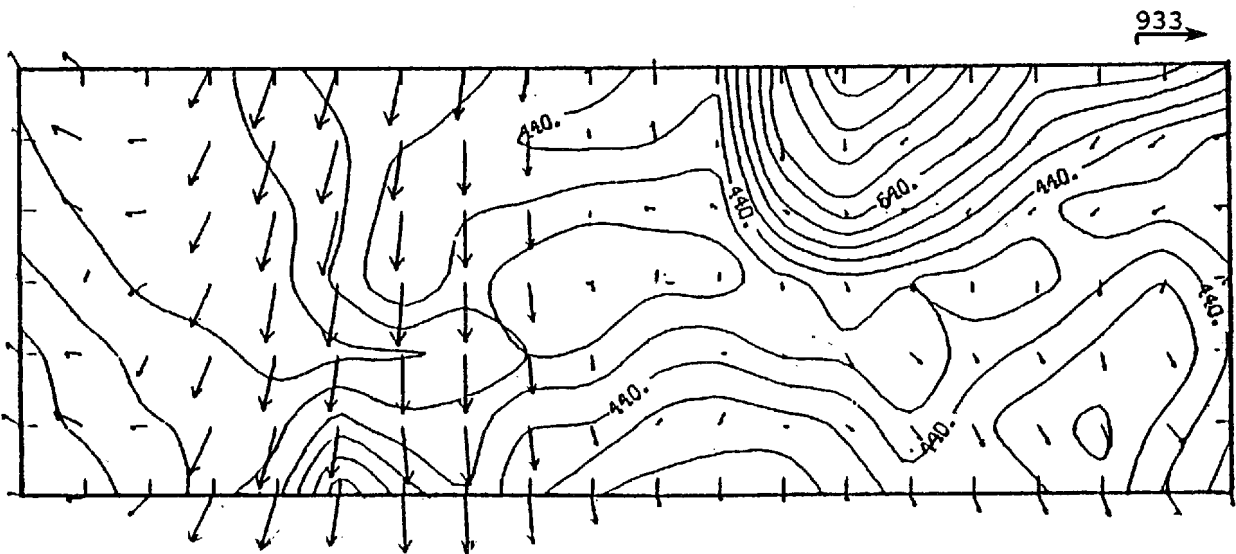


FIGURE 4b. Control run horizontal wind at 300 m elevation at 0507 sun time. The magnitude of the maximum wind vector (cm/s) in the field is shown in the upper right-hand corner.

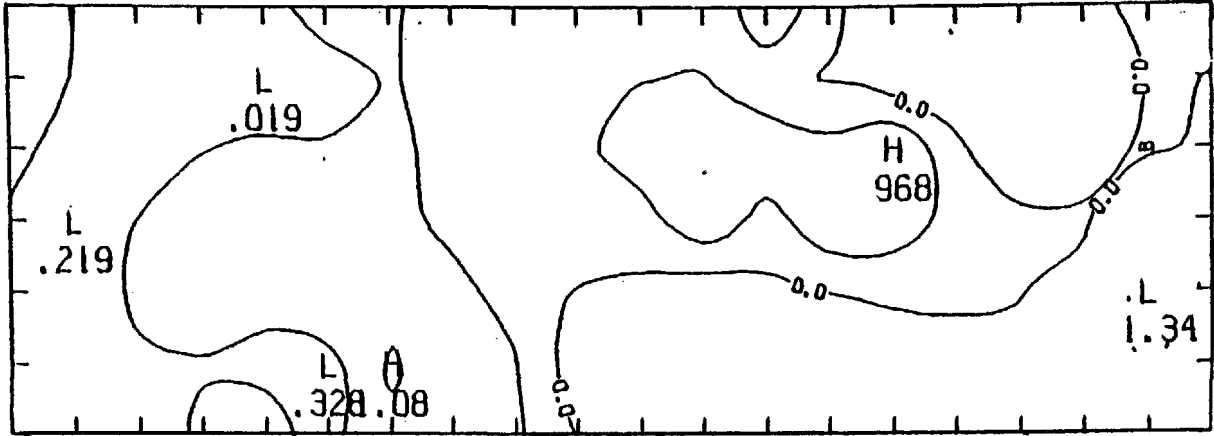


FIGURE 5a. Temperature difference dry cooling tower minus control run at 8 meters at 1707 sun time.

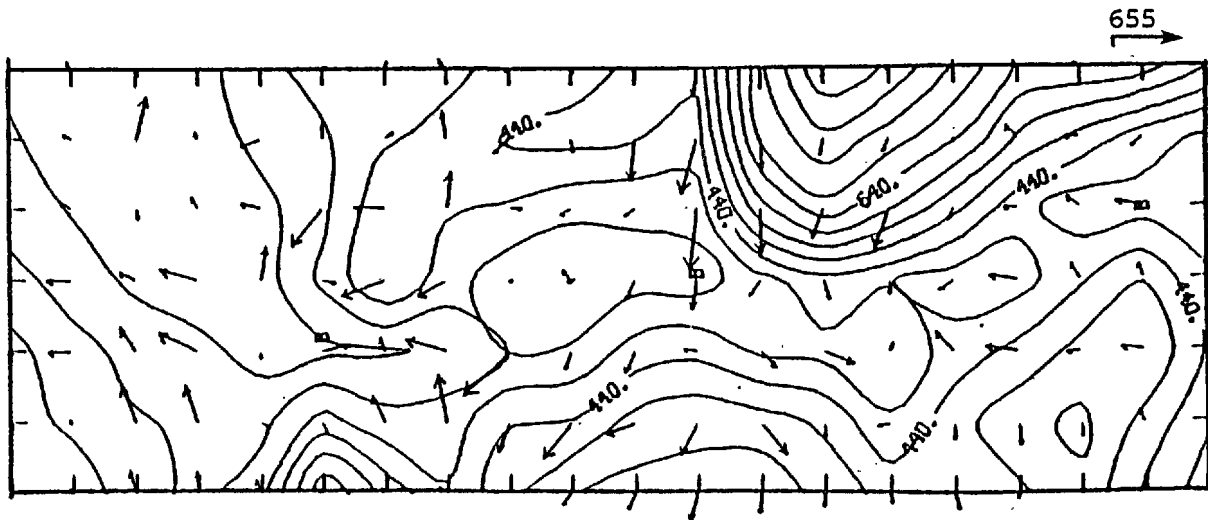


FIGURE 5b. Horizontal wind vector difference dry cooling tower minus control run at 8 meters at 1707 sun time. The magnitude of the maximum wind vector (cm/s) in the field is shown in the upper right-hand corner.

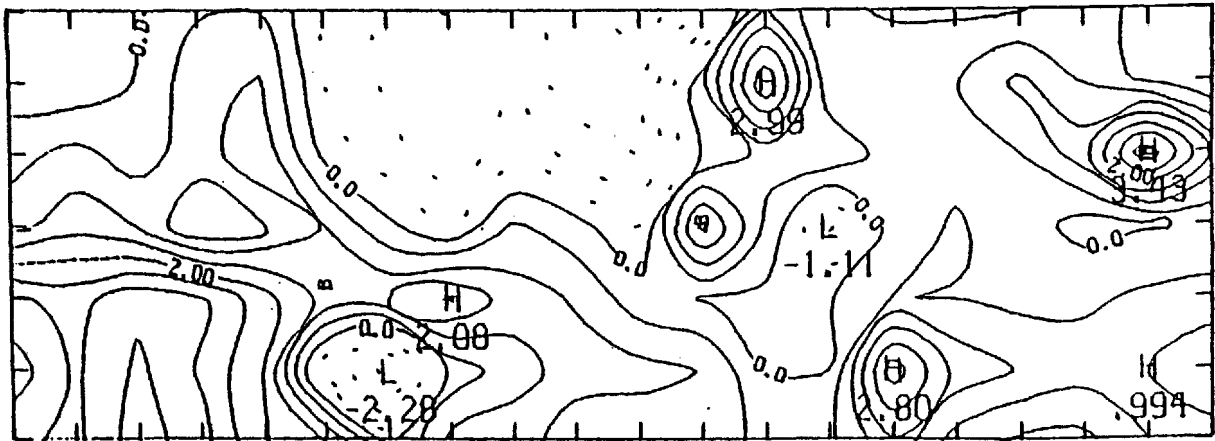


FIGURE 6a. Temperature difference dry cooling tower minus control run at 8 meters at 0507 sun time.

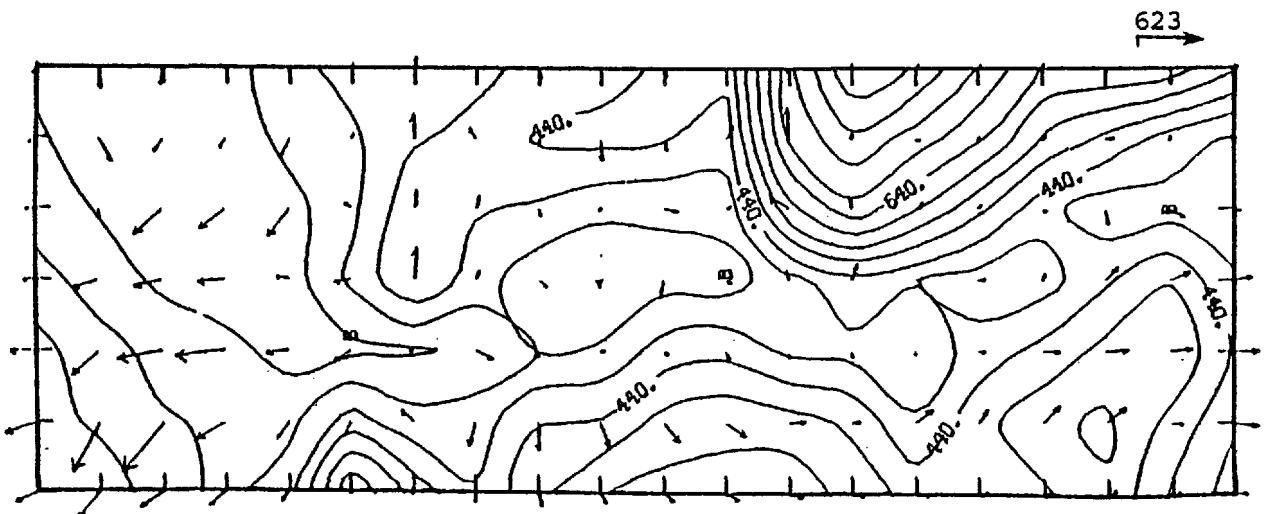


FIGURE 6b. Horizontal wind vector difference dry cooling tower minus control run at 0507 sun time. The magnitude of the maximum wind vector (cm/s) in the field is shown in the upper right-hand corner.

# A NUMERICAL SIMULATION OF WASTE HEAT EFFECTS ON SEVERE STORMS

H. D. Orville and P. A. Eckhoff  
Institute of Atmospheric Sciences  
South Dakota School of Mines and Technology  
Rapid City, South Dakota U.S.A.

## ABSTRACT

A two-dimensional, time-dependent model has been developed which gives realistic simulations of many severe storm processes -- such as heavy rains, hail, and strong winds. The model is a set of partial differential equations describing time changes of momentum, energy, and mass (air and various water substances such as water vapor, cloud liquid, cloud ice, rainwater, and hail). In addition, appropriate boundary and initial conditions (taken from weather sounding data) are imposed on a domain approximately 20 km high by 20 km wide with 200 m grid intervals to complete the model.

Cases have been run which depict realistic severe storm situations. One atmospheric sounding has a strong middle-level inversion which tend to inhibit the first convective clouds but give rise later to a severe storm with hail and heavy rains. One other sounding is taken from a day in which a severe storm occurred in the Miami area.

The results indicate that a power park emitting 80% latent heat and 20% sensible heat has little effect on the simulated storm. A case with 100% sensible heat emission leads to a much different solution, with the simulated storm reduced in severity and the rain and hail redistributed.

## INTRODUCTION

A two-dimensional, time-dependent cloud model has been modified to simulate the addition of heat and vapor from a hypothetical power park. The cloud model has been under development for many years and successfully applied to several convective situations. The most recent application was a simulation of a hailstorm reported by Orville and Kopp [1].

For this study, the model was run using two types of severe storm atmospheric soundings. The first type can be classified as Type I using the classification system established by Fawbush and Miller [2]. This type of sounding generally produces a family of tornadoes. The atmospheric sounding from the well documented Fleming Storm [3] was used as a Type I sounding. This was a dangerous hailstorm which eventually produced a tornado in its twelve plus hours of existence.

The second sounding used can be classified as a Type 2 atmospheric sounding [2]. The sounding used was taken three hours prior to a tornado touching down in downtown Miami, Florida [4]. This storm is typical of a Type 2 which produces a single tornadic event.

For each sounding, the total effluent from the cooling towers in the power park was calculated and inserted into the model in a cross sectional area of the park's heating and moistening volume (see Fig. 1).

The model was run until all the precipitation had fallen or until the simulation had progressed where valid comparisons could be made. Then the model was run again using the same initial sounding except that the effluent (vapor and heat) from the power park was excluded. Several other effluent variations were also simulated. For the Fleming storm cases, three other runs were made. One involved doubling the power park concentration of effluent which, in effect, halved the area of the power park. Another involved using an effluent that was made up of 100% sensible heat which is designated to simulate a park made up of dry natural draft cooling towers [5]. The last case in this series involved placing the power park on the other side of the ridge. This was done to see the effects location had on storm development.

The Miami storm cases were done in a similar manner with fewer park variations. In the end, there were seven cases that could be analyzed.

## RESULTS

### Fleming Storm

The cross sections for 66 min. and 102 min. show the general development of the storm in the 5 Fleming storm cases.

The first four cases (Figs. 2a-d) show the main cloud being fed by air from both the right and left. The strength of the main updraft in Figs. 2a-e draws in air from the lower left-hand corner into the main cloud.

In the first four cases of Fig. 2, the closed circulation pattern just to the right of the main updraft is a main feature. Each pattern is shaped differently, and the contours indicate that the flow of air in the main updraft is weakest in the natural case (Fig. 2a), followed by the 100% sensible heat case (Fig. 2e). The standard park and double flux cases (Figs. 2b and d) are strong but of about equal strength. The main updraft is the strongest in the left park case (Fig. 2c). Also notice the shape of the zero contour below the main cloud in Figs. 2a-e, and that the zero contour is in a different position in each case. The 100% sensible heat case has formed a strong secondary circulation over the right side of the grid, causing a second cloud to form.

The sequences at 102 min. (Fig. 3) show significant differences in most of the cases. The standard park case is most like the natural case. The storm in the left park case has moved further to the right in the domain and is weakening. The double flux case shows slightly less rain and hail, with most of the precipitation distributed below 5 km. The 100% sensible heat case exhibits the greatest differences. The major convection has ceased and precipitation has nearly all fallen to the ground.

The dynamics of each storm is slightly, to almost completely, different from that of the natural case. This difference in dynamics is evident in the accumulated rain and hailfall and the time at which the storms end. Figure 4 compares the natural case rainfall with that of the standard park, the left park cases, the 100% sensible heat, and the double flux cases.

Notice the similarity in rainwater distribution between the natural case and the standard park and double flux cases. However, the latter two cases exhibit a small distribution shift to the right. The left park case does not show the two-peak distribution of these three cases. The 100% sensible heat shows greatly reduced rainfall. The total accumulated rain on the ground for the Fleming storm cases shows the natural case with  $178.2 \text{ kT km}^{-1}$ . This is followed closely by the standard park and double park cases with  $174.6$  and  $174.9 \text{ kT km}^{-1}$ , a decrease of about 2% for both cases when compared to the natural case. The left park case shows a rainfall accumulation of  $151.6 \text{ kT km}^{-1}$ , a decrease of rainfall when compared to the natural case. The smallest rainfall amount was produced in the 100% sensible heat case. This case produced  $65.13 \text{ kT km}^{-1}$ , which is a 64% drop from the natural case.

Each case shows a maxima of hail at 10 km on the horizontal axis (the ridge line); however, the park and 100% sensible heat cases show a second maxima to the right. The total accumulated hail for the natural case is  $47.4 \text{ kT km}^{-1}$ . The standard park shows the next highest accumulation with  $41.3 \text{ kT km}^{-1}$ , or a 13% drop in hail. Next highest is the left park case with  $31.5 \text{ kT km}^{-1}$ , followed very closely by the double flux case with  $31.3 \text{ kT km}^{-1}$ . Both cases show a drop of about 34% when compared to the natural case. The case with the smallest hail accumulation is the 100% sensible heat case with  $3.8 \text{ kT km}^{-1}$ , or a decrease of 92% when compared to the natural case.

#### Miami Storm

The Miami storm results are shown in Figs. 4b-5a-b. The natural case at 141 min. (Fig. 5a) shows a vigorous, active convective storm, with convergent inflow (flow from both left and right in the lower levels). The power park case storm is nearly as big (Fig. 5c), but not as broad as the natural case. In addition, the power park case is being fed by low-level flow primarily from the right side. Figure 5b shows the natural case storm still active, with copious amounts of rain and precipitating ice. However, 5d shows that the power park case storm has nearly dissipated,

mostly anvil cloud remaining. Figure 4b shows the accumulated rainfall; much more has fallen in the natural case. There were reports of over 6 inches of rain in some south Florida areas on this day.

#### DISCUSSIONS AND CONCLUSIONS

The seven runs have shown some of the influence of power parks on severe storm development. Storm development was different and was affected to varying degrees by the effluents of the power park. The power parks create their own dynamics which interact with the flow of the developing storm to produce storms of less, to greatly less, precipitation output.

One of the really significant changes comes about after 66 min. of real-time simulation in the Fleming storm case. This is a time when the heat and/or moisture from the various parks had enough time to develop and interact with the natural dynamics to produce readily noticeable changes. The addition of heat and moisture from the wet cooling towers have supplied enough moisture to sustain the growth of the original cloud. In the dry cooling tower or 100% sensible heat case, there was enough heat affecting the dynamics to create a more vigorous cloud growth to the right of the original cloud development. The vigorous cloud developed a downdraft that interacted with the downdraft from the cloud system to the left. The result was a cessation of low-level moisture into both cloud systems and the premature death of both systems.

The cloud in the natural case was very weak at 66 min., and the new development to the rear saved the original cloud from dying slowly. The new development took over with good growth characteristics and rejuvenated the natural case. However, the wet cooling tower cases grew faster, and by 102 min. their gust fronts were more developed. This can be attributed to the effects of the power parks.

One of the more noticeable changes is the quantity and distribution of the rain and hail. All the power park cases produced less rain and hail, with the 100% sensible heat case showing around a 75% decrease in both rain and hail maximums. The wet cooling tower cases show a small decrease in precipitation with a shift in the location of rainfall. The standard power park case shows less differences than any of the other cases in its rain and hail distribution for the Fleming storm series of cases. The double park case showed slightly more of a change with a little less rain and hail than in the standard park case. However, the distributions of rain and hail were very similar to the standard case. The left park case showed a total rainfall slightly less than the natural case in the Fleming storm series, but the distribution shows a large single peak instead of the double peaks as in the other wet tower cases. The 100% sensible heat has rain and hail peak amounts that are 30% and 13% of the natural case. This can be directly attributed to the rapid cloud development in front of the storm, which saps the energy of the storm leading to early dissipation of the storm system.

One point brought out in the left park case is the earlier cloud formation if the power park is under the area where initial cloud development would normally take place.

In the two Miami runs, the power park effluents interact significantly with a cloud developing overhead. The clouds develop more rapidly in the power park case, but never become as organized a system as in the natural case. The flow that develops is not "complementary" to the flow in the natural case. This results in a 50% decrease in the rain maximum and a 66% decrease in accumulated rain at 174 min. in the power park case. Hail develops in the storms, but hail accumulation on the ground is insignificant.

Results of this study indicate that the incorporation of the added heat and moisture in a developing storm is a very nonlinear process and does not necessarily yield a more severe storm.

Other studies, one by Orville et al. [6], showed that slight increases in rain could occur if all of the added moisture were stored in the region and released to the storm at one time, such as might occur in a very stagnant flow condition.

The ultimate effects of power park effluents on severe storms are not readily determined by simple additive calculations. Complex interactions occur which can only be tested through realistic numerical simulations. Careful observations of the long term climatological changes near large power plants should be maintained for long periods of time to determine the actual effects of the plants on the weather.

#### ACKNOWLEDGMENTS

This research was sponsored by the U.S. Nuclear Regulatory Commission under Contract No. NRC-04-76-350. Acknowledgment is given to the National Center for Atmospheric Research, which is sponsored by the National Science Foundation, for granting us use of their computing facilities.

#### REFERENCES

1. Orville, H. D., and F. J. Kopp, 1977: Numerical simulation of the life history of a hailstorm. J. Atmos. Sci., 34, 1596-1618.
2. Fawbush, E. J., and R. C. Miller, 1954: The types of air masses in which North American tornadoes form. Bull. Amer. Meteor. Soc., 35, 154-165.

3. Browning, K. A., and G. B. Foote, 1975: Airflow and hail growth in supercell storms and some implications for hail suppression. National Hail Research Experiment Technical Report No. 75/1, May 1975, 75 pp.
4. Hiser, H. W., 1967: Radar and synoptic analysis of the Miami tornado of 17 June 1959. Preprints 5th Conf. Severe Local Storms, St. Louis, Missouri, Amer. Meteor. Soc., 260-269.
5. Lee, J. L., 1978: Potential weather modification caused by waste heat release from large dry cooling towers. Proposed for presentation at the 2nd AIAA/ASME Thermophysics and Heat Transfer Conf., May 24-26, 1978, Palo Alto, California.
6. Orville, H. D., F. J. Kopp, and P. A. Eckhoff, 1977: The application of a numerical model to determine the effects of waste heat on severe weather. Preprints 10th Conf. Severe Local Storms, Omaha, Nebraska, Amer. Meteor. Soc., 271-276.

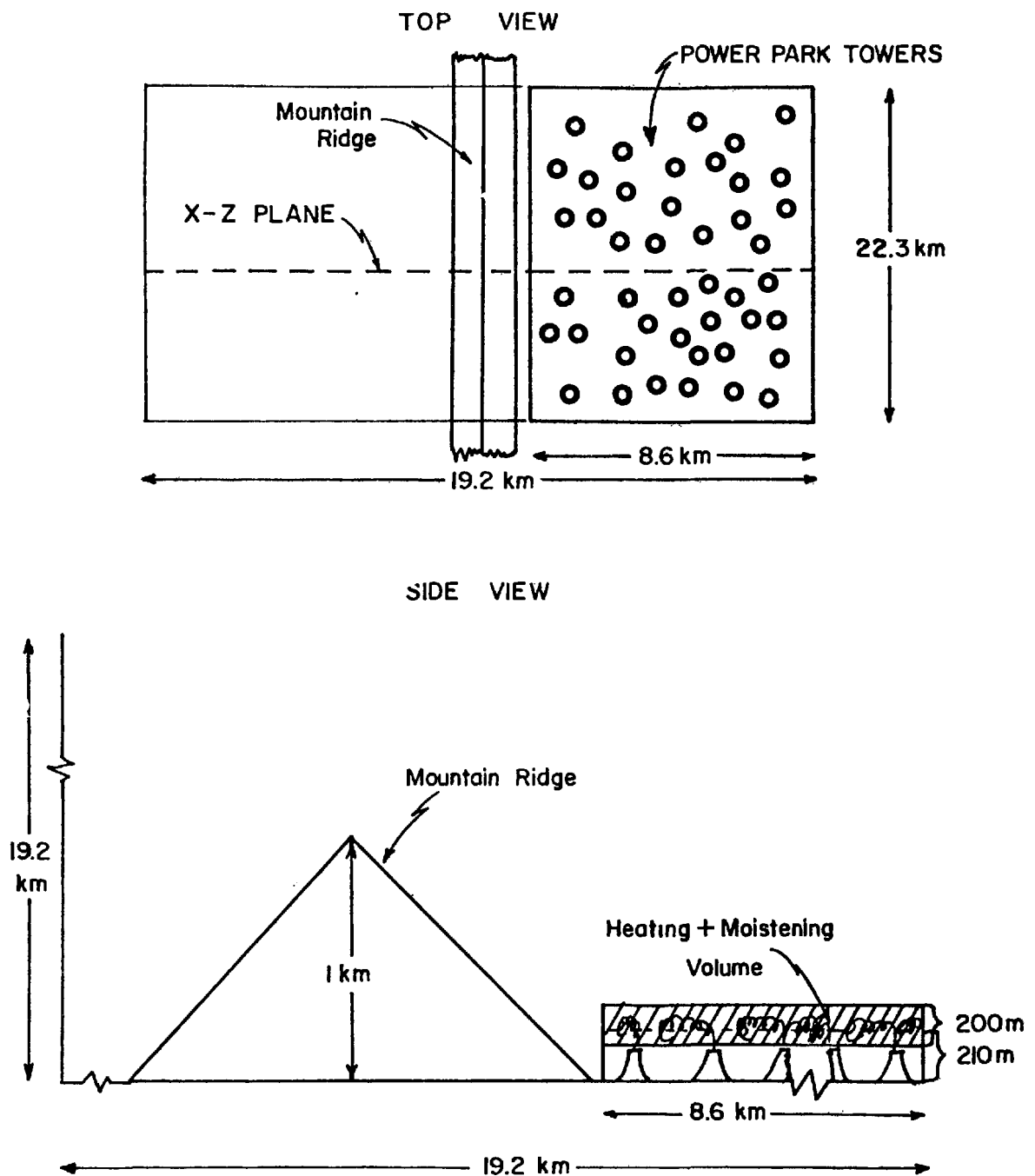


Fig. 1: The top view shows the standard park configuration to the right of the ridge. The side view shows the volume into which the moisture and heat is added.

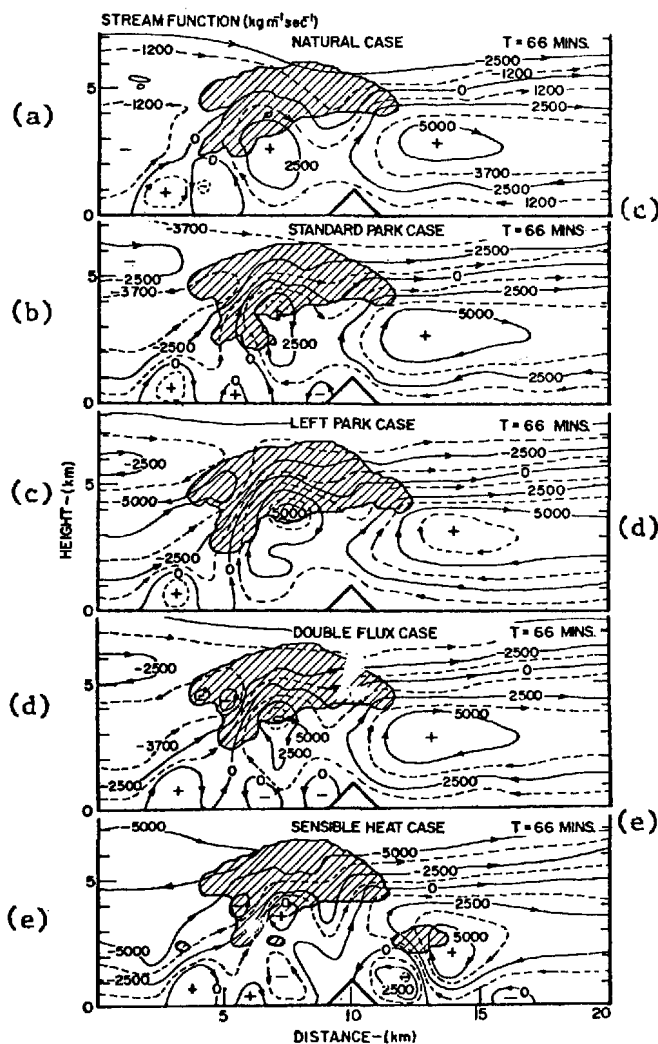


Fig. 2: The stream function field of the Fleming storm cases at 66 minutes. The clouds are the shaded areas.

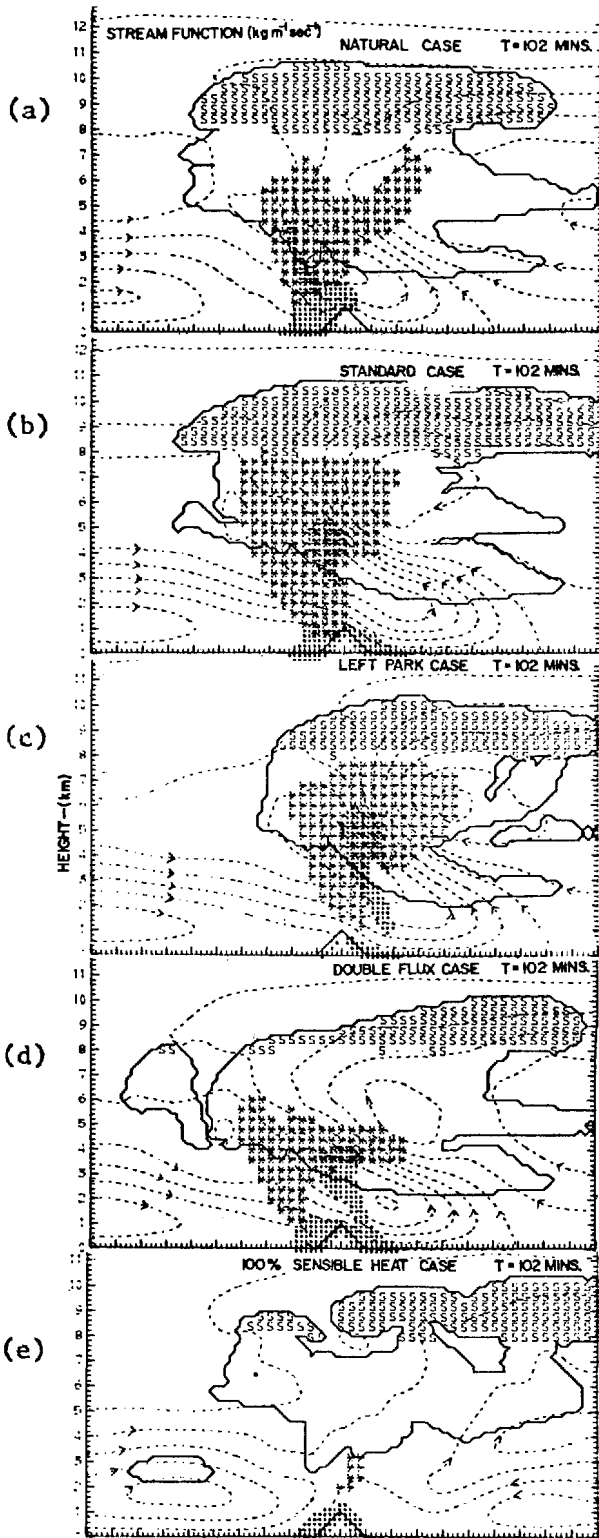


Fig. 3: Same as Fig. 2 but for a contour interval of  $5000 \text{ kg m}^{-2} \text{ sec}^{-1}$ . Rain and hail over  $1 \text{ gm kg}^{-1}$  are depicted as dots and asterisks, respectively.

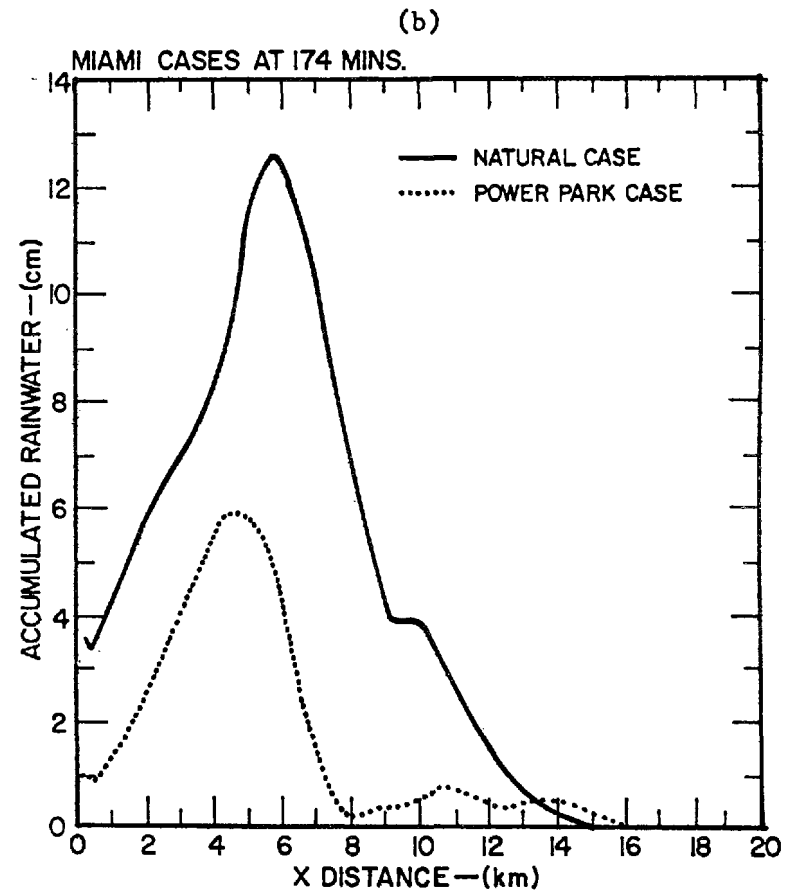
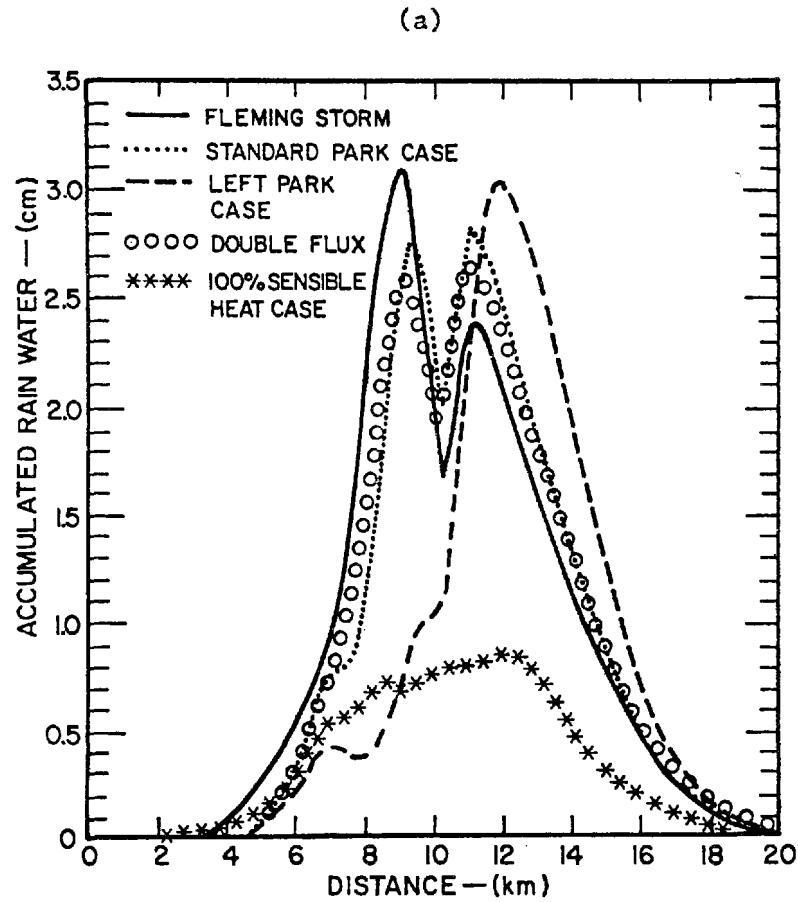


Fig. 4: (a) This compares the natural case rainfall with that of the standard park, the left park cases, the 100% sensible heat, and the double flux cases. (b) This compares the rainfall of the two Miami storm cases at 174 minutes.

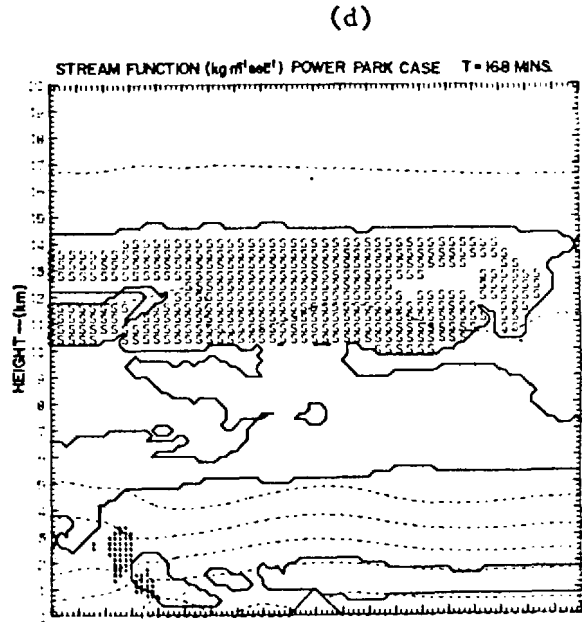
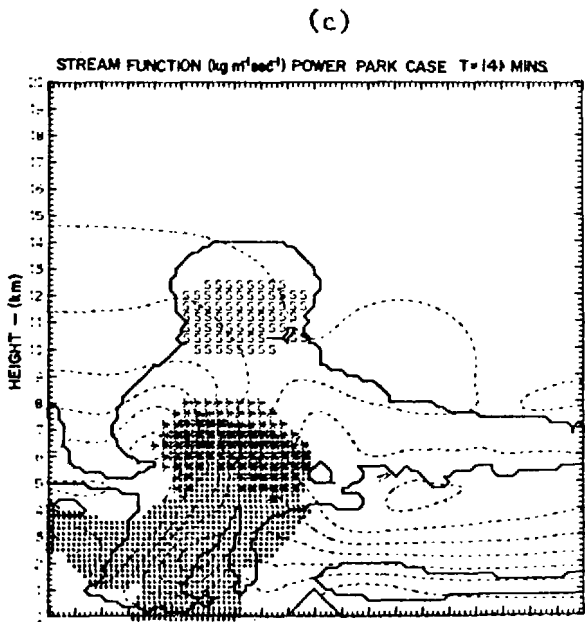
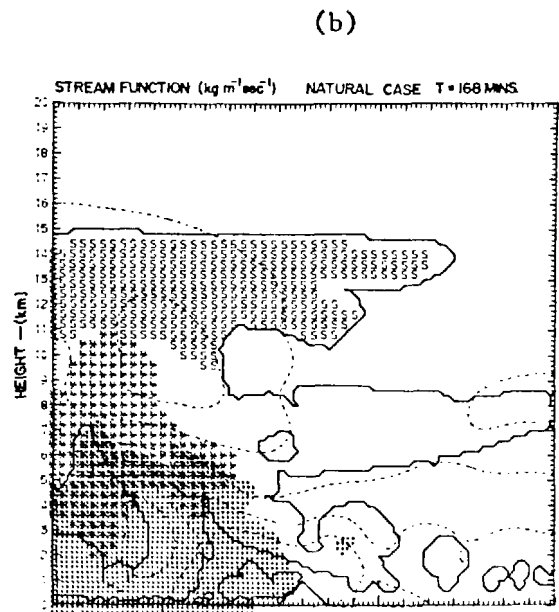
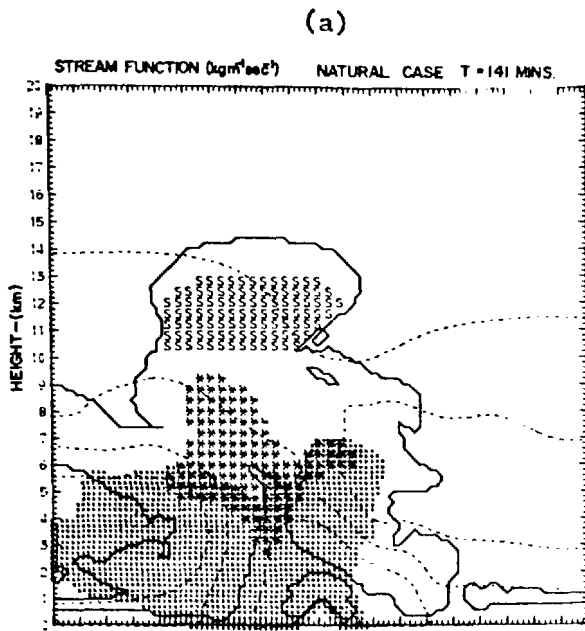


Fig. 5: The stream function for the natural (a & b) and power park (c & d) cases of the Miami storm at 141 and 168 minutes. Contouring is  $10000 \text{ kg m}^{-1} \text{ sec}^{-1}$  for a, b, & d and  $5000 \text{ kg m}^{-1} \text{ sec}^{-1}$  for c.

# ON THE PREDICTION OF LOCAL EFFECTS OF PROPOSED COOLING PONDS

B. B. Hicks

Radiological and Environmental Research Division  
Argonne National Laboratory, Argonne, Illinois U.S.A.

## ABSTRACT

A Fog Excess Water (FEW) Index has been shown to provide a good measure of the likelihood for steam fog to occur at specific cooling pond installations. The FEW Index is derived from the assumption that the surface boundary layer over a cooling pond will be strongly convective, and that highly efficient vertical transport mechanisms will result in a thorough mixing of air saturated at surface temperature with ambient air aloft. Available data support this assumption. An extension of this approach can be used to derive a simple indicator for use in predicting the formation of rime ice in the immediate downwind environs of a cooling pond. In this case, it is supposed that rime ice will be deposited whenever steam fog and sub-freezing surface temperatures are predicted. This provides a convenient method for interpreting pre-existing meteorological information in order to assess possible icing effects while in the early design stages of the planning process. However, it remains necessary to derive accurate predictions of the cooling pond water surface temperature. Once a suitable and proven procedure for this purpose has been demonstrated, it is then a simple matter to employ the FEW Index in evaluations of the relative merits of alternative cooling pond designs, with the purpose of minimizing overall environmental impact.

## INTRODUCTION

Industrial cooling ponds often give rise to localized environmental effects, particularly in winter when steam fog and rime ice can become problems downwind of the hottest areas. Fog generation above artificially-heated water surfaces has been the subject of a number of studies<sup>1,2,3</sup>, but similar studies of rime ice have not been found. A preliminary study of the matter demonstrated the practical difficulties likely to confront experimental investigations of riming<sup>4,5</sup>. This study, performed at the Commonwealth Edison Dresden plant (near Morris, Illinois) during the winter of 1976/7, provides a four-month record of the occurrence and intensity of fog and rime associated with the operation of a fairly typical industrial cooling lake.

Earlier studies at Dresden succeeded in obtaining direct measurements of turbulent fluxes of sensible and latent heat from the heated water<sup>6</sup>. The resulting improved formulations of these convective and evaporative heat losses can be used in much

the same way as the familiar wind speed functions that are used in most contemporary cooling pond design studies. In this regard the earlier Dresden experiments, which were conducted over the three-year period 1973-1976, addressed the question of how to predict the water temperature characteristics of cooling pond installations. Subsequent studies have refined these techniques by parameterizing the subsurface thermal boundary layer<sup>7</sup>, which effectively limits heat exchange between deep water and the air. The premise of the present study is, therefore, that we can predict the temperature characteristics of a proposed cooling pond, but need to assess the potential environmental impact.

## STEAM FOG

Hicks<sup>2</sup> introduced a Fog Excess Water Index,  $e_{xs}$ , based on the supposition that air saturated at surface temperature rises and mixes with equal quantities of ambient, background air. The excess vapor pressure  $e_{xs}$  of the mixture can be written as

$$e_{xs} = (e_s(T_s) + e_a)/2 - e_s((T_s + T_a)/2)$$

where  $e_s(T)$  is the saturated vapor pressure at temperature  $T$ ,  $T_s$  is the ambient air temperature and  $e_a$  is the air vapor pressure. When tested against the data of Currier<sup>a</sup> et al.<sup>1</sup>, the FEW Index was found to provide a good indication of the occurrence of steam fog, as well as some measure of its intensity. The FEW Index was further verified by use of observations of fog generated by cooling-pond simulators at Argonne National Laboratory and by data from Dresden.

Figure 1 is a further test of the FEW Index, again largely based on observations made at Dresden but supplemented by a series of measurements made at the Cal-Sag shipping canal, a major inland waterway which passes conveniently near Argonne. Canal water temperatures in winter are typically more than 20°C higher than in nearby lakes and streams, due to heavy industrial usage. The data illustrated in the diagram give further support for the validity of the FEW Index method.

## RIME ICE DEPOSITION

A few obvious (and perhaps trivial) considerations should be set down at the outset. Firstly, it is clear that rime ice deposition is a cold-weather phenomenon which is constrained, by definition, to occasions when the surface temperature is below freezing. This constraint does not apply to the generation of steam fog, and hence rime deposition might well be considered as a sub-set of steam fog cases. Secondly, it follows that riming will be mainly a wintertime phenomenon, most often at night. In the nocturnal case, it seems likely that accurate prediction of riming will prove extremely demanding, since nocturnal surface temperatures

are highly variable both in space and in time and thus great care must be taken in selecting an appropriate data base.

Figure 2(a) illustrates the first point; the Dresden 1976/7 winter data do indeed show riming to be a subset of the fog occurrences. Observations were made on a total of 84 mornings. On no occasion was the observation of overnight rime deposition not accompanied by steam fog from the pond. Furthermore, the amount of rime deposited is well correlated with a measure of steam fog intensity. To show this, rime deposits have been quantified according to the visual observations; none = 0, slight rime = 1, moderate rime = 2, heavy rime = 3. The fog intensity is conveniently quantified by the reported depth of the fog layer over the hottest part of the cooling pond, estimated from a comparison with the known heights of surrounding obstacles. Figure 3 demonstrates the correlation. Thus, it appears reasonable to expect the FEW Index to be an appropriate measure of the intensity of rime deposit, since it has already been shown to be an indicator of steam fog intensity. The present limited set of data do not allow direct investigation of the interrelation between rime intensity and  $e_{xs}$ , since reliable nocturnal evaluations of  $e_{xs}$  at the Dresden site are not available<sup>8</sup>

Figure 2(b) shows the frequency of occurrence of fog and rime that would have been expected on the basis of the arguments presented above. It is assumed that steam fog will occur when  $e_{xs} > 0$ , based on the observed Dresden water temperatures and overnight air temperatures and humidities measured some 40 km away at Argonne National Laboratory. Rime is then predicted on each of those occasions for which sub-freezing overnight temperatures were reported. Comparison between Figures 2(a) and 2(b) shows fairly good agreement: the rime curves are drawn to be identical.

## DISCUSSION AND CONCLUSIONS

Although it is clear that the depth of steam fog and the amount of rime deposited are well correlated, there is no strong dependence of riming upon meteorological quantities such as wind speed, nocturnal net radiation, etc. To a considerable extent, this is as must be expected as a consequence of the lack of correlation between  $e_{xs}$  and wind speed (see Figure 1). The 1976/7 results are not suitable for investigating this matter with confidence. Nor is it clear that the physics involved will permit a clear-cut conclusion to be obtained. Nevertheless, it is intended to proceed with investigations of the thermal and moisture plumes arising from heated water surfaces, in part to derive better methods for predicting the frequency of events in the design stage but also to investigate the role of steam fog as an interference with the natural infrared radiation regime of a water surface.

## ACKNOWLEDGEMENTS

The work performed at Dresden was made possible by the complete cooperation of the Commonwealth Edison Company. The Dresden data reported here were obtained during a field program directed by Dr. J. D. Shannon. Dr. P. Frenzen obtained the canal data. This study was supported by the U. S. Department of Energy, as part of an investigation of the Meteorological Effects of Thermal Energy Release.

## REFERENCES

1. Currier, E. L., J. B. Knox, and T. V. Crawford, Cooling pond steam fog, J. Air. Poll. Cont. Assoc., 24, 860-864, 1974.
2. Hicks, B. B., The prediction of fog over cooling ponds, J. Air Poll. Cont. Assoc., 27, 140-142, 1977.
3. Leahey, D. M., M. J. E. Davies, and L. A. Panek, A study of cooling pond fog generation, Paper #78-40.2 presented at the 71st. Annual Meeting of the Air Pollution Control Association, Houston, Texas, June 25-30, 1978.
4. Everett, R. G., and G. A. Zerbe, Winter field program at the Dresden cooling ponds, Argonne National Laboratory Radiological and Environmental Research Division Annual Report, January-December 1976, ANL-76-88 Part IV, 108-113, 1976.
5. Shannon, J. D. and R. G. Everett, Effect of a severe winter upon a cooling pond fog study, Bull. Amer. Meteorol. Soc., 59, 60-61, 1978.
6. Hicks, B. B., M. L. Wesely, and C. M. Sheih, A study of heat transfer processes above a cooling pond, Water Resources Res., 13, 901-908, 1977.
7. Wesely, M. L., Behavior of the thermal skin of cooling pond waters subjected to moderate wind speeds, Proceedings, Second Conference on Waste Heat Management and Utilization, Miami Beach, FL, XI-A-40 (1-8), December 4-6, 1978.
8. Hicks, B. B., The generation of steam fog over cooling ponds, Environmental Effects of Atmospheric Heat/Moisture Releases, Proceedings of the Second AIAA/ASME Thermophysics and Heat Transfer Conference, Palo Alto, California, 24-26 May 1978 (Library of Congress Catalog Card Number 78-52527).

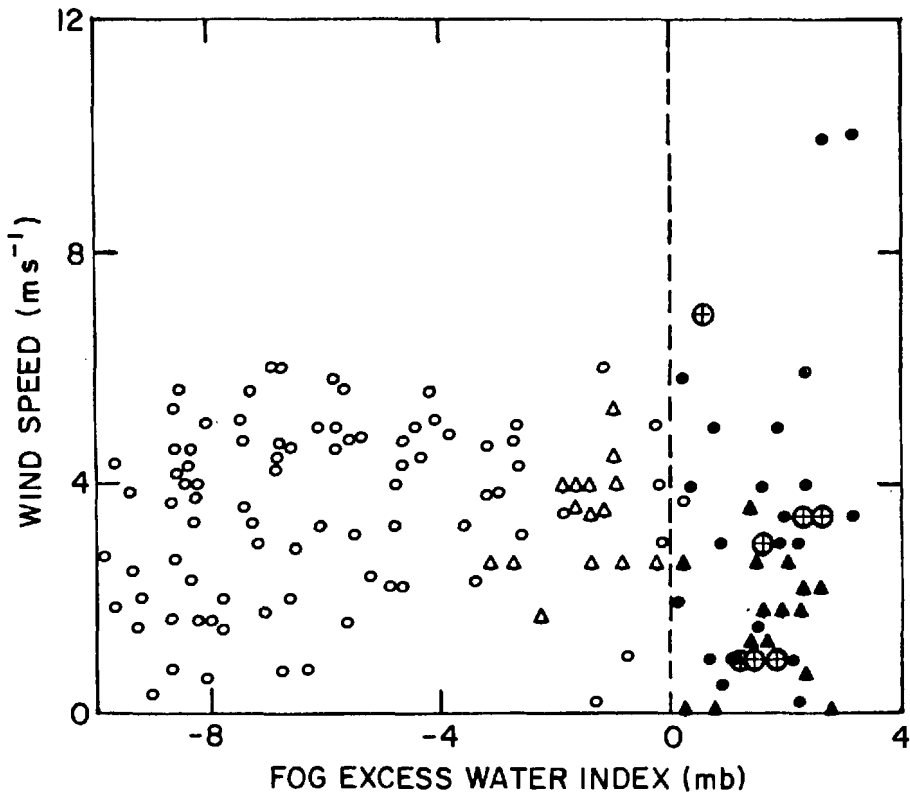


Fig. 1. Observations of the Fog Excess Water Index made at the Dresden cooling lake (circles), over cooling pond simulators at Argonne<sup>8</sup> (triangles), and above a shipping canal near Argonne (circles and crosses). Except in the last case, solid symbols indicate that fog was observed; fog was always observed over the canal.

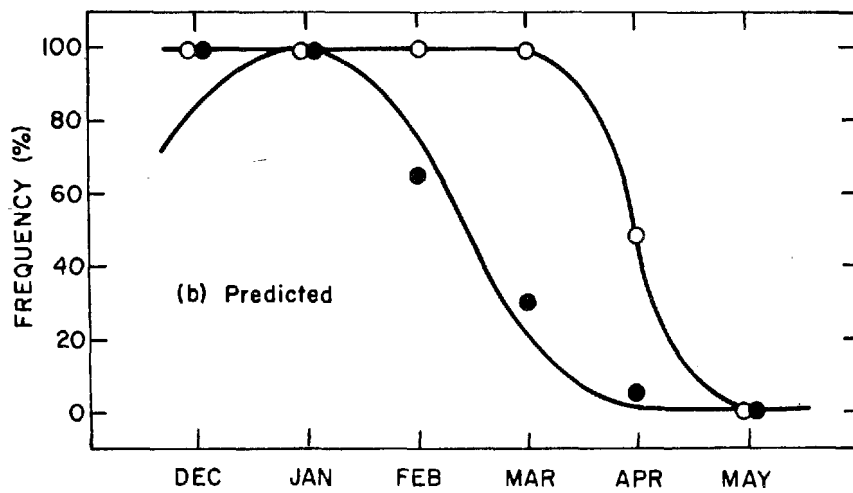
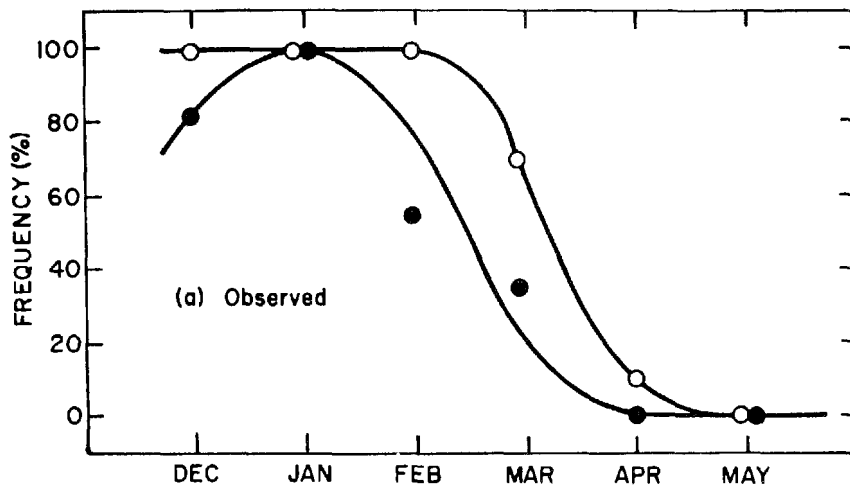


Fig. 2. Observed (a) and predicted (b) frequencies of occurrence of overnight steam fog (open circles) and local rime ice deposition (solid circles) at the Dresden cooling lake.

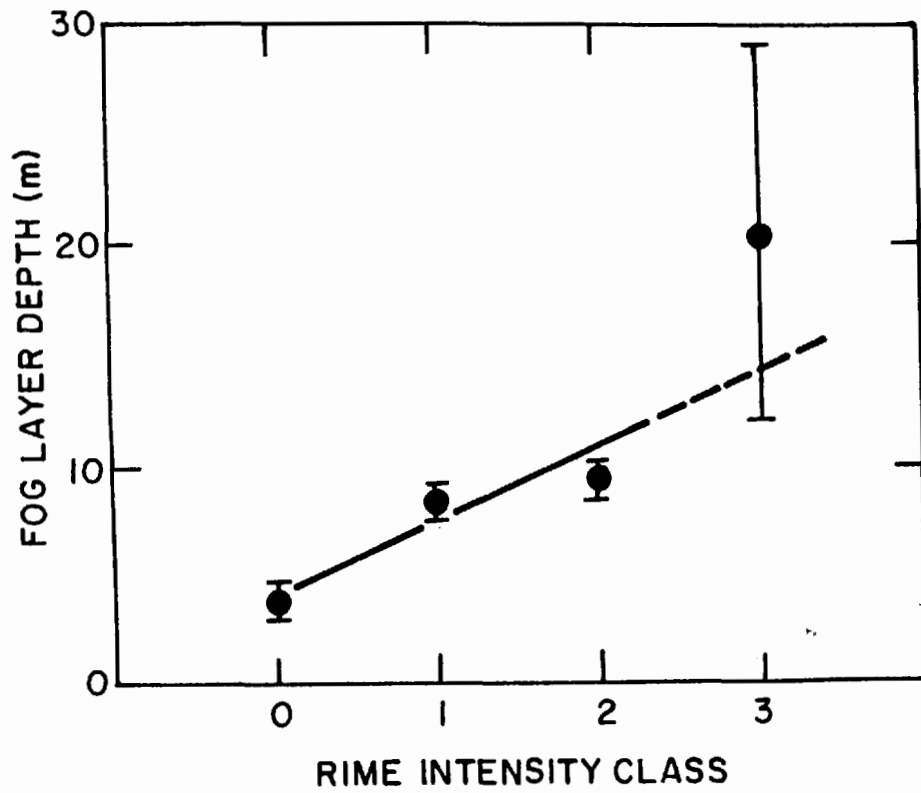


Fig. 3. The relationship between the intensity of overnight rime deposition and the reported depth of the fog layer at Dresden.

MEASUREMENT AND EVALUATION OF THERMAL  
EFFECTS IN THE INTERMIXING ZONE AT  
LOW POWER NUCLEAR STATION OUTFALL

P. R. KAMATH, R. P. GURG, I. S. BHAT and P. V. VYAS  
ENVIRONMENTAL STUDIES SECTION, H. P. DIVISION  
BHABHA ATOMIC RESEARCH CENTRE, BOMBAY 400085

ABSTRACT

The paper reports observations and evaluation of thermal effects in the Rana Pratap Sagar Lake in Rajasthan, India where one unit (200 MWe) of the Rajasthan Atomic Power Station is in operation. The coolant waters are drawn 8-10 m below the lake surface through a conduit and discharged through an open discharge channel with a temperature rise of 10°C. There was a small increase in lake water temperature in the vicinity of the outfall. Temperature profiles and spread were mapped using insitu monitors.

These studies showed evidence of thermal stratification in the period following winter and the existence of a well established thermocline. Thermal stratification brought out specific advantages for thermal abatement when the hypolimnion waters were well below the temperature of surface waters. Parasitism and eutrophication were observed. The thermal effects were accentuated by photosynthetic effects. Proposal to utilise waste heat for algal culture in the Kalpakkam nuclear site in South and mariculture (Lobsters, Prawns) in the heated effluents canal at the Tarapur Atomic Power Station near Bombay are discussed.

INTRODUCTION

The fresh water nuclear site in operation in India is in Rajasthan on the R. Chambal drawing its coolant water from the man made lake Rana Pratap Sagar (RPS). Only one reactor unit of 200 MWe is commissioned. Of the two coastal sites, the Tarapur Atomic Power Station has two reactors 200 MWe each commissioned in 1970. Kalpakkam Atomic Project is under construction. Monitoring of heat distribution in foreshore waters, assessment of thermal effects and investigations for waste heat utilisation are at present carried out by the Environmental Survey Laboratories installed on each site.<sup>1</sup>

RAJASTHAN ATOMIC POWER SITE (RAPS)

The RPS lake is about 3 km wide at the reactor site and extends

to 5 km downstream upto the Dam. It receives about 8000 cfs of water as tailings from a Dam located 32 km upstream. The lake is in the main fed by R Chambal and its tributaries. The cooling waters from the lake are drawn through a conduit 8-10 m below the surface and 300 m off shore. The warm condenser effluents are discharged through a canal which is open and virtually discharges to the lake surface.

The water movement in the RPS is dependent on wind speed and its direction. When the wind speed is less than 8-10 km/hr, the lake waters are stagnant. The discharges remain close to the bank at that time and spread along gradually. At wind speeds 15-17 km/hr there is a conspicuous movement of water on surface in the direction of wind. At speeds greater than 20 km/hr there is good turbulence and mixing.<sup>2</sup>

RAPS is an inland site located in the central part of the country subjected to large differences (10-15°C) between day and night air temperatures and about 25°C between peak day temperatures between summer and winter. Temperature stratification in the lake depends on the severity of winter which is considered acute when the air temperatures reach 15-18°C at noon.

Stagnancy of water movement in the lake and design of the condenser circulation system in RAPS held out interesting possibilities of heat build up. Torrid summers when air temperatures touched 39°C and lake water, 31.9°C at surface, showed the chance of thermal pollution effects being observed attributable directly to the power station reject heat.

#### Materials and Methods:

The condenser discharge was identified as it moved along or spread over the lake surface by spiking the effluent stream with Rhodamine B dye for visual marking.<sup>3</sup>

#### Electronic Temperature Meter

An insitu temperature meter for taking vertical temperature profiles was developed on the temperature dependent characteristics of a semiconductor diode. The system used matched pair of diodes as temperature sensors(°C). The response time is 80 secs for a difference of 25°C. The sensitivity is 0.1°C. Cable reach 20 m.

#### Dissolved Oxygen (DO) Meter<sup>4</sup>

Field Lab Oxygen analyser supplied by Beckman Instruments, USA

was used for DO measurement in the laboratory study. The In situ monitor employed in the field was also obtained from USA - YSI DO Meter model. The dual probe has a built in temperature sensor for in situ measurement. DO concentration is read in ppm or as percentage of saturation at the set temperature.

### Observations -Results

Temperatures at surface observed during set hours of the day in the different months following winter are presented in Table 1. The temperature readings have to be read bearing in mind that the intake is obtained from the hypolimnion (Elevation 335 m) and the condenser discharge is made to the surface of the lake. Table 2 is important because it gives the basic water quality change and indicates what happens when water from the hypolimnion goes through a churning motion in the condenser tubing. Values of DO(as percent saturation), COD and BOD are given in the intake and discharge streams.<sup>5</sup> Fig 2 gives the horizontal spread of heated effluents giving the different Thermal zones. Fig.3 gives the vertical profiles of temperatures in the different seasons to illustrate the formation of thermocline and its gradual disappearance.<sup>6</sup>

### DISCUSSION-EVALUATION

Data presented in Table 1 has brought out the important features of the environment which go a long way to effect thermal abatement. Even as the lake surface temperature reached 23.5°C in February, the hypolimnion waters were nearly 5.6°C lower than surface. The intake waters were cooler than if the design was a surface intake. The difference between the intake water and surface temperatures (5.3°C) was greater than that between condenser intake and discharge (4.3°C), resulting a station output of heated effluents at one degree celsius less than the lake surface temperature. This situation continued till peak summer temperature was reached in air (39°C). In the last week of May there were stray showers which brought in the welcome change in air (air temperature dropped by 4°C 39 to 35). There was a sudden change also in the lake water temperature profile. After the rains came down the picture changed entirely because the lake received plenty of water supply from hinterland and tributaries (Fig 3 for profiles).

Fig 2 gives the different thermal zones around the outfall. There is a 1°C rise in the close vicinity of outfall and then an intermixing or a well spread out mixing zone where at the peripheri the temperature was hardly above the ambient. The stretch of the mixing zone was about 1.3 km along the bank and 0.3 km off shore. As

the Fig 3 recorded 8 km/hr wind speed, the condition was a stagnancy in the lake. The lake stretched to about 3 km in the off shore direction - and the thermal impact was therefore felt only upto a tenth of available width.

### Comments

Thermal Water Quality standards are generally set round the following criteria.<sup>7, 8</sup>

1. Mixing Zone - an area where water quality standards are not applicable. This depends on the limited spread of affected region as a small fraction of the width at outfall.
2. Temperature standard - In cold climates a temperature maximum of 32-32.2°C is recommended ; at any time however the increase in temperature should not be greater than 2.5°C. in any part of the river system. In summer such increases shall be less than 1.1°C.

In conditions available in tropics namely, wide differences in diurnal and seasonal temperatures, and summer water temperatures at surface exceeding 35-38°C, the above criteria are not relevant. Except where the fishes get trapped or sedentary organisms are present, the impact of heated effluents is not likely to be felt on fish life directly at a low power nuclear station sites.

3. Table 2 suggests that under the prevailing circumstances of design, the intake waters drawn from the hypolimnion and discharged to surface, there was an enhancement in its DO content in the process of circulation through the condenser. This effect is demonstrated in the last four columns of Table 2. High C.O.D and B.O.D of intake waters can be caused because of pollution at depth (away from sunlight) and because the lake contained rotting wood.

4. There is a matted growth of *Velvetaria* grass in the outfall region which was found to be spreading and needed removal. This may not be a direct impact of thermal discharge.

### INVESTIGATIONS CARRIED OUT AT E.S. LABORATORY(ESL)

#### Gas supersaturation

Long hours of day light in tropical and subtropical regions can cause algal growth in stagnant reservoirs. Photosynthesis can lead to increased oxygen output in waters. If heated effluents are also discharged, oxygen supersaturation can result because of elevated temperature. These effects were studied in the ESL experimental tank as follows :

20,000 litres of raw water were transferred to a concrete tank of size 9.6 m x 5.2 m x 0.5 m. The waters were inoculated with

culture of Sconedesmus and dosed with urea and other nutrients. Measurements of DO, pH and temperatures were made throughout the duration of experiment. DO rose from 8.2 to 15 ppm and pH 8.9 to 11.1. After 12 days exposure in sun and when the water appeared as a pea soup from algal growth, fingerlings of Indian carp (*C.mrigala*-8; *L.rohita*-4) were introduced in the tank. In a week's time DO concentration exceeded 100% over the saturation limit and the fishes progressively died. An examination of dying fish showed that the fishes were breathing with difficulty and the fish died from excess of oxygen. Laceration of tissue in the gill region was seen in the dead fish.

The outfall region cannot be treated as stagnant because of turbulence but these observations are likely to be met with in the intermixing zone (Gas supersaturation) under tropical conditions. Gas bubbles were seen to escape from the tank waters during the day (14.00 hrs).

#### Parasitism

Two 'happas' (floating cages) were fabricated from nylon netting built around a wooden frame 180 cm x 80 cm x 60 cm. The happas were tied loosely to fixed pegs on the bank and released, one, into the discharge canal and the other (control) in the lake upstream. The nylon cages were weighted to submerge partially so that the introduced fishes always remained under heated effluents in the 'test' cage, as the waters flowed through the net. Each happa was charged with 20 numbers each of *C.carpio*, *L.rohita* and *C.mrigala*. The experiment had to be given up as the large fishes chewed away chunks of nylon. A set of improvised cages was prepared with steel wires and placed as before, in the discharge canal and upstream as Test and Control respectively. 50 fingerlings of *L.rohita* each were placed in each cage. The cages were provided with slit opening in the top cover for addition of fish feed and to conduct periodical examination. All the fishes were found dead in a month - severely mauled in belly and mouth.

The experiment was repeated with fingerlings of *L.rohita* and *C.mrigal* - weighing them before placing them in the cage :

| <u>Species</u>  | <u>No</u> | <u>Discharge Canal</u> |           | <u>Control</u> |           |
|-----------------|-----------|------------------------|-----------|----------------|-----------|
|                 |           | Av. Wt-g               | Length-cm | Av. Wt-g       | Length-cm |
| <i>L.rohita</i> | 13        | 238                    | 26 (av )  | 215            | 25        |
| <i>C.mrigal</i> | 11        | 210                    | 26        | 234            | 27        |

5 fingerlings from the Test and Control were taken out for examination. *L. rohita* had suffered very severely in the Test cage losing nearly 70g weight. The controls were steady. *C. mrigala* were also similarly affected but not to the same extent. On closer scrutiny, the fishes were found to be infested with an Ectoparasite identified as *Alitropus typus*. The parasite *Alitropus Typus* is a blood sucking type and it attacks the soft parts of the fish. <sup>9</sup>

#### Twin Aquaria Assemblies-Synergesis

The study of parasite proliferation, and synergesis caused by waste heat as primary pollutant, are being conducted in ESL attached to nuclear sites. For this purpose two sets of aquaria experimental tanks were electronically connected in such a way that the water temperature in one is 2.5°C higher than in the other which represents unaffected water of lake, upstream of outfall. The temperature difference represents the peak temperature increase in the intermixing zone. The experiments under way are of two types, namely, where

- 1- Both the control and heated one are charged with 5 fingerlings and 5 parasites (parasite behaviour and proliferation), and
- 2- In addition to heat other pollutants are added to the control and the Test aquaria e.g., H<sub>2</sub>S, Cl<sub>2</sub>, Hg, Chromates etc. to study synergistic effects.

#### TARAPUR ATOMIC POWER STATION

The Tarapur Atomic Power Station is 100 km north of Bombay on the West Coast. The station output of 400 MWe is generated by two BWR units. The reactors are located on a promontory jutting out about 200 m into the sea. The intake is an open channel drawing waters from upto one fathom depth, the channel sloping into a stilling pool after a silt trap. The intake waters are about 1°C less than the ambient sea water temperature. The condenser discharge which has a temperature of 10°C above the intake water, across the condenser ends, flows out to the sea through two discharge canals - one north of and the other south of the intake. <sup>3</sup> Although originally intended to prevent recirculation of heated effluents by directing the discharge to follow the tidal flow-at present the discharge flows out of both the canals. The discharge canals are 14 m wide, 4 m deep and nearly one kilometer long and do not contribute to thermal abatement by themselves, except in high tides because of

dilution and intermixing with on rushing waters. During other periods the wind cooling takes place only to the extent of lowering by 1°C as the water reaches the end of the canal.

Two important natural factors that help control thermal pollution are i) monsoon rains lasting for 3 months and strong breeze, and ii) turbulence caused by semidiurnal tides which may rise upto 5-6 m, giving effective mixing and dilution.<sup>2</sup>

There is no evidence as yet to demonstrate the negative effects of thermal discharges at Tarapur. Even in the many sedentary species present along the coastline and creeks, no accelerated growth of vegetation or radioactivity uptake in fish have been observed. The temperatures of heated effluents drop suddenly by about 3°C, even under neap conditions, when the effluent stream meets the sea at the discharge canal end in the first abatement step. Under low tide conditions about 400 m of the shelf are virtually bare and the effluents flow over the exposed rocks. Thermal monitoring did not show any increase in temperature beyond 1.5 km from the discharge canal end.

#### WASTE HEAT UTILISATION

Studies on Waste Heat Utilisation have been initiated for sometime in ESLs and it may take sometime before effective techniques for waste heat utilisation are developed for commercial exploitation.

At the Kalpakkam E S Laboratory, where the Madras Atomic Power Station is located it is intended to use waste heat for large scale production of algal cultures. An algal pond of size 12 m x 9 m is in operation from last 3 years using solar heat and domestic waste nutrients. When the power station goes into operation, waste heat will come up as an additional source of lowly rated heat flow. Mariculture is on the cards- particularly growth of shrimps, prawns and lobsters.

Prawns form a major exchange earning industry in the country.<sup>10</sup> Among the different species Penaeus indicus and Penaeus monodon are widely employed for developing creek and estuarine fisheries. Experiments are being initiated in co-operation with Tamilnadu mariculture teams for setting up

experimental assemblies in the discharge canals at Tarapur for production of Prawns and Lobsters. Laboratory study is also being planned at the Rajasthan -E S Laboratory for production of fresh water prawns-type *M. rosenbergii*.

Acknowledgements : The authors desire to acknowledge assistance from several colleagues and particularly of Mr K V K Nair (ESL-Kalpakkam) Mr B Dube (ESL-Rajasthan) and Shri S. Chandramouli (ESL-Tarapur). The authors gratefully acknowledge support received from Dr. A.K. Ganguly, Director, Chemical Group and Mr.S.D. Soman, Head H.P. Division, BARC.

## REFERENCES

1. Kamath, P.R., 'Environmental Surveillance at Nuclear sites in India', NUCLEAR INDIA April-May 1978 (Publ: DAE, Bombay 400 001)
2. Kamath, P.R., Bhat, I.S., Gurg, R.P., Adiga, B.B., and S.Chandramouli. 'Seasonal Features of Thermal Abatement of Shoreline Discharges at Nuclear sites' presented at the IAEA Symposium on Environmental Effects of Cooling Systems at Nuclear Power Plants; OSLO 26-30; Aug 1974.
3. Kamath, P.R., Bhat, I.S., and Ganguly, A.K., 'Environmental Behaviour of discharged Radioactive Effluents At Tarapur Atomic Power Station' IAEA-USAEC Symposium on Environmental Aspects of Nuclear Power Stations; 10-14 Aug 1970 N.Y., USA.
4. Gurg, R.P., Bhat, I.S., and Kamath, P.R. -Progress report of ESL Rajasthan Atomic Power Station - BARC report No I-369, 1975.
5. Gurg, R.P., Bhat, I.S., and Kamath, P.R. 'Thermal Pollution from Nuclear Power Production under Tropical Conditions' Presented at the symposium on Operating Experience of Nuclear Reactors and Power Plants. Feb 7-9, 1977 Bombay, DAE.
6. Kamath, P.R., Gurg, R.P., Sebastian, T.A., Vyas, P.V., Dube, B., and Nair, K.V.K., 'Impact on water quality from Discharge of Thermal Effluents in RPS Lake' Presented at the IAEA Research Coordination Meeting on Thermal Pollution, Kalpakkam Dec 5-9, 1977.
7. Miller, D.C., and Beck, A.D. 'Development and Application of Criteria for Marine Cooling Waters' Paper IAEA -SM-187/10 in Symposium mentioned in Ref 2 above.
8. Jeter, C 'An Approach to Thermal Water Quality Standards' Presented at the Conference on Waste Heat Management and Utilisation, 9-11 May 1976, Miami Beach, Florida, University of Miami.
9. Chaudhary, R.S., and Walker M.F., 'Parasitic Behaviour of Fresh Water ISOPOD ALITROPUS TYPUS in fishes of Rana Pratap Sagar India' (In press) 1978. Preprint communicated.
10. Fishes and Fisheries - publication of CSIR, New Delhi 1962 Supplement to 'The Wealth of India' Vol IV.

Table - 1

RAJASTHAN: SEASONAL VARIATION IN AMBIENT  
AND COOLING TEMPERATURES

| Date<br>and time<br>(hrs) | Power<br>MW | Ambient temp. °C |                 | Coolant<br>intake<br>°C | Coolant<br>outlet<br>°C |
|---------------------------|-------------|------------------|-----------------|-------------------------|-------------------------|
|                           |             | Air              | Lake<br>surface |                         |                         |
| 26.2.74<br>(11.00)        | 130         | 23.8             | 23.5            | 18.2                    | 22.5                    |
| 9.3.74<br>(11.10)         | 155         | 32.2             | 26.0            | 17.2                    | 22.4                    |
| 18.3.74<br>(14.30)        | 150         | 32.5             | 24.7            | 18.1                    | 24.2                    |
| 10.4.74<br>(15.30)        | 170         | 36.5             | 29.2            | 19.2                    | 28.5                    |
| 25.4.74<br>(13.00)        | 170         | 37.0             | 28.5            | 19.6                    | 27.8                    |
| 20.5.74<br>(15.30)        | 175         | 39.3             | 31.7            | 19.0                    | 30.0                    |
| 25.5.74<br>(10.30)        | 150         | 35.0             | 30.0            | 21.5                    | 32.0                    |
| 1.6.74<br>(11.30)         | 180         | 35.0             | 30.0            | 24.0                    | 36.0                    |
| 5.6.74<br>(17.15)         | 160         | 36.0             | 30.0            | 26.0                    | 37.0                    |
| 13.6.74<br>(10.30)        | 175         | 35.5             | 31.0            | 23.0                    | 35.0                    |
| 27.6.74<br>(14.10)        | 125         | 38.8             | 29.7            | 27.5                    | 29.7                    |

Table - 2

COOLANT WATER QUALITY AT RAPS

| Date     | Reactor<br>Power<br>MWe | Temp.<br>differ-<br>ence<br>dt °C | Dissolved<br>oxygen ppm<br>percent<br>saturation |                        | C. O. D<br>Intake -<br>Disch-<br>arge<br>(ppm) | B. O. D.<br>Intake -<br>Disch-<br>arge<br>(ppm) |
|----------|-------------------------|-----------------------------------|--|------------------------|--|---|
|          |                         |                                   | <u>Int-<br/>ake</u>                              | <u>Disch-<br/>arge</u> |  |   |
| 30.6.76  | 165                     | 10.5                              | 92.1   | 105.5                  | + 1.2  | + 1.2   |
| 11.8.76  | 170                     | 11.0                              | 91.0   | 110.8                  | + 0  | + 0.5   |
| 27.8.76  | 0                       | 2.0                               | 76.9   | 81.6                   | + 0.3  | + 1.1   |
| 25.9.76  | 172                     | 10.5                              | 83.5   | 100.0                  | + 0.7  | + 0.5   |
| 6.10.76  | 160                     | 10.5                              | 75.6   | 92.4                   | + 2.0  | + 1.5   |
| 3.11.76  | 180                     | 8.0                               | 85.0   | 95.7                   | + 1.1  | + 0.9   |
| 11.11.76 | 175                     | 11.0                              | 72.8   | 101.5                  | + 0.3  | + 0.3   |

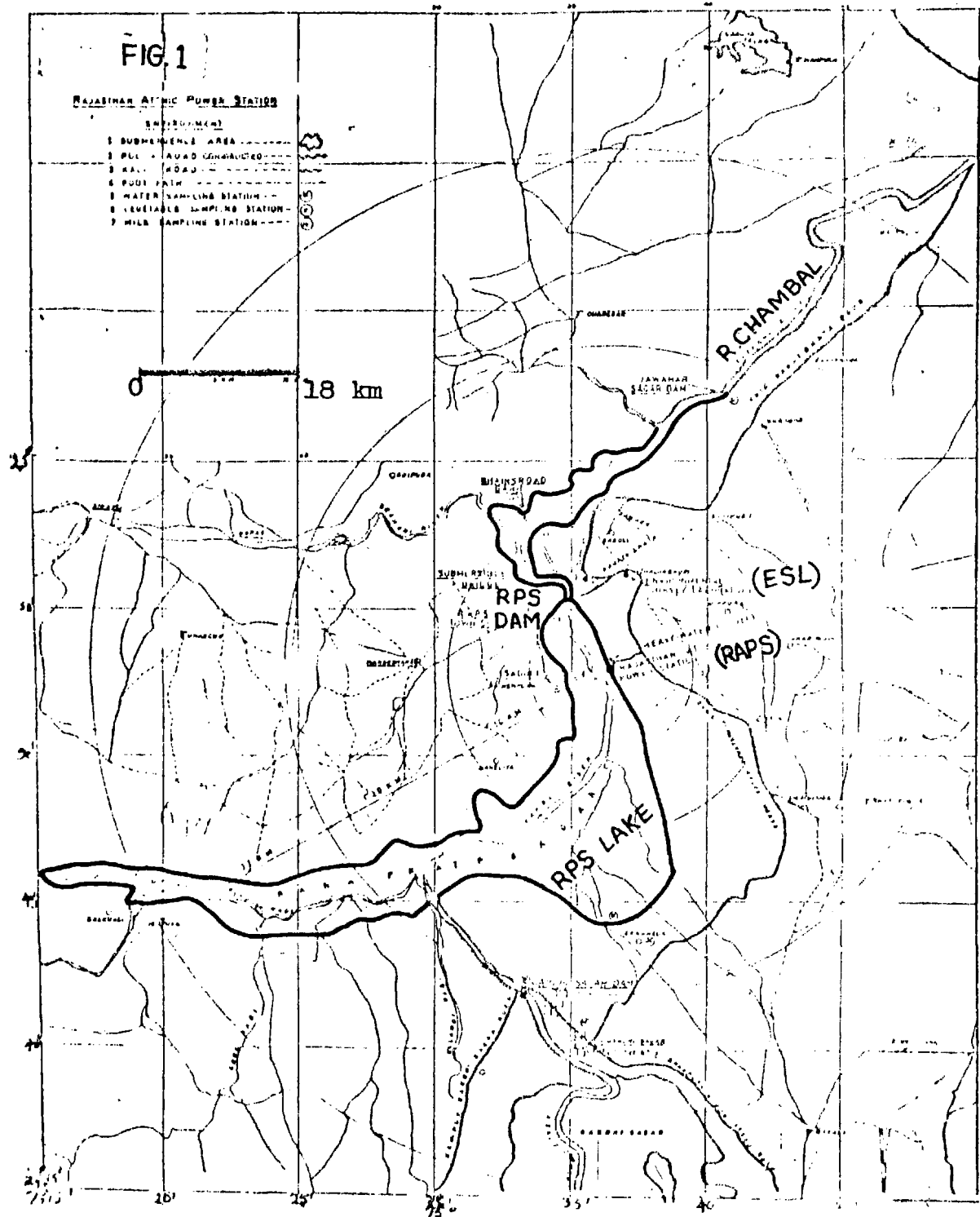


FIG. 2 THERMAL ZONE OF RAPS DISCHARGE (10-1-77)

|                     |         |             |
|---------------------|---------|-------------|
| POWER LEVEL         | 170 MWe | PLUME DEPTH |
| CONDENSER INTAKE    | 18°C    | AT A 3.0 M  |
| CONDENSER DISCHARGE | 28°C    | AT B 1.5 M  |
| AMBIENT TEMP        | 24°C    | AT C 11.0 M |
| WIND SPEED          | 3 Km/Hr | AT D 13.5 M |
| WIND DIRECTION      | SE      |             |

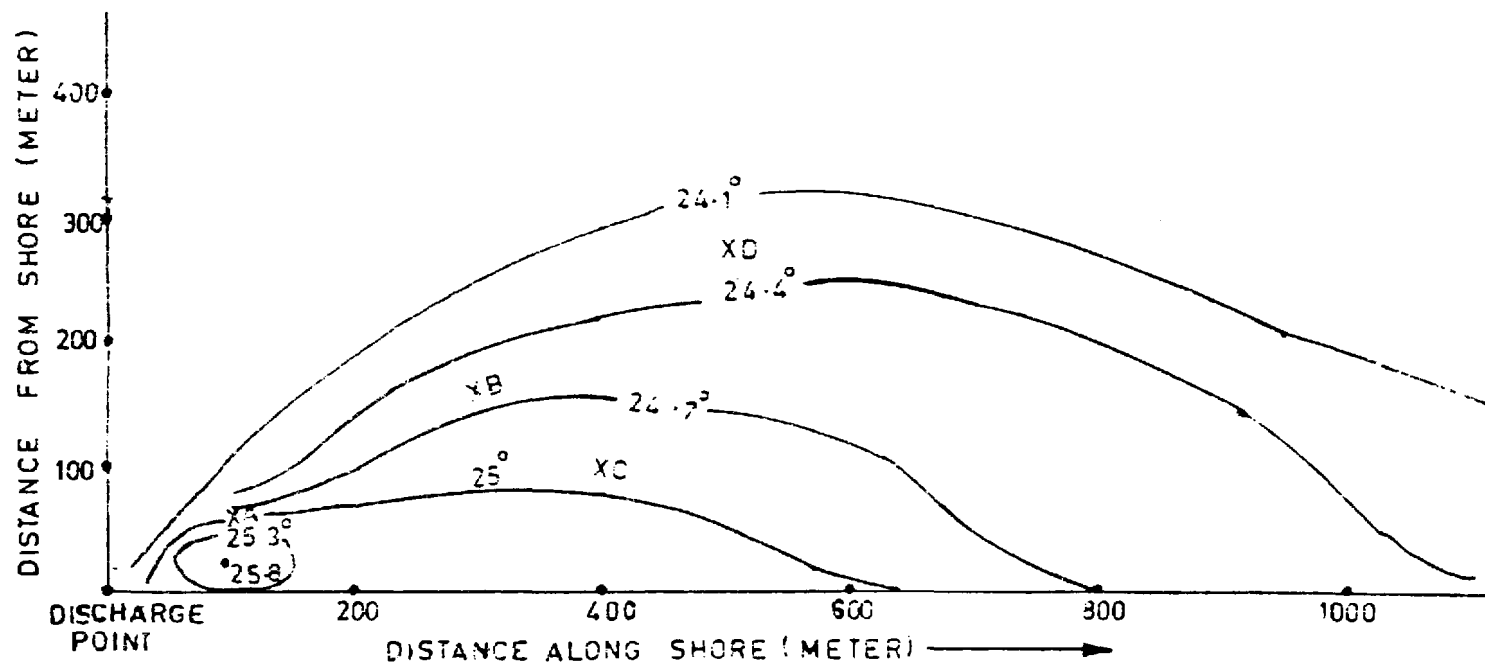
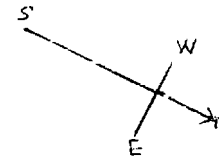


FIG. 3 THERMAL PROFILE IN LAKE RPS DAM

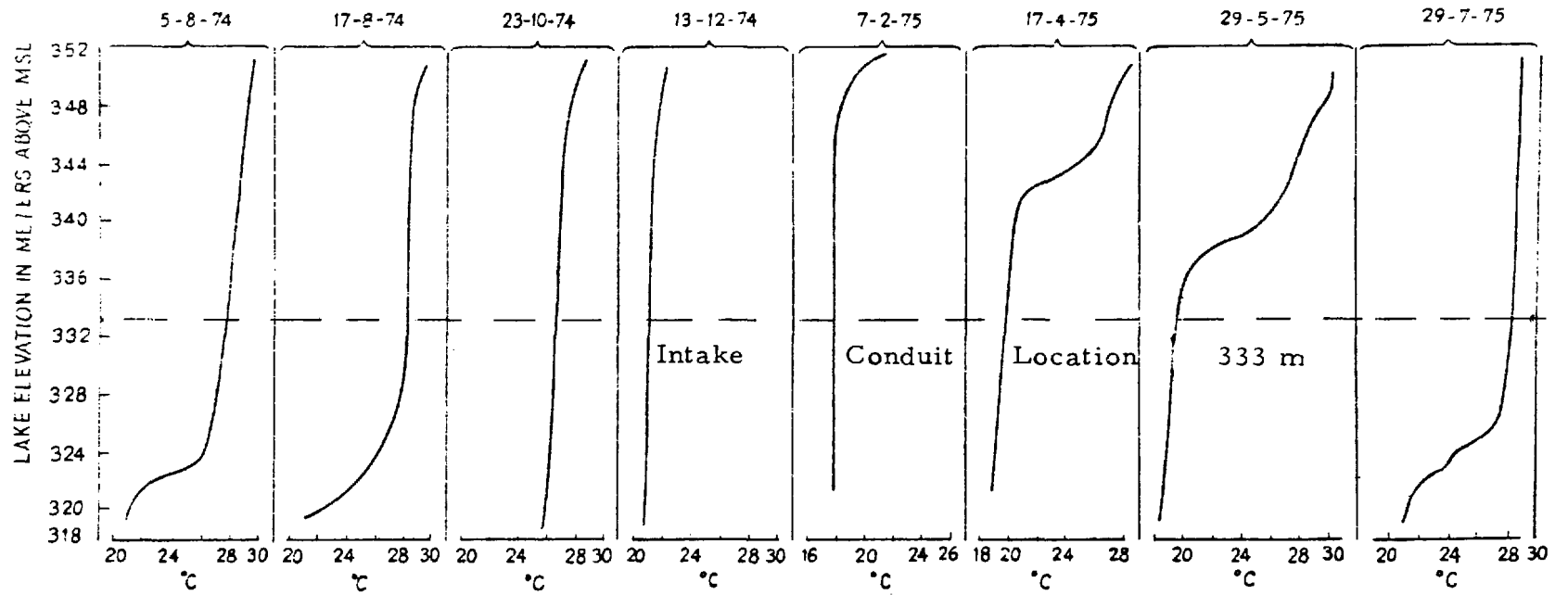
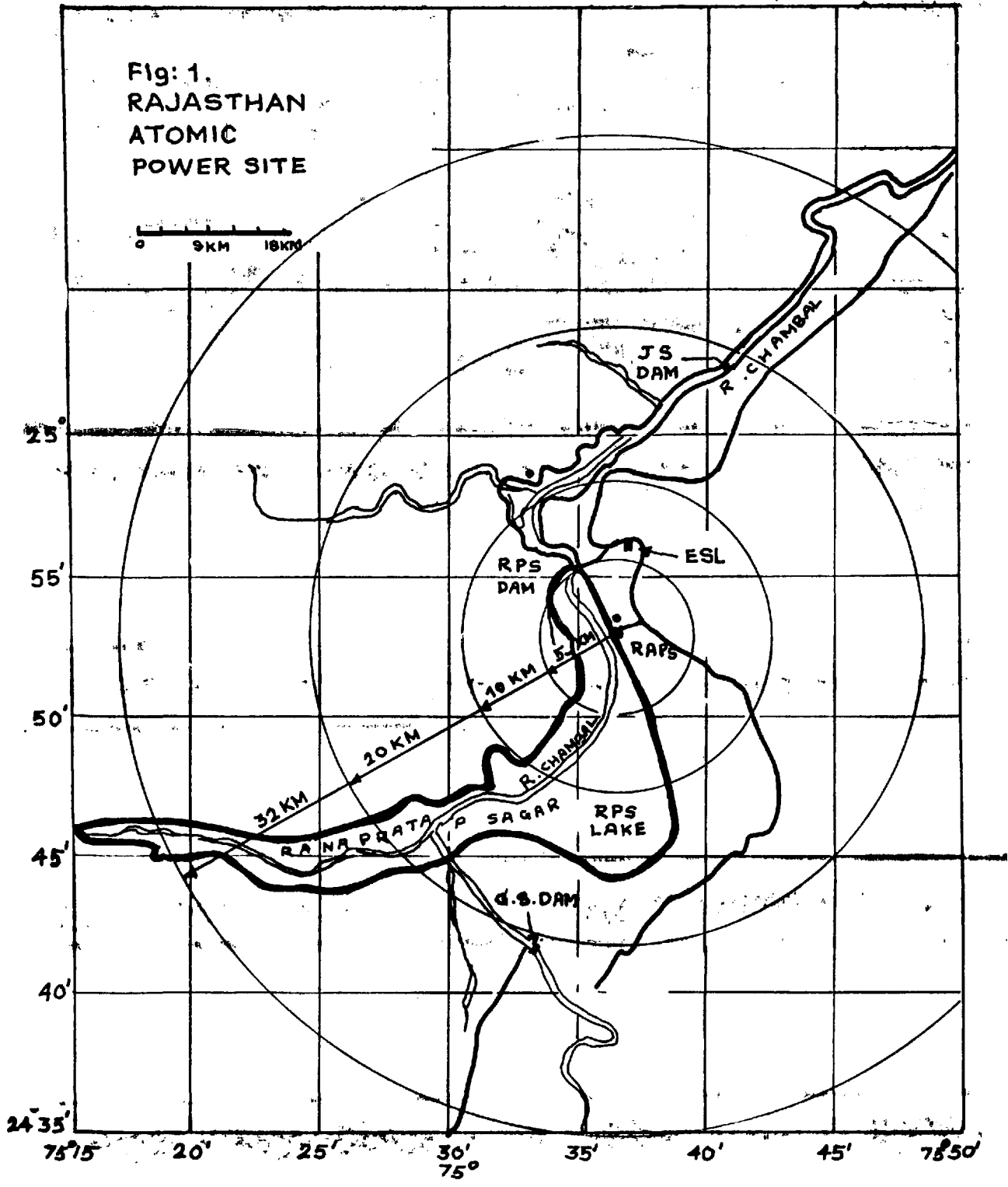


Fig: 1.  
RAJASTHAN  
ATOMIC  
POWER SITE



RIVER THERMAL STANDARDS EFFECTS ON COOLING-RELATED  
POWER PRODUCTION COSTS

by

T.E. Croley II, A.R. Giaquinta,  
M.P. Cherian, and R.A. Woodhouse

Iowa Institute of Hydraulic Research  
The University of Iowa  
Iowa City, Iowa USA

ABSTRACT

Power plant cooling costs and water consumption for various river temperature standards are presented for existing and proposed future power plants located along the Upper Mississippi River. Three models previously developed at the Iowa Institute of Hydraulic Research are combined to evaluate the cooling-related costs of river thermal standards. These costs depend on the meteorological conditions at each power plant site, and they are summed for the river reach of interest. The existing thermal standards case, the free-discharge or no-thermal-standard case (all plants employ open-cycle-cooling), and the extreme case of no allowable discharges are chosen to show the dependency of power-production-related cooling costs and water consumption on various criteria. A critical appraisal of the worth of thermal standards in terms of water consumption and other costs is thereby possible, so that subjective assessments of the standards can proceed with full knowledge of the trade-offs involved between the costs of power production and environmental impacts.

INTRODUCTION

A joint meeting of state and federal governmental agencies on Mississippi River temperature standards was held in St. Louis, Missouri, on March 3, 1971. Temperature standards were proposed because it was felt that heated effluents from nuclear-and fossil-fueled power plants could raise river temperatures enough to harm the biota. The report recommended that the maximum "artificial" rise in water temperature not exceed a prescribed limit above the recorded natural temperature, nor should the actual temperature exceed the maximum safe temperature, whichever constraint dominates. It was decided at this meeting that power plants could easily comply with the standards with closed-cycle cooling being the most economically feasible means.

The existing standards now governing thermal discharges into the Mississippi River include a specified maximum allowable water temperature for each month of the year and a maximum allowable temperature rise of 5°F along the entire length of the river. Future regulations will further limit thermal discharges into the river. The U.S. Environmental Protection Agency has mandated that

thermal discharges into natural rivers from power plants placed into service after 1 January 1970 (or 1974 depending on the size of the plant) will not be permitted after 1 July 1983 [1].

The standards were aimed at environmental enhancement with little consideration of resultant costs. It is extremely difficult to determine a set of standards which adequately represents both the environmental and beneficial use viewpoints. The difficulty stems from a lack of knowledge about the level of environmental preservation (or beneficial use) to be maintained by the standards and how that level should be measured. There have been many studies of the environmental ramifications of thermal loads on rivers. The common characteristic of them all is that the environmental impacts either are not quantifiable or are multidimensional, or both. In any event, it has been impossible to associate a numerical indication of environmental impact with a set of river standards. However, the environmental impact is real and must be addressed in any intelligent determination of river temperature regulations. This problem of evaluating alternate standards in terms of their environmental impacts is typical of situations requiring subjective evaluations to be made.

If the economic impacts of environmental standards are understood by decision makers, then alternate sets of standards can be evaluated in terms of the "costs" required to meet those standards and the amount of environmental protection consequent to those constraints. In other words, trade-off "costs" of providing different levels of environmental protection (resulting from different sets of thermal standards) can be investigated. The question can be asked for each set of standards to be evaluated: "Are the environmental gains justified in relation to the expenditures?" This question still involves a subjective choice, but it is much easier to answer than the original question: "How much environmental protection should be provided?" The trade-off question can be asked over and over for increasingly stringent sets of standards until a desired balance between environmental objectives and consequent economic penalties and water consumption is established.

This study looks at the question of the "costs" (both economic and water consumption) to the utilities (and the public) of meeting various thermal standards for the Upper Mississippi River from the source to the southern Iowa border. The costs of the existing thermal standards are assessed by computing the marginal increases in monetary expenditure and water consumption over the "free-discharge" or no-standards case wherein all utilities are assumed to utilize the most economical and lowest water consumptive system: the once-through cooling system. The additional "costs" (over the existing standards and over the free-discharge case) of more restrictive thermal standards (the "zero-discharge" thermal standard) are also assessed for a complete realization of the implications of impacts of these standards. It is extremely important to realize that the figures given herein are illustrative only since fixed unit costs were assumed across-the-board for all utilities along the study reach and fixed assumptions were made for the operation of all plants. The numbers cannot be taken

as indicative of true costs of any one utility but serve to indicate the generalized total costs for the entire study region. The power plants included in the study are those presently operating and those proposed for future construction (through 1994) having capacities of 25 MW or greater; all of the utilities lie in the Mid-Continent Area Power Pool (MAPP) geographical area, and most are MAPP members. The computational scheme to assess the worth of thermal standards requires the use of three models previously developed at the Iowa Institute of Hydraulic Research. The first model examines the steady-state thermal regime along the study reach of the Upper Mississippi River. The model is used to locate regions where river temperatures exceed the allowable limits for any prescribed set of thermal standards, and to assess river evaporation for heat loadings consequent with those thermal standards. The second model evaluates cooling-related costs of backfitting existing power plants (identified as requiring backfitting with the first model under a set of thermal standards) with mechanical draft wet cooling towers. The third model computes cooling-related costs of outfitting proposed power plants (identified as requiring outfitting with the first model for a set of standards) with once-through and closed-cycle (wet tower) cooling systems.

#### COMPUTATIONAL MODELS

##### Iowa Thermal Regime Model (ITRM)

A predictive computational model for computing temperature distributions along natural rivers (ITRM) was developed by Paily and Kennedy [2]. The steady-state version presented by Paily et al. [3] is used to compute the thermal regimes for the natural, free-discharge, existing, and no-discharge cases.

The model is based on a numerical solution of the one-dimensional convection-diffusion equation, and it predicts the longitudinal distribution of cross-sectional average temperature along a river. The total river length is divided into smaller reaches, and temperature distributions are computed for each reach separately. The solutions for adjacent reaches are linked by the common conditions at the junction points connecting them. Each reach of the river can have multiple thermal inputs and tributary inflows. The formulation allows for changes in the channel characteristics and the river flow rate. Variations in weather data from place to place also are taken into account. The model is one-dimensional and assumes complete mixing of the heated effluent with the river. To compute thermal discharges of proposed plants, the model assumes in-plant efficiencies of 85 and 95 percent, an overall plant efficiency of 32 and 36 percent, and a condenser temperature rise of 18°F and 25°F for fossil-fueled and nuclear power plants, respectively.

Based on these assumptions, it is clear that the steady-state thermal regime model presents only an overview of the aggregate thermal profile of a river; it does not yield a detailed assessment of the actual temperature

distribution. However, this model does give adequate representation of the river temperature distribution.

The thermal regime model is used to determine the temperature profile along the Mississippi River in the MAPP geographical area corresponding to average flow and weather conditions. The input data used for the computations are the following:

1. heat loads from power plants of rated capacity 25 MW or greater, industries, and municipalities located on the main stem of the river;
2. monthly mean values of daily flow rates measured at 12 U.S. Geological Survey gaging stations along the river;
3. monthly mean values of daily weather conditions including air temperature, wind speed, relative humidity, atmospheric pressure, cloud cover, and solar radiation measured at 6 first-order weather stations of the National Weather Service; and
4. channel top widths at approximately ten-mile intervals determined from river profiles developed by the U.S. Army Corps of Engineers.

Temperature profiles also were determined for the 7-day, 10-year low flow along the river combined with average weather conditions for the months of August and November to compute the extreme assimilation capacity of the river at locations of proposed power plants. Evaporation rates along the river were computed for the average flow thermal regimes. The river discharge, climatological variables, and channel geometry parameters were assumed to vary linearly between adjacent measuring stations.

#### Backfitting Model

This model evaluates the cost of backfitting a power plant or unit currently operating on open-cycle cooling with a mechanical draft wet cooling tower [4]. The major factors considered in the economic assessment of backfitting an existing unit are:

1. the cost of installing the cooling tower, including materials, labor, site acquisition, and preparation;
2. the plant downtime for system changeover;
3. the provision of additional generating capacity to replace the power consumed by the cooling system;
4. the operation and maintenance costs of the cooling-system; and
5. the additional cost of power generation due to limitations imposed by the use of the closed-cycle system.

The first three of these quantities are capital costs and the last two are operating costs incurred over the remaining lifetime of the plant. Once these factors have been determined, the total cost may be computed by using the fixed-charge-rate method [5]. It is possible to design mechanical draft wet towers of any size, but realistically the lowest-cost tower would be built in practice. Therefore, a range of tower sizes must be investigated at each site to determine the optimum design. The characteristics of the power plant required for backfitting calculations are the accredited

capacity of the unit, the type of plant (fossil or nuclear), the thermodynamics of the existing turbine and condenser systems, and the economic situation of the utility operating the unit. Simplifications and assumptions made in the development of the model are:

1. the power plant is operating at 80 percent of the accredited capacity throughout the year to satisfy a constant demand of the same amount;
2. the plant or unit is considered to be operating with a constant, relatively low, turbine back pressure, and the corresponding heat rejection rate is known for an existing open-cycle cooling system;
3. the existing condensers are retained without modification; and
4. the same capacity factor is used both before and after backfitting.

With these assumptions, computation of capital and operating costs of backfitting with a mechanical-draft wet cooling tower may be achieved by using calculation procedures outlined by Croley et al. [4] and described briefly in the following subsection on outfitting. Of foremost importance in the backfitting calculations are the capacity loss, the energy loss, the excess fuel consumption (the difference between the fuel consumption with an open-cycle cooling system and the backfitted system) and the excess maintenance cost. The model also may be used for the computation of water consumption by the cooling tower.

#### Outfitting Model for Once-Through and Closed-Cycle Cooling Systems

The economics of power plant cooling performance is mainly dependent on the turbine-condenser subsystem characteristics and on the size and type of cooling system. Two basic types of turbines are considered in this study as representative of those currently in use. The first type is a high back-end loaded unit of contemporary design, and the second type is a low back-end loaded unit primarily used in older plants. Operating characteristics of these turbines are given in reference [5].

Cooling characteristics curves may be determined for any specified size and type of cooling system using the appropriate model. The size of a once-through cooling system is primarily determined by the condenser flow rate and by the design heat assimilation capacity of the receiving water body. The cooling characteristics curve is determined by the size of the system and by the actual heat assimilation capacity of the stream. For mechanical draft wet cooling towers, the size of the cooling system is specified by the dimensions of the tower and the design meteorological conditions chosen at the site. The cooling characteristics may then be determined from the basic thermodynamic model described elsewhere [6]. The operation point of the cooling tower is defined as the intersection point obtained by superimposing the appropriate cooling characteristics curve on the turbine characteristics curve as described in reference [6]. This operation point completely describes the performance of the power plant cooling system in terms of hot water temperature, heat rejection rate, power output, and turbine back pressure for any given set of meteorological conditions and power loading. Condenser sizing is obtained from the operation point

corresponding to the design characteristics curves using design meteorological and stream conditions. Capacity loss is obtained from the operation point corresponding to the extreme characteristics curve evaluated using extreme meteorological and stream conditions. Fuel consumption, make-up water (water evaporation), energy loss, and other quantities may be obtained from the operation point corresponding to the "prevailing or existing" characteristics curve. If the cooling system is smaller or if the meteorological or stream conditions become more adverse, the operation point will shift such that the resulting power output will decrease. The model has the capability of computing fuel consumption, water evaporation, energy loss, and other parameters for a given distribution of meteorological and stream conditions.

Power plant cooling costs are composed of capital costs which include the cost of tower structures, once-through cooling structures, condensers, pump and pipe systems, and replacement capacity; and operating costs which consist of the costs of fuel, make-up water, water treatment, maintenance, and replacement energy. These costs are determined by using appropriate unit costs and monographs, (see TABLE I and reference [7]). The unit costs are expressed in terms of 1976 dollars and are valid only for the MAPP region. The total cooling-related cost of power production is computed using the fixed-charge-rate method.

#### PROCEDURE

Changes in thermal standards would alter existing assimilation capacities of the river and, hence, the operation of once-through cooling systems located along the river. Thermal violations (defined as cases where the maximum river temperature or the increase of river temperature due to heated effluents exceeds the allowable limit) which occur as a result of a change in thermal standards would require these power plants to derate or to backfit a closed-cycle cooling system. Associated with these alternatives are high energy losses and capital expenditures in terms of cooling tower construction and associated changes in operating cost, and water evaporation as a result of the closed-cycle operation. To relate thermal standards to the cooling-related costs of power production and water consumption, the following procedure was developed:

1. Determine the thermal regime of the river for the heat loads from existing and proposed power plants at average flow conditions. Compute net evaporation resulting from thermal discharges.
2. Choose a specified set of thermal standards.
3. Determine cases where thermal standards are exceeded, if any.
4. Backfit power plants with mechanical draft wet cooling towers wherever thermal violations occur, and compute annual backfitting costs (including all capital costs). Calculate the corresponding annual water consumption.
5. Determine the annual energy loss at plants where thermal standards are exceeded, and determine the corresponding cost of purchasing replacement energy, without adding auxiliary cooling capacity.
6. Choose the more economical alternative of steps 4 and 5 at each affected location.

7. Compute the annual operating costs of existing power plants that do not violate thermal regulations. (The capital costs of these cooling systems are not considered.) Determine the corresponding annual water evaporation.
8. Size cooling systems of proposed power plants (the capital costs of these cooling systems are considered). Determine total annual costs and water evaporation.
9. Compute the total annual cooling-related costs of power production and the total water consumption corresponding to the specified thermal standard.
10. Repeat the computations for other thermal standards.

Computations in steps 1 and 3 are carried out for the months of February, May, August, and November. These four months are assumed to adequately represent the meteorological and hydrological conditions that exist throughout the year. Backfitting is carried out at an existing plant if thermal standards are exceeded during any one of these months. Annual operating costs for existing and proposed power plants are computed corresponding to meteorological and stream conditions that exist during the chosen study months.

Proposed plants are sized corresponding to extreme meteorological conditions and the 7-day, 10-year low flow hydrological condition. Capital costs of proposed power plants are added to annual operating costs by using the fixed-charge-rate method. For existing power plants a uniform remaining life of 20 years is assumed; for proposed power plants the expected life horizon is assumed to be 35 years.

## RESULTS

The cost of meeting a specified thermal standard is defined as the difference in total cooling-related costs associated with the thermal standard and the total cooling-related costs associated with no thermal standards. In the latter case, all existing and proposed power plants utilizing a closed-cycle cooling system are considered as employing once-through cooling, as noted earlier. Marginal cost changes are computed and the worth of the thermal standard is evaluated; also changes in water consumption that occur as a result of variations in thermal standards are presented. The three thermal standards considered herein are the existing regulations, the "no-discharge" standard, and a free-discharge condition.

### Water Consumption

Water consumption resulting from power plant operation is due to the increased river temperatures caused by heated effluents and to evaporation from wet cooling towers. Natural evaporation from the study reach (without power plants) was obtained from the ITRM with the appropriate data set and is shown in Fig. 1. The annual equivalent of this figure integrated over the river and the year is 257.1 million m<sup>3</sup>. The variations in natural evaporation are a result of the natural variations of the top width of the river. To eliminate

the effects of top width from this and succeeding figures, the unit evaporation is calculated by dividing evaporation by the river width. Unit natural evaporation is depicted in Fig. 2. Now, the dips and peaks in the curve are seen to correspond to the locations of the weather stations which are labeled at the tops of Figs. 1 and 2. It is noted that natural evaporation for the month of February and most of November is zero because of the presence of ice cover on the river during these months. Sublimation from ice is neglected in this study.

The actual river evaporation corresponding to the existing and proposed power plants with existing thermal standards was computed with the ITRM and appropriate data sets on a unit basis, and the unit natural evaporation of Fig. 2 was subtracted to give the unit net evaporation on the river, which is plotted for August conditions in Fig. 3. It is important to note that this figure pertains to unit net river evaporation only and does not include the other cooling-related evaporation losses from wet cooling towers since it is not possible to present those losses on a unit basis. Sudden spikes in the evaporation curve are a result of thermal discharges at those locations. Certain interesting features can be observed in the unit net evaporation for the month of February, Fig. 4. As a result of ice cover, no evaporation occurs unless the temperature of the river water is above 0°C as a consequence of heated discharges from power plants. Water temperatures above freezing are not sustained over any long reach of the river because of adverse meteorological conditions; therefore, the unit net evaporation abruptly drops to zero. It also should be noticed that the magnitude of the evaporation rates is much greater than the corresponding rates for August. This increase is primarily due to the fact that the air temperature in February is below the water temperature at these locations; other meteorological conditions are also conducive to this phenomenon during February.

By integrating the net river evaporation along the river and over the year and adding the total evaporation from wet cooling towers (if there are any), the total annual evaporation can be calculated for each set of thermal standards. This calculation was made for the free-discharge condition, the existing thermal standard, and the no-discharge thermal standard; the results are tabulated in TABLE II. It is seen from this table that the existing standards result in an annual increase of about 2.60 million m<sup>3</sup> over the free-discharge condition of 156.9 million m<sup>3</sup> (an increase of 1.67 percent). The no-discharge standard represents an annual increase of 5.68 million m<sup>3</sup> over the free-discharge condition (an increase of 3.62 percent) and an annual increase of 3.08 million m<sup>3</sup> over the existing thermal standards of 159.5 million m<sup>3</sup> (an increase of 1.93 percent). Net evaporation for the free-discharge condition represents total evaporation (no cooling tower evaporation) and is smaller than the total annual evaporation for the existing thermal standards. For the no-discharge thermal standard, net evaporation is zero. On the other hand, evaporation from wet towers is higher for the no-discharge condition. Thus, it is easily seen that total annual evaporation is greater with the no-discharge standard since water consumption from wet towers is higher than evaporation from the river surface for comparable cooling duties.

## Economic Costs

Costs for the various thermal standard conditions are computed from the backfitting and outfitting models for each utility identified as exceeding the thermal standards with ITRM. Costs for existing thermal standards are presented in TABLE III. These computed results indicate that the average cooling-related cost of power production in the region of study is of the order of 15.20 mills/kw-hr for the present thermal standards, which represents a relative increase of about 1.58 mills/kw-hr over the free-discharge case. The value of 1.58 mills/kw-hr may then be considered as the average "cost" of the existing thermal standards. Details of the cost reduction as a result of the free-discharge thermal standard are presented in TABLE IV. It should be mentioned that the fuel consumption cost with the once-through cooling system is higher than the corresponding cost for the same power plant outfitted with a mechanical-draft wet cooling tower. This phenomenon also is observed in the backfitting operation and is due to the fact that with a wet tower, the power plant is derated at certain times as a result of adverse meteorological conditions. Consequently, fuel consumption is lower with the wet tower. Under these conditions, however, large amounts of replacement energy are required which result in high replacement energy costs. The decrease in fuel consumption of plants with cooling towers is, of course, counteracted by an increased fuel consumption of the plants supplying the replacement energy.

The no-discharge thermal standard involves additional costs incurred as a result of backfitting once-through cooling systems with wet cooling towers; the cost increases are listed in TABLE V. These costs must be added to the costs obtained with the existing thermal standards to compute the cost of the no-discharge standard. It is seen that the no-discharge thermal standard represents an average increase of 2.042 mills/kw-hr over the existing average annual cost. The "cost" of the no-discharge standard is, therefore, of the order of 3.62 mills/kw-hr as compared to the free-discharge condition. All regional cost figures are summarized in TABLE VI.

## CONCLUSION

The knowledge of costs and water consumption associated with the free-discharge, existing, and no-discharge thermal standards should provide a useful guide in reexamining present criteria and perhaps setting up new thermal regulations for the Upper Mississippi River. If the "worth" of these thermal standards in environmental terms has been established, the standards can be assessed with regard to their "costs" and the trade-offs between the costs of power production and environmental impacts is made clear. Undoubtedly, it is extremely difficult to determine the level of environmental protection required; however, subjective assessments can be made with an understanding of the costs associated with thermal standards. The procedure and the results presented in this paper should help in enabling intelligent decision-making with regard to the establishment of thermal standards. The costs cannot be judged as accurate on a site-to-site basis, but serve to illustrate the general impact of various standards for the entire study reach.

## ACKNOWLEDGEMENTS

This project was financed in part by a grant from the Mid-Continent Area Power Pool (MAPP) and by a grant from the U.S. Department of the Interior, Office of Water Research and Technology under Public Law 88-379 as amended, and made available through the Iowa State Water Resources Research Institute. Funds for computer time were provided by the Graduate College of The University of Iowa.

## REFERENCES

1. U.S. Environmental Protection Agency, "Development Document for Effluent Limitations and Guidelines and New Source Performance Standards for the Steam Electric Power Generating Point Source Category," United States Environmental Protection Agency, Washington, D.C., Oct. 1974.
2. Paily, P.P. and Kennedy, J.F., "A Computational Model for Predicting the Thermal Regimes of Rivers," IIHR Report No. 169, Iowa Institute of Hydraulic Research, The University of Iowa, Iowa City, Iowa, Nov. 1974.
3. Paily, P.P., Su, T.Y., Giaquinta, A.R., and Kennedy, J.F., "The Thermal Regimes of the Upper Mississippi and Missouri Rivers," IIHR Report No. 182, Iowa Institute of Hydraulic Research, The University of Iowa, Iowa City, Iowa, Oct. 1976.
4. Croley, T.E., II, Giaquinta, A.R., and Patel, V.C., "Wet Cooling Tower Backfitting Economics," Journal of the Power Division, ASCE, Vol. 104, No. PO2, Apr. 1978, pp. 115-130.
5. Giaquinta, A.R., et al., "Economic Assessment of Backfitting Power Plants with Closed-Cycle Cooling Systems," Report No. EPA-600/2-76-050, U.S. Environmental Protection Agency, Research Triangle Park, North Carolina, Mar. 1976.
6. Croley, T.E., II, Patel, V.C., and Cheng, M.-S., "Thermodynamic Models of Dry-Wet Cooling Towers," Journal of the Power Division, ASCE, Vol. 102, No. PO1, Jan. 1976, pp. 1-19.
7. Croley, T.E., II, Giaquinta, A.R., Lee, R.M.-H., and Hsu, T.D., "Optimum Combinations of Cooling Alternatives for Steam-Electric Power Plants," IIHR Report No. 212, Iowa Institute of Hydraulic Research, The University of Iowa, Iowa City, Iowa, July 1978.

TABLE I

UNIT COSTS  
(assumed to be spatially uniform in the region of study)

| Description                         | Cost                           |
|-------------------------------------|--------------------------------|
| Unit cost of wet towers             | \$21/TU                        |
| Unit condenser cost                 | \$12/sq. ft of<br>surface area |
| Unit replacement capacity cost      | \$400,000/MW                   |
| Unit land cost                      | \$5,000/acre                   |
| Unit make-up water cost             | \$1.8/1000 gals                |
| Unit waste-water treatment cost     | \$0.15/1000 gals               |
| Unit fuel cost                      | \$0.004/kw-hr                  |
| Unit maintenance cost of wet towers | \$300/yr/cell                  |
| Unit replacement energy cost        | \$0.02/kw-hr                   |

TABLE II

WATER CONSUMPTION COMPARISON OF DIFFERENT THERMAL STANDARDS

| Thermal Standard | Net Annual<br>Evaporation from<br>River Surface, m <sup>3</sup> | Annual<br>Water Consumption<br>of Wet Towers, m <sup>3</sup> | Total Annual<br>Evaporation<br>m <sup>3</sup> |
|------------------|---|--|---|
| Free-discharge   | 156,923,000   | 0  | 156,923,000                                   |
| Existing         | 68,851,000  | 90,670,000   | 159,521,000                                   |
| No-discharge     | 0   | 162,600,000  | 162,600,000                                   |

TABLE III

COMPUTED COSTS OF EXISTING THERMAL STANDARDS (1976 dollars)

| Plant & Unit No.        | Location (R. Mile) | Capacity (MW) | Cod. <sup>a</sup> | Capital Costs (million dollars) |                    |           |                        |                     |       | Annual Operating Costs (million dollars) |        |             |       |                   |               |                 |             | Tot. An. Cost, 1976 |             |        |             |
|-------------------------|--------------------|---------------|-------------------|---------------------------------|--------------------|-----------|------------------------|---------------------|-------|--|--------|-------------|-------|-------------------|---------------|-----------------|-------------|---------------------|-------------|--------|-------------|
|                         |                    |               |                   | Type                            | Pum. & Pipe System | Condenser | Once-through (cooling) | Replacment Capacity | Land  | Total                                    | Annual |             | Fuel  | Replacment Energy | Make-up Water | Water Treatment | Maintenance | Total               | mills/kw-hr | Total  | Mills/kw-hr |
|                         |                    |               |                   |                                 |                    |           |                        |                     |       |  | Total  | Mills/kw-hr |       |                   |               |                 |             |                     |             |        |             |
| Clay Boswell #1-2       | 1187               | 150           | F2GE              |                                 |                    |           |                        |                     |       |  | 13.82  | 0           | --    | --                | 0.0276        | 13.85           | 13.176      | 13.85               | 13.176      |        |             |
| Clay Boswell #3         | 1187               | 350           | F1WE              |                                 |                    |           |                        |                     |       |  | 36.24  | 0.3502      | 2.878 | 0.0727            | 0.0027        | 35.55           | 14.492      | 35.55               | 14.492      |        |             |
| Clay Boswell #4         | 1187               | 500           | F1WE              | 1.350                           | 3.120              | 4.290     | 2.161                  | 4.740               | 0.25  | 19.96                                    | 2.944  | 0.840       | 44.11 | 3.601             | 4.026         | 0.1015          | 0.0054      | 52.04               | 14.852      | 54.99  | 15.692      |
| Sherburne County #1-2   | 906                | 1420          | F1WE              |                                 |                    |           |                        |                     |       |  | 124.0  | 13.09       | 10.17 | 0.3074            | 0.0141        | 149.5           | 15.028      | 149.5               | 15.028      |        |             |
| Sherburne County #3-4   | 906                | 1600          | F1WE              | 7.400                           | 13.7               | 0.880     | 20.20                  | 0.80                | 65.28 | 9.629                                    | 0.859  | 139.7       | 14.79 | 13.72             | 0.3464        | 0.0159          | 168.6       | 15.032              | 178.2       | 15.891 |             |
| Monticello              | 906                | 568.8         | R2CE              |                                 |                    |           |                        |                     |       |  | 51.19  | 0           |       |                   | 0.0051        | 56.63           | 14.208      | 56.63               | 14.208      |        |             |
| Lik River #1-3          | 891                | 49.95         | F2OE              |                                 |                    |           |                        |                     |       |  | 4.403  | 0           |       |                   | 0.0030        | 4.606           | 13.159      | 4.606               | 13.159      |        |             |
| Riverside #8            | 651.7              | 239.36        | F2OE              |                                 |                    |           |                        |                     |       |  | 22.06  | 0           |       |                   | 0.0883        | 22.15           | 13.203      | 22.15               | 13.203      |        |             |
| High Bridge #5-6        | 641.7              | 277.64        | F2OE              |                                 |                    |           |                        |                     |       |  | 25.59  | 0           |       |                   | 0.0579        | 25.64           | 13.186      | 25.64               | 13.186      |        |             |
| Prairie Island #1-2     | 764.8              | 1123.10       | R2CE              |                                 |                    |           |                        |                     |       |  | 100.6  | 11.89       | 8.714 | 0.2201            | 0.0162        | 121.5           | 15.436      | 121.5               | 15.436      |        |             |
| Aima #1-5               | 752.1              | 209.9         | F2OF              |                                 |                    |           |                        |                     |       |  | 19.34  | 0           |       |                   | 0.0037        | 19.35           | 13.153      | 19.35               | 13.153      |        |             |
| Aima #6                 | 752.1              | 350           | F1OF              |                                 |                    |           |                        |                     |       |  | 16.24  | 0           |       |                   | 0.0742        | 32.32           | 13.175      | 32.99               | 13.451      |        |             |
| Genoa #1A-4D.1          | 752.1              | 363.5         | F2CE              |                                 |                    | 1.672     | 0                      |                     | 4.585 | 0.676                                    | 31.41  | 0           |       |                   | 0.0634        | 33.47           | 13.175      | 33.47               | 13.175      |        |             |
| Genoa #2                | 752.1              | 50            | N2GE              |                                 |                    |           |                        |                     |       |  | 4.613  | 0           |       |                   | 0.0087        | 4.621           | 13.189      | 4.621               | 13.189      |        |             |
| Genoa #3                | 752.1              | 62.8          | F4L               |                                 |                    |           |                        |                     |       |  | 5.707  | 0           |       |                   | 0.2626        | 5.814           | 13.232      | 5.814               | 13.210      |        |             |
| Labadie #4              | 677                | 255           | F1W               |                                 |                    |           |                        |                     |       |  | 21.49  | 0           |       |                   | 0.0559        | 23.55           | 13.176      | 23.55               | 13.176      |        |             |
| Stoneman #1-2           | 677                | 51.75         | F2GE              |                                 |                    |           |                        |                     |       |  | 4.769  | 0           |       |                   | 0.0030        | 4.773           | 13.160      | 4.773               | 13.160      |        |             |
| Neilon Dewey            | 625                | 227           | F2OE              |                                 |                    |           |                        |                     |       |  | 26.94  | 0           |       |                   | 0.0691        | 21.01           | 13.205      | 21.01               | 13.205      |        |             |
| Dubaque #2-4            | 580                | 80            | F2OL              |                                 |                    |           |                        |                     |       |  | 7.373  | 0           |       |                   | 0.0282        | 7.401           | 13.2        | 7.401               | 13.2        |        |             |
| Carroll County #1       | 537                | 1100          | F1OF              |                                 |                    | 10.00     | 4.934                  | 190.6               |       | 111.6                                    | 31.24  | 4.052       | 102.0 | 0                 | 0.1786        | 102.2           | 13.259      | 133.5               | 17.311      |        |             |
| M.L. Kapp #1-2          | 516                | 236.5         | F2OE              |                                 |                    |           |                        |                     |       |  | 11.98  | 0           |       |                   | 0.0501        | 22.03           | 13.18       | 22.03               | 13.18       |        |             |
| Quad-Cities             | 502                | 1600          | N2GE              |                                 |                    |           |                        |                     |       |  | 0.786  | 0           |       |                   | 0.0043        | 196.0           | 17.479      | 196.0               | 17.479      |        |             |
| Moline #7-7             | 463                | 73.64         | F2OE              |                                 |                    |           |                        |                     |       |  | 20.60  | 0           |       |                   | 0.0363        | 6.791           | 13.139      | 6.790               | 13.139      |        |             |
| Riverside #3, 3HS, 4, 5 | 463                | 233.50        | F2GL              |                                 |                    |           |                        |                     |       |  | 5.990  | 0           |       |                   | 0.0192        | 20.64           | 13.173      | 20.64               | 13.173      |        |             |
| Fair #1-4               | 463                | 65            | F2GE              |                                 |                    |           |                        |                     |       |  | 11.39  | 0           |       |                   | 0.0287        | 11.42           | 13.183      | 11.42               | 13.183      |        |             |
| Muscataine #5-8         | 457.1              | 123.6         | F1GE              |                                 |                    |           |                        |                     |       |  | 13.82  | 0           |       |                   | 0.0178        | 13.84           | 13.162      | 14.16               | 13.410      |        |             |
| Muscataine #9           | 457.1              | 150           | F1OF              |                                 |                    | 1.120     | 0.640                  |                     |       | 1.772                                    | 0.2613 | 3.2490      | 57.13 | 5.329             | 5.276         | 0.1333          | 0.0069      | 67.87               | 14.900      | 71.66  | 15.776      |
| Louisa #1               | 457.2              | 650           | F1W               | 1.700                           | 5.470              | 2.800     | 7.587                  | 0.325               | 27.05 | 13.990                                   | 19.54  | 0           |       |                   | 0.2386        | 32.57           | 13.172      | 32.57               | 13.172      |        |             |
| Burlington              | 404                | 210           | F1W               |                                 |                    |           |                        |                     |       |  | 19.54  | 0           |       |                   |               |                 |             |                     |             |        |             |

<sup>a</sup> First quantity indicates fuel type, F = Fossil, N = Nuclear; the second refers to assumed turbine type, Type 1 or Type 2; the third quantity denotes the type of cooling system, C = Once-through, W = Mechanical draft wet tower, D = Combined Once-through/Wet tower, D = Combined Once-through/Wet tower; the last quantity indicates whether the plant is existing (E) or proposed (P).

<sup>b</sup> Includes cooling system operation cost for the once-through cooling tank.

<sup>c</sup> Estimate based on equivalent wet tower operation.

TABLE IV

COST REDUCTIONS OF FREE-DISCHARGE THERMAL STANDARD (1976 dollars)

| Plant & Unit No.      | Capital Costs                   |             | Operating Costs                 |             | Total Cost Reduction      |             |
|-----------------------|---------------------------------|-------------|---------------------------------|-------------|---------------------------|-------------|
|                       | Total Annual 10 <sup>6</sup> \$ | mills/kw-hr | Total Annual 10 <sup>6</sup> \$ | mills/kw-hr | Annual 10 <sup>6</sup> \$ | mills/kw-hr |
| Clay Boswell #3       |                                 |             | 3.287                           | 3.127       | 3.287                     | 3.127       |
| Clay Boswell #4       | 1.681                           | 0.480       | 5.907                           | 1.686       | 7.588                     | 2.166       |
| Sherburne County #1-2 |                                 |             | 18.51                           | 1.860       | 18.51                     | 1.860       |
| Sherburne County #3-4 | 6.847                           | 0.611       | 20.90                           | 1.864       | 27.74                     | 2.475       |
| Monticello            |                                 |             | 4.077                           | 1.023       | 4.077                     | 1.023       |
| Prairie Island        |                                 |             | 17.70                           | 2.248       | 17.70                     | 2.248       |
| Quad-Cities           |                                 |             | 18.41                           | 1.642       | 18.41                     | 1.642       |
| Carroll County #1     | 29.02                           | 3.765       |                                 |             | 29.02                     | 3.765       |
| Louisa #1             | 2.857                           | 0.627       | 7.893                           | 1.733       | 10.75                     | 2.360       |

TABLE V

ZERO-DISCHARGE COST INCREASES ABOVE COSTS OF EXISTING THERMAL STANDARDS (1976 dollars)

| Plant & Unit No.     | Capital Costs                   |             | Operating Costs                 |             | Total Cost Increase       |             |
|----------------------|---------------------------------|-------------|---------------------------------|-------------|---------------------------|-------------|
|                      | Total Annual 10 <sup>6</sup> \$ | mills/kw-hr | Total Annual 10 <sup>6</sup> \$ | mills/kw-hr | Annual 10 <sup>6</sup> \$ | mills/kw-hr |
| Clay Boswell #1-2    | 2.060                           | 1.961       | 2.160                           | 2.054       | 4.221                     | 4.015       |
| Monticello           |                                 |             | 17.938                          | 4.500       | 17.94                     | 4.500       |
| Elk River #1-3       | 0.7935                          | 2.267       | 0.6743                          | 1.926       | 1.468                     | 4.193       |
| Riverside #8         | 7.032                           | 4.192       | 4.582                           | 2.731       | 11.61                     | 6.923       |
| High Bridge #5-6     | 7.002                           | 3.600       | 4.644                           | 2.387       | 11.65                     | 5.987       |
| Prairie Island #1-2  |                                 |             | 5.153                           | 0.655       | 5.153                     | 0.655       |
| Alma #1-6            | 9.693                           | 3.008       | 8.600                           | 2.668       | 18.29                     | 5.676       |
| Genoa #1A-2D,2,3     | 6.808                           | 2.335       | 6.453                           | 2.232       | 13.26                     | 4.568       |
| Lansing #1-4         | 5.424                           | 2.435       | 4.846                           | 2.176       | 10.27                     | 4.611       |
| Stoneman             | 0.7727                          | 2.131       | 0.7985                          | 2.202       | 1.571                     | 4.333       |
| Nelson Dewey         | 6.489                           | 4.079       | 4.214                           | 2.649       | 10.70                     | 6.728       |
| Dubuque #2-4         | 1.304                           | 2.326       | 1.124                           | 2.004       | 2.428                     | 4.330       |
| Carroll County #1    | 6.398                           | 0.830       | 16.01                           | 2.077       | 22.41                     | 2.907       |
| M.L. Kapp #1-2       | 6.023                           | 3.604       | 4.107                           | 2.457       | 10.13                     | 6.061       |
| Moline #5-7          | 1.254                           | 2.430       | 1.185                           | 2.295       | 2.439                     | 4.725       |
| Riverside #3,3HS,4,5 | 3.901                           | 2.490       | 3.584                           | 2.288       | 7.485                     | 4.778       |
| Fair #1-2            | 1.126                           | 2.473       | 1.064                           | 2.336       | 2.190                     | 4.809       |
| Muscatine #5-9       | 4.937                           | 2.515       | 4.640                           | 2.420       | 9.576                     | 4.995       |
| Burlington           | 8.726                           | 5.873       | 5.368                           | 3.613       | 14.09                     | 9.486       |

TABLE VI

REGIONAL COST COMPARISONS OF DIFFERENT THERMAL STANDARDS

| Thermal Standard | Total Costs               |             | Incremental "Cost" of Standard above Free-Discharge |             |
|------------------|---------------------------|-------------|---|-------------|
|                  | Annual 10 <sup>6</sup> \$ | mills/kw-hr | Annual 10 <sup>6</sup> \$                           | mills/kw-hr |
| Free-Discharge   | 1180.3                    | 13.622      | ---   | ---         |
| Existing         | 1317.4                    | 15.204      | 118.7   | 1.582       |
| No-Discharge     | 1494.3                    | 17.246      | 295.6   | 3.623       |

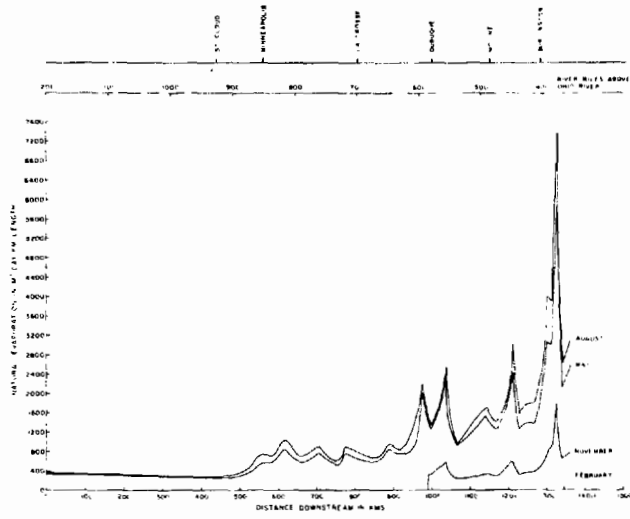


Figure 1 Natural Evaporation Along the Upper Mississippi River

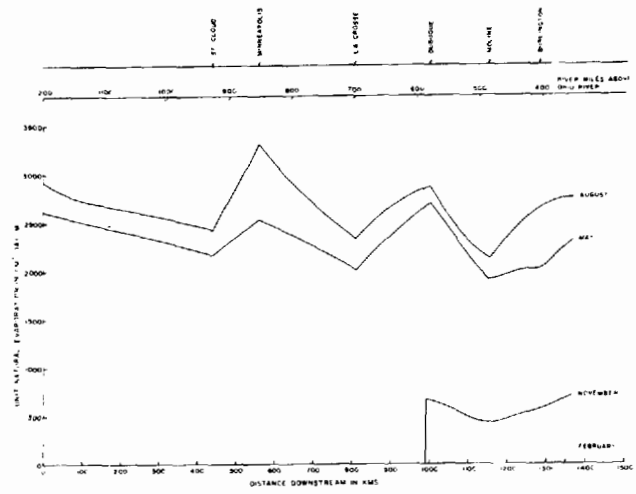


Figure 2 Unit Natural Evaporation Along the Upper Mississippi River

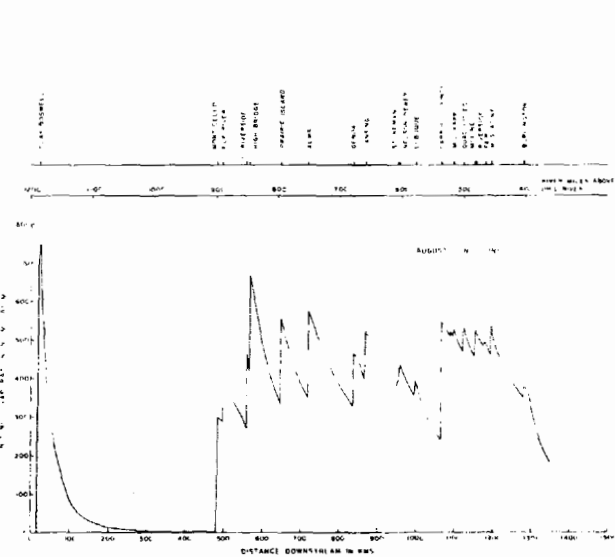


Figure 3 Unit Net Evaporation for August Along the Upper Mississippi River

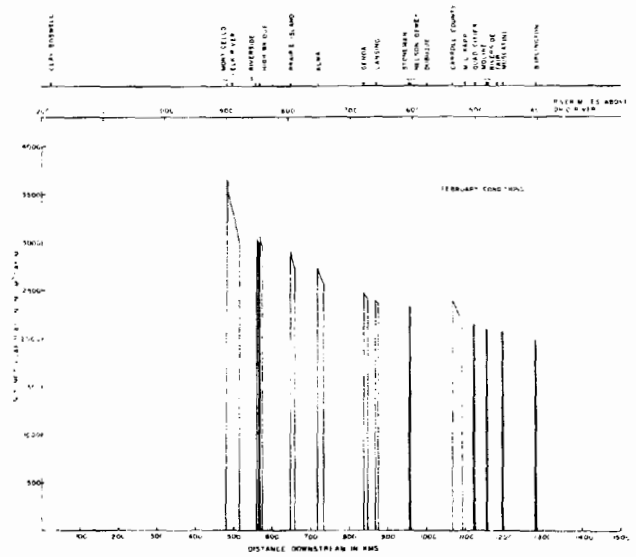


Figure 4 Unit Net Evaporation for February Along the Upper Mississippi River

## THERMAL PLUME MAPPING

J.R. Jackson and A.P. Verma  
Envirosphere Company, Division of Ebasco Services Incorporated  
Atlanta, Ga. and New York, N.Y., U.S.A.

### ABSTRACT

An accurate description of thermal plume characteristics is fundamental to the evaluation of plant performance as it relates to technical specifications and state imposed mixing zone criteria. This paper presents a generalized approach for mapping thermal plumes with considerations given to discharges in different types of receiving water bodies, variability of ambient conditions, and other parameters which must be measured. Rivers, lakes, estuaries and oceans all present widely varying conditions for which several alternative methods of sampling and positioning are available. Also, any single receiving water body type can be sampled in several ways due to the wide variety that exists in instrumentation and data logging equipment.

The basic elements of a thermal plume survey can be grouped in three phases. These phases consist of (1) logistics and planning, (2) execution, and (3) data reduction and evaluation. The criticality and interrelationship between them are highlighted.

### INTRODUCTION

Before the planning phase of any survey can begin, it is necessary to carefully examine the client's needs with respect to not only the means and extent of data acquisition but also the uses to which the data will ultimately be applied. Quite often the client is not fully aware of his own needs in terms of the level of effort required to insure the adequacy of the data and the degree of scrutiny to which the results will be subjected. There will also be cases in which the client will only supply a general requirement, leaving the responsibility of detailed planning to the surveyor. In any event, it is imperative, when one's client must ultimately deal with the federal and state regulatory process, that the mediocre or "cost effective" survey does not become adequate after the fact.

The most critical piece of information needed but not always asked for by the client is a precise definition of the end product of the survey effort. For the purpose of this paper, we shall define this initially in terms of a set of maps or map overlays which show the following data:

- Isotherms, in terms of temperature or temperature variation ( T) over ambient and/or contours of other simultaneously measured data such as dissolved oxygen or dye concentration,
- Wind and current vectors,
- Ambient (if definable), intake, discharge and air temperatures,
- Calculated area within critical isotherms (where required),
- Tide or stage level data,
- Time, date and depth(s) of the survey(s).

Certain basic items must also appear on the maps or in the title block including:

- Shoreline and discharge structure outlines (unnecessary on an overlay),
- Scale and north arrow,
- Grid reference points and an explanation of the coordinate system.

Other pieces of information which might be included or discussed separately in an accompanying report are:

- Positioning system reference station locations or control points,
- In situ meter and vertical profile station locations,
- Plant operational data for the time of the survey,
- Vertical profile data and/or receiving water body temperature cross-sections,
- Plant structure outline,
- Bathymetry,
- Drogue plots,
- A discussion of field and analytical methodology,
- Any subsequent analytical results,
- An evaluation of discharge performance with respect to mathematical models and/or thermal water quality criteria,

Discussions with the client prior to detailed planning of the survey should include not only the appearance and content of the finished maps, but also and of even greater importance the adequacy of the information being presented. Considerations such as sample density and data redundancy must be dealt with and agreed upon, primarily due to their obvious impact upon the survey cost, before detailed planning can begin.

#### OPERATIONAL ELEMENTS

The basic elements of a thermal plume survey can be grouped in three phases. The first and most critical phase consists of logistics and planning. The success and credibility of the survey will directly depend upon adequate preparation in terms of equipment and supplies, timing and coordination with respect to ambient conditions and plant operating schedules, as well as pre-plotting of tracklines and profile locations, arranging for accurately surveyed horizontal control and, if necessary, site reconnaissance. The need for redundancy in data collection for certain parameters is also an important planning consideration, particularly when operational constraints are imposed by economic factors.

With a reasonable effort during the planning phase, the next phase, execution of the actual survey, becomes reasonably straightforward with the exception of unavoidable scheduling difficulties which often arise as a result of weather or changes in plant operation. With the more sophisticated equipment now available, much of the data reduction and evaluation, the third and final phase of the survey, can be accomplished in the field. This is not always economically feasible, however, when surveys are of limited duration and scope.

## DATA REQUIREMENTS AND PLANNING

### Preliminary Background Investigation

The complete thermal survey should include the definition of effects of natural and man-made variability of environmental conditions on plume characteristics. Consequently, thermal mapping is not confined to the measurement and mapping of temperature alone. Other important parameters include ambient current, tides, water mass distribution, bathymetry, wind conditions for heat transfer considerations and accurate locations for the discharge and any other structure or naturally occurring object which may affect the plume's shape. Additional considerations include horizontal and vertical ambient temperature fluctuations, variations in plant heat output, interference from other heat sources, extrapolation between normal and extreme thermal conditions and definition of ambient conditions with respect to regulatory agency requirements. Many of these parameters can be anticipated and evaluated for their relative importance prior to the field work. The most immediate source of site specific information is the plant operator who may be able to make available the results of previous or ongoing data collection programs. Available parameters might include intake and discharge temperatures, stage or tide, and meteorological conditions. In addition, the operator should provide horizontal control (plant or state grid) information, charts or plans of the plant and discharge areas, any hydrological information obtained through studies conducted during pre-operational phases, a plant operating schedule as it effects the operation of the circulating water system and/or blowdown flow, the heat rejection rate, thermal criteria and technical specifications to which the effluent is subject and an understanding of any local political sensitivities which might affect the way survey operations are to be conducted. Other potential sources of information include but are not necessarily restricted to:

- U.S. Geological Survey,
- Corps of Engineers,
- National Oceanic and Atmospheric Administration,
- State and local agencies including water management and irrigation boards,
- Privately-owned reservoir managements,
- Universities and private research institutions.

Adequate attention given to background data collection will make possible a proper definition of the scope and duration of the study and the conditions leading to the definition of critical situations.

### Logistics and Support Arrangements

Most problems connected with field programs can be prevented or alleviated by applying anticipation, communication, and money. Furthermore, a weakness in any one factor, usually the latter, will proportionately increase a need for the others. The following is, therefore, an attempt to anticipate at least the basic field planning steps necessary in advance of survey execution. While some may seem obvious, they are listed for the sake of completeness. In that any two surveys may have as many differences as similarities, greater detail in the area of general arrangements is beyond the scope of this paper.

- Survey Boat selection:

While the selection and layout of the boat to be used is often a matter of institutional or personal preference (not always that of the surveyor), a few basic points should be mentioned. The size of the vessel should be large enough to provide adequate protection as well as mounting and working space for the instrumentation. In addition, space should be available for working over the side along with, if possible, some light lifting capability in the form of a davit for lowering and raising line depressors or profiling instruments. The boat should also be small enough to have a high degree of maneuverability for work in and around the plume but not so small as to make it overly sensitive to weather and sea conditions. The draft should be shallow and wake small to minimize surface water (plume) displacement and, of course, appropriate safety and emergency equipment, including extra protection for the instruments, should be on board at all times. If diving is involved with, for example, the placement of in situ recorders or inspection of the discharge structure, facilities should be provided according to Occupational Health and Safety Administration Requirements as set forth in the Federal Register, July 22, 1977. Finally, berthing, launching, fueling and insurance should also be prearranged.

- Preparation, shipping and calibration of equipment:

A thermal survey can involve a wide variety of types of instrumentation including in situ and onboard monitoring devices, vertical profiling and towed sensors, electronic positioning systems and a variety of recording equipment (strip chart, magnetic tape, film and x-y plot). Additional support equipment might consist of communications and navigation equipment, diving and mooring gear plus testing and calibration instruments. Since each individual piece of equipment may have its own distinct preparatory requirements, only general rules

can be stated to cover this phase of the effort. Most importantly, any and all setup, maintenance and calibration procedures and logs should be pre-defined, recoverable and meticulously documented, even in those areas where the client has not imposed specific quality assurance guidelines. Where possible, pre-operational checks and calibrations should be performed after shipping and as close as possible to the time of deployment. While these procedures are best left to the responsible technician, it is imperative that the principal investigator be familiar with and able to defend the selection and preparation of the equipment should questions arise, as they often do, concerning the credibility of his or her methods and data. One more consideration in the preparation of equipment is, simply, how much to use. Whenever possible backup equipment for onboard systems should be available along with redundant data collection by in situ instruments. This must of course, be weighed against limitations of time, space and budget. Finally, a common mistake in the shipping of equipment is inadequate insurance coverage. The automatic coverage generally provided by airlines and other carriers is minimal. While additional coverage is often expensive, the high replacement costs of much of the equipment involved generally justifies the expense.

- Local support and purchase arrangements:

In addition to the arrangement for plant data which is concurrent with the many operations, several mundane but ever-present problems must be addressed. These include lodging, security for the boat, positioning equipment and in situ instruments, local availability of moving materials, marine supplies and rental equipment and land access permission, if necessary, for the location of shore stations. Finally, arrangements must be made for land surveyors to establish the positioning system reference points.

## POSITIONING ALTERNATIVES AND REQUIREMENTS

Several methods exist for the determination of a moving boat's position while crossing and recording the temperature distribution of the thermal plume. The selection of any one necessitates the weighing of the need for accuracy and data density against cost and level of sophistication of equipment and personnel. It is not always less expensive to resort to the simpler visual (versus electronic) positioning methods when one considers the often greater time requirements for setup and data reduction and the extended use of land survey parties. These methods might include:

- Shore based surveyors (two or more with radio communication) continuously turning angles on the boat's position as it moves and recording fix locations which must be later calculated individually,
- Recording horizontal angles between shore landmarks (at least three) from the boat for each fix location,

- Steering along predetermined and surveyor fixed transects by means of buoys or aligned range stakes on the shore.

All of these methods share the disadvantages discussed above. Electronic positioning, however, provides the capability of instantaneous position determinations as little as one-half second apart which, when coordinated with continuously measuring temperature or other sensors, can provide enormous amounts of information over large areas not necessarily constrained by visibility limitation. Unfortunately, this costly piece of equipment cannot be utilized to its fullest potential without a reasonably sophisticated digitizing and recording system which is capable of assimilating all of the parameters being measured, properly sequencing and tagging them with times, and recording them in analog or preferably digital format which can be later recovered by a computer and in hand copy. At this point one must also consider the use of an onboard processor which, in addition to its ability to key, organize and feed the data to a tape recorder, can also instantaneously process incoming position information, converting it to a simultaneous track plot by which the boat operator can steer. This enables the surveyor to preplot the survey tracklines and simply over-print these lines on an x-y plotter during the actual survey. The obvious advantages are the completeness of coverage made possible by close, regularly spaced tracklines without overlap, repeatability and increased ease of survey operation. Likewise, data reduction time can be greatly reduced as a result of the system's computer compatibility. There are several further variations and refinements to this system but all produce the same end result.

#### SURVEY TIMING AND AMBIENT CONDITION VARIABILITY

The inherent differences between rivers, lakes, estuaries and oceans with their varying levels of complexity determine the timing of a thermal survey and the number of surveys required to sufficiently define the plume. In general, the timing should reflect the periodic fluctuations of plume characteristics, from seasonal to tidal, in terms of conditions surrounding the critical case(s). Aperiodically changing conditions such as storm effects are more difficult by far to plan around and can only be marginally predicted on a seasonal basis.

Some of the more important variables to consider include:

- Periodic and aperiodic changes in direction of flow,
- Velocity, magnitude of flow and dispersive characteristics,
- Degree of natural stratification,
- Presence of vertical water mass boundaries,
- Potential heat accumulation or ponding areas which occur only under certain conditions,
- Conditions of maximum thermal impact,
- Occurrences of heat input from sources other than the plant,
- Relative location of ecologically sensitive areas,

- Minimum levels of wave action and atmospheric heat transfer,
- Worst case basin configuration in the receiving water body,
- Plant operating conditions producing maximum temperature elevation.

#### FINAL CONSIDERATIONS

Once on board the survey boat, it is generally too late to significantly modify the program to account for oversights. However, there are certain questions that can be raised during initial survey activities which may expedite a successful completion.

- Are the instrument preparations and calibrations complete and traceable?
- Are in situ instruments and profiling stations adequate in terms of location and density to properly define the system?
- Have variations in plant output been accounted for?
- Is there sufficient definition of the wind and air temperature conditions over the actual plume?
- Is there interference from other heat sources present and, if so, can it be discriminated from the plume under study?
- If the discharge is subsurface, has it been accurately located in terms of the survey positioning system?
- Is a detailed bathymetric survey available or necessary?
- Is the minimum temperature elevation to be measured within the range of horizontal ambient temperature variability?
- Are the depth settings of the temperature sensors such that they will skip in and out of a thin surface plume layer?
- Is the deepest sensor consistently below the far-field plume or are vertical temperature profiles along the longitudinal plume axis necessary?
- Can the boil area location and migration from a subsurface discharge be accurately determined?
- Have the short term periodic ambient temperature fluctuations been adequately defined?
- What are the thermal characteristics relative to both the normal and extremes and can they be extrapolated with respect to ambient conditions and plant output?

# THERMAL SURVEYS NEW HAVEN HARBOR

SUMMER AND FALL, 1976

W. Owen

College of Marine Science, University of Delaware  
Lewes, Delaware, U.S.A.

J. Monk

Normandeau Associates, Inc.  
Bedford, New Hampshire U.S.A.

## ABSTRACT

Thermal surveys conducted in New Haven Harbor, Connecticut during July, August and October 1976 were designed to define the thermal plume of the New Haven Harbor Station as required by the National Pollution Discharge Elimination System (NPDES) Permit to Discharge. Since New Haven Harbor has a complex temperature structure due to both natural and man-made sources of heat, Rhodamine WT dye was used in conjunction with a three dimensional temperature sampling program to distinguish the thermal load introduced by the New Haven Harbor Station from other natural and man-made thermal influences. The results of a dye and thermal study conducted in October were used to interpret the data from the July and August thermal surveys. This report includes a presentation and analysis of the assumptions upon which the dye study design, calculations and projections were made.

## INTRODUCTION

Dyes and more specifically Rhodamine dye have been successful as tracers in studies of transport, dispersal and dilution patterns of solids or liquids subjected to the naturally occurring forces of a water system. Since 1960 this technique has been adapted to profiling the movement of effluent discharges in receiving waters. In the present study the dye was used as a tracer of heat input to New Haven Harbor resulting from operation of the New Haven Harbor Station, a 460 MW oil fired power plant.

Given the temperature increase across the condensers ( $\Delta t$ ) and the cooling water flow, dye concentration can be related to temperature and it is possible to calculate  $\Delta t^1$  per part per billion of measured dye concentration. Dye concentration was measured in the field using standard, continuous sampling fluorometric techniques in conjunction with temperature measurements. The dye distribution was converted to a

---

<sup>1</sup> $\Delta t$  is used here to describe the elevated temperature due to the cooling water discharge from the New Haven Station only.  $\Delta t$  is a function of position and time.

temperature distribution indicating the  $\Delta t$  independent of other thermal sources. This method is based on the assumption that the temporal and spatial distribution of dye and temperature will be the same. For this assumption to hold, the following conditions must be met: (1) the density of the receiving water must not be affected by the tracer material, (2) the power plant must be operating under normal conditions to ensure a representative density difference between the thermal discharge and the receiving water, and (3) the dilution of the thermal discharge water must occur rapidly enough to ensure that the effects of cooling to the atmosphere can be neglected.

The first condition (1) was satisfied by the method of discharge of dye. The proof of the validity of conditions (2) and (3) lies in the base temperature computations which serve as a check on the correspondence of dye and temperature. Base temperature is defined as the temperature the water would have been if it were thermally unaffected by the New Haven Harbor Station but still affected by natural thermal sources and man-made sources of heat other than the power plant in question. The base temperatures were determined by subtracting the  $\Delta t$  computed from dye concentration from the actual temperatures measured in the Harbor (If the dye concentration and the temperatures were not similarly distributed, the assumptions would be invalid to the extent that the base temperature was perturbed). Conditions (2) and (3) can only be checked by the base temperature's agreement with temperature distribution expected in the body of water in question at the time of the survey. If there was a region of anomalously low temperatures observed in the computed base temperature distribution, the implication is that the plant has not run long enough to create a quasi-steady state in temperature. Thus there was too much dye for the given temperature. The opposite effect would be caused by interruption in the impact of dye.

### Experimental Procedure

#### Instrumentation

Instrumentation and material used in the study included Turner Designs Model 10-000 full flow fluorometer and an NAI Model 3100-TD temperature profiling system (BT), and Rhodamine WT dye, 20% aqueous solution. The dye was injected into the plant cooling water just downstream of its intake. Other equipment and materials used were all standard off the shelf items commonly employed in this sort of work.

## Measurements at Cooling Water Intake

During the October dye study, water was pumped continuously from in front of the New Haven Harbor Station intake through the fluorometer set up in the pump house. A Rustrak 1332 temperature probe was in the line downstream of the fluorometer. Fluorescence and temperature were recorded on a 3 channel Rustrak recorder. This set up is shown in Figure 1.

## Shipboard Measurements

During the thermal surveys, vertical temperature profiles were obtained at a series of stations whose positions were established using a mini-ranger (August) or sextant as a pelorus (July). The stations were occupied at each critical phase of the tide on two successive days each month. While the vessel was on station, the BT submarine unit was lowered from the surface to the bottom using the hand winch; the vertical temperature profile was recorded on the x-y plotter set in its temperature-depth mode.

Shipboard measurements during the October dye/temperature surveys were of two types:

- a. Horizontal continuous sampling of surface dye concentration and temperature.
- b. Vertical profiles of dye concentration and temperature.

Both types of measurements were made during each of the four critical tide phases. The equipment set up for both types of measurement is shown in Figure 2. Water was pumped continuously through a hose to the deck where it passed through the shipboard fluorometer and a housing containing a Rustrak 1332 temperature probe. The hose was clamped to the submarine unit of the BT system, which was also used during shipboard measurements. Outputs from the fluorometer and the temperature probe were recorded on a Rustrak recorder. BT system output was recorded on a Houston Instruments x-y recorder. The purpose of the Rustrak temperature system was to correct the fluorometer. The purpose of the Rosemount temperature system was to provide an accurate temperature measurement of the water at the hose intake for the fluorometer.

To obtain continuous horizontal data, the research vessel traversed a series of pre-selected transects (Figure 3). Start, end and intermediate positions on all transects were established using the mini-ranger navigation system. While the vessel was underway, water was pumped through the instruments and data were recorded as described above. The x-y plotter was set in its time sweep mode so the BT system served as a continuous temperature monitor.

For the vertical profiles (Figure 3) the research vessel occupied a series of stations. The positions of these stations were established using the mini-ranger. While the vessel was on station, water was pumped through the instruments, fluorescence data were read from the fluorometer and recorded by hand and temperature was recorded on the x-y plotter. The plotter was set in its temperature-depth mode so that temperature was recorded on the y-axis and depth was recorded on the x-axis.

## RESULTS

### October Dye and Thermal Survey

Figures 4a through 11a are maps of surface  $\Delta t$  prepared from dye concentration measurements made on October 13, 14 and 15, 1976. Included are two sets of data obtained for each phase of the tide. The attendant maps of actual measured temperature are contained in Appendix B. In these and all other figures the caption block includes wind speed and direction and power generated by the station. Figures 4b through 11b, which accompany the  $\Delta t$  maps, indicate the respective surface base temperatures. The purpose of the base temperature determination is to assess the validity of the assumptions made in using the method and to look for problems which may have occurred during the survey. The computed base temperature distributions agreed well with what was expected. Generally they indicated the weak surface temperature gradients characteristic of autumn with the following exception: on October 14 the dye pump failed from 0452 to 0652 EST due to the destruction of the foam cushion around the motor. The base temperature for the ensuing low water slack measurements clearly showed a warm spot (insufficient dye). The  $\Delta t$  map for the corresponding tide was not used in this report. It was replaced by data from low water slack measurements made on October 15, 1976. This exception and the normal base temperatures determination previously discussed all serve as verification of the assumptions made above.

Figure 4 is the  $\Delta t$  map determined from field measurements during low water slack on October 13, 1976. The wind was from the southwest at 13 knots. The plume, as would be expected, was in the immediate vicinity of the discharge, but there was also evidence of warmer water on the west side of the harbor. Results of the second low water slack survey (October 15) are presented in Figure 5a. The wind (southwest, 14 knots) was nearly the same as during the earlier low water slack survey, but the plume was larger. This is due at least partially to the higher power output of the plant on October 15 (463 MWH, 3 hr average) compared to output on October 13 (446 MWH).

The  $\Delta t$  maps developed from flood tide surveys are shown in Figure 6a (October 13) and 7a (October 14). On October 13 the wind was 15 knots from the south-southwest, and, as such, it had a sizeable component in the same direction as the flood tide. Wind and tide combined to create the narrow, elongated plume seen streaming to the north in Figure 6a. On October 14, the wind was from the west-northwest at 19 knots. This opposed the flood tide and the resultant plume was smaller than it had been on the day before even though the average power output of the plant was higher (463 MWH on October 14 and 447 MWH on October 13). Also in Figure 7a there is a small patch of water on the west side of the harbor characterized by a  $\Delta t$  of 2F. This may be a remnant of the ebb tide plume which broke away from the main plume as a result of the turning tide and the vigorous wind.

The  $\Delta t$  distributions for high water slack are illustrated in Figure 8a (October 13) and 9a (October 14). On October 13 the wind during high water slack was nearly the same as it had been during the previous flood tide, and the elongated character of the plume was still evident, although it covered a smaller area. On October 14 the wind had diminished somewhat from mid ebb to high water slack when it was 14 knots from the west-northwest. The plume had broadened considerably compared to its shape during flood, and, because of the wind, it extended further south than the high water slack plume on the day before.

There was a substantial difference in the relative extents of the ebb-tide plume on October 13 and 14. On October 13 (Figure 10a) the plume swung far down stream despite the continued brisk wind from the south-southwest. In contrast, the ebb-tide plume on the next day (Figure 11a) was very small. The reason for the large difference was the sharp reduction in power on October 14, when the average plant output was only 288 MWH during the ebb-tide survey. Plant output during the ebb survey on October 13 was 420 MWH. If the plant had been operating at full power on October 14, the plume would have extended far downstream (i.e., like Figure 10a), and it would have been narrower than the October 13 ebb plume because of the 18 knot west wind that blew during the ebb survey on October 14.

It is clear that the position of the plume varied greatly. This variability resulted from two effects: the wind's direct effect on the harbor and the wind's effect on the ocean and Long Island Sound which in turn directly affect the tide in the harbor.

Figure 12 is an example of the cross-sectional  $\Delta t$  observations in the harbor. Higher subsurface temperatures were found only in the immediate vicinity of the discharge (Transect F). The lower temperature water of the plume did spread further but did not extend across the harbor. The percentages of the cross-sectional area affected by the plume are discussed below. The  $\Delta t$ 's in the cross sections were determined by the same method as was used for the surface maps.

### July Temperature Survey

During the July survey the power plant was slow to come on line each morning. On July 21, it was operating at about 31% power early in the day, and on July 22 it was operating at 60% power early in the day. These times correspond to high water slack surveys, which were conducted from 0540 to 0741 EST on July 21 and from 0640 to 0826 on July 22. For the remainder of each day the plant operated at between 80% and 83% power. Nevertheless, there was generally no readily recognizable plume on the surface and only slight indications of a subsurface plume.

Since there was no clearly defined plume, the techniques used for computing base temperatures in Section 3.1 cannot be applied here. Instead, base temperatures for the July survey were determined by analyzing the plant records of intake temperature, correcting them for recirculation effects and by examining the far-field temperatures measured while the plant was coming on line. These analyses disclosed surface base temperatures which generally were in the range of 69-70F and subsurface base temperatures which ranged between 67F and 69F. The results of the dye study suggested that with the power plant operating at 100% the highest maximum  $\Delta t$  was about 5F. A  $\Delta t$  of 5F would have produced a maximum surface temperature in the harbor of 75F during the July survey. The subsurface maximum would have been between 72F and 74F, except in the immediate vicinity of the discharge where it would probably be higher.

### August Temperature Survey

The power plant was not operating during the August survey; therefore the temperatures measured were base temperatures. To determine the nature of the plume that would have existed had New Haven Station been operating, results of the October dye study were applied to the August temperature data. The principal assumption was that if dye had been pumped during the August survey then the distribution of dye (and  $\Delta t$ ) in the harbor would have been the same as it was in October if the winds were the same. In reality, the winds were not the same, but the differences were taken into account in hindcasting the positions of the August plume at the various phases. No adjustments were made in the plume projections to allow for natural cooling of the discharge water during a given tidal phase, so actual areal extent of the plume would likely be smaller than that depicted.

### Recirculation Effects

Recirculation is defined here as the ratio of the dye concentration measured at the intake structure, well upstream of the dye injection point, to the dye concentration at the discharge (expressed as a percentage). Recirculation is a function of the tidal current and the wind; tidal current is the dominant factor. Figure 13 displays recirculation plotted against time on October 13, 14 and 15. The range of the recirculation was from 0 to 12.9% which is equivalent to a temperature range

of 0F to 1.9F. Because of the upstream location of the intake, recirculation is usually highest near the time of high tide. Variations in recirculation during the same tide phases on different days are primarily the result of wind effects.

## DISCUSSION

Characteristic maximum discharge plume surface temperatures observed or predicted during the three months included in the survey were as follows: July -- 75F; August -- 80F; October -- 64F. The maxima for the individual tide phases generally ranged no more than 1 or 2F from the average for each study. Table 1 lists the observed maximum surface temperature for each of the surveys. The maximum temperatures for the July survey are all 74-75F and were obtained by adding a  $\Delta t$  of 5F to an assumed maximum base temperature of 69-70F. Maxima for the August survey were determined by the superposition of the  $\Delta t$ 's calculated from the October dye study onto the August measurements; maximum predicted temperature was 82F during low water slack on August 25. Maximum temperatures for the October survey were determined by actual measurements; the maximum observed temperature of 65F occurred during high water slack on October 14.

Generally, the percentage of the surface area of the inner harbor subjected to a temperature rise of 1 to 4F was small. This is indicated in Table 2 which is a compilation of the percentage of the surface area of the inner harbor bounded by  $\Delta t$ 's of 1, 2, 3 and 4F. In each case the area bounded by a  $\Delta t$  of 4F was equal to or less than one tenth of one percent of the total inner harbor area. The areas bounded by  $\Delta t$ 's of 3F ranged from zero to 0.4% in October and from 0.1% to 0.5% in August. Much more area was bounded by the 2F  $\Delta t$  isotherm; the percentage affected ranged from less than 0.1% to 3% in October and from 0.5% to 5.5% in August. The percentage of the surface area bounded by a  $\Delta t$  of 1F ranged between 0.7% and 12.6% in October and between 2.7% and 11.2% in August.

In discussing the cross-sectional area affected by temperature rises of 1 to 4F, attention will be limited to Transect F. This transect corresponds to the position of the New Haven Harbor Station discharge; therefore, it shows far more subsurface plume effects than any other. Table 3 lists the percentage of cross-sectional area of Transect F bounded by  $\Delta t$ 's of 1, 1.5, 2, 3 and 4F at the various phases of the tide. The total cross-sectional area of the harbor at Transect F is, of course, a function of tide height, so average values were determined for each tide phase during both the October and August surveys. Specifically, this was done by drawing cross sections of the harbor at Transect F for each tide phase and determining the areas by planimetry. Predicted tides and tidal heights obtained from National Ocean survey tide tables are listed in Appendix D.

In October the percentage bounded by 4F was zero during four of the eight tide phases studied, and it ranged to a maximum of 2.9% during low water

slack on October 13. For August the range was between zero and 3.2%. The 3F  $\Delta t$  contour bounded up to 6.7% and 8.5% of Transect F in October and August, respectively. The extent of the 2F  $\Delta t$  contour was highly variable in October but somewhat less variable in August. The area bounded by the 2F isotherm ranged from 1.9% to 22.8% in October and from 10.4% to 20.6% in August. The areal extent of the 1F  $\Delta t$  was also quite variable in October, ranging from 7.4% to 40.2%. Again, August showed less variability; the range then was from 22.3% to 41.6%.

The percent of cross-sectional area bounded by the 1.5°F contour of  $\Delta t$  was also included in Table 3 as Connecticut water quality regulations use this temperature in defining a "mixing zone". The percentages of Transect F bounded by the 1.5F  $\Delta t$  ranged from 3% to 27.6% in October with an average of 17.4%. In August the range was from 15.8% to 30% with an average of 22.6%.

Generally, the data reported herein have shown surface and cross-sectional contours of  $\Delta t$  in which the 3F and 4F contours encompassed a relatively small area. Since power plant design specifies a  $\Delta t$  of about 3.75F where the discharge jet impinges on the surface (and near field is the immediate vicinity of the discharge jet), it is reasonable to represent the near field as the 3F and 4F contours of  $\Delta t$ . Therefore, the 1.5F  $\Delta t$  contour is included in the far field, and it will probably not be affected by any change in plant operation as long as the heat input to the harbor does not change.

#### LITERATURE CITED

- Fan, L.N. Numerical solutions of turbulent buoyant jet problems.  
W.M. Keck Laboratory of Water Resources and Hydraulics Report  
No. KH-R-15. California Institute of Technology. June 1967.
- Pritchard, D.W. and H.H. Carter, 1965. On the prediction of the  
distribution of excess temperature from a heated discharge in an  
estuary. Chesapeake Bay Institute. Technical Report No. ~~33~~ 33  
Res. 65-1. 45 p.

TABLE 1. MAXIMUM SURFACE TEMPERATURES. THERMAL SURVEYS NEW HAVEN HARBOR, SUMMER AND FALL, 1976.

| DATE                         | TIDE PHASE <sup>†</sup> | MAXIMUM SURFACE TEMPERATURE (F) |
|------------------------------|-------------------------|---------------------------------|
| July 21, 1976                | HWS                     | 74-75 <sup>Δ</sup>              |
|                              | ME                      |                                 |
|                              | LWS                     |                                 |
|                              | MF                      |                                 |
| July 22, 1976                | HWS                     | 74-75 <sup>Δ</sup>              |
|                              | ME                      |                                 |
|                              | LWS                     |                                 |
|                              | MF                      |                                 |
| August 24, 1976 <sup>*</sup> | MF                      | 78                              |
|                              | HWS                     | 80                              |
|                              | ME                      | 80                              |
|                              | LWS                     | 81                              |
| August 25, 1976 <sup>*</sup> | MF                      | 79                              |
|                              | HWS                     | 80                              |
|                              | ME                      | 81                              |
|                              | LWS                     | 82                              |
| October 13, 1976             | LWS                     | 63                              |
|                              | MF                      | 64                              |
|                              | HWS                     | 64                              |
|                              | ME                      | 64                              |
| October 14, 1976             | ME                      | 64                              |
|                              | MF                      | 64                              |
|                              | HWS                     | 65                              |
| October 15, 1976             | LWS                     | 63                              |

† HWS = High water slack  
 ME = Mid ebb  
 LWS = Low water slack  
 MF = Mid flood

\* Temperatures are estimated.

Δ See Section 4.2 for discussion.

TABLE 2. PERCENTAGE OF THE SURFACE AREA OF THE INNER HARBOR BOUNDED BY  $\Delta t$ 's of 4F OR LESS. THERMAL SURVEYS, NEW HAVEN HARBOR, SUMMER AND FALL, 1976.

| DATE     | TIDE PHASE | 4F   | 3F   | 2F   | 1F   |
|----------|------------|------|------|------|------|
| 8/24/76* | MF         | <0.1 | 0.1  | 0.8  | 2.8  |
|          | HWS        | <0.1 | 0.3  | 0.8  | 3.4  |
|          | ME         | <0.1 | 0.4  | 5.5  | 11.2 |
|          | LWS        | <0.1 | 0.3  | 0.7  | 4.7  |
| 8/25/76* | MF         | <0.1 | 0.2  | 1.1  | 4.7  |
|          | HWS        | <0.1 | 0.1  | 0.5  | 2.7  |
|          | ME         | 0.1  | 0.5  | 2.3  | 6.5  |
|          | LWS        | <0.1 | 0.2  | 0.8  | 5.4  |
| 10/13/76 | LWS        | 0.1  | 0.4  | 0.6  | 1.0  |
|          | MF         | 0.0  | <0.1 | 0.3  | 2.4  |
|          | HWS        | 0.0  | 0.0  | <0.1 | 2.2  |
|          | ME         | <0.1 | 0.4  | 3.0  | 12.6 |
| 10/14/76 | ME         | <0.1 | <0.1 | 0.2  | 0.7  |
|          | MF         | <0.1 | 0.1  | 1.0  | 1.2  |
|          | HWS        | <0.1 | 0.1  | 0.6  | 3.7  |
| 10/15/76 | LWS        | <0.1 | 0.1  | 0.5  | 10.1 |

\* Predictions based on dye study

TABLE 3. PERCENTAGES OF THE CROSS-SECTIONAL AREA OF TRANSECT F BOUNDED BY  $\Delta t$ 's OF 1F, 1.5F, 2F, 3F AND 4F. THERMAL SURVEYS, NEW HAVEN HARBOR, SUMMER AND FALL, 1976.

| DATE     | TIDE PHASE | 4F  | 3F  | 2F   | 1.5F | 1F   |
|----------|------------|-----|-----|------|------|------|
| 8/24/76  | MF         | 3.2 | 8.5 | 17.0 | 25.2 | 34.1 |
|          | HWS        | 2.8 | 8.5 | 20.6 | 30.0 | 41.6 |
|          | ME         | 0.0 | 2.4 | 12.8 | 22.2 | 35.8 |
|          | LWS        | 1.6 | 4.8 | 11.3 | 22.1 | 36.5 |
| 8/25/76  | MF         | 1.4 | 5.5 | 15.7 | 23.5 | 34.1 |
|          | HWS        | 2.1 | 5.6 | 12.4 | 19.7 | 28.8 |
|          | ME         | 2.1 | 5.6 | 10.4 | 15.8 | 22.3 |
|          | LWS        | 1.1 | 3.8 | 12.5 | 22.7 | 36.5 |
| 10/13/76 | LWS        | 2.9 | 6.7 | 17.4 | 20.8 | 24.4 |
|          | MF         | 0.0 | 0.5 | 1.9  | 3.0  | 15.1 |
|          | HWS        | 0.6 | 2.0 | 21.3 | 26.3 | 30.5 |
|          | ME         | 0.0 | 1.6 | 3.9  | 5.4  | 7.4  |
| 10/14/76 | ME         | 0.0 | 0.0 | 22.8 | 27.6 | 32.7 |
|          | MF         | 0.7 | 3.4 | 9.6  | 16.3 | 24.9 |
|          | HWS        | 1.1 | 5.9 | 11.7 | 14.9 | 20.3 |
| 10/15/76 | LWS        | 0.0 | 0.0 | 3.1  | 24.7 | 40.2 |

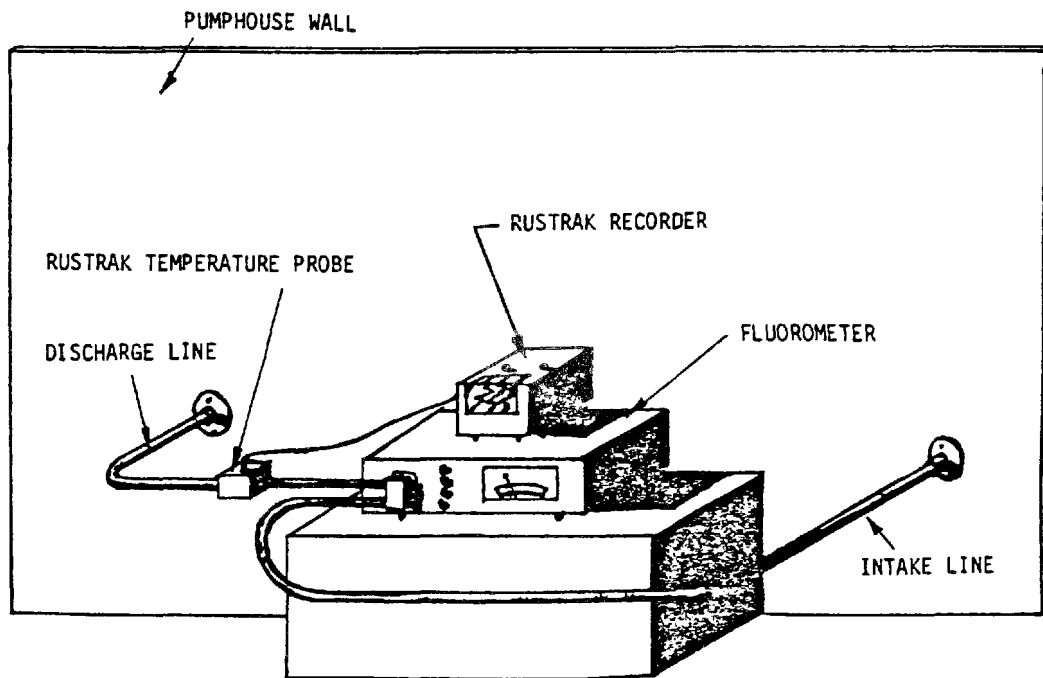


Figure 1. Illustration of instrumentation set up in intake pump house. Thermal Surveys, New Haven Harbor, Summer and Fall, 1976.

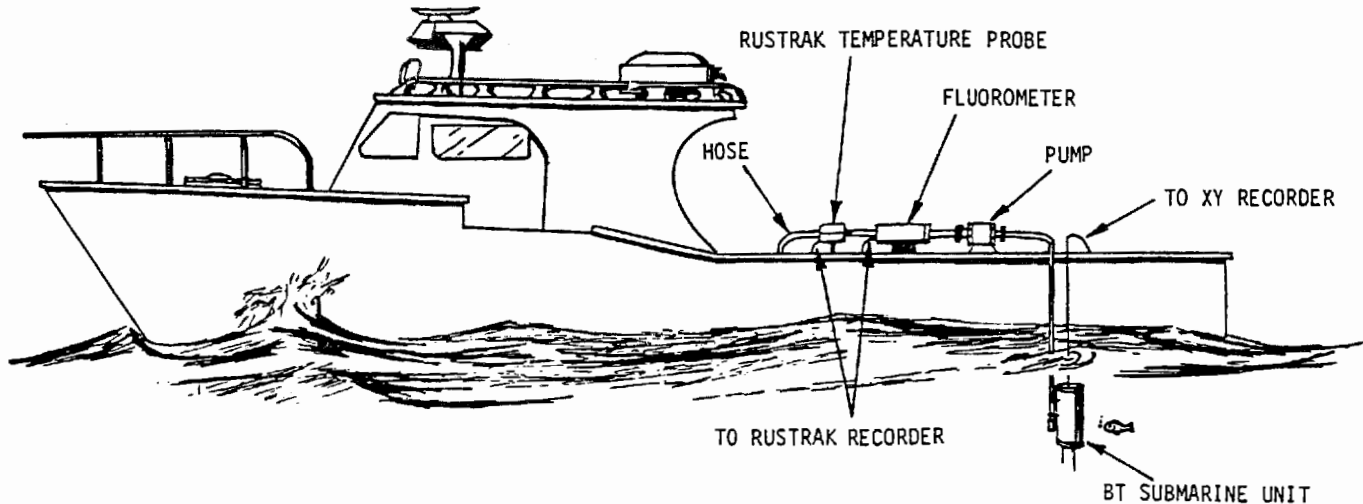


Figure 2. Illustration of instrumentation set up aboard the R/V Gale. Thermal Surveys, New Haven Harbor, Summer and Fall, 1976.

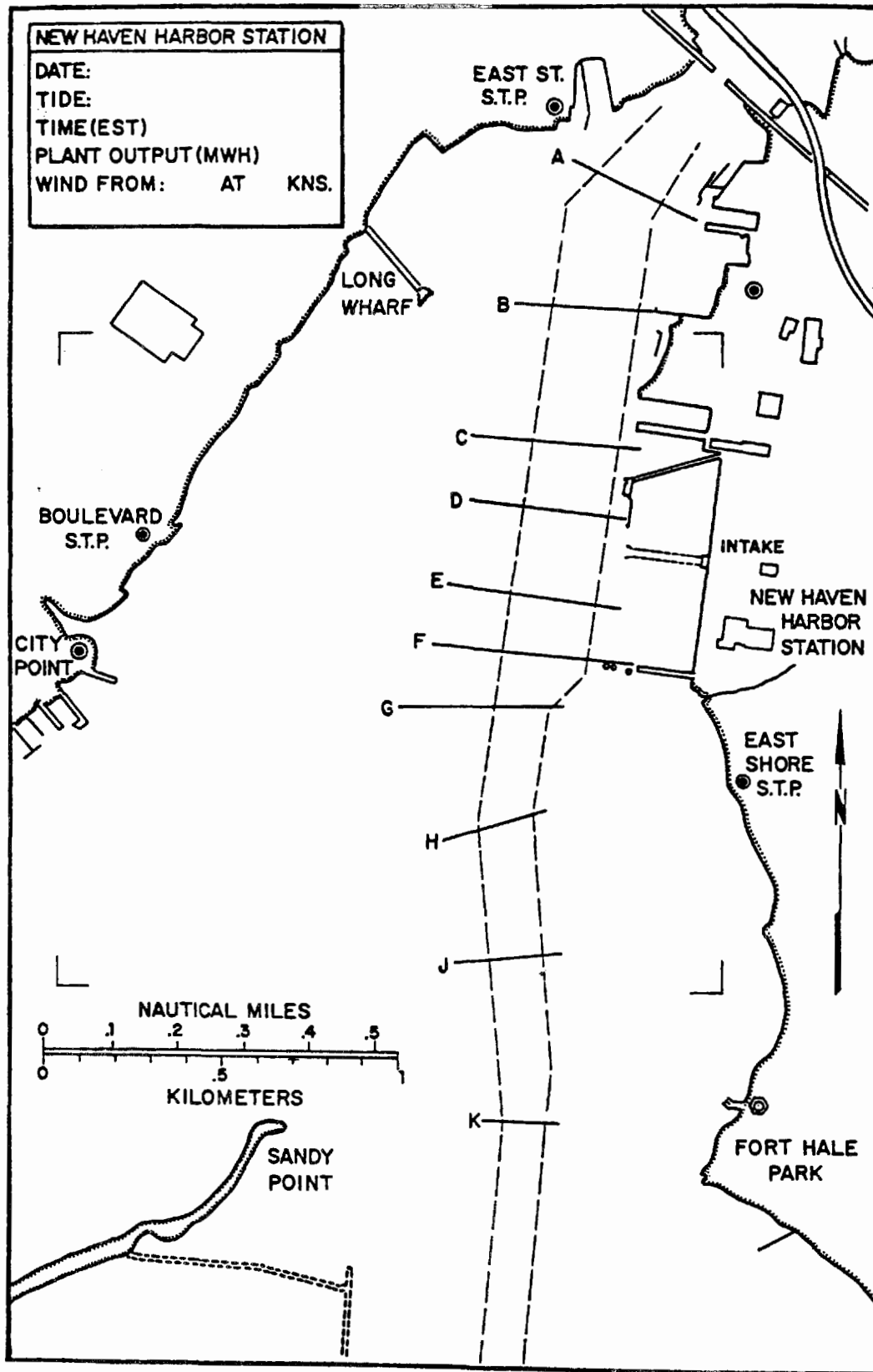


Figure 3. Transect locator map. Thermal Surveys, New Haven Harbor, Summer and Fall, 1976.

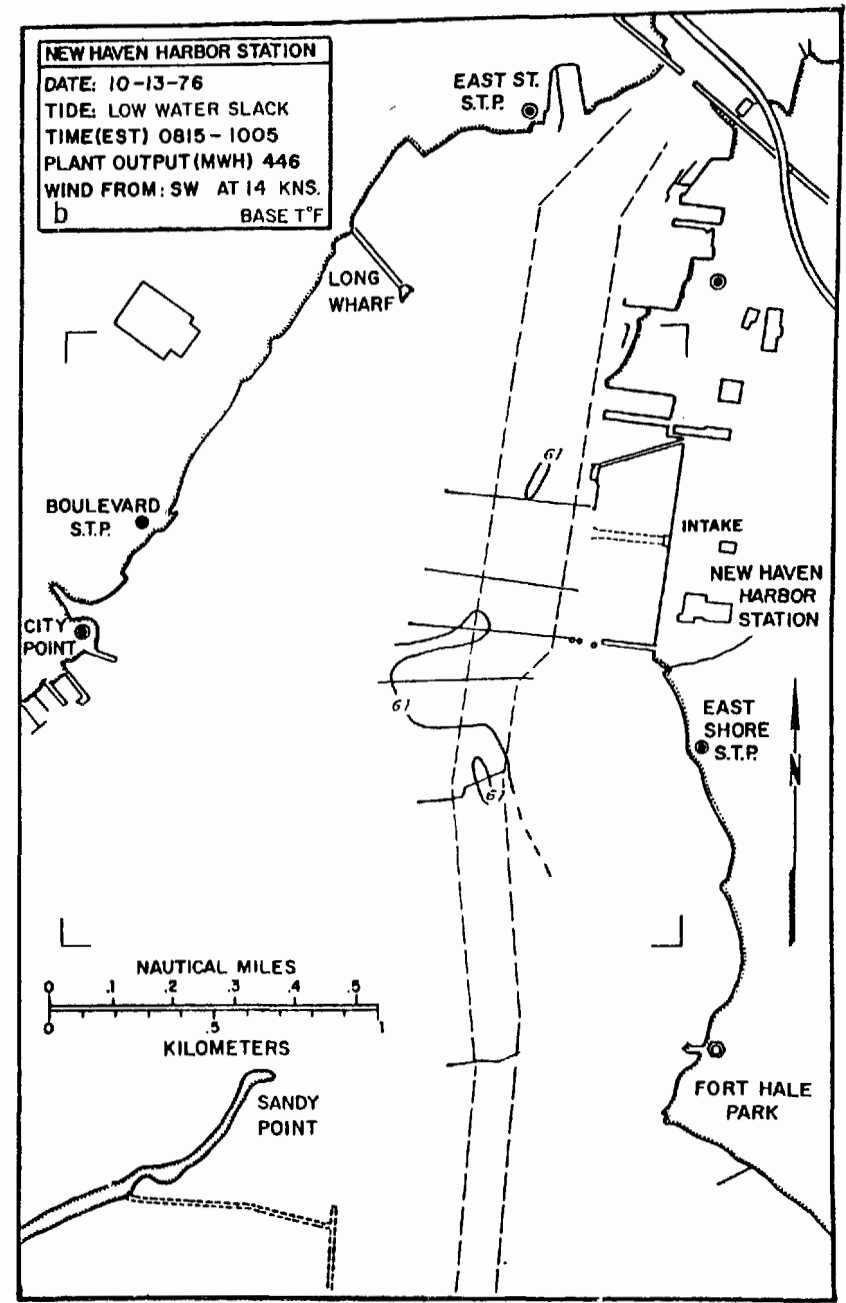
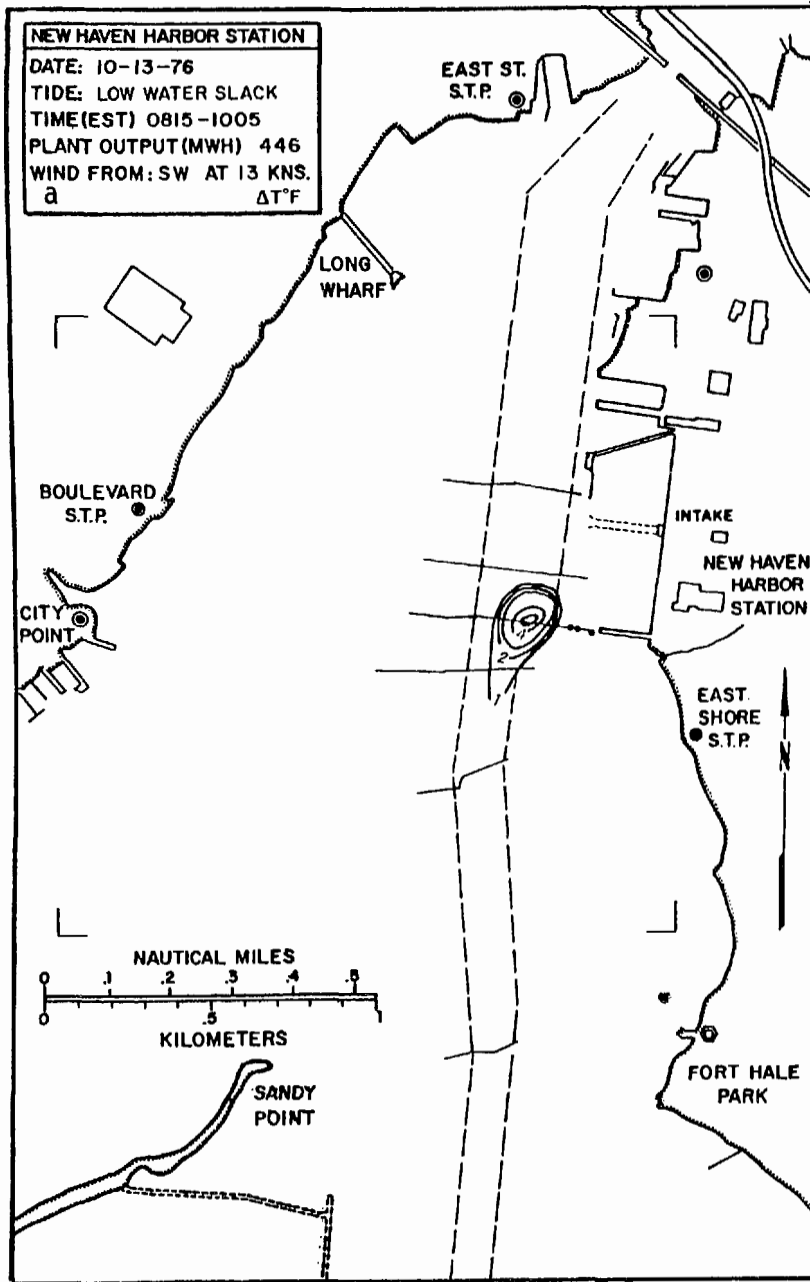


Figure 4. Surface  $\Delta t$ , (a) and surface base temperature (b), October 13, 1976 - Low Water Slack. Thermal Surveys, New Haven Harbor, Summer and Fall, 1976.

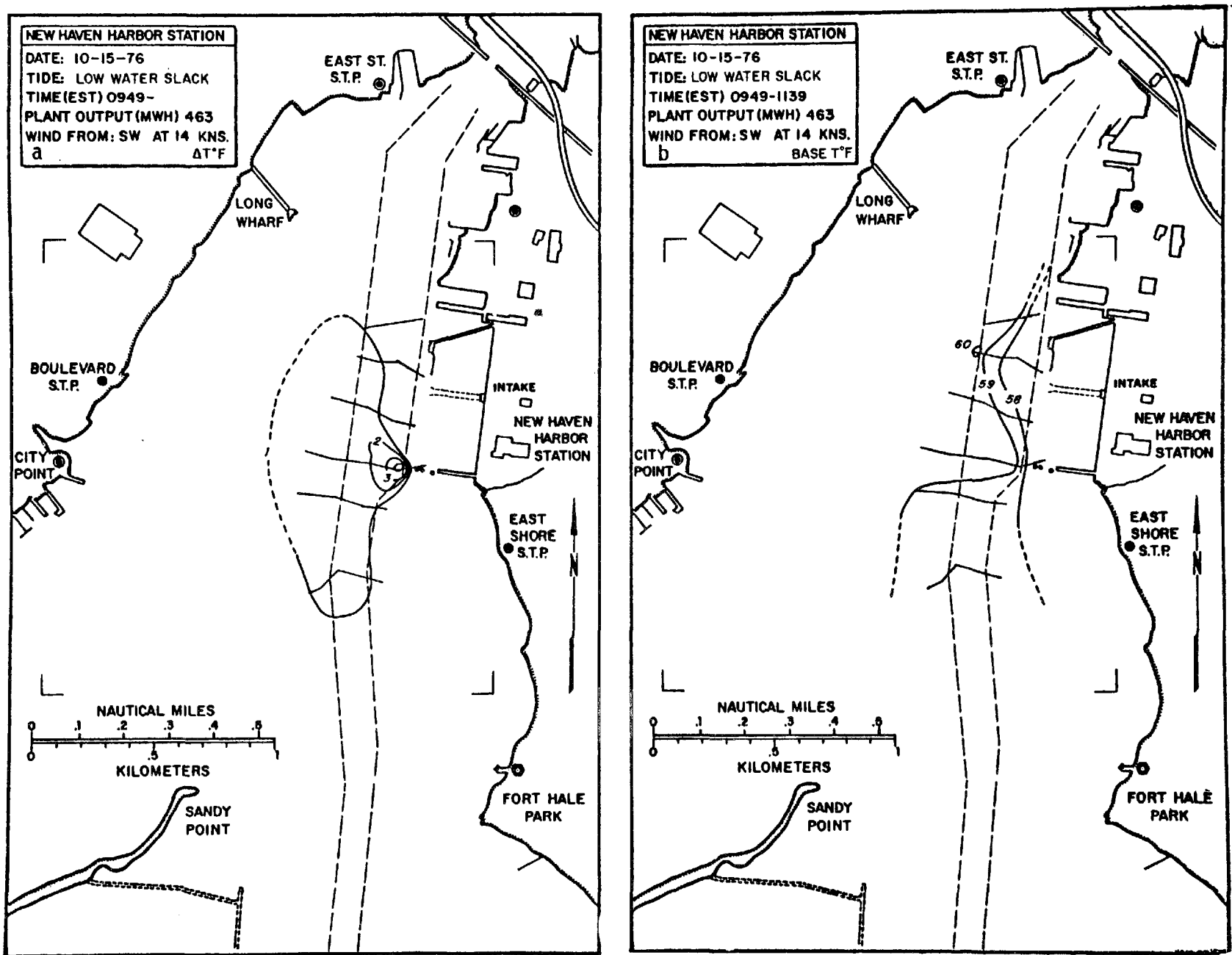


Figure 5. Surface  $\Delta t$ , (a) and surface base temperature (b), October 15, 1976 - Low Water Slack. Thermal Surveys, New Haven Harbor, Summer and Fall, 1976.

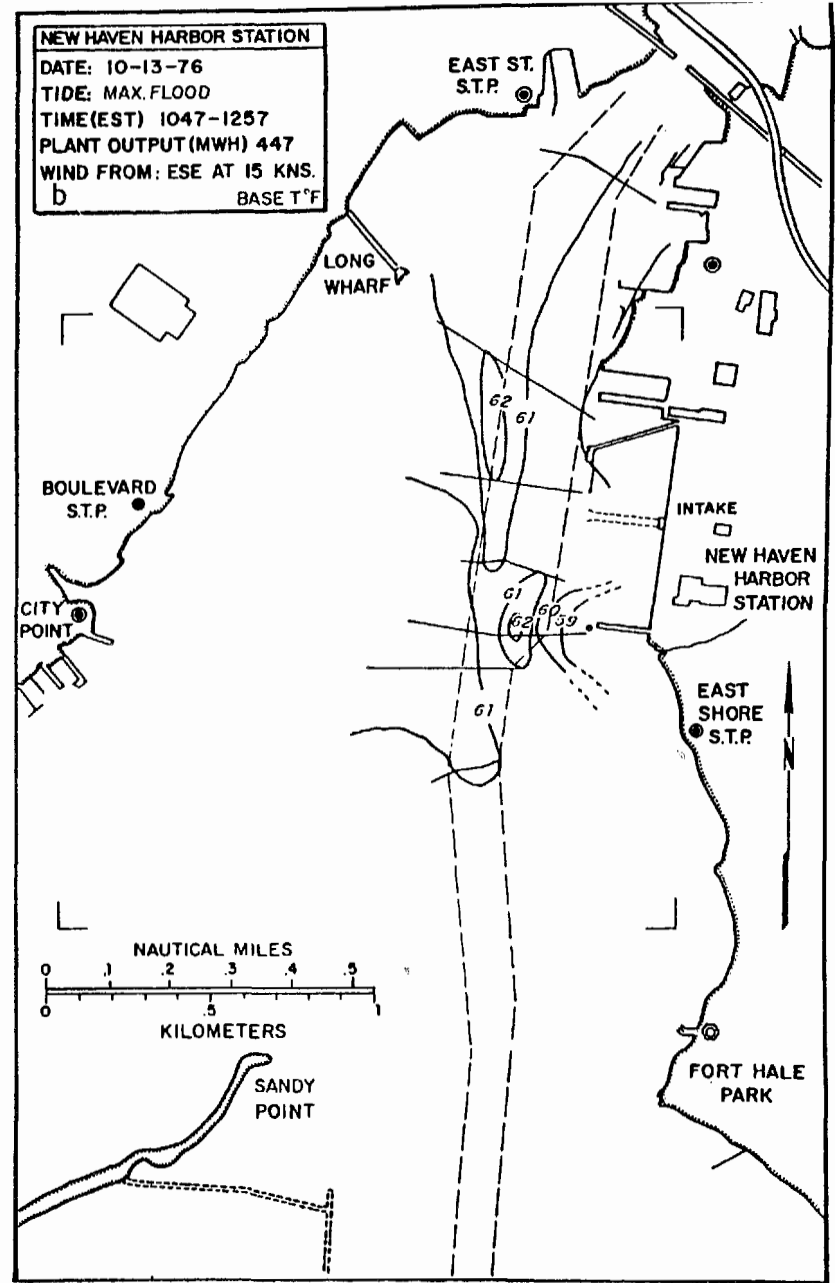
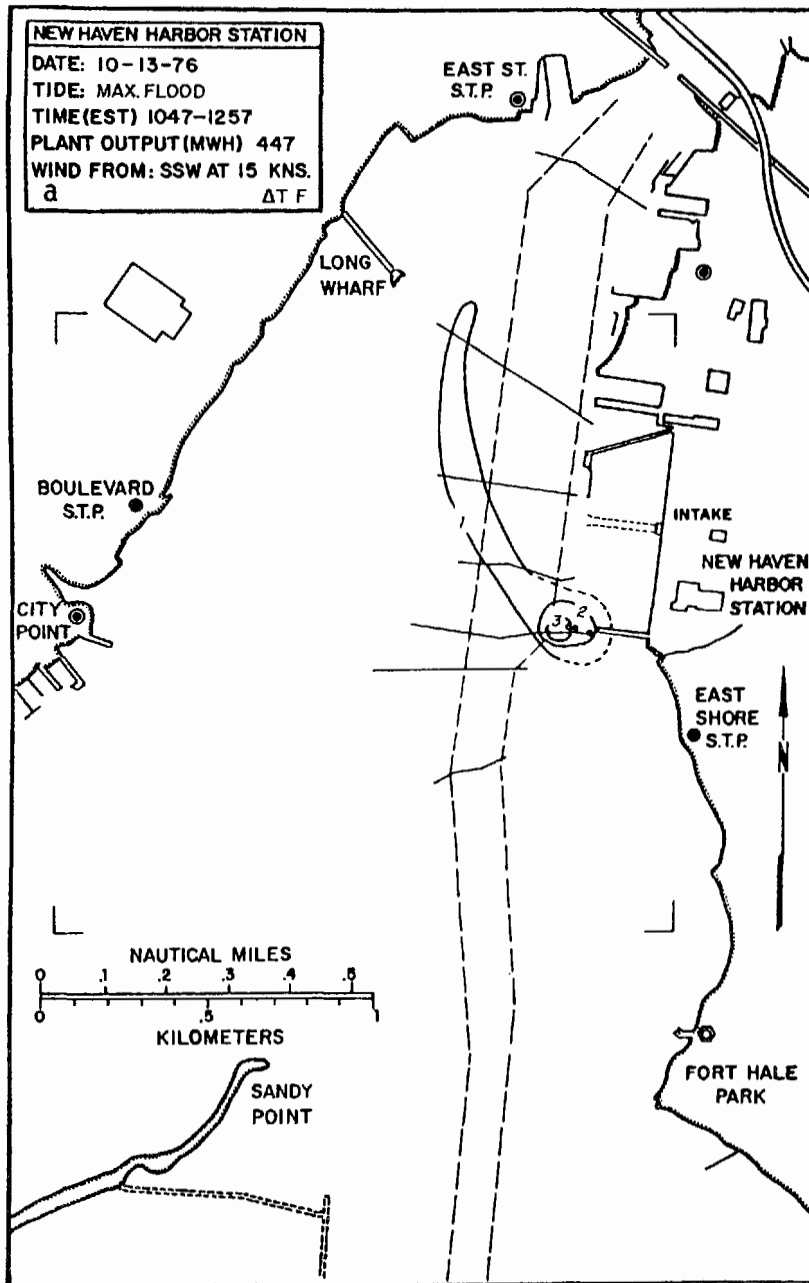


Figure 6. Surface  $\Delta t$ , (a) and surface base temperature (b), October 13, 1976 - Mid-Flood. Thermal Surveys, New Haven Harbor, Summer and Fall, 1976.

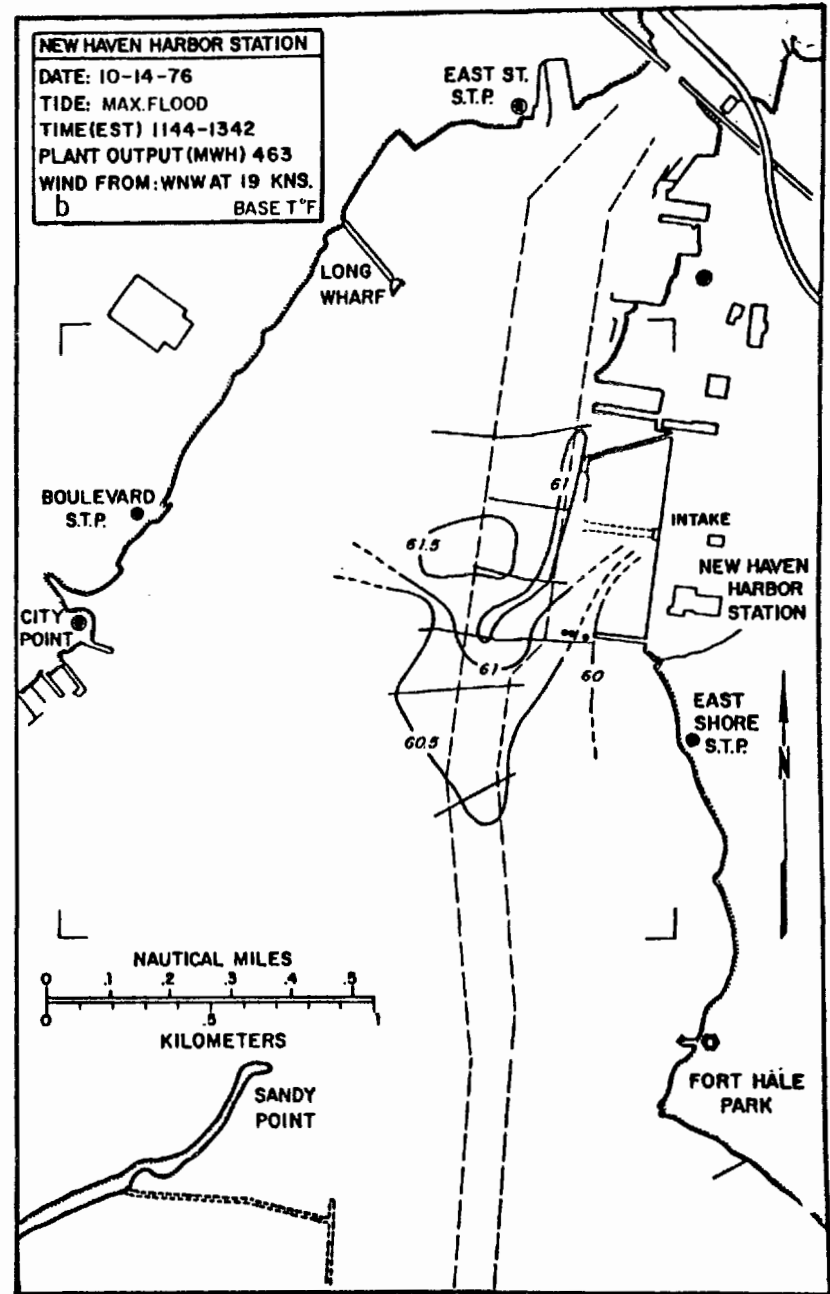
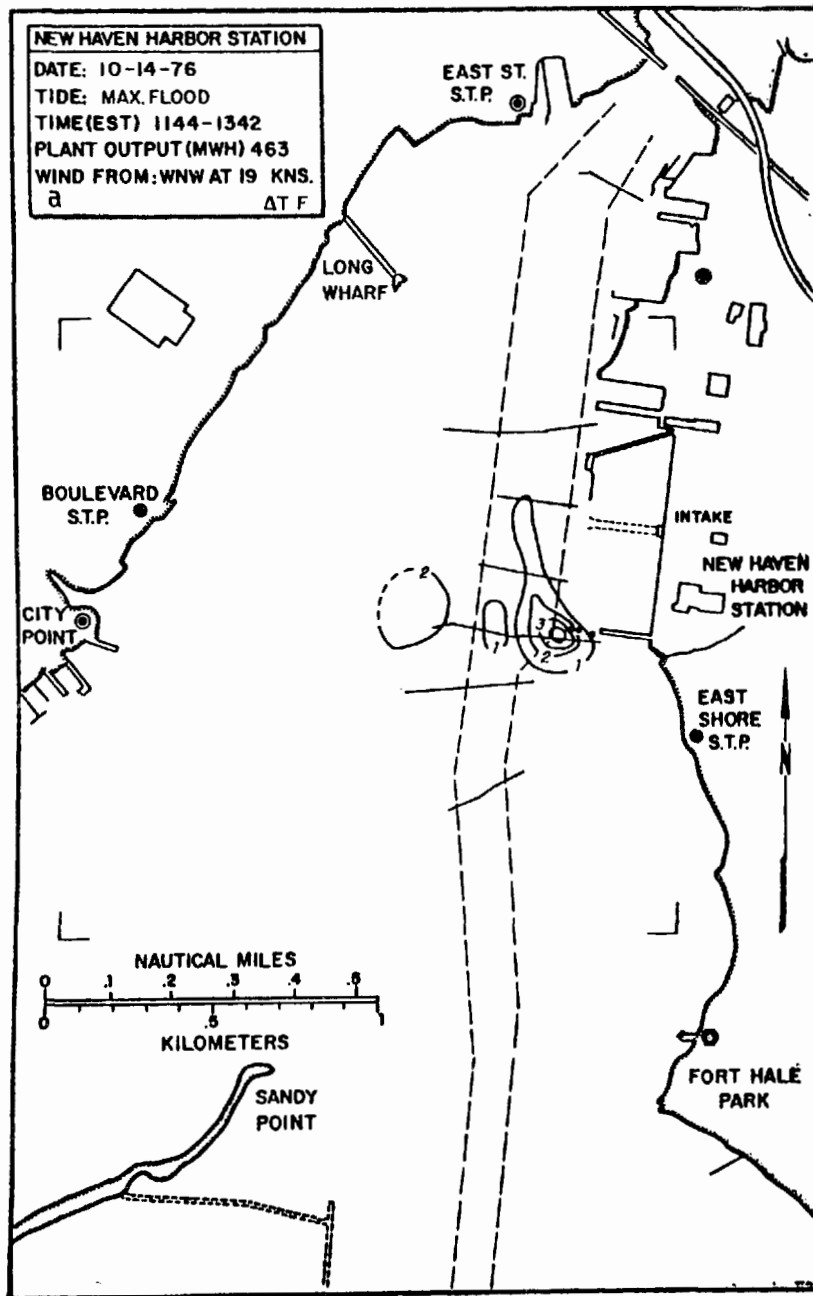


Figure 7. Surface  $\Delta t$ , (a) and surface base temperature (b), October 14, 1976 - Mid-Flood. Thermal Surveys, New Haven Harbor, Summer and Fall, 1976.

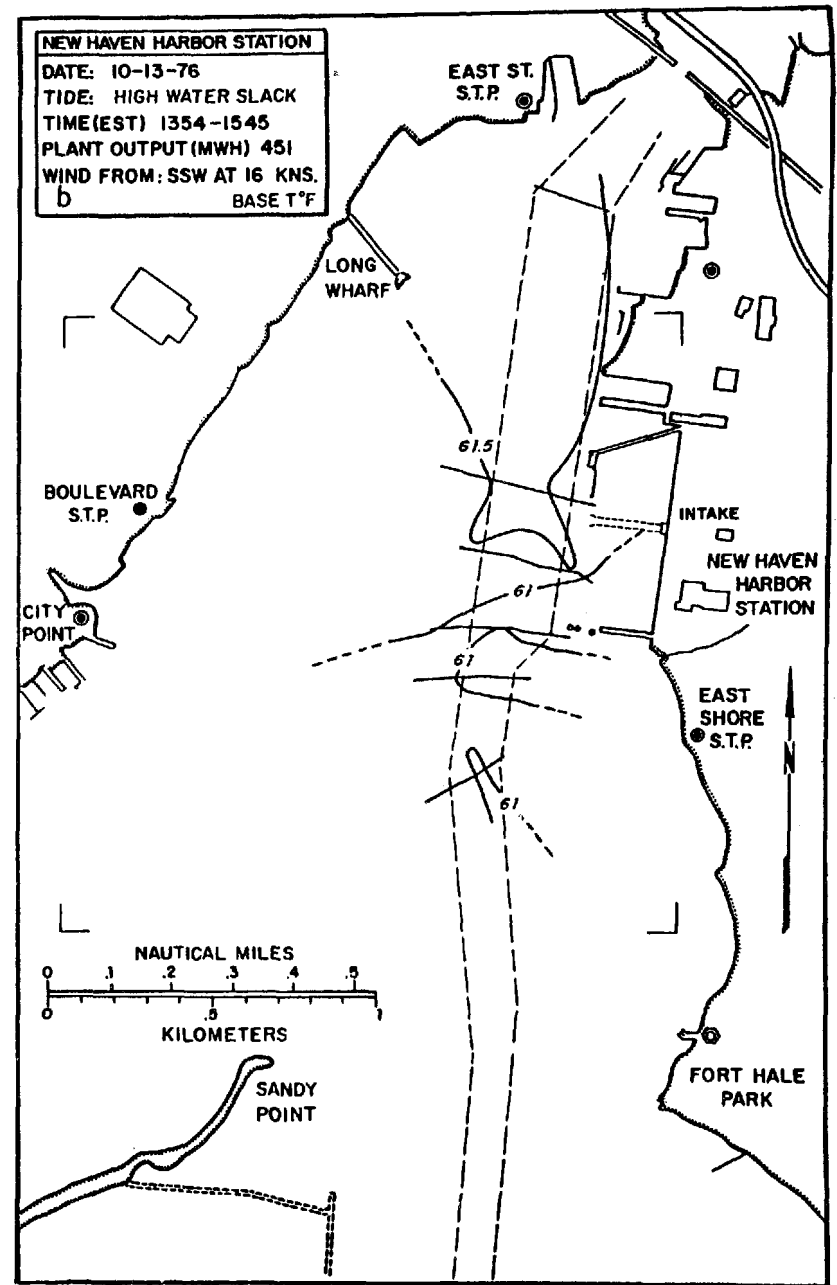
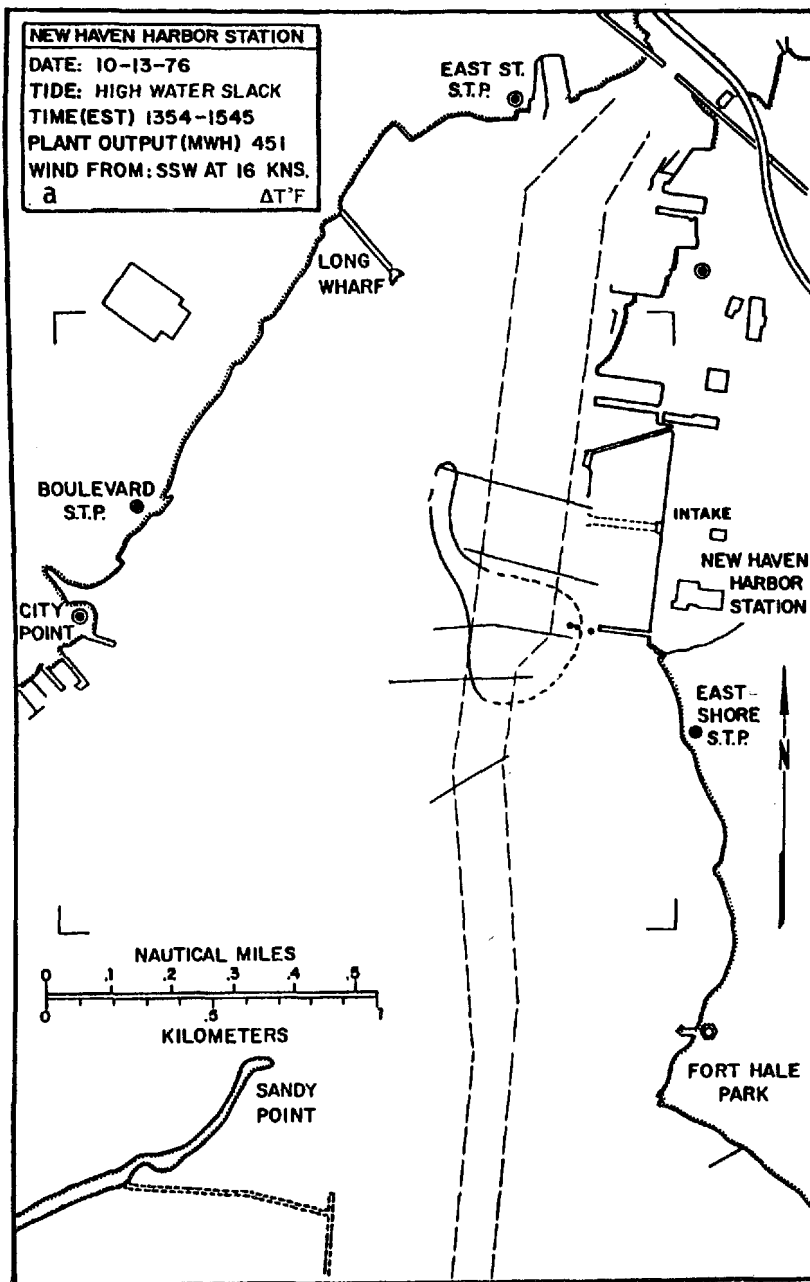


Figure 8. Surface  $\Delta t$ , (a) and surface base temperature (b), October 13, 1976 - High-Water Slack. Thermal Surveys, New Haven Harbor, Summer and Fall, 1976.

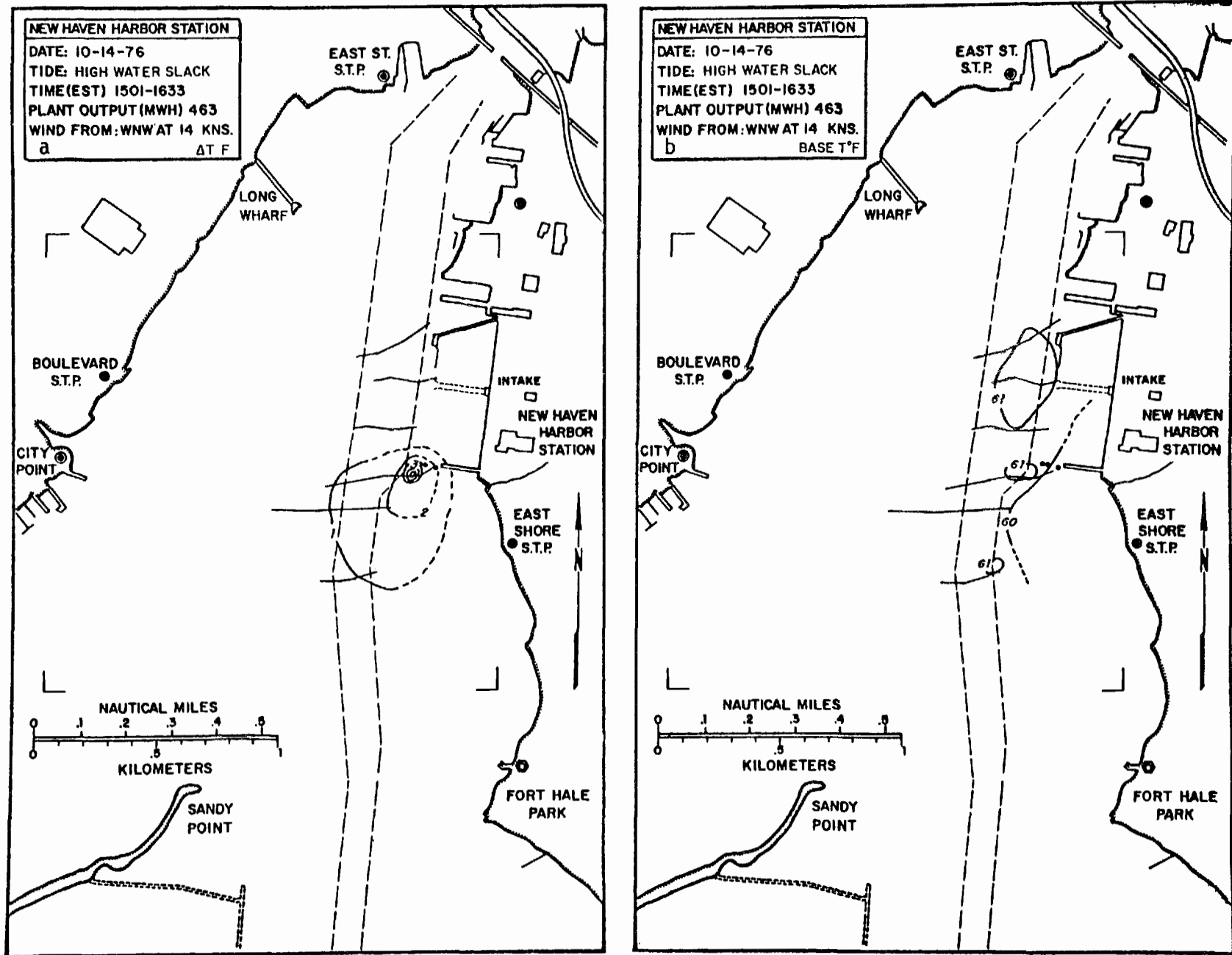


Figure 9. Surface  $\Delta t$ , (a) and surface base temperature (b), October 14, 1976 - High-Water Slack. Thermal Surveys, New Haven Harbor, Summer and Fall, 1976.

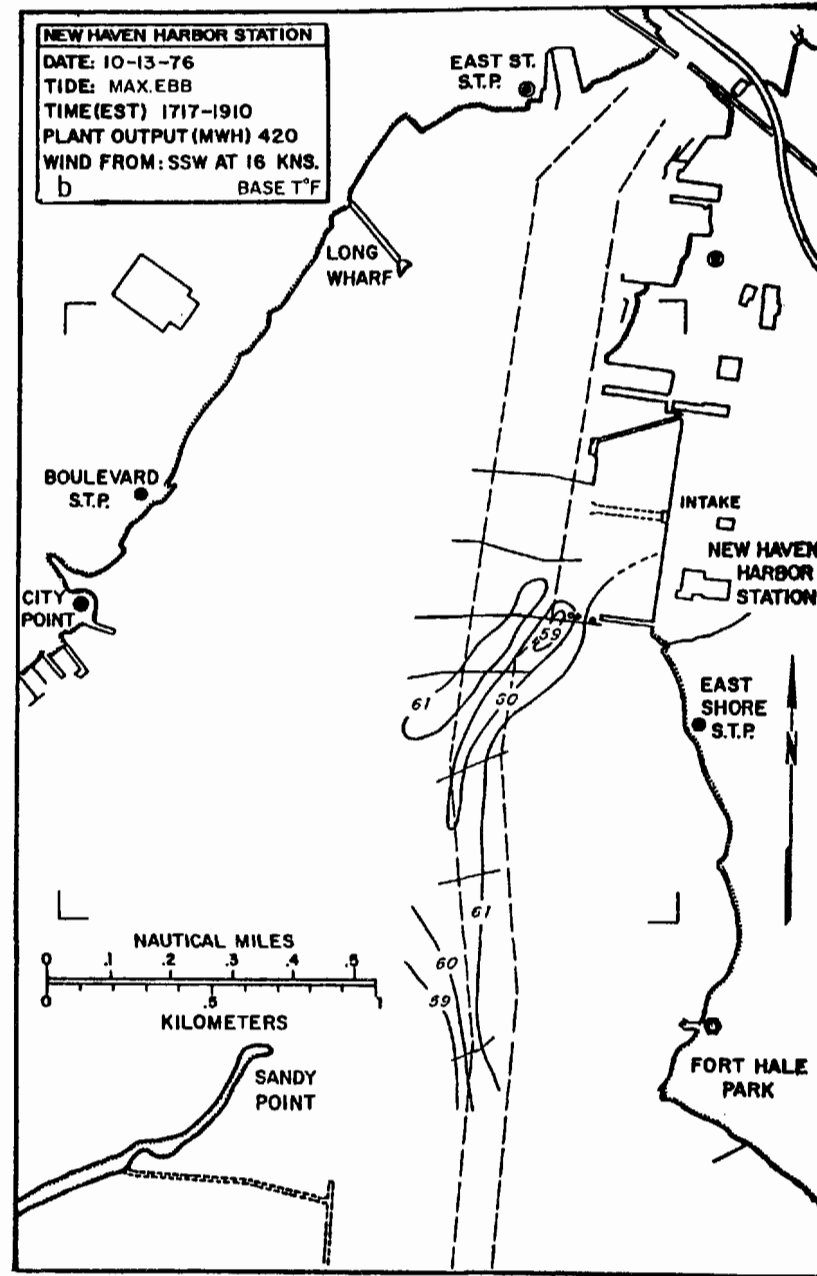
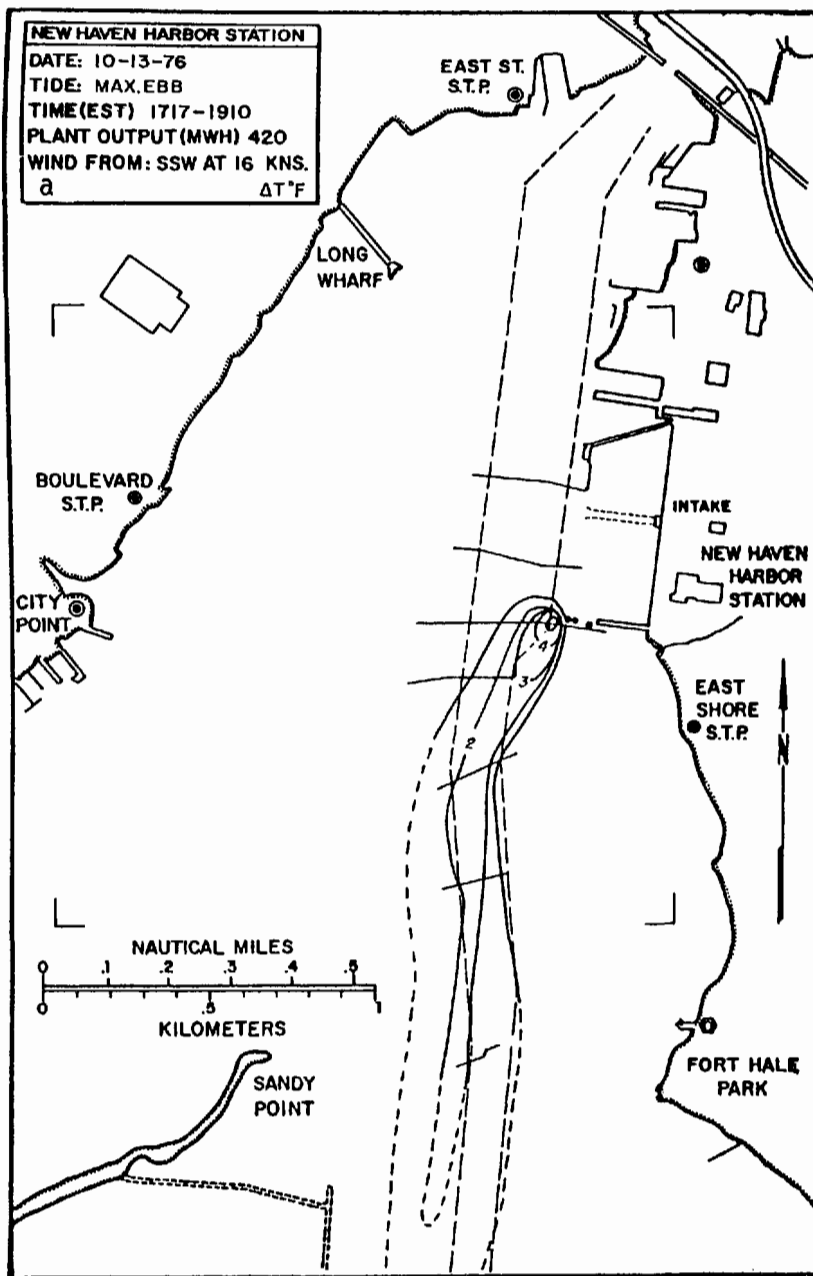


Figure 10. Surface  $\Delta t$ , (a) and surface base temperature (b), October 13, 1976 - Mid-Ebb. Thermal Surveys, New Haven Harbor, Summer and Fall, 1976.

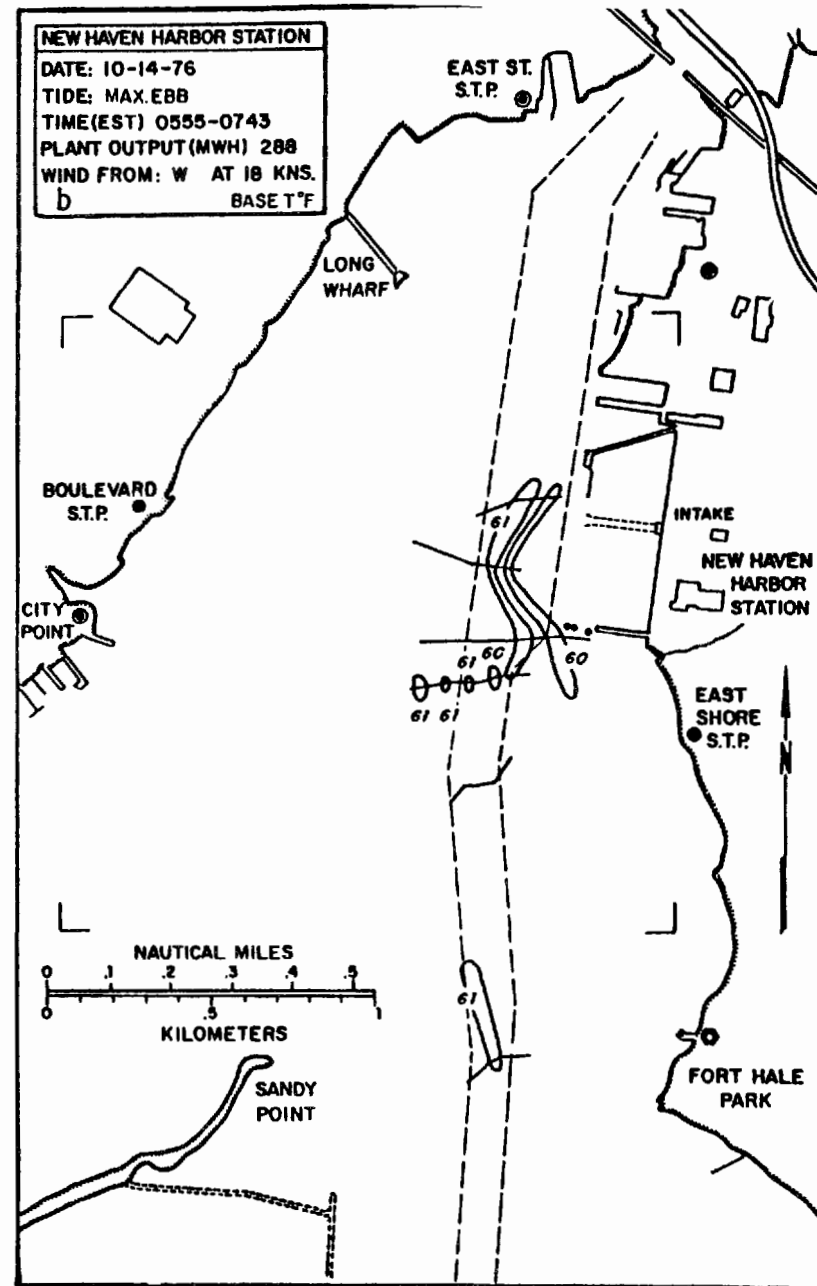
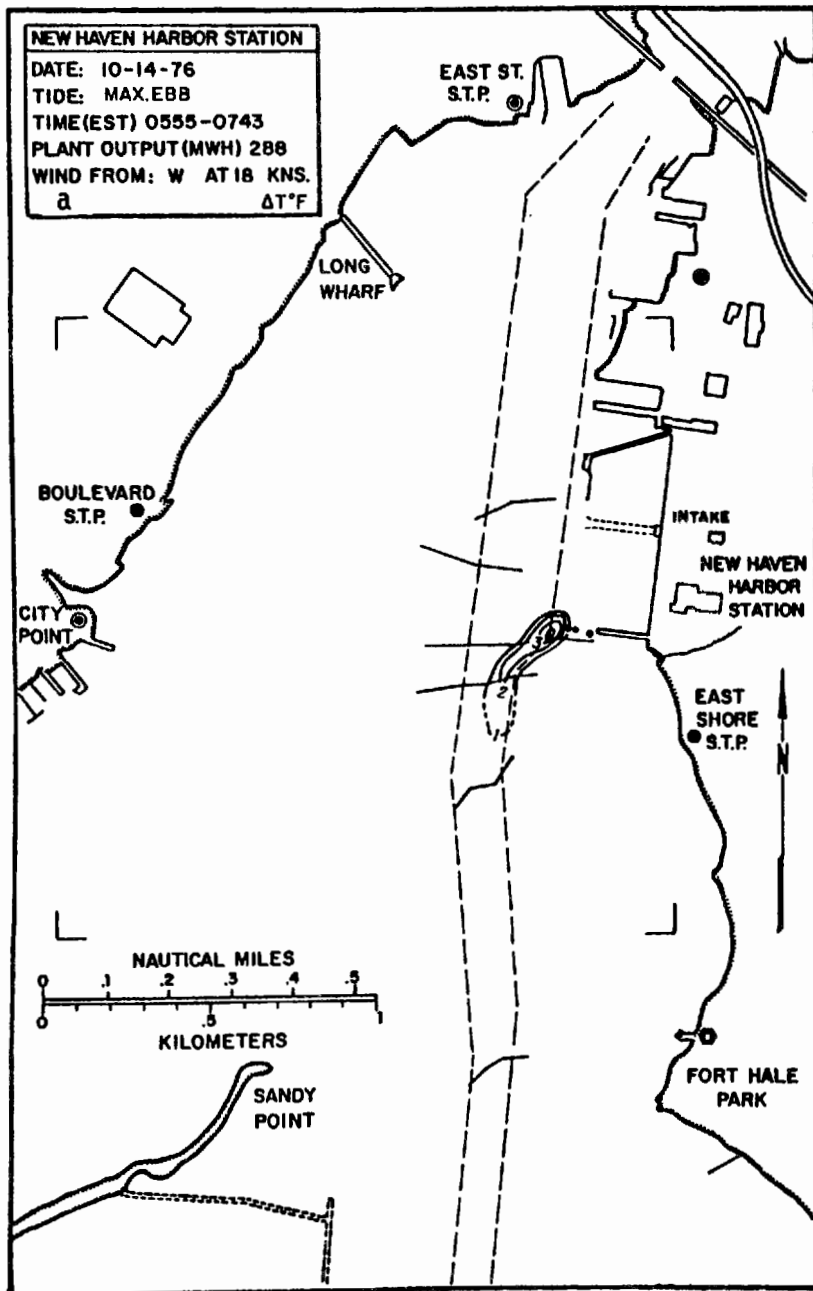


Figure 11. Surface  $\Delta t$ , (a) and surface base temperature (b), October 14, 1976 - Mid-Ebb. Thermal Surveys, New Haven Harbor, Summer and Fall, 1976.

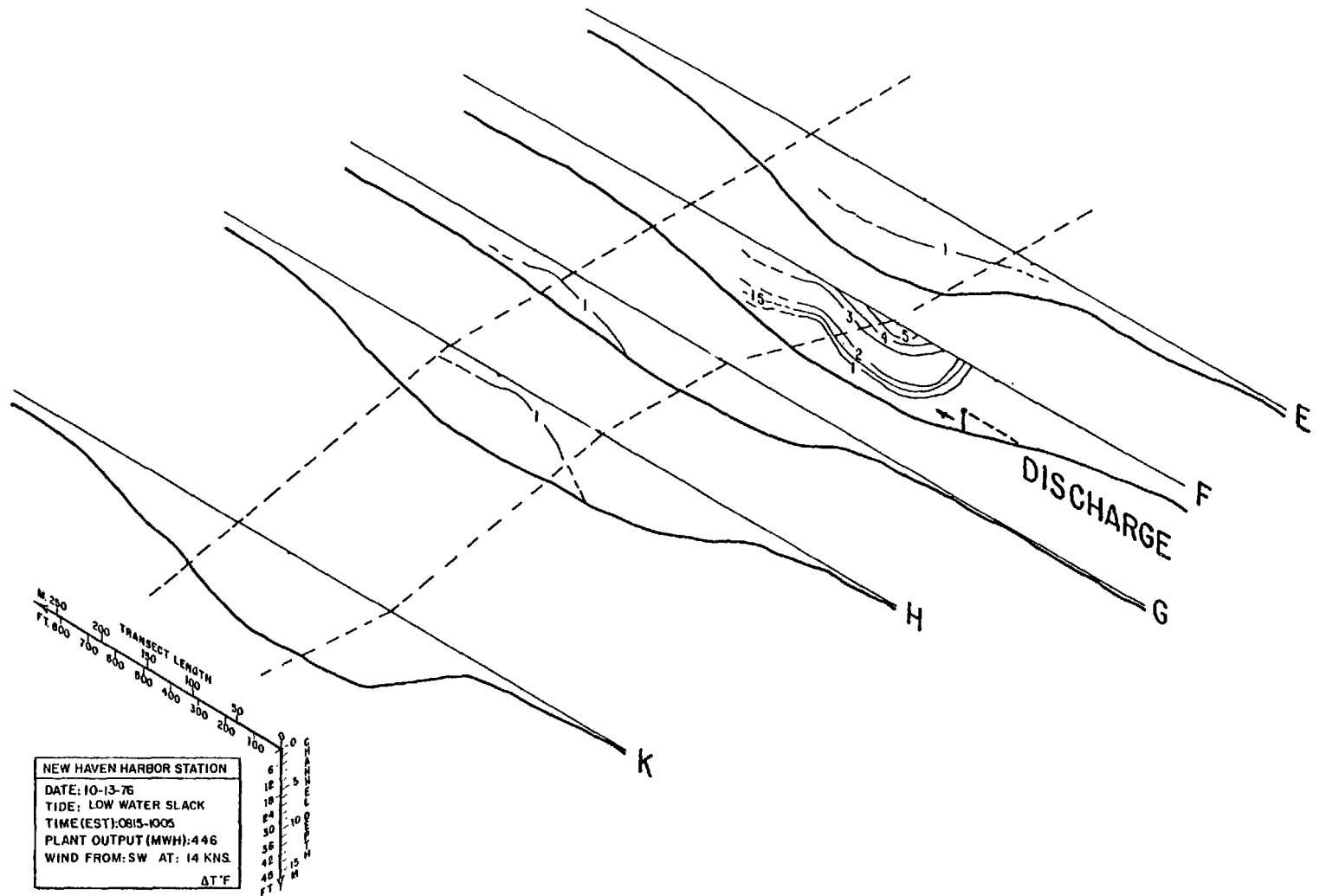


Figure 12. Cross sectional  $\Delta t$ , October 13, 1976-Low Water Slack. Thermal Surveys, New Haven Harbor, Summer and Fall, 1976.

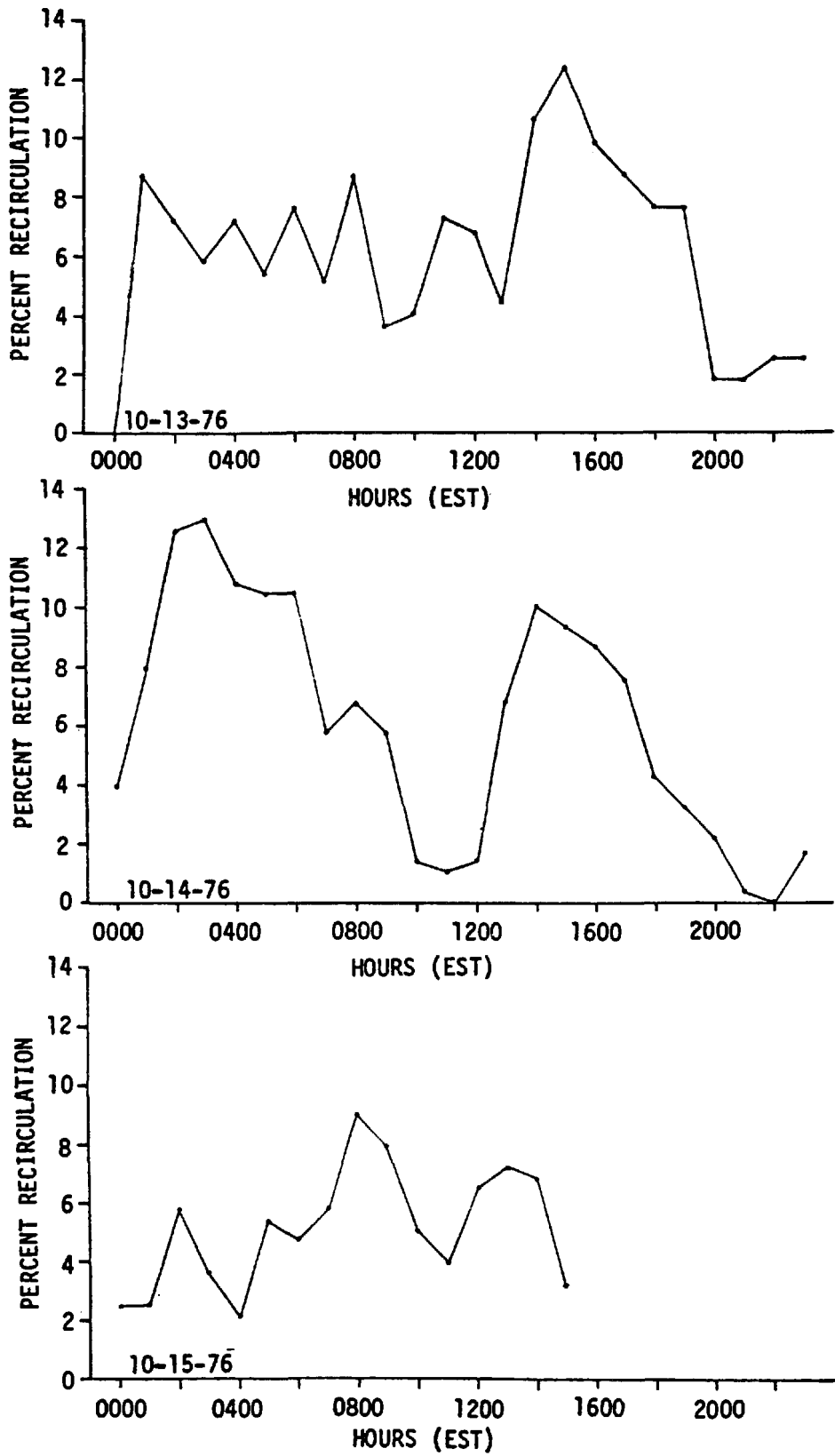


Figure 13. Percent recirculation as a function of time. Thermal Surveys, New Haven Harbor, Summer and Fall, 1976.

# BEHAVIOR OF THE THERMAL SKIN OF COOLING POND WATERS SUBJECTED TO MODERATE WIND SPEEDS

M. L. Wesely  
Radiological and Environmental Research Division  
Argonne National Laboratory, Argonne, Illinois U.S.A.

## ABSTRACT

The temperature difference  $\Delta T_{\delta}$  across the partially laminar skin of water on the surface of a water body is determined by the total heat transfer  $Q$  through the skin, the wind speed  $u$ , and the mean temperature  $T_{\delta}$  of the skin. Systematic measurements of these variables were made over a wide range of conditions at a cooling pond in northeastern Illinois. Waves were present in all cases; the wind speeds were  $u = 2.5-7.0 \text{ m s}^{-1}$  at a height of 1 m and water temperatures were  $T_{\delta} = 18-37.5^{\circ}\text{C}$ . The main result is the equation

$$\Delta T_{\delta} = 11.5 \gamma^{2/3} \kappa^{1/3} Q k^{-1} (\tau / \rho_w)^{-1/3},$$

where  $\gamma$  is the water viscosity,  $\kappa$  is the thermal diffusivity of water,  $k$  is the water thermal conductivity,  $\tau$  is the wind shearing stress, and  $\rho_w$  is the water density.

## INTRODUCTION

The transfer of heat across the uppermost millimeter of a body of water is limited partially by the slow rate of molecular heat diffusion in this poorly-mixed cool skin. In the relatively warm water of industrial cooling ponds, the magnitude of the temperature drop across the skin can approach  $1^{\circ}\text{C}$ . Use of bulk water temperature instead of actual surface temperature can cause significant errors both in estimating the total heat loss by use of bulk aerodynamic formulae<sup>1</sup>, and in predicting the onset and severity of steam fog<sup>2</sup>. For oceanic waters, the temperature drop from the surface to the water beneath the skin is usually much less than  $1.0^{\circ}\text{C}$ . Although of ten small, this difference is significant because the gradient of air temperature above is also usually very small. Thus, significant errors in the estimate of sensible heat flux (and evaporation) from the sea can result if water temperature below the skin is used instead of surface temperature.

In the present study, an attempt is made to determine the relationship of the temperature drop across the cool skin to atmospheric conditions and water properties at a cooling pond. Only a wavy surface subjected to moderate wind speeds is considered. The rather wide range of water temperatures encountered allows a systematic examination of the effects of varying (molecular) water viscosity and thermal diffusivity.

## SIMPLE THEORETICAL DESCRIPTIONS

This section reviews some of the past work on the behavior of the cool skin. A common formula for relating the temperature difference  $\Delta T_\delta$  across the depth  $\delta$  of the thermal skin to the total heat flux  $Q$  through the skin is

$$Q = k\Delta T_\delta / \delta, \quad (1)$$

where  $k$  is the thermal conductivity of the water. Rather than a fixed value,  $\delta$  is considered the variable to be determined. According to the measurements of Khundzhua and Andreyev<sup>3</sup>,  $\delta$  is the depth at which the remaining temperature drop is about 37% of  $\Delta T_\delta$ . Rather than a detailed examination of profile descriptions<sup>4-7</sup>, a parameterization of the bulk properties is considered here. To do so, we will assume initially that flow in the skin is mostly laminar, as would be the case if the air-sea interface were a smooth, nonmobile surface, although opinions have been expressed that excessively turbulent flow might exist when waves are present<sup>8</sup>. If the flow is mostly laminar, the viscosity of the water and thus its temperature strongly affects the depth of the thermal skin.

With the assumption that the depth of the skin for heat is proportional to that for momentum, dimensional arguments<sup>9</sup> lead to the relationship

$$\delta \sim \gamma(\tau_w / \rho_w)^{-\frac{1}{2}} \quad (2)$$

where  $\tau_w$  is the viscous stress,  $\gamma$  is the viscosity of water, and  $\rho_w$  is the water density. By combining (1) and (2) and assuming that  $\tau_w$  is proportional to the shearing stress  $\tau$  aloft in the atmospheric surface layer, Saunders<sup>9</sup> finds the relationship

$$Q = k(\tau / \rho_w)^{\frac{1}{2}} \Delta T_\delta / (\lambda \gamma), \quad (3)$$

where  $\lambda$  is a numerical coefficient that absorbs the relationship between  $\tau_w$  and  $\tau$  and other unknown factors. Resorting to this empirically-derived coefficient may be one of the disadvantages that result from the assumption that a rigid boundary exists when in fact waves are present. One limited data set<sup>10</sup> indicates that  $\tau_w$  is considerably less than  $\tau$ , perhaps by about 80%, when waves are present.

For the case of forced convection in the skin, (3) appears acceptable except that no adjustment has been directly for the difference between the thickness of the thermal boundary layer in the skin and the depth of the viscous boundary layer. Since the Prandtl number  $Pr = \gamma / \kappa$ , where  $\kappa$  is the thermal diffusivity of water, is greater than one, the thermal layer should be smaller than the viscous layer. Approximately, this can be taken into account in accordance with the theory of flow near a rigid boundary layer by multiplying the right-hand side of (2) by  $Pr^{\frac{1}{3}}$ . This is equivalent to replacing  $\lambda$  in (3) by a new

coefficient  $\Lambda$  such that  $\lambda = \Lambda \text{Pr}^{-\frac{1}{3}}$ . The resulting formulae is

$$Q = k(\tau/\rho_w)^{\frac{1}{2}} \Delta T_{\delta} / (\Lambda r^{\frac{2}{3}} \kappa^{\frac{1}{3}}). \quad (4)$$

One of the aims of the present experimental effort is to determine if  $\Lambda$  is better suited than  $\lambda$  to relate  $\Delta T_{\delta}$  to  $Q$ .

Deacon<sup>11</sup> derives an equation similar to (4), but with modifications that allow consideration of cases when  $\Delta T_{\delta}$  is across depths much greater than  $\delta$  are considered. We shall neglect such elaborations here. His equation in the present notation becomes, after rearrangement,

$$Q = k(\tau/\rho_w)^{\frac{1}{2}} \Delta T_{\delta} [\gamma \phi(\text{Pr})]^{-1} \quad (5)$$

where  $\phi(\text{Pr})$  is given by his Figure 1, about equal to  $15.2 \text{Pr}^{-0.39}$  for water.

Another somewhat similar approach for describing the thermal skin is given by Hasse<sup>12</sup>, who finds that a temperature difference across the upper 35 cm of sea water not exposed to solar radiation can be represented by

$$\Delta T = C_{10} Q / u_{10}, \quad (6)$$

where  $C_{10}$  is a constant appropriate for wind speed  $u_{10}$  measured at a height of 10 m. Saunders<sup>8</sup> has found this to be roughly in agreement with (3), provided absorption of solar radiation in the water layer is not significant. Although a fairly large amount of solar radiation can be absorbed by a water layer of 35 cm, absorption by layer of depths of  $\delta \approx 1$  mm can usually be ignored.

## MEASUREMENTS

All measurements were taken at the cooling pond complex of Commonwealth Edison's Dresden nuclear power generating facility near Morris, Illinois, U.S.A. Many aspects of the cooling lake have been described in a previous publication<sup>13</sup>. Briefly, it is a man-made lake of about  $5.3 \text{ km}^2$  surface area divided into five pools connected by narrow channels. Typically, the warmest pool is about  $10^\circ\text{C}$  warmer than ambient air and the coolest is within  $5^\circ\text{C}$  of air temperature. Thus, the heat fluxes from most of the lake are large and can be measured by use of atmospheric bulk techniques with a relative accuracy better than above most natural, unheated water bodies.

A wide range of temperatures and wind speeds at the Dresden cooling pond can be found if samples are taken over an entire year. The measurements considered here were taken on various occasions when no steam fog was present during 1973-1978. For the 64 10-min samples taken, the temperature  $T_{\delta}$  of the surface skin ranged from 18 to  $37.5^\circ\text{C}$  and averaged  $27.5^\circ\text{C}$ , where

each  $T_{\delta}$  was determined as the average of the surface and the bulk water temperatures. Wind speeds at a height of 1 m varied from 2.5 to 7.0  $\text{m s}^{-1}$  (which extrapolates to about 3.0–8.5  $\text{m s}^{-1}$  at a height of 10 m), with an average of 5.1  $\text{m s}^{-1}$ . Atmospheric conditions above the pond were unstable during all data collection periods, with a heat flux upward through the water skin. The temperature difference  $\Delta T_{\delta}$  across the skin varied from 0.3 to 1.5°C.

In all cases, measurements were taken aboard a pontoon boat positioned 200–1500 m downwind from the nearest shoreline. A cup anemometer measured wind speeds at heights of 0.5–1.5 m above the surface, usually supported on a shaft about 2 m to the side and cross wind of the low-slung boat faced into the wind. At a height of 0.5 m at the upwind edge of the boat, an aspirated psychrometer provided wet- and dry-bulb air temperatures. An immersed mercury-in-glass thermometer supplied water temperatures at a depth of 2–5 cm, and a hand-held infrared thermometer detected the surface temperature.

The temperature difference  $\Delta T_{\delta}$  across the skin was found by several techniques, usually by vigorously stirring the water in the field of view of the hand-held infrared device. Other techniques, somewhat less successful, were employed also. For example, using stirred water in an insulated container as a reference, the experimenter could obtain a fairly accurate measurement of surface temperature, so that  $\Delta T_{\delta}$  could be determined as the difference between the surface and the immersed temperature.

A difficulty encountered in measuring  $\Delta T_{\delta}$  is that it varies in magnitude as different portions of the wave field are viewed, and is highly responsive to wind speed variations. Breaking waves might cause serious aberrations, but if breaking waves were present during sampling at the Dresden pond, the breaking portion of the wave usually was not included in the view of the thermometer. Typical variations were noted during one 10 min data-collection period. With the total heat flux  $Q$  across the skin averaging 418  $\text{W m}^{-2}$  and the mean wind velocity being  $u = 4.1 \text{ m s}^{-1}$  at a height of 0.5 m,  $\Delta T_{\delta}$  fluctuated within the range 0.55–0.85°C as the wind speed varied from 6.7 to 2.7  $\text{m s}^{-1}$ . The values of  $\Delta T_{\delta}$  appeared to be roughly proportional to  $u^{-1}$ . How should one properly average these variables? The present approach is that common in studies of momentum, heat and mass transfer in the atmospheric surface layer. That is, while gradients of horizontal wind speed, temperatures and humidities can vary greatly from minute to minute (especially during unstable conditions), valid relationships of fluxes to mean gradients can be found by simple linear averaging of the measured variable over periods of 10–60 min. Admittedly, the results are partially empirical and do not explain the details of the transfer mechanisms involved.

## RESULTS

For each 10 min run, the friction velocity  $u_* = (\tau/\rho_a)$ , sensible heat flux  $H$ , and latent heat flux  $LE$  is calculated by use of a low-level bulk aerodynamic

method as described by Hicks<sup>1</sup> with minor modifications as given by Hicks et al.<sup>13</sup>. The upward infrared energy flux density is calculated as

$$R_u = \epsilon \sigma T_s^4, \quad (7)$$

where  $\epsilon \cong 0.95$  is the emissivity of the water surface,  $\sigma$  is the Stephan-Boltzman constant, and  $T_s$  is the surface temperature. The downward infrared flux is estimated (in unit of watts per square meter) as

$$R_d = 5.31 T_a^6 \cdot 10^{-13} - 20 - 0.3 \epsilon_c \sigma T_c^4 c, \quad (8)$$

which is Swinbank's<sup>15</sup> formula as modified by Paltridge<sup>16</sup> and Paltridge and Platt<sup>17</sup>. The numerical coefficients are empirical,  $T_a$  is the average air temperature,  $\epsilon_c \cong 1$  is the thermal emissivity of clouds present,  $T_c$  is the estimated temperature of the cloud lower surfaces, and  $c$  is the fraction of cloudiness. For most of the data taken,  $c$  was zero. Combining the atmospheric estimates of fluxes results in

$$Q = H + LE + R_u - R_d. \quad (9)$$

This estimate of  $Q$  is independent of the procedures used to examine directly the cool skin, as in the discussion to follow.

Upon inspection of (4) it becomes evident that  $Q$  should be unique function of  $\Delta T_\delta$ , wind speed ( $u_1$  at a height of one meter), and  $T_\delta$ . A simple multiple linear regression of the 64 data points results in the equation

$$Q = -631 + 457 \Delta T_\delta + 88u_1 + 17.1 T_\delta. \quad (10)$$

Figure 1 compares the results of (10) with the atmospheric estimates given by (9). Although the correlation coefficient for the 64 samples is a highly significant 0.92, wide scatter in the data is evident. This is most likely due to the errors in obtaining a reliable average of  $\Delta T_\delta$  during each 10 min run. Because of this scatter, statistical techniques will be used to obtain values of  $\Lambda$ ,  $\lambda$ , and  $C_{10}$ .

First, to test the expectation that  $\delta \sim u_*^{-1}$  as given by (1), Figure 2 shows the relationship between  $\delta$  and  $u_*$ . For this case,  $\delta$  is calculated as

$$\delta = Q / (k \Delta T_\delta). \quad (11)$$

Even though a rather extensive range of water temperatures were encountered (18-37.5°C), the range of  $u_*$  for each small interval of water temperature was rather large, so that no systematic change of  $\delta$  with  $u_*$  due to a correlation of  $u_*$  with  $T_\delta$  should have resulted. Figure 2 seems to verify that  $\delta \sim u_*^{-1}$ . Since waves $\delta$  were present in all cases, the aerodynamically smooth case is not considered. These results do not compare well with the results of Hill<sup>18</sup>

who used a wind-water tunnel. His estimates of  $\delta$  are considerably greater for  $u_* < 35 \text{ cm s}^{-1}$ , for which the tunnel produced aerodynamically smooth flow. Extrapolation of the results of Figure 2 for  $u_* > 35 \text{ cm s}^{-1}$  yield present estimates of  $\delta$  considerably greater than Hill's values. Further comparisons can be made by examination of Figure 5 of Kondo<sup>19</sup>, in which the present data would follow very well the theoretical calculations derived from Brutsaert<sup>6</sup> for  $u_* = 15\text{-}30 \text{ cm s}^{-1}$ .

Figure 3 shows the values of  $\Lambda$ ,  $\lambda$ , and  $C_{10}$  determined at the Dresden cooling pond and plotted as a function of  $T_\delta$ . The variability of  $k$ ,  $\gamma$ , and  $\kappa$  with temperatures are taken into account by application of readily-available, published estimates. The density  $\rho$  is estimated for a height of about 0.5 m, and  $\rho_w$  is assumed to be  $1 \text{ g cm}^{-3}$ . Also,  $C_{10}$  is computed on the basis of an extrapolation to wind speeds at a height of 10 m. The regression lines in Figure 3 show the dependency of  $\Lambda$ ,  $\lambda$ , and  $C_{10}$  on  $T_\delta$ . It appears that  $C_{10}$  is negatively correlated with  $T_\delta$ , with a correlation coefficient of  $-0.27$  for the 64 runs, while  $\lambda$  and  $\Lambda$  are positively correlated with  $T_\delta$ , yielding correlation coefficients of  $0.22$  and  $0.06$ , respectively. Thus,  $\lambda$  seems to suffer from overadjustment relative to  $C_{10}$ , but  $\Lambda$  is not significantly correlated with  $T_\delta$ . Additionally, analyses indicate that  $\phi(\text{Pr})$  from (5) is about  $12.8\text{Pr}^{-0.39}$ , if the exponent is fixed at  $-0.39$ . The numerical coefficient  $12.8$  has a behavior very similar to  $\Lambda$ ; the use of  $\Lambda \text{Pr}^{-\frac{1}{3}}$  or  $\phi(\text{Pr}) = 12.8\text{Pr}^{-0.39}$  provide equally good fits in a statistical sense.

The present estimate of  $\lambda \approx 6$  is very near to the estimate of about 7 given by Saunders (1967) for the oceanic case, and to the value of about 8 that can be inferred from the oceanic data of Hasse<sup>12</sup> for temperatures near  $15^\circ\text{C}$ . Grassl<sup>20</sup> recomputes a value of  $\lambda \approx 6$  for Hasse's data by choice of a different drag coefficient. For his own data at sea with surface temperatures near  $26.5^\circ\text{C}$ , Grassl obtains  $\lambda$  increasing with wind speeds, with  $\lambda \approx 4$  at  $u_{10} = 3 \text{ m s}^{-1}$  and  $\lambda \approx 5.5$  at  $u_{10} = 8.5 \text{ m s}^{-1}$  corresponding to the approximate range of wind speeds in the present study. On the other hand, Hill<sup>18</sup> obtains  $\lambda \approx 4$  for waves present and  $\lambda \approx 11$  at lower wind speeds without waves in a wind-water tunnel; Paulson and Parker<sup>21</sup> discuss Hill's results more fully. The Dresden data do not indicate a significant correlation of  $\lambda$  (or  $\Lambda$  and  $C_{10}$ ) with wind speed; the scatter in the data over the relatively small range of wind speeds would prevent detection of this correlation if it were only slightly significant.

For all 64 runs obtained at the Dresden cooling pond, the average value of  $C_{10}$  is  $5.1^\circ\text{C m s}^{-1}/(\text{ly min}^{-1})$ , which corresponds to  $0.0073^\circ\text{C m}^3 \text{ W}^{-1} \text{ s}^{-1}$ . Hasse's value of about  $9.2^\circ\text{C m s}^{-1}/(\text{ly min}^{-1})$  is larger, as it should be because the temperature difference was measured over a much greater depth (35 cm versus the present 2-5 cm). The average value of  $C_{10}$  can be used to derive a simple expression for  $\delta$ . That is, (1) and (6) can be combined to form the expression

$$\delta = kC_{10}f_c/u_* \quad (12)$$

where  $f_c$  is the friction coefficient suitable for a 10 m height, inferred from the aerodynamic calculations<sup>18</sup> to be about 0.0349 for the unstable conditions at the Dresden lake. With use of  $k = 0.637 \text{ W m}^{-1} \text{ }^\circ\text{K}$  corresponding to an overall mean water skin temperature of about  $27.5^\circ\text{C}$  encountered,  $\delta$  is found to be

$$\delta = 16.2/u_* \quad (13)$$

The curve drawn in Figure 1 shows that (13) presents an acceptable fit to the data.

## CONCLUSIONS

Data collected at the Dresden cooling pond indicate that expressions for the transport of heat through a viscous layer appear to describe sufficiently the temperature differences found when waves are present. While the range of windspeeds examined is small ( $3\text{--}8.5 \text{ m s}^{-1}$  at  $z = 10 \text{ m}$ ), the rather wide range of water temperatures encountered ( $18\text{--}37.5^\circ\text{C}$ ) allows determination statistically of the temperature dependency of empirical numerical coefficients. Values of  $\lambda$  appear to increase slightly with temperature from 6 to 7, and  $C_{10}$  decreases from 6 to 4.5. When the ratio of the viscous to thermal boundary layer thicknesses is assumed to be approximately proportional to  $\text{Pr}^{1/3}$ , which is appropriate for a rigid boundary, the resulting coefficient  $\Lambda$  is found to be roughly independent of temperature. The overall result is verification of (4), which can be rearranged to show that the temperature drop across the skin is

$$\Delta T_\delta = 11.5 Q \gamma^{2/3} \kappa^{1/3} [k(\tau/\rho_w)^{1/2}]^{-1} \quad (14)$$

The measured thermal skin thickness is in fair agreement with some theoretical predictions, indicating that the assumption of a rigid, smooth boundary at the air-water interface appears valid for the wavy surface. As stated by Saunders<sup>8</sup>, this might be fortuitous if the effect of possibly significant transfer of wind stress to the waves by normal pressure forces is compensated by the effects of turbulence in the water near the surface. Whether fortuitous or not, a working relationship has been found.

Similar relationships can be found to describe the transfer of nonreactive gases across the viscous water layer. Because the transfer is greatly impeded by the low diffusivity of gases in water, the main problems that need to be addressed deal with the transfer through the water rather than in the lower atmosphere, especially if reactions in the surface water can substantially increase the uptake rate.

## ACKNOWLEDGEMENTS

Data were collected at the Dresden cooling pond with the permission and cooperation of the Commonwealth Edison Company.

## REFERENCES

1. Hicks, B. B., A procedure for the formulation of bulk transfer coefficients over water, Boundary-Layer Meteorol., 8, 515-524, 1975.
2. Hicks, B. B., The prediction of fog over cooling ponds, J. Air Pollut. Contr. Assoc., 27, 140-142, 1977.
3. Khundzhua, G. G., and Ye. G. Andreyev, An experimental study of heat exchange between the ocean and the atmosphere in small-scale interaction, Izv. Acad. Sci. USSR Atmos. Oceanic Phys., Engl. Transl., 10, 685-687, 1974.
4. Owen, P. R., and W. R. Thomson, Heat transfer across rough surfaces, J. Fluid Mech., 15, 321-334, 1963.
5. Yaglom, A. M., and B. A. Kader, Heat and mass transfer between a rough wall and turbulent fluid flow at high Reynolds and Peclet numbers, J. Fluid Mech., 62, 601-623, 1974.
6. Brutsaert, W., A theory for local evaporation (or heat transfer) from rough and smooth surfaces at ground level, Water Resour. Res., 11, 543-550, 1975.
7. Liu, W. T., and J. A. Businger, Temperature profile in the molecular sublayer near the interface of a fluid in turbulent motion. Geophys. Res. Lett., 2, 403-404, 1975.
8. Saunders, P. M., Space and time variability of temperature in the upper ocean, Deep-Sea Res., 19, 467-480, 1973.
9. Saunders, P. M., The temperature at the ocean-air interface, J. Atmos. Sci., 24, 269-273, 1967.
10. Dobson, F. W., Measurements of atmospheric pressure on wind-generated sea waves, J. Fluid Mech., 48, 91-127, 1971.
11. Deacon, E. L., Gas transfer to and across an air-water interface, Tellus, 29, 363-374, 1977.

12. Hasse, L., The sea surface temperature deviation and the heat flow at the sea-air interface, Boundary-Layer Meteorol., 1, 368-379, 1971.
13. Hicks, B. B., M. L. Wesely, and C. M. Sheih, A study of heat transfer processes above a cooling pond, Water Resour. Res., 13, 901-908, 1977.
14. McLeish, W., On the mechanism of wind-slick generation, Deep-Sea Res., 15, 461-469, 1968.
15. Swinbank, W. C., Long-wave radiation from clear skies, Quart. J. Roy. Meteorol. Soc., 89, 339-348, 1963.
16. Paltridge, G. W., Day-time long-wave radiation from the sky, Quart. J. Roy. Meteorol. Soc., 96, 645-653, 1970.
17. Paltridge, G. W., and C. M. R. Platt, Radiative Processes in Meteorology and Climatology, Developments in Atmospheric Science 5, Elsevier, New York, 1976.
18. Hill, R. H., Laboratory measurement of heat transfer and thermal structure near an air-water interface, J. Phys. Oceanogr., 2, 190-198, 1972.
19. Kondo, J., Parameterization of turbulent transport in the top meter of the ocean, J. Phys. Oceanogr., 6, 712-720, 1976.
20. Grassl, H., The dependence of the measured cool skin of the ocean on wind stress and total heat flux, Boundary-Layer Meteorol., 10, 465-474, 1976.
21. Paulson, C. A., and T. W. Parker, Cooling of a water surface by evaporation, radiation, and heat transfer, J. Geophys. Res., 77, 491-495, 1972.

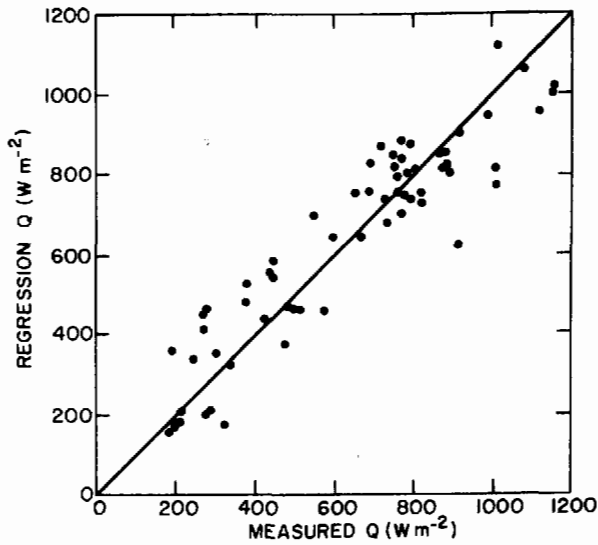


Fig. 1. Comparison of total heat transfer through the skin as computed from the regression equation (10), to Q estimated from measurements as given by (9).

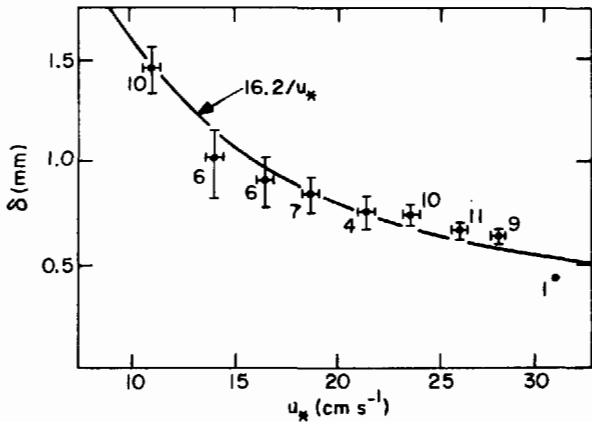


Fig. 2. Values of  $\delta$  estimated via (11) versus  $u_*$  calculated from bulk aerodynamic relationships. The numbers near the points and the standard error bars are the numbers of 10 min samples.

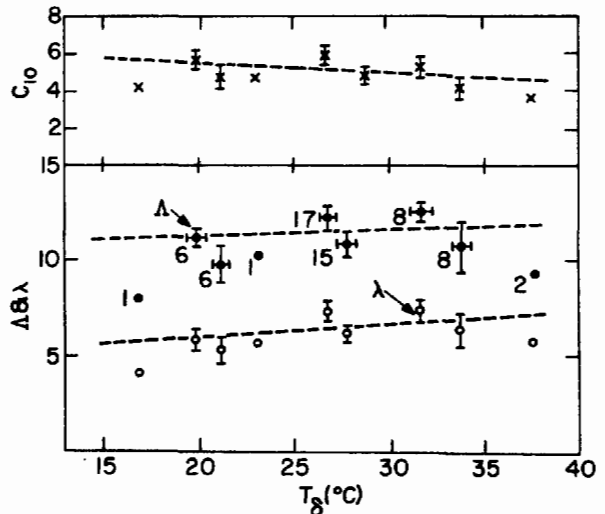


Fig. 3. Measurements of coefficients as a function of skin temperature. The numbers give the number of 10 min samples for each skin temperature interval and standard error bars are shown. The dashed lines represent a linear regressions.

Alternate Energy Conservation Applications for Industry\*

Lawrence J. Schmerzler

Increasing costs of electrical energy and fuel requires management to evaluate alternate methods of providing their total energy requirement with a view towards saving money as well as fuel.

A number of energy conservation illustrations are presented utilizing cogeneration, regenerators, recompression, and heat pumps. Thermoeconomic analysis is made for a few industrial cogeneration applications from 50 to 1200 kw.

While cogeneration systems may not always be practical or economical, it was found possible to obtain payback periods of under 4 years. In addition to possible economy, cogeneration systems have other merits such as reliability, uninterrupted service, and national security.

\*This paper was not presented.

Mineral Cycling Model of the Thalassia Community as Affected by Thermal Effluents.

By Peter B. Schroeder and Anitra Thorhaug, Department of Biological Science, Florida International University, Tamiami Campus, Miami, Florida 33199.

ABSTRACT

The cooling water effluents from fossil fuel and nuclear power stations often contain low levels of heavy metals from nuclear plants and potentially contain radionuclides. When these effluents discharge into subtropical or tropical estuaries in the Caribbean area and the Gulf of Mexico, the biological community most directly affected is the tropical seagrass bed dominated by the marine angiosperm, Thalassia testudinum. These seagrass beds are very productive and form the basis of a food chain which supports many marine organisms harvested by man. In order to understand the process and explore the possible consequences of introducing pollutants at the base of a food chain leading to man we have prepared an energy circuit diagram and mathematical model of the flow of heavy metal and radiopollutants through a tropical seagrass community and into higher tropic levels.

The model comprises seven compartments: water, substrate, seagrasses, macroalgae, epiphytes, detritus and macroanimals. The model will be translated into CSSL (Continuous Systems Simulation Language) and coupled to a productivity-biomass model which is also presented. Simulations of different size communities under various environmental conditions and different levels of energy-related pollution will be made.

## INTRODUCTION

"The importance of seagrass meadows to coastal marine ecosystems is not fully understood and is generally underestimated...Despite the extensive studies on seagrass productivity and on the temporal and spatial variability in biological composition of seagrass communities, little is known of the general principles of ecosystem function and factors controlling 'ecological success' of the communities" (Thayer, et al., 1975).

Because of the location of seagrass communities in estuaries and often directly adjacent to the shoreline, they are one of the marine systems most directly impacted by man's activities. Seagrasses are directly subjected to increased nutrient loads, heavy metal, thermal, and radioactive pollutants, dredge and fill; and the effects of recreational activities, such as boating in the estuaries. The seagrass communities are the major basis of a food web that leads in many locations to man. Destruction of seagrasses leads to a great decrease in invertebrate and fish species (Thorhaug et al., 1974). In particular, as energy related industry expands in the coastal regions, increasing impact occurs on marine grassbeds. One of the large impacts of **energy** related industry is the release of trace metals into the environment. A number of studies have been made on the uptake and content of trace metals by specific marine organisms. Goldberg (1965) summarized these findings. A major deficiency in these studies is that most of the environmental parameters that might have affected the results were unrecorded .

In chemical studies in the subtropical estuary, Biscayne Bay, Florida, the seagrasses and macroalgae were found to contain a significant proportion of trace metals and to cycle significant fractions of the amount each year (Segar, et al., 1971, Gilio and Segar, 1976). Studies by

Parker (1962, 1966) indicate that two compartments, 'the sediment and the seagrass Thalassia testudinum KÜnig, constitute prime reservoirs for radio-nuclides added to the estuary and there can be a rapid flux between these two.

To understand trace metal flux in the seagrasses, one must consider the plants' physiology. Research on absorption of trace metals and other elements by aquatic plants was reviewed by Sutcliffe (1962). Early work was done with Vallisneria, Elodea and Lemna species, all fresh water aquatics not subjected normally to environments of fluctuating salinities. Submerged marine angiosperms such as Thalassia secondarily migrated to the sea; in readapting to an environment of fluctuating salinity, they have developed complex osmoregulatory microstructures and are able to maintain a steep electrochemical gradient with the surrounding water through selective exchange of ions (Jagels, 1973; Gessner, 1971). The result is a highly dynamic system dependent primarily on the maintenance of osmotic balance by the seagrasses. Osmoregulation in seagrasses is not only a function of salinity, but also of temperature and the molecular or ionic state of the minerals in the water (Schroeder, 1975), and possibly of light and other factors (Bachmann and Odum, 1960). Unless mineral cycling in these systems is studied as a dynamic function of interacting environmental parameters such as light, temperature, salinity; and biological factors such as photosynthesis and plant growth and senescence, at best it can be only partially understood.

Schroeder (1975) and Schroeder and Thorhaug (in press) found that radioactive cation uptake by the seagrass Thalassia testudinum occurred primarily by absorption on cation exchange sites and was largely reversible

by a wash with a solution of the nonradioactive isotope. A two step process of uptake was suggested. Initially, there was a large uptake, probably on the cation exchange sites located in the "outer space" of the plant. This process was readily reversible. A slower uptake of lesser magnitude also occurred, thought to represent cations which had been transported into the cell by the cell membrane.

Elemental content of this subtropical and tropical marine angiosperm was found to be concentration and temperature dependent; uptake may be increased several times by a temperature change of less than 5°C (Thorhaug and Schroeder, this volume). Gessner (1971) showed that Thalassia cells overcame plasmolysis resulting from increased salinity by uptake of cations. Bachmann and Odum (1960) strongly suggested that zinc-65 uptake by macroalgae was light controlled. Parker (1966) found that cobalt-60 content in Thalassia may be five times greater at night than during the day. As indicated by Walsh and Grow (1973), and Pulich et al. (1976) and others, sampling surveys of the distribution of elements in seagrass communities collected at only one discrete time may lead to erroneous conclusions concerning mineral cycling because of the magnitude of seasonal or diurnal changes. We conclude that the cycling of minerals through seagrass beds and the exchange of elements between the compartments in these ecosystems are dynamic processes and must be studied as a function of time and environmental variables.

#### The Model

The Thalassia seagrass community is a highly diverse system comprised of many species of plants and animals comparable to coral reefs in diversity (Thorhaug and Roessler, 1977 ). The composition and numbers of organisms

comprising the system change and shift with the seasons, especially in subtropical locations, complicating the statistical analysis of the effects of stress.

However, as a first approximation, the seagrass community can be conceptualized as a limited number of separate compartments which can be treated as components representing the entire system. Changes in the composition and functions of the organisms comprising a compartment can be interpreted as a quantitative change in the function of the compartment, *i.e.*, the interchange of the compartment with the other compartments in the system.

Because it is possible to compartmentalize the Thalassia seagrass system and quantify the flows between the compartments under different environmental conditions, it is possible to create mathematical models of productivity and mineral cycling in the Thalassia community. These models were created not only to simulate the response of the system to environmental change but also to provide a structure on which to design future research.

Two interlocking conceptual models were made. One is an energy flow model (Figure 1) used to quantify a representative Thalassia bed, and describe annual changes in its composition. The second is a model of the interchange of minerals (heavy metals, radiopollutants, micronutrients) between the compartments of the Thalassia seagrass system. It will be used as the basis for simulations of micronutrient cycling in the system and the biological concentration in marine food chains of pollutants released into nearshore waters or estuaries dominated by the Thalassia seagrass community.

Figures 1 and 2 show the biomass-productivity model and the model of mineral cycling respectively diagrammed in the symbolic modelling language

developed by H.T. Odum (1971). Both models are composed of major compartments: water, substrate, seagrasses, their epiphytes, macroalgae, detritus, and the macroscopic animals. The seagrass compartment is composed of two sub-compartments: the sub-sediment parts of the plant (roots and rhizomes) and the above-sediment parts (vertical short shoots, living and attached dead leaves).

The variable names used in the models are found in Table 1. The coefficients that pertain to each flow or exchange are shown as labels on the arrows indicating the pathways in the diagrams. Definitions of the rate symbols used in the biomass-productivity model are given in Table 2. Definitions of the rate symbols used in the mineral cycling model are given in Table 3. Values for all rates used in the models are dependent on environmental parameters, principally temperature and salinity.

The biomass-productivity model expressed in mathematical equations is found in Table 4. This model is relatively straightforward. A Michaelis-Menten expression is used to describe energy flow to Thalassia, the epiphytes, and the macroalgae. The  $K_m$  symbol used in these equations follows the convention of Michaelis-Menten equations and represents the level of light or nutrients allowing one-half maximum growth. A logistic expression is used to describe energy flow to the heterotrophic compartments. Respiration is assumed to be a simple exponential decay function of each biomass compartment. As a first approximation, epiphyte and Thalassia leaf conversion to detritus is assumed to be a mutually dependent function; when leaves are heavily epiphytized, they die and slough off, carrying their epiphytes with them.

The mineral cycling model expressed in mathematical equations is given in Table 5. Biomass values used in this model are generated by the biomass-productivity model previously described. Otherwise it is a simple mass

balance model. The water compartment is volume dependent as would be the case in tank microcosm studies. When used to simulate an actual or field situation, the water compartment would be considered infinite in volume. Losses by other compartments to the water would be considered losses from the system, and concentration of the mineral or element under study would remain unaffected in the water. The concentration in the water would be determined from a table function which would simulate the change in concentration in the water as it passed over the seagrass bed affected only by the source of the mineral and the flow of the water.

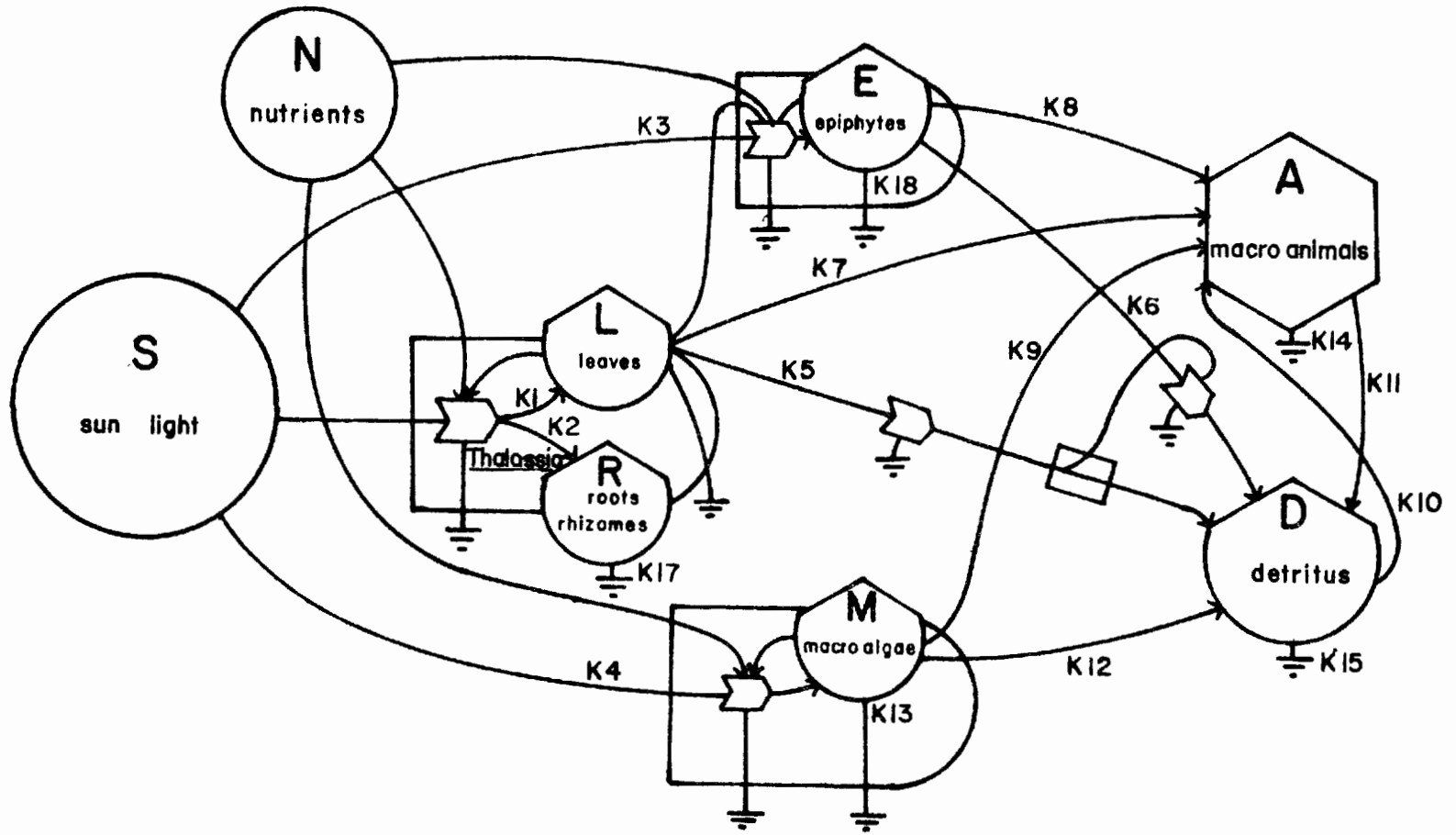
The mathematical models are presently being translated into Continuous Systems Simulation Language (CSSL) in order to produce computer simulations with the UNIVAC 1106 at the University of Miami Computer Center in Coral Gables, Florida.

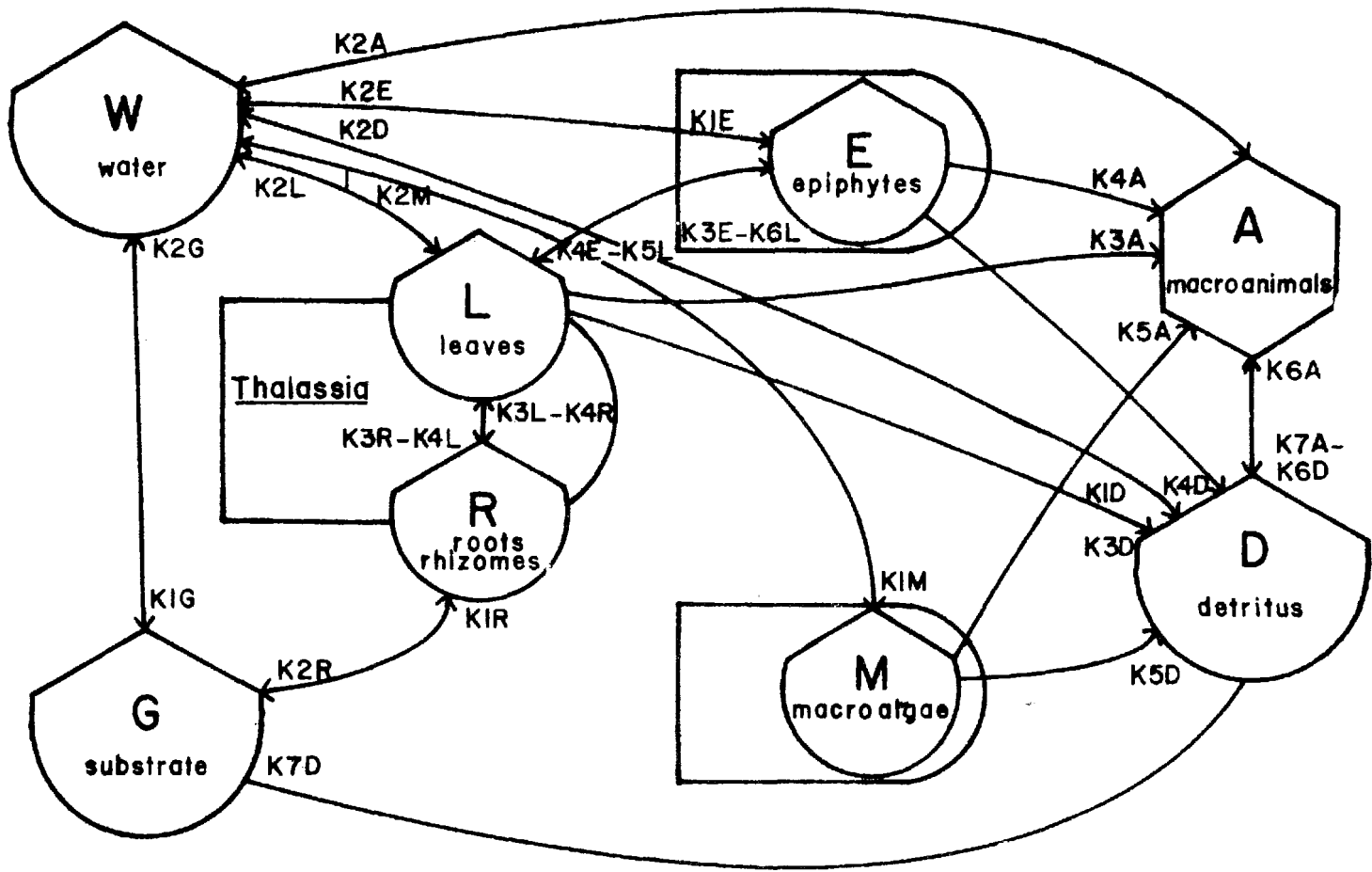
Coefficients for the mineral cycling model are being determined by a series of microcosm studies using radiotracers. Initial values of elemental content in the compartments are being taken from existing studies (Eisler et al., 1972; Gilio and Segar, 1976; Goldberg, 1965; Schroeder, 1975; Windom, 1972).

Coefficients for the biomass productivity model are also available for previous reports (Jones, 1968; Thorhaug and Garcia-Gomez, 1972; Thorhaug and Kellar, 1972; Bach, 1975; Josselyn, 1965; Penhale, 1976; Edwards, 1977; Greenway, 1977; Thorhaug and Roessler, 1977; Thorhaug, 1977). Initial conditions for simulations of this model will reflect actual conditions in the particular seagrass bed under study, or conditions in typical Thalassia communities will be used. Seagrass community data from upper subtropical (Thorhaug et al., in preparation), subtropical (Thorhaug and

Roessler, 1977; Thorhaug et al., 1973; Thorhaug and Stearns, 1972), and tropical (Puerto Rico - Schroeder, 1975; Jamaica - Greenway, 1977; Cuba - Buesa, 1974) can be compared for effects of energy-related industry.

1210





1211

Table 1. List of Variable Names Used in the Models.

---

S=SUN LIGHT

N=NUTRIENTS

I=TOTAL ACTIVITY OF COMPARTMENT

B=BIOMASS OF COMPARTMENT

V=VOLUME OR WEIGHT OF COMPARTMENT (SURFACE AREA OF SEDIMENT)

C=CONCENTRATION PER UNIT (GRAM-MILLILITER-AREA) IN COMPARTMENT

$\dot{B}$ =CHANGE IN BIOMASS (B) WITH TIME

$\dot{V}$ =CHANGE IN VOLUME (V) WITH TIME

$\dot{C}$ =CHANGE IN CONCENTRATION (C) WITH TIME

Subscripts

L=LEAVES

R=ROOTS-RHIZOMES

E=EPIPHYTES

M=MACROALGAE

A=ANIMALS

F=FECES

D=DETRITUS

W=WATER

G=SEDIMENT

O=INITIAL CONDITIONS

I=NEW CONDITIONS

Rates

K=Rates

Table 2. Definitions of Rate Symbols Used in Biomass-Productivity Model.

---

k1=Coefficient of above substrate Thalassia parts growth  
k2=Coefficient of below substrate Thalassia parts growth  
k3=Coefficient of epiphyte growth  
k4=Coefficient of macroalgae growth  
k5=Coefficient of conversion of above sediment Thalassia parts to detritus  
k6=Coefficient of conversion of epiphytes to detritus  
k7=Coefficient of macroanimal feeding on Thalassia  
k8=Coefficient of macroanimal feeding on epiphytes  
k9=Coefficient of macroanimal feeding on macroalgae  
k10=Coefficient of macroanimal feeding on detritus  
k11=Coefficient of conversion of macroanimals to detritus  
k12=Coefficient of conversion of macroalgae to detritus  
k13=Coefficient of macroalgae respiration  
k14=Coefficient of macroanimal respiration  
k15=Coefficient of respiration in detritus  
k16=Coefficient of respiration by above sediment Thalassia  
k17=Coefficient of respiration by below sediment Thalassia  
k18=Coefficient of respiration by epiphytes

Table 3. Definitions of Rate Symbols Used in Mineral Cycling Model.

---

k1L=Rate of uptake by leaves from water  
k2L=Rate of loss to water from leaves  
k3L=Rate of translocation from root-rhizomes to leaves=k4R  
k4L=Rate of translocation from leaves to root-rhizomes=k3R  
k5L=Rate of translocation from epiphytes to leaves=k4E  
k6L=Rate of translocation from leaves to epiphytes=k3E

k1R=Rate of uptake by roots from sediment  
k2R=Rate of loss to sediment from roots  
k3R=k4B  
k4R=k3B

k1E=Rate of uptake by epiphytes from water  
k2E=Rate of loss to water from epiphytes  
k3E=k6L  
k4E=k5L

k1M=Rate of uptake by macroalgae from water  
k2M=Rate of loss to water from macroalgae

k1A=Rate of uptake by animals from water  
k2A=Rate of loss to water by animals  
k3A=Rate of feeding on leaves  
k4A=Rate of feeding on epiphytes  
k5A=Rate of feeding on macroalgae  
k6A=Rate of feeding on detritus  
k7A=Rate of excretion=k6D

k1D=Rate of uptake by detritus from water  
k2D=Rate of loss to water from detritus  
k3D=Rate of conversion of leaves to detritus  
k4D=Rate of conversion of epiphytes to detritus  
k5D=Rate of conversion of macroalgae to detritus  
k6D=k7A  
k7D=Rate of mineralization of detritus

k1G=Rates of uptake by sediment from water  
k2G=Rate of loss to water from sediment

Table 4. Biomass-Productivity Model.

$$\dot{L} = k_1 NL \left( \frac{N}{K_{mn1} + N} \right) \left( \frac{S}{K_{ms1} + S} \right) - k_{16}L - k_5LE - k_7LA(1-cA)$$

$$\dot{R} = k_2 NL \left( \frac{N}{K_{mn2} + N} \right) \left( \frac{S}{K_{ms2} + S} \right) - k_{17}R$$

$$\dot{E} = k_3 NE \left( \frac{N}{K_{mn3} + N} \right) \left( \frac{S}{K_{ms3} + S} \right) - k_5k_6LE - k_8EA(1-cA) - k_{18}E$$

$$\dot{M} = k_4 NM \left( \frac{N}{K_{mn4} + N} \right) \left( \frac{S}{K_{ms4} + S} \right) - k_{12}D - k_{13}M - k_9MA(1-cA)$$

$$\dot{A} = (k_7L + k_8E + k_9M + k_{10}D)(1-cA)A - k_{11}A - k_{14}A$$

$$\dot{D} = k_5LE + k_6k_5LE + k_{11}A + k_{12}M - k_{15}D$$

Table 5. Mineral Cycling Model.

---

Leaves-Vertical Shoots

$$ILI = ILO + \dot{C}L \text{ BL} + CL \dot{B}L$$

$$CL = K1L \text{ CW} - K2L \text{ CL} + K3L \text{ CR} - K4L \text{ CL} + K5L \text{ CE} - K6L \text{ CL}$$

Roots-Rhizomes

$$IRI = IRO + \dot{C}R \text{ BR} + CR \text{ BR}$$

$$CR = K1R \text{ CG} - K2R \text{ CR} + K3R \text{ CL} - K4R \text{ CR}$$

Epiphytes

$$IEI = IEO + \dot{C}E \text{ BE} + CE \dot{B}E$$

$$CE = K1E \text{ CW} - K2E \text{ CE} + K3E \text{ CL} - K4E \text{ CE}$$

Macroalgae

$$IMI = IMO + \dot{C}M \text{ BM} + CM \dot{B}M$$

$$CM = K1M \text{ CW} - K2M \text{ CM}$$

Macroanimals

$$IAI = IAO + \dot{C}A \text{ BA} + CA \dot{B}A$$

$$CA = K1A \text{ CW} - K2A \text{ CA} + K3A \text{ CL} + K4A \text{ CE} + K5A \text{ CM} + K6A \text{ CD} - K7A \text{ CA}$$

Detritus

$$IDI = IDO + \dot{C}D \text{ BD} + CD \dot{B}D$$

$$CD = K1D \text{ CW} - K2D \text{ CD} + K3D \text{ CL} + K4D \text{ CE} + K5D \text{ CM} + K6D \text{ CA} - K7D \text{ CD}$$

Water

$$IWI = IWO + \dot{C}W \text{ VW} + CW \dot{V}W$$

$$\dot{C}W = K2L \text{ CL} - K1L \text{ CW} + K2E \text{ CE} - K1E \text{ CW} + K2M \text{ CM} - K1M \text{ CW} + K2A \text{ CA} - K1A \text{ CW} \\ + K2D \text{ CD} - K1D \text{ CW} + K2G \text{ CG} - K1G \text{ CW}$$

Substrate

$$IGI = ISO + \dot{C}G \text{ VG} + CG \dot{V}G$$

$$CG = K1G \text{ CW} - K2G \text{ CG} + K2R \text{ CR} - K1R \text{ CG} + K7D \text{ CD}$$

Captions for Illustrations

Fig. 1 Thalassia testudinum Biomass-productivity model

Fig. 2 Thalassia testudinum Mineral cycling model

LITERATURE CITED

- Bach, S.D. 1975. The Distribution and Production of Calcareous Macroalgae in Card Sound, Florida. Ph.D. Dissertation. . University of Michigan, Michigan.
- Bachmann, R.W. and E.P. Odum. 1960. Uptake of zinc-65 and primary productivity in marine benthic algae. Limnol. Oceanogr., 5(4):349-355.
- Buesa, R.J. 1974. Population and biological data on turtle grass (Thalassia testudinum König, 1805) on the Northwestern Cuban shelf. Aquaculture, 4(2):207-226.
- Edwards, R.E. 1977. Respiration of a Shallow-water Benthic Community Associated with the Seagrass Halodule wrightii. Masters Thesis. University of Miami, Florida.
- Eisler, R., G.E. Zoroogian and R.J. Hennekey. 1972. Cadmium uptake by marine organisms. J. Fish. Res. Bd. Canada, 29:1367-1369.
- Gessner, F. 1971. The water economy of the seagrass Thalassia testudinum. Mar. Biol., 10:258-260.
- Gilio, J.L. and D.A. Segar. 1976. Biogeochemistry of trace elements in Card Sound, Florida. Inventory and annual turnover. IN: Symposium on Biscayne Bay, University of Miami, Florida.
- Goldberg, E.D. 1965. Review of Trace Element Concentrations in Marine Organisms. 2 vol. P.R. Nuclear Center, Mayaguez, P.R.
- Greenway, M. 1977. The Production and Utilization of Thalassia testudinum in Kingston Harbor, Jamaica. Ph.D. Dissertation. University of West Indies, Kingston, Jamaica.
- Jagels, R. 1973. Studies of the marine grass Thalassia testudinum. I. Ultrastructure of the osmoregulatory leaf cells. Amer. J. Bot., 60(10): 1003-1009.

- Jones, J.A. 1968. Primary Productivity by the Tropical Marine Turtle Grass, *Thalassia testudinum* König and Its Epiphytes. Ph.D. Dissertation. University of Miami, Florida.
- Josselyn, M.N. 1975. The Growth and Distribution of Two Species of *Laurencia*, a Red Macroalgae, in Card Sound, Florida. Masters Thesis. University of Miami, Florida.
- Odum, H.T. 1971. Environment, Power, and Society. John Wiley & Sons, N.Y.
- Parker, P.L. 1966. \_\_\_\_\_ in a Texas bay. Publ. Inst. Mar. Sci. Univ. Texas, 8:75-79.
- \_\_\_\_\_. 1966. Movement of radioisotopes in a marine bay: cobalt-60, iron-59, manganese-54, zinc-65, sodium-22. Publ. Inst. Mar. Sci. Univ. Texas, 11:102-107.
- Penhale, P.A. 1976. Primary Productivity, Dissolved Organic Carbon Excretion, and Nutrient Transport in an Epiphyte-Eelgrass (*Zostera marina*) System. Ph.D. Dissertation. N.C. State University, N.C.
- Pulich, W., S. Barnes and P. Parker. 1976. Trace metal cycles in seaweed communities, in Wiley, M. (ed.). Estuarine Processes. I. Academic Press, N.Y.
- Schroeder, P.B. 1975. Thermal Stress in *Thalassia testudinum*. Ph.D. Dissertation. University of Miami, Florida.
- \_\_\_\_\_, and A. Thorhaug. (in press) Uptake of zinc-65 by *Thalassia testudinum*. Mar. Biol.
- Segar, D., S. Gerchakov and T. Johnson. 1971. Chemistry, in R.G. Bader and M. Roessler (eds.). Ecological Study of South Biscayne Bay and Card Sound. University of Miami, Florida.

- Sutcliffe, J.F. 1962. Mineral Salts Absorption in Plants. Pergamon Press, N.Y.
- Thayer, G.W., D.A. Wolfe and R.B. Williams. 1975. The impact of man on seagrass systems. Amer. Scientist, 63:288-295.
- Thorhaug, A. (in preparation) Primary production measured on a long term basis of the seagrass Thalassia testudinum in two subtropical estuaries fringing the tropics.
- \_\_\_\_\_, and J. Garcia-Gomez. 1972. Preliminary laboratory and field growth studies of Laurencia complex. J. Phycol., 8(S):10.
- \_\_\_\_\_, and K.F. Kellar. 1972. Laboratory and field growth studies of four green calcareous algae. I. Preliminary results. J. Phycol., 8(S):10.
- \_\_\_\_\_, and M.A. Roessler. 1977. Seagrass community dynamics in a subtropical estuarine lagoon. Aquaculture, 12:253-277.
- \_\_\_\_\_. M.A. Roessler, and D.A. Segar. 1973. Impact of a power plant on a subtropical estuarine environment. Bull. Mar. Poll., 7(11):166-169.
- \_\_\_\_\_. and P.B. Schroeder. 1977. Synergistic effect of temperature, salinity and heavy metals on subtropical versus tropical populations of the seagrass Thalassia testudinum. Energy and Environmental Stress on Aquatic Systems; ERDA Symposium, Augusta, Georgia.
- \_\_\_\_\_ and R.D. Stearns. 1972. A preliminary field and laboratory study of physiological aspects of growth and reproduction of Thalassia testudinum. Amer. J. Bot., 59:670.
- Walsh, G.E. and T.E. Grow. 1973. Composition of Thalassia testudinum and Nuppia maritima. Quart. J. Fla. Acad. Sci., 35:97-108.
- Window, H.L. 1972. Arsenic, cadmium, copper, lead, mercury and zinc in marine biota - North Atlantic Ocean, in Baseline Studies of Pollutants in Marine Environment. Background papers for IDOE Workshop, Brookhaven Nat. Lab. May 1972. Unpublished.

Synergistic Effects of Substances Emitted from Power Plants on Subtropical and Tropical Populations of the Seagrass Thalassia testudinum: Temperature, Salinity and Heavy Metals.

By Anitra Thorhaug and Peter B. Schroeder, Department of Biological Science, Florida International University, Tamiami Campus, Miami, Florida 33199.

ABSTRACT

The seagrass Thalassia testudinum is the dominant species in much of the Gulf of Mexico and Caribbean nearshore marine system. Dense meadows of seagrasses appear immediately adjacent to the shoreline where energy related industry has often been sited. Power plants have released their heated effluents accompanied by salinity changes (dilution causing lower salinity, or waters evaporated in cooling ponds raising salinities) along with heavy metals on seagrasses causing damage. Although the effect of temperature on the heated effluents in the tropics and subtropics is of fundamental importance in mortality of organisms, it has been shown that there are sublethal temperature regimes where synergistic effects of other effluent components probably figure importantly. Field data from two subtropical and on tropical effluent canals have recently been compared (Thorhaug, Blake and Schroeder, 1978). Unfortunately, measurements of all parameters are usually not frequent enough in field situations to delineate the entire topological surface of synergy. Therefore, detailed laboratory experiments using tropical and subtropical Thalassia were undertaken to describe synergistic effects. Temperature versus uptake of heavy metals appears fairly similar and predictable for most cations in the 20° to 30° C range; there are minima in all cationic uptake examined at 30° to 32°C; above this there is a strongly accelerated rate of uptake of metals. High salinities (50%) lower the upper lethal temperature by one to two degrees centigrade; lower salinities (20%) have a much smaller effect. A comparison of power plant effluents from Gulf of Mexico to Central Caribbean shows summer effluent temperatures are in the range of 31° to 35°C, which is the sublethal to lethal area of maximum effect of synergy examined in laboratory experiments. This emphasizes that the tropics are "on the brink of disaster."

## I. INTRODUCTION

Throughout the Gulf of Mexico, Caribbean and southeastern Florida coast, the seagrass Thalassia testudinum is the dominant nearshore species. It is most dense very close to shore, decreasing in productivity and abundance as one goes seaward. Thus, energy-related industry, often sited on estuaries or marine shorelines, has in the past impacted this densest zone of Thalassia in a series of sites (Thorhaug, 1974; Thorhaug et al., 1977; Thorhaug and Schroeder, 1977). Heated effluents from cooling canals have been shown to have a lethal effect on Thalassia populations from the subtropics and tropics above 35°C for extended time periods such as ten days (most recently reviewed by Thorhaug et al., 1977). However, it is in the sublethal temperature regime, where temperature (usually the dominant factor from heated effluents from power plants) is not lethal, that interests us. At sublethal temperatures, the synergistic effects of other substances, such as salinity and/or heavy metals, come into focus.

There has been little quantified field evidence for the effects of heavy metals and/or salinity changes on such populations. The critical question is "How long does the maximum or minimum condition impinge on the population?" The question of lethal substances at power plants has usually been answered by data which reports the average salinity or average heavy metal concentration during a certain season, or gives the yearly limits, but not their duration. Because detailed series of measurements of heavy metals and other pollutants at power plants were not available during the summer months when the sublethal effects were encountered, and also due to the many interaction factors present in thermal effluents, we have necessarily resorted to laboratory measurements to understand the detailed synergistic effects of high temperature, salinity and heavy metals.

The effect of heavy metals on Thalassia has received little attention in the literature. Biogeochemists have examined the cycling of radionuclides. Parker (1962, 1963, 1966) in a Texas Bay showed zinc was important in the mineral cycling in these shallow waters. Gilio and Segar (1976) showed a good deal of the trace element content in the Card Sound estuary was accumulated in Thalassia in an inventory of the major trace metal components (Tables 1 and 2) and these authors extrapolated the rate of cycling through Thalassia would be a critical factor in mineral cycling in Card Sound (Table 3).

Schroeder and Thorhaug (in press) showed that Thalassia seedlings take up zinc-65 both through roots and leaves, dependent on which organ is exposed to the radionuclides. Cations such as zinc can be translocated from the root to the leaf or vice versa. Seeds do not have a significant role in uptake. Much of the original cation concentration is adsorbed to exchange sites on the surface and can be washed off. Heavy metals can be concentrated in tissues up to 500 times ambient sediment water concentration within 10 days in these seagrasses which form the base of the detrital food chain in subtropical and tropical estuaries. Pumping effects of heavy metals from sediment to water or vice versa did not appear significant. Previously McRoy et al. (1972) have postulated a phosphate pump by another seagrass Zostera, which mechanism was suggested by Gilio and Segar (1976) as possibly occurring with the cations in Thalassia.

In this present discussion we examine the combined effect of temperature and salinity on the uptake of metals in Thalassia from the tropics and from the subtropics to begin a determination of synergistic effects of temperature dependencies which might be found in sites impacted by energy-related industry.

## II. METHODS

### A. Radiotracer Experiments

The ability to grow Thalassia under laboratory conditions has been demonstrated in the past (Thorhaug, 1971, 1972, 1974). Large plugs of the seagrass Thalassia testudinum with sediment were removed from the field in snug fitting vessels and returned to the laboratory. Glass tanks into which these plugs fit snugly were provided with grow-lux lights (eight hours on, sixteen hours off), calcareous sediment, and aeration.

Temperature was controlled by aquarium immersion heaters ( $\pm 0.5^{\circ}\text{C}$ ). Filtered seawater was used; salinity was adjusted by using artificial seawater diluted to the appropriate salinity level in daily checks.

A cocktail of salts of zinc-65, cobalt-57, cobalt-60, cesium-137, manganese-54, silver-108, and iron-59 was prepared so that all isotopes would have approximately the same radioactivity. The mixture was added to tanks of unfiltered seawater 35‰; pH was adjusted to normal within a short time period. All cations except cobalt-60 (added as cobaltamine) were introduced as elemental ions.

At 4, 11, 18, 23 and 31 days, plant samples were removed, rinsed thoroughly, fractionated into roots, rhizomes, blades and seeds, dried at  $105^{\circ}\text{C}$  and weighed. Samples were then placed mixed with plaster of Paris in petrie dishes to provide the same geometry for all samples.

Counting procedures included counting on a shielded germanium semiconductor detector. Multichannel pulse height analyzer separated counts into 1024 channels of which 299 were used for analysis. Energy intervals were 1.5KeV. 120 samples and 8 standard spectra were used. A computer program analyzed disintegrations per minute per g dry weight for each radionuclide. Two cobalt radio-

isotopes provided an additional internal check for running a dummy sample spectrum.

## B. Salinity-temperature Experiments

Plants collected as seeds in the Florida and Bahamas areas by methods of Thorhaug (1974) were held in out-of-door running-seawater tanks with six inches of peat sediment (described also in Thorhaug, 1974) replanted in these tanks for observation.

Two types of temperature control devices were utilized to determine upper temperature limits: polythermostats and controlled temperature baths. The procedure and apparatus have been thoroughly described by Thorhaug (1976). Basically Millipore filtered (Whatman #42) seawater was adjusted to appropriate salinity with "Instant Ocean," then equilibrated in the temperature device. In the two polythermostats, six small seedlings per cuvette were utilized; large numbers of seedlings or mature plants could be used in the temperature baths. Specimens were exposed to a steady-state temperature for a given time, at the conclusion of which specimens were carefully examined, tagged and planted in a second outdoor running-seawater tank for observation of death (1 month holding time). Two to four month seedlings and mature plants with rhizomes and roots intact were utilized. Time of exposure was 12, 24, and 48 hours; salinities 20, 36 and 50‰,  $\pm 0.5\%$ ; temperature 30° to 45°C,  $\pm 0.05^\circ\text{C}$ .

## III. RESULTS

### A. Trace Metal Uptake

In experiments at ambient salinity with Puerto Rican specimens, uptake rates of cations to whole plants (fractionated into blades and roots) showed

one dependency from 30° (or 32°C) to 37° (or 38°C) and usually around 37° to 38°C an abruptly decreasing dependency (Figures 1 and 2), which is the accumulated data of four trials, six plants per temperature per trial. In some cases (Co-57, Co-60, Fe-59, Na-22, Zn-65, Bi-207) there was little dependency on temperature below 30°C. In most cases 30° to 32°C was a minimum and 35° to 37°C was a maximum for uptake. It should be noted that in a second study of uptake, between 38° and 40°C the uptake markedly decreased, probably representing mortality processes occurring within the plant. Bismuth showed the least strong temperature dependency; cesium, cobalt, manganese and sodium the most.

Those cations in the transition groups of the periodic table appeared to have a similar temperature dependency as did sodium (note abscissa of sodium is  $10^6$  while all others are  $10^5$ ) with cesium. The later two were strangely temperature dependent. Table 4 is a regression analysis of activities of each radiotracer versus each other as a function of temperature and time. Especially notable are close correlations of bismuth, cesium, sodium. One should note that cobalt-60 was introduced as cobaltamine while others were introduced as elemental ions

The introduction of the radionuclide into the seawater did not increase the total content of the elements to any appreciable extent, except bismuth (24.6%) and cesium (22.6%), which were very low in ambient seawater. In no case in these results were the concentrations of trace metals near the toxification levels. Due to a germanium-gel detector being used for analyses, water radioactive concentrations were below the limits of detection.

#### B. Salinity-temperature Experiments.

These 92 experiments on both Thalassia seedling and mature specimens,

between 20 and 50‰ salinity, 25°C to 40°C, and 6 to 96 hours showed that upper temperature lethal limits were more sensitive to salinities 15‰ above (i.e., 50‰) mean than 15‰ below (Figure 3). The temperature-mortality curve resembled a step-function for 20 and 36‰, while the 50‰ resembled a skewed Gaussian curve. At 36‰ for 12 hours the upper survival temperature limit was 36°C, which dropped to 35°C at 48 hours, and was the same at 20‰, while at 50‰, 48 hours, the limit was 33°C. Tests showed no difference between seedling and ~~nature plant~~ lethal limits.

The two cobalt isotopes acted as an internal check on the methodology itself. Behavior of these two radioisotopes in leaves, roots and rhizomes was quite similar.

#### IV. DISCUSSION

The effect of temperature on the survival and physiology of the seagrass Thalassia is profound. In many subtropical and tropical estuarine areas, ambient summer temperatures are near a mean of 30°C with mid-afternoon excursions in shallow water to 33° or 34°C. Yet the upper tolerance limits for Thalassia over a long time period are 34° to 36°C (Thorhaug et al., in press), very close to non-impacted summer temperatures. High salinity (50‰) as seen in our results, affects this upper temperature limit, causing it to fall to 33°C. Lower salinities (in the range of 20‰) do not have much effect from normal (34‰) on upper temperature tolerance, perhaps indicating less adaptation to saline conditions than the brackish water from which ancestors of Thalassia arose.

The sublethal temperature area from 31°C upward is particularly of interest to those concerned with thermal effluents from power plants. The uptake of most of the radioisotopic cations investigated is highly temperature dependent above

31° to 32°C. A minimum occurs at about 30° to 32° C with a maximum near 35° to 38°C. Below 30°C, the temperature dependency varies from a low temperature coefficient in elements such as zinc-65 and bismuth-207 to high temperature coefficients in cesium-137 and sodium-22. Both above and below 30°C, bismuth showed less strong temperature dependency than the other elements. Temperatures in the range above 31° to 32°C produce higher uptake of the heavy metals than temperatures below 30°C in general. This is significant for thermal effluents of semitropical and tropical power plants, which release both heavy metals and cause temperature regimes above 31° to 32°C for periods of three to five months in the semitropics and longer in the tropics.

There are several levels of information to be obtained from this data including implications for: the organismic level of Thalassia functioning; and cooling canal operation.

The major implications for Thalassia plant physiology are several. Trace metals accumulate rapidly from external sources in Thalassia tissue. Within hours concentrations of several times ambient appear and within days, accumulations build to several hundred times ambient. The elements can enter through either roots and rhizomes from sediment concentrations of metals or from the water column via leaves. Translocation between tissues occurs rapidly within hours within the plant (Schroeder and Thorhaug, in press). Coefficient of uptake in roots and leaves differs but the effect of temperature on uptake in roots and leaves is fairly similar.

The implications of these studies to cooling canals from power plants are several. First, 15% concentration of salts in normal seawater (32 to 35%) such as released from cooling ponds (or other evaporating devices) appears to have an effect in lowering Thalassia lethal temperature limits, whereas lowering

the salt in seawater 15‰, such as occurs in dilution processes with fresh or brackish water, has little effect on thermal lethal limits. A caveat here is that salinities below 20‰ have not yet been studied, nor have longterm (greater than 72 hour) cycles been studied. The effect of temperatures found in tropical effluent waters and in summer effluent waters in the subtropics is to increase the rate of uptake and thus the accumulation rate of heavy metals. Some elements are accumulated several times in concentration and rate of uptake in ranges of thermal effluents (32° to 35°C) than in lower, normal temperature ranges. The accumulation of these cations appears to be proportional to the concentrations present in water or sediments (within the ranges studied). Accumulation rates from sediment through roots/rhizomes or from the water column through leaves have similar temperature dependencies for a particular element. Heavy metals enter Thalassia either through the blades or through the roots/rhizomes so that accumulations in the sediment or spikes of elements (such as might occur during spills or cleaning processes) into the water column would cause accumulation in Thalassia.

It should be noted that in the above discussion on cooling canal effluents that temperature and temperature-salinity relations for Thalassia are in full accord with field data found at Turkey Point and Guayanilla Bay (Thorhaug and Schroeder, 1977), but that the heavy metal accumulation rates have not yet been tested under field conditions. Results are in progress for synergistic comparison of temperature, salinity and heavy metal uptake in tropical versus subtropical populations.

#### ACKNOWLEDGEMENTS

The authors appreciate the support of ERDA grant # E(40-1) 4493 for the support of the bulk of the reported work. Part of the Puerto Rican work was sponsored by the Puerto Rican Nuclear Center in Mayaguez, Puerto Rico and the laboratory graduate participation program of the Oak Ridge Associated Universities, Inc., to Dr. Schroeder.

#### LITERATURE CITED

- Gilio, J. L. and D. A. Segar. 1974. Biogeochemistry of trace elements in Card Sound, Florida. Inventory and annual turnover. pp. 1-17. IN: A. Thorhaug (ed.) Biscayne Bay: Past, Present and Future. Sea Grant Sp. Report No.5, Univ. of Miami, Miami, Florida.
- McRoy, C., R. Barsdate and Nebert. 1972. Phosphorus cycling in an eelgrass (Zostera marina L.) ecosystem. *Limn. Oceanogr.* 17:58-67.
- Parker, P. L. 1962. Zinc in a Texas bay. *Publ. Inst. Mar. Sci., Univ. Texas.* 8:75-79.
- Parker, P. L., A. Gibbs and R. Lowler. 1963. Cobalt, iron and manganese in a Texas bay. *Publ. Inst. Mar. Sci. Univ. Texas.* 9:28-32.
- Parker, P. L. 1966. Movement of radioisotopes in marine bay: cobalt-60, iron-59, manganese-54, zinc-65, sodium-22. *Publ. Inst. Mar. Sci. Univ. Texas.* 11:102-107.
- Thorhaug, A. 1971. Grasses and macroalgae. IN: R. G. Bader and M. A. Roessler (eds.) An Ecological Study of South Biscayne Bay and Card Sound. Progrs. Rpt. to AEC (AT(40-1)-3801-3) and FPL Co. ML 71066.
- Thorhaug, A. 1972. Laboratory thermal studies. IN: R. G. Bader and M. A. Roessler (eds.) An Ecological Study of South Biscayne Bay and Card Sound. Prgrs. Rpt. to AEC (AT(40-1)-3801-4) and FPL Co. RSMAS 72060.
- Thorhaug, A. 1974. Effect of thermal effluents on the marine biology of southeastern Florida. pp. 518-531. IN: J. W. Gibbons and R.R. Sharitz (eds.) Thermal Ecology. AEC Symp. Series (Conf. 730505).
- Thorhaug, A. 1976. Tropical macroalgae as pollution indicator organisms. *Micronesica* 12(1):49-68.

Thorhaug, A., N. Blake and P. Schroeder. 1977. The effects of heated effluents from power plants on the seagrass Thalassia testudinum quantitatively comparing estuaries in the subtropics to the tropics. Mar. Poll. Bull. 9(7):181-187.

Thorhaug, A. and P. Schroeder. 1977. A comparison of the biological effects of heated effluents from two fossil fuel plants: Biscayne Bay, Florida, in the subtropics; Guayanilla Bay, Puerto Rico, in the tropics. Vol 3, 11B:133-164. IN: S. Lee and S. Sengupta (eds.). Waste Heat Management and Utilization. Miami, Florida.

Table 1. Trace element concentrations for marine organisms of Card Sound, Florida as determined by Gilio & Segar, 1976. Numbers in parenthesis are the number of samples. (from Gilio & Segar, 1976)

|  | Elements (ug/g dry weight) ± Standard Error of the Mean |           |               |           |              |              |
|--|---|-----------|---------------|-----------|--------------|--------------|
|  | V   | Fe        | Cu            | Zn        | Cd           | Pb           |
| <b>Macrophyta</b>                        |   |           |               |           |              |              |
| <u>Thalassia testudinum</u> (46)         | 8.5 ± 1.2   | 320 ± 46  | 1.6 ± 0.33(a) | 18 ± 1.3  | 0.20 ± 0.021 | 0.72 ± 0.16  |
| <u>Laurencia poitei</u> (14)             | 96.0 ± 58   | 420 ± 75  | 12 ± 2.4      | 34 ± 5.1  | 0.20 ± 0.047 | 0.59 ± 0.16  |
| <u>Penicillus capitatus</u> (34)         | 4.8 ± 0.72  | 560 ± 77  | 1.2 ± 0.17    | 12 ± 3.5  | 0.11 ± 0.012 | 1.1 ± 0.21   |
| <u>Halimeda incrassata</u> (4)           | 2.4 ± 0.78  | 230 ± 75  | 0.70 ± 0.26   | 3.7 ± 1.2 | 0.16 ± 0.12  | 1.2 ± 0.56   |
| <u>Rhizophora mangle</u> (7)             |   |           |               |           |              |              |
| Leaves (b)                               | .43 ± .29   | 100 ± 76  | 1.3 ± .67     | 3.1 ± .88 | .044 ± .028  | .39 ± .11    |
| (c)                                      | .52 ± .22   | 71 ± 20   | 5.8 ± 4.6     | 2.3 ± .52 | .24 ± .11    | .79 ± .23    |
| Seedlings in water (3)                   | .48 ± .41   | 12 ± 5.6  | 0.81 ± 0.79   | 2.2 ± .58 | .017 ± .0059 | .23 ± .17    |
| Decaying stems in water (2)              | .056 ± .055   | 140 ± 0   | 0.52 ± 0.46   | 8.1 ± 5.9 | .056 ± .055  | .099 ± .0072 |
| <b>Microphyta</b>                        |   |           |               |           |              |              |
| <u>Phytoplankton</u> (d)                 | 0.33  | 730       | 12 ± 8.0      | 180 ± 80  | .20          | .33          |
| <u>Epiphytes on Thalassia blades</u> (e) | 96  | 420       | 21 ± 9.4      | 150 ± 59  | .20          | 0.59         |
| <b>Macrofauna</b>                        |   |           |               |           |              |              |
| <u>Detritivores and Carnivores</u> (4)   | 0.77 ± 0.07   | 41 ± 8.9  | 7.4 ± 0.67    | 28 ± 20   | 0.19 ± 0.08  | 0.39 ± 0.15  |
| <u>Sponges</u> (7)                       | 2.8 ± 1.5   | 530 ± 150 | 3.7 ± 1.5     | 24 ± 9.8  | .44 ± .18    | .36 ± .15    |

Notes: (a) Possible error due to a high Cu blank; (b) Live leaves; (c) Dead leaves; (d) Values for V, Fe, Cd, and Pb, 15-fold lower than Bowen's 1966 data. Cu and Zn values determined in this study as 15-fold lower than Bowen's values; (e) Values same as Laurencia poitei.

Figure 2. Trace element inventory for Card Sound, Florida.  
(from Gilio & Segar, 1976)

| Compartment                 | Biomass <sub>2</sub><br>g dry wt/m <sup>2</sup> | V                        | Elements (mg/m <sup>2</sup> ) |                       |                       |                          |                          |
|-----------------------------|---|--------------------------|-------------------------------|-----------------------|-----------------------|--------------------------|--------------------------|
|                             |   |                          | Fe                            | Cu                    | Zn                    | Cd                       | Pb                       |
| Sediment (1)                | 3.4 x 10 <sup>5</sup>                           | 8.0 x 10 <sup>3</sup>    | 6.3 x 10 <sup>5</sup>         | 6.7 x 10 <sup>2</sup> | 1.4 x 10 <sup>3</sup> | 23                       | 3.4 x 10 <sup>2</sup>    |
| Water                       | 3.0 x 10 <sup>6</sup>                           | 2.6                      | 5.2 x 10 <sup>2</sup>         | 1.2 x 10 <sup>2</sup> | 2.6 x 10 <sup>2</sup> | 2.1                      | 15                       |
| <b>Biota</b>                |   |                          |                               |                       |                       |                          |                          |
| <u>macrophyta</u>           |   |                          |                               |                       |                       |                          |                          |
| <u>Thalassia testudinum</u> | 1.67 x 10 <sup>2</sup>                          | 1.4                      | 53                            | .27                   | 3.0                   | .033                     | .12                      |
| <u>Laurencia poitei</u>     | 6.1 (2)   | 0.23                     | 2.6                           | 0.073                 | 0.21                  | .0012                    | .0036                    |
| <u>Halimeda</u> group       | 8.7 (3)   | 0.023                    | 2.2                           | 0.0068                | 0.036                 | .0016                    | .012                     |
| <u>Penicillus</u> group     | 3.1 (4)   | 0.015                    | 1.7                           | 0.0037                | 0.037                 | .00034                   | .0034                    |
| <u>Microphyta</u>           |   |                          |                               |                       |                       |                          |                          |
| epiphytes                   | 10  | .96                      | 4.2                           | .21                   | 1.5                   | .002                     | .0059                    |
| phytoplankton               | 0.28  | .0092 x 10 <sup>-2</sup> | .064                          | .0034                 | .050                  | .0076 x 10 <sup>-3</sup> | .0092 x 10 <sup>-2</sup> |
| <u>Macrotauna</u>           |   |                          |                               |                       |                       |                          |                          |
| sponges                     | 1.1 x 10 <sup>2</sup>                           | 0.032                    | 89                            | 0.19                  | 2.1                   | .030                     | 0.014                    |
| <u>Detritivores</u>         |   |                          |                               |                       |                       |                          |                          |
| Carnivores                  | 0.18 (5)  | 0.021 x 10 <sup>-2</sup> | 0.011                         | 0.002                 | 0.075                 | .055 x 10 <sup>-3</sup>  | .011 x 10 <sup>-2</sup>  |
| <b>Biota Total</b>          | <b>3.1 x 10<sup>2</sup></b>                     | <b>2.7</b>               | <b>150</b>                    | <b>0.76</b>           | <b>7.0</b>            | <b>0.068</b>             | <b>0.16</b>              |

- Notes: (1) Calculated from concentration data of trace elements in Card Sound, Florida from Pellenberg (1973). Includes total sediment depth and total element concentrations
- (2) Josselyn (1975).
- (3) Calculated from Bach (1975). Includes Halimeda incrassata (5.5), H. monile (1.5), and H. opunta (1.4).
- (4) Calculated from Bach (1975). Includes Penicillus capitatus (1.7), Rhizocephalus phoenix (0.51) and Udotea flabellum (0.48).
- (5) Gilio et al. (in prep.).

Table 3. Trace element biological turnover potential. Derived from the product of annual net production data of Card Sound and trace element concentrations. (from Gilio & Segar, 1976)

Trace Element Biological Turnover Potential  $\text{mg/m}^2/\text{yr}$

| <u>Compartment</u>        | <u>Annual Net Production <math>\text{g/m}^2/\text{yr}</math></u> | <u>V</u>   | <u>Fe</u>   | <u>Cu</u>  | <u>Zn</u>  | <u>Cd</u>   | <u>Pb</u>   |
|---------------------------|--|------------|-------------|------------|------------|-------------|-------------|
| <b>Macrophyta</b>         |  |            |             |            |            |             |             |
| <u>Thalassia</u> (blades) | 609.   | 5.2        | 200.        | 0.97       | 11.        | 0.12        | 0.44        |
| <u>Laurencia</u>          | 11.  | 1.1        | 4.6         | 0.13       | 0.37       | 0.0022      | 0.0065      |
| <u>Penicillus</u>         | 4.3 (1)  | 0.021      | 2.4         | 0.0052     | 0.052      | 0.00047     | 0.0047      |
| <u>Halimeda</u>           | 8.6 (2)  | 0.021      | 2.0         | 0.0060     | 0.032      | 0.00014     | .010        |
| <b>Microphyta</b>         |  |            |             |            |            |             |             |
| epiphytes                 | 180.   | 17.        | 76.         | 3.8        | 27.        | 0.036       | 0.11        |
| phytoplankton             | 120.   | 0.040      | 28.         | 1.4        | 22.        | 0.024       | 0.040       |
| <b>Macrofauna</b>         |  |            |             |            |            |             |             |
| sponges                   | 21.  | 0.059      | 11.         | 0.078      | 0.50       | 0.0092      | 0.0076      |
| detritivores              |  |            |             |            |            |             |             |
| carnivores                | 6.6 (3)  | 0.0051     | 0.27        | 0.049      | 0.18       | 0.0043      | 0.0026      |
| <b>Total (4)</b>          | <b>960.</b>  | <b>24.</b> | <b>320.</b> | <b>6.4</b> | <b>61.</b> | <b>0.19</b> | <b>0.12</b> |

- Notes: (1) Calculated from Bach (1975) as Penicillus capitatus (56%), Rhipocephalus phoenix (37%), and Udotea flabellum (7%).
- (2) Calculated from Bach (1975) as H. incrassata (94%), and H. monile (6%).
- (3) Assumes ingestion of  $0.18 \text{ g m}^{-2} \text{ d}^{-1}$  since most members of this group are juveniles which ingest their own body weight/day (Jørgensen, 1966) of which 10% is net production.
- (4) Excludes detritivore and carnivore group as only initial uptake by primary production from either water or sediment is relevant to potential turnover.

Table 4. Correlation Coefficients of Radionuclide Uptake by Thalassia testudinum Including Mean Values of Activities (disintegrations per minute per gram dry weight).

| Leaf          | Silver-108 | Cesium-137 | Manganese-54 | Zinc-65 | Sodium-22 | Cobalt-57 | Cobalt-60 |
|---------------|------------|------------|--------------|---------|-----------|-----------|-----------|
| Bismuth-207   | .909       | .989       | .872         | .962    | .999      | .236      | .687      |
| Silver-108    |            | .886       | .738         | .873    | .895      | .242      | .664      |
| Cesium-137    |            |            | .894         | .958    | .991      | .272      | .703      |
| Manganese-54  |            |            |              | .894    | .877      | .580      | .805      |
| Zinc-65       |            |            |              |         | .958      | .331      | .721      |
| Sodium-22     |            |            |              |         |           | .221      | .675      |
| Cobalt-57     |            |            |              |         |           |           | .646      |
| Cobalt-60     |            |            |              |         |           |           |           |
| Root Material | Silver-108 | Cesium-137 | Manganese-54 | Zinc-65 | Sodium-22 | Cobalt-57 | Cobalt-60 |
| Bismuth-207   | .689       | .990       | .883         | .944    | .997      | .191      | .852      |
| Silver-108    |            | .662       | .552         | .648    | .656      | .222      | .625      |
| Cesium-137    |            |            | .883         | .943    | .991      | .188      | .846      |
| Manganese-54  |            |            |              | .900    | .869      | .495      | .870      |
| Zinc-65       |            |            |              |         | .929      | .372      | .890      |
| Sodium-22     |            |            |              |         |           | .141      | .834      |
| Cobalt-57     |            |            |              |         |           |           | .476      |
| Cobalt-60     |            |            |              |         |           |           |           |

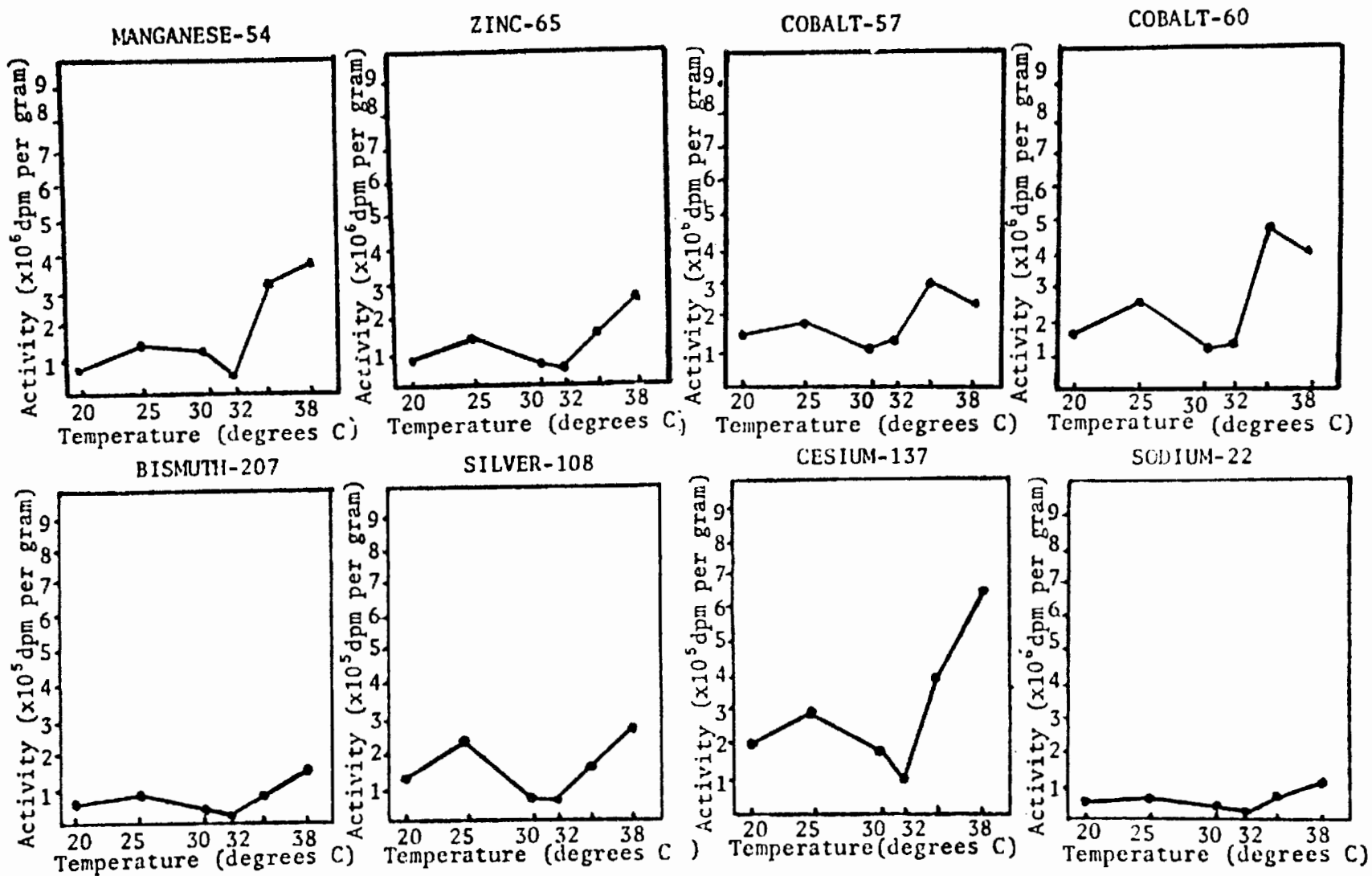


Figure 1. . Trace metal activities in disintegration per minute per g dry wt. in blades as a function of temperature. Each point represents mean of five samples.

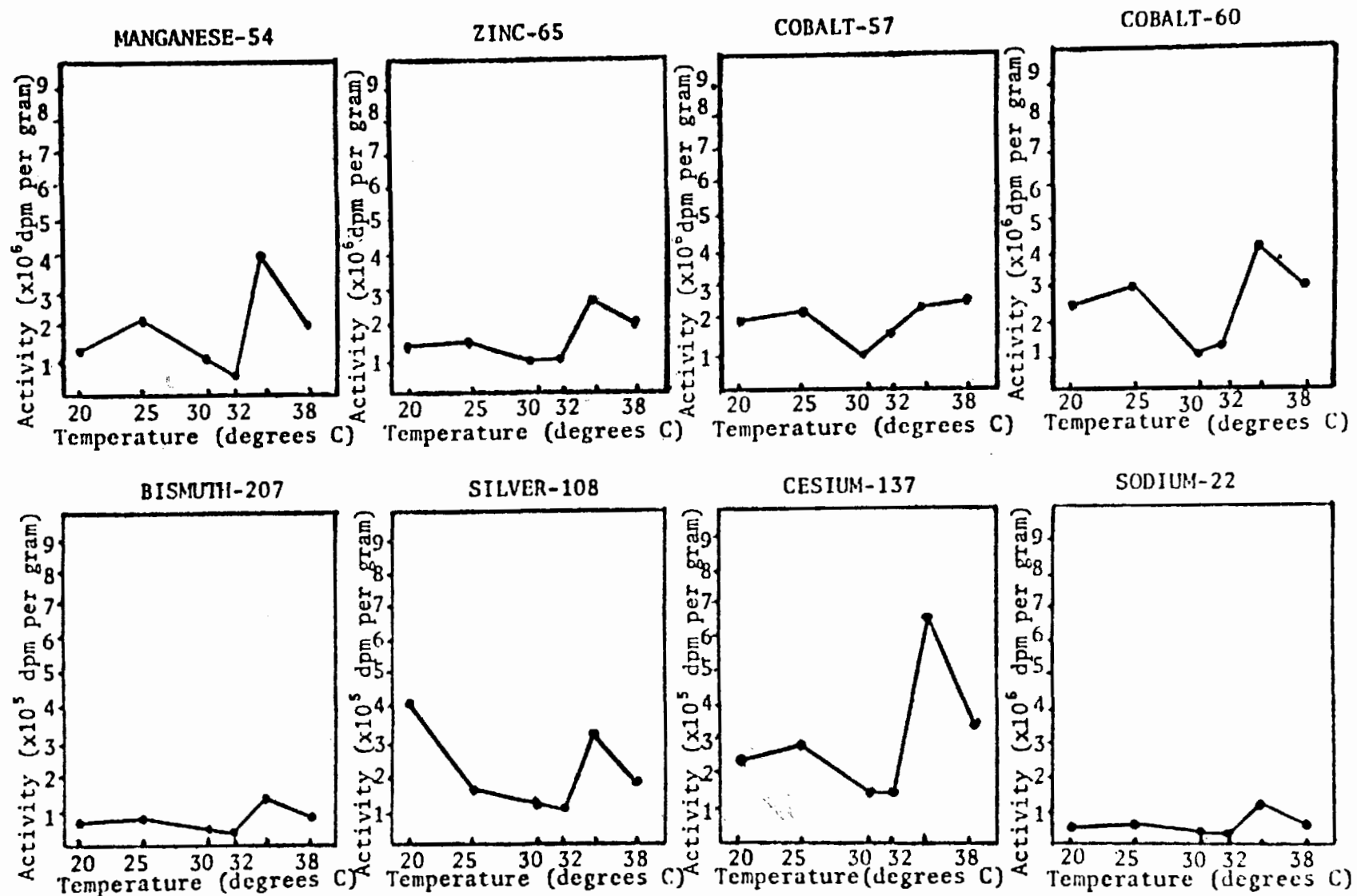
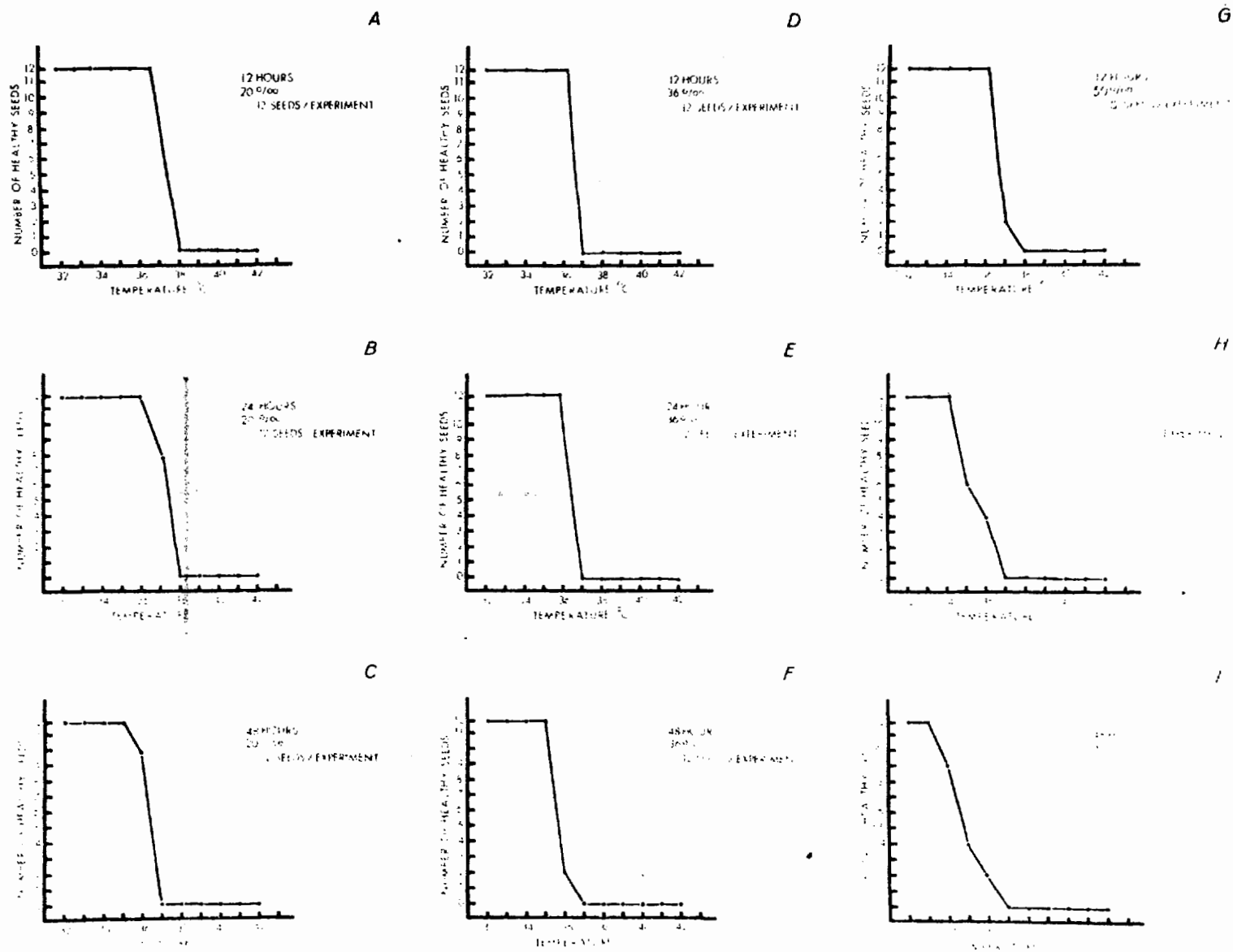


Figure 2. Trace metal activities in disintegration per minute per g dry wt. in roots as a function of temperature. Each point represents mean of five samples.

Figure 3. Mortality of Thalassia as a function of temperature and salinity.



WASTE HEAT MANAGEMENT AND UTILIZATION:  
SOME REGULATORY CONSTRAINTS \*

William A. Anderson, II  
P.O. Box 1535  
Richmond, Virginia 23212

ABSTRACT

The need for rational management and utilization of waste heat is undeniable. Yet conflicting governmental policies have resulted in regulatory constraints that often foreclose rational solutions. Effluent limitations and water quality standards under the Federal Water Pollution Control Act restrict use of surface waters, including cooling lakes, for waste heat management. Other regulatory constraints, including provisions of the Clean Air Act Amendments of 1977, may preclude the use of evaporative cooling towers under some circumstances due to salt drift emissions. Waste heat utilization schemes involving clusters of industrial facilities will also encounter environmental regulatory constraints. Provisions of both the Air Act and the Water Act will limit industrial concentration in any given locality. Thermal aquaculture may be possible under governing EPA regulations only in blowdown streams from closed-cycle systems. Concentrated contaminants in these blowdown streams may make the produce unmarketable.

\*This paper was not presented.

**TECHNICAL REPORT DATA**  
(Please read Instructions on the reverse before completing)

|   |  |   |  |   |
|---|--|---|--|---|
| 1. REPORT NO.<br><b>EPA-600/9-79-031b</b>   |  | 2.  | 3. RECIPIENT'S ACCESSION NO.                                       |   |
| 4. TITLE AND SUBTITLE<br><b>Proceedings: Second Conference on Waste Heat Management and Utilization (December 1978, Miami Beach, FL), Volume 2</b>  |  |   | 5. REPORT DATE<br><b>August 1979</b>                               |   |
| 7. AUTHOR(S)<br><b>S. S. Lee and Subrata Sengupta, Compilers</b>  |  |   | 6. PERFORMING ORGANIZATION CODE                                    |   |
| 9. PERFORMING ORGANIZATION NAME AND ADDRESS<br><b>University of Miami<br/>Department of Mechanical Engineering<br/>Coral Gables, Florida 33124</b>  |  |   | 8. PERFORMING ORGANIZATION REPORT NO.                              |   |
| 12. SPONSORING AGENCY NAME AND ADDRESS<br><b>EPA, Office of Research and Development*<br/>Industrial Environmental Research Laboratory<br/>Research Triangle Park, NC 27711</b>   |  |   | 10. PROGRAM ELEMENT NO.<br><b>EHE624A</b>                          |   |
|   |  |   | 11. CONTRACT/GRANT NO.<br><b>EPA Purchase Order<br/>DA86256J</b>   |   |
| 15. SUPPLEMENTARY NOTES<br><b>IERL-RTP project officer is Theodore G. Brna, MD-61, 919/541-2683. Cosponsors are: EPRI, Florida Power and Light Co., Univ. of Miami, U.S. DoE, U.S. EPA, and U.S. Nuclear Regulatory Commission.</b>   |  |   | 13. TYPE OF REPORT AND PERIOD COVERED<br><b>Proceedings; 12/78</b> |   |
| 16. ABSTRACT<br><b>The proceedings document most presentations made during the Second Conference on Waste Heat Management and Utilization, held December 4-6, 1978, at Miami Beach, FL. Presentations were grouped by areas of concern: general, utilization, mathematical modeling, ecological effects, cooling tower plumes, cooling towers, cogeneration, cooling systems, cooling lakes, recovery systems, aquatic thermal discharges, and atmospheric effects. Causes, effects, prediction, monitoring, utilization, and abatement of thermal discharges were represented. Utilization was of prime importance because of increased awareness that waste heat is a valuable resource. Cogeneration and recovery systems were added to reflect this emphasis.</b> |  |   | 14. SPONSORING AGENCY CODE<br><b>EPA/600/13</b>                    |   |
| 17. KEY WORDS AND DOCUMENT ANALYSIS   |  |   |  |   |
| a. DESCRIPTORS  |  | b. IDENTIFIERS/OPEN ENDED TERMS                         |  | c. COSATI Field/Group   |
| <b>Pollution<br/>Heat Recovery<br/>Management<br/>Utilization<br/>Mathematical Models<br/>Ecology</b>   |  | <b>Cooling Towers<br/>Plumes</b>                        |  | <b>Pollution Control<br/>Stationary Sources<br/>Cogeneration<br/>Cooling Lakes<br/>Thermal Discharges<br/>Atmospheric Effects</b> |
|   |  |   |  | <b>13B 07A, 13I<br/>20M, 13A 21B<br/>05A<br/>14B<br/>12A<br/>06F</b>  |
| 18. DISTRIBUTION STATEMENT<br><b>Release to Public</b>  |  | 19. SECURITY CLASS (This Report)<br><b>Unclassified</b> |  | 21. NO. OF PAGES<br><b>637</b>  |
|   |  | 20. SECURITY CLASS (This page)<br><b>Unclassified</b>   |  | 22. PRICE   |